Climate and Drought Exposure Supplementary Figures for Perennial Grasslands in Southeast Utah Group National Parks

John B. Bradford[1], Caroline A. Havrilla[2], Jessica A. Hartsell[1,3], Daniel R. Schlaepfer[1],Molly M. McCormick[1], Seth Munson[1], Charles B. Yackulic[1], Terry T. Fisk[4], David Thoma[5], Dusty Perkins[5], Dana Witwicki[5,] Matt VanScoyoc[4], Mike Duniway[1], and Sasha Reed[1]

[1]US Geological Survey, Southwest Biological Science Center, Flagstaff, Arizona
[2]Colorado State University, Fort Collins, Colorado
[3]Northern Arizona University, Flagstaff, Arizona
[4]Southeast Utah Group National Park Service, Moab, Utah
[5]Northern Colorado Plateau Network, National Park Service

Supplement to:
Bradford, J. B., C. A. Havrilla, J. A. Hartsell, D. R. Schlaepfer, M. M. McCormick, S. Munson, C. B. Yackulic, T. T. Fisk, D. Thoma, D. Perkins, D. Witwicki, M. VanScoyoc, M.Duniway, and S. Reed. 2022. Southeast Utah Group climate and drought adaptation report: Exposure and perennial grass sensitivity. Natural Resource Report NPS/NCPN/NRR—2022/2432. National Park Service, Fort Collins, Colorado.

Complete exposure figures for the Southeast Utah Group national park units (Arches, Canyonlands, Hovenweep and Natural Bridges). Variables include annual and/or seasonal values aggregations of mean temperature, minimum temperature, maximum temperature, frost days, potential evapotranspiration, precipitation, soil volumetric water content, soil water availability (soil moisture above -3.9 MPa), wet soil days (soil water potential in any soil layer > -1.5 MPa), dry soil days (soil water potential in all soil layers < -3.9 MPa), soil water availability during not dry soil days (days with soil water potential in any soil layer > -3.9 MPa), extreme short-term dry stress (mean daily maximum air temperature of the 10 hottest day when soil water potential of all soil layers < -3.9 MPa), semi-dry soil duration length (mean length of continuous days with soil water potential in all soil layers < -1.5 MPa), transpiration, and evaporation. Figures for each park and variable include timeseries and future distributions by climate model for both values and anomalies relative to historical mean. Maps for each park and variable include means across years under historical and future conditions and future changes relatively to historical conditions.

Underlying data are available from the US Geological Survey's digital repository, ScienceBase, at https://www.sciencebase.gov/catalog/item/61a6952fd34eb622f6978d9f.

Contents

Category	Variable	Units	Seasons	Pages			
				Arches	Canyonlands	Hovenweep[1]	Natural Bridges
Meteorological Conditions	Temperature	C	A, W, Sp, Su, F	3 - 12	127 - 136	251 - 260	375 - 384
	Minimum temperature	C	W, Sp, Su, F	13 - 20	137 - 144	261 - 268	385 - 392
	Maximum temperature	C	W, Sp, Su, F	21 - 28	145 - 152	269 - 276	393 - 400
	Frost Days	days	W, Sp, F	29 - 34	153 - 158	277 - 282	401 - 406
	Potential evapotranspiration	cm/cm	W, Sp, Su, F	35 - 42	159 - 166	283 - 290	407 - 414
	Precipitation	cm	A, W, Sp, Su, F	43 - 52	167 - 176	291 - 300	415 - 424
	Monthly T-P correlation	r	NA	53 - 54	177 - 178	301 - 302	425 - 426
Soil moisture	Soil water content top 50cm	cm/cm	W, Sp, Su, F	55 - 62	179 - 186	303 - 310	427 - 434
	Soil water content	cm/cm	W, Sp, Su, F	63 - 70	187 - 194	311 - 318	435 - 442
	Available soil water top 50cm	cm	W, Sp, Su, F	71 - 78	195 - 202	319 - 326	443 - 450
	Available soil water	cm	W, Sp, Su, F	79 - 86	203 - 210	327 - 334	451 - 458
Ecological drought conditions	Days with wet soil	days	W, Sp, Su, F	87 - 94	211 - 218	335 - 342	459 - 466
	Days with dry soil	days	Sp, Su, F	95 - 100	219 - 224	343 - 348	467 - 472
	Extreme short-term stress	C	W, Sp, Su, F	101 - 108	225 - 232	349 - 356	473 - 480
	Duration of semi-dry soil spells	days	NA	109 - 110	233 - 234	357 - 358	481 - 482
Water Balance	Evaporation	cm	W, Sp, Su, F	111 - 118	235 - 242	359 - 366	483 - 490
	Transpiration	cm	W, Sp, Su, F	119 - 126	243 - 250	367 - 374	491 - 498

[1] Detailed data for visualizing climate and drought exposure results at a larger scale in Hovenweep are available from the USGS digital repository, ScienceBase, at https://www.sciencebase.gov/catalog/item/61a6952fd34eb622f6978d9f.

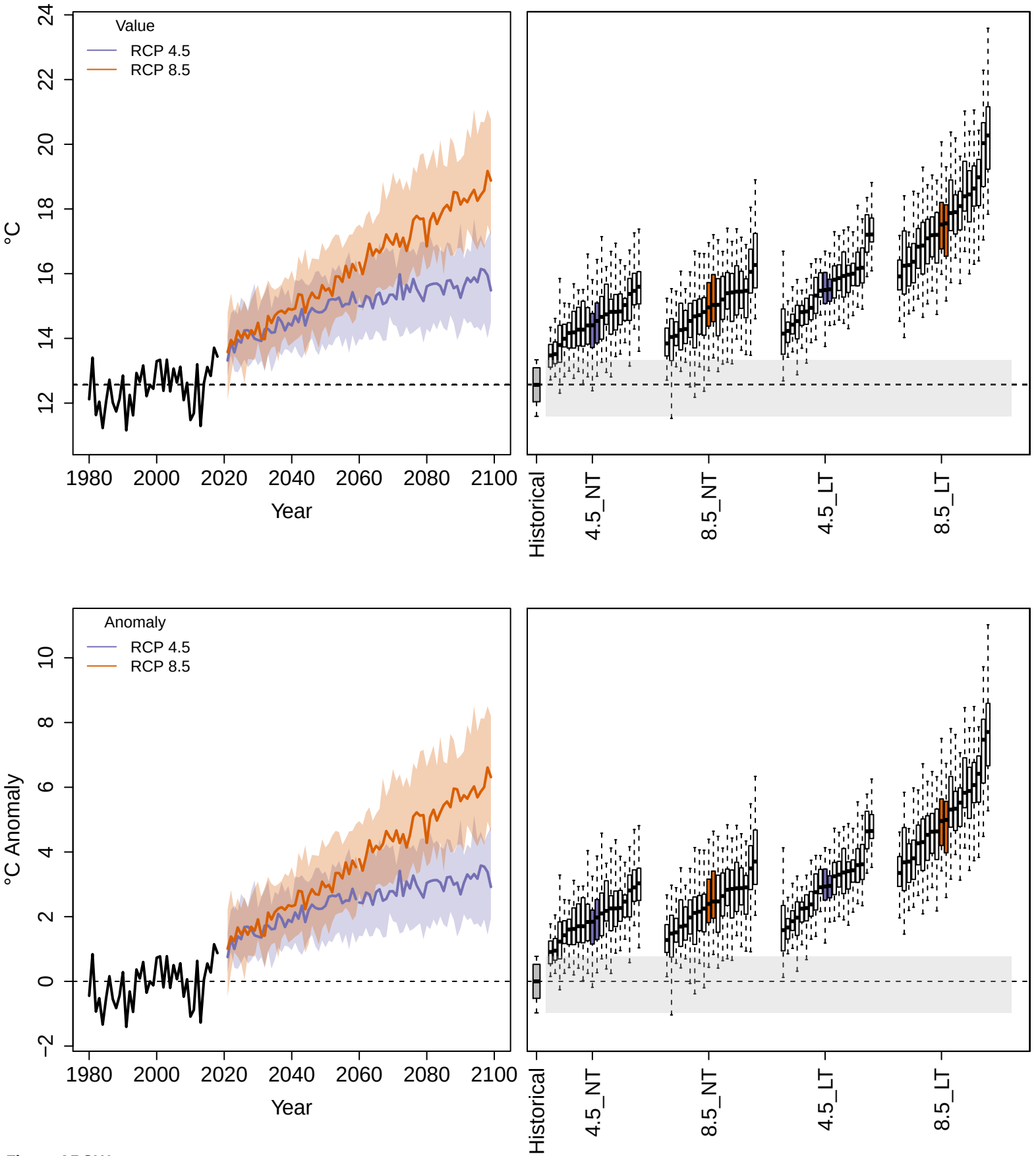


Figure ARCH1:
Past trends and future trajectories of park−wide mean values for Mean Annual Temperature in Arches. Top panels show values, bottom panels show changes from the long−term historical mean. Left: Time series of historical (black) and future projections for RCP 4.5 and 8.5. Shaded areas show spread among climate models. Right: Boxplots of temporal variability over 40−year periods under historical (left box) and individual climate models under two RCPs. Right: Historical time period is 1970−2010; near−term (NT) is 2020−2060; long−term (LT) is 2061−2100.

Arches: Mean Annual Temperature

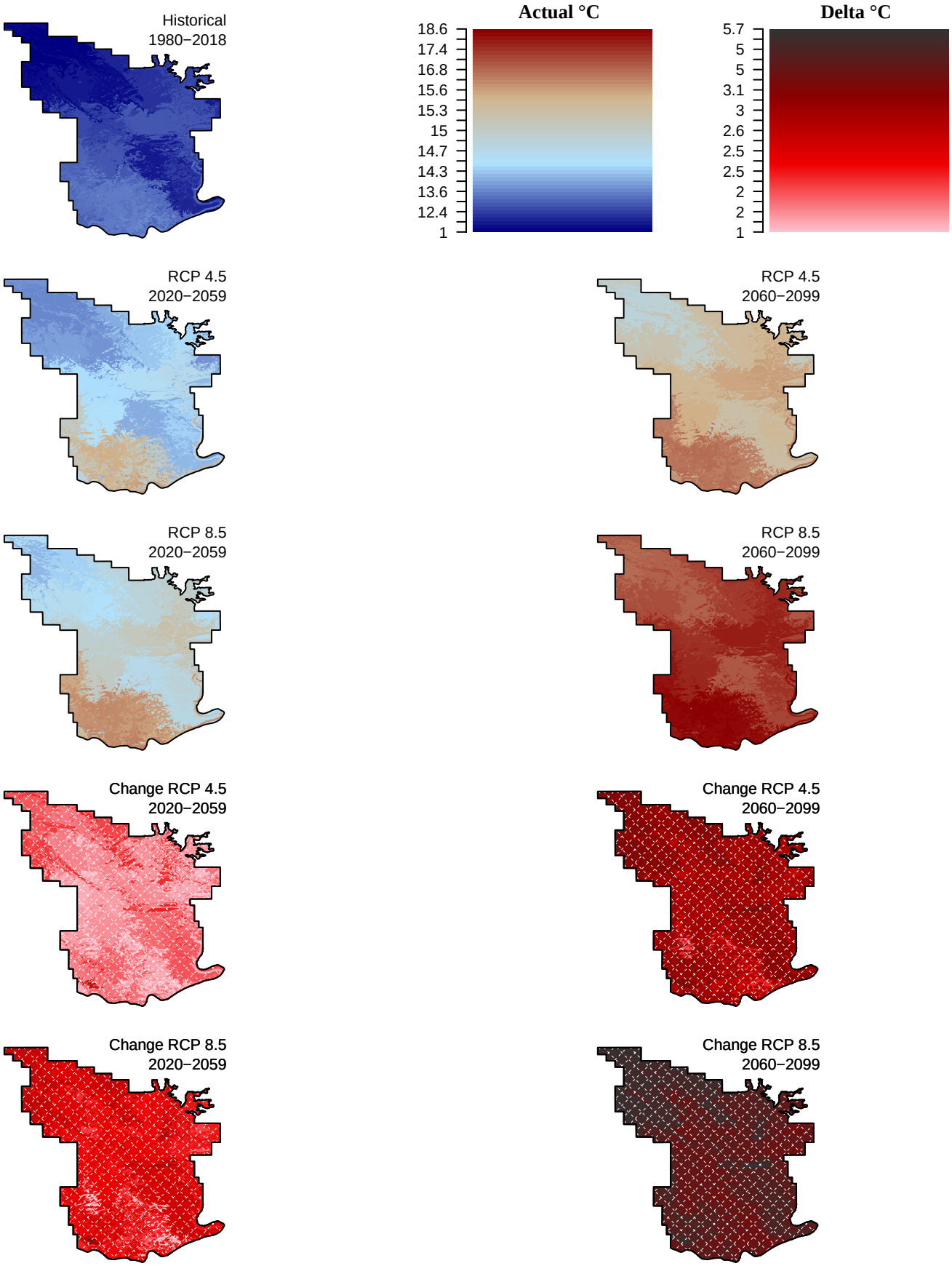


Figure ARCHmap1:
Past trends and future trajectories of park−wide mean values for Mean Annual Temperature in Arches. Topmost panel depicts the historical mean from 1980−2018. Lower four panels show the emission scenarios of RCP 4.5 and RCP 8.5 at near−term and long−term timeframes. Bottom four panels depict the change from the historical mean; cross hatching denotes areas of robust predicitons (90% of models agree in the direction of change).

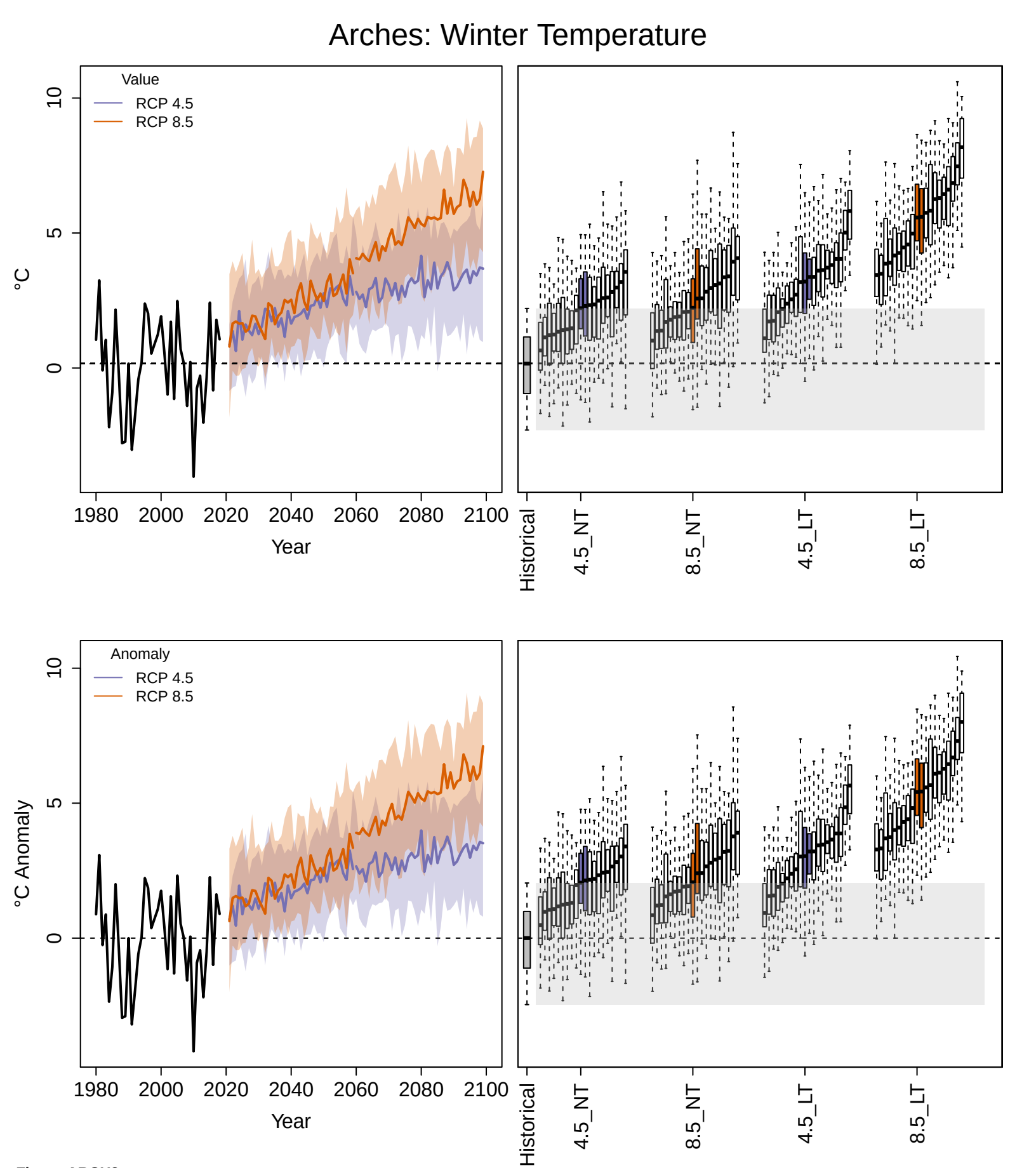


Figure ARCH3:
Past trends and future trajectories of park−wide mean values for Winter Temperature in Arches. Top panels show values, bottom panels show changes from the long−term historical mean. Left: Time series of historical (black) and future projections for RCP 4.5 and 8.5. Shaded areas show spread among climate models. Right: Boxplots of temporal variability over 40−year periods under historical (left box) and individual climate models under two RCPs. Right: Historical time period is 1970−2010; near−term (NT) is 2020−2060; long−term (LT) is 2061−2100.

Arches: Winter Temperature

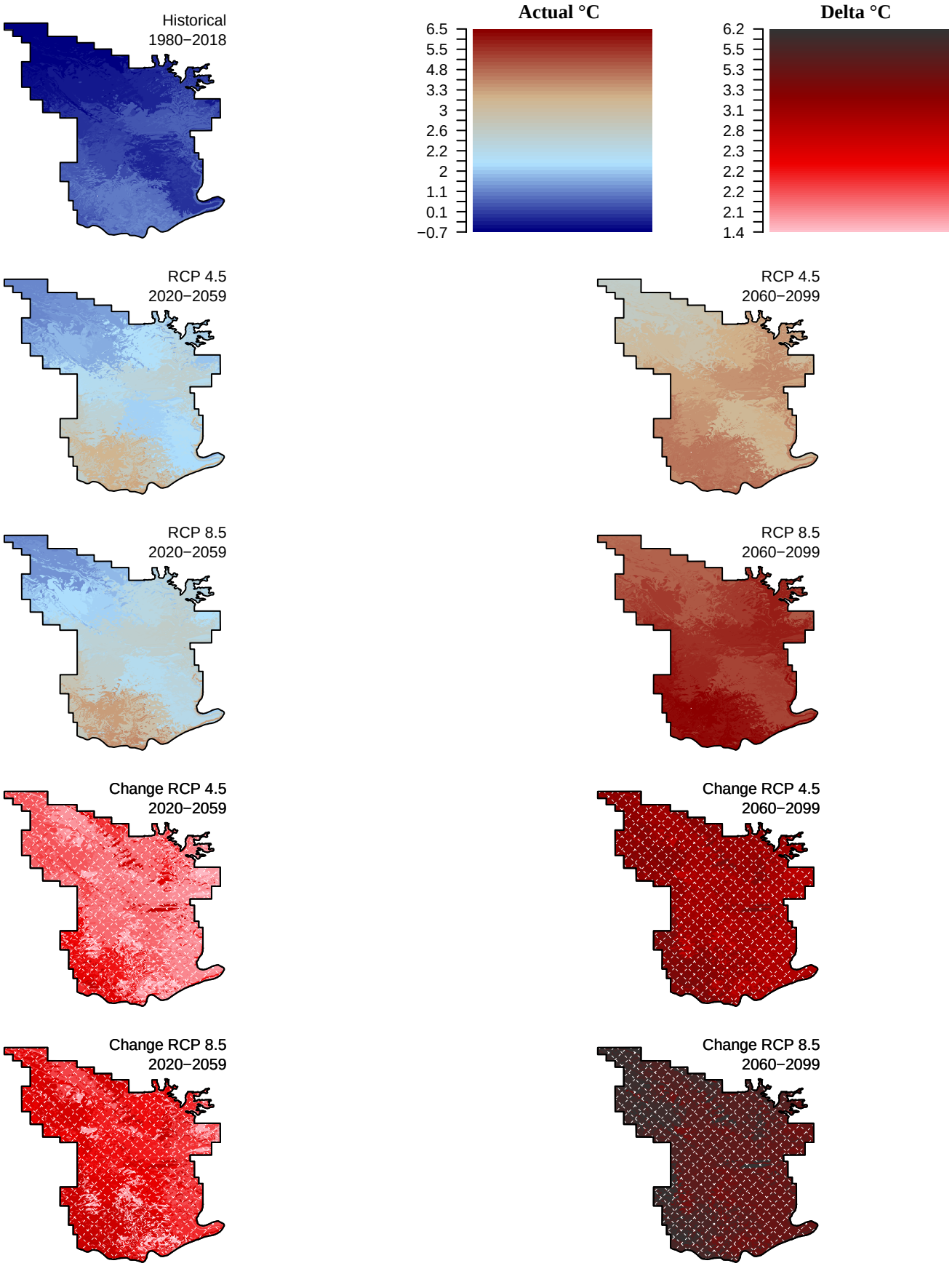


Figure ARCHmap3:
Past trends and future trajectories of park−wide mean values for Winter Temperature in Arches. Topmost panel depicts the historical mean from 1980−2018. Lower four panels show the emission scenarios of RCP 4.5 and RCP 8.5 at near−term and long−term timeframes. Bottom four panels depict the change from the historical mean; cross hatching denotes areas of robust predicitons (90% of models agree in the direction of change).

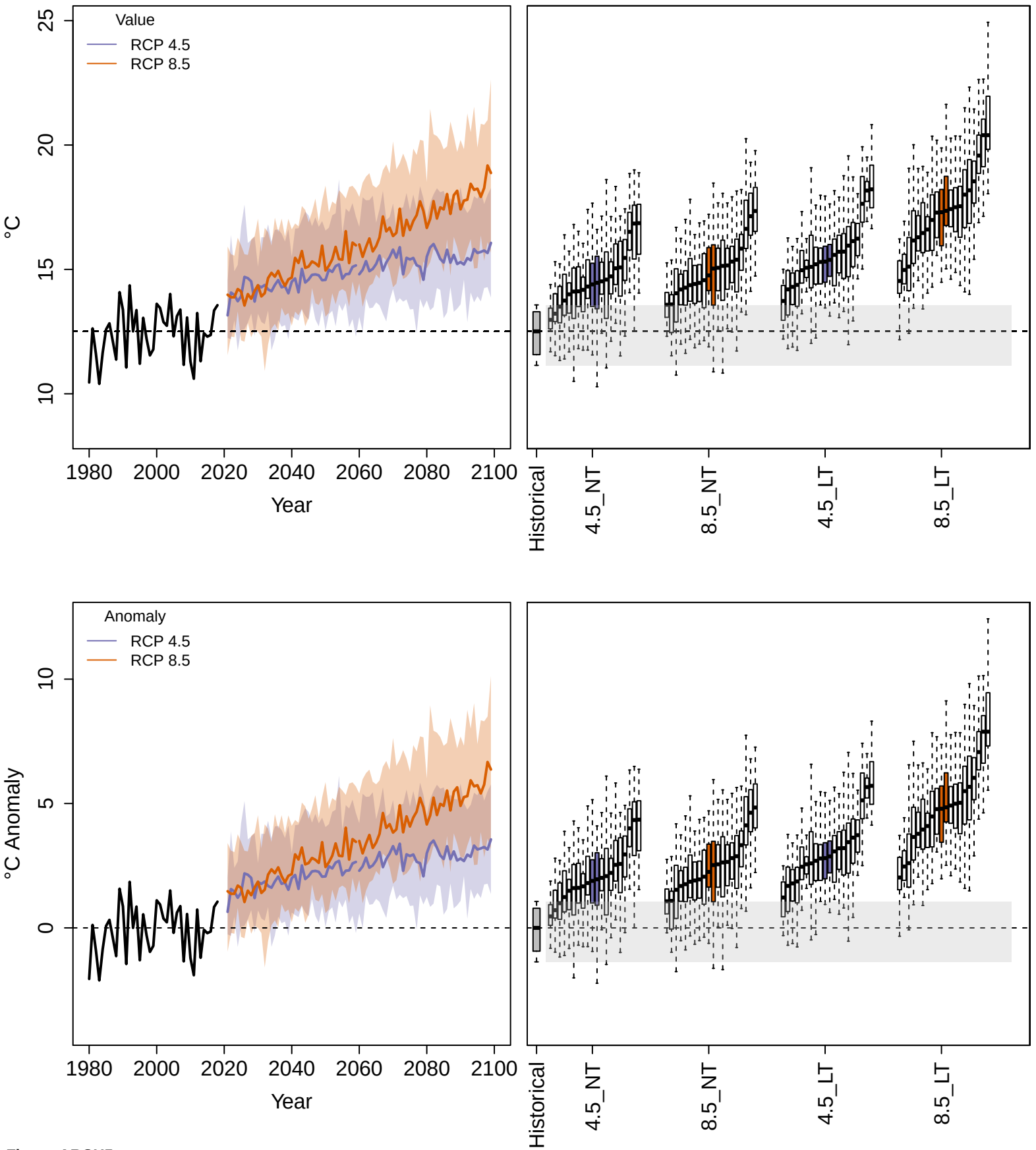


Figure ARCH5:
Past trends and future trajectories of park−wide mean values for Spring Temperature in Arches. Top panels show values, bottom panels show changes from the long−term historical mean. Left: Time series of historical (black) and future projections for RCP 4.5 and 8.5. Shaded areas show spread among climate models. Right: Boxplots of temporal variability over 40−year periods under historical (left box) and individual climate models under two RCPs. Right: Historical time period is 1970−2010; near−term (NT) is 2020−2060; long−term (LT) is 2061−2100.

Arches: Spring Temperature

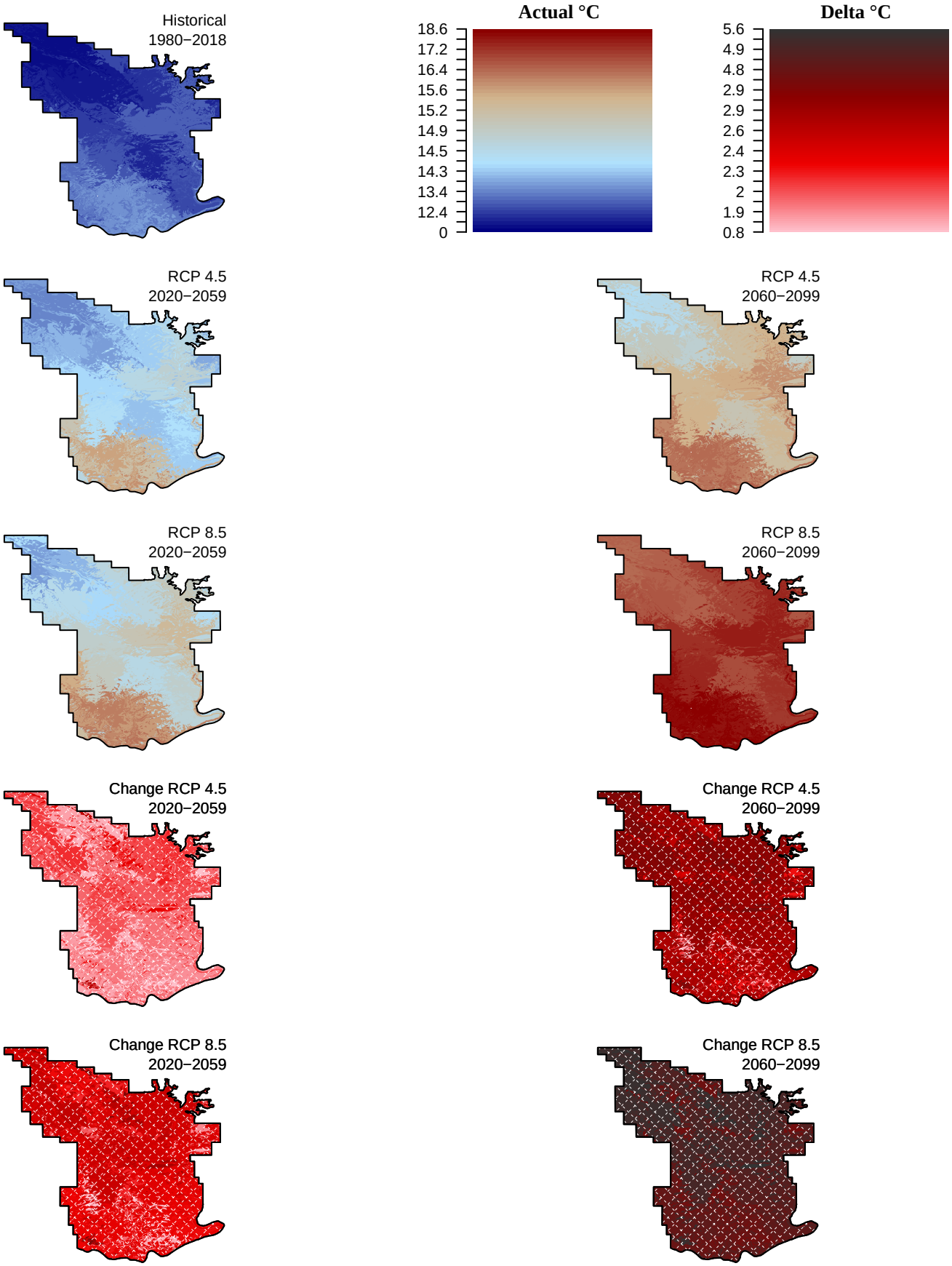


Figure ARCHmap5:
Past trends and future trajectories of park−wide mean values for Spring Temperature in Arches. Topmost panel depicts the historical mean from 1980−2018. Lower four panels show the emission scenarios of RCP 4.5 and RCP 8.5 at near−term and long−term timeframes. Bottom four panels depict the change from the historical mean; cross hatching denotes areas of robust predicitons (90% of models agree in the direction of change).

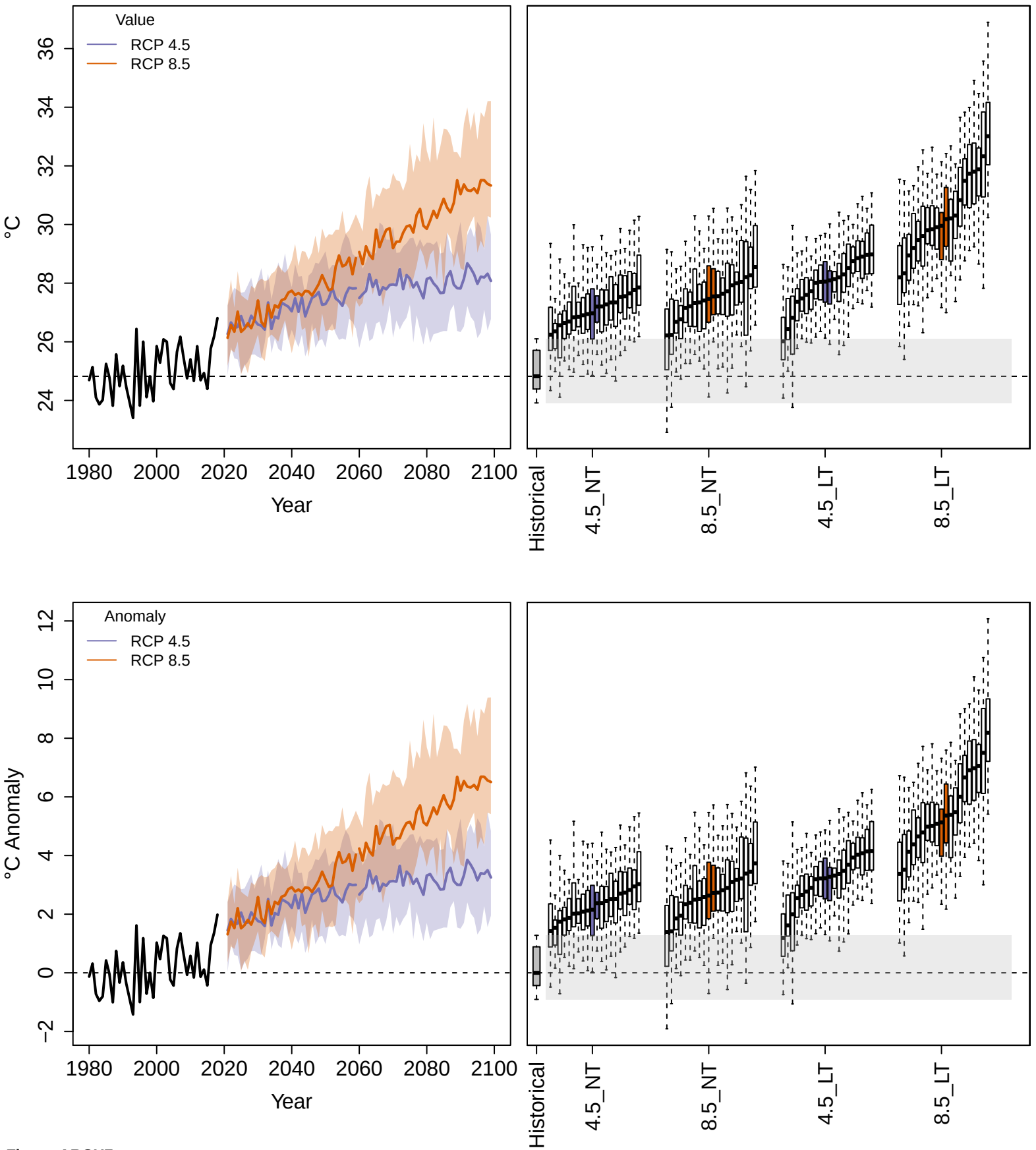


Figure ARCH7:
Past trends and future trajectories of park−wide mean values for Summer Temperature in Arches. Top panels show values, bottom panels show changes from the long−term historical mean. Left: Time series of historical (black) and future projections for RCP 4.5 and 8.5. Shaded areas show spread among climate models. Right: Boxplots of temporal variability over 40−year periods under historical (left box) and individual climate models under two RCPs. Right: Historical time period is 1970−2010; near−term (NT) is 2020−2060; long−term (LT) is 2061−2100.

Arches: Summer Temperature

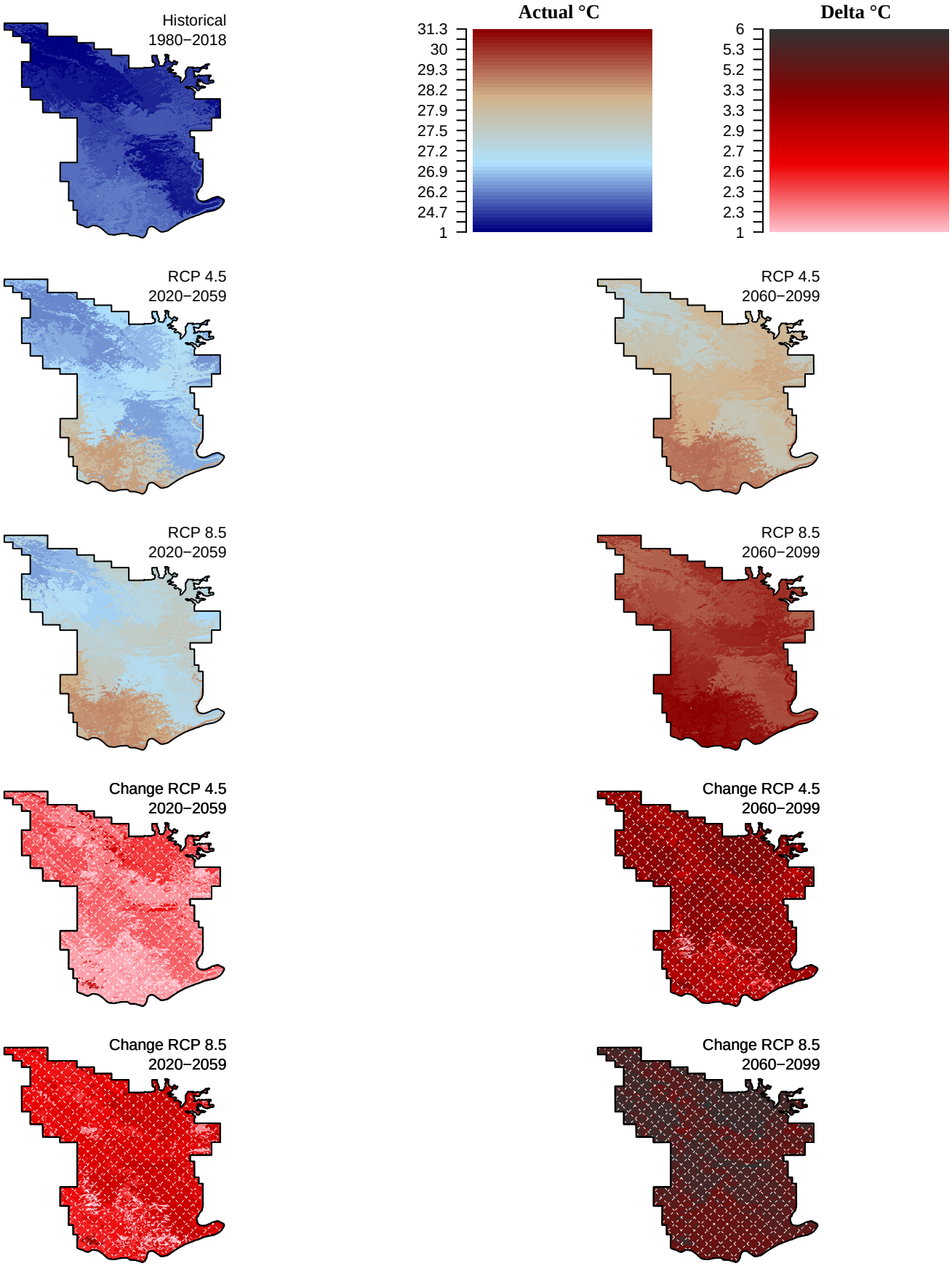


Figure ARCHmap7:
Past trends and future trajectories of park−wide mean values for Summer Temperature in Arches. Topmost panel depicts the historical mean from 1980−2018. Lower four panels show the emission scenarios of RCP 4.5 and RCP 8.5 at near−term and long−term timeframes. Bottom four panels depict the change from the historical mean; cross hatching denotes areas of robust predicitons (90% of models agree in the direction of change).

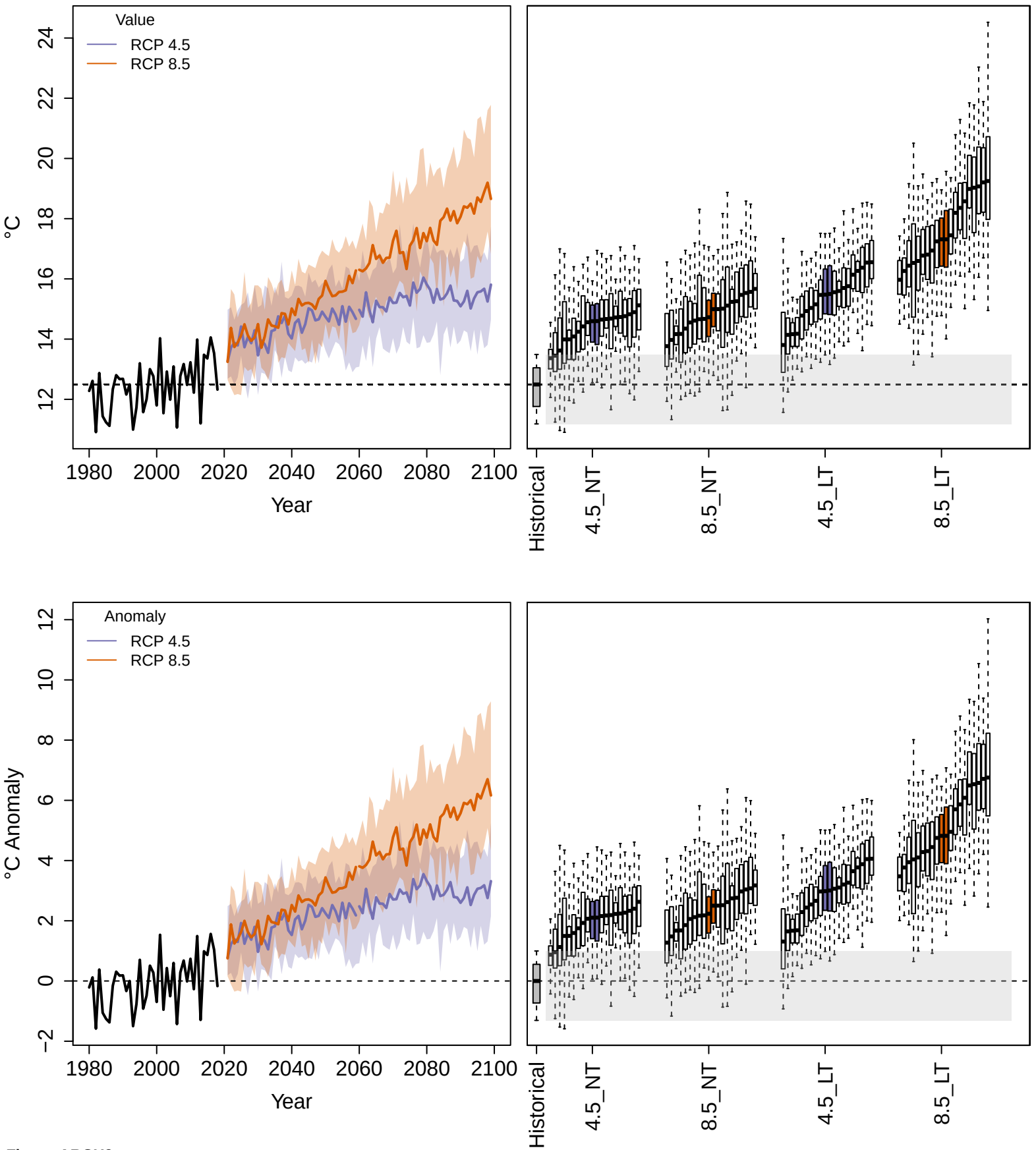


Figure ARCH9:
Past trends and future trajectories of park−wide mean values for Fall Temperature in Arches. Top panels show values, bottom panels show changes from the long−term historical mean. Left: Time series of historical (black) and future projections for RCP 4.5 and 8.5. Shaded areas show spread among climate models. Right: Boxplots of temporal variability over 40−year periods under historical (left box) and individual climate models under two RCPs. Right: Historical time period is 1970−2010; near−term (NT) is 2020−2060; long−term (LT) is 2061−2100.

Arches: Fall Temperature

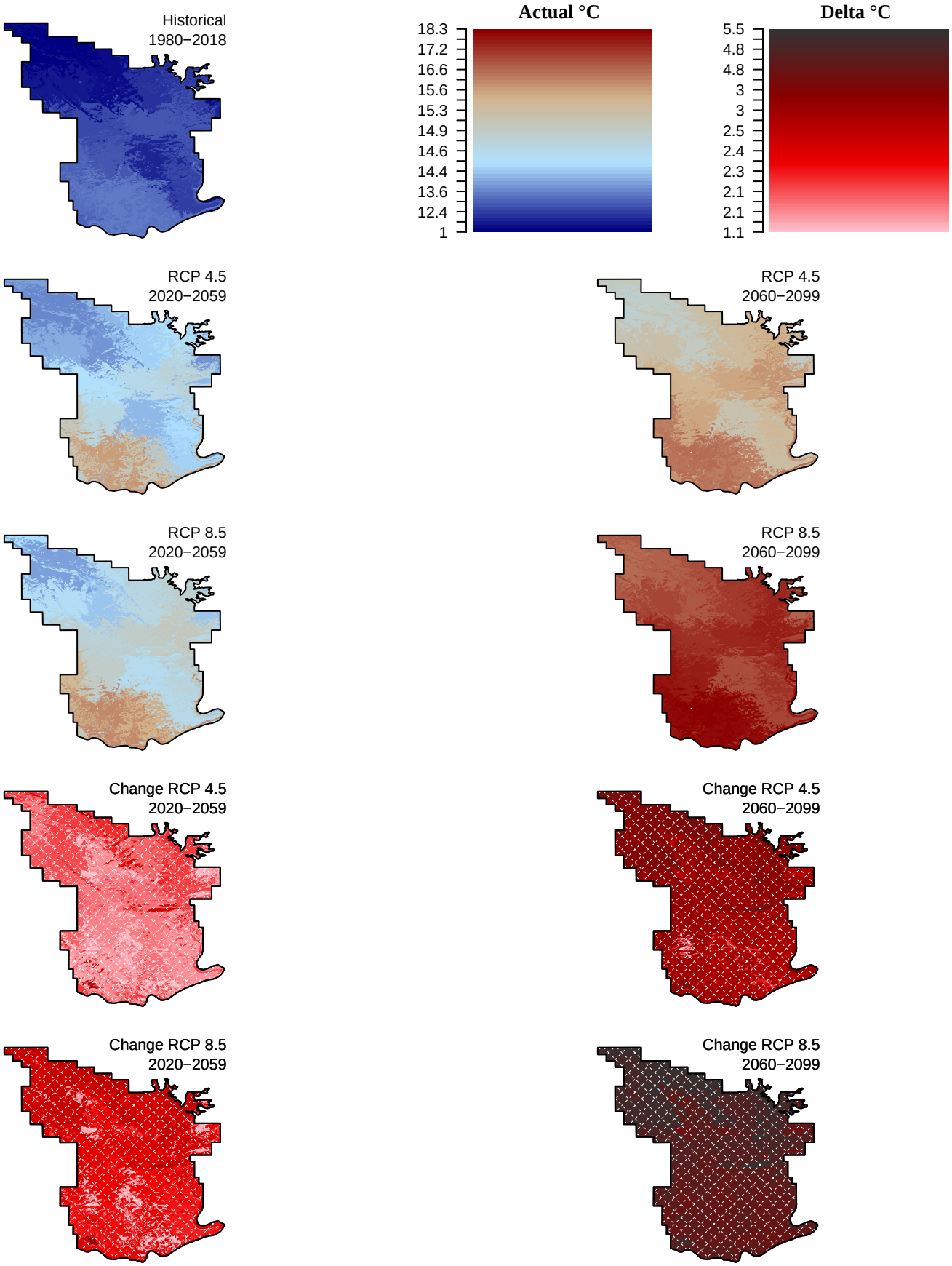


Figure ARCHmap9:
Past trends and future trajectories of park−wide mean values for Fall Temperature in Arches. Topmost panel depicts the historical mean from 1980−2018. Lower four panels show the emission scenarios of RCP 4.5 and RCP 8.5 at near−term and long−term timeframes. Bottom four panels depict the change from the historical mean; cross hatching denotes areas of robust predicitons (90% of models agree in the direction of change).

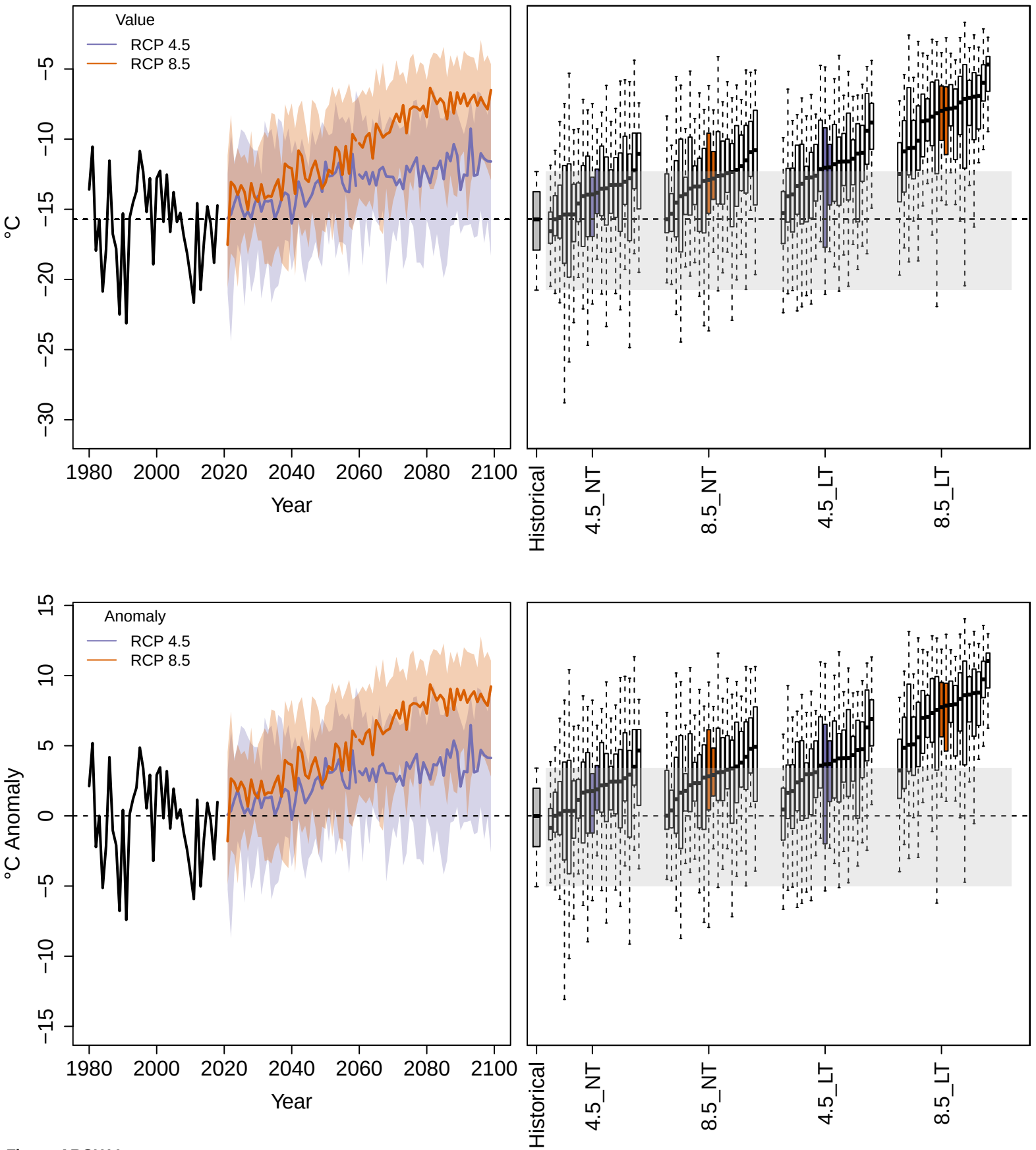


Figure ARCH11:
Past trends and future trajectories of park−wide mean values for Minimum winter temperature in Arches. Top panels show values, bottom panels show changes from the long−term historical mean. Left: Time series of historical (black) and future projections for RCP 4.5 and 8.5. Shaded areas show spread among climate models. Right: Boxplots of temporal variability over 40−year periods under historical (left box) and individual climate models under two RCPs. Right: Historical time period is 1970−2010; near−term (NT) is 2020−2060; long−term (LT) is 2061−2100.

Arches: Minimum winter temperature

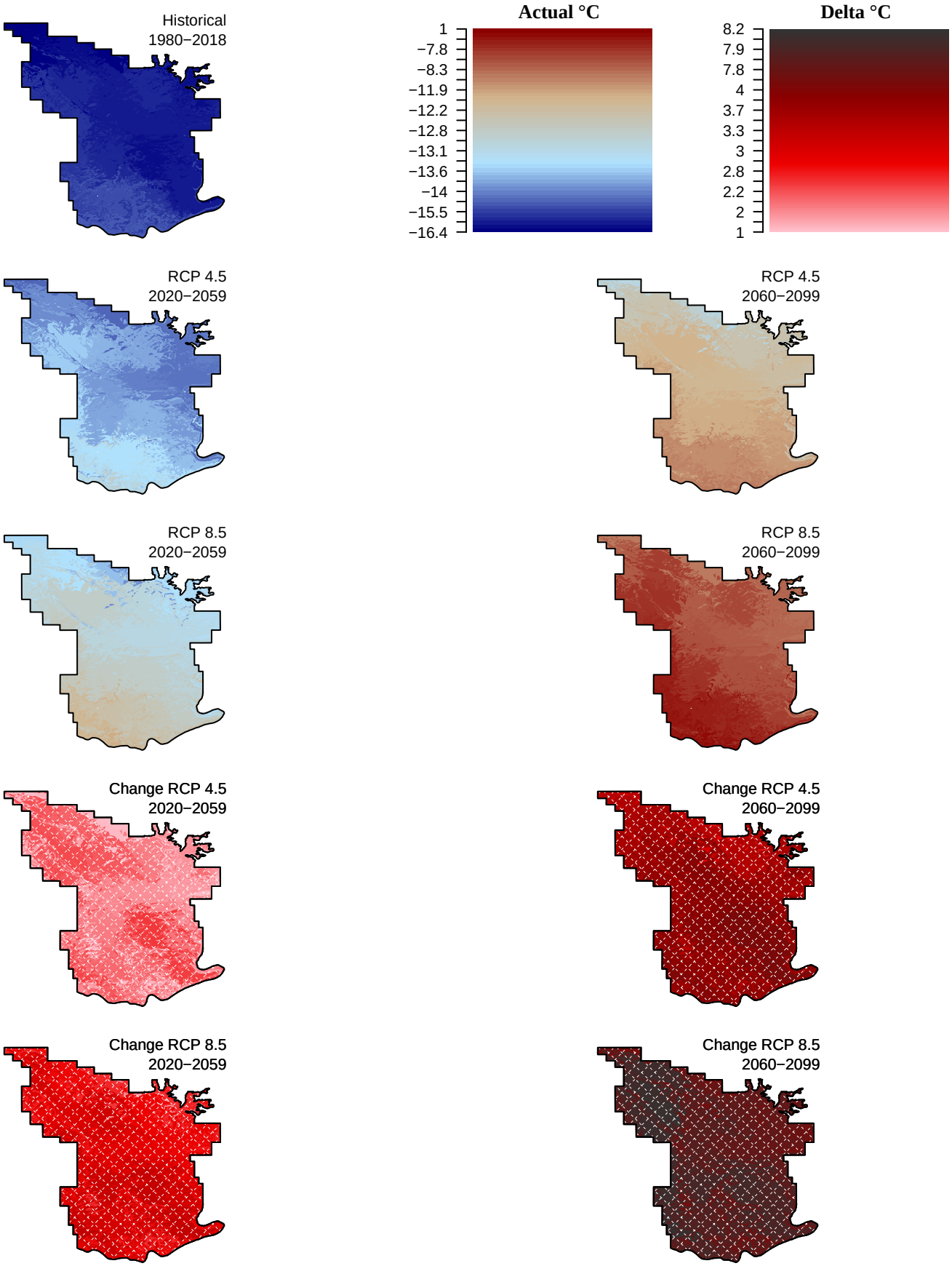


Figure ARCHmap11:
Past trends and future trajectories of park−wide mean values for Minimum winter temperature in Arches. Topmost panel depicts the historical mean from 1980−2018. Lower four panels show the emission scenarios of RCP 4.5 and RCP 8.5 at near−term and long−term timeframes. Bottom four panels depict the change from the historical mean; cross hatching denotes areas of robust predicitons (90% of models agree in the direction of change).

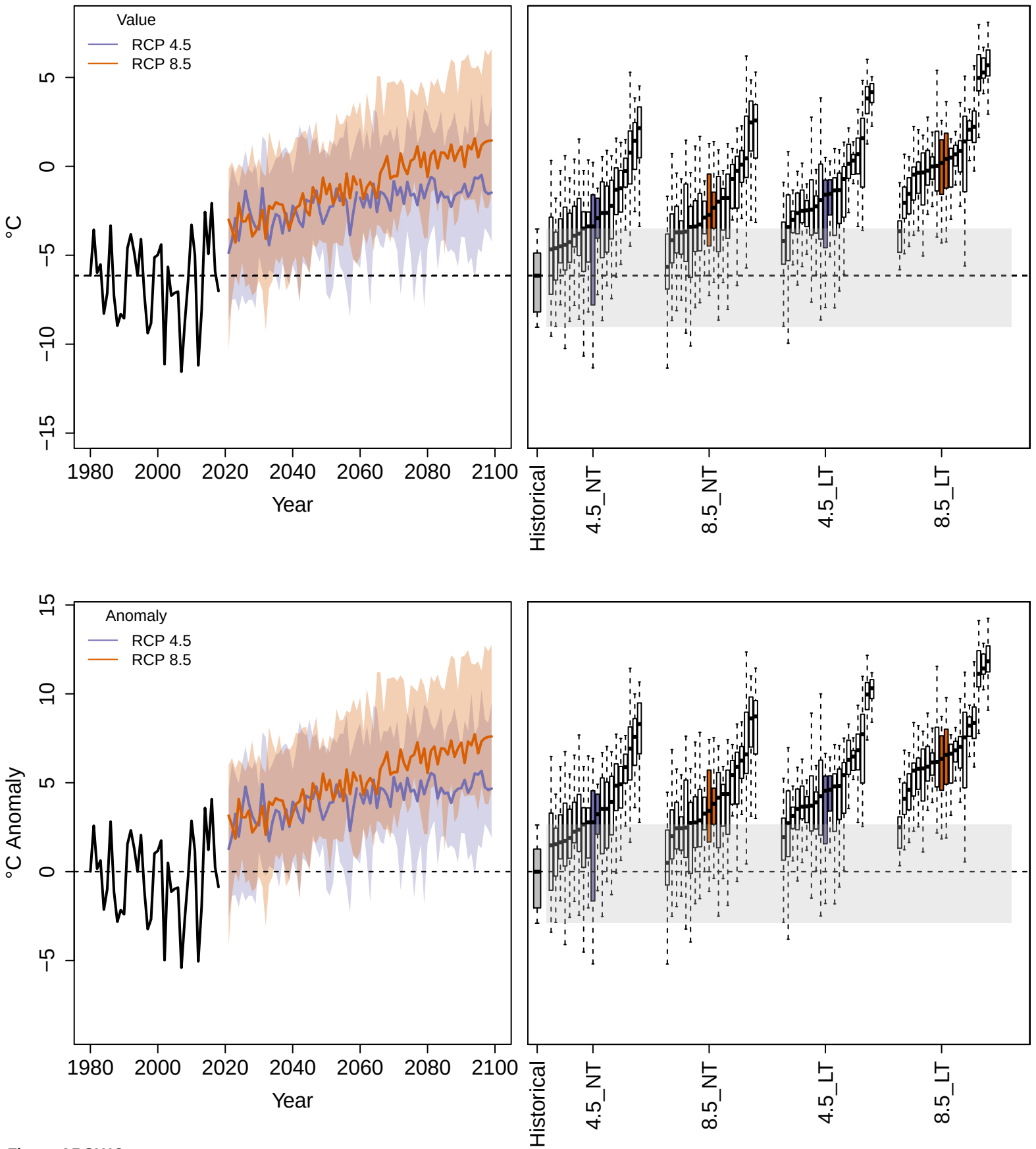


Figure ARCH13:
Past trends and future trajectories of park−wide mean values for Minimum spring temperature in Arches. Top panels show values, bottom panels show changes from the long−term historical mean. Left: Time series of historical (black) and future projections for RCP 4.5 and 8.5. Shaded areas show spread among climate models. Right: Boxplots of temporal variability over 40−year periods under historical (left box) and individual climate models under two RCPs. Right: Historical time period is 1970−2010; near−term (NT) is 2020−2060; long−term (LT) is 2061−2100.

Arches: Minimum spring temperature

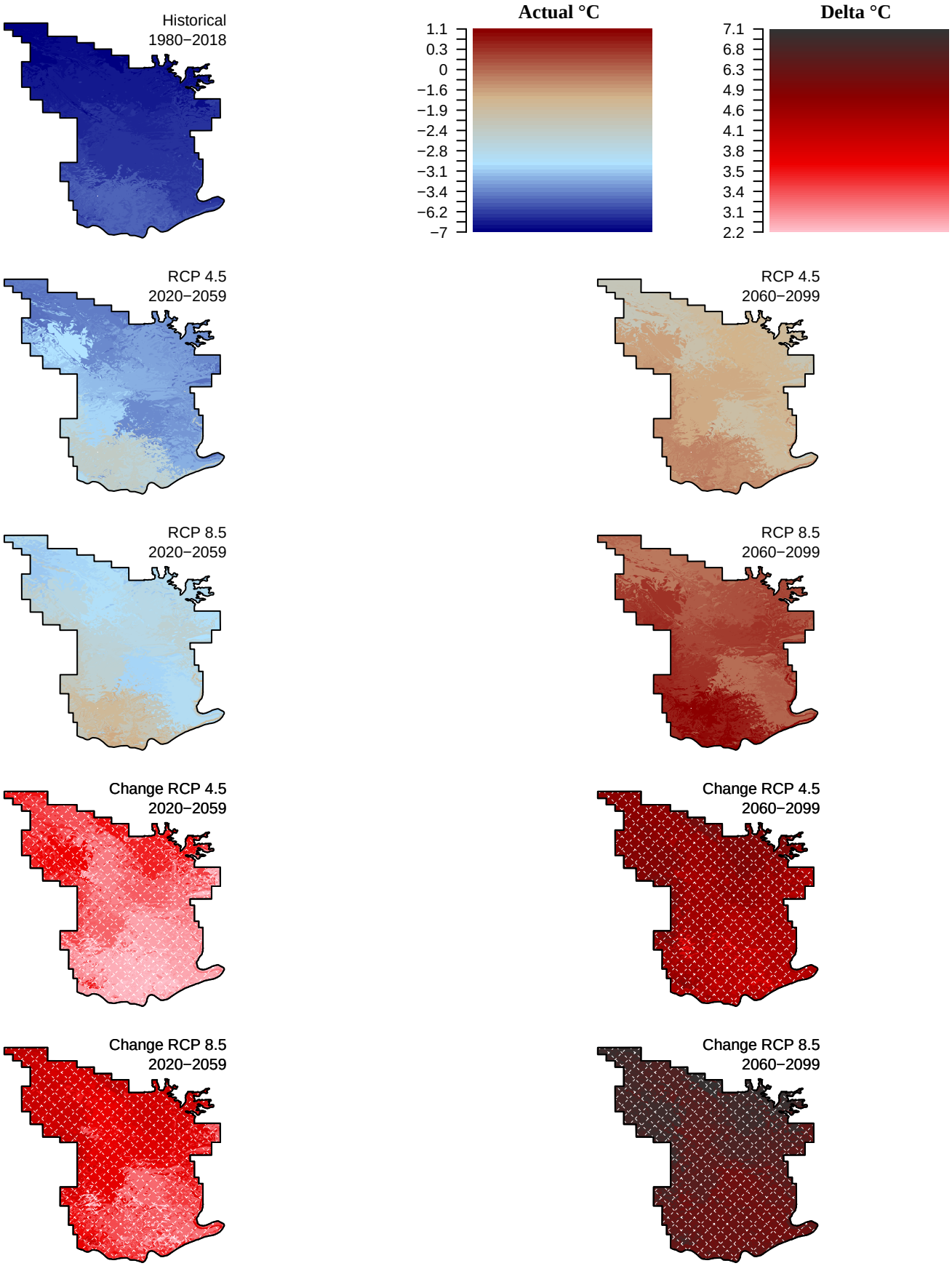


Figure ARCHmap13:
Past trends and future trajectories of park−wide mean values for Minimum spring temperature in Arches. Topmost panel depicts the historical mean from 1980−2018. Lower four panels show the emission scenarios of RCP 4.5 and RCP 8.5 at near−term and long−term timeframes. Bottom four panels depict the change from the historical mean; cross hatching denotes areas of robust predicitons (90% of models agree in the direction of change).

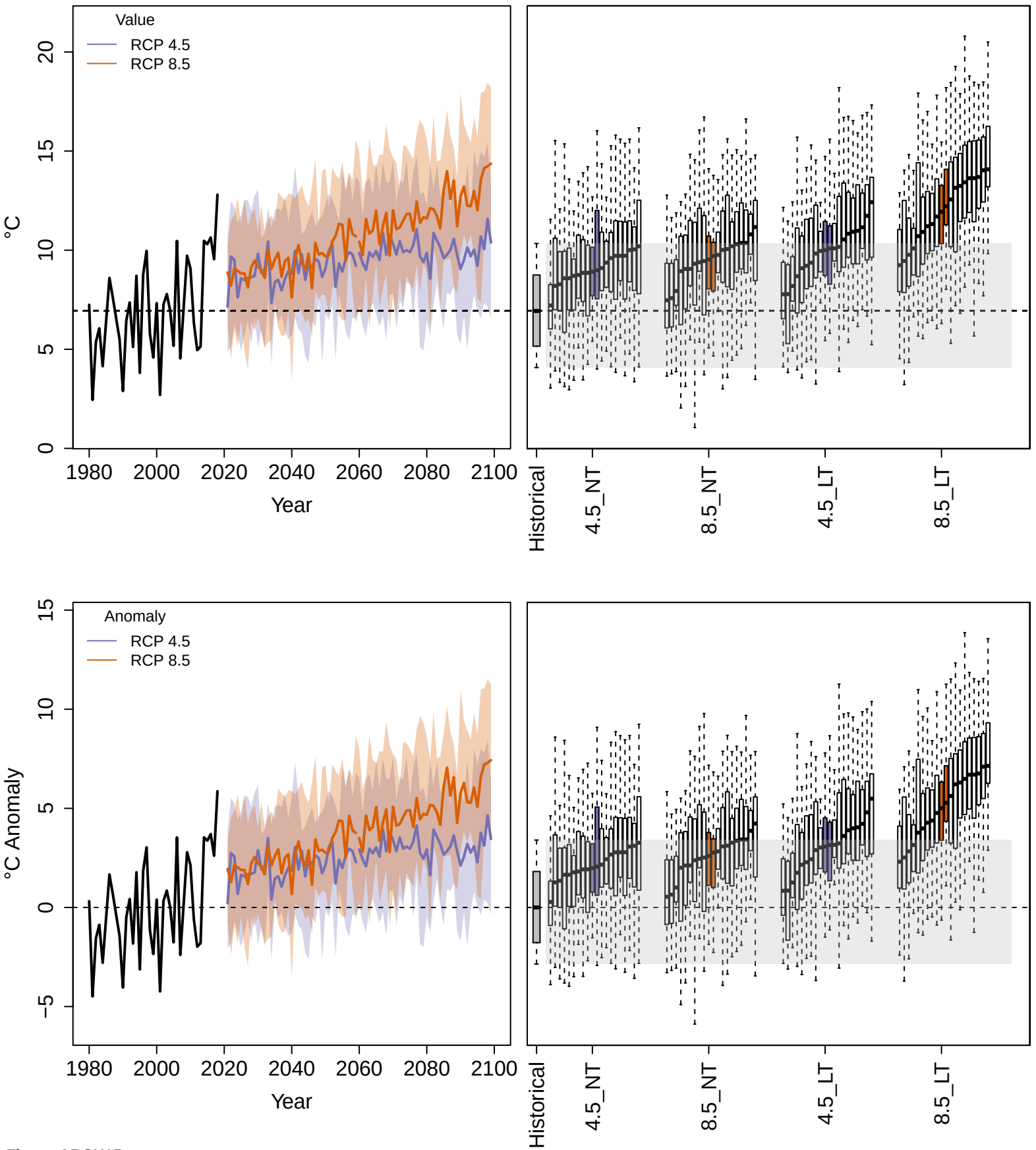


Figure ARCH15:
Past trends and future trajectories of park−wide mean values for Minimum summer temperature in Arches. Top panels show values, bottom panels show changes from the long−term historical mean. Left: Time series of historical (black) and future projections for RCP 4.5 and 8.5. Shaded areas show spread among climate models. Right: Boxplots of temporal variability over 40−year periods under historical (left box) and individual climate models under two RCPs. Right: Historical time period is 1970−2010; near−term (NT) is 2020−2060; long−term (LT) is 2061−2100.

Arches: Minimum summer temperature

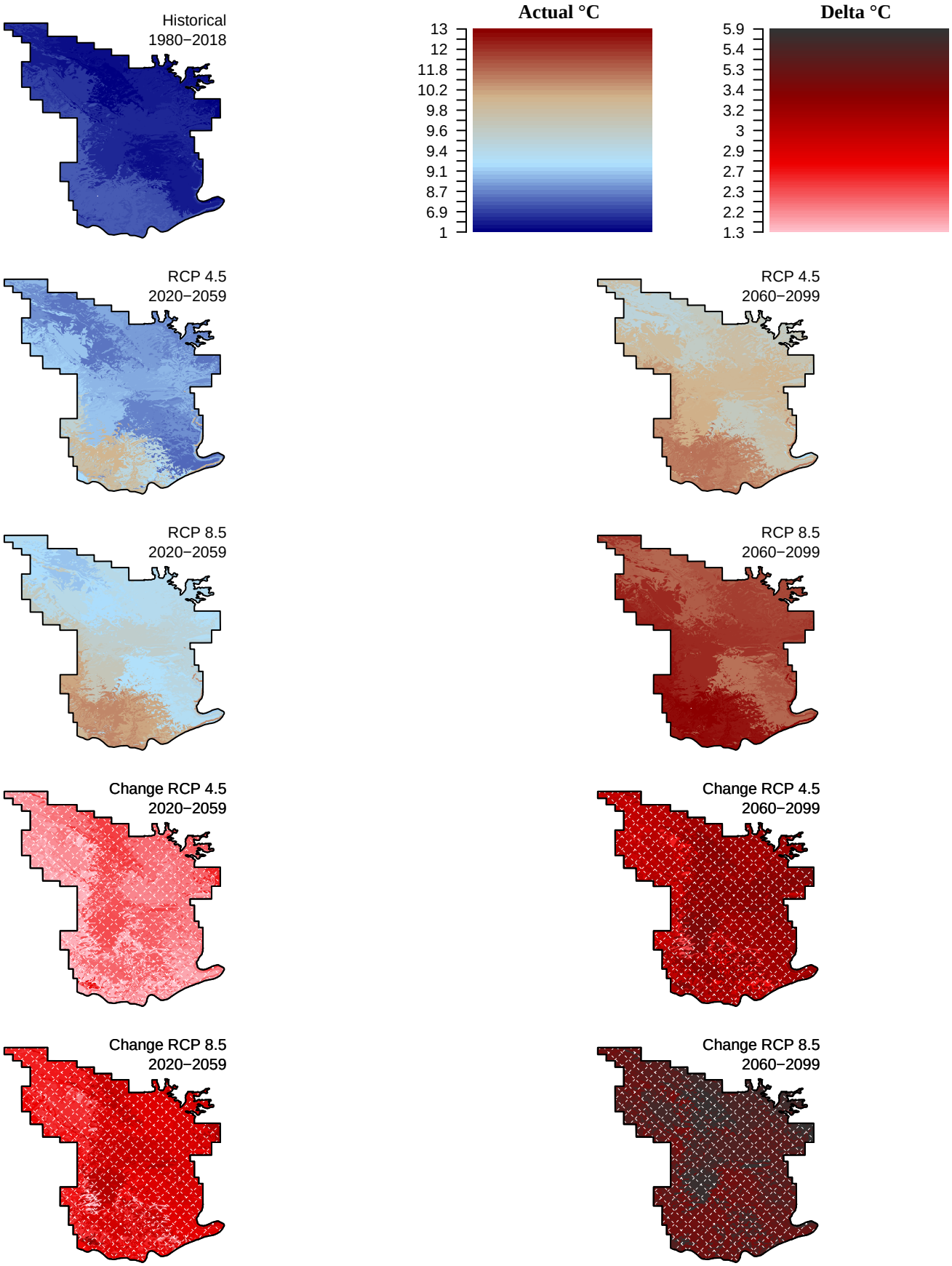


Figure ARCHmap15:
Past trends and future trajectories of park−wide mean values for Minimum summer temperature in Arches. Topmost panel depicts the historical mean from 1980−2018. Lower four panels show the emission scenarios of RCP 4.5 and RCP 8.5 at near−term and long−term timeframes. Bottom four panels depict the change from the historical mean; cross hatching denotes areas of robust predicitons (90% of models agree in the direction of change).

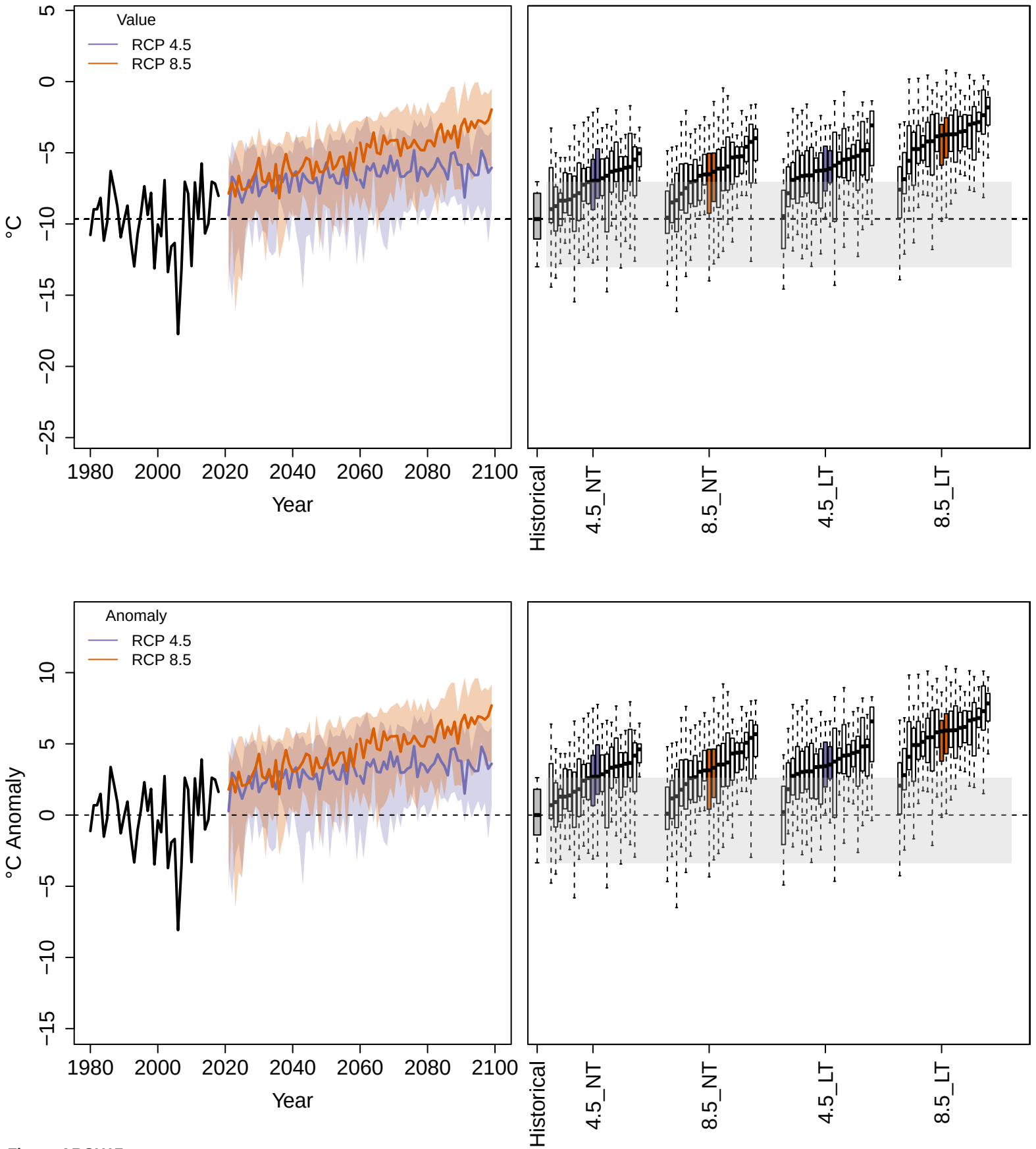


Figure ARCH17:
Past trends and future trajectories of park−wide mean values for Minimum fall temperature in Arches. Top panels show values, bottom panels show changes from the long−term historical mean. Left: Time series of historical (black) and future projections for RCP 4.5 and 8.5. Shaded areas show spread among climate models. Right: Boxplots of temporal variability over 40−year periods under historical (left box) and individual climate models under two RCPs. Right: Historical time period is 1970−2010; near−term (NT) is 2020−2060; long−term (LT) is 2061−2100.

Arches: Minimum fall temperature

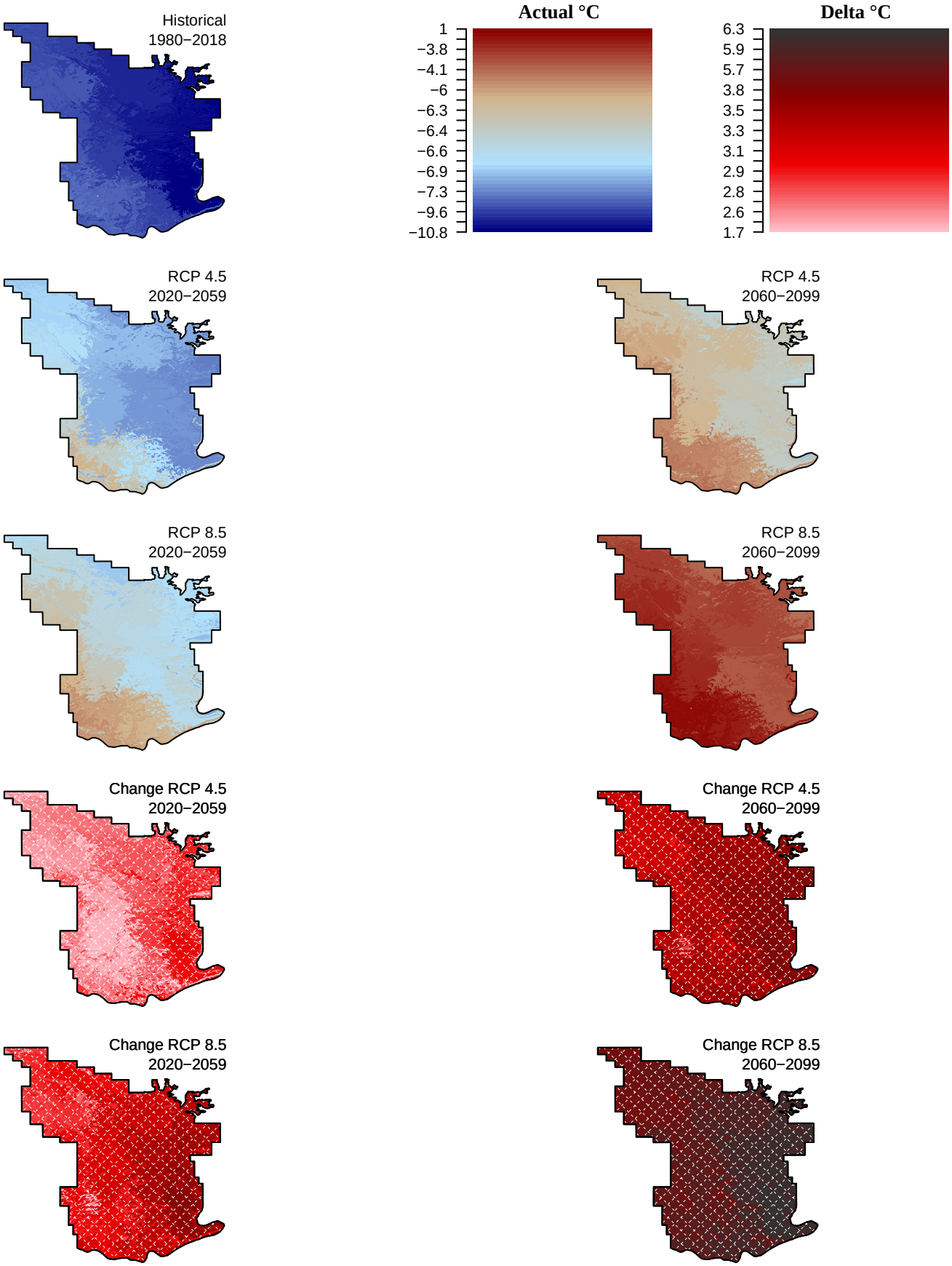


Figure ARCHmap17:
Past trends and future trajectories of park−wide mean values for Minimum fall temperature in Arches. Topmost panel depicts the historical mean from 1980−2018. Lower four panels show the emission scenarios of RCP 4.5 and RCP 8.5 at near−term and long−term timeframes. Bottom four panels depict the change from the historical mean; cross hatching denotes areas of robust predicitons (90% of models agree in the direction of change).

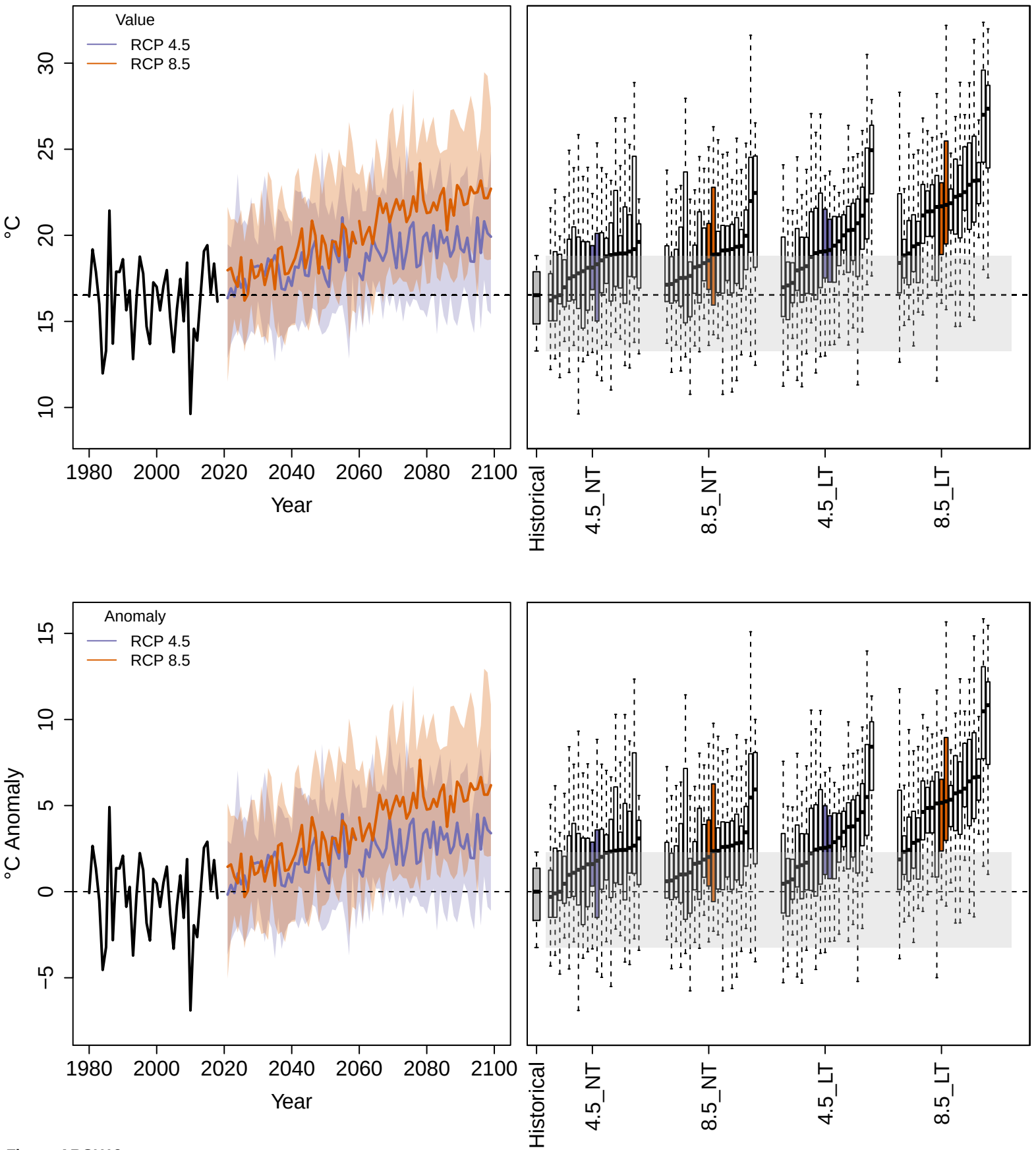


Figure ARCH19:
Past trends and future trajectories of park−wide mean values for Maximum winter temperature in Arches. Top panels show values, bottom panels show changes from the long−term historical mean. Left: Time series of historical (black) and future projections for RCP 4.5 and 8.5. Shaded areas show spread among climate models. Right: Boxplots of temporal variability over 40−year periods under historical (left box) and individual climate models under two RCPs. Right: Historical time period is 1970−2010; near−term (NT) is 2020−2060; long−term (LT) is 2061−2100.

Arches: Maximum winter temperature

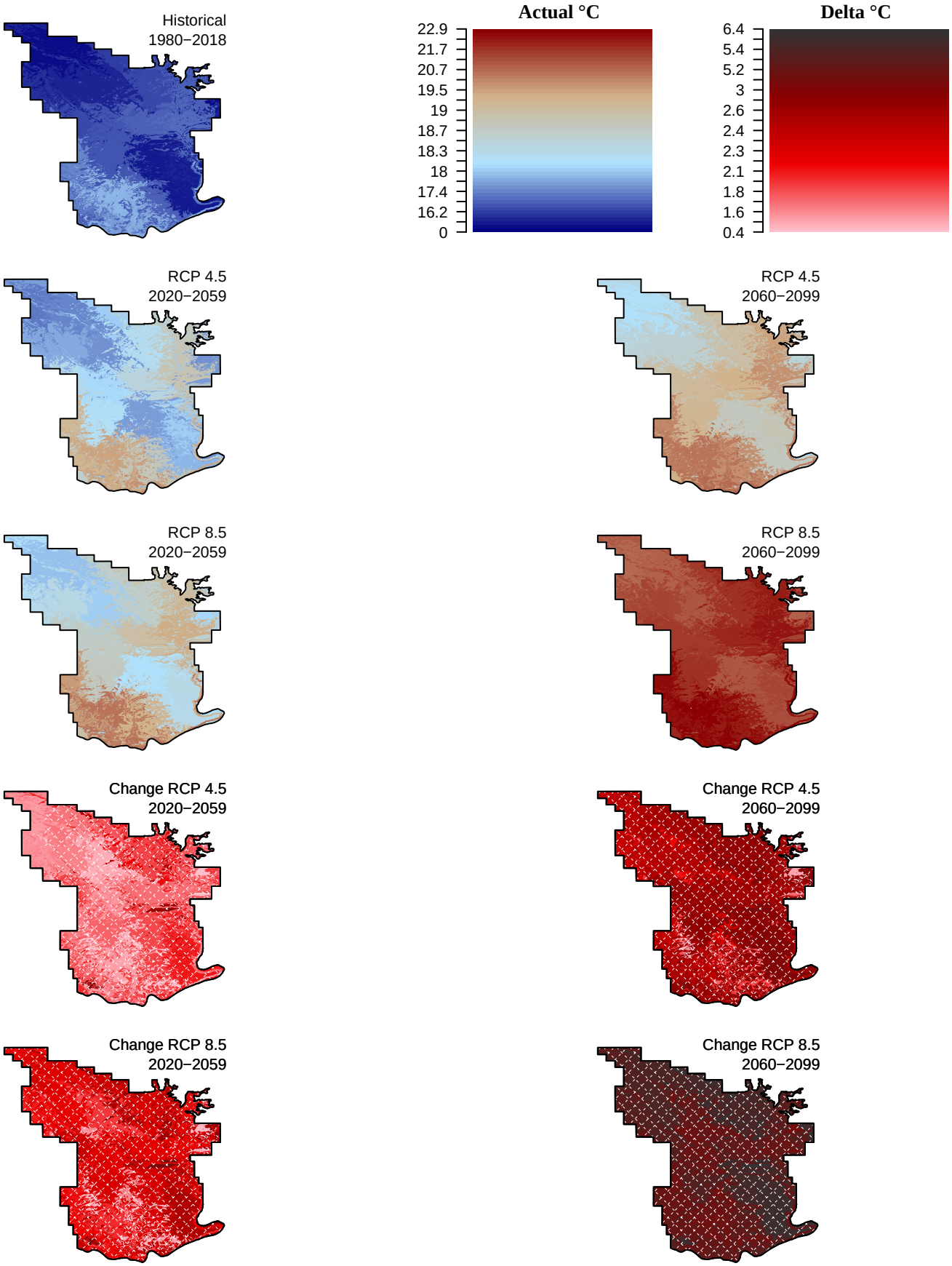


Figure ARCHmap19:
Past trends and future trajectories of park−wide mean values for Maximum winter temperature in Arches. Topmost panel depicts the historical mean from 1980−2018. Lower four panels show the emission scenarios of RCP 4.5 and RCP 8.5 at near−term and long−term timeframes. Bottom four panels depict the change from the historical mean; cross hatching denotes areas of robust predicitons (90% of models agree in the direction of change).

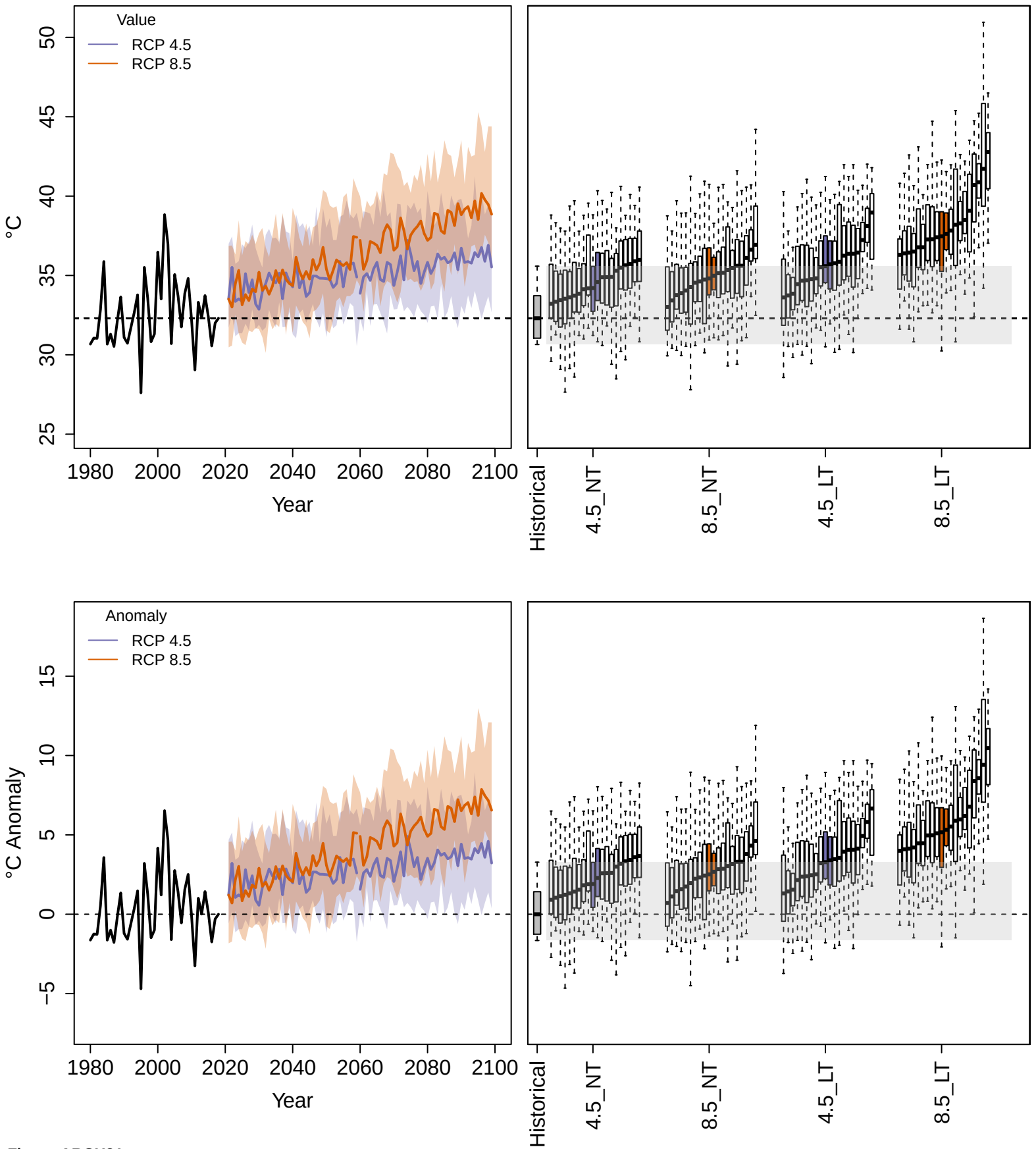


Figure ARCH21:
Past trends and future trajectories of park−wide mean values for Maximum spring temperature in Arches. Top panels show values, bottom panels show changes from the long−term historical mean. Left: Time series of historical (black) and future projections for RCP 4.5 and 8.5. Shaded areas show spread among climate models. Right: Boxplots of temporal variability over 40−year periods under historical (left box) and individual climate models under two RCPs. Right: Historical time period is 1970−2010; near−term (NT) is 2020−2060; long−term (LT) is 2061−2100.

Arches: Maximum spring temperature

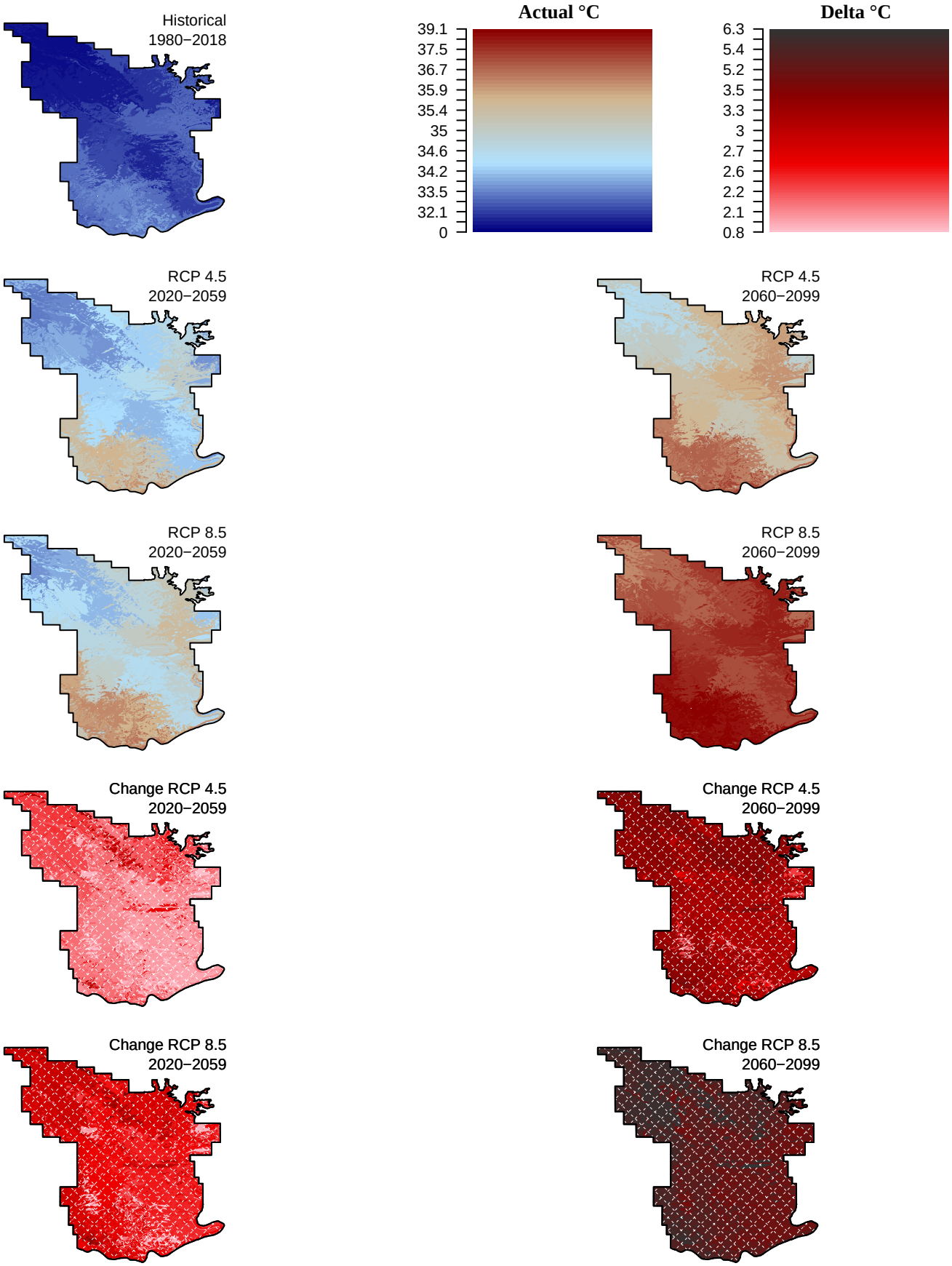


Figure ARCHmap21:
Past trends and future trajectories of park−wide mean values for Maximum spring temperature in Arches. Topmost panel depicts the historical mean from 1980−2018. Lower four panels show the emission scenarios of RCP 4.5 and RCP 8.5 at near−term and long−term timeframes. Bottom four panels depict the change from the historical mean; cross hatching denotes areas of robust predicitons (90% of models agree in the direction of change).

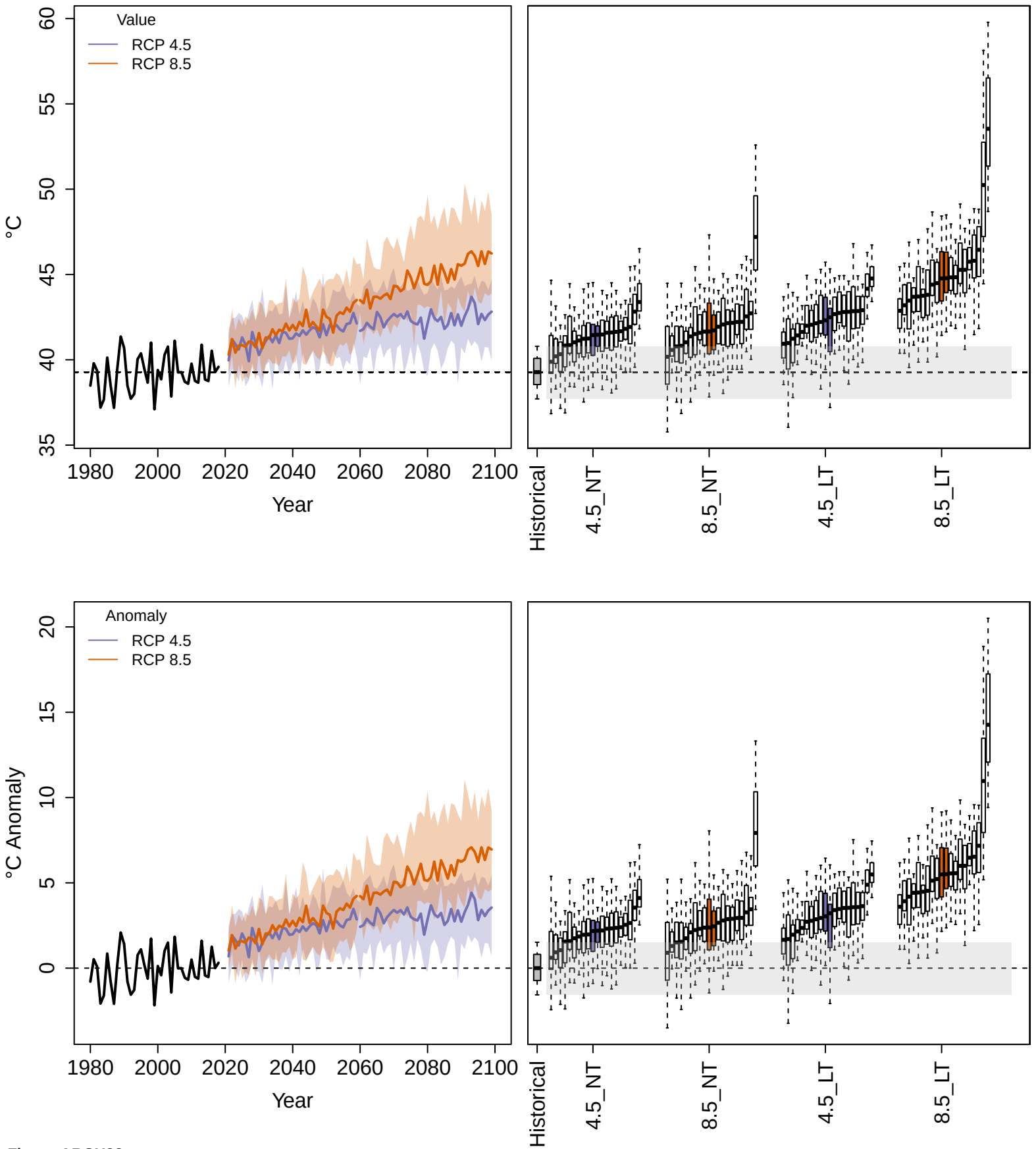


Figure ARCH23:
Past trends and future trajectories of park−wide mean values for Maximum summer temperature in Arches. Top panels show values, bottom panels show changes from the long−term historical mean. Left: Time series of historical (black) and future projections for RCP 4.5 and 8.5. Shaded areas show spread among climate models. Right: Boxplots of temporal variability over 40−year periods under historical (left box) and individual climate models under two RCPs. Right: Historical time period is 1970−2010; near−term (NT) is 2020−2060; long−term (LT) is 2061−2100.

Arches: Maximum summer temperature

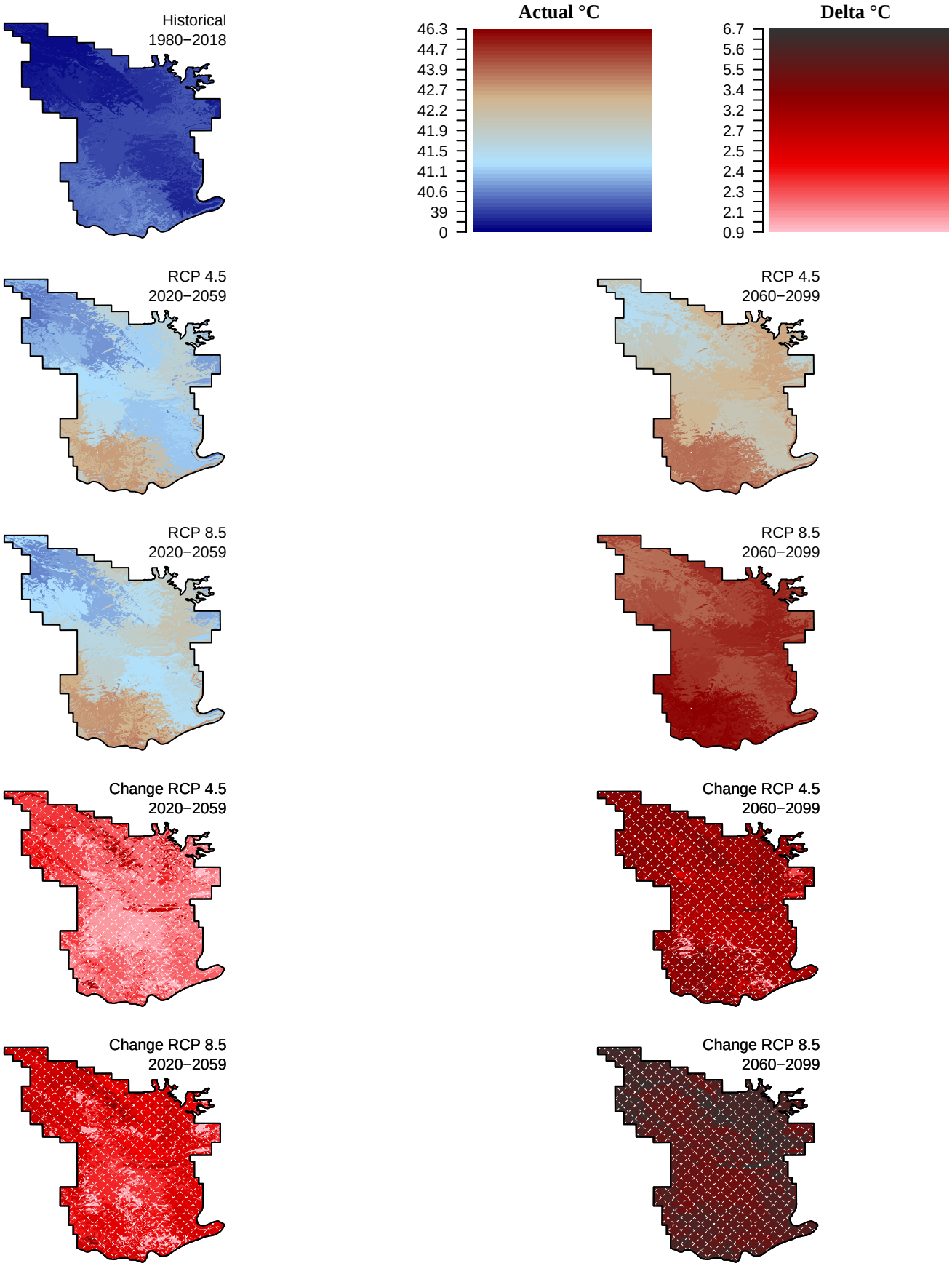


Figure ARCHmap23:
Past trends and future trajectories of park−wide mean values for Maximum summer temperature in Arches. Topmost panel depicts the historical mean from 1980−2018. Lower four panels show the emission scenarios of RCP 4.5 and RCP 8.5 at near−term and long−term timeframes. Bottom four panels depict the change from the historical mean; cross hatching denotes areas of robust predicitons (90% of models agree in the direction of change).

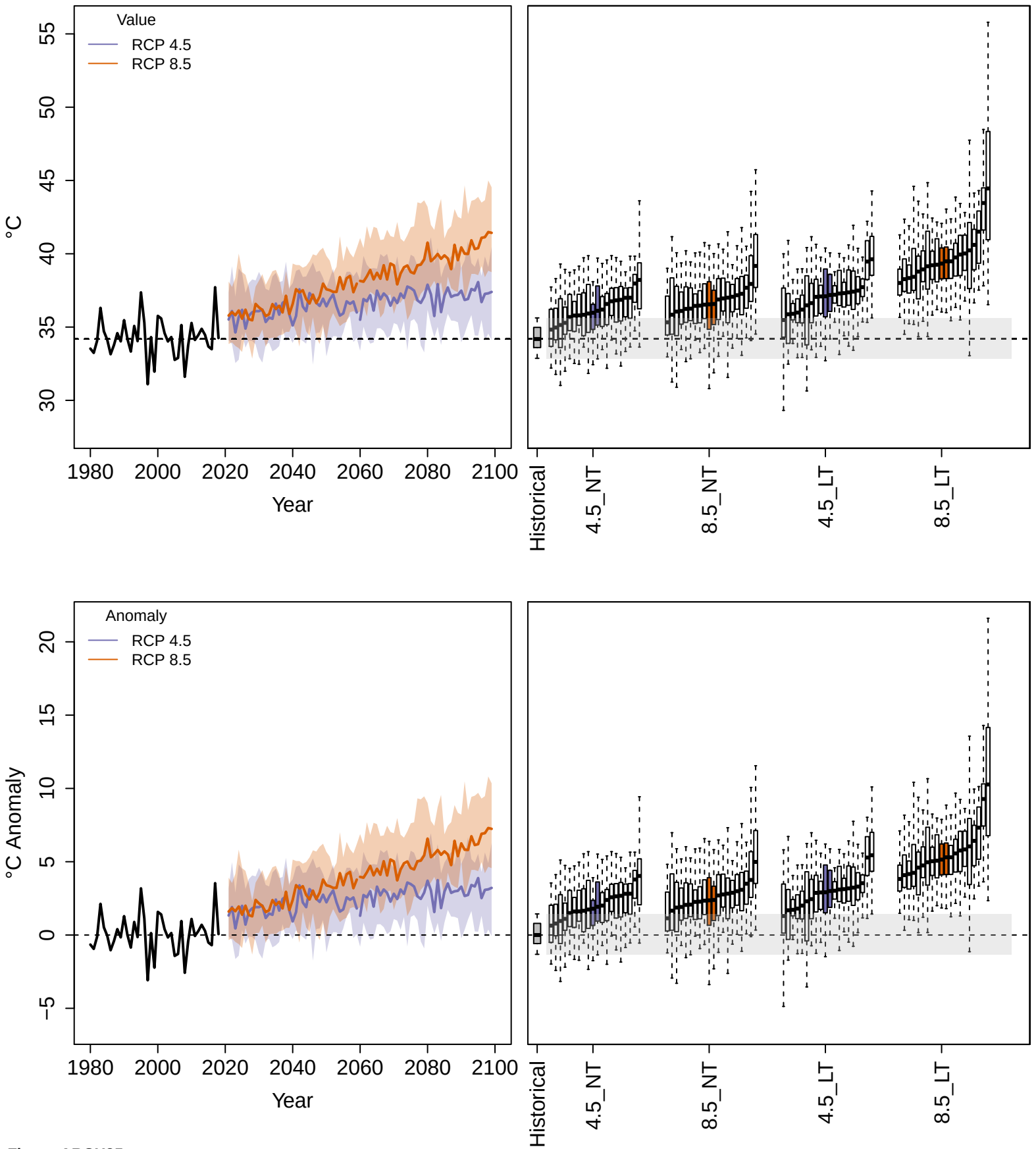


Figure ARCH25:
Past trends and future trajectories of park−wide mean values for Maximum fall temperature in Arches. Top panels show values, bottom panels show changes from the long−term historical mean. Left: Time series of historical (black) and future projections for RCP 4.5 and 8.5. Shaded areas show spread among climate models. Right: Boxplots of temporal variability over 40−year periods under historical (left box) and individual climate models under two RCPs. Right: Historical time period is 1970−2010; near−term (NT) is 2020−2060; long−term (LT) is 2061−2100.

Arches: Maximum fall temperature

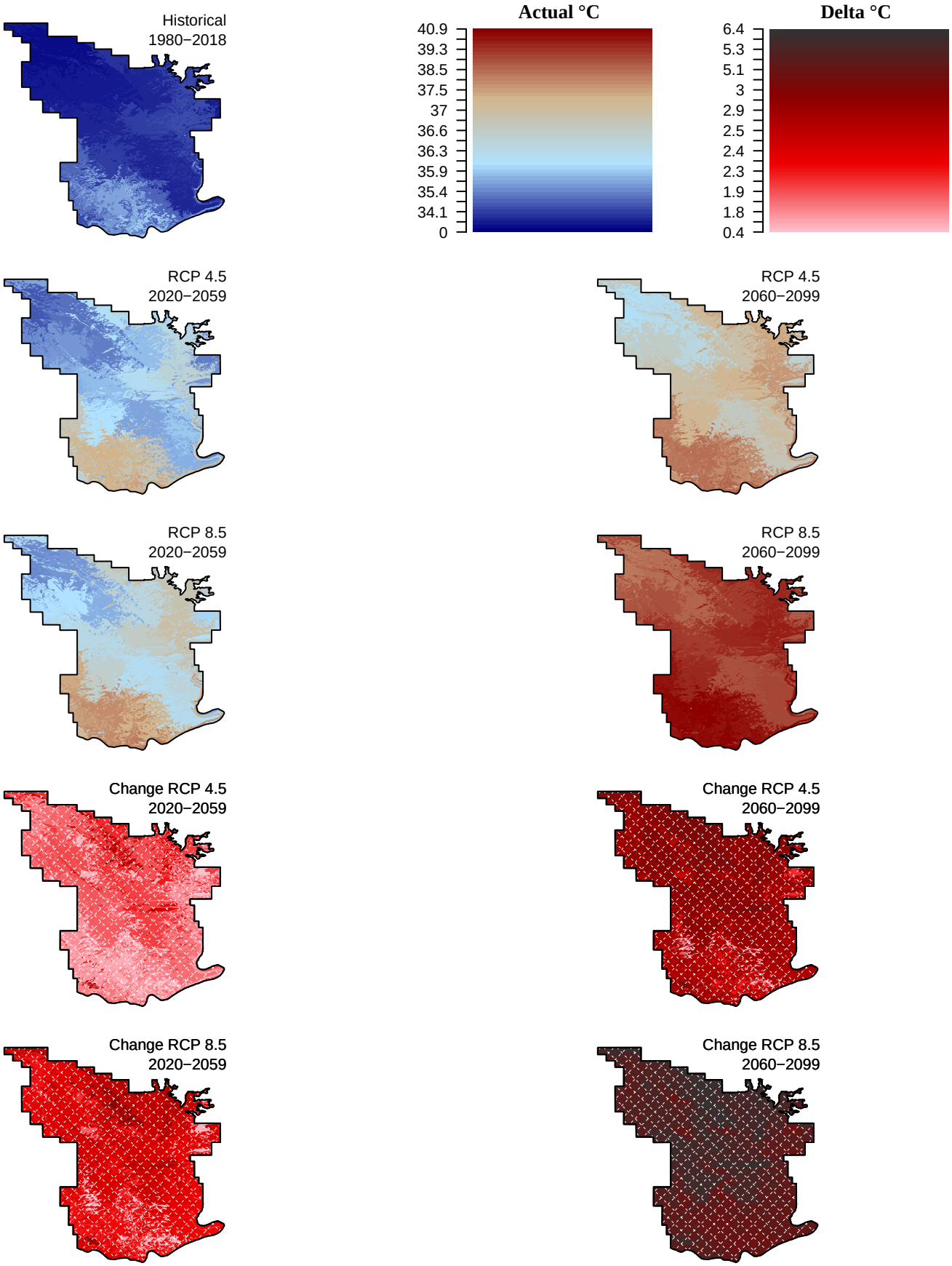


Figure ARCHmap25:
Past trends and future trajectories of park−wide mean values for Maximum fall temperature in Arches. Topmost panel depicts the historical mean from 1980−2018. Lower four panels show the emission scenarios of RCP 4.5 and RCP 8.5 at near−term and long−term timeframes. Bottom four panels depict the change from the historical mean; cross hatching denotes areas of robust predicitons (90% of models agree in the direction of change).

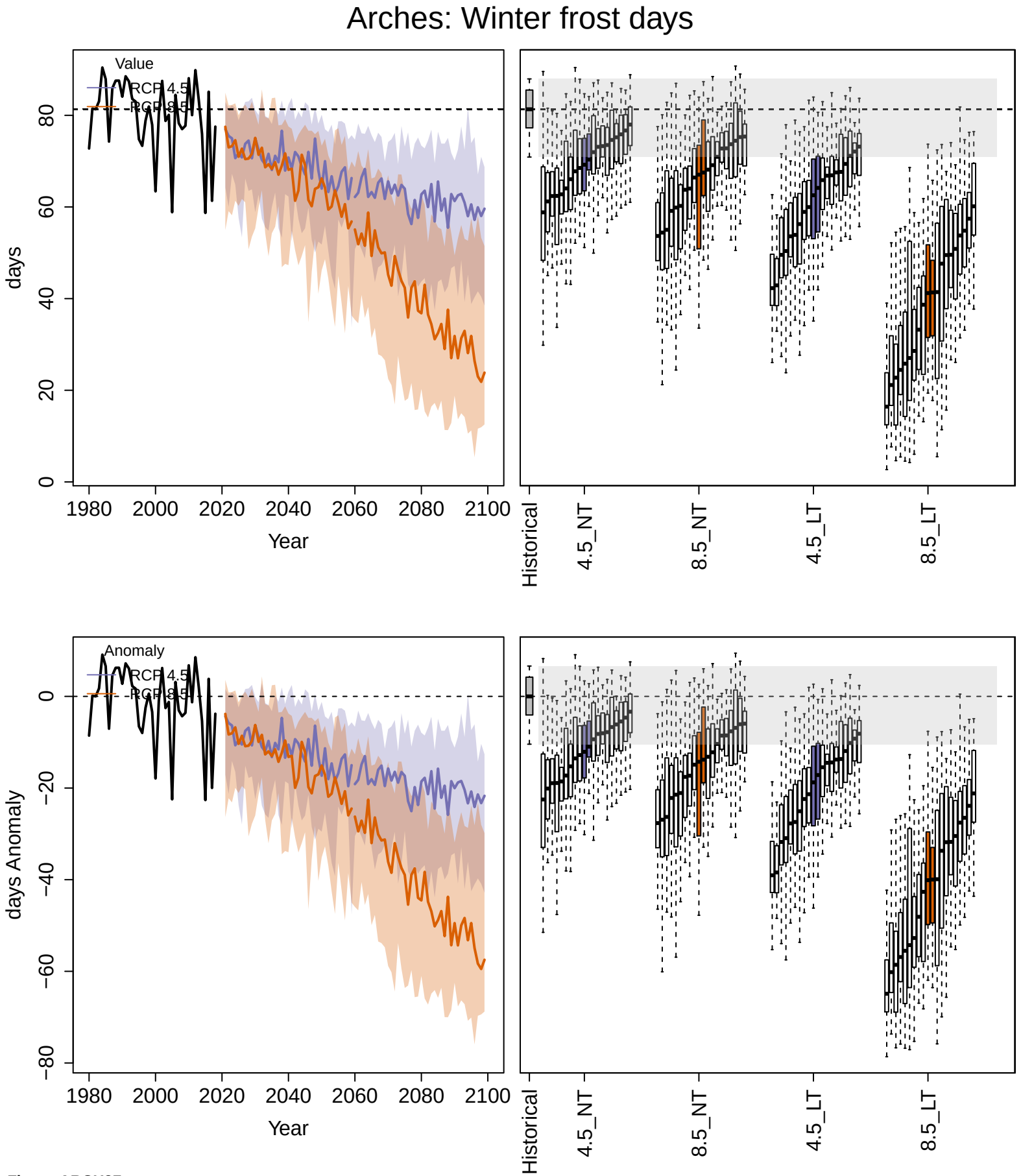


Figure ARCH27:
Past trends and future trajectories of park−wide mean values for Winter frost days in Arches. Top panels show values, bottom panels show changes from the long−term historical mean. Left: Time series of historical (black) and future projections for RCP 4.5 and 8.5. Shaded areas show spread among climate models. Right: Boxplots of temporal variability over 40−year periods under historical (left box) and individual climate models under two RCPs. Right: Historical time period is 1970−2010; near−term (NT) is 2020−2060; long−term (LT) is 2061−2100.

Arches: Winter frost days

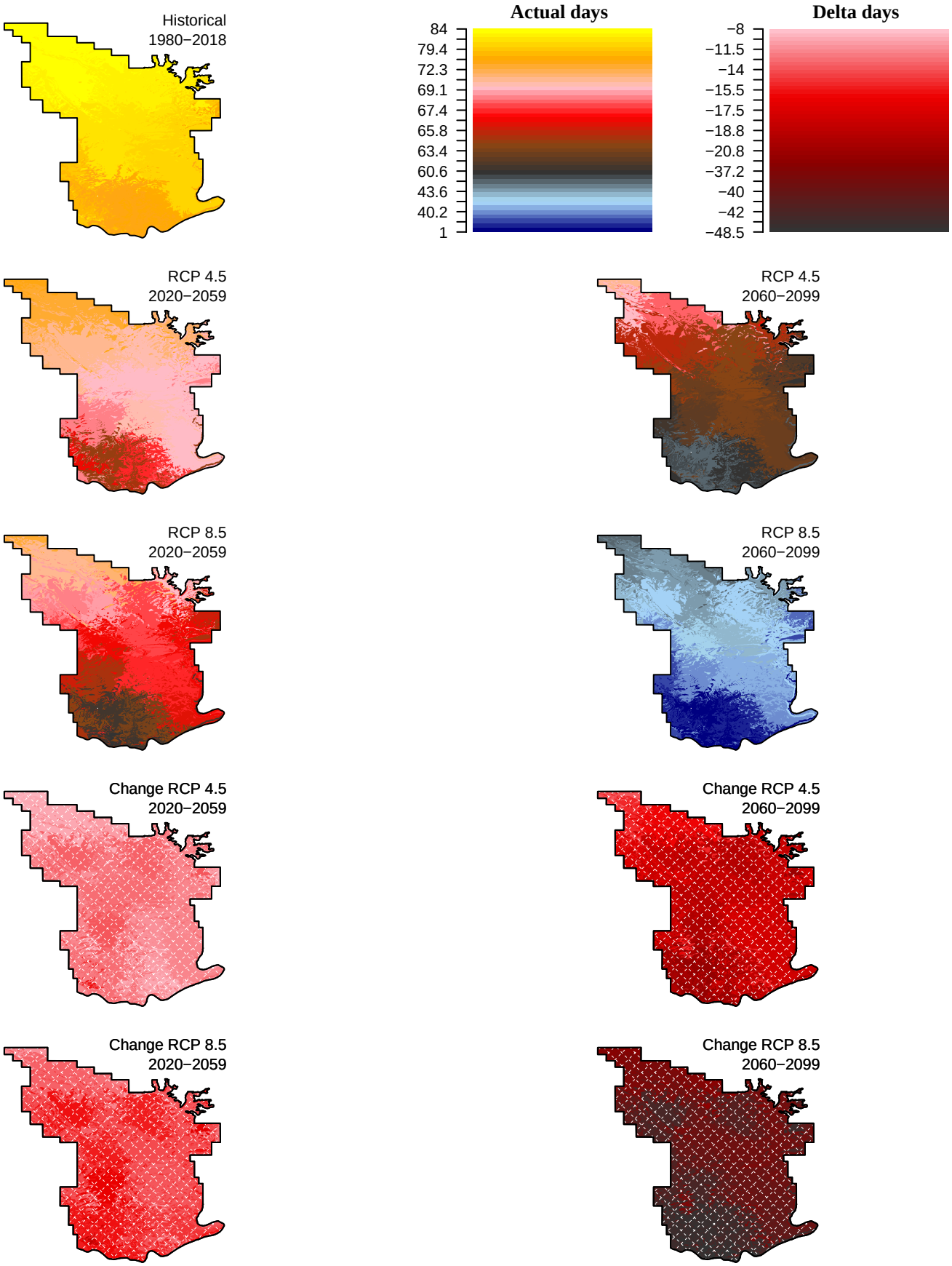


Figure ARCHmap27:
Past trends and future trajectories of park−wide mean values for Winter frost days in Arches. Topmost panel depicts the historical mean from 1980−2018. Lower four panels show the emission scenarios of RCP 4.5 and RCP 8.5 at near−term and long−term timeframes. Bottom four panels depict the change from the historical mean; cross hatching denotes areas of robust predicitons (90% of models agree in the direction of change).

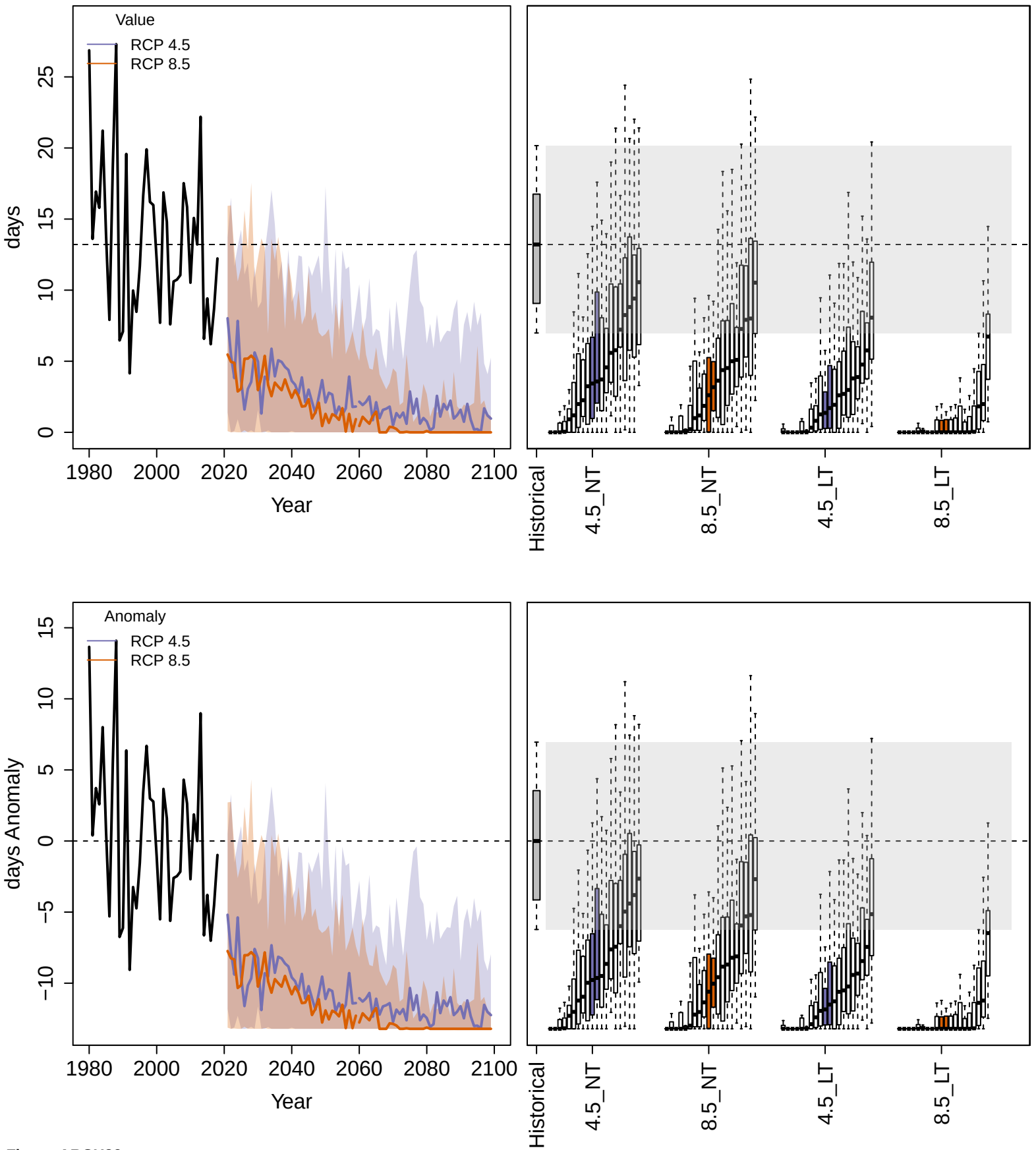


Figure ARCH29:
Past trends and future trajectories of park−wide mean values for Spring frost days in Arches. Top panels show values, bottom panels show changes from the long−term historical mean. Left: Time series of historical (black) and future projections for RCP 4.5 and 8.5. Shaded areas show spread among climate models. Right: Boxplots of temporal variability over 40−year periods under historical (left box) and individual climate models under two RCPs. Right: Historical time period is 1970−2010; near−term (NT) is 2020−2060; long−term (LT) is 2061−2100.

Arches: Spring frost days

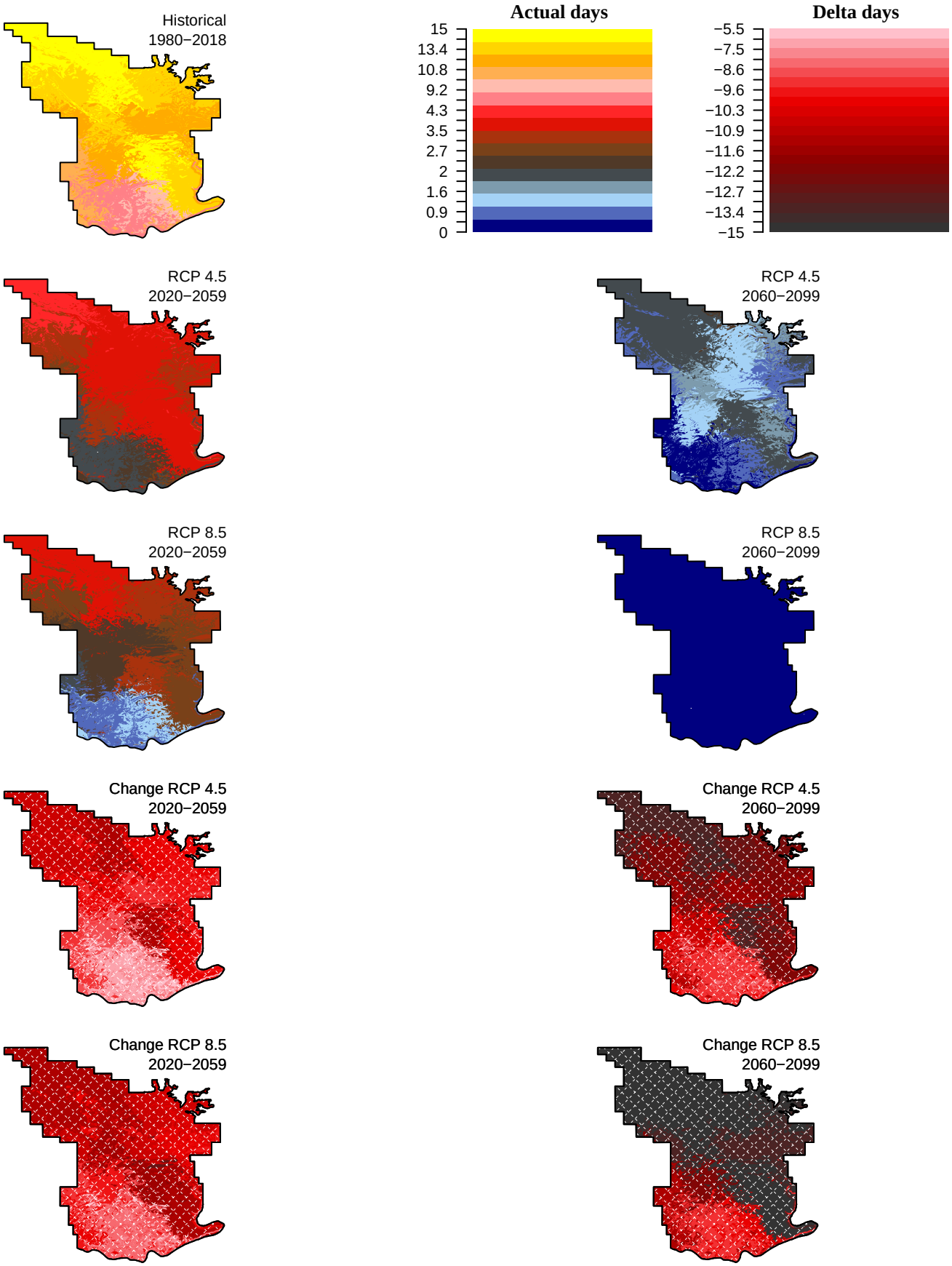


Figure ARCHmap29:
Past trends and future trajectories of park−wide mean values for Spring frost days in Arches. Topmost panel depicts the historical mean from 1980−2018. Lower four panels show the emission scenarios of RCP 4.5 and RCP 8.5 at near−term and long−term timeframes. Bottom four panels depict the change from the historical mean; cross hatching denotes areas of robust predicitons (90% of models agree in the direction of change).

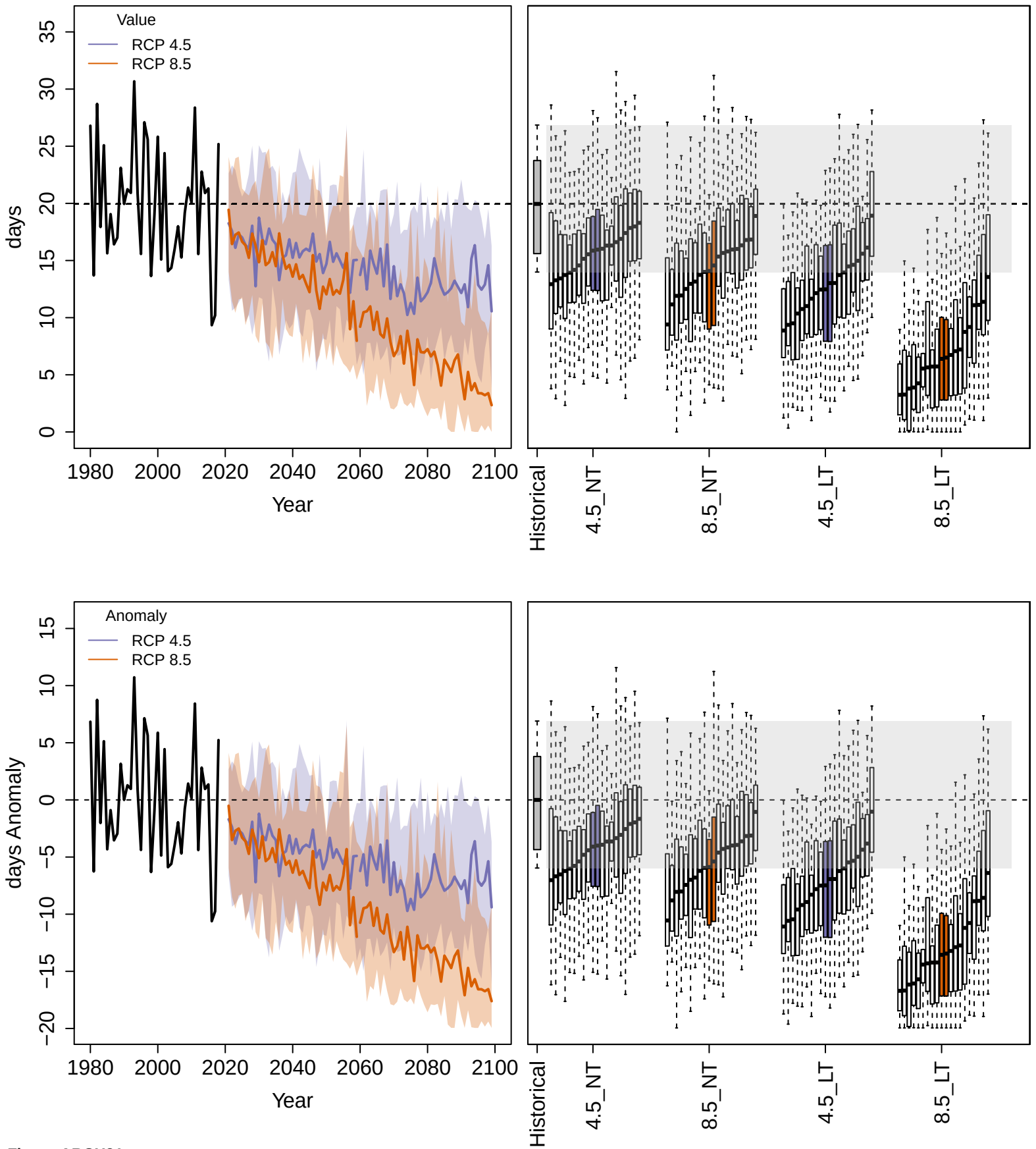


Figure ARCH31:
Past trends and future trajectories of park−wide mean values for Fall frost days in Arches. Top panels show values, bottom panels show changes from the long−term historical mean. Left: Time series of historical (black) and future projections for RCP 4.5 and 8.5. Shaded areas show spread among climate models. Right: Boxplots of temporal variability over 40−year periods under historical (left box) and individual climate models under two RCPs. Right: Historical time period is 1970−2010; near−term (NT) is 2020−2060; long−term (LT) is 2061−2100.

Arches: Fall frost days

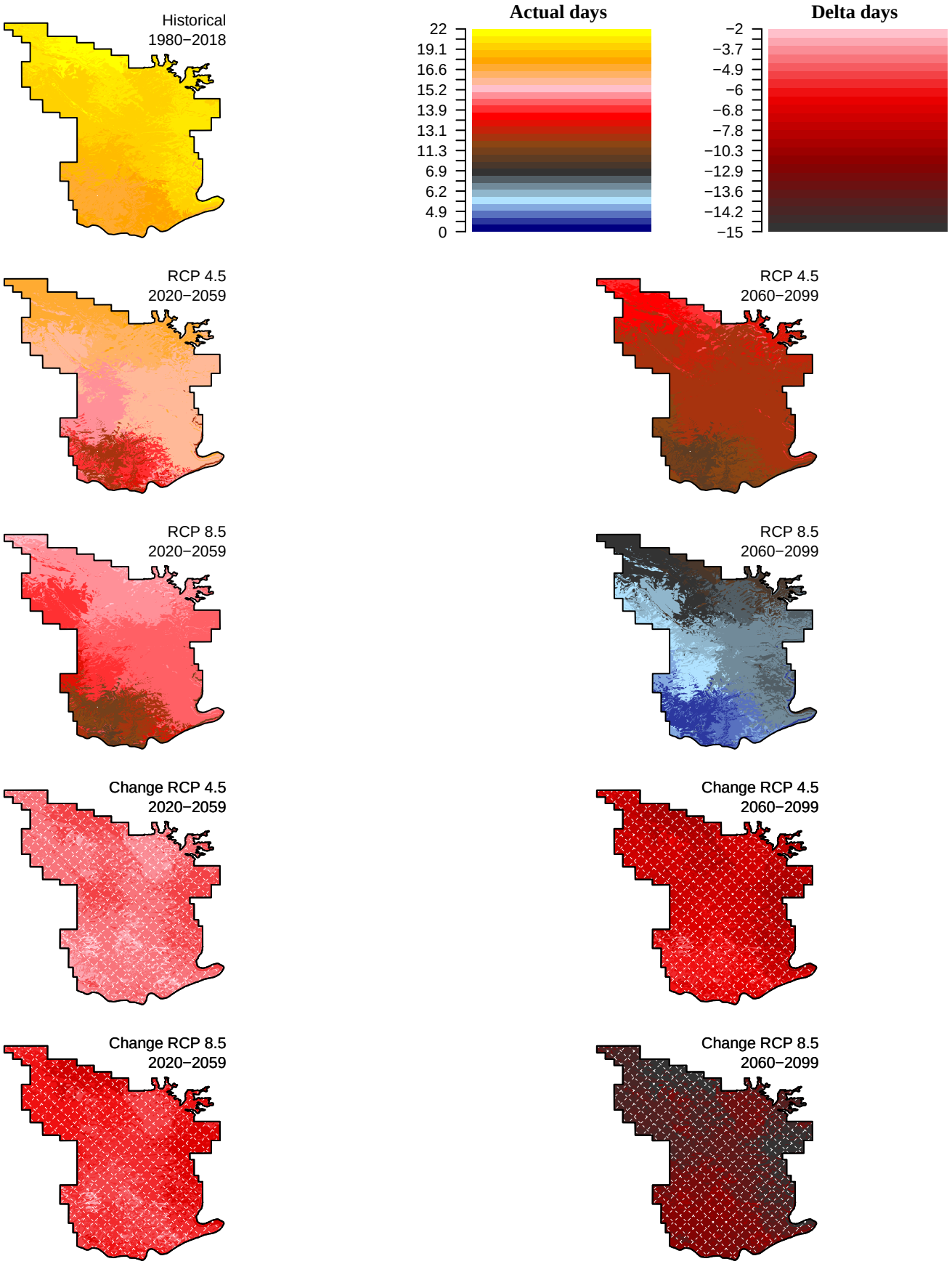


Figure ARCHmap31:
Past trends and future trajectories of park−wide mean values for Fall frost days in Arches. Topmost panel depicts the historical mean from 1980−2018. Lower four panels show the emission scenarios of RCP 4.5 and RCP 8.5 at near−term and long−term timeframes. Bottom four panels depict the change from the historical mean; cross hatching denotes areas of robust predicitons (90% of models agree in the direction of change).

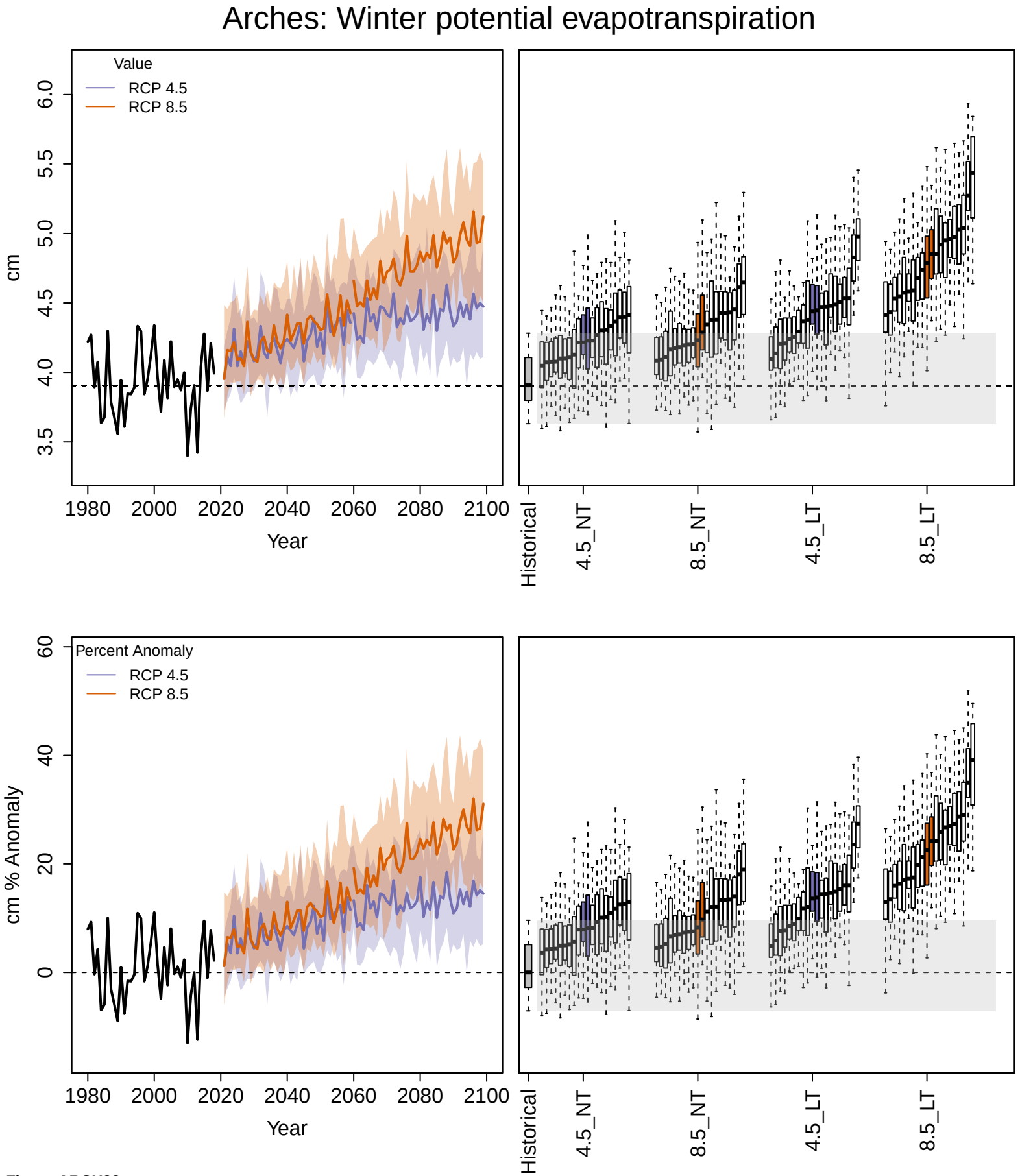


Figure ARCH33:
Past trends and future trajectories of park−wide mean values for Winter potential evapotranspiration in Arches. Top panels show values, bottom panels show changes from the long−term historical mean. Left: Time series of historical (black) and future projections for RCP 4.5 and 8.5. Shaded areas show spread among climate models. Right: Boxplots of temporal variability over 40−year periods under historical (left box) and individual climate models under two RCPs. Right: Historical time period is 1970−2010; near−term (NT) is 2020−2060; long−term (LT) is 2061−2100.

Arches: Winter potential evapotranspiration

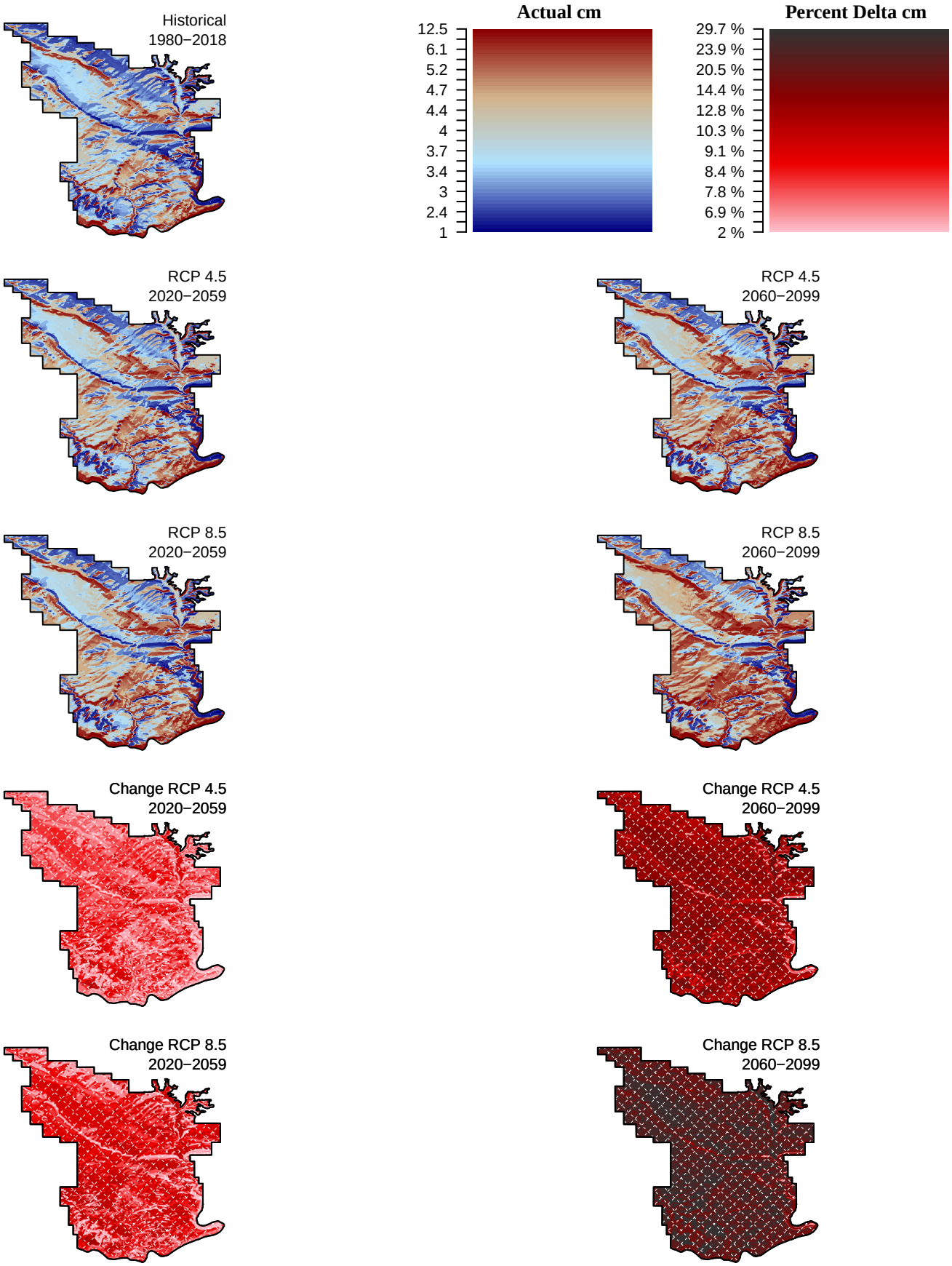


Figure ARCHmap33:
Past trends and future trajectories of park−wide mean values for Winter potential evapotranspiration in Arches. Topmost panel depicts the historical mean from 1980−2018. Lower four panels show the emission scenarios of RCP 4.5 and RCP 8.5 at near−term and long−term timeframes. Bottom four panels depict the change from the historical mean; cross hatching denotes areas of robust predicitons (90% of models agree in the direction of change).

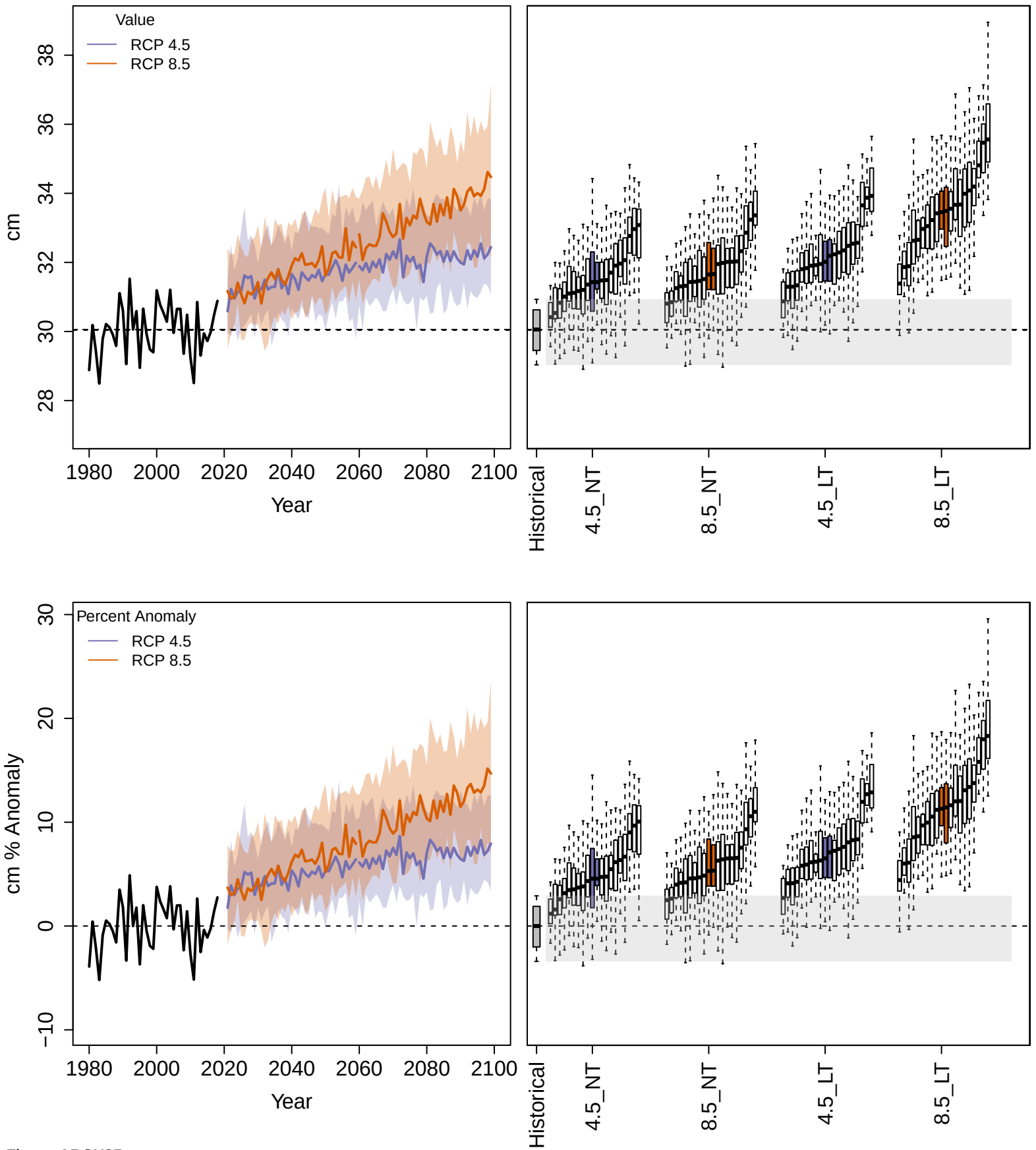


Figure ARCH35:
Past trends and future trajectories of park−wide mean values for Spring potential evapotranspiration in Arches. Top panels show values, bottom panels show changes from the long−term historical mean. Left: Time series of historical (black) and future projections for RCP 4.5 and 8.5. Shaded areas show spread among climate models. Right: Boxplots of temporal variability over 40−year periods under historical (left box) and individual climate models under two RCPs. Right: Historical time period is 1970−2010; near−term (NT) is 2020−2060; long−term (LT) is 2061−2100.

Arches: Spring potential evapotranspiration

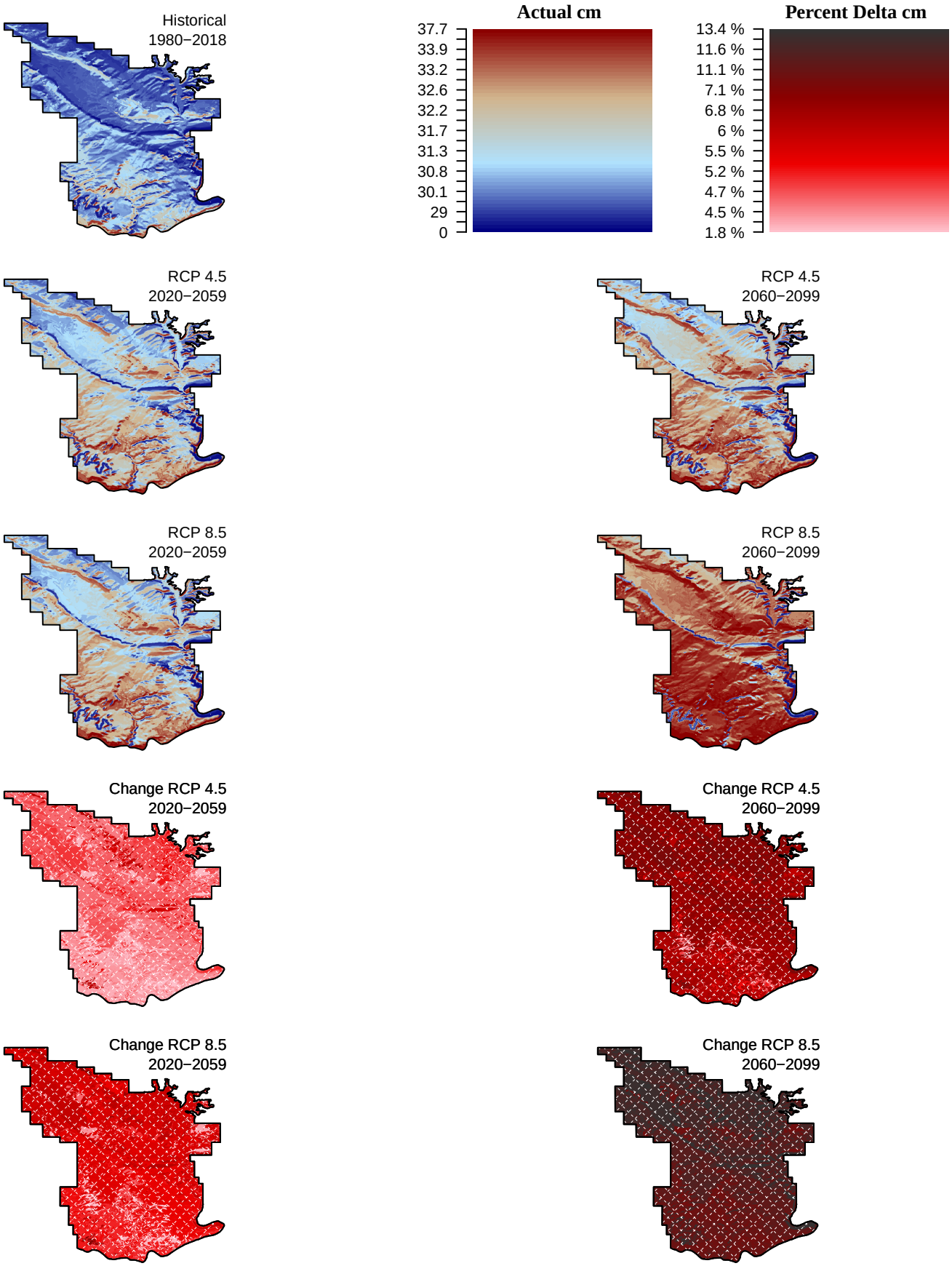


Figure ARCHmap35:
Past trends and future trajectories of park−wide mean values for Spring potential evapotranspiration in Arches. Topmost panel depicts the historical mean from 1980−2018. Lower four panels show the emission scenarios of RCP 4.5 and RCP 8.5 at near−term and long−term timeframes. Bottom four panels depict the change from the historical mean; cross hatching denotes areas of robust predicitons (90% of models agree in the direction of change).

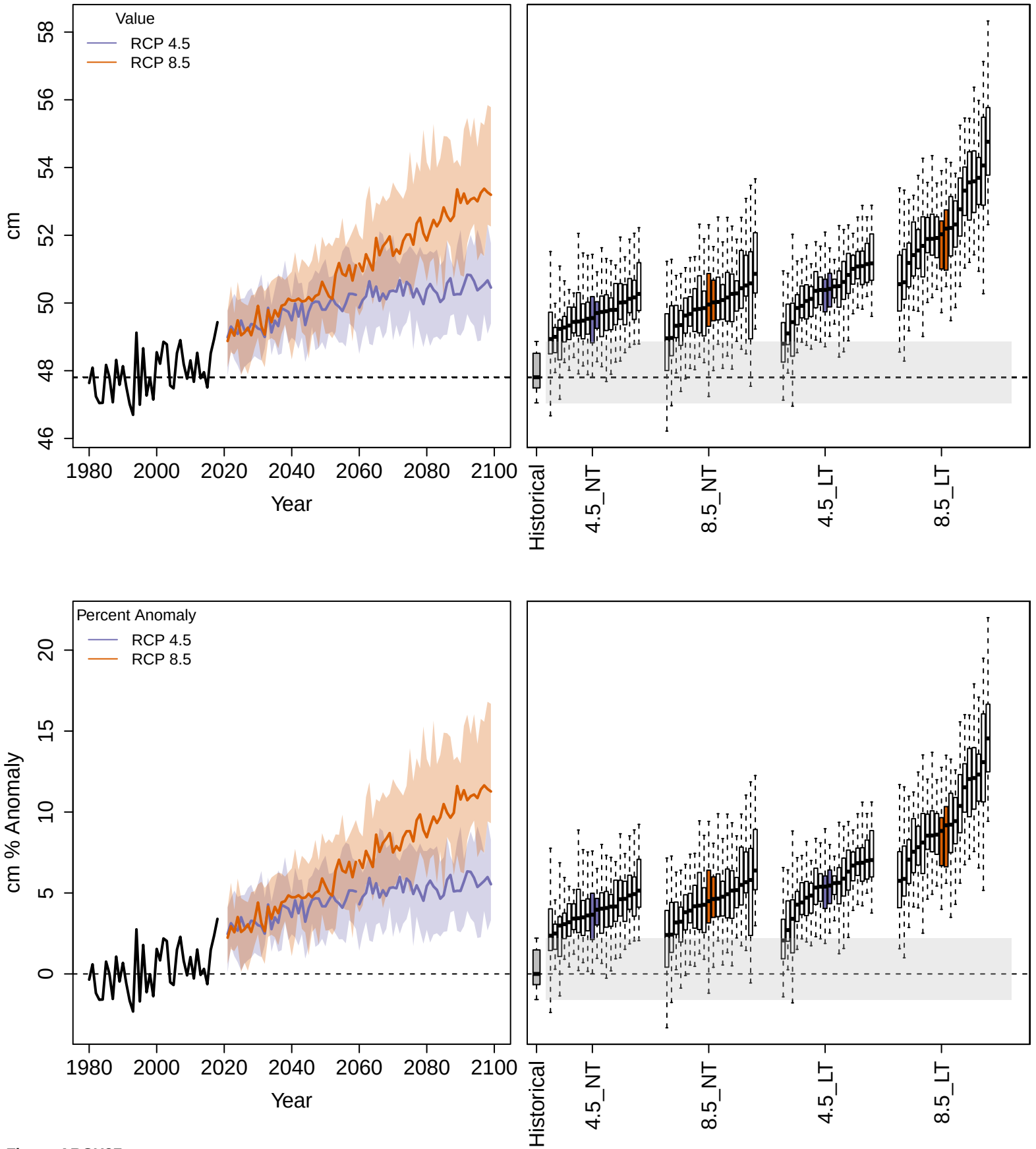


Figure ARCH37:
Past trends and future trajectories of park−wide mean values for Summer potential evapotranspiration in Arches. Top panels show values, bottom panels show changes from the long−term historical mean. Left: Time series of historical (black) and future projections for RCP 4.5 and 8.5. Shaded areas show spread among climate models. Right: Boxplots of temporal variability over 40−year periods under historical (left box) and individual climate models under two RCPs. Right: Historical time period is 1970−2010; near−term (NT) is 2020−2060; long−term (LT) is 2061−2100.

Arches: Summer potential evapotranspiration

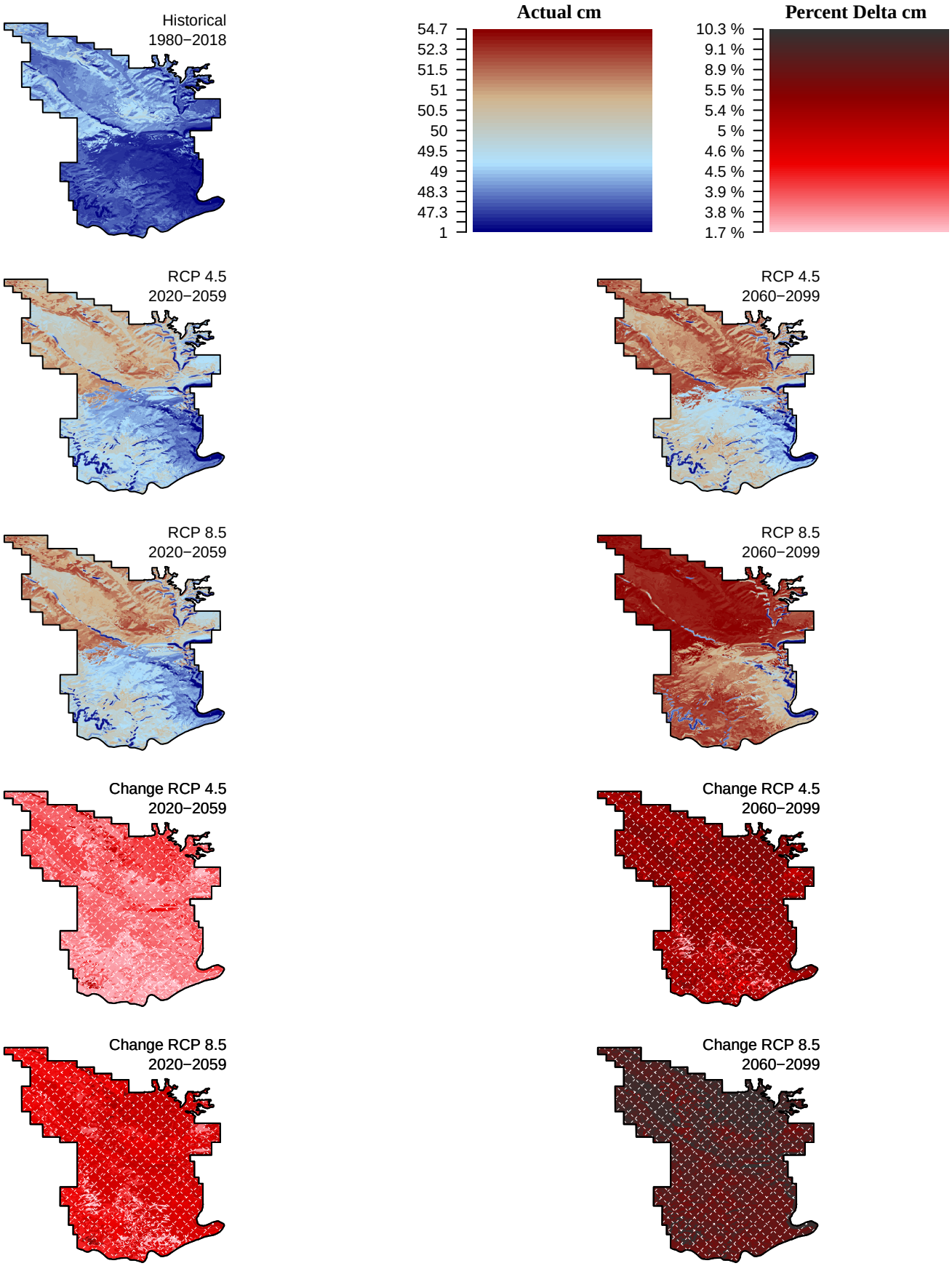


Figure ARCHmap37:
Past trends and future trajectories of park−wide mean values for Summer potential evapotranspiration in Arches. Topmost panel depicts the historical mean from 1980−2018. Lower four panels show the emission scenarios of RCP 4.5 and RCP 8.5 at near−term and long−term timeframes. Bottom four panels depict the change from the historical mean; cross hatching denotes areas of robust predicitons (90% of models agree in the direction of change).

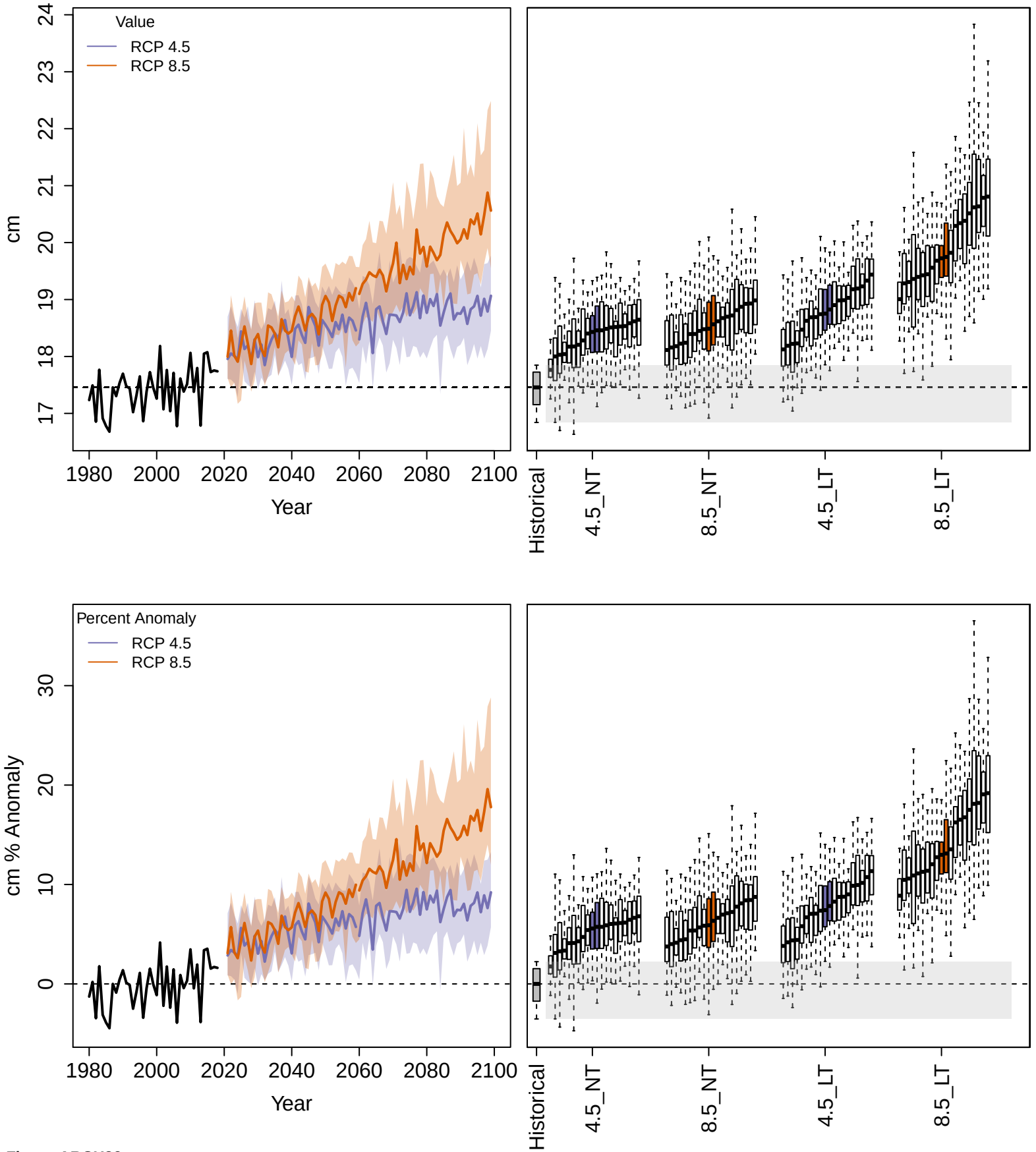


Figure ARCH39:
Past trends and future trajectories of park−wide mean values for Fall potential evapotranspiration in Arches. Top panels show values, bottom panels show changes from the long−term historical mean. Left: Time series of historical (black) and future projections for RCP 4.5 and 8.5. Shaded areas show spread among climate models. Right: Boxplots of temporal variability over 40−year periods under historical (left box) and individual climate models under two RCPs. Right: Historical time period is 1970−2010; near−term (NT) is 2020−2060; long−term (LT) is 2061−2100.

Arches: Fall potential evapotranspiration

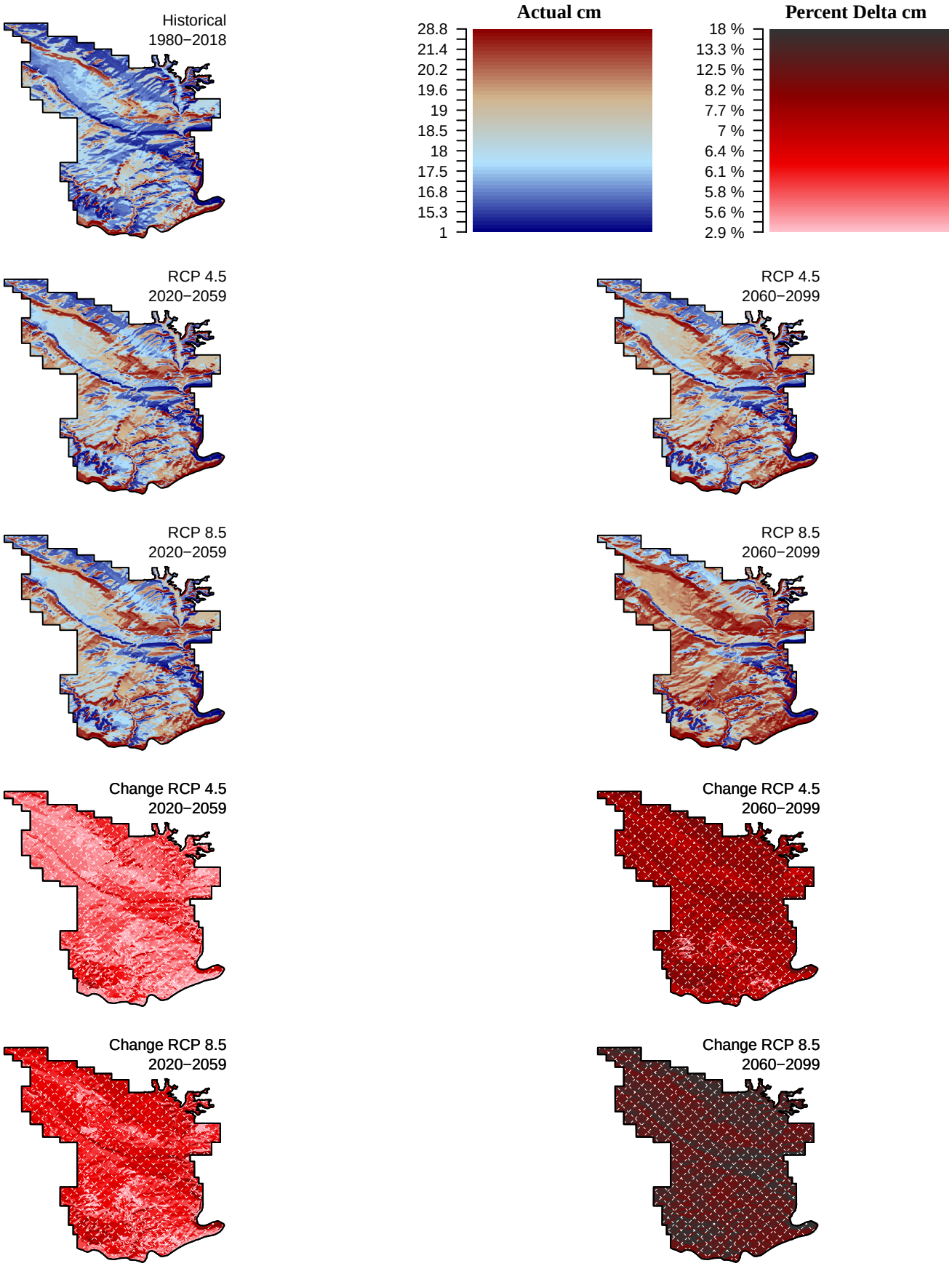


Figure ARCHmap39:
Past trends and future trajectories of park−wide mean values for Fall potential evapotranspiration in Arches. Topmost panel depicts the historical mean from 1980−2018. Lower four panels show the emission scenarios of RCP 4.5 and RCP 8.5 at near−term and long−term timeframes. Bottom four panels depict the change from the historical mean; cross hatching denotes areas of robust predicitons (90% of models agree in the direction of change).

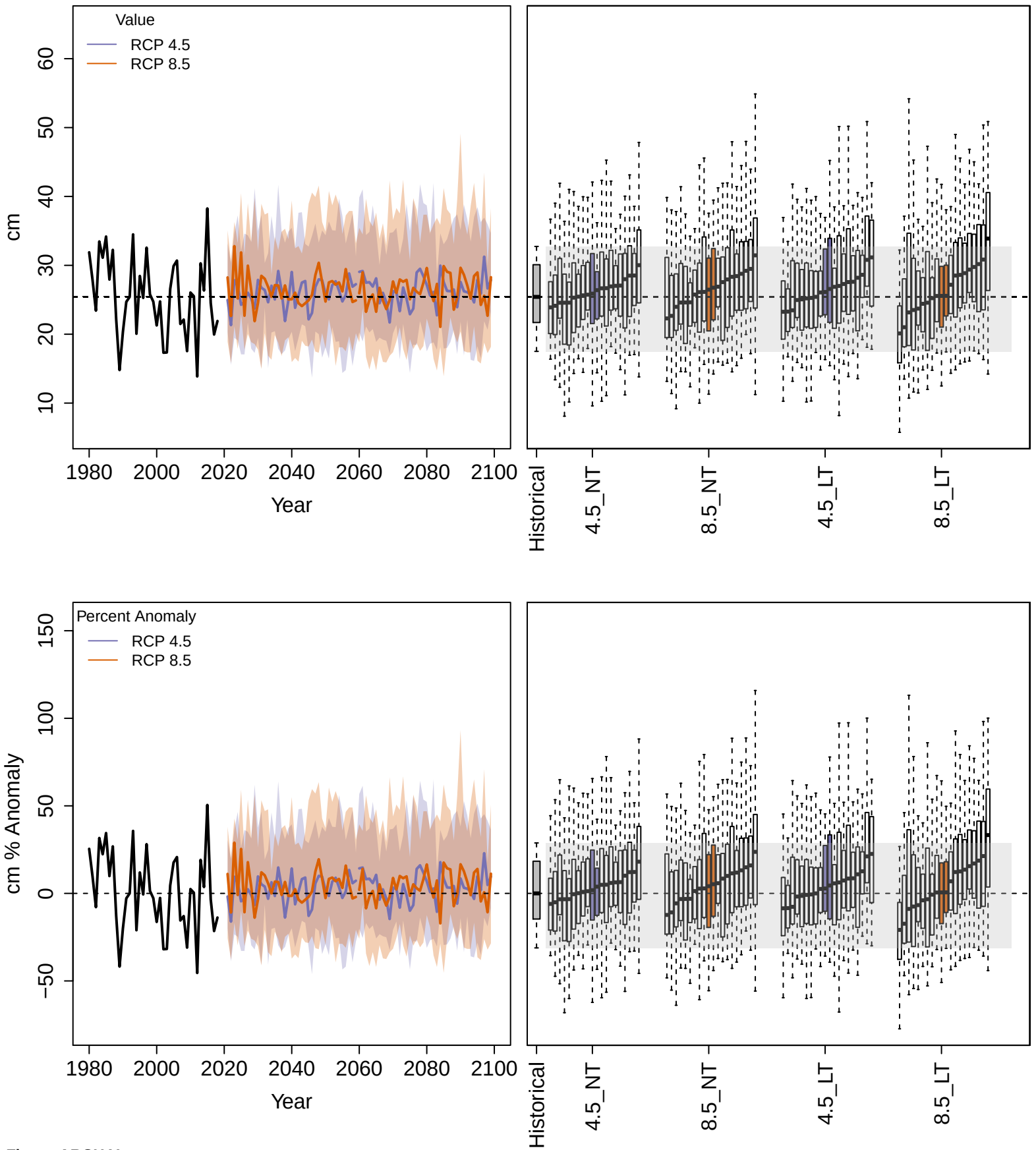


Figure ARCH41:
Past trends and future trajectories of park−wide mean values for Annual Precipitation in Arches. Top panels show values, bottom panels show changes from the long−term historical mean. Left: Time series of historical (black) and future projections for RCP 4.5 and 8.5. Shaded areas show spread among climate models. Right: Boxplots of temporal variability over 40−year periods under historical (left box) and individual climate models under two RCPs. Right: Historical time period is 1970−2010; near−term (NT) is 2020−2060; long−term (LT) is 2061−2100.

Arches: Annual Precipitation

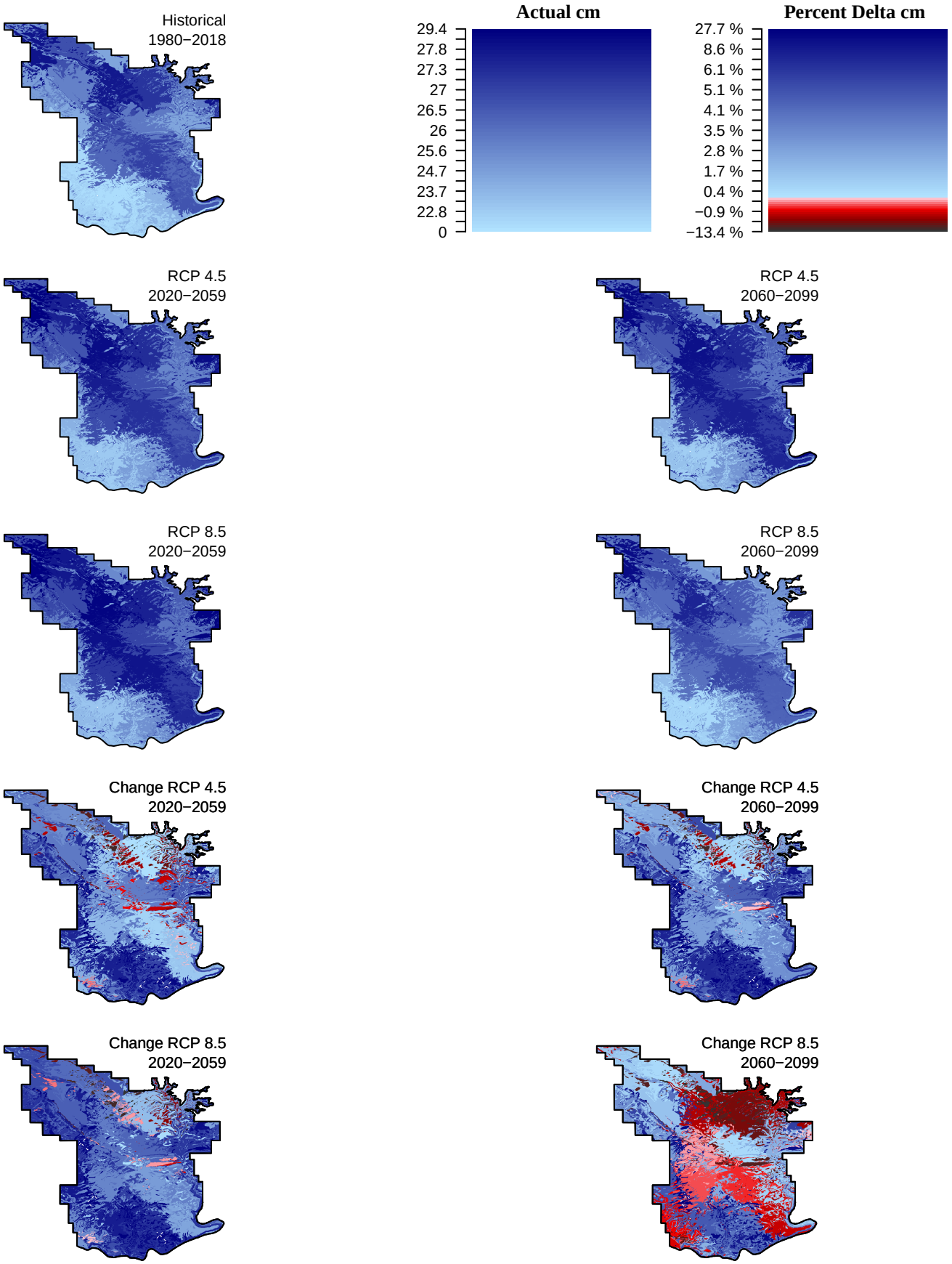


Figure ARCHmap41:
Past trends and future trajectories of park−wide mean values for Annual Precipitation in Arches. Topmost panel depicts the historical mean from 1980−2018. Lower four panels show the emission scenarios of RCP 4.5 and RCP 8.5 at near−term and long−term timeframes. Bottom four panels depict the change from the historical mean; cross hatching denotes areas of robust predicitons (90% of models agree in the direction of change).

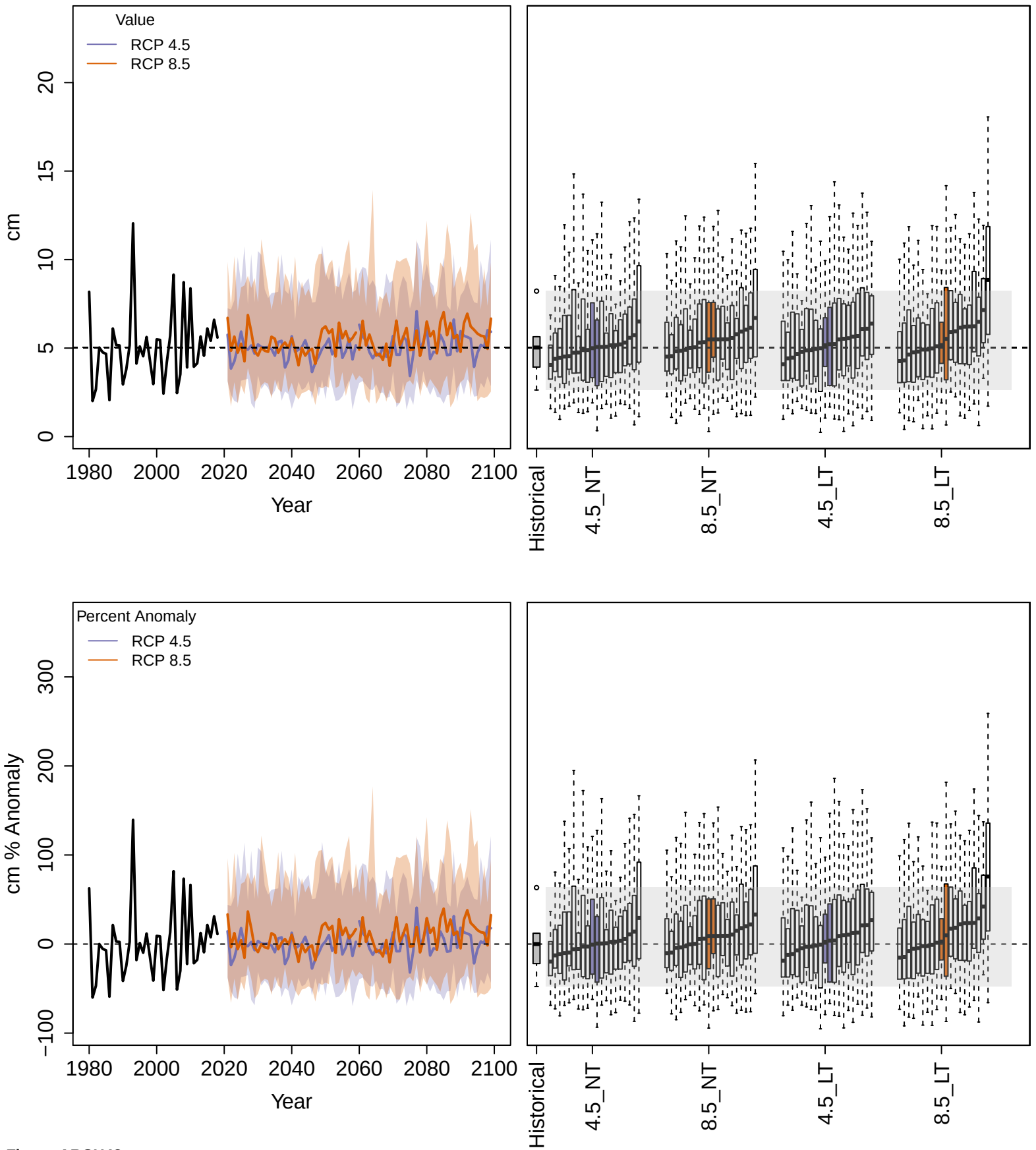


Figure ARCH43:
Past trends and future trajectories of park−wide mean values for Winter Precipitation in Arches. Top panels show values, bottom panels show changes from the long−term historical mean. Left: Time series of historical (black) and future projections for RCP 4.5 and 8.5. Shaded areas show spread among climate models. Right: Boxplots of temporal variability over 40−year periods under historical (left box) and individual climate models under two RCPs. Right: Historical time period is 1970−2010; near−term (NT) is 2020−2060; long−term (LT) is 2061−2100.

Arches: Winter Precipitation

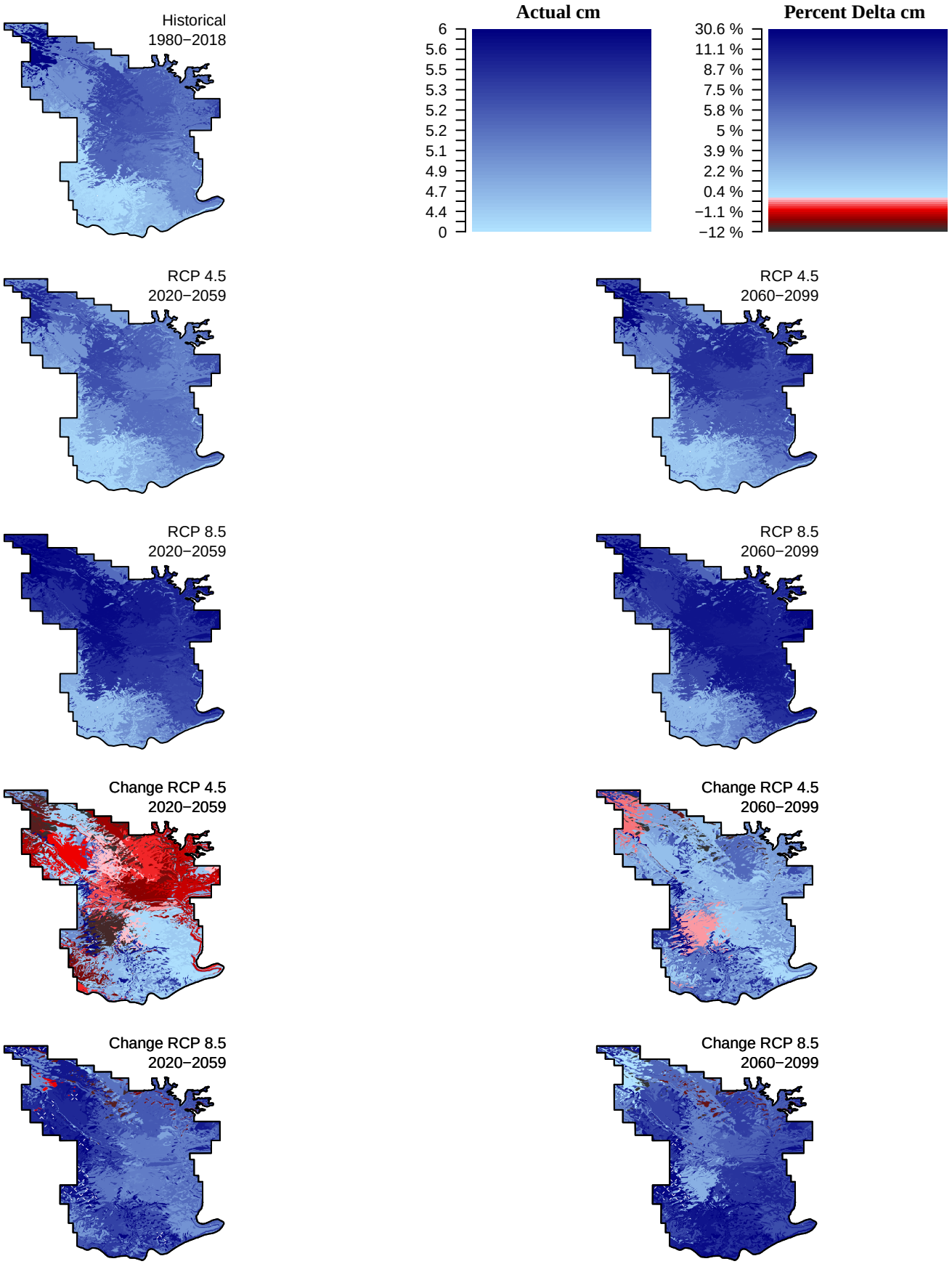


Figure ARCHmap43:
Past trends and future trajectories of park−wide mean values for Winter Precipitation in Arches. Topmost panel depicts the historical mean from 1980−2018. Lower four panels show the emission scenarios of RCP 4.5 and RCP 8.5 at near−term and long−term timeframes. Bottom four panels depict the change from the historical mean; cross hatching denotes areas of robust predicitons (90% of models agree in the direction of change).

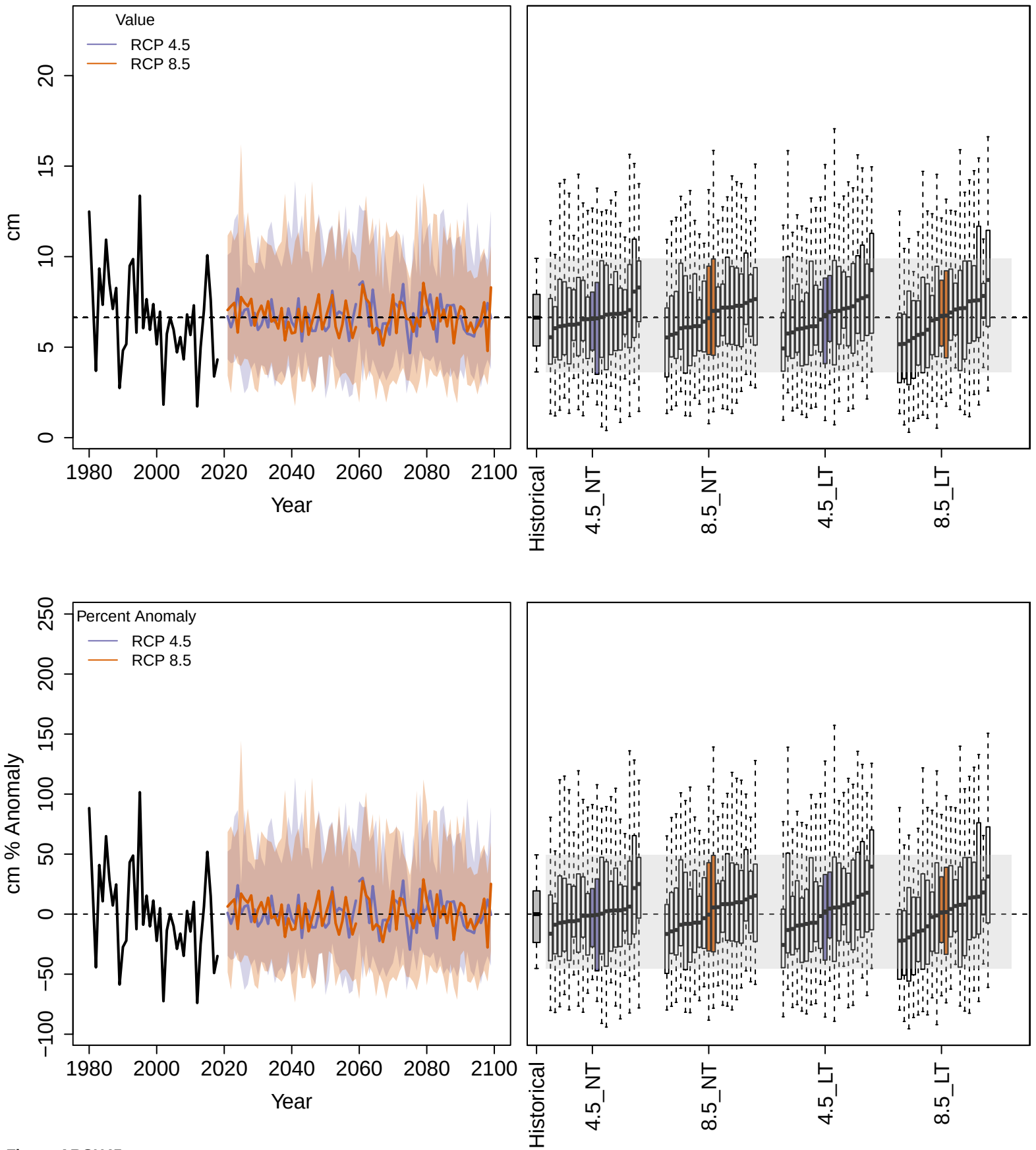


Figure ARCH45:
Past trends and future trajectories of park−wide mean values for Spring Precipitation in Arches. Top panels show values, bottom panels show changes from the long−term historical mean. Left: Time series of historical (black) and future projections for RCP 4.5 and 8.5. Shaded areas show spread among climate models. Right: Boxplots of temporal variability over 40−year periods under historical (left box) and individual climate models under two RCPs. Right: Historical time period is 1970−2010; near−term (NT) is 2020−2060; long−term (LT) is 2061−2100.

Arches: Spring Precipitation

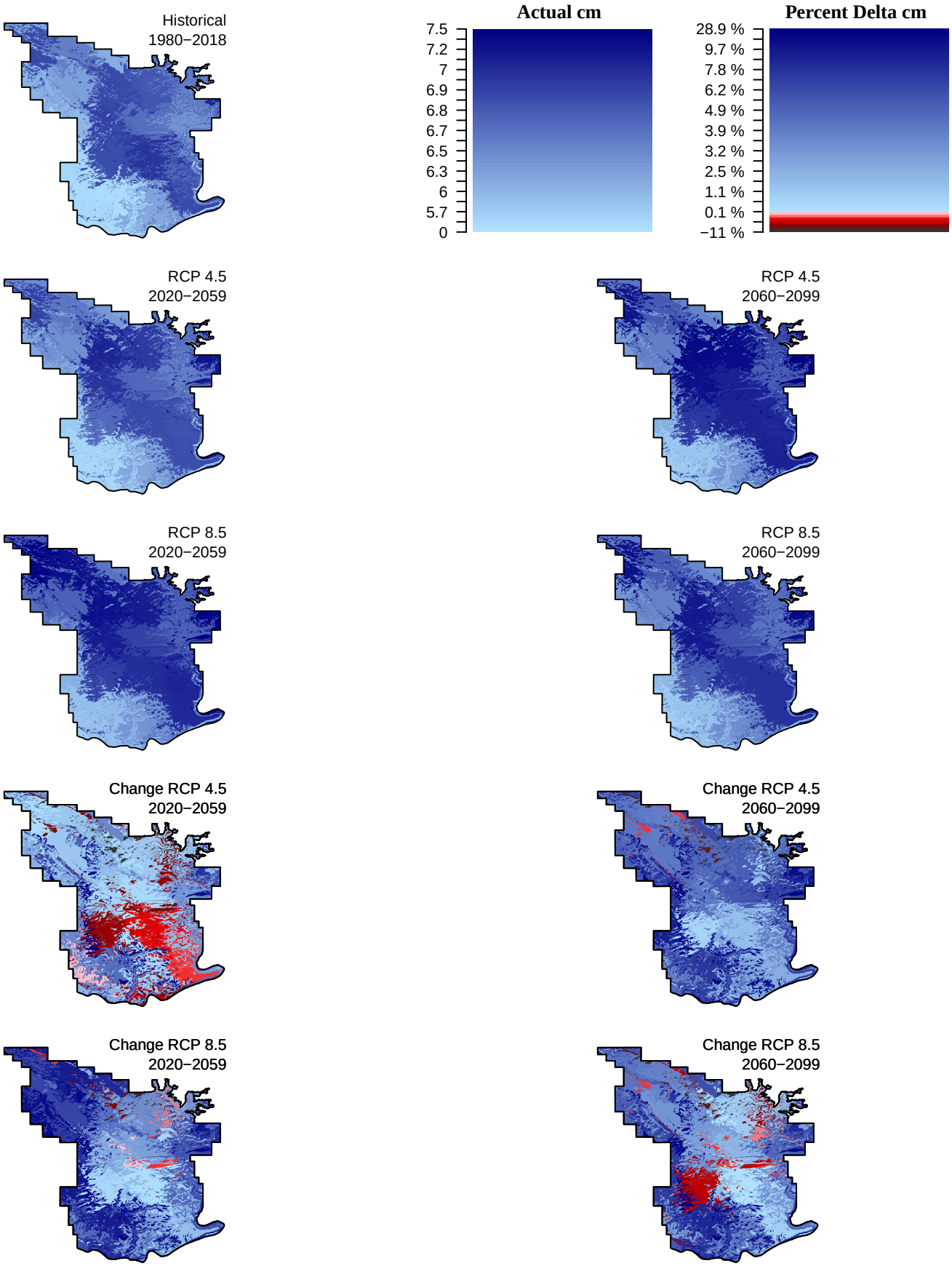


Figure ARCHmap45:
Past trends and future trajectories of park−wide mean values for Spring Precipitation in Arches. Topmost panel depicts the historical mean from 1980−2018. Lower four panels show the emission scenarios of RCP 4.5 and RCP 8.5 at near−term and long−term timeframes. Bottom four panels depict the change from the historical mean; cross hatching denotes areas of robust predicitons (90% of models agree in the direction of change).

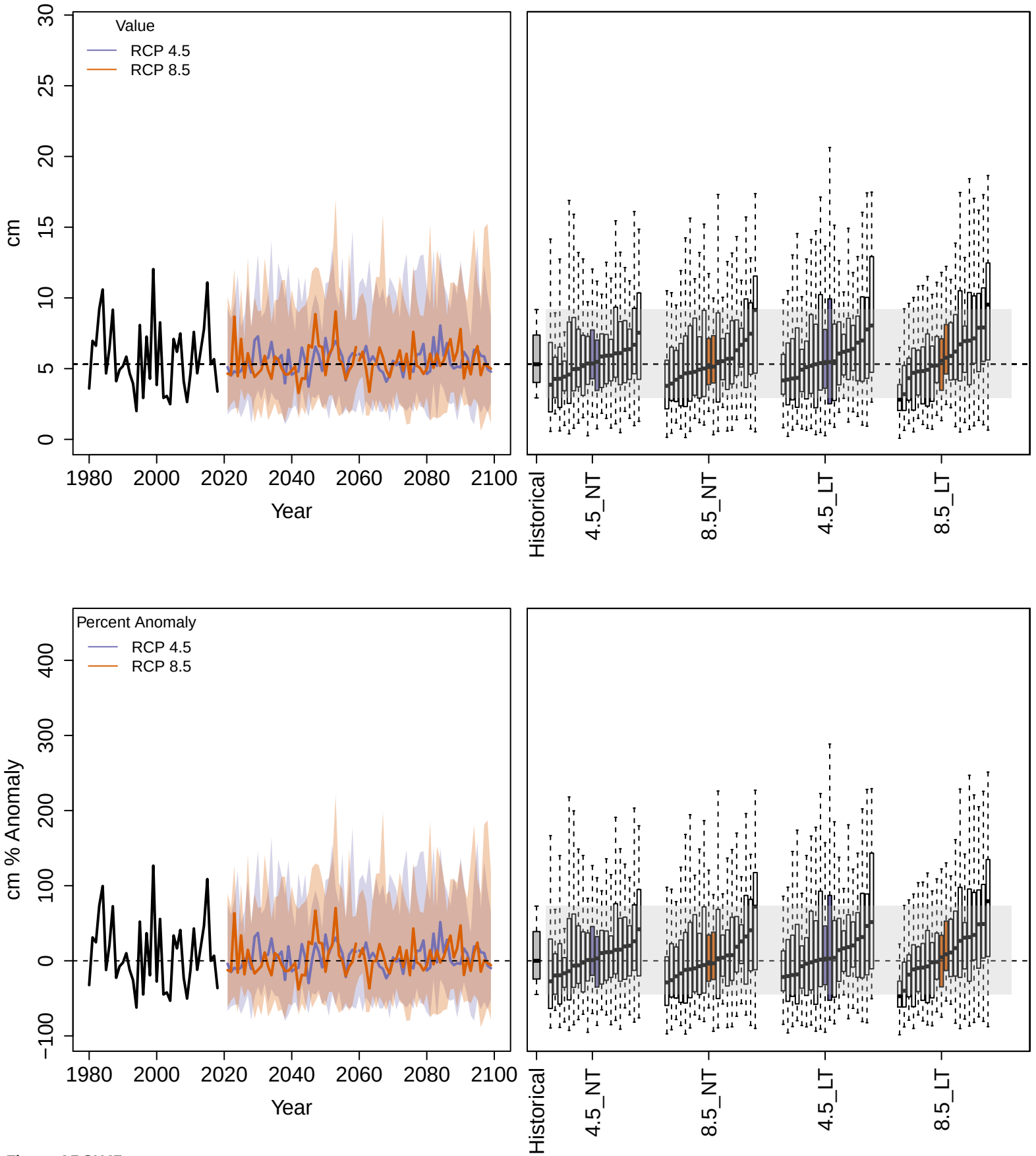


Figure ARCH47:
Past trends and future trajectories of park−wide mean values for Summer Precipitation in Arches. Top panels show values, bottom panels show changes from the long−term historical mean. Left: Time series of historical (black) and future projections for RCP 4.5 and 8.5. Shaded areas show spread among climate models. Right: Boxplots of temporal variability over 40−year periods under historical (left box) and individual climate models under two RCPs. Right: Historical time period is 1970−2010; near−term (NT) is 2020−2060; long−term (LT) is 2061−2100.

Arches: Summer Precipitation

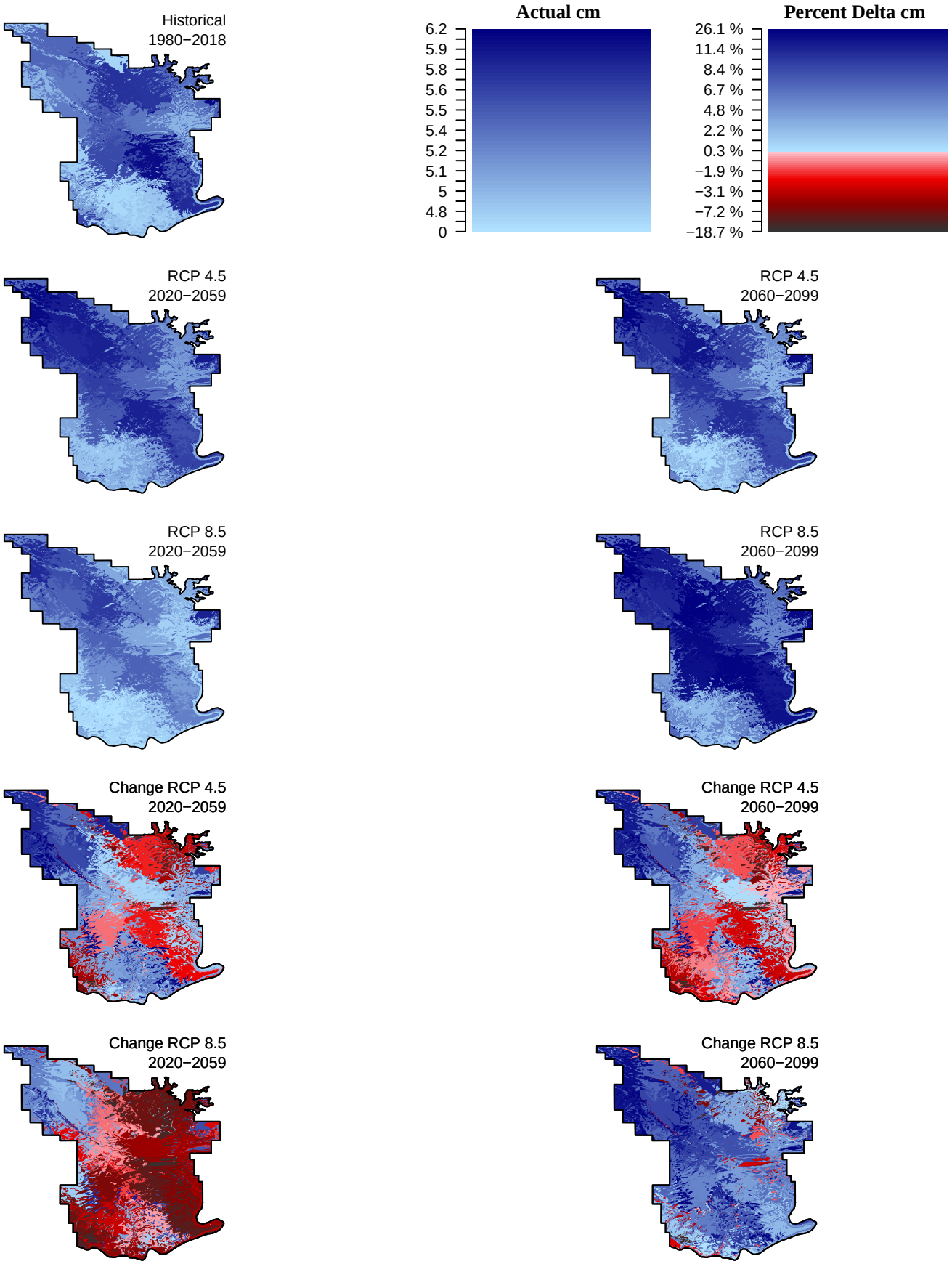


Figure ARCHmap47:
Past trends and future trajectories of park−wide mean values for Summer Precipitation in Arches. Topmost panel depicts the historical mean from 1980−2018. Lower four panels show the emission scenarios of RCP 4.5 and RCP 8.5 at near−term and long−term timeframes. Bottom four panels depict the change from the historical mean; cross hatching denotes areas of robust predicitons (90% of models agree in the direction of change).

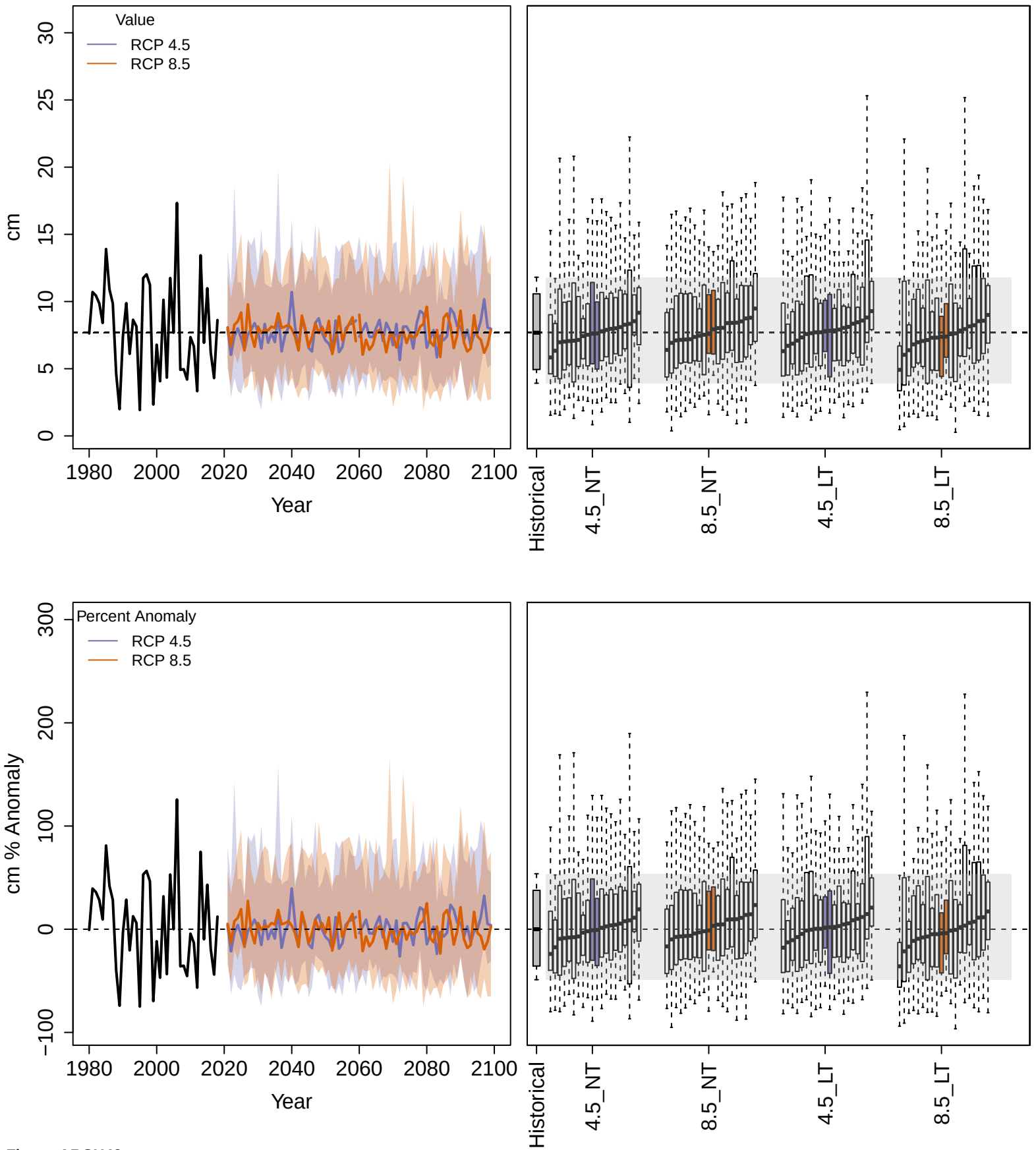


Figure ARCH49:
Past trends and future trajectories of park−wide mean values for Fall Precipitation in Arches. Top panels show values, bottom panels show changes from the long−term historical mean. Left: Time series of historical (black) and future projections for RCP 4.5 and 8.5. Shaded areas show spread among climate models. Right: Boxplots of temporal variability over 40−year periods under historical (left box) and individual climate models under two RCPs. Right: Historical time period is 1970−2010; near−term (NT) is 2020−2060; long−term (LT) is 2061−2100.

Arches: Fall Precipitation

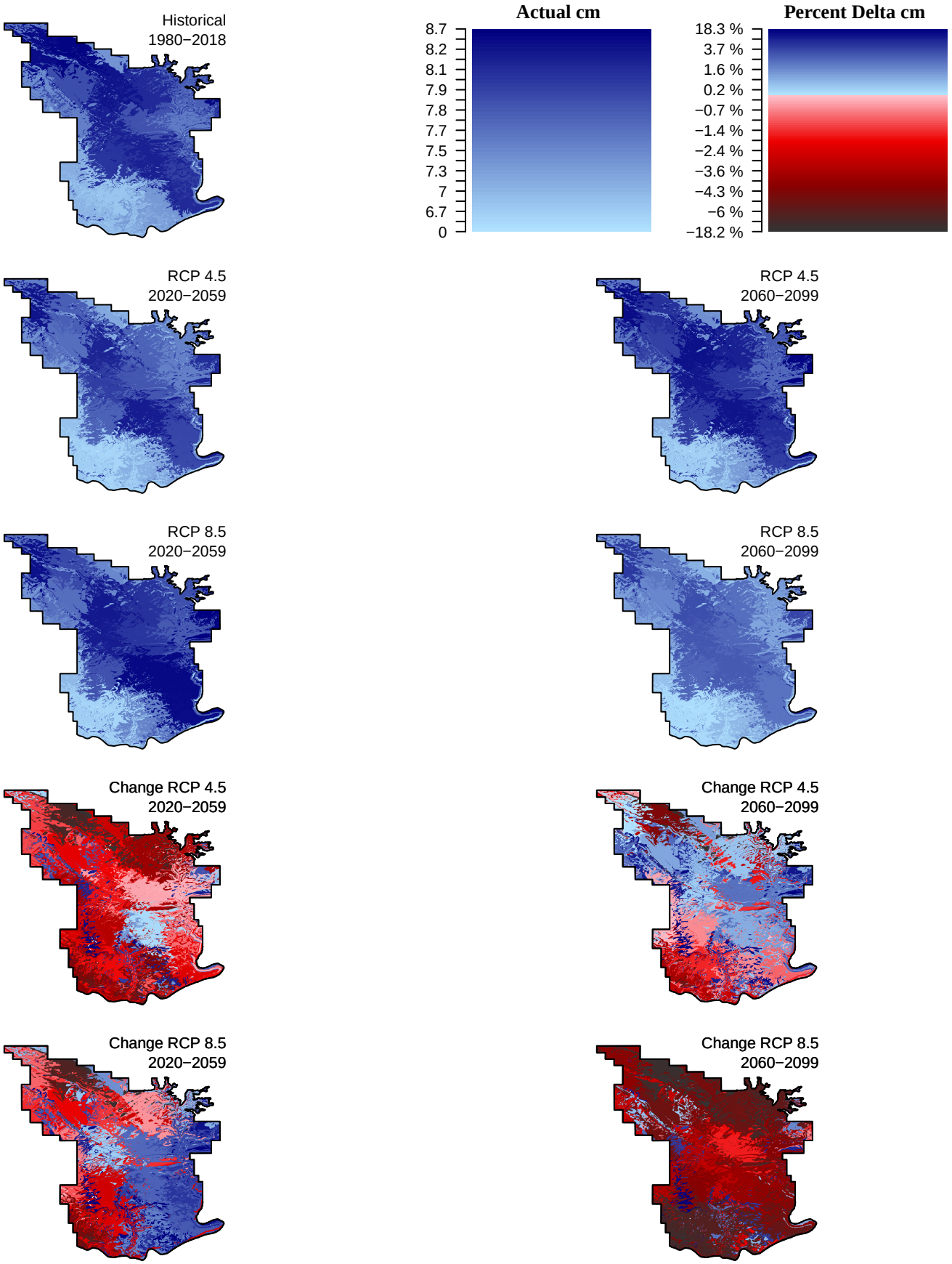


Figure ARCHmap49:
Past trends and future trajectories of park−wide mean values for Fall Precipitation in Arches. Topmost panel depicts the historical mean from 1980−2018. Lower four panels show the emission scenarios of RCP 4.5 and RCP 8.5 at near−term and long−term timeframes. Bottom four panels depict the change from the historical mean; cross hatching denotes areas of robust predicitons (90% of models agree in the direction of change).

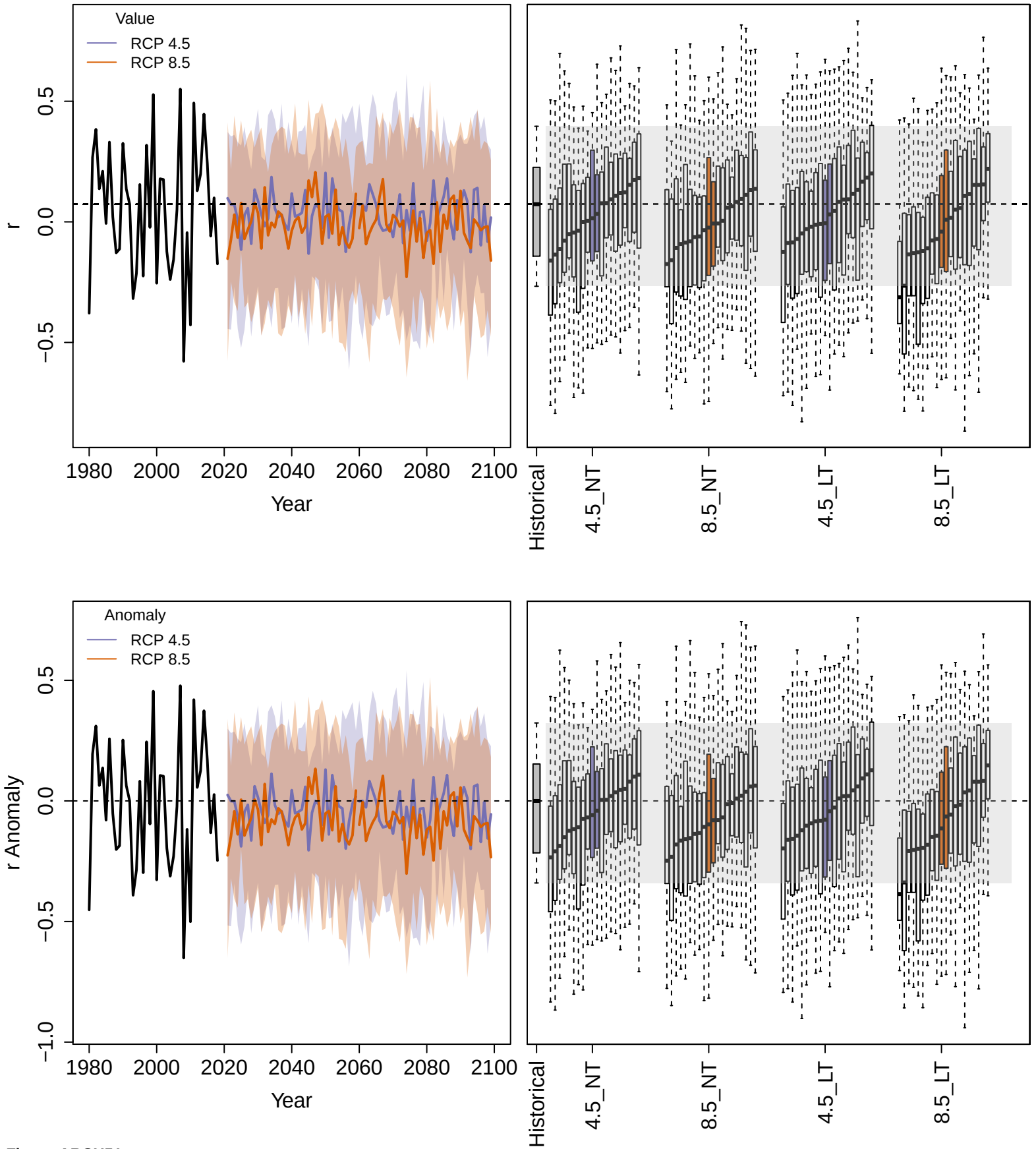


Figure ARCH51:
Past trends and future trajectories of park−wide mean values for Monthly temperature−precipitation correlation in Arches. Top panels show values, bottom panels show changes from the long−term historical mean. Left: Time series of historical (black) and future projections for RCP 4.5 and 8.5. Shaded areas show spread among climate models. Right: Boxplots of temporal variability over 40−year periods under historical (left box) and individual climate models under two RCPs. Right: Historical time period is 1970−2010; near−term (NT) is 2020−2060; long−term (LT) is 2061−2100.

Arches: Monthly temperature−precipitation correlation

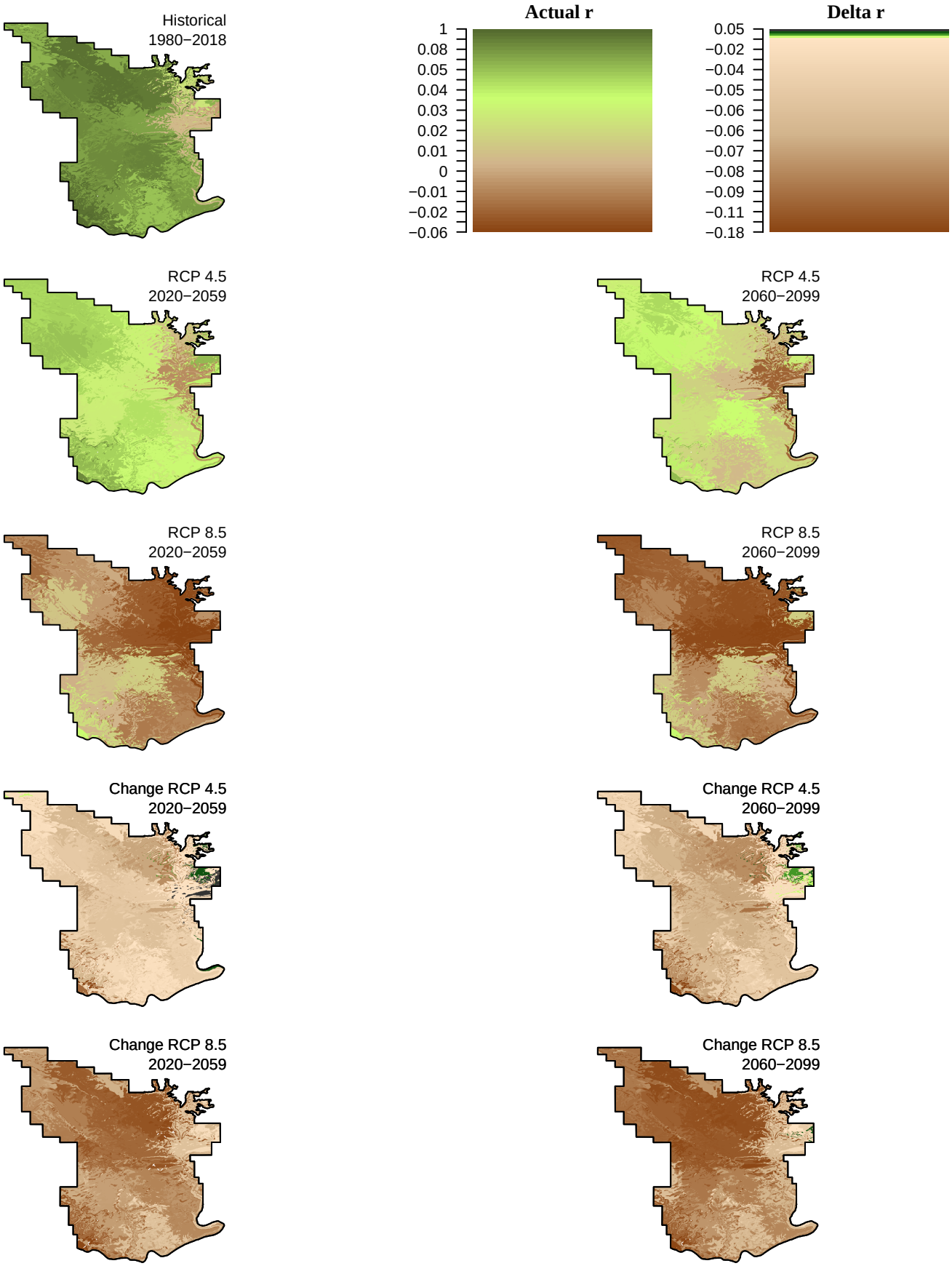


Figure ARCHmap51:
Past trends and future trajectories of park−wide mean values for Monthly temperature−precipitation correlation in Arches. Topmost panel depicts the historical mean from 1980−2018. Lower four panels show the emission scenarios of RCP 4.5 and RCP 8.5 at near−term and long−term timeframes. Bottom four panels depict the change from the historical mean; cross hatching denotes areas of robust predicitons (90% of models agree in the direction of change).

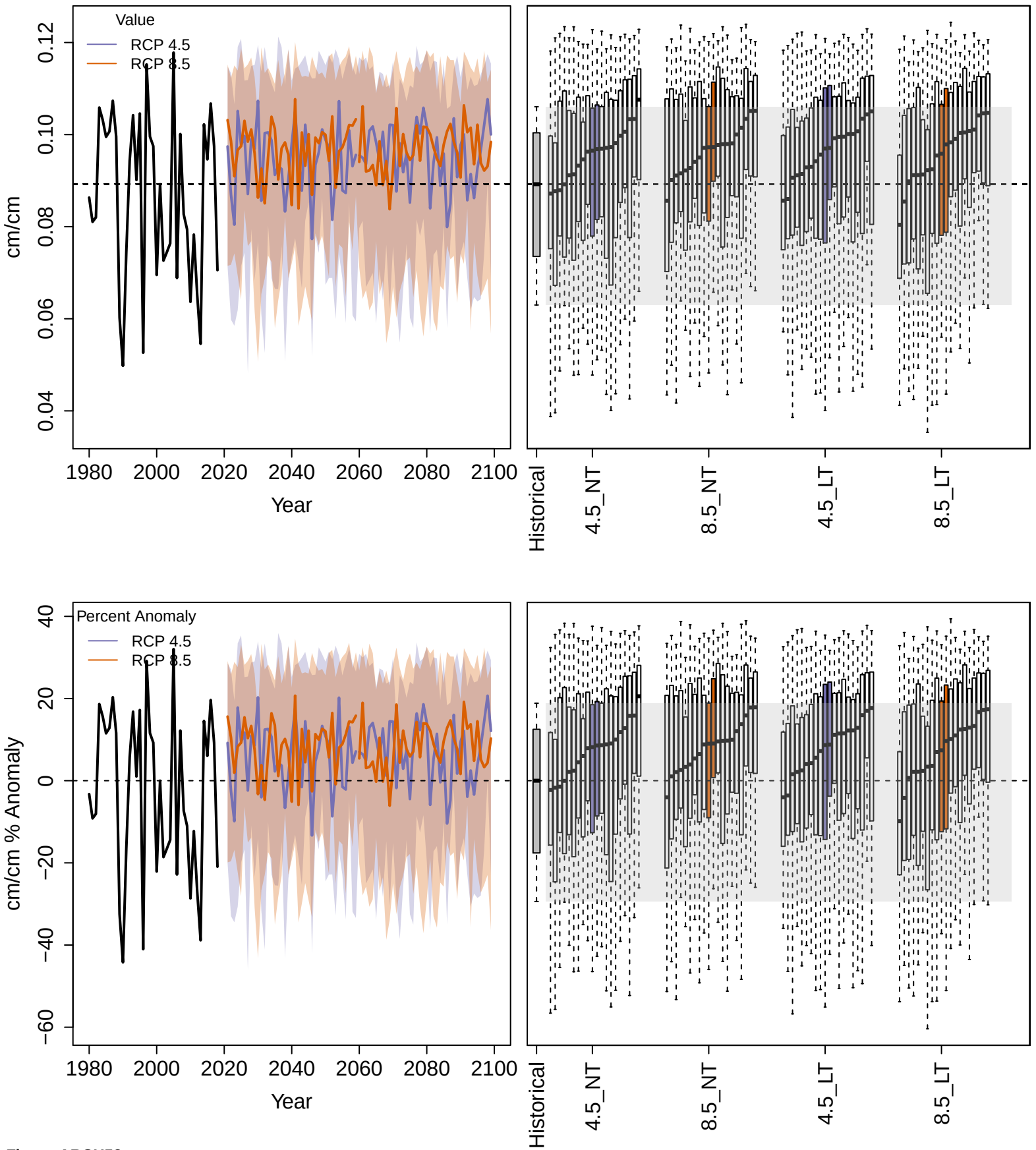


Figure ARCH53:
Past trends and future trajectories of park−wide mean values for Winter soil water content: Top 50cm in Arches. Top panels show values, bottom panels show changes from the long−term historical mean. Left: Time series of historical (black) and future projections for RCP 4.5 and 8.5. Shaded areas show spread among climate models. Right: Boxplots of temporal variability over 40−year periods under historical (left box) and individual climate models under two RCPs. Right: Historical time period is 1970−2010; near−term (NT) is 2020−2060; long−term (LT) is 2061−2100.

Arches: Winter soil water content: Top 50cm

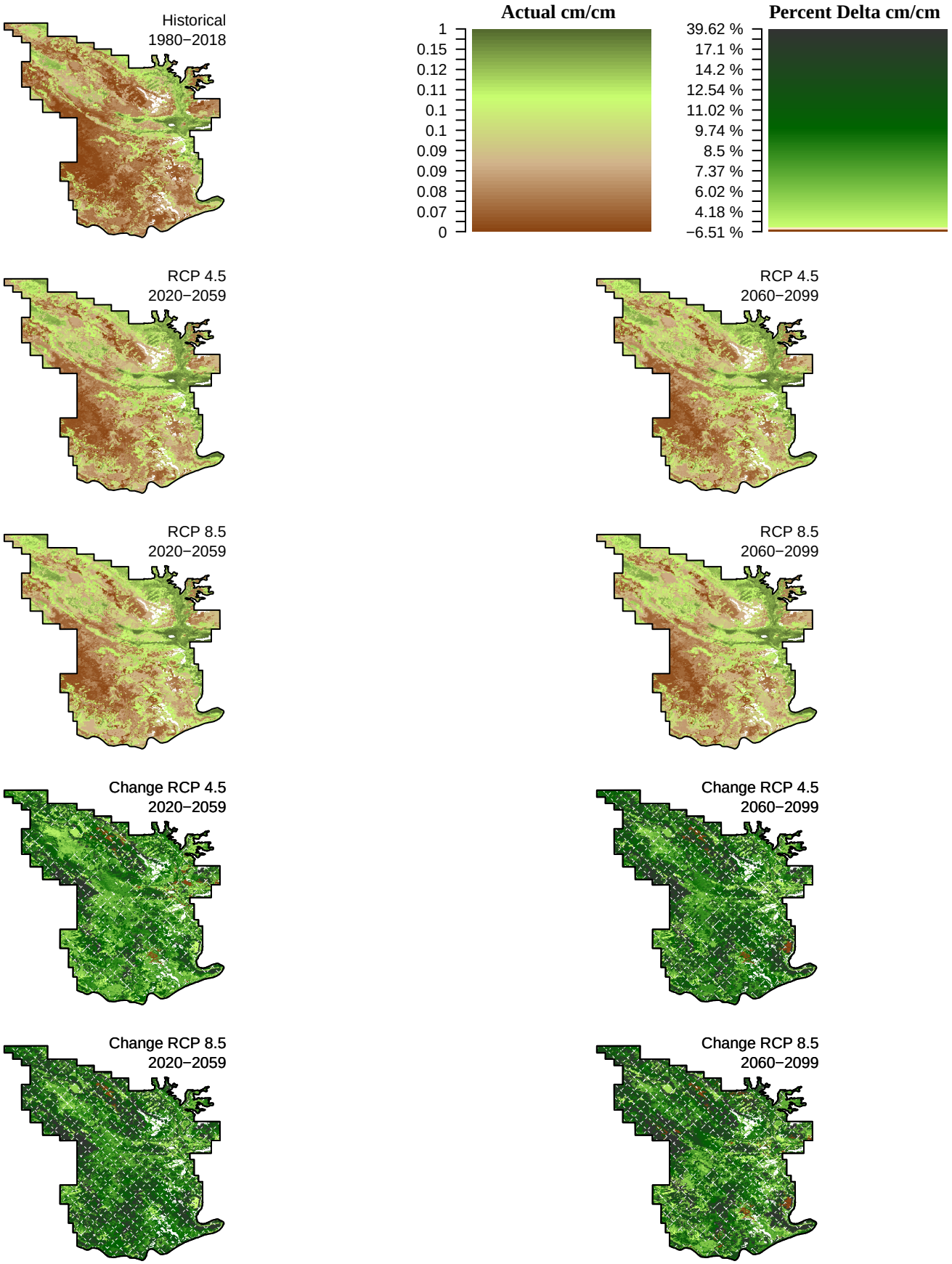


Figure ARCHmap53:
Past trends and future trajectories of park−wide mean values for Winter soil water content: Top 50cm in Arches. Topmost panel depicts the historical mean from 1980−2018. Lower four panels show the emission scenarios of RCP 4.5 and RCP 8.5 at near−term and long−term timeframes. Bottom four panels depict the change from the historical mean; cross hatching denotes areas of robust predicitons (90% of models agree in the direction of change).

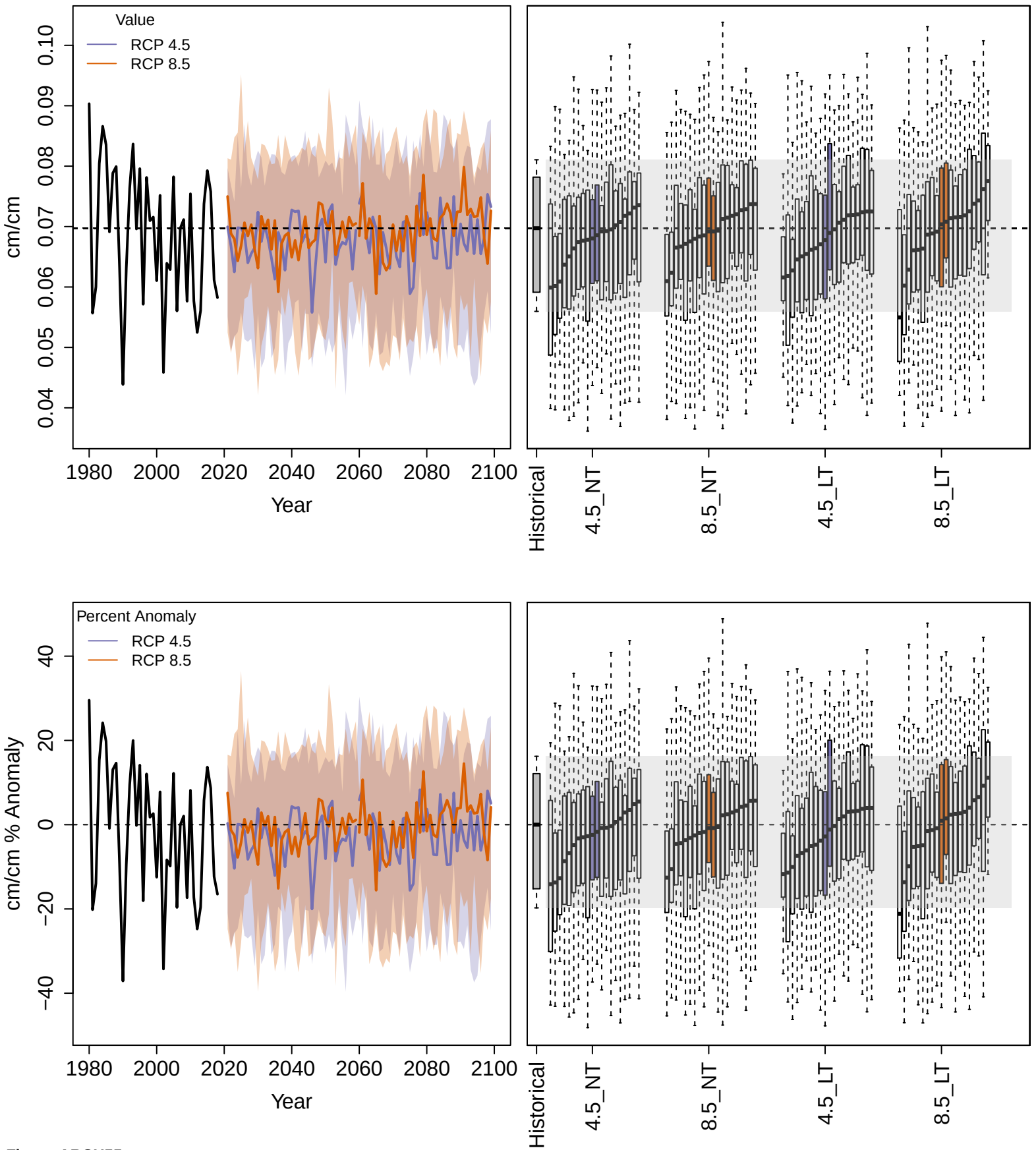


Figure ARCH55:
Past trends and future trajectories of park−wide mean values for Spring soil water content:Top 50cm in Arches. Top panels show values, bottom panels show changes from the long−term historical mean. Left: Time series of historical (black) and future projections for RCP 4.5 and 8.5. Shaded areas show spread among climate models. Right: Boxplots of temporal variability over 40−year periods under historical (left box) and individual climate models under two RCPs. Right: Historical time period is 1970−2010; near−term (NT) is 2020−2060; long−term (LT) is 2061−2100.

Arches: Spring soil water content:Top 50cm

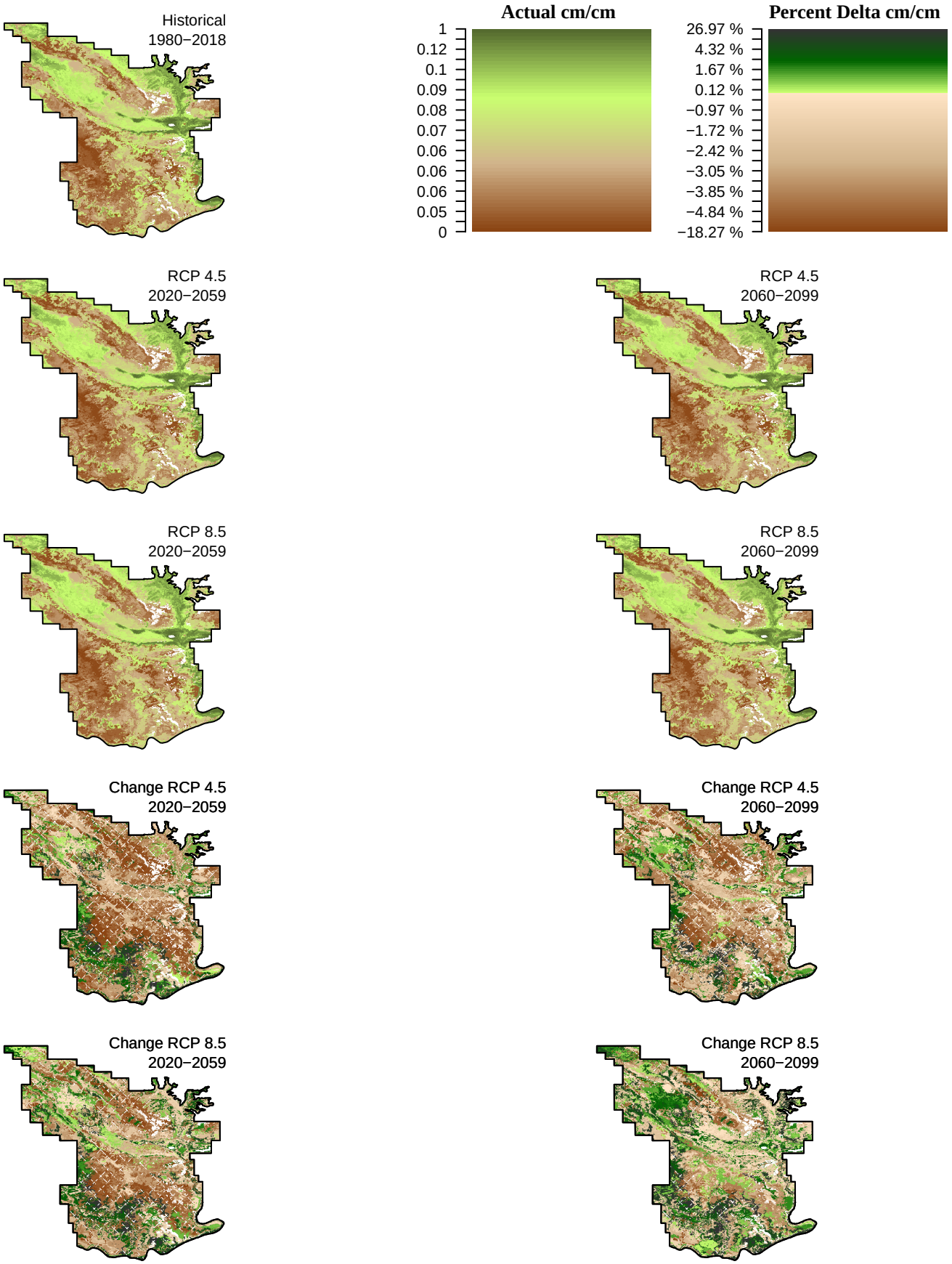


Figure ARCHmap55:
Past trends and future trajectories of park−wide mean values for Spring soil water content:Top 50cm in Arches. Topmost panel depicts the historical mean from 1980−2018. Lower four panels show the emission scenarios of RCP 4.5 and RCP 8.5 at near−term and long−term timeframes. Bottom four panels depict the change from the historical mean; cross hatching denotes areas of robust predicitons (90% of models agree in the direction of change).

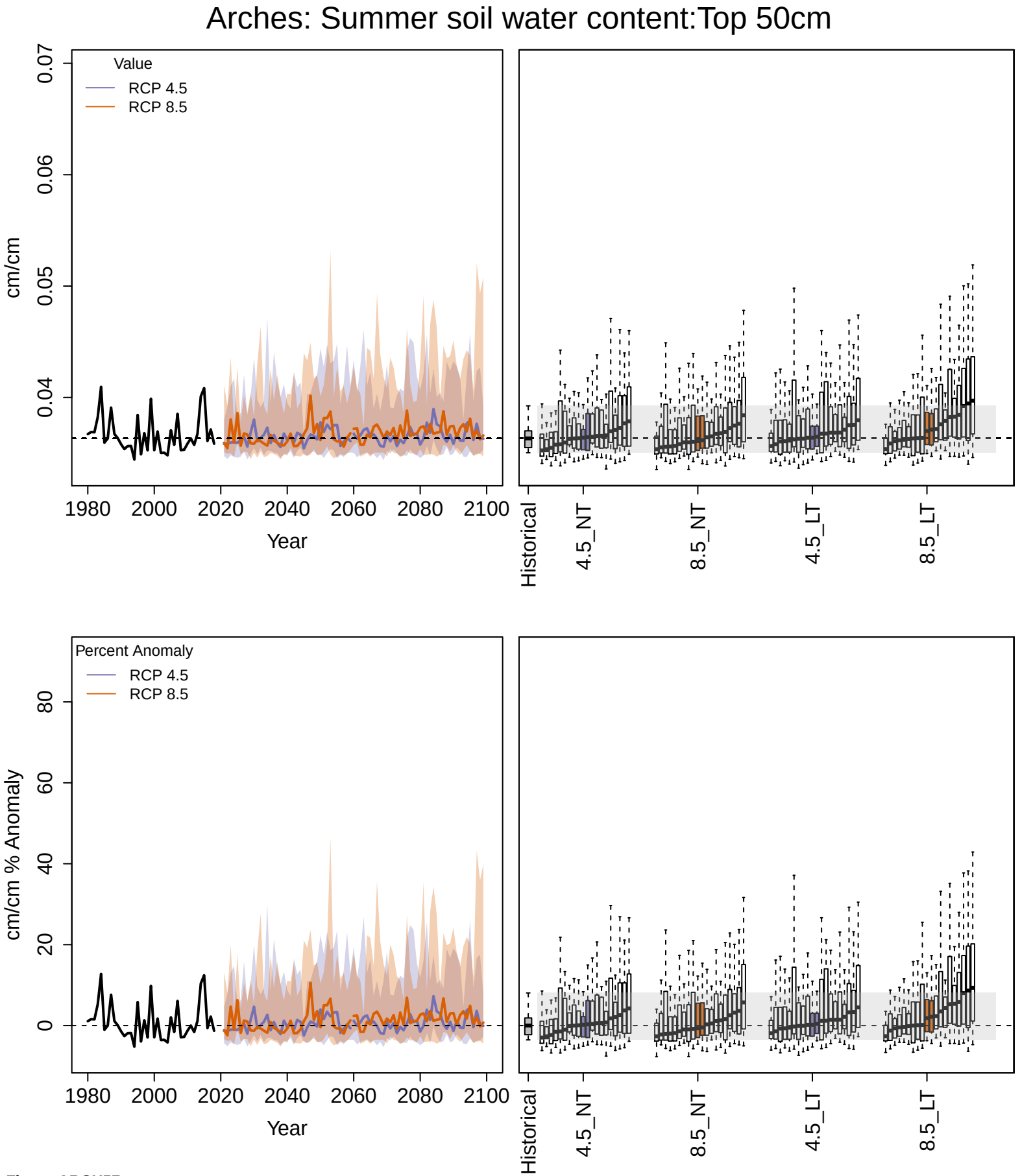


Figure ARCH57:
Past trends and future trajectories of park−wide mean values for Summer soil water content:Top 50cm in Arches. Top panels show values, bottom panels show changes from the long−term historical mean. Left: Time series of historical (black) and future projections for RCP 4.5 and 8.5. Shaded areas show spread among climate models. Right: Boxplots of temporal variability over 40−year periods under historical (left box) and individual climate models under two RCPs. Right: Historical time period is 1970−2010; near−term (NT) is 2020−2060; long−term (LT) is 2061−2100.

Arches: Summer soil water content:Top 50cm

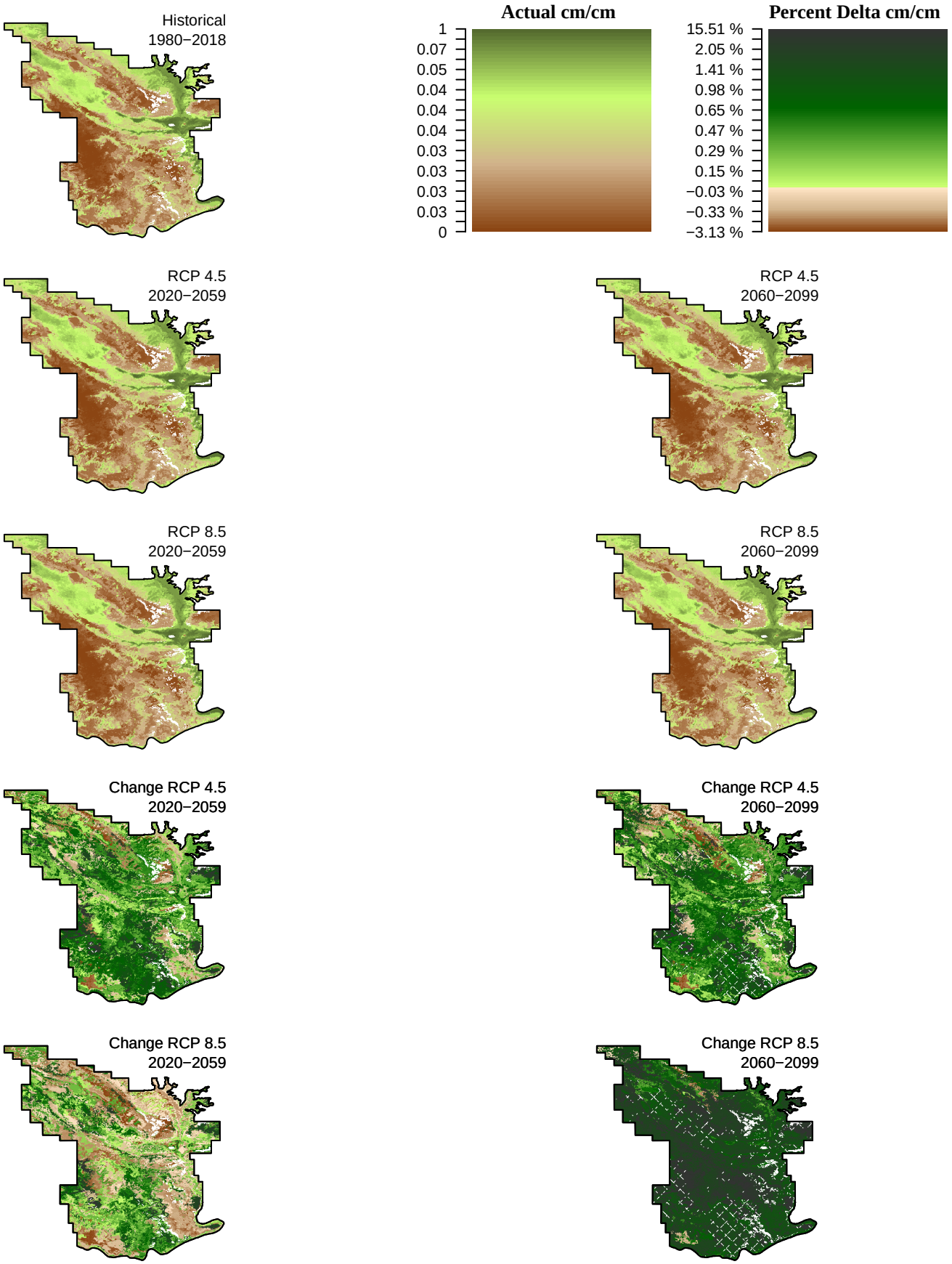


Figure ARCHmap57:
Past trends and future trajectories of park−wide mean values for Summer soil water content:Top 50cm in Arches. Topmost panel depicts the historical mean from 1980−2018. Lower four panels show the emission scenarios of RCP 4.5 and RCP 8.5 at near−term and long−term timeframes. Bottom four panels depict the change from the historical mean; cross hatching denotes areas of robust predicitons (90% of models agree in the direction of change).

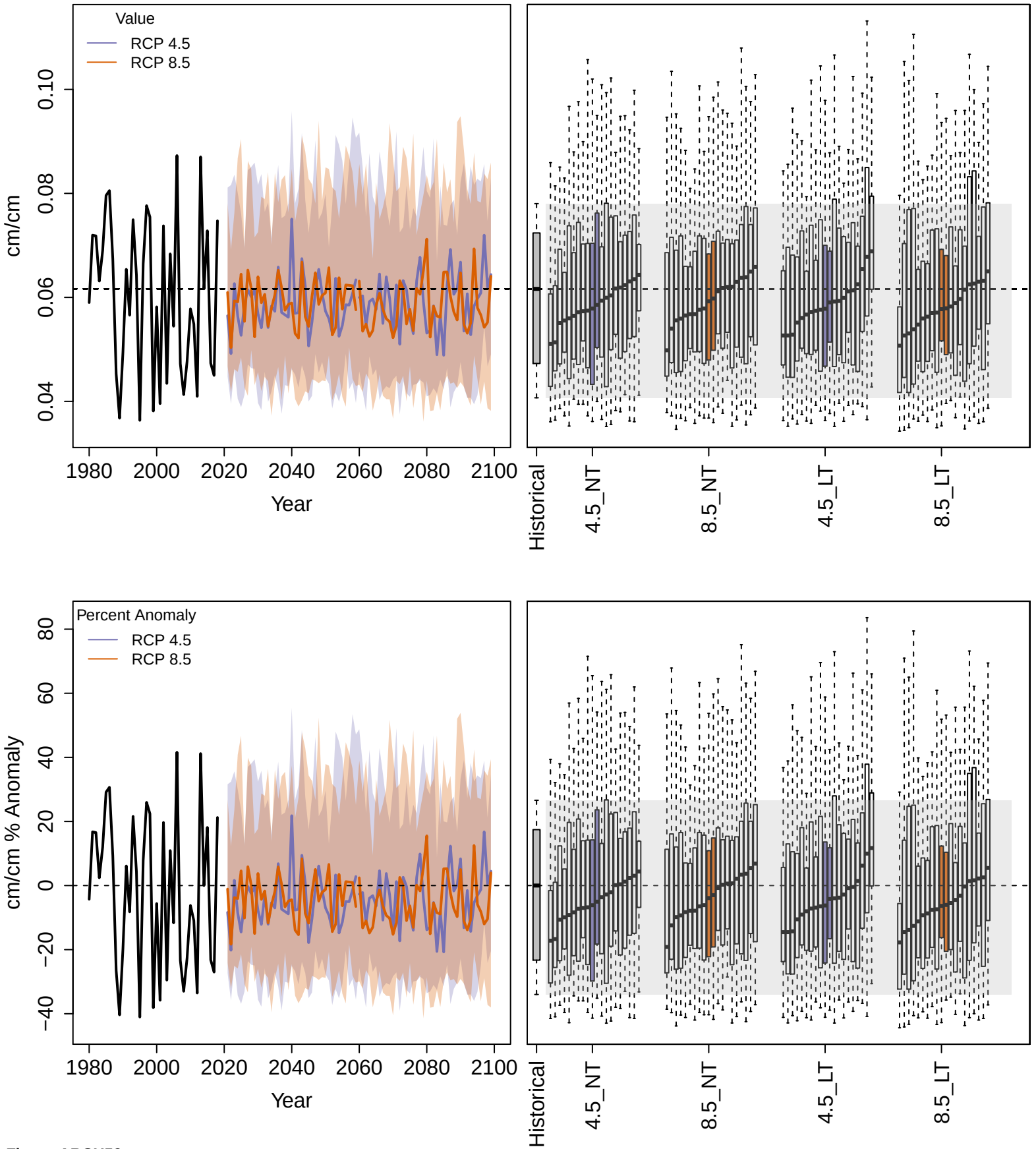


Figure ARCH59:
Past trends and future trajectories of park−wide mean values for Fall soil water content:Top 50cm in Arches. Top panels show values, bottom panels show changes from the long−term historical mean. Left: Time series of historical (black) and future projections for RCP 4.5 and 8.5. Shaded areas show spread among climate models. Right: Boxplots of temporal variability over 40−year periods under historical (left box) and individual climate models under two RCPs. Right: Historical time period is 1970−2010; near−term (NT) is 2020−2060; long−term (LT) is 2061−2100.

Arches: Fall soil water content:Top 50cm

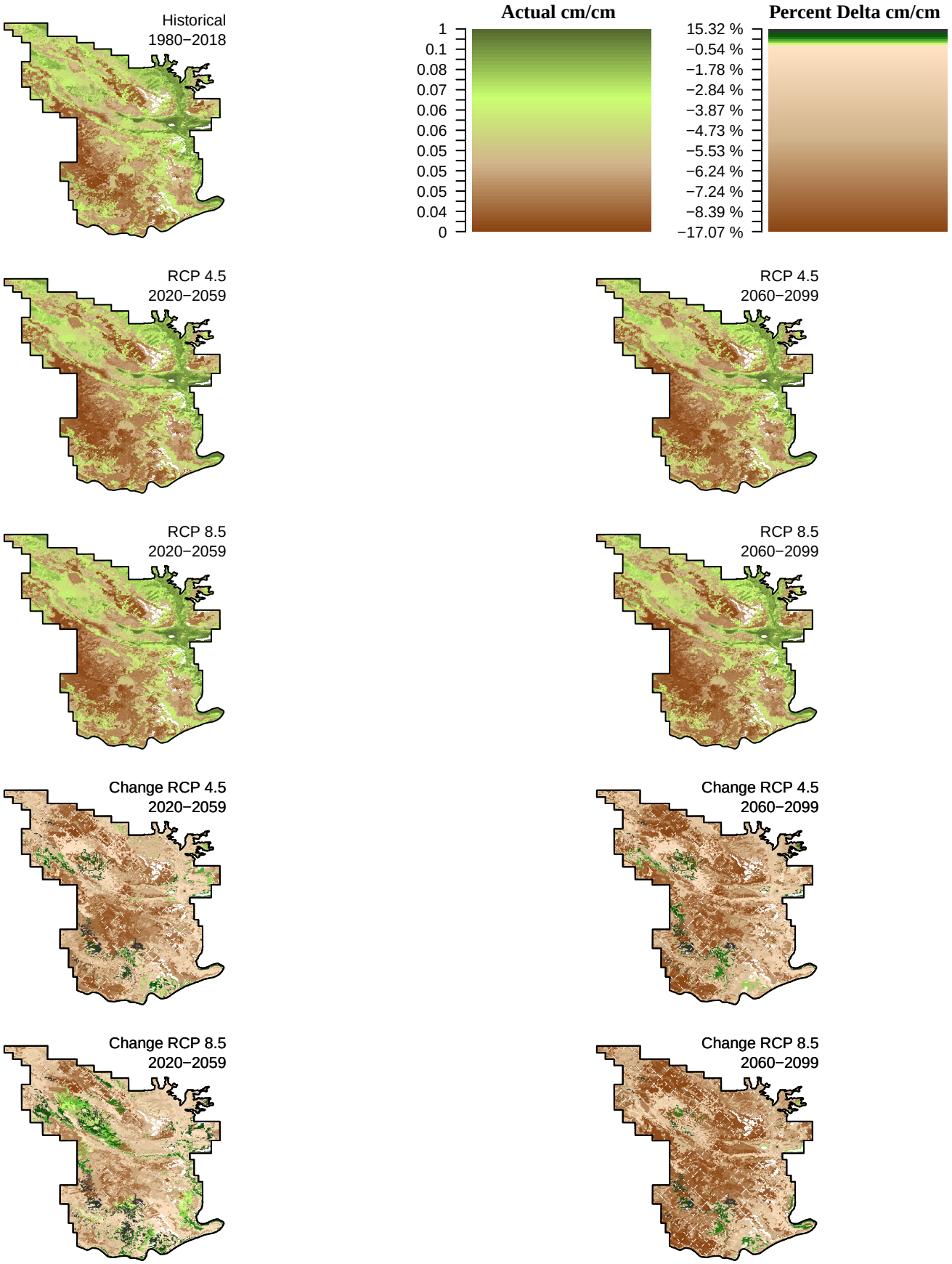


Figure ARCHmap59:
Past trends and future trajectories of park−wide mean values for Fall soil water content:Top 50cm in Arches. Topmost panel depicts the historical mean from 1980−2018. Lower four panels show the emission scenarios of RCP 4.5 and RCP 8.5 at near−term and long−term timeframes. Bottom four panels depict the change from the historical mean; cross hatching denotes areas of robust predicitons (90% of models agree in the direction of change).

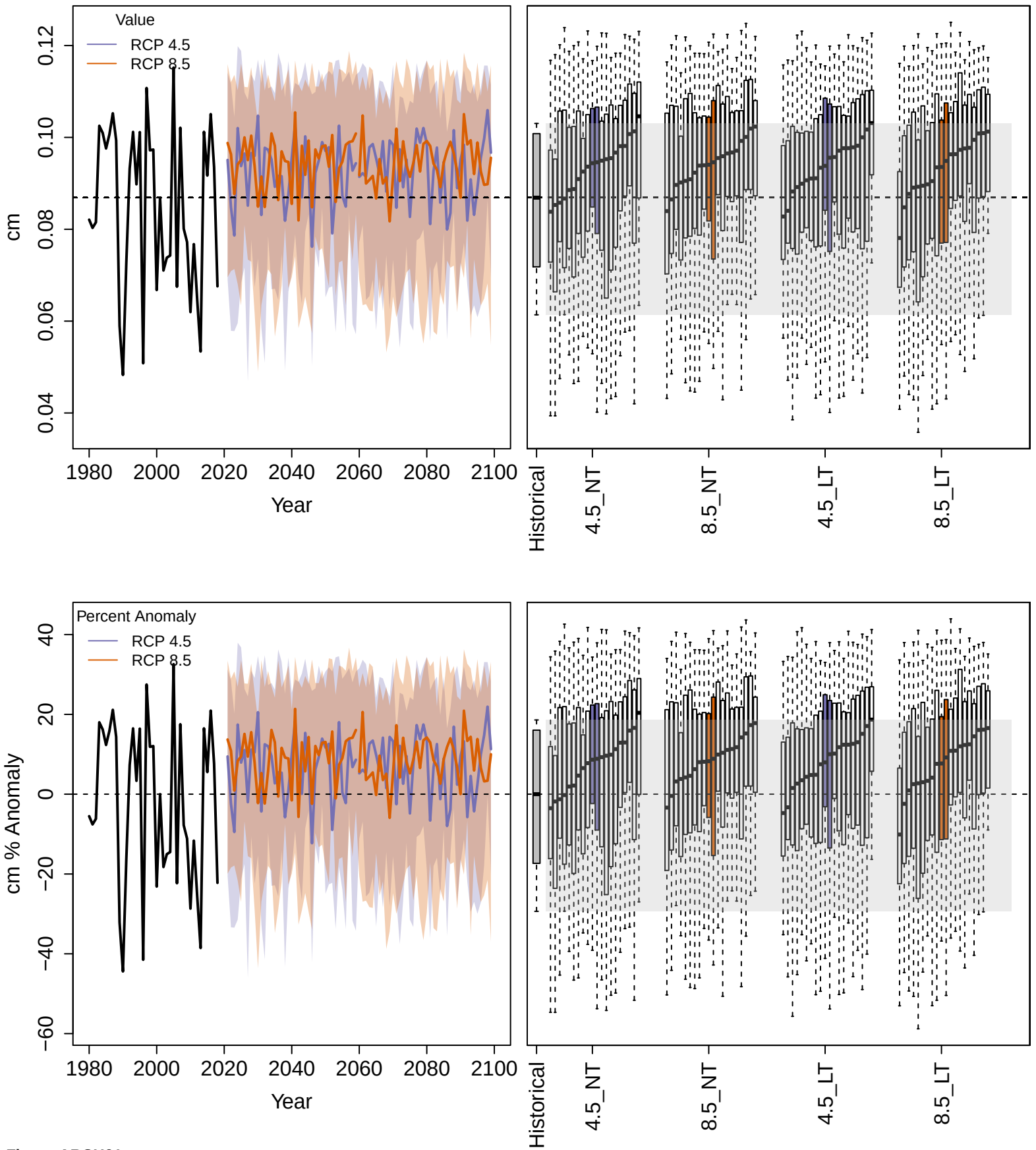


Figure ARCH61:
Past trends and future trajectories of park−wide mean values for Winter soil water content in Arches. Top panels show values, bottom panels show changes from the long−term historical mean. Left: Time series of historical (black) and future projections for RCP 4.5 and 8.5. Shaded areas show spread among climate models. Right: Boxplots of temporal variability over 40−year periods under historical (left box) and individual climate models under two RCPs. Right: Historical time period is 1970−2010; near−term (NT) is 2020−2060; long−term (LT) is 2061−2100.

Arches: Winter soil water content

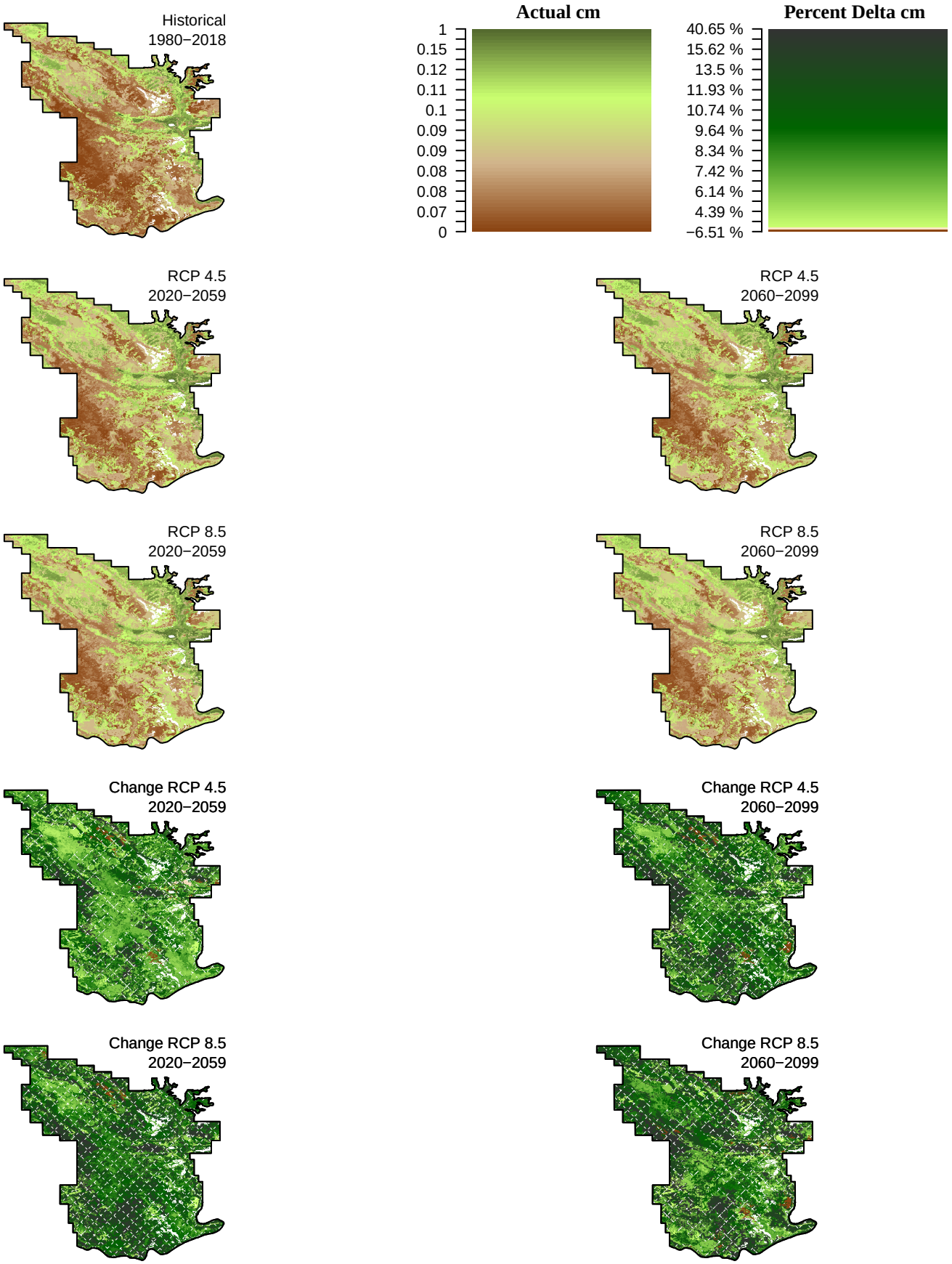


Figure ARCHmap61:
Past trends and future trajectories of park−wide mean values for Winter soil water content in Arches. Topmost panel depicts the historical mean from 1980−2018. Lower four panels show the emission scenarios of RCP 4.5 and RCP 8.5 at near−term and long−term timeframes. Bottom four panels depict the change from the historical mean; cross hatching denotes areas of robust predicitons (90% of models agree in the direction of change).

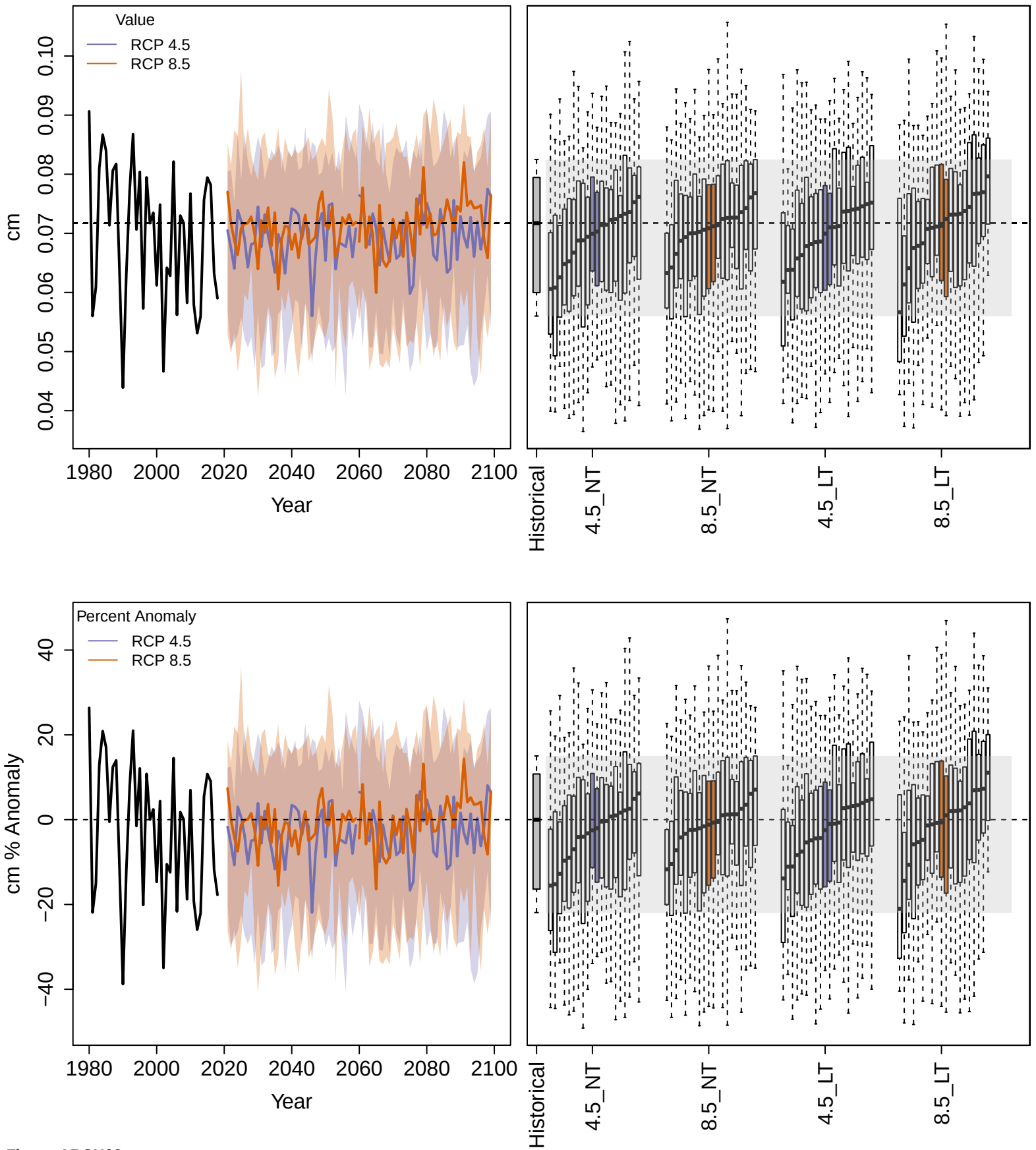


Figure ARCH63:
Past trends and future trajectories of park−wide mean values for Spring soil water content in Arches. Top panels show values, bottom panels show changes from the long−term historical mean. Left: Time series of historical (black) and future projections for RCP 4.5 and 8.5. Shaded areas show spread among climate models. Right: Boxplots of temporal variability over 40−year periods under historical (left box) and individual climate models under two RCPs. Right: Historical time period is 1970−2010; near−term (NT) is 2020−2060; long−term (LT) is 2061−2100.

Arches: Spring soil water content

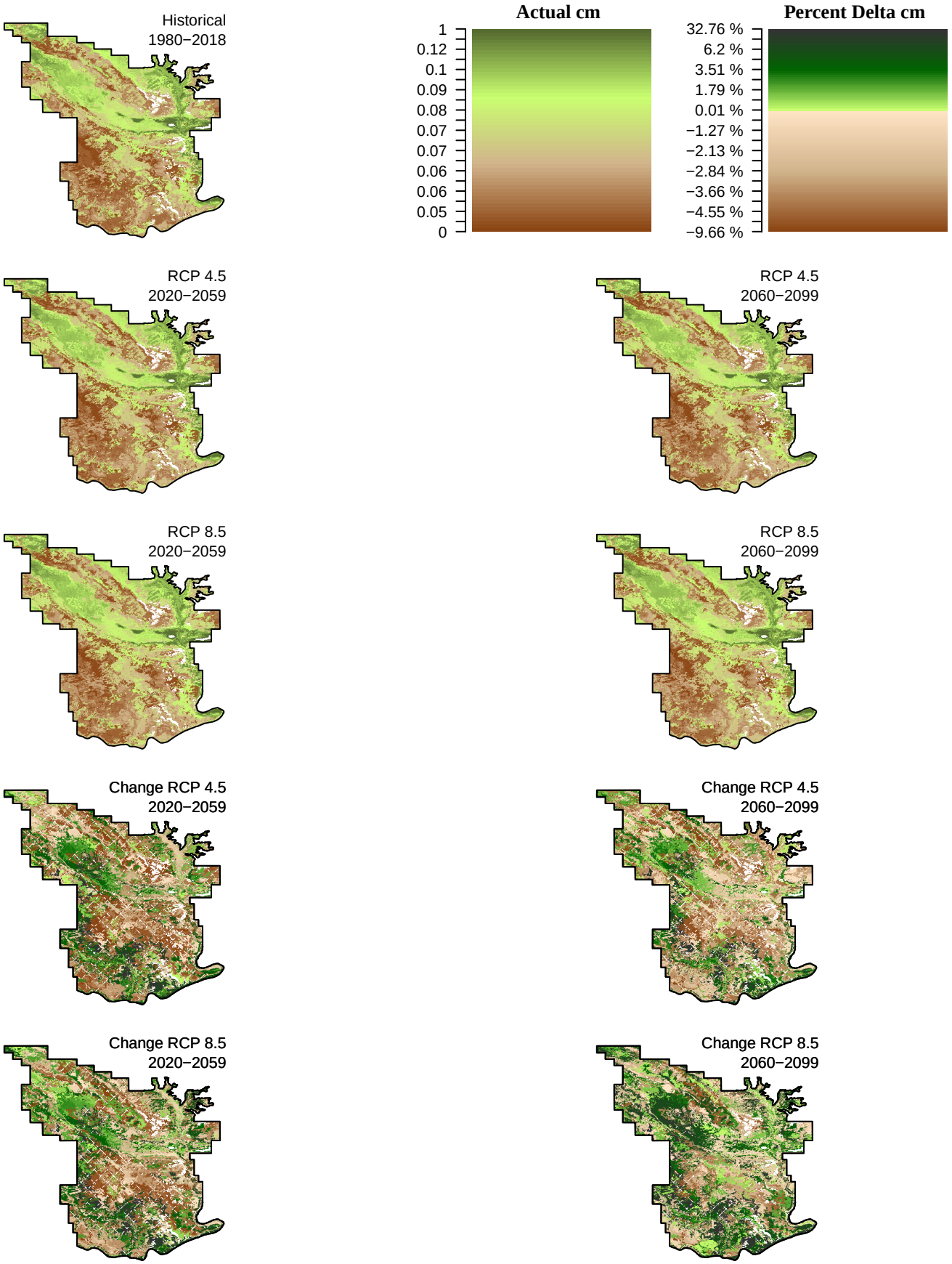


Figure ARCHmap63:
Past trends and future trajectories of park−wide mean values for Spring soil water content in Arches. Topmost panel depicts the historical mean from 1980−2018. Lower four panels show the emission scenarios of RCP 4.5 and RCP 8.5 at near−term and long−term timeframes. Bottom four panels depict the change from the historical mean; cross hatching denotes areas of robust predicitons (90% of models agree in the direction of change).

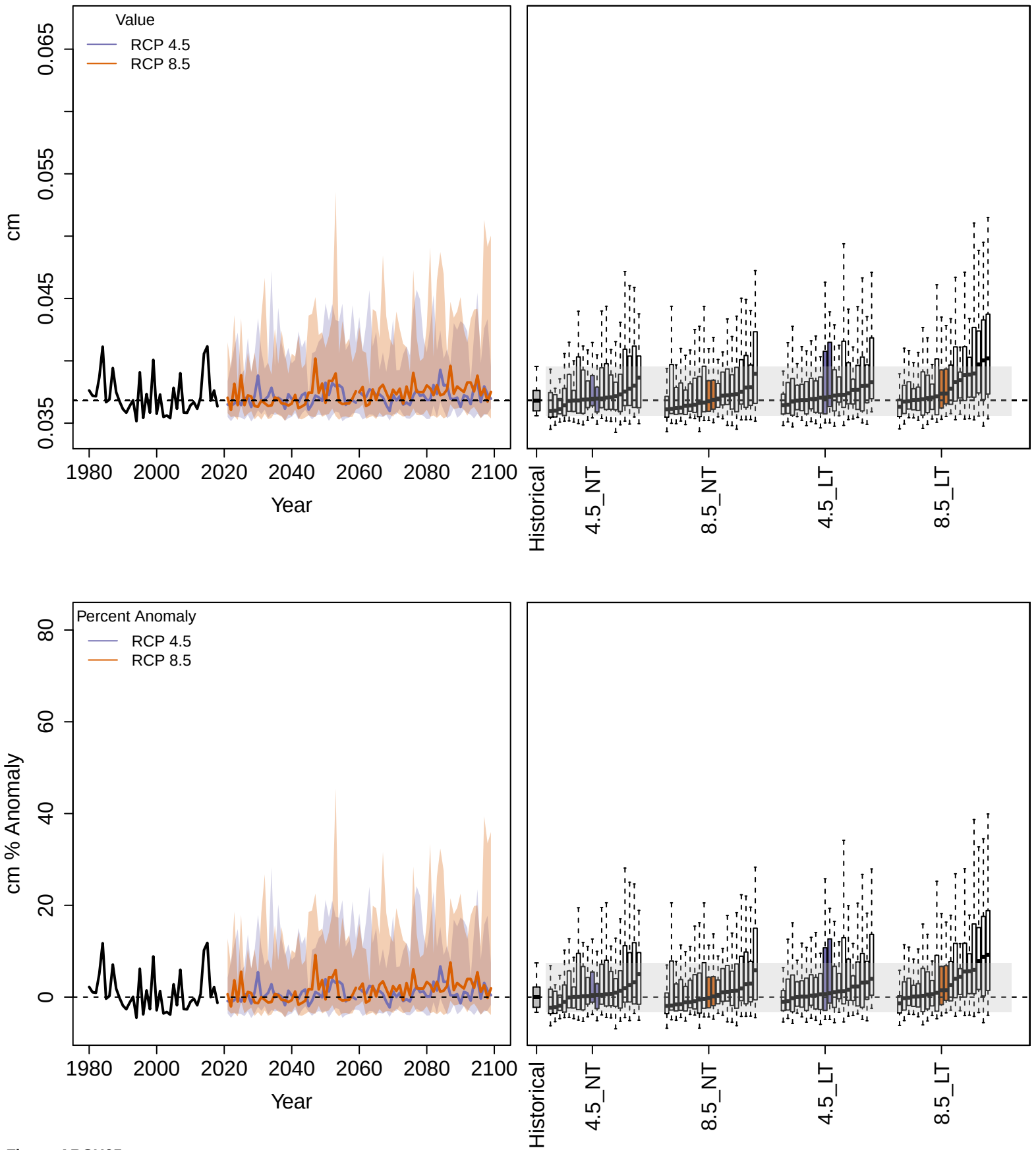


Figure ARCH65:
Past trends and future trajectories of park−wide mean values for Summer soil water content in Arches. Top panels show values, bottom panels show changes from the long−term historical mean. Left: Time series of historical (black) and future projections for RCP 4.5 and 8.5. Shaded areas show spread among climate models. Right: Boxplots of temporal variability over 40−year periods under historical (left box) and individual climate models under two RCPs. Right: Historical time period is 1970−2010; near−term (NT) is 2020−2060; long−term (LT) is 2061−2100.

Arches: Summer soil water content

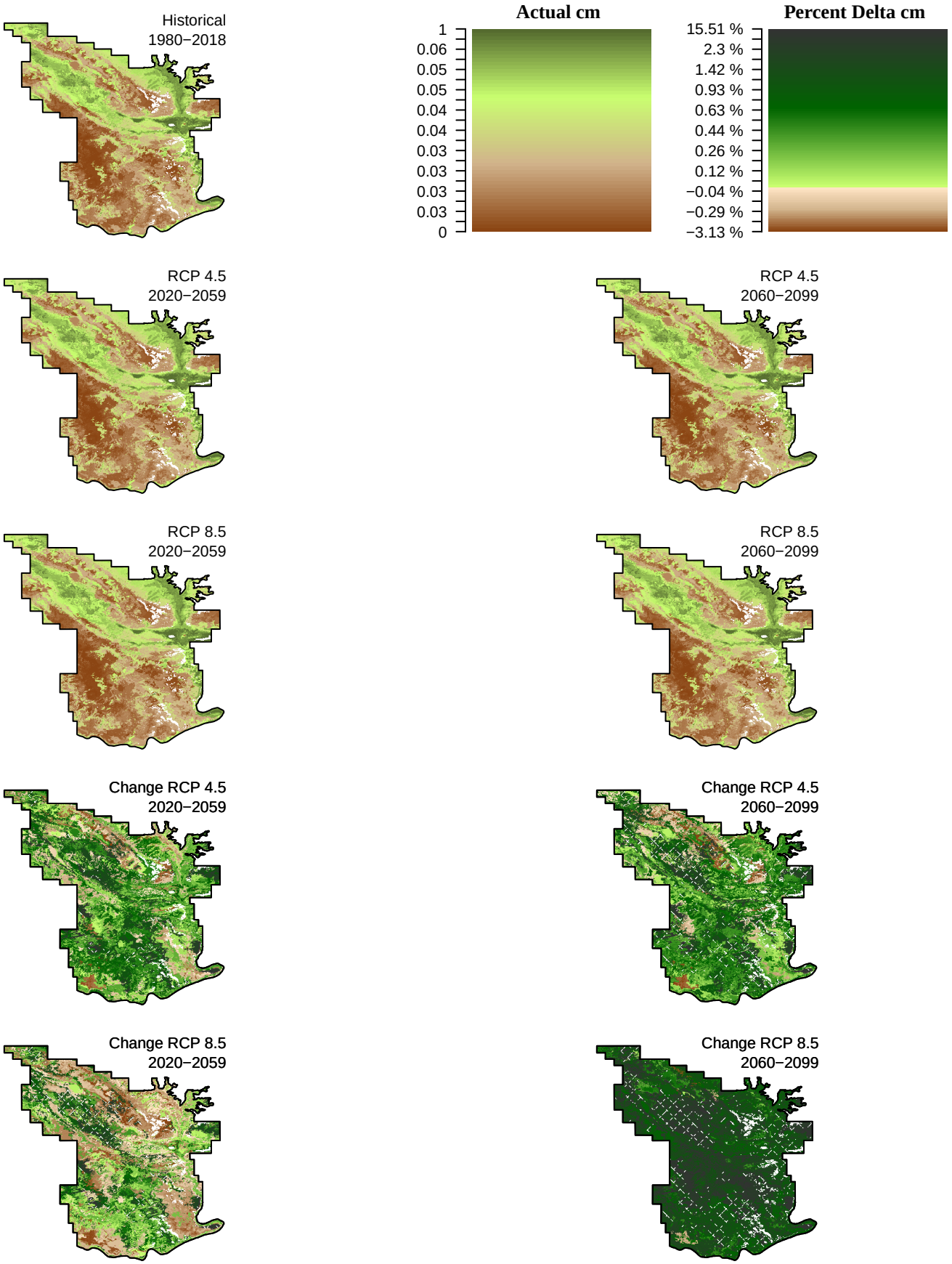


Figure ARCHmap65:
Past trends and future trajectories of park−wide mean values for Summer soil water content in Arches. Topmost panel depicts the historical mean from 1980−2018. Lower four panels show the emission scenarios of RCP 4.5 and RCP 8.5 at near−term and long−term timeframes. Bottom four panels depict the change from the historical mean; cross hatching denotes areas of robust predicitons (90% of models agree in the direction of change).

Arches: Fall soil water content

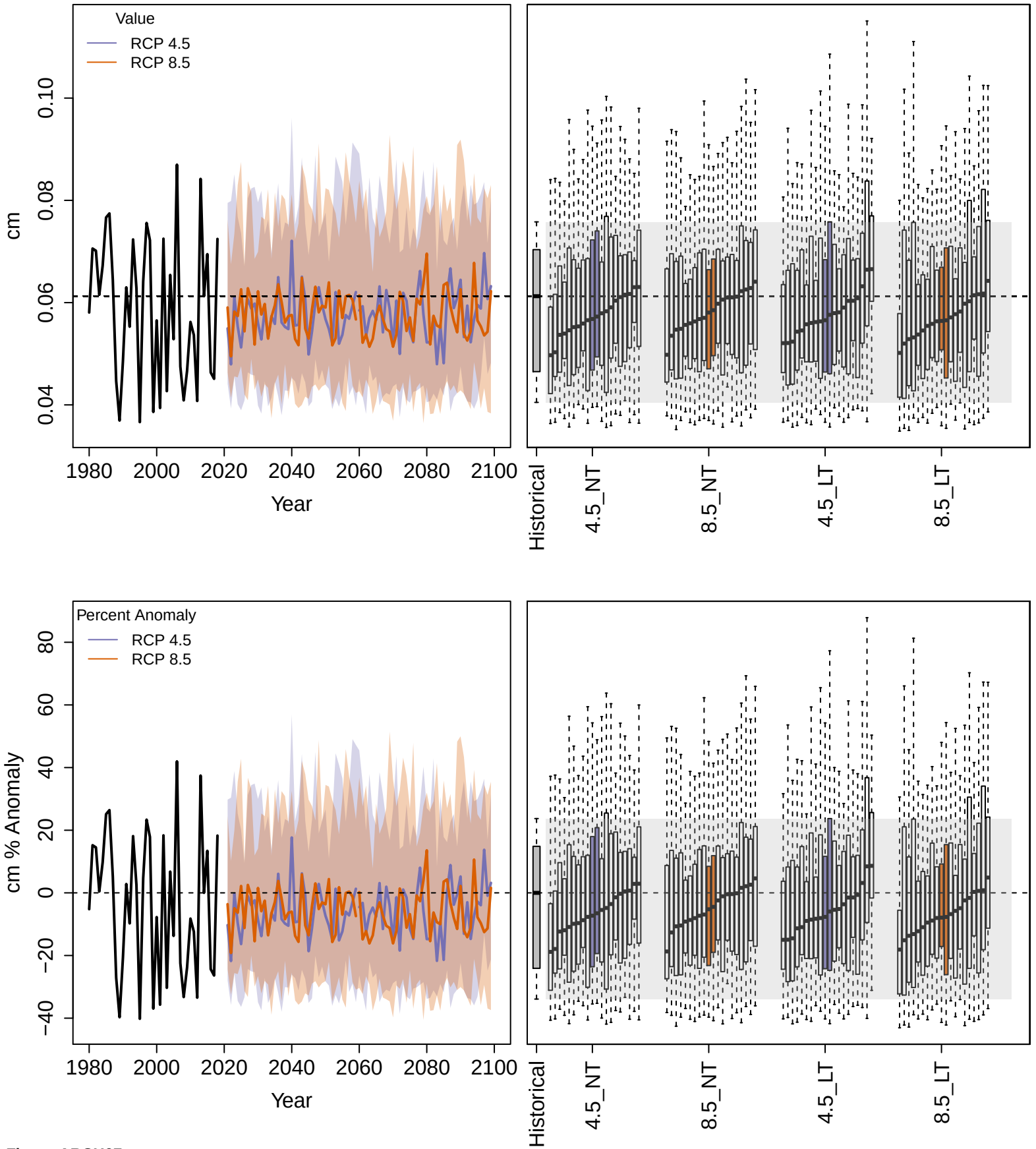


Figure ARCH67:
Past trends and future trajectories of park−wide mean values for Fall soil water content in Arches. Top panels show values, bottom panels show changes from the long−term historical mean. Left: Time series of historical (black) and future projections for RCP 4.5 and 8.5. Shaded areas show spread among climate models. Right: Boxplots of temporal variability over 40−year periods under historical (left box) and individual climate models under two RCPs. Right: Historical time period is 1970−2010; near−term (NT) is 2020−2060; long−term (LT) is 2061−2100.

Arches: Fall soil water content

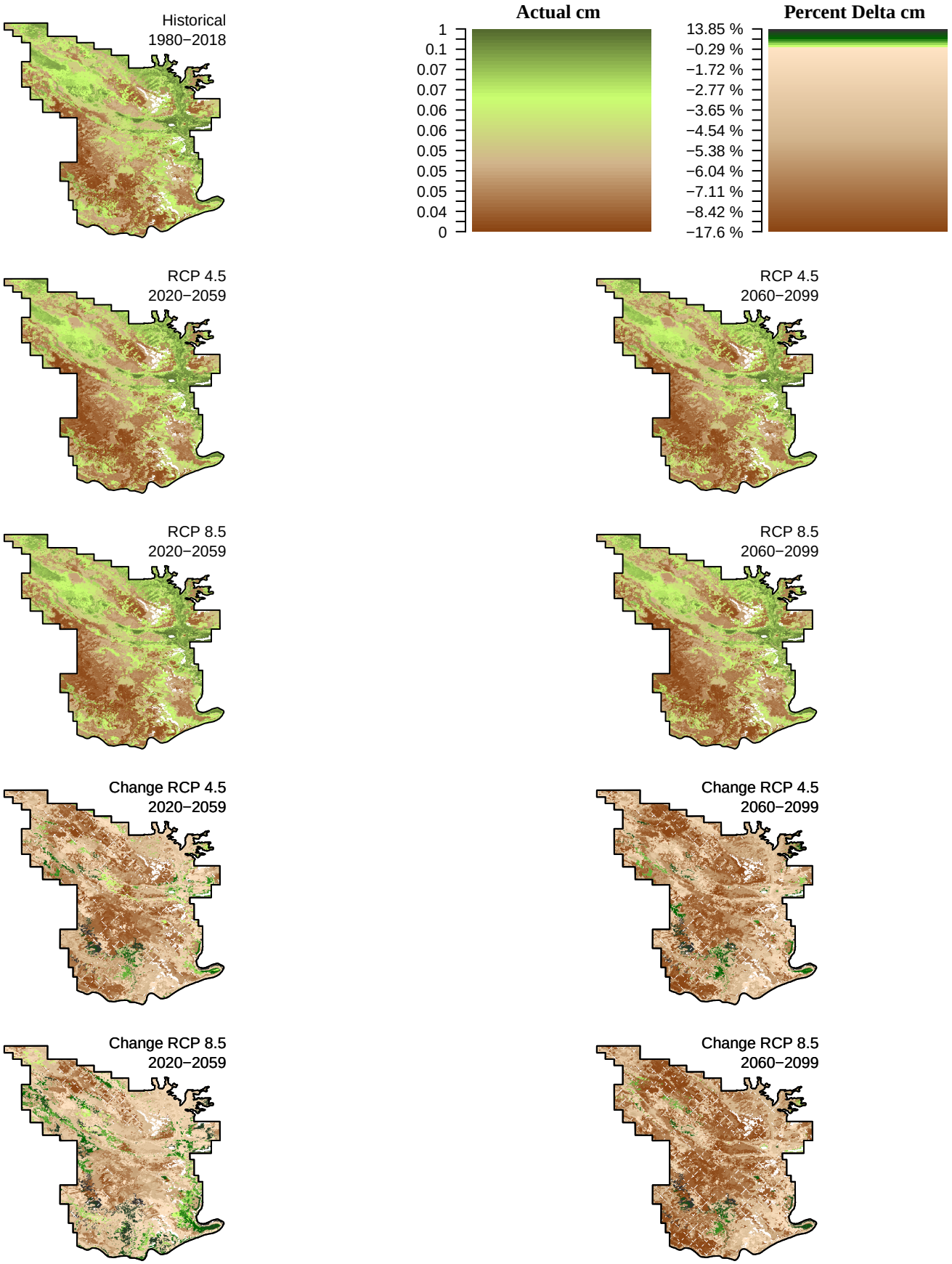


Figure ARCHmap67:
Past trends and future trajectories of park−wide mean values for Fall soil water content in Arches. Topmost panel depicts the historical mean from 1980−2018. Lower four panels show the emission scenarios of RCP 4.5 and RCP 8.5 at near−term and long−term timeframes. Bottom four panels depict the change from the historical mean; cross hatching denotes areas of robust predicitons (90% of models agree in the direction of change).

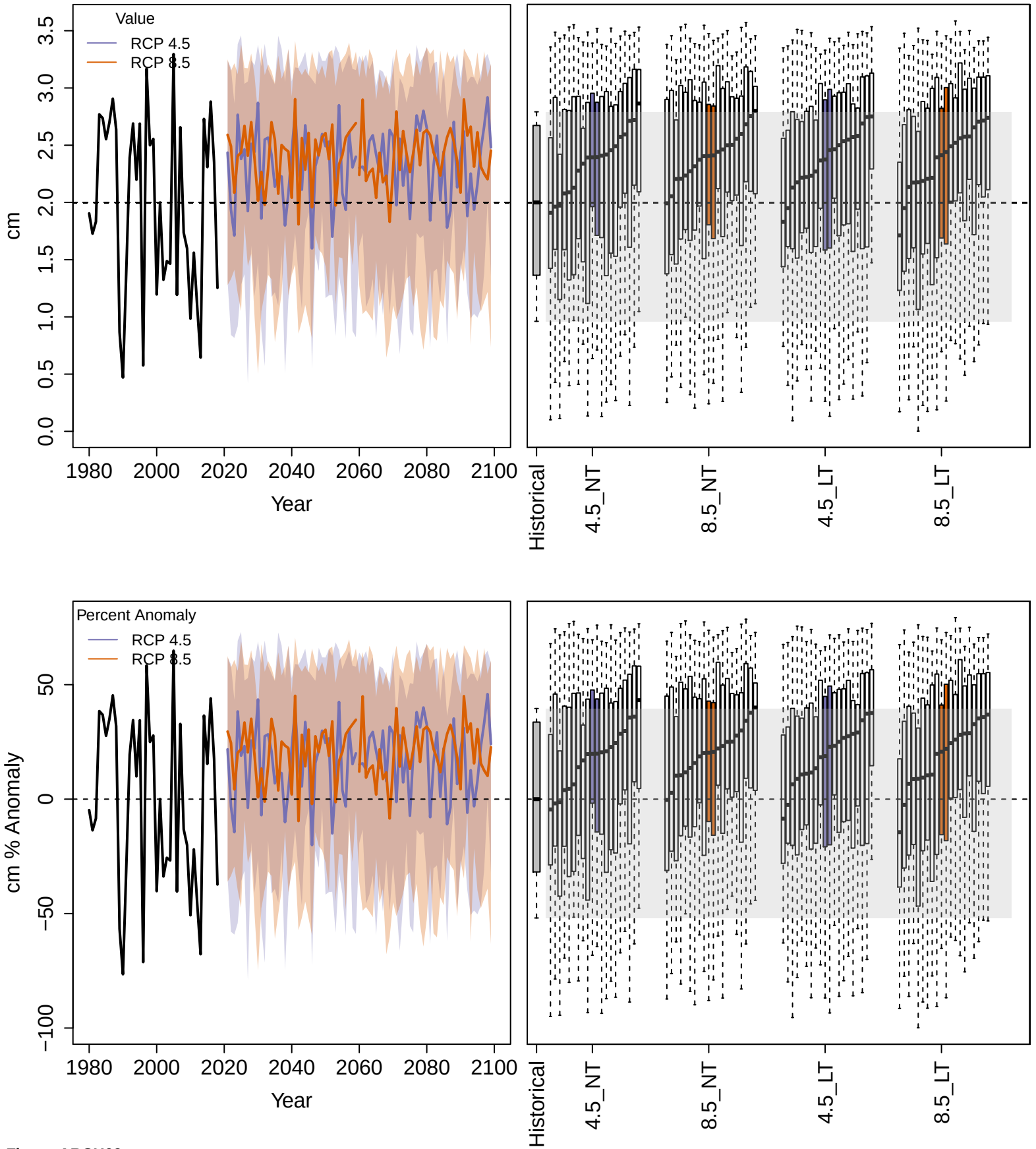


Figure ARCH69:
Past trends and future trajectories of park−wide mean values for Winter available soil moisture: top 50cm in Arches. Top panels show values, bottom panels show changes from the long−term historical mean. Left: Time series of historical (black) and future projections for RCP 4.5 and 8.5. Shaded areas show spread among climate models. Right: Boxplots of temporal variability over 40−year periods under historical (left box) and individual climate models under two RCPs. Right: Historical time period is 1970−2010; near−term (NT) is 2020−2060; long−term (LT) is 2061−2100.

Arches: Winter available soil moisture: top 50cm

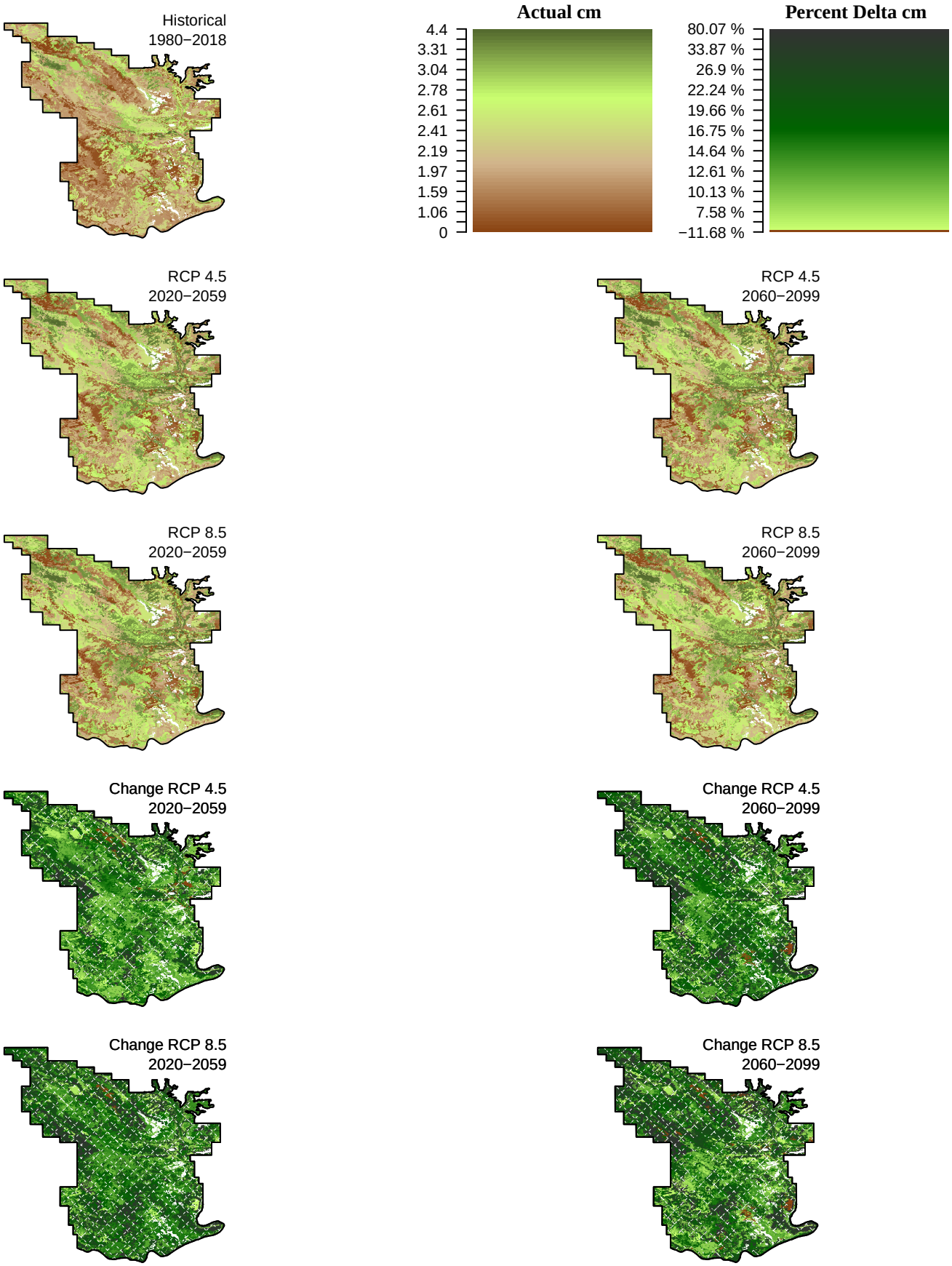


Figure ARCHmap69:
Past trends and future trajectories of park−wide mean values for Winter available soil moisture: top 50cm in Arches. Topmost panel depicts the historical mean from 1980−2018. Lower four panels show the emission scenarios of RCP 4.5 and RCP 8.5 at near−term and long−term timeframes. Bottom four panels depict the change from the historical mean; cross hatching denotes areas of robust predicitons (90% of models agree in the direction of change).

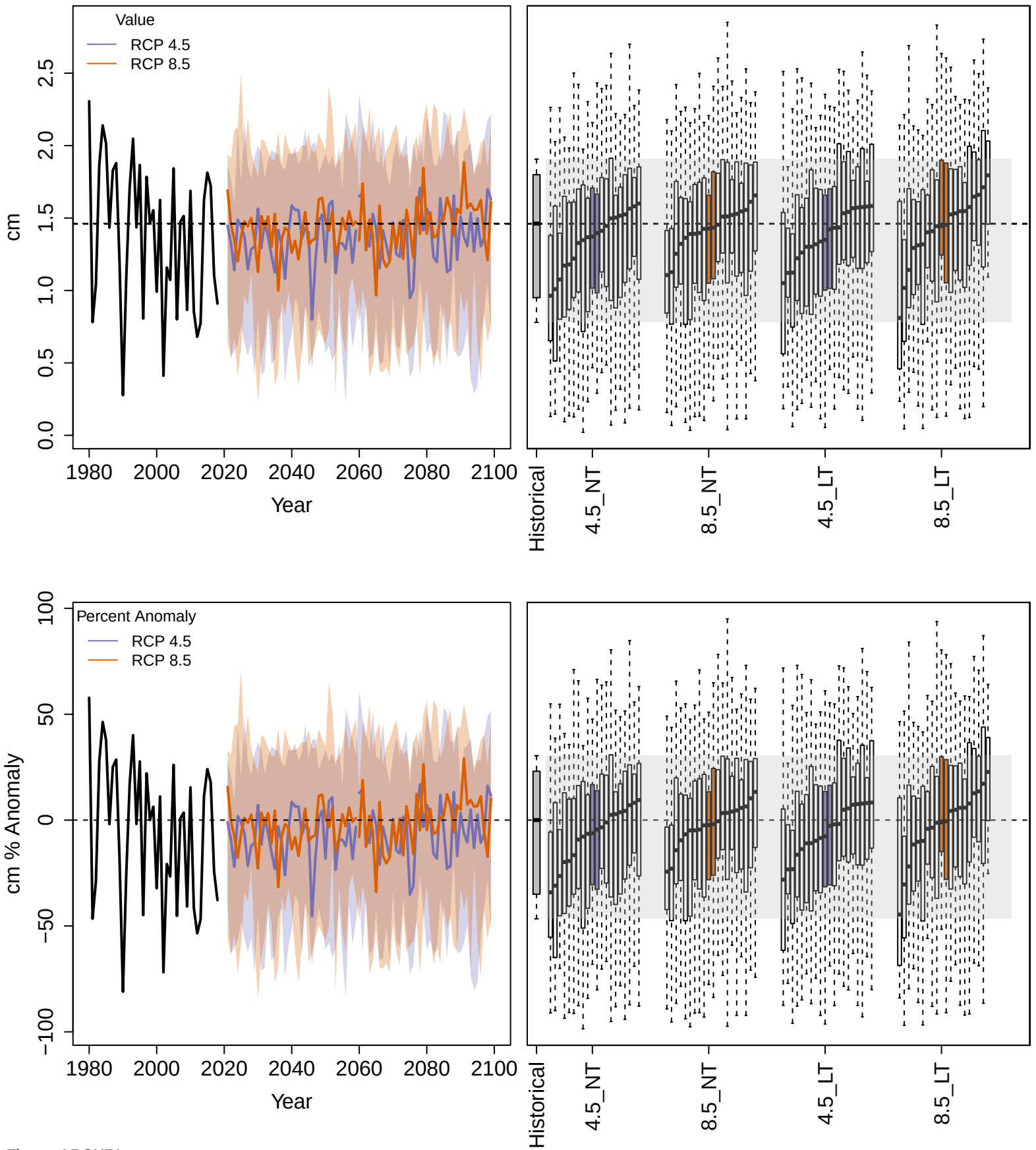


Figure ARCH71:
Past trends and future trajectories of park−wide mean values for Spring available soil moisture: top 50cm in Arches. Top panels show values, bottom panels show changes from the long−term historical mean. Left: Time series of historical (black) and future projections for RCP 4.5 and 8.5. Shaded areas show spread among climate models. Right: Boxplots of temporal variability over 40−year periods under historical (left box) and individual climate models under two RCPs. Right: Historical time period is 1970−2010; near−term (NT) is 2020−2060; long−term (LT) is 2061−2100.

Arches: Spring available soil moisture: top 50cm

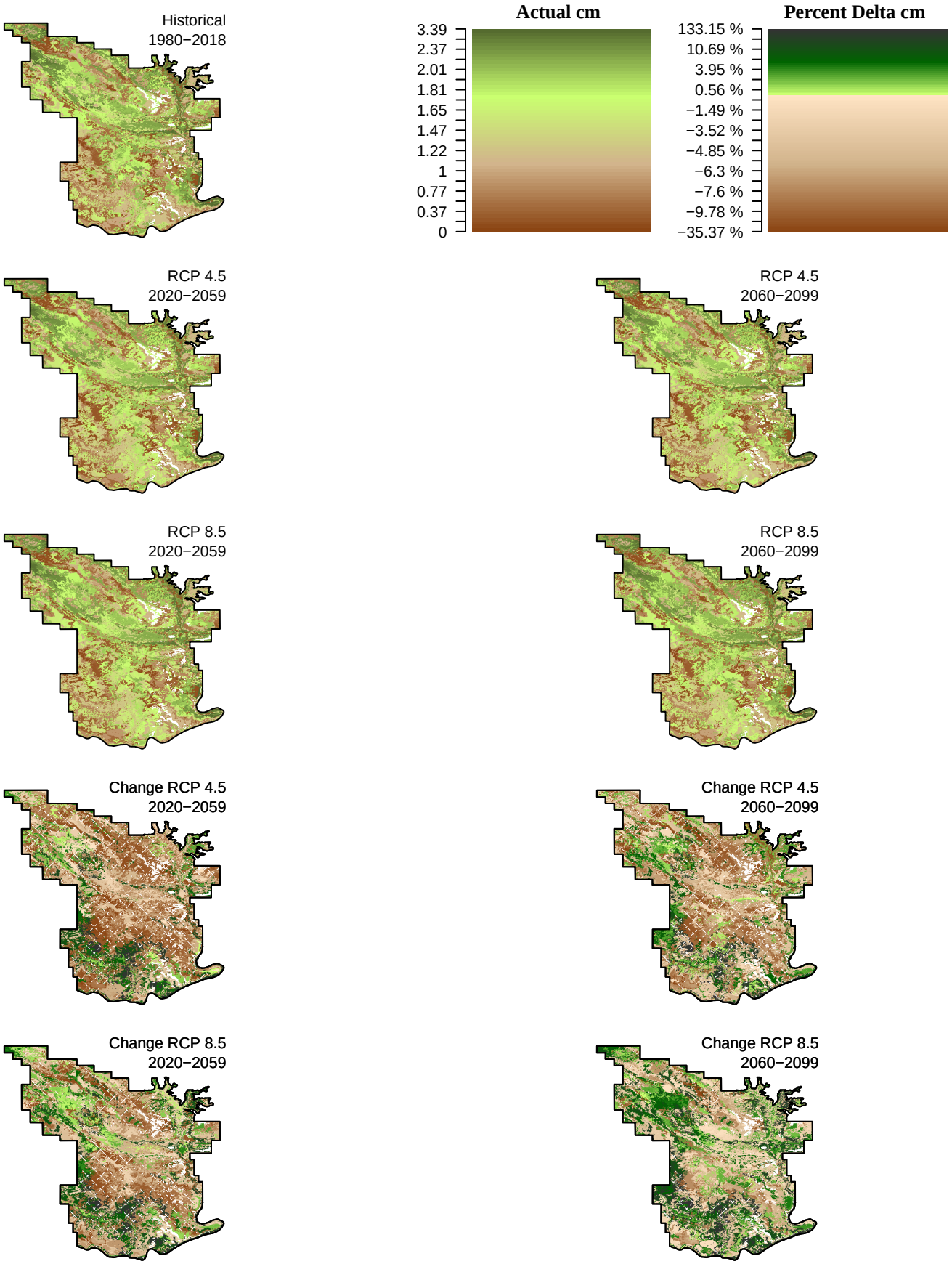


Figure ARCHmap71:
Past trends and future trajectories of park−wide mean values for Spring available soil moisture: top 50cm in Arches. Topmost panel depicts the historical mean from 1980−2018. Lower four panels show the emission scenarios of RCP 4.5 and RCP 8.5 at near−term and long−term timeframes. Bottom four panels depict the change from the historical mean; cross hatching denotes areas of robust predicitons (90% of models agree in the direction of change).

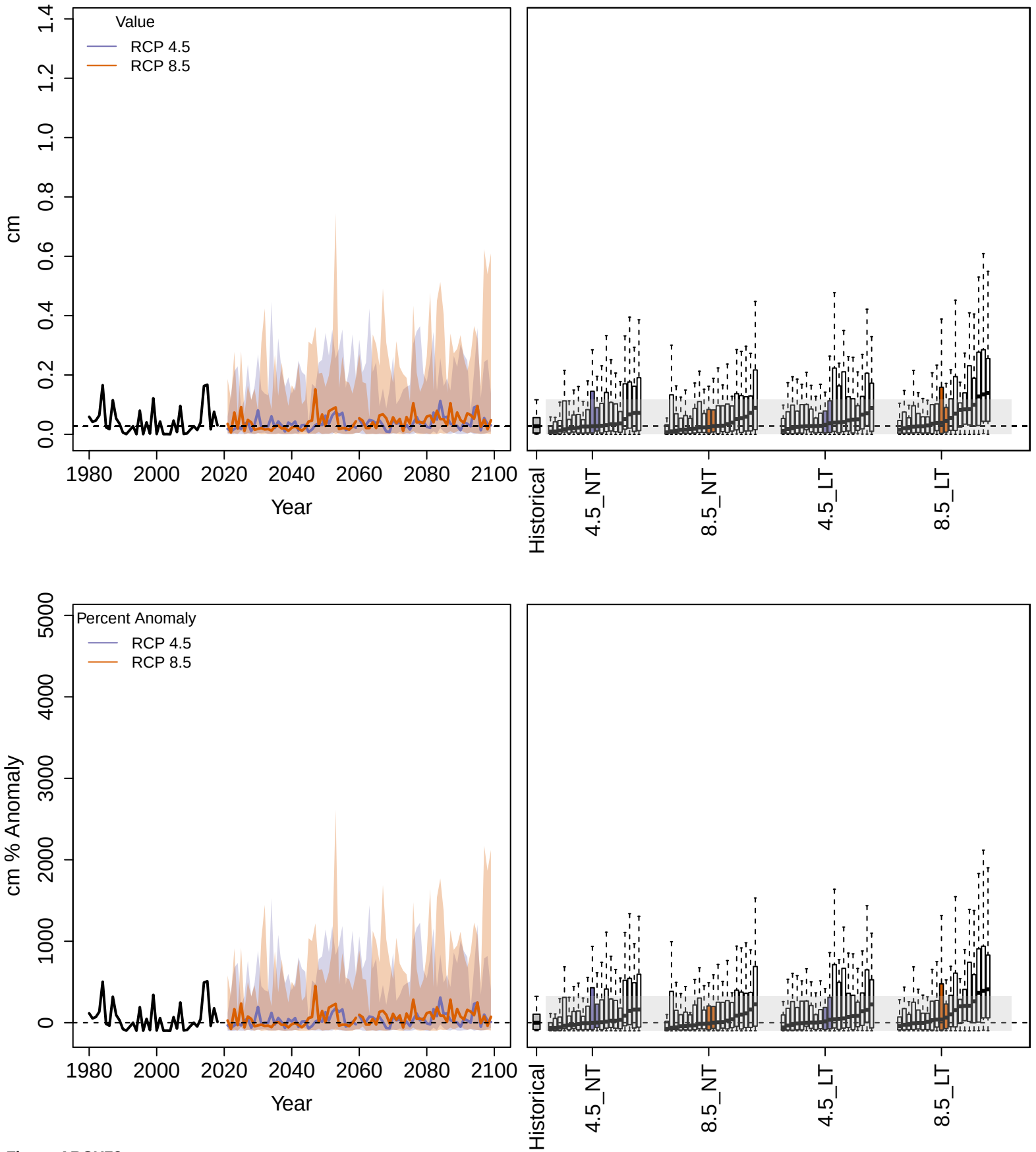


Figure ARCH73:
Past trends and future trajectories of park−wide mean values for Summer available soil moisture: top 50cm in Arches. Top panels show values, bottom panels show changes from the long−term historical mean. Left: Time series of historical (black) and future projections for RCP 4.5 and 8.5. Shaded areas show spread among climate models. Right: Boxplots of temporal variability over 40−year periods under historical (left box) and individual climate models under two RCPs. Right: Historical time period is 1970−2010; near−term (NT) is 2020−2060; long−term (LT) is 2061−2100.

Arches: Summer available soil moisture: top 50cm

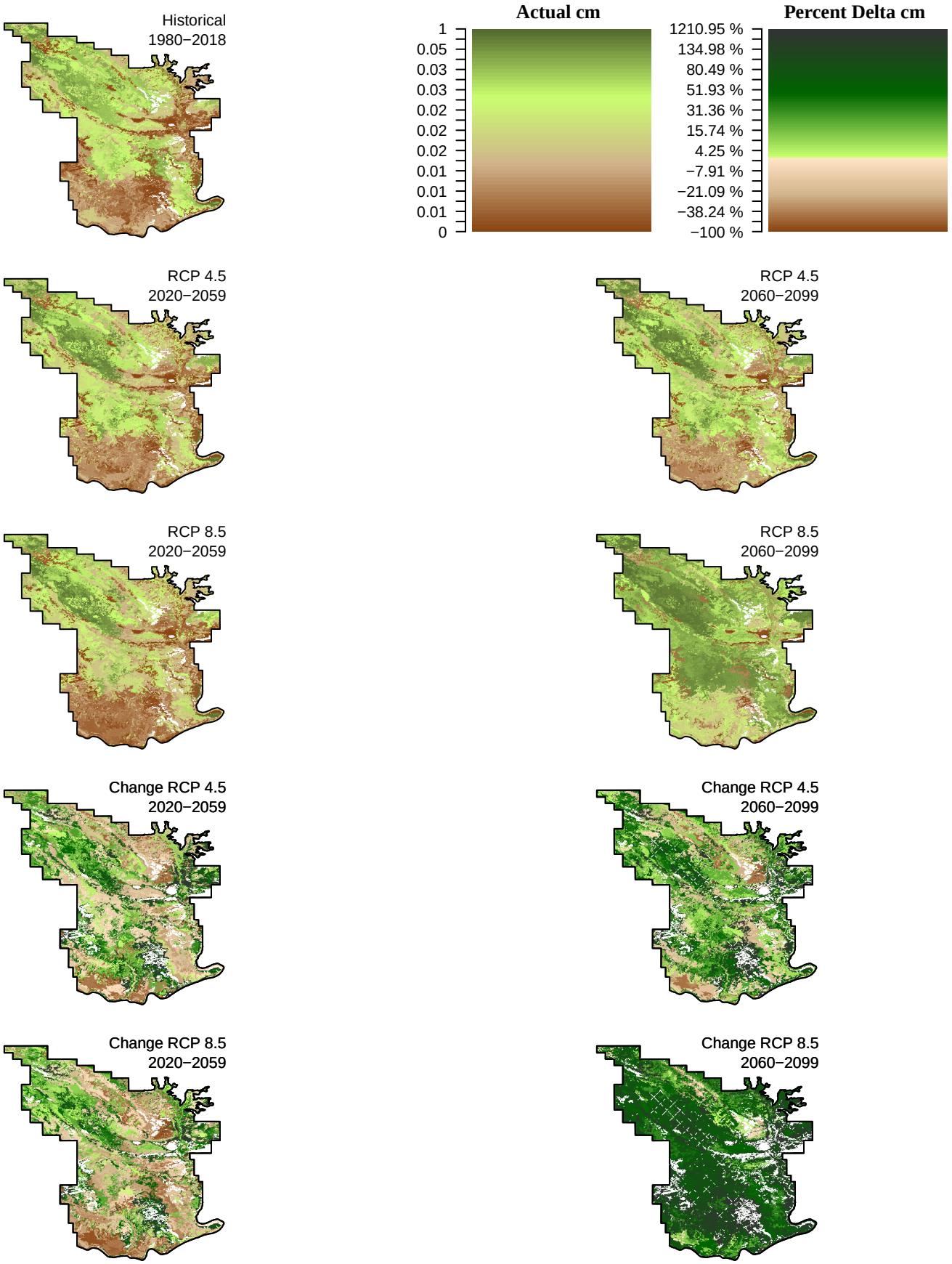


Figure ARCHmap73:
Past trends and future trajectories of park−wide mean values for Summer available soil moisture: top 50cm in Arches. Topmost panel depicts the historical mean from 1980−2018. Lower four panels show the emission scenarios of RCP 4.5 and RCP 8.5 at near−term and long−term timeframes. Bottom four panels depict the change from the historical mean; cross hatching denotes areas of robust predicitons (90% of models agree in the direction of change).

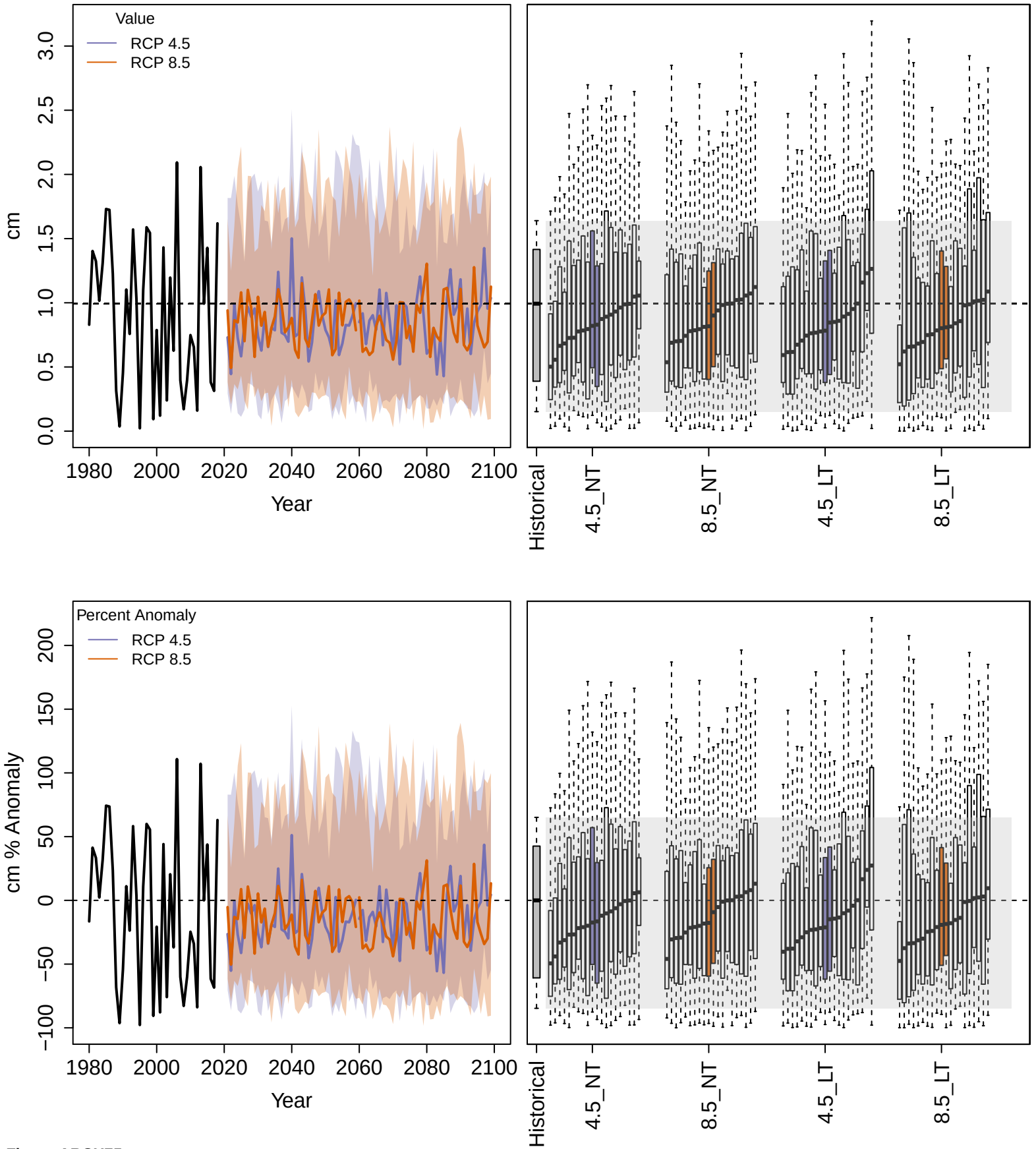


Figure ARCH75:
Past trends and future trajectories of park−wide mean values for Fall available soil moisture: top 50cm in Arches. Top panels show values, bottom panels show changes from the long−term historical mean. Left: Time series of historical (black) and future projections for RCP 4.5 and 8.5. Shaded areas show spread among climate models. Right: Boxplots of temporal variability over 40−year periods under historical (left box) and individual climate models under two RCPs. Right: Historical time period is 1970−2010; near−term (NT) is 2020−2060; long−term (LT) is 2061−2100.

Arches: Fall available soil moisture: top 50cm

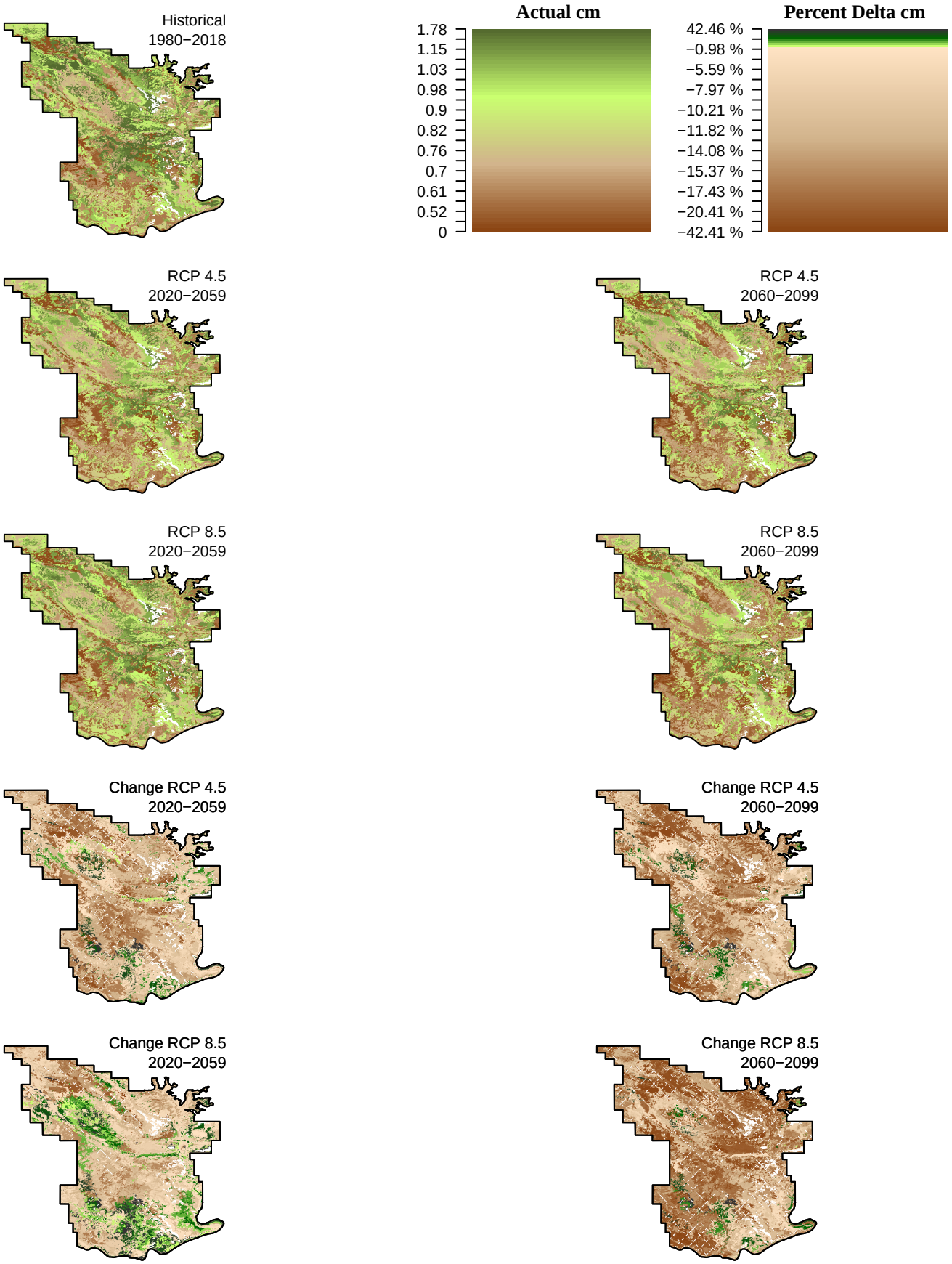


Figure ARCHmap75:
Past trends and future trajectories of park−wide mean values for Fall available soil moisture: top 50cm in Arches. Topmost panel depicts the historical mean from 1980−2018. Lower four panels show the emission scenarios of RCP 4.5 and RCP 8.5 at near−term and long−term timeframes. Bottom four panels depict the change from the historical mean; cross hatching denotes areas of robust predicitons (90% of models agree in the direction of change).

Arches: Winter available soil moisture

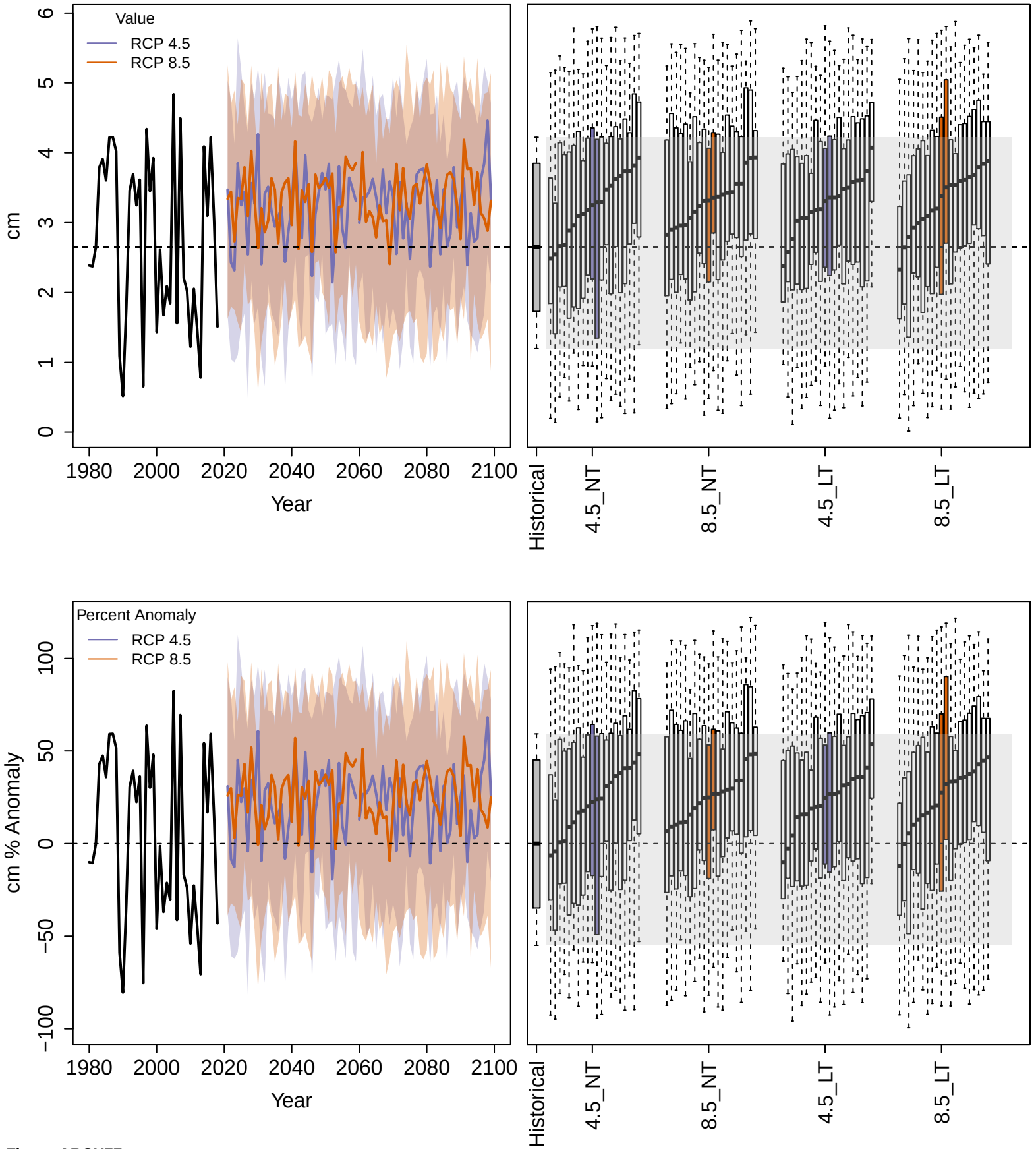


Figure ARCH77:
Past trends and future trajectories of park−wide mean values for Winter available soil moisture in Arches. Top panels show values, bottom panels show changes from the long−term historical mean. Left: Time series of historical (black) and future projections for RCP 4.5 and 8.5. Shaded areas show spread among climate models. Right: Boxplots of temporal variability over 40−year periods under historical (left box) and individual climate models under two RCPs. Right: Historical time period is 1970−2010; near−term (NT) is 2020−2060; long−term (LT) is 2061−2100.

Arches: Winter available soil moisture

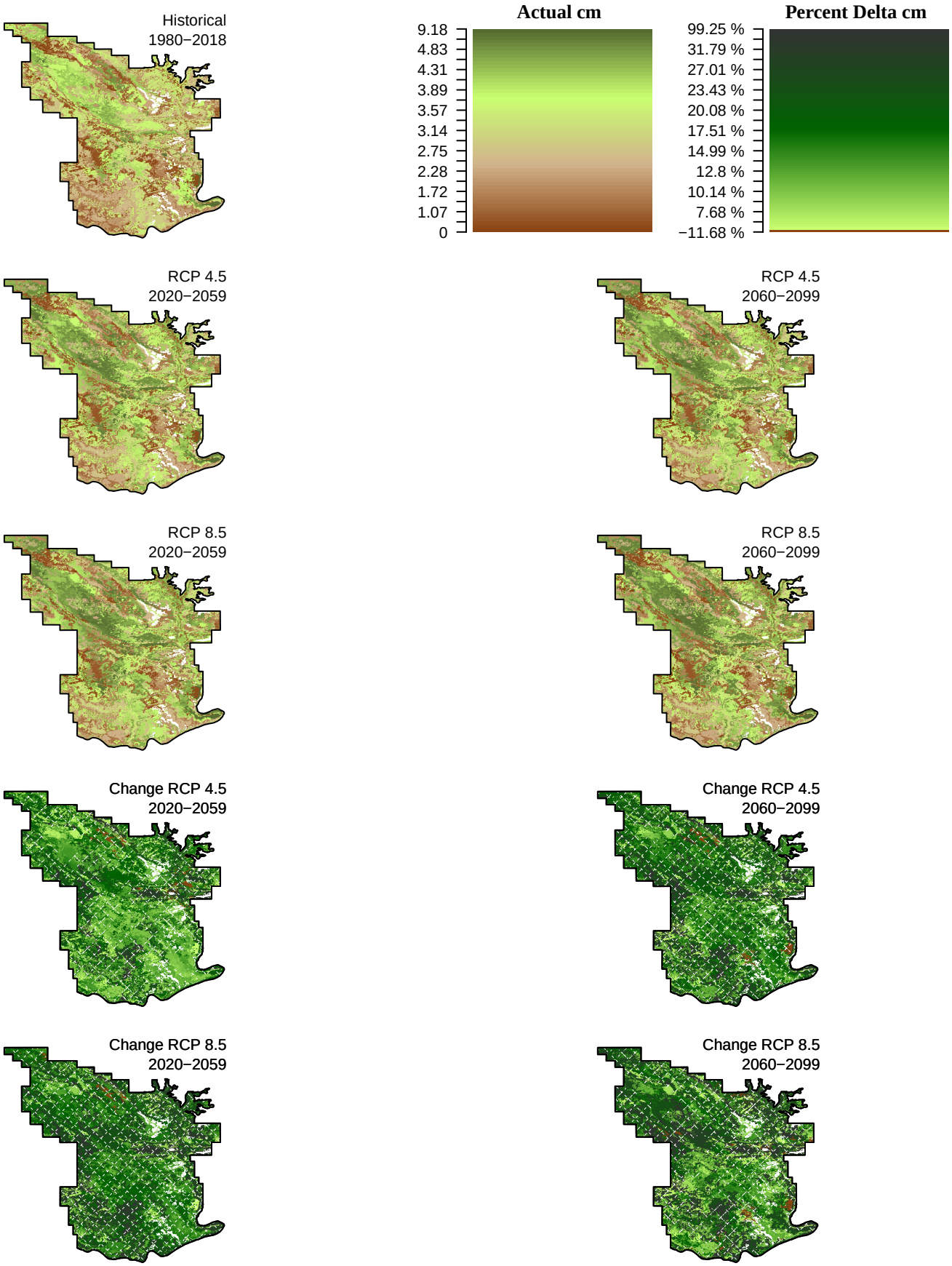


Figure ARCHmap77:
Past trends and future trajectories of park−wide mean values for Winter available soil moisture in Arches. Topmost panel depicts the historical mean from 1980−2018. Lower four panels show the emission scenarios of RCP 4.5 and RCP 8.5 at near−term and long−term timeframes. Bottom four panels depict the change from the historical mean; cross hatching denotes areas of robust predicitons (90% of models agree in the direction of change).

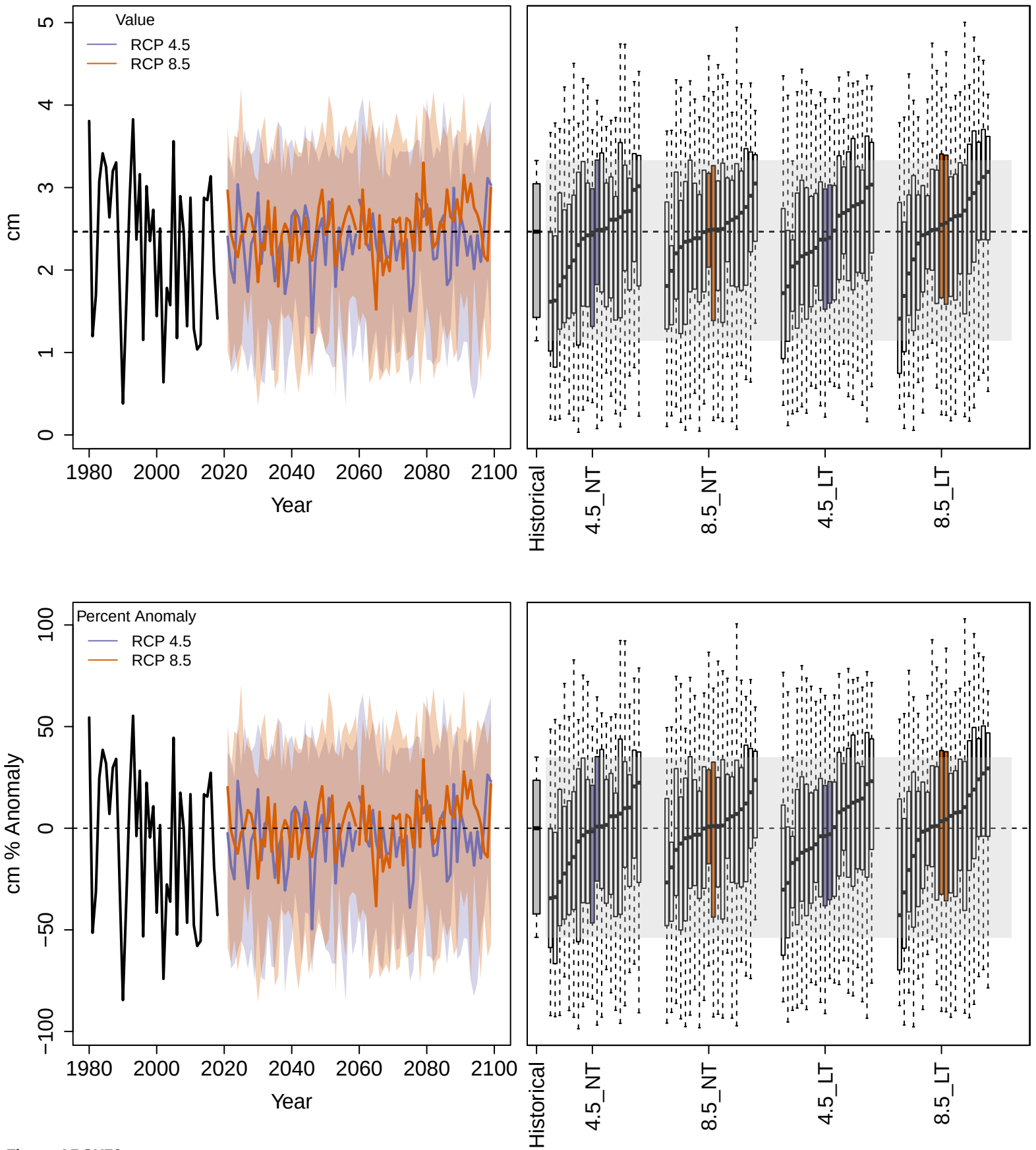


Figure ARCH79:
Past trends and future trajectories of park−wide mean values for Spring available soil moisture in Arches. Top panels show values, bottom panels show changes from the long−term historical mean. Left: Time series of historical (black) and future projections for RCP 4.5 and 8.5. Shaded areas show spread among climate models. Right: Boxplots of temporal variability over 40−year periods under historical (left box) and individual climate models under two RCPs. Right: Historical time period is 1970−2010; near−term (NT) is 2020−2060; long−term (LT) is 2061−2100.

Arches: Spring available soil moisture

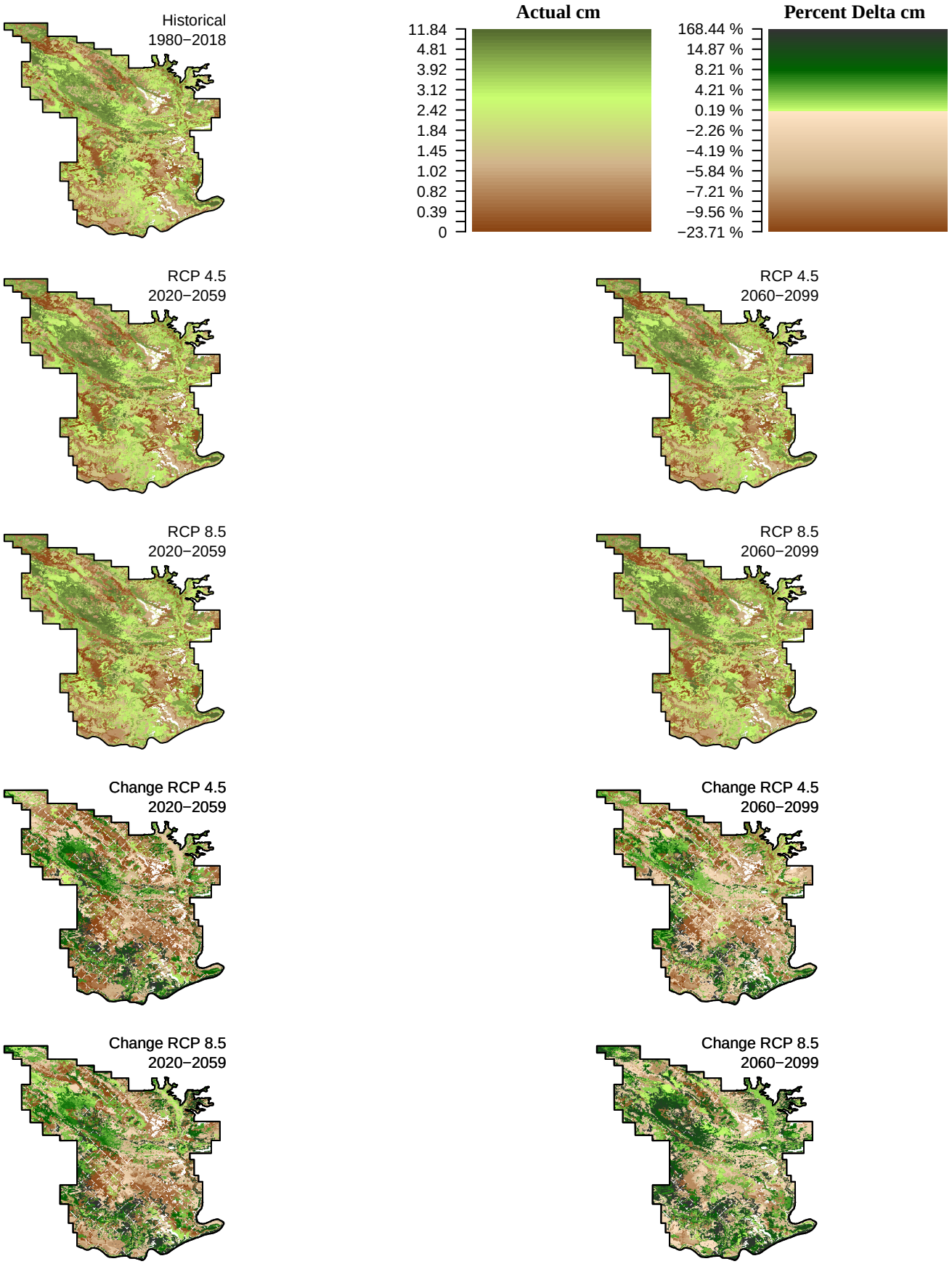


Figure ARCHmap79:
Past trends and future trajectories of park−wide mean values for Spring available soil moisture in Arches. Topmost panel depicts the historical mean from 1980−2018. Lower four panels show the emission scenarios of RCP 4.5 and RCP 8.5 at near−term and long−term timeframes. Bottom four panels depict the change from the historical mean; cross hatching denotes areas of robust predicitons (90% of models agree in the direction of change).

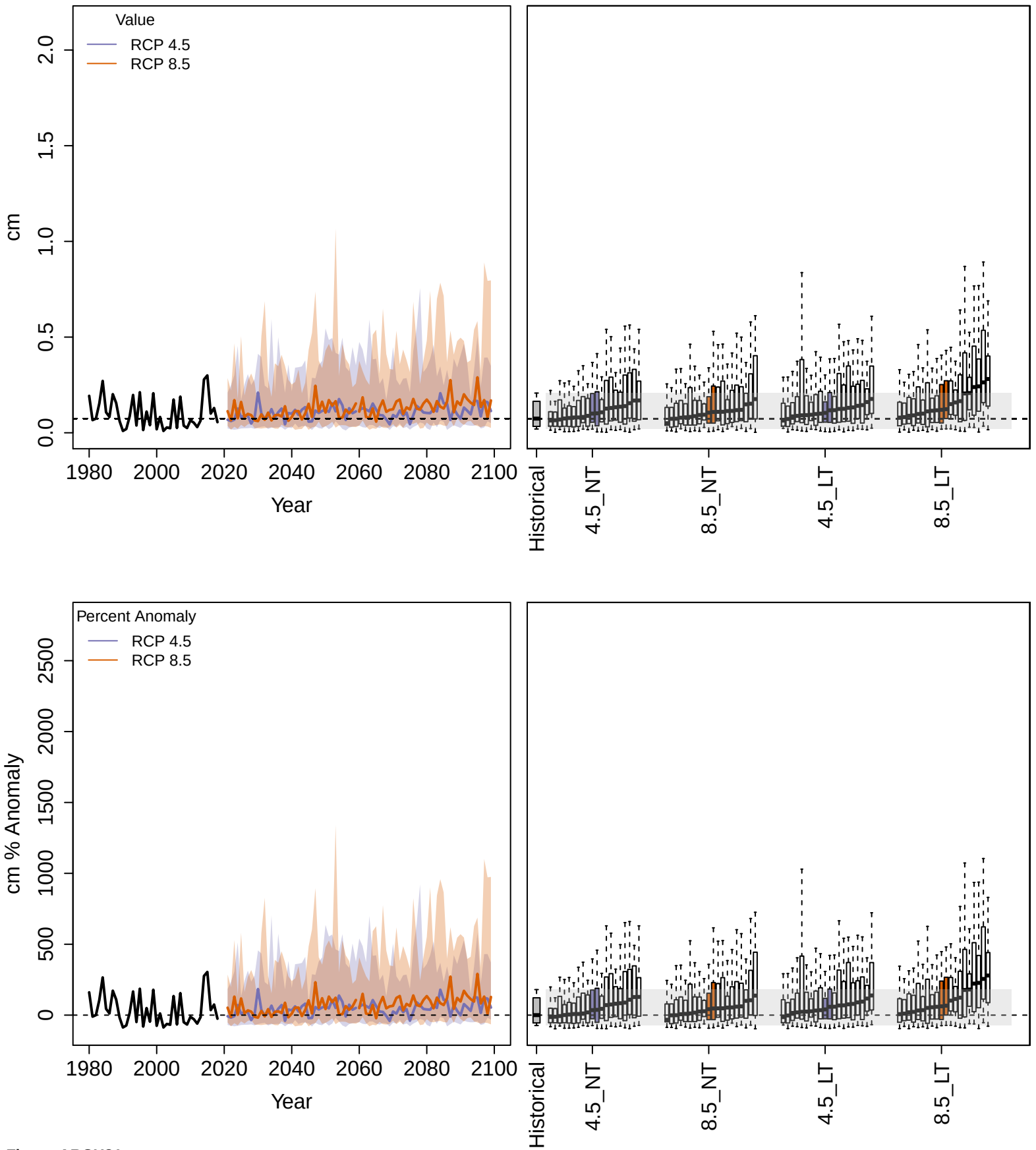


Figure ARCH81:
Past trends and future trajectories of park−wide mean values for Summer available soil moisture in Arches. Top panels show values, bottom panels show changes from the long−term historical mean. Left: Time series of historical (black) and future projections for RCP 4.5 and 8.5. Shaded areas show spread among climate models. Right: Boxplots of temporal variability over 40−year periods under historical (left box) and individual climate models under two RCPs. Right: Historical time period is 1970−2010; near−term (NT) is 2020−2060; long−term (LT) is 2061−2100.

Arches: Summer available soil moisture

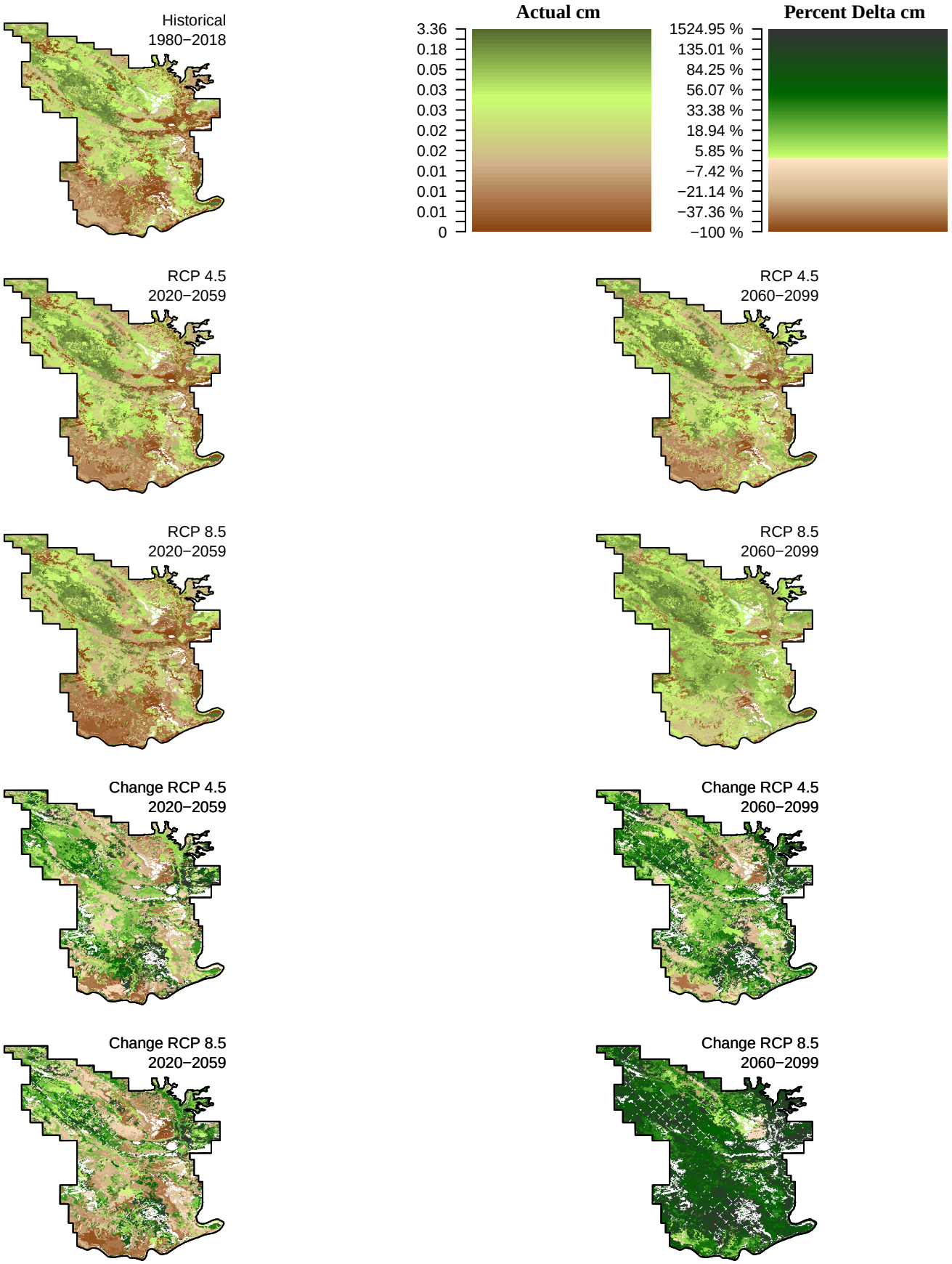


Figure ARCHmap81:
Past trends and future trajectories of park−wide mean values for Summer available soil moisture in Arches. Topmost panel depicts the historical mean from 1980−2018. Lower four panels show the emission scenarios of RCP 4.5 and RCP 8.5 at near−term and long−term timeframes. Bottom four panels depict the change from the historical mean; cross hatching denotes areas of robust predicitons (90% of models agree in the direction of change).

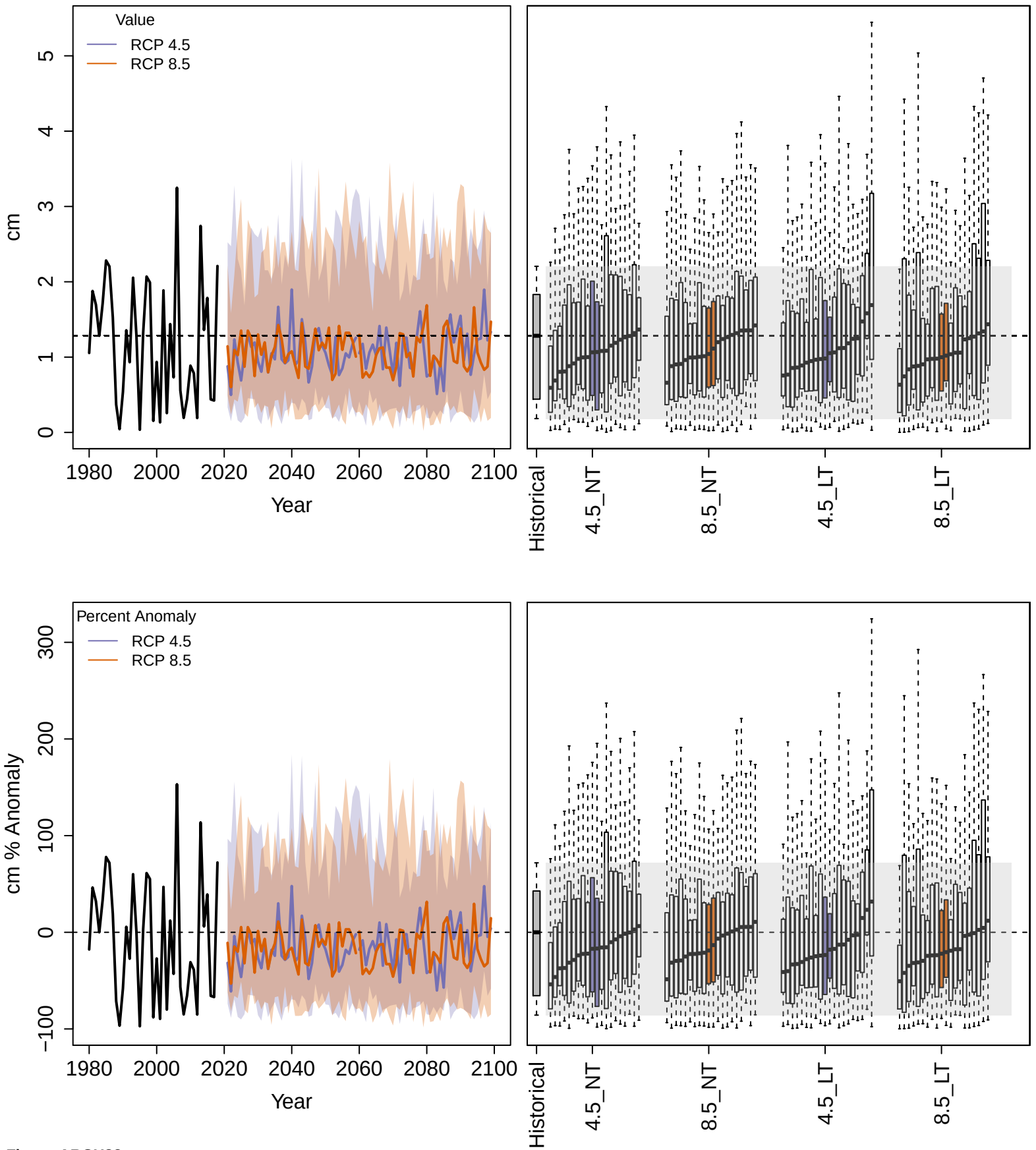


Figure ARCH83:
Past trends and future trajectories of park−wide mean values for Fall available soil moisture in Arches. Top panels show values, bottom panels show changes from the long−term historical mean. Left: Time series of historical (black) and future projections for RCP 4.5 and 8.5. Shaded areas show spread among climate models. Right: Boxplots of temporal variability over 40−year periods under historical (left box) and individual climate models under two RCPs. Right: Historical time period is 1970−2010; near−term (NT) is 2020−2060; long−term (LT) is 2061−2100.

Arches: Fall available soil moisture

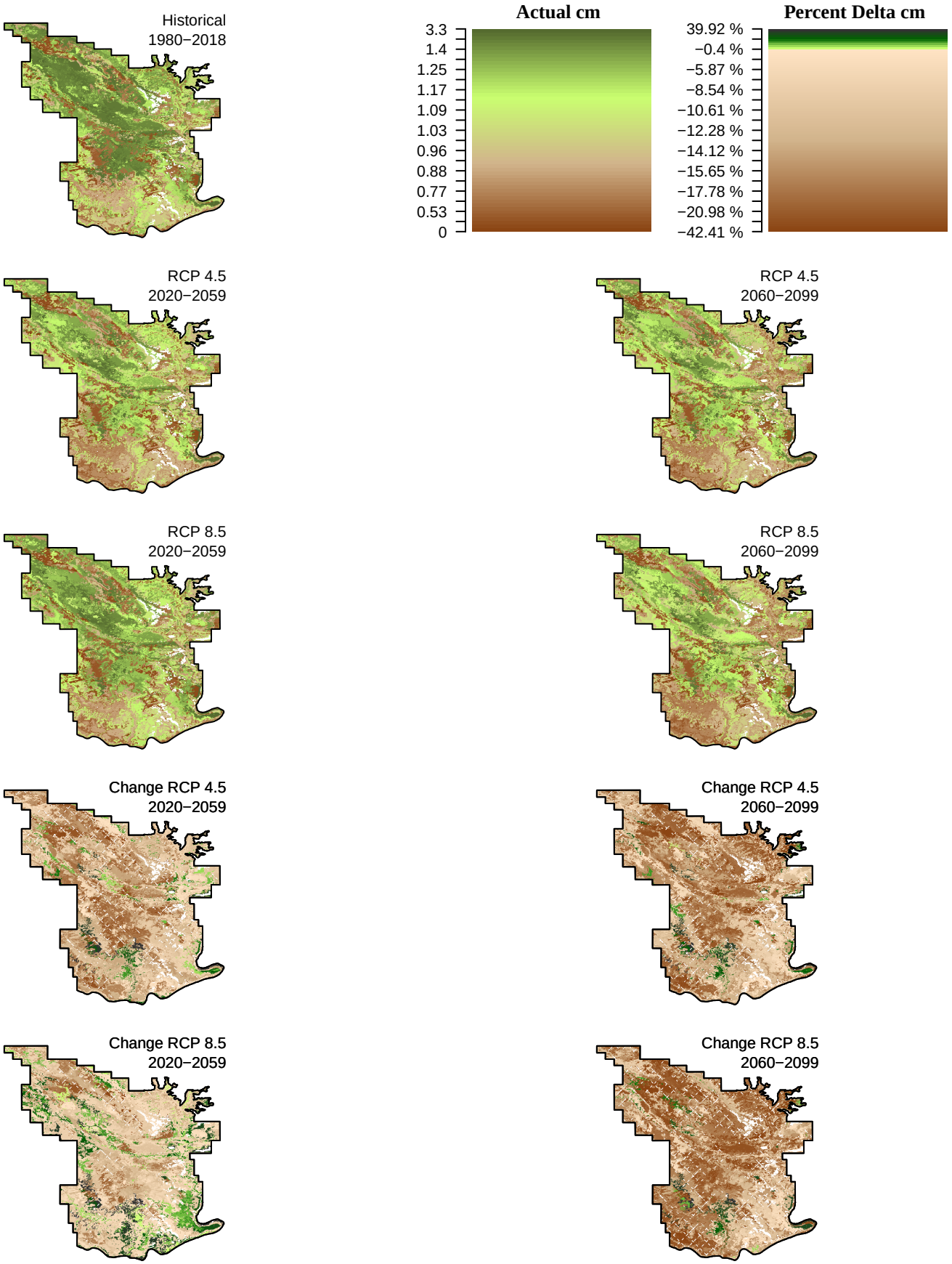


Figure ARCHmap83:
Past trends and future trajectories of park−wide mean values for Fall available soil moisture in Arches. Topmost panel depicts the historical mean from 1980−2018. Lower four panels show the emission scenarios of RCP 4.5 and RCP 8.5 at near−term and long−term timeframes. Bottom four panels depict the change from the historical mean; cross hatching denotes areas of robust predicitons (90% of models agree in the direction of change).

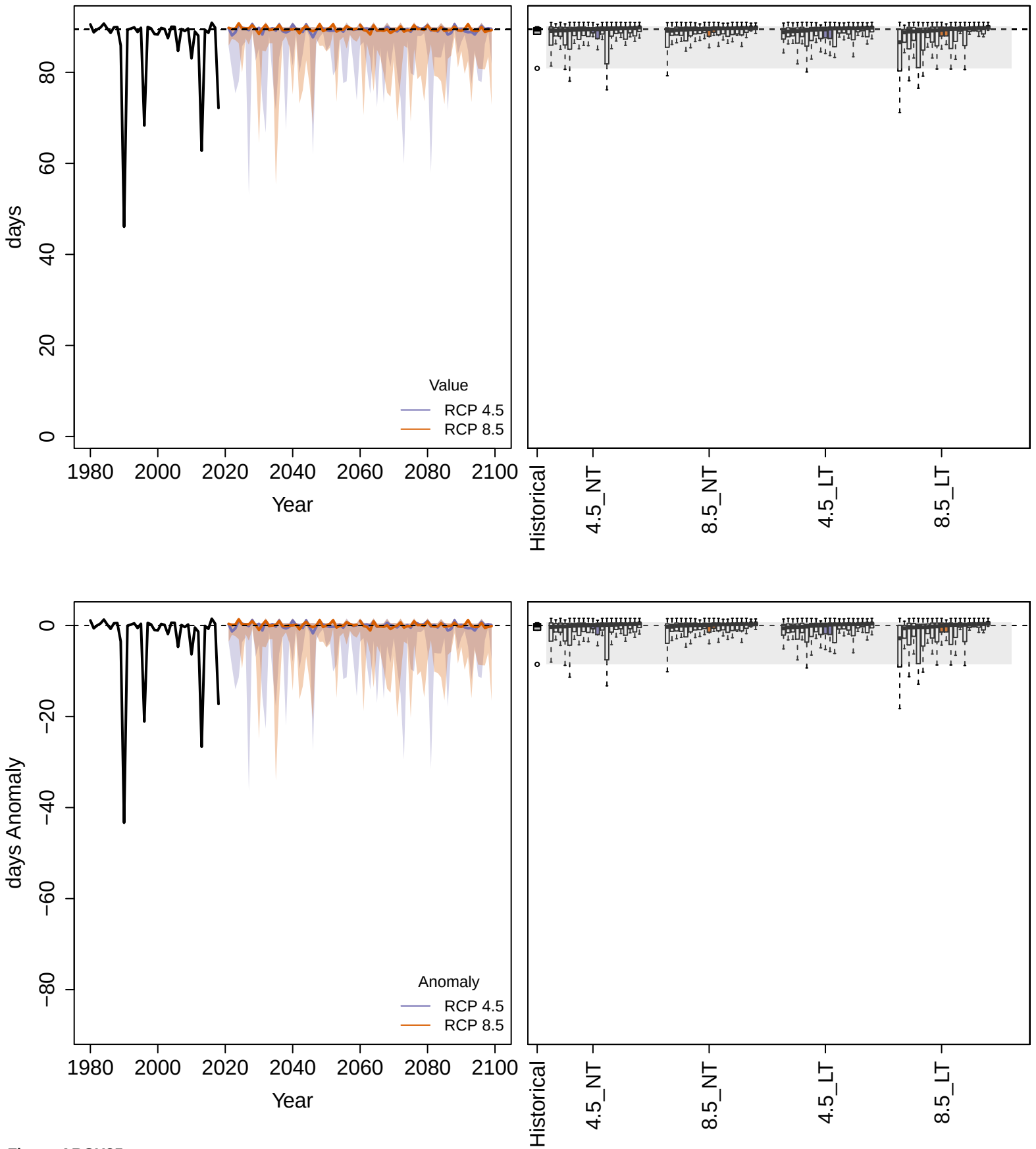


Figure ARCH85:
Past trends and future trajectories of park−wide mean values for Winter wet soil days in Arches. Top panels show values, bottom panels show changes from the long−term historical mean. Left: Time series of historical (black) and future projections for RCP 4.5 and 8.5. Shaded areas show spread among climate models. Right: Boxplots of temporal variability over 40−year periods under historical (left box) and individual climate models under two RCPs. Right: Historical time period is 1970−2010; near−term (NT) is 2020−2060; long−term (LT) is 2061−2100.

Arches: Winter wet soil days

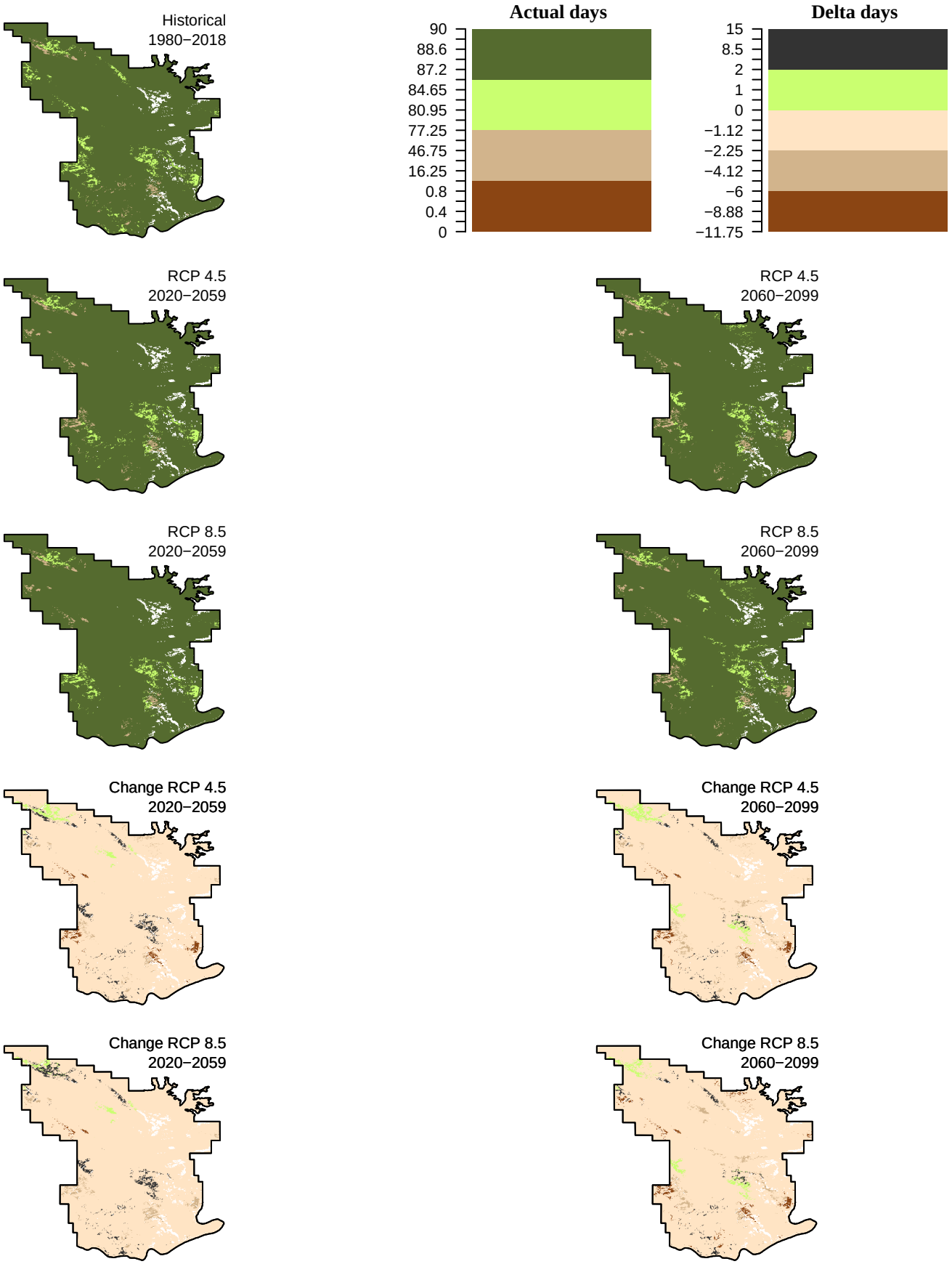


Figure ARCHmap85:
Past trends and future trajectories of park−wide mean values for Winter wet soil days in Arches. Topmost panel depicts the historical mean from 1980−2018. Lower four panels show the emission scenarios of RCP 4.5 and RCP 8.5 at near−term and long−term timeframes. Bottom four panels depict the change from the historical mean; cross hatching denotes areas of robust predicitons (90% of models agree in the direction of change).

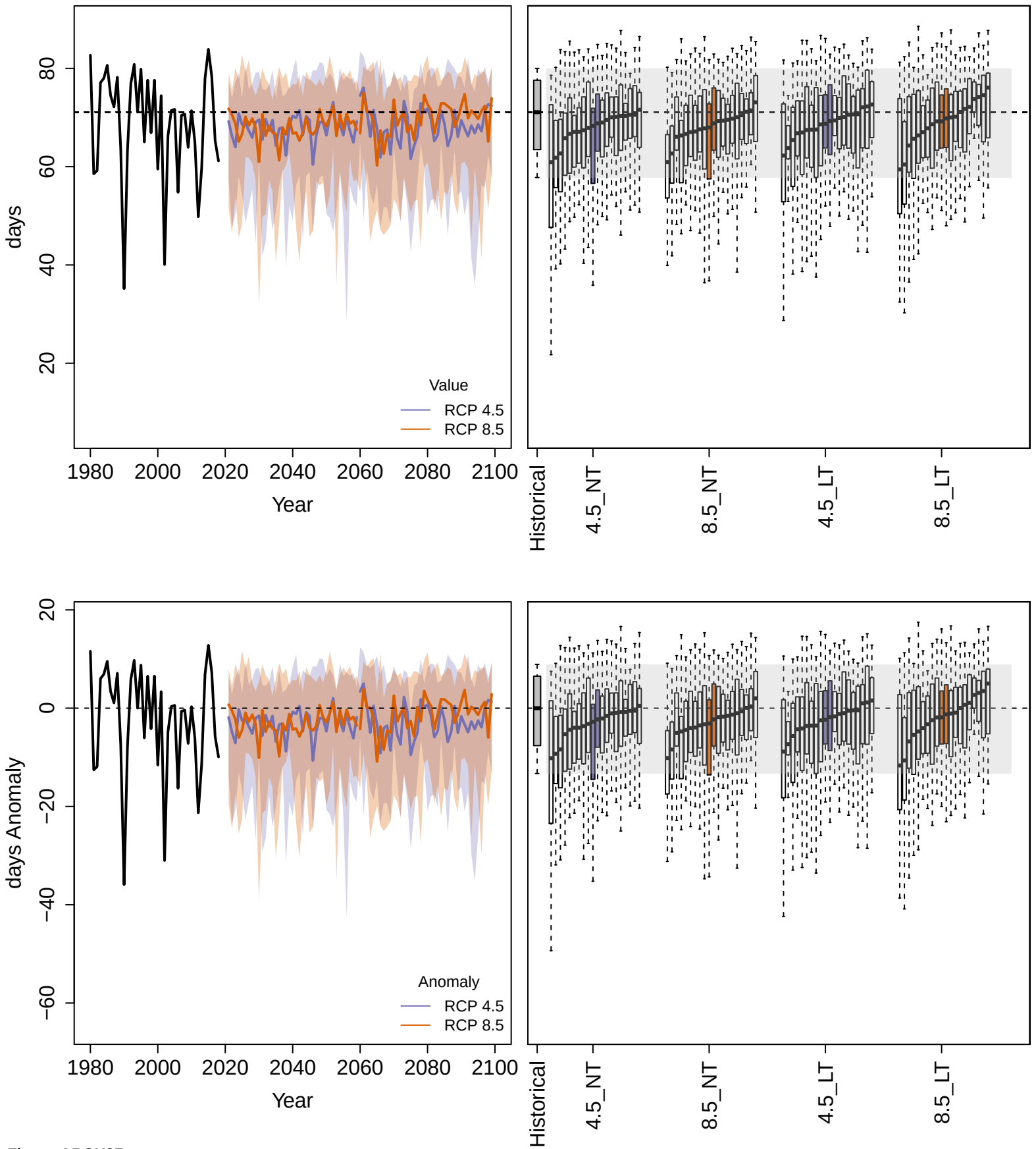


Figure ARCH87:
Past trends and future trajectories of park−wide mean values for Spring wet soil days in Arches. Top panels show values, bottom panels show changes from the long−term historical mean. Left: Time series of historical (black) and future projections for RCP 4.5 and 8.5. Shaded areas show spread among climate models. Right: Boxplots of temporal variability over 40−year periods under historical (left box) and individual climate models under two RCPs. Right: Historical time period is 1970−2010; near−term (NT) is 2020−2060; long−term (LT) is 2061−2100.

Arches: Spring wet soil days

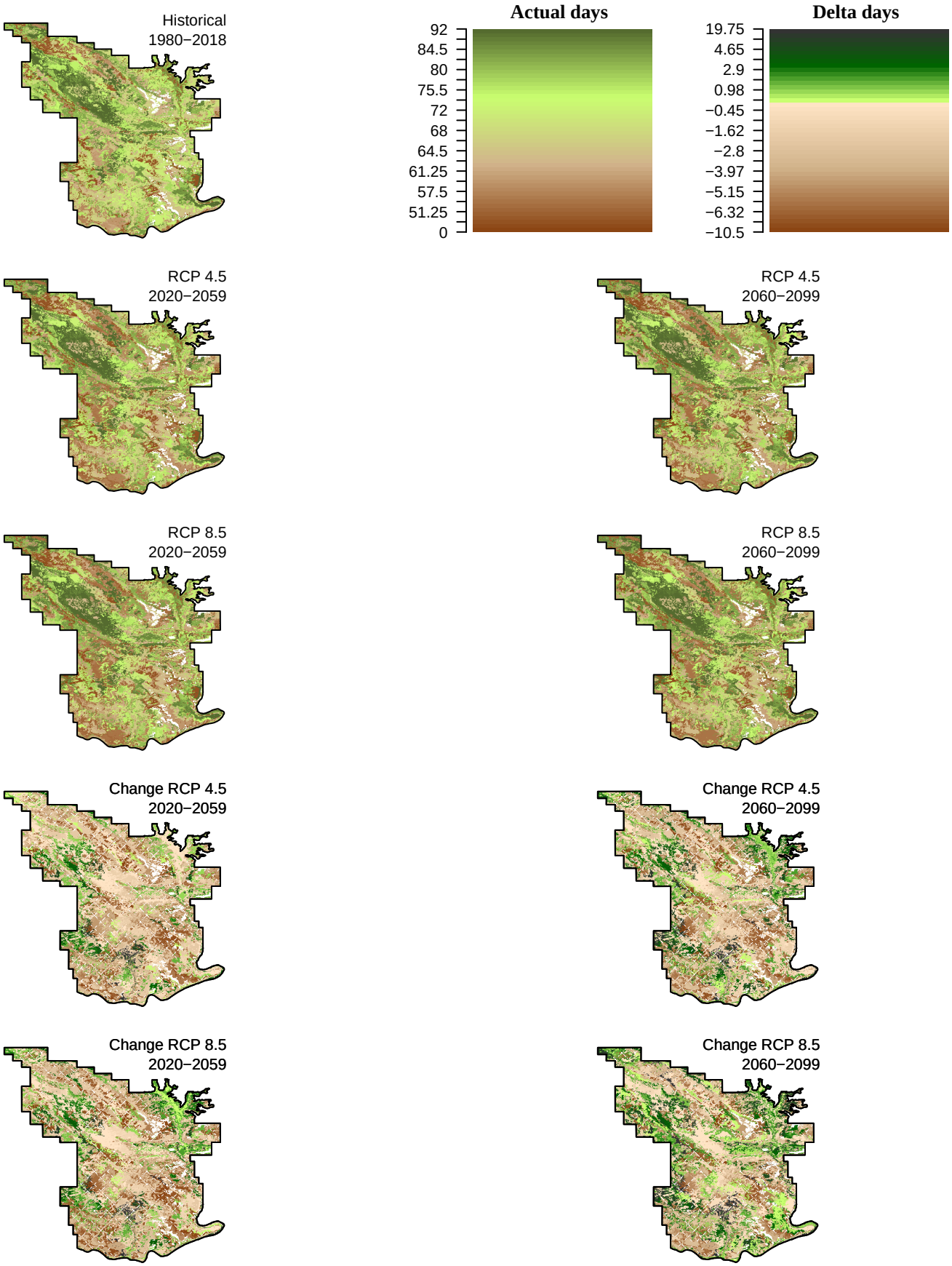


Figure ARCHmap87:
Past trends and future trajectories of park−wide mean values for Spring wet soil days in Arches. Topmost panel depicts the historical mean from 1980−2018. Lower four panels show the emission scenarios of RCP 4.5 and RCP 8.5 at near−term and long−term timeframes. Bottom four panels depict the change from the historical mean; cross hatching denotes areas of robust predicitons (90% of models agree in the direction of change).

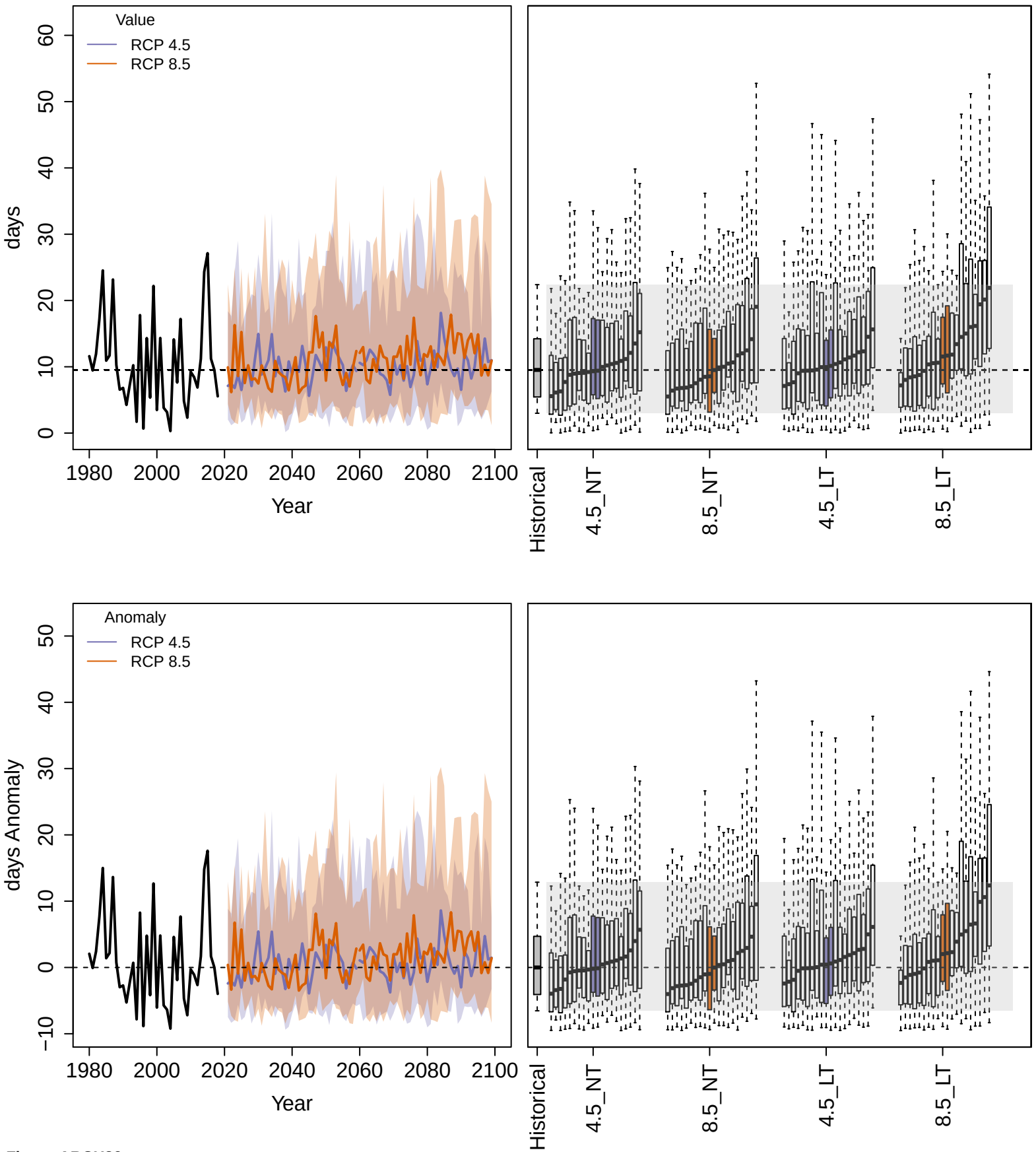


Figure ARCH89:
Past trends and future trajectories of park−wide mean values for Summer wet soil days in Arches. Top panels show values, bottom panels show changes from the long−term historical mean. Left: Time series of historical (black) and future projections for RCP 4.5 and 8.5. Shaded areas show spread among climate models. Right: Boxplots of temporal variability over 40−year periods under historical (left box) and individual climate models under two RCPs. Right: Historical time period is 1970−2010; near−term (NT) is 2020−2060; long−term (LT) is 2061−2100.

Arches: Summer wet soil days

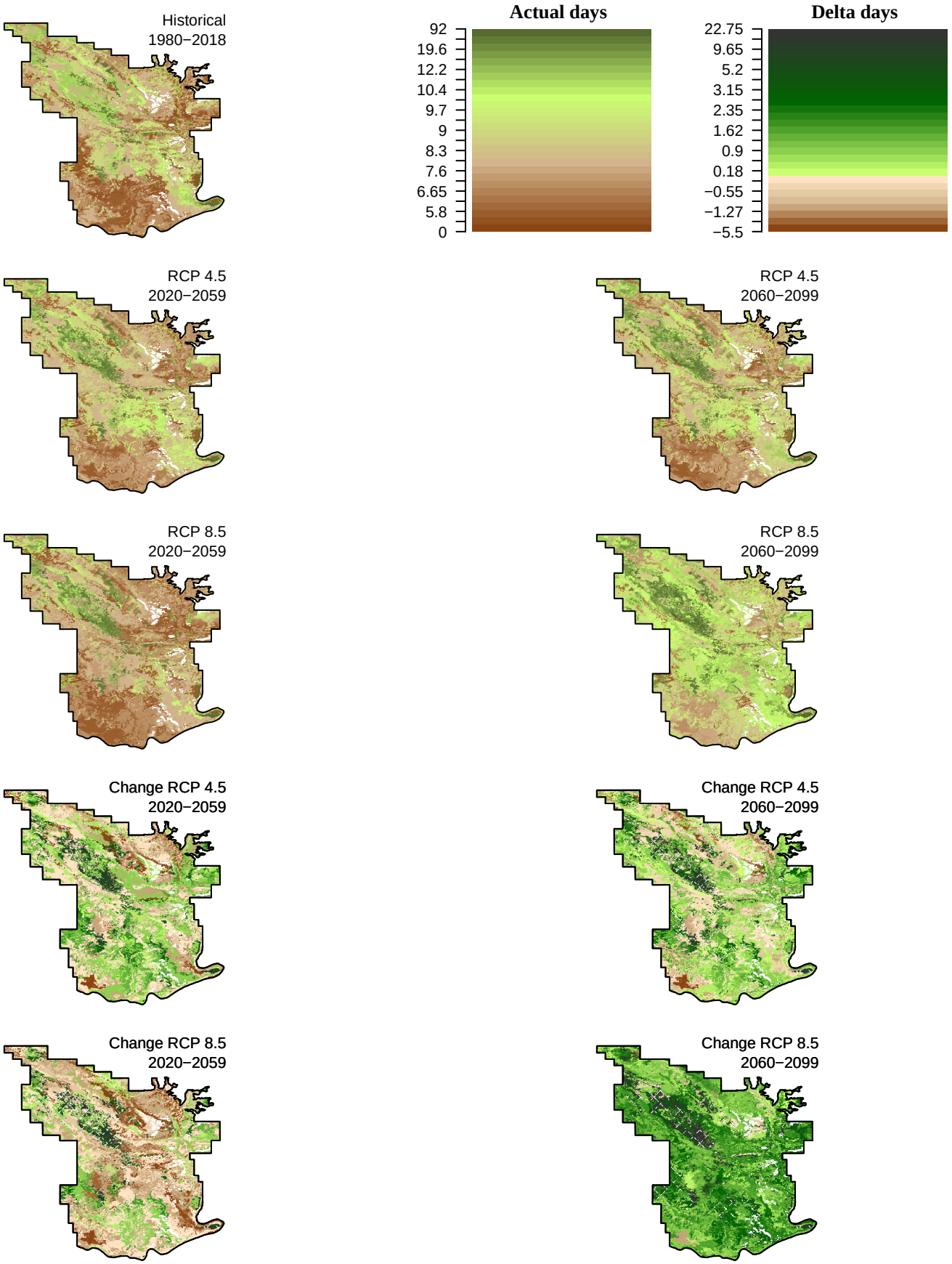


Figure ARCHmap89:
Past trends and future trajectories of park−wide mean values for Summer wet soil days in Arches. Topmost panel depicts the historical mean from 1980−2018. Lower four panels show the emission scenarios of RCP 4.5 and RCP 8.5 at near−term and long−term timeframes. Bottom four panels depict the change from the historical mean; cross hatching denotes areas of robust predicitons (90% of models agree in the direction of change).

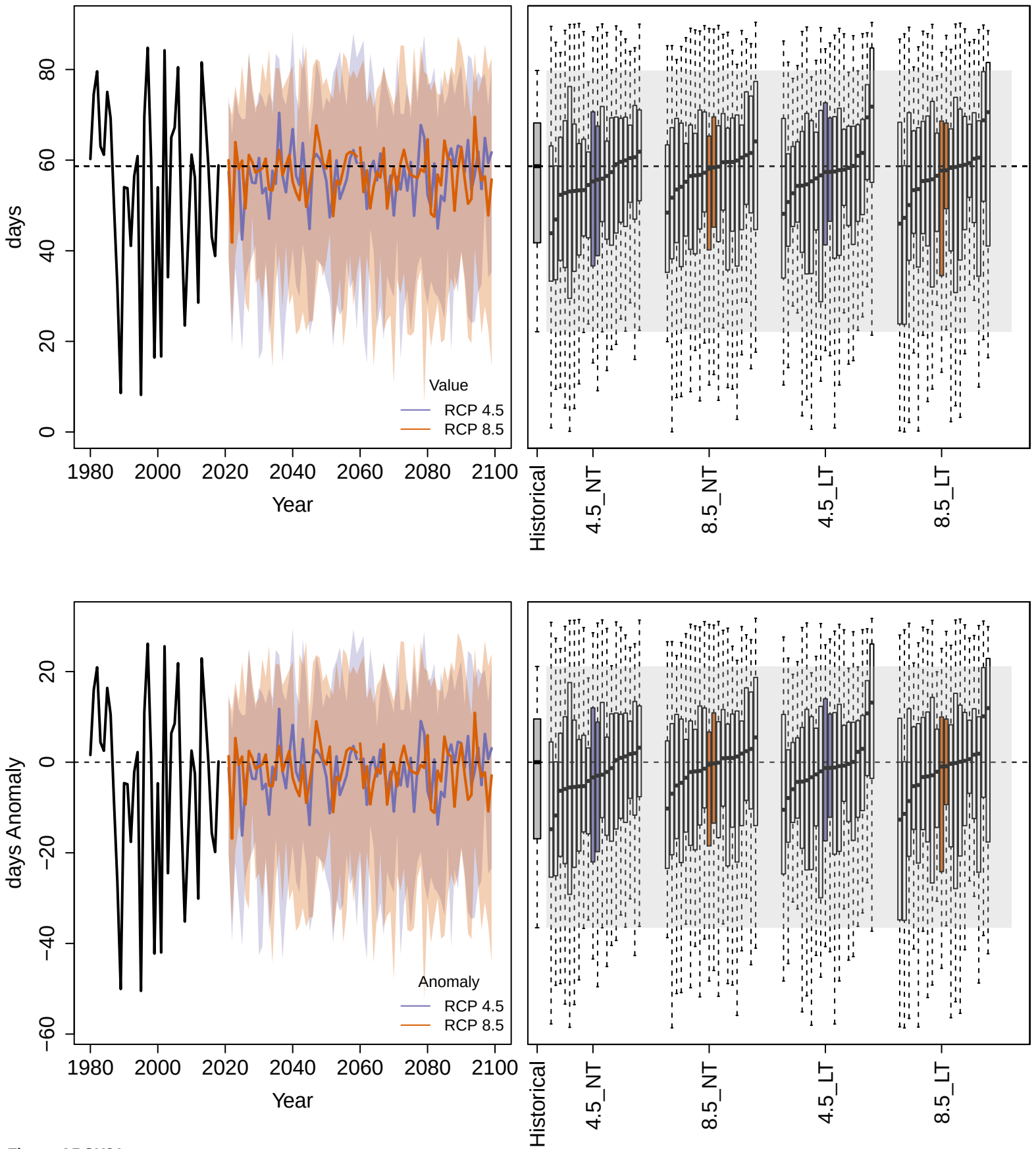


Figure ARCH91:
Past trends and future trajectories of park−wide mean values for Fall wet soil days in Arches. Top panels show values, bottom panels show changes from the long−term historical mean. Left: Time series of historical (black) and future projections for RCP 4.5 and 8.5. Shaded areas show spread among climate models. Right: Boxplots of temporal variability over 40−year periods under historical (left box) and individual climate models under two RCPs. Right: Historical time period is 1970−2010; near−term (NT) is 2020−2060; long−term (LT) is 2061−2100.

Arches: Fall wet soil days

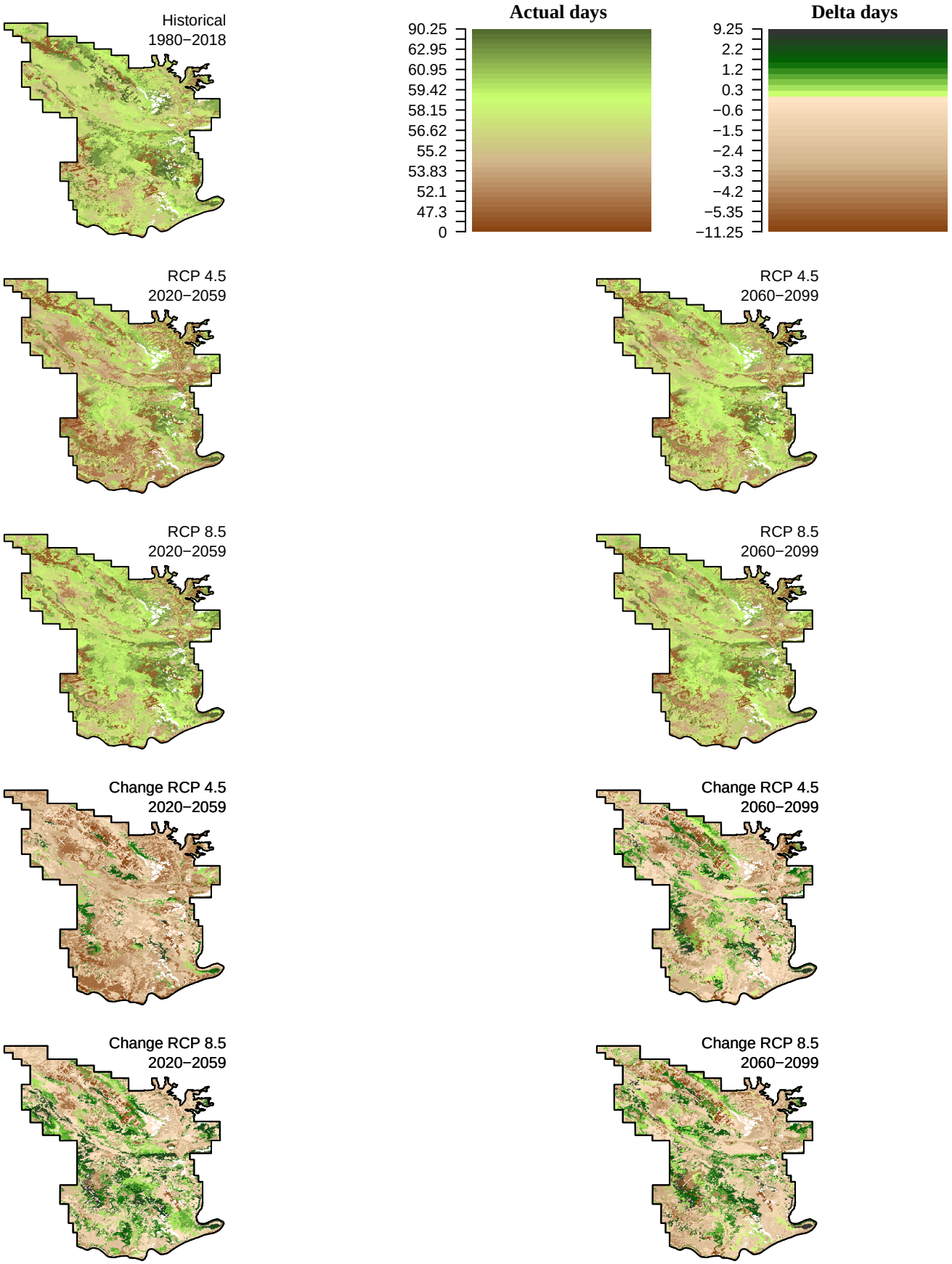


Figure ARCHmap91:
Past trends and future trajectories of park−wide mean values for Fall wet soil days in Arches. Topmost panel depicts the historical mean from 1980−2018. Lower four panels show the emission scenarios of RCP 4.5 and RCP 8.5 at near−term and long−term timeframes. Bottom four panels depict the change from the historical mean; cross hatching denotes areas of robust predicitons (90% of models agree in the direction of change).

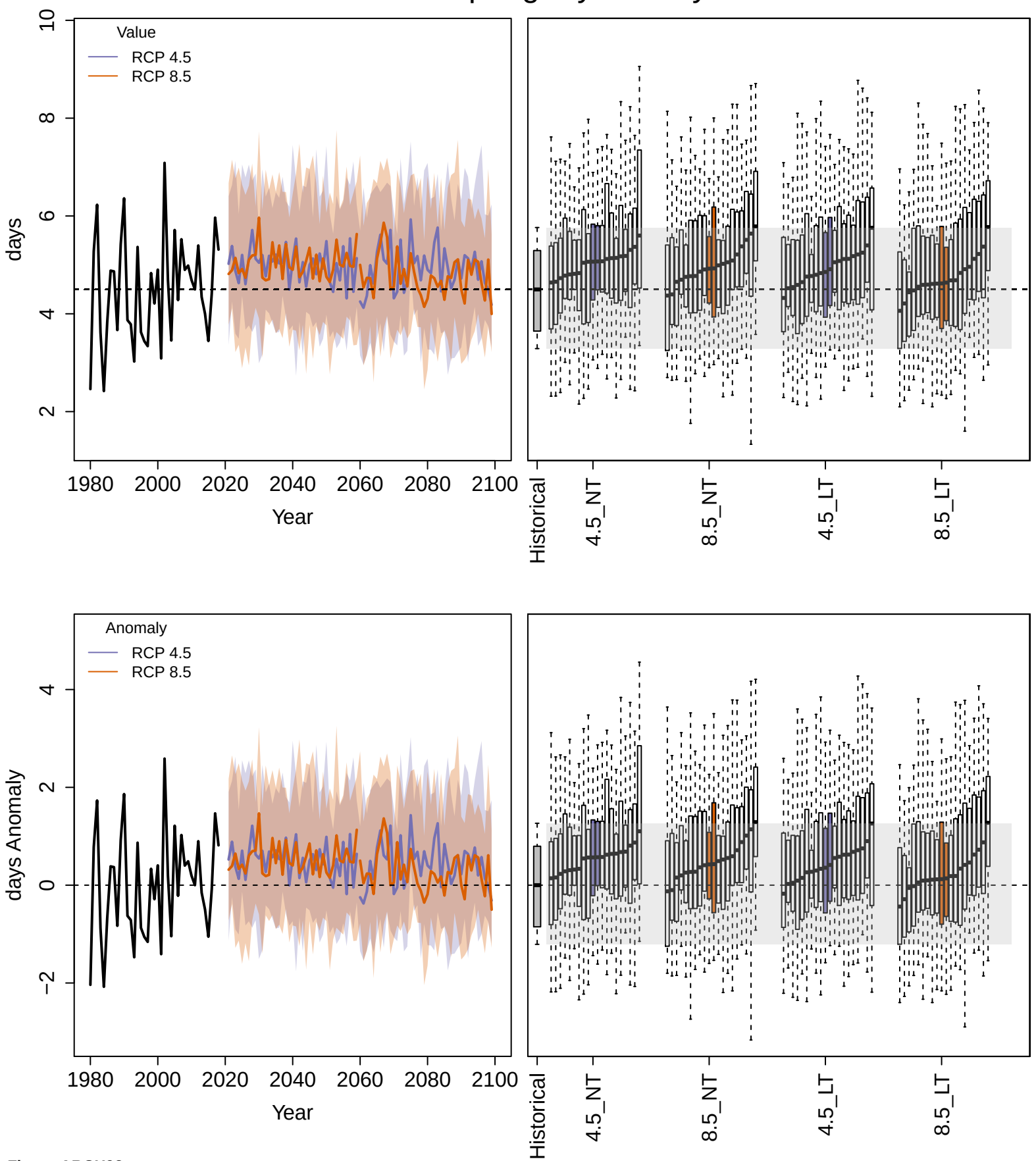


Figure ARCH93:
Past trends and future trajectories of park−wide mean values for Spring dry soil days in Arches. Top panels show values, bottom panels show changes from the long−term historical mean. Left: Time series of historical (black) and future projections for RCP 4.5 and 8.5. Shaded areas show spread among climate models. Right: Boxplots of temporal variability over 40−year periods under historical (left box) and individual climate models under two RCPs. Right: Historical time period is 1970−2010; near−term (NT) is 2020−2060; long−term (LT) is 2061−2100.

Arches: Spring dry soil days

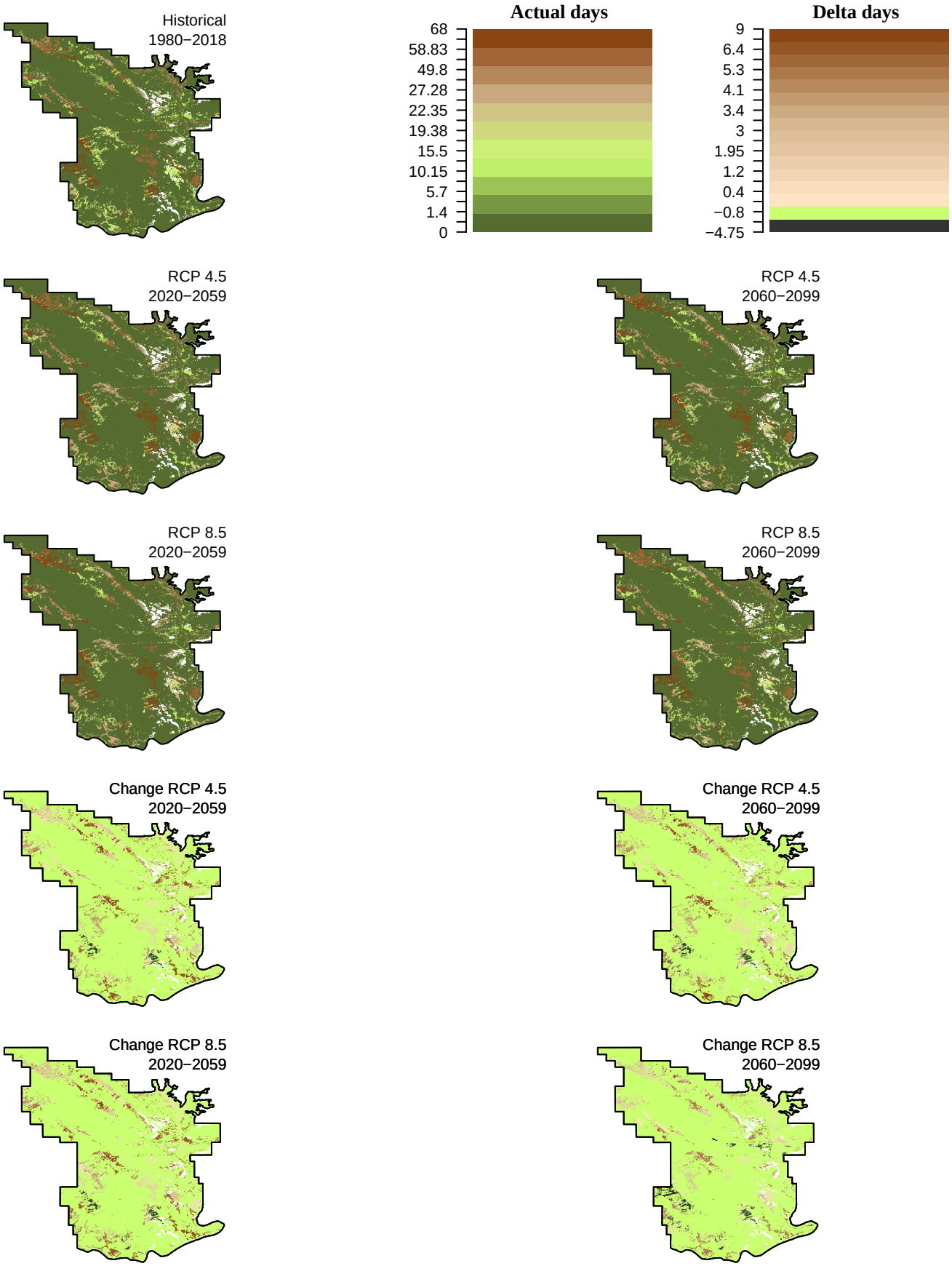


Figure ARCHmap93:
Past trends and future trajectories of park−wide mean values for Spring dry soil days in Arches. Topmost panel depicts the historical mean from 1980−2018. Lower four panels show the emission scenarios of RCP 4.5 and RCP 8.5 at near−term and long−term timeframes. Bottom four panels depict the change from the historical mean; cross hatching denotes areas of robust predicitons (90% of models agree in the direction of change).

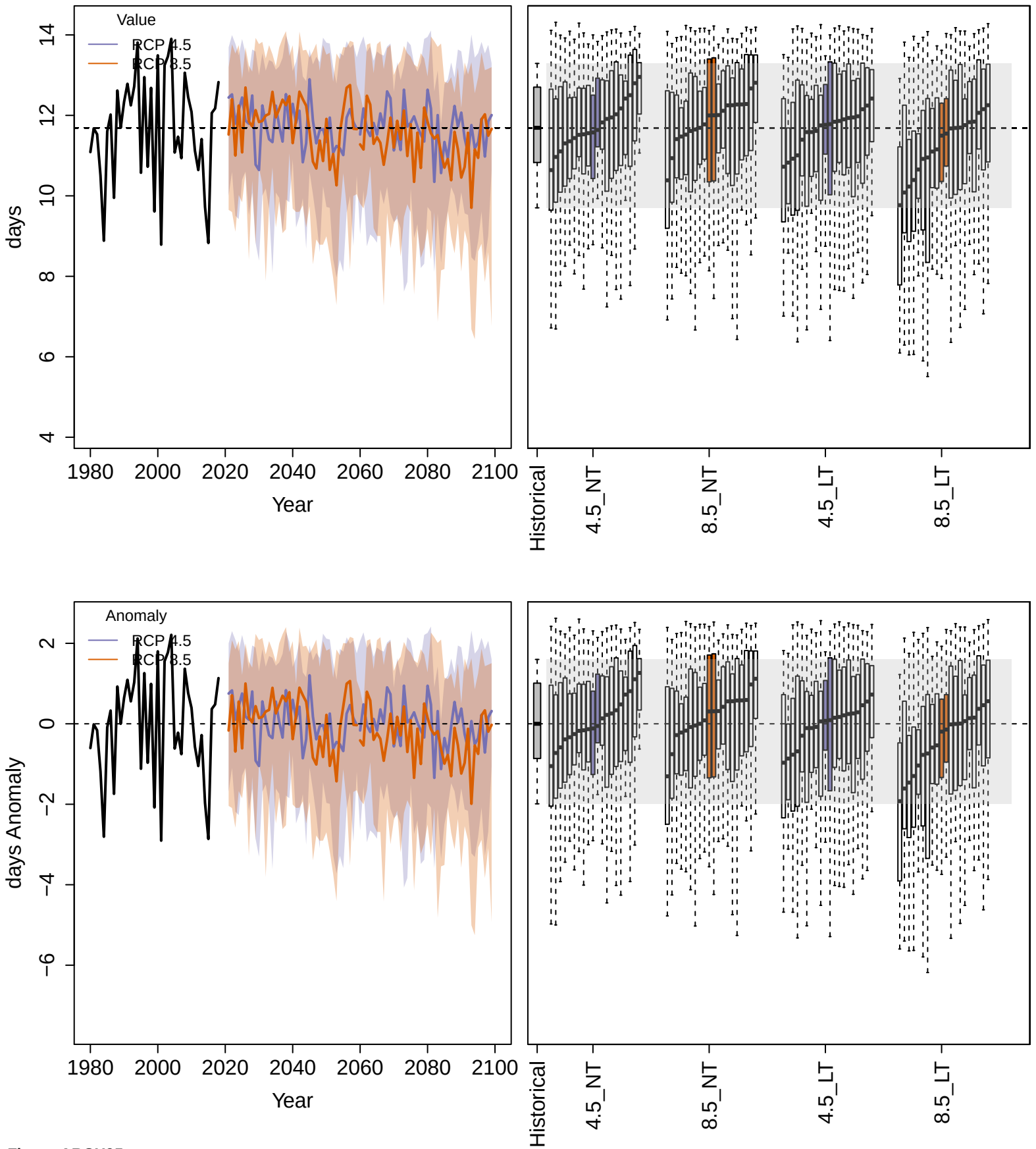


Figure ARCH95:
Past trends and future trajectories of park−wide mean values for Summer dry soil days in Arches. Top panels show values, bottom panels show changes from the long−term historical mean. Left: Time series of historical (black) and future projections for RCP 4.5 and 8.5. Shaded areas show spread among climate models. Right: Boxplots of temporal variability over 40−year periods under historical (left box) and individual climate models under two RCPs. Right: Historical time period is 1970−2010; near−term (NT) is 2020−2060; long−term (LT) is 2061−2100.

Arches: Summer dry soil days

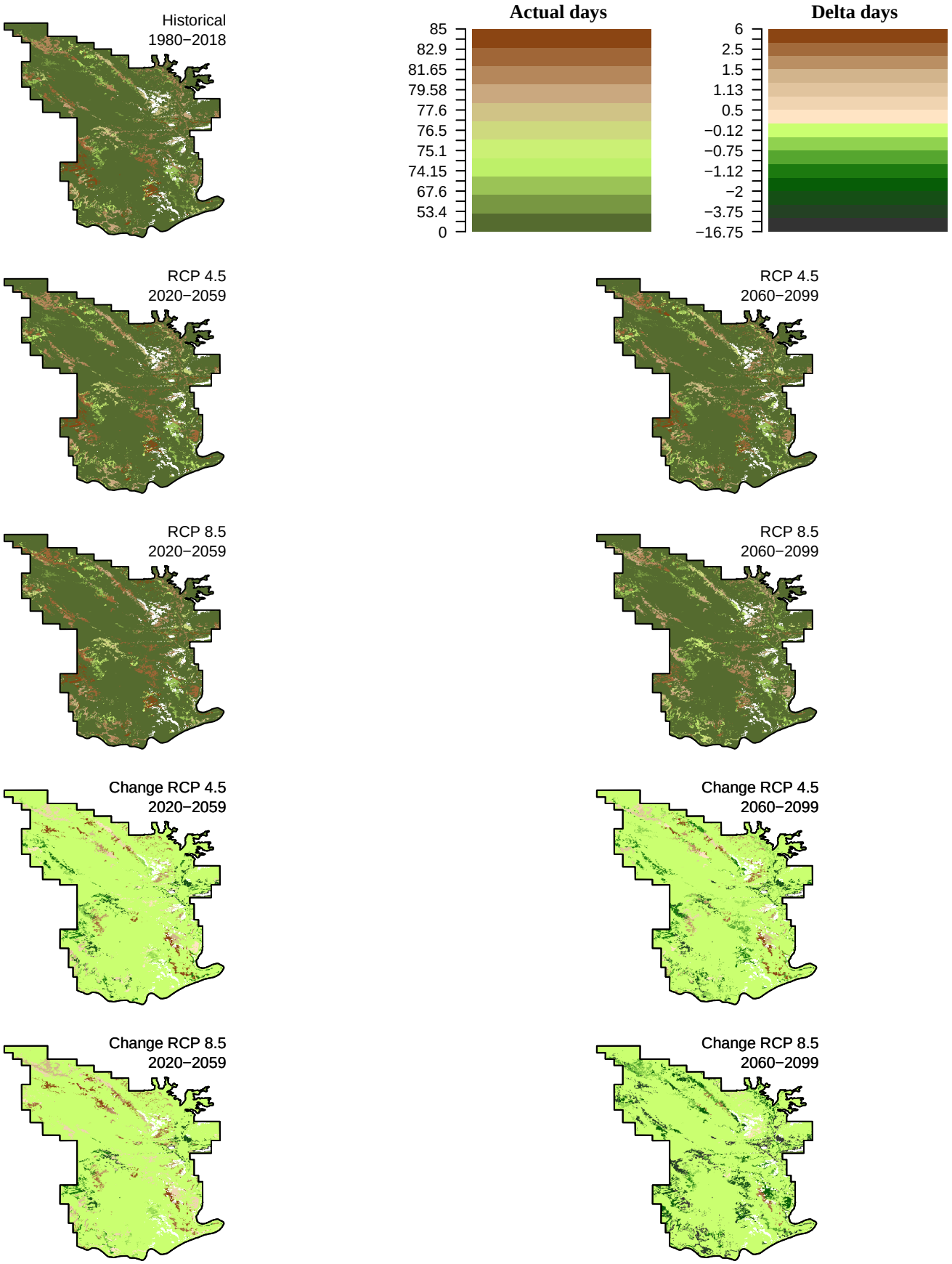


Figure ARCHmap95:
Past trends and future trajectories of park−wide mean values for Summer dry soil days in Arches. Topmost panel depicts the historical mean from 1980−2018. Lower four panels show the emission scenarios of RCP 4.5 and RCP 8.5 at near−term and long−term timeframes. Bottom four panels depict the change from the historical mean; cross hatching denotes areas of robust predicitons (90% of models agree in the direction of change).

Arches: Fall dry soil days

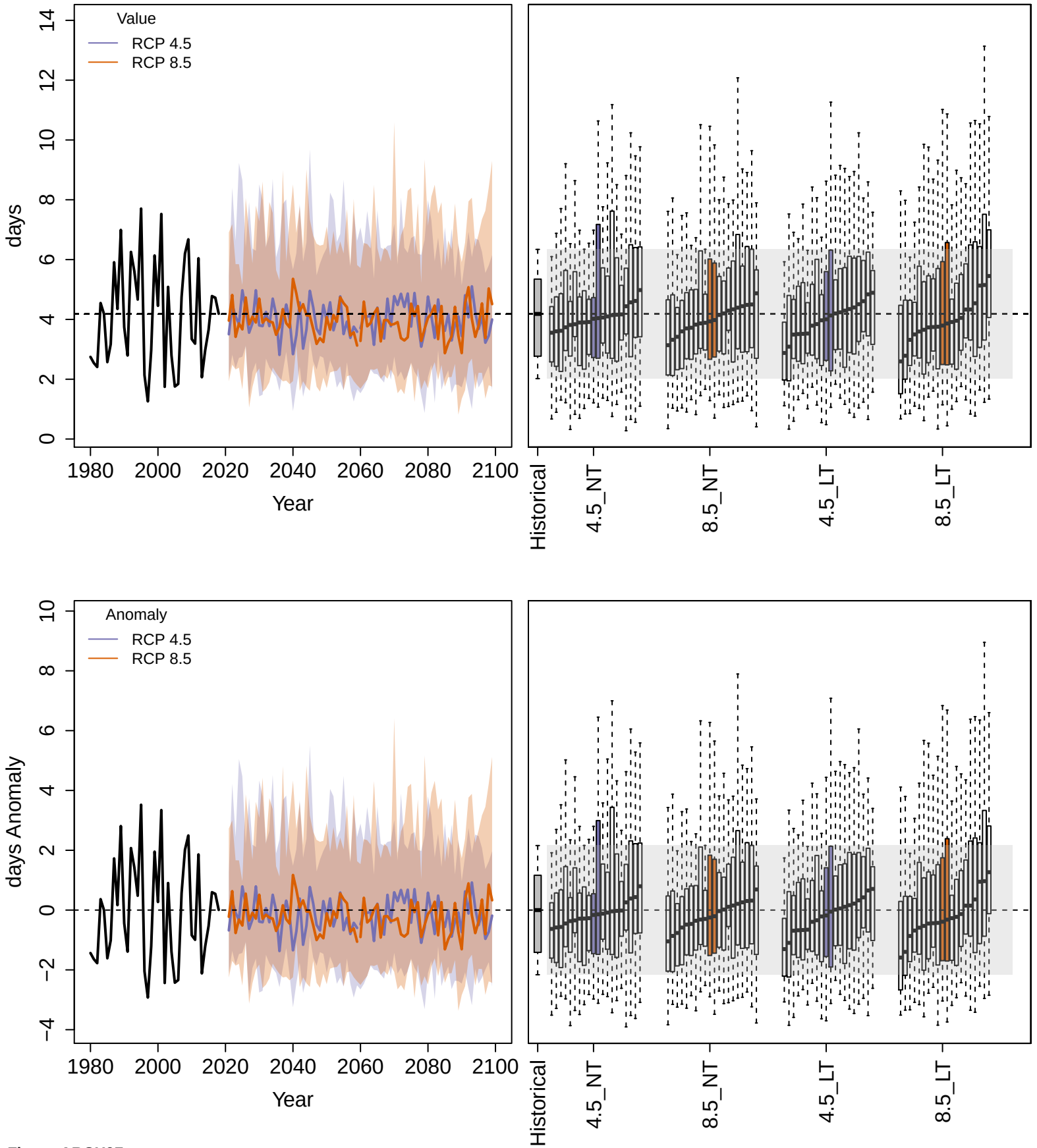


Figure ARCH97:
Past trends and future trajectories of park−wide mean values for Fall dry soil days in Arches. Top panels show values, bottom panels show changes from the long−term historical mean. Left: Time series of historical (black) and future projections for RCP 4.5 and 8.5. Shaded areas show spread among climate models. Right: Boxplots of temporal variability over 40−year periods under historical (left box) and individual climate models under two RCPs. Right: Historical time period is 1970−2010; near−term (NT) is 2020−2060; long−term (LT) is 2061−2100.

Arches: Fall dry soil days

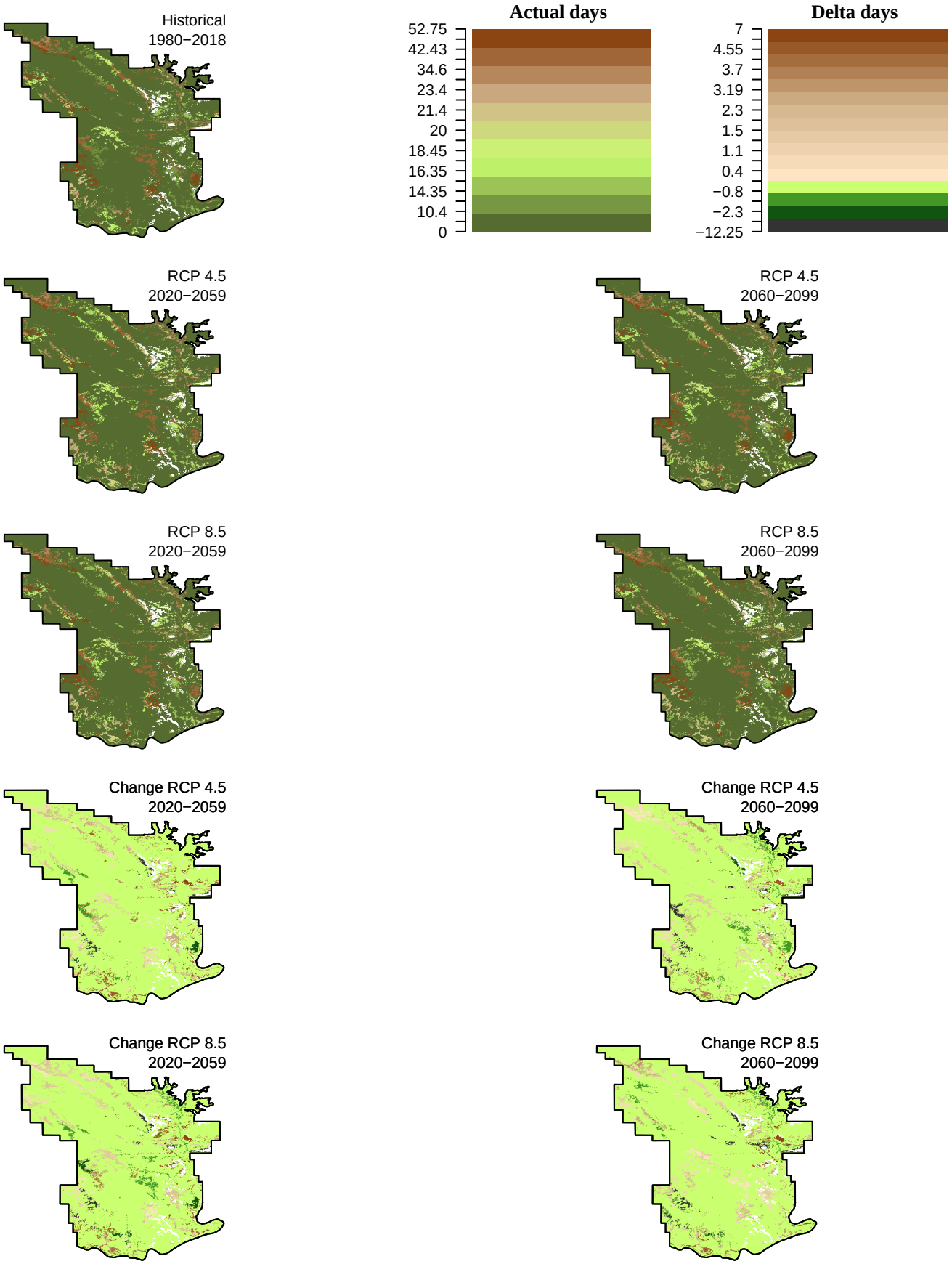


Figure ARCHmap97:
Past trends and future trajectories of park−wide mean values for Fall dry soil days in Arches. Topmost panel depicts the historical mean from 1980−2018. Lower four panels show the emission scenarios of RCP 4.5 and RCP 8.5 at near−term and long−term timeframes. Bottom four panels depict the change from the historical mean; cross hatching denotes areas of robust predicitons (90% of models agree in the direction of change).

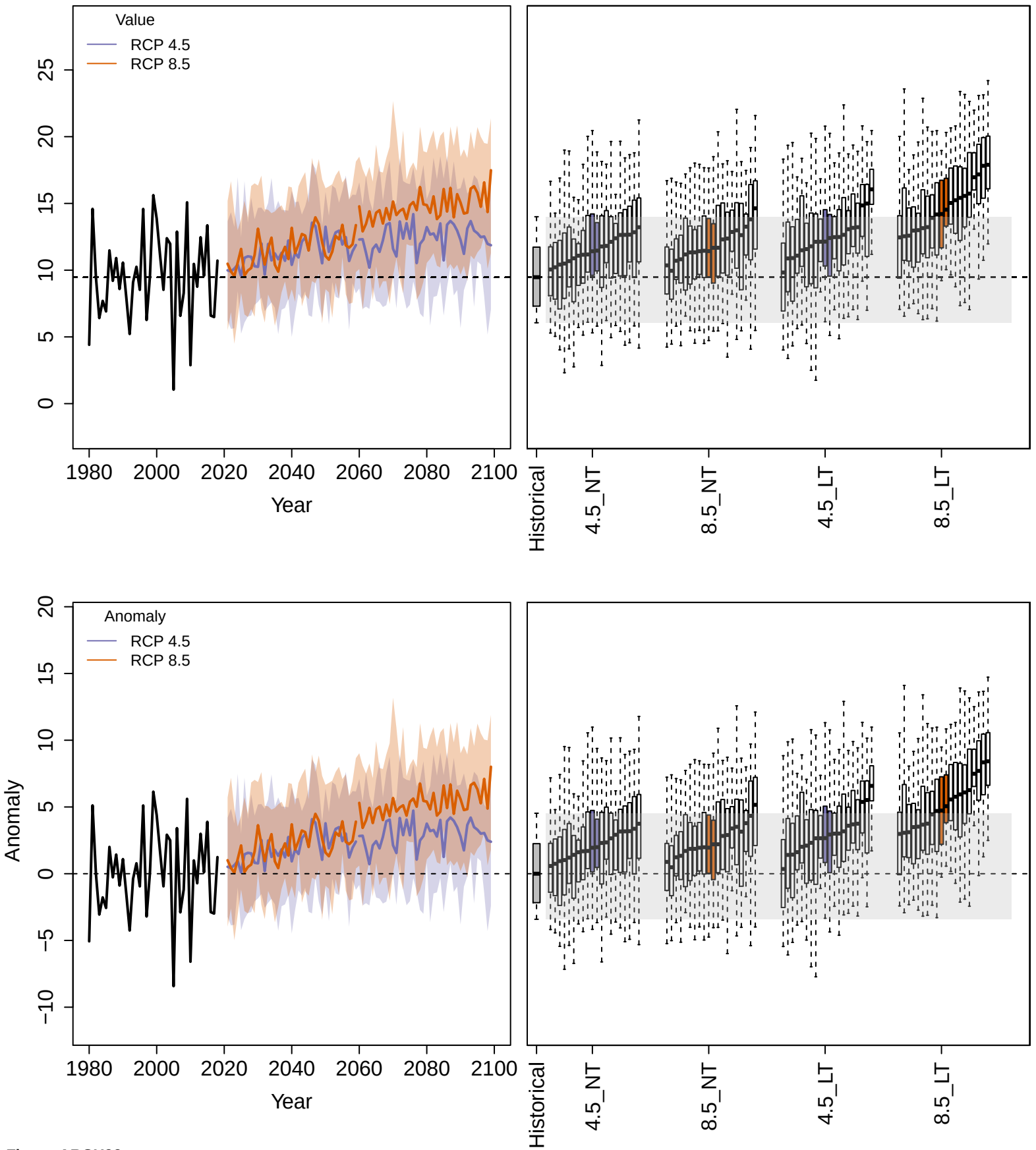


Figure ARCH99:
Past trends and future trajectories of park−wide mean values for Winter extreme short−term dry stress in Arches. Top panels show values, bottom panels show changes from the long−term historical mean. Left: Time series of historical (black) and future projections for RCP 4.5 and 8.5. Shaded areas show spread among climate models. Right: Boxplots of temporal variability over 40−year periods under historical (left box) and individual climate models under two RCPs. Right: Historical time period is 1970−2010; near−term (NT) is 2020−2060; long−term (LT) is 2061−2100.

Arches: Winter extreme short−term dry stress

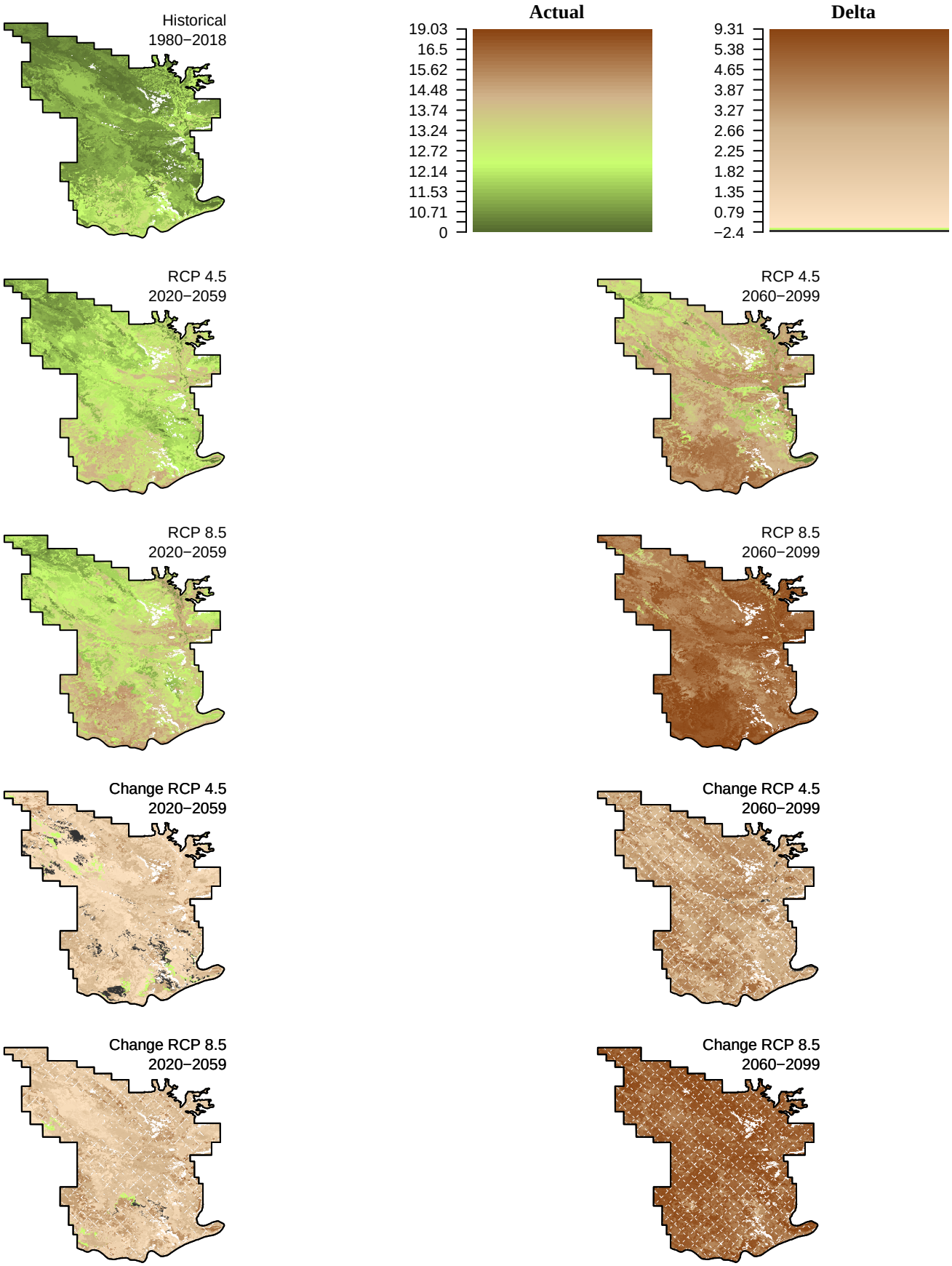


Figure ARCHmap99:
Past trends and future trajectories of park−wide mean values for Winter extreme short−term dry stress in Arches. Topmost panel depicts the historical mean from 1980−2018. Lower four panels show the emission scenarios of RCP 4.5 and RCP 8.5 at near−term and long−term timeframes. Bottom four panels depict the change from the historical mean; cross hatching denotes areas of robust predicitons (90% of models agree in the direction of change).

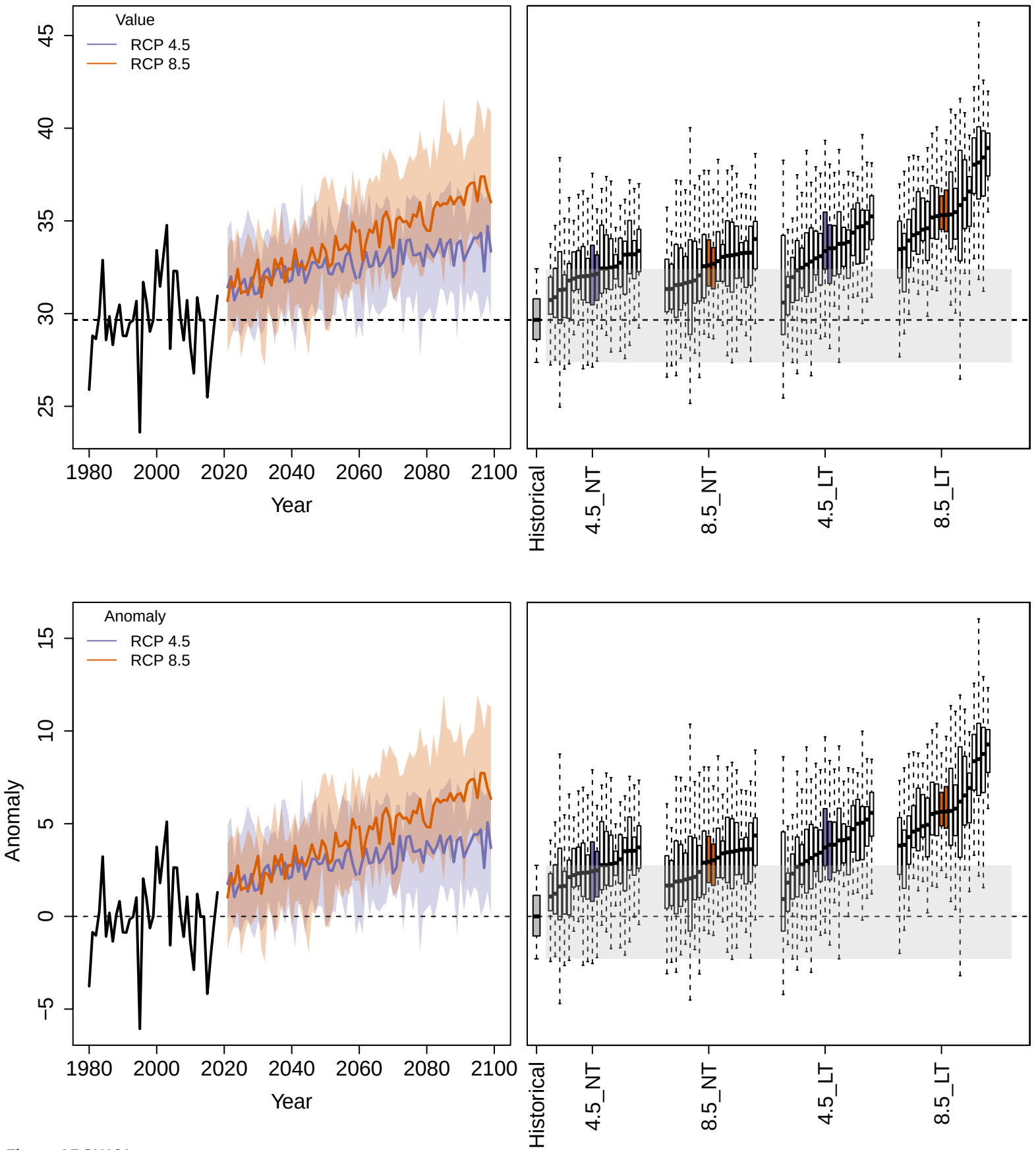


Figure ARCH101:
Past trends and future trajectories of park−wide mean values for Spring extreme short−term dry stress in Arches. Top panels show values, bottom panels show changes from the long−term historical mean. Left: Time series of historical (black) and future projections for RCP 4.5 and 8.5. Shaded areas show spread among climate models. Right: Boxplots of temporal variability over 40−year periods under historical (left box) and individual climate models under two RCPs. Right: Historical time period is 1970−2010; near−term (NT) is 2020−2060; long−term (LT) is 2061−2100.

Arches: Spring extreme short−term dry stress

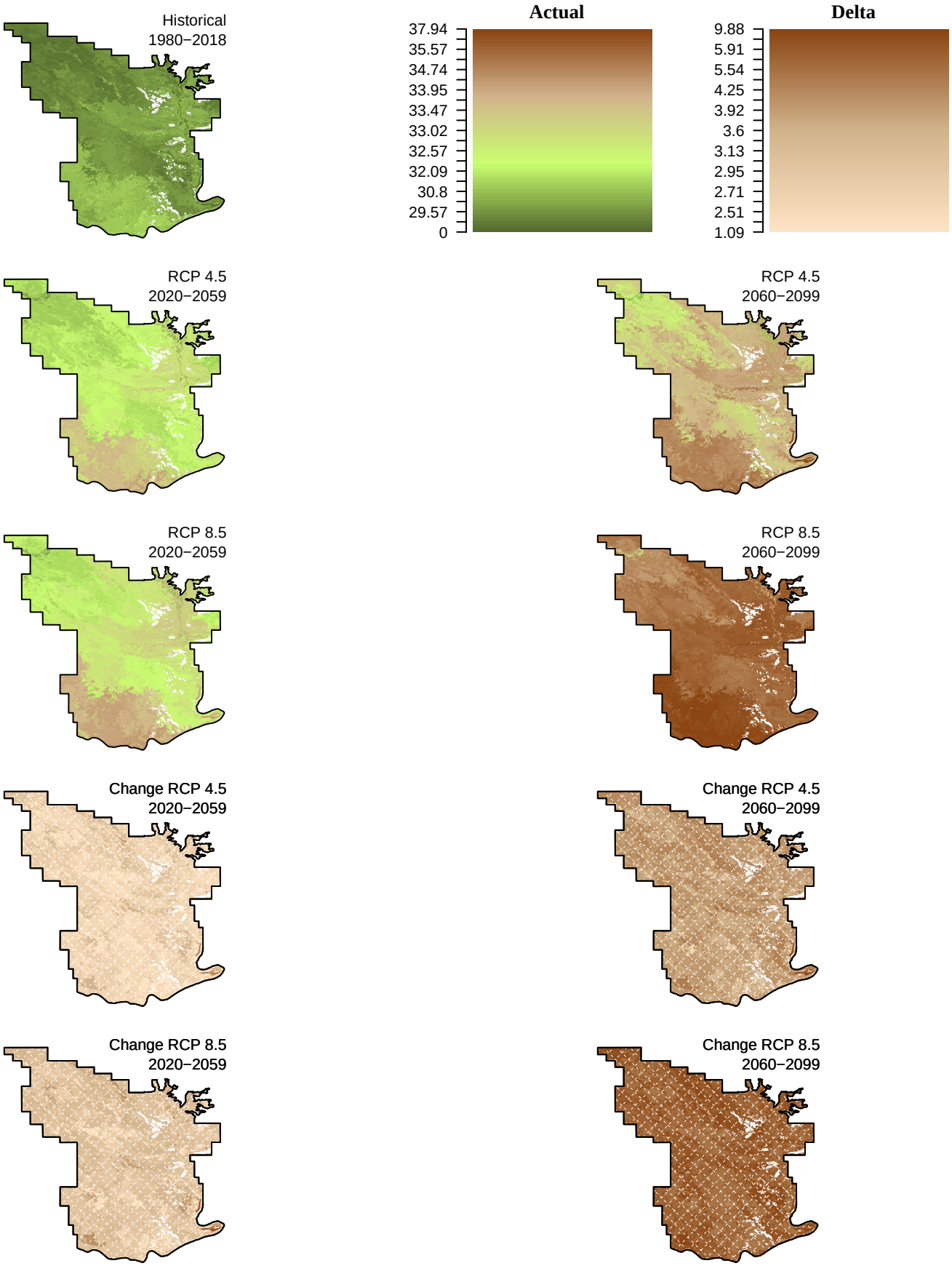


Figure ARCHmap101:
Past trends and future trajectories of park−wide mean values for Spring extreme short−term dry stress in Arches. Topmost panel depicts the historical mean from 1980−2018. Lower four panels show the emission scenarios of RCP 4.5 and RCP 8.5 at near−term and long−term timeframes. Bottom four panels depict the change from the historical mean; cross hatching denotes areas of robust predicitons (90% of models agree in the direction of change).

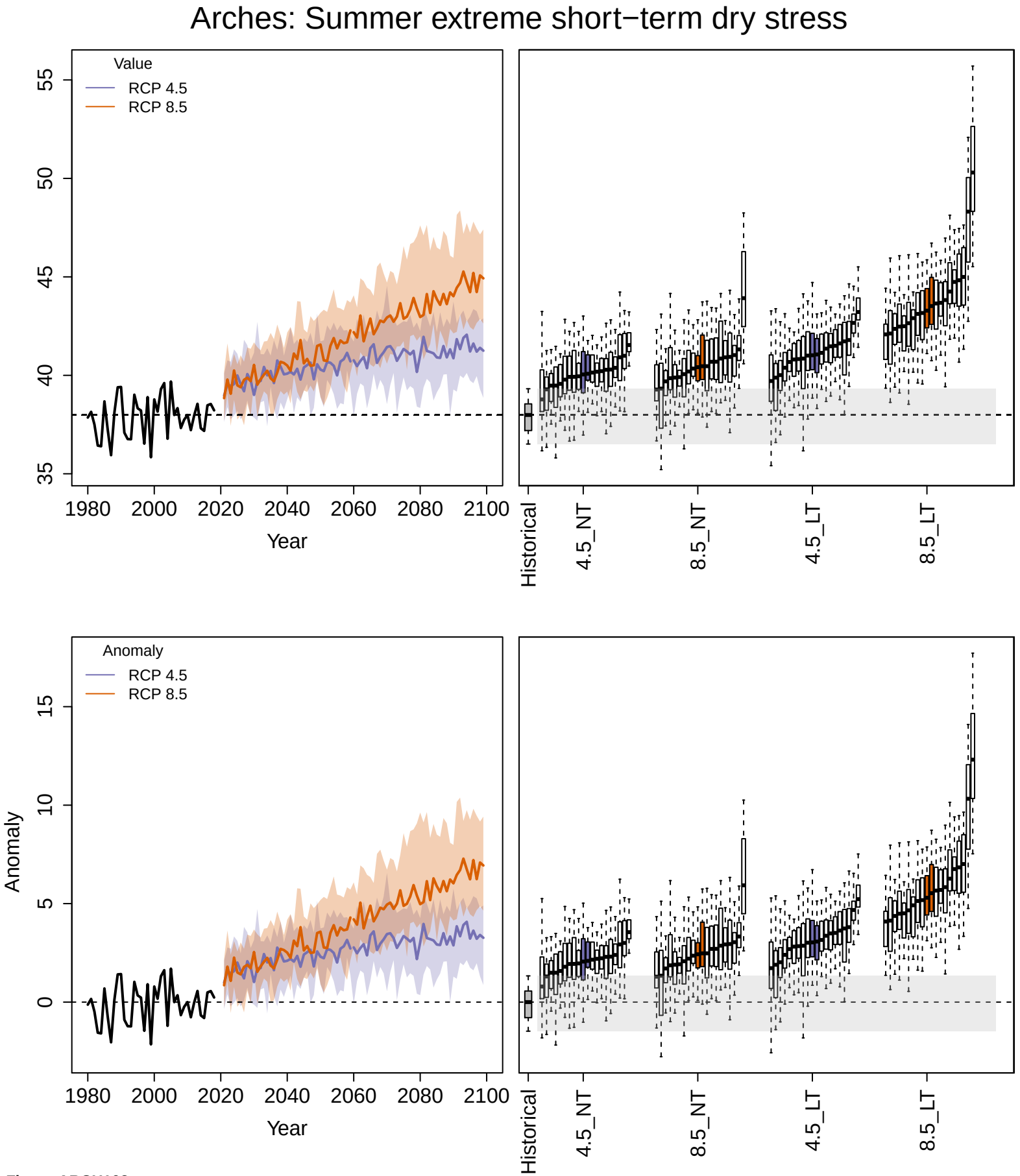


Figure ARCH103:
Past trends and future trajectories of park−wide mean values for Summer extreme short−term dry stress in Arches. Top panels show values, bottom panels show changes from the long−term historical mean. Left: Time series of historical (black) and future projections for RCP 4.5 and 8.5. Shaded areas show spread among climate models. Right: Boxplots of temporal variability over 40−year periods under historical (left box) and individual climate models under two RCPs. Right: Historical time period is 1970−2010; near−term (NT) is 2020−2060; long−term (LT) is 2061−2100.

Arches: Summer extreme short−term dry stress

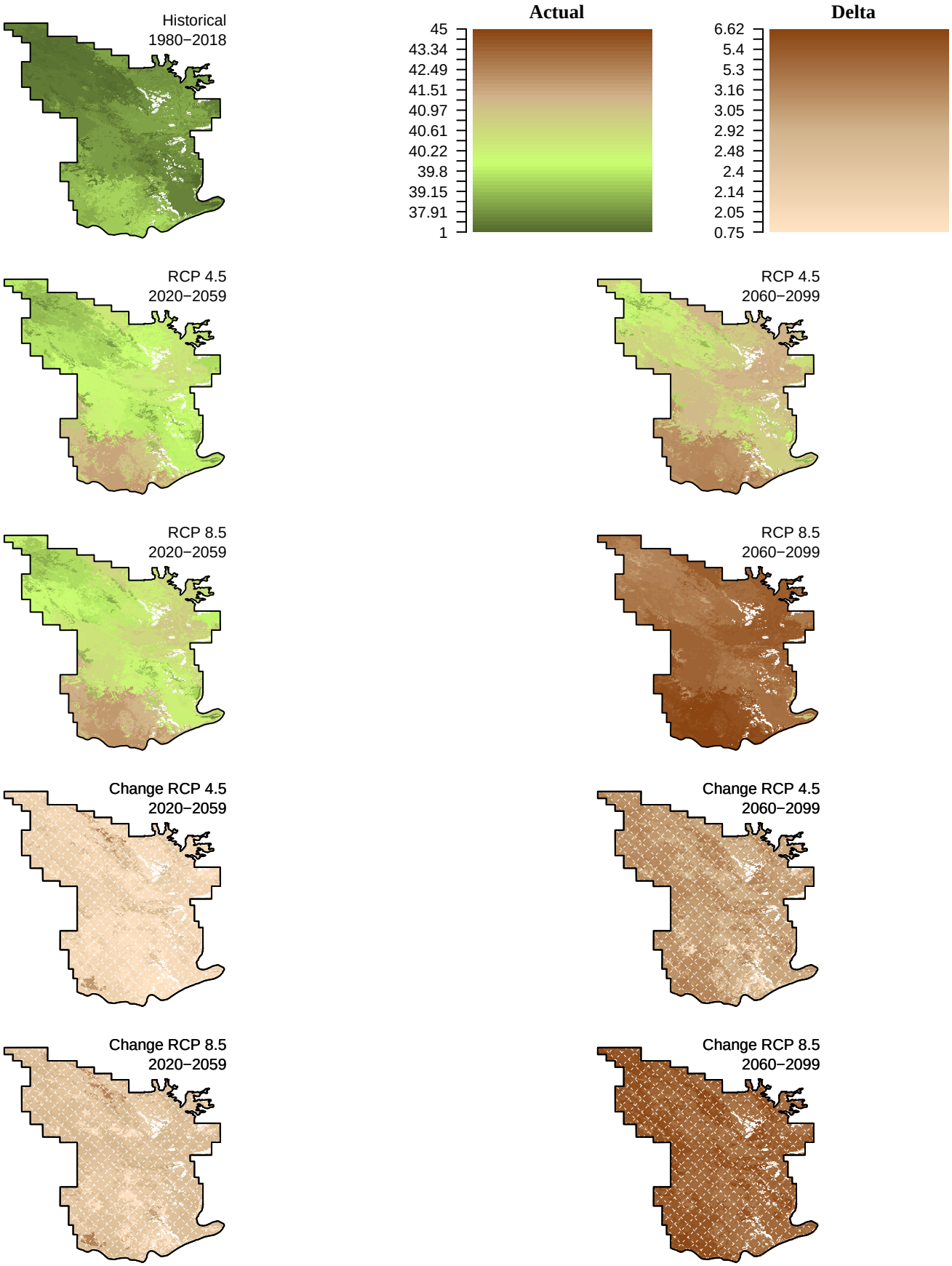


Figure ARCHmap103:
Past trends and future trajectories of park−wide mean values for Summer extreme short−term dry stress in Arches. Topmost panel depicts the historical mean from 1980−2018. Lower four panels show the emission scenarios of RCP 4.5 and RCP 8.5 at near−term and long−term timeframes. Bottom four panels depict the change from the historical mean; cross hatching denotes areas of robust predicitons (90% of models agree in the direction of change).

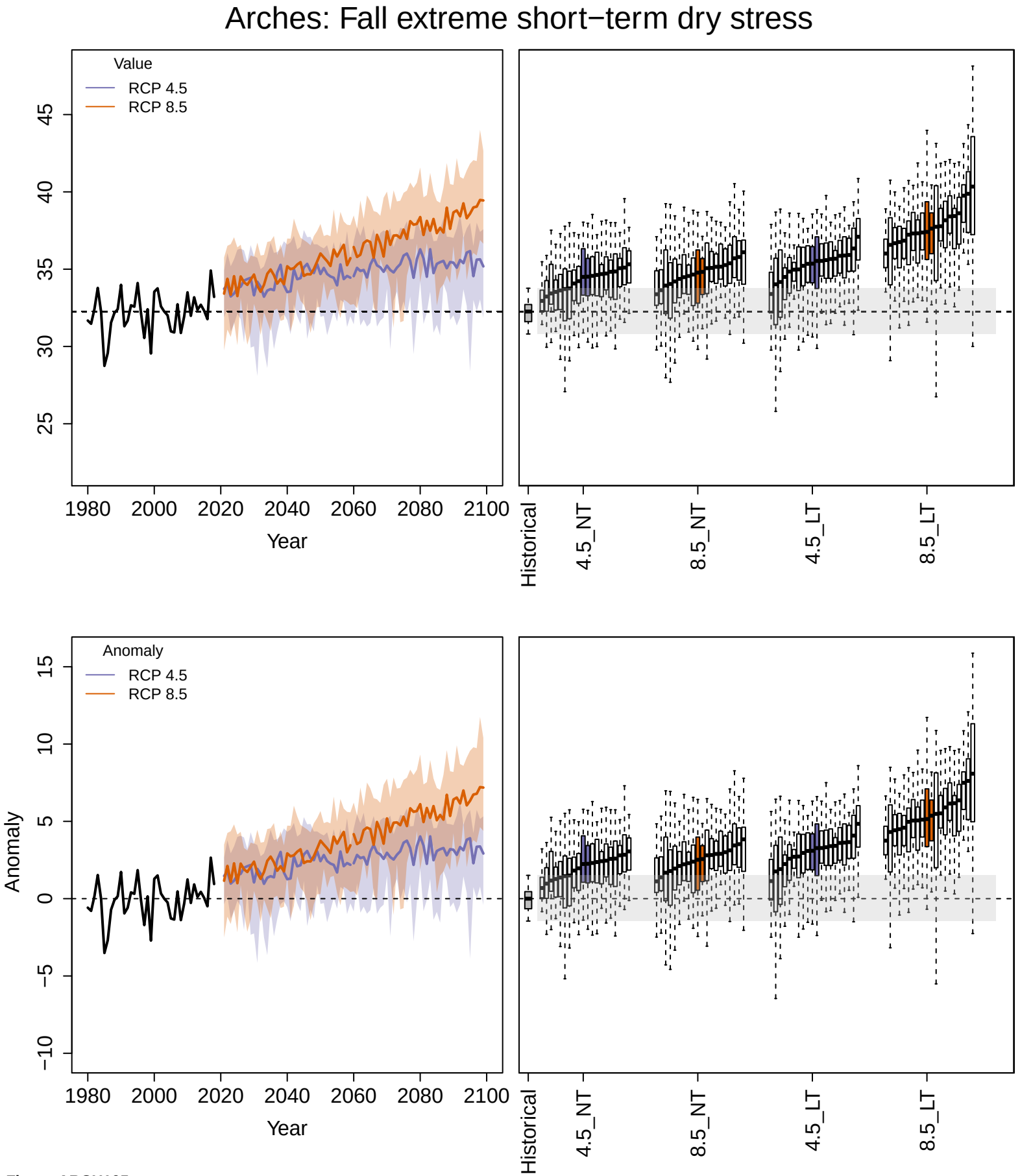


Figure ARCH105:
Past trends and future trajectories of park−wide mean values for Fall extreme short−term dry stress in Arches. Top panels show values, bottom panels show changes from the long−term historical mean. Left: Time series of historical (black) and future projections for RCP 4.5 and 8.5. Shaded areas show spread among climate models. Right: Boxplots of temporal variability over 40−year periods under historical (left box) and individual climate models under two RCPs. Right: Historical time period is 1970−2010; near−term (NT) is 2020−2060; long−term (LT) is 2061−2100.

Arches: Fall extreme short−term dry stress

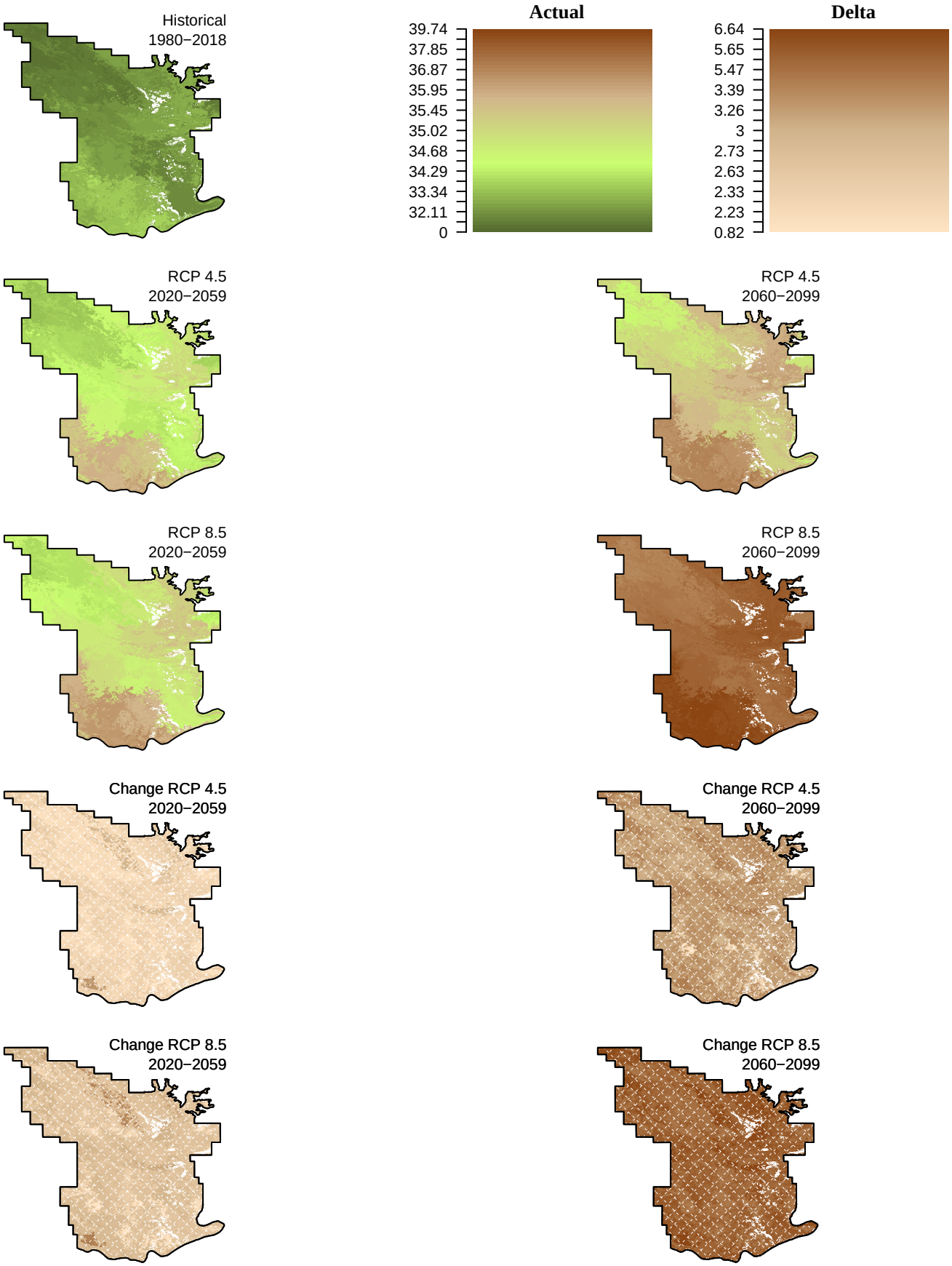


Figure ARCHmap105:
Past trends and future trajectories of park−wide mean values for Fall extreme short−term dry stress in Arches. Topmost panel depicts the historical mean from 1980−2018. Lower four panels show the emission scenarios of RCP 4.5 and RCP 8.5 at near−term and long−term timeframes. Bottom four panels depict the change from the historical mean; cross hatching denotes areas of robust predicitons (90% of models agree in the direction of change).

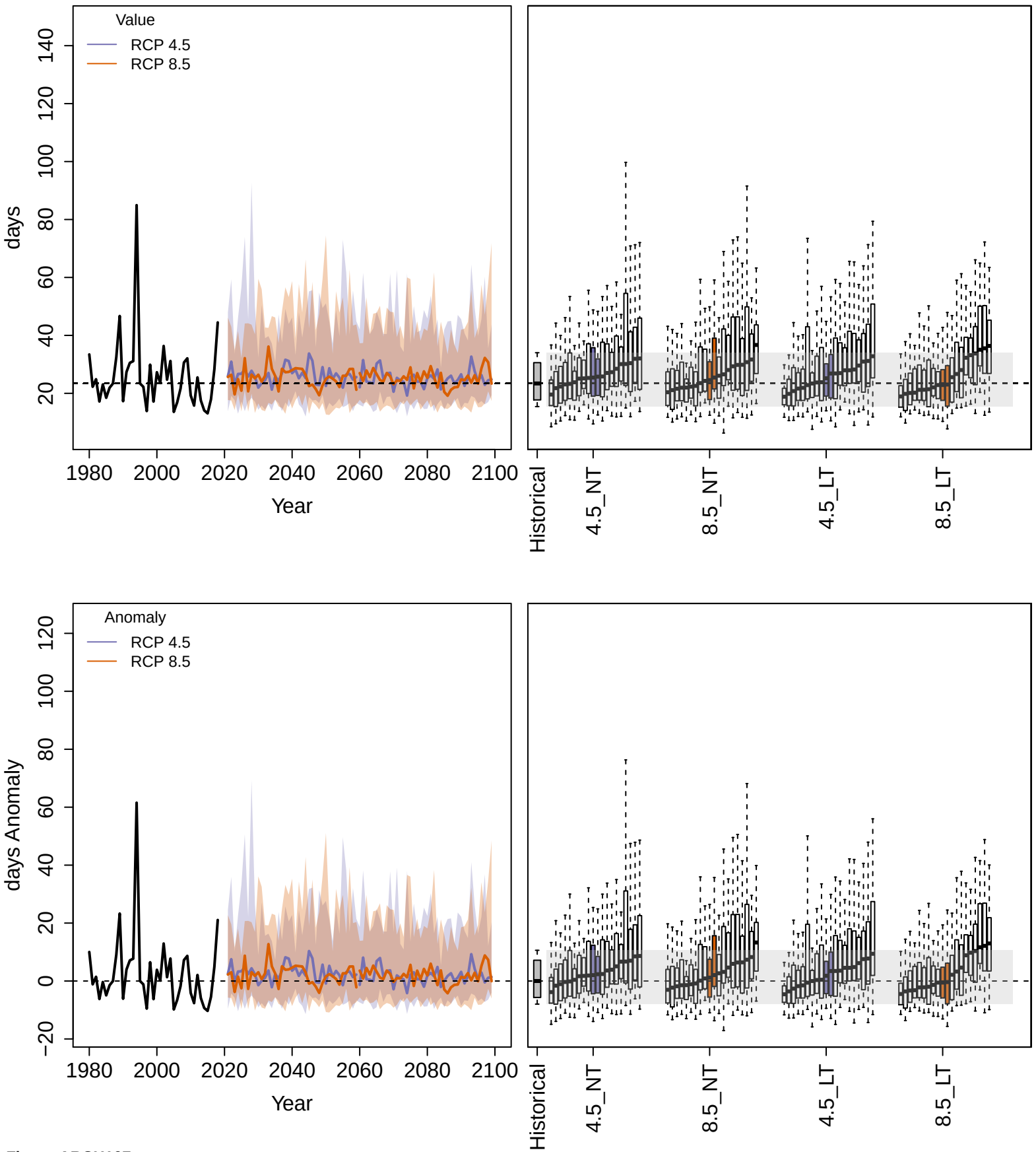


Figure ARCH107:
Past trends and future trajectories of park−wide mean values for Semi−dry soil duration in Arches. Top panels show values, bottom panels show changes from the long−term historical mean. Left: Time series of historical (black) and future projections for RCP 4.5 and 8.5. Shaded areas show spread among climate models. Right: Boxplots of temporal variability over 40−year periods under historical (left box) and individual climate models under two RCPs. Right: Historical time period is 1970−2010; near−term (NT) is 2020−2060; long−term (LT) is 2061−2100.

Arches: Semi−dry soil duration

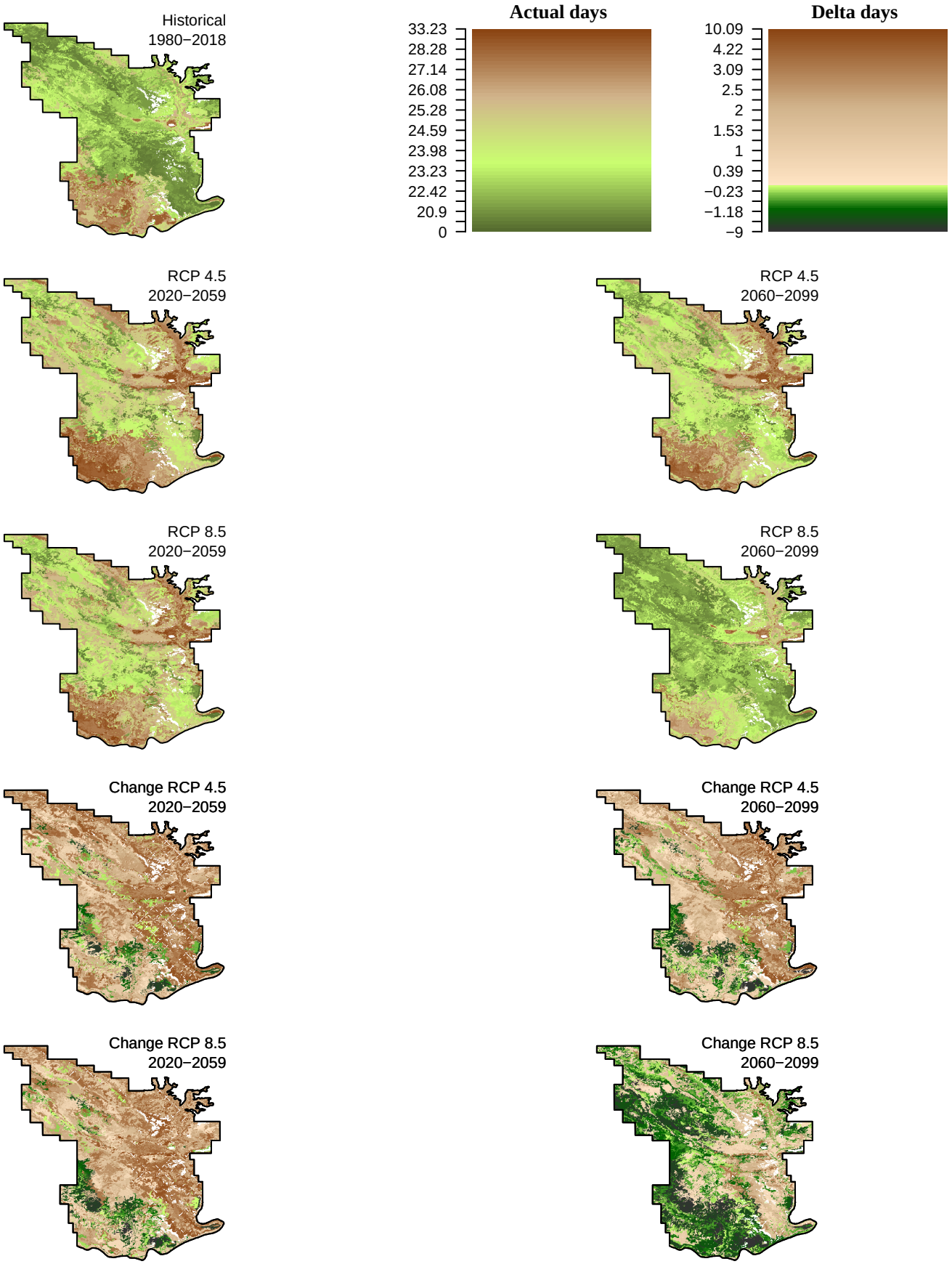


Figure ARCHmap107:
Past trends and future trajectories of park−wide mean values for Semi−dry soil duration in Arches. Topmost panel depicts the historical mean from 1980−2018. Lower four panels show the emission scenarios of RCP 4.5 and RCP 8.5 at near−term and long−term timeframes. Bottom four panels depict the change from the historical mean; cross hatching denotes areas of robust predicitons (90% of models agree in the direction of change).

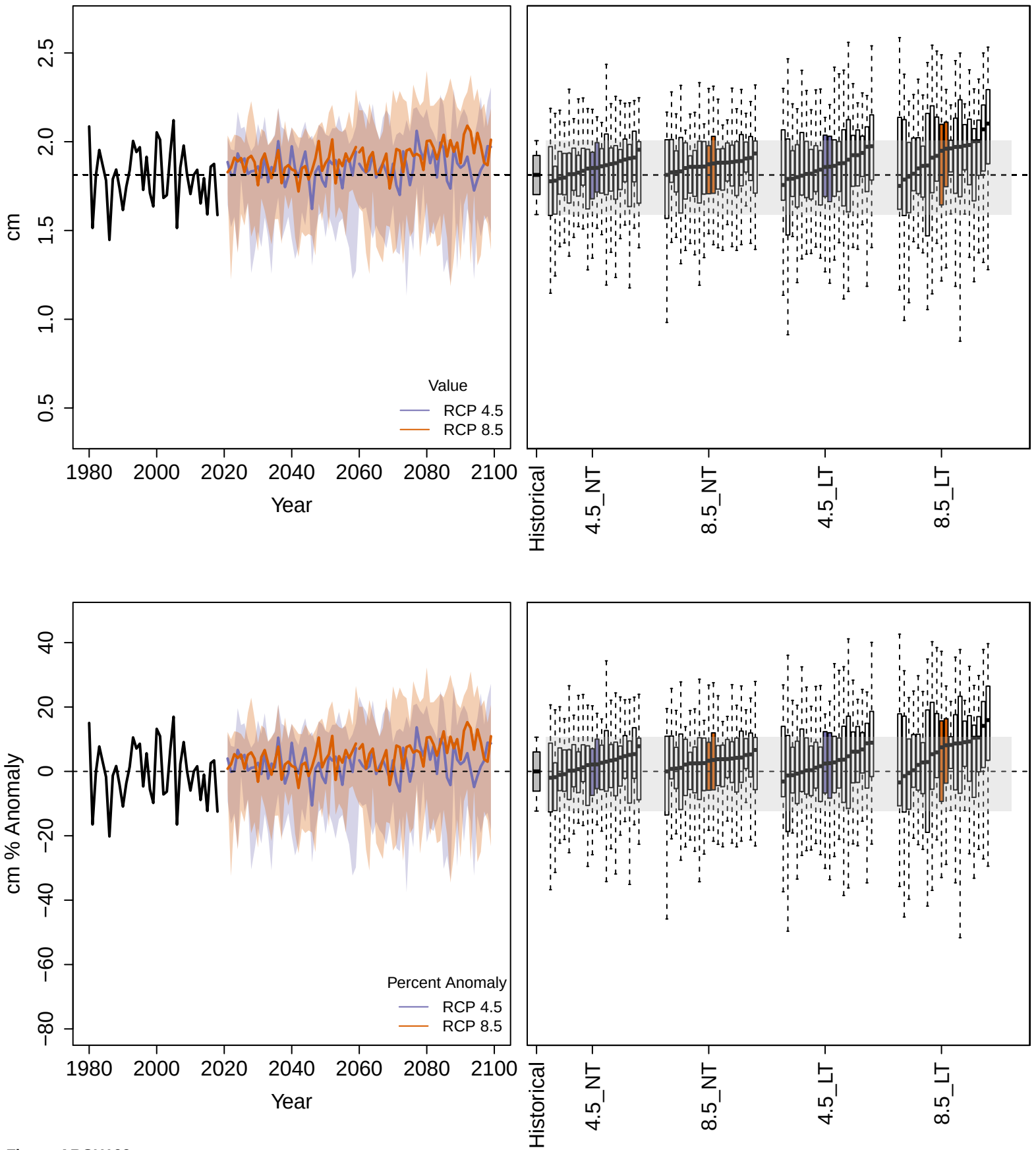


Figure ARCH109:
Past trends and future trajectories of park−wide mean values for Winter evaporation in Arches. Top panels show values, bottom panels show changes from the long−term historical mean. Left: Time series of historical (black) and future projections for RCP 4.5 and 8.5. Shaded areas show spread among climate models. Right: Boxplots of temporal variability over 40−year periods under historical (left box) and individual climate models under two RCPs. Right: Historical time period is 1970−2010; near−term (NT) is 2020−2060; long−term (LT) is 2061−2100.

Arches: Winter evaporation

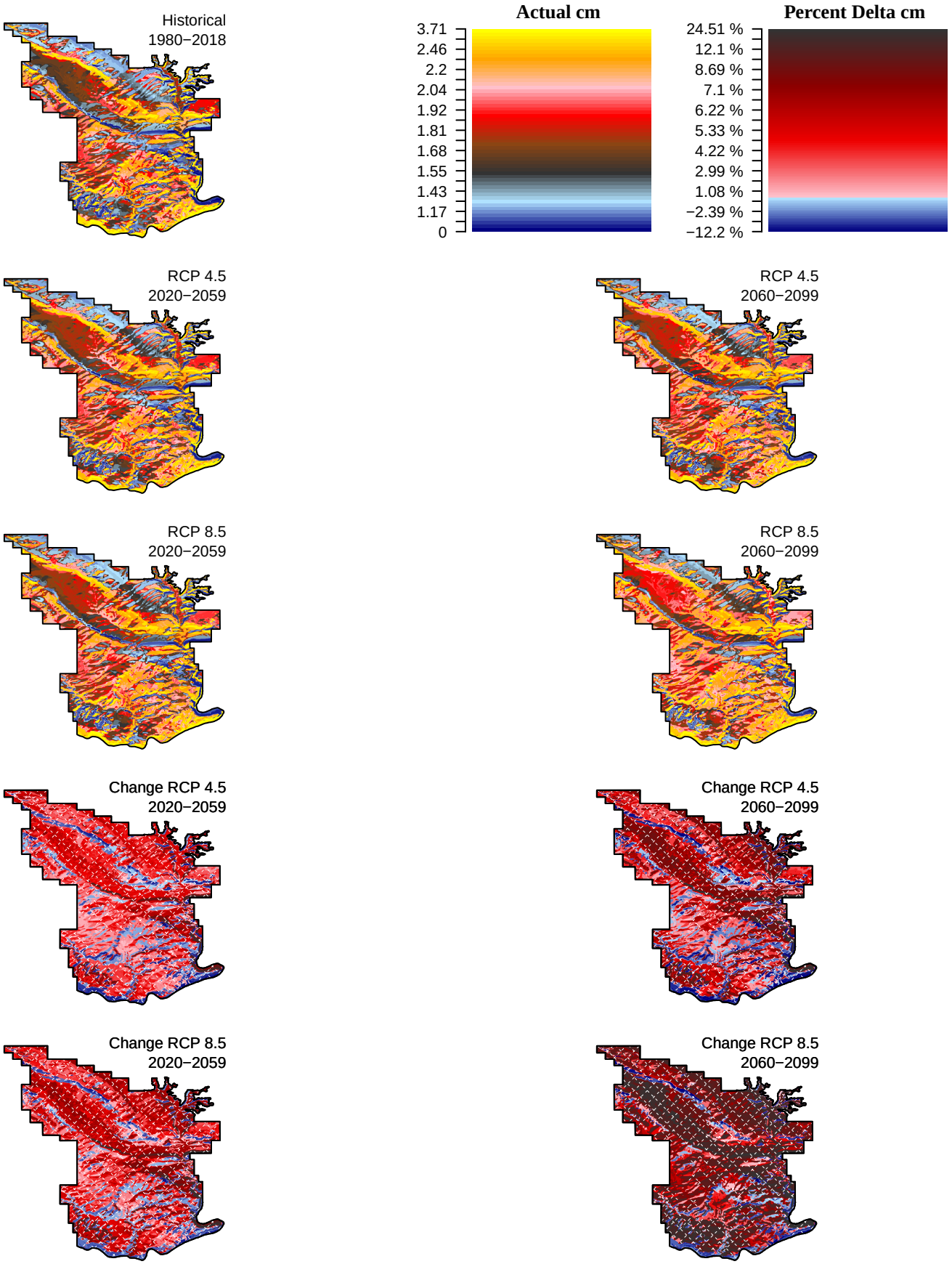


Figure ARCHmap109:
Past trends and future trajectories of park−wide mean values for Winter evaporation in Arches. Topmost panel depicts the historical mean from 1980−2018. Lower four panels show the emission scenarios of RCP 4.5 and RCP 8.5 at near−term and long−term timeframes. Bottom four panels depict the change from the historical mean; cross hatching denotes areas of robust predicitons (90% of models agree in the direction of change).

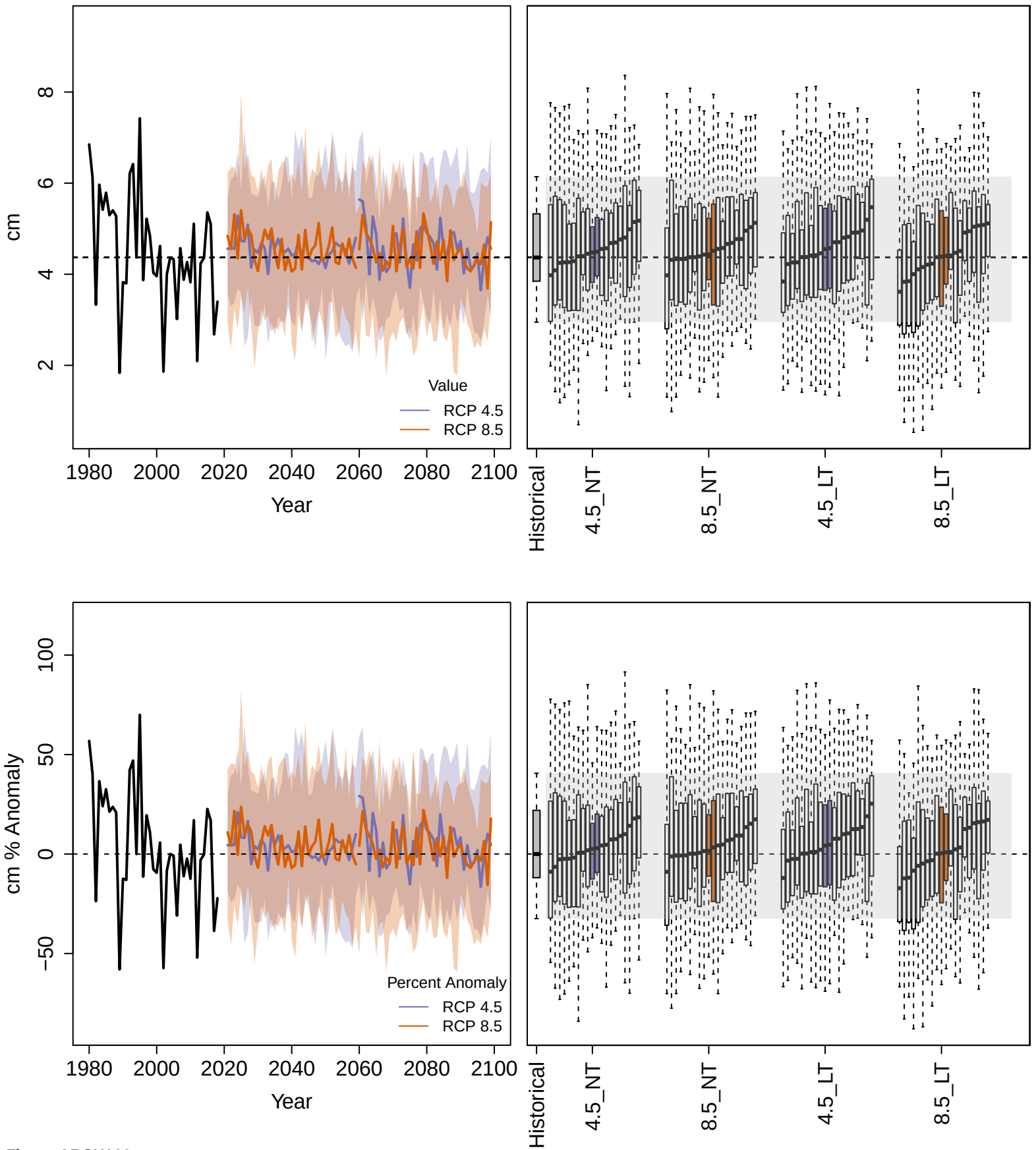


Figure ARCH111:
Past trends and future trajectories of park−wide mean values for Spring evaporation in Arches. Top panels show values, bottom panels show changes from the long−term historical mean. Left: Time series of historical (black) and future projections for RCP 4.5 and 8.5. Shaded areas show spread among climate models. Right: Boxplots of temporal variability over 40−year periods under historical (left box) and individual climate models under two RCPs. Right: Historical time period is 1970−2010; near−term (NT) is 2020−2060; long−term (LT) is 2061−2100.

Arches: Spring evaporation

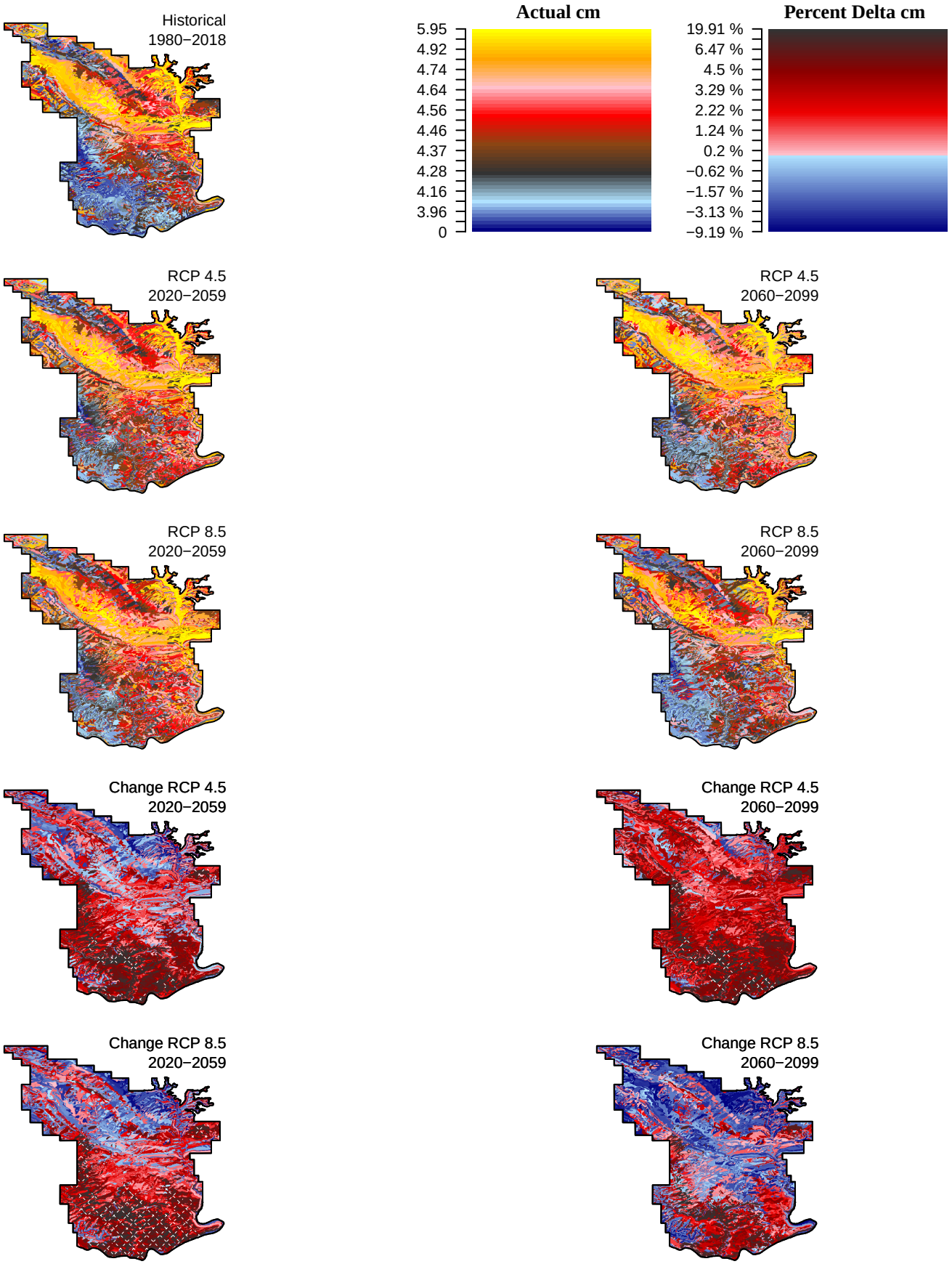


Figure ARCHmap111:
Past trends and future trajectories of park−wide mean values for Spring evaporation in Arches. Topmost panel depicts the historical mean from 1980−2018. Lower four panels show the emission scenarios of RCP 4.5 and RCP 8.5 at near−term and long−term timeframes. Bottom four panels depict the change from the historical mean; cross hatching denotes areas of robust predicitons (90% of models agree in the direction of change).

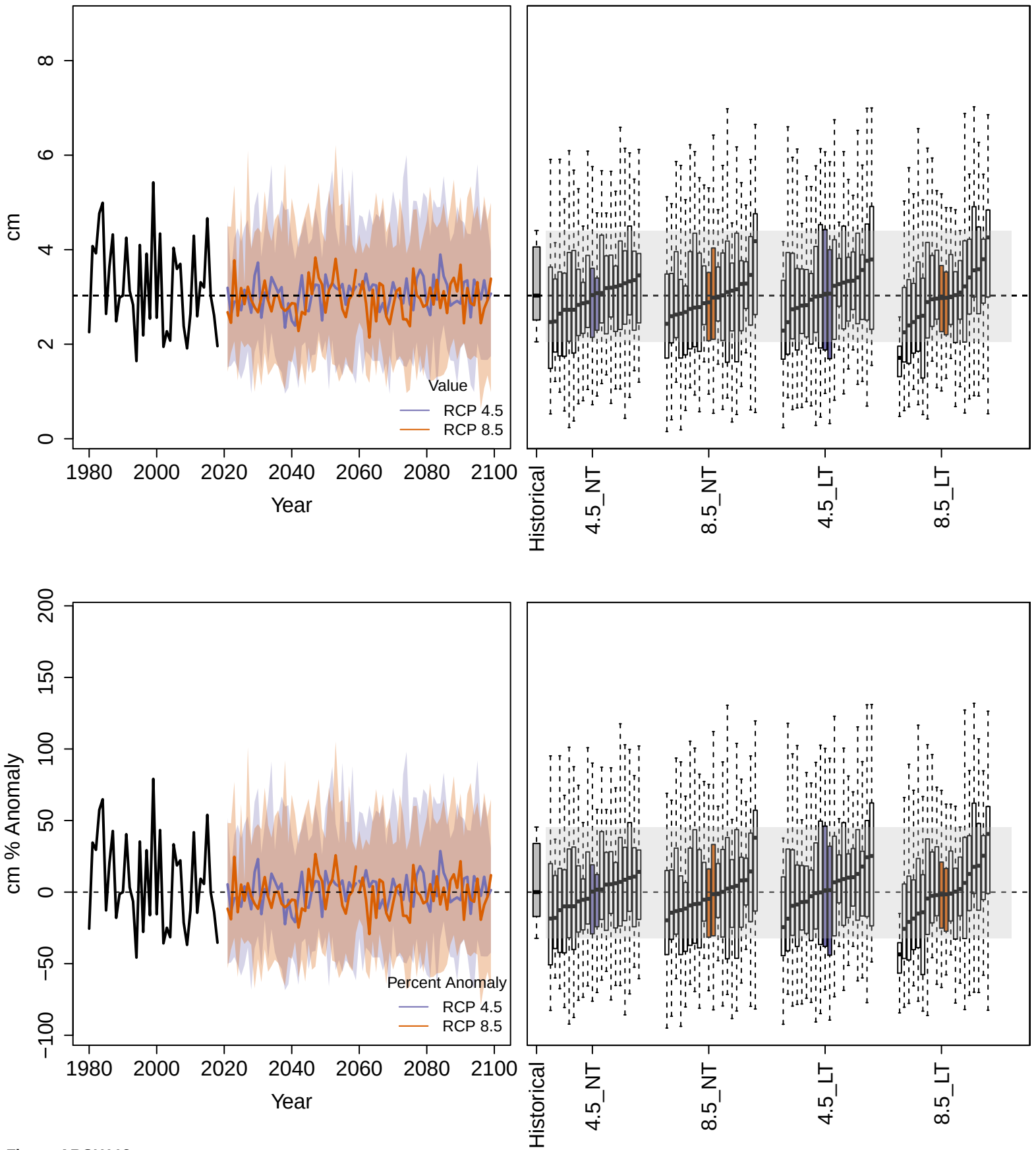


Figure ARCH113:
Past trends and future trajectories of park−wide mean values for Summer evaporation in Arches. Top panels show values, bottom panels show changes from the long−term historical mean. Left: Time series of historical (black) and future projections for RCP 4.5 and 8.5. Shaded areas show spread among climate models. Right: Boxplots of temporal variability over 40−year periods under historical (left box) and individual climate models under two RCPs. Right: Historical time period is 1970−2010; near−term (NT) is 2020−2060; long−term (LT) is 2061−2100.

Arches: Summer evaporation

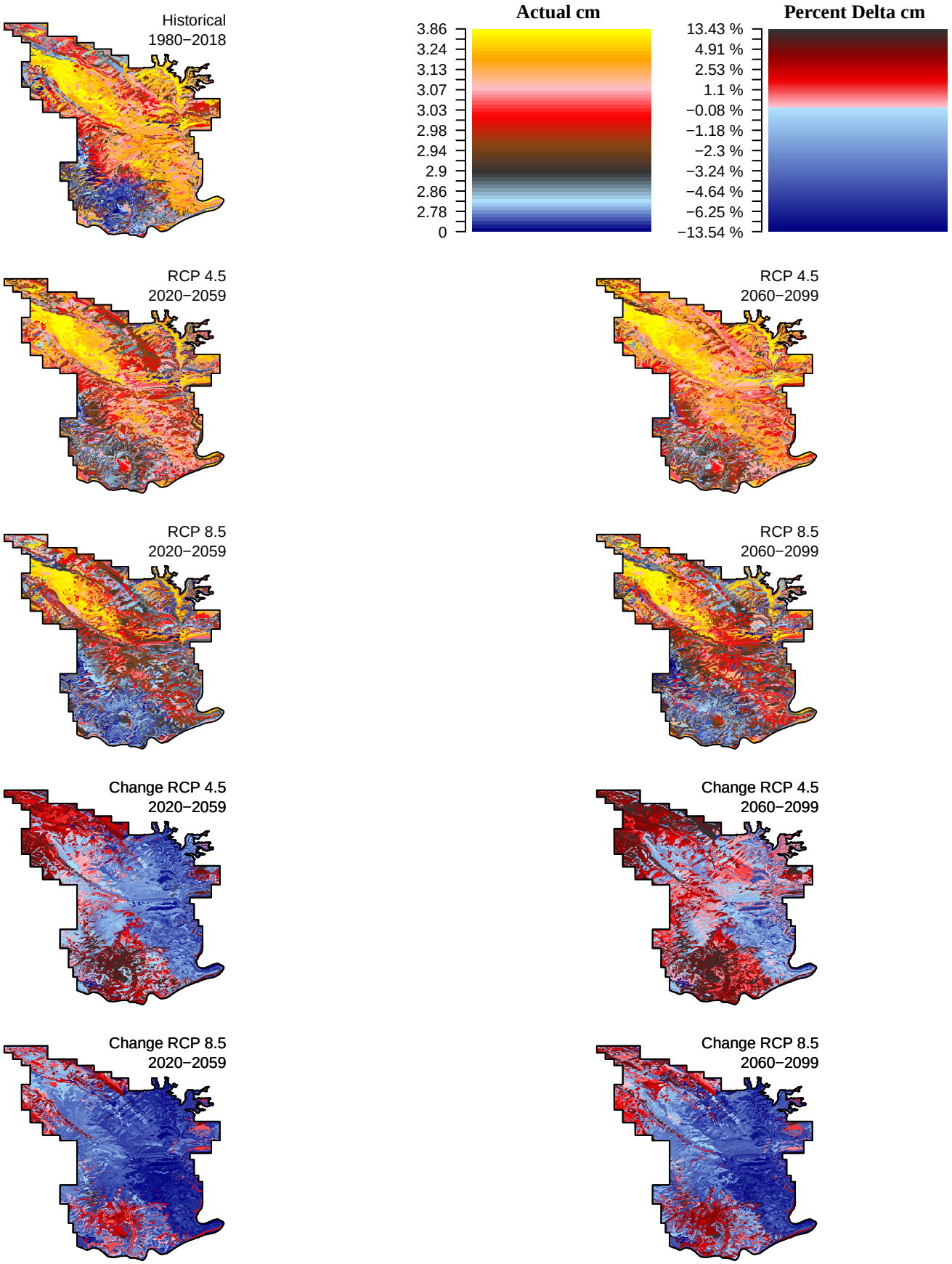


Figure ARCHmap113:
Past trends and future trajectories of park−wide mean values for Summer evaporation in Arches. Topmost panel depicts the historical mean from 1980−2018. Lower four panels show the emission scenarios of RCP 4.5 and RCP 8.5 at near−term and long−term timeframes. Bottom four panels depict the change from the historical mean; cross hatching denotes areas of robust predicitons (90% of models agree in the direction of change).

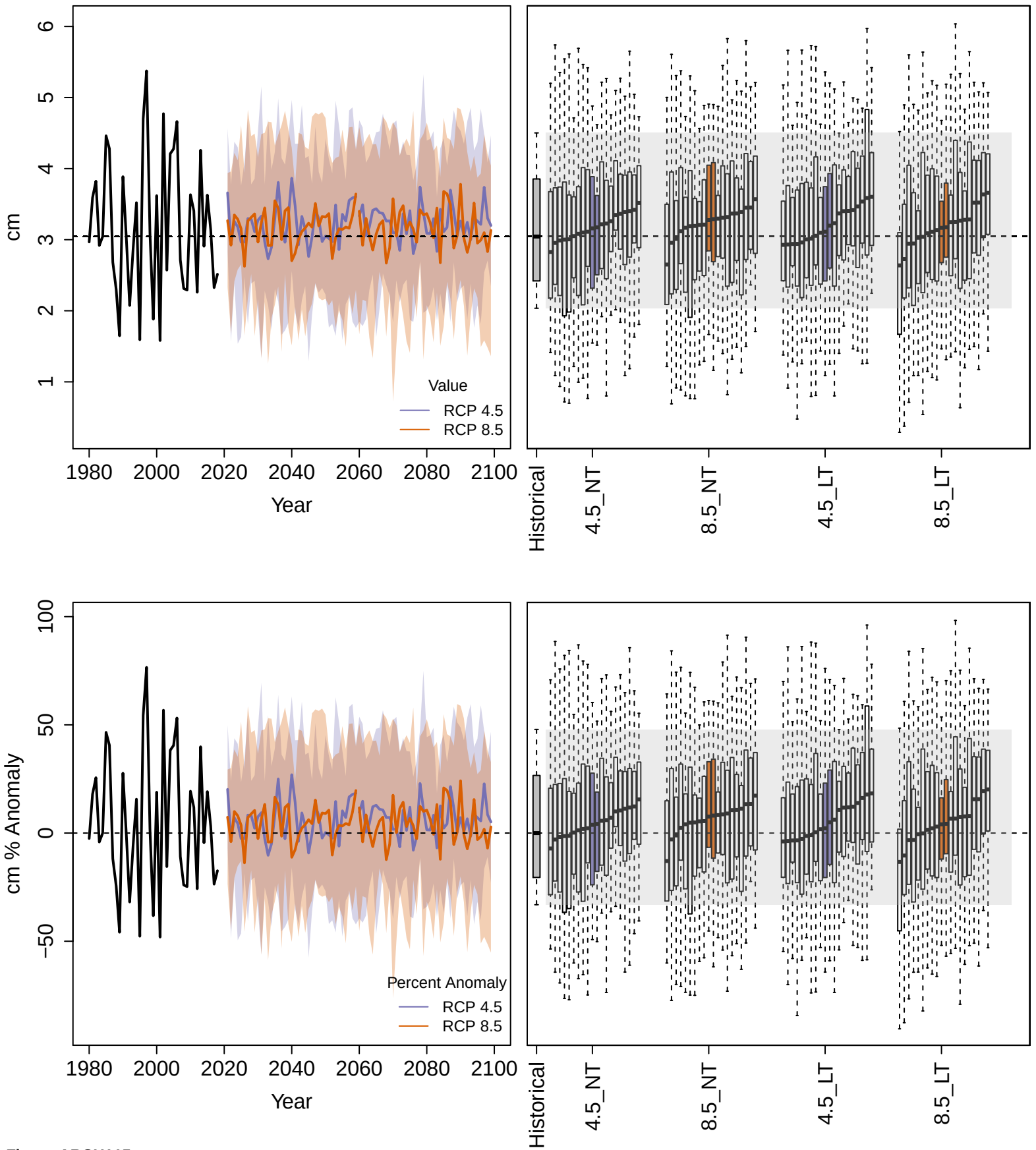


Figure ARCH115:
Past trends and future trajectories of park−wide mean values for Fall evaporation in Arches. Top panels show values, bottom panels show changes from the long−term historical mean. Left: Time series of historical (black) and future projections for RCP 4.5 and 8.5. Shaded areas show spread among climate models. Right: Boxplots of temporal variability over 40−year periods under historical (left box) and individual climate models under two RCPs. Right: Historical time period is 1970−2010; near−term (NT) is 2020−2060; long−term (LT) is 2061−2100.

Arches: Fall evaporation

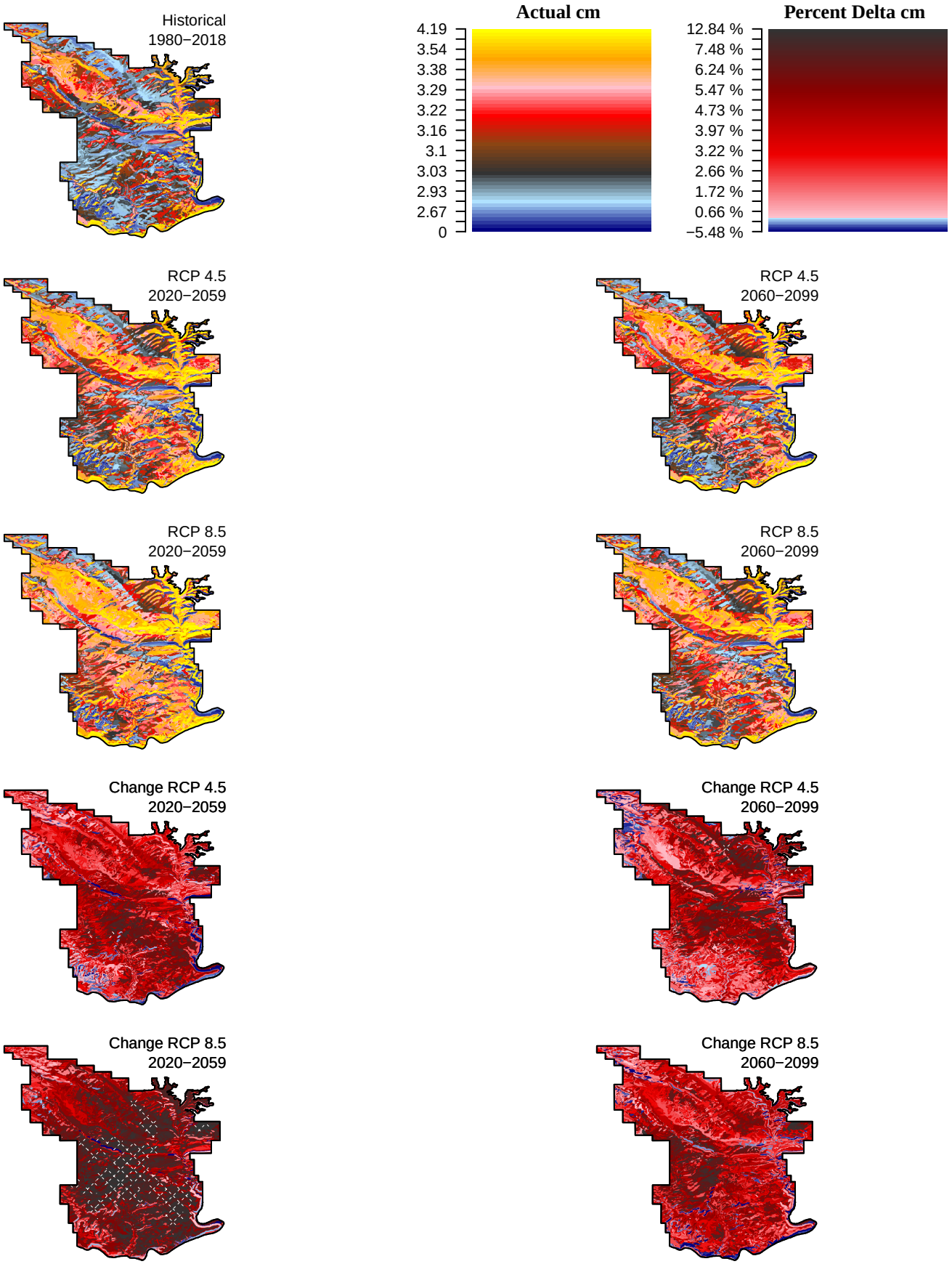


Figure ARCHmap115:
Past trends and future trajectories of park−wide mean values for Fall evaporation in Arches. Topmost panel depicts the historical mean from 1980−2018. Lower four panels show the emission scenarios of RCP 4.5 and RCP 8.5 at near−term and long−term timeframes. Bottom four panels depict the change from the historical mean; cross hatching denotes areas of robust predicitons (90% of models agree in the direction of change).

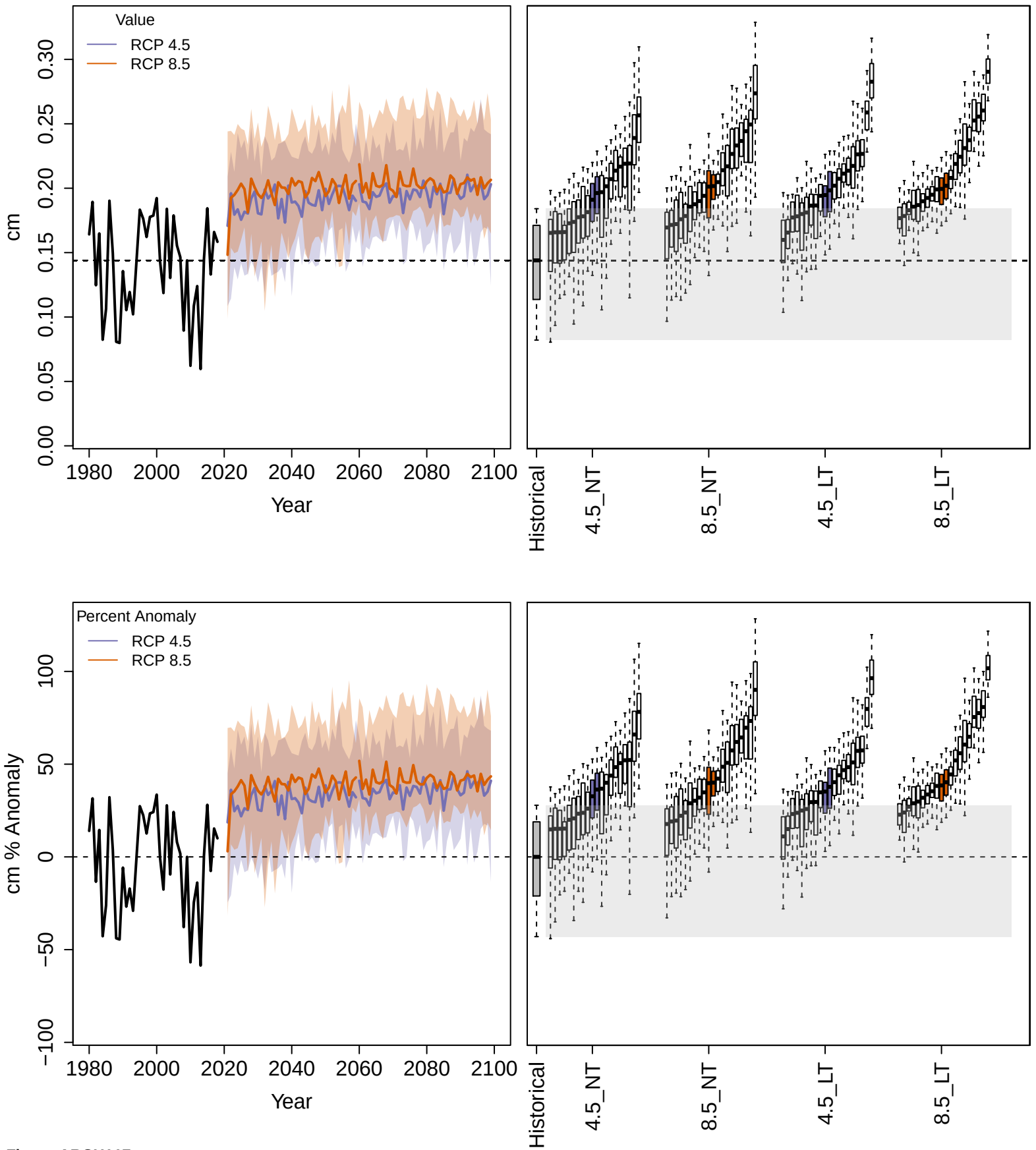


Figure ARCH117:
Past trends and future trajectories of park−wide mean values for Winter transpiration in Arches. Top panels show values, bottom panels show changes from the long−term historical mean. Left: Time series of historical (black) and future projections for RCP 4.5 and 8.5. Shaded areas show spread among climate models. Right: Boxplots of temporal variability over 40−year periods under historical (left box) and individual climate models under two RCPs. Right: Historical time period is 1970−2010; near−term (NT) is 2020−2060; long−term (LT) is 2061−2100.

Arches: Winter transpiration

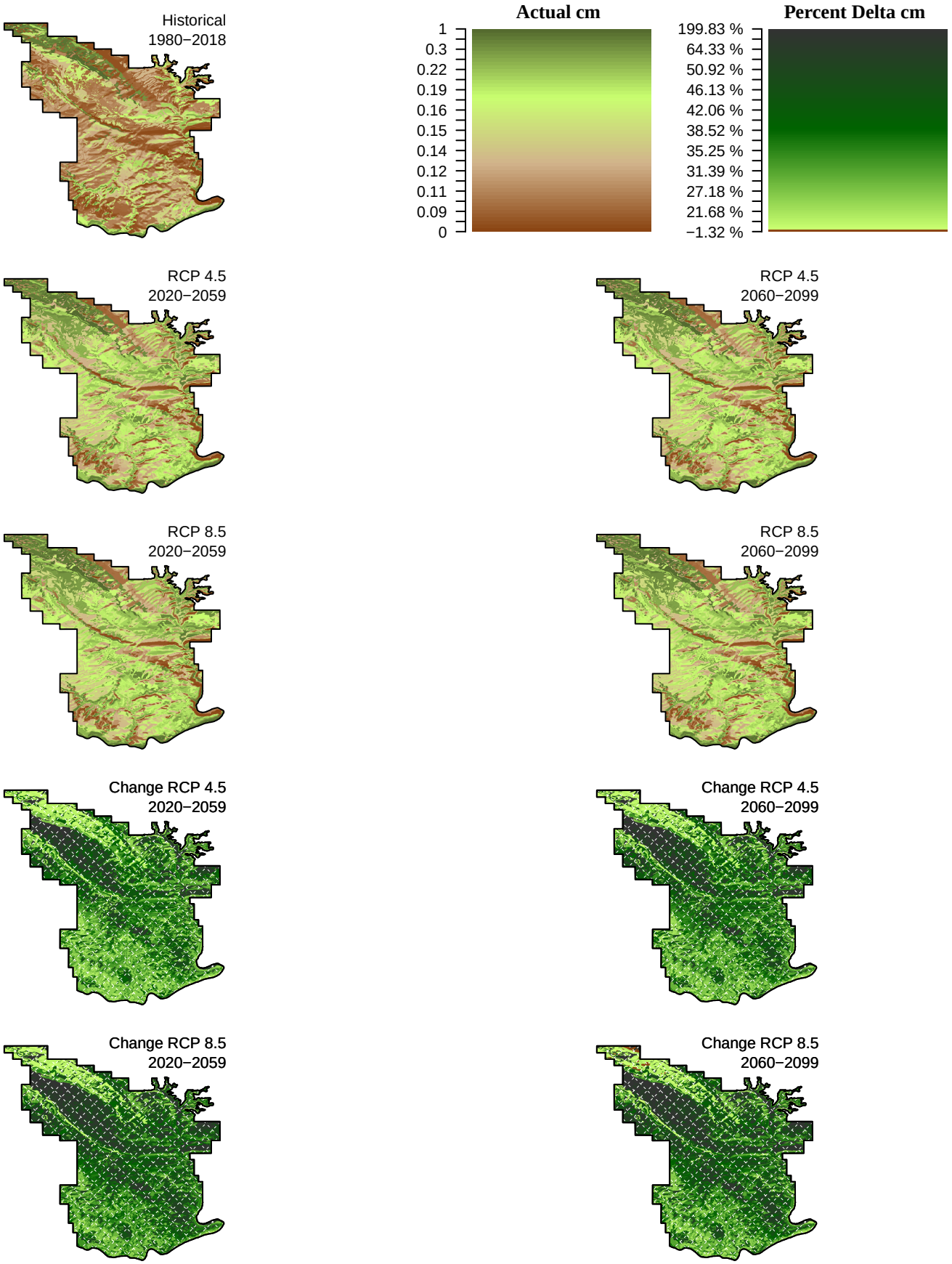


Figure ARCHmap117:
Past trends and future trajectories of park−wide mean values for Winter transpiration in Arches. Topmost panel depicts the historical mean from 1980−2018. Lower four panels show the emission scenarios of RCP 4.5 and RCP 8.5 at near−term and long−term timeframes. Bottom four panels depict the change from the historical mean; cross hatching denotes areas of robust predicitons (90% of models agree in the direction of change).

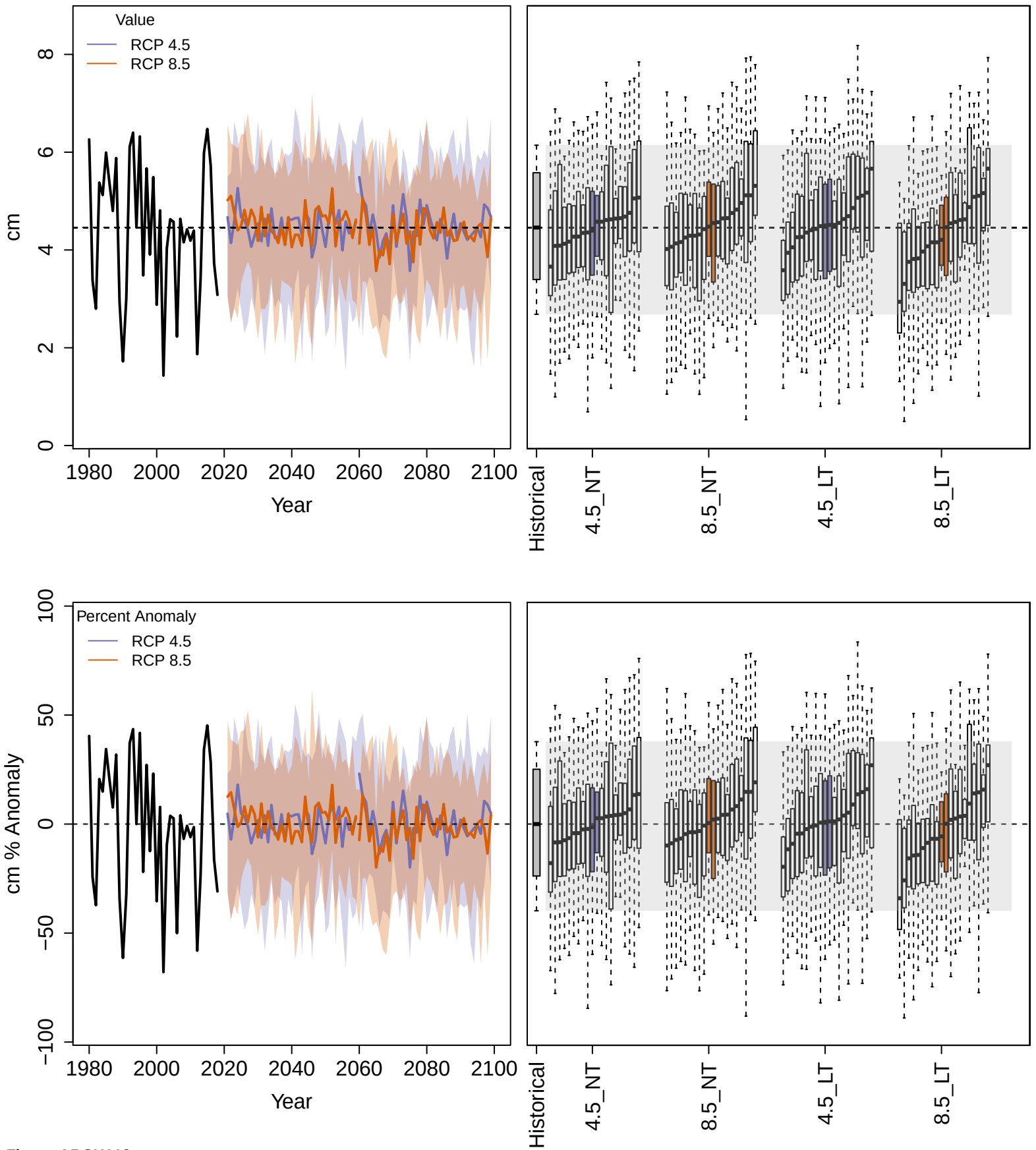


Figure ARCH119:
Past trends and future trajectories of park−wide mean values for Spring transpiration in Arches. Top panels show values, bottom panels show changes from the long−term historical mean. Left: Time series of historical (black) and future projections for RCP 4.5 and 8.5. Shaded areas show spread among climate models. Right: Boxplots of temporal variability over 40−year periods under historical (left box) and individual climate models under two RCPs. Right: Historical time period is 1970−2010; near−term (NT) is 2020−2060; long−term (LT) is 2061−2100.

Arches: Spring transpiration

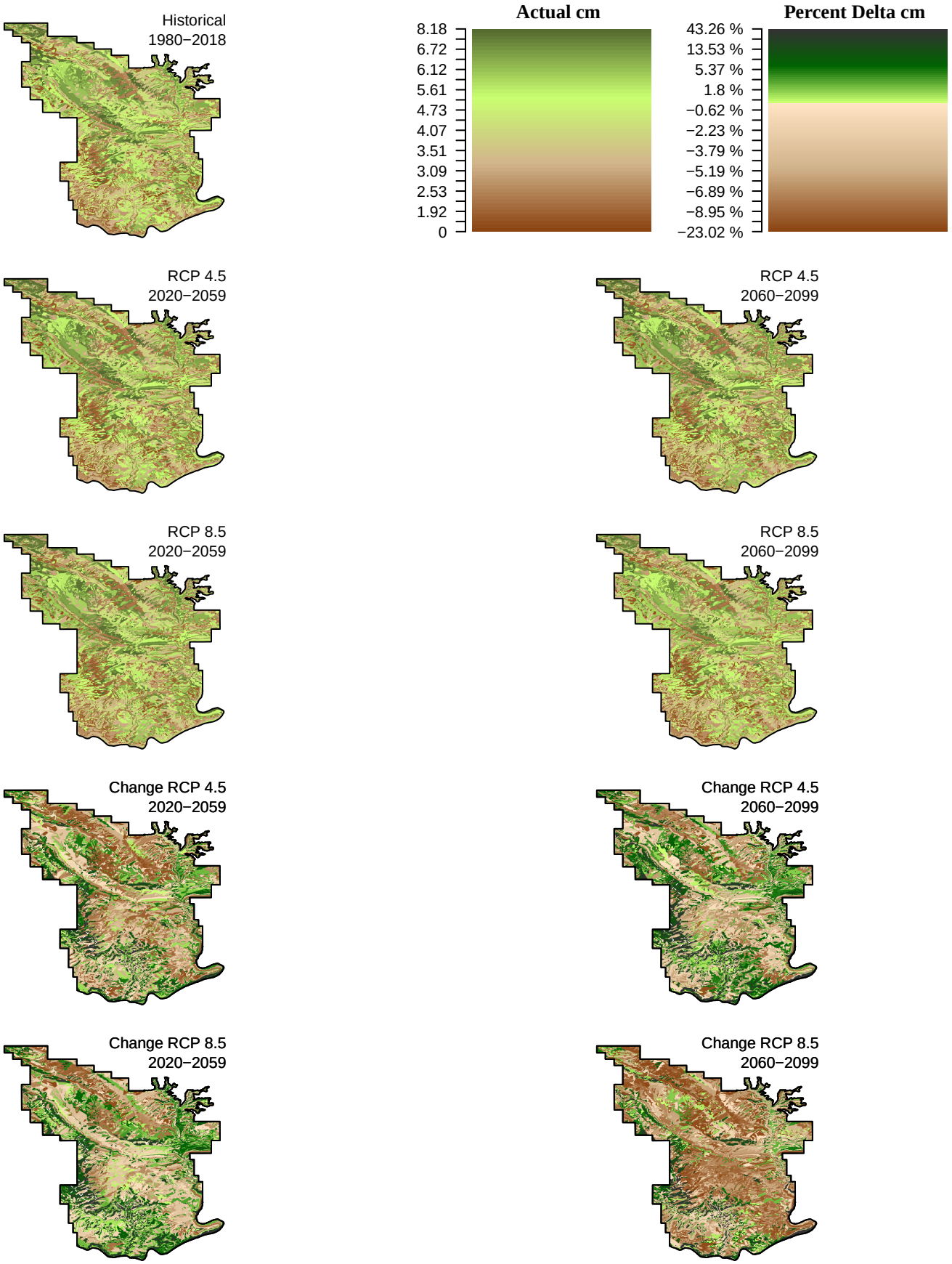


Figure ARCHmap119:
Past trends and future trajectories of park−wide mean values for Spring transpiration in Arches. Topmost panel depicts the historical mean from 1980−2018. Lower four panels show the emission scenarios of RCP 4.5 and RCP 8.5 at near−term and long−term timeframes. Bottom four panels depict the change from the historical mean; cross hatching denotes areas of robust predicitons (90% of models agree in the direction of change).

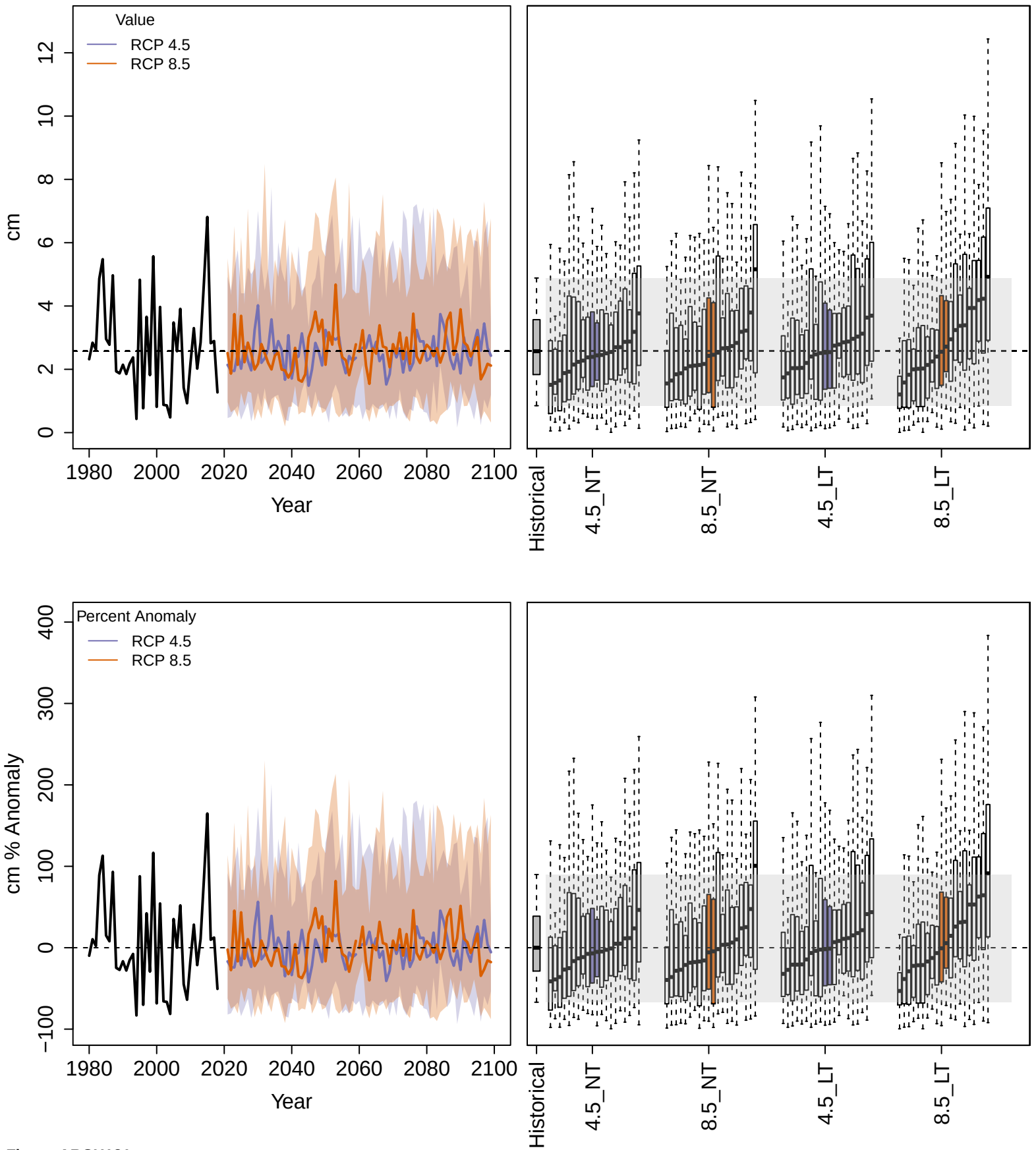


Figure ARCH121:
Past trends and future trajectories of park−wide mean values for Summer transpiration in Arches. Top panels show values, bottom panels show changes from the long−term historical mean. Left: Time series of historical (black) and future projections for RCP 4.5 and 8.5. Shaded areas show spread among climate models. Right: Boxplots of temporal variability over 40−year periods under historical (left box) and individual climate models under two RCPs. Right: Historical time period is 1970−2010; near−term (NT) is 2020−2060; long−term (LT) is 2061−2100.

Arches: Summer transpiration

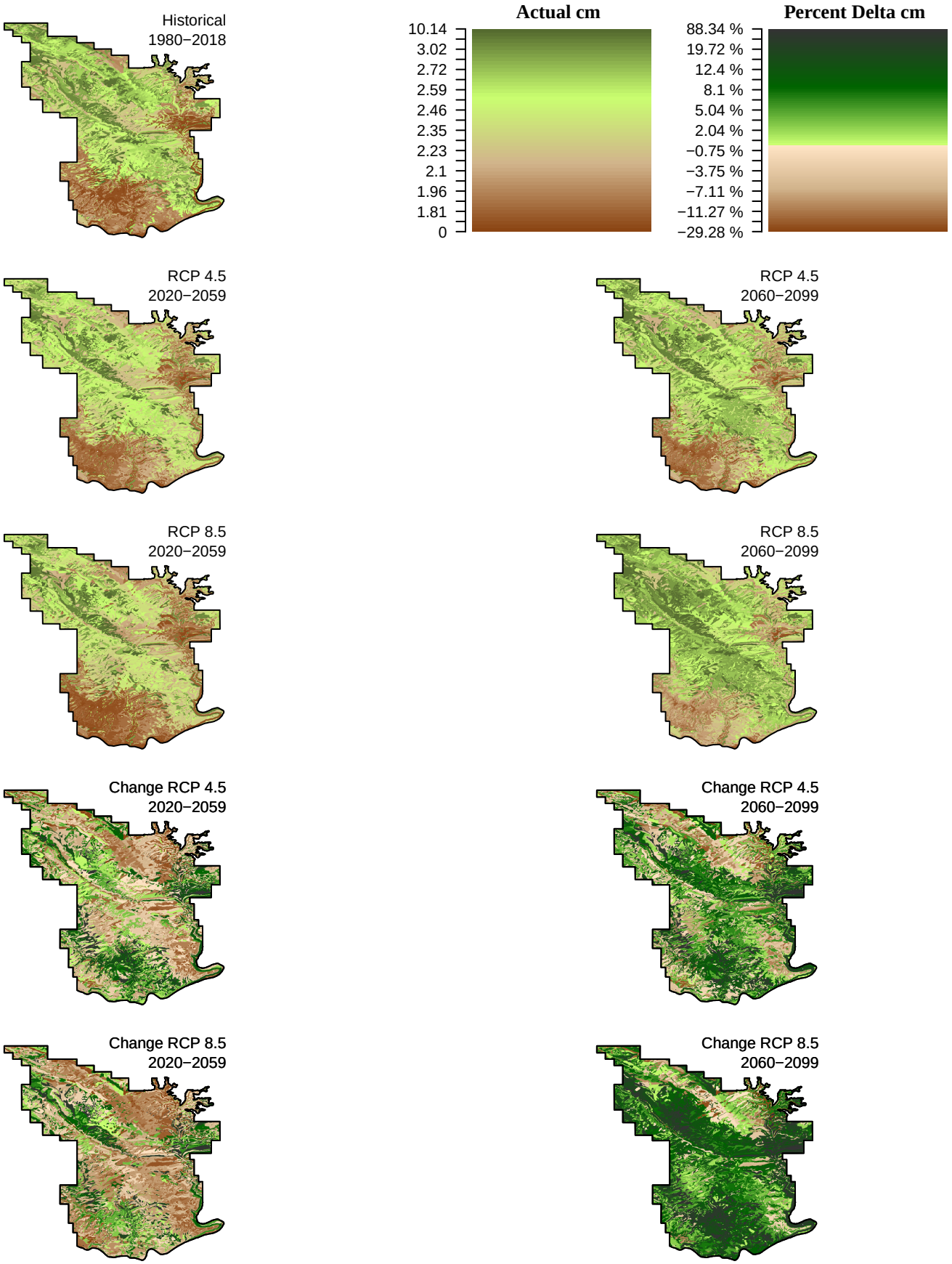


Figure ARCHmap121:
Past trends and future trajectories of park−wide mean values for Summer transpiration in Arches. Topmost panel depicts the historical mean from 1980−2018. Lower four panels show the emission scenarios of RCP 4.5 and RCP 8.5 at near−term and long−term timeframes. Bottom four panels depict the change from the historical mean; cross hatching denotes areas of robust predicitons (90% of models agree in the direction of change).

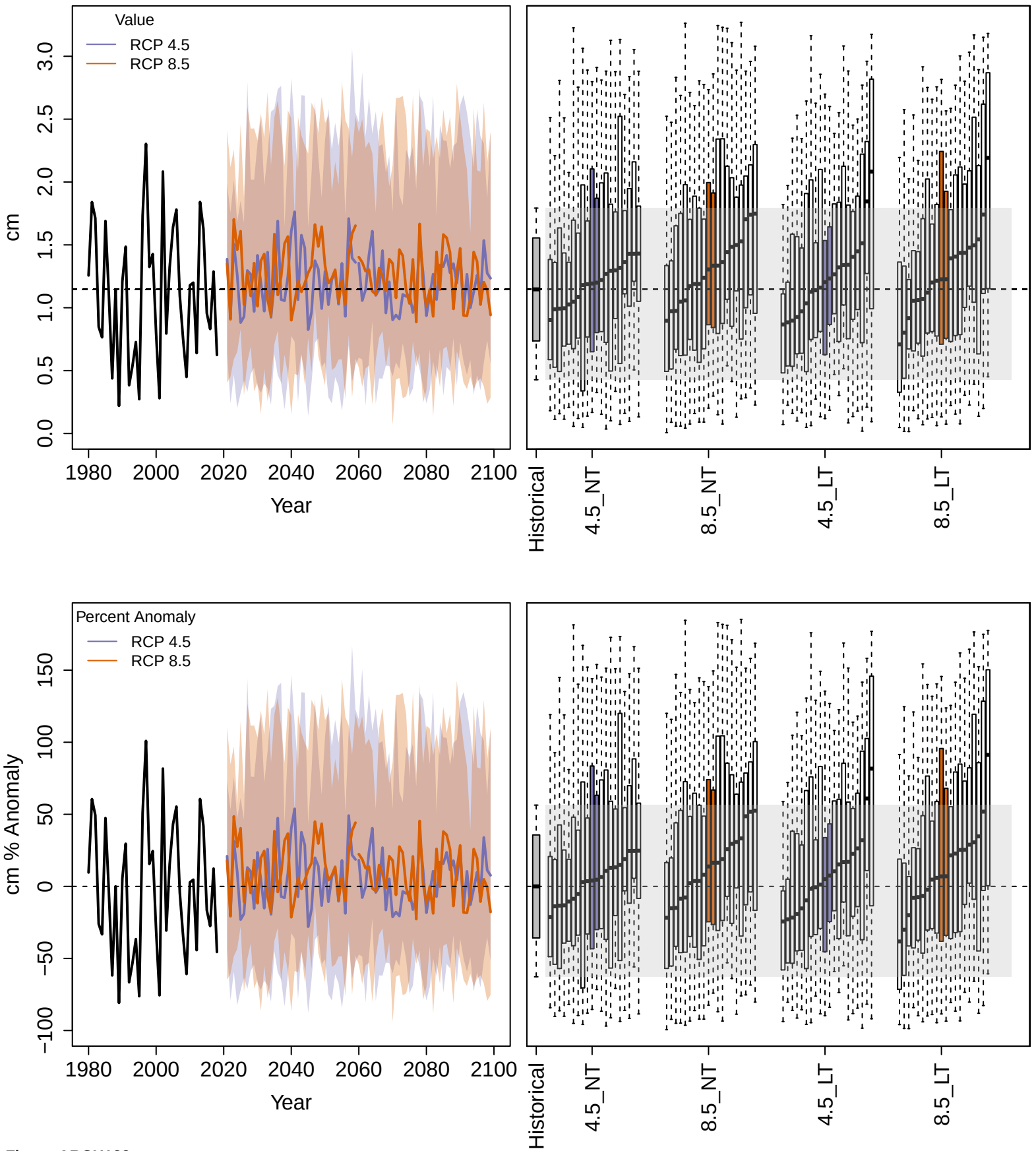


Figure ARCH123:
Past trends and future trajectories of park−wide mean values for Fall transpiration in Arches. Top panels show values, bottom panels show changes from the long−term historical mean. Left: Time series of historical (black) and future projections for RCP 4.5 and 8.5. Shaded areas show spread among climate models. Right: Boxplots of temporal variability over 40−year periods under historical (left box) and individual climate models under two RCPs. Right: Historical time period is 1970−2010; near−term (NT) is 2020−2060; long−term (LT) is 2061−2100.

Arches: Fall transpiration

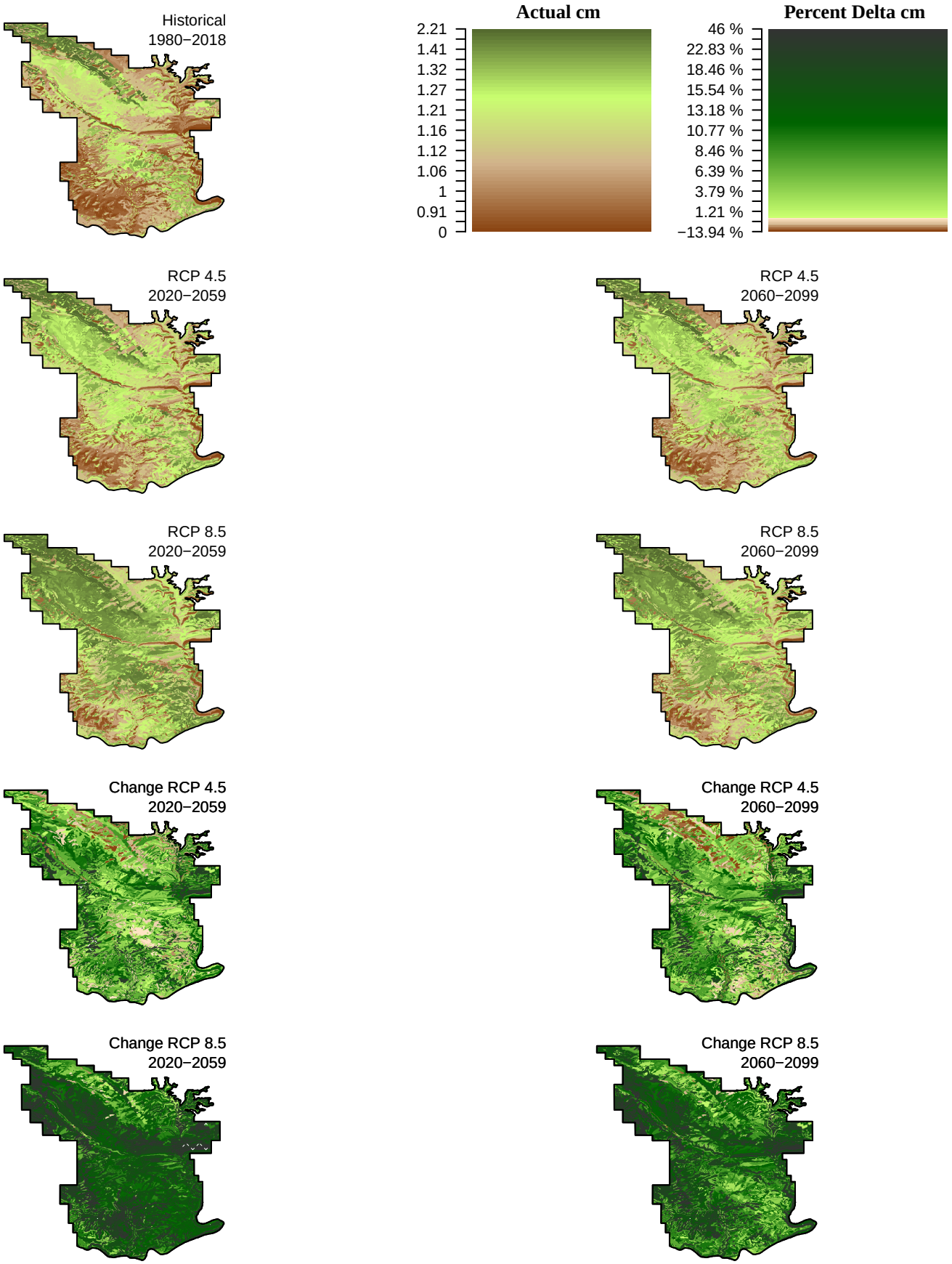


Figure ARCHmap123:
Past trends and future trajectories of park−wide mean values for Fall transpiration in Arches. Topmost panel depicts the historical mean from 1980−2018. Lower four panels show the emission scenarios of RCP 4.5 and RCP 8.5 at near−term and long−term timeframes. Bottom four panels depict the change from the historical mean; cross hatching denotes areas of robust predicitons (90% of models agree in the direction of change).

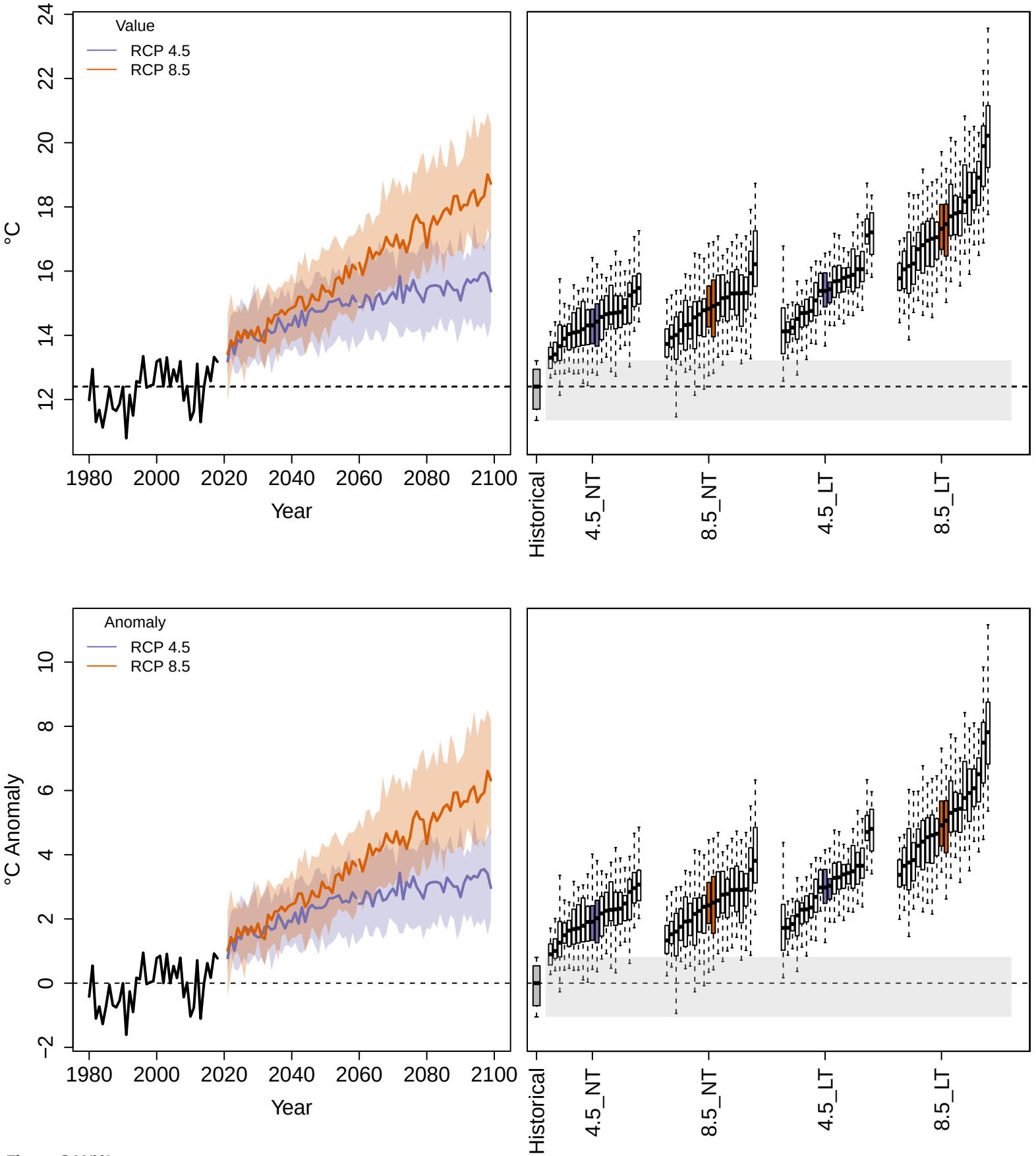


Figure CANY1:
Past trends and future trajectories of park−wide mean values for Mean Annual Temperature in Canyonlands. Top panels show values, bottom panels show changes from the long−term historical mean. Left: Time series of historical (black) and future projections for RCP 4.5 and 8.5. Shaded areas show spread among climate models. Right: Boxplots of temporal variability over 40−year periods under historical (left box) and individual climate models under two RCPs. Right: Historical time period is 1970−2010; near−term (NT) is 2020−2060; long−term (LT) is 2061−2100.

Canyonlands: Mean Annual Temperature

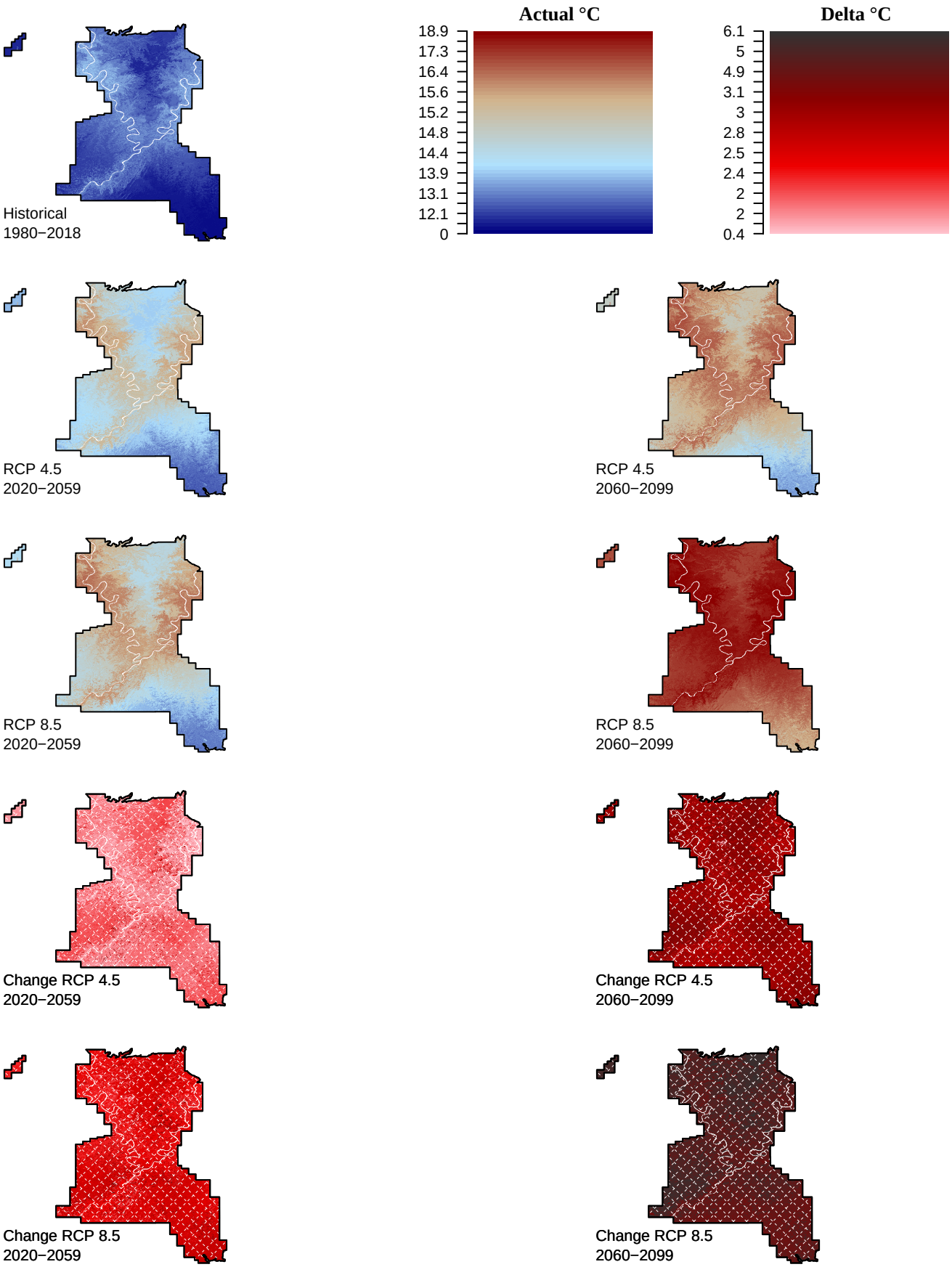


Figure CANYmap1:
Past trends and future trajectories of park−wide mean values for Mean Annual Temperature in Canyonlands. Topmost panel depicts the historical mean from 1980−2018. Lower four panels show the emission scenarios of RCP 4.5 and RCP 8.5 at near−term and long−term timeframes. Bottom four panels depict the change from the historical mean; cross hatching denotes areas of robust predicitons (90% of models agree in the direction of change).

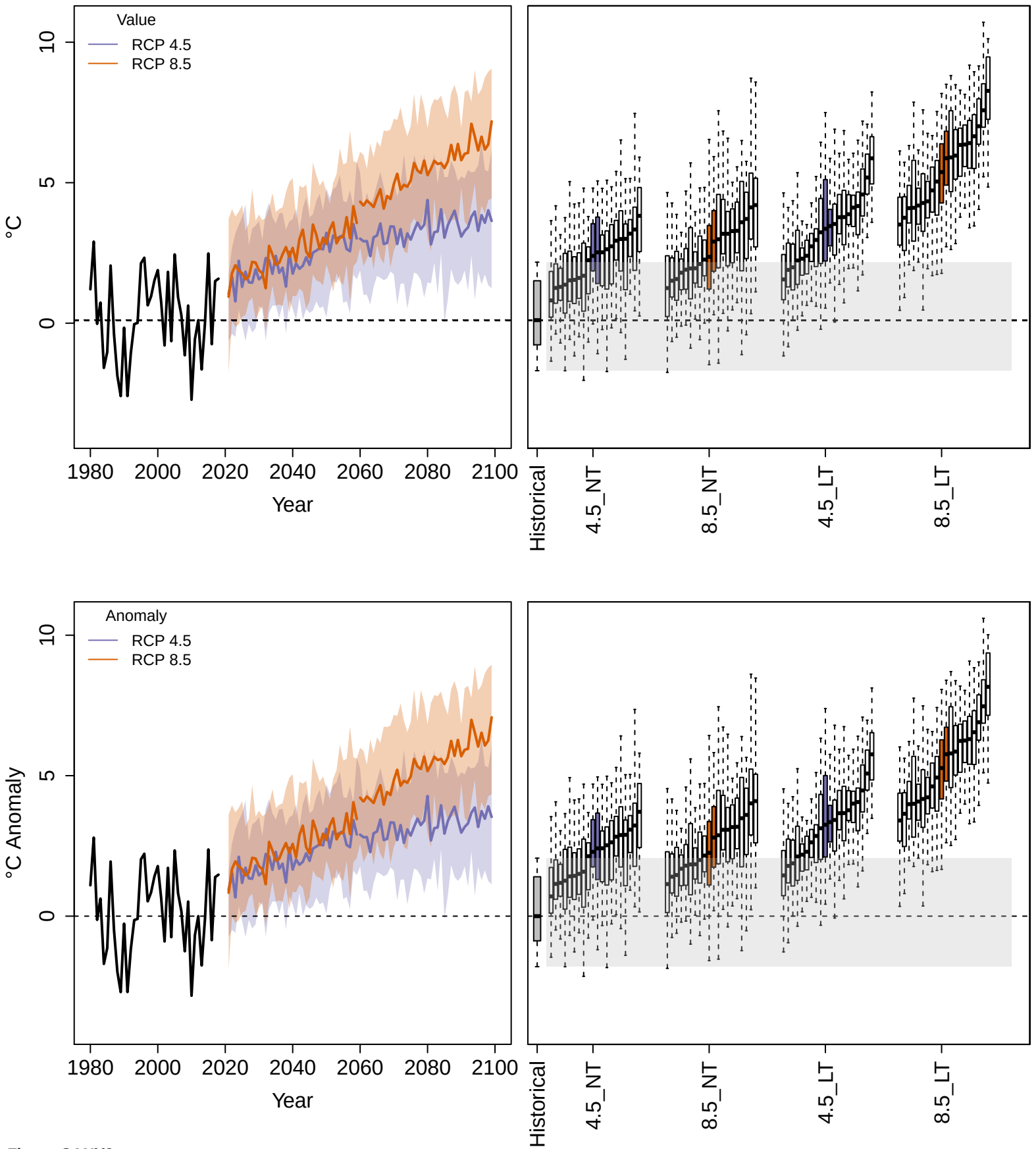


Figure CANY3:
Past trends and future trajectories of park−wide mean values for Winter Temperature in Canyonlands. Top panels show values, bottom panels show changes from the long−term historical mean. Left: Time series of historical (black) and future projections for RCP 4.5 and 8.5. Shaded areas show spread among climate models. Right: Boxplots of temporal variability over 40−year periods under historical (left box) and individual climate models under two RCPs. Right: Historical time period is 1970−2010; near−term (NT) is 2020−2060; long−term (LT) is 2061−2100.

Canyonlands: Winter Temperature

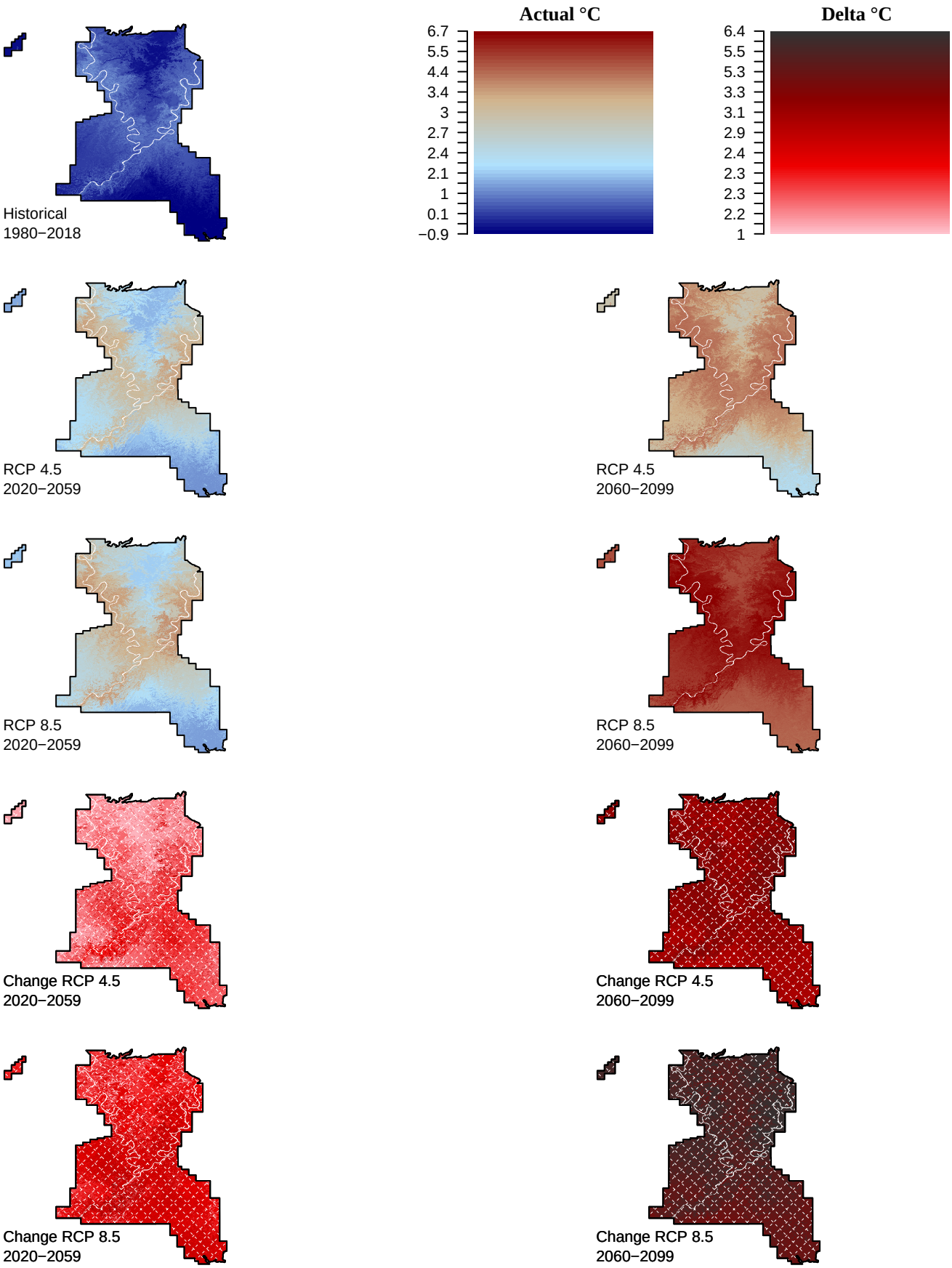


Figure CANYmap3:
Past trends and future trajectories of park−wide mean values for Winter Temperature in Canyonlands. Topmost panel depicts the historical mean from 1980−2018. Lower four panels show the emission scenarios of RCP 4.5 and RCP 8.5 at near−term and long−term timeframes. Bottom four panels depict the change from the historical mean; cross hatching denotes areas of robust predicitons (90% of models agree in the direction of change).

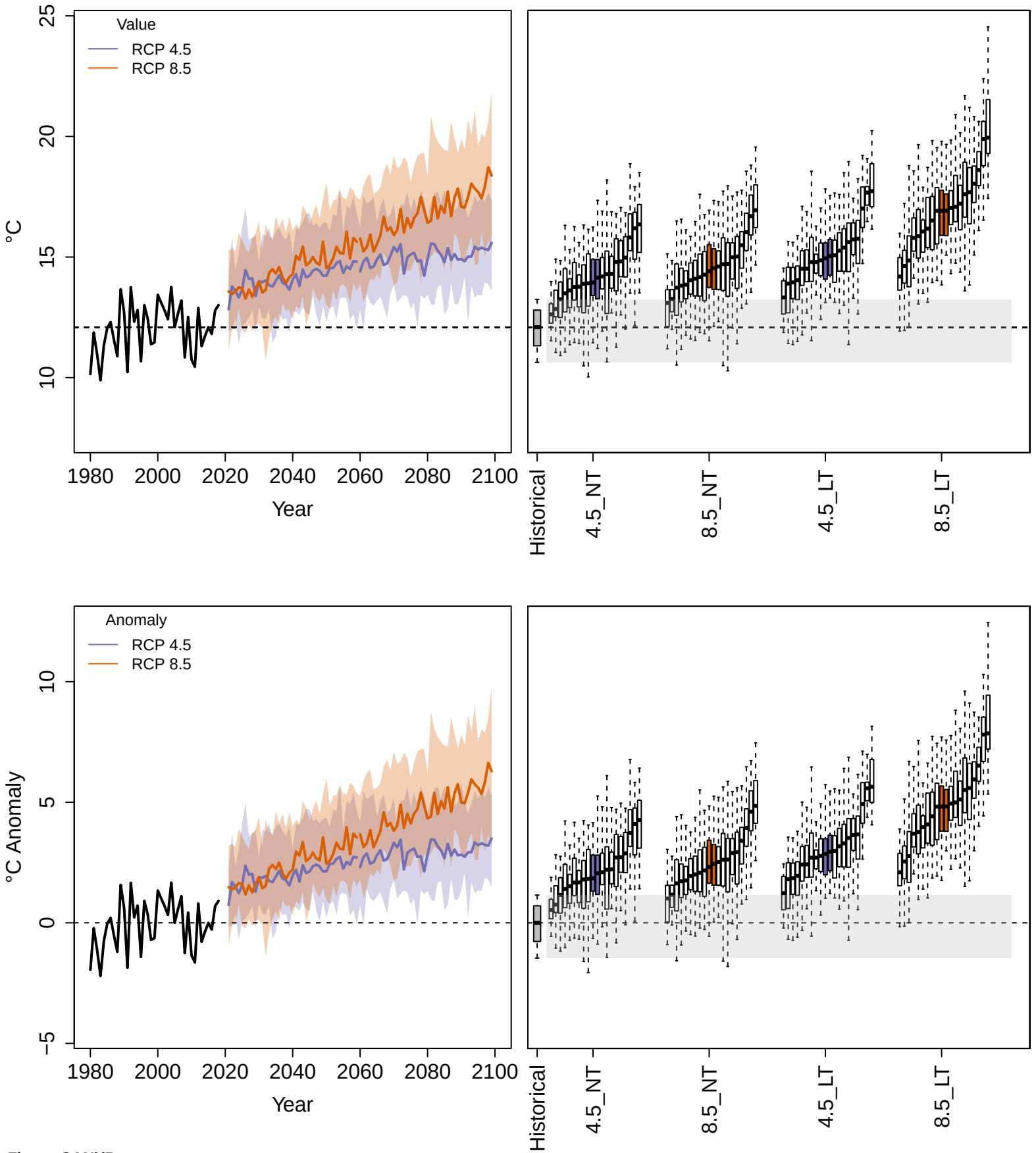


Figure CANY5:
Past trends and future trajectories of park−wide mean values for Spring Temperature in Canyonlands. Top panels show values, bottom panels show changes from the long−term historical mean. Left: Time series of historical (black) and future projections for RCP 4.5 and 8.5. Shaded areas show spread among climate models. Right: Boxplots of temporal variability over 40−year periods under historical (left box) and individual climate models under two RCPs. Right: Historical time period is 1970−2010; near−term (NT) is 2020−2060; long−term (LT) is 2061−2100.

Canyonlands: Spring Temperature

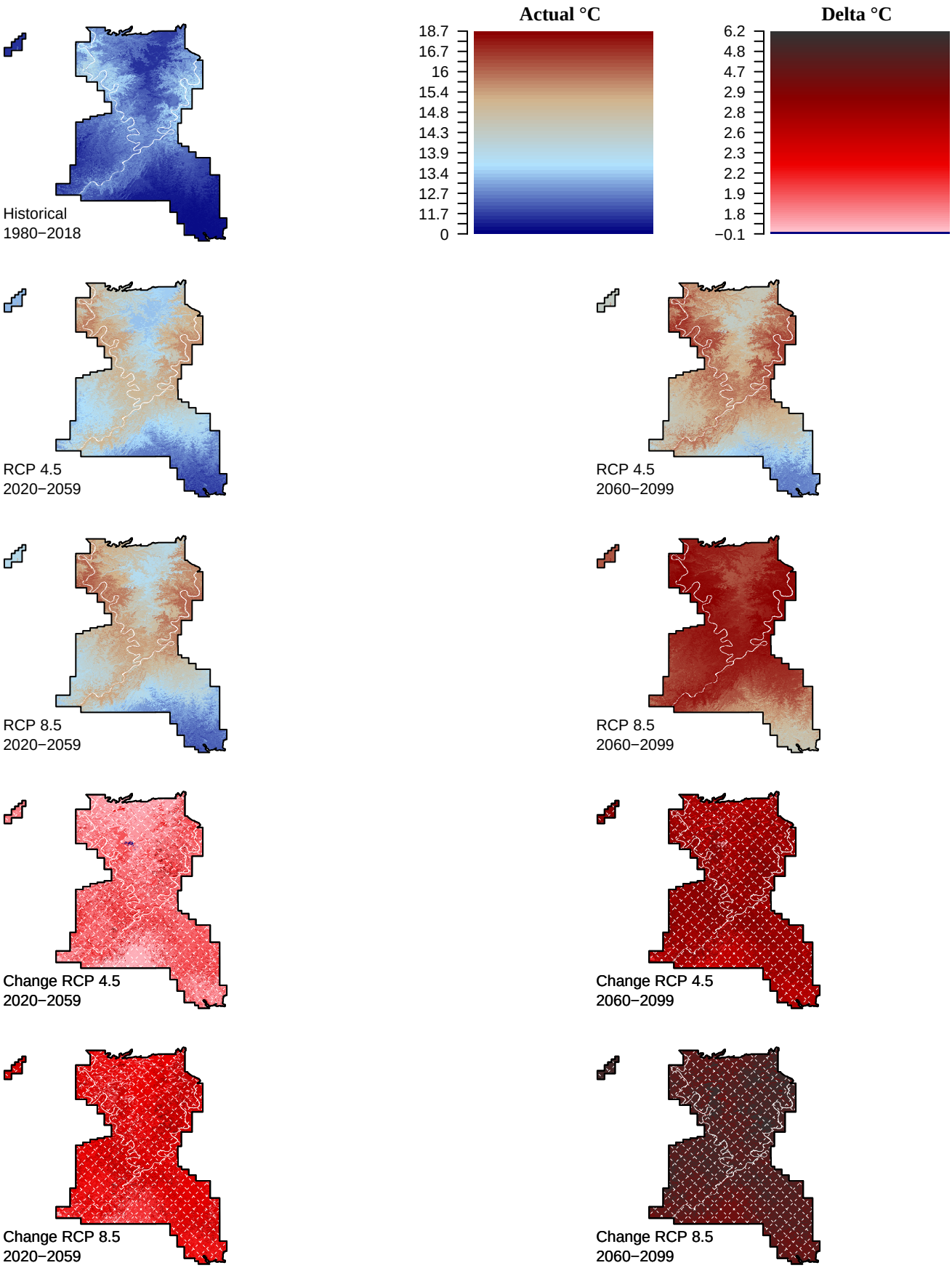


Figure CANYmap5:
Past trends and future trajectories of park−wide mean values for Spring Temperature in Canyonlands. Topmost panel depicts the historical mean from 1980−2018. Lower four panels show the emission scenarios of RCP 4.5 and RCP 8.5 at near−term and long−term timeframes. Bottom four panels depict the change from the historical mean; cross hatching denotes areas of robust predicitons (90% of models agree in the direction of change).

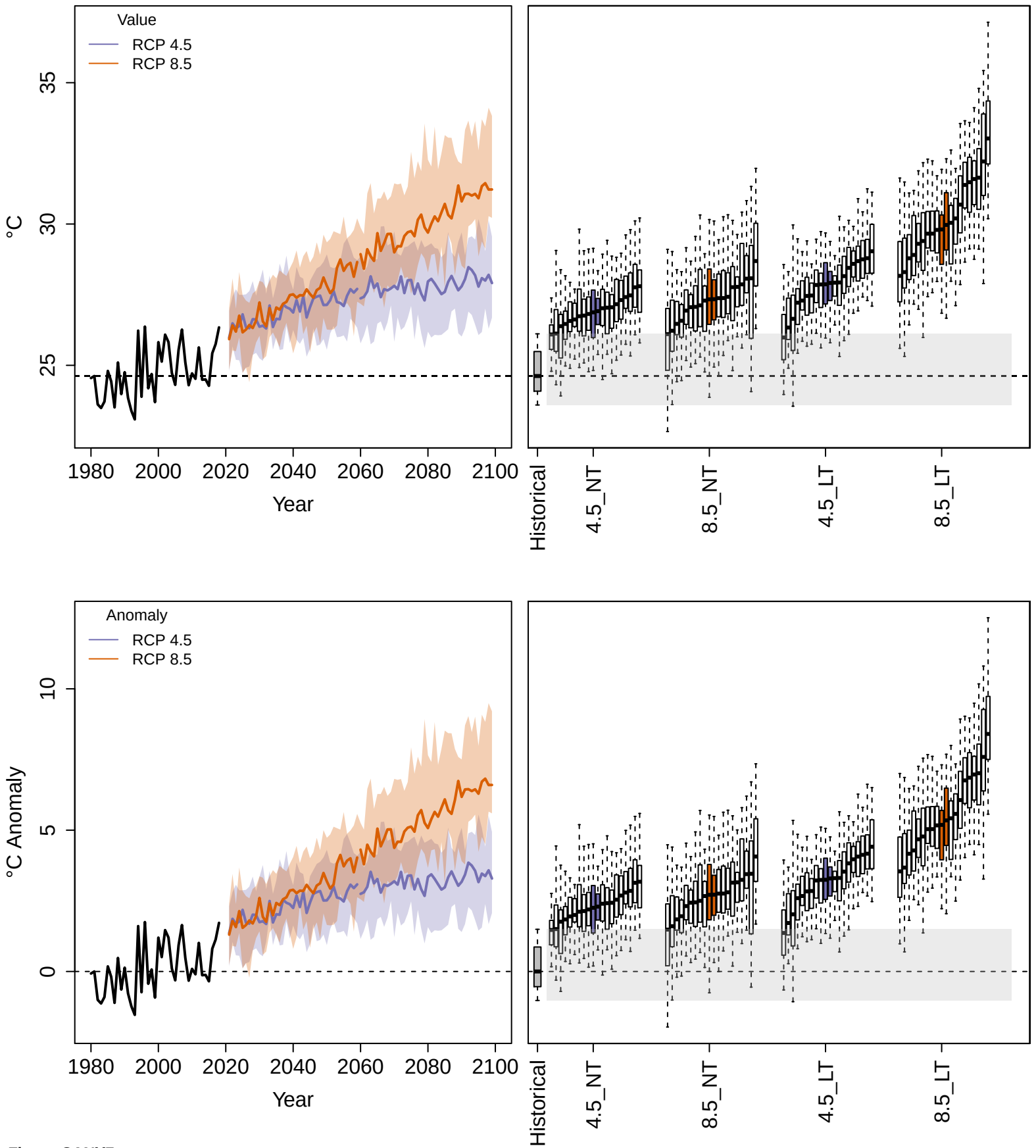


Figure CANY7:
Past trends and future trajectories of park−wide mean values for Summer Temperature in Canyonlands. Top panels show values, bottom panels show changes from the long−term historical mean. Left: Time series of historical (black) and future projections for RCP 4.5 and 8.5. Shaded areas show spread among climate models. Right: Boxplots of temporal variability over 40−year periods under historical (left box) and individual climate models under two RCPs. Right: Historical time period is 1970−2010; near−term (NT) is 2020−2060; long−term (LT) is 2061−2100.

Canyonlands: Summer Temperature

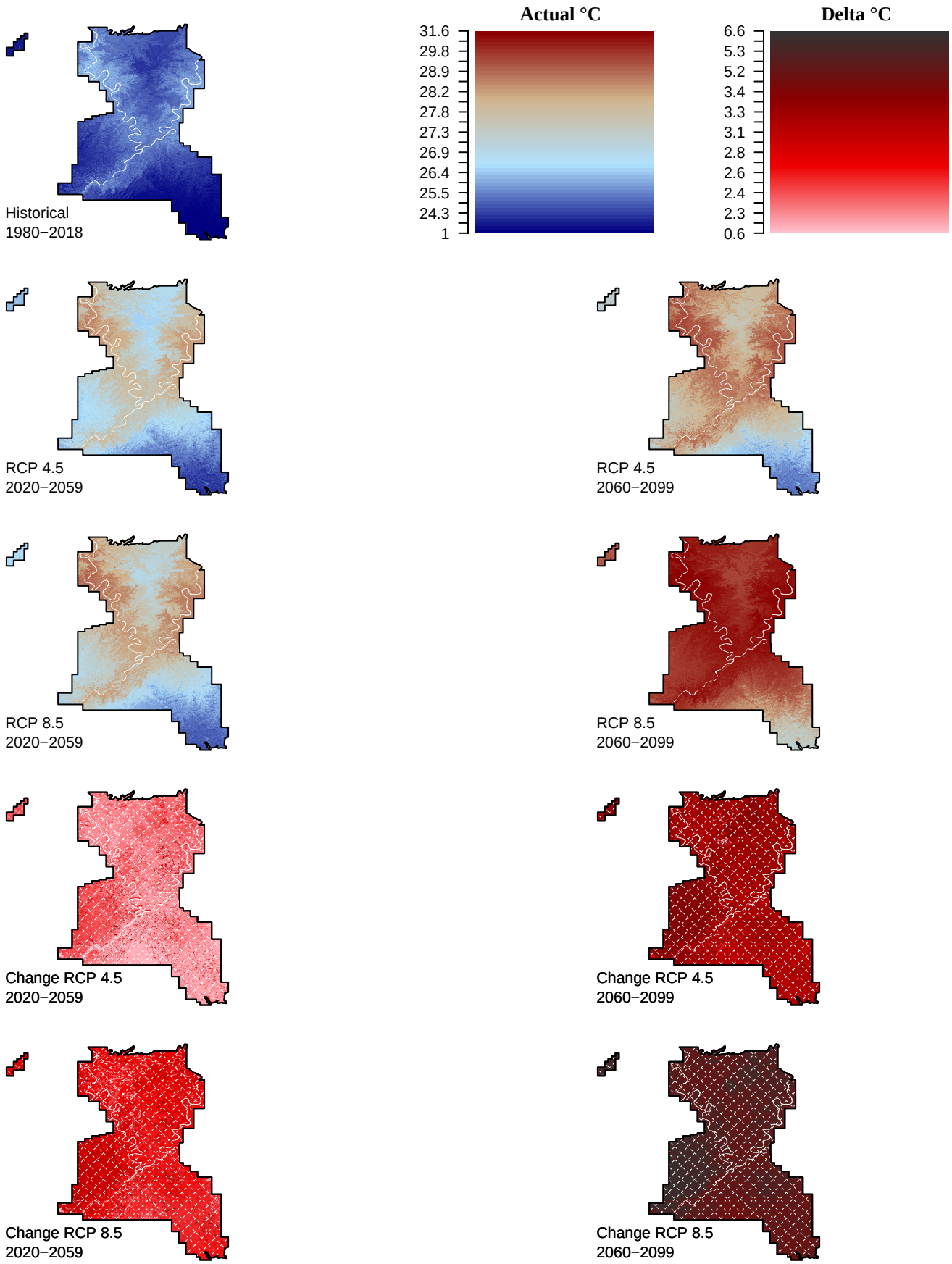


Figure CANYmap7:
Past trends and future trajectories of park−wide mean values for Summer Temperature in Canyonlands. Topmost panel depicts the historical mean from 1980−2018. Lower four panels show the emission scenarios of RCP 4.5 and RCP 8.5 at near−term and long−term timeframes. Bottom four panels depict the change from the historical mean; cross hatching denotes areas of robust predicitons (90% of models agree in the direction of change).

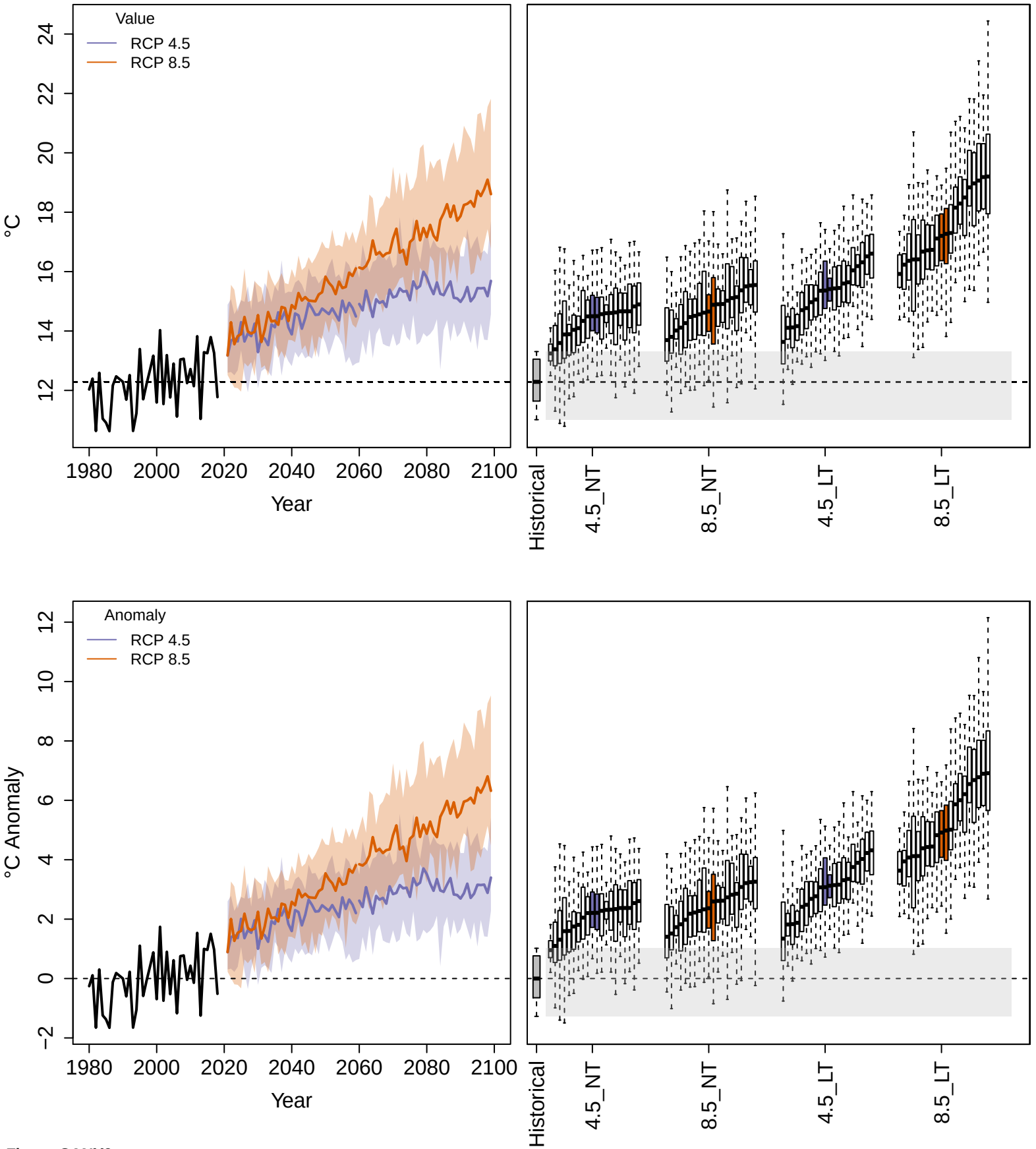


Figure CANY9:
Past trends and future trajectories of park−wide mean values for Fall Temperature in Canyonlands. Top panels show values, bottom panels show changes from the long−term historical mean. Left: Time series of historical (black) and future projections for RCP 4.5 and 8.5. Shaded areas show spread among climate models. Right: Boxplots of temporal variability over 40−year periods under historical (left box) and individual climate models under two RCPs. Right: Historical time period is 1970−2010; near−term (NT) is 2020−2060; long−term (LT) is 2061−2100.

Canyonlands: Fall Temperature

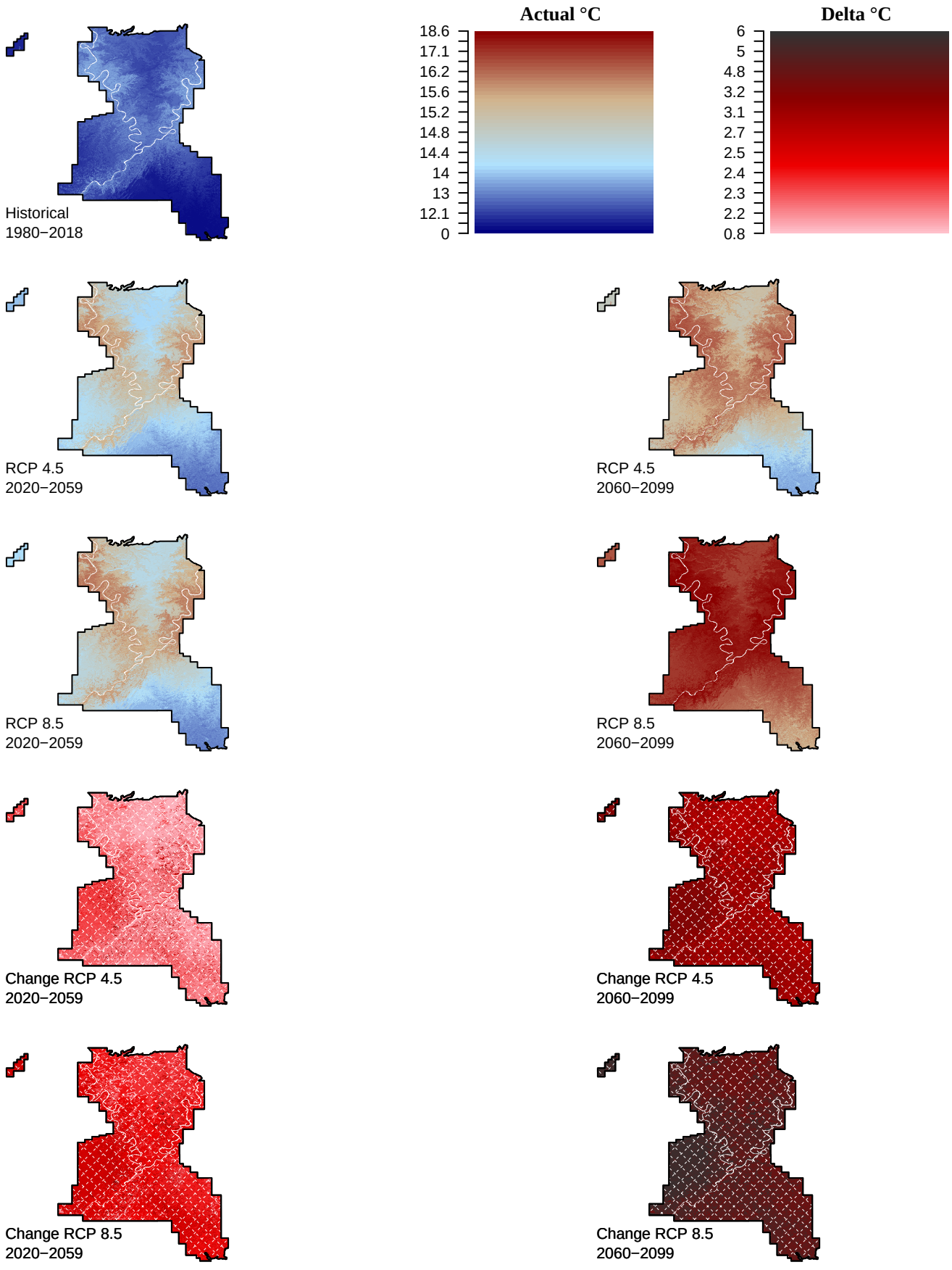


Figure CANYmap9:
Past trends and future trajectories of park−wide mean values for Fall Temperature in Canyonlands. Topmost panel depicts the historical mean from 1980−2018. Lower four panels show the emission scenarios of RCP 4.5 and RCP 8.5 at near−term and long−term timeframes. Bottom four panels depict the change from the historical mean; cross hatching denotes areas of robust predicitons (90% of models agree in the direction of change).

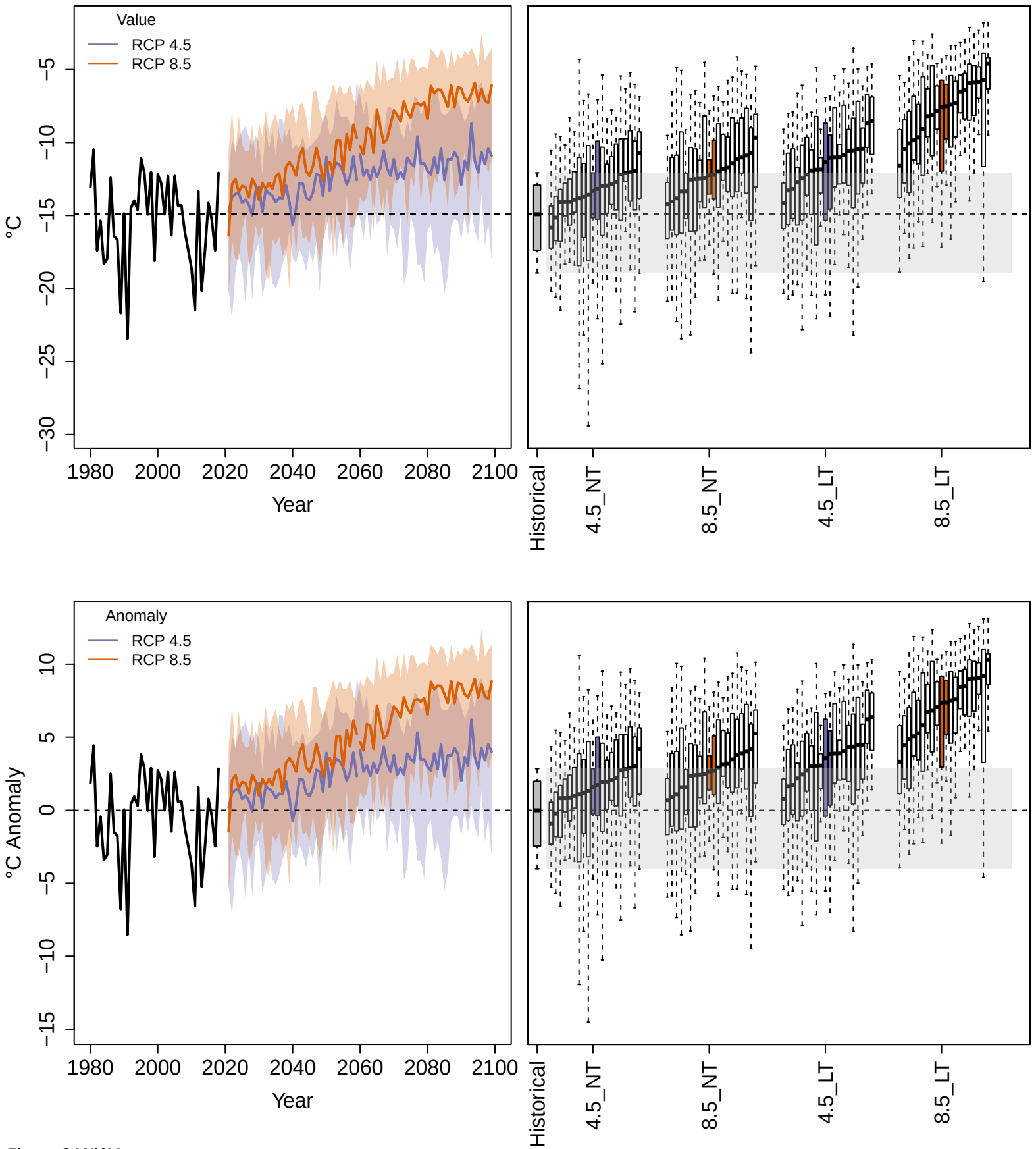


Figure CANY11:
Past trends and future trajectories of park−wide mean values for Minimum winter temperature in Canyonlands. Top panels show values, bottom panels show changes from the long−term historical mean. Left: Time series of historical (black) and future projections for RCP 4.5 and 8.5. Shaded areas show spread among climate models. Right: Boxplots of temporal variability over 40−year periods under historical (left box) and individual climate models under two RCPs. Right: Historical time period is 1970−2010; near−term (NT) is 2020−2060; long−term (LT) is 2061−2100.

Canyonlands: Minimum winter temperature

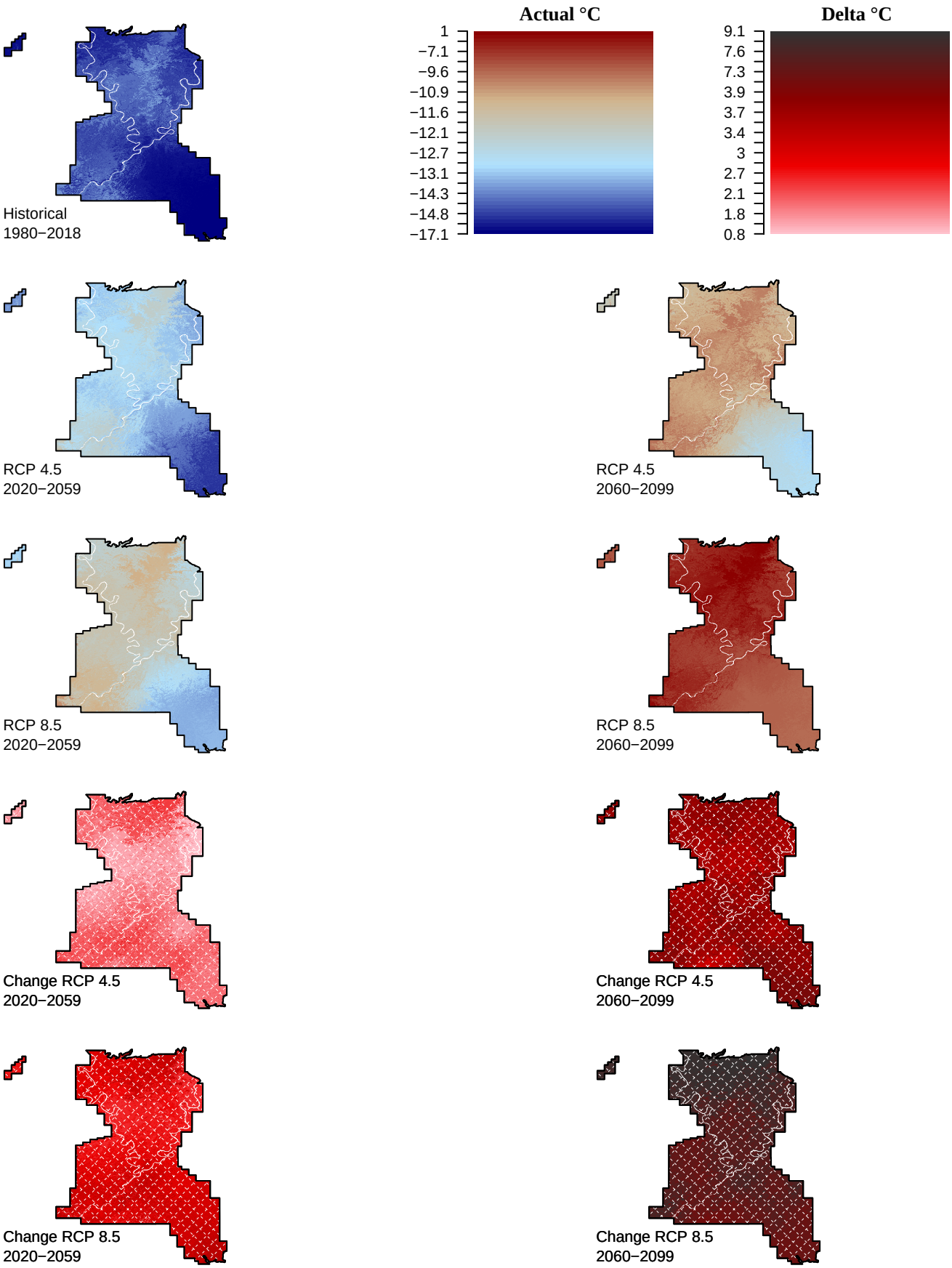


Figure CANYmap11:
Past trends and future trajectories of park−wide mean values for Minimum winter temperature in Canyonlands. Topmost panel depicts the historical mean from 1980−2018. Lower four panels show the emission scenarios of RCP 4.5 and RCP 8.5 at near−term and long−term timeframes. Bottom four panels depict the change from the historical mean; cross hatching denotes areas of robust predicitons (90% of models agree in the direction of change).

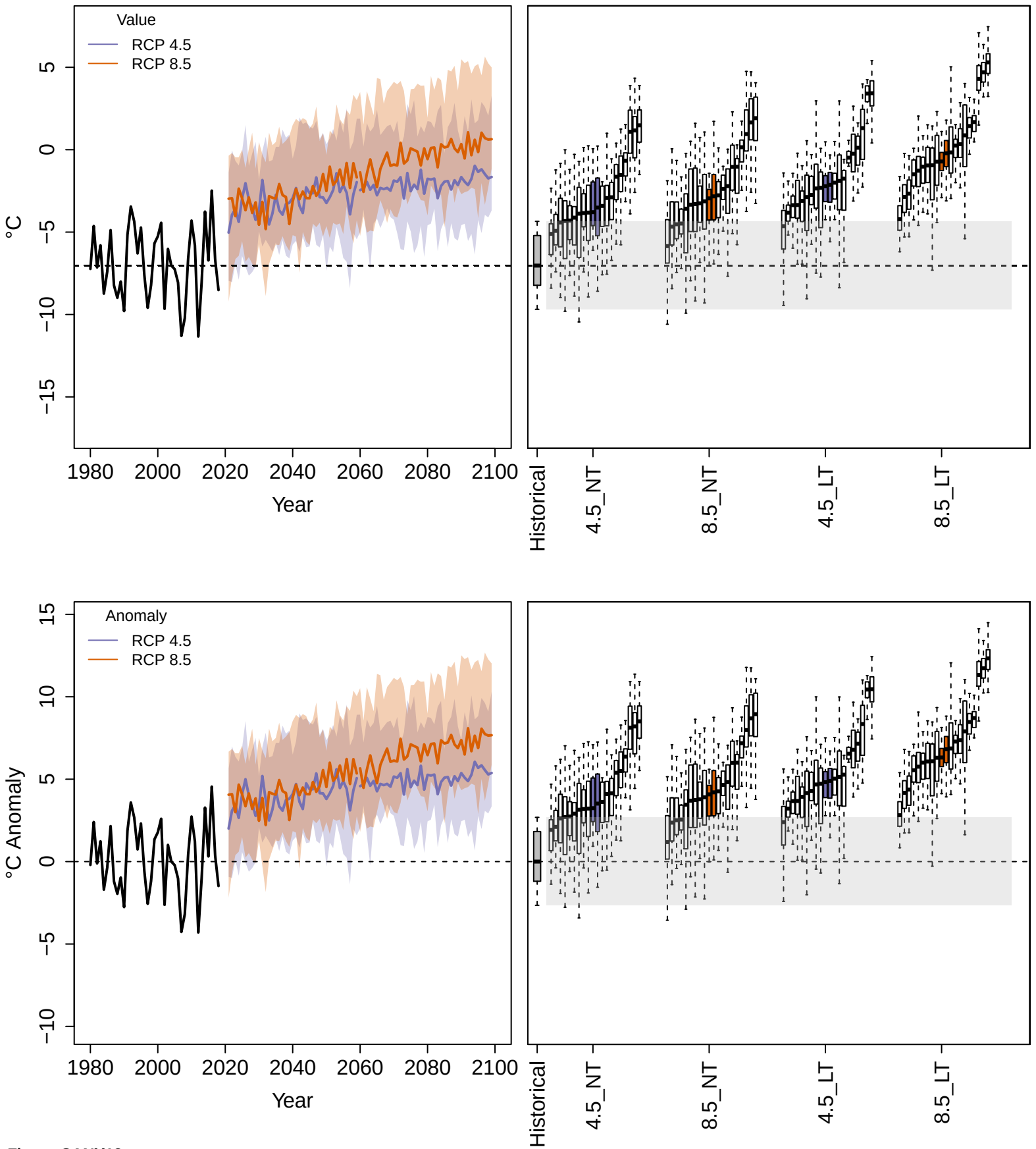


Figure CANY13:
Past trends and future trajectories of park−wide mean values for Minimum spring temperature in Canyonlands. Top panels show values, bottom panels show changes from the long−term historical mean. Left: Time series of historical (black) and future projections for RCP 4.5 and 8.5. Shaded areas show spread among climate models. Right: Boxplots of temporal variability over 40−year periods under historical (left box) and individual climate models under two RCPs. Right: Historical time period is 1970−2010; near−term (NT) is 2020−2060; long−term (LT) is 2061−2100.

Canyonlands: Minimum spring temperature

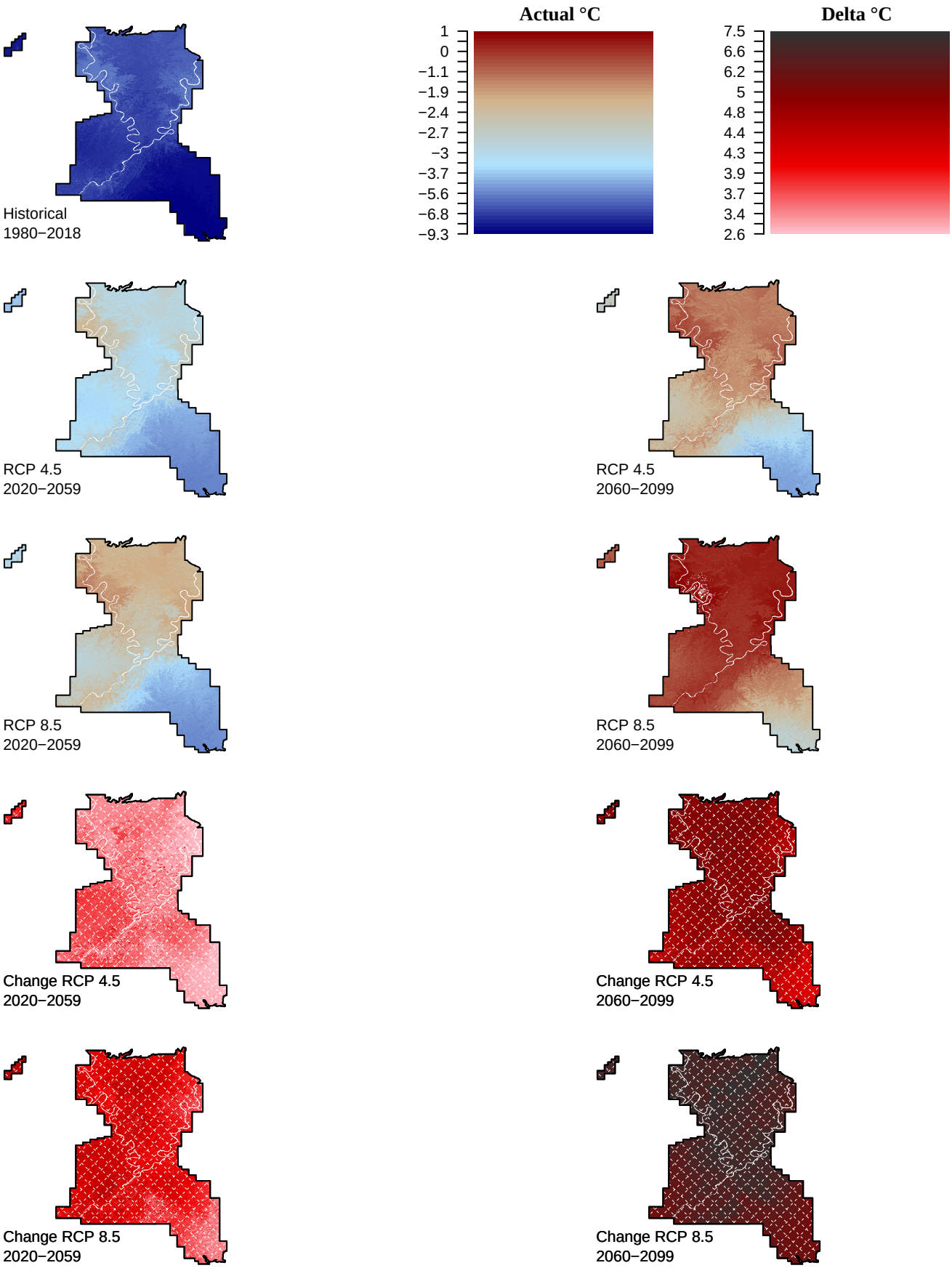


Figure CANYmap13:
Past trends and future trajectories of park−wide mean values for Minimum spring temperature in Canyonlands. Topmost panel depicts the historical mean from 1980−2018. Lower four panels show the emission scenarios of RCP 4.5 and RCP 8.5 at near−term and long−term timeframes. Bottom four panels depict the change from the historical mean; cross hatching denotes areas of robust predicitons (90% of models agree in the direction of change).

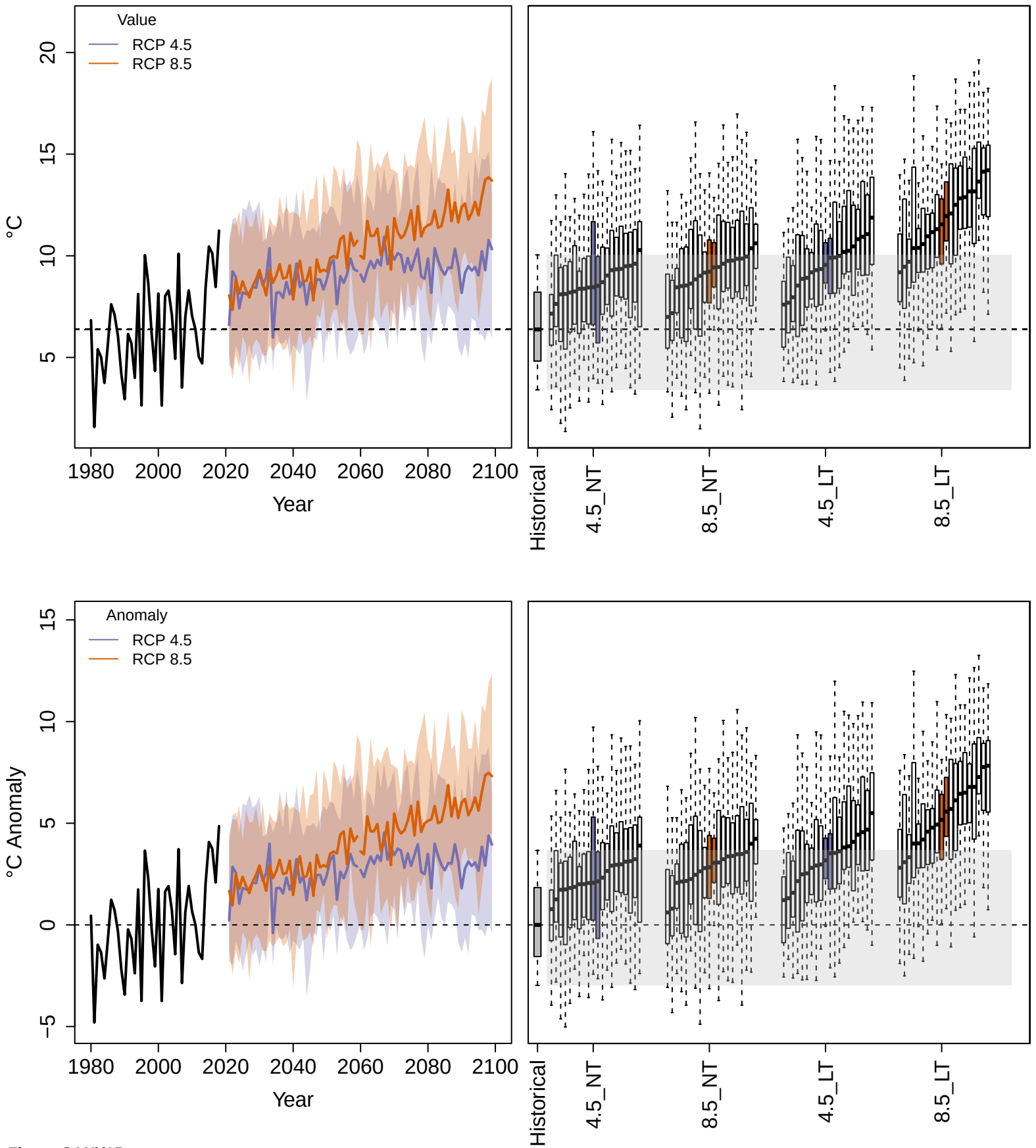


Figure CANY15:
Past trends and future trajectories of park−wide mean values for Minimum summer temperature in Canyonlands. Top panels show values, bottom panels show changes from the long−term historical mean. Left: Time series of historical (black) and future projections for RCP 4.5 and 8.5. Shaded areas show spread among climate models. Right: Boxplots of temporal variability over 40−year periods under historical (left box) and individual climate models under two RCPs. Right: Historical time period is 1970−2010; near−term (NT) is 2020−2060; long−term (LT) is 2061−2100.

Canyonlands: Minimum summer temperature

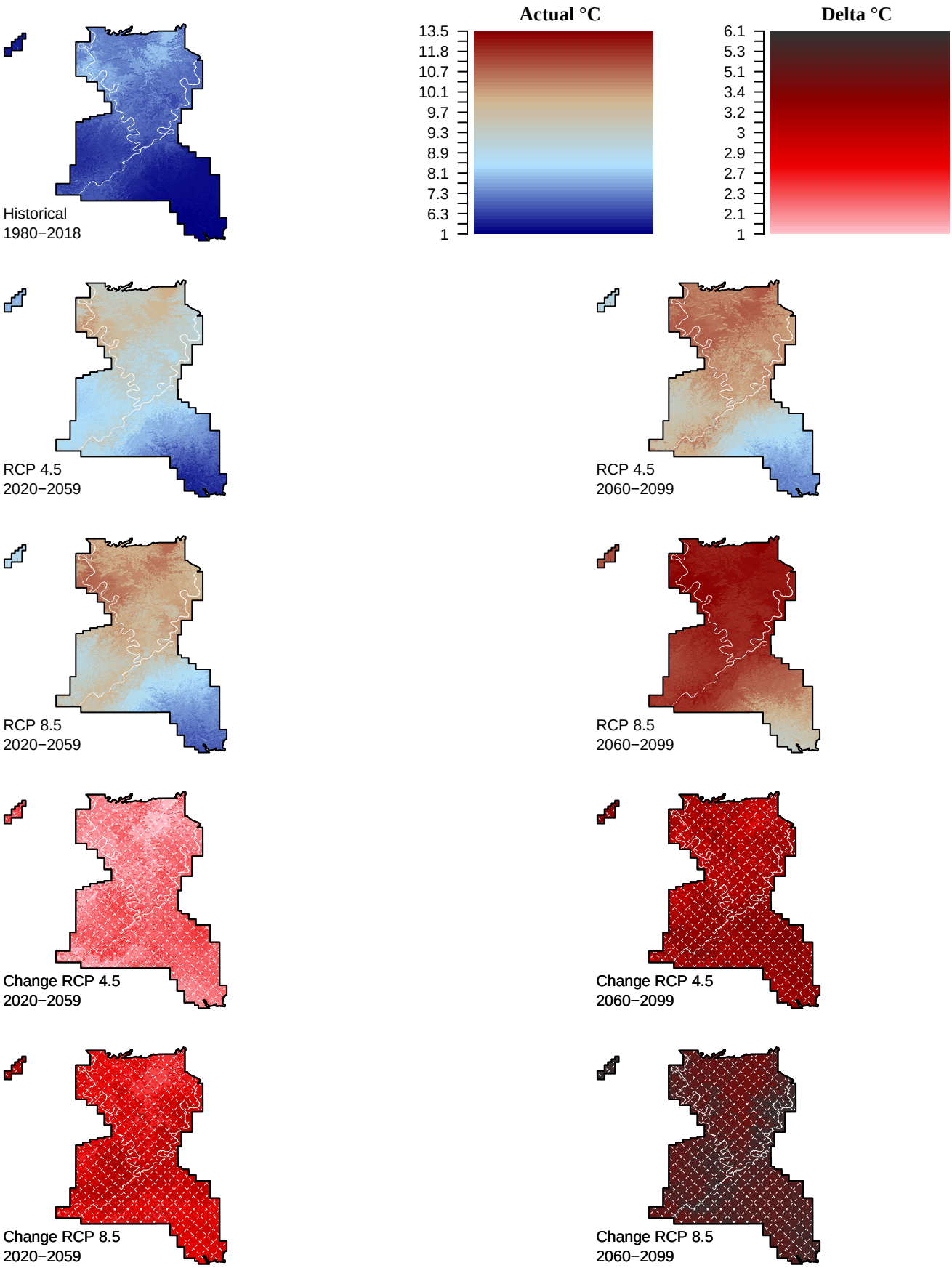


Figure CANYmap15:
Past trends and future trajectories of park−wide mean values for Minimum summer temperature in Canyonlands. Topmost panel depicts the historical mean from 1980−2018. Lower four panels show the emission scenarios of RCP 4.5 and RCP 8.5 at near−term and long−term timeframes. Bottom four panels depict the change from the historical mean; cross hatching denotes areas of robust predicitons (90% of models agree in the direction of change).

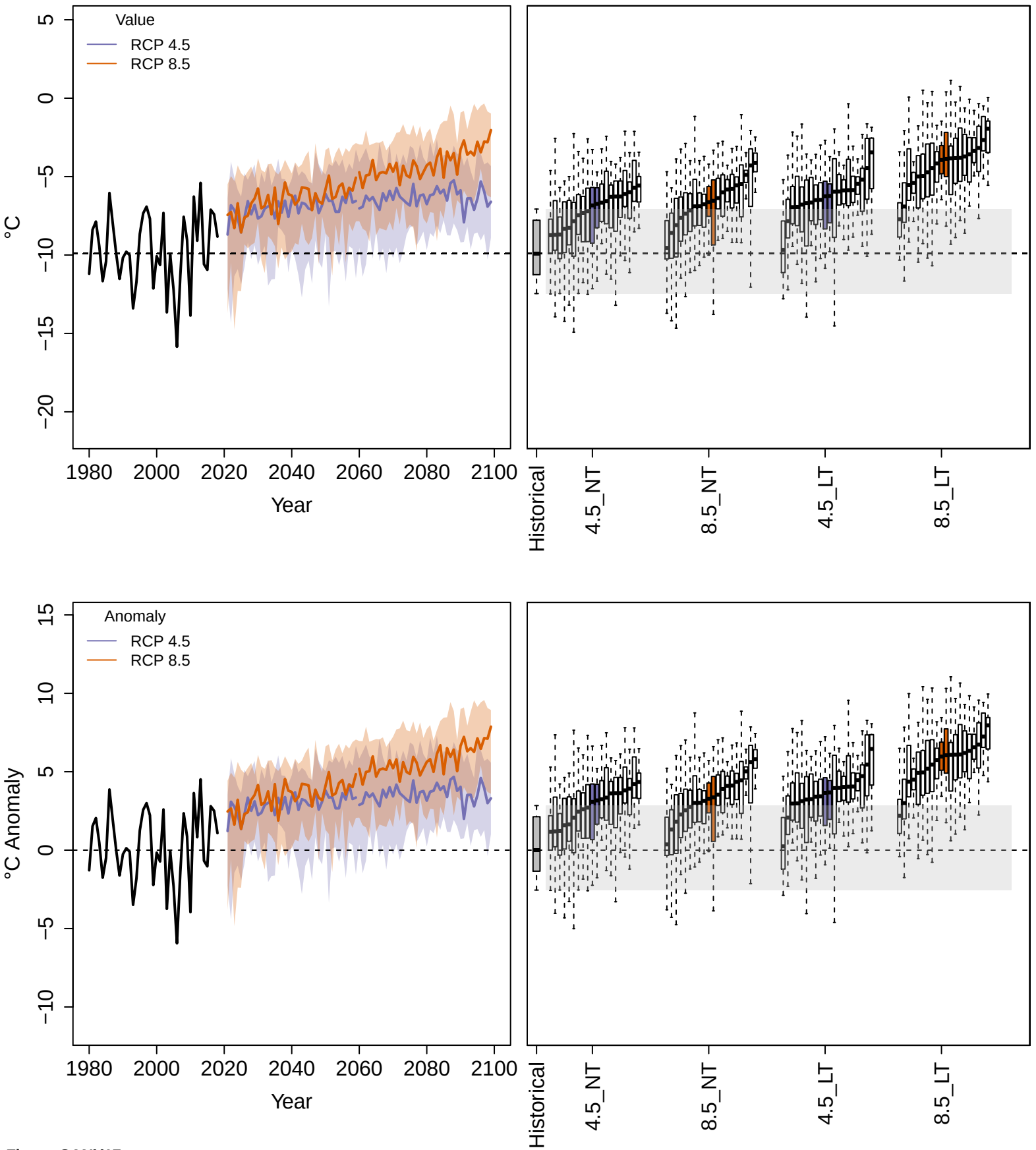


Figure CANY17:
Past trends and future trajectories of park−wide mean values for Minimum fall temperature in Canyonlands. Top panels show values, bottom panels show changes from the long−term historical mean. Left: Time series of historical (black) and future projections for RCP 4.5 and 8.5. Shaded areas show spread among climate models. Right: Boxplots of temporal variability over 40−year periods under historical (left box) and individual climate models under two RCPs. Right: Historical time period is 1970−2010; near−term (NT) is 2020−2060; long−term (LT) is 2061−2100.

Canyonlands: Minimum fall temperature

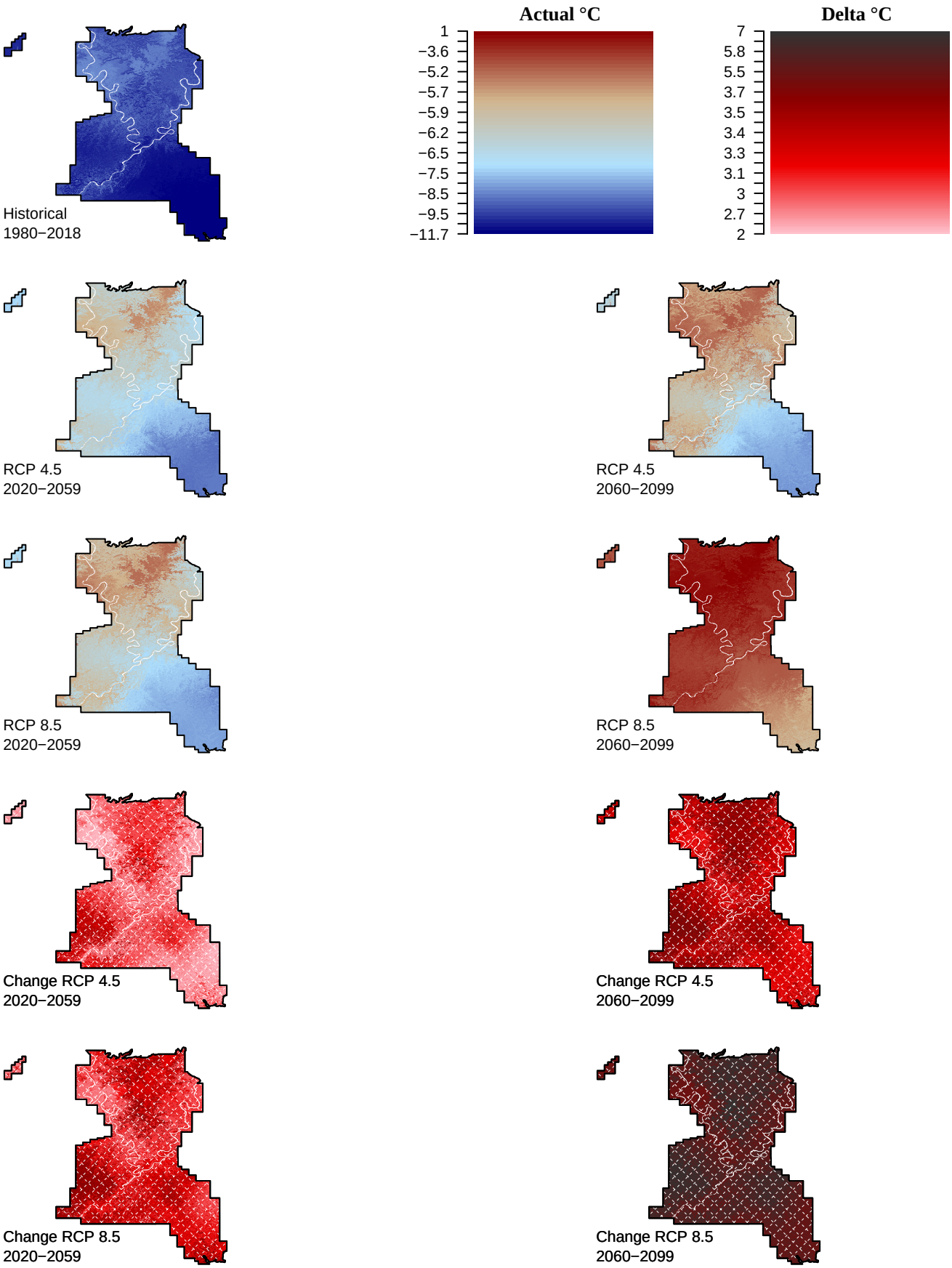


Figure CANYmap17:
Past trends and future trajectories of park−wide mean values for Minimum fall temperature in Canyonlands. Topmost panel depicts the historical mean from 1980−2018. Lower four panels show the emission scenarios of RCP 4.5 and RCP 8.5 at near−term and long−term timeframes. Bottom four panels depict the change from the historical mean; cross hatching denotes areas of robust predicitons (90% of models agree in the direction of change).

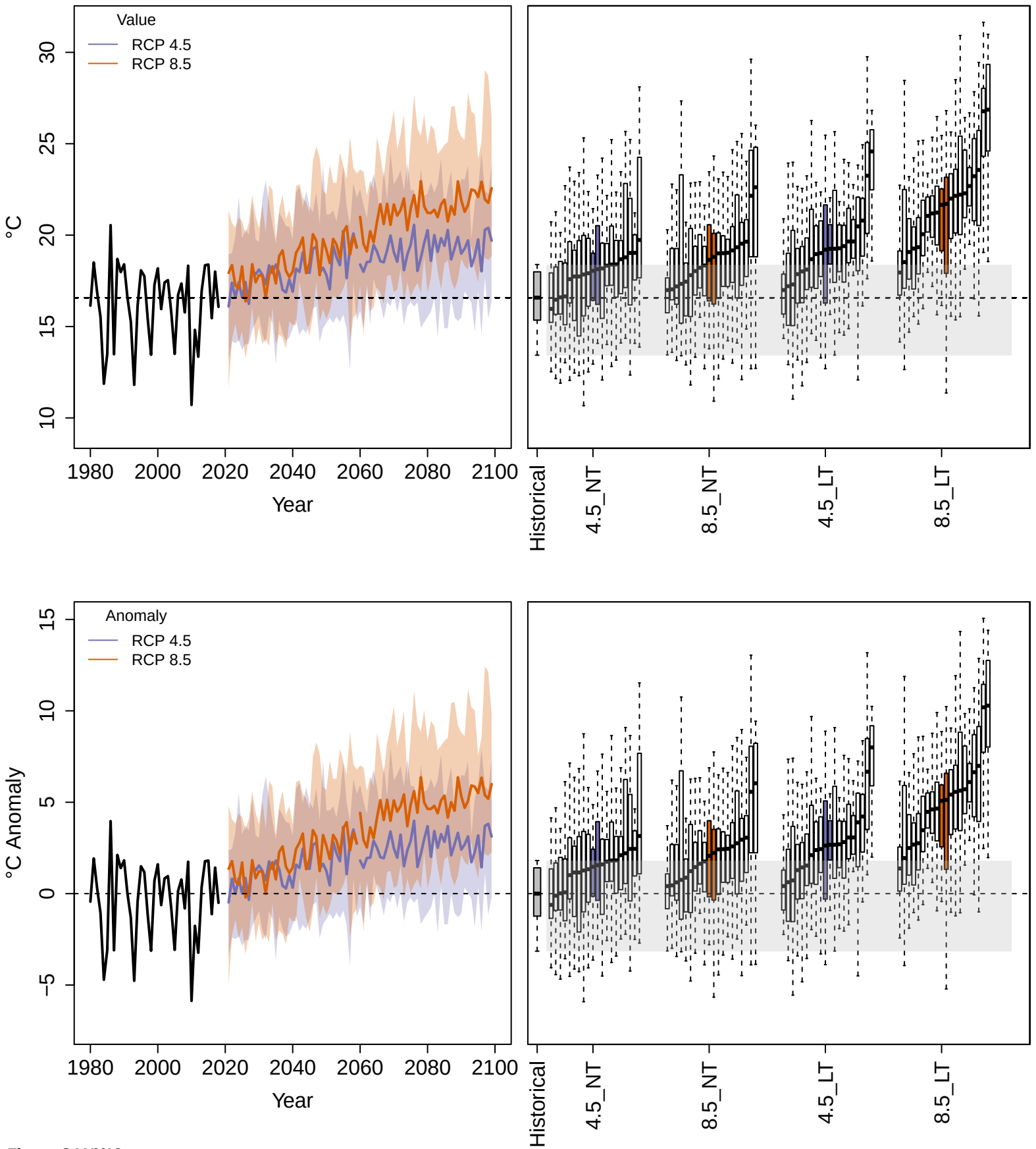


Figure CANY19:
Past trends and future trajectories of park−wide mean values for Maximum winter temperature in Canyonlands. Top panels show values, bottom panels show changes from the long−term historical mean. Left: Time series of historical (black) and future projections for RCP 4.5 and 8.5. Shaded areas show spread among climate models. Right: Boxplots of temporal variability over 40−year periods under historical (left box) and individual climate models under two RCPs. Right: Historical time period is 1970−2010; near−term (NT) is 2020−2060; long−term (LT) is 2061−2100.

Canyonlands: Maximum winter temperature

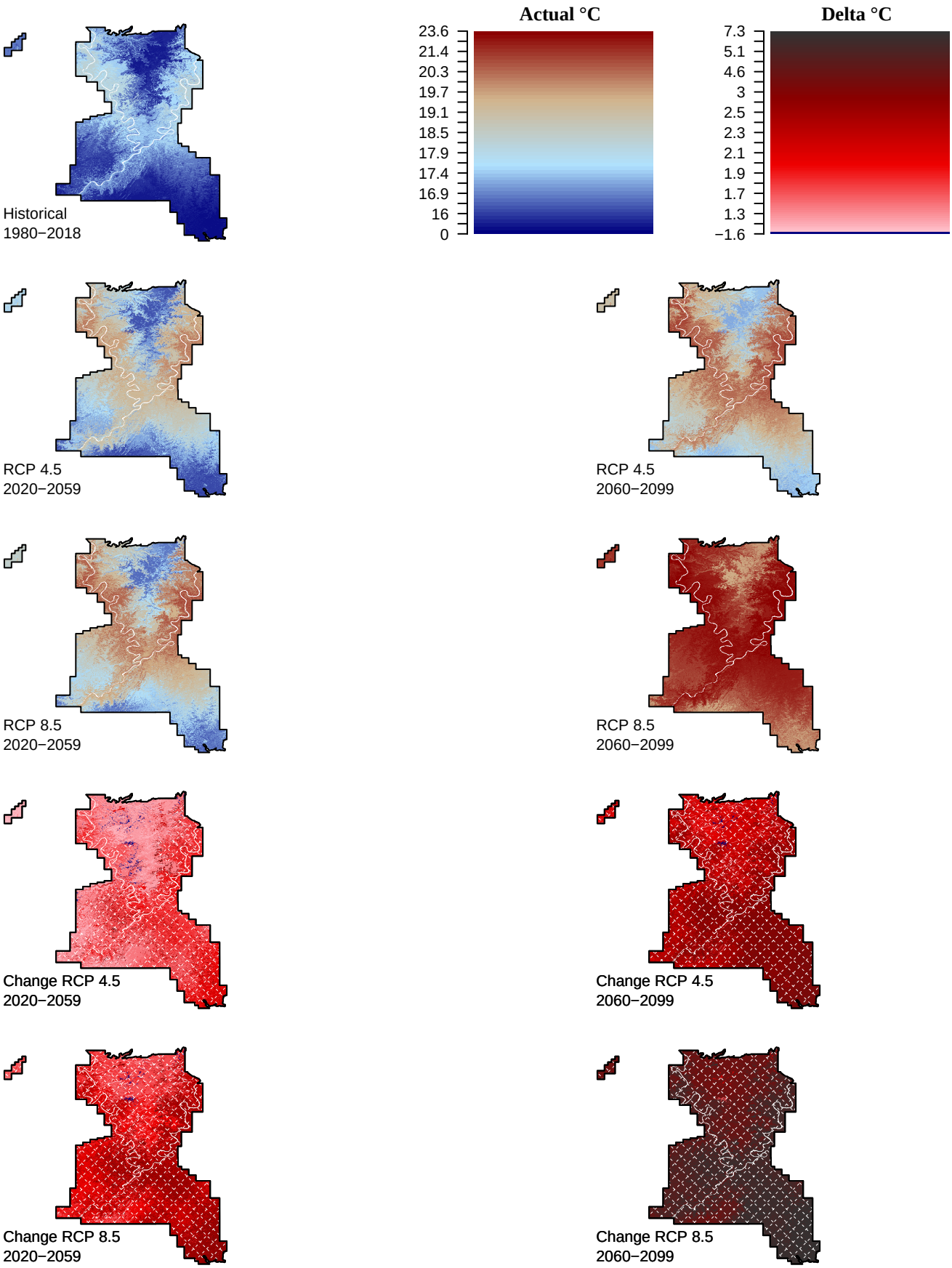


Figure CANYmap19:
Past trends and future trajectories of park−wide mean values for Maximum winter temperature in Canyonlands. Topmost panel depicts the historical mean from 1980−2018. Lower four panels show the emission scenarios of RCP 4.5 and RCP 8.5 at near−term and long−term timeframes. Bottom four panels depict the change from the historical mean; cross hatching denotes areas of robust predicitons (90% of models agree in the direction of change).

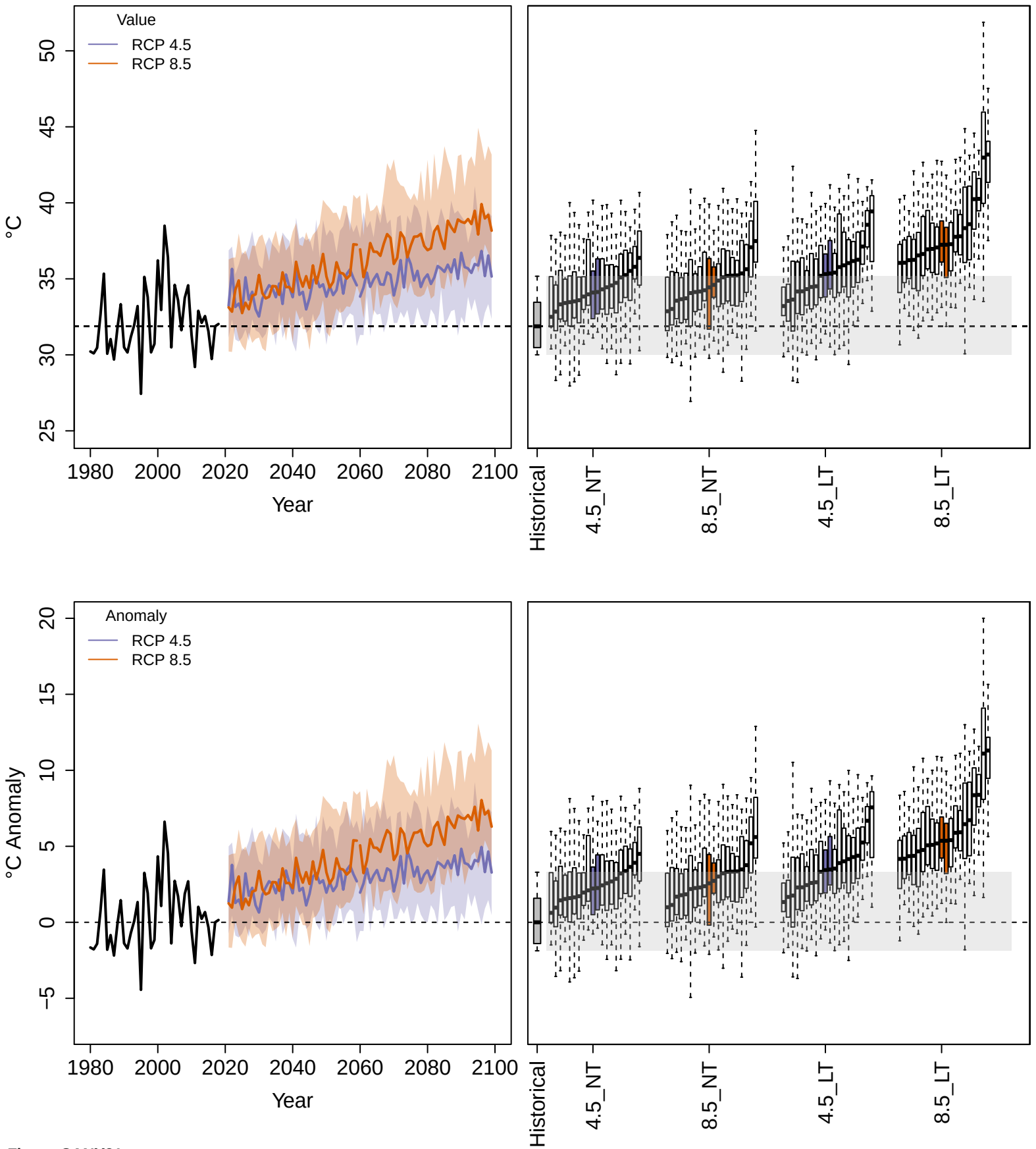


Figure CANY21:
Past trends and future trajectories of park−wide mean values for Maximum spring temperature in Canyonlands. Top panels show values, bottom panels show changes from the long−term historical mean. Left: Time series of historical (black) and future projections for RCP 4.5 and 8.5. Shaded areas show spread among climate models. Right: Boxplots of temporal variability over 40−year periods under historical (left box) and individual climate models under two RCPs. Right: Historical time period is 1970−2010; near−term (NT) is 2020−2060; long−term (LT) is 2061−2100.

Canyonlands: Maximum spring temperature

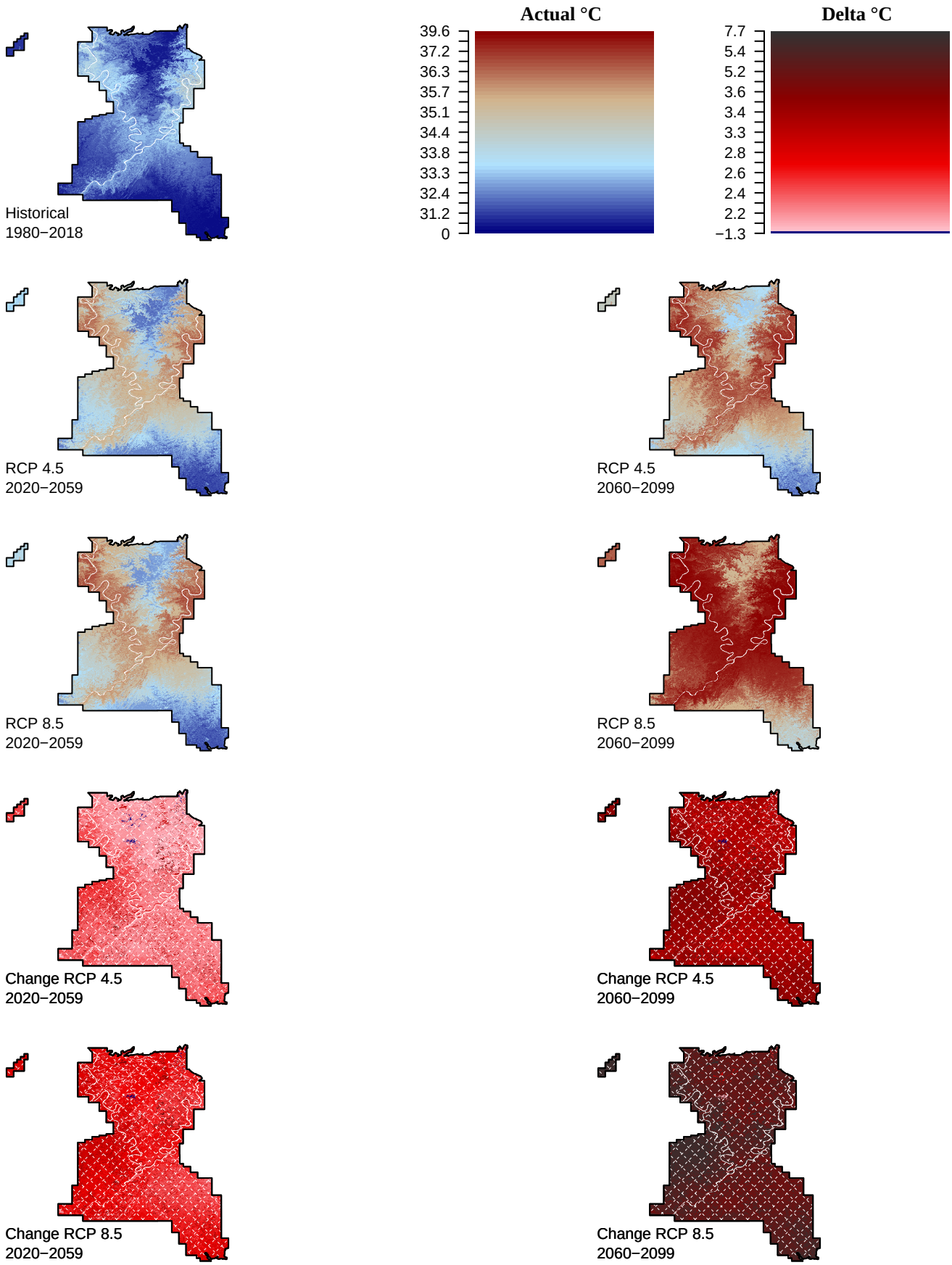


Figure CANYmap21:
Past trends and future trajectories of park−wide mean values for Maximum spring temperature in Canyonlands. Topmost panel depicts the historical mean from 1980−2018. Lower four panels show the emission scenarios of RCP 4.5 and RCP 8.5 at near−term and long−term timeframes. Bottom four panels depict the change from the historical mean; cross hatching denotes areas of robust predicitons (90% of models agree in the direction of change).

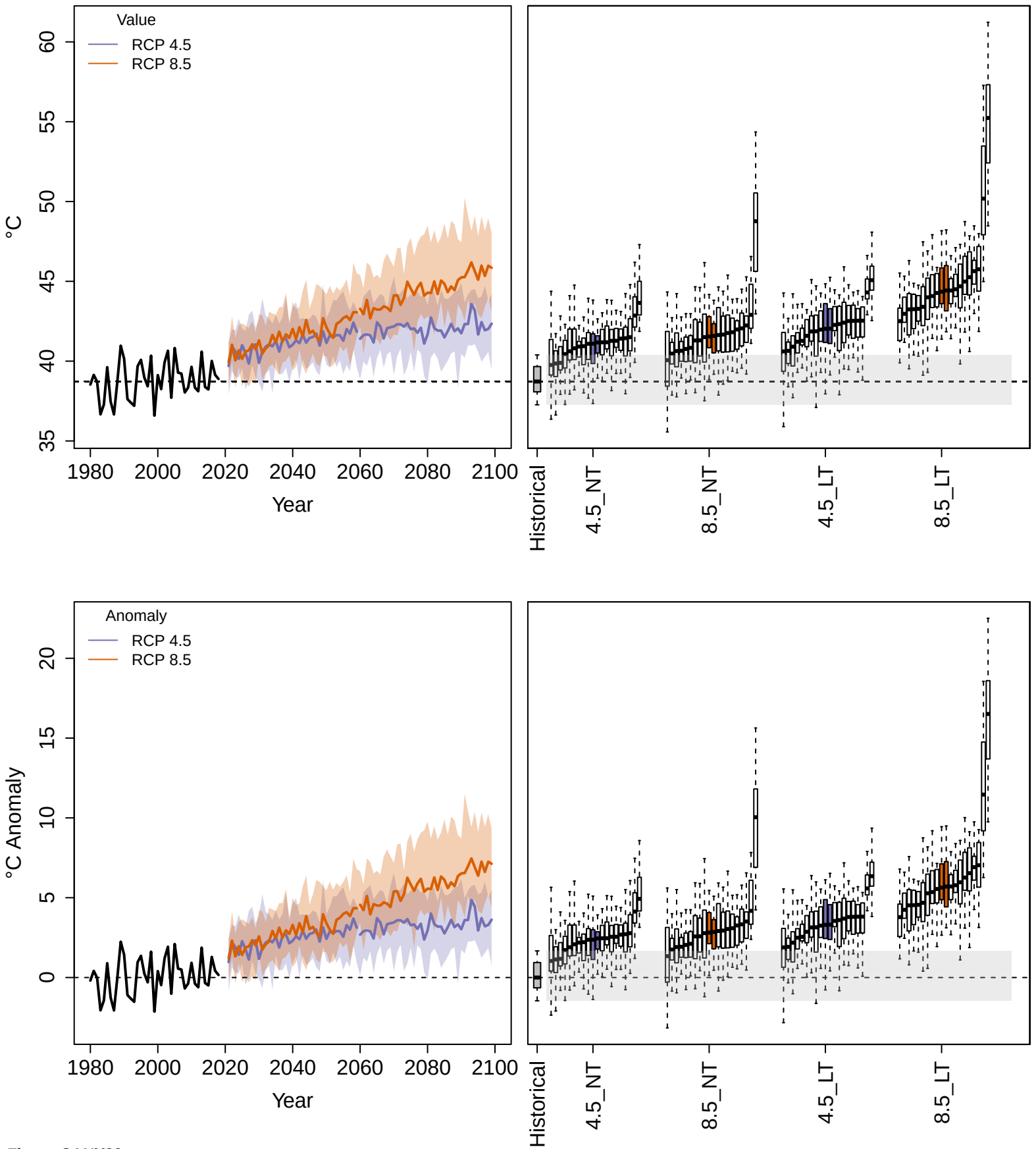


Figure CANY23:
Past trends and future trajectories of park−wide mean values for Maximum summer temperature in Canyonlands. Top panels show values, bottom panels show changes from the long−term historical mean. Left: Time series of historical (black) and future projections for RCP 4.5 and 8.5. Shaded areas show spread among climate models. Right: Boxplots of temporal variability over 40−year periods under historical (left box) and individual climate models under two RCPs. Right: Historical time period is 1970−2010; near−term (NT) is 2020−2060; long−term (LT) is 2061−2100.

Canyonlands: Maximum summer temperature

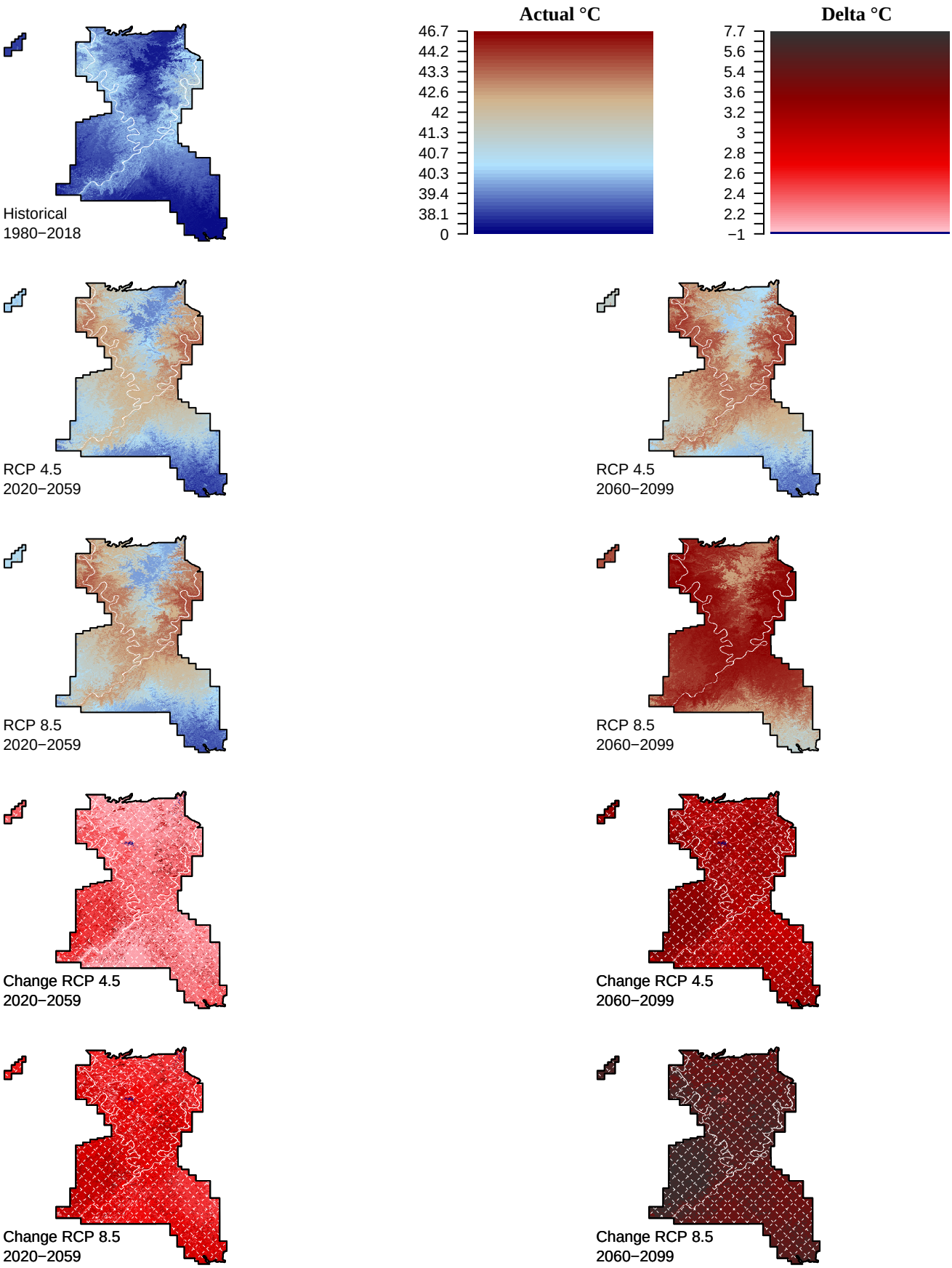


Figure CANYmap23:
Past trends and future trajectories of park−wide mean values for Maximum summer temperature in Canyonlands. Topmost panel depicts the historical mean from 1980−2018. Lower four panels show the emission scenarios of RCP 4.5 and RCP 8.5 at near−term and long−term timeframes. Bottom four panels depict the change from the historical mean; cross hatching denotes areas of robust predicitons (90% of models agree in the direction of change).

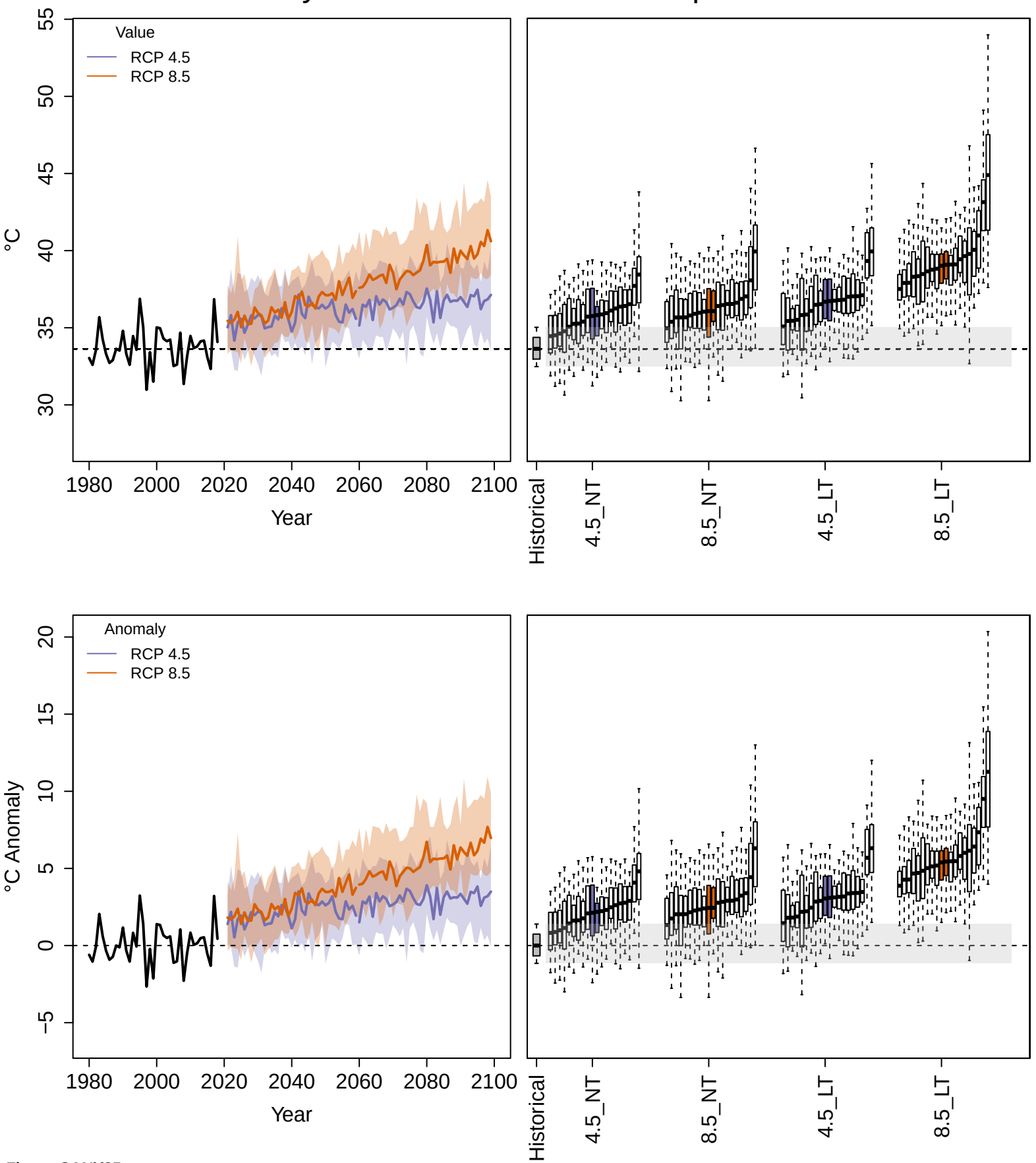


Figure CANY25:
Past trends and future trajectories of park−wide mean values for Maximum fall temperature in Canyonlands. Top panels show values, bottom panels show changes from the long−term historical mean. Left: Time series of historical (black) and future projections for RCP 4.5 and 8.5. Shaded areas show spread among climate models. Right: Boxplots of temporal variability over 40−year periods under historical (left box) and individual climate models under two RCPs. Right: Historical time period is 1970−2010; near−term (NT) is 2020−2060; long−term (LT) is 2061−2100.

Canyonlands: Maximum fall temperature

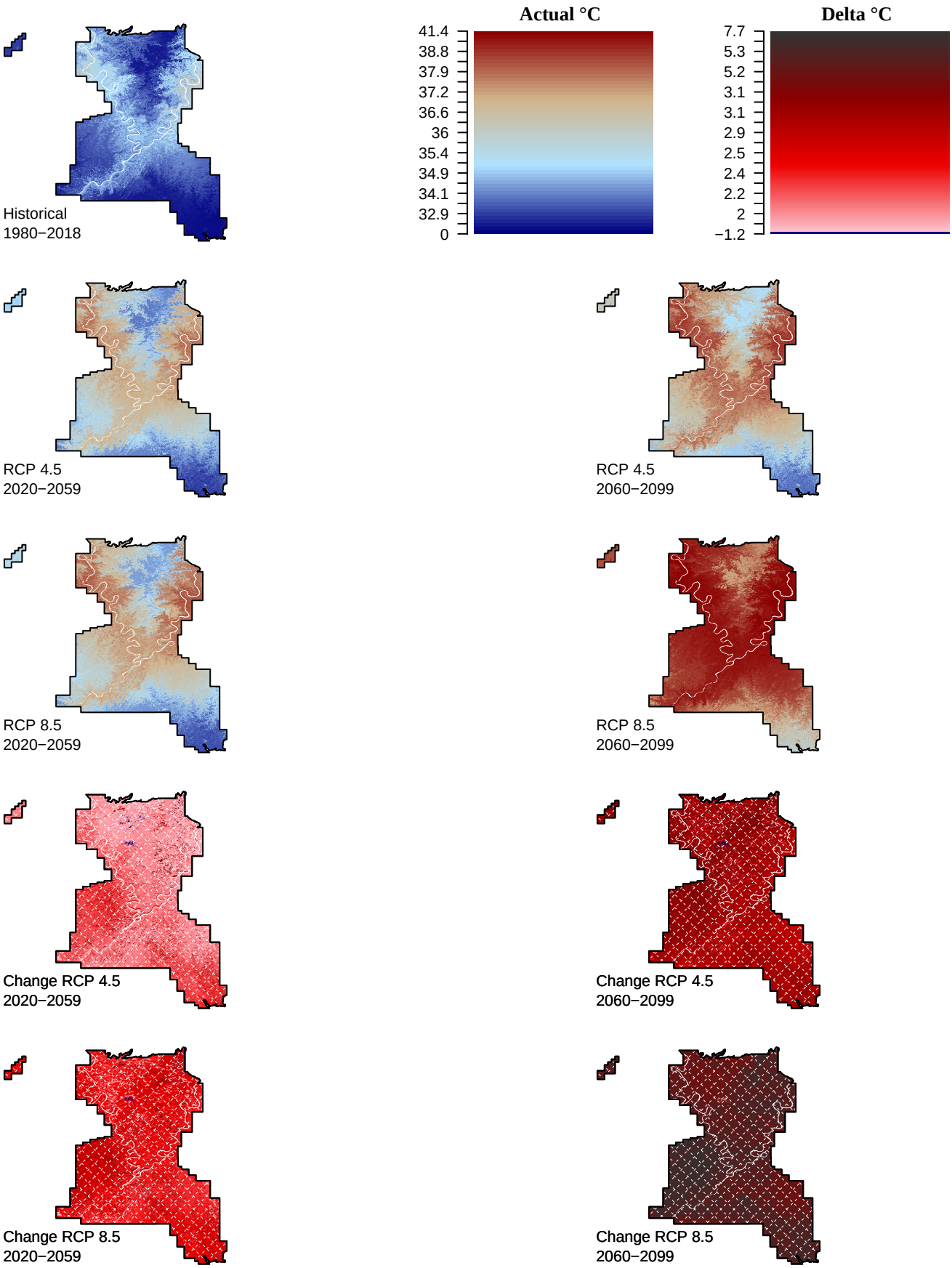


Figure CANYmap25:
Past trends and future trajectories of park−wide mean values for Maximum fall temperature in Canyonlands. Topmost panel depicts the historical mean from 1980−2018. Lower four panels show the emission scenarios of RCP 4.5 and RCP 8.5 at near−term and long−term timeframes. Bottom four panels depict the change from the historical mean; cross hatching denotes areas of robust predicitons (90% of models agree in the direction of change).

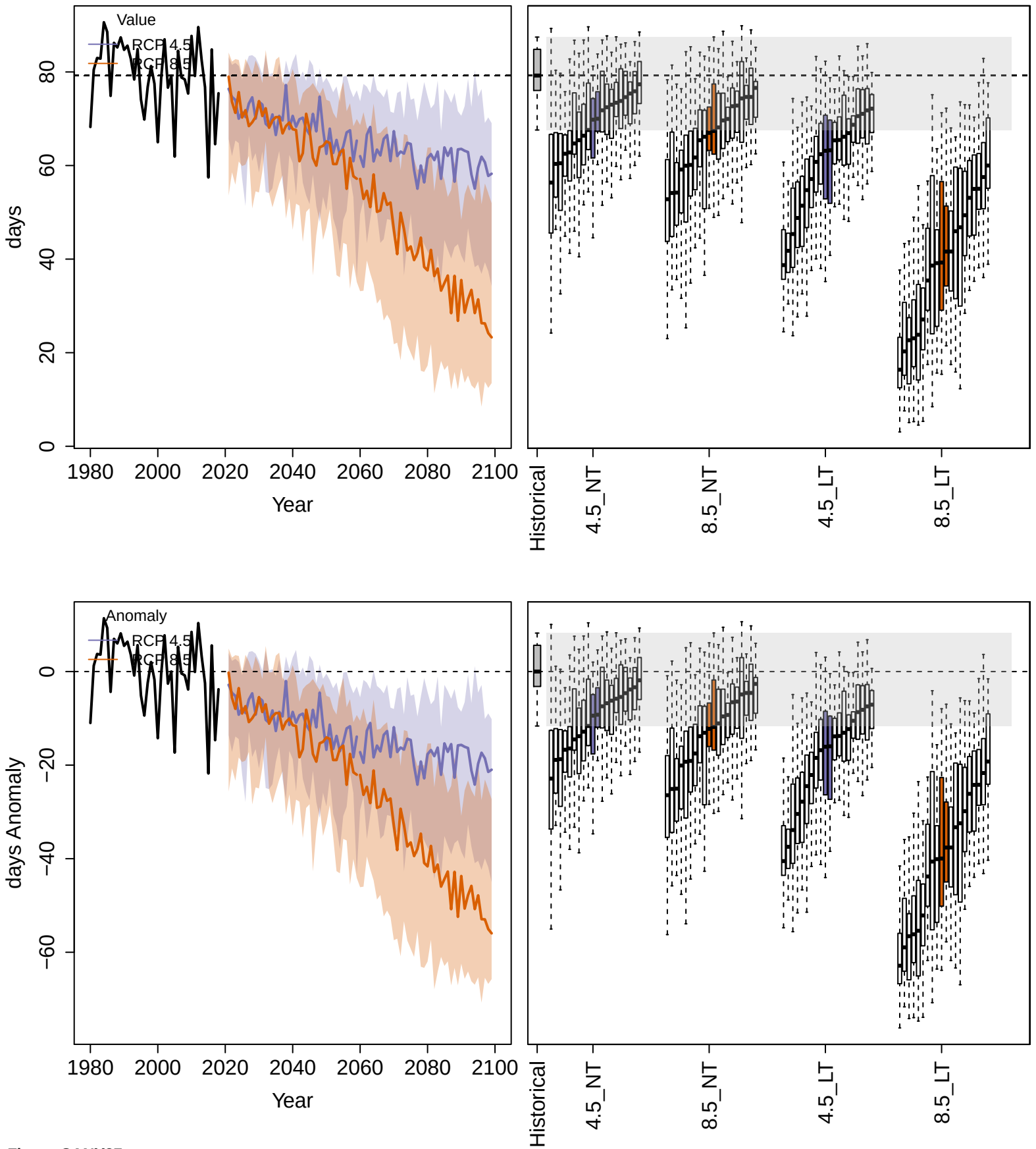


Figure CANY27:
Past trends and future trajectories of park−wide mean values for Winter frost days in Canyonlands. Top panels show values, bottom panels show changes from the long−term historical mean. Left: Time series of historical (black) and future projections for RCP 4.5 and 8.5. Shaded areas show spread among climate models. Right: Boxplots of temporal variability over 40−year periods under historical (left box) and individual climate models under two RCPs. Right: Historical time period is 1970−2010; near−term (NT) is 2020−2060; long−term (LT) is 2061−2100.

Canyonlands: Winter frost days

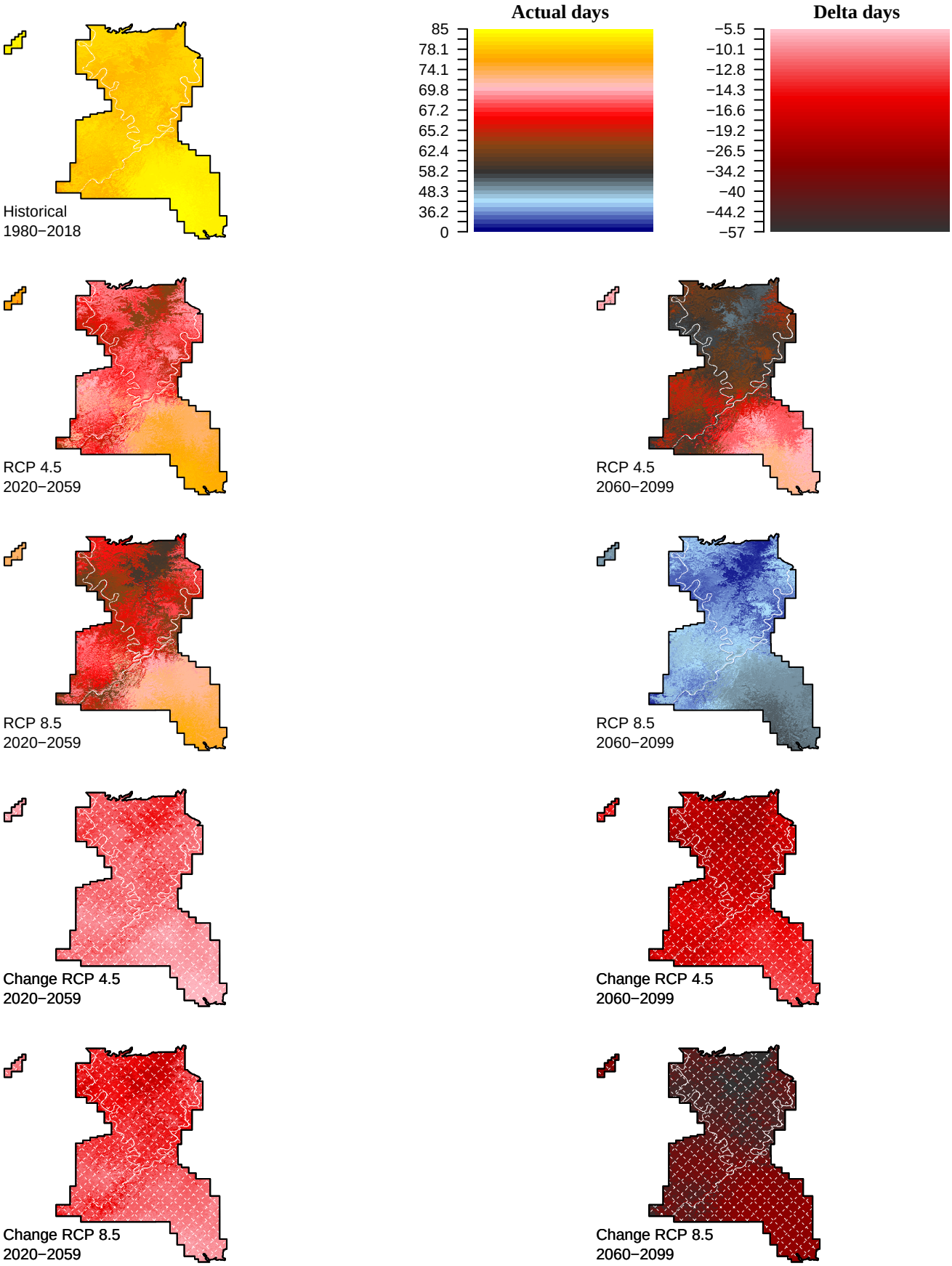


Figure CANYmap27:
Past trends and future trajectories of park−wide mean values for Winter frost days in Canyonlands. Topmost panel depicts the historical mean from 1980−2018. Lower four panels show the emission scenarios of RCP 4.5 and RCP 8.5 at near−term and long−term timeframes. Bottom four panels depict the change from the historical mean; cross hatching denotes areas of robust predicitons (90% of models agree in the direction of change).

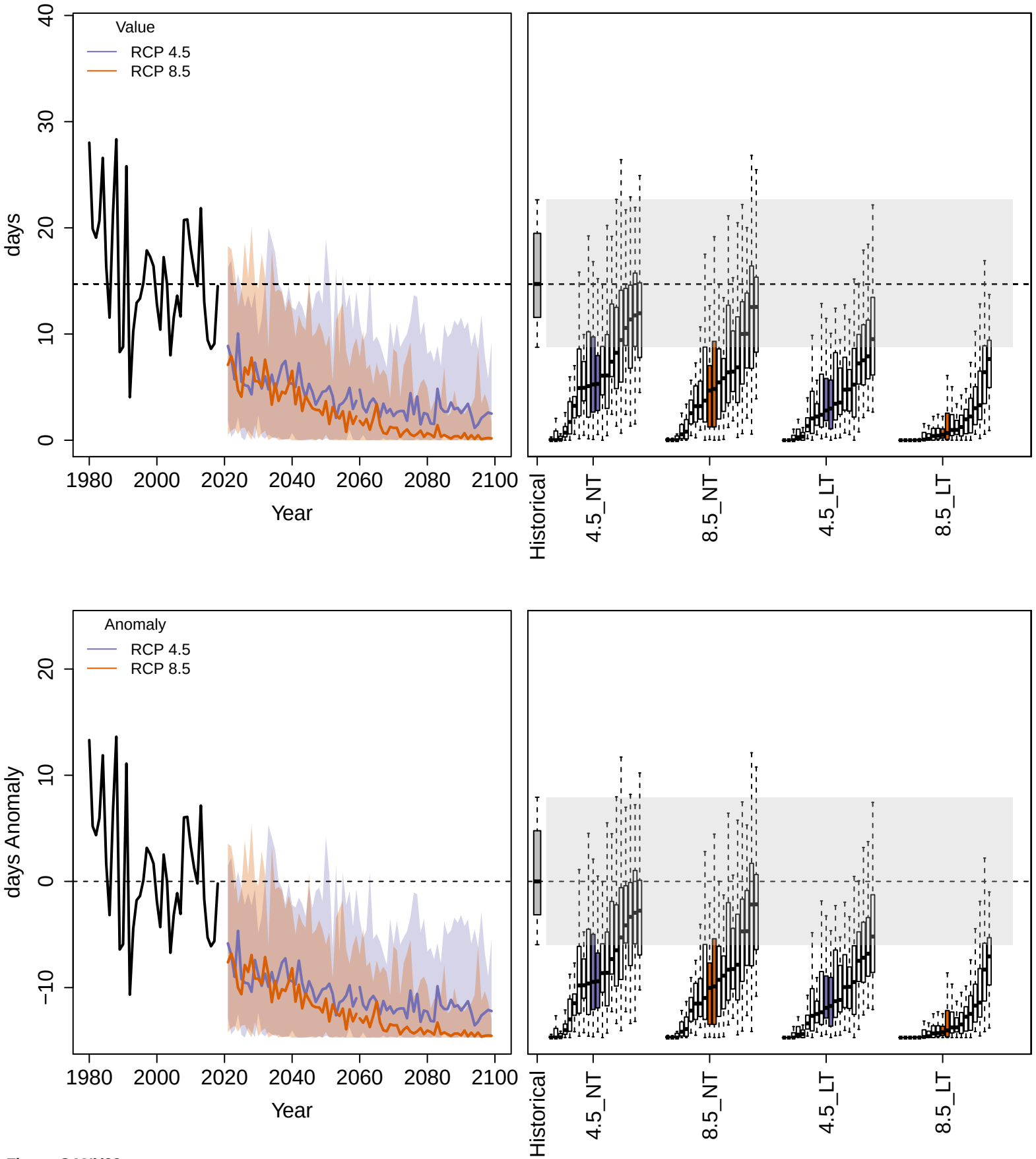


Figure CANY29:
Past trends and future trajectories of park−wide mean values for Spring frost days in Canyonlands. Top panels show values, bottom panels show changes from the long−term historical mean. Left: Time series of historical (black) and future projections for RCP 4.5 and 8.5. Shaded areas show spread among climate models. Right: Boxplots of temporal variability over 40−year periods under historical (left box) and individual climate models under two RCPs. Right: Historical time period is 1970−2010; near−term (NT) is 2020−2060; long−term (LT) is 2061−2100.

Canyonlands: Spring frost days

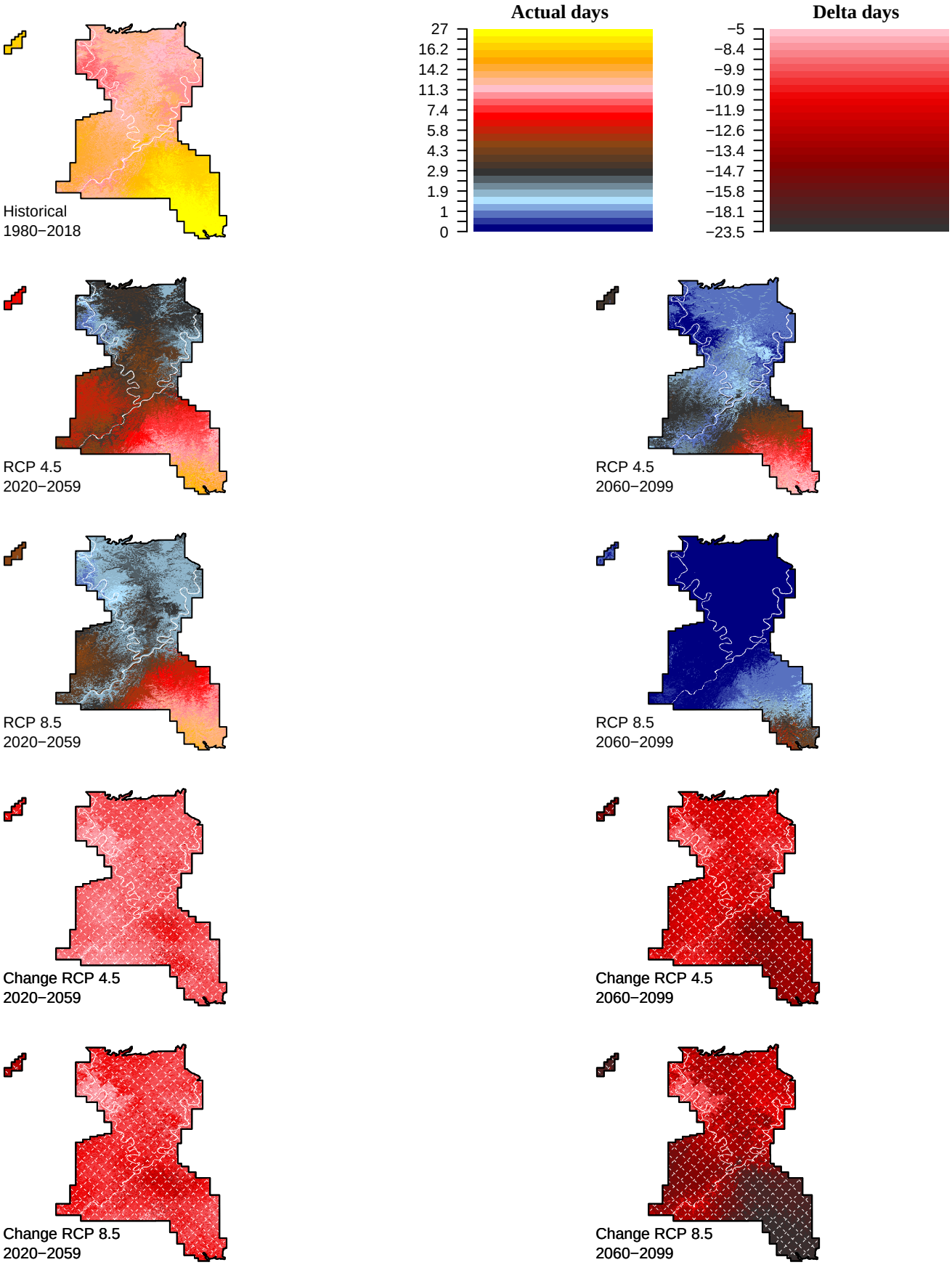


Figure CANYmap29:
Past trends and future trajectories of park−wide mean values for Spring frost days in Canyonlands. Topmost panel depicts the historical mean from 1980−2018. Lower four panels show the emission scenarios of RCP 4.5 and RCP 8.5 at near−term and long−term timeframes. Bottom four panels depict the change from the historical mean; cross hatching denotes areas of robust predicitons (90% of models agree in the direction of change).

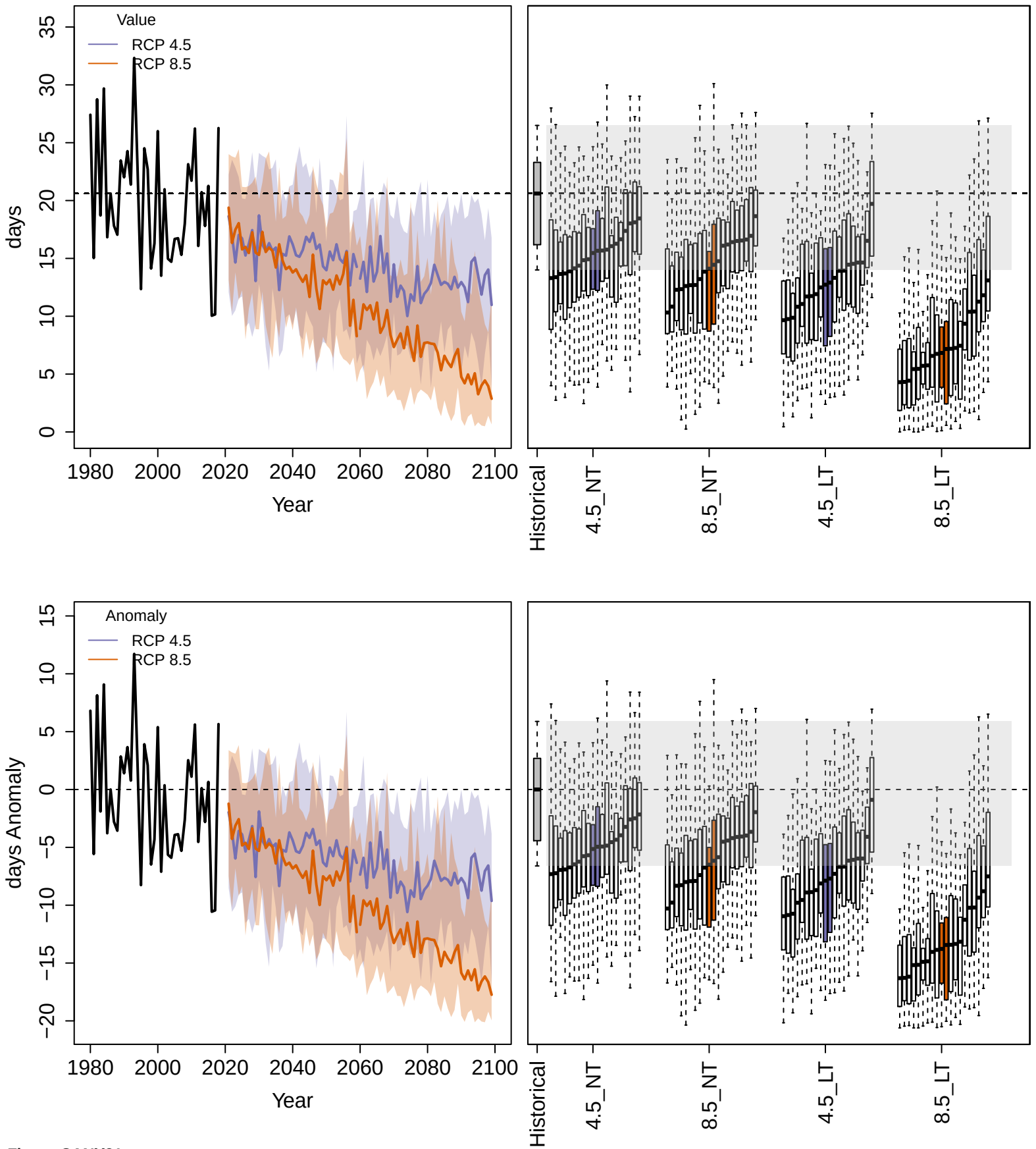


Figure CANY31:
Past trends and future trajectories of park−wide mean values for Fall frost days in Canyonlands. Top panels show values, bottom panels show changes from the long−term historical mean. Left: Time series of historical (black) and future projections for RCP 4.5 and 8.5. Shaded areas show spread among climate models. Right: Boxplots of temporal variability over 40−year periods under historical (left box) and individual climate models under two RCPs. Right: Historical time period is 1970−2010; near−term (NT) is 2020−2060; long−term (LT) is 2061−2100.

Canyonlands: Fall frost days

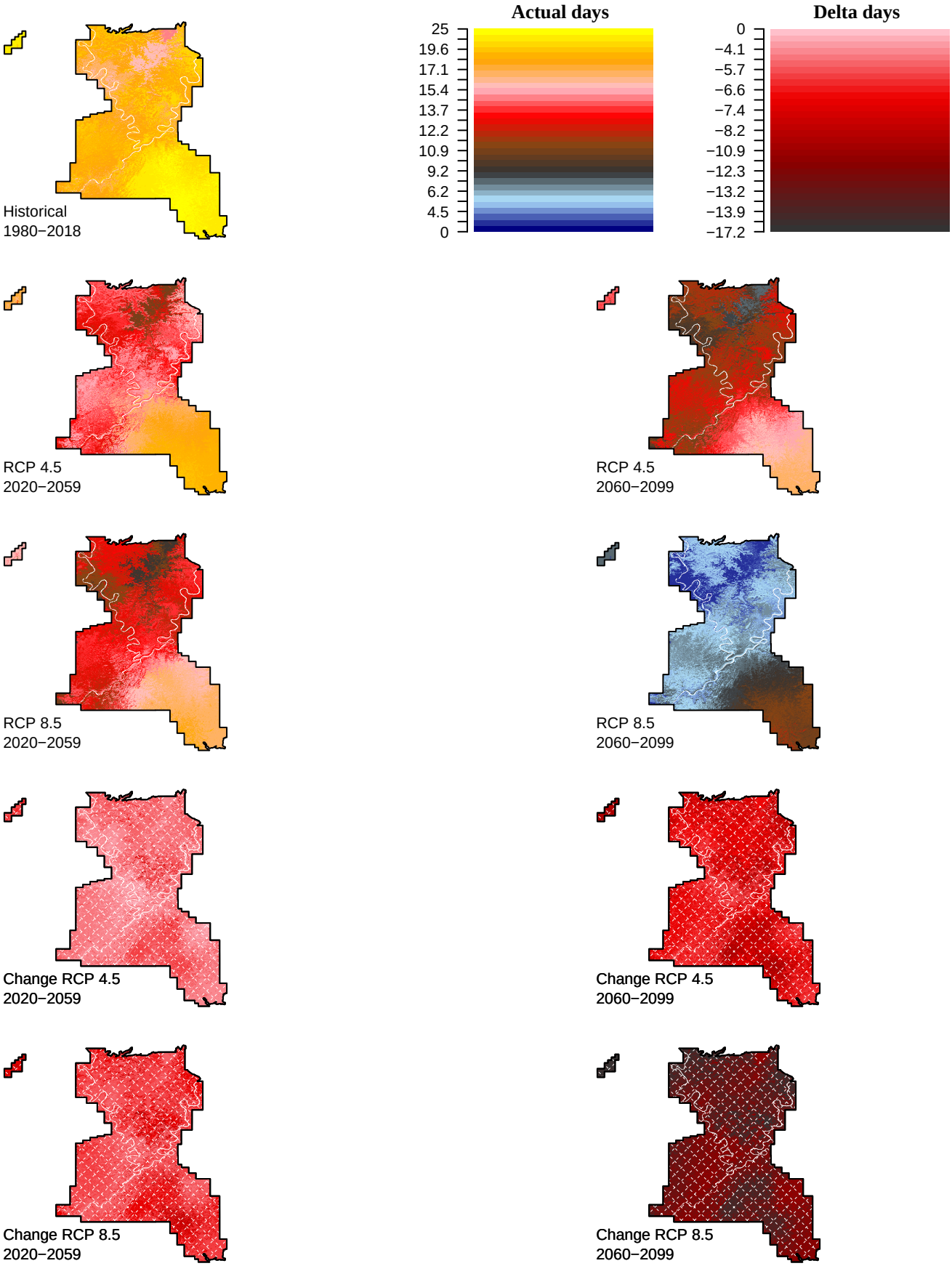


Figure CANYmap31:
Past trends and future trajectories of park−wide mean values for Fall frost days in Canyonlands. Topmost panel depicts the historical mean from 1980−2018. Lower four panels show the emission scenarios of RCP 4.5 and RCP 8.5 at near−term and long−term timeframes. Bottom four panels depict the change from the historical mean; cross hatching denotes areas of robust predicitons (90% of models agree in the direction of change).

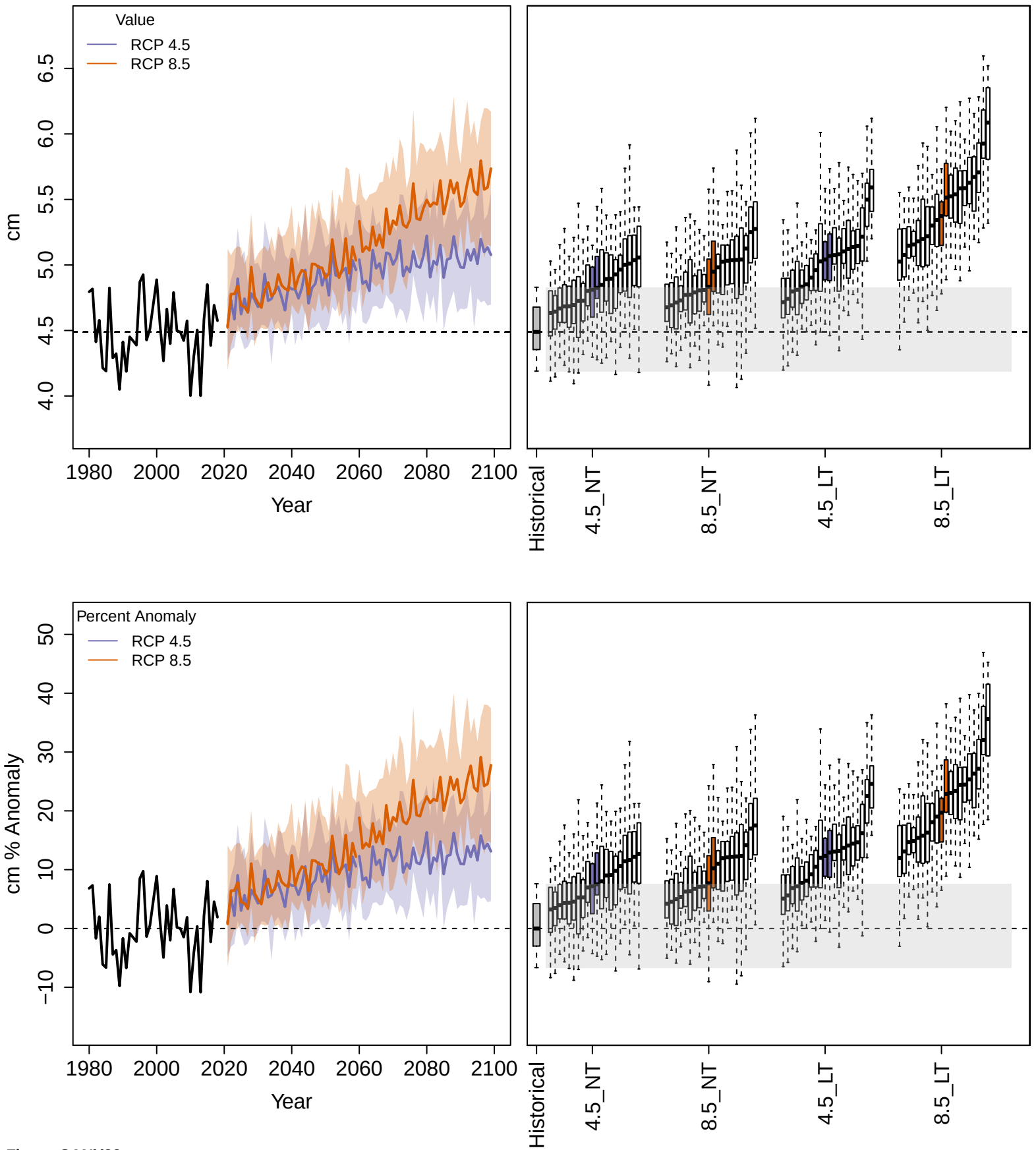


Figure CANY33:
Past trends and future trajectories of park−wide mean values for Winter potential evapotranspiration in Canyonlands. Top panels show values, bottom panels show changes from the long−term historical mean. Left: Time series of historical (black) and future projections for RCP 4.5 and 8.5. Shaded areas show spread among climate models. Right: Boxplots of temporal variability over 40−year periods under historical (left box) and individual climate models under two RCPs. Right: Historical time period is 1970−2010; near−term (NT) is 2020−2060; long−term (LT) is 2061−2100.

Canyonlands: Winter potential evapotranspiration

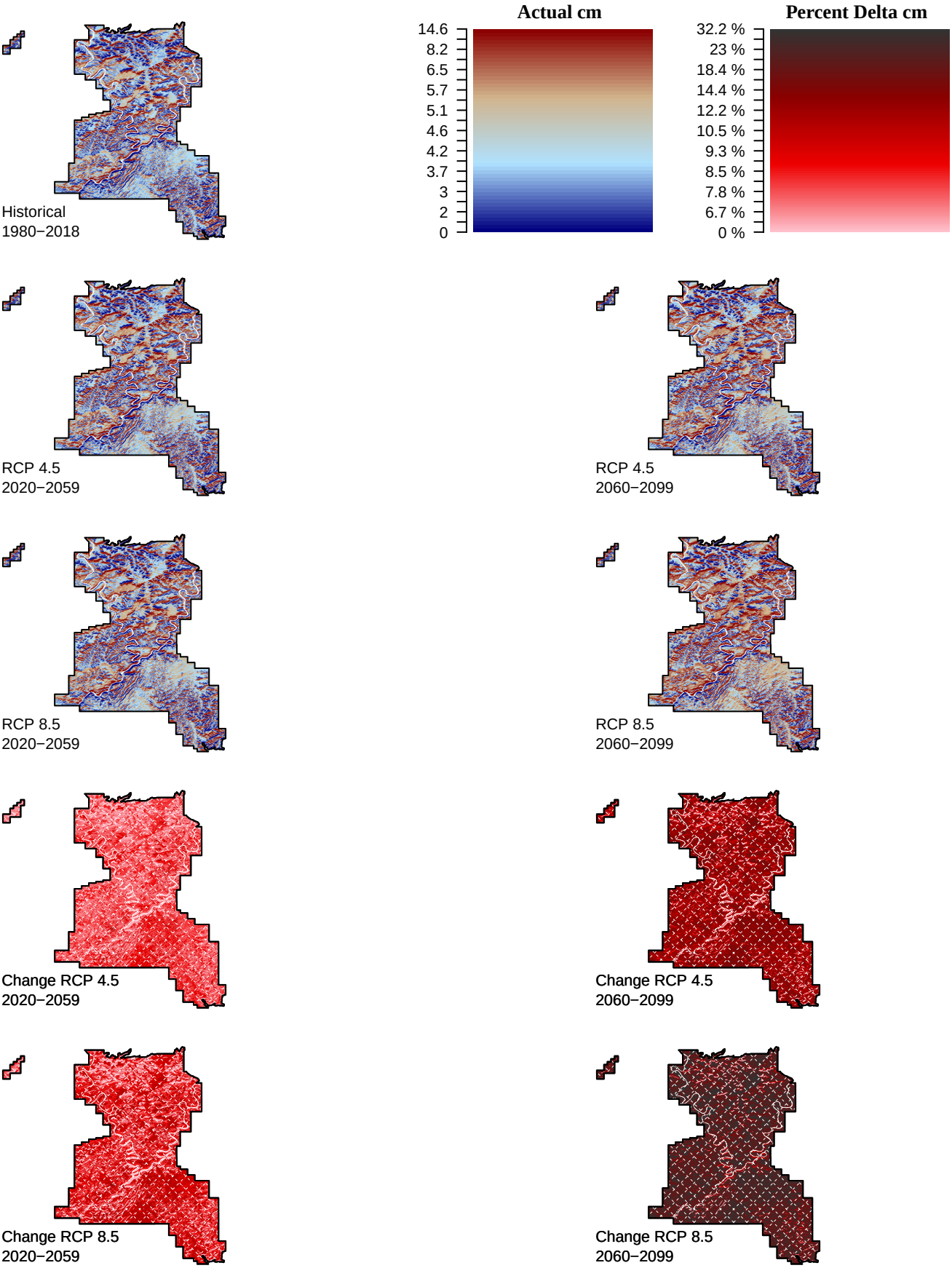


Figure CANYmap33:
Past trends and future trajectories of park−wide mean values for Winter potential evapotranspiration in Canyonlands. Topmost panel depicts the historical mean from 1980−2018. Lower four panels show the emission scenarios of RCP 4.5 and RCP 8.5 at near−term and long−term timeframes. Bottom four panels depict the change from the historical mean; cross hatching denotes areas of robust predicitons (90% of models agree in the direction of change).

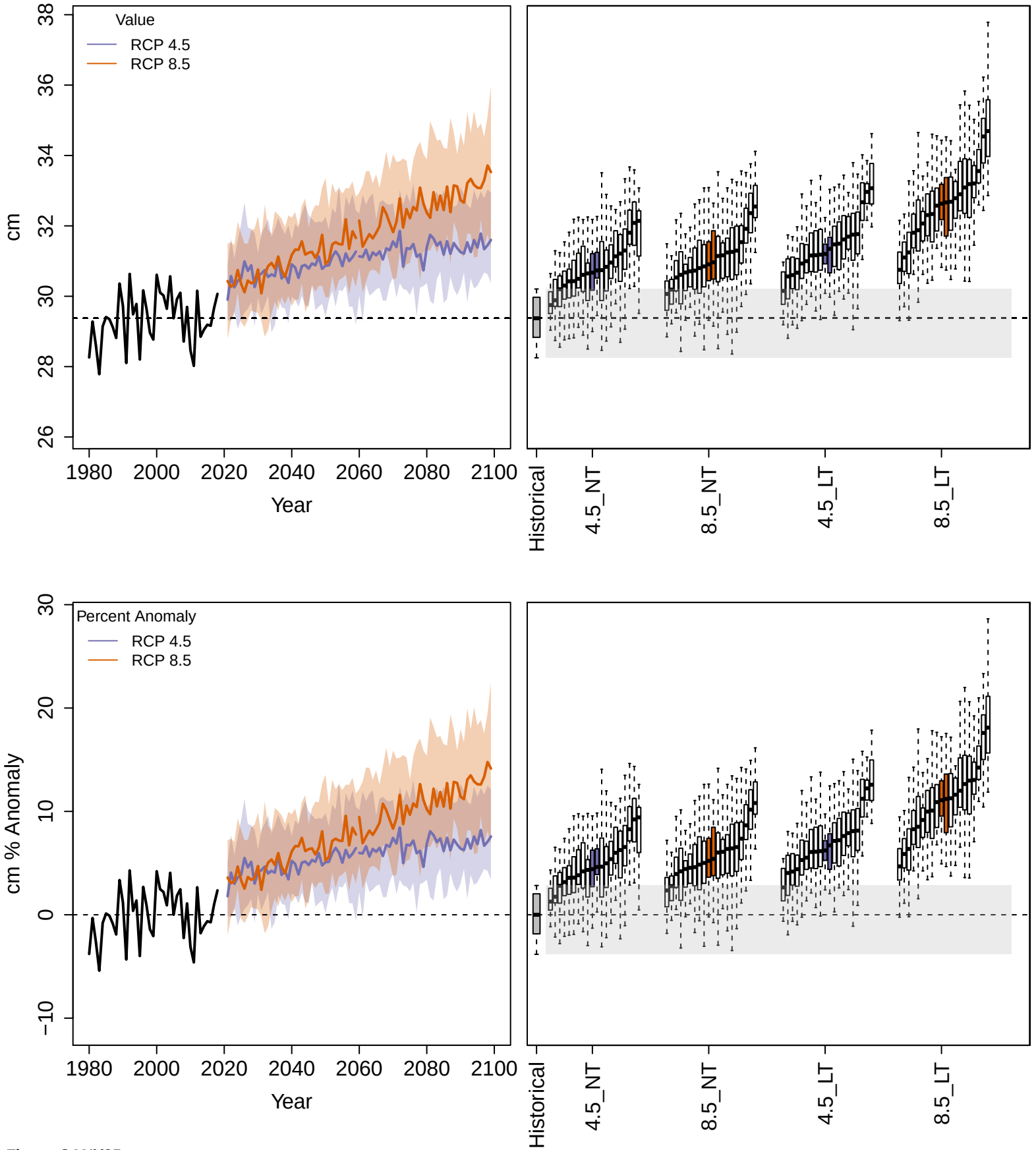


Figure CANY35:
Past trends and future trajectories of park−wide mean values for Spring potential evapotranspiration in Canyonlands. Top panels show values, bottom panels show changes from the long−term historical mean. Left: Time series of historical (black) and future projections for RCP 4.5 and 8.5. Shaded areas show spread among climate models. Right: Boxplots of temporal variability over 40−year periods under historical (left box) and individual climate models under two RCPs. Right: Historical time period is 1970−2010; near−term (NT) is 2020−2060; long−term (LT) is 2061−2100.

Canyonlands: Spring potential evapotranspiration

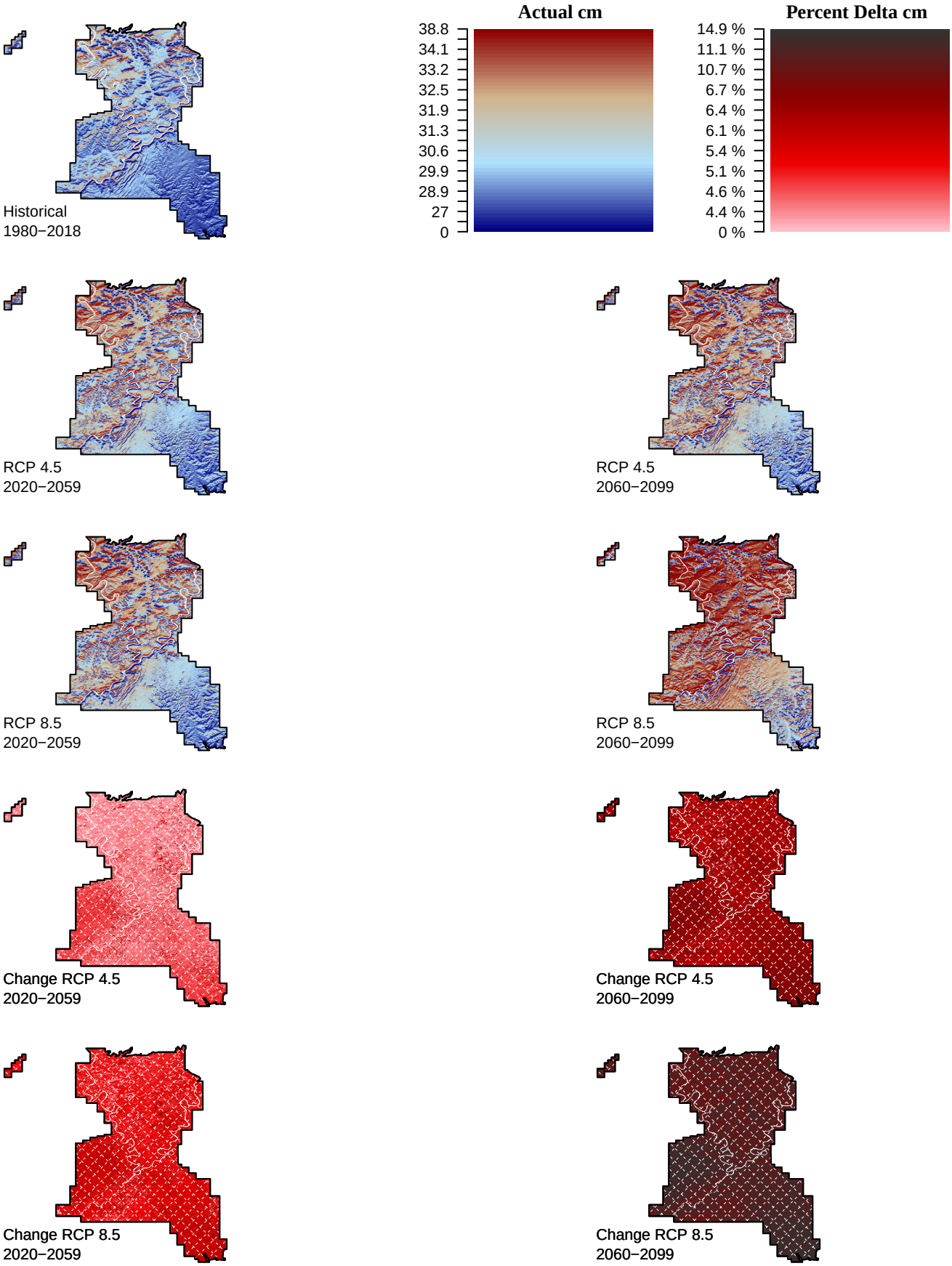


Figure CANYmap35:
Past trends and future trajectories of park−wide mean values for Spring potential evapotranspiration in Canyonlands. Topmost panel depicts the historical mean from 1980−2018. Lower four panels show the emission scenarios of RCP 4.5 and RCP 8.5 at near−term and long−term timeframes. Bottom four panels depict the change from the historical mean; cross hatching denotes areas of robust predicitons (90% of models agree in the direction of change).

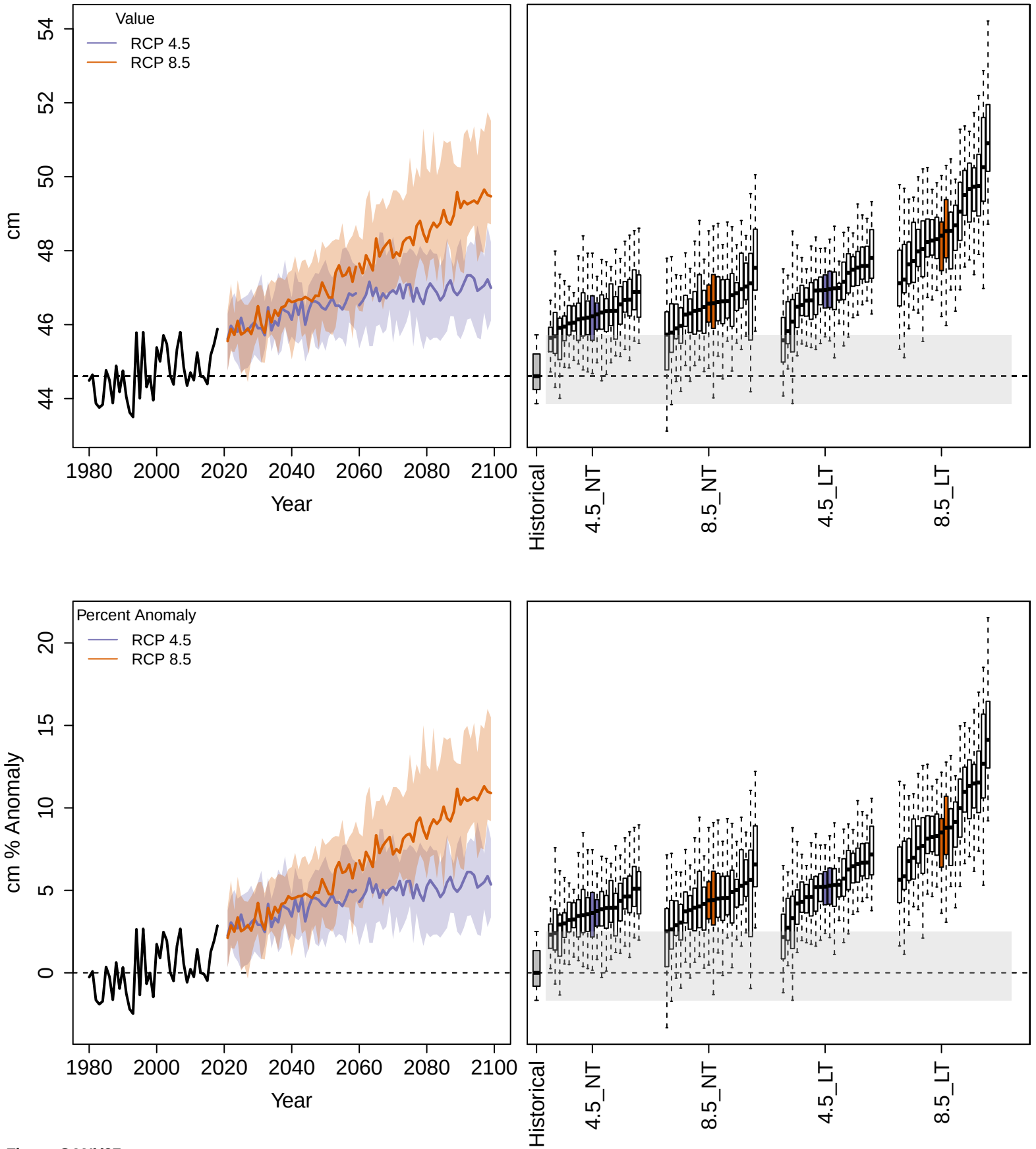


Figure CANY37:
Past trends and future trajectories of park−wide mean values for Summer potential evapotranspiration in Canyonlands. Top panels show values, bottom panels show changes from the long−term historical mean. Left: Time series of historical (black) and future projections for RCP 4.5 and 8.5. Shaded areas show spread among climate models. Right: Boxplots of temporal variability over 40−year periods under historical (left box) and individual climate models under two RCPs. Right: Historical time period is 1970−2010; near−term (NT) is 2020−2060; long−term (LT) is 2061−2100.

Canyonlands: Summer potential evapotranspiration

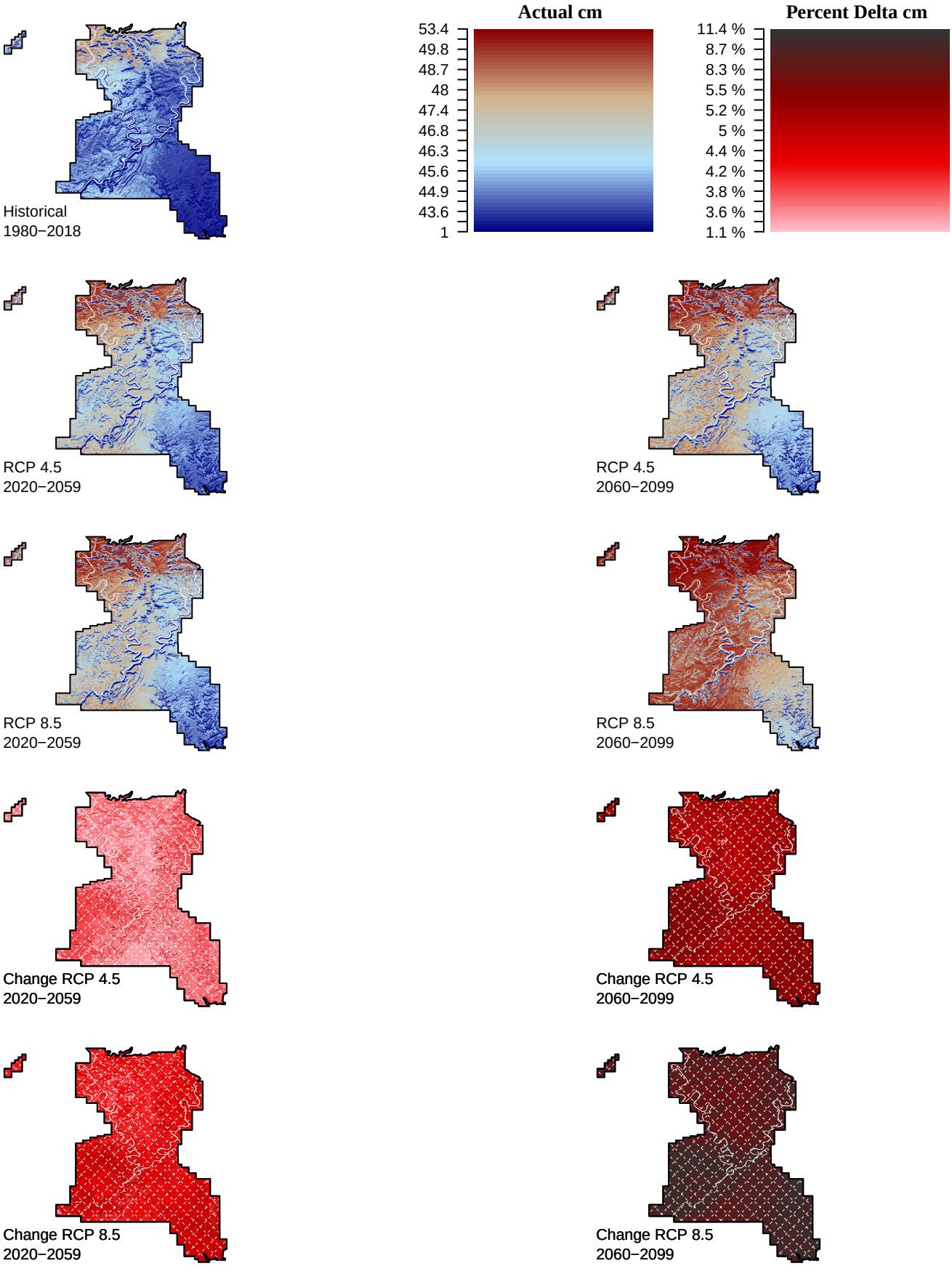


Figure CANYmap37:
Past trends and future trajectories of park−wide mean values for Summer potential evapotranspiration in Canyonlands. Topmost panel depicts the historical mean from 1980−2018. Lower four panels show the emission scenarios of RCP 4.5 and RCP 8.5 at near−term and long−term timeframes. Bottom four panels depict the change from the historical mean; cross hatching denotes areas of robust predicitons (90% of models agree in the direction of change).

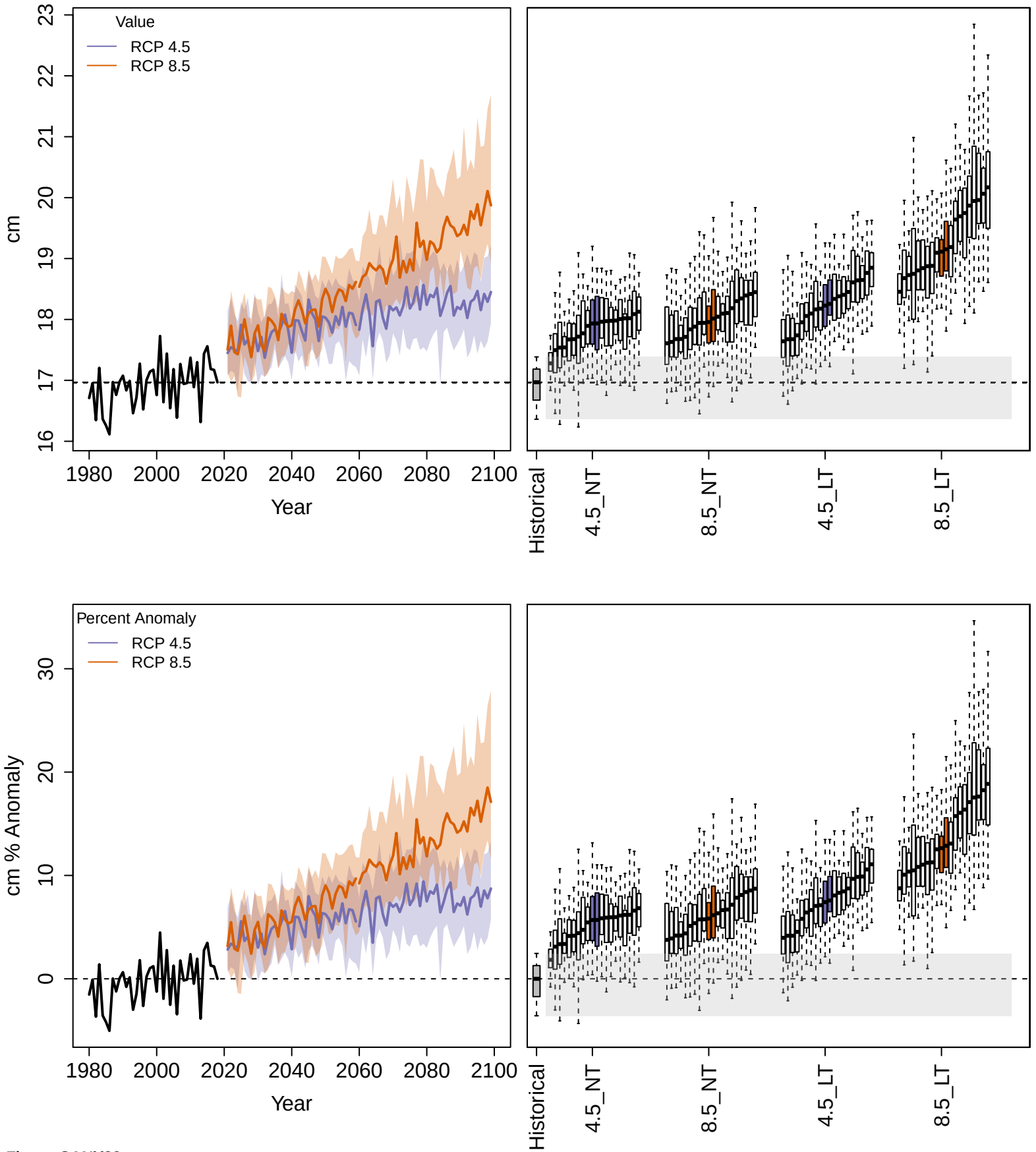


Figure CANY39:
Past trends and future trajectories of park−wide mean values for Fall potential evapotranspiration in Canyonlands. Top panels show values, bottom panels show changes from the long−term historical mean. Left: Time series of historical (black) and future projections for RCP 4.5 and 8.5. Shaded areas show spread among climate models. Right: Boxplots of temporal variability over 40−year periods under historical (left box) and individual climate models under two RCPs. Right: Historical time period is 1970−2010; near−term (NT) is 2020−2060; long−term (LT) is 2061−2100.

Canyonlands: Fall potential evapotranspiration

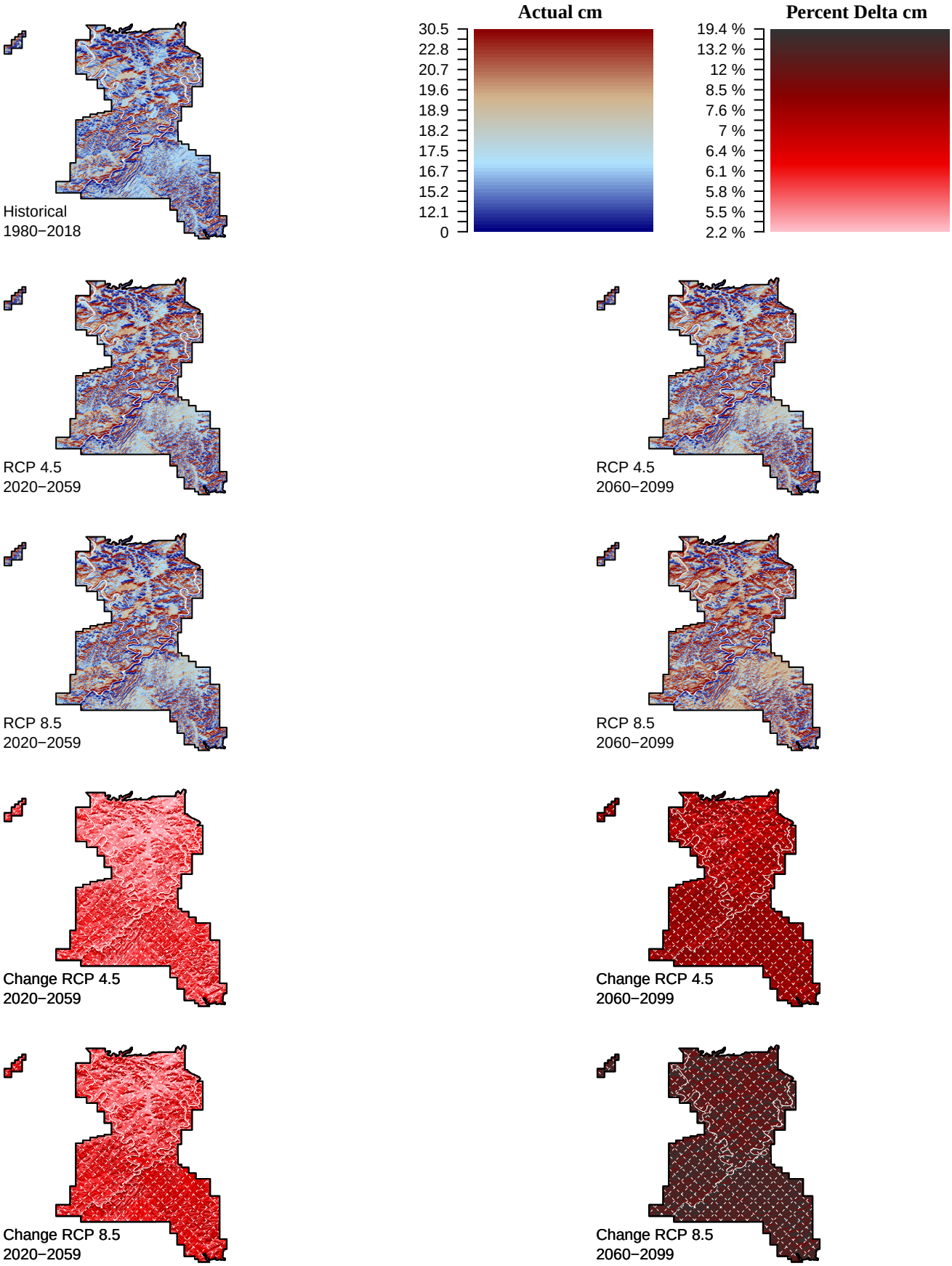


Figure CANYmap39:
Past trends and future trajectories of park−wide mean values for Fall potential evapotranspiration in Canyonlands. Topmost panel depicts the historical mean from 1980−2018. Lower four panels show the emission scenarios of RCP 4.5 and RCP 8.5 at near−term and long−term timeframes. Bottom four panels depict the change from the historical mean; cross hatching denotes areas of robust predicitons (90% of models agree in the direction of change).

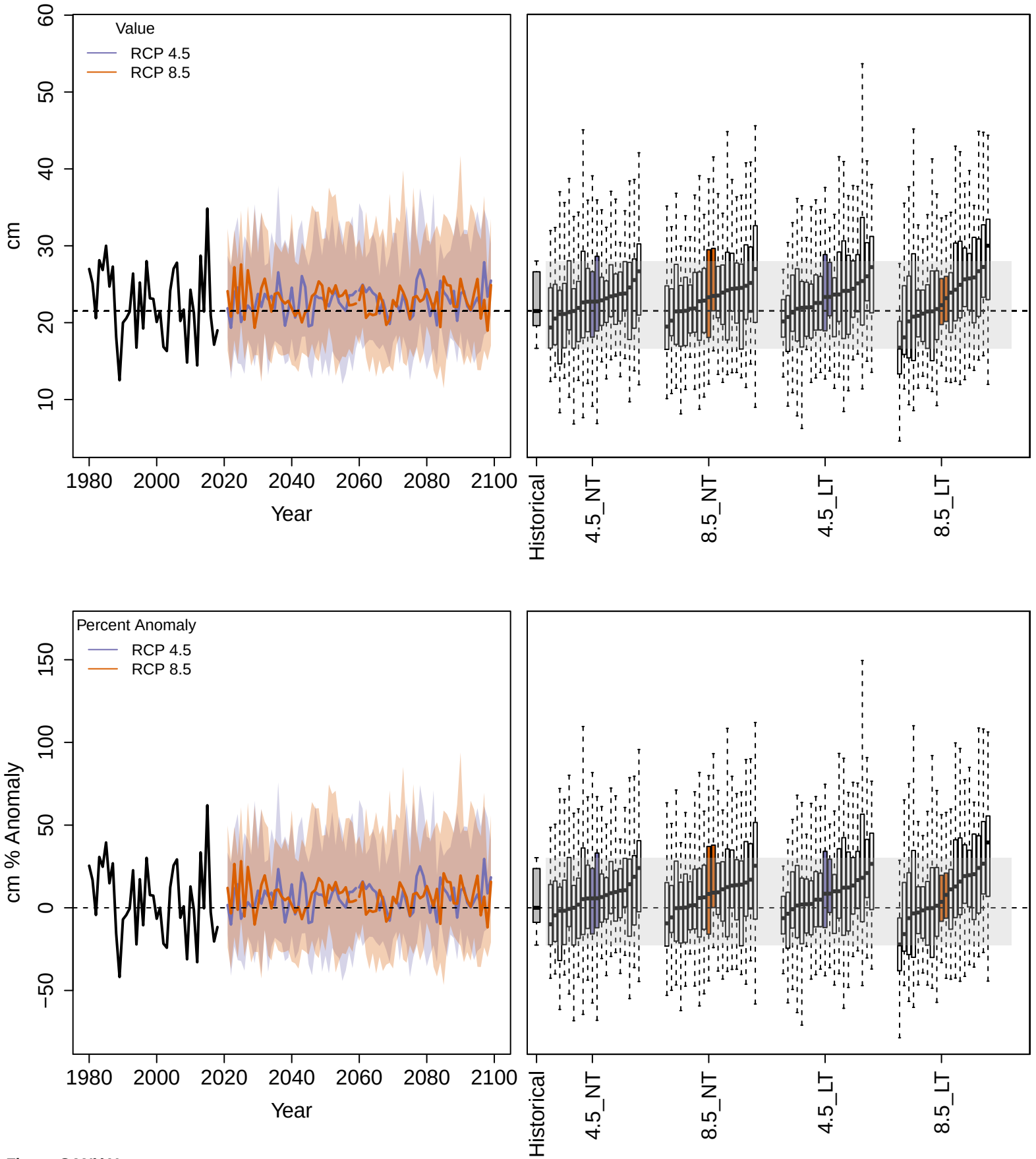


Figure CANY41:
Past trends and future trajectories of park−wide mean values for Annual Precipitation in Canyonlands. Top panels show values, bottom panels show changes from the long−term historical mean. Left: Time series of historical (black) and future projections for RCP 4.5 and 8.5. Shaded areas show spread among climate models. Right: Boxplots of temporal variability over 40−year periods under historical (left box) and individual climate models under two RCPs. Right: Historical time period is 1970−2010; near−term (NT) is 2020−2060; long−term (LT) is 2061−2100.

Canyonlands: Annual Precipitation

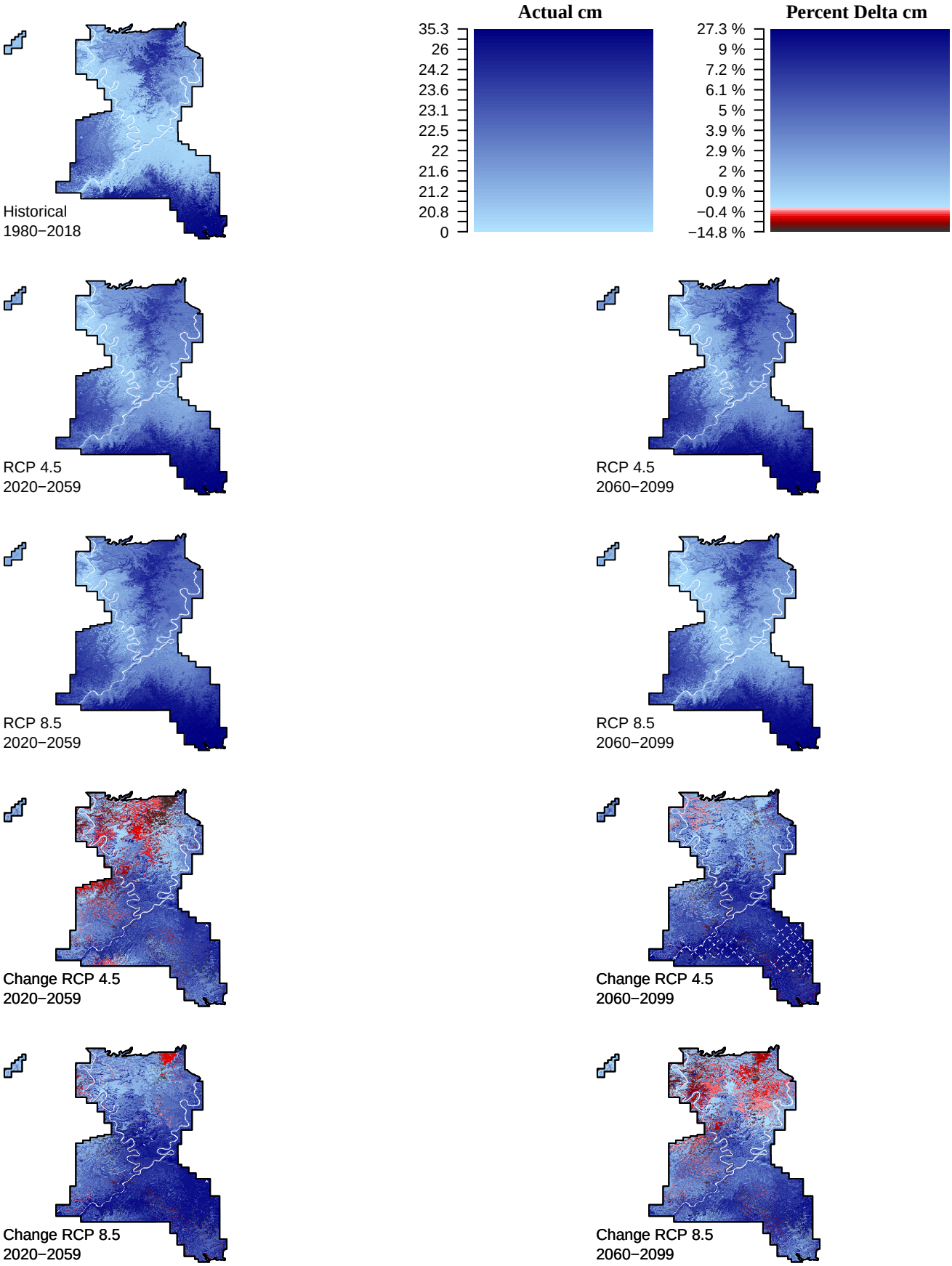


Figure CANYmap41:
Past trends and future trajectories of park−wide mean values for Annual Precipitation in Canyonlands. Topmost panel depicts the historical mean from 1980−2018. Lower four panels show the emission scenarios of RCP 4.5 and RCP 8.5 at near−term and long−term timeframes. Bottom four panels depict the change from the historical mean; cross hatching denotes areas of robust predicitons (90% of models agree in the direction of change).

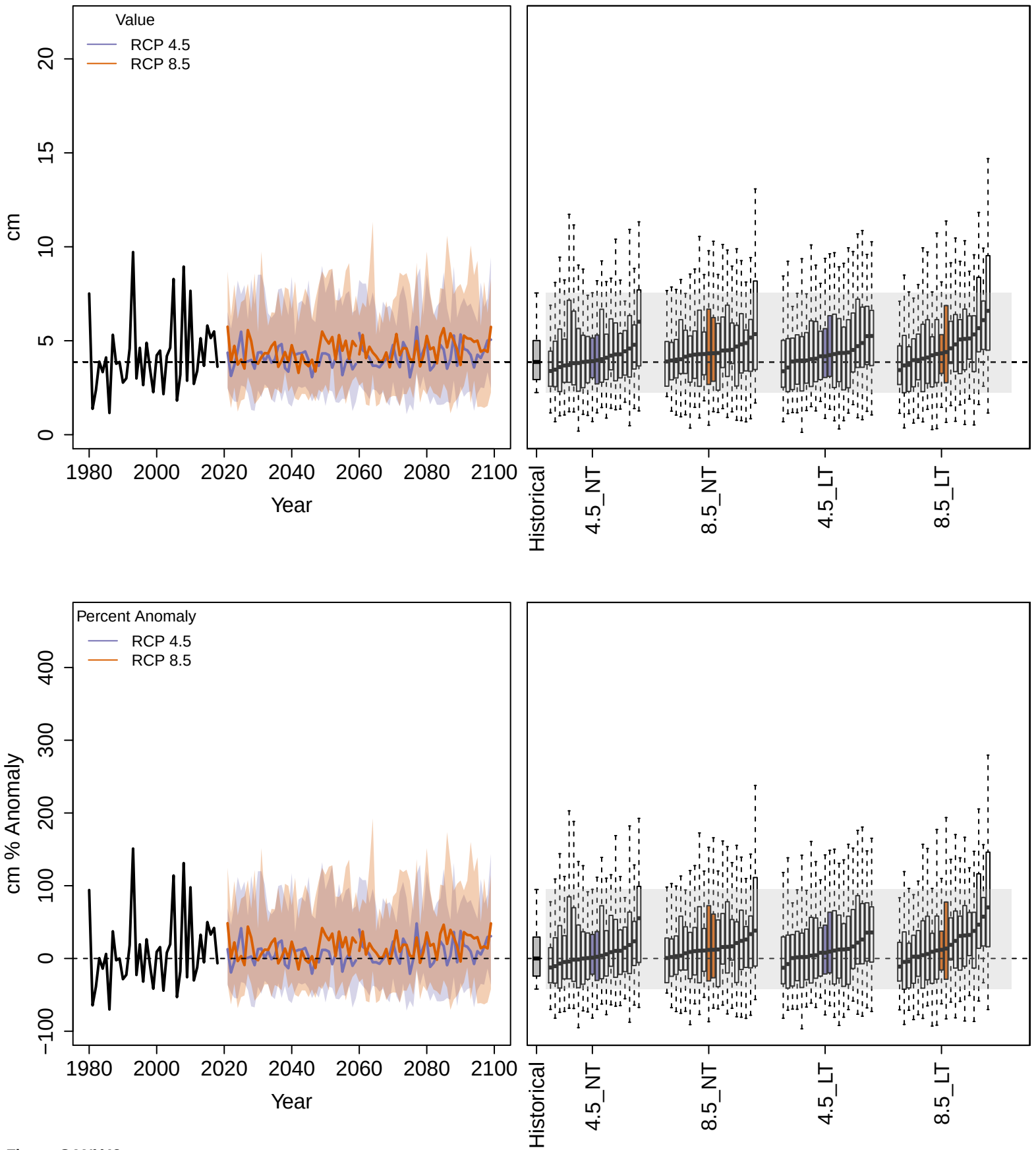


Figure CANY43:
Past trends and future trajectories of park−wide mean values for Winter Precipitation in Canyonlands. Top panels show values, bottom panels show changes from the long−term historical mean. Left: Time series of historical (black) and future projections for RCP 4.5 and 8.5. Shaded areas show spread among climate models. Right: Boxplots of temporal variability over 40−year periods under historical (left box) and individual climate models under two RCPs. Right: Historical time period is 1970−2010; near−term (NT) is 2020−2060; long−term (LT) is 2061−2100.

Canyonlands: Winter Precipitation

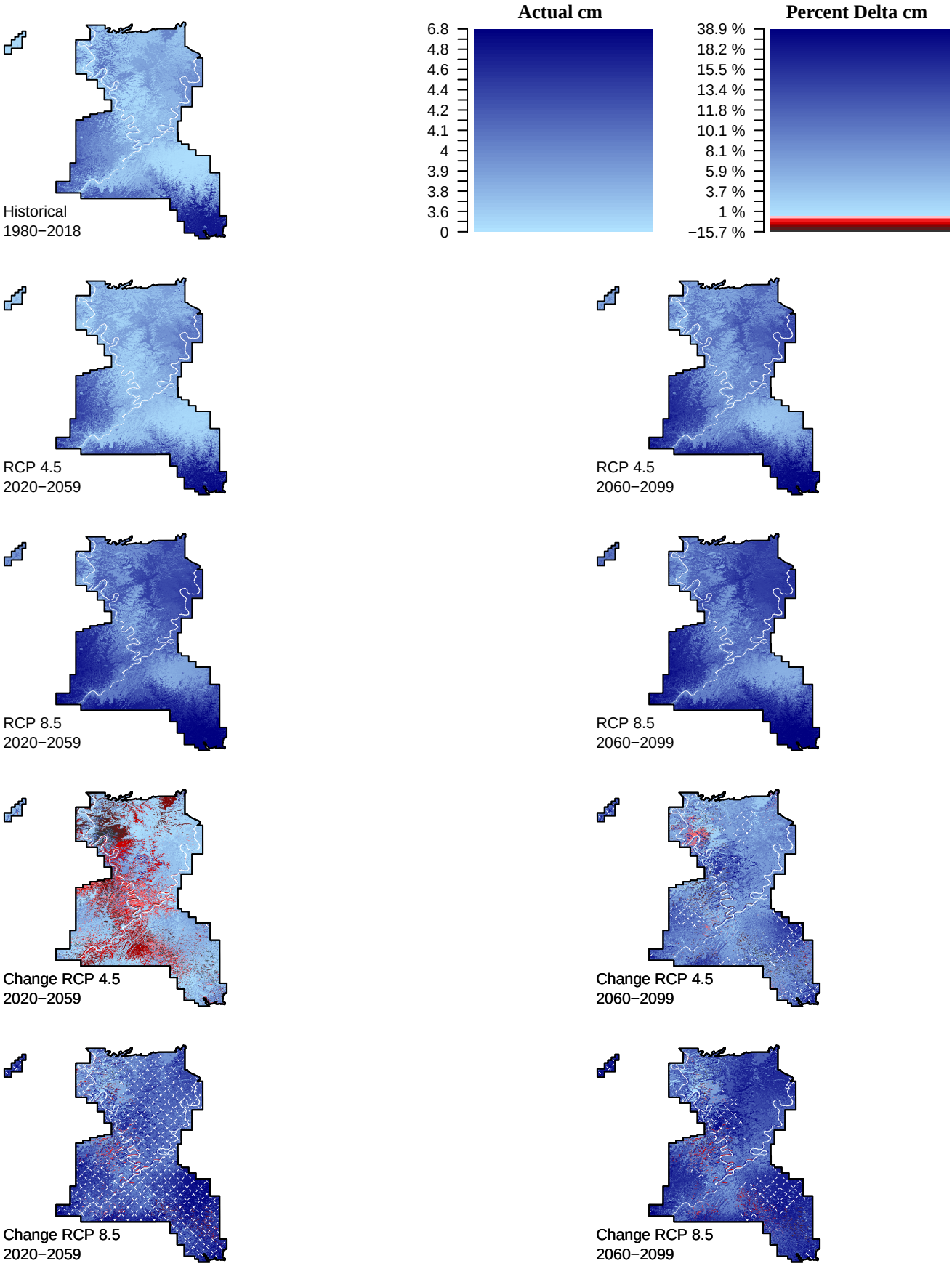


Figure CANYmap43:
Past trends and future trajectories of park−wide mean values for Winter Precipitation in Canyonlands. Topmost panel depicts the historical mean from 1980−2018. Lower four panels show the emission scenarios of RCP 4.5 and RCP 8.5 at near−term and long−term timeframes. Bottom four panels depict the change from the historical mean; cross hatching denotes areas of robust predicitons (90% of models agree in the direction of change).

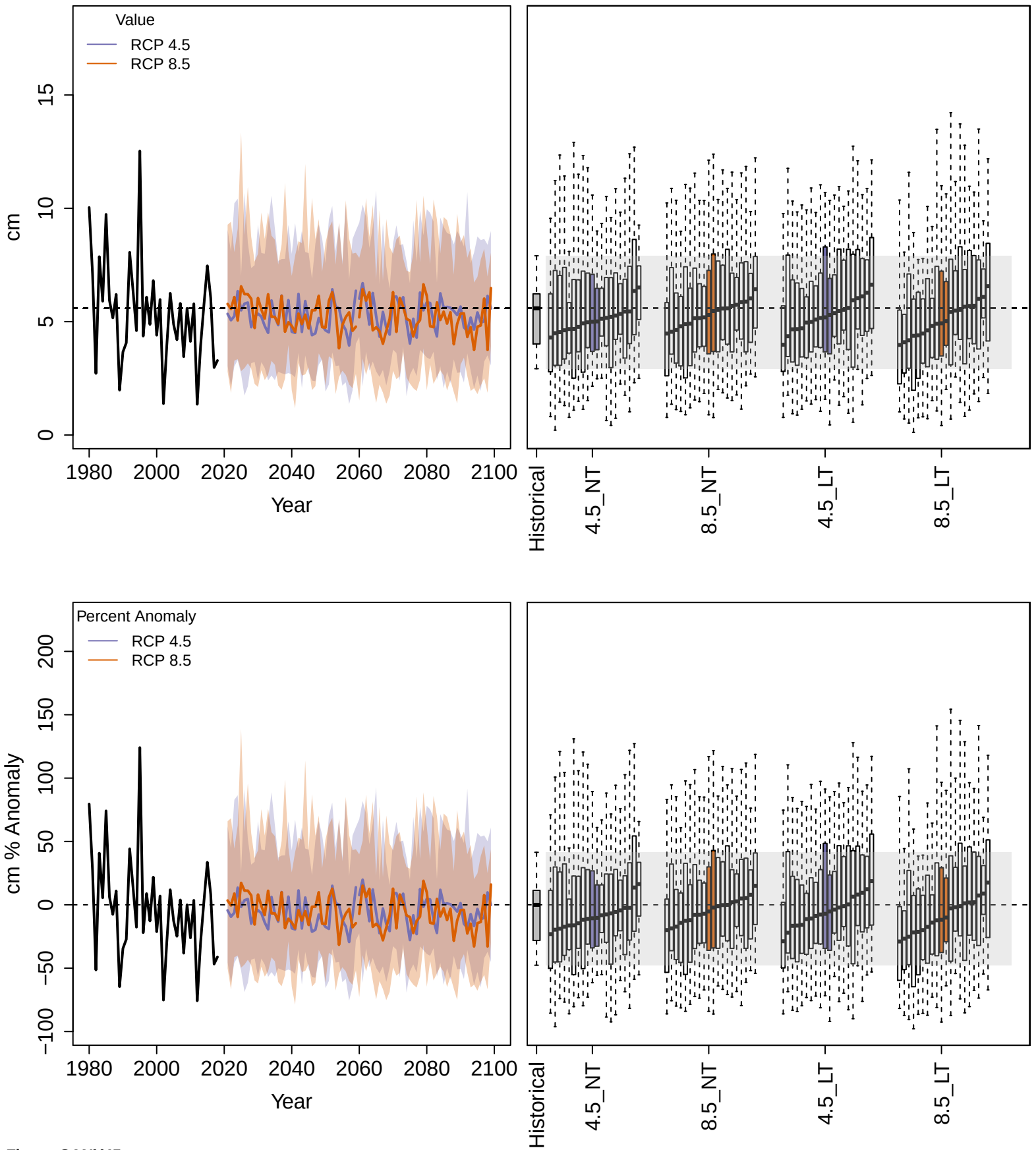


Figure CANY45:
Past trends and future trajectories of park−wide mean values for Spring Precipitation in Canyonlands. Top panels show values, bottom panels show changes from the long−term historical mean. Left: Time series of historical (black) and future projections for RCP 4.5 and 8.5. Shaded areas show spread among climate models. Right: Boxplots of temporal variability over 40−year periods under historical (left box) and individual climate models under two RCPs. Right: Historical time period is 1970−2010; near−term (NT) is 2020−2060; long−term (LT) is 2061−2100.

Canyonlands: Spring Precipitation

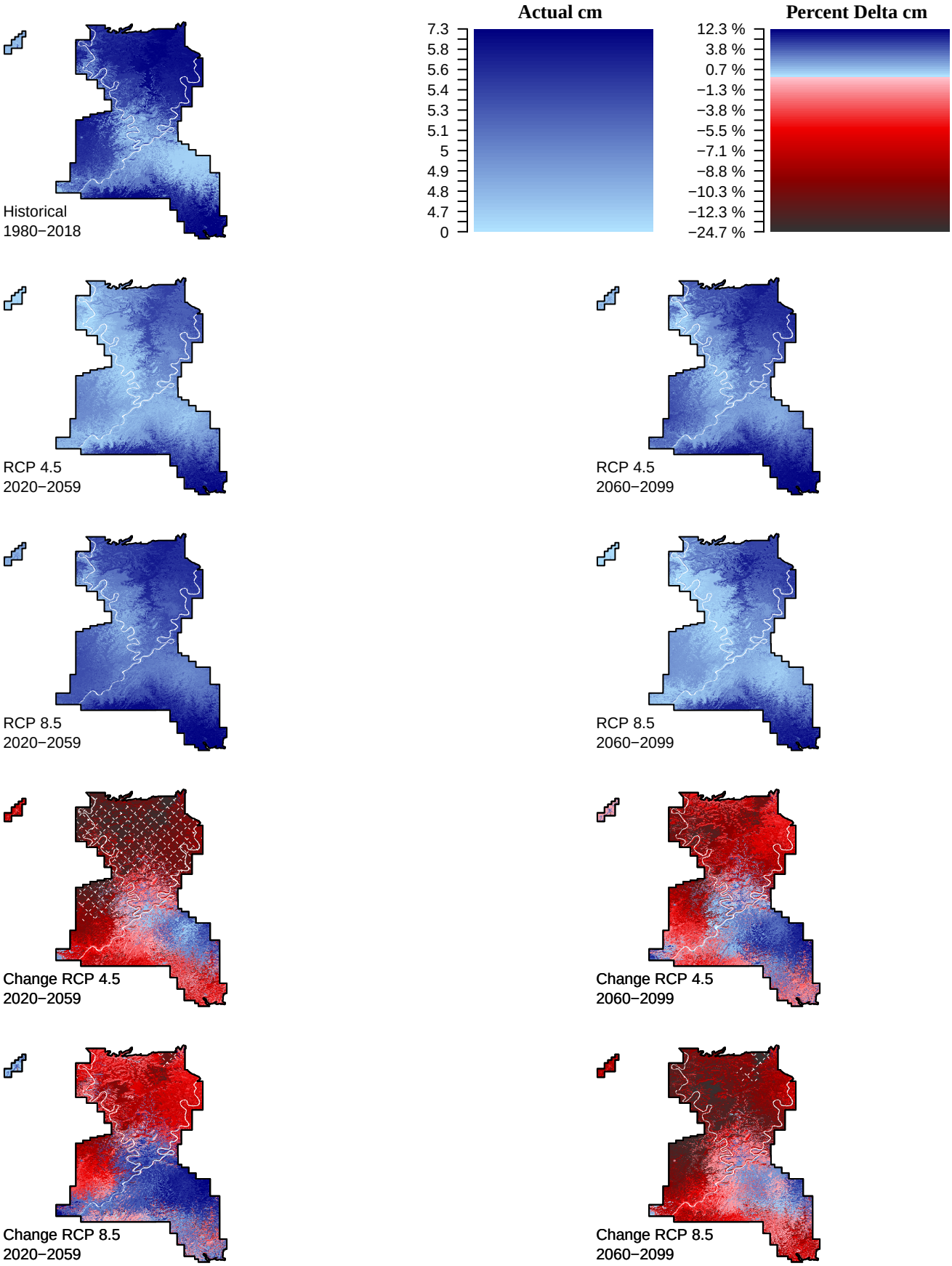


Figure CANYmap45:
Past trends and future trajectories of park−wide mean values for Spring Precipitation in Canyonlands. Topmost panel depicts the historical mean from 1980−2018. Lower four panels show the emission scenarios of RCP 4.5 and RCP 8.5 at near−term and long−term timeframes. Bottom four panels depict the change from the historical mean; cross hatching denotes areas of robust predicitons (90% of models agree in the direction of change).

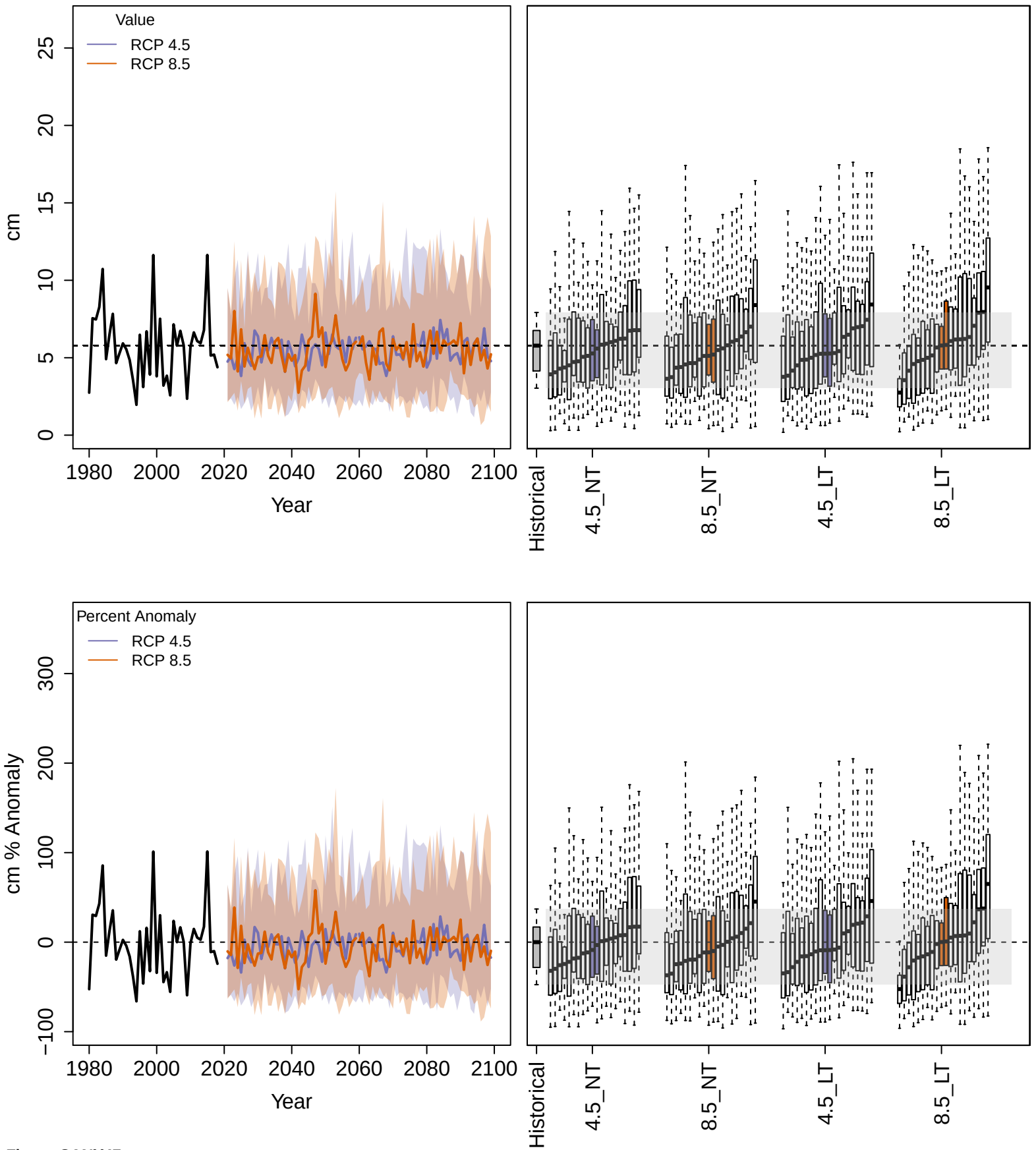


Figure CANY47:
Past trends and future trajectories of park−wide mean values for Summer Precipitation in Canyonlands. Top panels show values, bottom panels show changes from the long−term historical mean. Left: Time series of historical (black) and future projections for RCP 4.5 and 8.5. Shaded areas show spread among climate models. Right: Boxplots of temporal variability over 40−year periods under historical (left box) and individual climate models under two RCPs. Right: Historical time period is 1970−2010; near−term (NT) is 2020−2060; long−term (LT) is 2061−2100.

Canyonlands: Summer Precipitation

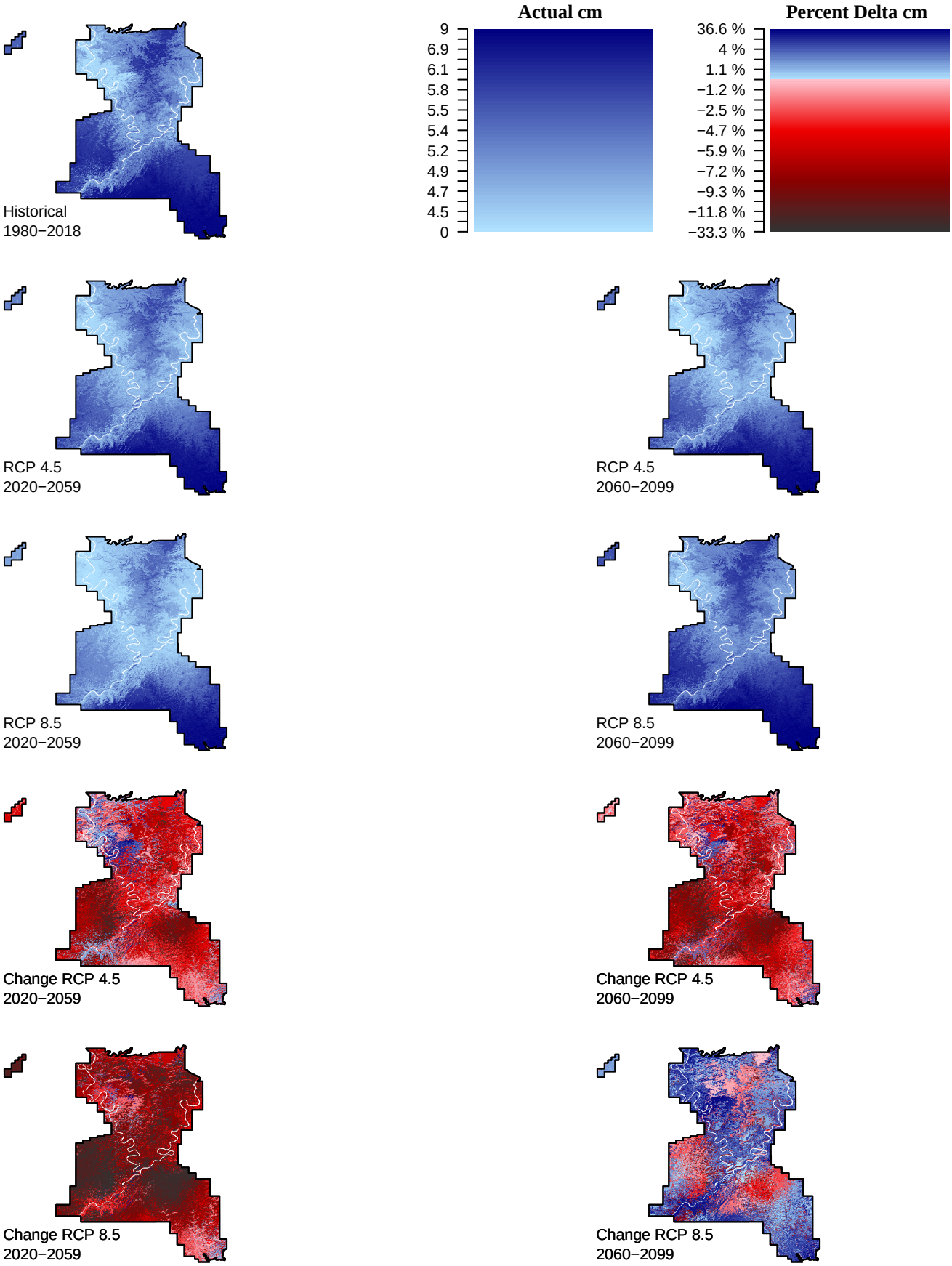


Figure CANYmap47:
Past trends and future trajectories of park−wide mean values for Summer Precipitation in Canyonlands. Topmost panel depicts the historical mean from 1980−2018. Lower four panels show the emission scenarios of RCP 4.5 and RCP 8.5 at near−term and long−term timeframes. Bottom four panels depict the change from the historical mean; cross hatching denotes areas of robust predicitons (90% of models agree in the direction of change).

Canyonlands: Fall Precipitation

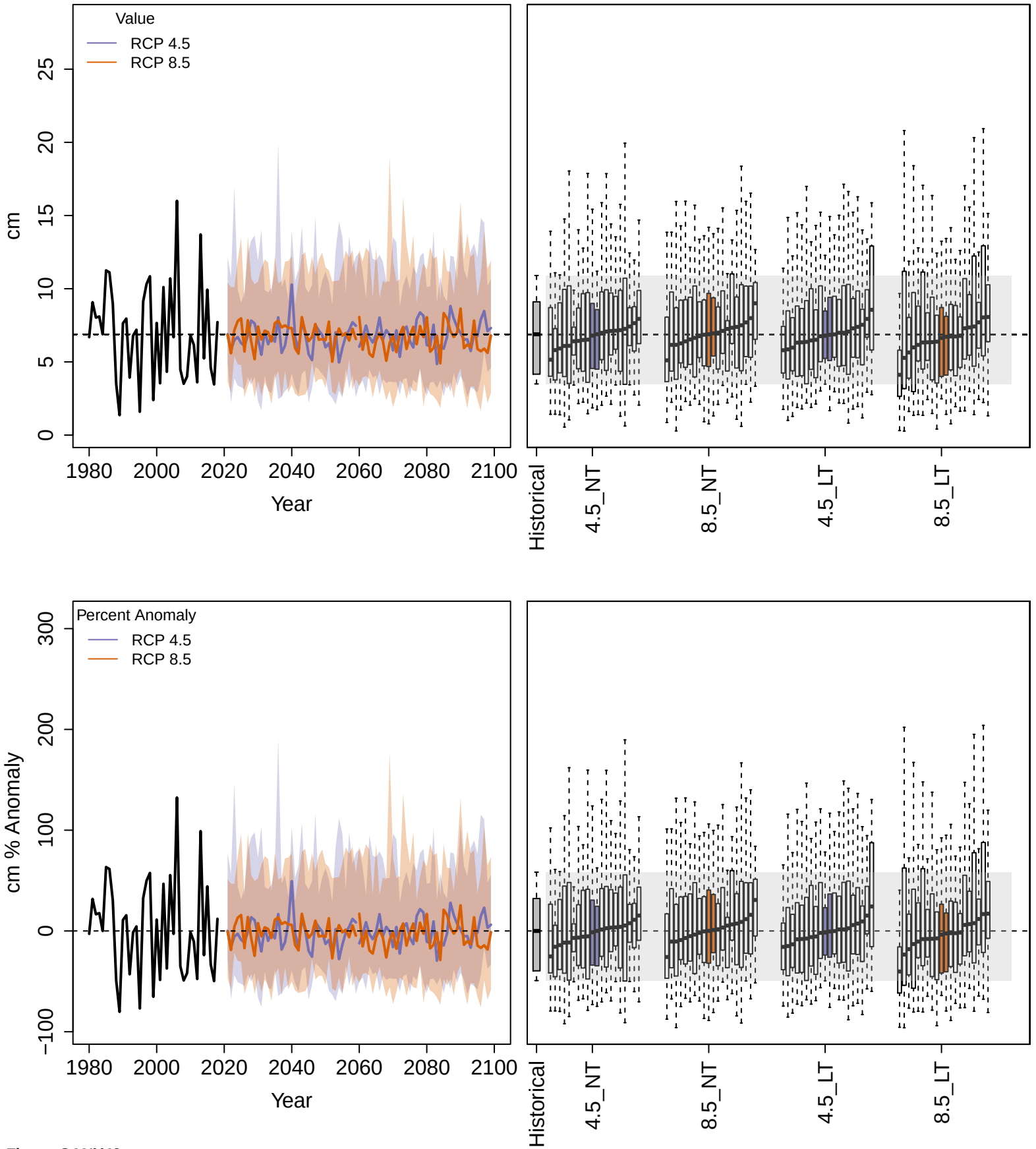


Figure CANY49:
Past trends and future trajectories of park−wide mean values for Fall Precipitation in Canyonlands. Top panels show values, bottom panels show changes from the long−term historical mean. Left: Time series of historical (black) and future projections for RCP 4.5 and 8.5. Shaded areas show spread among climate models. Right: Boxplots of temporal variability over 40−year periods under historical (left box) and individual climate models under two RCPs. Right: Historical time period is 1970−2010; near−term (NT) is 2020−2060; long−term (LT) is 2061−2100.

Canyonlands: Fall Precipitation

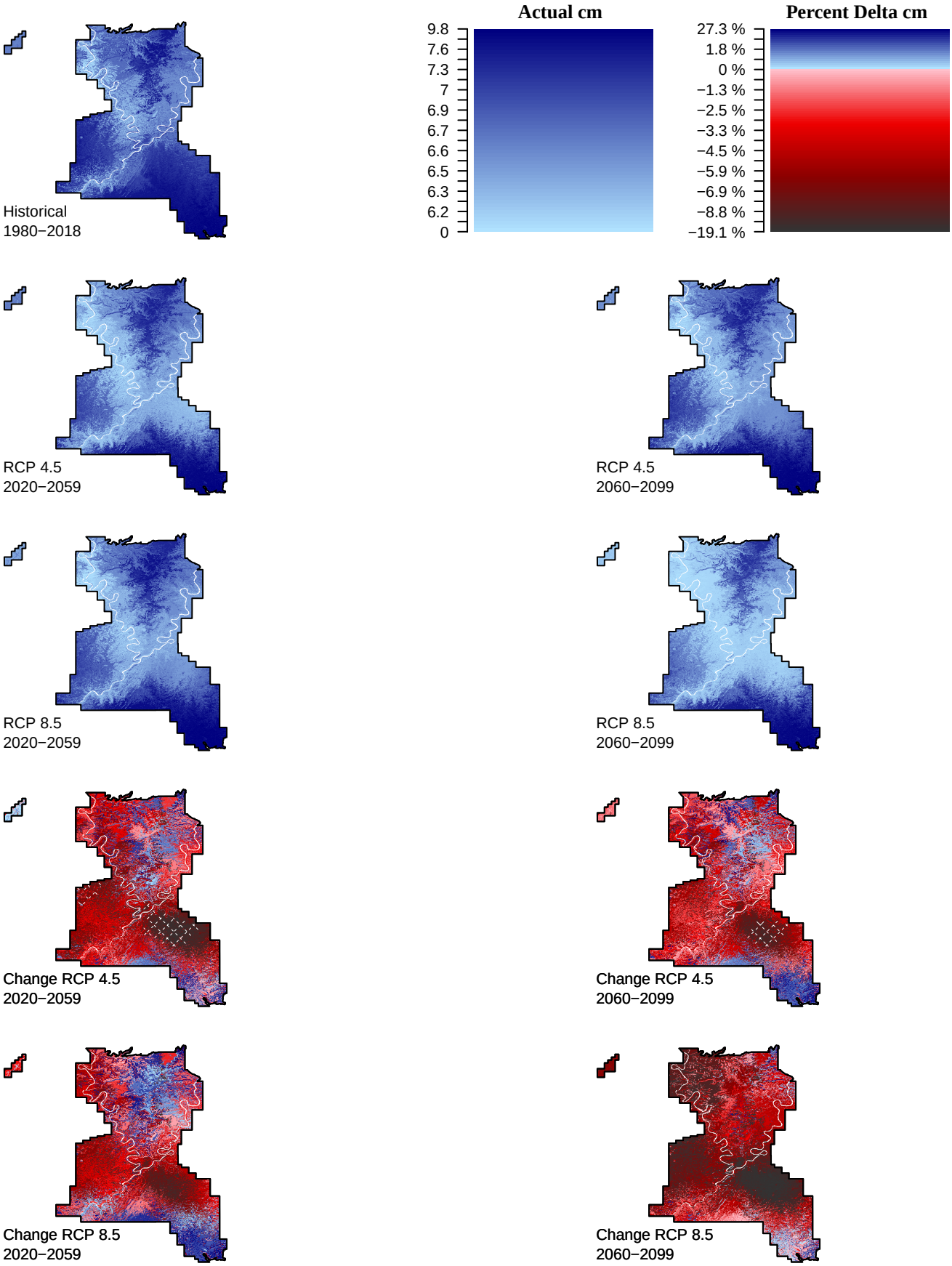


Figure CANYmap49:
Past trends and future trajectories of park−wide mean values for Fall Precipitation in Canyonlands. Topmost panel depicts the historical mean from 1980−2018. Lower four panels show the emission scenarios of RCP 4.5 and RCP 8.5 at near−term and long−term timeframes. Bottom four panels depict the change from the historical mean; cross hatching denotes areas of robust predicitons (90% of models agree in the direction of change).

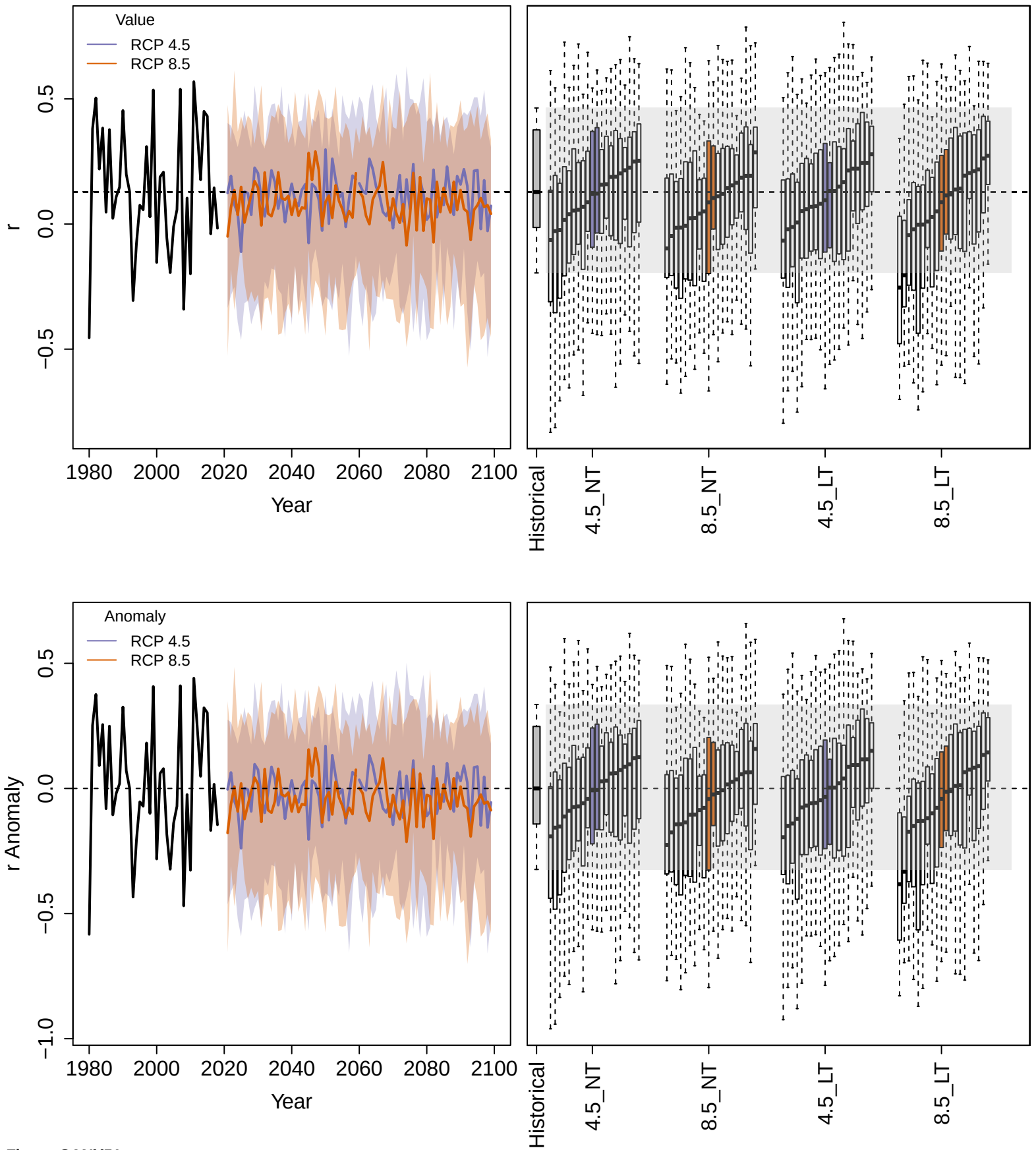


Figure CANY51:
Past trends and future trajectories of park−wide mean values for Monthly temperature−precipitation correlation in Canyonlands. Top panels show values, bottom panels show changes from the long−term historical mean. Left: Time series of historical (black) and future projections for RCP 4.5 and 8.5. Shaded areas show spread among climate models. Right: Boxplots of temporal variability over 40−year periods under historical (left box) and individual climate models under two RCPs. Right: Historical time period is 1970−2010; near−term (NT) is 2020−2060; long−term (LT) is 2061−2100.

Canyonlands: Monthly temperature−precipitation correlation

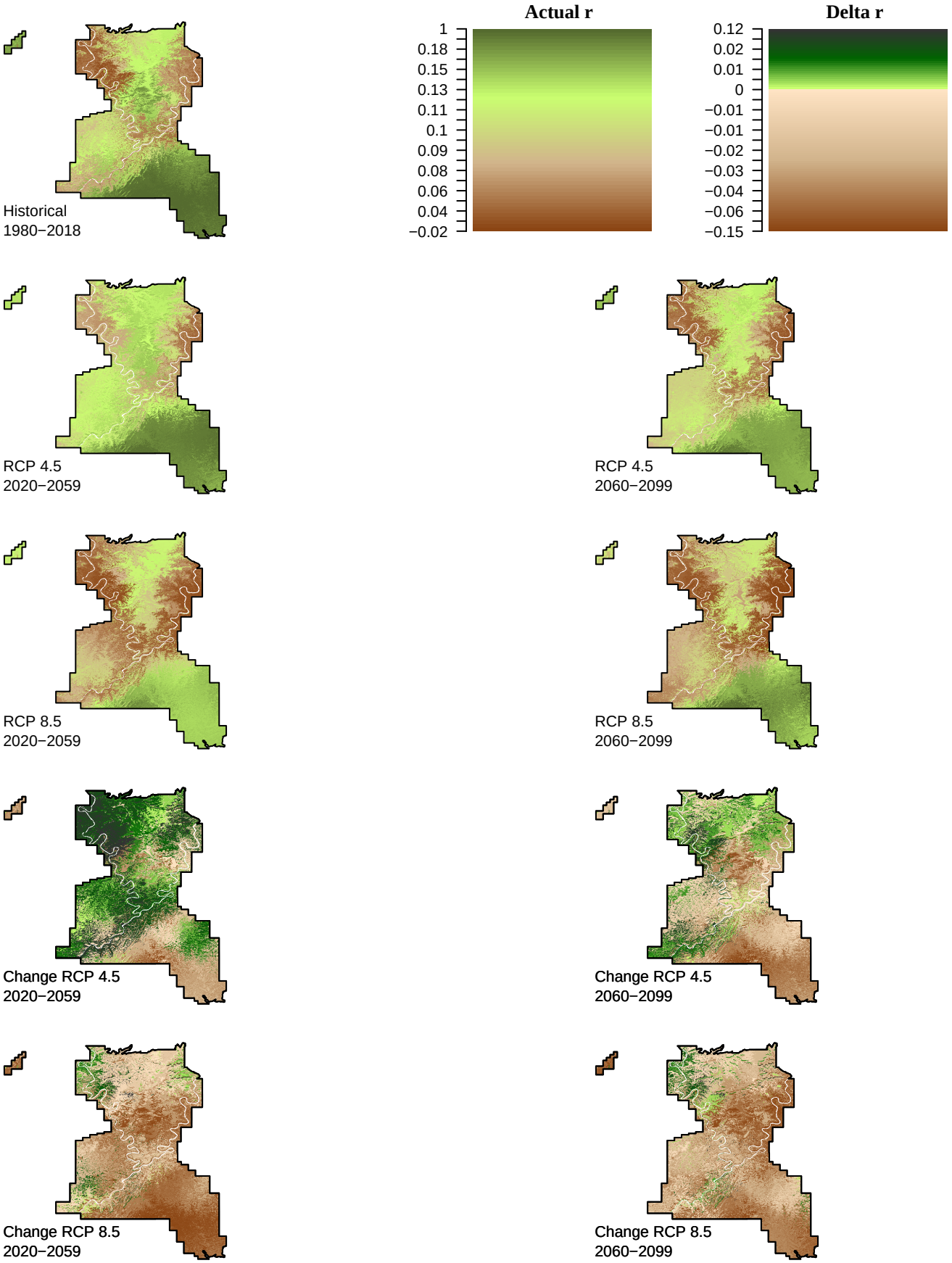


Figure CANYmap51:
Past trends and future trajectories of park−wide mean values for Monthly temperature−precipitation correlation in Canyonlands. Topmost panel depicts the historical mean from 1980−2018. Lower four panels show the emission scenarios of RCP 4.5 and RCP 8.5 at near−term and long−term timeframes. Bottom four panels depict the change from the historical mean; cross hatching denotes areas of robust predicitons (90% of models agree in the direction of change).

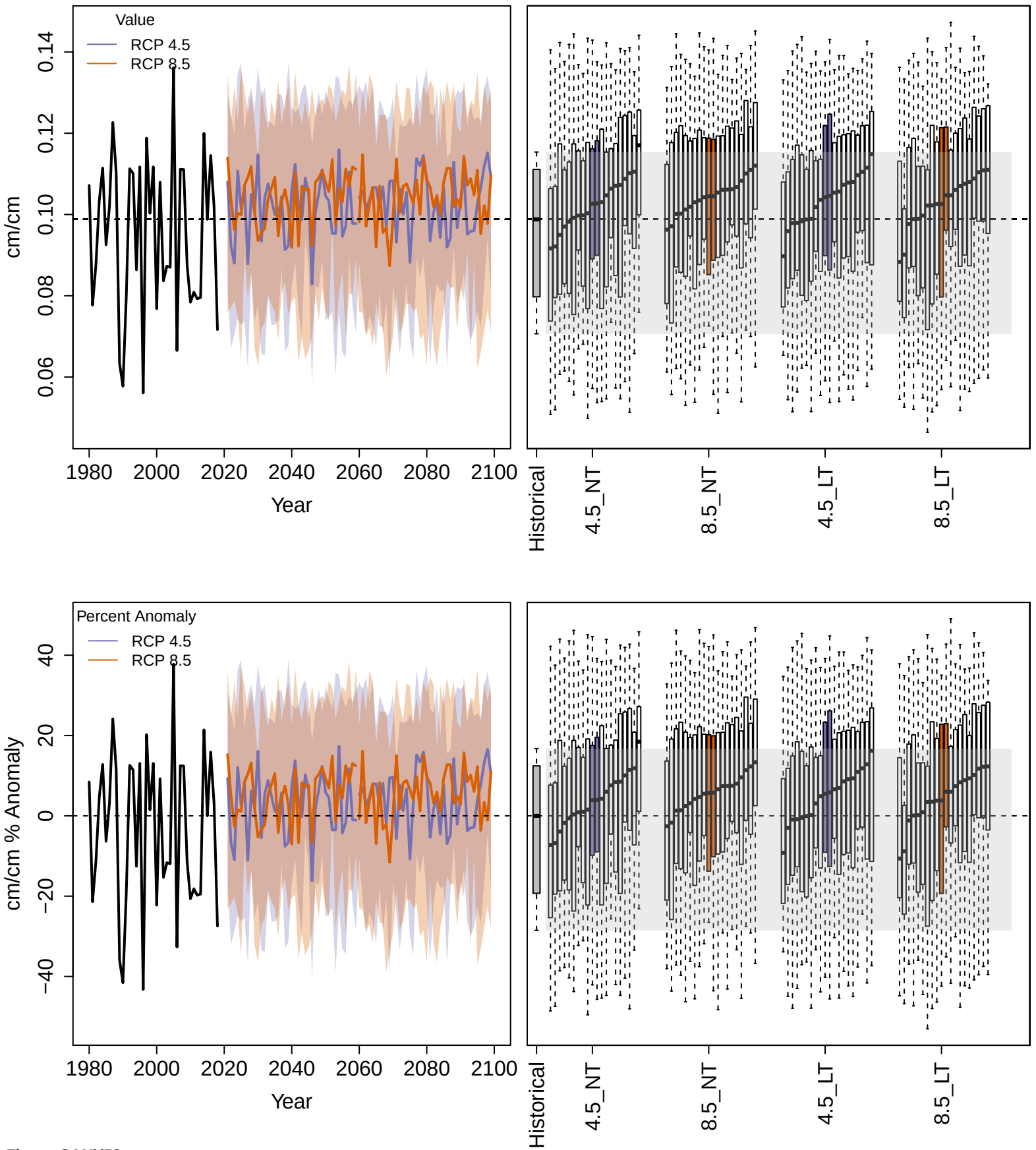


Figure CANY53:
Past trends and future trajectories of park−wide mean values for Winter soil water content: Top 50cm in Canyonlands. Top panels show values, bottom panels show changes from the long−term historical mean. Left: Time series of historical (black) and future projections for RCP 4.5 and 8.5. Shaded areas show spread among climate models. Right: Boxplots of temporal variability over 40−year periods under historical (left box) and individual climate models under two RCPs. Right: Historical time period is 1970−2010; near−term (NT) is 2020−2060; long−term (LT) is 2061−2100.

Canyonlands: Winter soil water content: Top 50cm

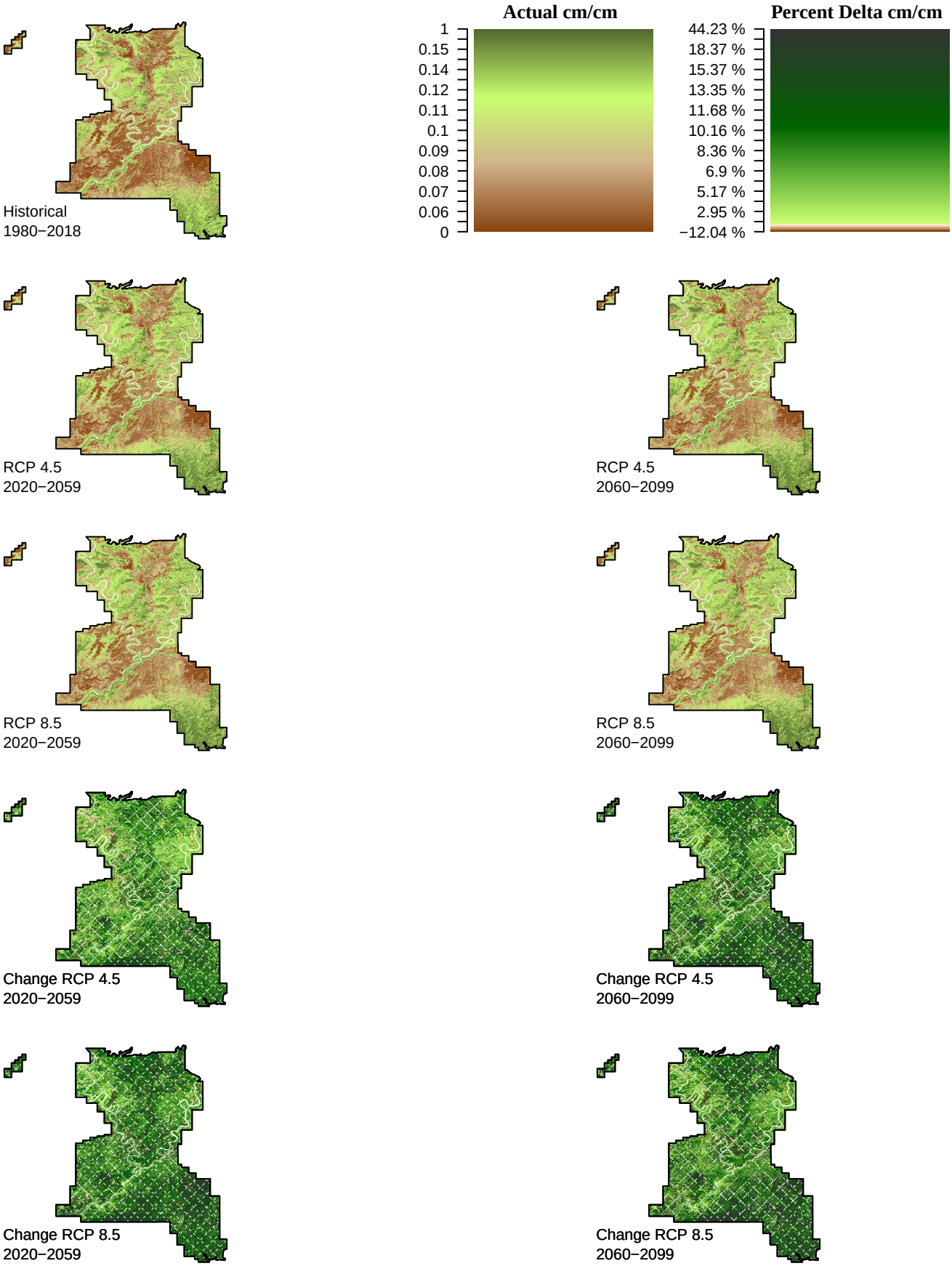


Figure CANYmap53:
Past trends and future trajectories of park−wide mean values for Winter soil water content: Top 50cm in Canyonlands. Topmost panel depicts the historical mean from 1980−2018. Lower four panels show the emission scenarios of RCP 4.5 and RCP 8.5 at near−term and long−term timeframes. Bottom four panels depict the change from the historical mean; cross hatching denotes areas of robust predicitons (90% of models agree in the direction of change).

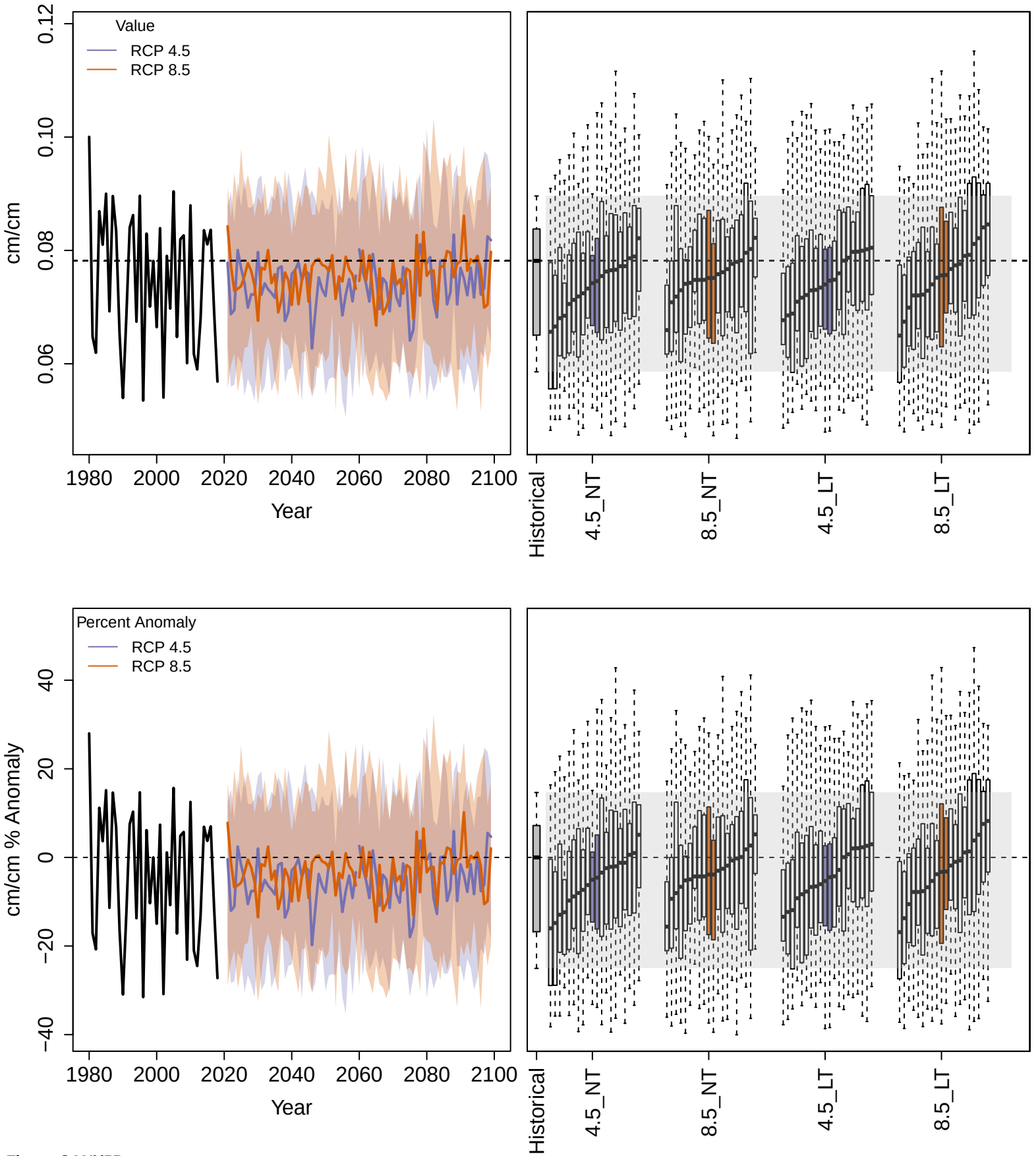


Figure CANY55:
Past trends and future trajectories of park−wide mean values for Spring soil water content:Top 50cm in Canyonlands. Top panels show values, bottom panels show changes from the long−term historical mean. Left: Time series of historical (black) and future projections for RCP 4.5 and 8.5. Shaded areas show spread among climate models. Right: Boxplots of temporal variability over 40−year periods under historical (left box) and individual climate models under two RCPs. Right: Historical time period is 1970−2010; near−term (NT) is 2020−2060; long−term (LT) is 2061−2100.

Canyonlands: Spring soil water content:Top 50cm

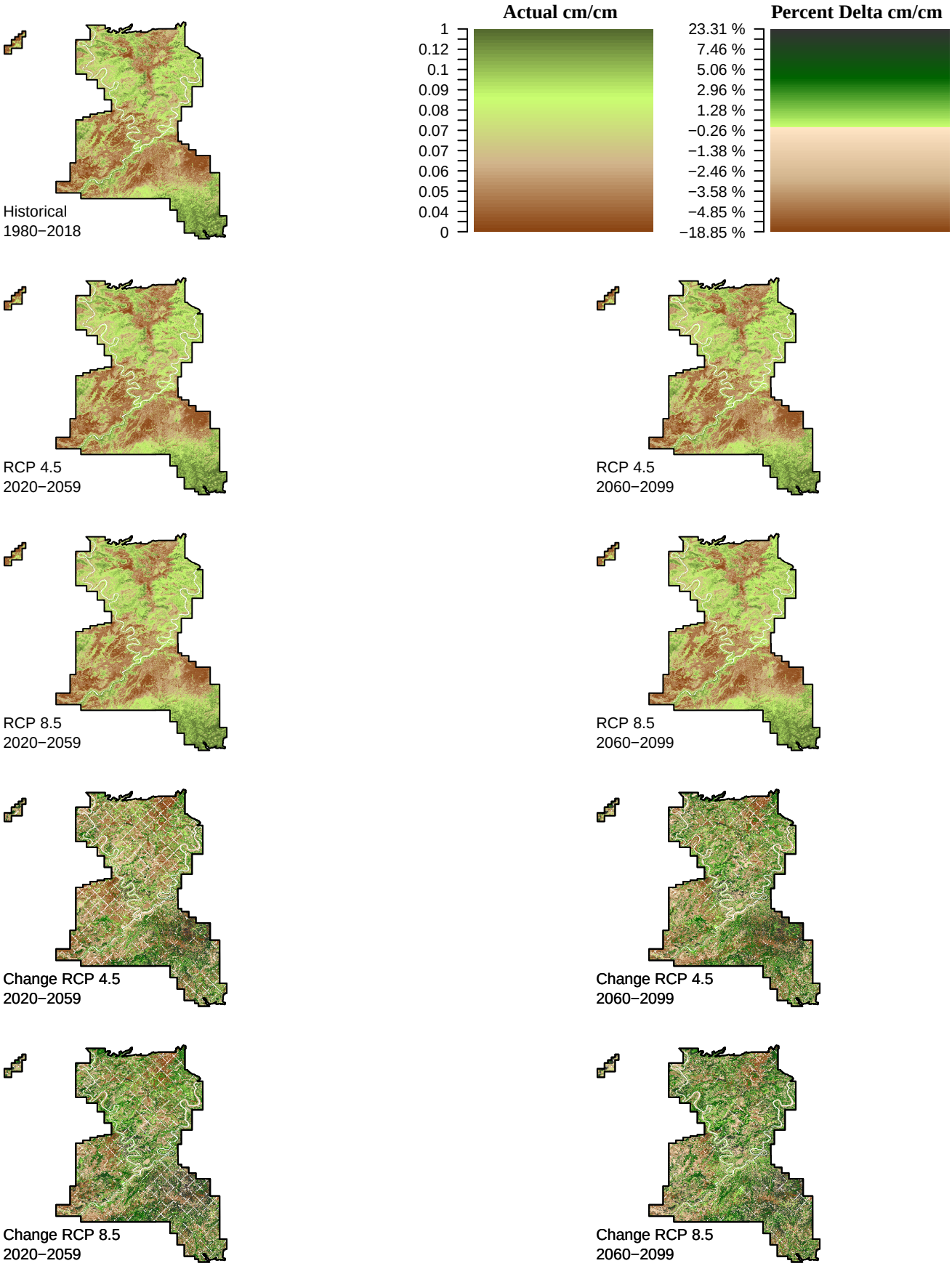


Figure CANYmap55:
Past trends and future trajectories of park−wide mean values for Spring soil water content:Top 50cm in Canyonlands. Topmost panel depicts the historical mean from 1980−2018. Lower four panels show the emission scenarios of RCP 4.5 and RCP 8.5 at near−term and long−term timeframes. Bottom four panels depict the change from the historical mean; cross hatching denotes areas of robust predicitons (90% of models agree in the direction of change).

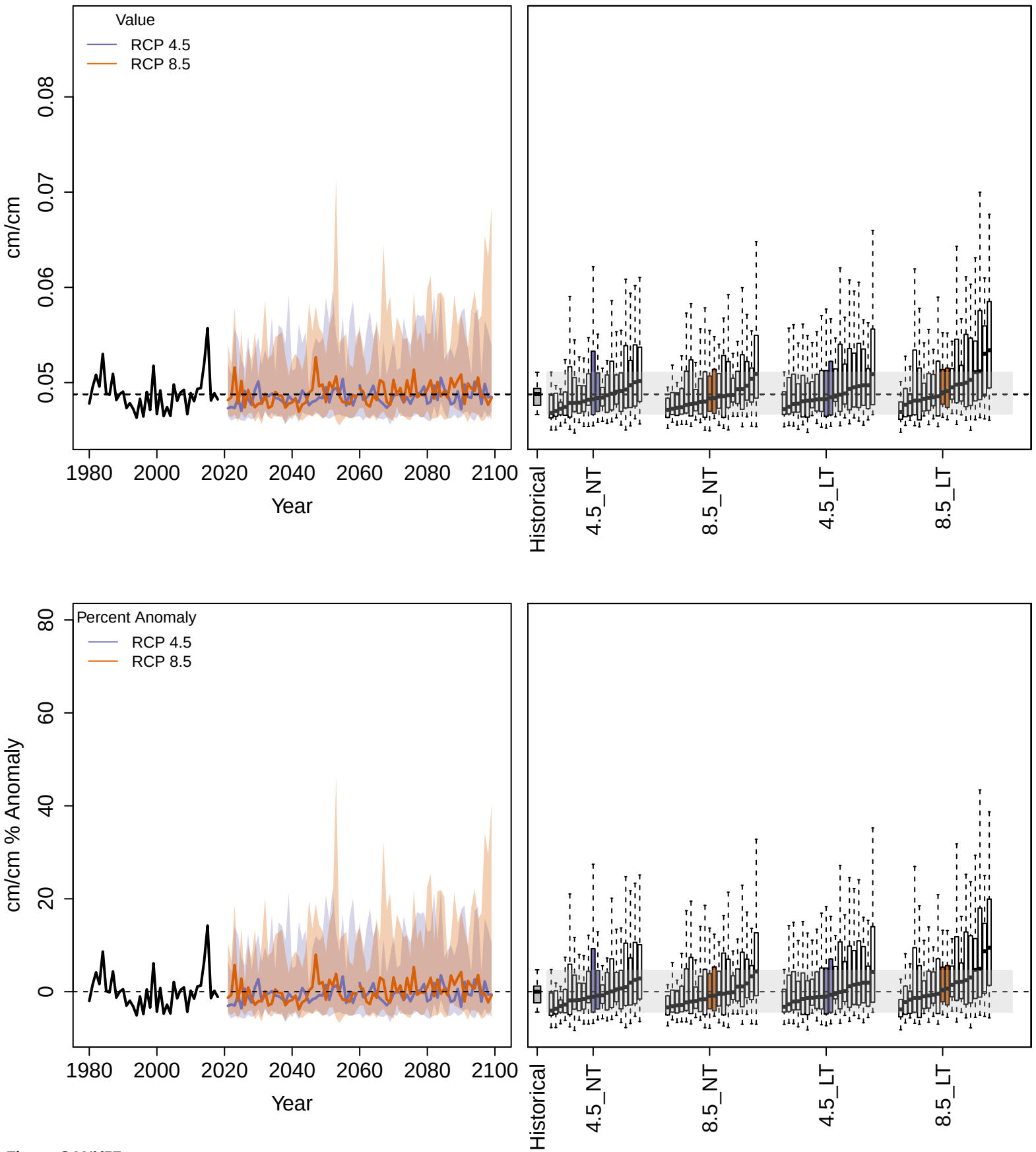


Figure CANY57:
Past trends and future trajectories of park−wide mean values for Summer soil water content:Top 50cm in Canyonlands. Top panels show values, bottom panels show changes from the long−term historical mean. Left: Time series of historical (black) and future projections for RCP 4.5 and 8.5. Shaded areas show spread among climate models. Right: Boxplots of temporal variability over 40−year periods under historical (left box) and individual climate models under two RCPs. Right: Historical time period is 1970−2010; near−term (NT) is 2020−2060; long−term (LT) is 2061−2100.

Canyonlands: Summer soil water content:Top 50cm

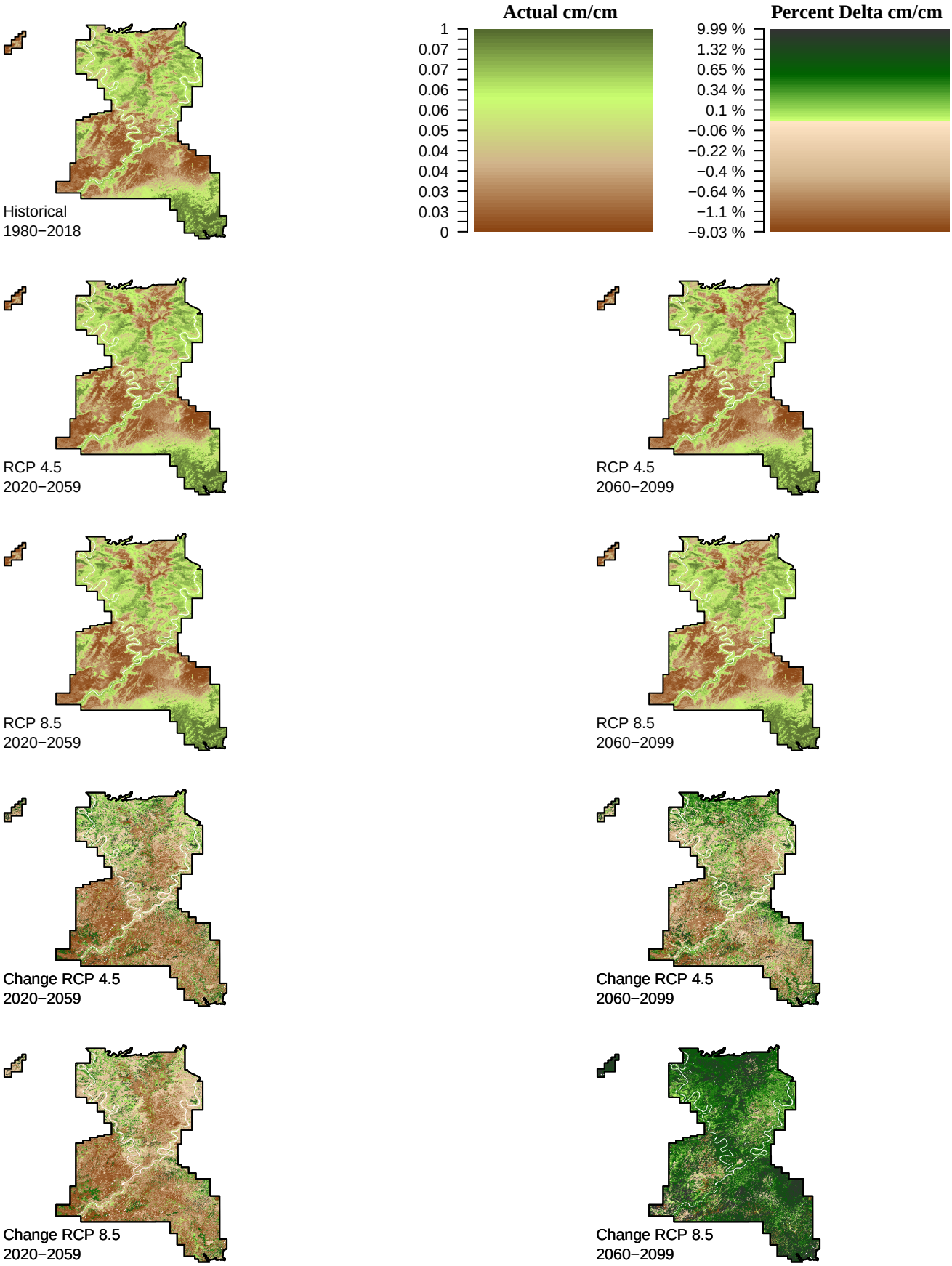


Figure CANYmap57:
Past trends and future trajectories of park−wide mean values for Summer soil water content:Top 50cm in Canyonlands. Topmost panel depicts the historical mean from 1980−2018. Lower four panels show the emission scenarios of RCP 4.5 and RCP 8.5 at near−term and long−term timeframes. Bottom four panels depict the change from the historical mean; cross hatching denotes areas of robust predicitons (90% of models agree in the direction of change).

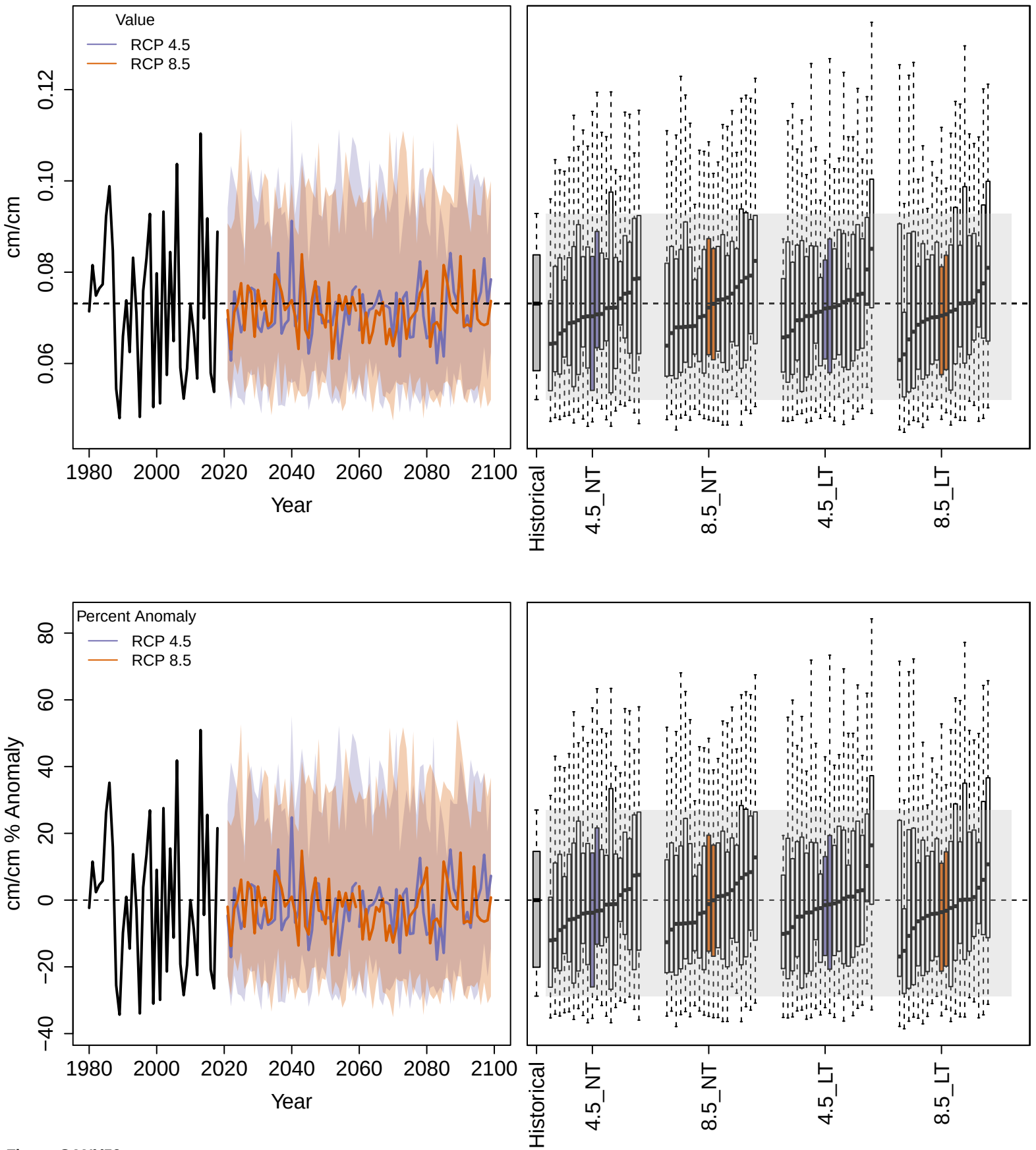


Figure CANY59:
Past trends and future trajectories of park−wide mean values for Fall soil water content:Top 50cm in Canyonlands. Top panels show values, bottom panels show changes from the long−term historical mean. Left: Time series of historical (black) and future projections for RCP 4.5 and 8.5. Shaded areas show spread among climate models. Right: Boxplots of temporal variability over 40−year periods under historical (left box) and individual climate models under two RCPs. Right: Historical time period is 1970−2010; near−term (NT) is 2020−2060; long−term (LT) is 2061−2100.

Canyonlands: Fall soil water content:Top 50cm

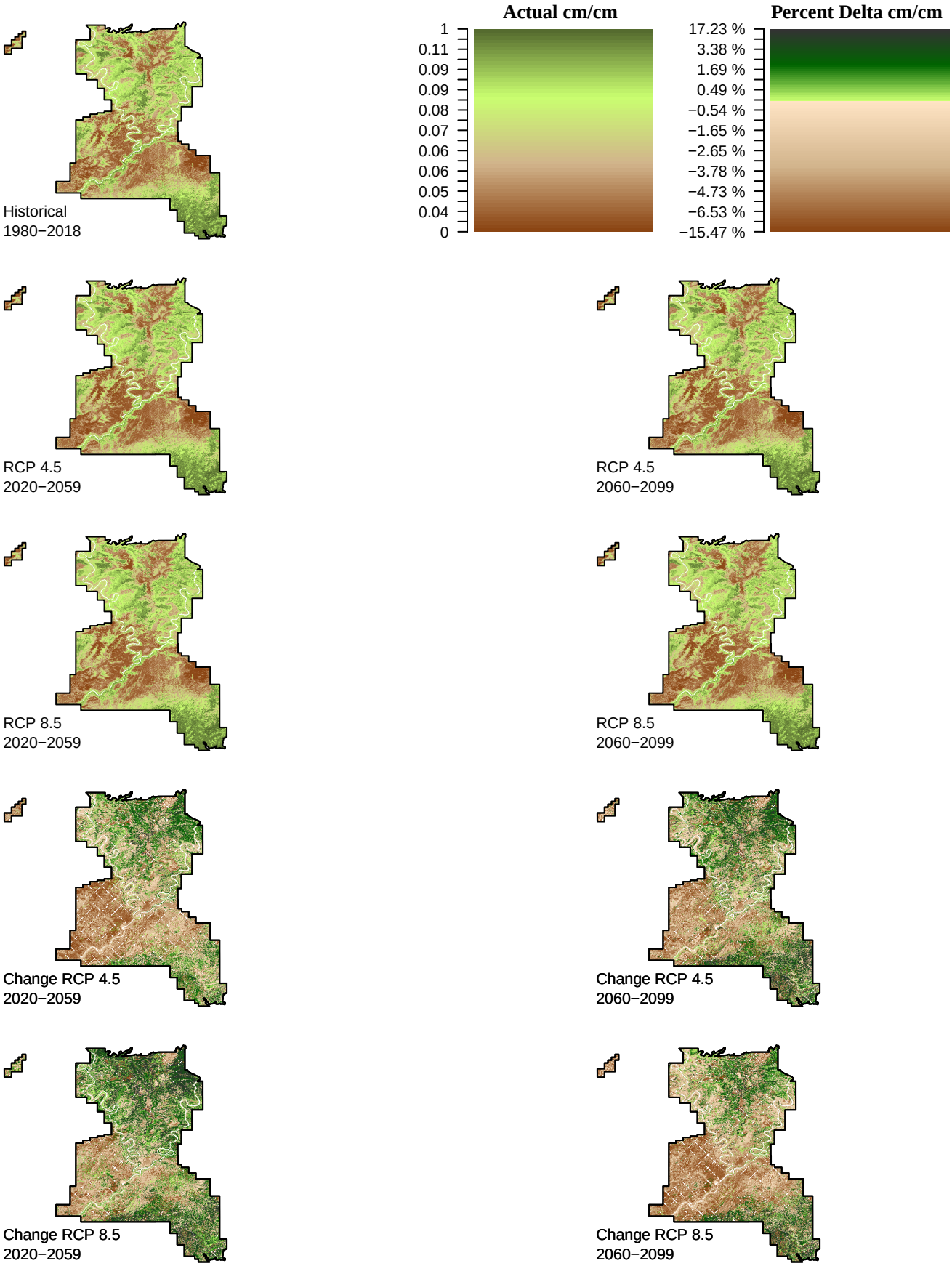


Figure CANYmap59:
Past trends and future trajectories of park−wide mean values for Fall soil water content:Top 50cm in Canyonlands. Topmost panel depicts the historical mean from 1980−2018. Lower four panels show the emission scenarios of RCP 4.5 and RCP 8.5 at near−term and long−term timeframes. Bottom four panels depict the change from the historical mean; cross hatching denotes areas of robust predicitons (90% of models agree in the direction of change).

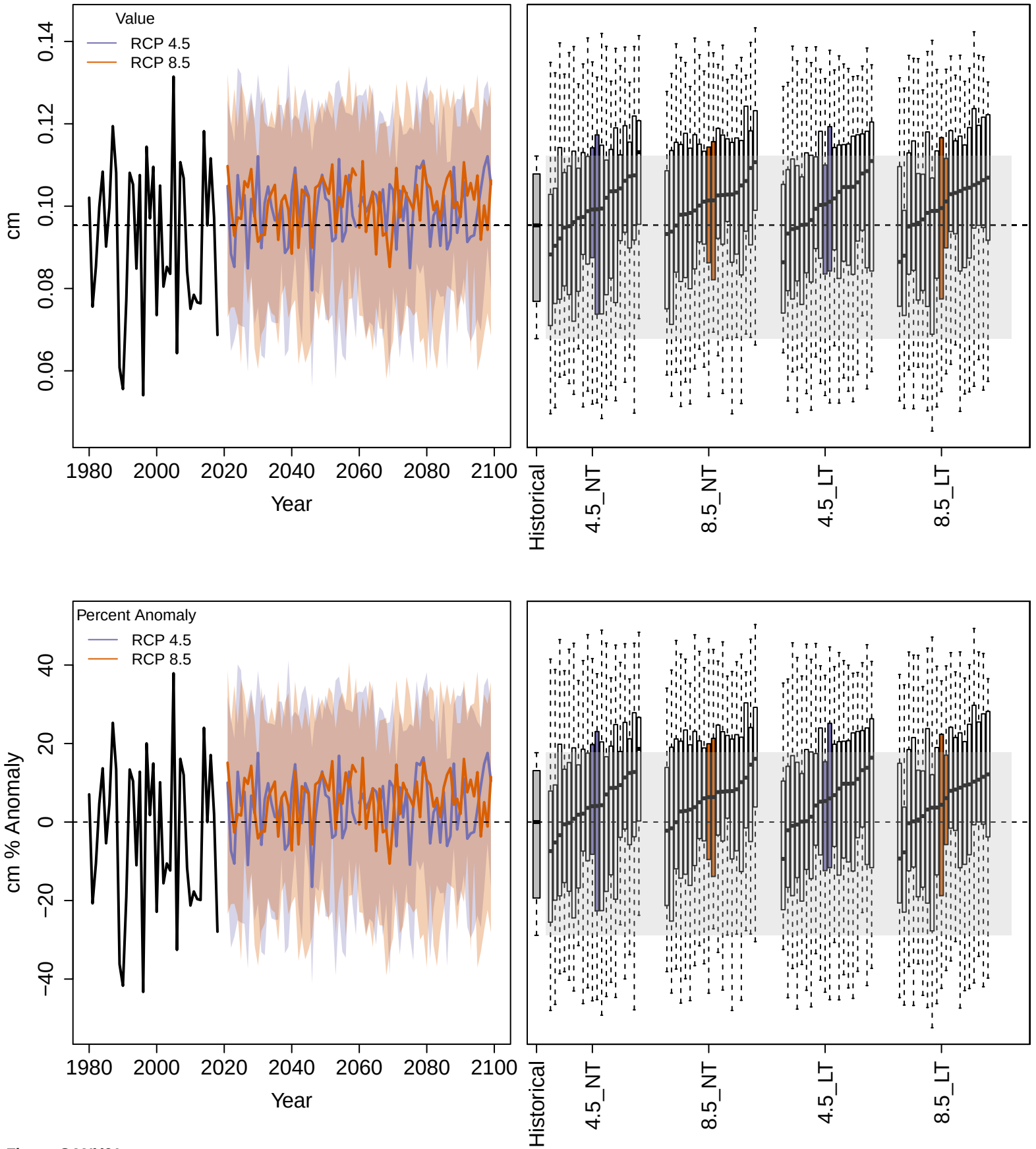


Figure CANY61:
Past trends and future trajectories of park−wide mean values for Winter soil water content in Canyonlands. Top panels show values, bottom panels show changes from the long−term historical mean. Left: Time series of historical (black) and future projections for RCP 4.5 and 8.5. Shaded areas show spread among climate models. Right: Boxplots of temporal variability over 40−year periods under historical (left box) and individual climate models under two RCPs. Right: Historical time period is 1970−2010; near−term (NT) is 2020−2060; long−term (LT) is 2061−2100.

Canyonlands: Winter soil water content

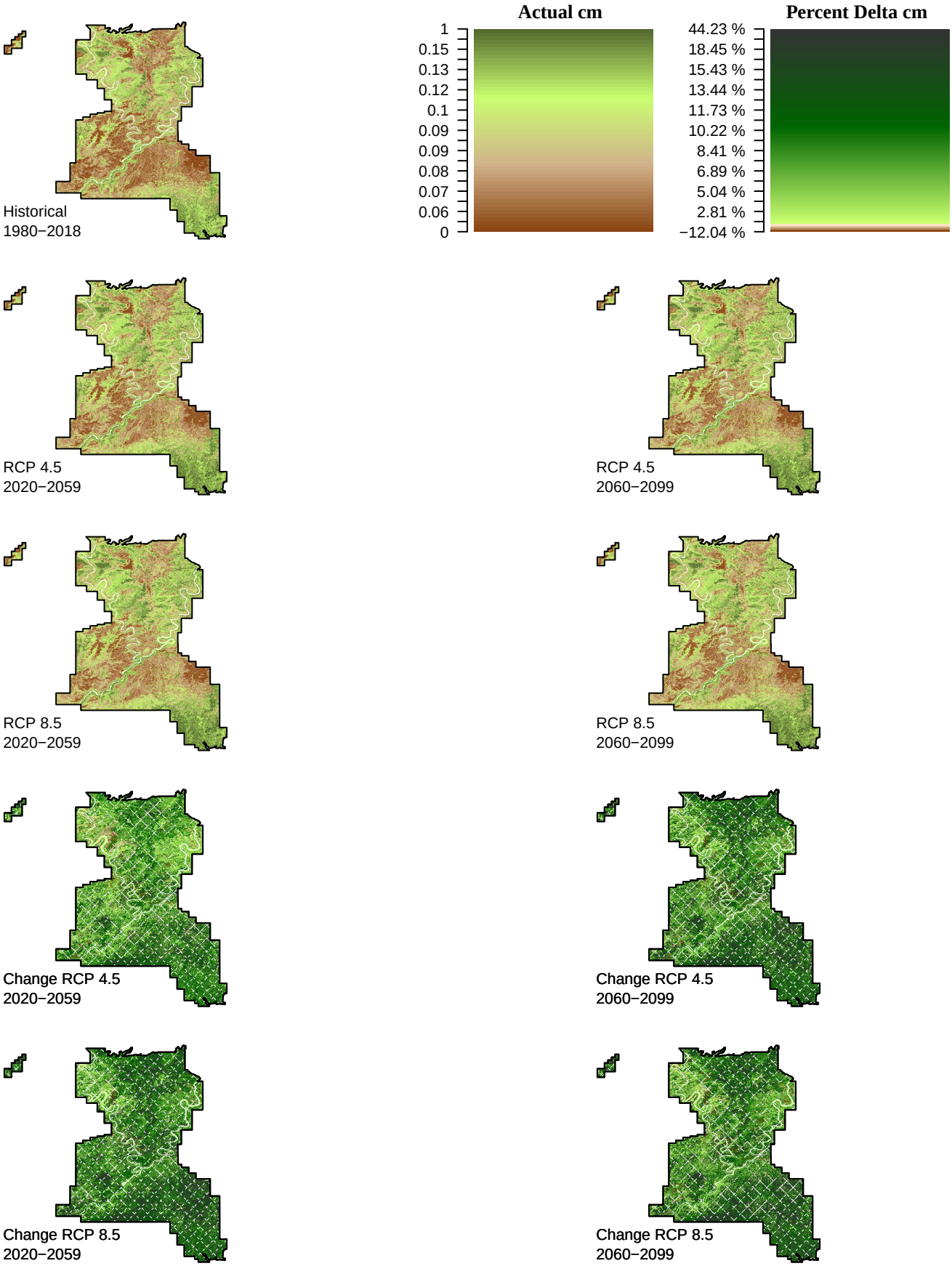


Figure CANYmap61:
Past trends and future trajectories of park−wide mean values for Winter soil water content in Canyonlands. Topmost panel depicts the historical mean from 1980−2018. Lower four panels show the emission scenarios of RCP 4.5 and RCP 8.5 at near−term and long−term timeframes. Bottom four panels depict the change from the historical mean; cross hatching denotes areas of robust predicitons (90% of models agree in the direction of change).

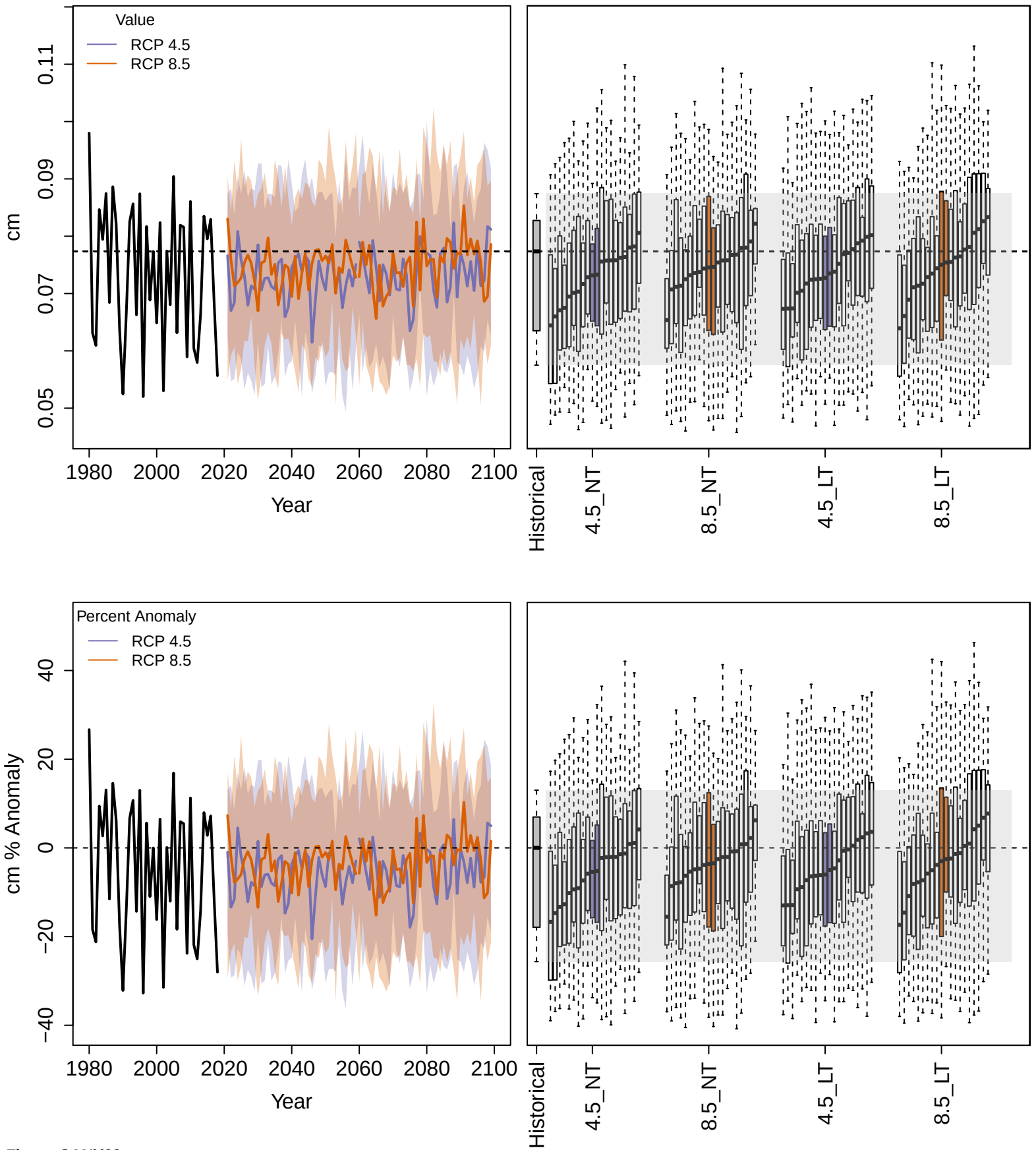


Figure CANY63:
Past trends and future trajectories of park−wide mean values for Spring soil water content in Canyonlands. Top panels show values, bottom panels show changes from the long−term historical mean. Left: Time series of historical (black) and future projections for RCP 4.5 and 8.5. Shaded areas show spread among climate models. Right: Boxplots of temporal variability over 40−year periods under historical (left box) and individual climate models under two RCPs. Right: Historical time period is 1970−2010; near−term (NT) is 2020−2060; long−term (LT) is 2061−2100.

Canyonlands: Spring soil water content

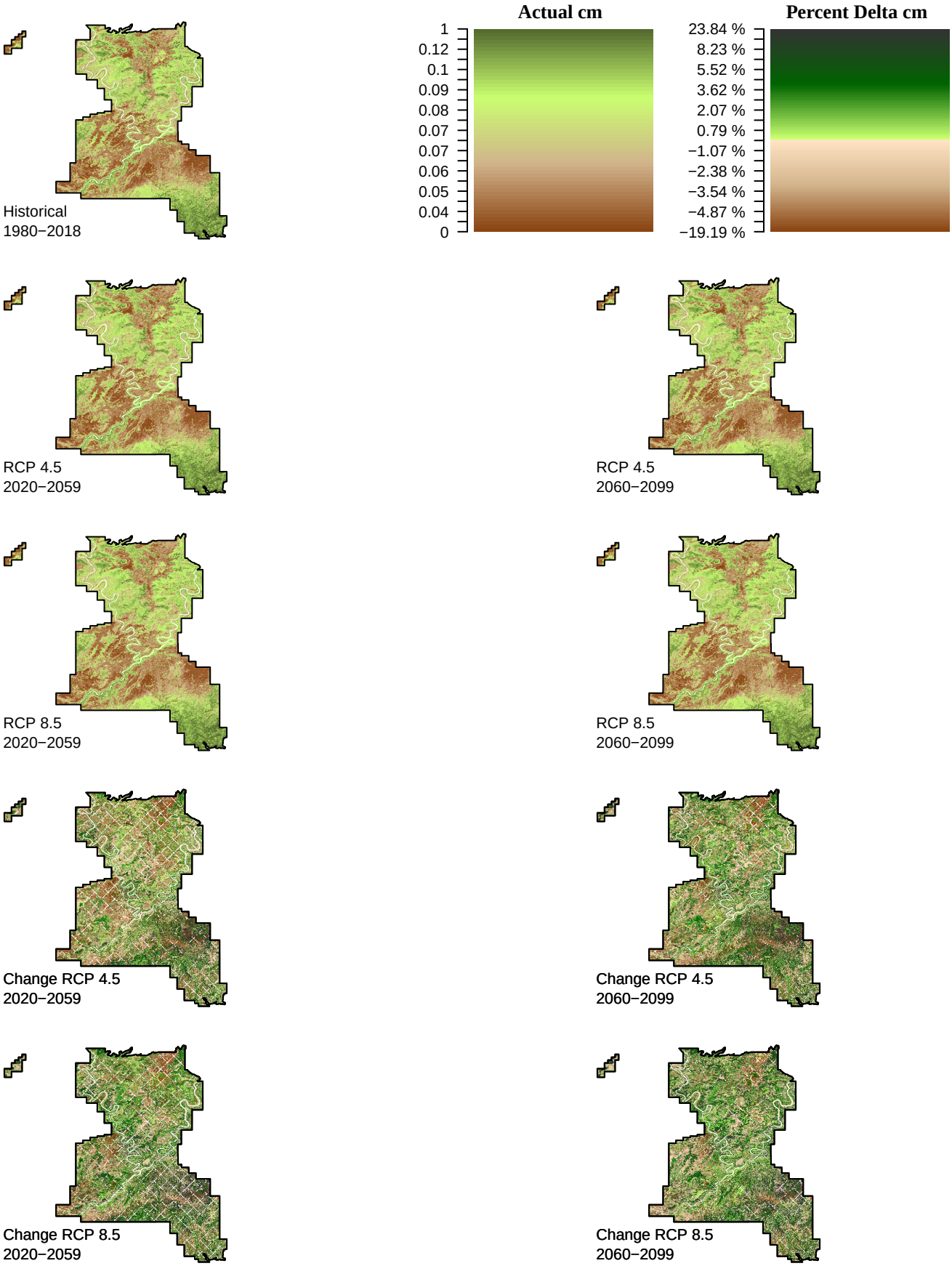


Figure CANYmap63:
Past trends and future trajectories of park−wide mean values for Spring soil water content in Canyonlands. Topmost panel depicts the historical mean from 1980−2018. Lower four panels show the emission scenarios of RCP 4.5 and RCP 8.5 at near−term and long−term timeframes. Bottom four panels depict the change from the historical mean; cross hatching denotes areas of robust predicitons (90% of models agree in the direction of change).

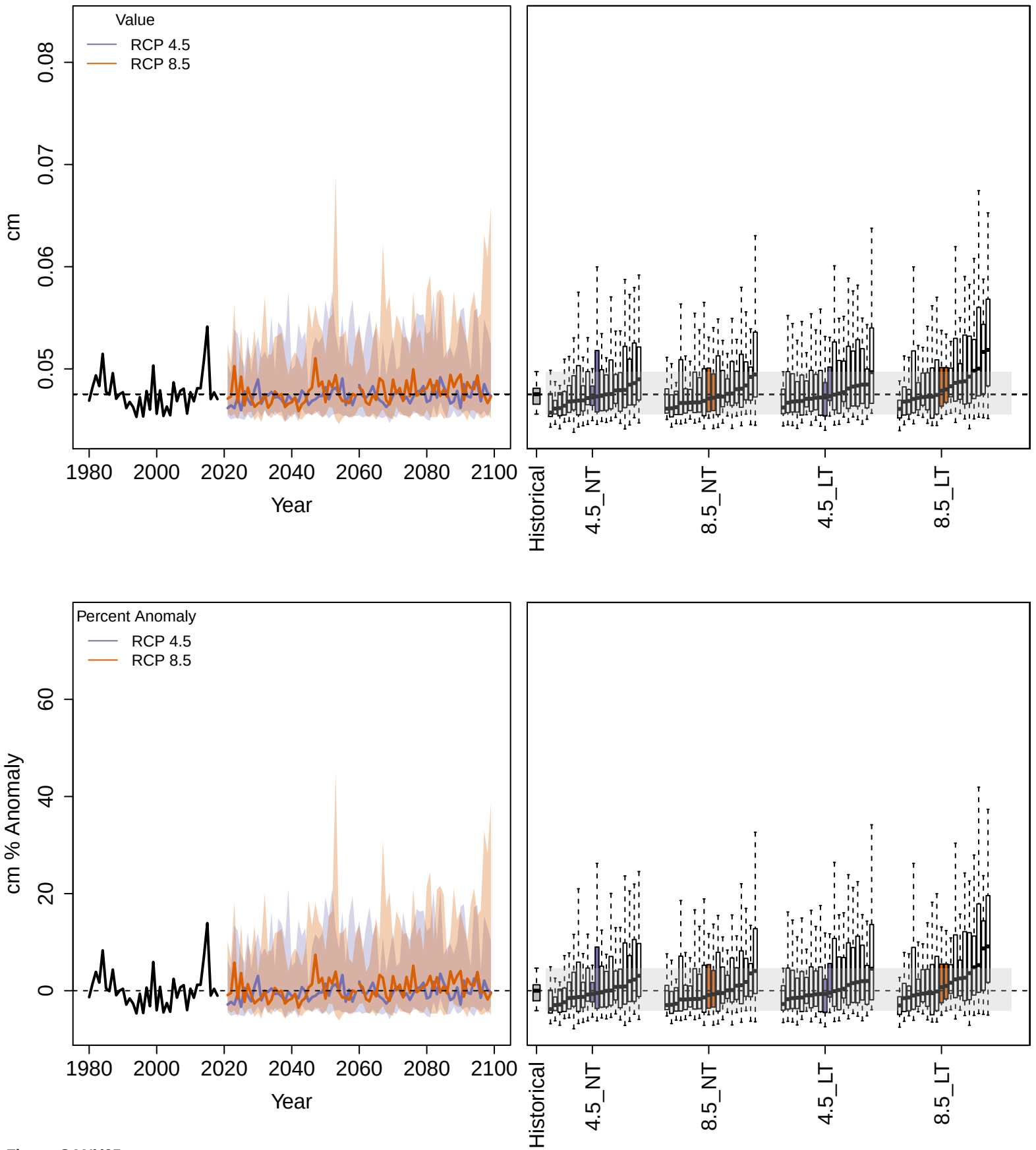


Figure CANY65:
Past trends and future trajectories of park−wide mean values for Summer soil water content in Canyonlands. Top panels show values, bottom panels show changes from the long−term historical mean. Left: Time series of historical (black) and future projections for RCP 4.5 and 8.5. Shaded areas show spread among climate models. Right: Boxplots of temporal variability over 40−year periods under historical (left box) and individual climate models under two RCPs. Right: Historical time period is 1970−2010; near−term (NT) is 2020−2060; long−term (LT) is 2061−2100.

Canyonlands: Summer soil water content

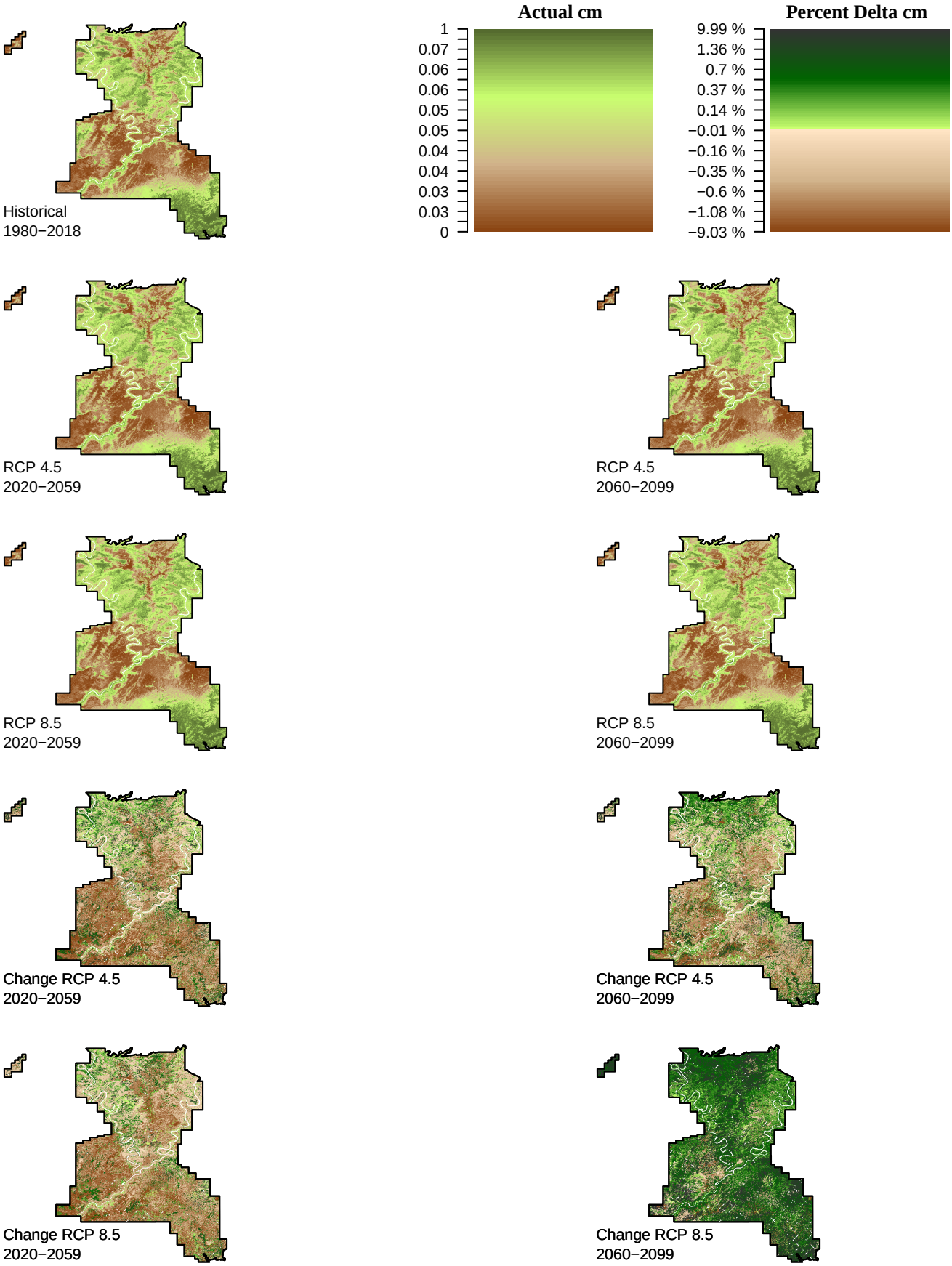


Figure CANYmap65:
Past trends and future trajectories of park−wide mean values for Summer soil water content in Canyonlands. Topmost panel depicts the historical mean from 1980−2018. Lower four panels show the emission scenarios of RCP 4.5 and RCP 8.5 at near−term and long−term timeframes. Bottom four panels depict the change from the historical mean; cross hatching denotes areas of robust predicitons (90% of models agree in the direction of change).

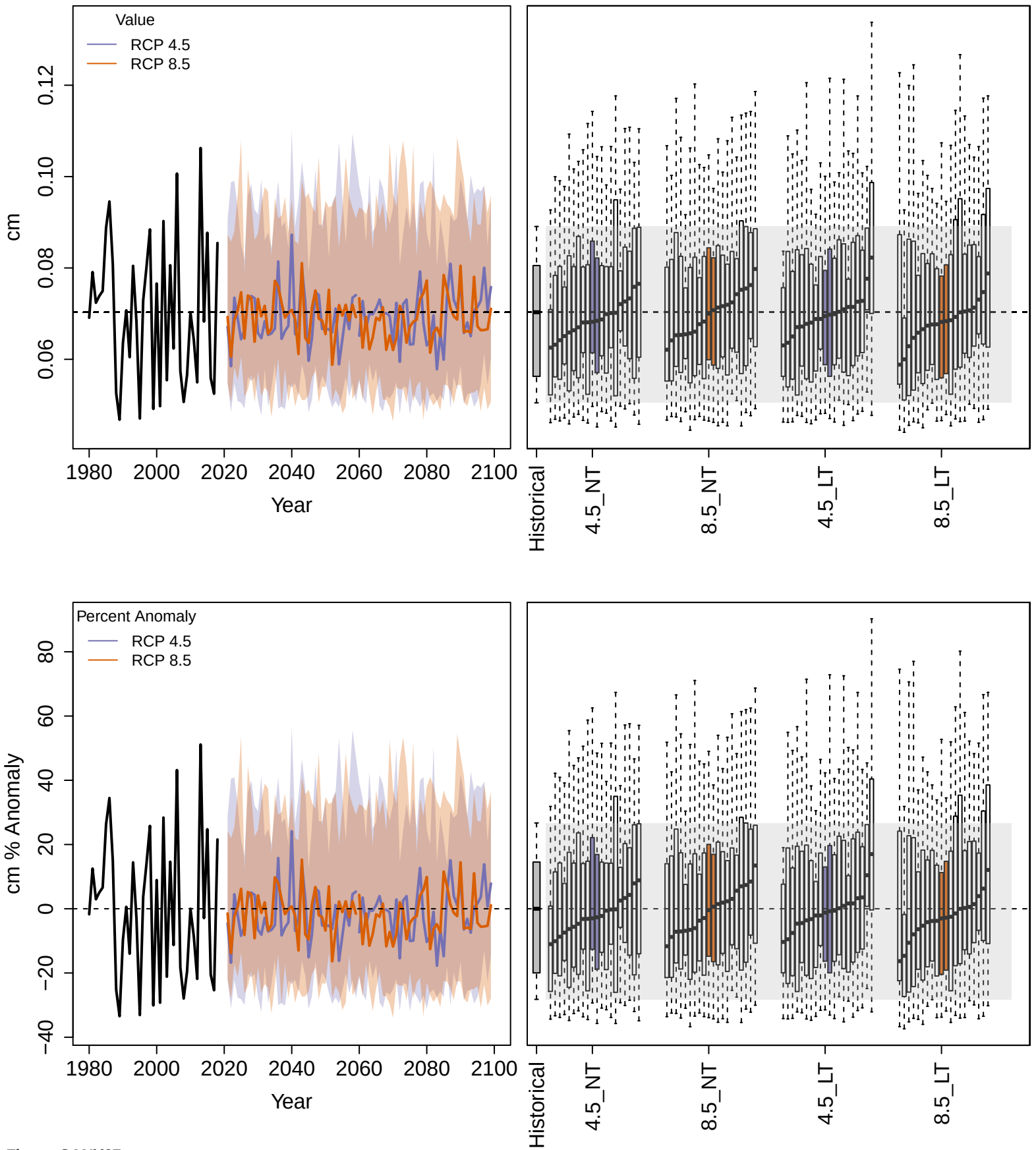


Figure CANY67:
Past trends and future trajectories of park−wide mean values for Fall soil water content in Canyonlands. Top panels show values, bottom panels show changes from the long−term historical mean. Left: Time series of historical (black) and future projections for RCP 4.5 and 8.5. Shaded areas show spread among climate models. Right: Boxplots of temporal variability over 40−year periods under historical (left box) and individual climate models under two RCPs. Right: Historical time period is 1970−2010; near−term (NT) is 2020−2060; long−term (LT) is 2061−2100.

Canyonlands: Fall soil water content

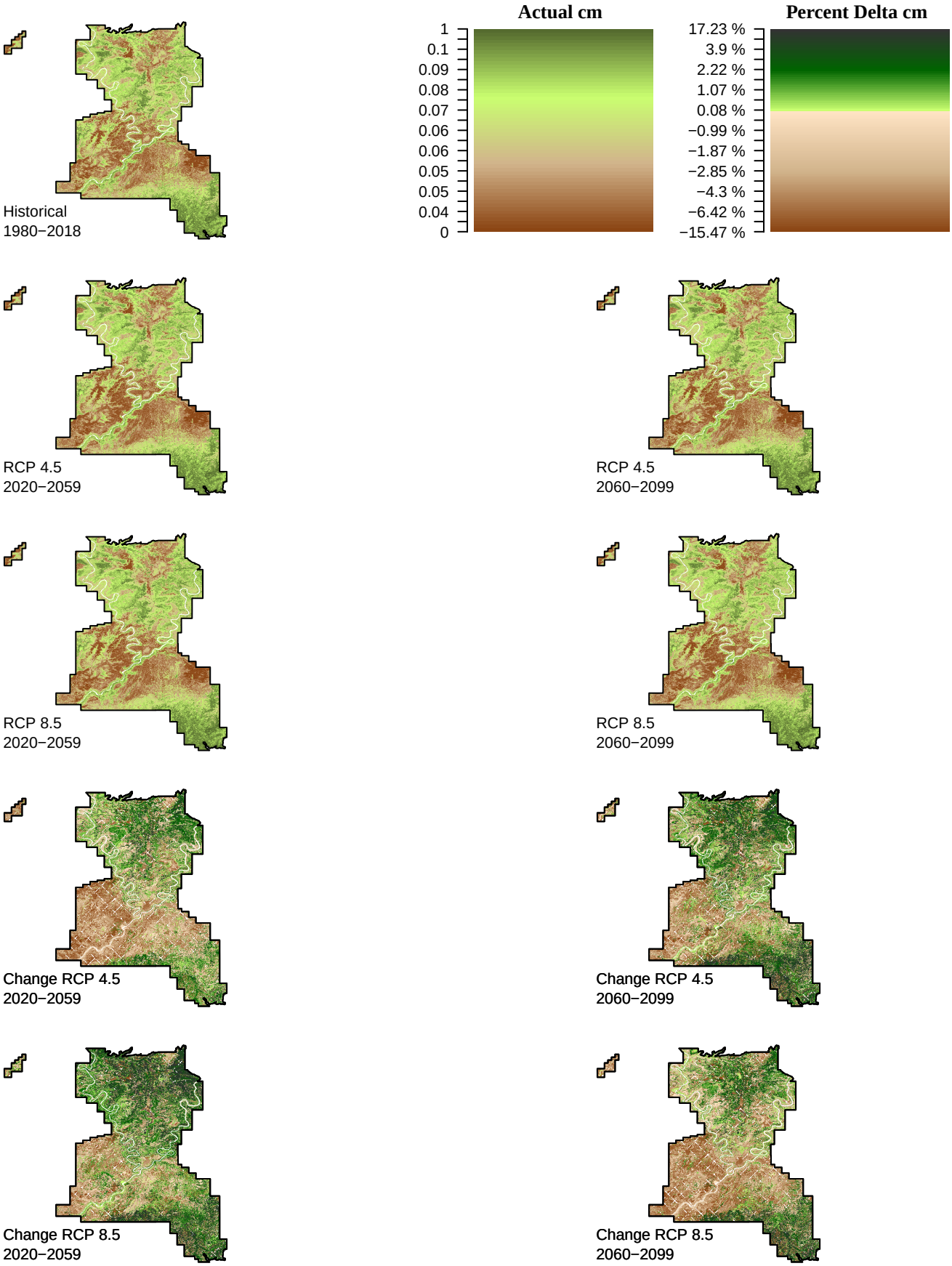


Figure CANYmap67:
Past trends and future trajectories of park−wide mean values for Fall soil water content in Canyonlands. Topmost panel depicts the historical mean from 1980−2018. Lower four panels show the emission scenarios of RCP 4.5 and RCP 8.5 at near−term and long−term timeframes. Bottom four panels depict the change from the historical mean; cross hatching denotes areas of robust predicitons (90% of models agree in the direction of change).

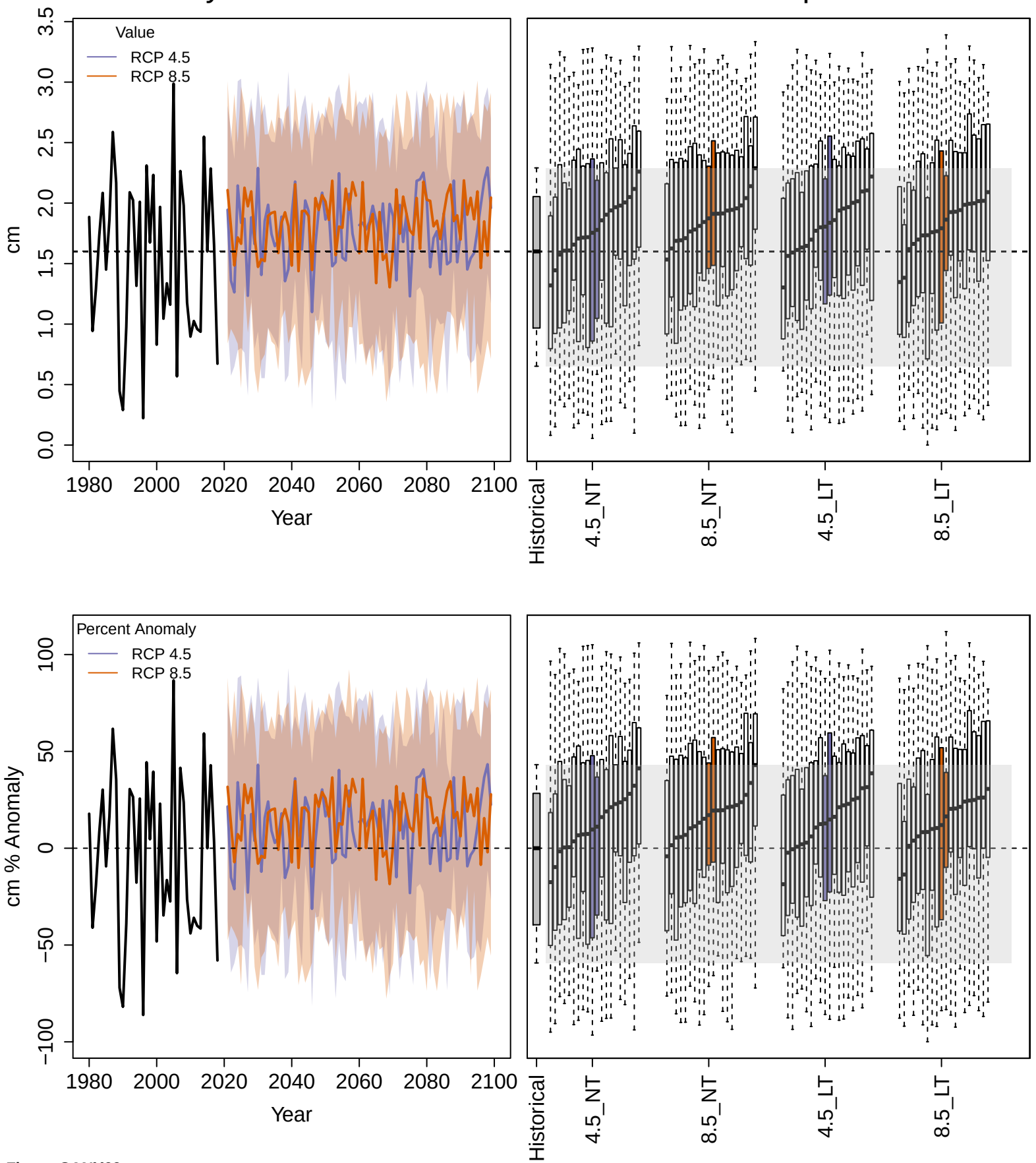


Figure CANY69:
Past trends and future trajectories of park−wide mean values for Winter available soil moisture: top 50cm in Canyonlands. Top panels show values, bottom panels show changes from the long−term historical mean. Left: Time series of historical (black) and future projections for RCP 4.5 and 8.5. Shaded areas show spread among climate models. Right: Boxplots of temporal variability over 40−year periods under historical (left box) and individual climate models under two RCPs. Right: Historical time period is 1970−2010; near−term (NT) is 2020−2060; long−term (LT) is 2061−2100.

Canyonlands: Winter available soil moisture: top 50cm

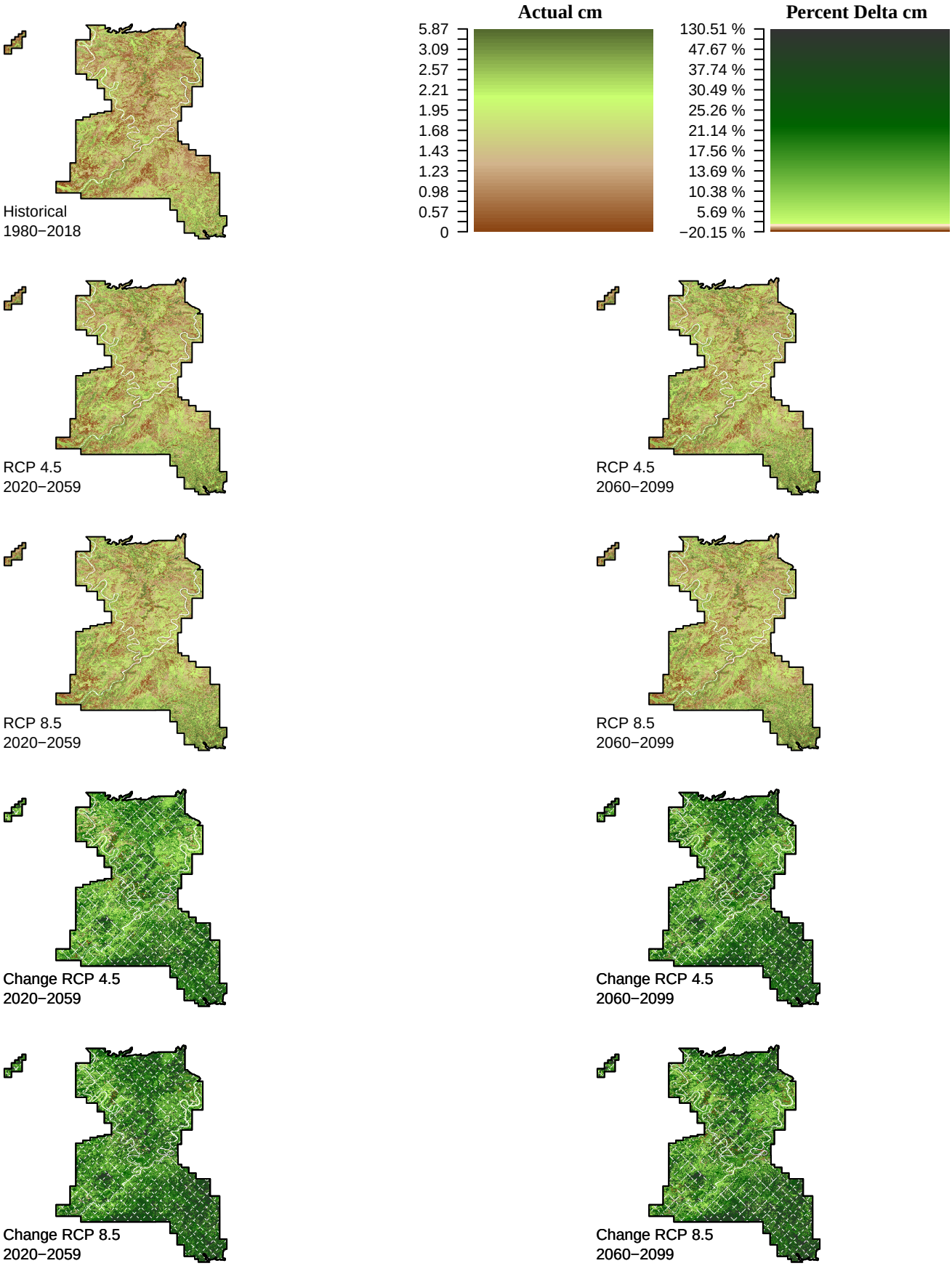


Figure CANYmap69:
Past trends and future trajectories of park−wide mean values for Winter available soil moisture: top 50cm in Canyonlands. Topmost panel depicts the historical mean from 1980−2018. Lower four panels show the emission scenarios of RCP 4.5 and RCP 8.5 at near−term and long−term timeframes. Bottom four panels depict the change from the historical mean; cross hatching denotes areas of robust predicitons (90% of models agree in the direction of change).

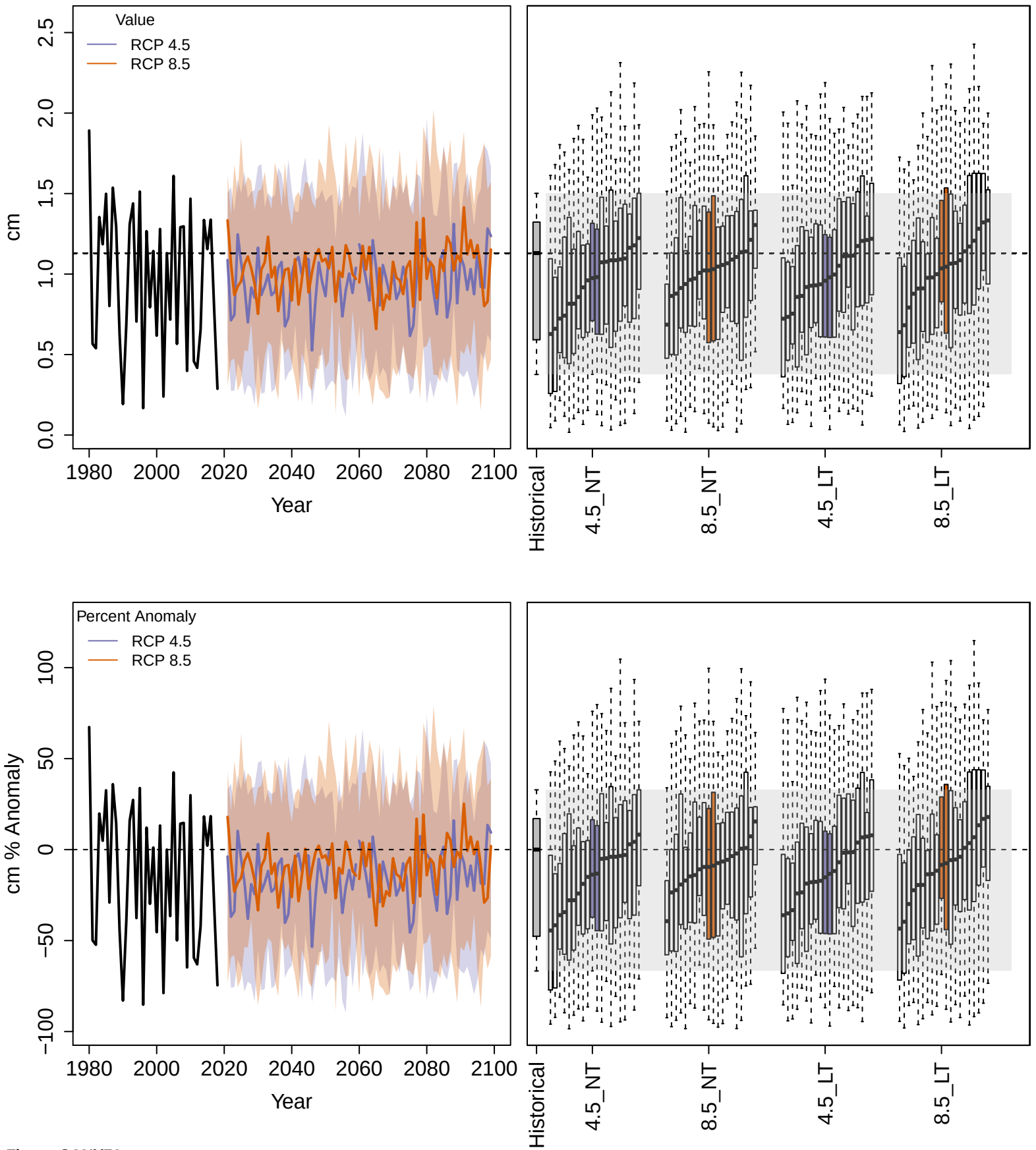


Figure CANY71:
Past trends and future trajectories of park−wide mean values for Spring available soil moisture: top 50cm in Canyonlands. Top panels show values, bottom panels show changes from the long−term historical mean. Left: Time series of historical (black) and future projections for RCP 4.5 and 8.5. Shaded areas show spread among climate models. Right: Boxplots of temporal variability over 40−year periods under historical (left box) and individual climate models under two RCPs. Right: Historical time period is 1970−2010; near−term (NT) is 2020−2060; long−term (LT) is 2061−2100.

Canyonlands: Spring available soil moisture: top 50cm

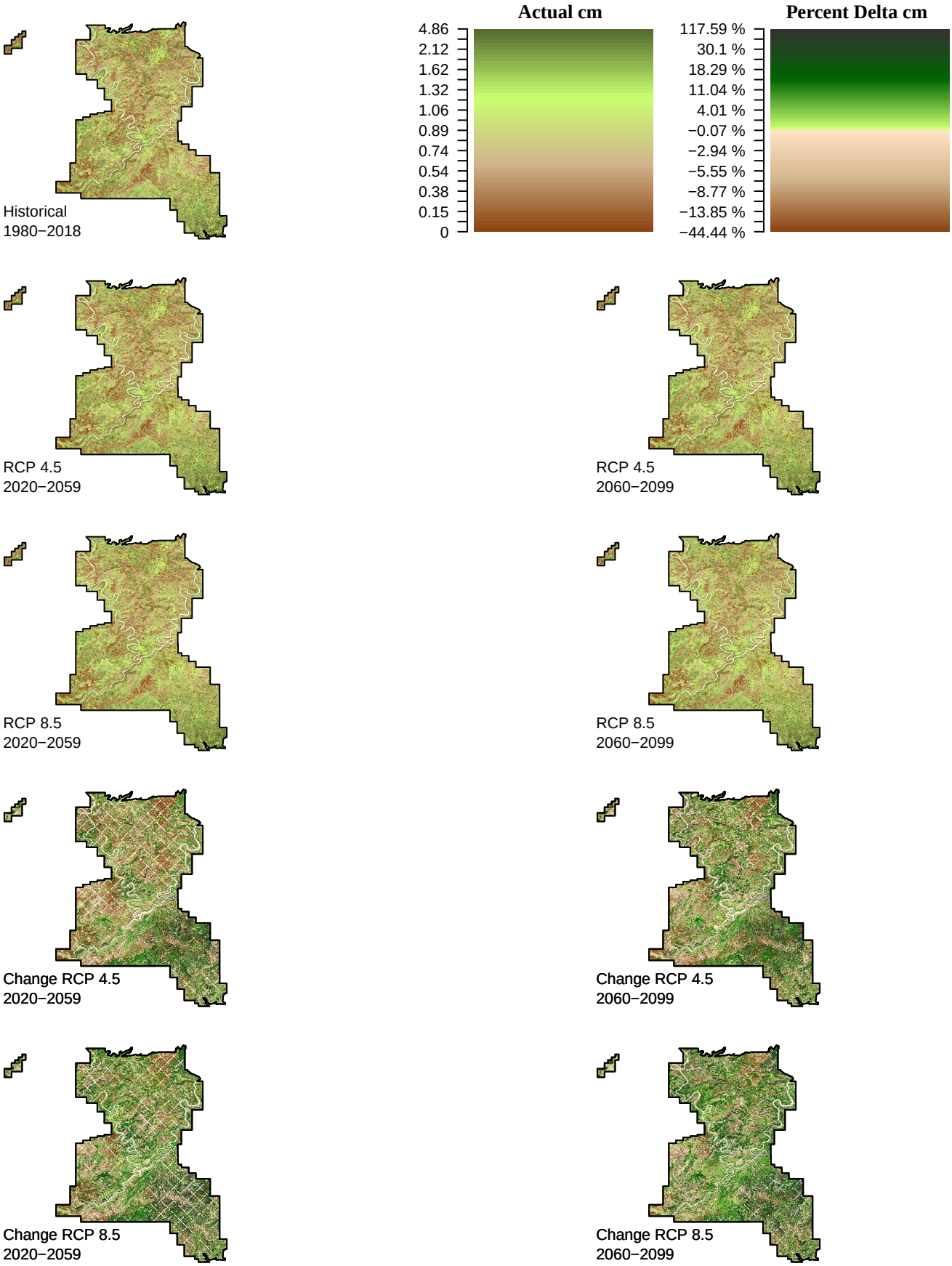


Figure CANYmap71:
Past trends and future trajectories of park−wide mean values for Spring available soil moisture: top 50cm in Canyonlands. Topmost panel depicts the historical mean from 1980−2018. Lower four panels show the emission scenarios of RCP 4.5 and RCP 8.5 at near−term and long−term timeframes. Bottom four panels depict the change from the historical mean; cross hatching denotes areas of robust predicitons (90% of models agree in the direction of change).

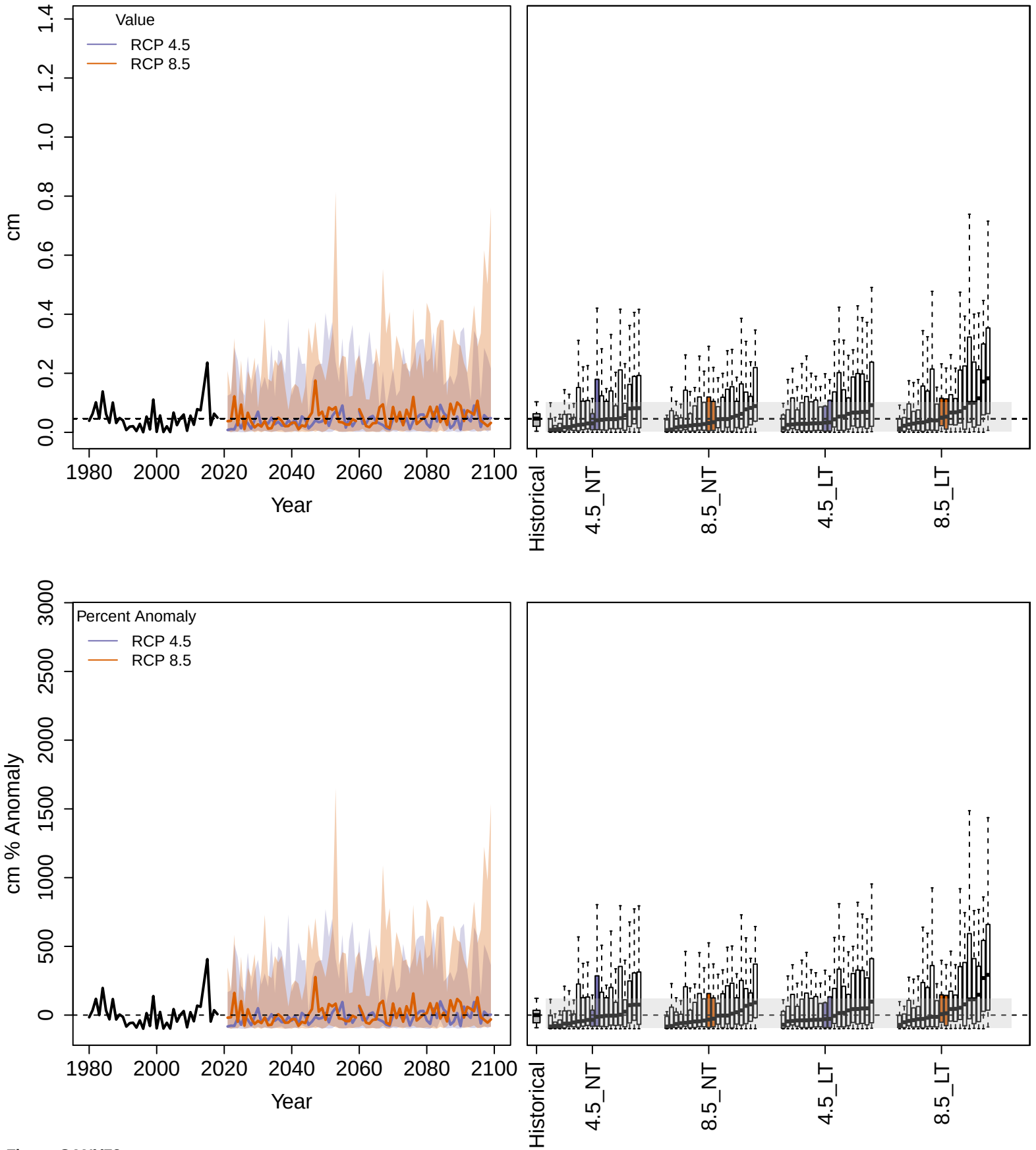


Figure CANY73:
Past trends and future trajectories of park−wide mean values for Summer available soil moisture: top 50cm in Canyonlands. Top panels show values, bottom panels show changes from the long−term historical mean. Left: Time series of historical (black) and future projections for RCP 4.5 and 8.5. Shaded areas show spread among climate models. Right: Boxplots of temporal variability over 40−year periods under historical (left box) and individual climate models under two RCPs. Right: Historical time period is 1970−2010; near−term (NT) is 2020−2060; long−term (LT) is 2061−2100.

Canyonlands: Summer available soil moisture: top 50cm

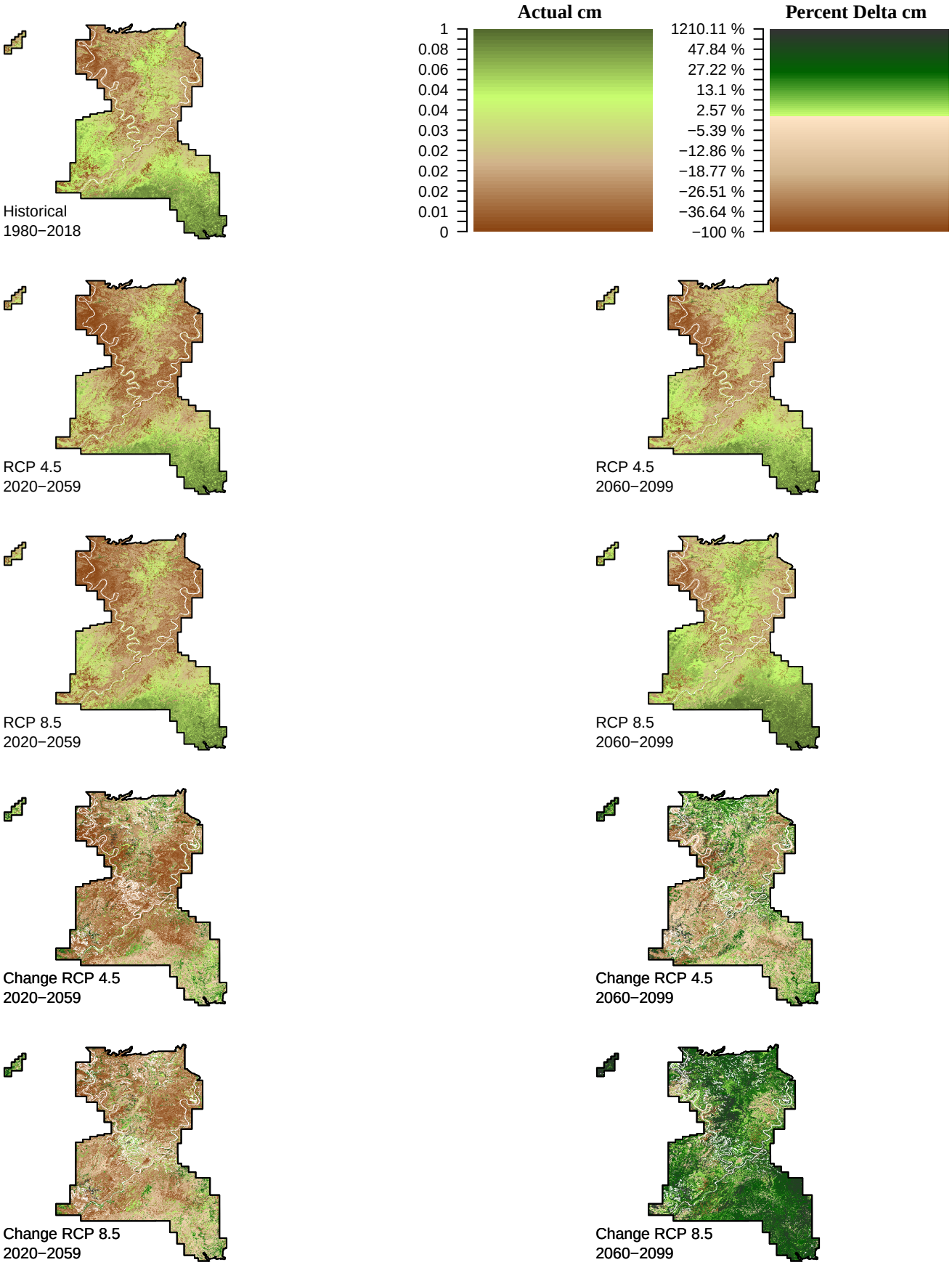


Figure CANYmap73:
Past trends and future trajectories of park−wide mean values for Summer available soil moisture: top 50cm in Canyonlands. Topmost panel depicts the historical mean from 1980−2018. Lower four panels show the emission scenarios of RCP 4.5 and RCP 8.5 at near−term and long−term timeframes. Bottom four panels depict the change from the historical mean; cross hatching denotes areas of robust predicitons (90% of models agree in the direction of change).

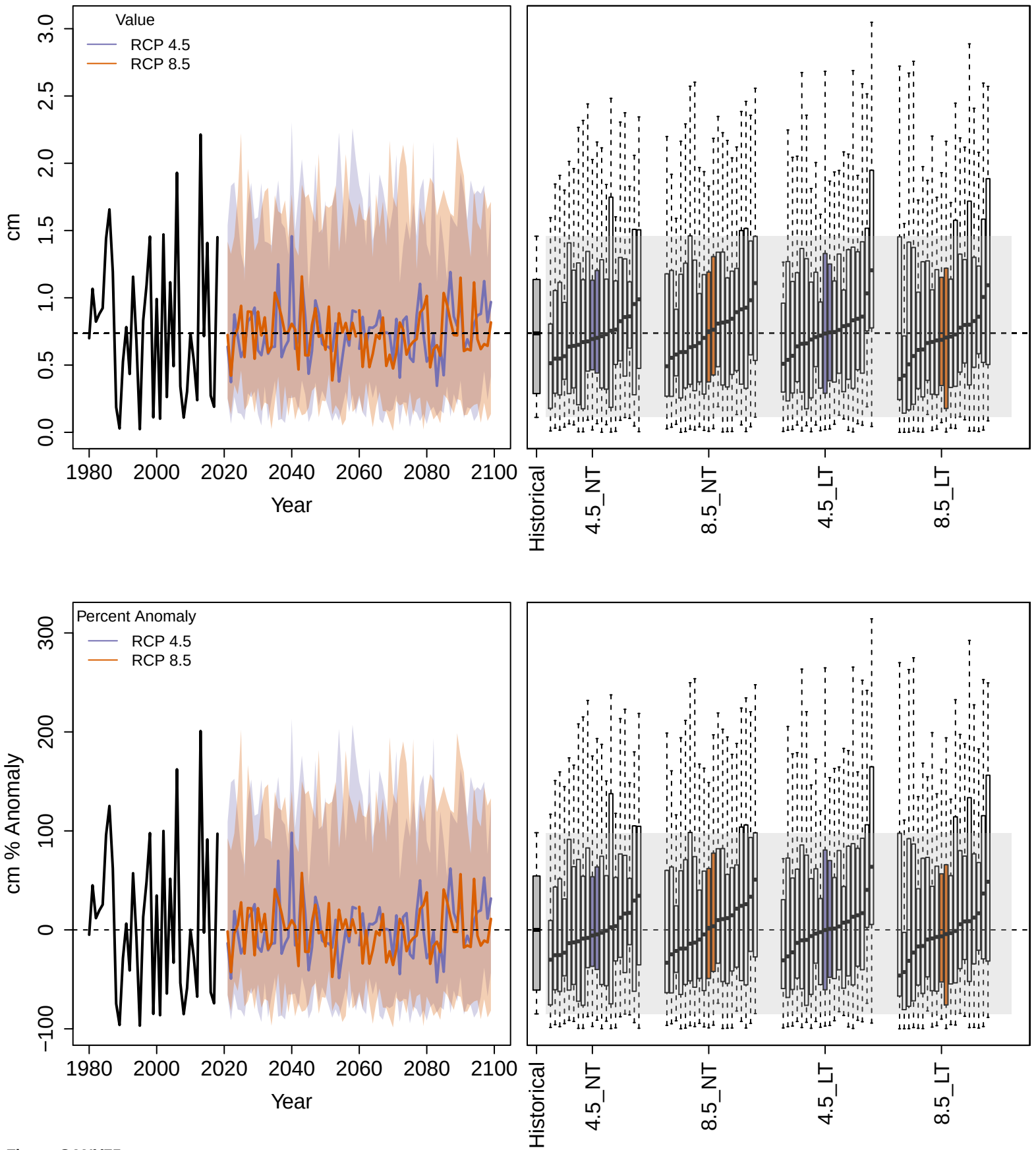


Figure CANY75:
Past trends and future trajectories of park−wide mean values for Fall available soil moisture: top 50cm in Canyonlands. Top panels show values, bottom panels show changes from the long−term historical mean. Left: Time series of historical (black) and future projections for RCP 4.5 and 8.5. Shaded areas show spread among climate models. Right: Boxplots of temporal variability over 40−year periods under historical (left box) and individual climate models under two RCPs. Right: Historical time period is 1970−2010; near−term (NT) is 2020−2060; long−term (LT) is 2061−2100.

Canyonlands: Fall available soil moisture: top 50cm

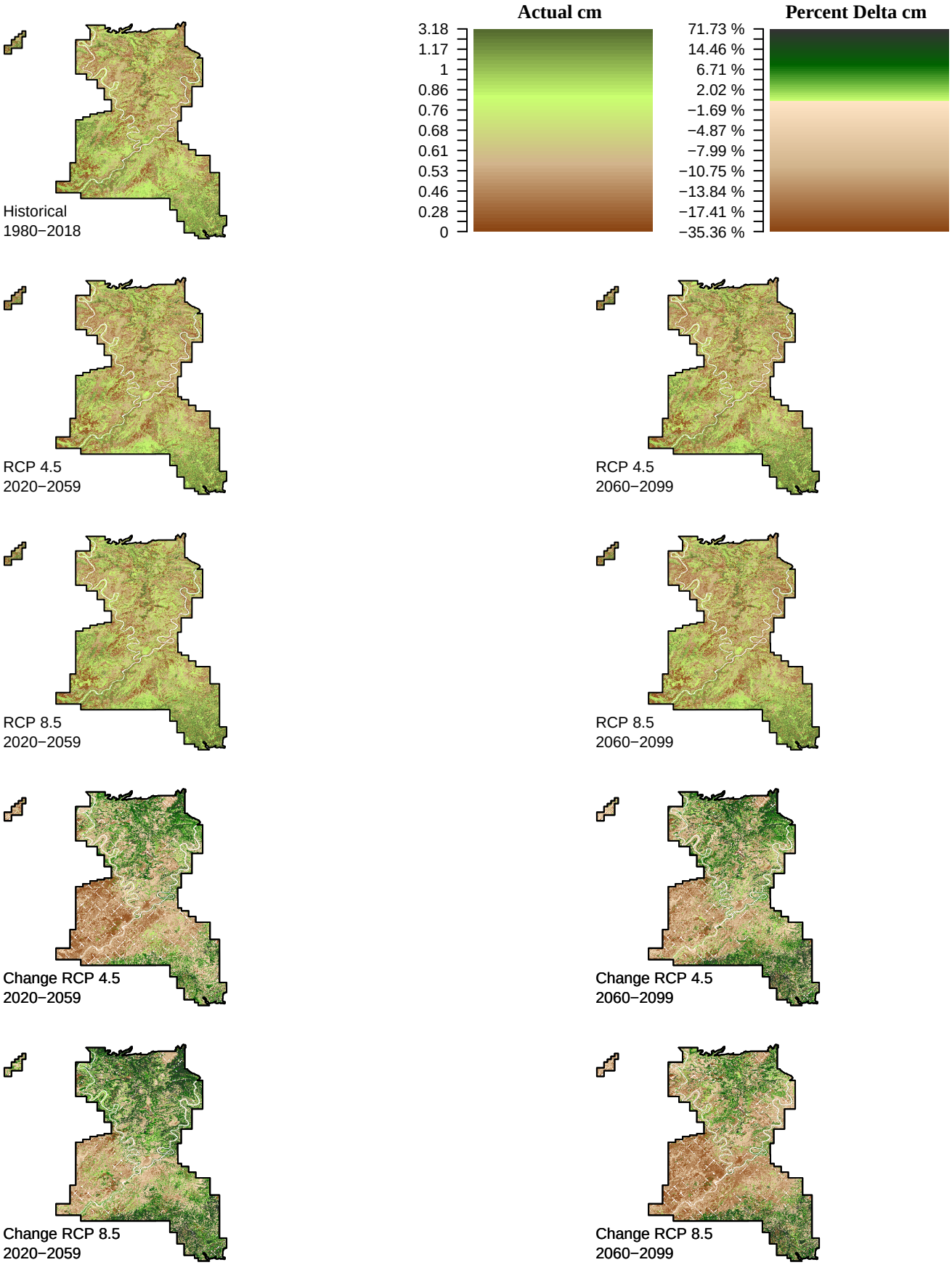


Figure CANYmap75:
Past trends and future trajectories of park−wide mean values for Fall available soil moisture: top 50cm in Canyonlands. Topmost panel depicts the historical mean from 1980−2018. Lower four panels show the emission scenarios of RCP 4.5 and RCP 8.5 at near−term and long−term timeframes. Bottom four panels depict the change from the historical mean; cross hatching denotes areas of robust predicitons (90% of models agree in the direction of change).

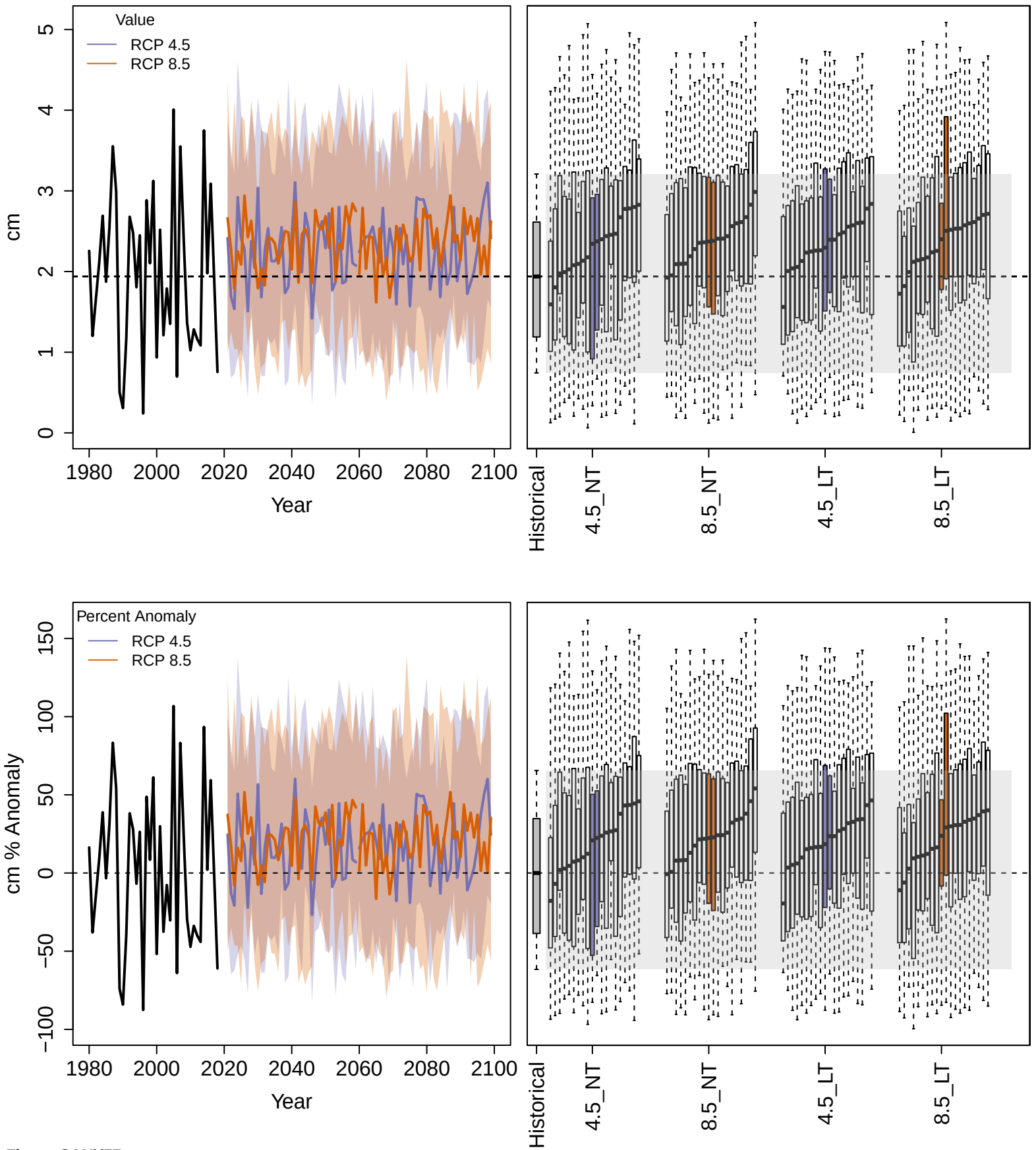


Figure CANY77:
Past trends and future trajectories of park−wide mean values for Winter available soil moisture in Canyonlands. Top panels show values, bottom panels show changes from the long−term historical mean. Left: Time series of historical (black) and future projections for RCP 4.5 and 8.5. Shaded areas show spread among climate models. Right: Boxplots of temporal variability over 40−year periods under historical (left box) and individual climate models under two RCPs. Right: Historical time period is 1970−2010; near−term (NT) is 2020−2060; long−term (LT) is 2061−2100.

Canyonlands: Winter available soil moisture

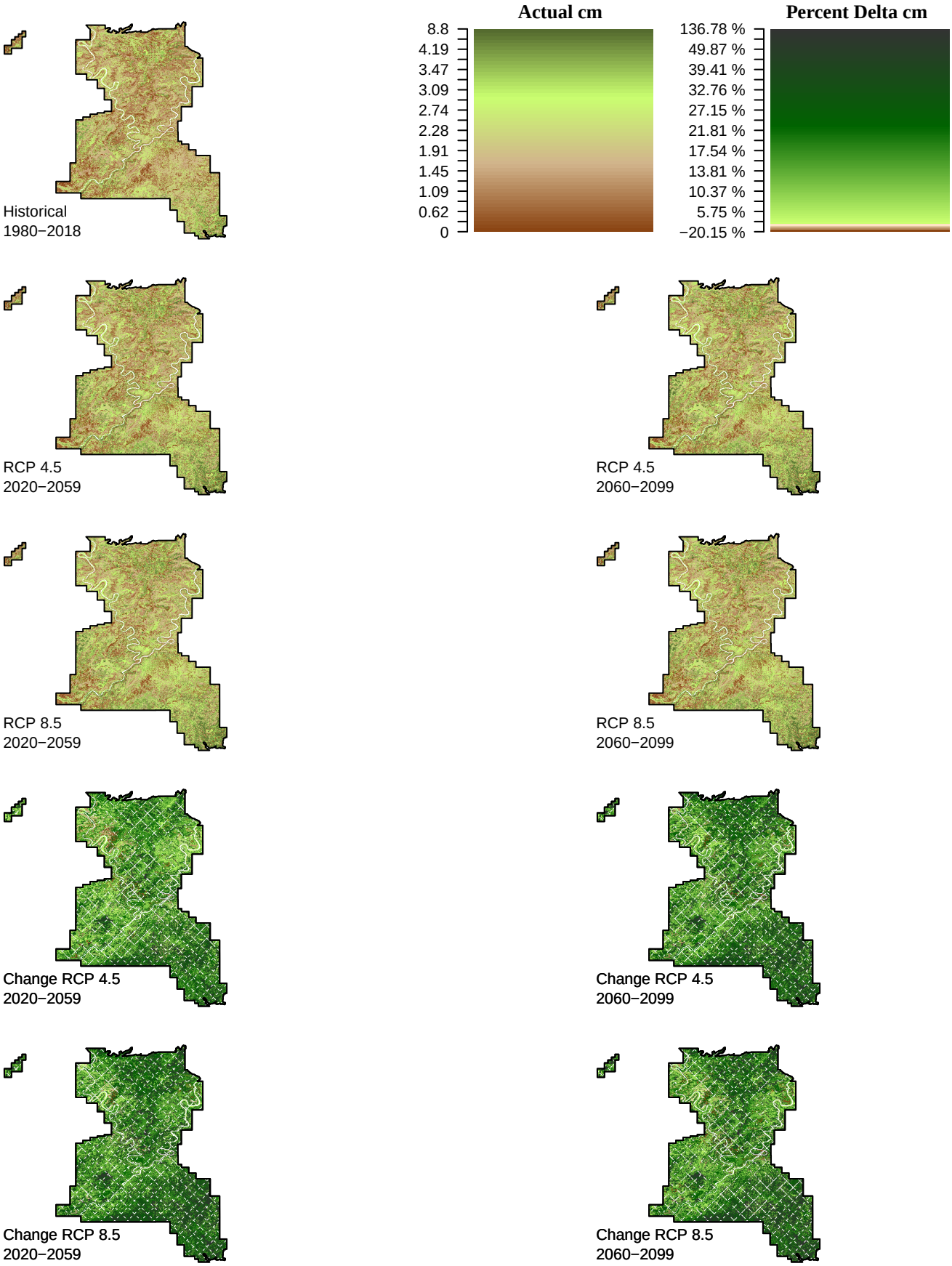


Figure CANYmap77:
Past trends and future trajectories of park−wide mean values for Winter available soil moisture in Canyonlands. Topmost panel depicts the historical mean from 1980−2018. Lower four panels show the emission scenarios of RCP 4.5 and RCP 8.5 at near−term and long−term timeframes. Bottom four panels depict the change from the historical mean; cross hatching denotes areas of robust predicitons (90% of models agree in the direction of change).

Canyonlands: Spring available soil moisture

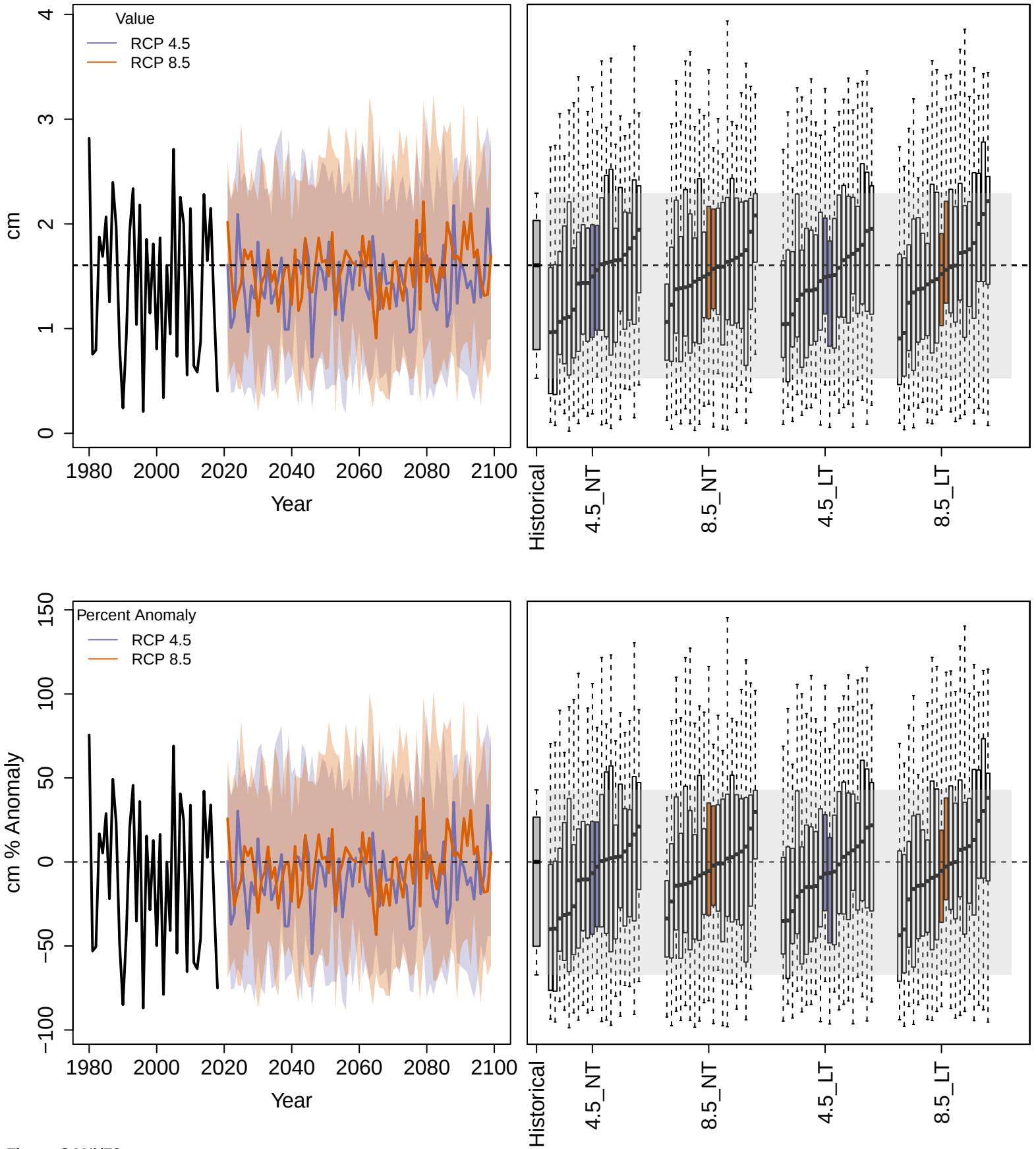


Figure CANY79:
Past trends and future trajectories of park−wide mean values for Spring available soil moisture in Canyonlands. Top panels show values, bottom panels show changes from the long−term historical mean. Left: Time series of historical (black) and future projections for RCP 4.5 and 8.5. Shaded areas show spread among climate models. Right: Boxplots of temporal variability over 40−year periods under historical (left box) and individual climate models under two RCPs. Right: Historical time period is 1970−2010; near−term (NT) is 2020−2060; long−term (LT) is 2061−2100.

Canyonlands: Spring available soil moisture

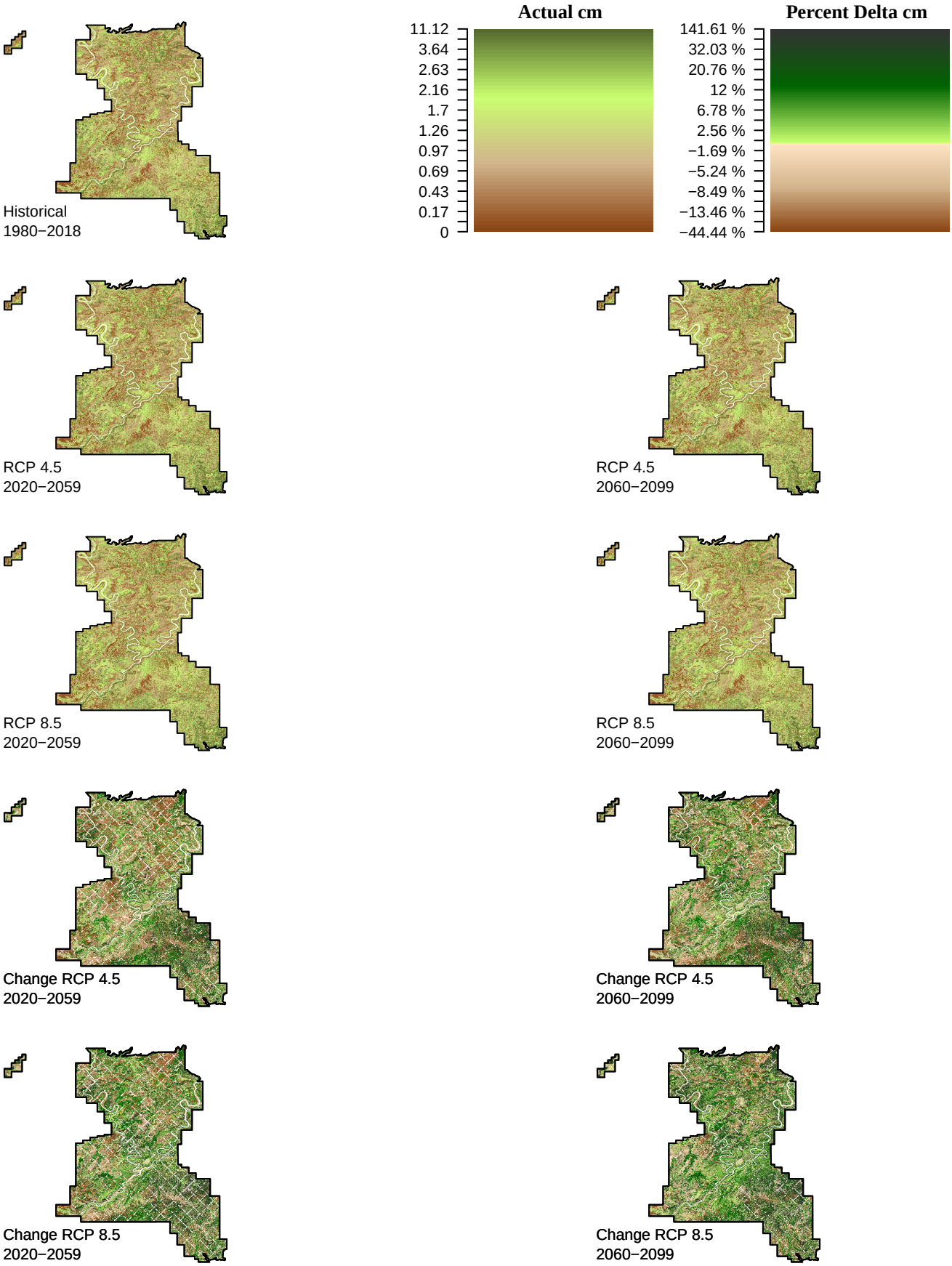


Figure CANYmap79:
Past trends and future trajectories of park−wide mean values for Spring available soil moisture in Canyonlands. Topmost panel depicts the historical mean from 1980−2018. Lower four panels show the emission scenarios of RCP 4.5 and RCP 8.5 at near−term and long−term timeframes. Bottom four panels depict the change from the historical mean; cross hatching denotes areas of robust predicitons (90% of models agree in the direction of change).

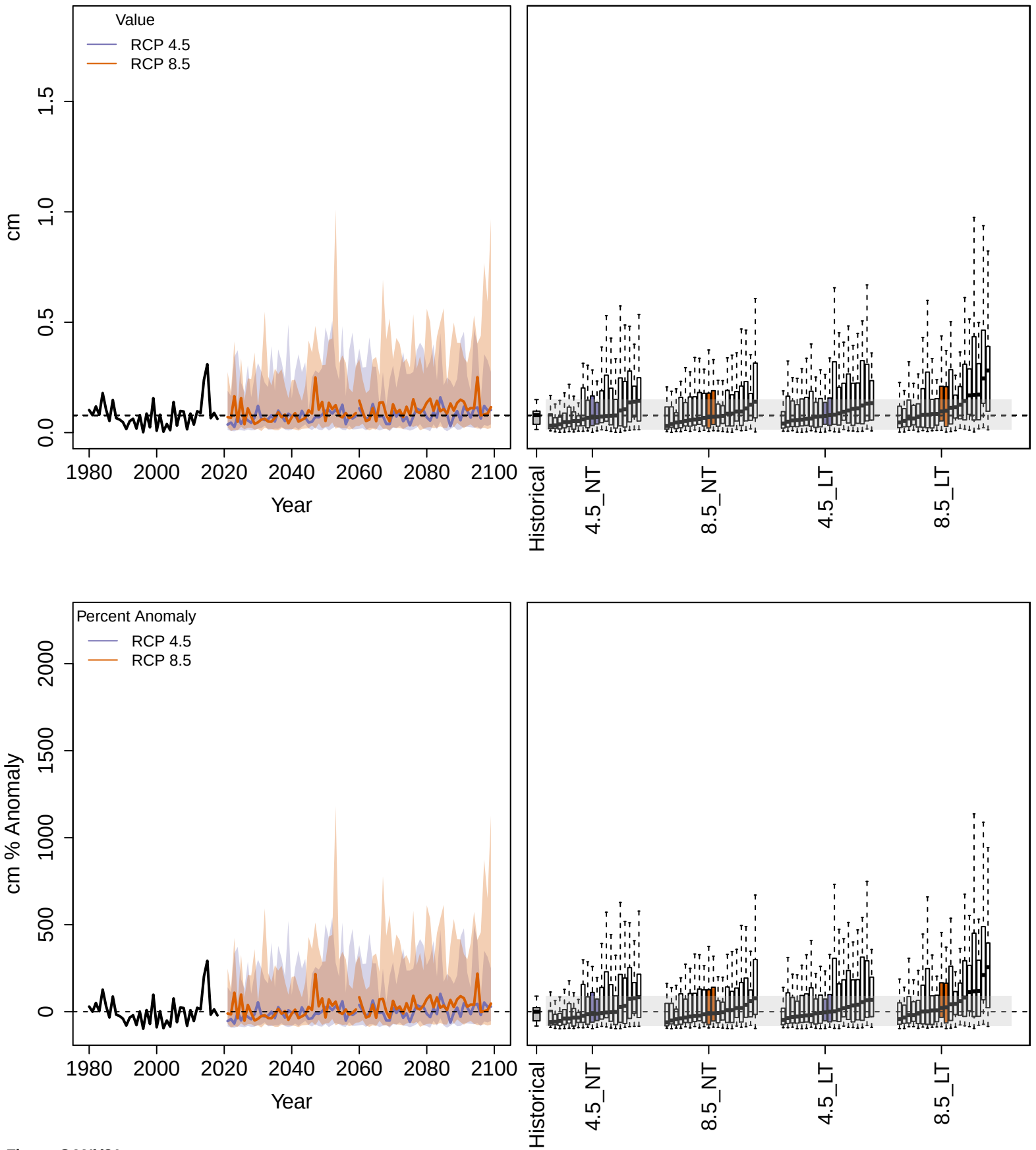


Figure CANY81:
Past trends and future trajectories of park−wide mean values for Summer available soil moisture in Canyonlands. Top panels show values, bottom panels show changes from the long−term historical mean. Left: Time series of historical (black) and future projections for RCP 4.5 and 8.5. Shaded areas show spread among climate models. Right: Boxplots of temporal variability over 40−year periods under historical (left box) and individual climate models under two RCPs. Right: Historical time period is 1970−2010; near−term (NT) is 2020−2060; long−term (LT) is 2061−2100.

Canyonlands: Summer available soil moisture

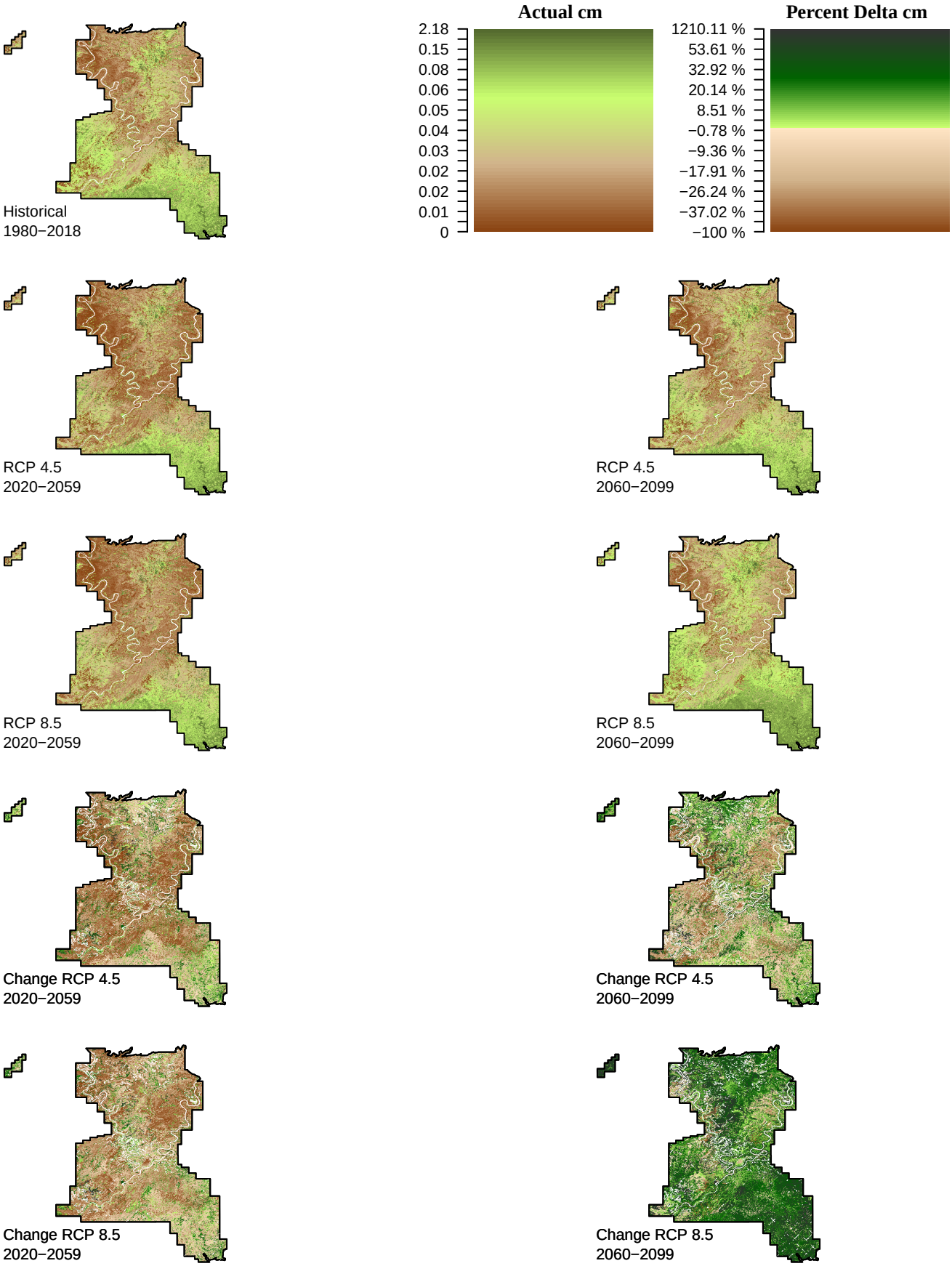


Figure CANYmap81:
Past trends and future trajectories of park−wide mean values for Summer available soil moisture in Canyonlands. Topmost panel depicts the historical mean from 1980−2018. Lower four panels show the emission scenarios of RCP 4.5 and RCP 8.5 at near−term and long−term timeframes. Bottom four panels depict the change from the historical mean; cross hatching denotes areas of robust predicitons (90% of models agree in the direction of change).

Canyonlands: Fall available soil moisture

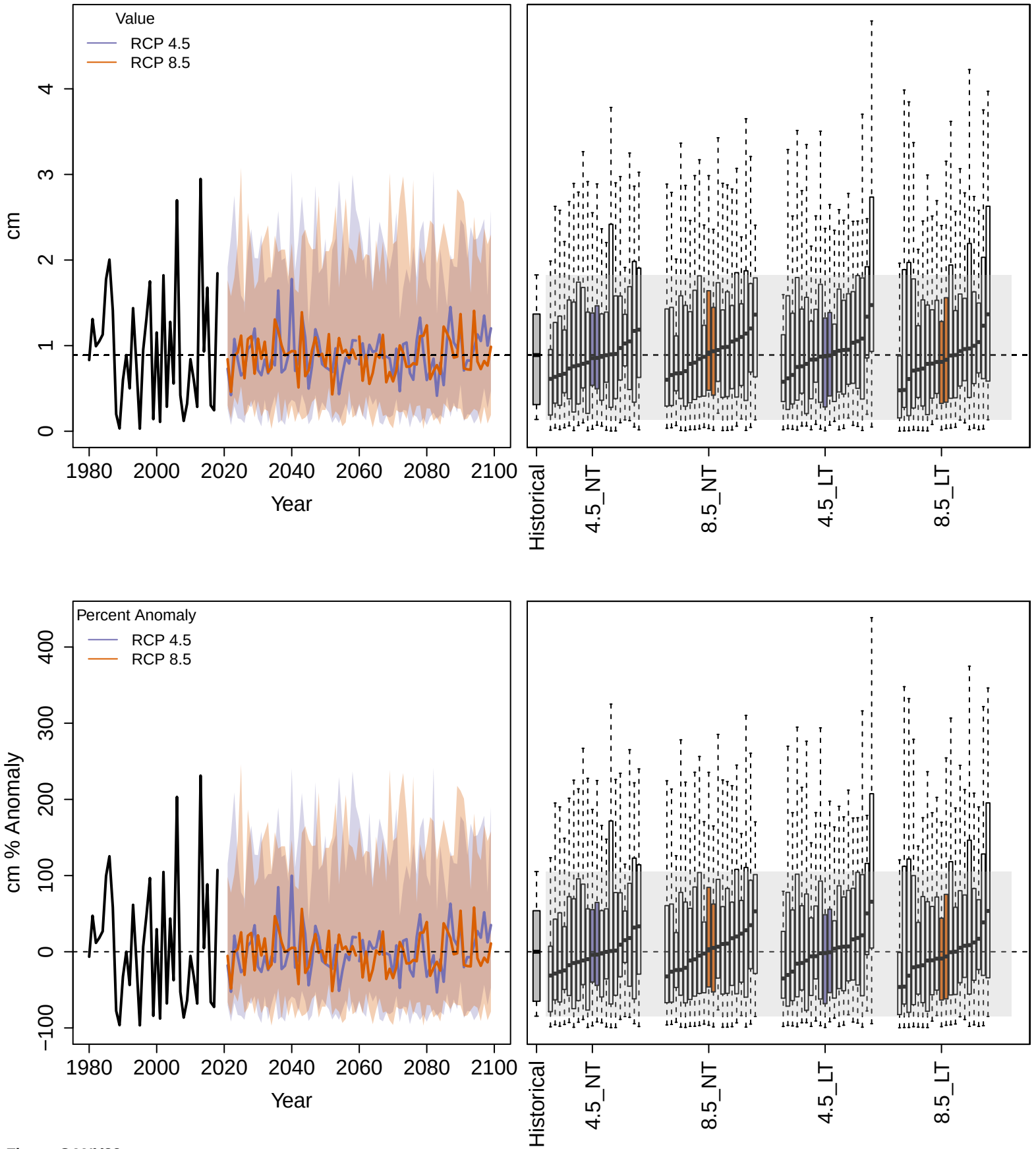


Figure CANY83:
Past trends and future trajectories of park−wide mean values for Fall available soil moisture in Canyonlands. Top panels show values, bottom panels show changes from the long−term historical mean. Left: Time series of historical (black) and future projections for RCP 4.5 and 8.5. Shaded areas show spread among climate models. Right: Boxplots of temporal variability over 40−year periods under historical (left box) and individual climate models under two RCPs. Right: Historical time period is 1970−2010; near−term (NT) is 2020−2060; long−term (LT) is 2061−2100.

Canyonlands: Fall available soil moisture

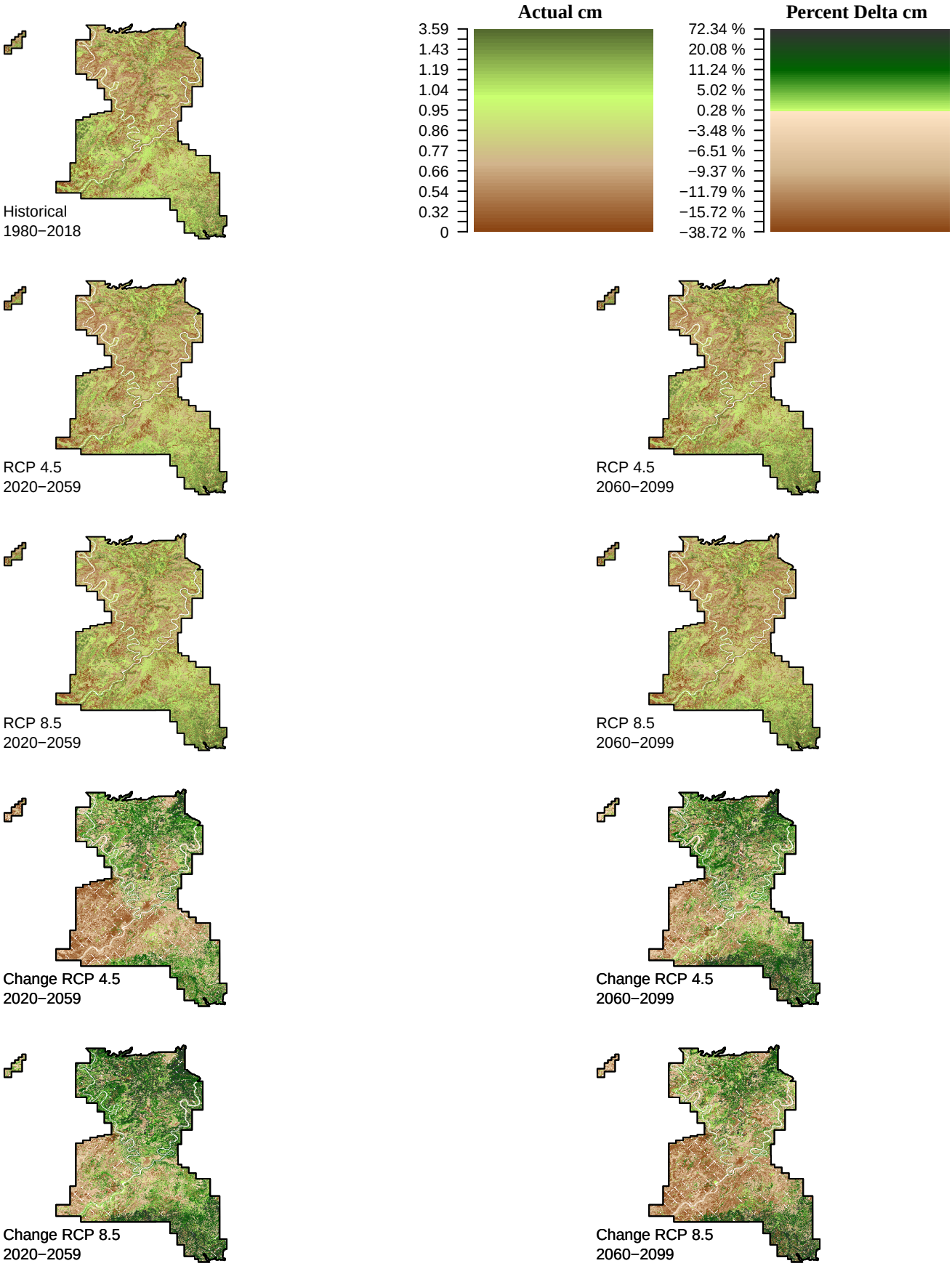


Figure CANYmap83:
Past trends and future trajectories of park−wide mean values for Fall available soil moisture in Canyonlands. Topmost panel depicts the historical mean from 1980−2018. Lower four panels show the emission scenarios of RCP 4.5 and RCP 8.5 at near−term and long−term timeframes. Bottom four panels depict the change from the historical mean; cross hatching denotes areas of robust predicitons (90% of models agree in the direction of change).

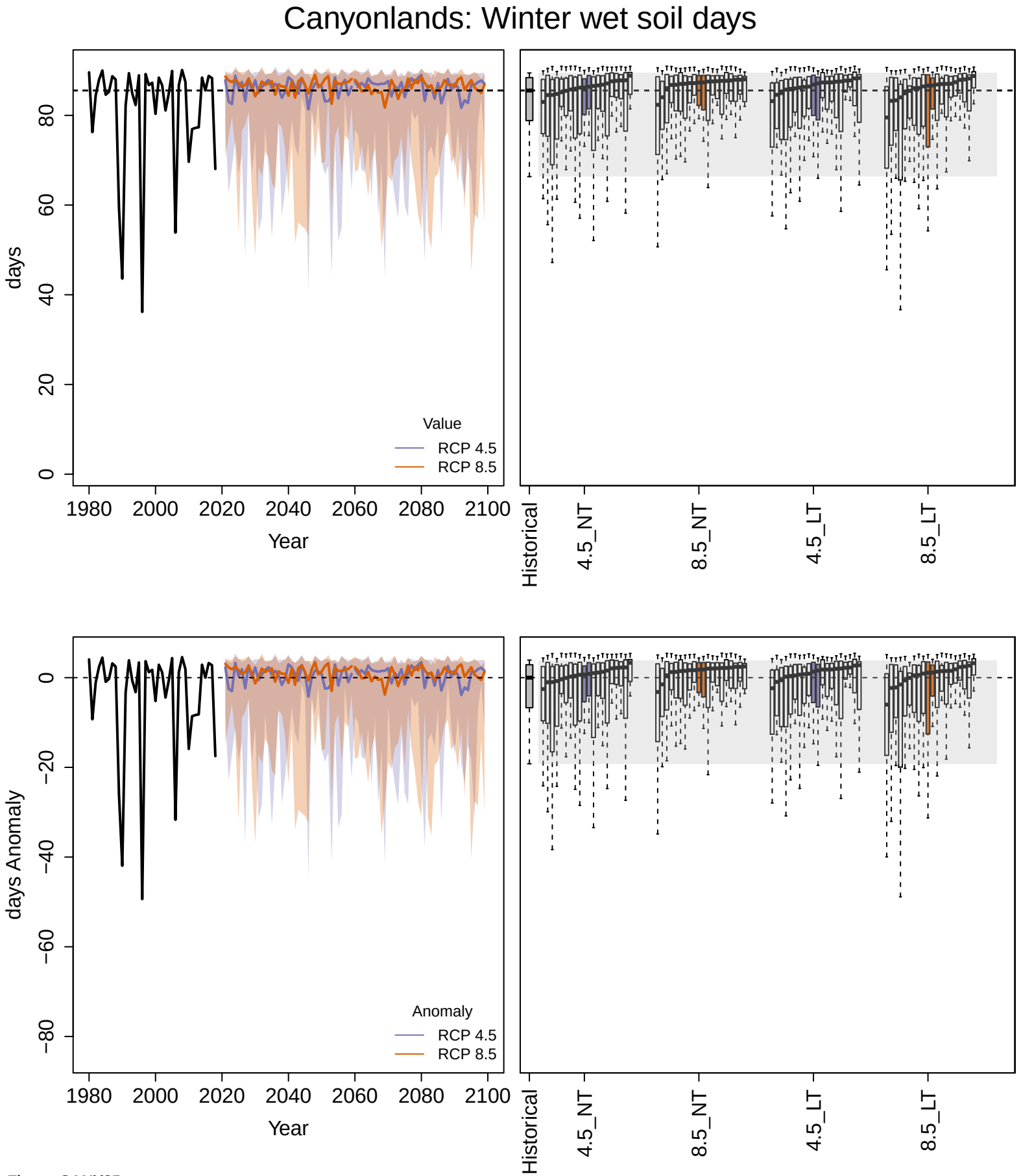


Figure CANY85:
Past trends and future trajectories of park−wide mean values for Winter wet soil days in Canyonlands. Top panels show values, bottom panels show changes from the long−term historical mean. Left: Time series of historical (black) and future projections for RCP 4.5 and 8.5. Shaded areas show spread among climate models. Right: Boxplots of temporal variability over 40−year periods under historical (left box) and individual climate models under two RCPs. Right: Historical time period is 1970−2010; near−term (NT) is 2020−2060; long−term (LT) is 2061−2100.

Canyonlands: Winter wet soil days

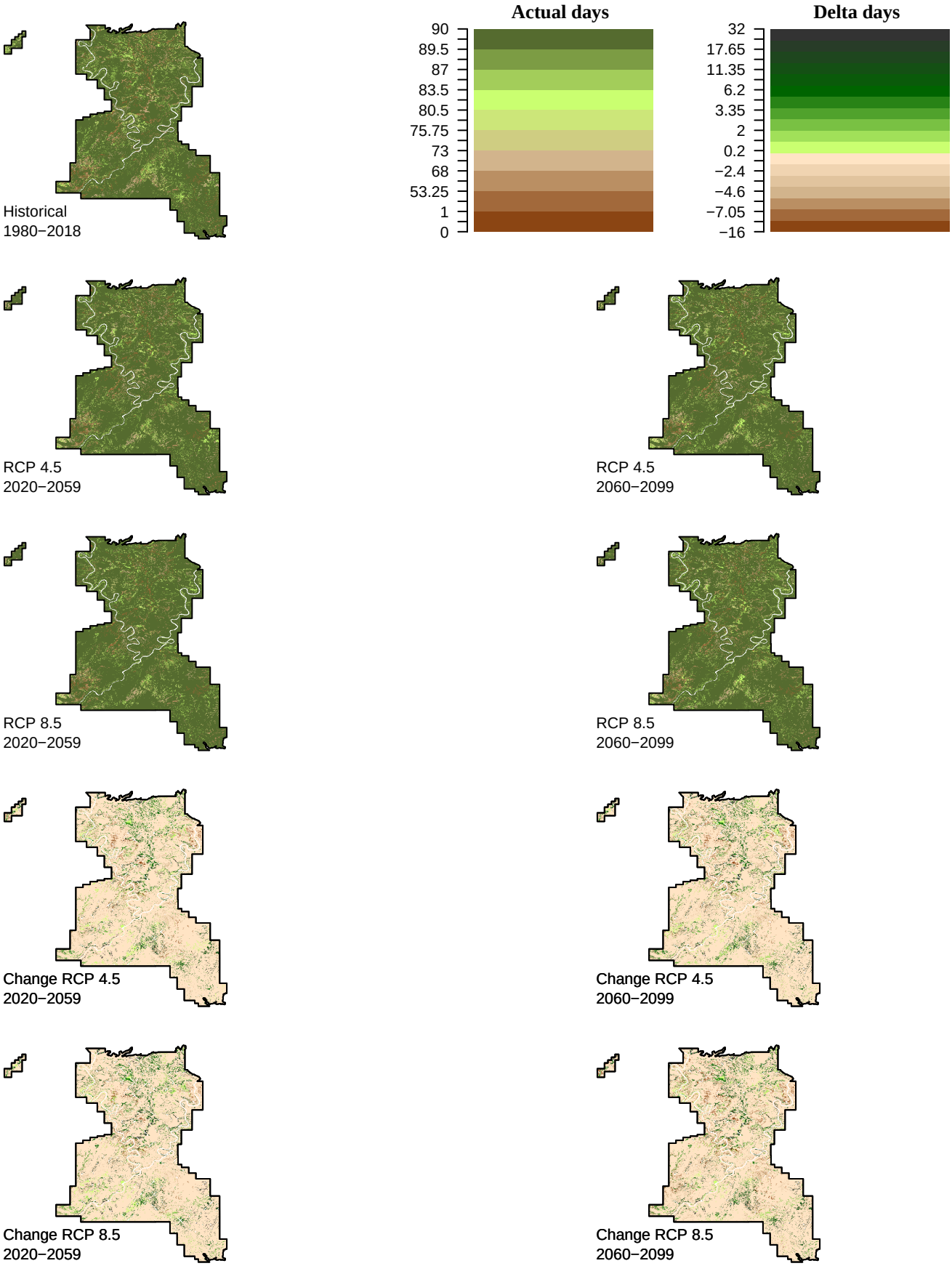


Figure CANYmap85:
Past trends and future trajectories of park−wide mean values for Winter wet soil days in Canyonlands. Topmost panel depicts the historical mean from 1980−2018. Lower four panels show the emission scenarios of RCP 4.5 and RCP 8.5 at near−term and long−term timeframes. Bottom four panels depict the change from the historical mean; cross hatching denotes areas of robust predicitons (90% of models agree in the direction of change).

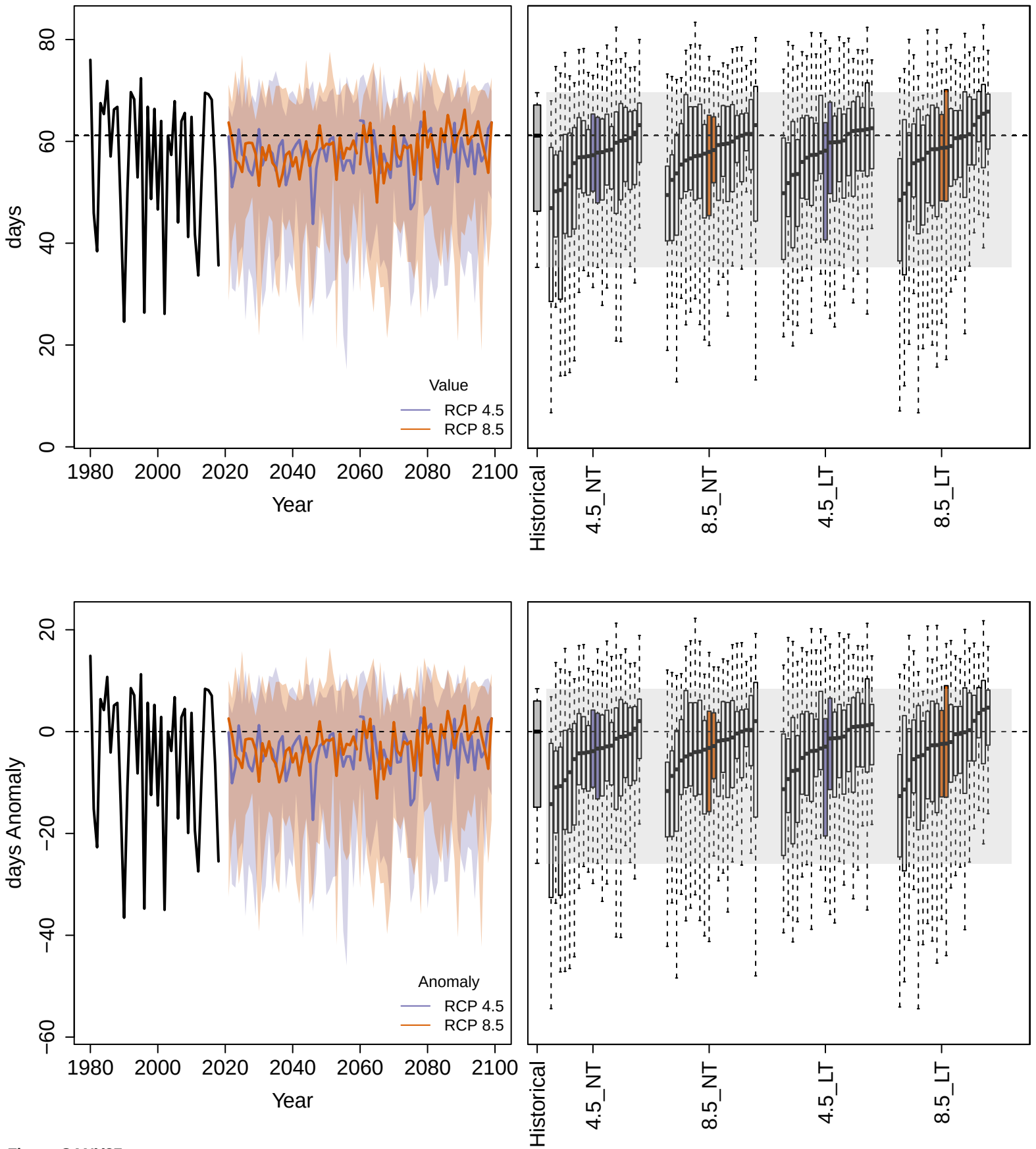


Figure CANY87:
Past trends and future trajectories of park−wide mean values for Spring wet soil days in Canyonlands. Top panels show values, bottom panels show changes from the long−term historical mean. Left: Time series of historical (black) and future projections for RCP 4.5 and 8.5. Shaded areas show spread among climate models. Right: Boxplots of temporal variability over 40−year periods under historical (left box) and individual climate models under two RCPs. Right: Historical time period is 1970−2010; near−term (NT) is 2020−2060; long−term (LT) is 2061−2100.

Canyonlands: Spring wet soil days

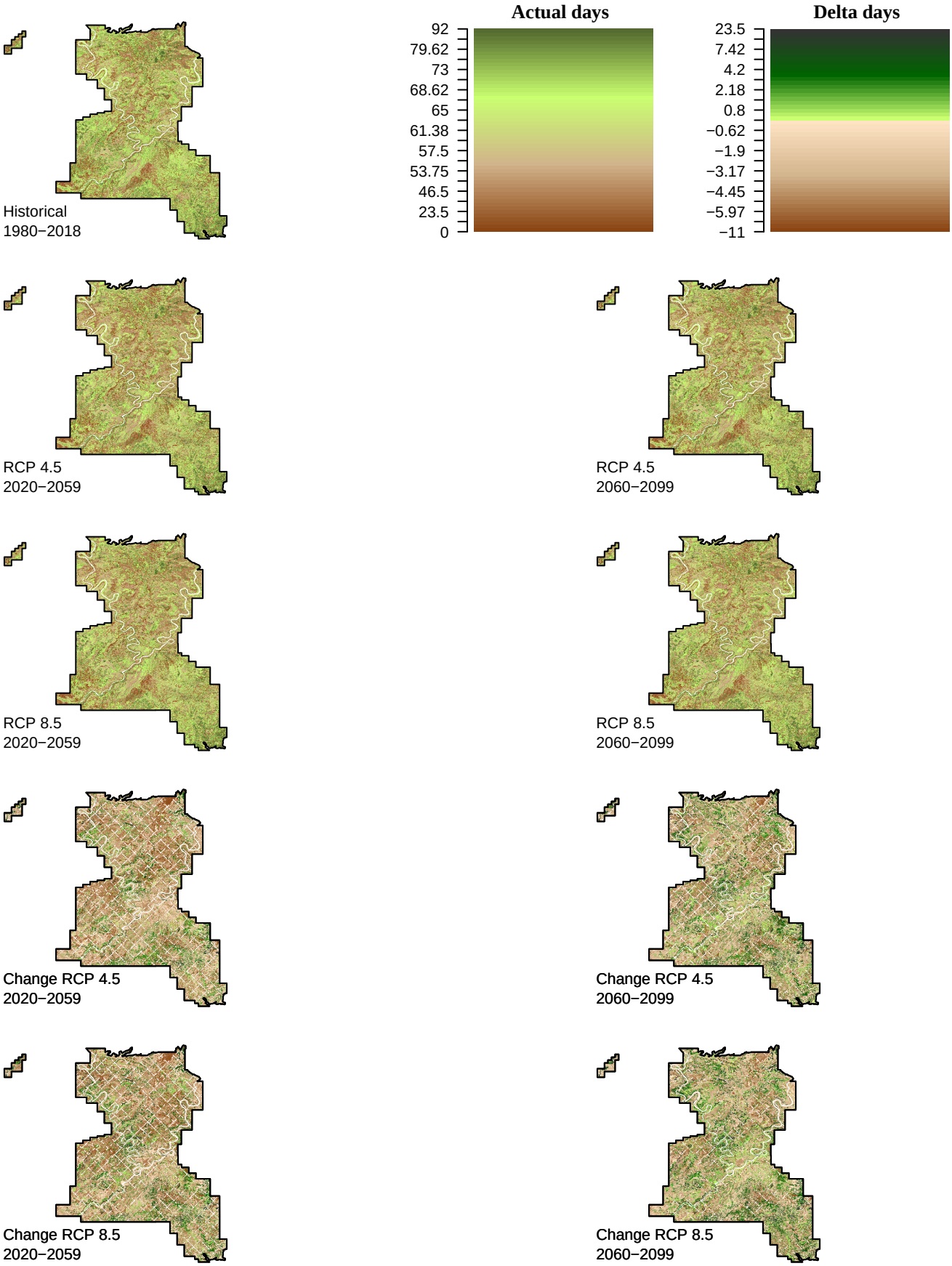


Figure CANYmap87:
Past trends and future trajectories of park−wide mean values for Spring wet soil days in Canyonlands. Topmost panel depicts the historical mean from 1980−2018. Lower four panels show the emission scenarios of RCP 4.5 and RCP 8.5 at near−term and long−term timeframes. Bottom four panels depict the change from the historical mean; cross hatching denotes areas of robust predicitons (90% of models agree in the direction of change).

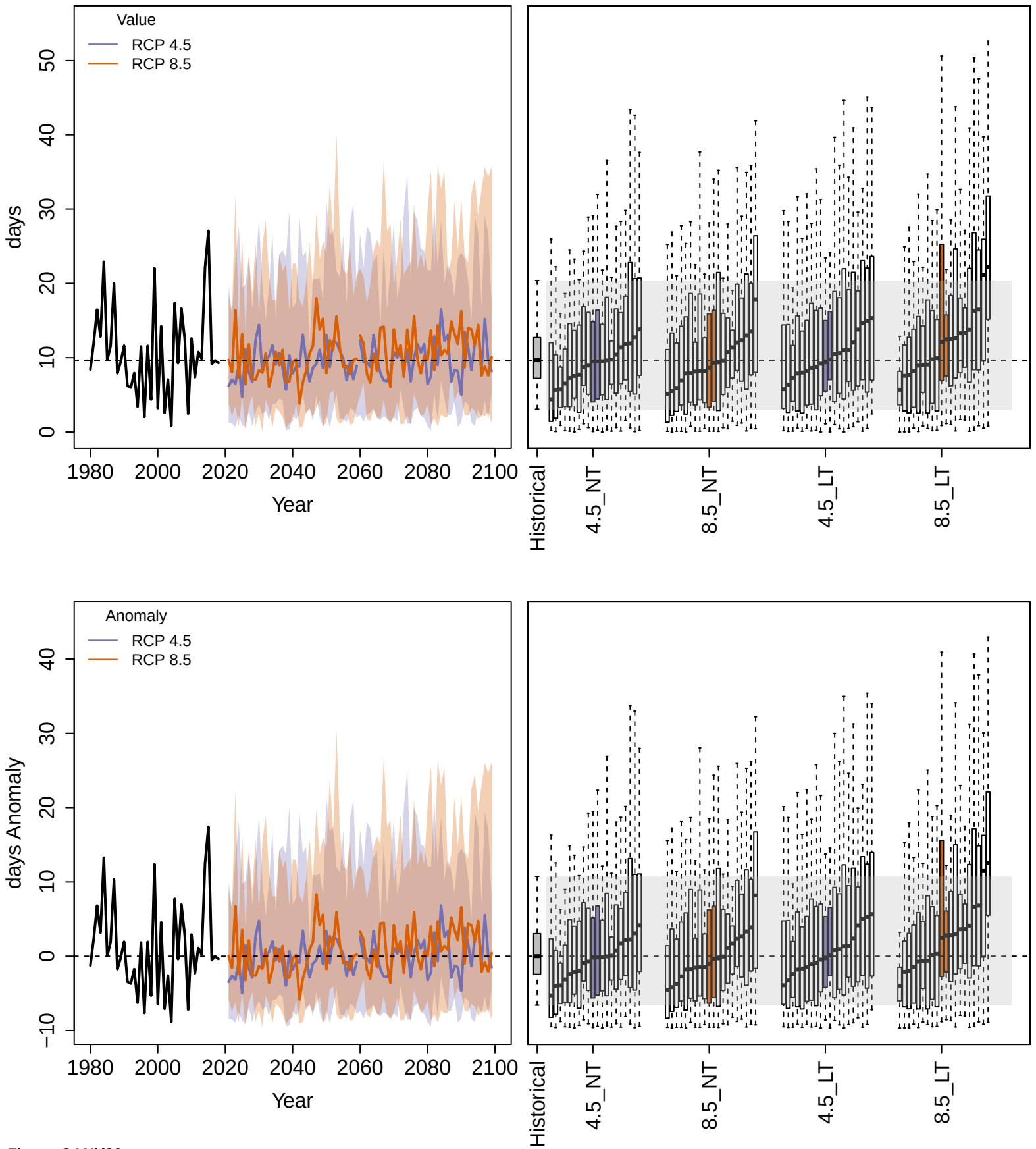


Figure CANY89:
Past trends and future trajectories of park−wide mean values for Summer wet soil days in Canyonlands. Top panels show values, bottom panels show changes from the long−term historical mean. Left: Time series of historical (black) and future projections for RCP 4.5 and 8.5. Shaded areas show spread among climate models. Right: Boxplots of temporal variability over 40−year periods under historical (left box) and individual climate models under two RCPs. Right: Historical time period is 1970−2010; near−term (NT) is 2020−2060; long−term (LT) is 2061−2100.

Canyonlands: Summer wet soil days

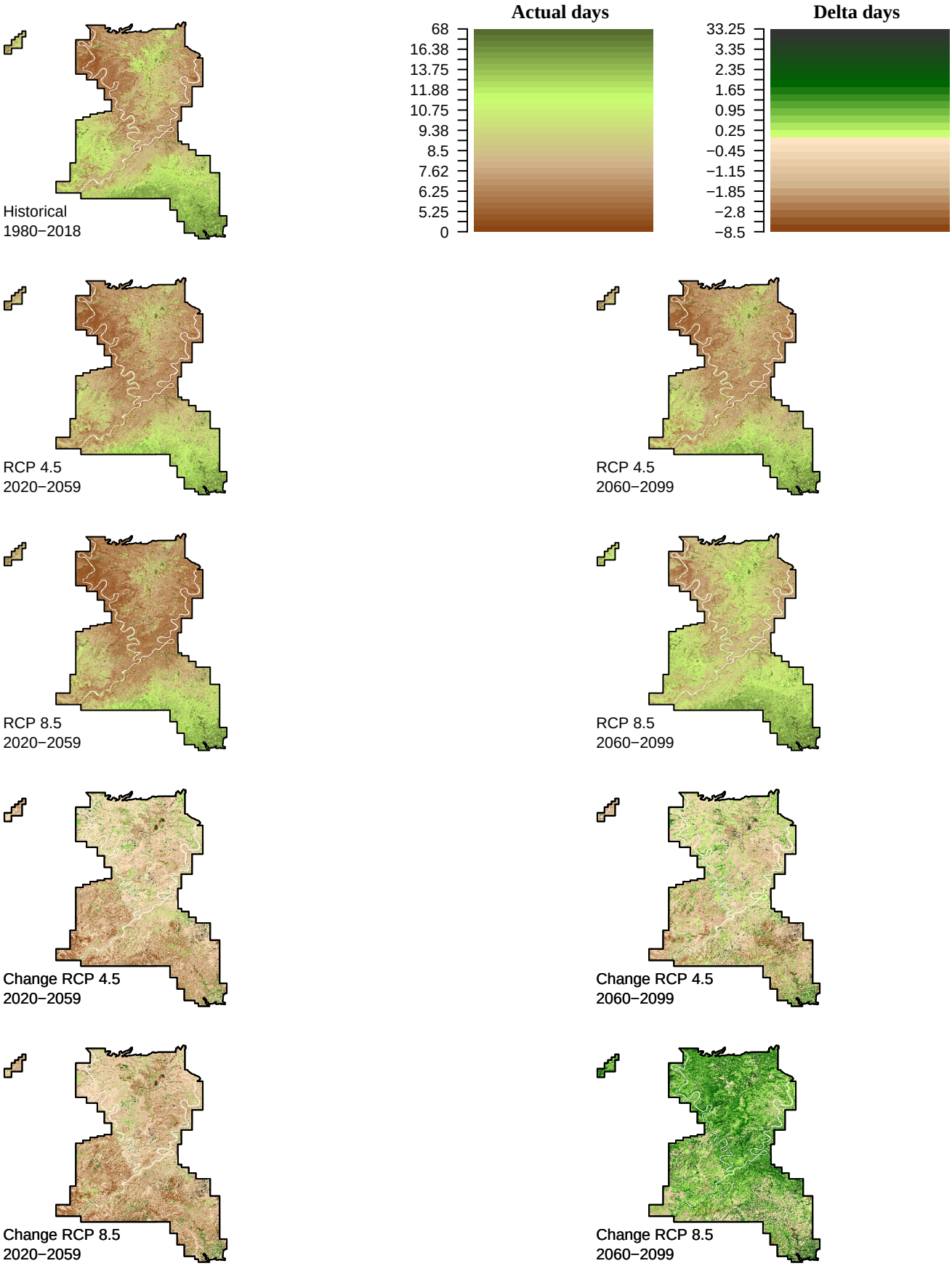


Figure CANYmap89:
Past trends and future trajectories of park−wide mean values for Summer wet soil days in Canyonlands. Topmost panel depicts the historical mean from 1980−2018. Lower four panels show the emission scenarios of RCP 4.5 and RCP 8.5 at near−term and long−term timeframes. Bottom four panels depict the change from the historical mean; cross hatching denotes areas of robust predicitons (90% of models agree in the direction of change).

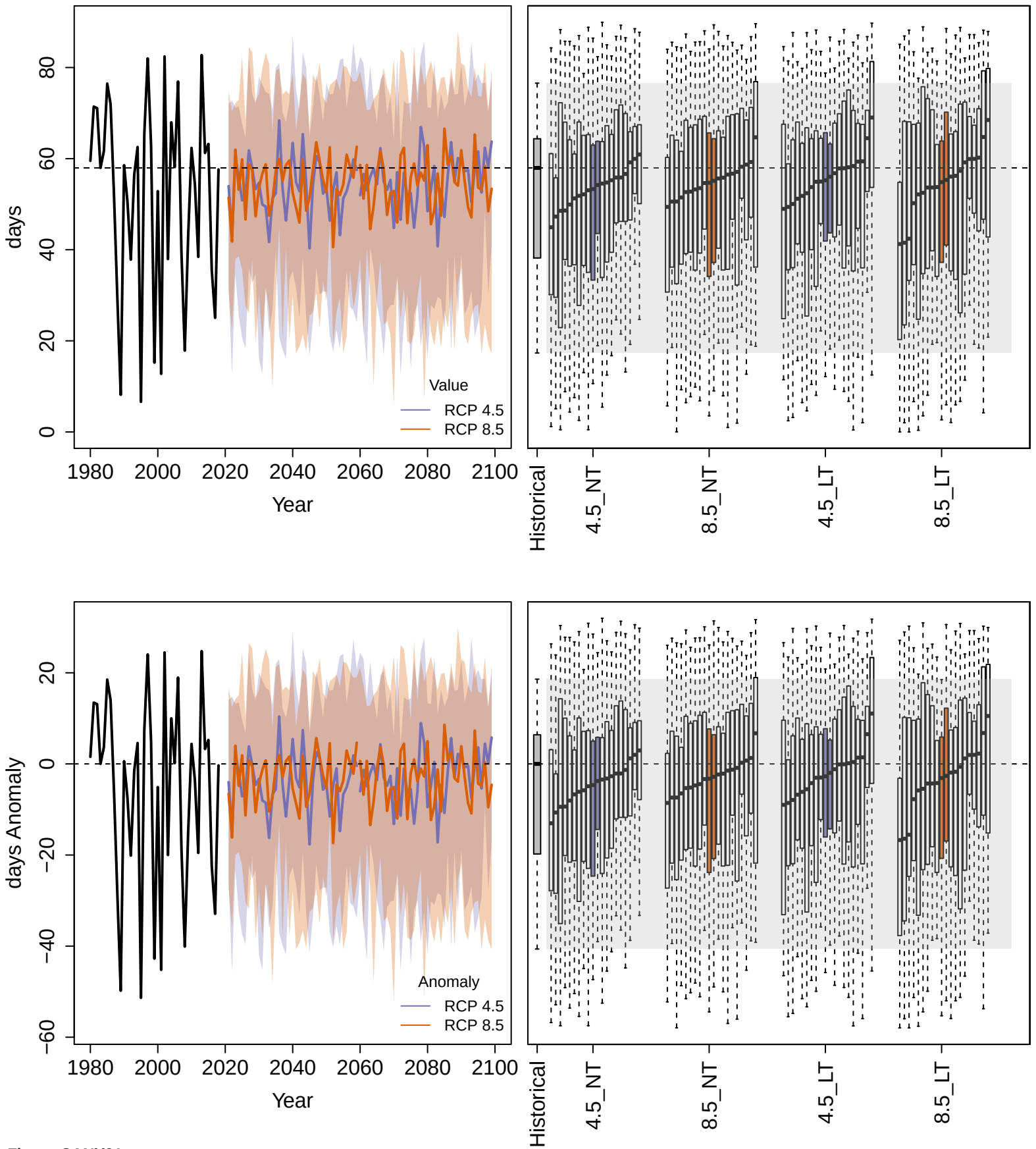


Figure CANY91:
Past trends and future trajectories of park−wide mean values for Fall wet soil days in Canyonlands. Top panels show values, bottom panels show changes from the long−term historical mean. Left: Time series of historical (black) and future projections for RCP 4.5 and 8.5. Shaded areas show spread among climate models. Right: Boxplots of temporal variability over 40−year periods under historical (left box) and individual climate models under two RCPs. Right: Historical time period is 1970−2010; near−term (NT) is 2020−2060; long−term (LT) is 2061−2100.

Canyonlands: Fall wet soil days

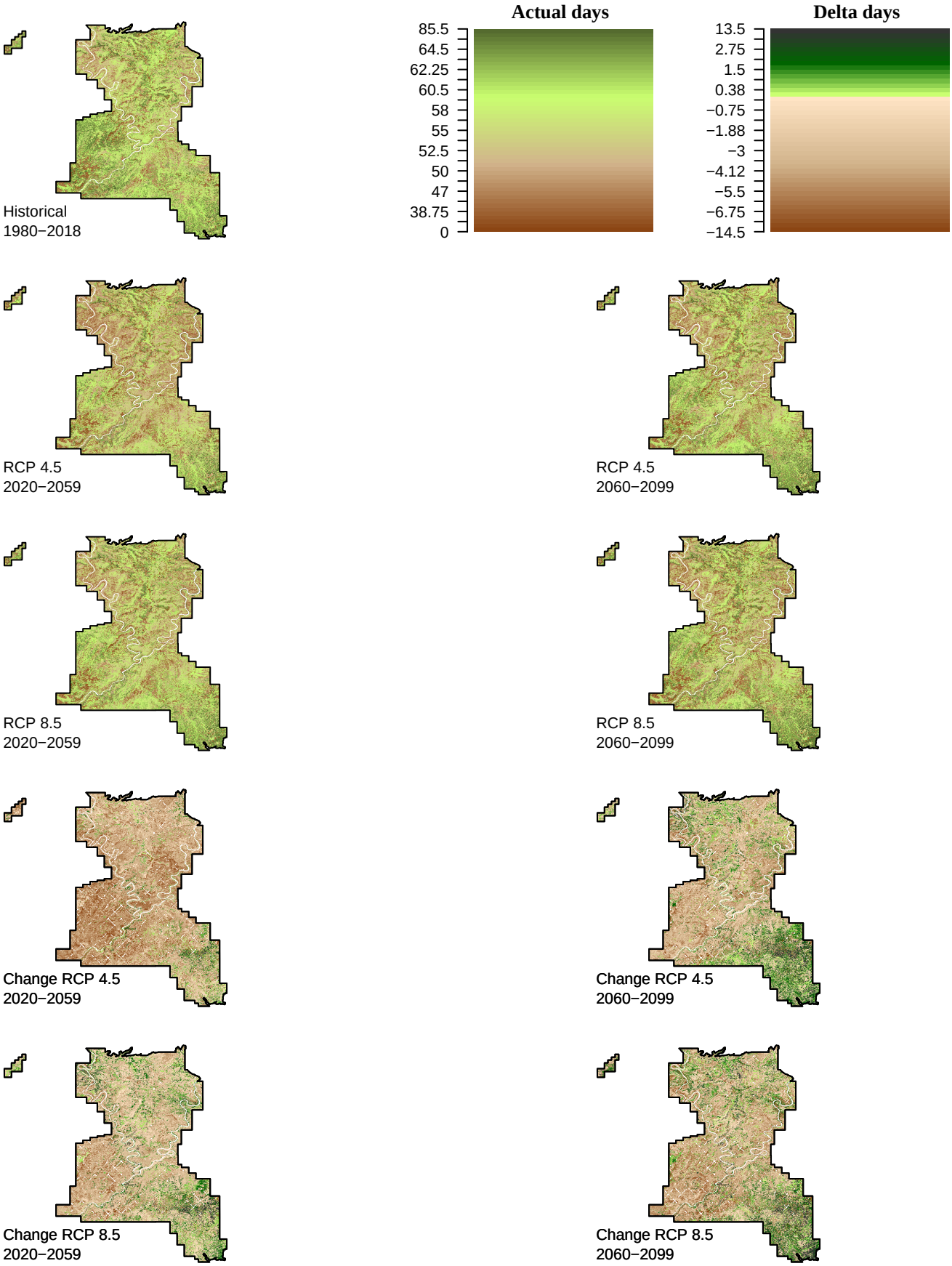


Figure CANYmap91:
Past trends and future trajectories of park−wide mean values for Fall wet soil days in Canyonlands. Topmost panel depicts the historical mean from 1980−2018. Lower four panels show the emission scenarios of RCP 4.5 and RCP 8.5 at near−term and long−term timeframes. Bottom four panels depict the change from the historical mean; cross hatching denotes areas of robust predicitons (90% of models agree in the direction of change).

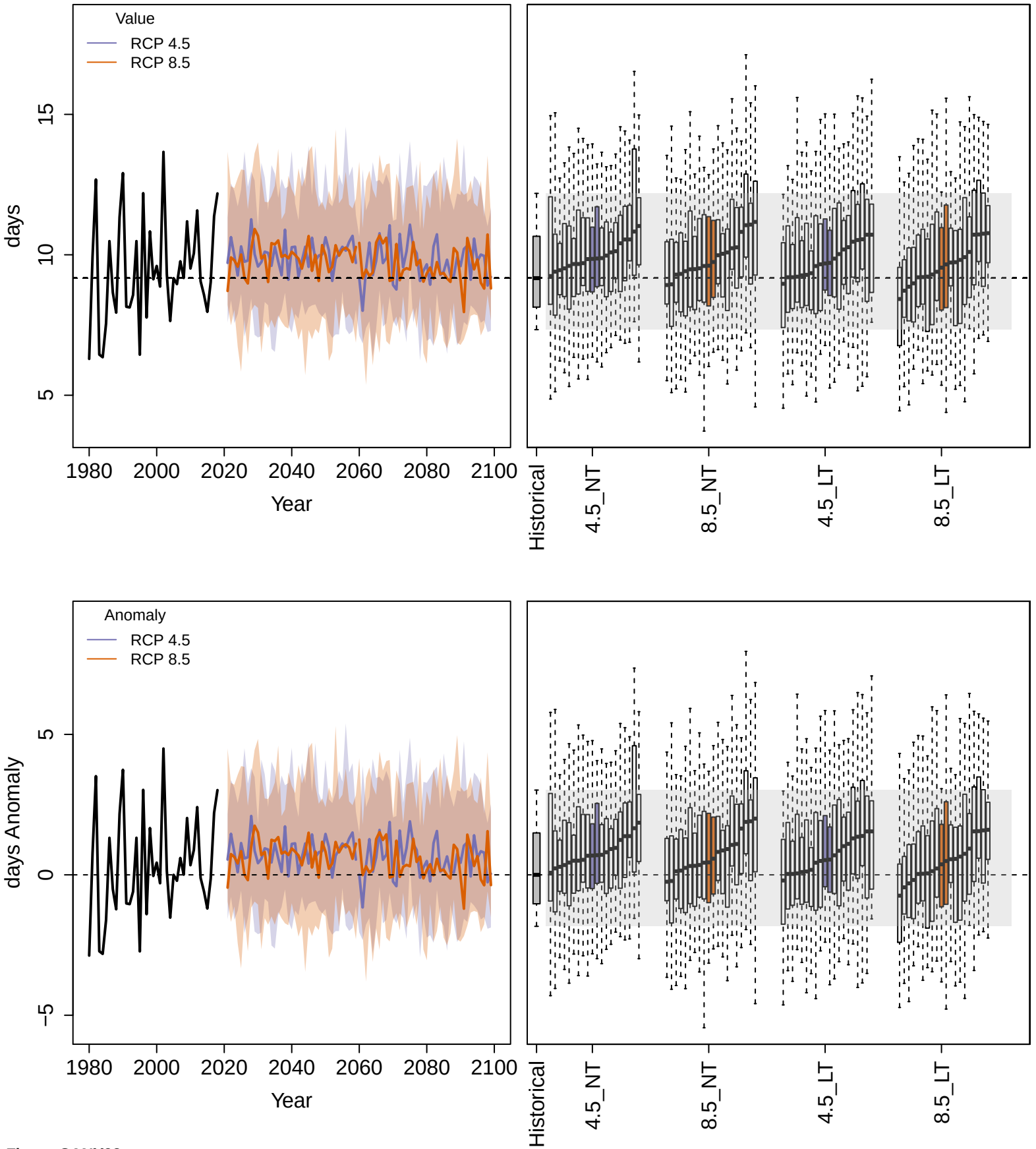


Figure CANY93:
Past trends and future trajectories of park−wide mean values for Spring dry soil days in Canyonlands. Top panels show values, bottom panels show changes from the long−term historical mean. Left: Time series of historical (black) and future projections for RCP 4.5 and 8.5. Shaded areas show spread among climate models. Right: Boxplots of temporal variability over 40−year periods under historical (left box) and individual climate models under two RCPs. Right: Historical time period is 1970−2010; near−term (NT) is 2020−2060; long−term (LT) is 2061−2100.

Canyonlands: Spring dry soil days

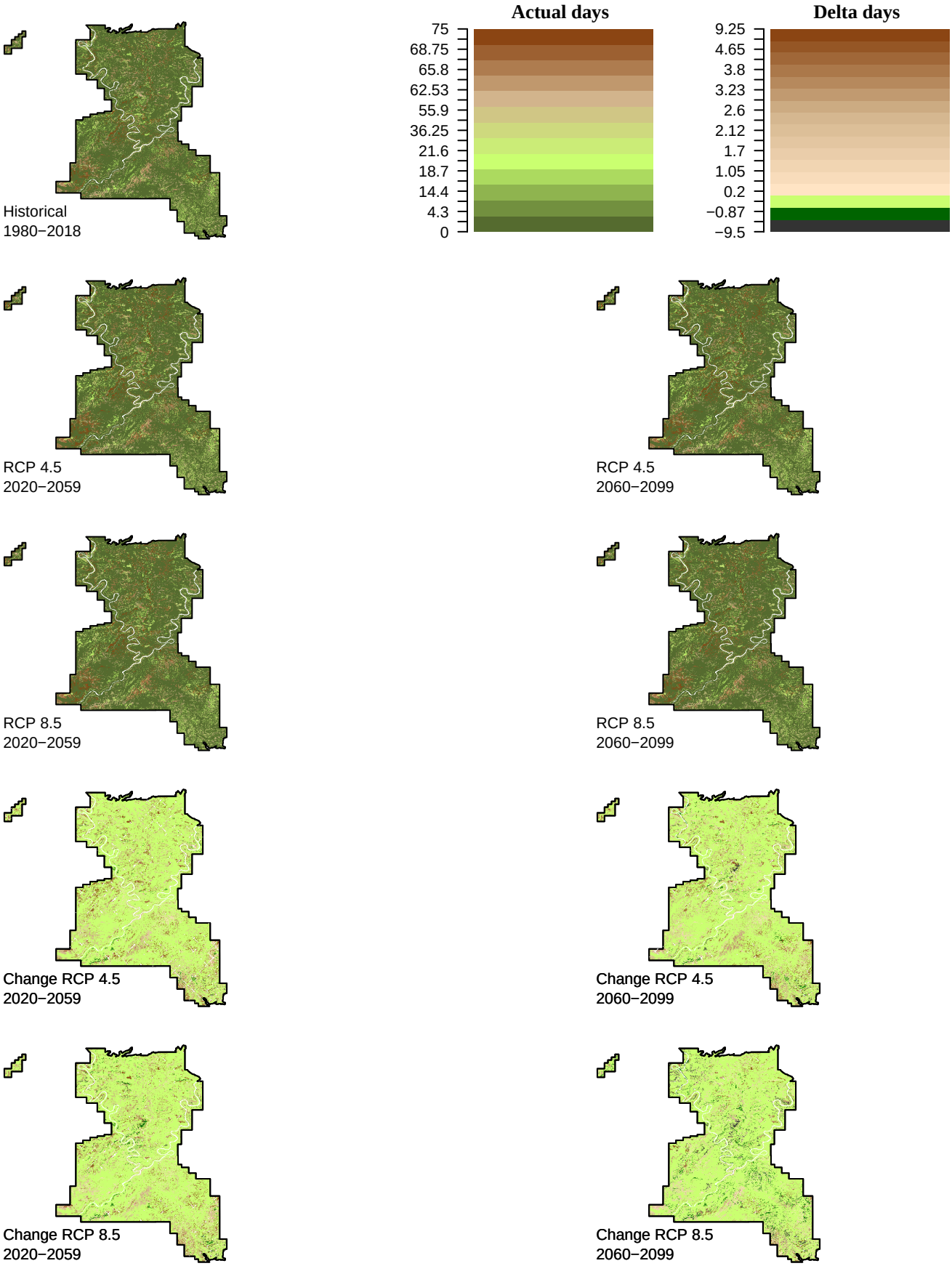


Figure CANYmap93:
Past trends and future trajectories of park−wide mean values for Spring dry soil days in Canyonlands. Topmost panel depicts the historical mean from 1980−2018. Lower four panels show the emission scenarios of RCP 4.5 and RCP 8.5 at near−term and long−term timeframes. Bottom four panels depict the change from the historical mean; cross hatching denotes areas of robust predicitons (90% of models agree in the direction of change).

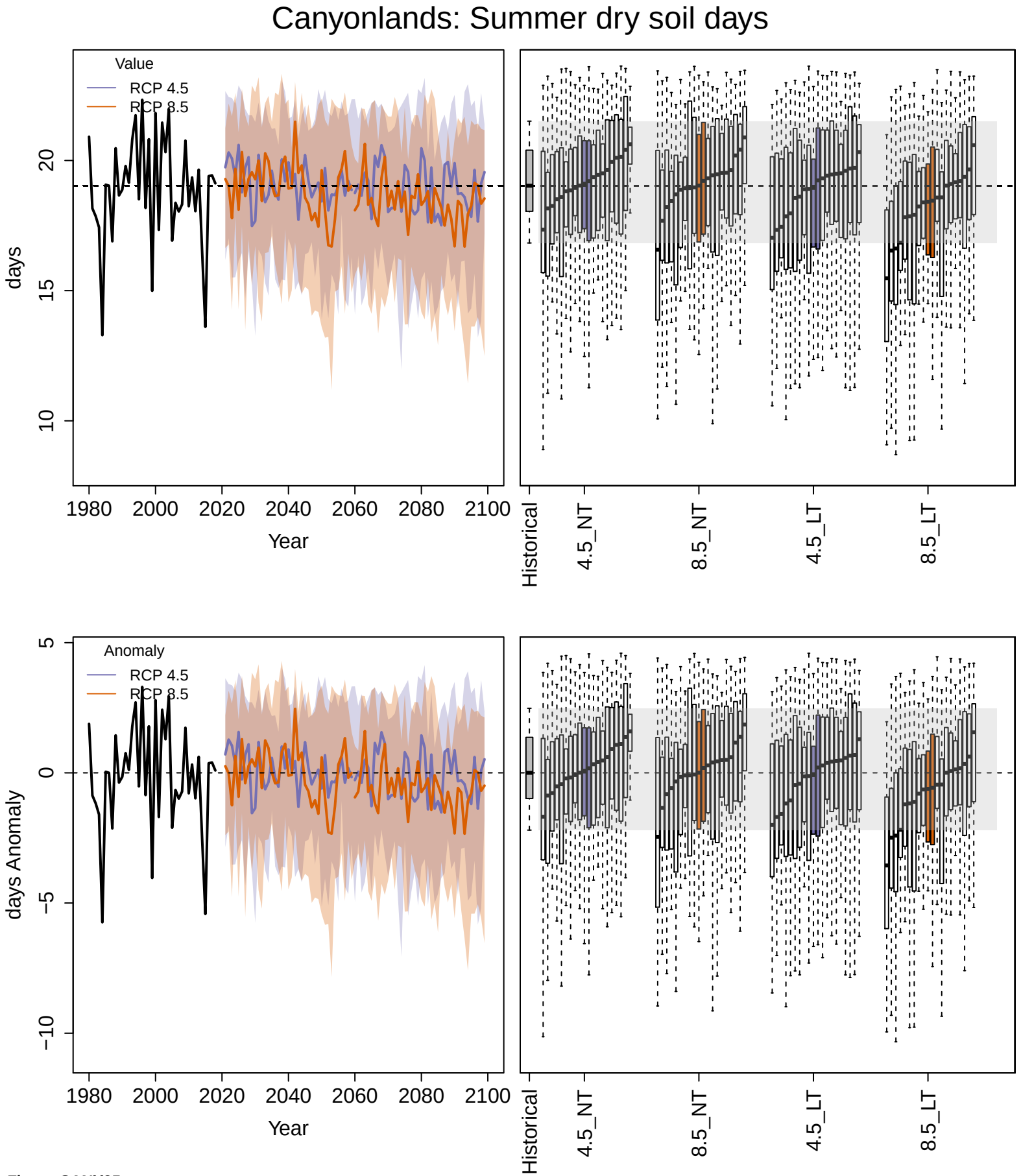


Figure CANY95:
Past trends and future trajectories of park−wide mean values for Summer dry soil days in Canyonlands. Top panels show values, bottom panels show changes from the long−term historical mean. Left: Time series of historical (black) and future projections for RCP 4.5 and 8.5. Shaded areas show spread among climate models. Right: Boxplots of temporal variability over 40−year periods under historical (left box) and individual climate models under two RCPs. Right: Historical time period is 1970−2010; near−term (NT) is 2020−2060; long−term (LT) is 2061−2100.

Canyonlands: Summer dry soil days

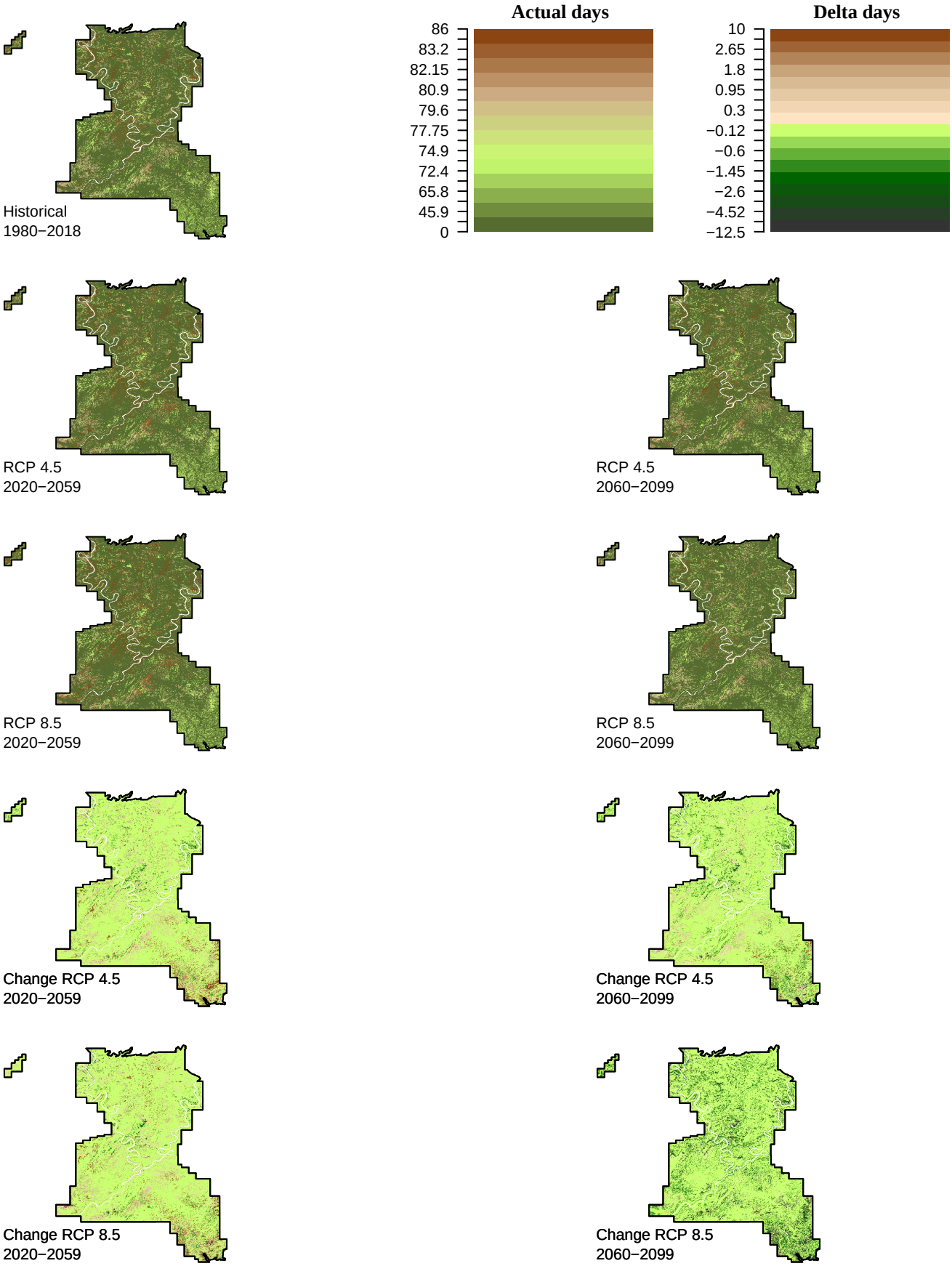


Figure CANYmap95:
Past trends and future trajectories of park−wide mean values for Summer dry soil days in Canyonlands. Topmost panel depicts the historical mean from 1980−2018. Lower four panels show the emission scenarios of RCP 4.5 and RCP 8.5 at near−term and long−term timeframes. Bottom four panels depict the change from the historical mean; cross hatching denotes areas of robust predicitons (90% of models agree in the direction of change).

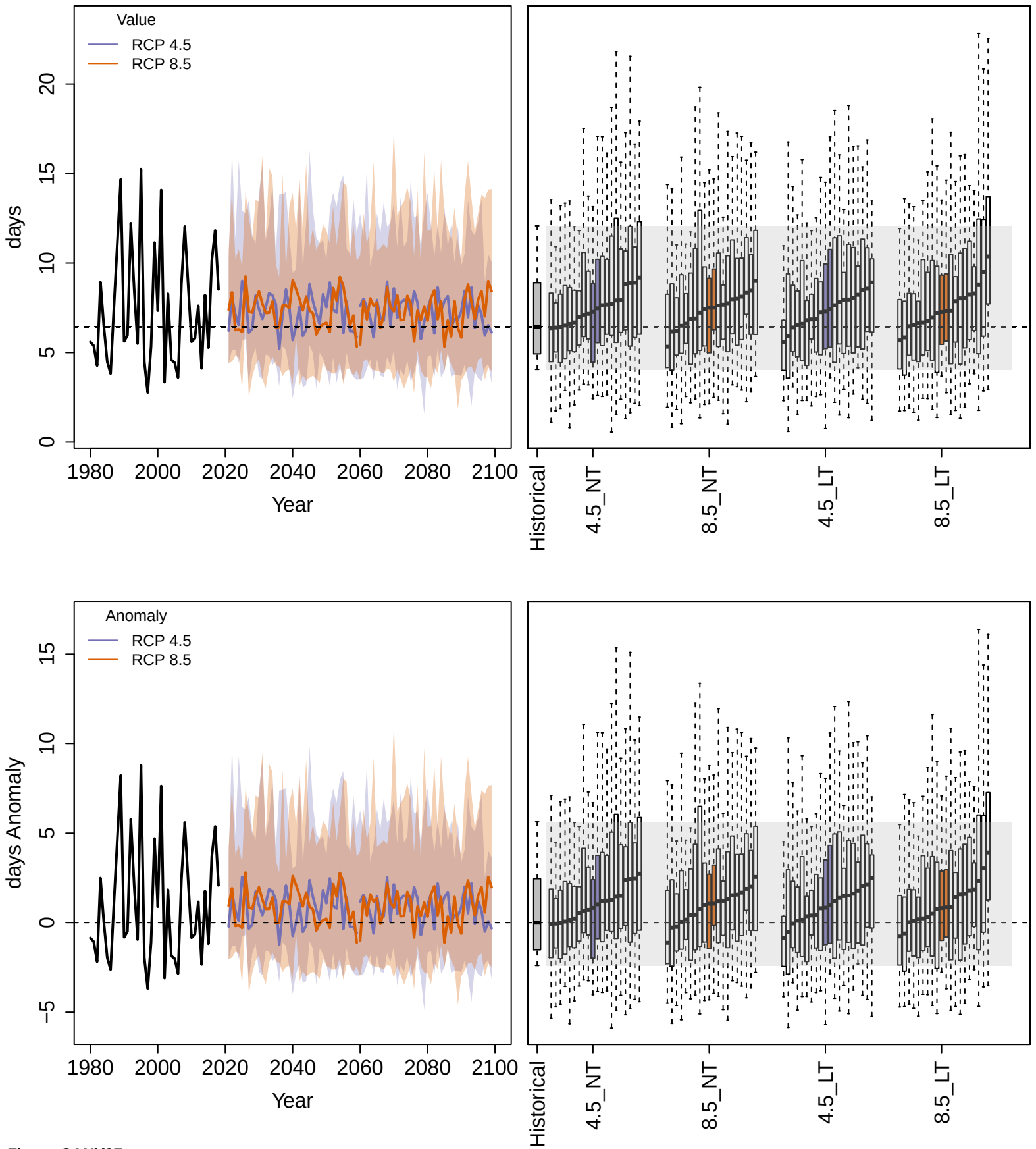


Figure CANY97:
Past trends and future trajectories of park−wide mean values for Fall dry soil days in Canyonlands. Top panels show values, bottom panels show changes from the long−term historical mean. Left: Time series of historical (black) and future projections for RCP 4.5 and 8.5. Shaded areas show spread among climate models. Right: Boxplots of temporal variability over 40−year periods under historical (left box) and individual climate models under two RCPs. Right: Historical time period is 1970−2010; near−term (NT) is 2020−2060; long−term (LT) is 2061−2100.

Canyonlands: Fall dry soil days

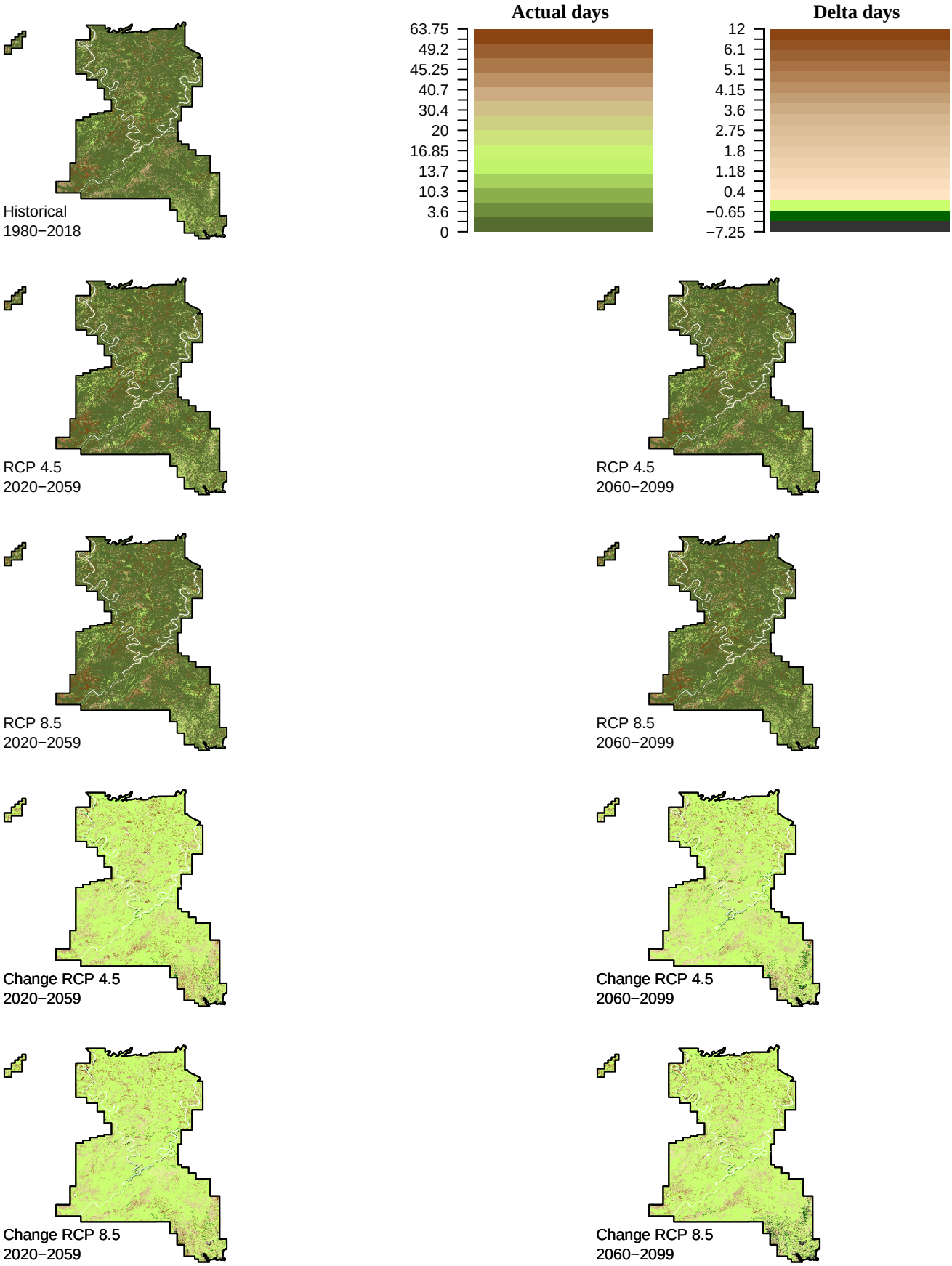


Figure CANYmap97:
Past trends and future trajectories of park−wide mean values for Fall dry soil days in Canyonlands. Topmost panel depicts the historical mean from 1980−2018. Lower four panels show the emission scenarios of RCP 4.5 and RCP 8.5 at near−term and long−term timeframes. Bottom four panels depict the change from the historical mean; cross hatching denotes areas of robust predicitons (90% of models agree in the direction of change).

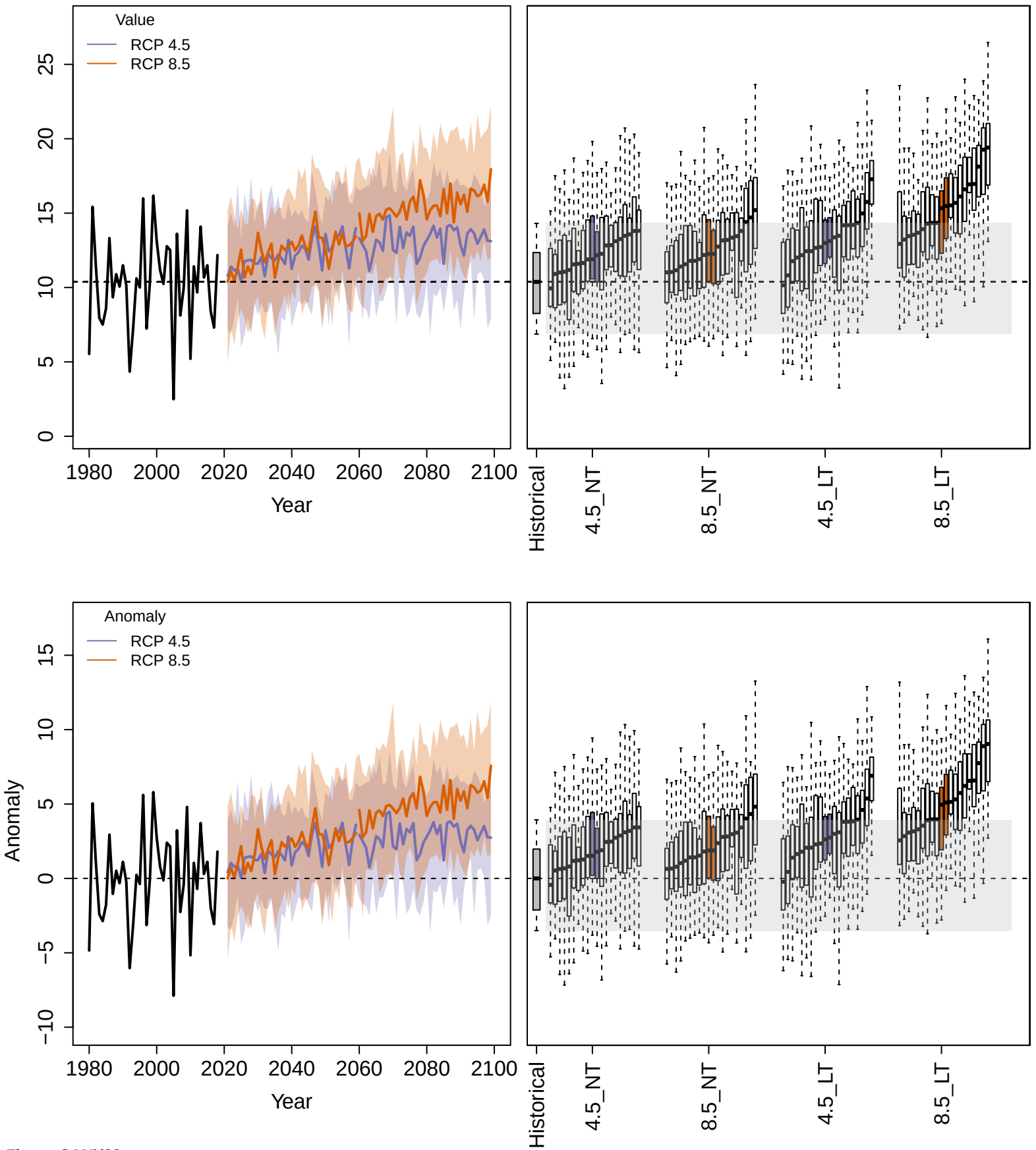


Figure CANY99:
Past trends and future trajectories of park−wide mean values for Winter extreme short−term dry stress in Canyonlands. Top panels show values, bottom panels show changes from the long−term historical mean. Left: Time series of historical (black) and future projections for RCP 4.5 and 8.5. Shaded areas show spread among climate models. Right: Boxplots of temporal variability over 40−year periods under historical (left box) and individual climate models under two RCPs. Right: Historical time period is 1970−2010; near−term (NT) is 2020−2060; long−term (LT) is 2061−2100.

Canyonlands: Winter extreme short−term dry stress

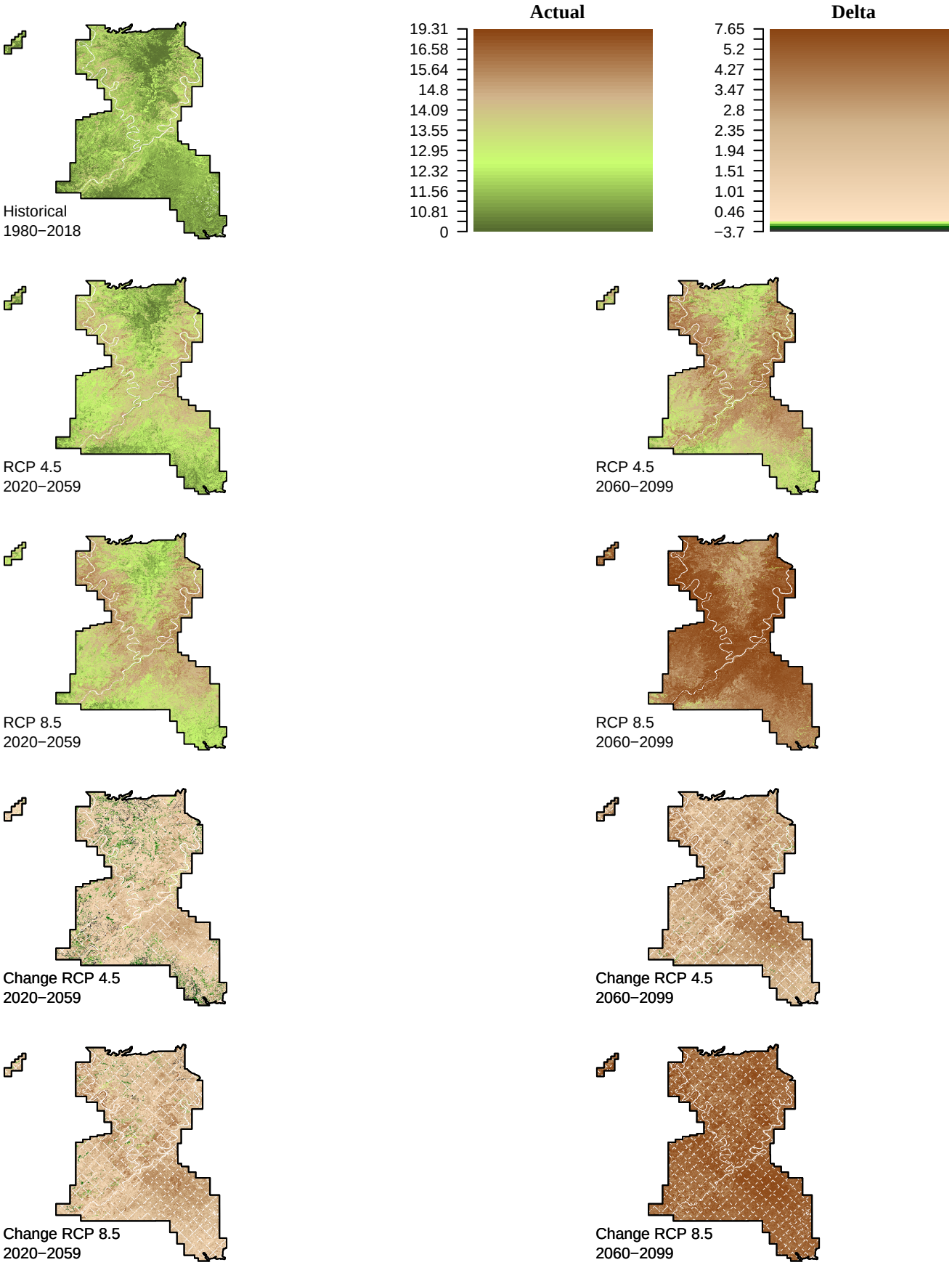


Figure CANYmap99:
Past trends and future trajectories of park−wide mean values for Winter extreme short−term dry stress in Canyonlands. Topmost panel depicts the historical mean from 1980−2018. Lower four panels show the emission scenarios of RCP 4.5 and RCP 8.5 at near−term and long−term timeframes. Bottom four panels depict the change from the historical mean; cross hatching denotes areas of robust predicitons (90% of models agree in the direction of change).

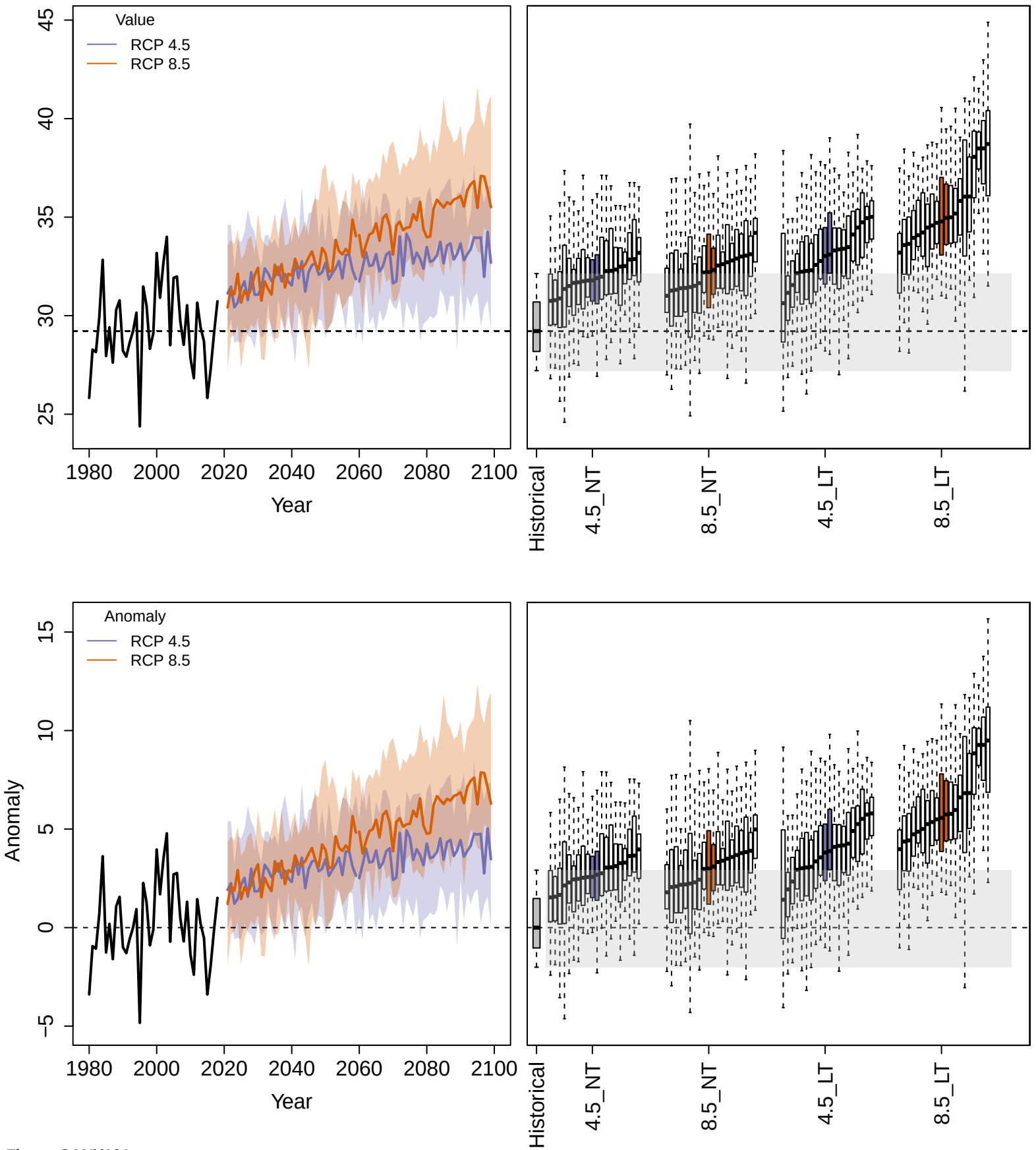


Figure CANY101:
Past trends and future trajectories of park−wide mean values for Spring extreme short−term dry stress in Canyonlands. Top panels show values, bottom panels show changes from the long−term historical mean. Left: Time series of historical (black) and future projections for RCP 4.5 and 8.5. Shaded areas show spread among climate models. Right: Boxplots of temporal variability over 40−year periods under historical (left box) and individual climate models under two RCPs. Right: Historical time period is 1970−2010; near−term (NT) is 2020−2060; long−term (LT) is 2061−2100.

Canyonlands: Spring extreme short−term dry stress

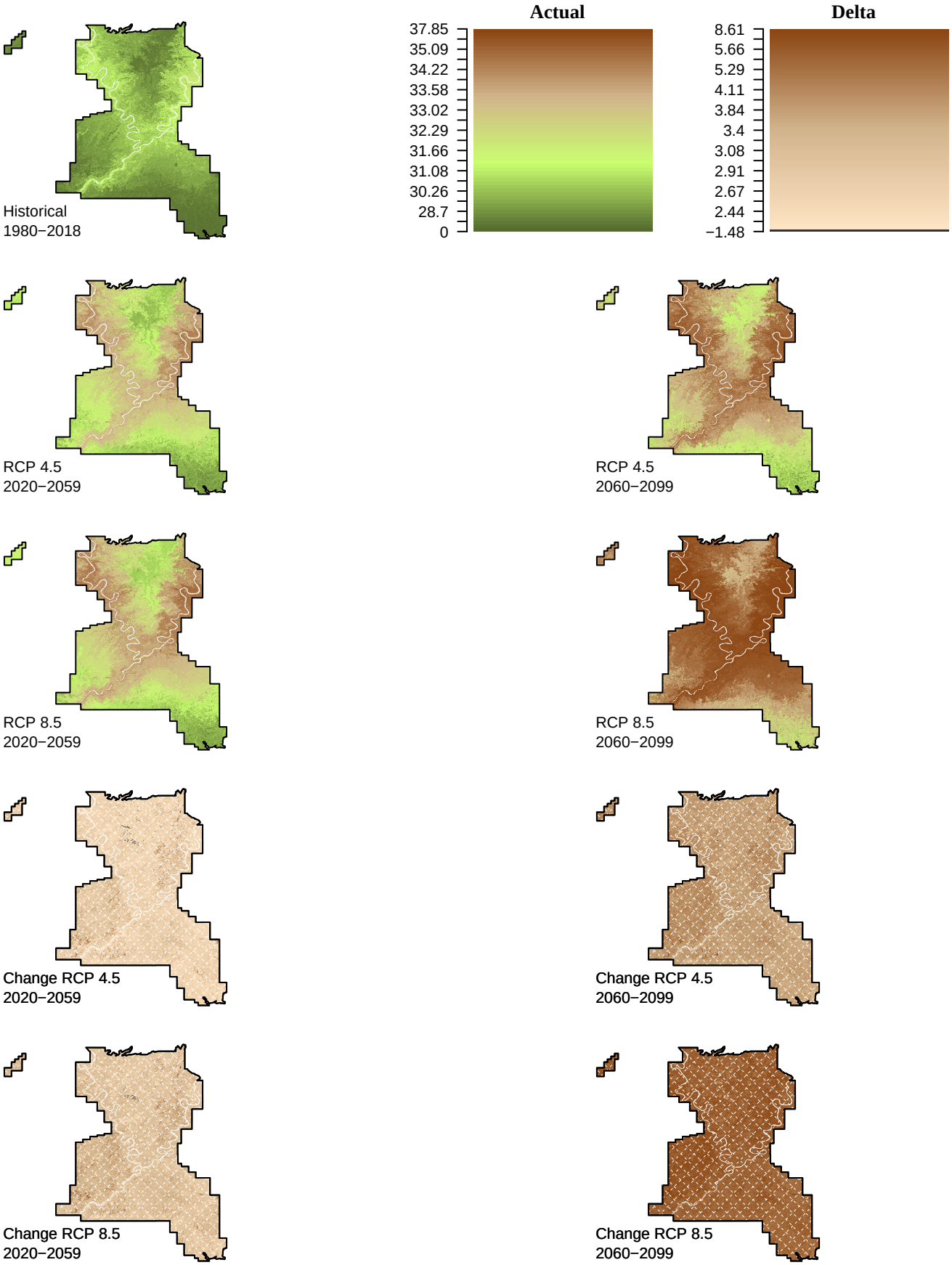


Figure CANYmap101:
Past trends and future trajectories of park−wide mean values for Spring extreme short−term dry stress in Canyonlands. Topmost panel depicts the historical mean from 1980−2018. Lower four panels show the emission scenarios of RCP 4.5 and RCP 8.5 at near−term and long−term timeframes. Bottom four panels depict the change from the historical mean; cross hatching denotes areas of robust predicitons (90% of models agree in the direction of change).

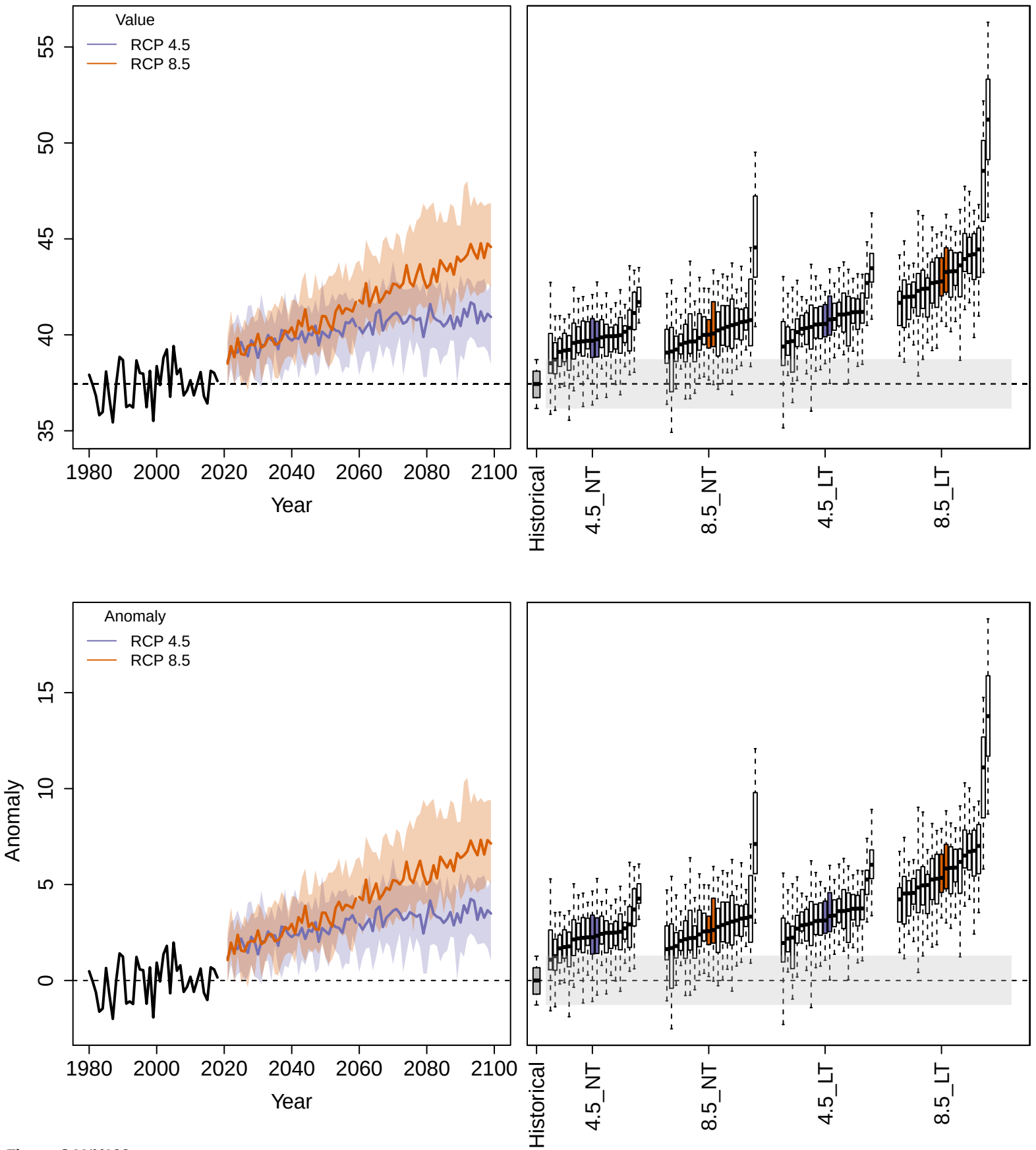


Figure CANY103:
Past trends and future trajectories of park−wide mean values for Summer extreme short−term dry stress in Canyonlands. Top panels show values, bottom panels show changes from the long−term historical mean. Left: Time series of historical (black) and future projections for RCP 4.5 and 8.5. Shaded areas show spread among climate models. Right: Boxplots of temporal variability over 40−year periods under historical (left box) and individual climate models under two RCPs. Right: Historical time period is 1970−2010; near−term (NT) is 2020−2060; long−term (LT) is 2061−2100.

Canyonlands: Summer extreme short−term dry stress

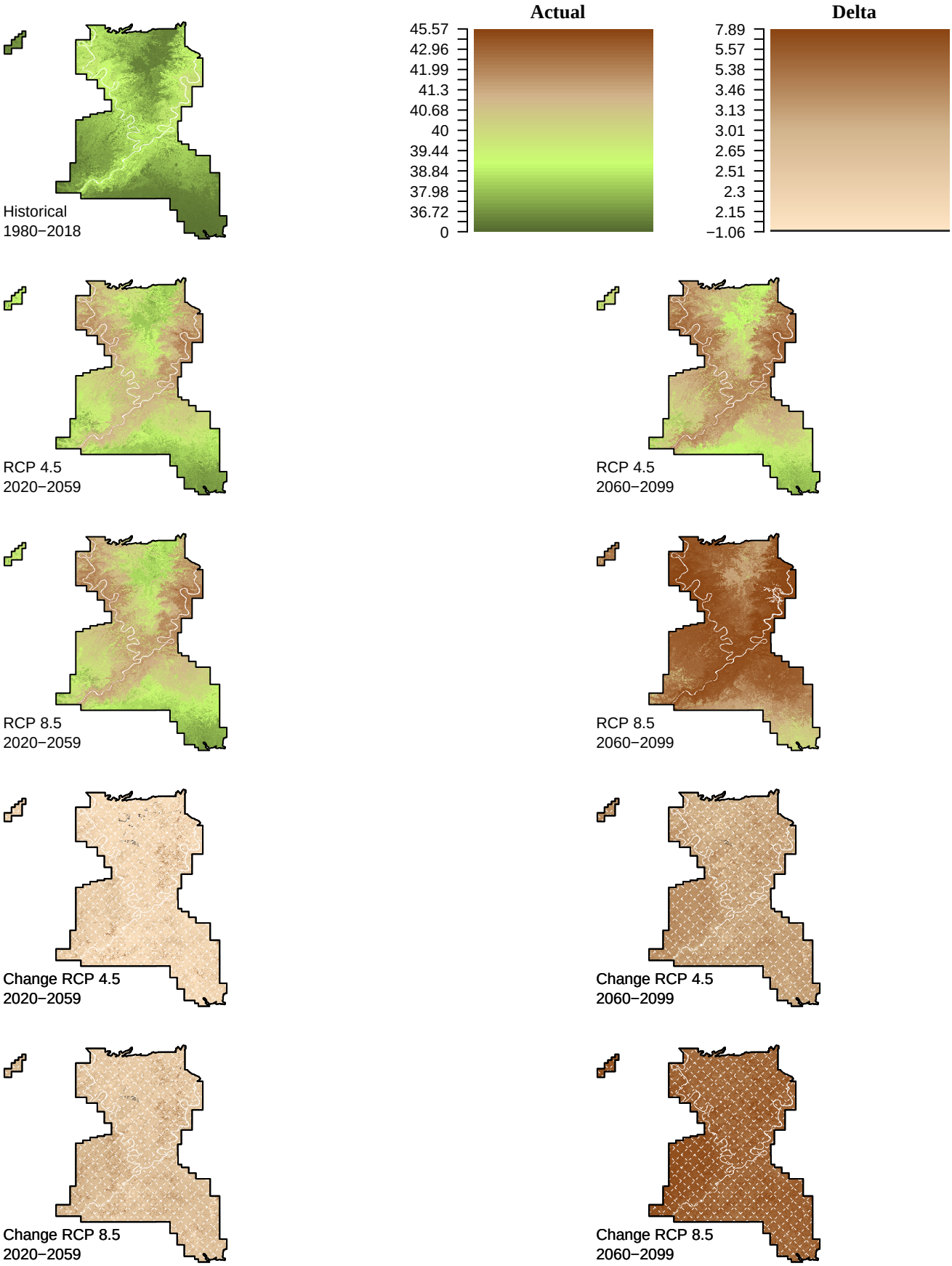


Figure CANYmap103:
Past trends and future trajectories of park−wide mean values for Summer extreme short−term dry stress in Canyonlands. Topmost panel depicts the historical mean from 1980−2018. Lower four panels show the emission scenarios of RCP 4.5 and RCP 8.5 at near−term and long−term timeframes. Bottom four panels depict the change from the historical mean; cross hatching denotes areas of robust predicitons (90% of models agree in the direction of change).

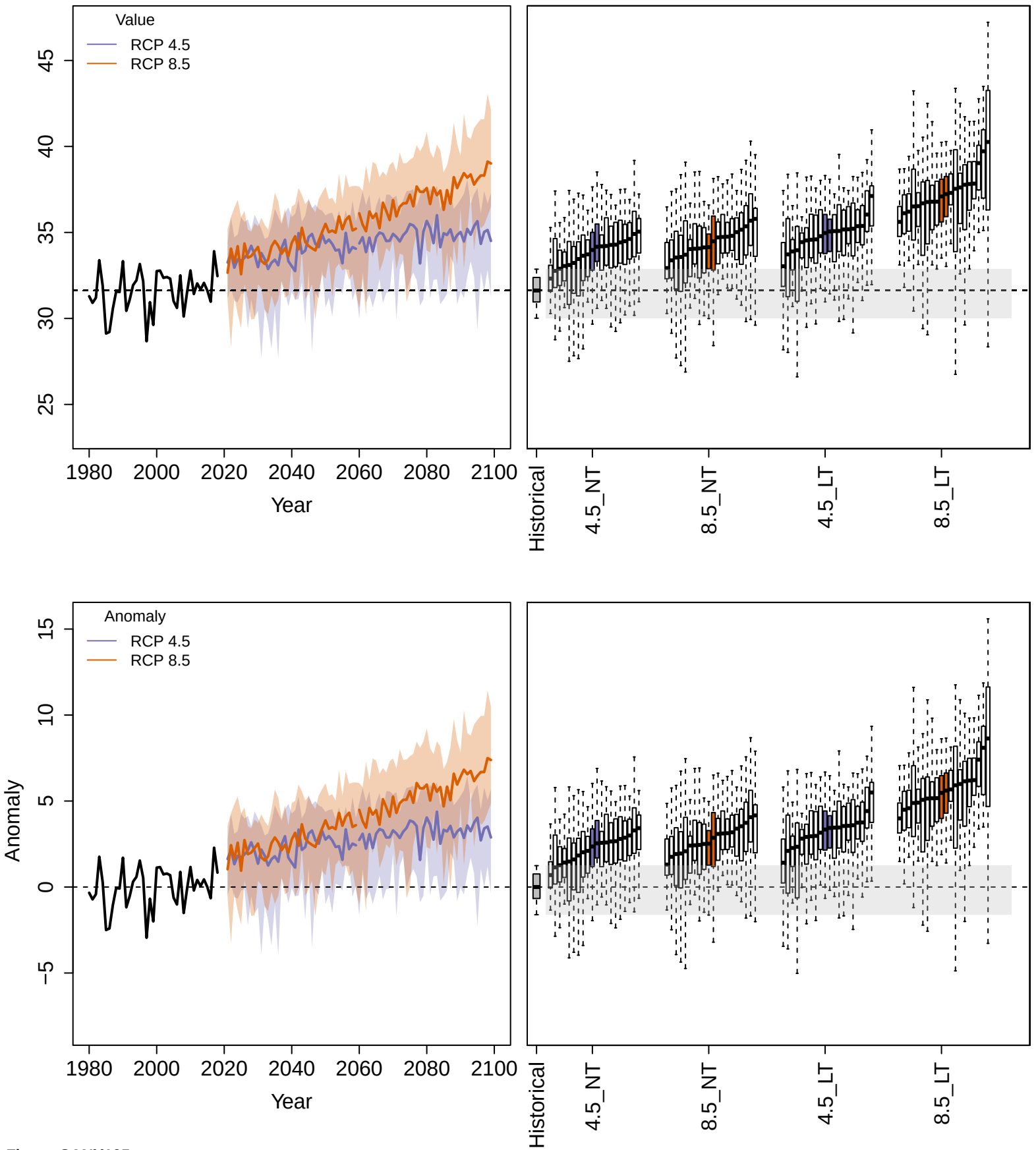


Figure CANY105:
Past trends and future trajectories of park−wide mean values for Fall extreme short−term dry stress in Canyonlands. Top panels show values, bottom panels show changes from the long−term historical mean. Left: Time series of historical (black) and future projections for RCP 4.5 and 8.5. Shaded areas show spread among climate models. Right: Boxplots of temporal variability over 40−year periods under historical (left box) and individual climate models under two RCPs. Right: Historical time period is 1970−2010; near−term (NT) is 2020−2060; long−term (LT) is 2061−2100.

Canyonlands: Fall extreme short−term dry stress

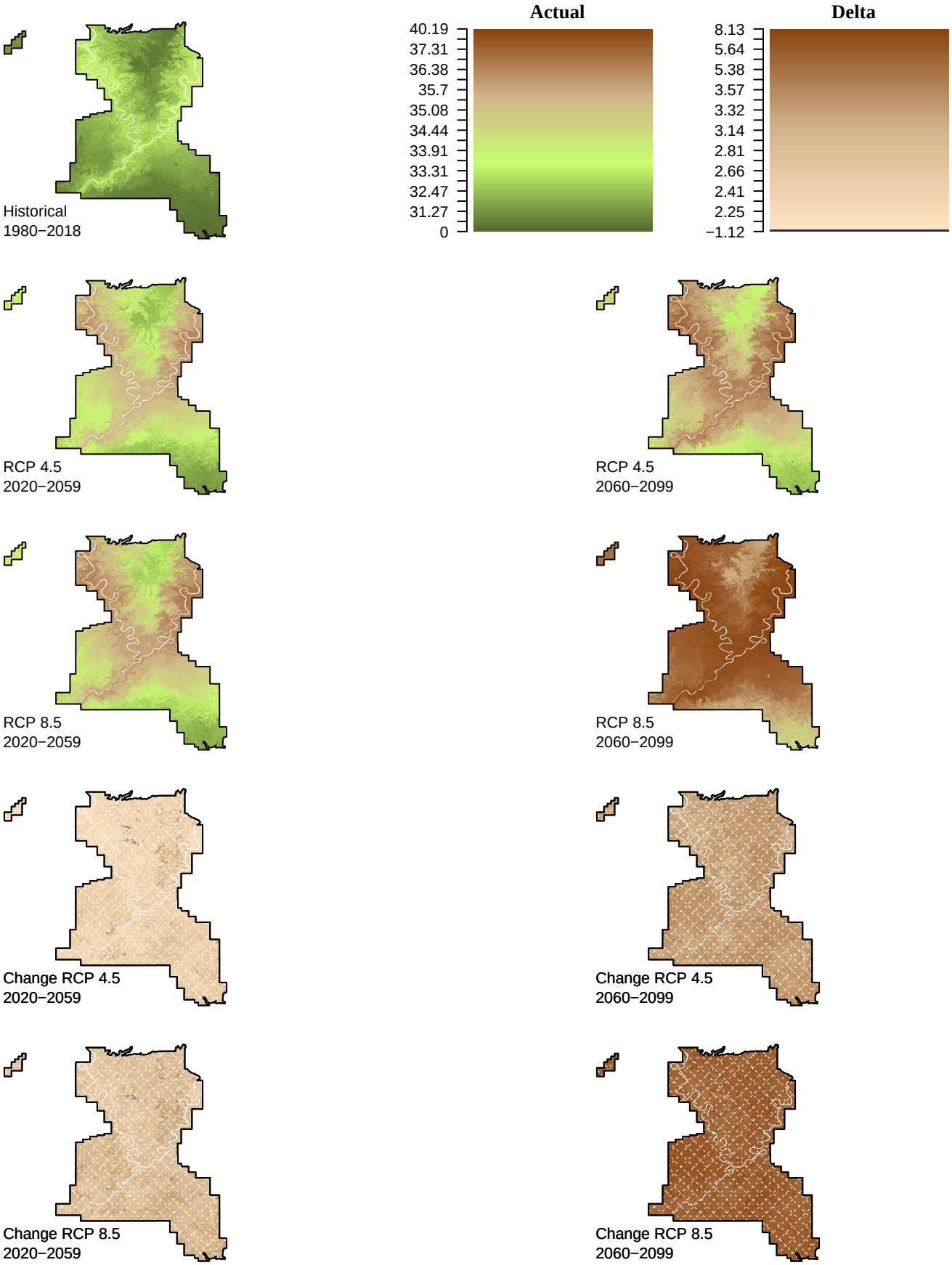


Figure CANYmap105:
Past trends and future trajectories of park−wide mean values for Fall extreme short−term dry stress in Canyonlands. Topmost panel depicts the historical mean from 1980−2018. Lower four panels show the emission scenarios of RCP 4.5 and RCP 8.5 at near−term and long−term timeframes. Bottom four panels depict the change from the historical mean; cross hatching denotes areas of robust predicitons (90% of models agree in the direction of change).

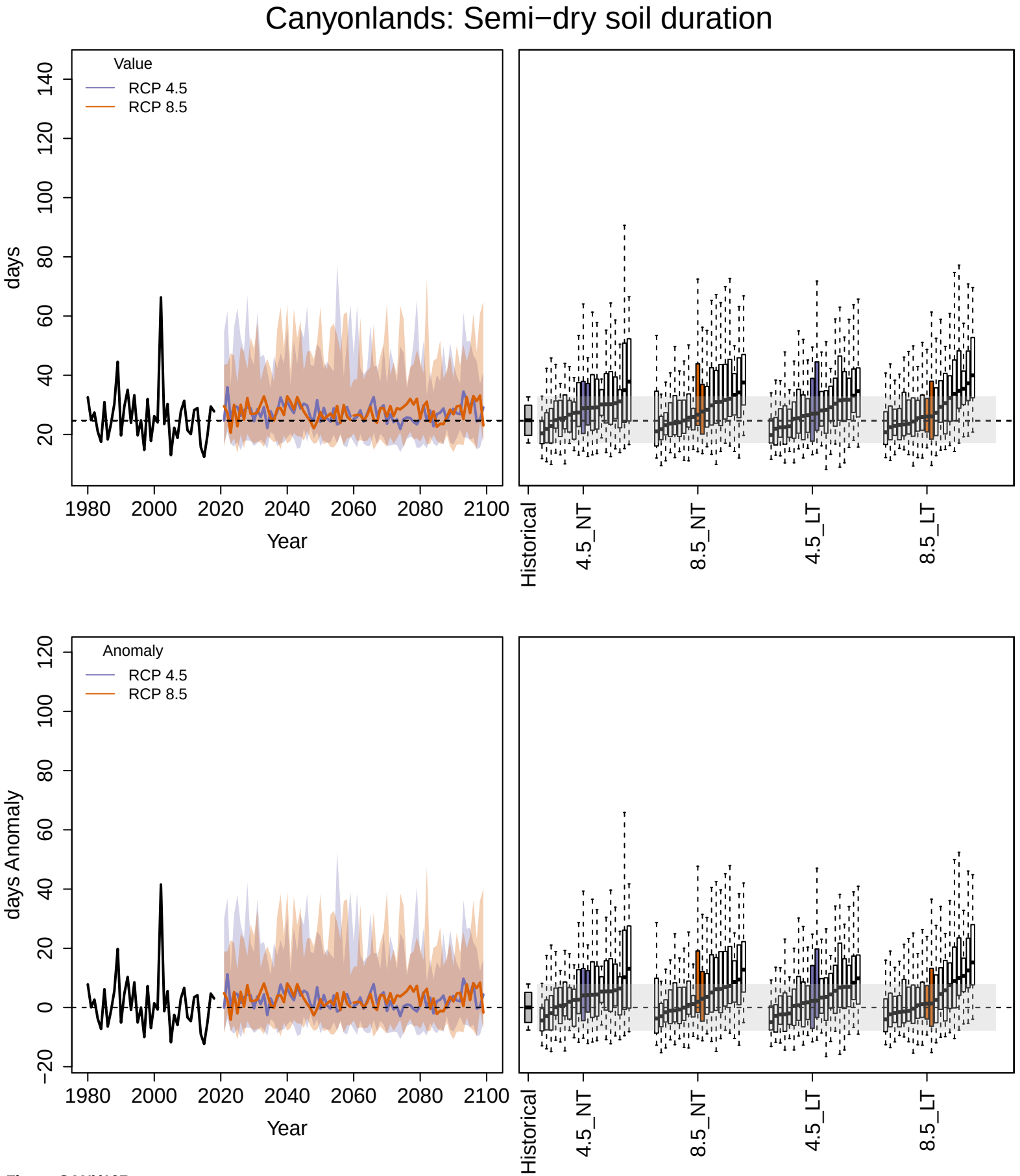


Figure CANY107:
Past trends and future trajectories of park−wide mean values for Semi−dry soil duration in Canyonlands. Top panels show values, bottom panels show changes from the long−term historical mean. Left: Time series of historical (black) and future projections for RCP 4.5 and 8.5. Shaded areas show spread among climate models. Right: Boxplots of temporal variability over 40−year periods under historical (left box) and individual climate models under two RCPs. Right: Historical time period is 1970−2010; near−term (NT) is 2020−2060; long−term (LT) is 2061−2100.

Canyonlands: Semi−dry soil duration

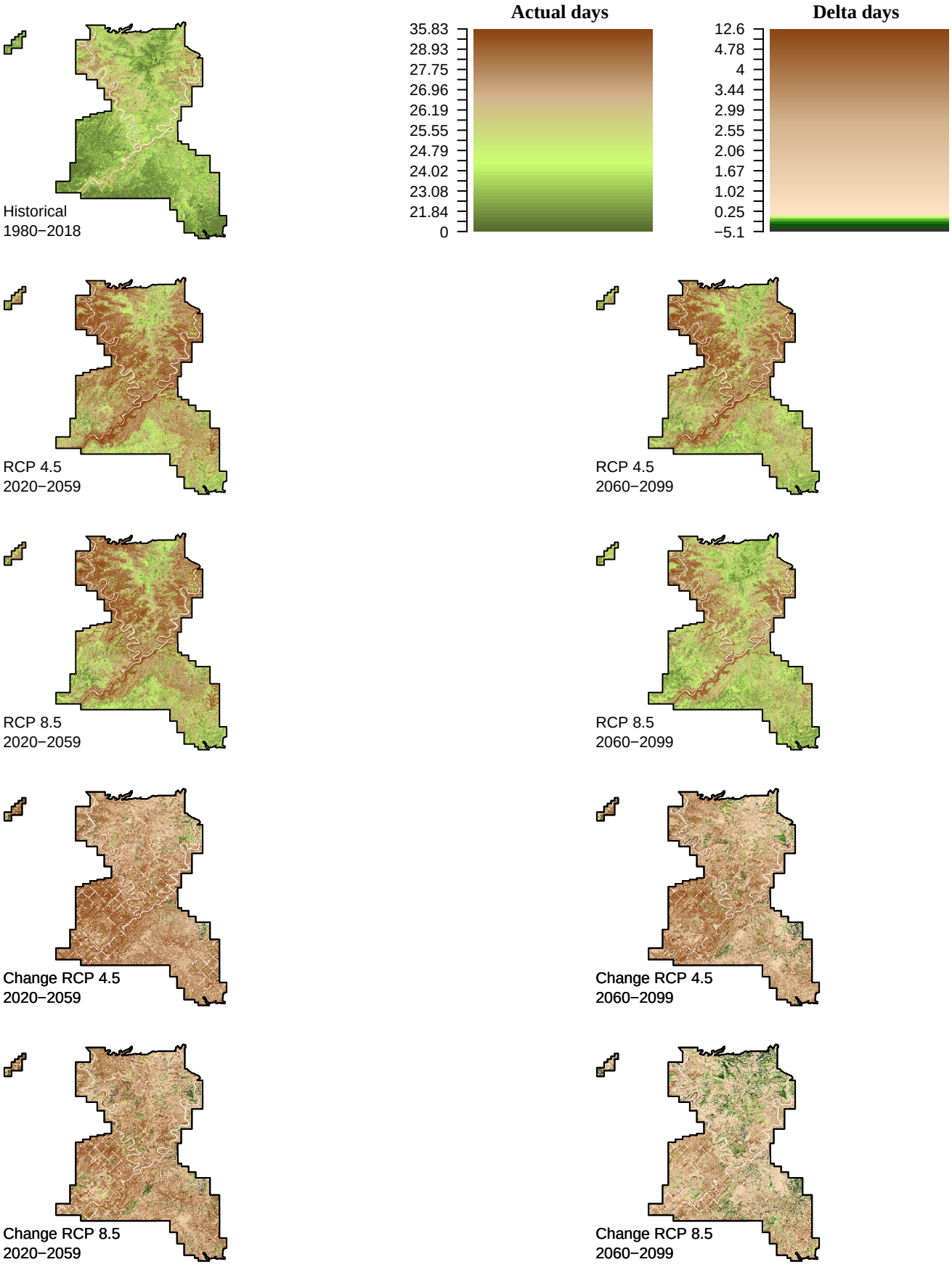


Figure CANYmap107:
Past trends and future trajectories of park−wide mean values for Semi−dry soil duration in Canyonlands. Topmost panel depicts the historical mean from 1980−2018. Lower four panels show the emission scenarios of RCP 4.5 and RCP 8.5 at near−term and long−term timeframes. Bottom four panels depict the change from the historical mean; cross hatching denotes areas of robust predicitons (90% of models agree in the direction of change).

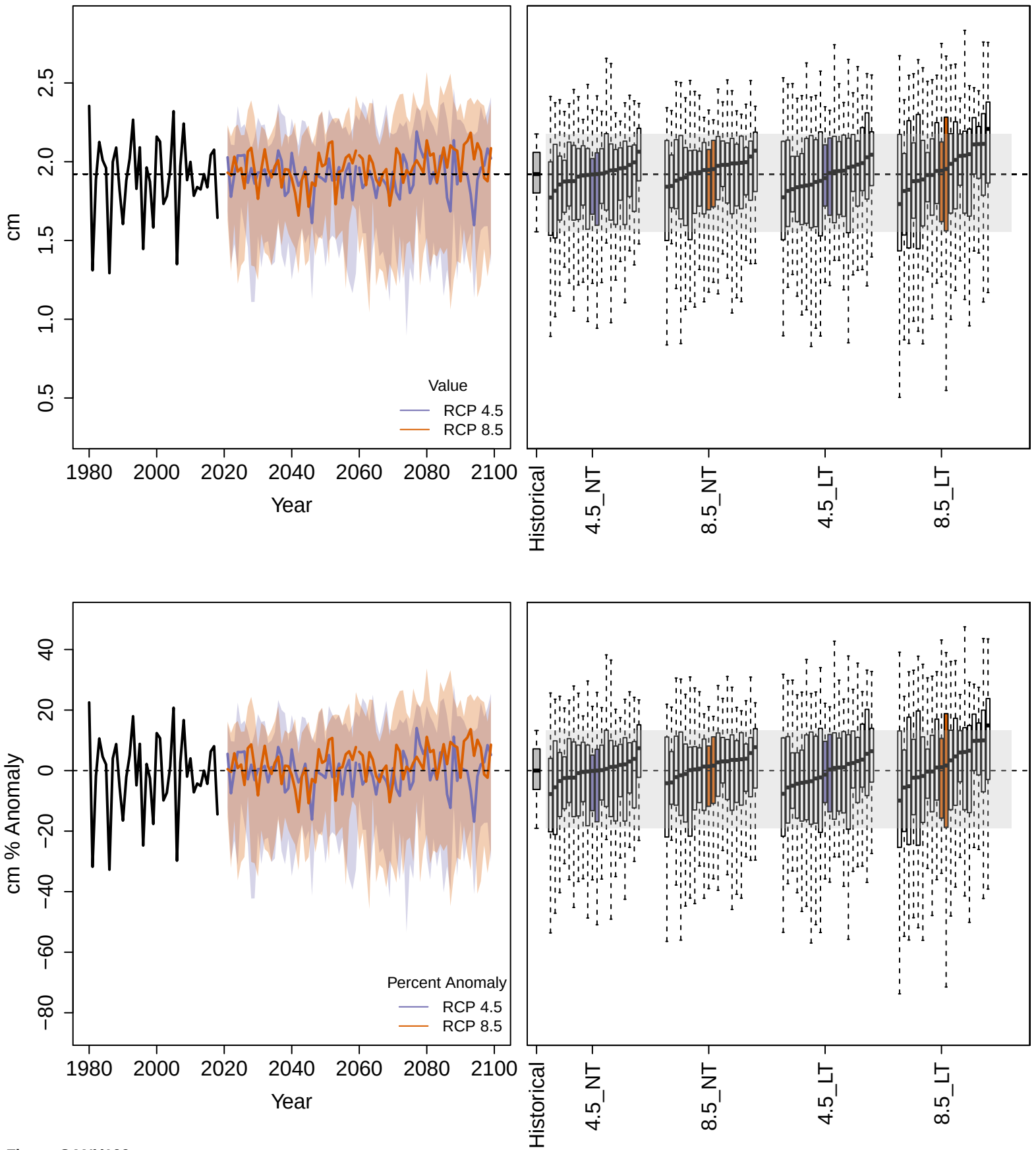


Figure CANY109:
Past trends and future trajectories of park−wide mean values for Winter evaporation in Canyonlands. Top panels show values, bottom panels show changes from the long−term historical mean. Left: Time series of historical (black) and future projections for RCP 4.5 and 8.5. Shaded areas show spread among climate models. Right: Boxplots of temporal variability over 40−year periods under historical (left box) and individual climate models under two RCPs. Right: Historical time period is 1970−2010; near−term (NT) is 2020−2060; long−term (LT) is 2061−2100.

Canyonlands: Winter evaporation

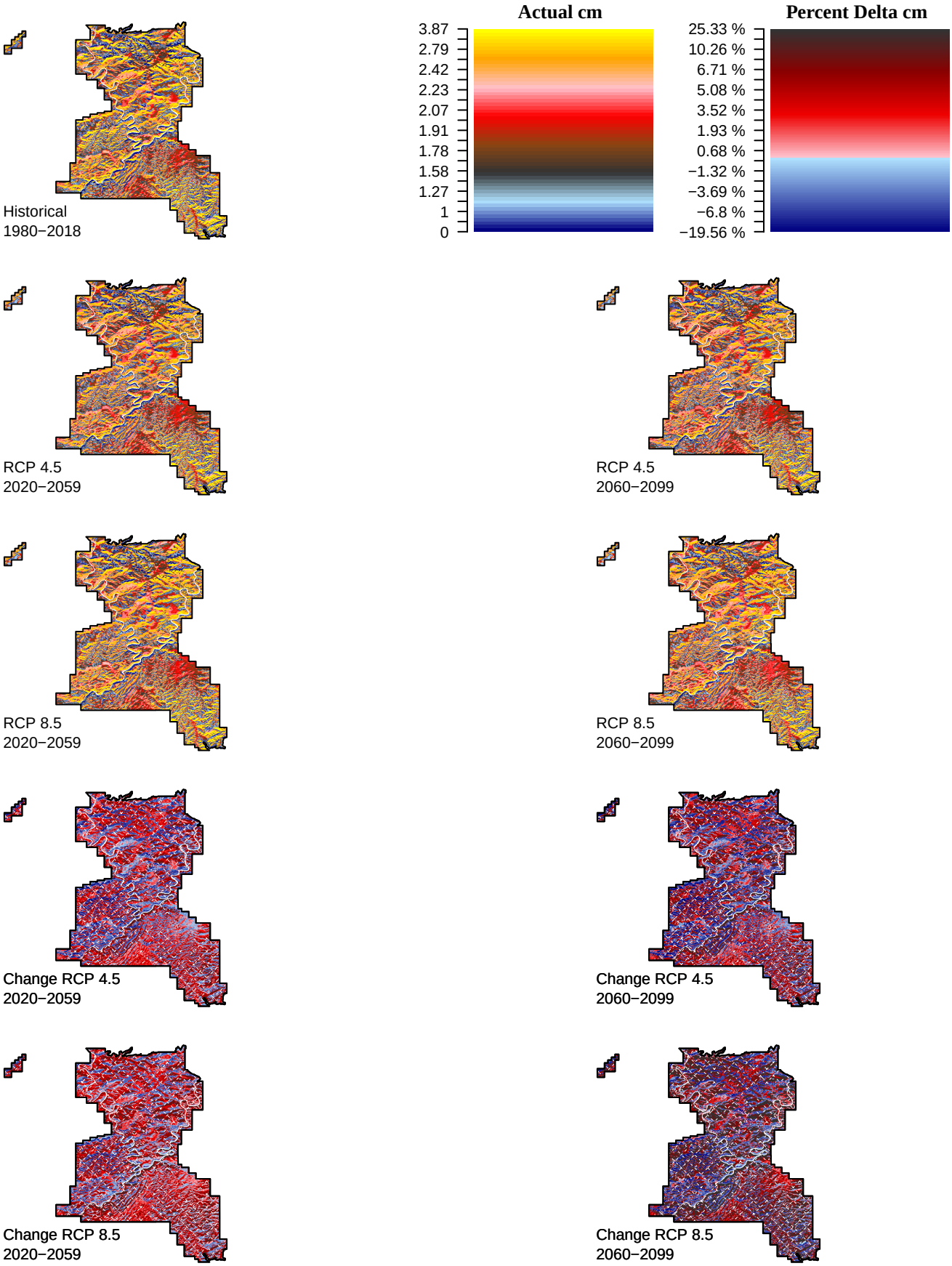


Figure CANYmap109:
Past trends and future trajectories of park−wide mean values for Winter evaporation in Canyonlands. Topmost panel depicts the historical mean from 1980−2018. Lower four panels show the emission scenarios of RCP 4.5 and RCP 8.5 at near−term and long−term timeframes. Bottom four panels depict the change from the historical mean; cross hatching denotes areas of robust predicitons (90% of models agree in the direction of change).

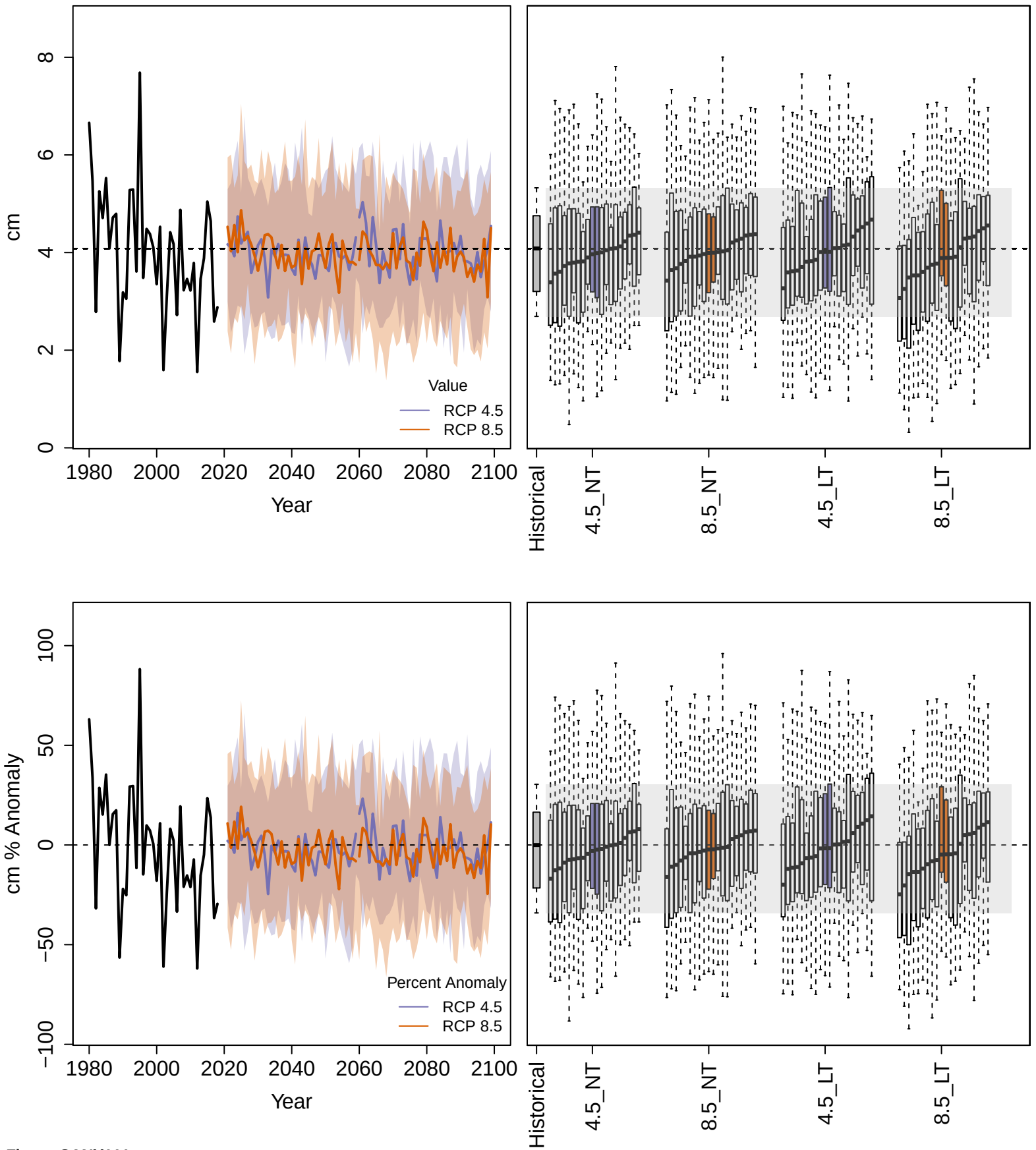


Figure CANY111:
Past trends and future trajectories of park−wide mean values for Spring evaporation in Canyonlands. Top panels show values, bottom panels show changes from the long−term historical mean. Left: Time series of historical (black) and future projections for RCP 4.5 and 8.5. Shaded areas show spread among climate models. Right: Boxplots of temporal variability over 40−year periods under historical (left box) and individual climate models under two RCPs. Right: Historical time period is 1970−2010; near−term (NT) is 2020−2060; long−term (LT) is 2061−2100.

Canyonlands: Spring evaporation

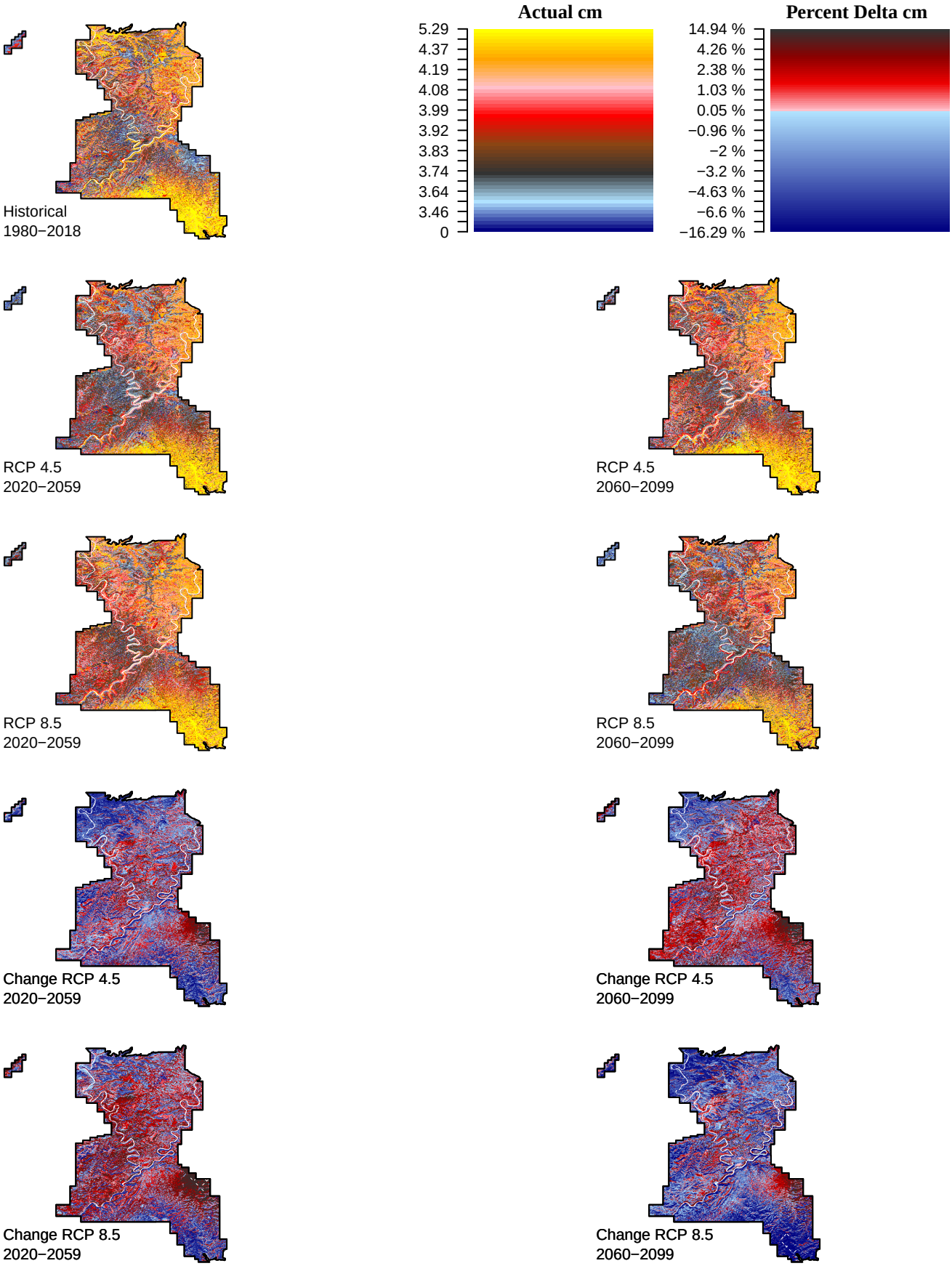


Figure CANYmap111:
Past trends and future trajectories of park−wide mean values for Spring evaporation in Canyonlands. Topmost panel depicts the historical mean from 1980−2018. Lower four panels show the emission scenarios of RCP 4.5 and RCP 8.5 at near−term and long−term timeframes. Bottom four panels depict the change from the historical mean; cross hatching denotes areas of robust predicitons (90% of models agree in the direction of change).

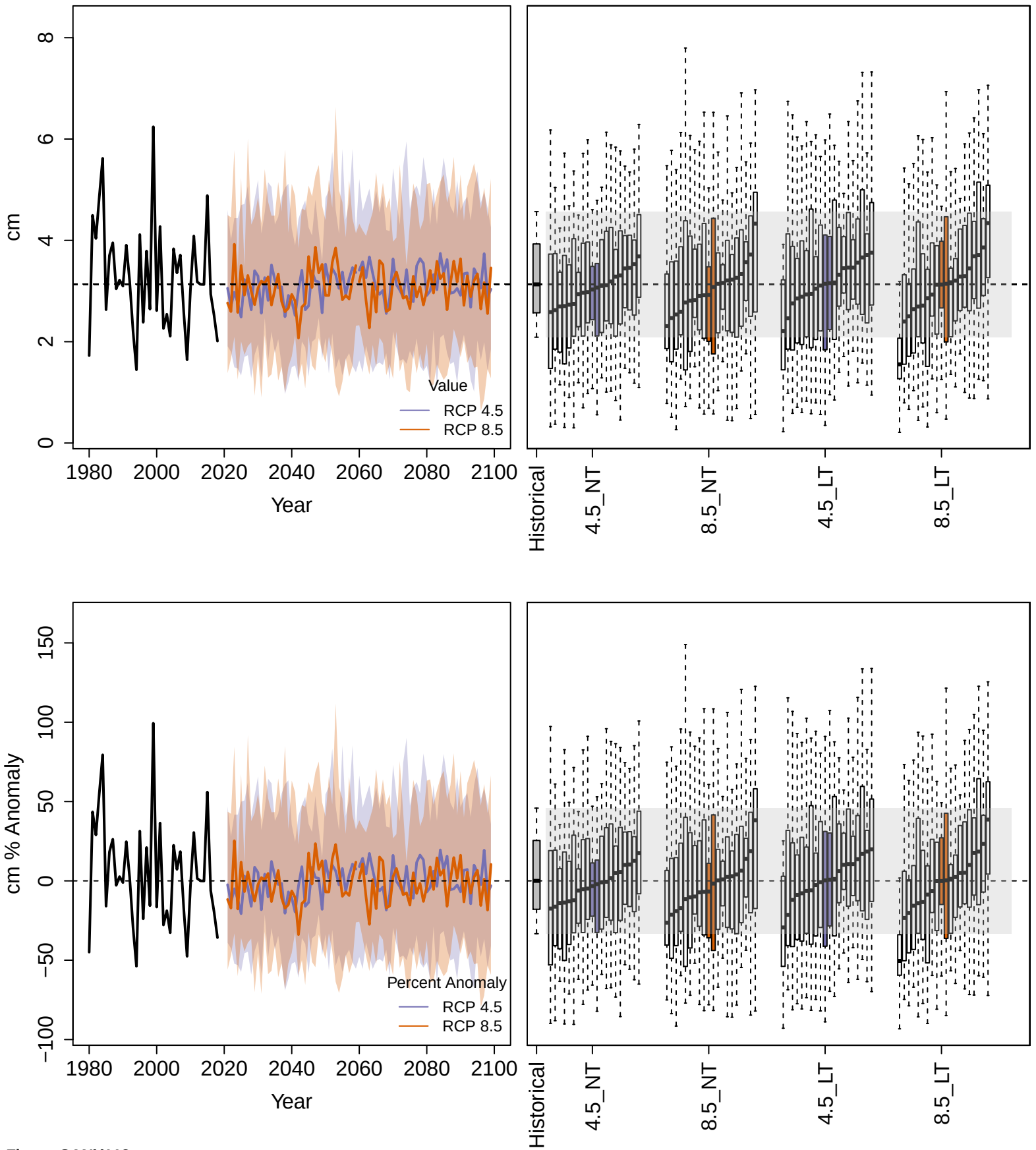


Figure CANY113:
Past trends and future trajectories of park−wide mean values for Summer evaporation in Canyonlands. Top panels show values, bottom panels show changes from the long−term historical mean. Left: Time series of historical (black) and future projections for RCP 4.5 and 8.5. Shaded areas show spread among climate models. Right: Boxplots of temporal variability over 40−year periods under historical (left box) and individual climate models under two RCPs. Right: Historical time period is 1970−2010; near−term (NT) is 2020−2060; long−term (LT) is 2061−2100.

Canyonlands: Summer evaporation

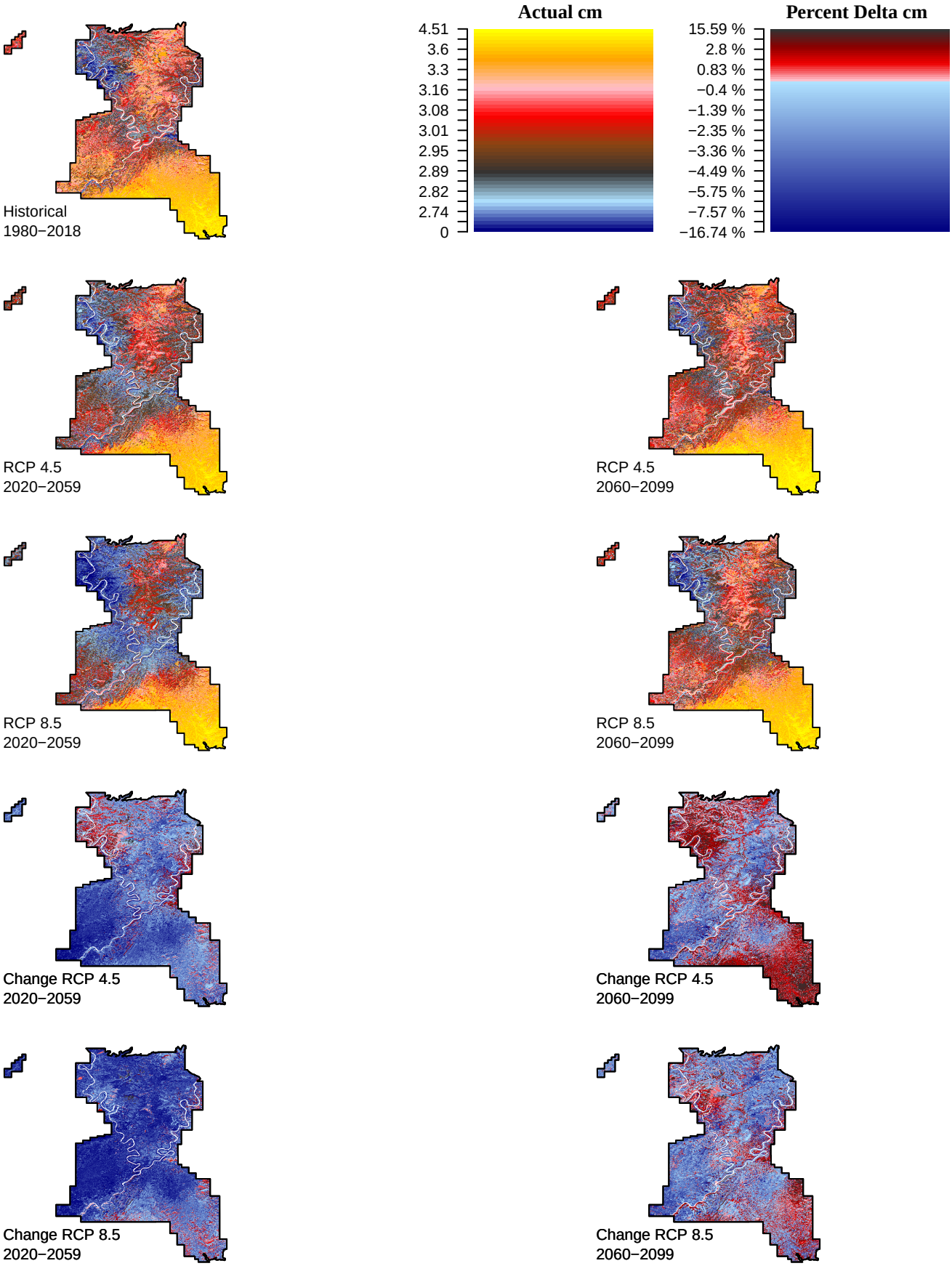


Figure CANYmap113:
Past trends and future trajectories of park−wide mean values for Summer evaporation in Canyonlands. Topmost panel depicts the historical mean from 1980−2018. Lower four panels show the emission scenarios of RCP 4.5 and RCP 8.5 at near−term and long−term timeframes. Bottom four panels depict the change from the historical mean; cross hatching denotes areas of robust predicitons (90% of models agree in the direction of change).

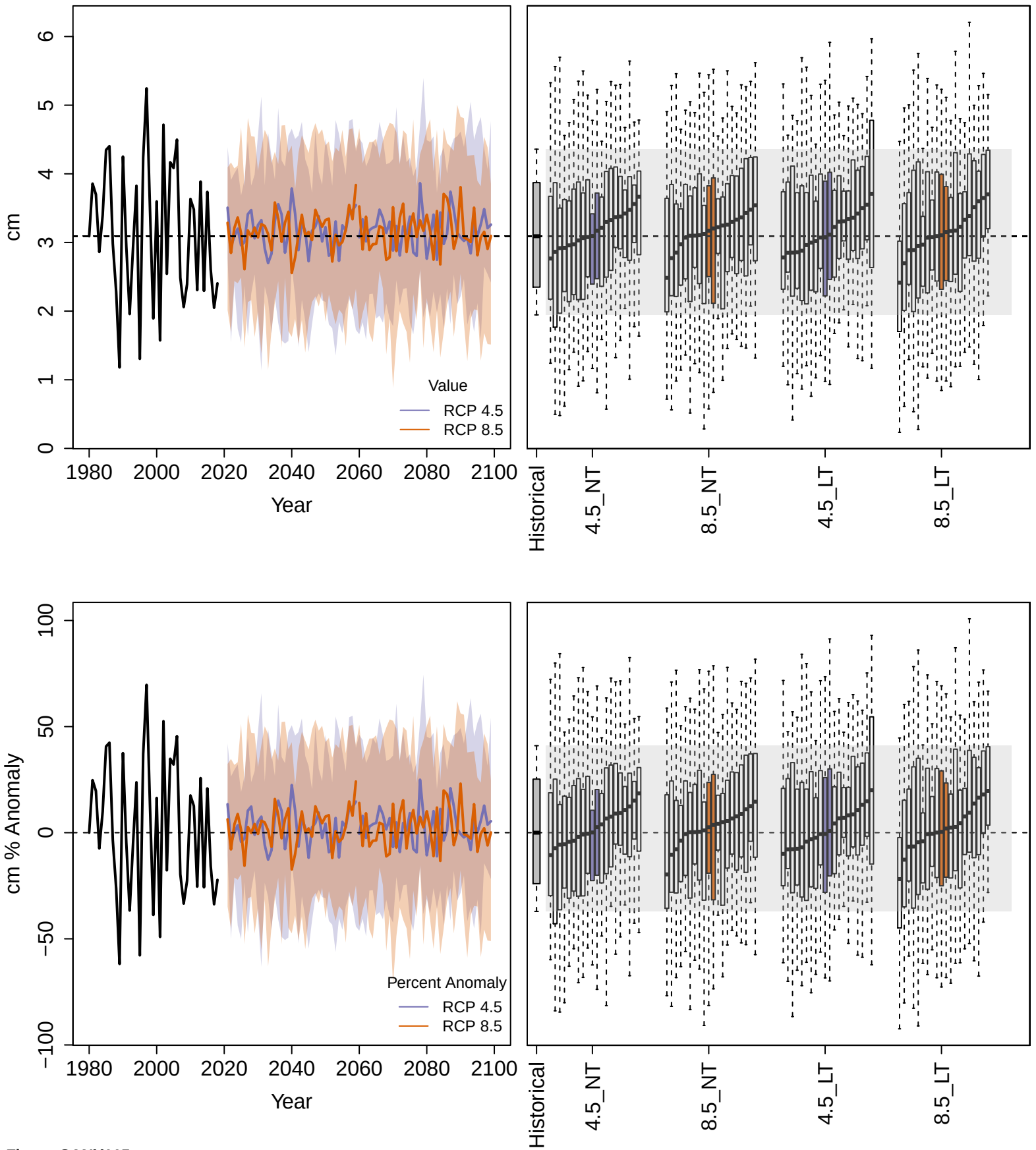


Figure CANY115:
Past trends and future trajectories of park−wide mean values for Fall evaporation in Canyonlands. Top panels show values, bottom panels show changes from the long−term historical mean. Left: Time series of historical (black) and future projections for RCP 4.5 and 8.5. Shaded areas show spread among climate models. Right: Boxplots of temporal variability over 40−year periods under historical (left box) and individual climate models under two RCPs. Right: Historical time period is 1970−2010; near−term (NT) is 2020−2060; long−term (LT) is 2061−2100.

Canyonlands: Fall evaporation

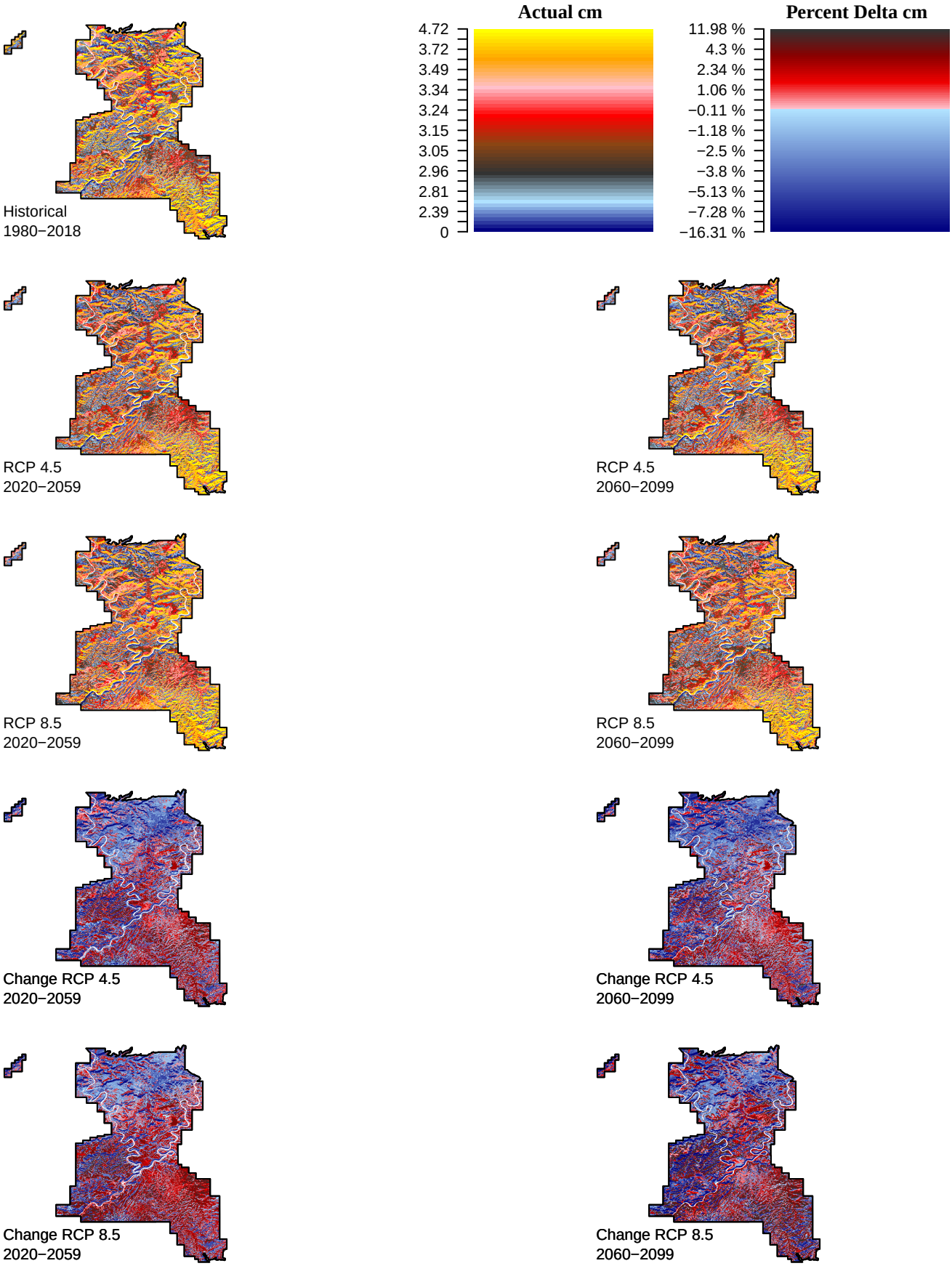


Figure CANYmap115:
Past trends and future trajectories of park−wide mean values for Fall evaporation in Canyonlands. Topmost panel depicts the historical mean from 1980−2018. Lower four panels show the emission scenarios of RCP 4.5 and RCP 8.5 at near−term and long−term timeframes. Bottom four panels depict the change from the historical mean; cross hatching denotes areas of robust predicitons (90% of models agree in the direction of change).

Canyonlands: Winter transpiration

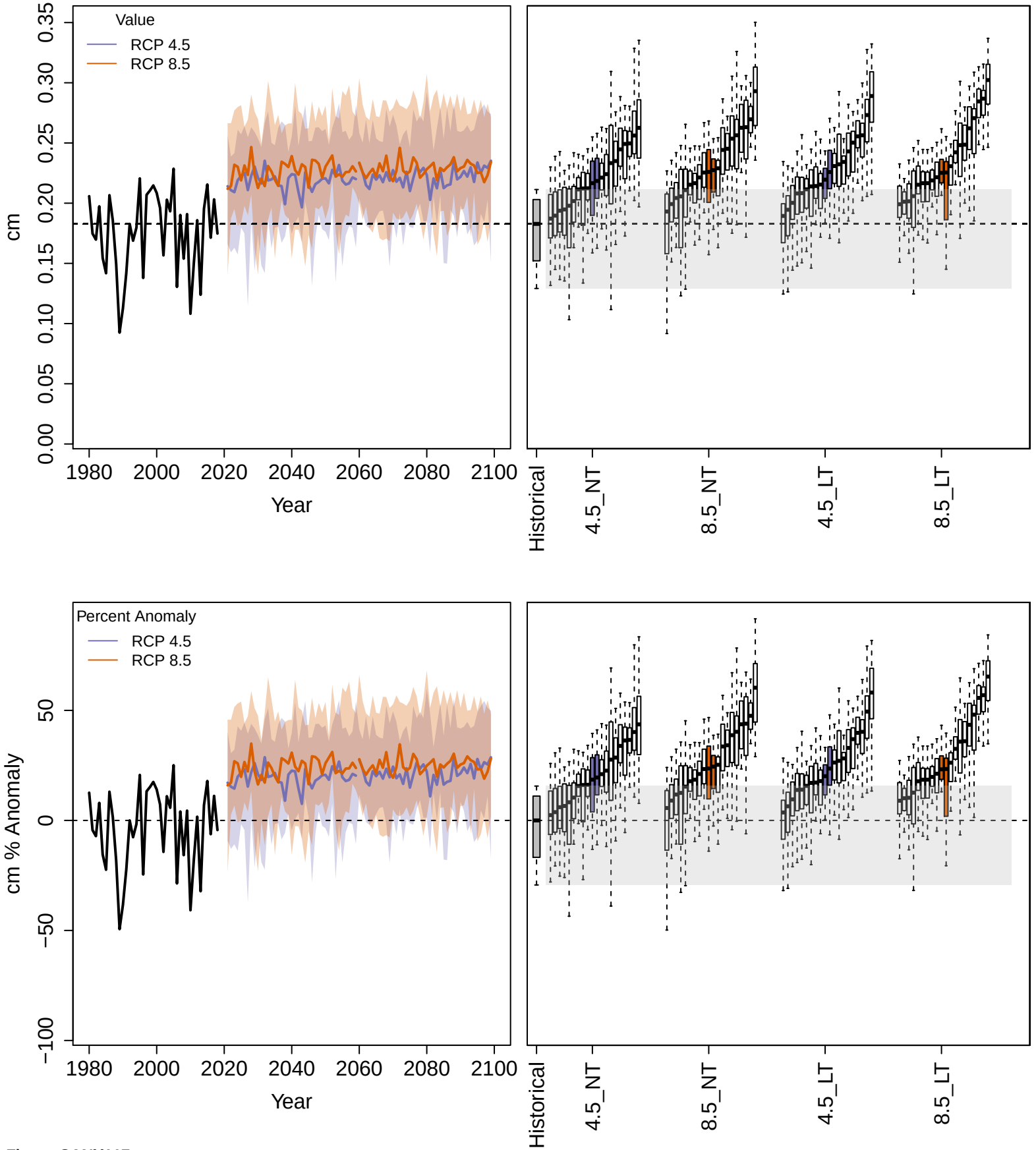


Figure CANY117:
Past trends and future trajectories of park−wide mean values for Winter transpiration in Canyonlands. Top panels show values, bottom panels show changes from the long−term historical mean. Left: Time series of historical (black) and future projections for RCP 4.5 and 8.5. Shaded areas show spread among climate models. Right: Boxplots of temporal variability over 40−year periods under historical (left box) and individual climate models under two RCPs. Right: Historical time period is 1970−2010; near−term (NT) is 2020−2060; long−term (LT) is 2061−2100.

Canyonlands: Winter transpiration

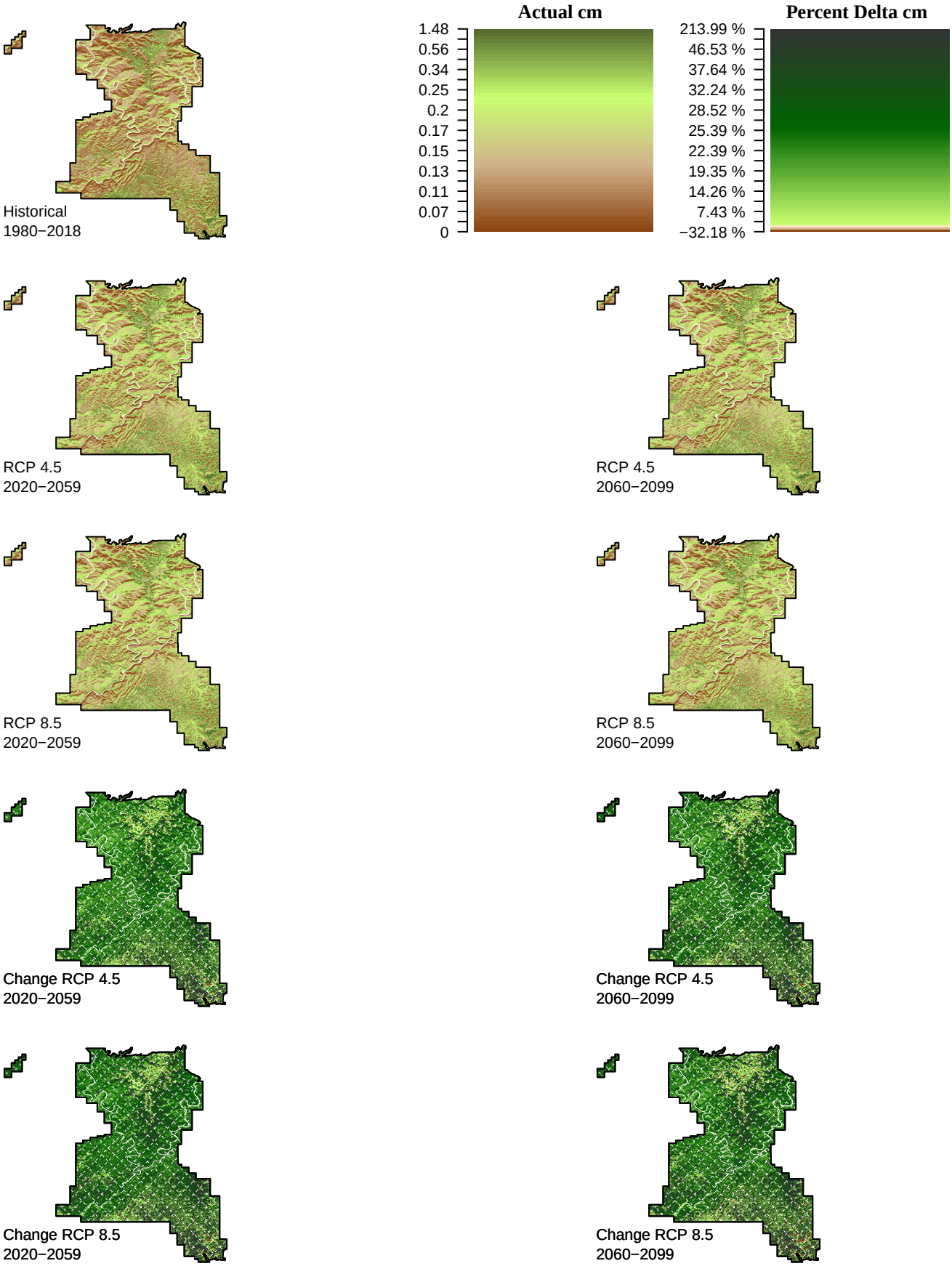


Figure CANYmap117:
Past trends and future trajectories of park−wide mean values for Winter transpiration in Canyonlands. Topmost panel depicts the historical mean from 1980−2018. Lower four panels show the emission scenarios of RCP 4.5 and RCP 8.5 at near−term and long−term timeframes. Bottom four panels depict the change from the historical mean; cross hatching denotes areas of robust predicitons (90% of models agree in the direction of change).

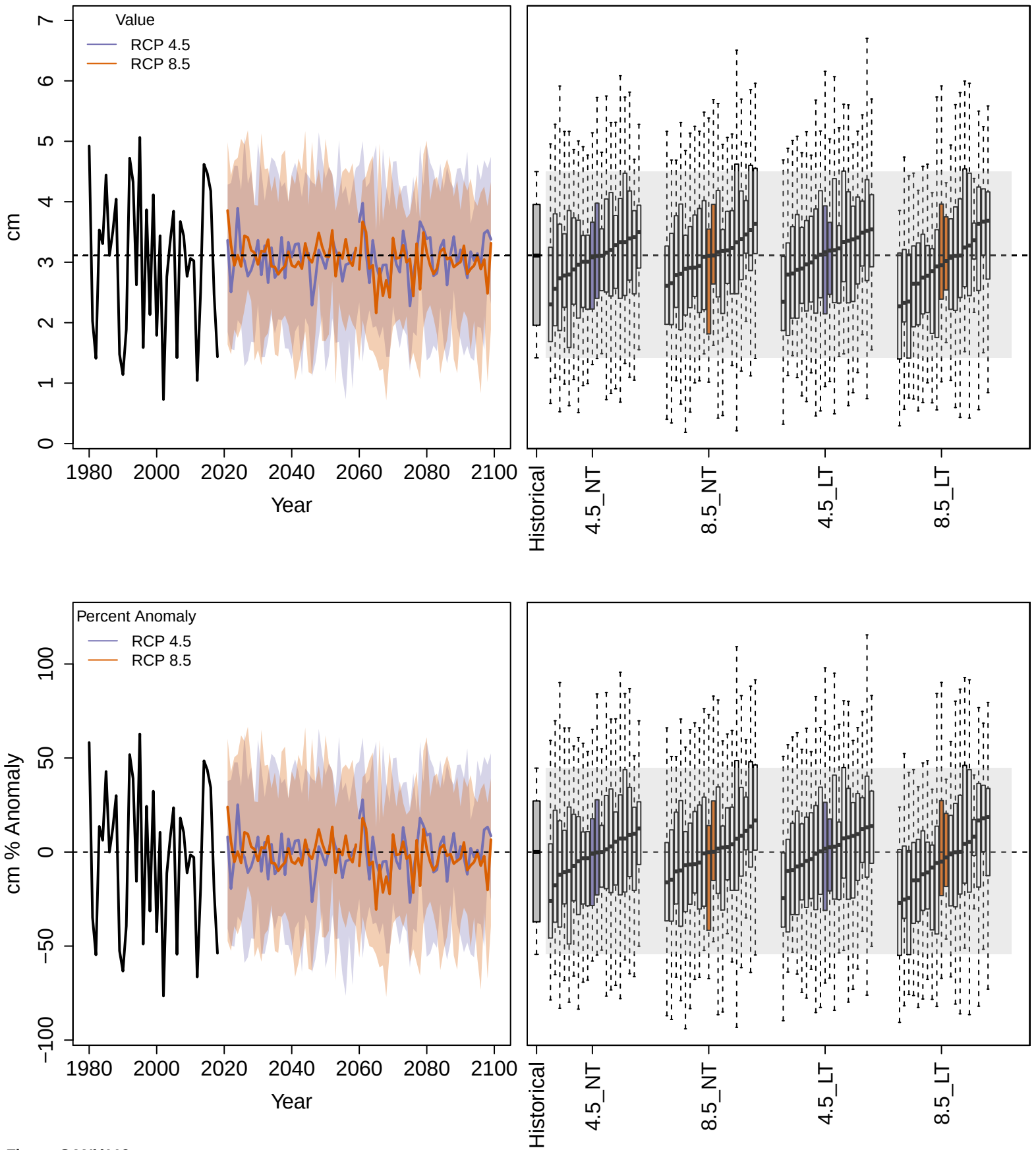


Figure CANY119:
Past trends and future trajectories of park−wide mean values for Spring transpiration in Canyonlands. Top panels show values, bottom panels show changes from the long−term historical mean. Left: Time series of historical (black) and future projections for RCP 4.5 and 8.5. Shaded areas show spread among climate models. Right: Boxplots of temporal variability over 40−year periods under historical (left box) and individual climate models under two RCPs. Right: Historical time period is 1970−2010; near−term (NT) is 2020−2060; long−term (LT) is 2061−2100.

Canyonlands: Spring transpiration

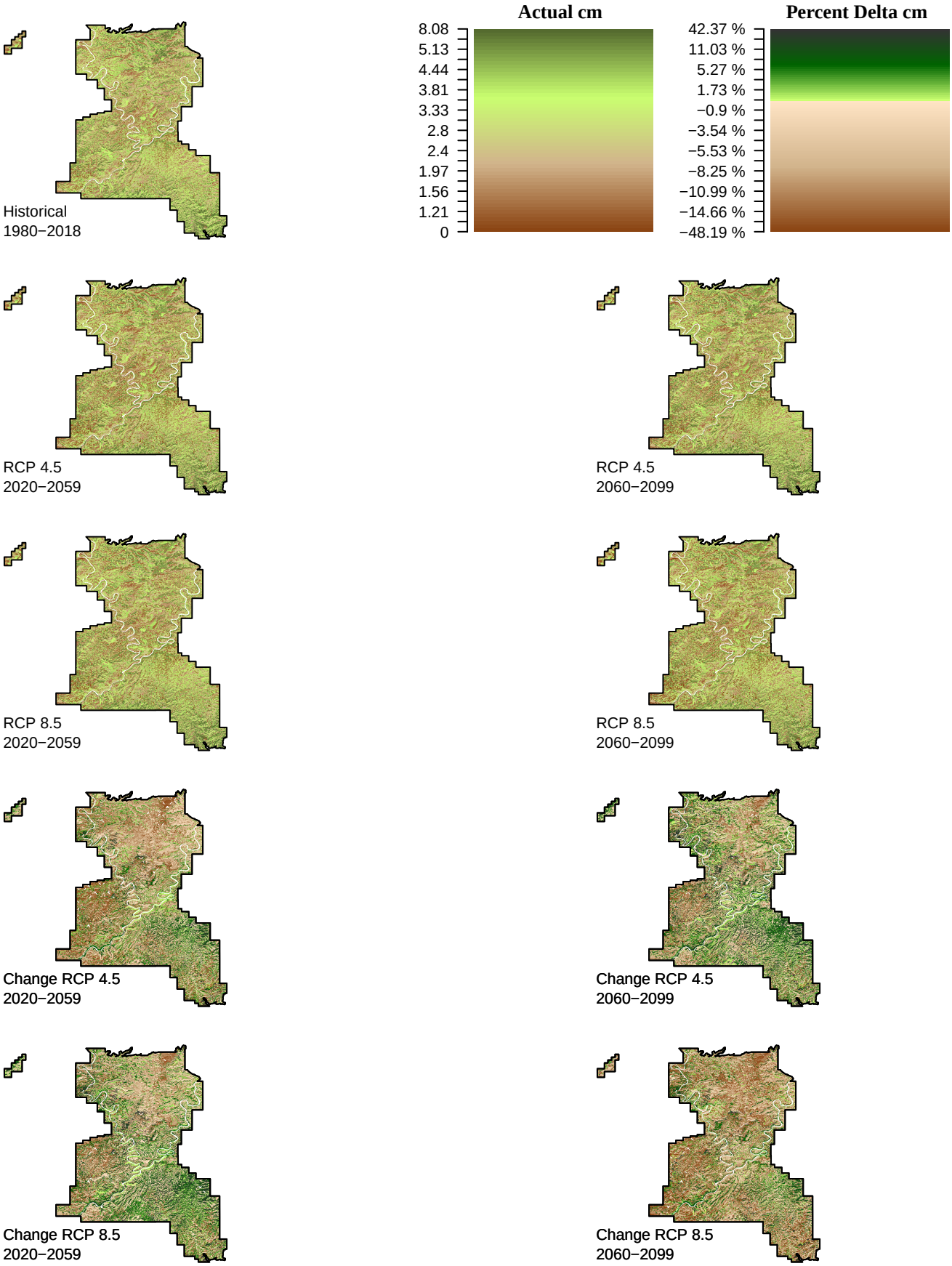


Figure CANYmap119:
Past trends and future trajectories of park−wide mean values for Spring transpiration in Canyonlands. Topmost panel depicts the historical mean from 1980−2018. Lower four panels show the emission scenarios of RCP 4.5 and RCP 8.5 at near−term and long−term timeframes. Bottom four panels depict the change from the historical mean; cross hatching denotes areas of robust predicitons (90% of models agree in the direction of change).

Canyonlands: Summer transpiration

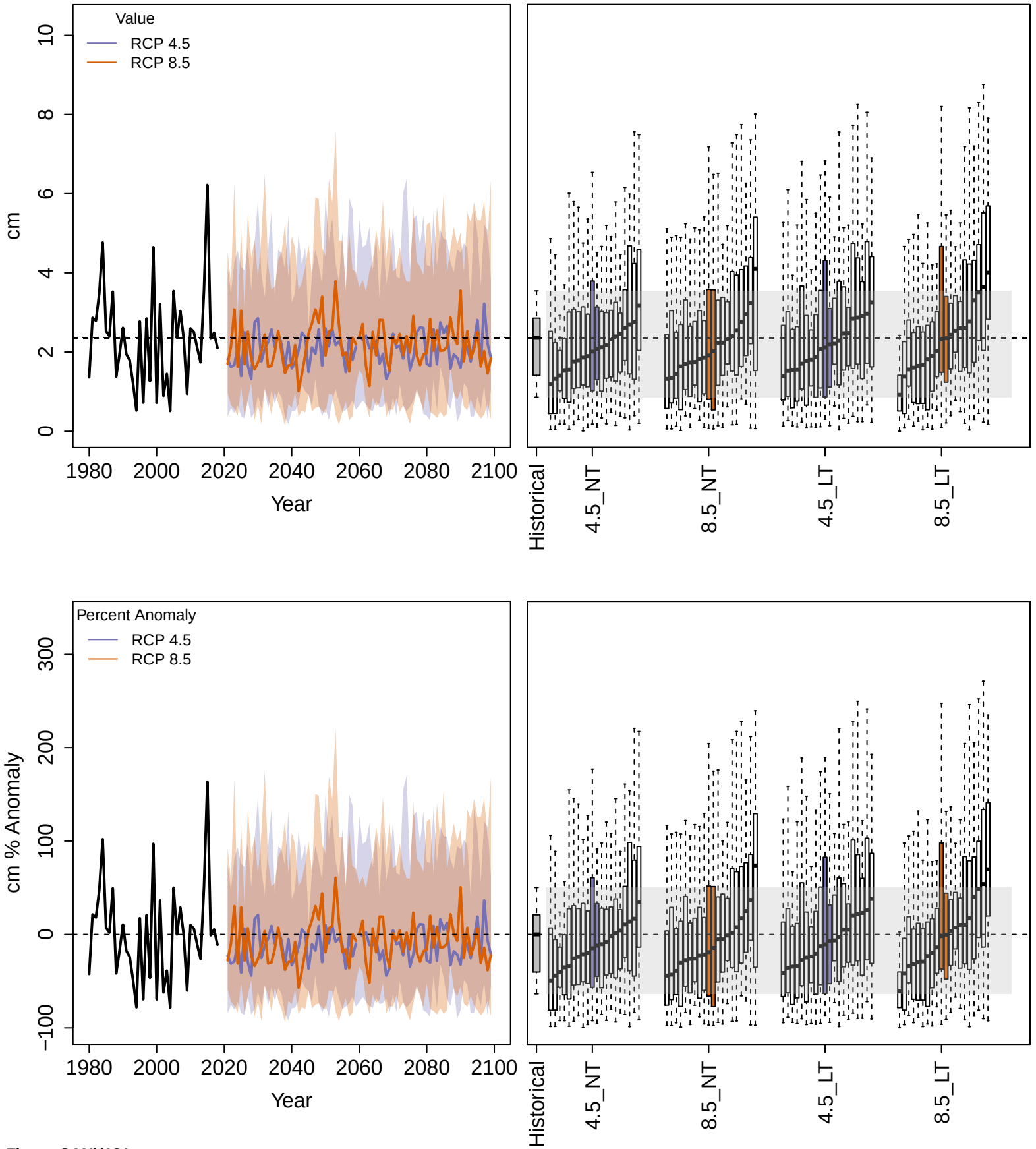


Figure CANY121:
Past trends and future trajectories of park−wide mean values for Summer transpiration in Canyonlands. Top panels show values, bottom panels show changes from the long−term historical mean. Left: Time series of historical (black) and future projections for RCP 4.5 and 8.5. Shaded areas show spread among climate models. Right: Boxplots of temporal variability over 40−year periods under historical (left box) and individual climate models under two RCPs. Right: Historical time period is 1970−2010; near−term (NT) is 2020−2060; long−term (LT) is 2061−2100.

Canyonlands: Summer transpiration

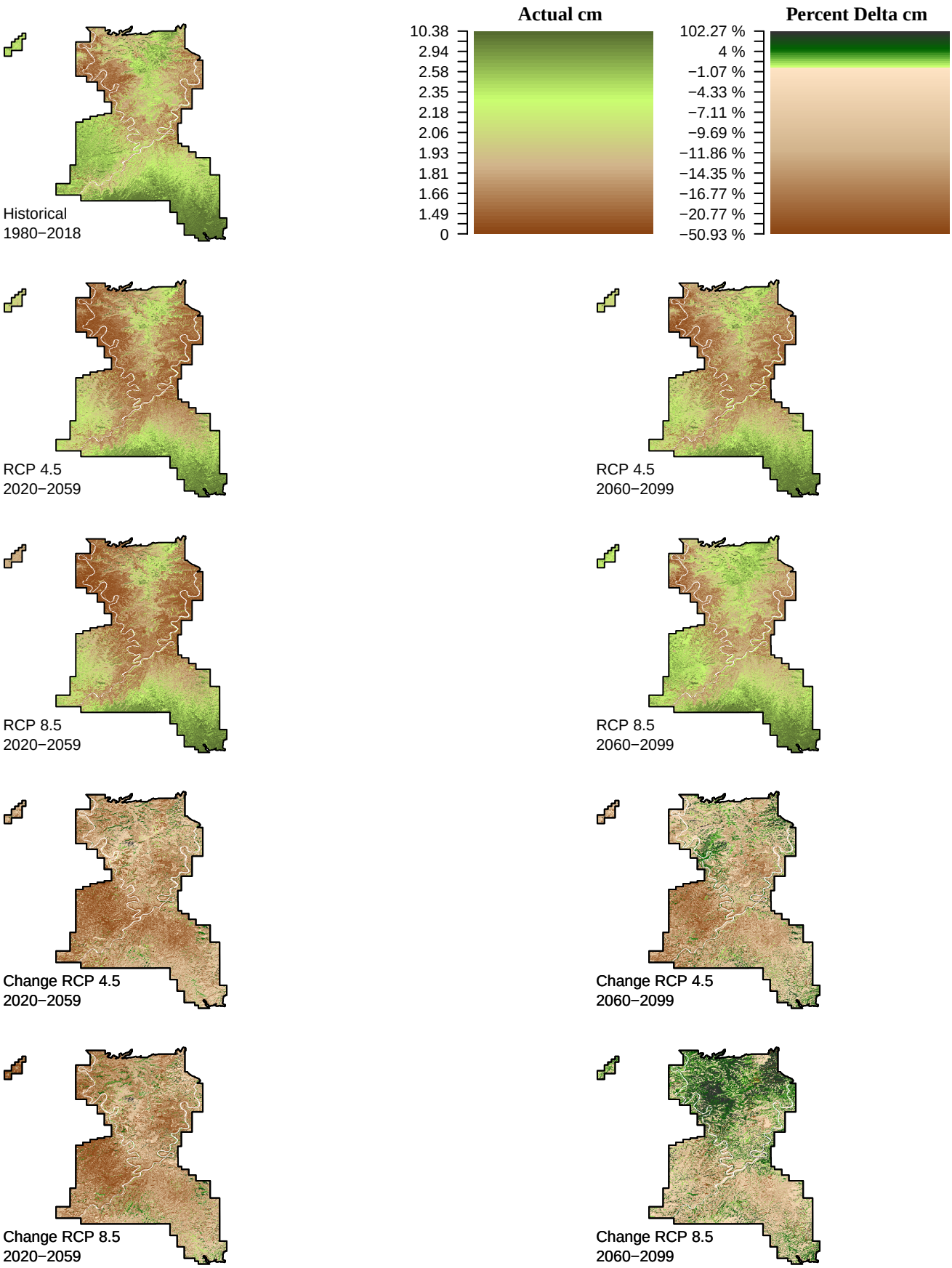


Figure CANYmap121:
Past trends and future trajectories of park−wide mean values for Summer transpiration in Canyonlands. Topmost panel depicts the historical mean from 1980−2018. Lower four panels show the emission scenarios of RCP 4.5 and RCP 8.5 at near−term and long−term timeframes. Bottom four panels depict the change from the historical mean; cross hatching denotes areas of robust predicitons (90% of models agree in the direction of change).

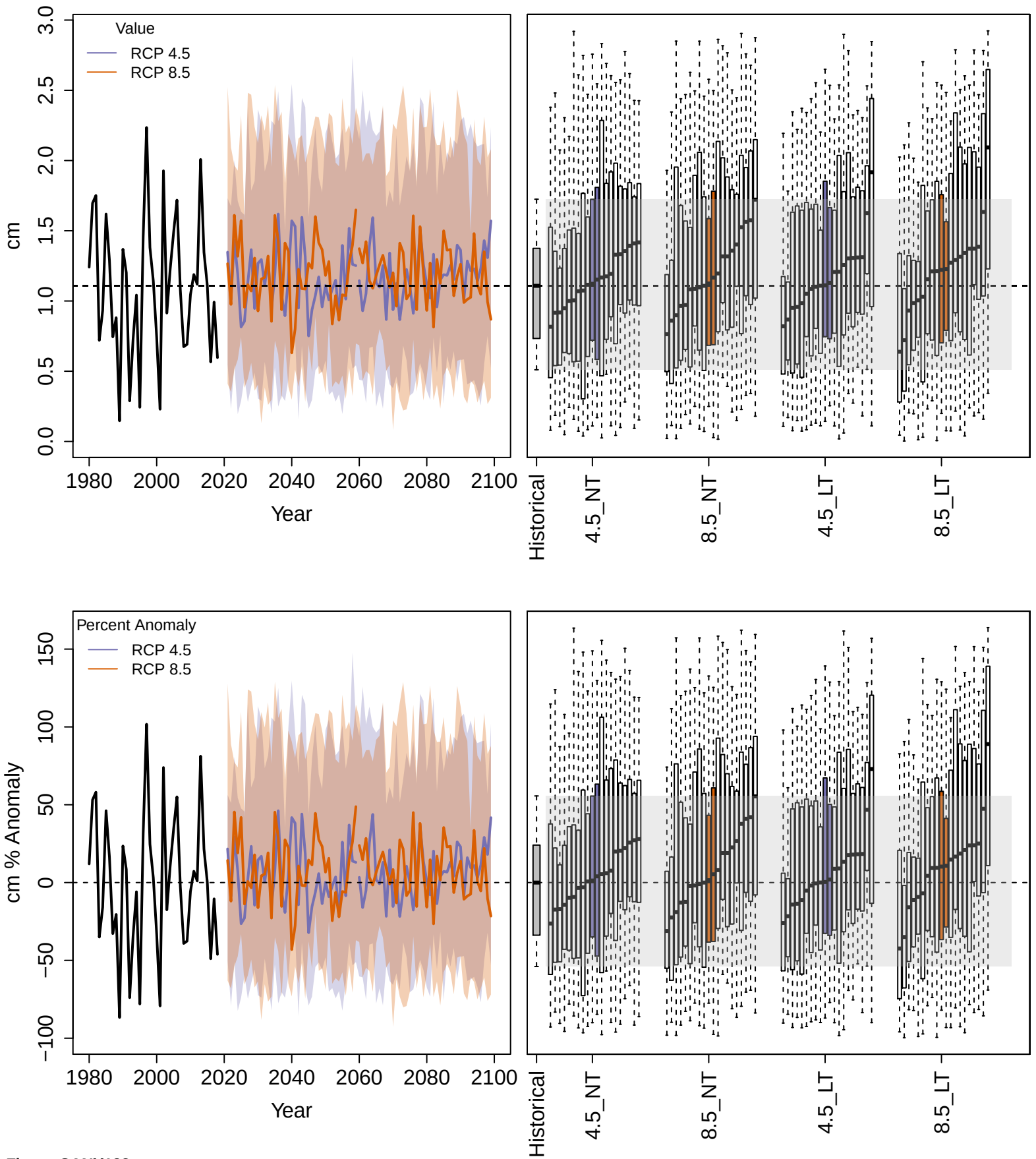


Figure CANY123:
Past trends and future trajectories of park−wide mean values for Fall transpiration in Canyonlands. Top panels show values, bottom panels show changes from the long−term historical mean. Left: Time series of historical (black) and future projections for RCP 4.5 and 8.5. Shaded areas show spread among climate models. Right: Boxplots of temporal variability over 40−year periods under historical (left box) and individual climate models under two RCPs. Right: Historical time period is 1970−2010; near−term (NT) is 2020−2060; long−term (LT) is 2061−2100.

Canyonlands: Fall transpiration

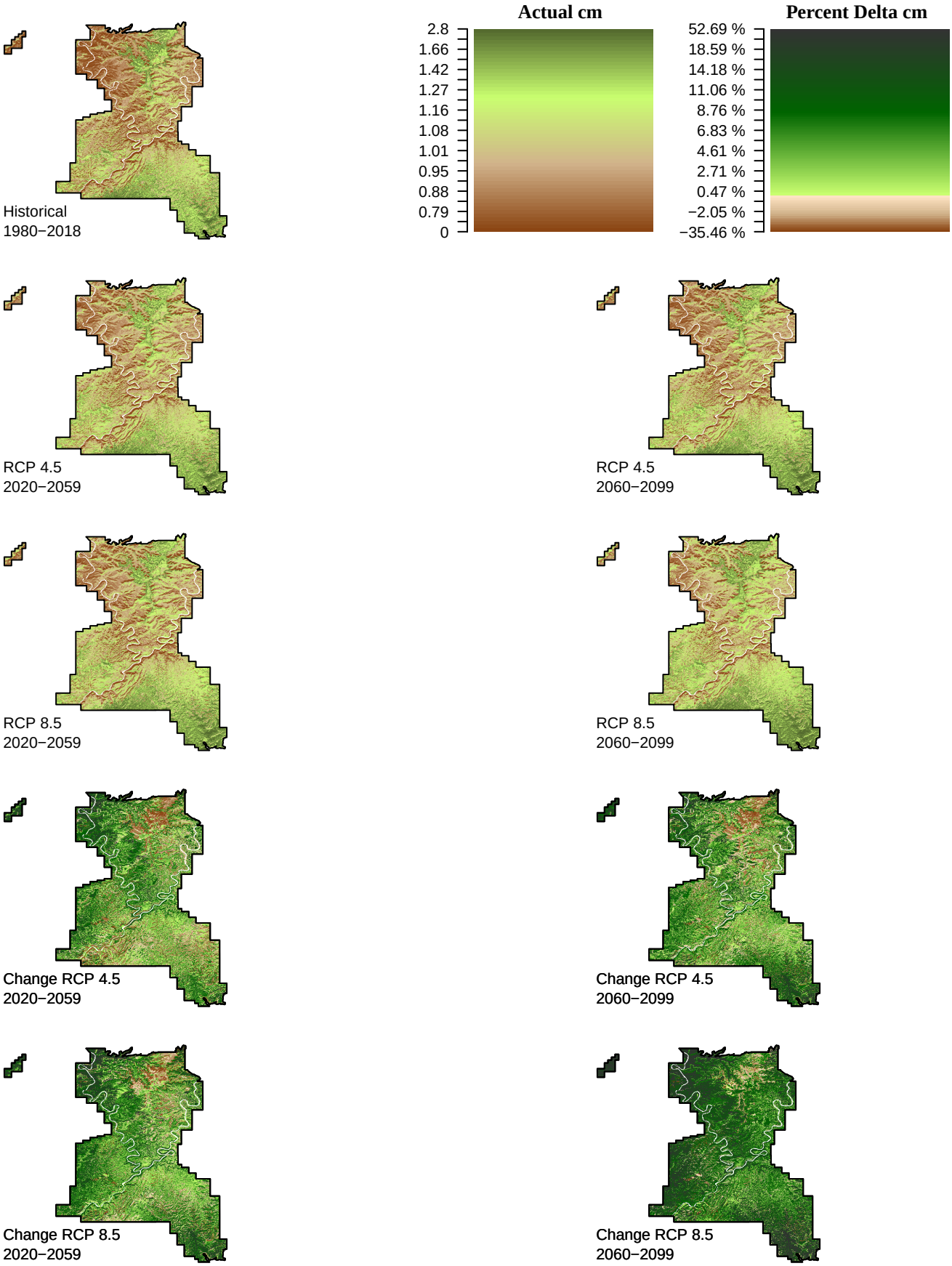


Figure CANYmap123:
Past trends and future trajectories of park−wide mean values for Fall transpiration in Canyonlands. Topmost panel depicts the historical mean from 1980−2018. Lower four panels show the emission scenarios of RCP 4.5 and RCP 8.5 at near−term and long−term timeframes. Bottom four panels depict the change from the historical mean; cross hatching denotes areas of robust predicitons (90% of models agree in the direction of change).

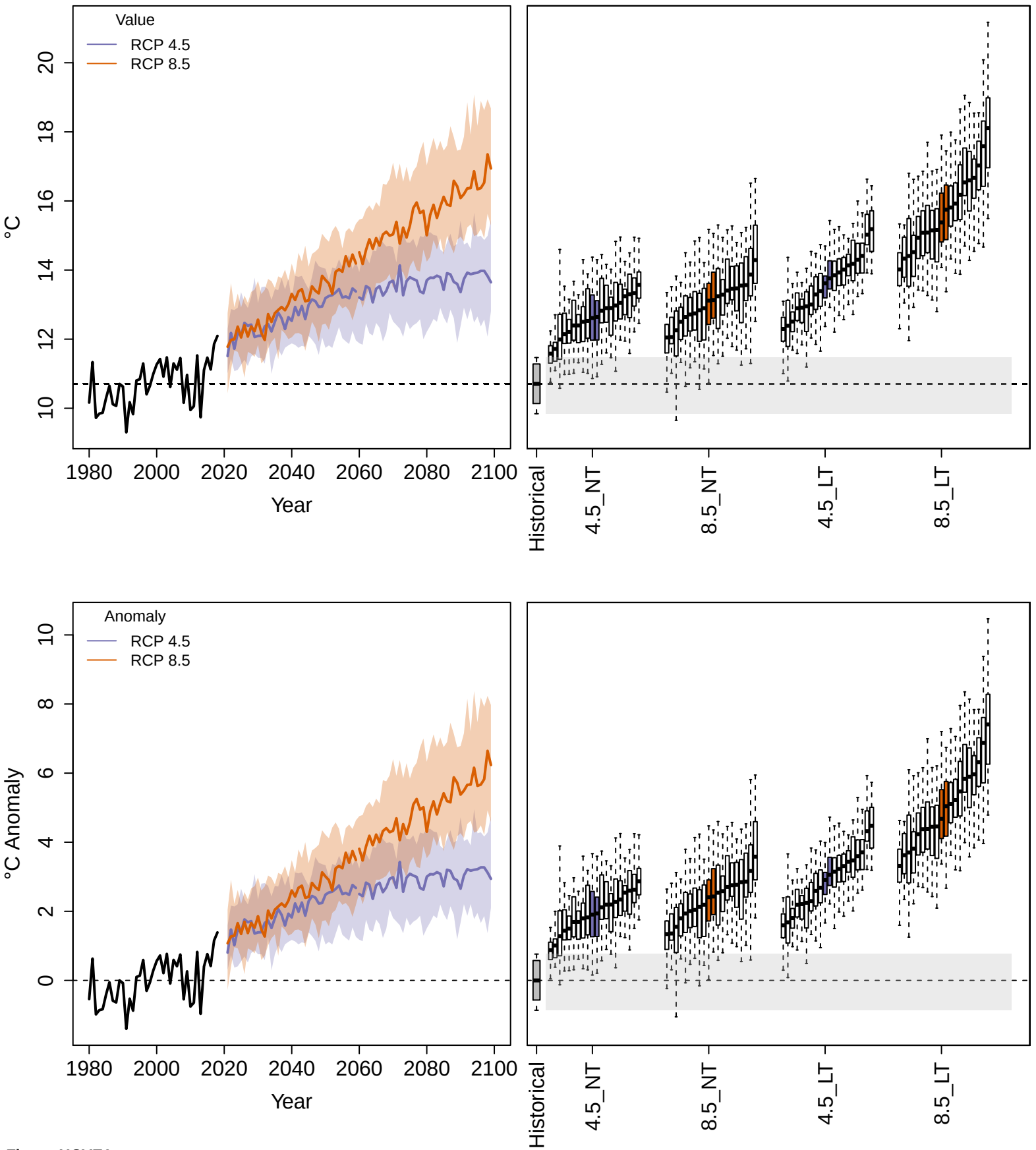


Figure HOVE1:
Past trends and future trajectories of park−wide mean values for Mean Annual Temperature in Hovenweep. Top panels show values, bottom panels show changes from the long−term historical mean. Left: Time series of historical (black) and future projections for RCP 4.5 and 8.5. Shaded areas show spread among climate models. Right: Boxplots of temporal variability over 40−year periods under historical (left box) and individual climate models under two RCPs. Right: Historical time period is 1970−2010; near−term (NT) is 2020−2060; long−term (LT) is 2061−2100.

Hovenweep: Mean Annual Temperature

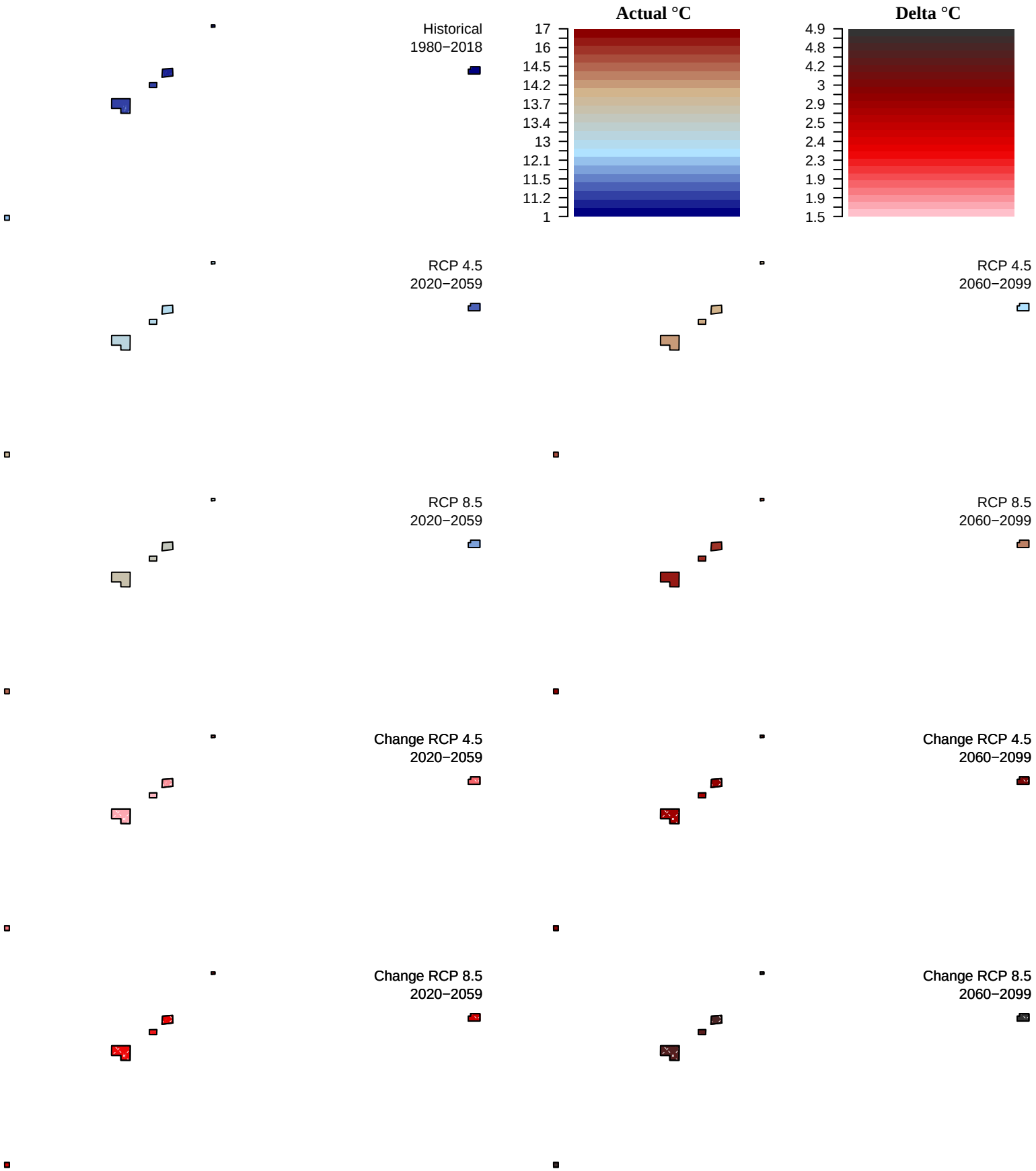


Figure HOVEmap1:
Past trends and future trajectories of park−wide mean values for Mean Annual Temperature in Hovenweep. Topmost panel depicts the historical mean from 1980−2018. Lower four panels show the emission scenarios of RCP 4.5 and RCP 8.5 at near−term and long−term timeframes. Bottom four panels depict the change from the historical mean; cross hatching denotes areas of robust predicitons (90% of models agree in the direction of change).

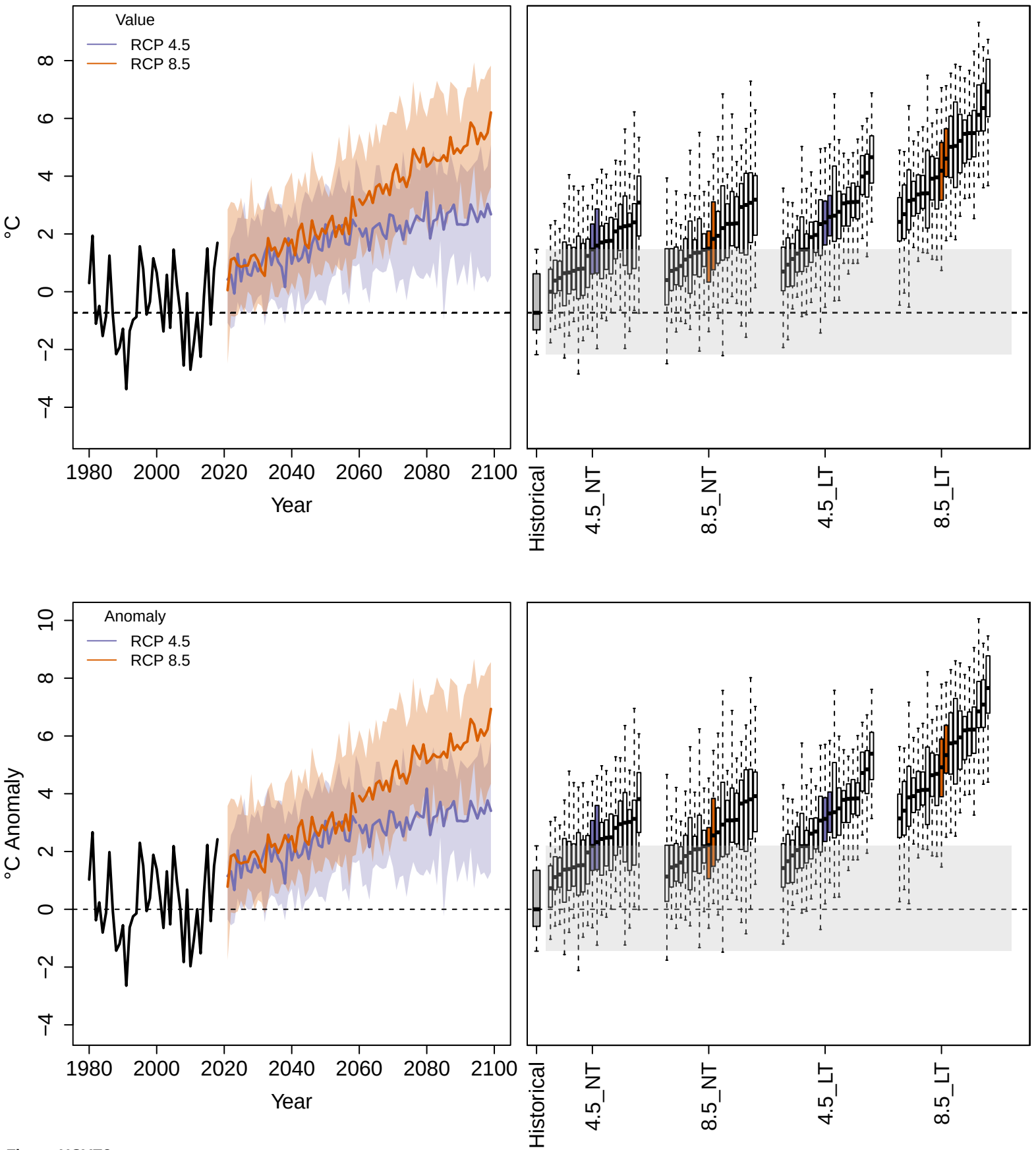


Figure HOVE3:
Past trends and future trajectories of park−wide mean values for Winter Temperature in Hovenweep. Top panels show values, bottom panels show changes from the long−term historical mean. Left: Time series of historical (black) and future projections for RCP 4.5 and 8.5. Shaded areas show spread among climate models. Right: Boxplots of temporal variability over 40−year periods under historical (left box) and individual climate models under two RCPs. Right: Historical time period is 1970−2010; near−term (NT) is 2020−2060; long−term (LT) is 2061−2100.

Hovenweep: Winter Temperature

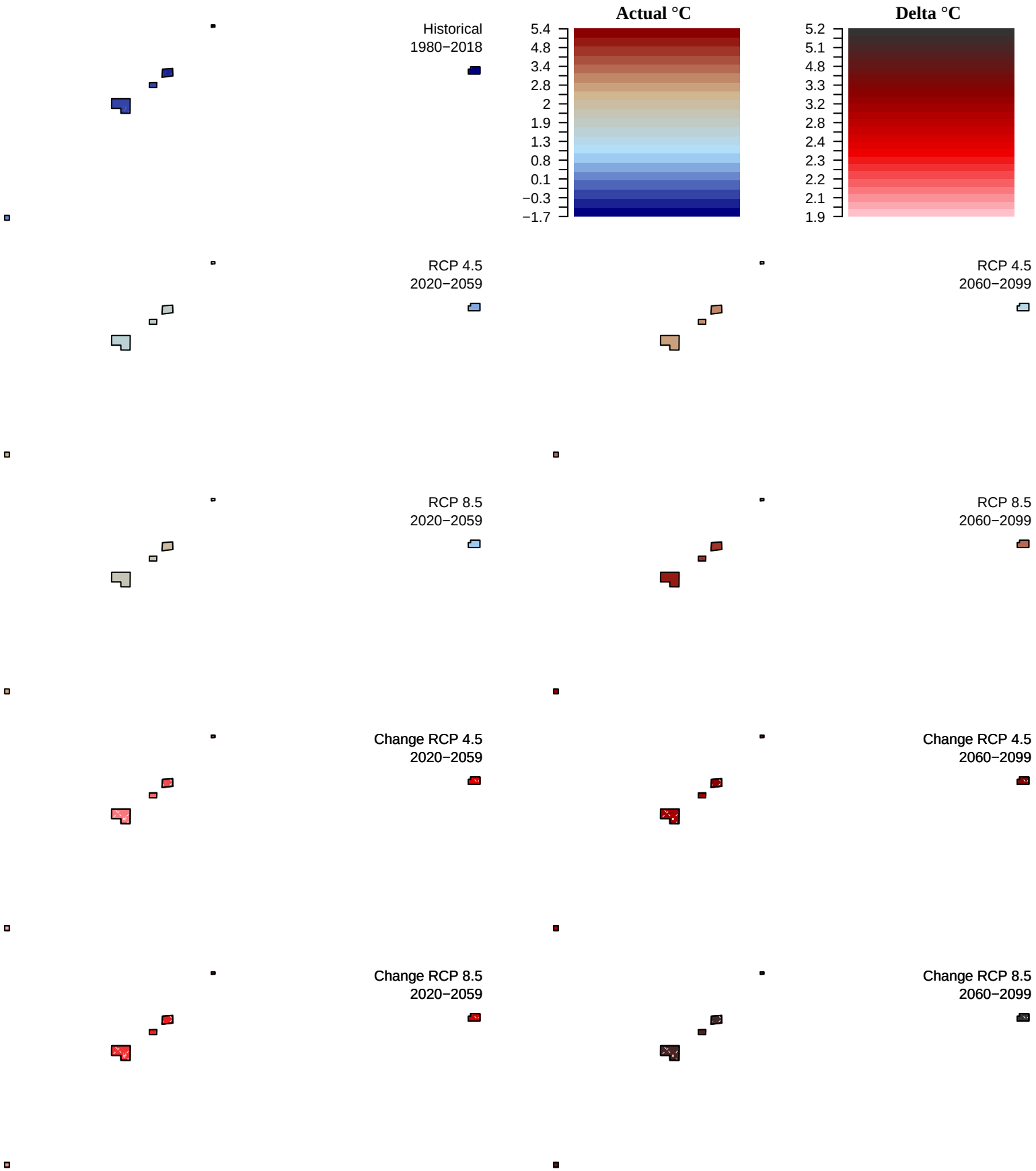


Figure HOVEmap3:
Past trends and future trajectories of park−wide mean values for Winter Temperature in Hovenweep. Topmost panel depicts the historical mean from 1980−2018. Lower four panels show the emission scenarios of RCP 4.5 and RCP 8.5 at near−term and long−term timeframes. Bottom four panels depict the change from the historical mean; cross hatching denotes areas of robust predicitons (90% of models agree in the direction of change).

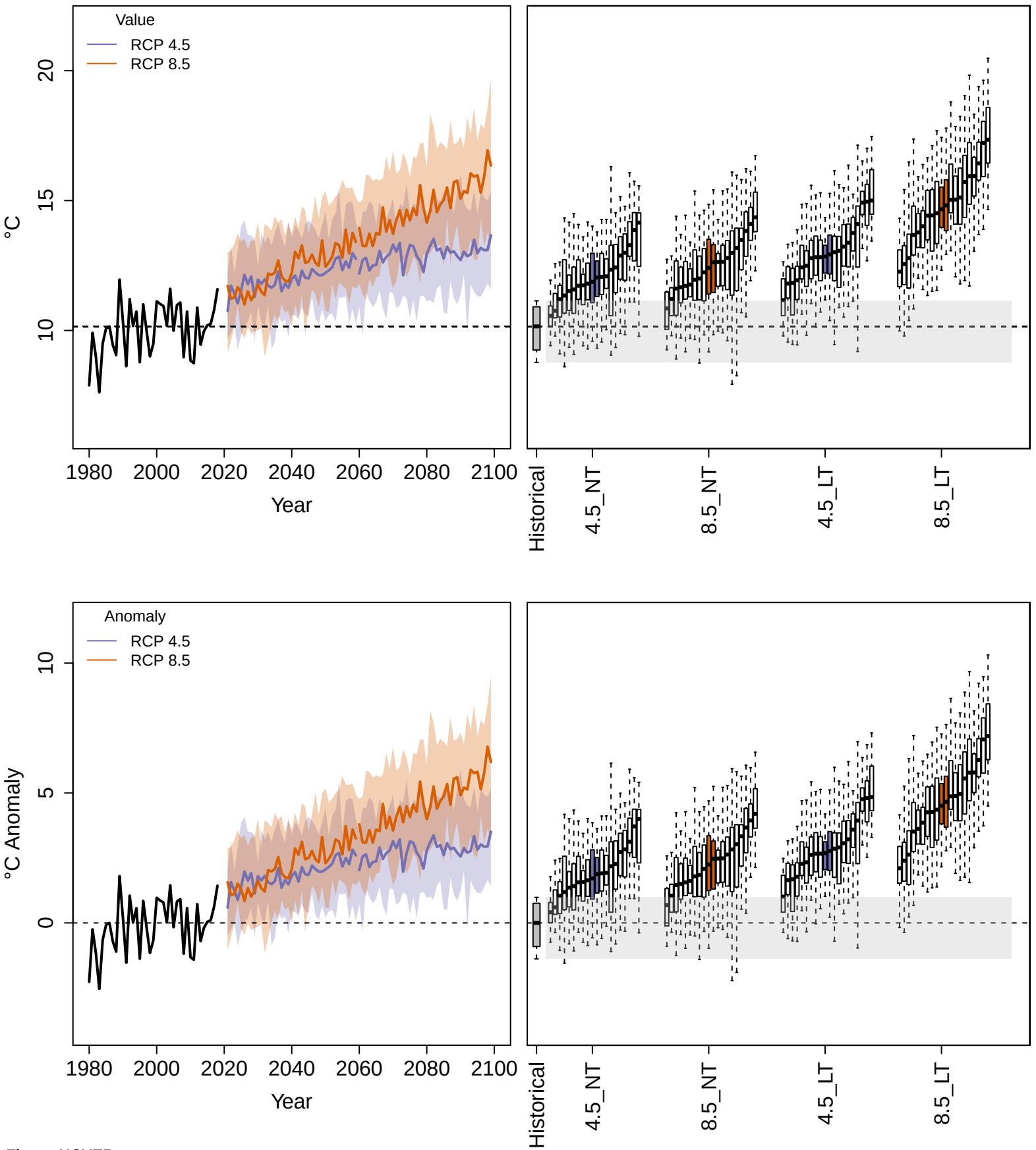


Figure HOVE5:
Past trends and future trajectories of park−wide mean values for Spring Temperature in Hovenweep. Top panels show values, bottom panels show changes from the long−term historical mean. Left: Time series of historical (black) and future projections for RCP 4.5 and 8.5. Shaded areas show spread among climate models. Right: Boxplots of temporal variability over 40−year periods under historical (left box) and individual climate models under two RCPs. Right: Historical time period is 1970−2010; near−term (NT) is 2020−2060; long−term (LT) is 2061−2100.

Hovenweep: Spring Temperature

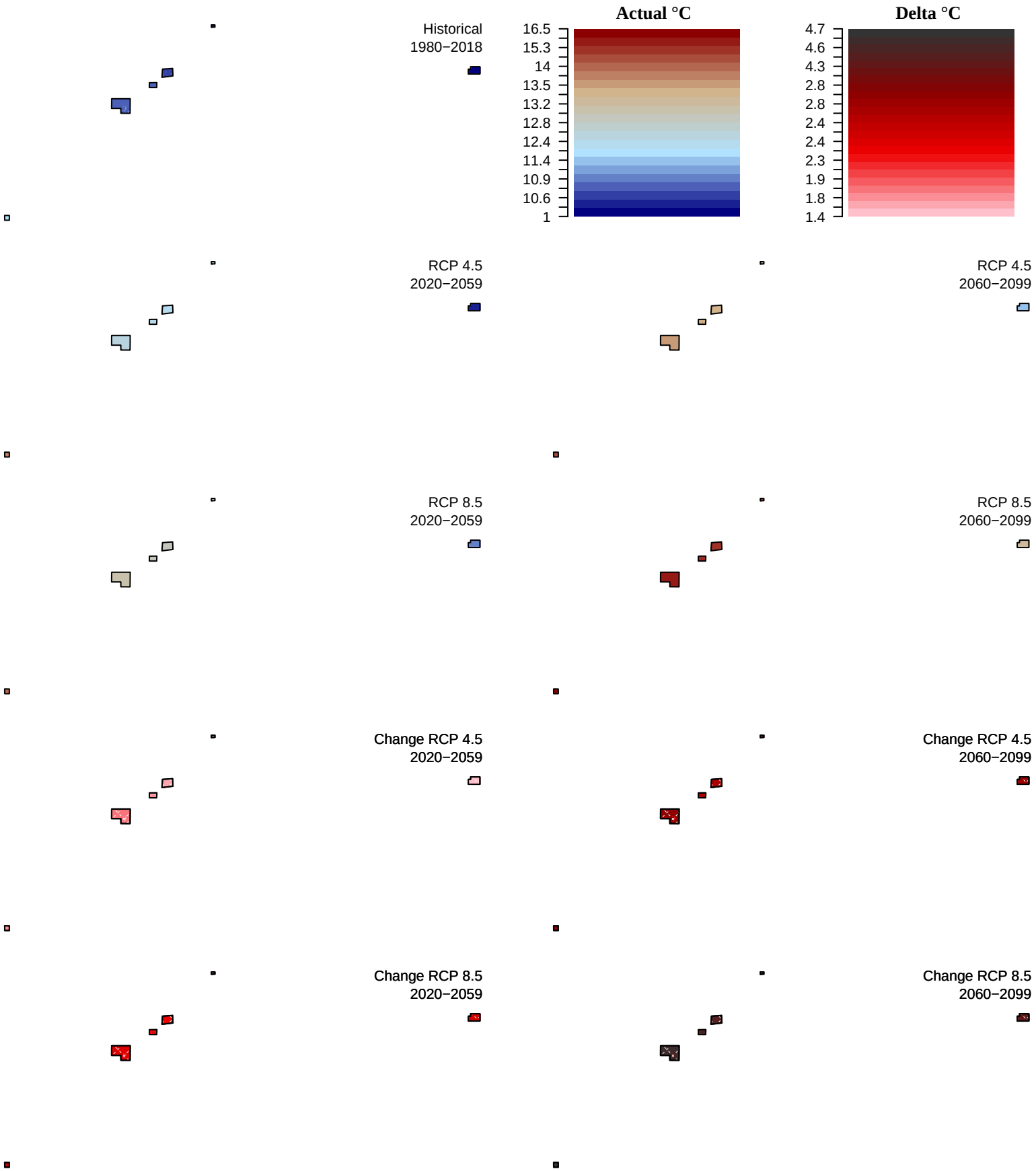


Figure HOVEmap5:
Past trends and future trajectories of park−wide mean values for Spring Temperature in Hovenweep. Topmost panel depicts the historical mean from 1980−2018. Lower four panels show the emission scenarios of RCP 4.5 and RCP 8.5 at near−term and long−term timeframes. Bottom four panels depict the change from the historical mean; cross hatching denotes areas of robust predicitons (90% of models agree in the direction of change).

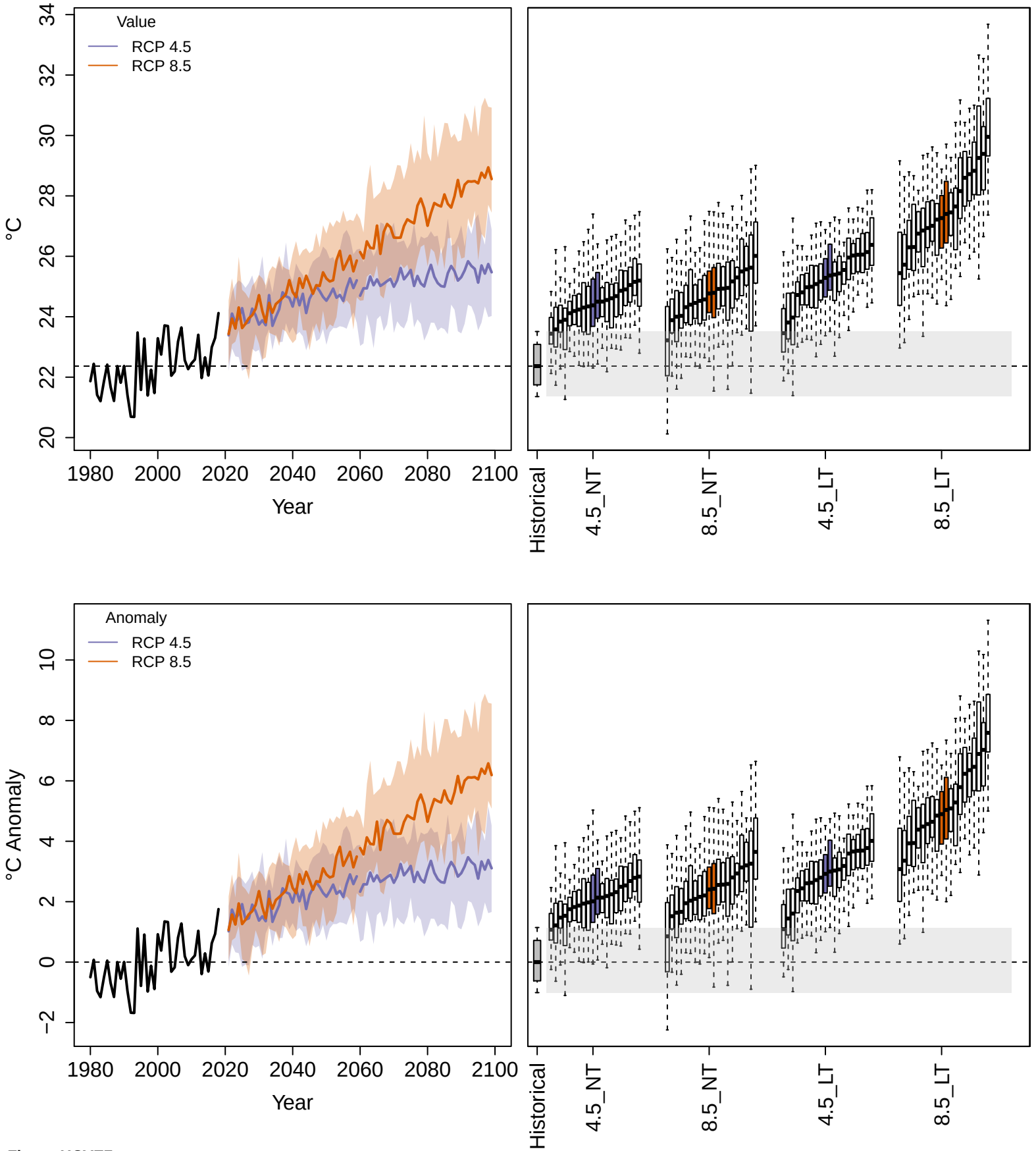


Figure HOVE7:
Past trends and future trajectories of park−wide mean values for Summer Temperature in Hovenweep. Top panels show values, bottom panels show changes from the long−term historical mean. Left: Time series of historical (black) and future projections for RCP 4.5 and 8.5. Shaded areas show spread among climate models. Right: Boxplots of temporal variability over 40−year periods under historical (left box) and individual climate models under two RCPs. Right: Historical time period is 1970−2010; near−term (NT) is 2020−2060; long−term (LT) is 2061−2100.

Hovenweep: Summer Temperature

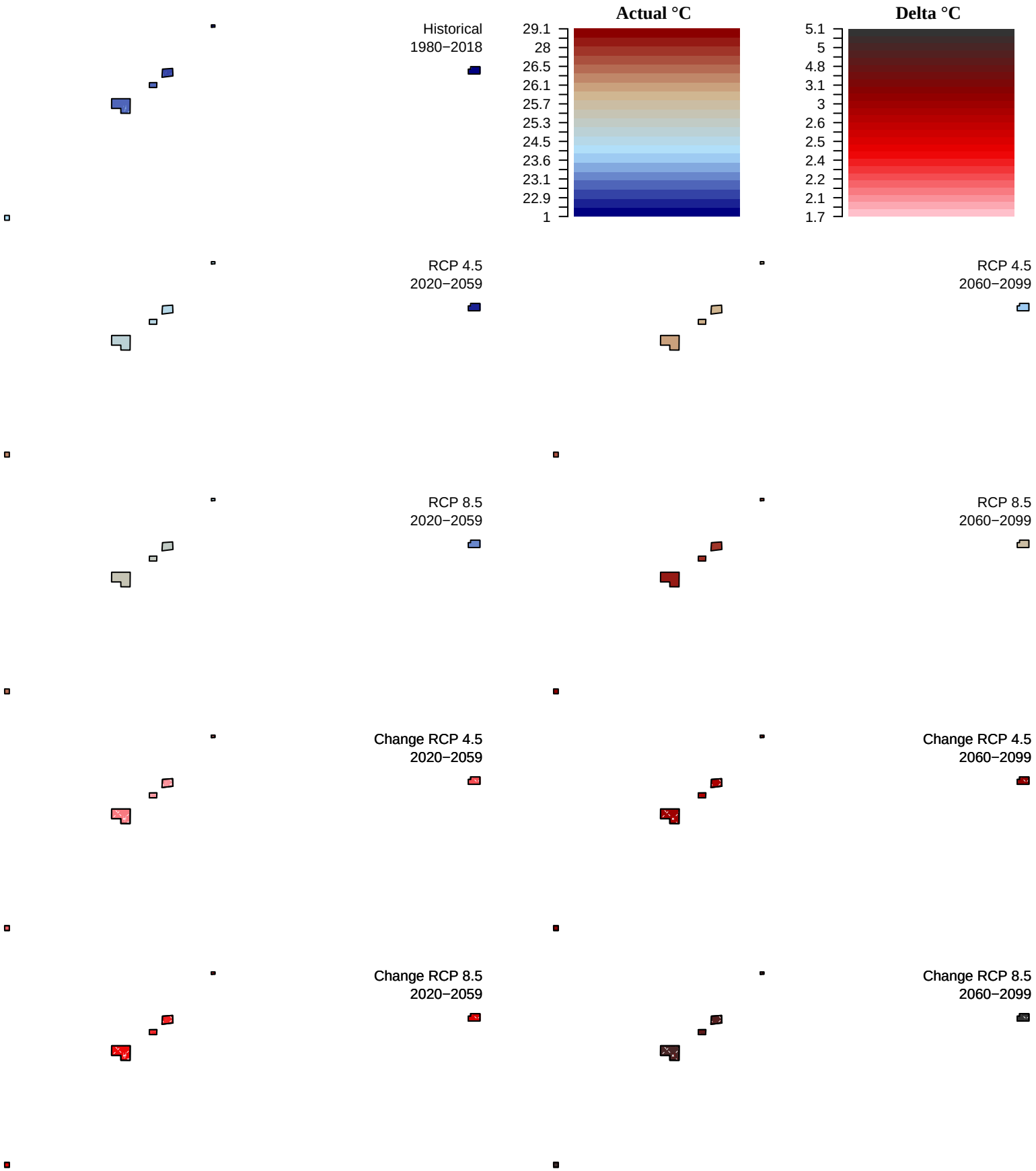


Figure HOVEmap7:
Past trends and future trajectories of park−wide mean values for Summer Temperature in Hovenweep. Topmost panel depicts the historical mean from 1980−2018. Lower four panels show the emission scenarios of RCP 4.5 and RCP 8.5 at near−term and long−term timeframes. Bottom four panels depict the change from the historical mean; cross hatching denotes areas of robust predicitons (90% of models agree in the direction of change).

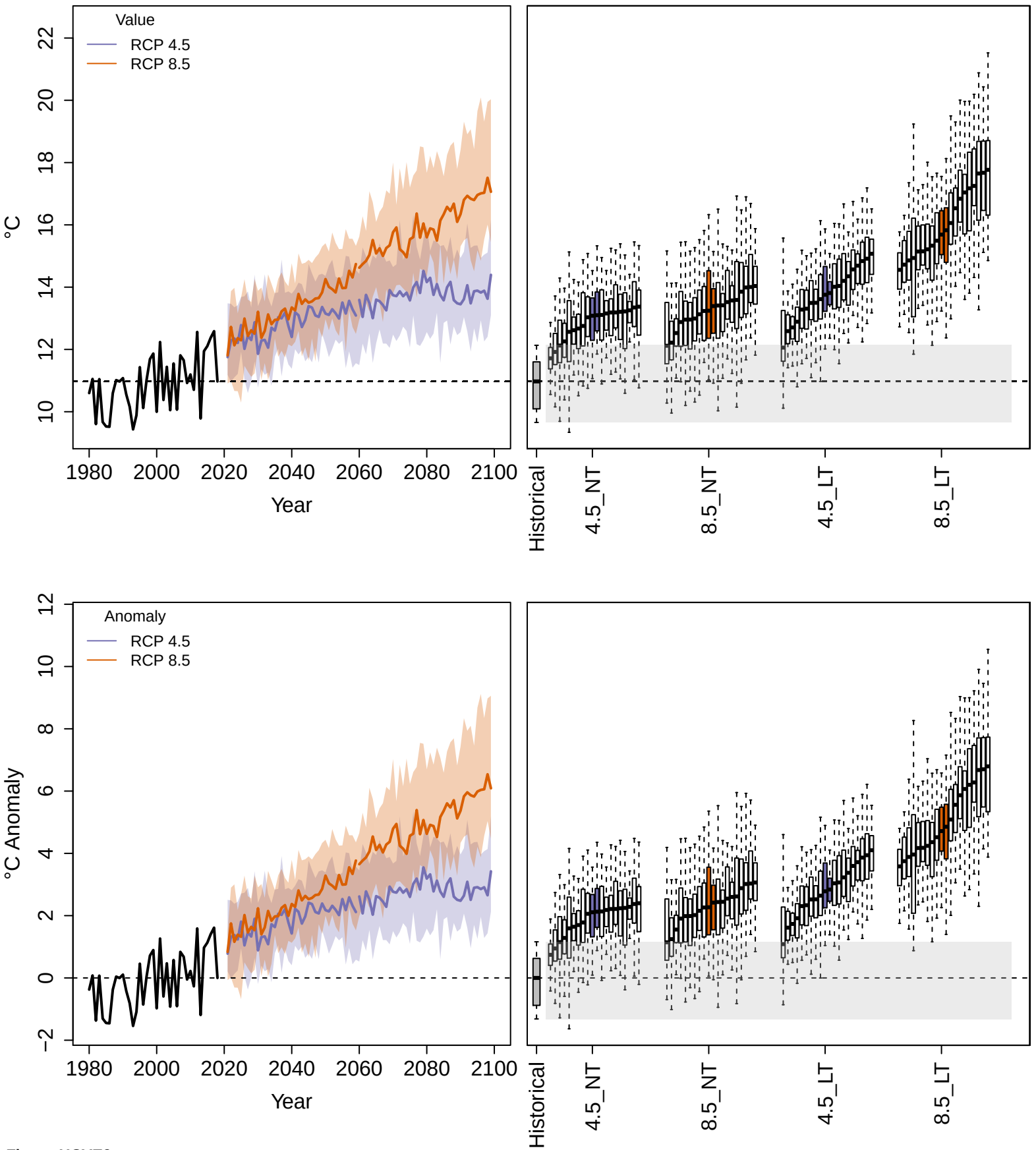


Figure HOVE9:
Past trends and future trajectories of park−wide mean values for Fall Temperature in Hovenweep. Top panels show values, bottom panels show changes from the long−term historical mean. Left: Time series of historical (black) and future projections for RCP 4.5 and 8.5. Shaded areas show spread among climate models. Right: Boxplots of temporal variability over 40−year periods under historical (left box) and individual climate models under two RCPs. Right: Historical time period is 1970−2010; near−term (NT) is 2020−2060; long−term (LT) is 2061−2100.

Hovenweep: Fall Temperature

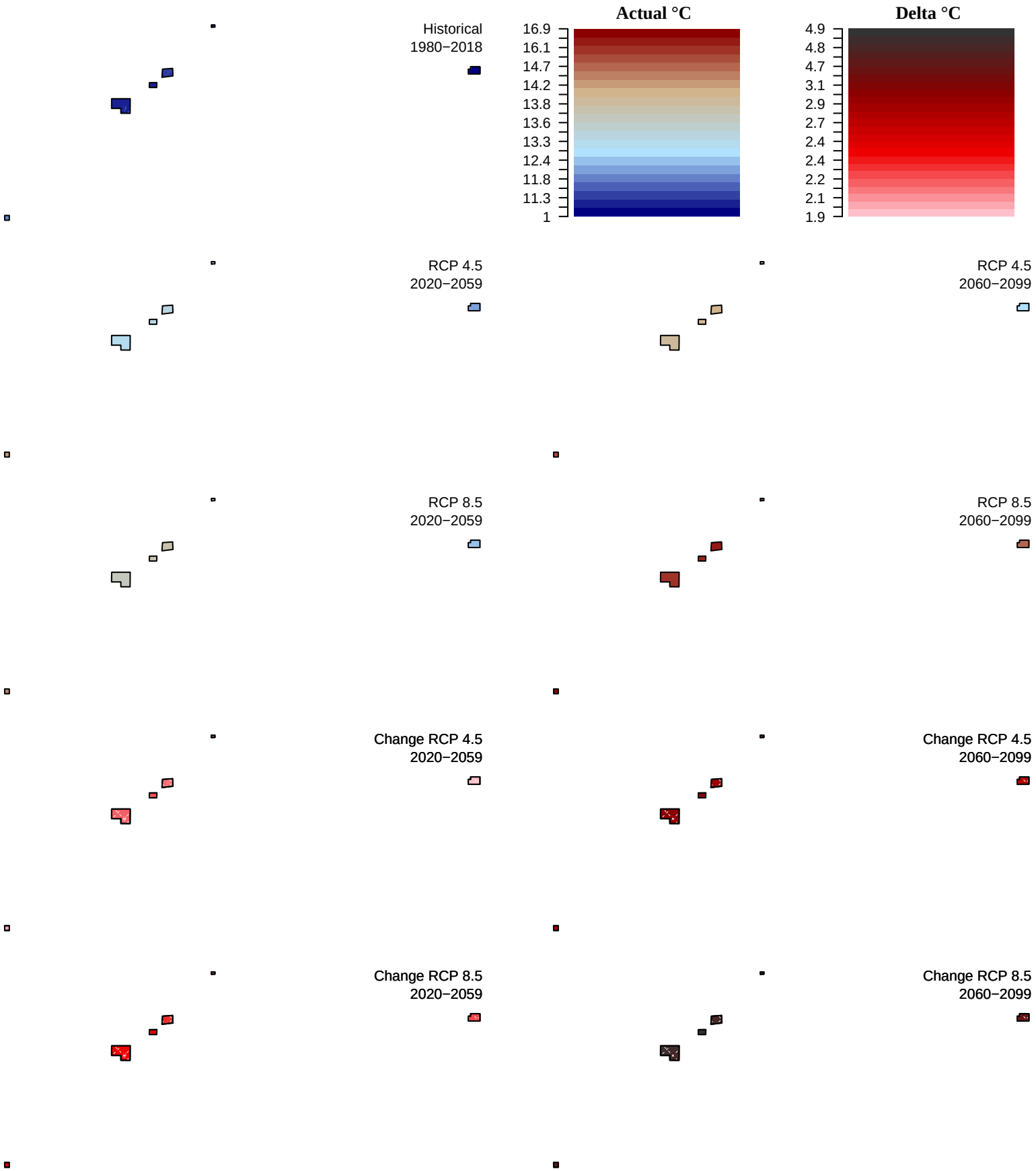


Figure HOVEmap9:
Past trends and future trajectories of park−wide mean values for Fall Temperature in Hovenweep. Topmost panel depicts the historical mean from 1980−2018. Lower four panels show the emission scenarios of RCP 4.5 and RCP 8.5 at near−term and long−term timeframes. Bottom four panels depict the change from the historical mean; cross hatching denotes areas of robust predicitons (90% of models agree in the direction of change).

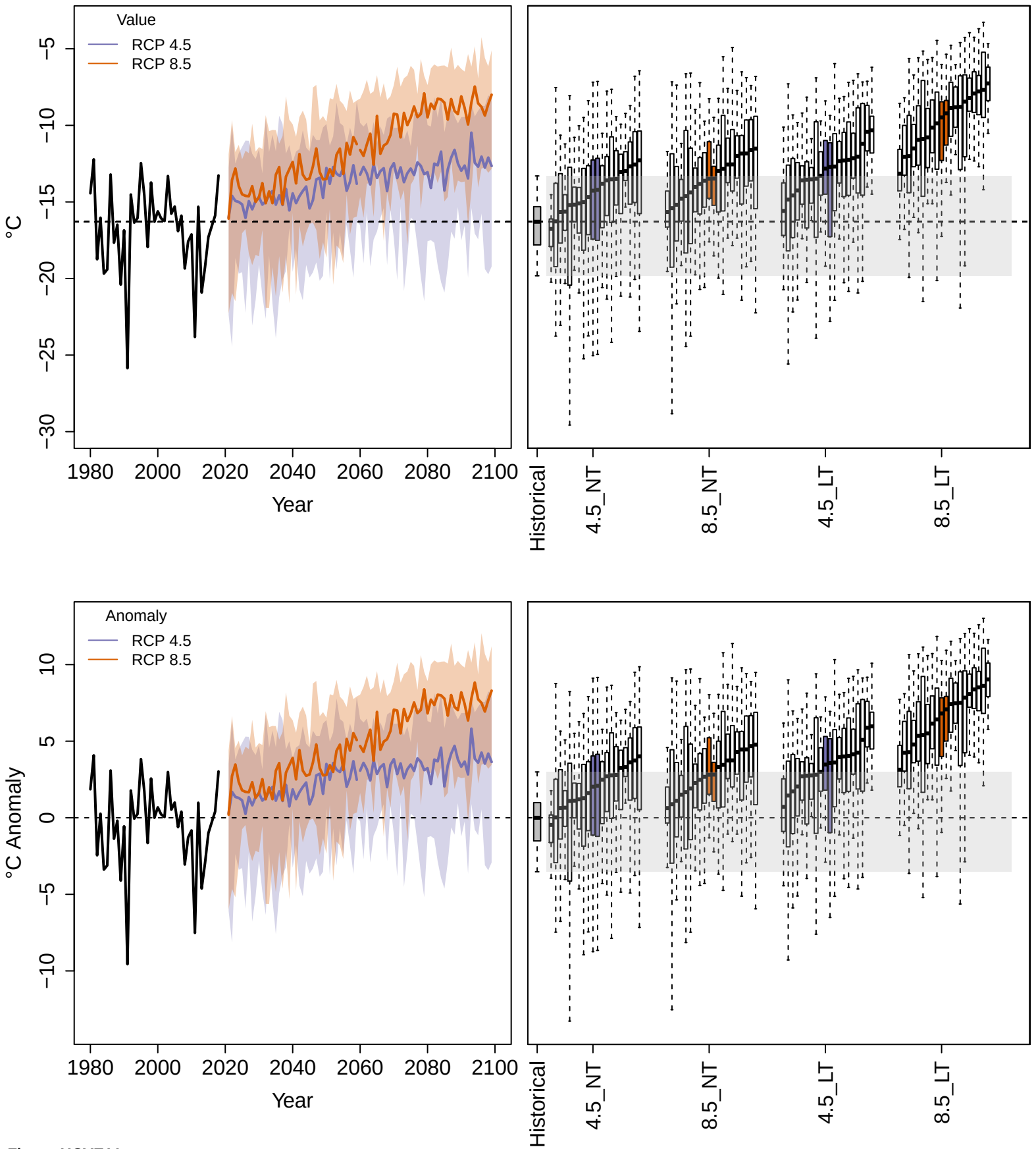


Figure HOVE11:
Past trends and future trajectories of park−wide mean values for Minimum winter temperature in Hovenweep. Top panels show values, bottom panels show changes from the long−term historical mean. Left: Time series of historical (black) and future projections for RCP 4.5 and 8.5. Shaded areas show spread among climate models. Right: Boxplots of temporal variability over 40−year periods under historical (left box) and individual climate models under two RCPs. Right: Historical time period is 1970−2010; near−term (NT) is 2020−2060; long−term (LT) is 2061−2100.

Hovenweep: Minimum winter temperature

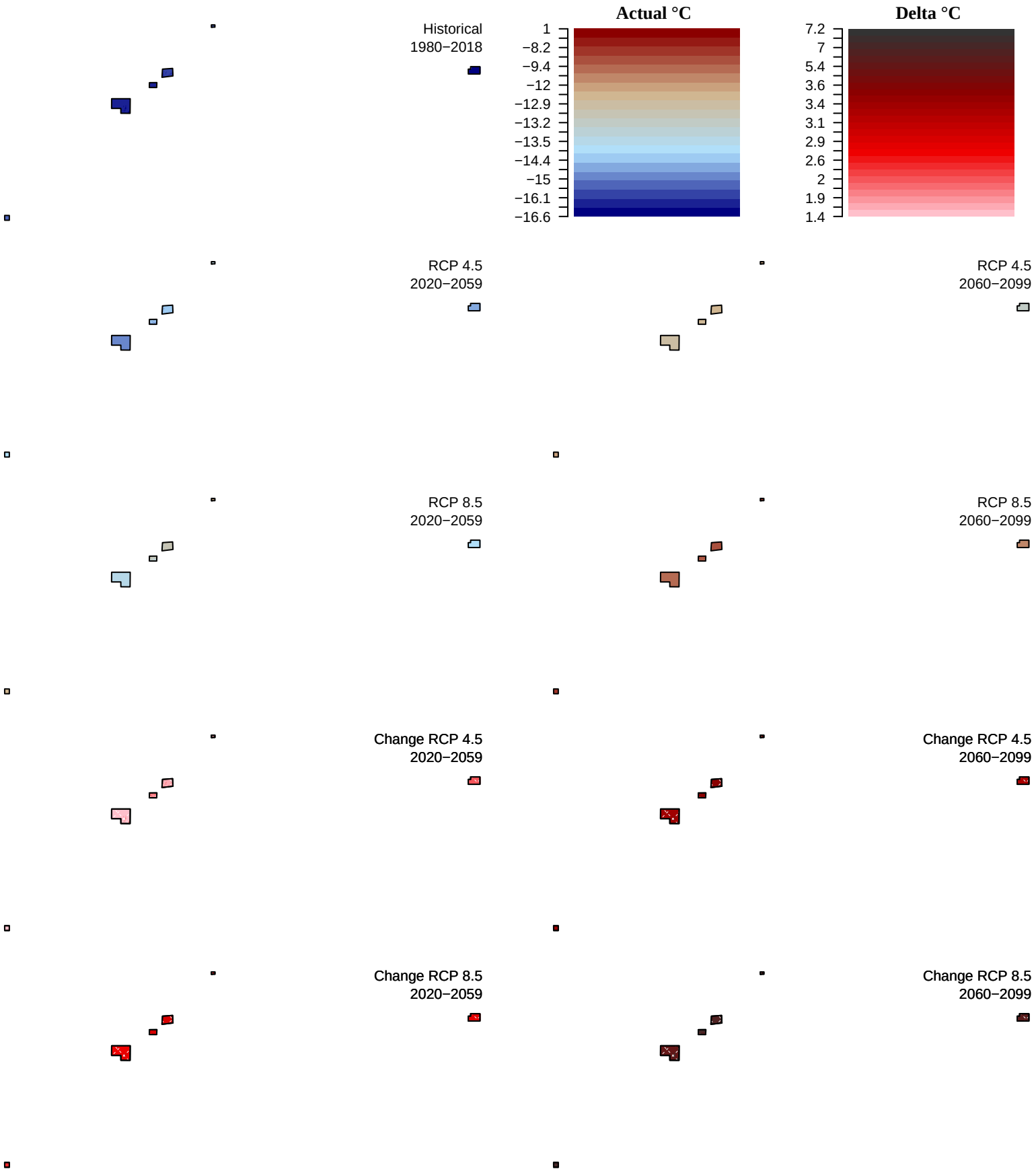


Figure HOVEmap11:
Past trends and future trajectories of park−wide mean values for Minimum winter temperature in Hovenweep. Topmost panel depicts the historical mean from 1980−2018. Lower four panels show the emission scenarios of RCP 4.5 and RCP 8.5 at near−term and long−term timeframes. Bottom four panels depict the change from the historical mean; cross hatching denotes areas of robust predicitons (90% of models agree in the direction of change).

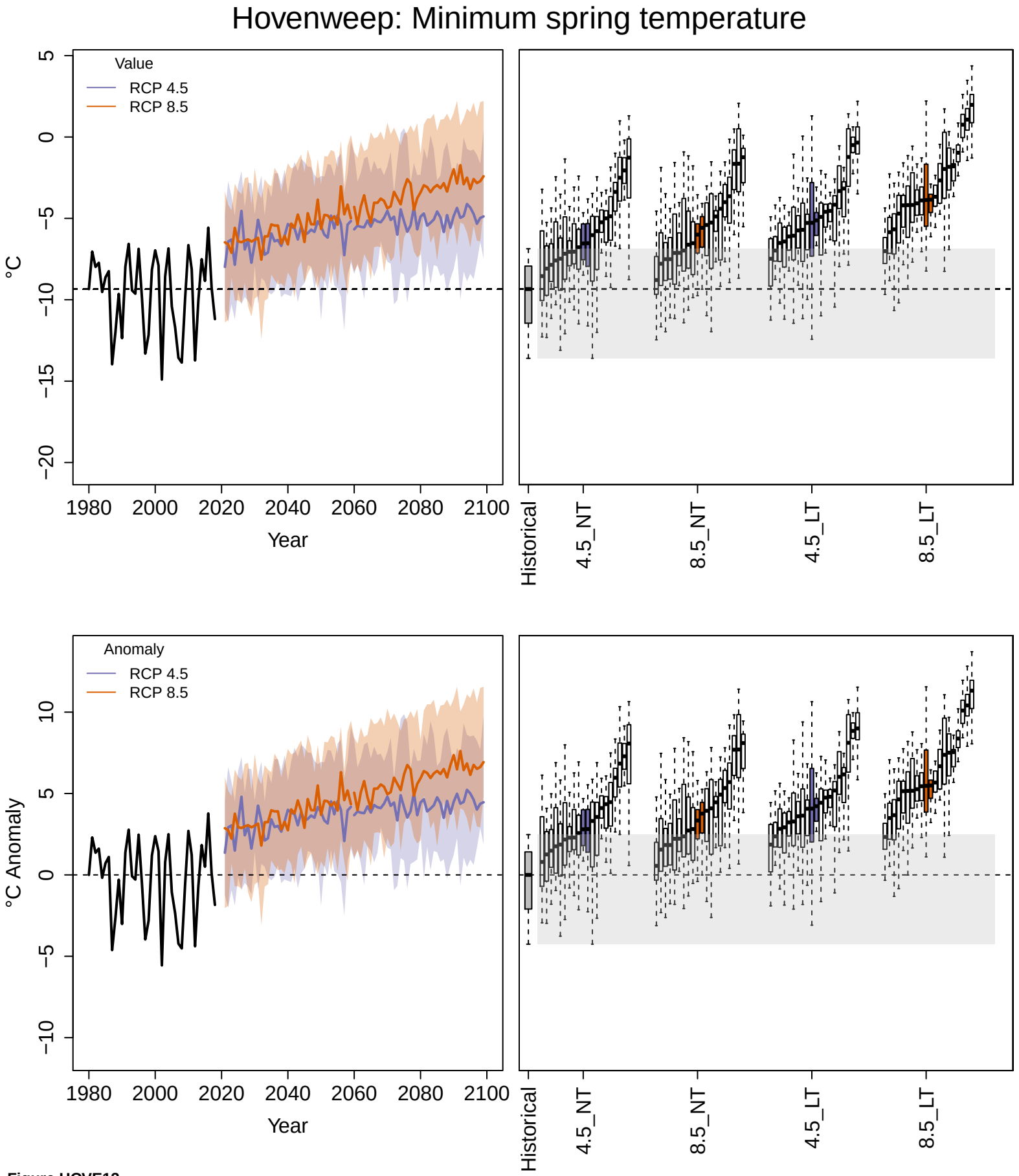


Figure HOVE13:
Past trends and future trajectories of park−wide mean values for Minimum spring temperature in Hovenweep. Top panels show values, bottom panels show changes from the long−term historical mean. Left: Time series of historical (black) and future projections for RCP 4.5 and 8.5. Shaded areas show spread among climate models. Right: Boxplots of temporal variability over 40−year periods under historical (left box) and individual climate models under two RCPs. Right: Historical time period is 1970−2010; near−term (NT) is 2020−2060; long−term (LT) is 2061−2100.

Hovenweep: Minimum spring temperature

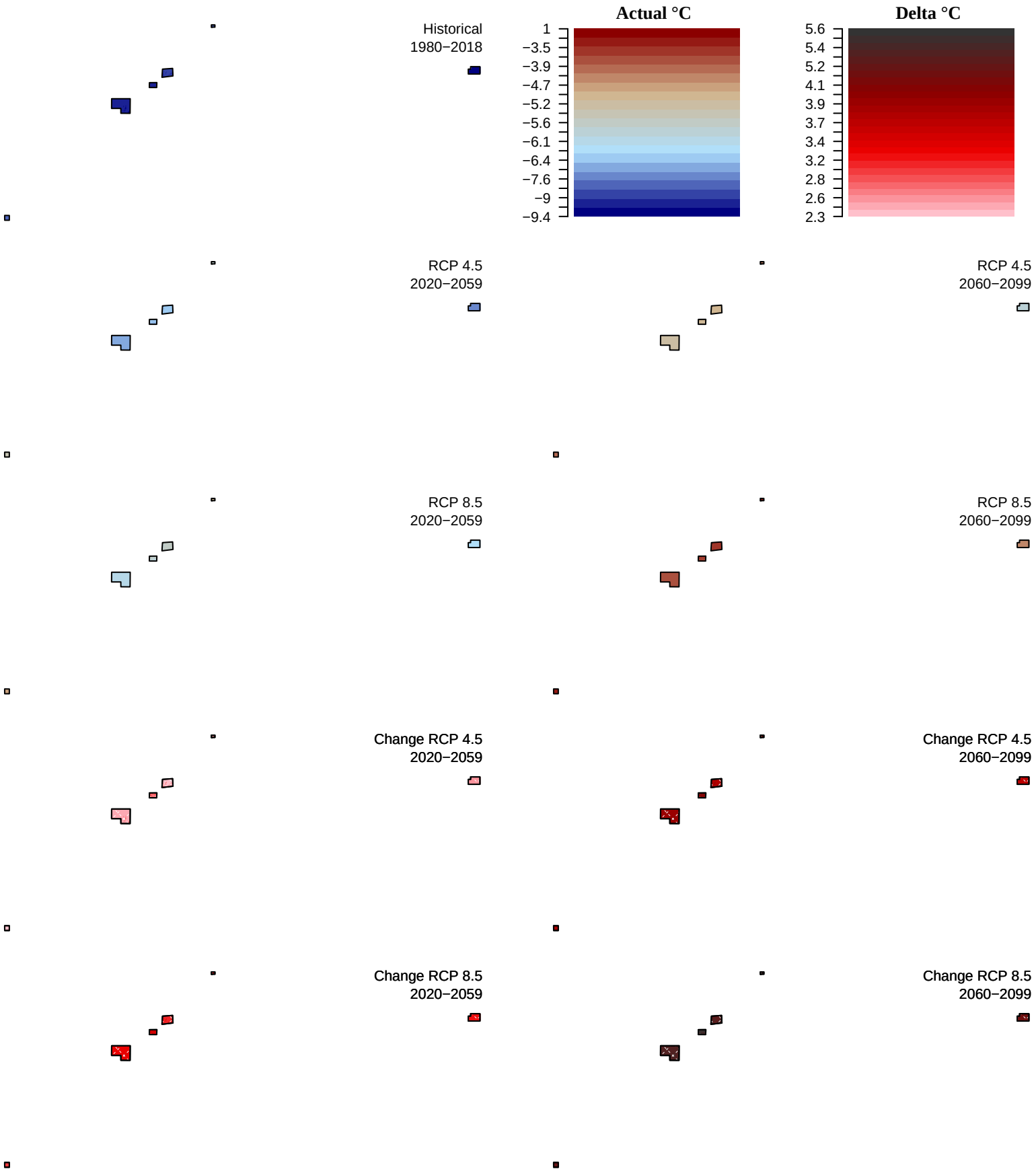


Figure HOVEmap13:
Past trends and future trajectories of park−wide mean values for Minimum spring temperature in Hovenweep. Topmost panel depicts the historical mean from 1980−2018. Lower four panels show the emission scenarios of RCP 4.5 and RCP 8.5 at near−term and long−term timeframes. Bottom four panels depict the change from the historical mean; cross hatching denotes areas of robust predicitons (90% of models agree in the direction of change).

Hovenweep: Minimum summer temperature

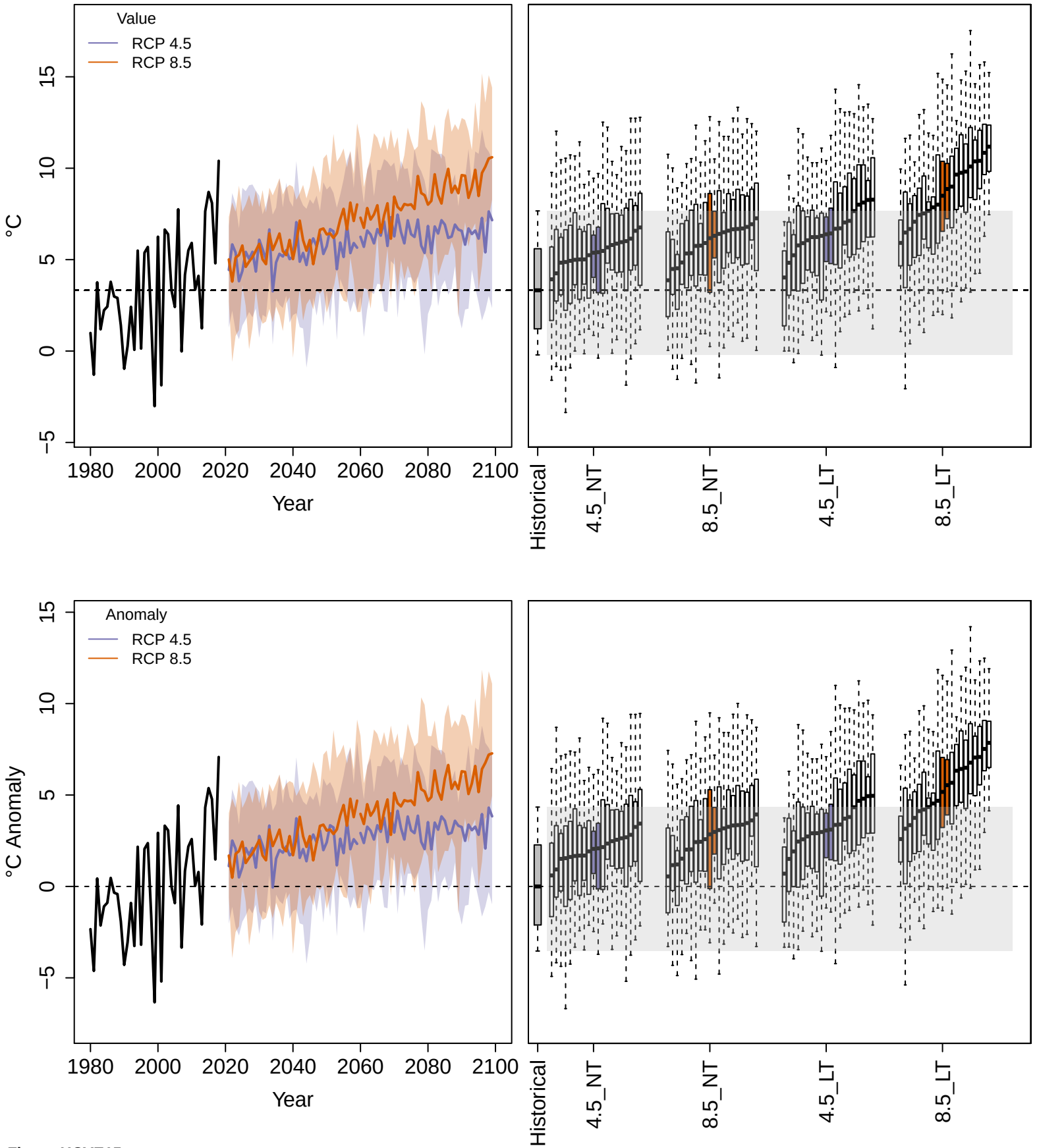


Figure HOVE15:
Past trends and future trajectories of park−wide mean values for Minimum summer temperature in Hovenweep. Top panels show values, bottom panels show changes from the long−term historical mean. Left: Time series of historical (black) and future projections for RCP 4.5 and 8.5. Shaded areas show spread among climate models. Right: Boxplots of temporal variability over 40−year periods under historical (left box) and individual climate models under two RCPs. Right: Historical time period is 1970−2010; near−term (NT) is 2020−2060; long−term (LT) is 2061−2100.

Hovenweep: Minimum summer temperature

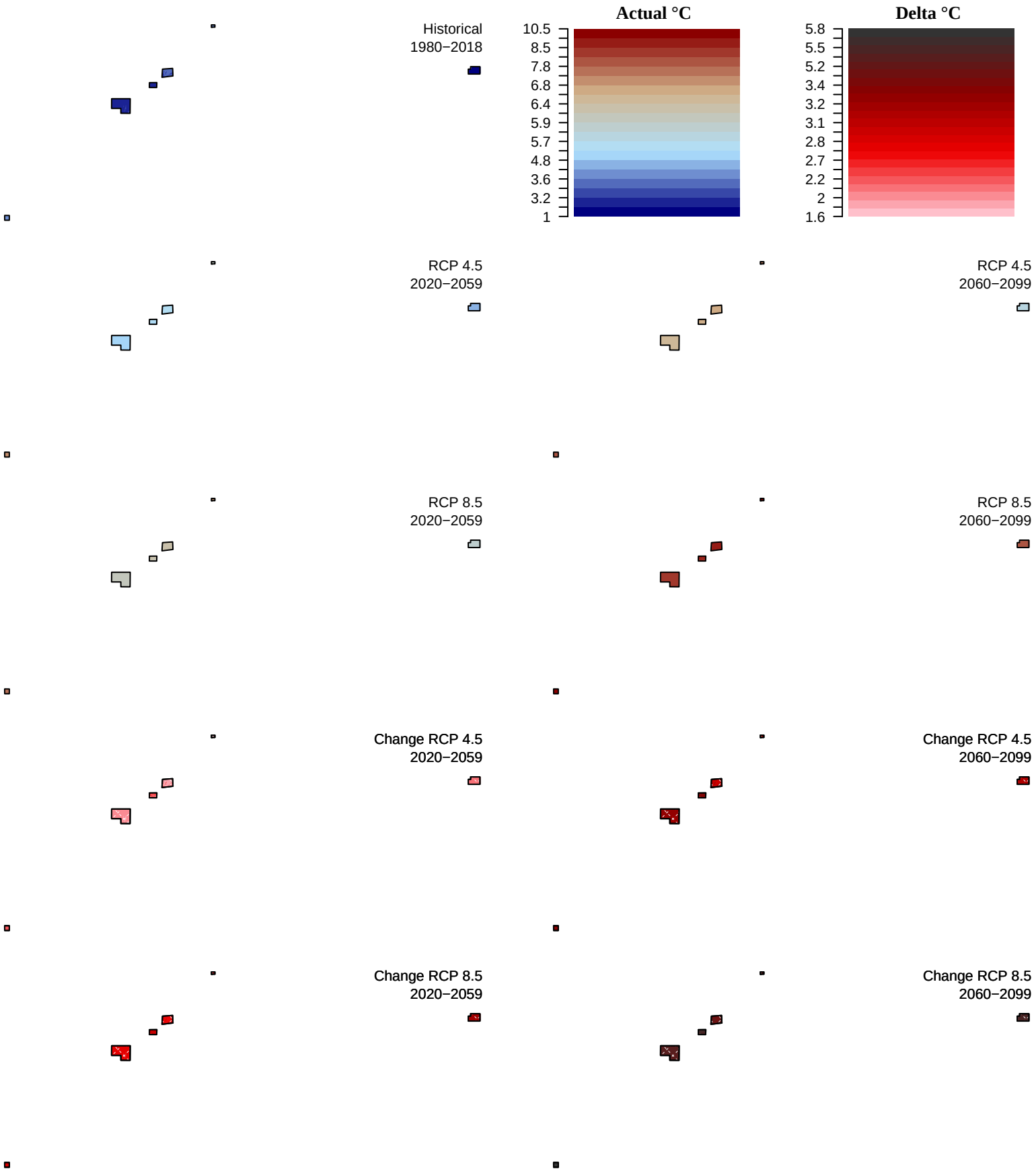


Figure HOVEmap15:
Past trends and future trajectories of park−wide mean values for Minimum summer temperature in Hovenweep. Topmost panel depicts the historical mean from 1980−2018. Lower four panels show the emission scenarios of RCP 4.5 and RCP 8.5 at near−term and long−term timeframes. Bottom four panels depict the change from the historical mean; cross hatching denotes areas of robust predicitons (90% of models agree in the direction of change).

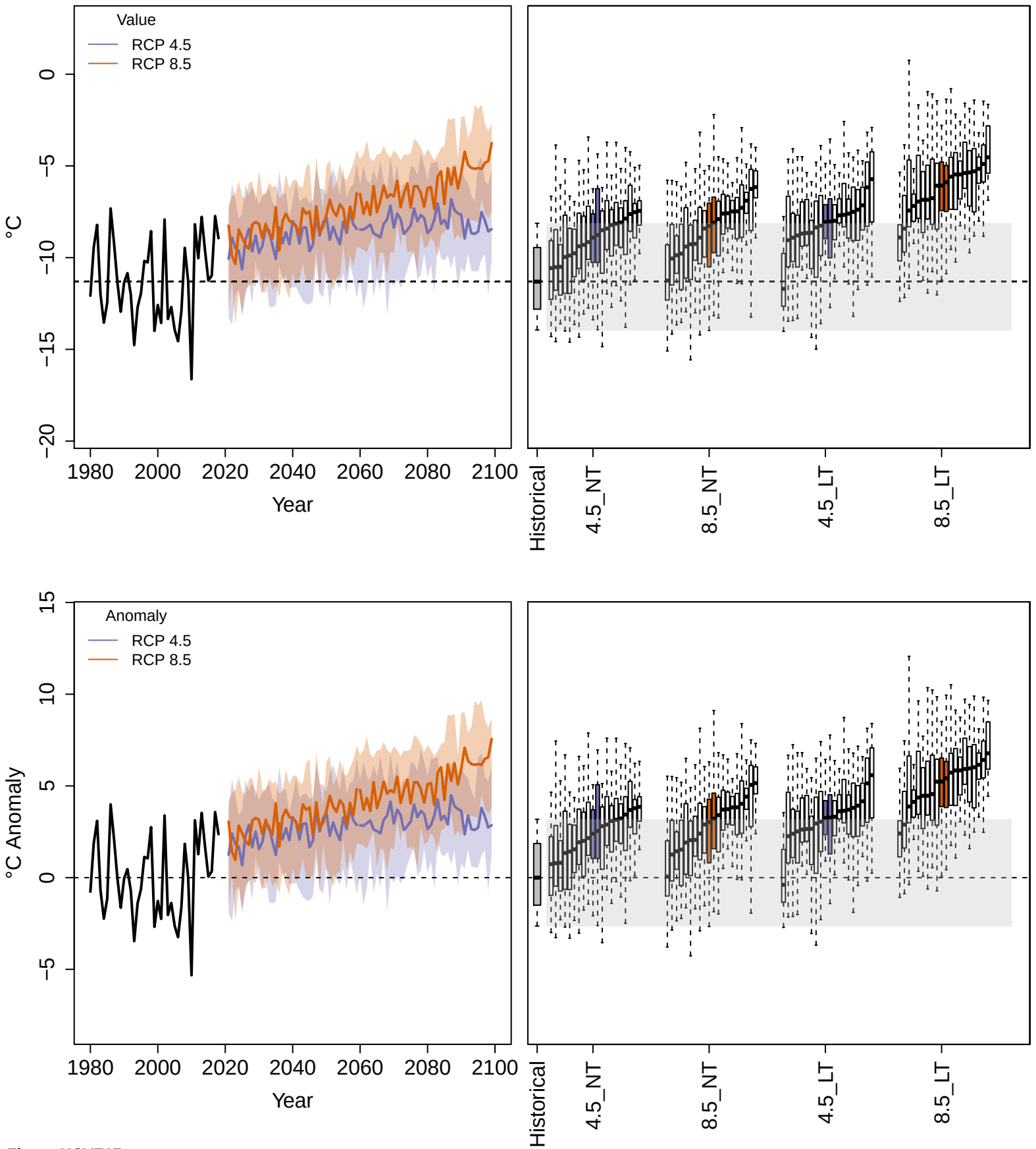


Figure HOVE17:
Past trends and future trajectories of park−wide mean values for Minimum fall temperature in Hovenweep. Top panels show values, bottom panels show changes from the long−term historical mean. Left: Time series of historical (black) and future projections for RCP 4.5 and 8.5. Shaded areas show spread among climate models. Right: Boxplots of temporal variability over 40−year periods under historical (left box) and individual climate models under two RCPs. Right: Historical time period is 1970−2010; near−term (NT) is 2020−2060; long−term (LT) is 2061−2100.

Hovenweep: Minimum fall temperature

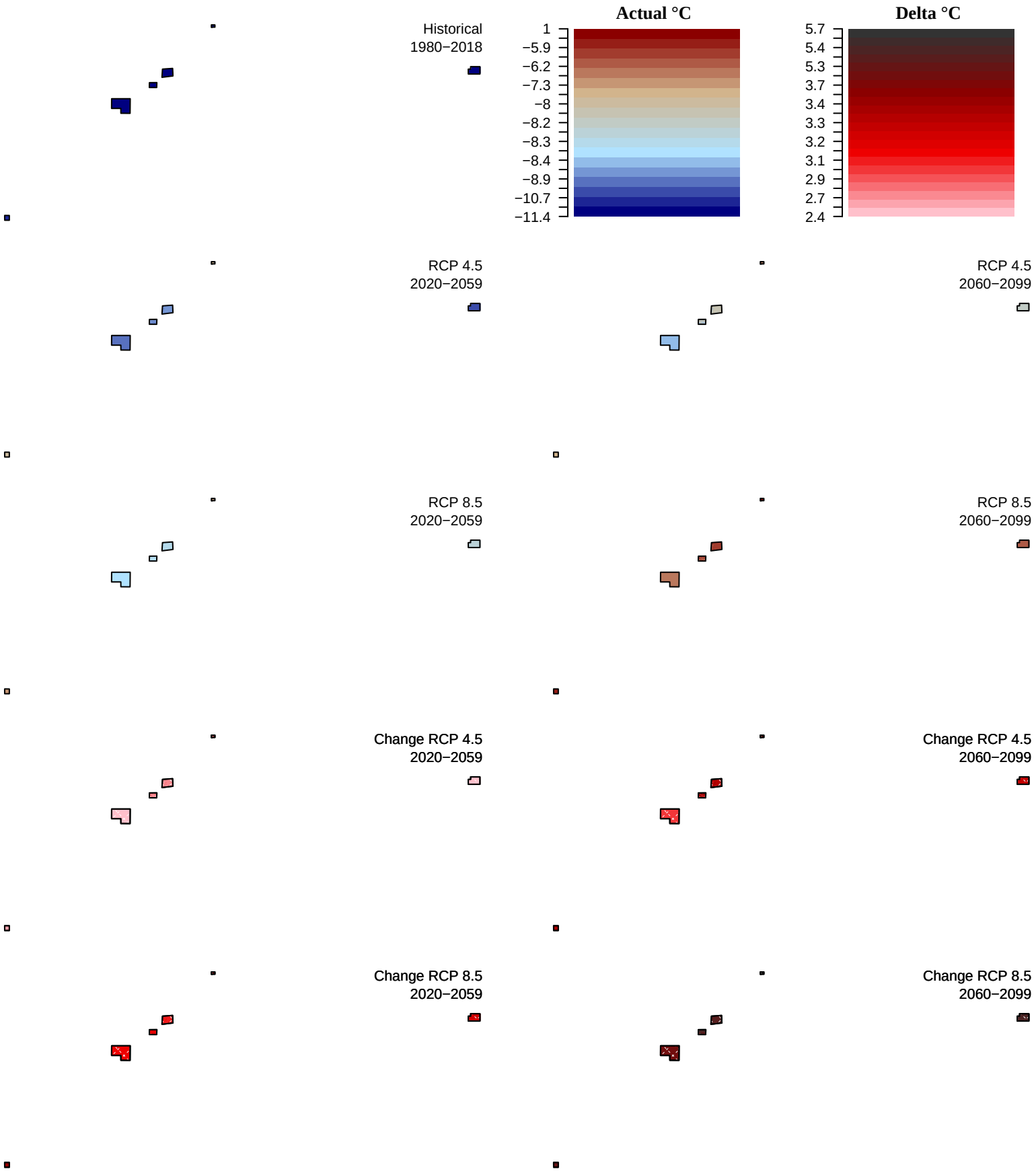


Figure HOVEmap17:
Past trends and future trajectories of park−wide mean values for Minimum fall temperature in Hovenweep. Topmost panel depicts the historical mean from 1980−2018. Lower four panels show the emission scenarios of RCP 4.5 and RCP 8.5 at near−term and long−term timeframes. Bottom four panels depict the change from the historical mean; cross hatching denotes areas of robust predicitons (90% of models agree in the direction of change).

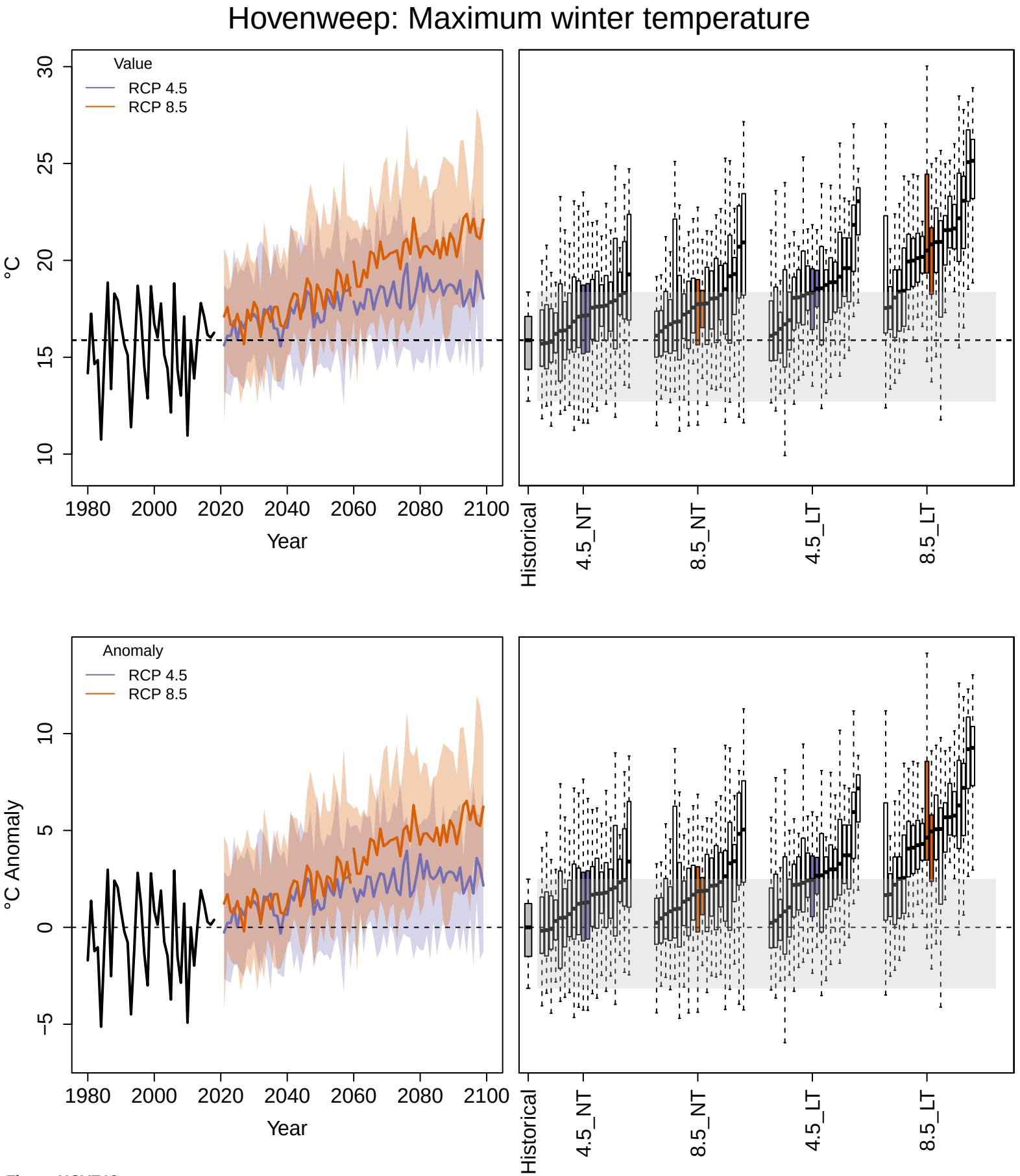


Figure HOVE19:
Past trends and future trajectories of park−wide mean values for Maximum winter temperature in Hovenweep. Top panels show values, bottom panels show changes from the long−term historical mean. Left: Time series of historical (black) and future projections for RCP 4.5 and 8.5. Shaded areas show spread among climate models. Right: Boxplots of temporal variability over 40−year periods under historical (left box) and individual climate models under two RCPs. Right: Historical time period is 1970−2010; near−term (NT) is 2020−2060; long−term (LT) is 2061−2100.

Hovenweep: Maximum winter temperature

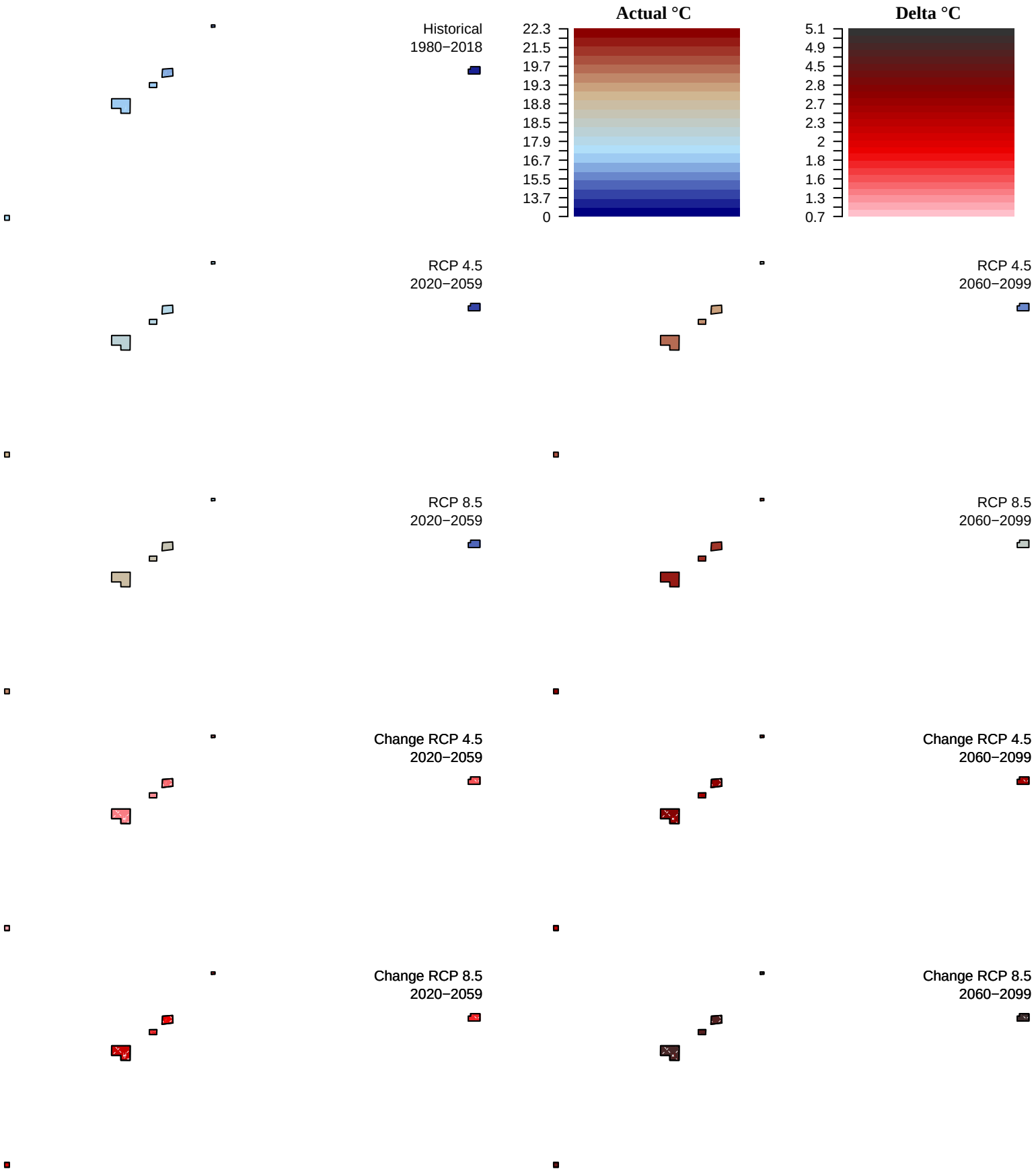


Figure HOVEmap19:
Past trends and future trajectories of park−wide mean values for Maximum winter temperature in Hovenweep. Topmost panel depicts the historical mean from 1980−2018. Lower four panels show the emission scenarios of RCP 4.5 and RCP 8.5 at near−term and long−term timeframes. Bottom four panels depict the change from the historical mean; cross hatching denotes areas of robust predicitons (90% of models agree in the direction of change).

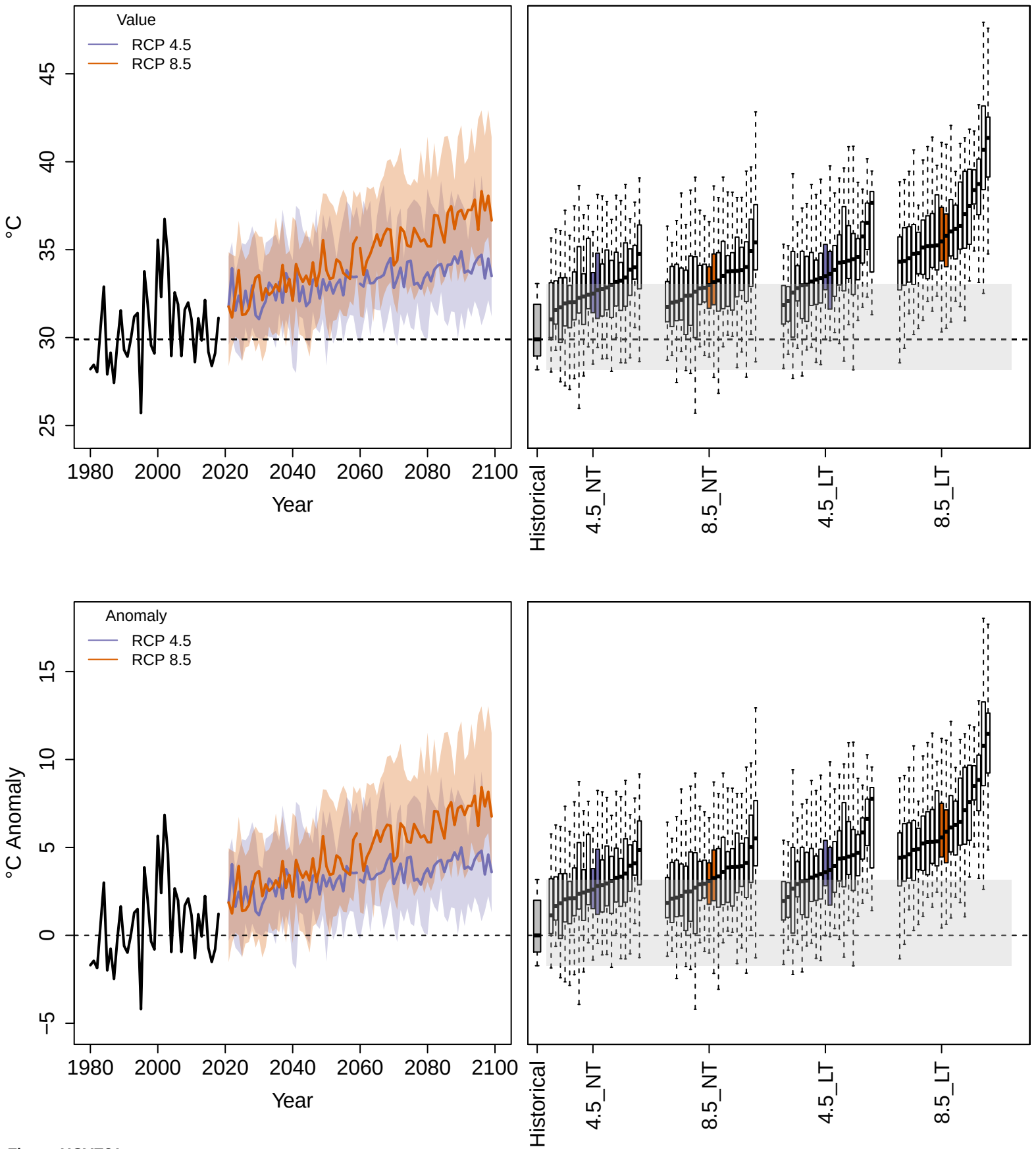


Figure HOVE21:
Past trends and future trajectories of park−wide mean values for Maximum spring temperature in Hovenweep. Top panels show values, bottom panels show changes from the long−term historical mean. Left: Time series of historical (black) and future projections for RCP 4.5 and 8.5. Shaded areas show spread among climate models. Right: Boxplots of temporal variability over 40−year periods under historical (left box) and individual climate models under two RCPs. Right: Historical time period is 1970−2010; near−term (NT) is 2020−2060; long−term (LT) is 2061−2100.

Hovenweep: Maximum spring temperature

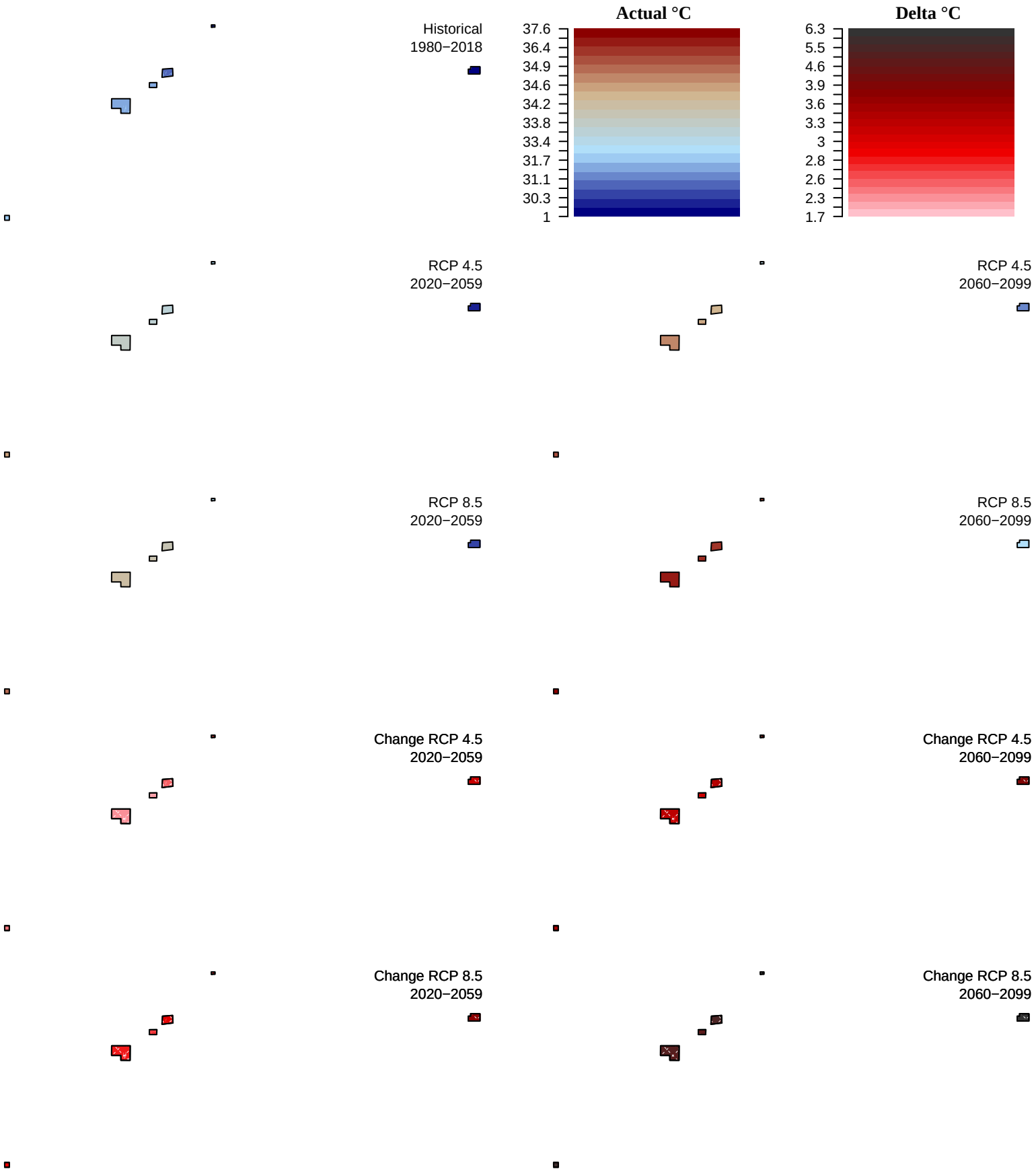


Figure HOVEmap21:
Past trends and future trajectories of park−wide mean values for Maximum spring temperature in Hovenweep. Topmost panel depicts the historical mean from 1980−2018. Lower four panels show the emission scenarios of RCP 4.5 and RCP 8.5 at near−term and long−term timeframes. Bottom four panels depict the change from the historical mean; cross hatching denotes areas of robust predicitons (90% of models agree in the direction of change).

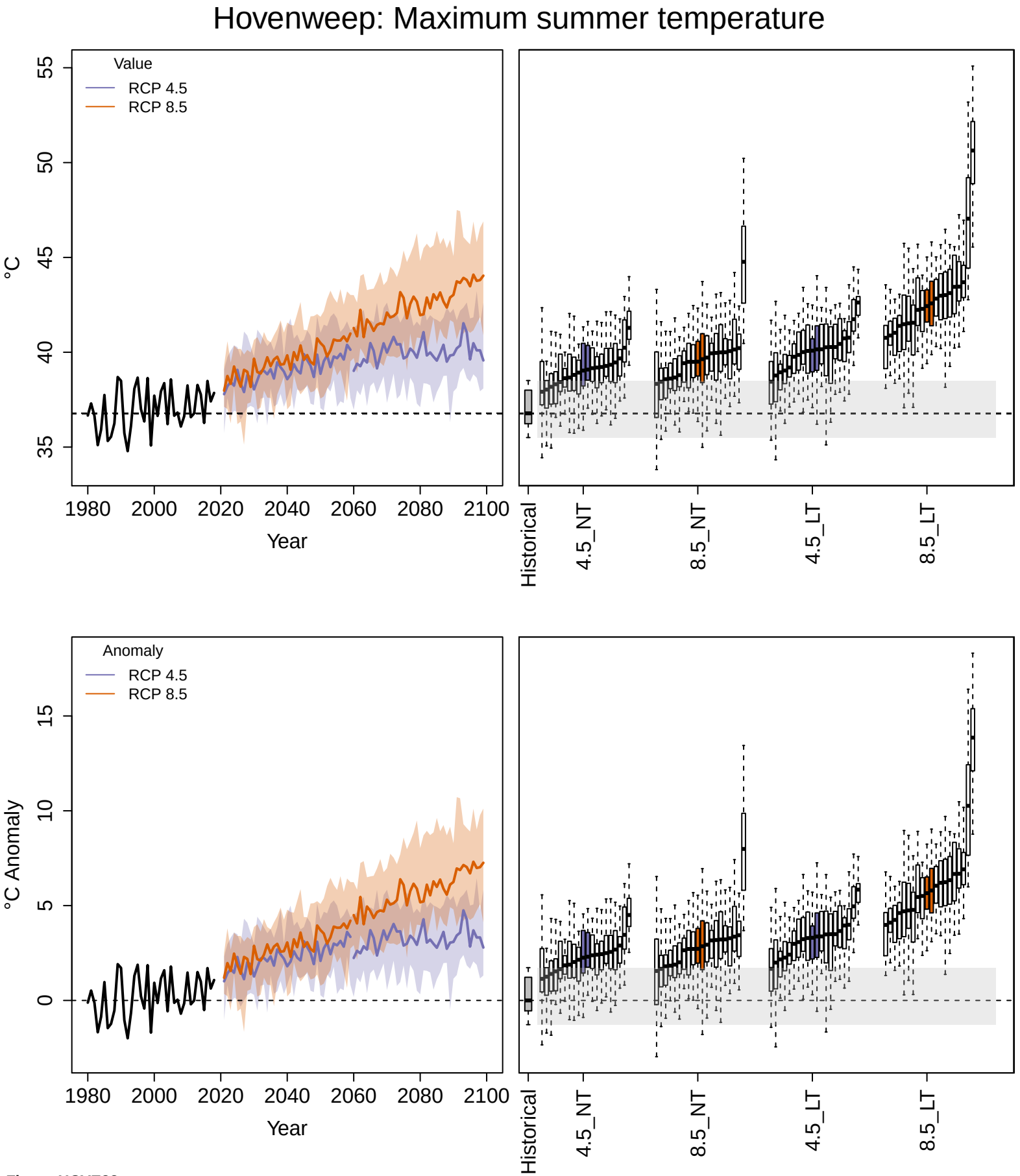


Figure HOVE23:
Past trends and future trajectories of park−wide mean values for Maximum summer temperature in Hovenweep. Top panels show values, bottom panels show changes from the long−term historical mean. Left: Time series of historical (black) and future projections for RCP 4.5 and 8.5. Shaded areas show spread among climate models. Right: Boxplots of temporal variability over 40−year periods under historical (left box) and individual climate models under two RCPs. Right: Historical time period is 1970−2010; near−term (NT) is 2020−2060; long−term (LT) is 2061−2100.

Hovenweep: Maximum summer temperature

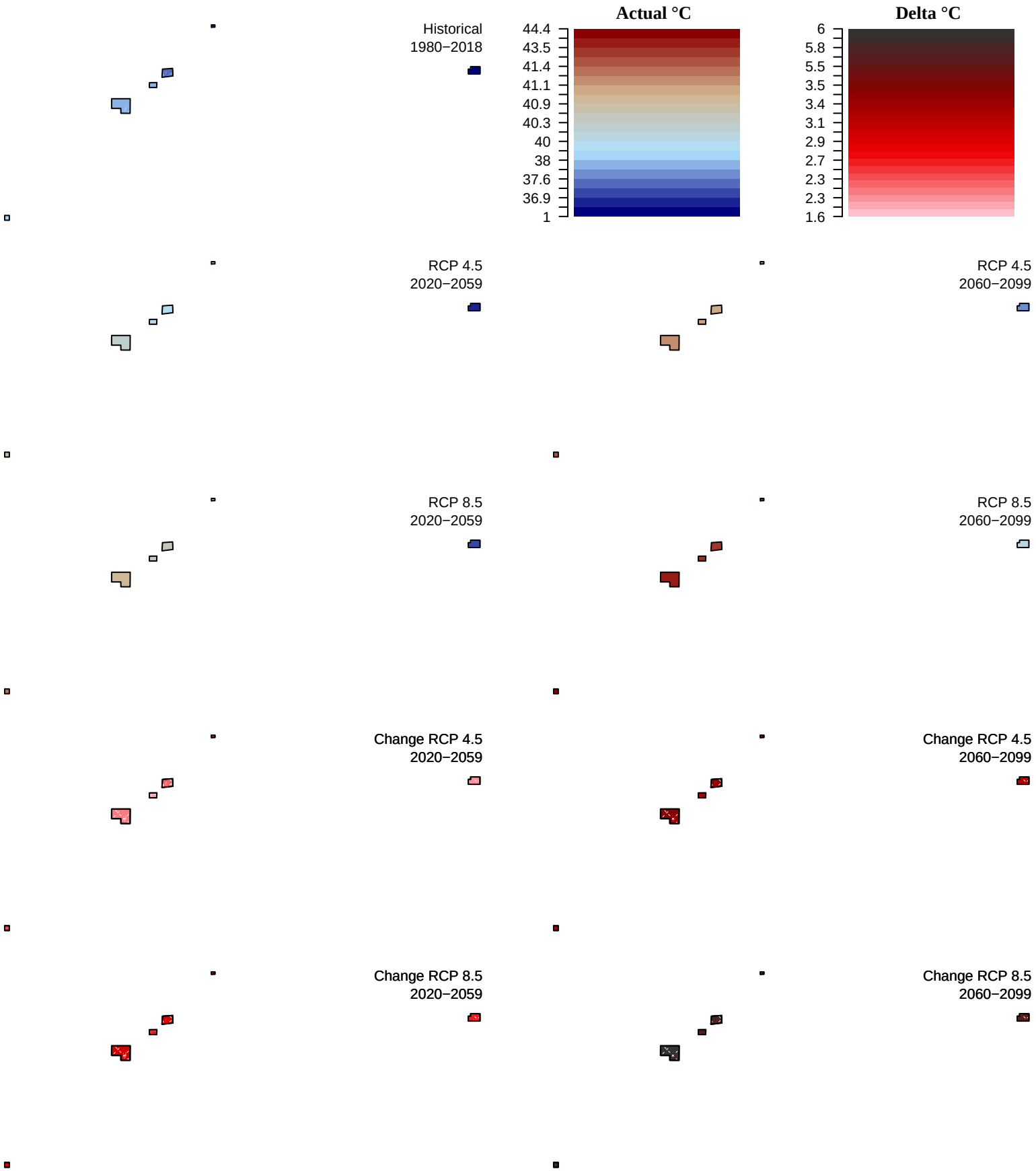


Figure HOVEmap23:
Past trends and future trajectories of park−wide mean values for Maximum summer temperature in Hovenweep. Topmost panel depicts the historical mean from 1980−2018. Lower four panels show the emission scenarios of RCP 4.5 and RCP 8.5 at near−term and long−term timeframes. Bottom four panels depict the change from the historical mean; cross hatching denotes areas of robust predicitons (90% of models agree in the direction of change).

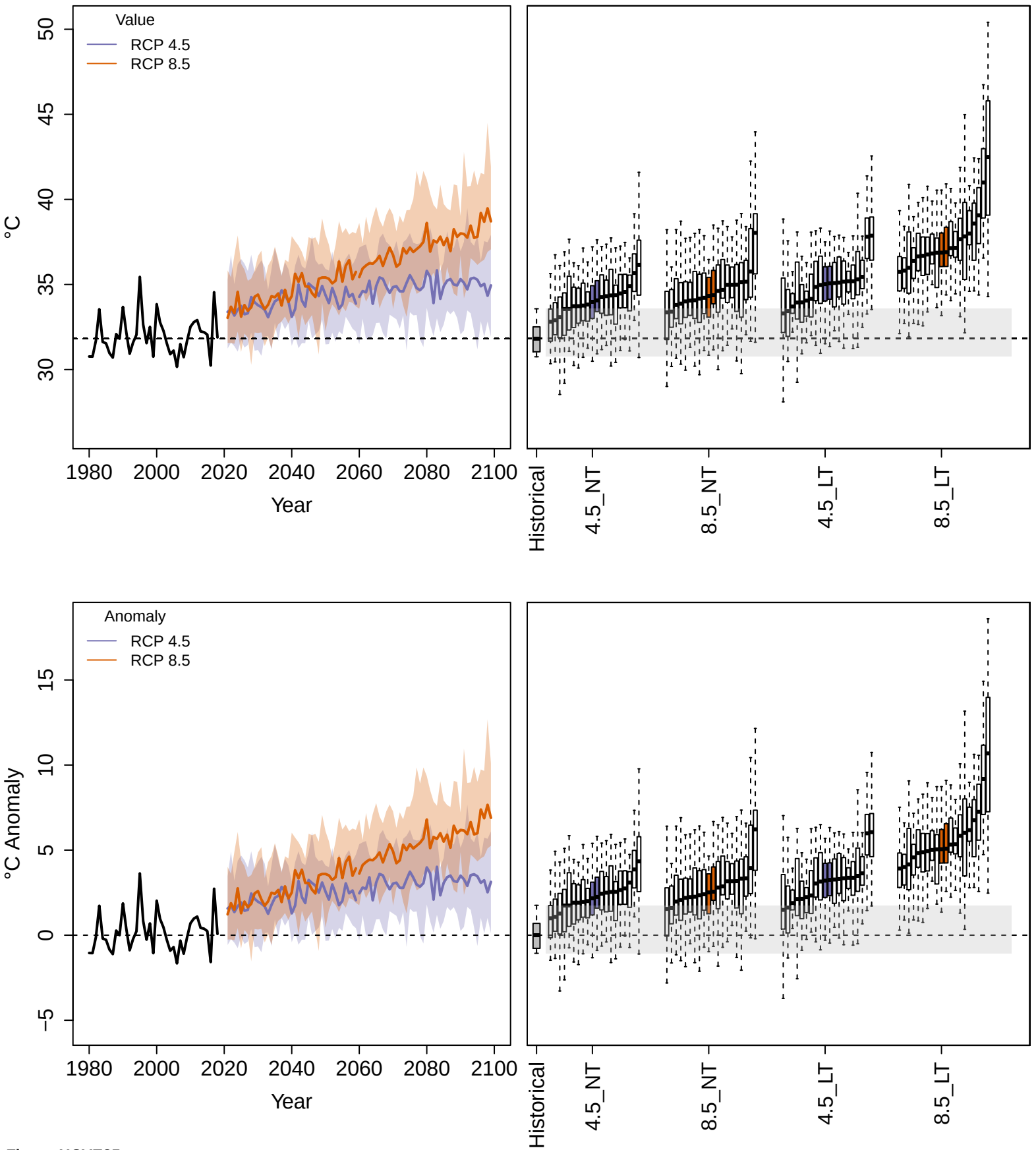


Figure HOVE25:
Past trends and future trajectories of park−wide mean values for Maximum fall temperature in Hovenweep. Top panels show values, bottom panels show changes from the long−term historical mean. Left: Time series of historical (black) and future projections for RCP 4.5 and 8.5. Shaded areas show spread among climate models. Right: Boxplots of temporal variability over 40−year periods under historical (left box) and individual climate models under two RCPs. Right: Historical time period is 1970−2010; near−term (NT) is 2020−2060; long−term (LT) is 2061−2100.

Hovenweep: Maximum fall temperature

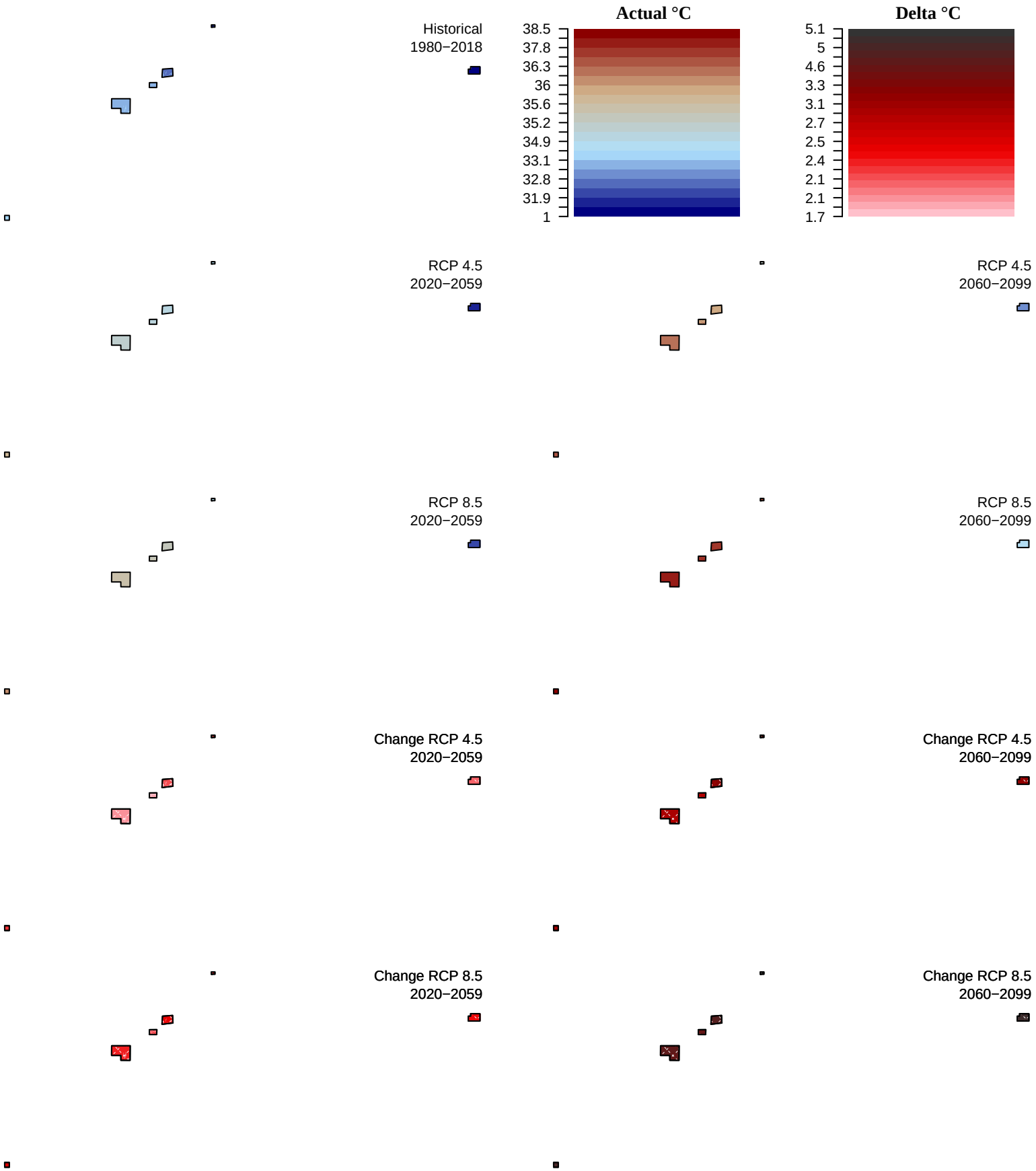


Figure HOVEmap25:
Past trends and future trajectories of park−wide mean values for Maximum fall temperature in Hovenweep. Topmost panel depicts the historical mean from 1980−2018. Lower four panels show the emission scenarios of RCP 4.5 and RCP 8.5 at near−term and long−term timeframes. Bottom four panels depict the change from the historical mean; cross hatching denotes areas of robust predicitons (90% of models agree in the direction of change).

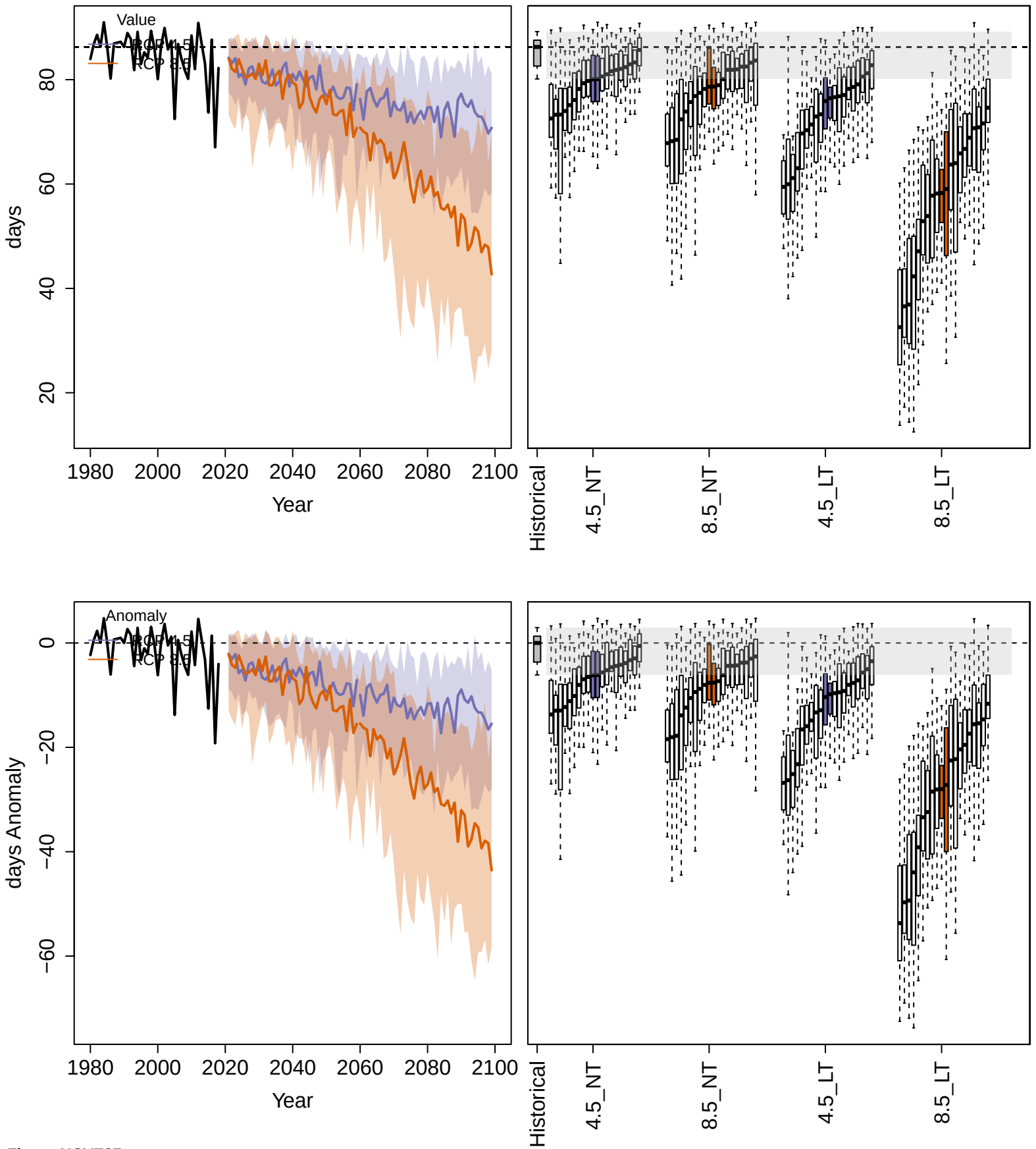


Figure HOVE27:
Past trends and future trajectories of park−wide mean values for Winter frost days in Hovenweep. Top panels show values, bottom panels show changes from the long−term historical mean. Left: Time series of historical (black) and future projections for RCP 4.5 and 8.5. Shaded areas show spread among climate models. Right: Boxplots of temporal variability over 40−year periods under historical (left box) and individual climate models under two RCPs. Right: Historical time period is 1970−2010; near−term (NT) is 2020−2060; long−term (LT) is 2061−2100.

Hovenweep: Winter frost days

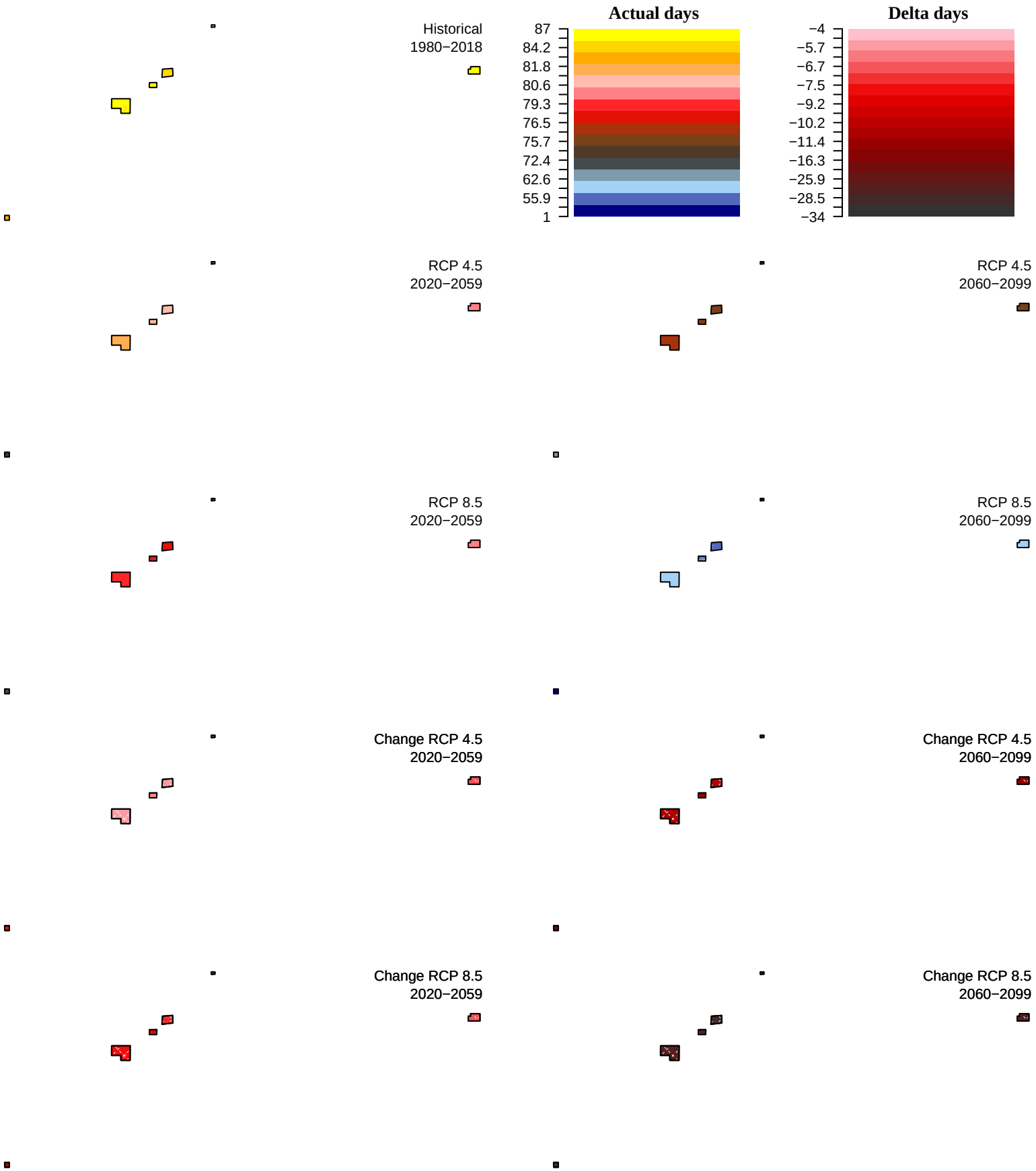


Figure HOVEmap27:
Past trends and future trajectories of park−wide mean values for Winter frost days in Hovenweep. Topmost panel depicts the historical mean from 1980−2018. Lower four panels show the emission scenarios of RCP 4.5 and RCP 8.5 at near−term and long−term timeframes. Bottom four panels depict the change from the historical mean; cross hatching denotes areas of robust predicitons (90% of models agree in the direction of change).

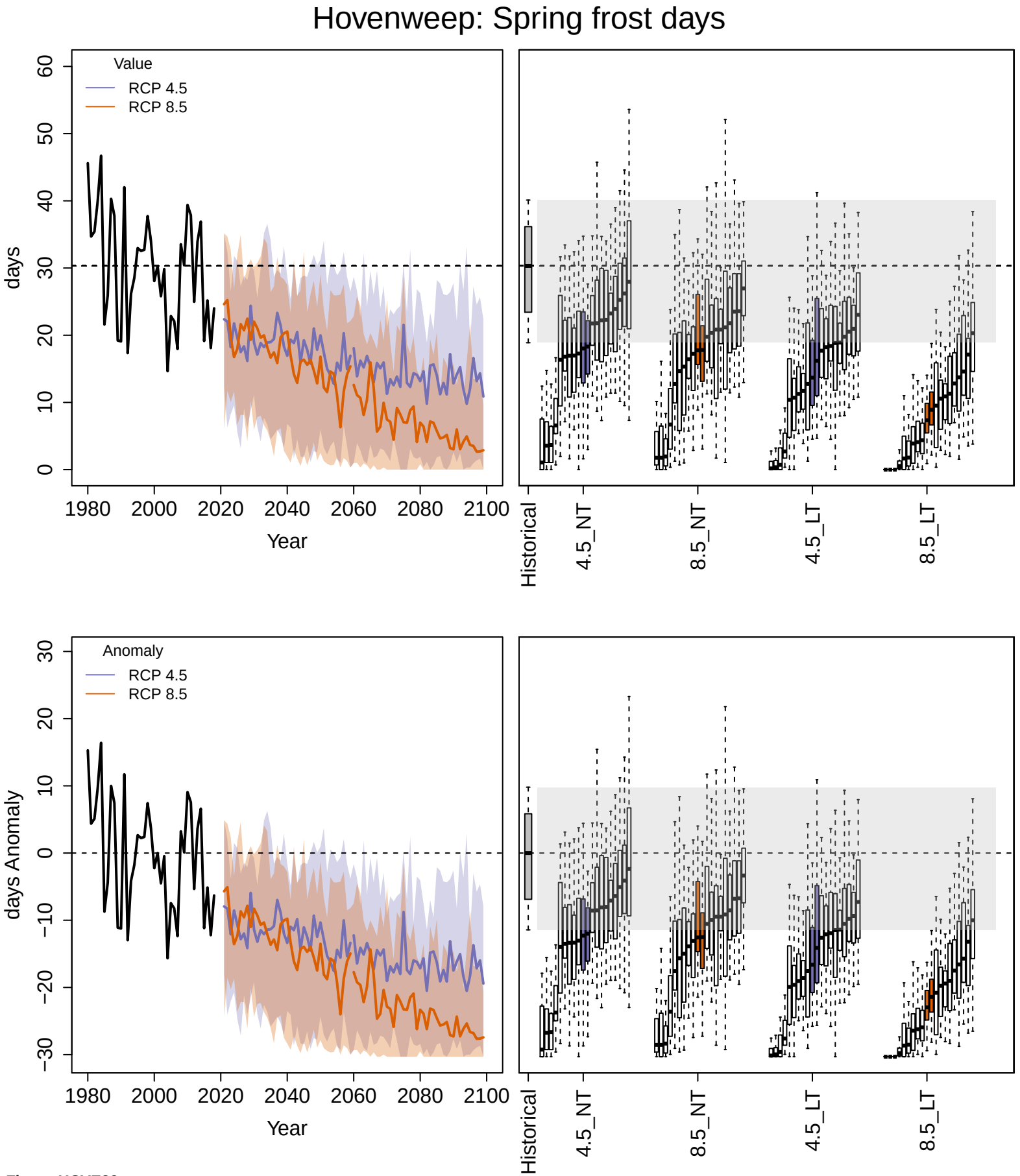


Figure HOVE29:
Past trends and future trajectories of park−wide mean values for Spring frost days in Hovenweep. Top panels show values, bottom panels show changes from the long−term historical mean. Left: Time series of historical (black) and future projections for RCP 4.5 and 8.5. Shaded areas show spread among climate models. Right: Boxplots of temporal variability over 40−year periods under historical (left box) and individual climate models under two RCPs. Right: Historical time period is 1970−2010; near−term (NT) is 2020−2060; long−term (LT) is 2061−2100.

Hovenweep: Spring frost days

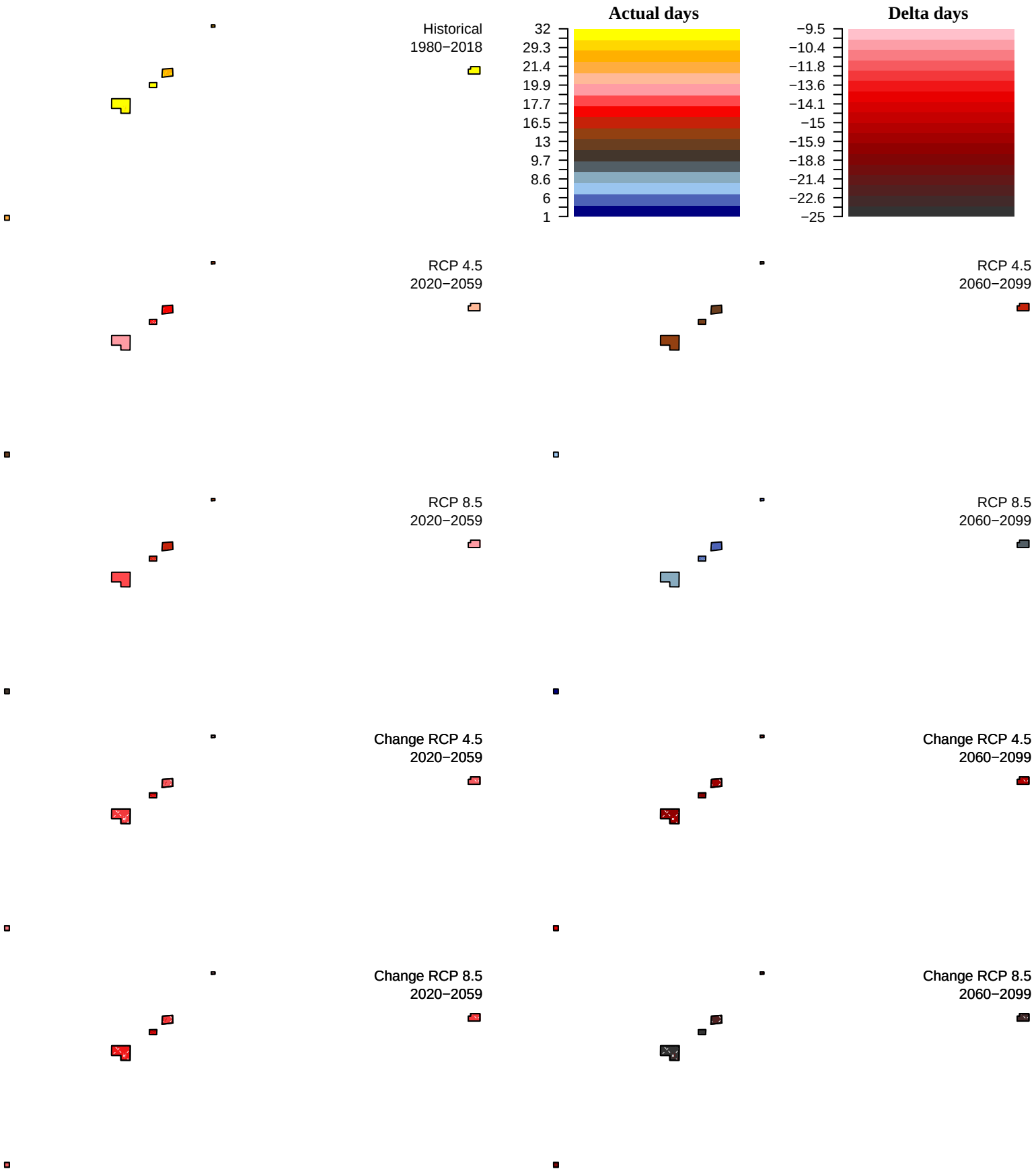


Figure HOVEmap29:
Past trends and future trajectories of park−wide mean values for Spring frost days in Hovenweep. Topmost panel depicts the historical mean from 1980−2018. Lower four panels show the emission scenarios of RCP 4.5 and RCP 8.5 at near−term and long−term timeframes. Bottom four panels depict the change from the historical mean; cross hatching denotes areas of robust predicitons (90% of models agree in the direction of change).

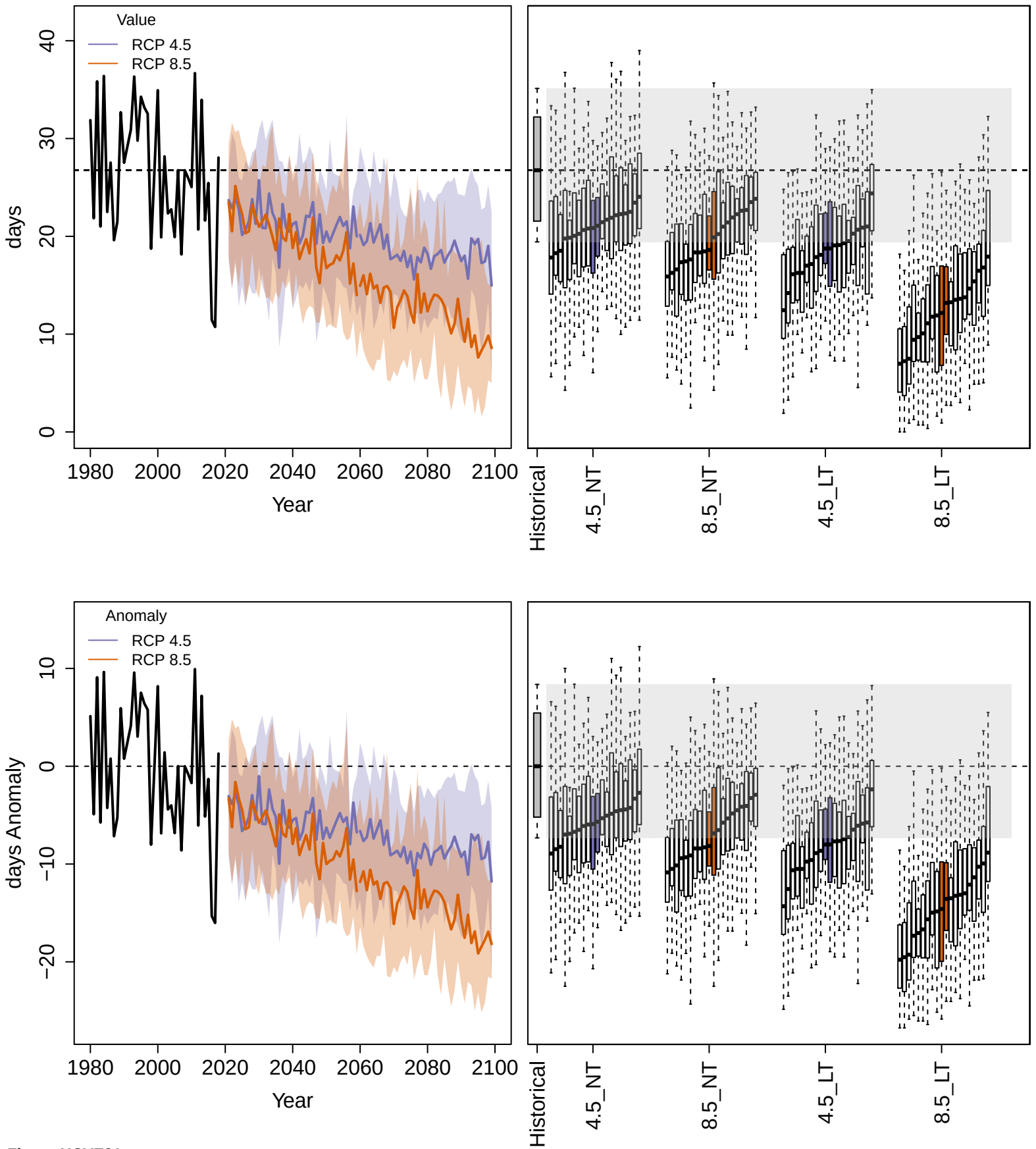


Figure HOVE31:
Past trends and future trajectories of park−wide mean values for Fall frost days in Hovenweep. Top panels show values, bottom panels show changes from the long−term historical mean. Left: Time series of historical (black) and future projections for RCP 4.5 and 8.5. Shaded areas show spread among climate models. Right: Boxplots of temporal variability over 40−year periods under historical (left box) and individual climate models under two RCPs. Right: Historical time period is 1970−2010; near−term (NT) is 2020−2060; long−term (LT) is 2061−2100.

Hovenweep: Fall frost days

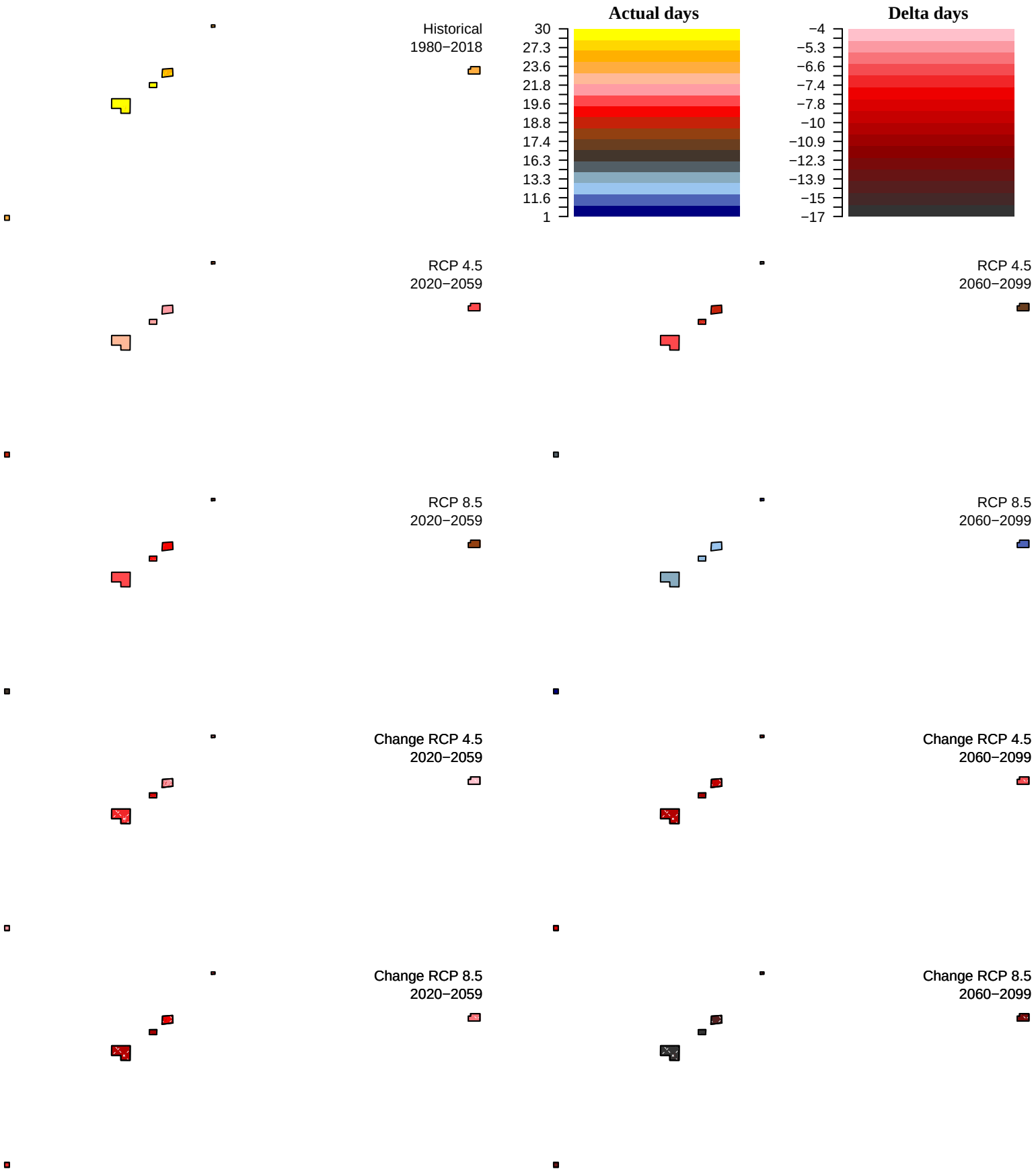


Figure HOVEmap31:
Past trends and future trajectories of park−wide mean values for Fall frost days in Hovenweep. Topmost panel depicts the historical mean from 1980−2018. Lower four panels show the emission scenarios of RCP 4.5 and RCP 8.5 at near−term and long−term timeframes. Bottom four panels depict the change from the historical mean; cross hatching denotes areas of robust predicitons (90% of models agree in the direction of change).

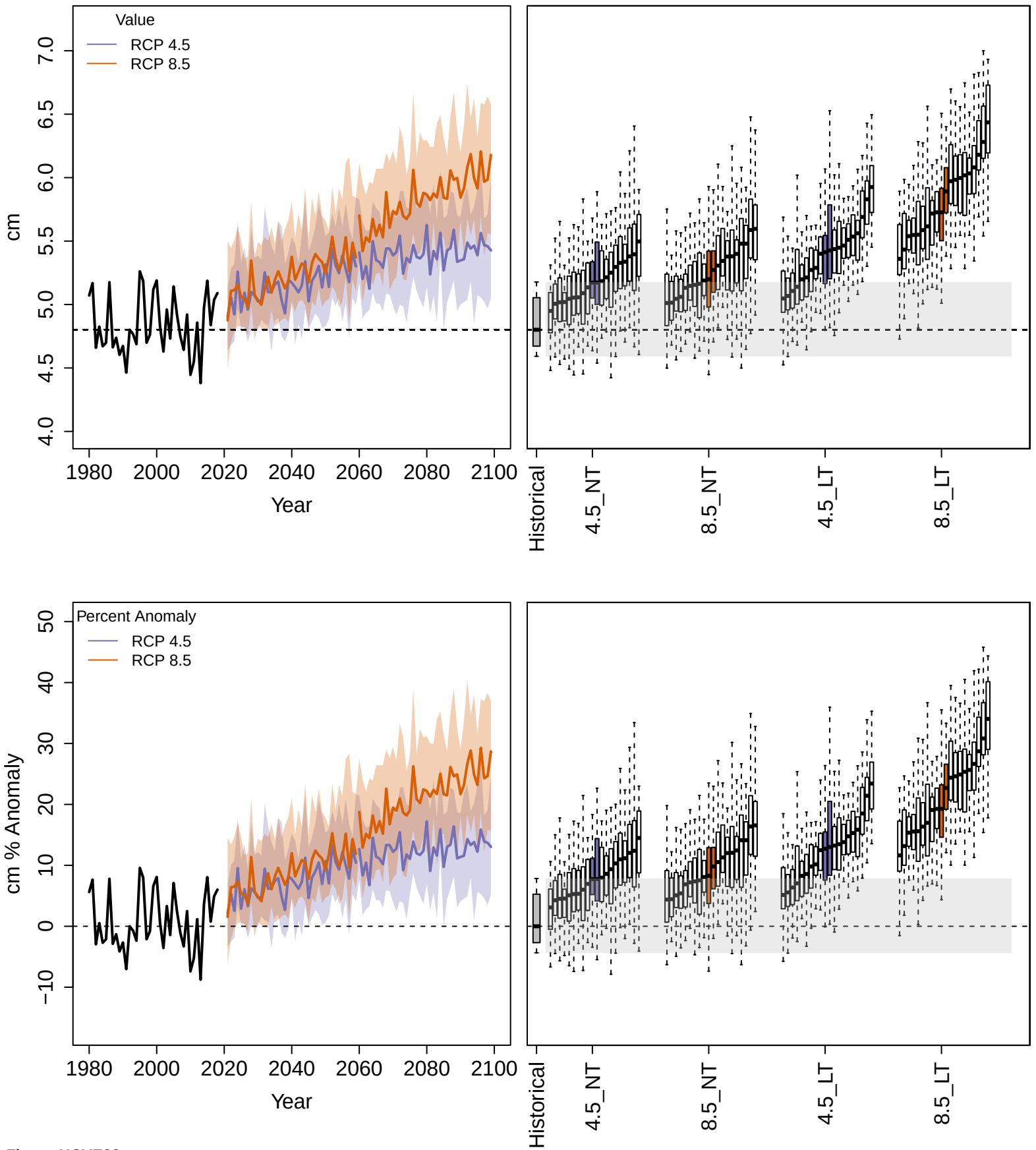


Figure HOVE33:
Past trends and future trajectories of park−wide mean values for Winter potential evapotranspiration in Hovenweep. Top panels show values, bottom panels show changes from the long−term historical mean. Left: Time series of historical (black) and future projections for RCP 4.5 and 8.5. Shaded areas show spread among climate models. Right: Boxplots of temporal variability over 40−year periods under historical (left box) and individual climate models under two RCPs. Right: Historical time period is 1970−2010; near−term (NT) is 2020−2060; long−term (LT) is 2061−2100.

Hovenweep: Winter potential evapotranspiration

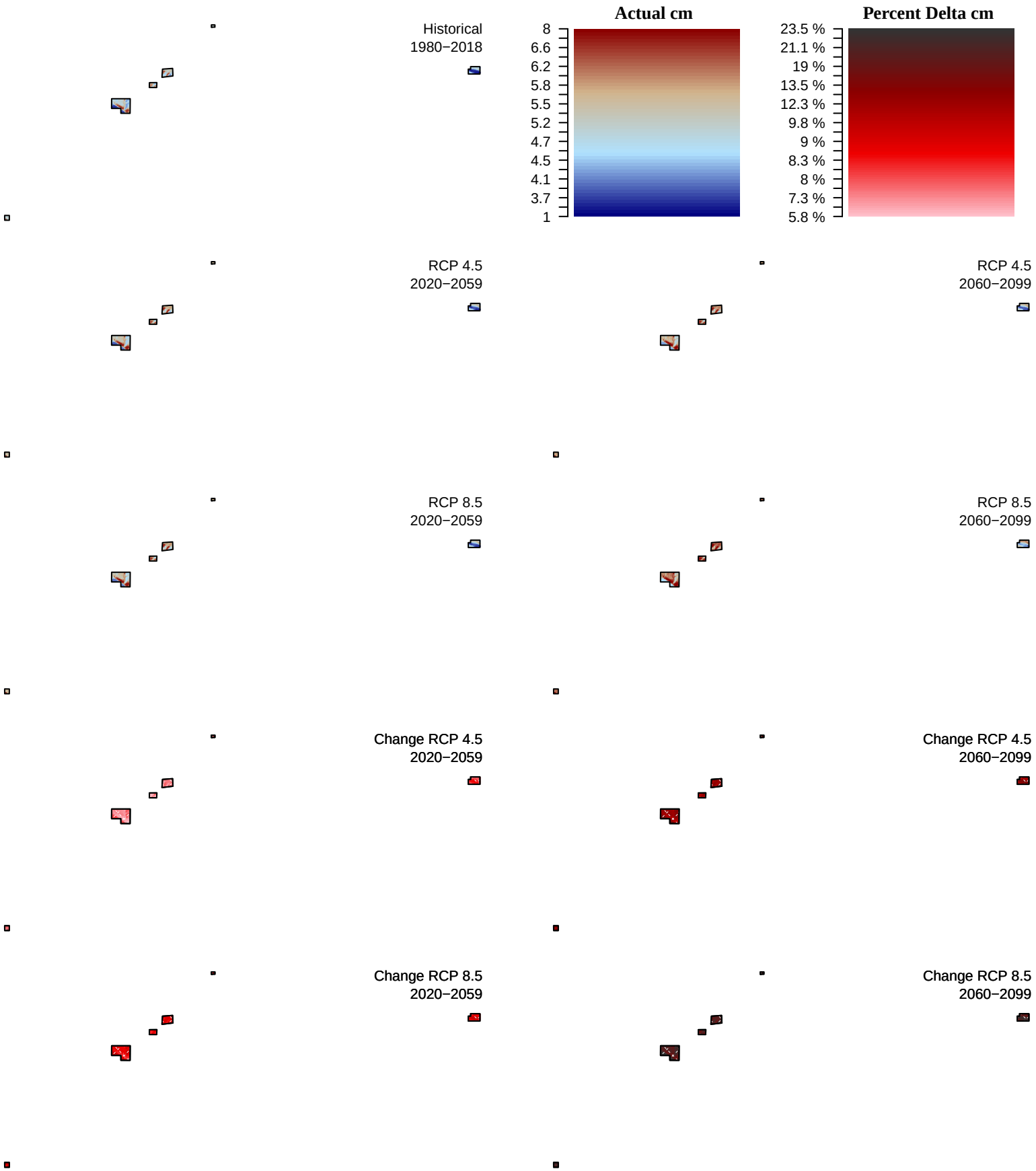


Figure HOVEmap33:
Past trends and future trajectories of park−wide mean values for Winter potential evapotranspiration in Hovenweep. Topmost panel depicts the historical mean from 1980−2018. Lower four panels show the emission scenarios of RCP 4.5 and RCP 8.5 at near−term and long−term timeframes. Bottom four panels depict the change from the historical mean; cross hatching denotes areas of robust predicitons (90% of models agree in the direction of change).

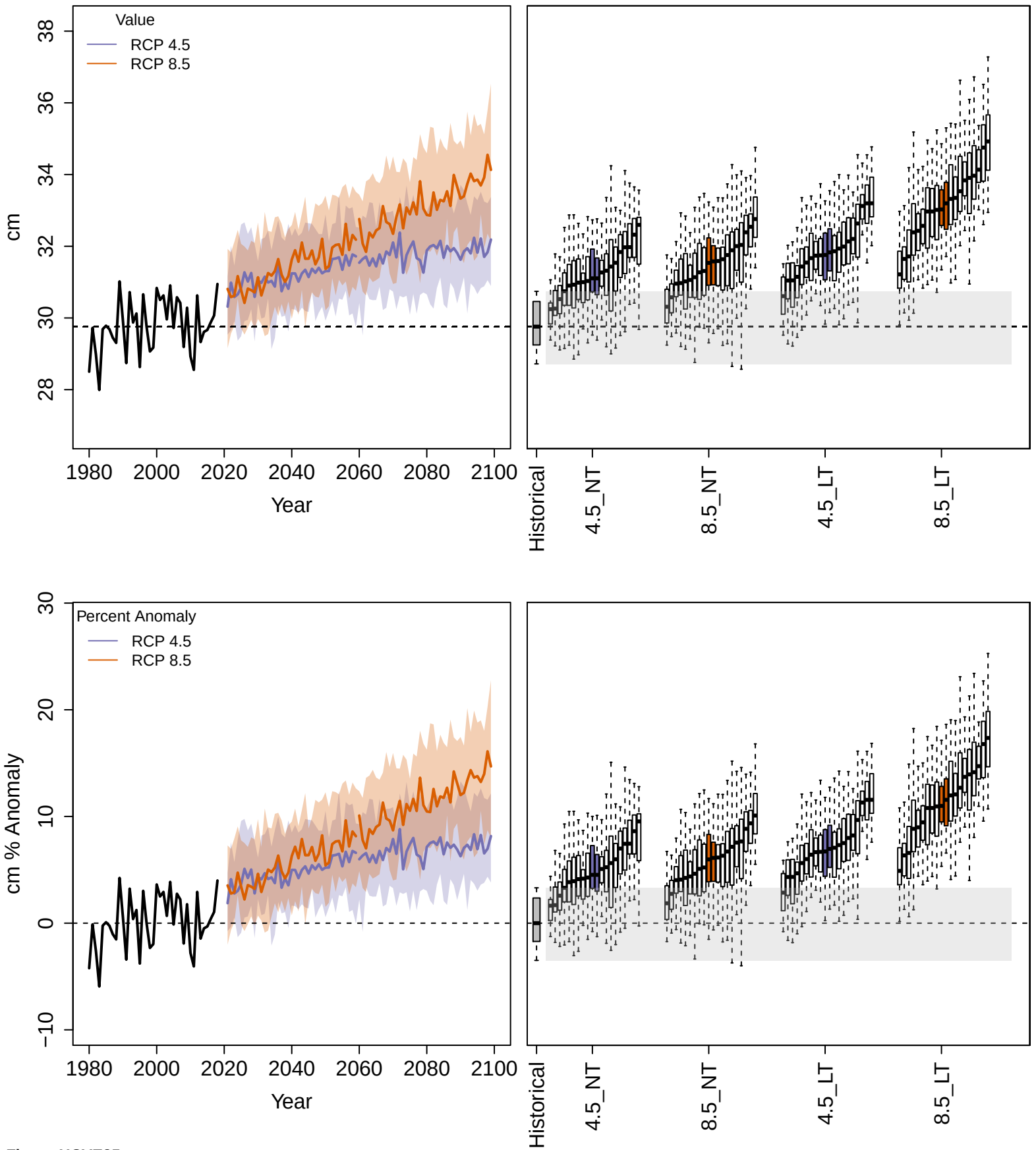


Figure HOVE35:
Past trends and future trajectories of park−wide mean values for Spring potential evapotranspiration in Hovenweep. Top panels show values, bottom panels show changes from the long−term historical mean. Left: Time series of historical (black) and future projections for RCP 4.5 and 8.5. Shaded areas show spread among climate models. Right: Boxplots of temporal variability over 40−year periods under historical (left box) and individual climate models under two RCPs. Right: Historical time period is 1970−2010; near−term (NT) is 2020−2060; long−term (LT) is 2061−2100.

Hovenweep: Spring potential evapotranspiration

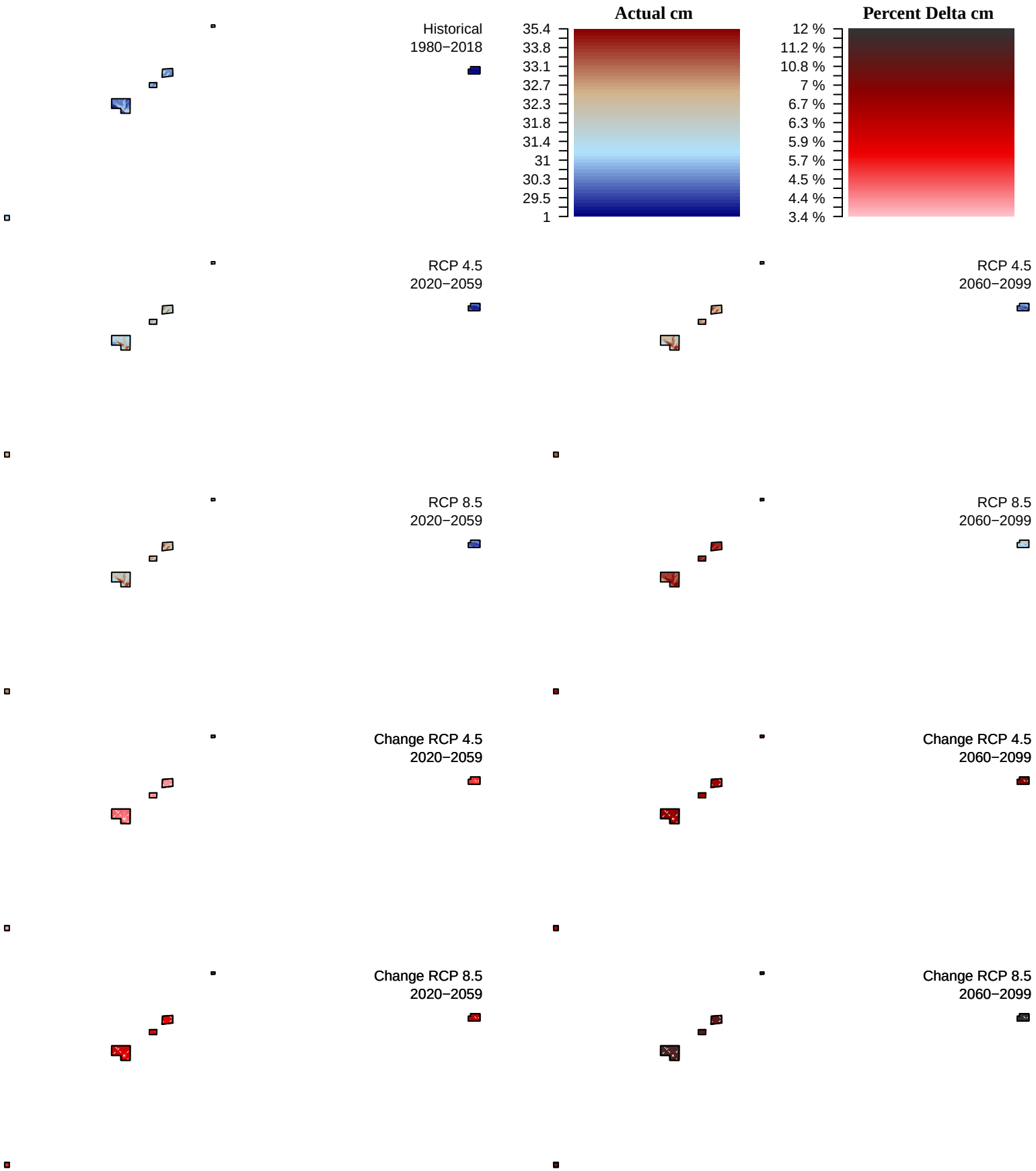


Figure HOVEmap35:
Past trends and future trajectories of park−wide mean values for Spring potential evapotranspiration in Hovenweep. Topmost panel depicts the historical mean from 1980−2018. Lower four panels show the emission scenarios of RCP 4.5 and RCP 8.5 at near−term and long−term timeframes. Bottom four panels depict the change from the historical mean; cross hatching denotes areas of robust predicitons (90% of models agree in the direction of change).

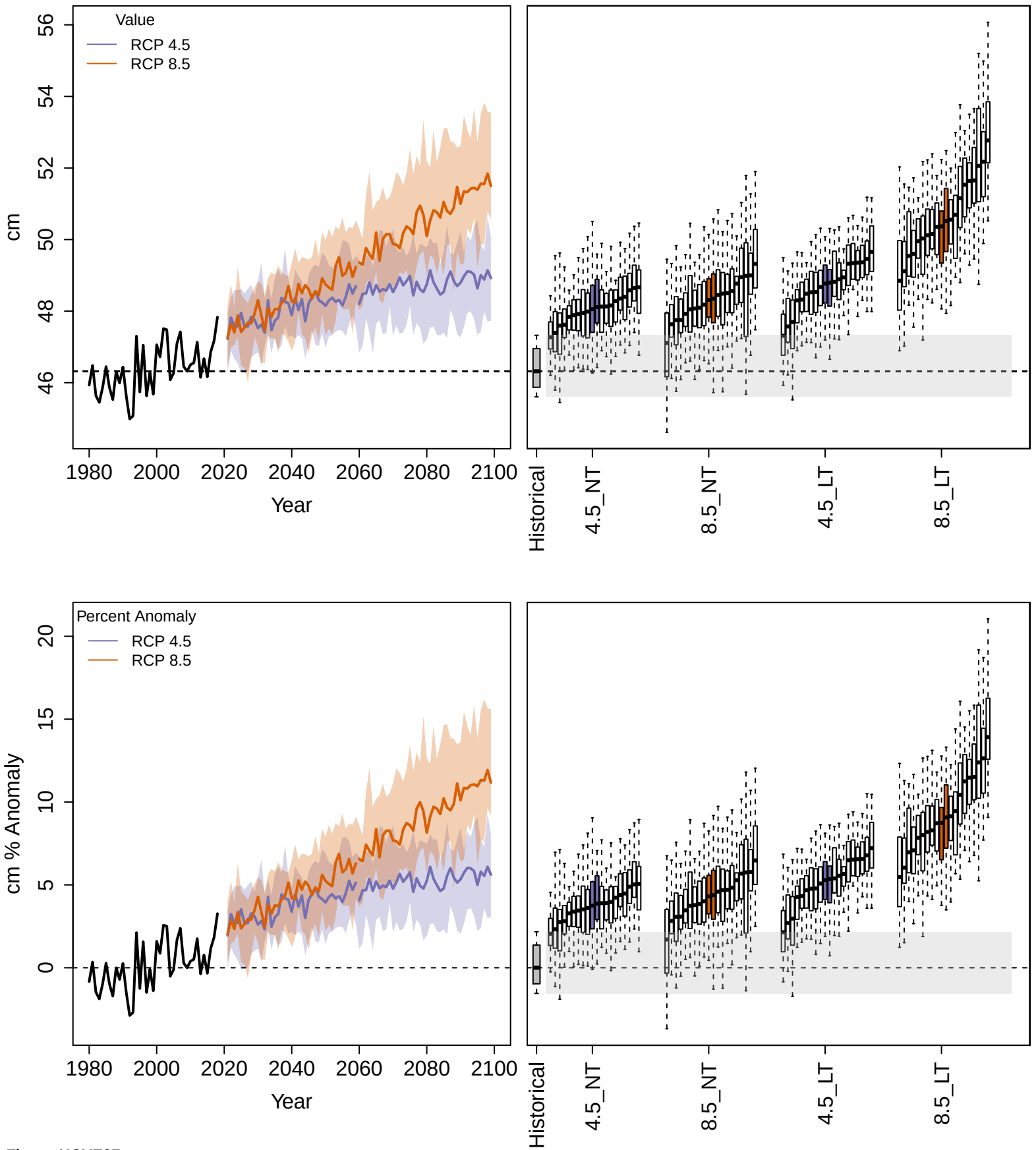


Figure HOVE37:
Past trends and future trajectories of park−wide mean values for Summer potential evapotranspiration in Hovenweep. Top panels show values, bottom panels show changes from the long−term historical mean. Left: Time series of historical (black) and future projections for RCP 4.5 and 8.5. Shaded areas show spread among climate models. Right: Boxplots of temporal variability over 40−year periods under historical (left box) and individual climate models under two RCPs. Right: Historical time period is 1970−2010; near−term (NT) is 2020−2060; long−term (LT) is 2061−2100.

Hovenweep: Summer potential evapotranspiration

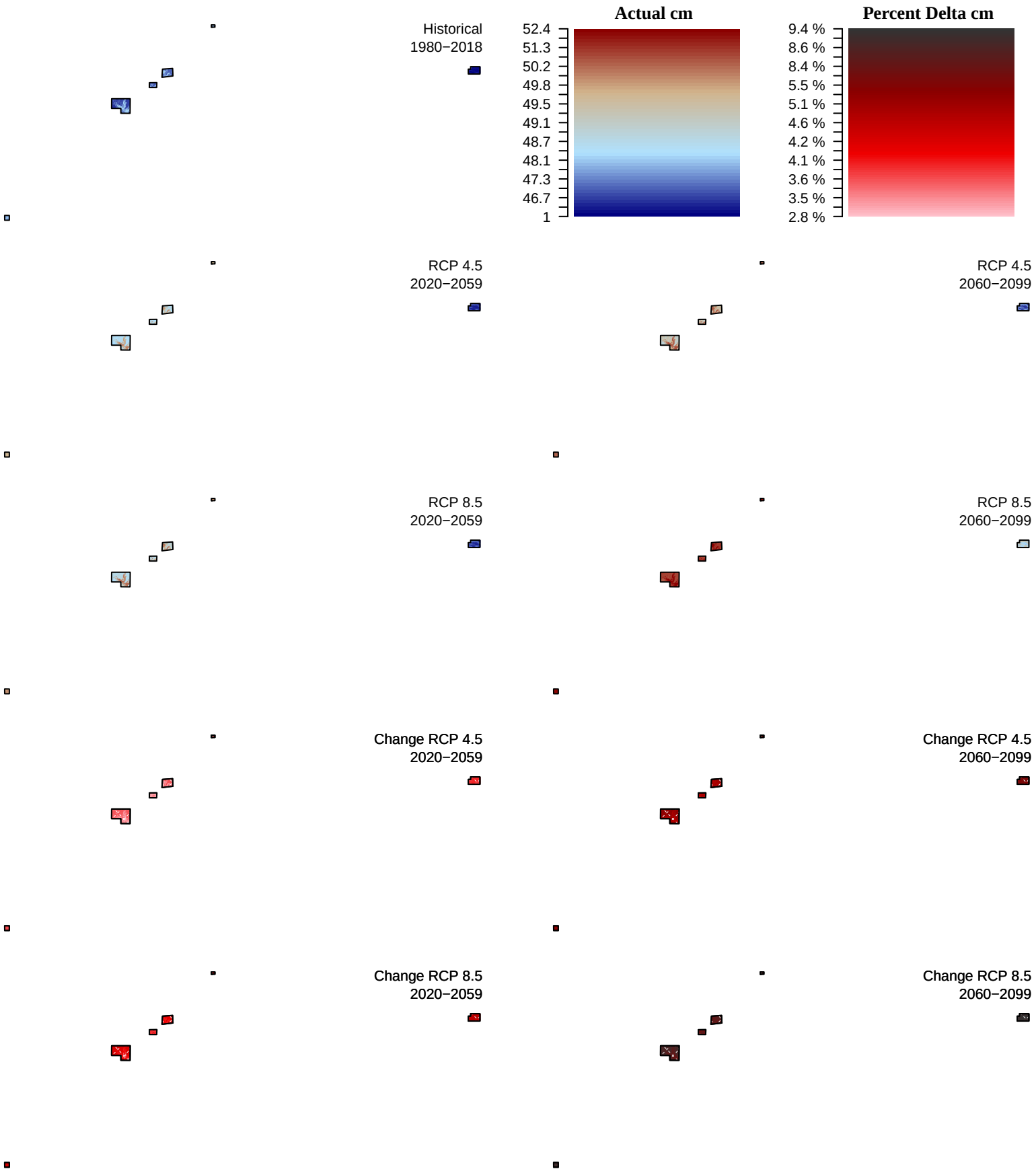


Figure HOVEmap37:
Past trends and future trajectories of park−wide mean values for Summer potential evapotranspiration in Hovenweep. Topmost panel depicts the historical mean from 1980−2018. Lower four panels show the emission scenarios of RCP 4.5 and RCP 8.5 at near−term and long−term timeframes. Bottom four panels depict the change from the historical mean; cross hatching denotes areas of robust predicitons (90% of models agree in the direction of change).

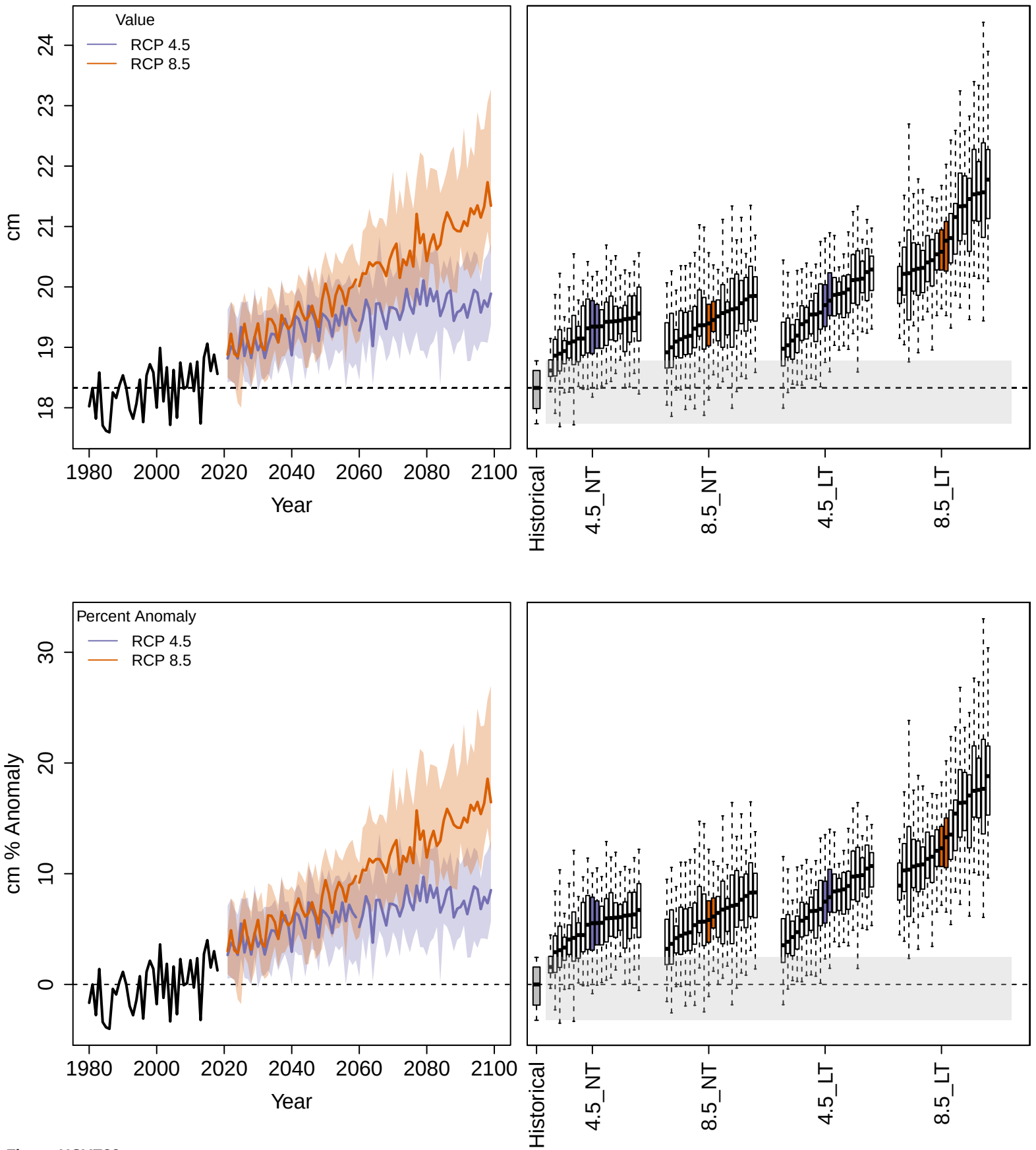


Figure HOVE39:
Past trends and future trajectories of park−wide mean values for Fall potential evapotranspiration in Hovenweep. Top panels show values, bottom panels show changes from the long−term historical mean. Left: Time series of historical (black) and future projections for RCP 4.5 and 8.5. Shaded areas show spread among climate models. Right: Boxplots of temporal variability over 40−year periods under historical (left box) and individual climate models under two RCPs. Right: Historical time period is 1970−2010; near−term (NT) is 2020−2060; long−term (LT) is 2061−2100.

Hovenweep: Fall potential evapotranspiration

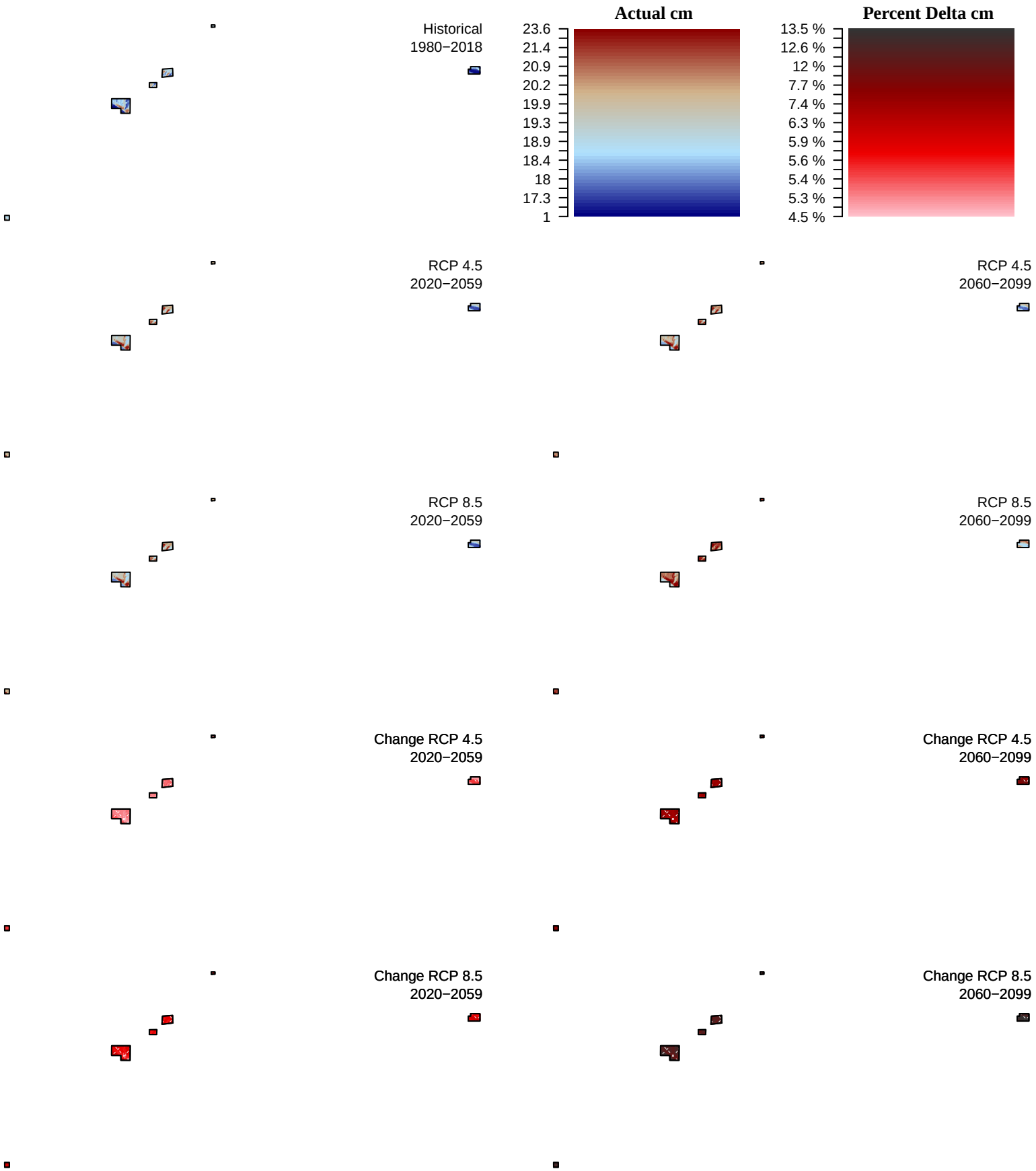


Figure HOVEmap39:
Past trends and future trajectories of park−wide mean values for Fall potential evapotranspiration in Hovenweep. Topmost panel depicts the historical mean from 1980−2018. Lower four panels show the emission scenarios of RCP 4.5 and RCP 8.5 at near−term and long−term timeframes. Bottom four panels depict the change from the historical mean; cross hatching denotes areas of robust predicitons (90% of models agree in the direction of change).

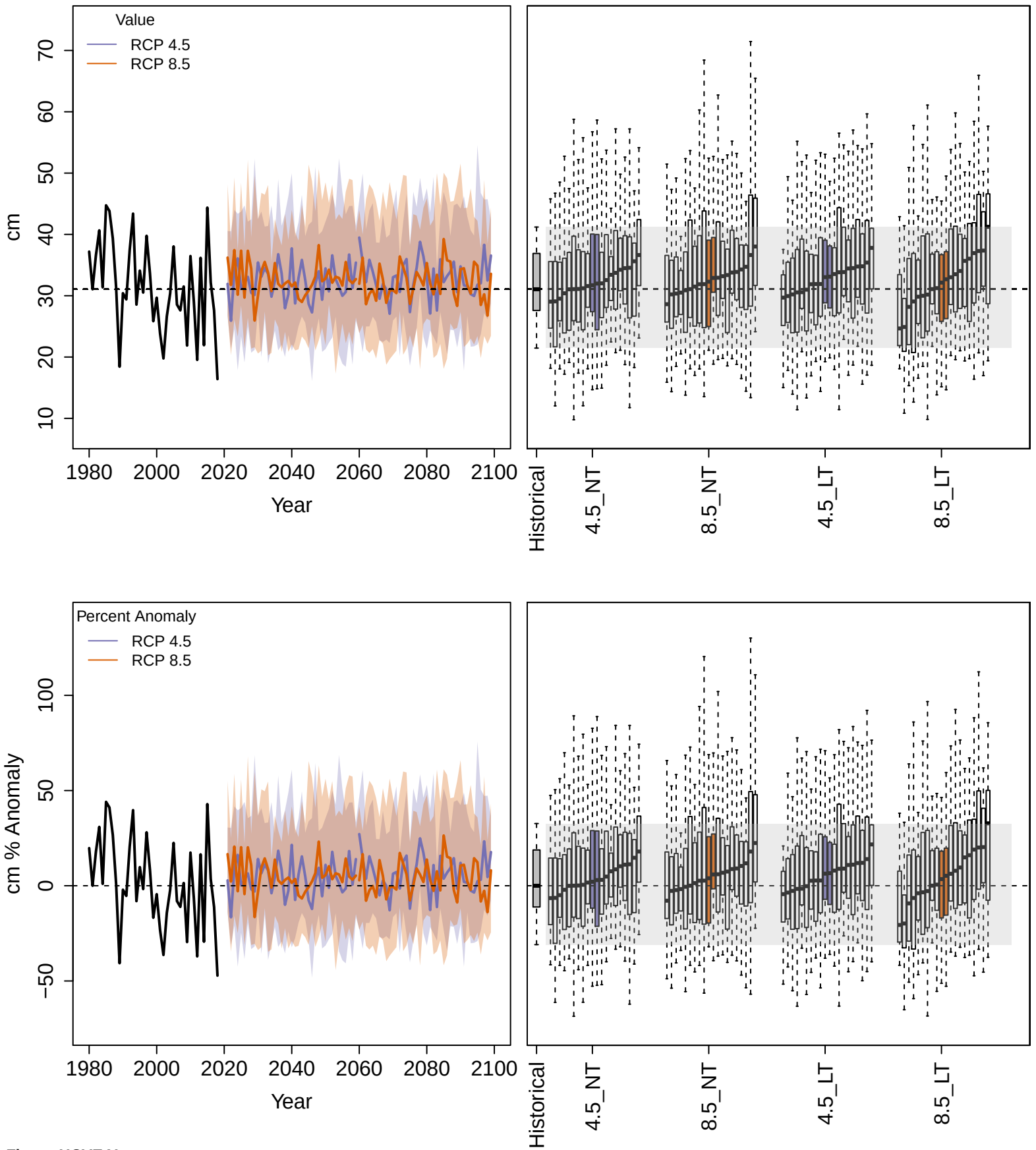


Figure HOVE41:
Past trends and future trajectories of park−wide mean values for Annual Precipitation in Hovenweep. Top panels show values, bottom panels show changes from the long−term historical mean. Left: Time series of historical (black) and future projections for RCP 4.5 and 8.5. Shaded areas show spread among climate models. Right: Boxplots of temporal variability over 40−year periods under historical (left box) and individual climate models under two RCPs. Right: Historical time period is 1970−2010; near−term (NT) is 2020−2060; long−term (LT) is 2061−2100.

Hovenweep: Annual Precipitation

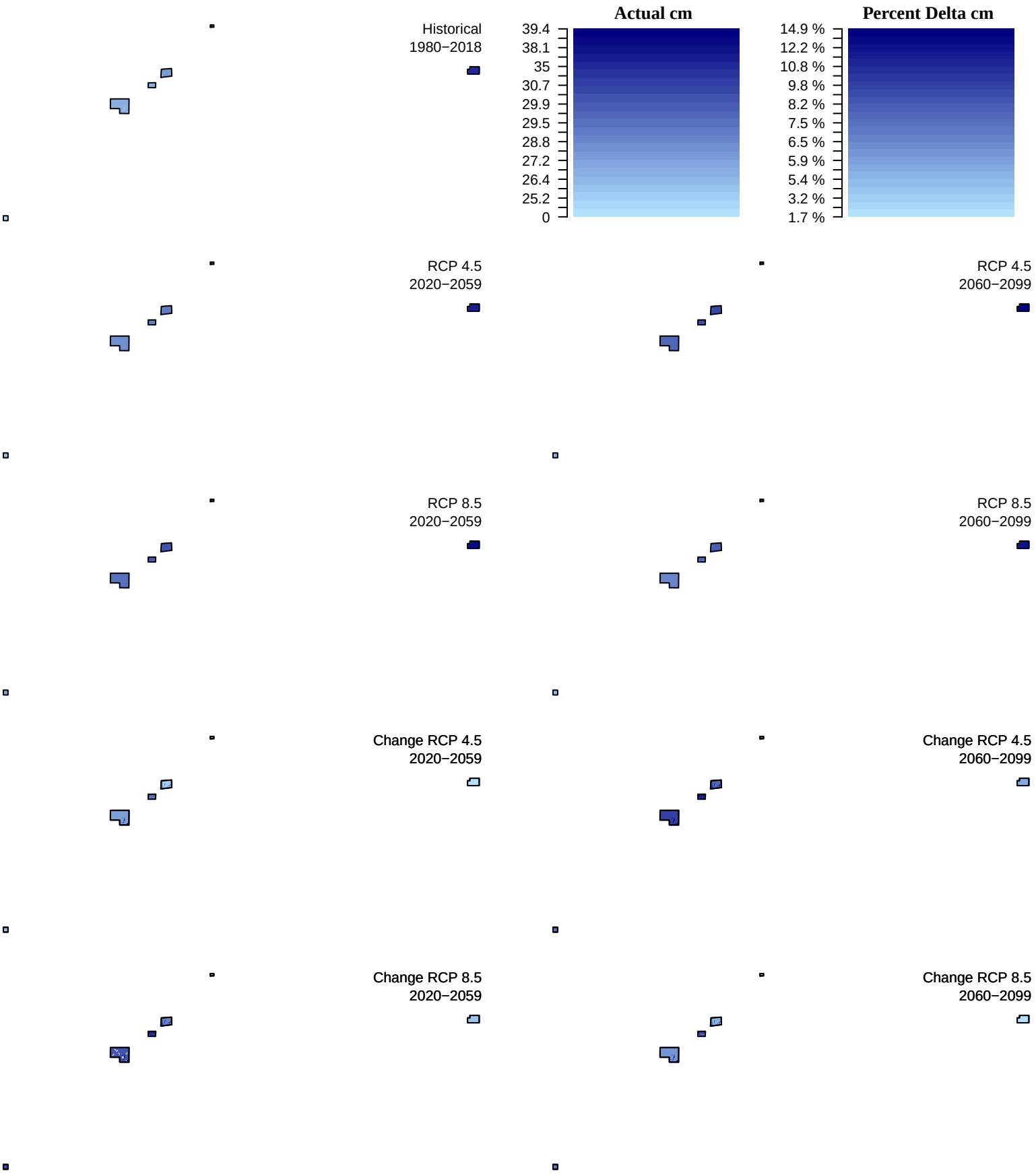


Figure HOVEmap41:
Past trends and future trajectories of park−wide mean values for Annual Precipitation in Hovenweep. Topmost panel depicts the historical mean from 1980−2018. Lower four panels show the emission scenarios of RCP 4.5 and RCP 8.5 at near−term and long−term timeframes. Bottom four panels depict the change from the historical mean; cross hatching denotes areas of robust predicitons (90% of models agree in the direction of change).

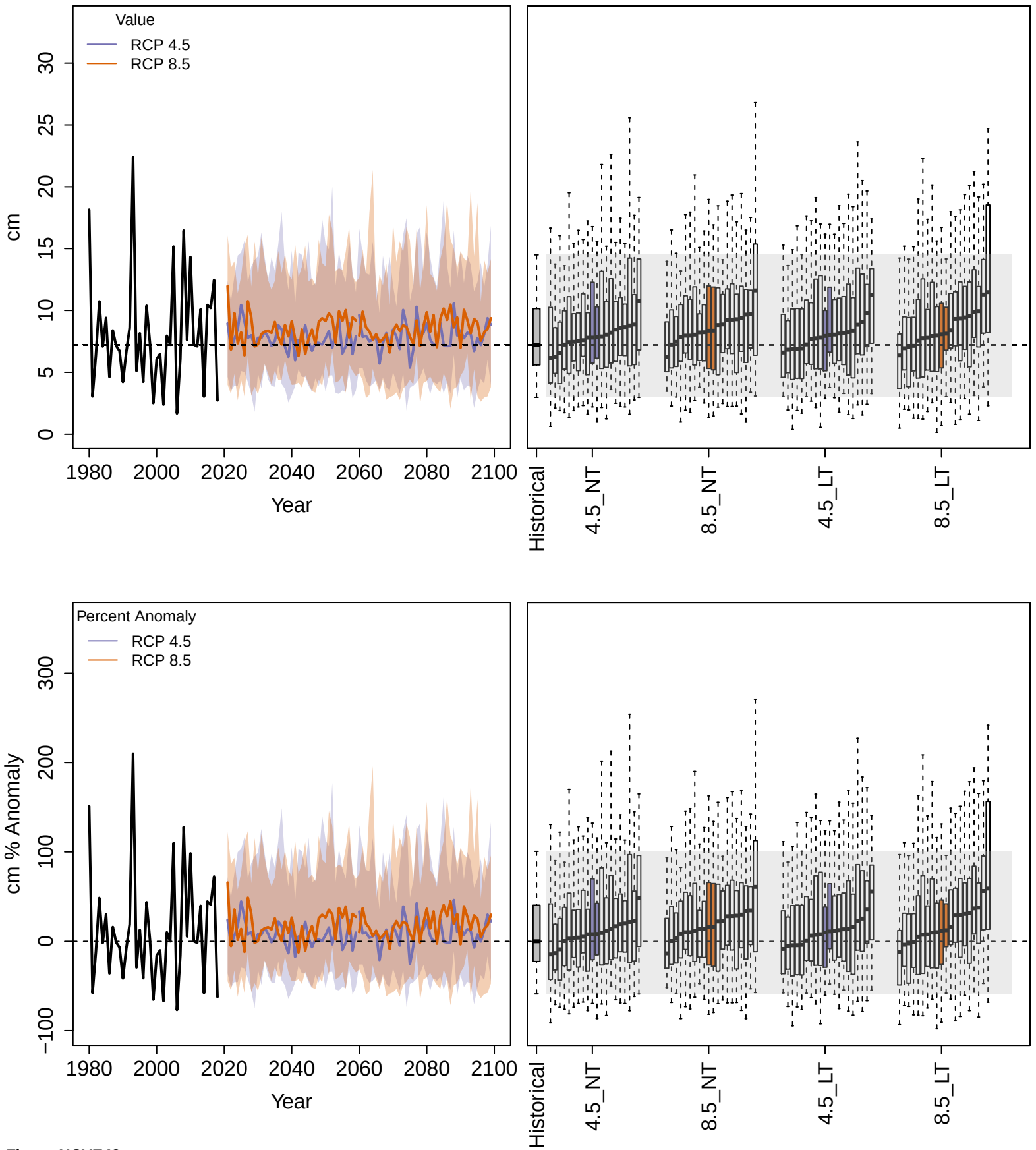


Figure HOVE43:
Past trends and future trajectories of park−wide mean values for Winter Precipitation in Hovenweep. Top panels show values, bottom panels show changes from the long−term historical mean. Left: Time series of historical (black) and future projections for RCP 4.5 and 8.5. Shaded areas show spread among climate models. Right: Boxplots of temporal variability over 40−year periods under historical (left box) and individual climate models under two RCPs. Right: Historical time period is 1970−2010; near−term (NT) is 2020−2060; long−term (LT) is 2061−2100.

Hovenweep: Winter Precipitation

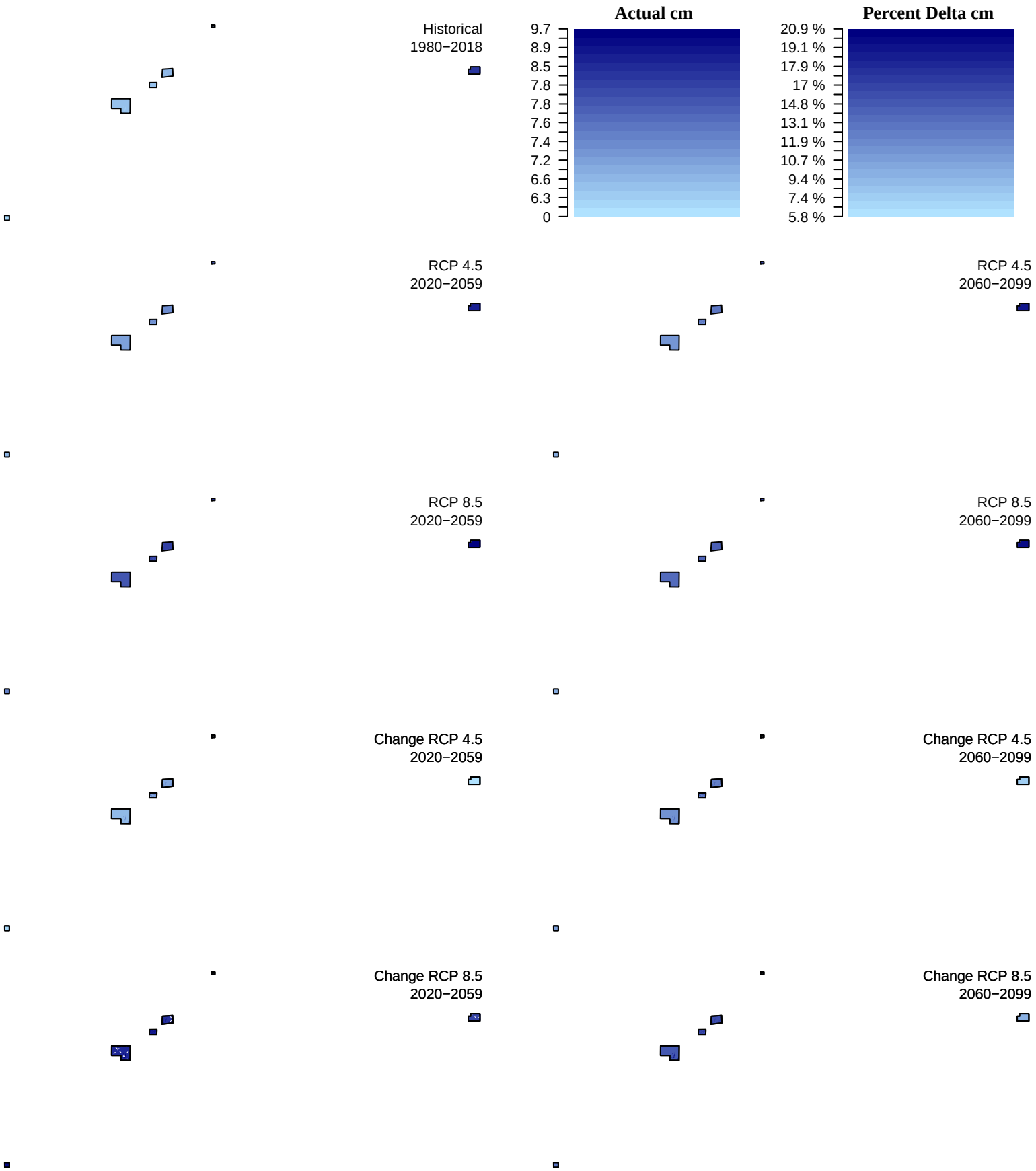


Figure HOVEmap43:
Past trends and future trajectories of park−wide mean values for Winter Precipitation in Hovenweep. Topmost panel depicts the historical mean from 1980−2018. Lower four panels show the emission scenarios of RCP 4.5 and RCP 8.5 at near−term and long−term timeframes. Bottom four panels depict the change from the historical mean; cross hatching denotes areas of robust predicitons (90% of models agree in the direction of change).

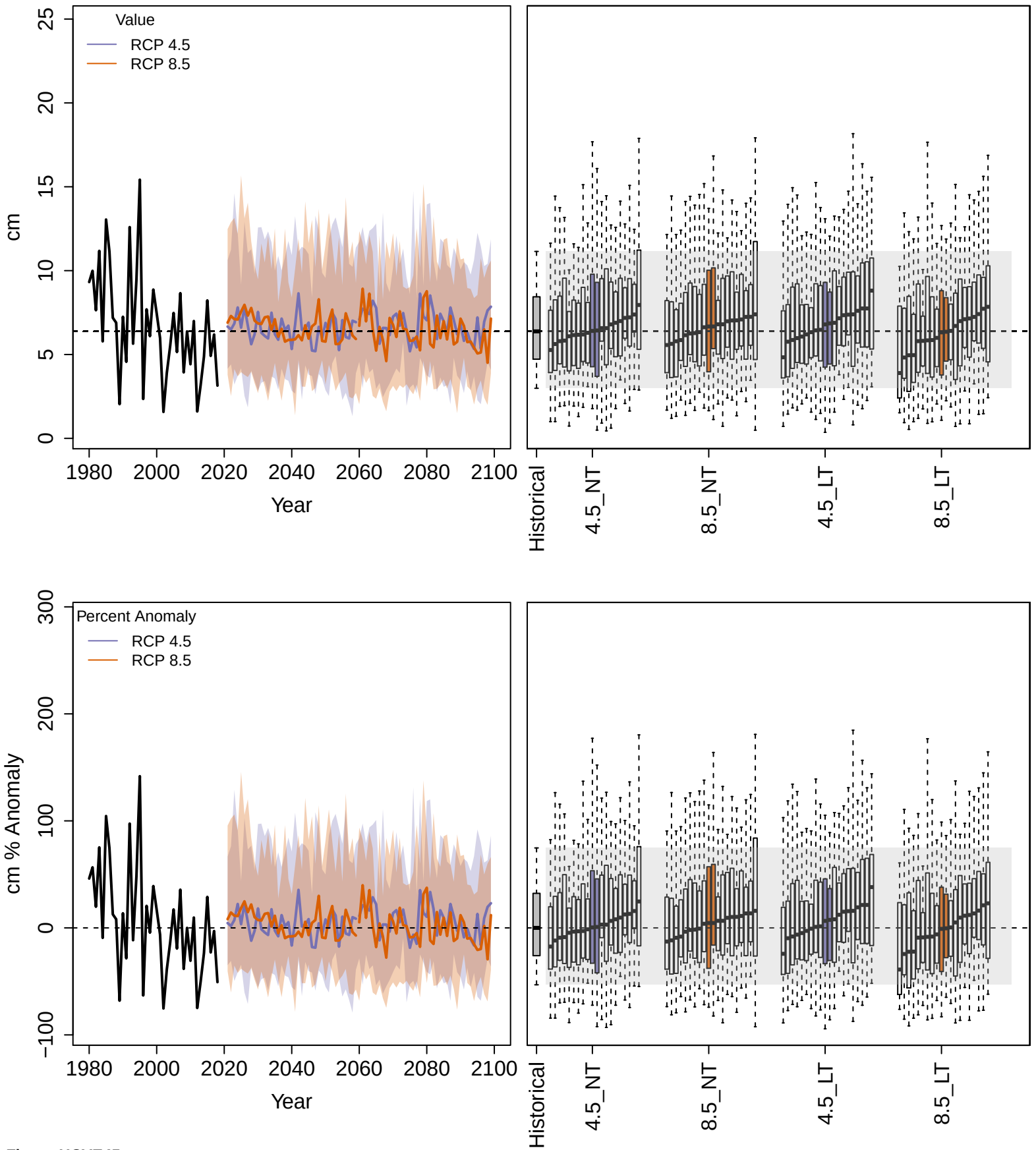


Figure HOVE45:
Past trends and future trajectories of park−wide mean values for Spring Precipitation in Hovenweep. Top panels show values, bottom panels show changes from the long−term historical mean. Left: Time series of historical (black) and future projections for RCP 4.5 and 8.5. Shaded areas show spread among climate models. Right: Boxplots of temporal variability over 40−year periods under historical (left box) and individual climate models under two RCPs. Right: Historical time period is 1970−2010; near−term (NT) is 2020−2060; long−term (LT) is 2061−2100.

Hovenweep: Spring Precipitation

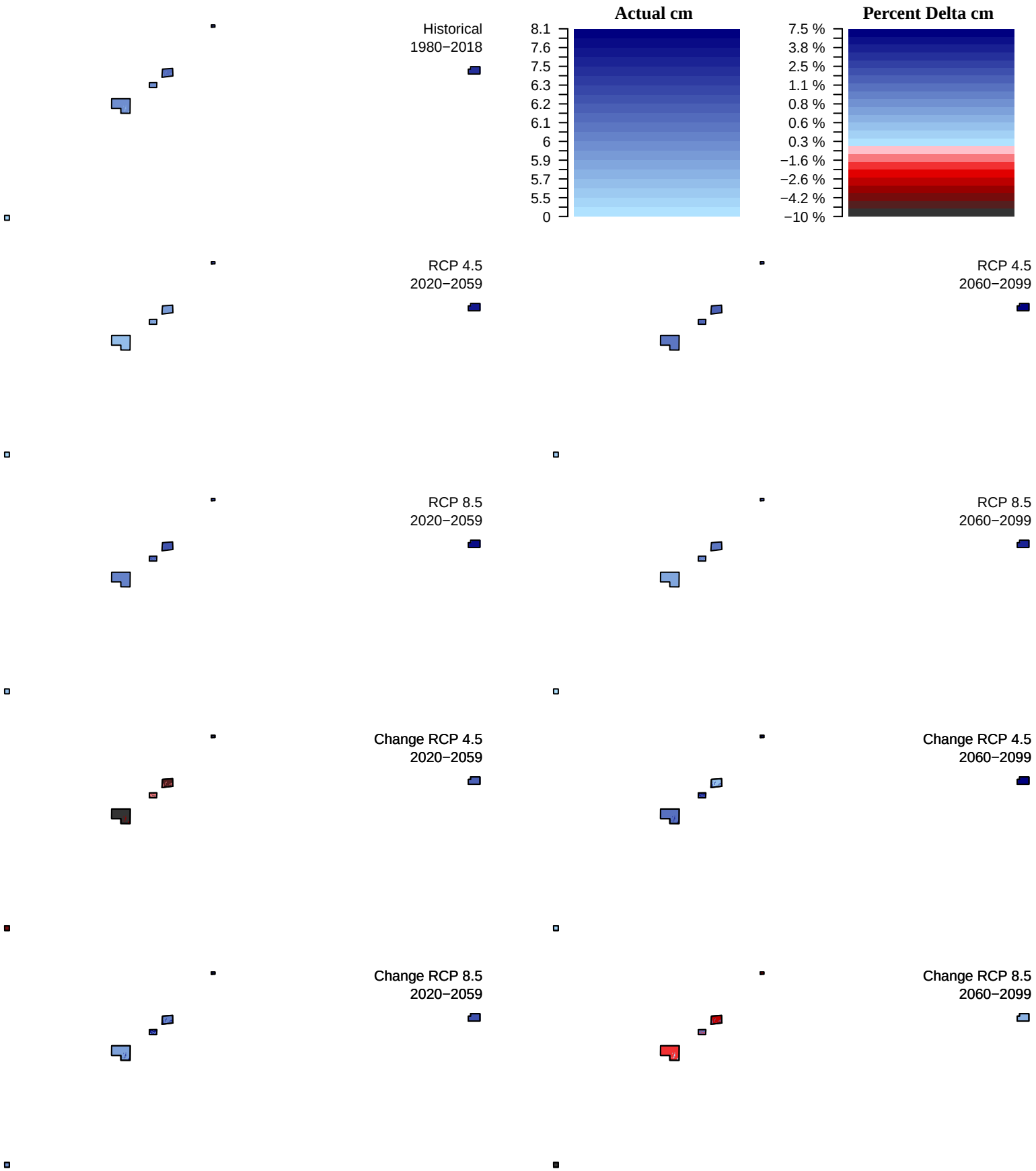


Figure HOVEmap45:
Past trends and future trajectories of park−wide mean values for Spring Precipitation in Hovenweep. Topmost panel depicts the historical mean from 1980−2018. Lower four panels show the emission scenarios of RCP 4.5 and RCP 8.5 at near−term and long−term timeframes. Bottom four panels depict the change from the historical mean; cross hatching denotes areas of robust predicitons (90% of models agree in the direction of change).

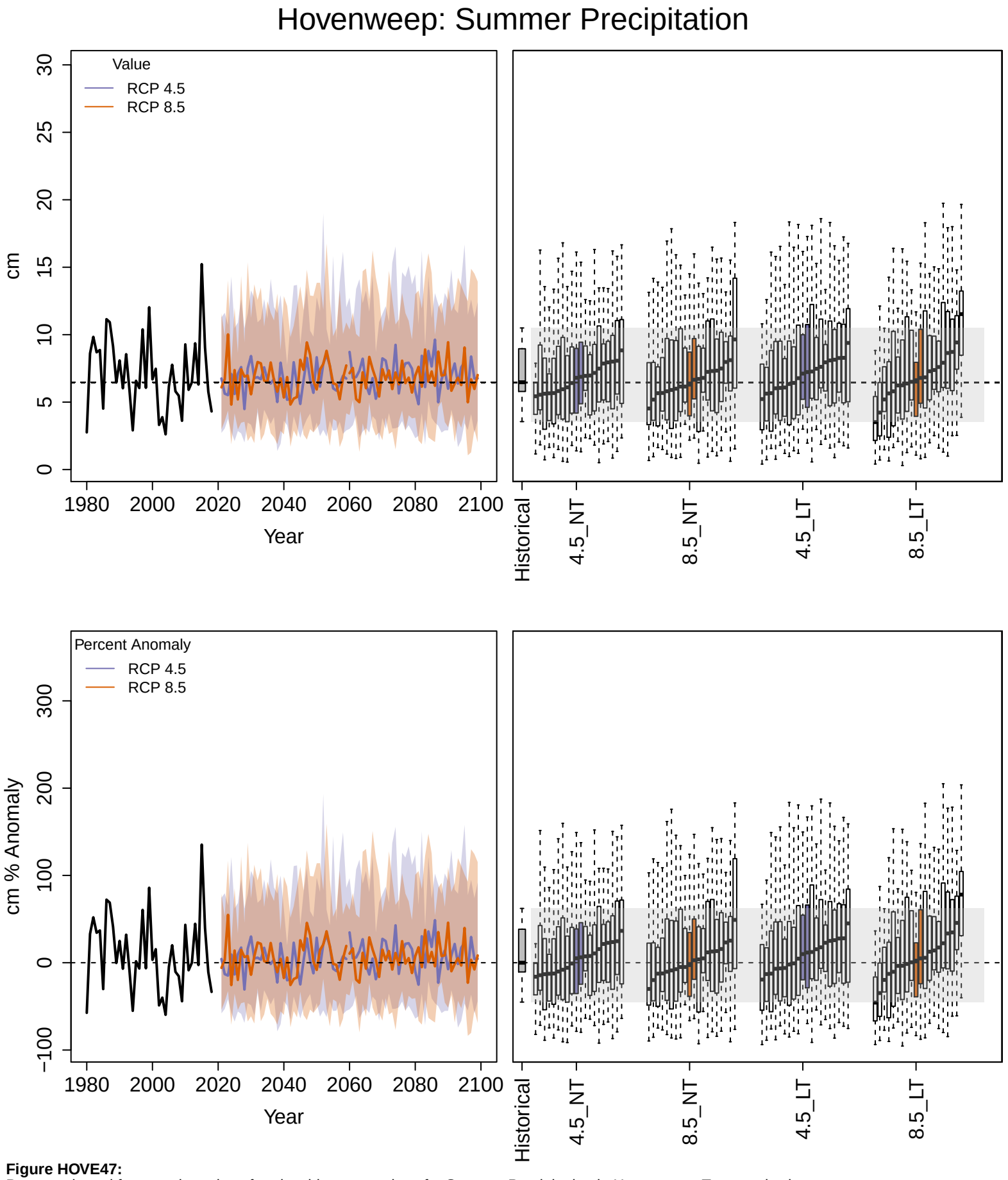


Figure HOVE47:
Past trends and future trajectories of park−wide mean values for Summer Precipitation in Hovenweep. Top panels show values, bottom panels show changes from the long−term historical mean. Left: Time series of historical (black) and future projections for RCP 4.5 and 8.5. Shaded areas show spread among climate models. Right: Boxplots of temporal variability over 40−year periods under historical (left box) and individual climate models under two RCPs. Right: Historical time period is 1970−2010; near−term (NT) is 2020−2060; long−term (LT) is 2061−2100.

Hovenweep: Summer Precipitation

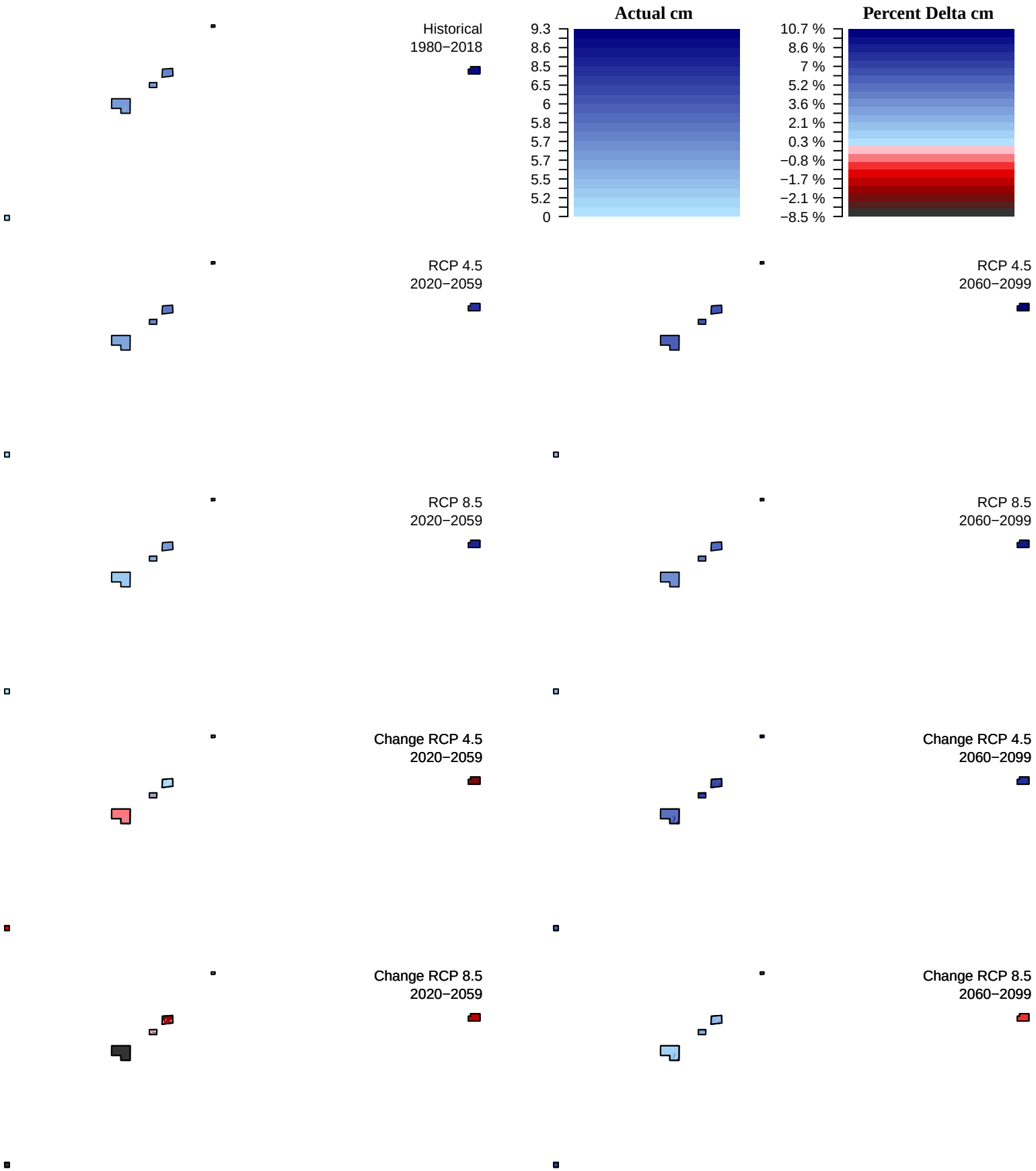


Figure HOVEmap47:
Past trends and future trajectories of park−wide mean values for Summer Precipitation in Hovenweep. Topmost panel depicts the historical mean from 1980−2018. Lower four panels show the emission scenarios of RCP 4.5 and RCP 8.5 at near−term and long−term timeframes. Bottom four panels depict the change from the historical mean; cross hatching denotes areas of robust predicitons (90% of models agree in the direction of change).

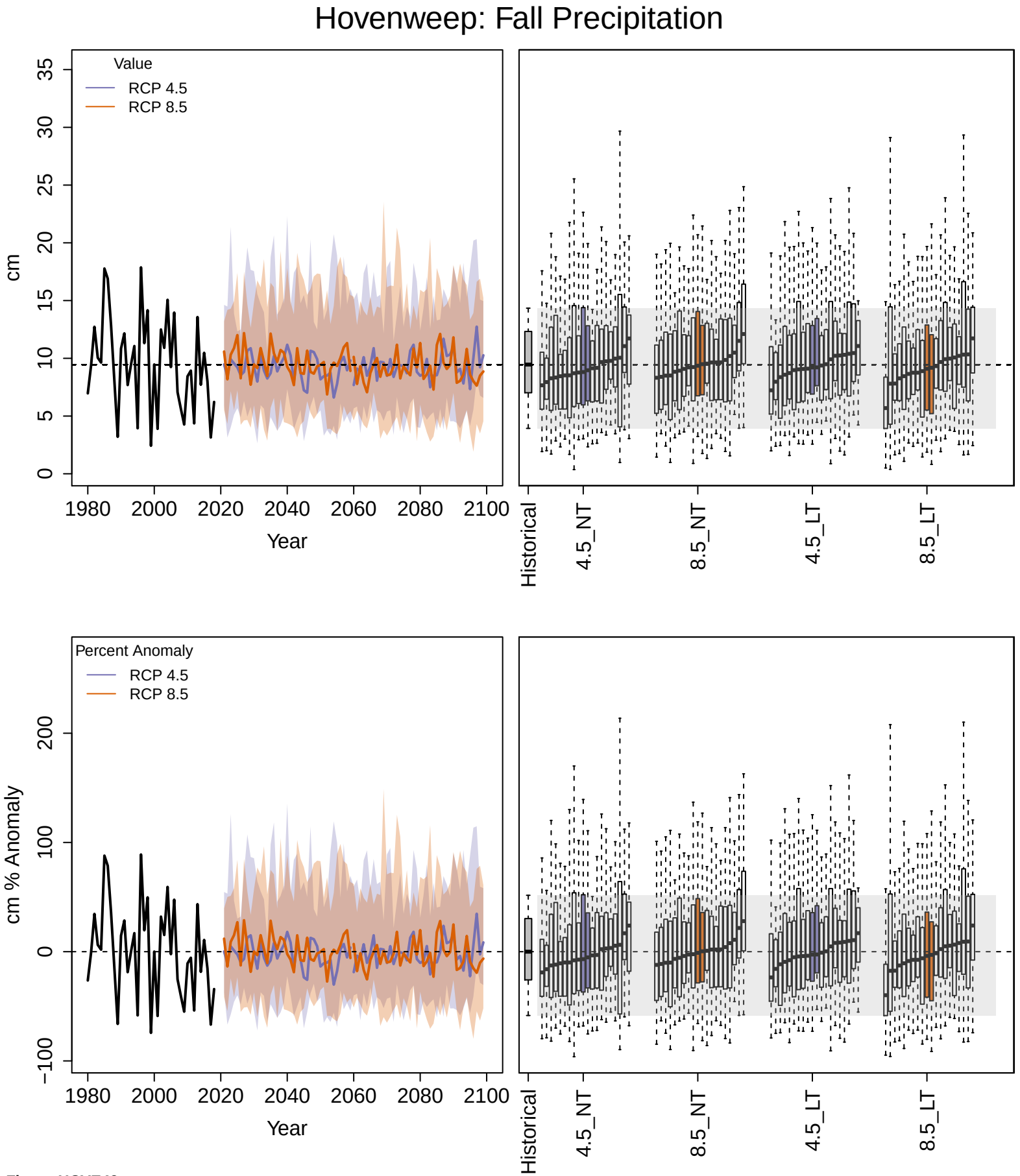


Figure HOVE49:
Past trends and future trajectories of park−wide mean values for Fall Precipitation in Hovenweep. Top panels show values, bottom panels show changes from the long−term historical mean. Left: Time series of historical (black) and future projections for RCP 4.5 and 8.5. Shaded areas show spread among climate models. Right: Boxplots of temporal variability over 40−year periods under historical (left box) and individual climate models under two RCPs. Right: Historical time period is 1970−2010; near−term (NT) is 2020−2060; long−term (LT) is 2061−2100.

Hovenweep: Fall Precipitation

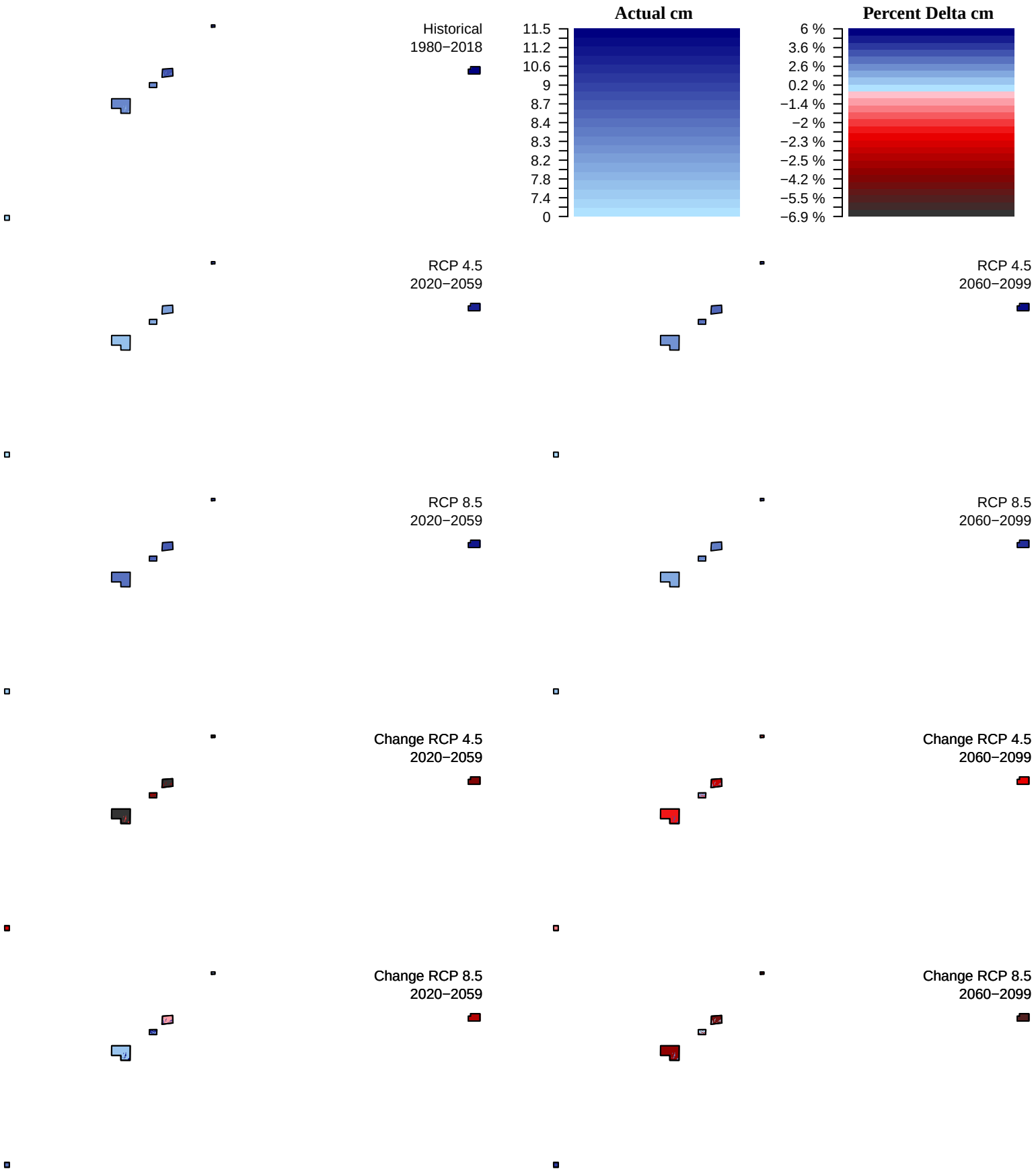


Figure HOVEmap49:
Past trends and future trajectories of park−wide mean values for Fall Precipitation in Hovenweep. Topmost panel depicts the historical mean from 1980−2018. Lower four panels show the emission scenarios of RCP 4.5 and RCP 8.5 at near−term and long−term timeframes. Bottom four panels depict the change from the historical mean; cross hatching denotes areas of robust predicitons (90% of models agree in the direction of change).

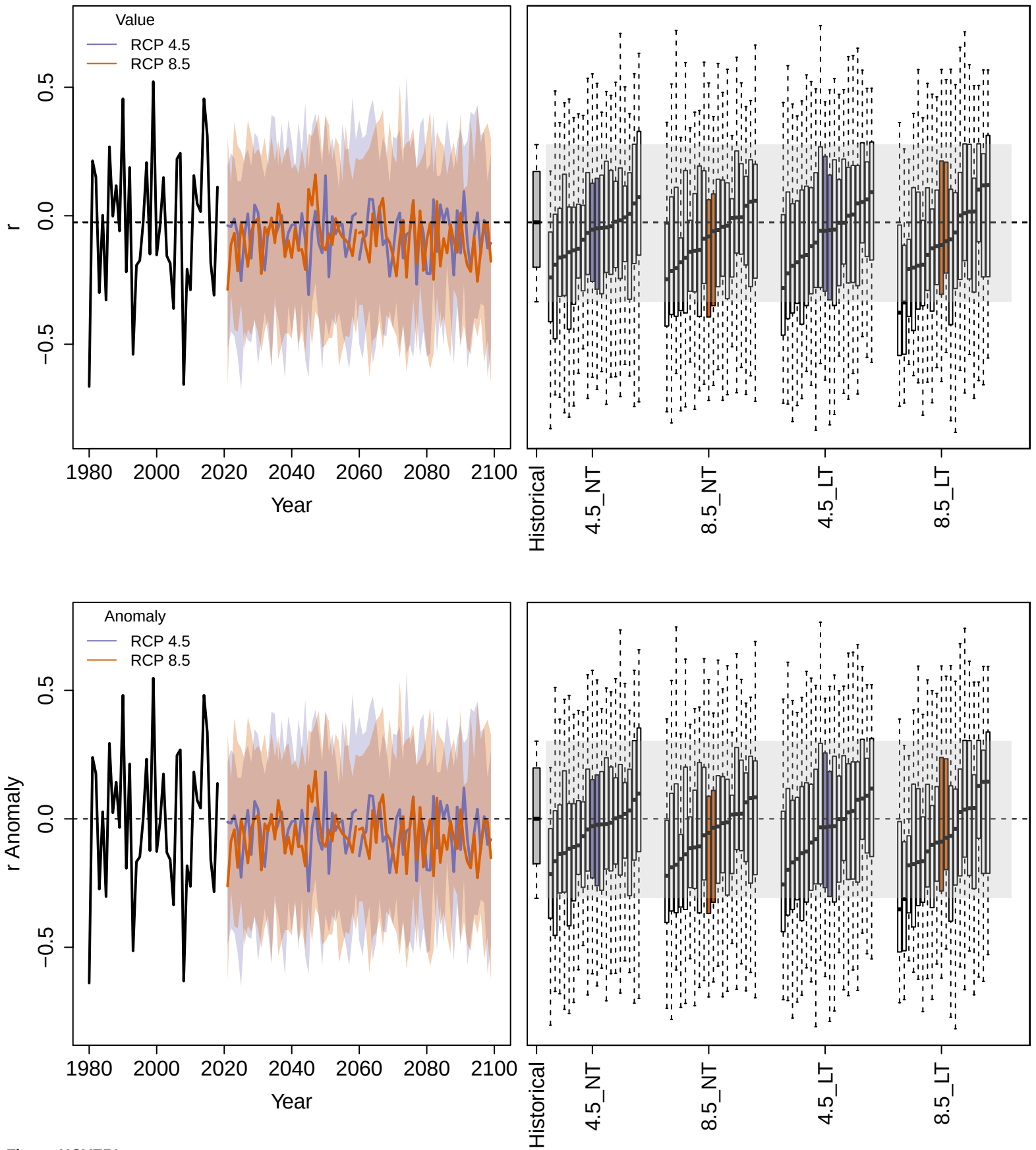


Figure HOVE51:
Past trends and future trajectories of park−wide mean values for Monthly temperature−precipitation correlation in Hovenweep. Top panels show values, bottom panels show changes from the long−term historical mean. Left: Time series of historical (black) and future projections for RCP 4.5 and 8.5. Shaded areas show spread among climate models. Right: Boxplots of temporal variability over 40−year periods under historical (left box) and individual climate models under two RCPs. Right: Historical time period is 1970−2010; near−term (NT) is 2020−2060; long−term (LT) is 2061−2100.

Hovenweep: Monthly temperature−precipitation correlation

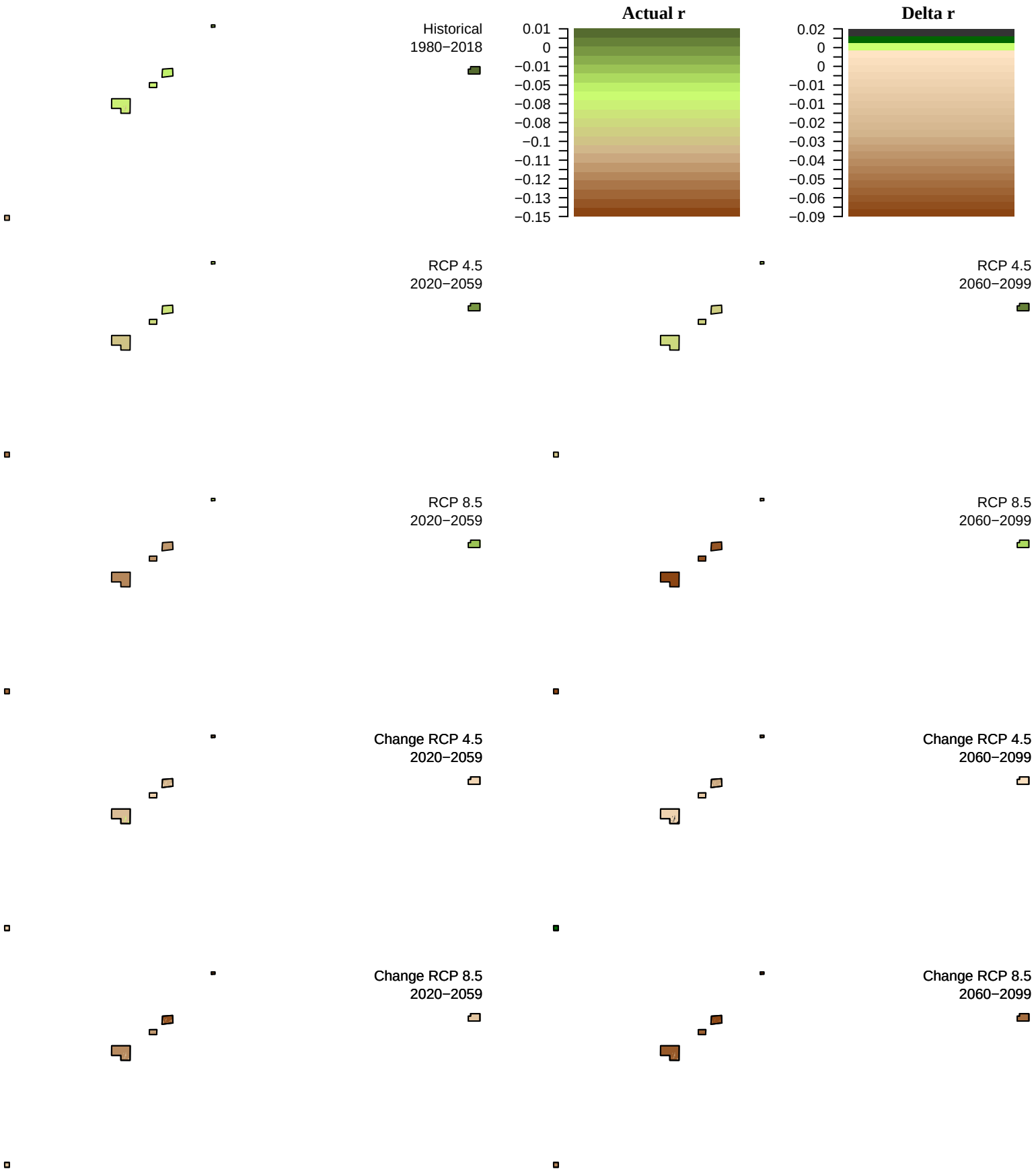


Figure HOVEmap51:
Past trends and future trajectories of park−wide mean values for Monthly temperature−precipitation correlation in Hovenweep. Topmost panel depicts the historical mean from 1980−2018. Lower four panels show the emission scenarios of RCP 4.5 and RCP 8.5 at near−term and long−term timeframes. Bottom four panels depict the change from the historical mean; cross hatching denotes areas of robust predicitons (90% of models agree in the direction of change).

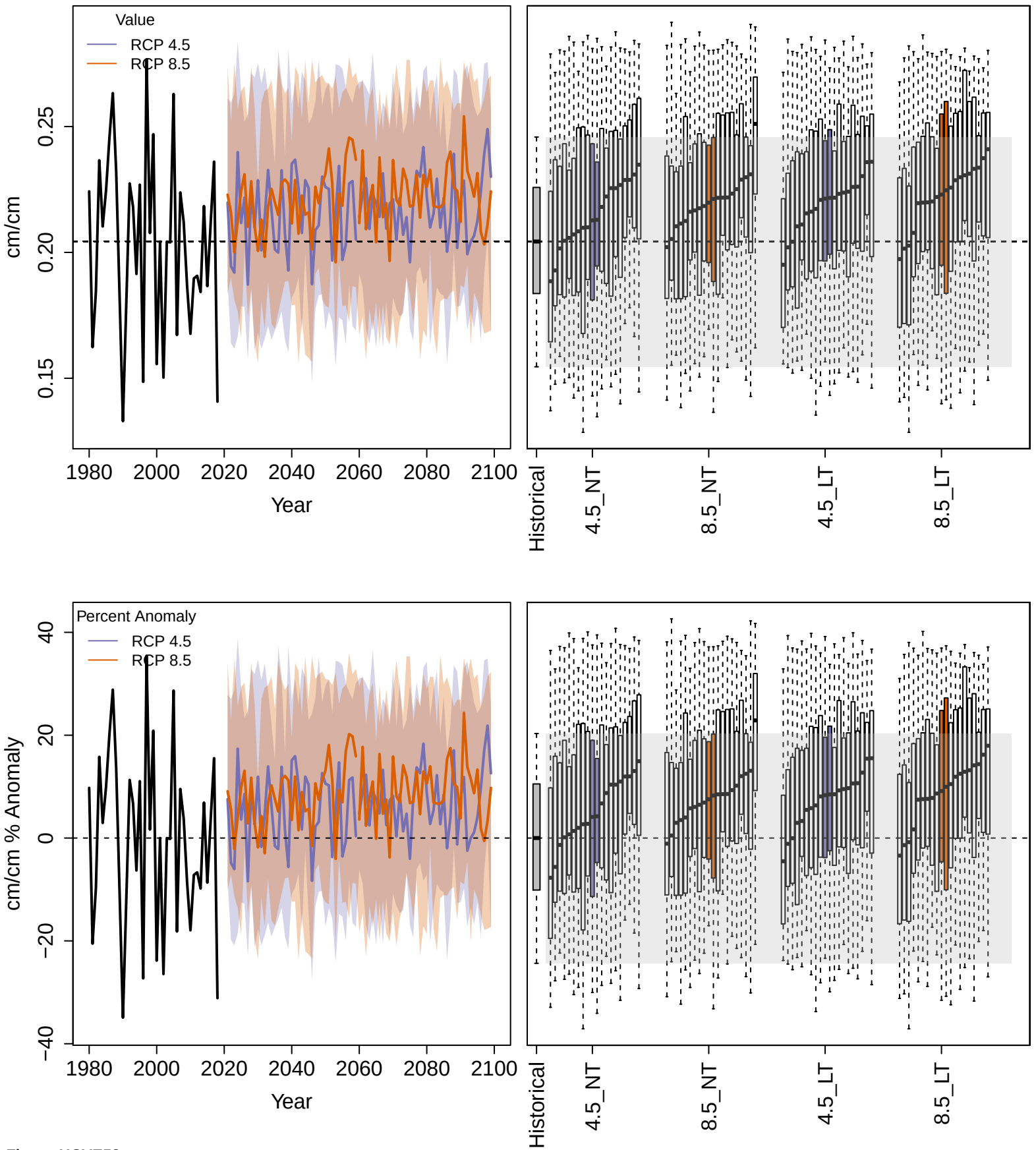


Figure HOVE53:
Past trends and future trajectories of park−wide mean values for Winter soil water content: Top 50cm in Hovenweep. Top panels show values, bottom panels show changes from the long−term historical mean. Left: Time series of historical (black) and future projections for RCP 4.5 and 8.5. Shaded areas show spread among climate models. Right: Boxplots of temporal variability over 40−year periods under historical (left box) and individual climate models under two RCPs. Right: Historical time period is 1970−2010; near−term (NT) is 2020−2060; long−term (LT) is 2061−2100.

Hovenweep: Winter soil water content: Top 50cm

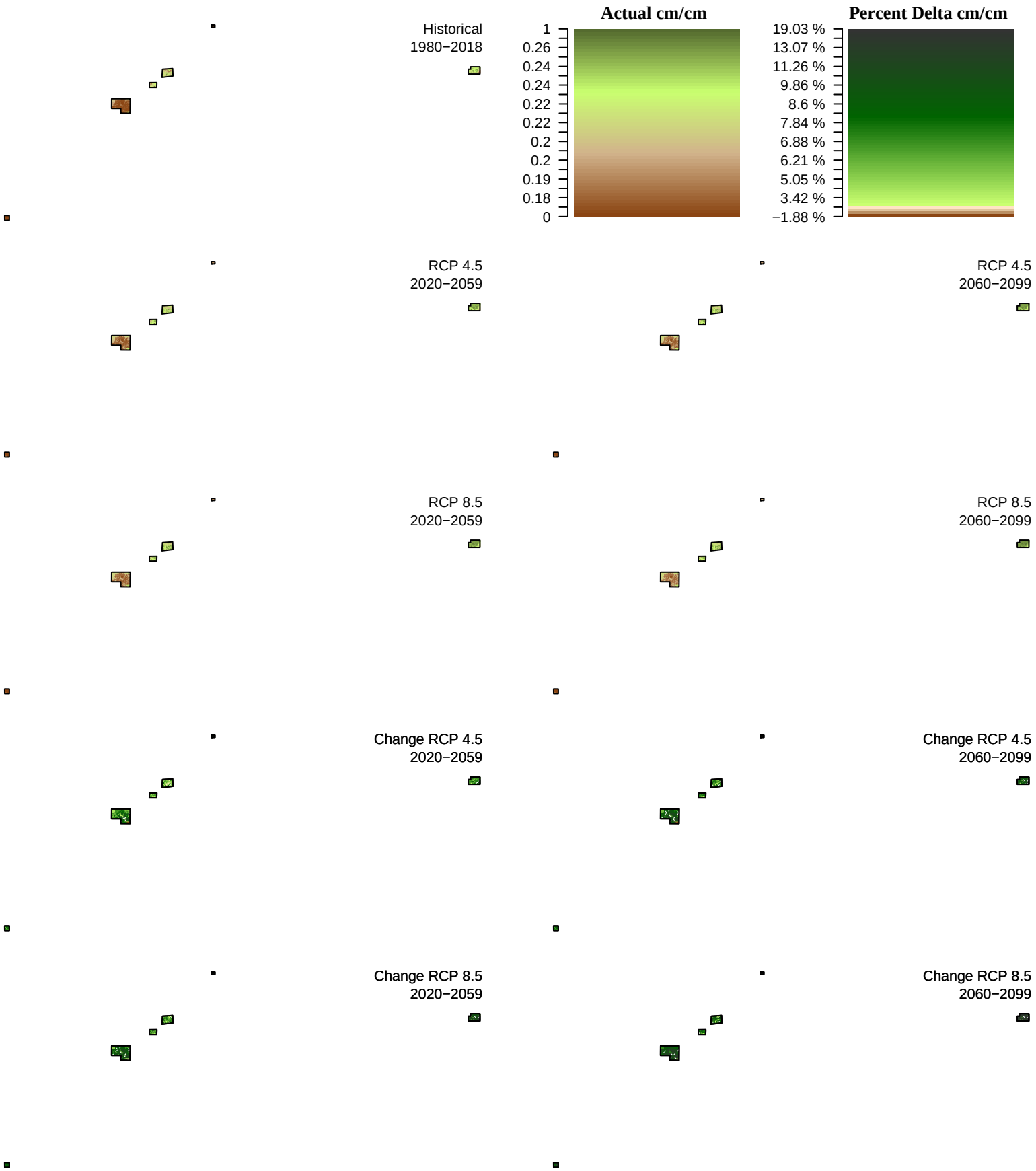


Figure HOVEmap53:
Past trends and future trajectories of park−wide mean values for Winter soil water content: Top 50cm in Hovenweep. Topmost panel depicts the historical mean from 1980−2018. Lower four panels show the emission scenarios of RCP 4.5 and RCP 8.5 at near−term and long−term timeframes. Bottom four panels depict the change from the historical mean; cross hatching denotes areas of robust predicitons (90% of models agree in the direction of change).

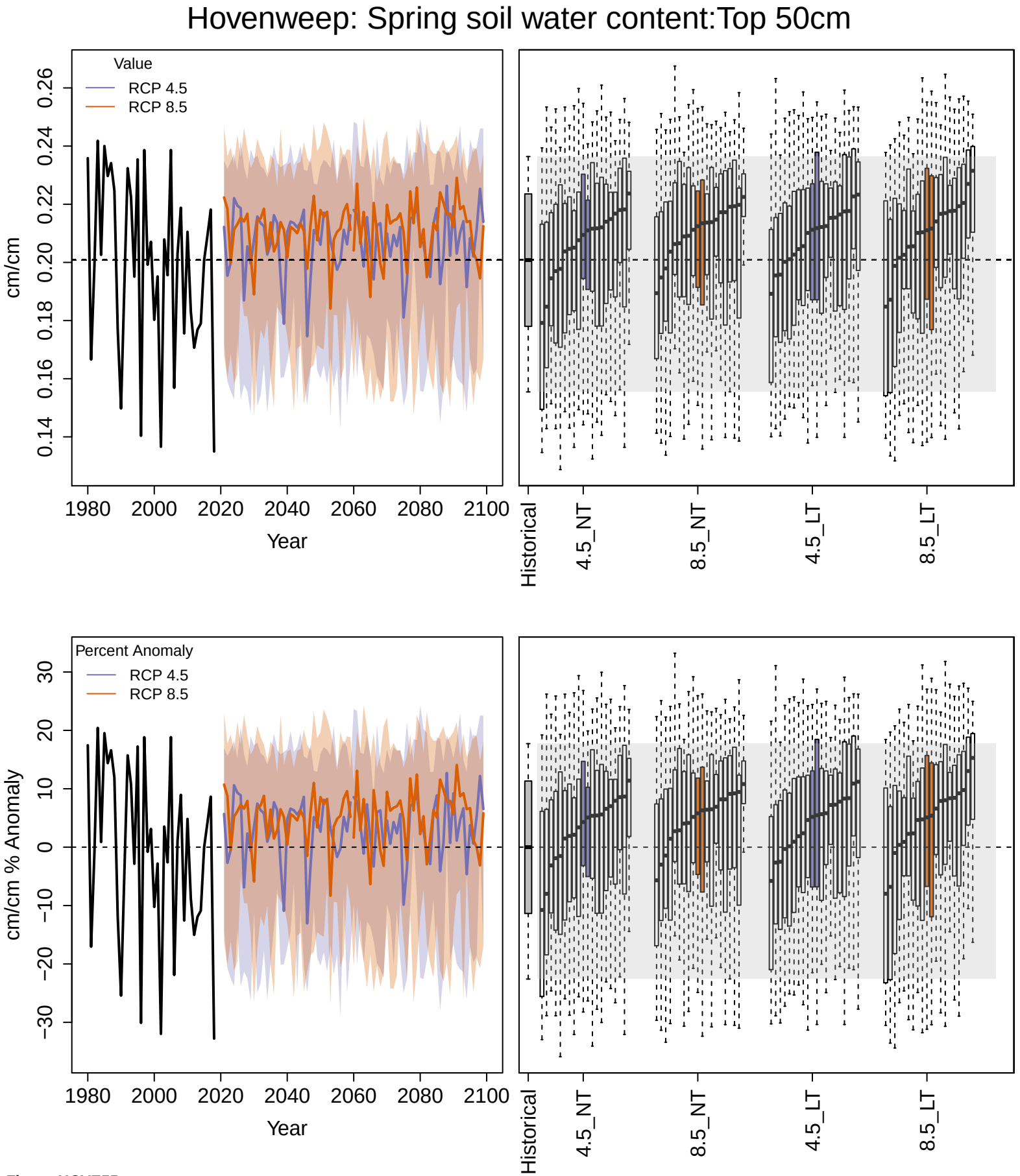


Figure HOVE55:
Past trends and future trajectories of park−wide mean values for Spring soil water content:Top 50cm in Hovenweep. Top panels show values, bottom panels show changes from the long−term historical mean. Left: Time series of historical (black) and future projections for RCP 4.5 and 8.5. Shaded areas show spread among climate models. Right: Boxplots of temporal variability over 40−year periods under historical (left box) and individual climate models under two RCPs. Right: Historical time period is 1970−2010; near−term (NT) is 2020−2060; long−term (LT) is 2061−2100.

Hovenweep: Spring soil water content:Top 50cm

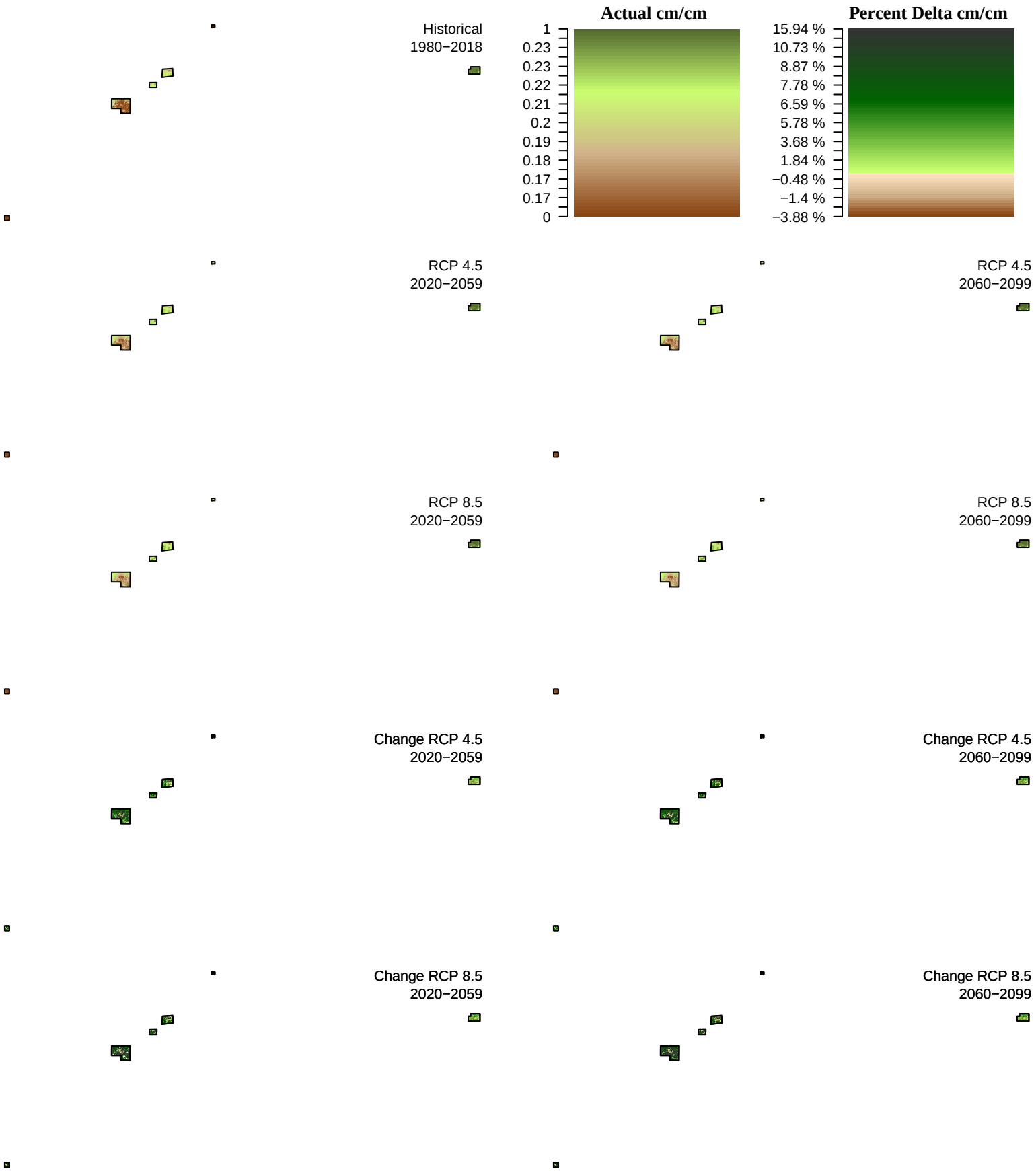


Figure HOVEmap55:
Past trends and future trajectories of park−wide mean values for Spring soil water content:Top 50cm in Hovenweep. Topmost panel depicts the historical mean from 1980−2018. Lower four panels show the emission scenarios of RCP 4.5 and RCP 8.5 at near−term and long−term timeframes. Bottom four panels depict the change from the historical mean; cross hatching denotes areas of robust predicitons (90% of models agree in the direction of change).

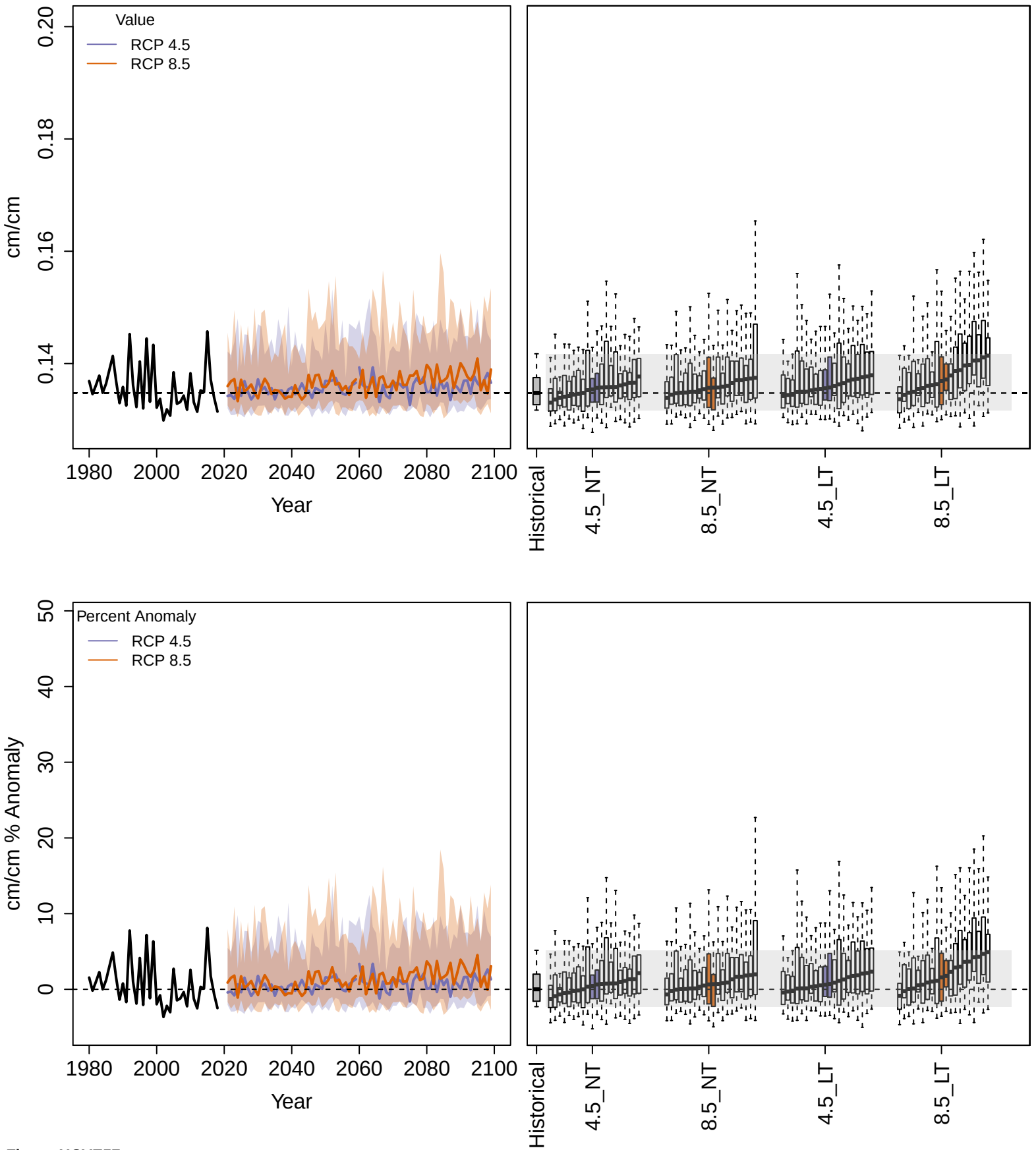


Figure HOVE57:
Past trends and future trajectories of park−wide mean values for Summer soil water content:Top 50cm in Hovenweep. Top panels show values, bottom panels show changes from the long−term historical mean. Left: Time series of historical (black) and future projections for RCP 4.5 and 8.5. Shaded areas show spread among climate models. Right: Boxplots of temporal variability over 40−year periods under historical (left box) and individual climate models under two RCPs. Right: Historical time period is 1970−2010; near−term (NT) is 2020−2060; long−term (LT) is 2061−2100.

Hovenweep: Summer soil water content:Top 50cm

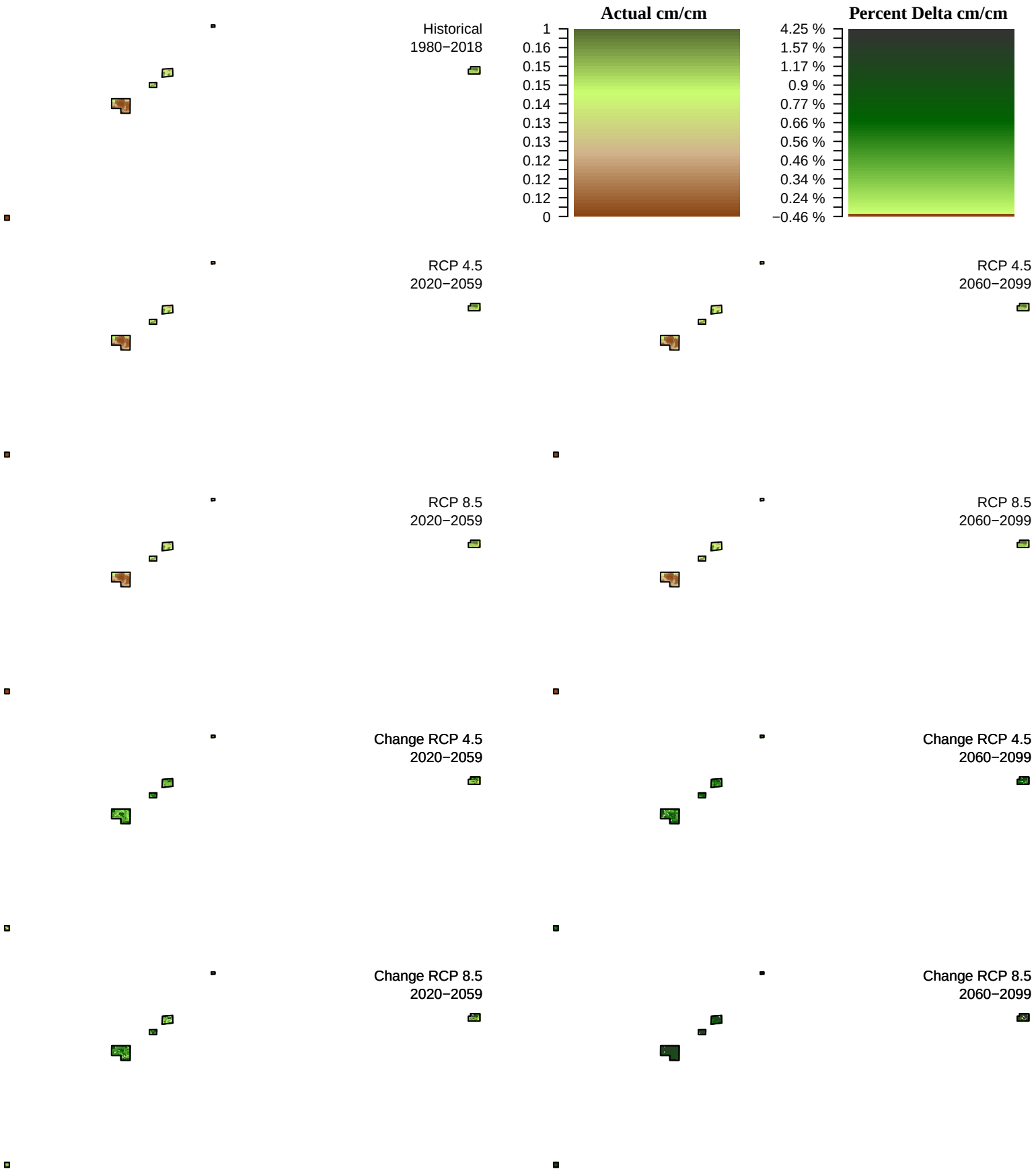


Figure HOVEmap57:
Past trends and future trajectories of park−wide mean values for Summer soil water content:Top 50cm in Hovenweep. Topmost panel depicts the historical mean from 1980−2018. Lower four panels show the emission scenarios of RCP 4.5 and RCP 8.5 at near−term and long−term timeframes. Bottom four panels depict the change from the historical mean; cross hatching denotes areas of robust predicitons (90% of models agree in the direction of change).

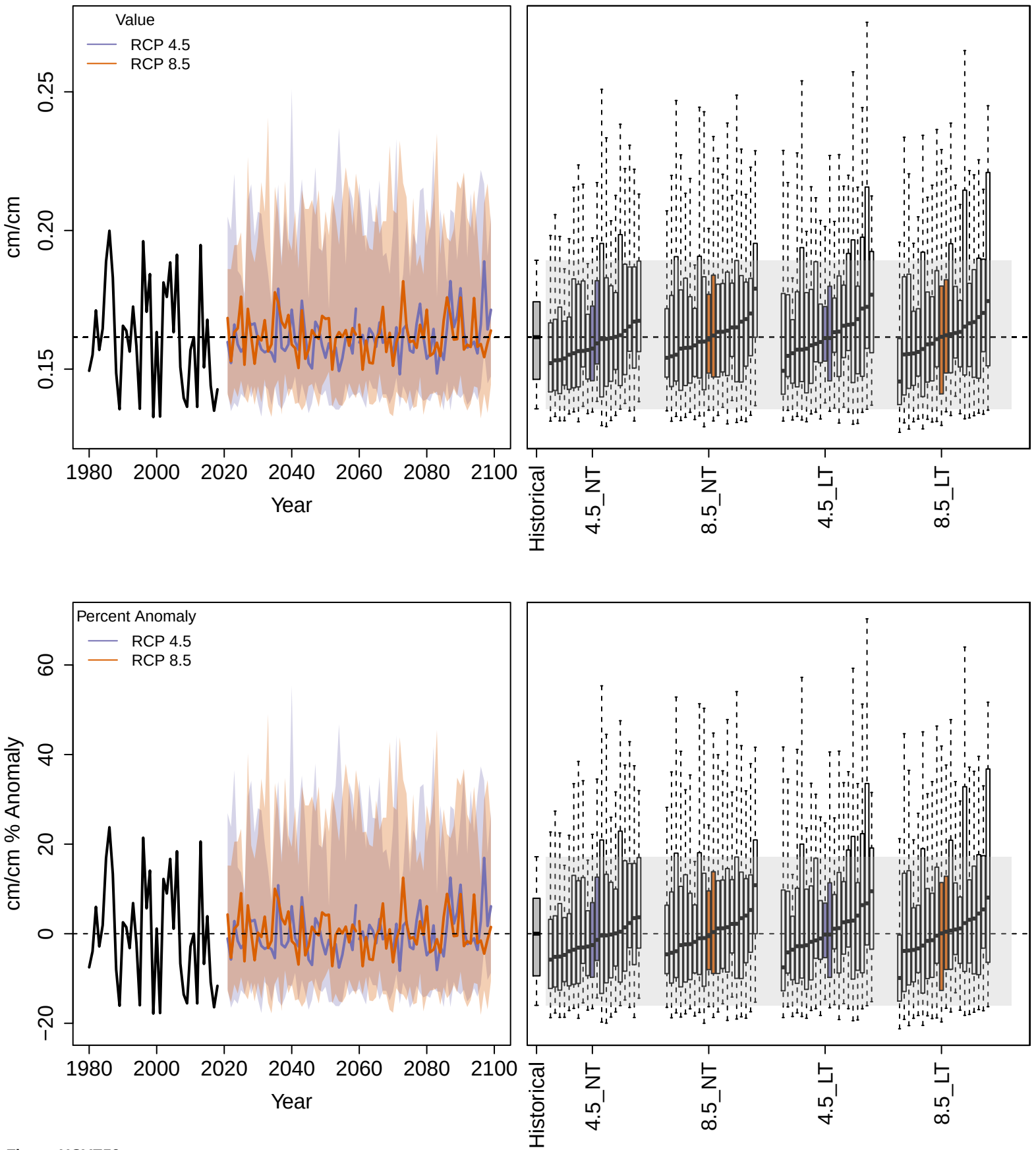


Figure HOVE59:
Past trends and future trajectories of park−wide mean values for Fall soil water content:Top 50cm in Hovenweep. Top panels show values, bottom panels show changes from the long−term historical mean. Left: Time series of historical (black) and future projections for RCP 4.5 and 8.5. Shaded areas show spread among climate models. Right: Boxplots of temporal variability over 40−year periods under historical (left box) and individual climate models under two RCPs. Right: Historical time period is 1970−2010; near−term (NT) is 2020−2060; long−term (LT) is 2061−2100.

Hovenweep: Fall soil water content:Top 50cm

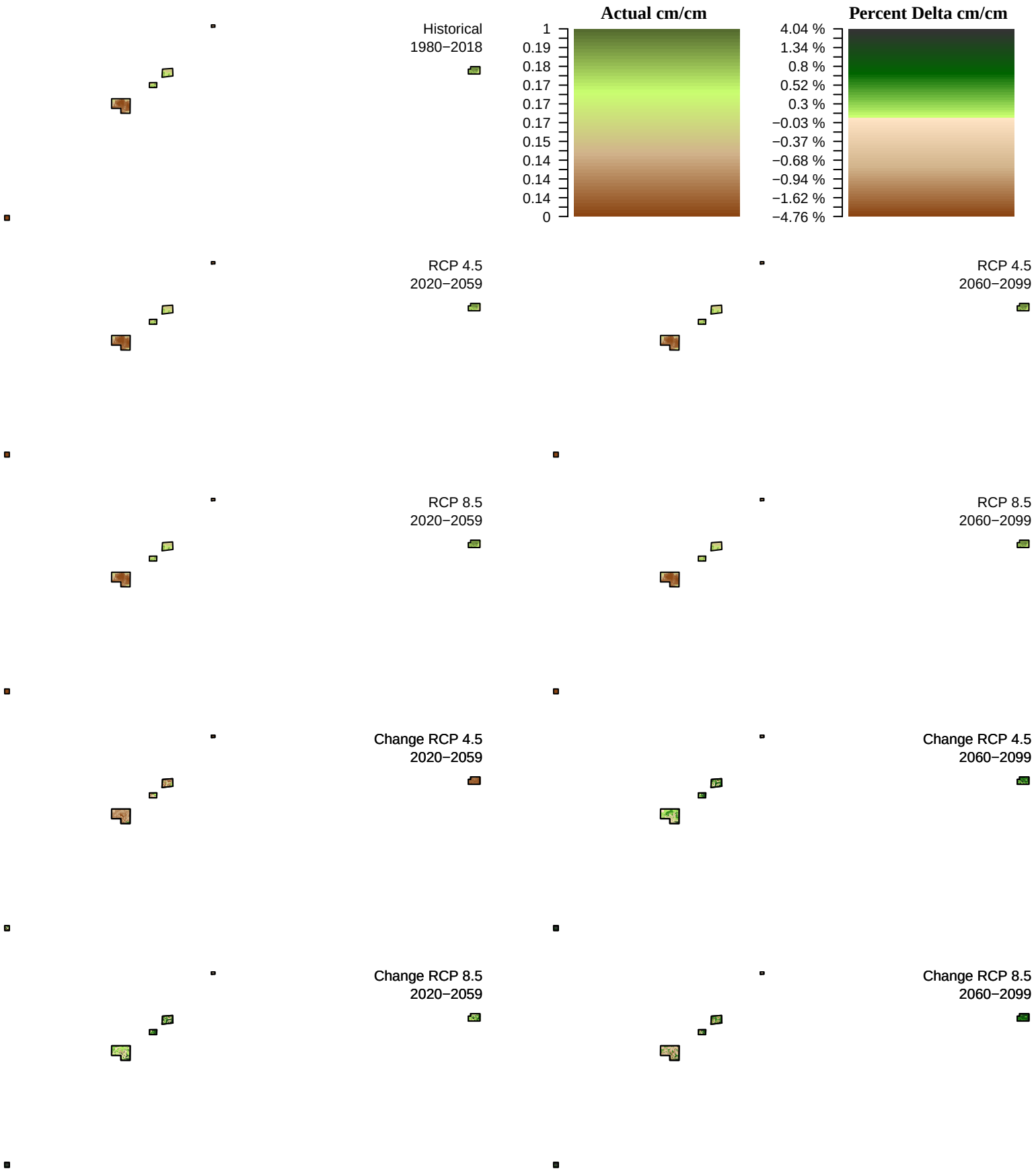


Figure HOVEmap59:
Past trends and future trajectories of park−wide mean values for Fall soil water content:Top 50cm in Hovenweep. Topmost panel depicts the historical mean from 1980−2018. Lower four panels show the emission scenarios of RCP 4.5 and RCP 8.5 at near−term and long−term timeframes. Bottom four panels depict the change from the historical mean; cross hatching denotes areas of robust predicitons (90% of models agree in the direction of change).

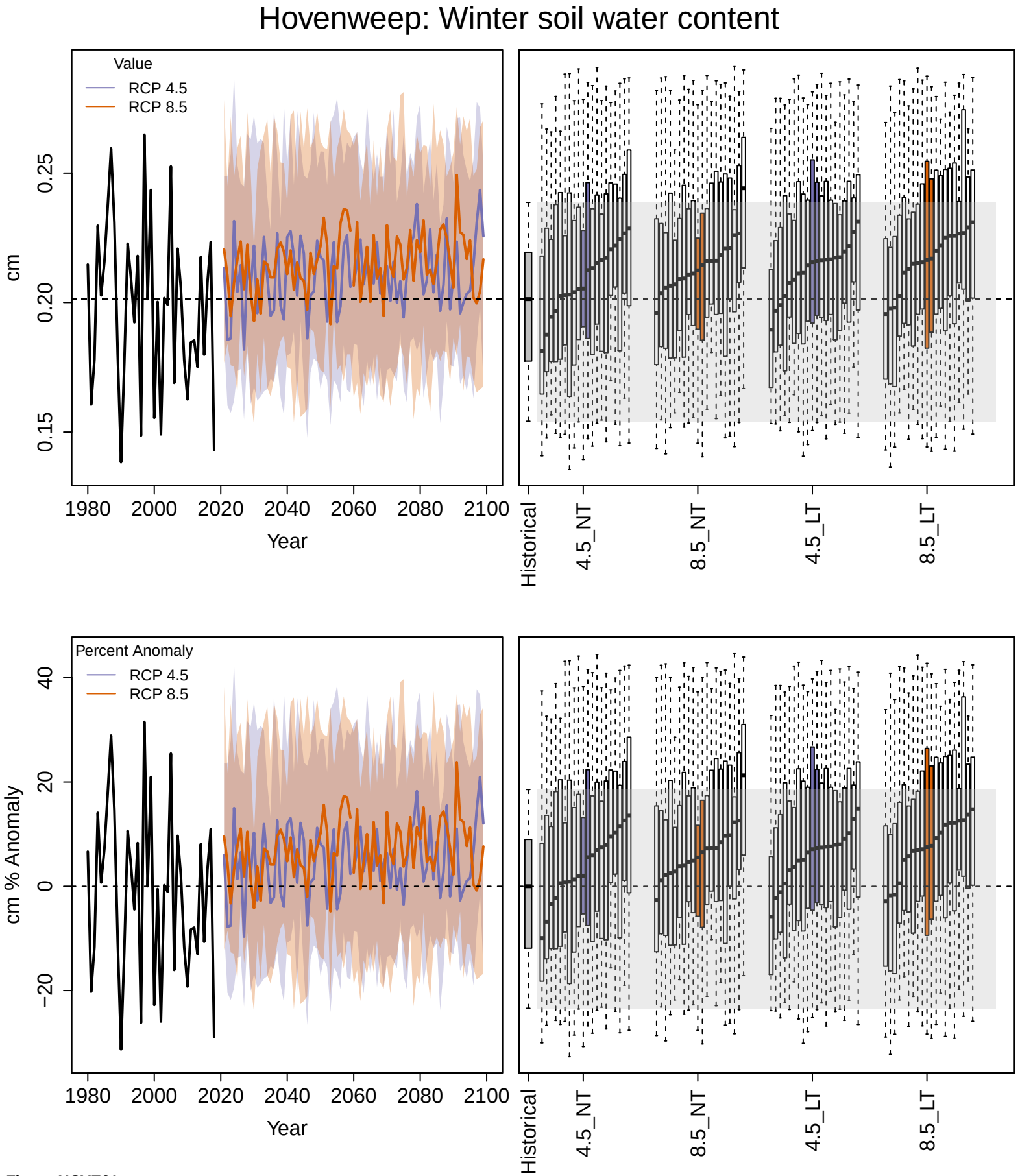


Figure HOVE61:
Past trends and future trajectories of park−wide mean values for Winter soil water content in Hovenweep. Top panels show values, bottom panels show changes from the long−term historical mean. Left: Time series of historical (black) and future projections for RCP 4.5 and 8.5. Shaded areas show spread among climate models. Right: Boxplots of temporal variability over 40−year periods under historical (left box) and individual climate models under two RCPs. Right: Historical time period is 1970−2010; near−term (NT) is 2020−2060; long−term (LT) is 2061−2100.

Hovenweep: Winter soil water content

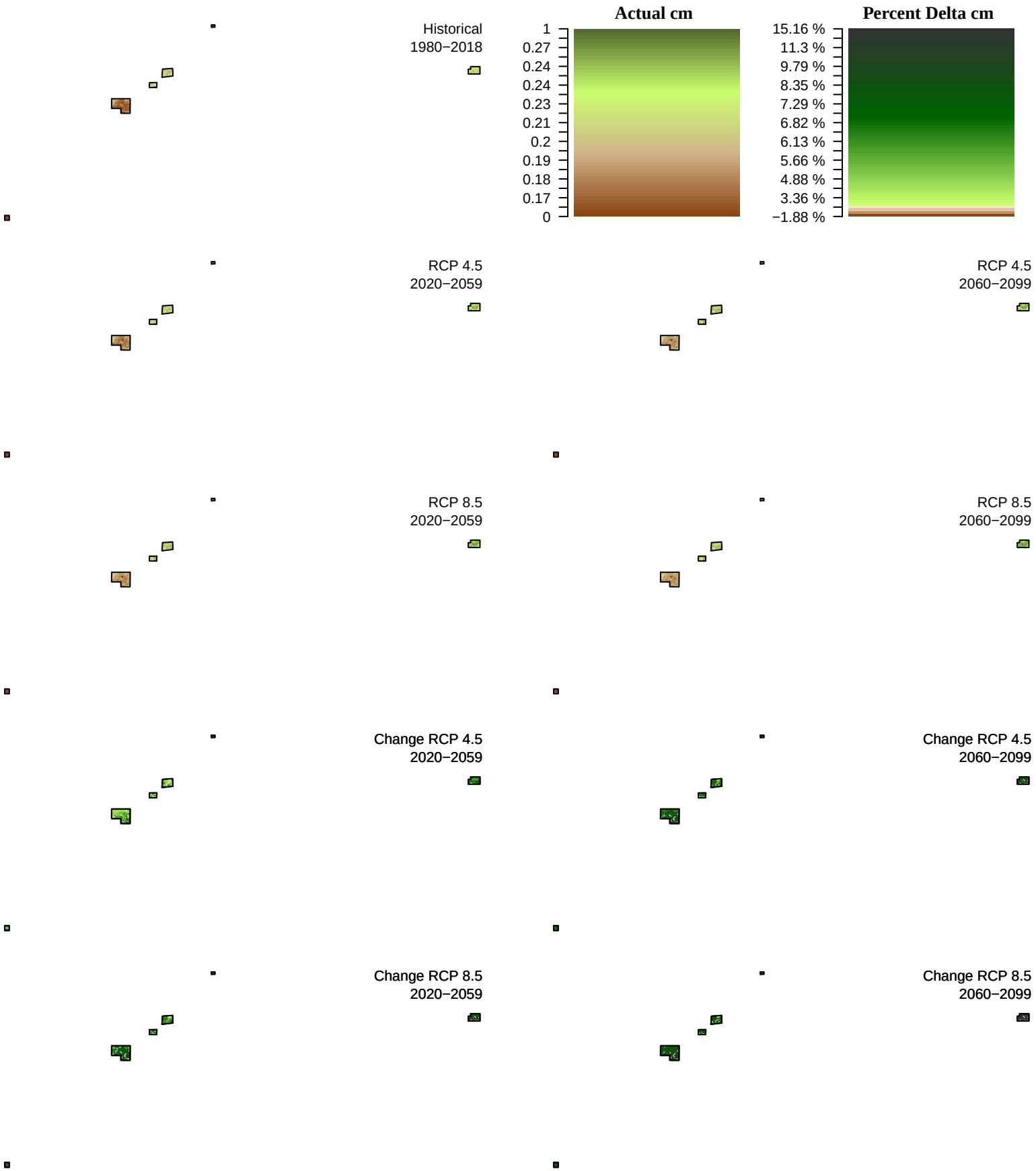


Figure HOVEmap61:
Past trends and future trajectories of park−wide mean values for Winter soil water content in Hovenweep. Topmost panel depicts the historical mean from 1980−2018. Lower four panels show the emission scenarios of RCP 4.5 and RCP 8.5 at near−term and long−term timeframes. Bottom four panels depict the change from the historical mean; cross hatching denotes areas of robust predicitons (90% of models agree in the direction of change).

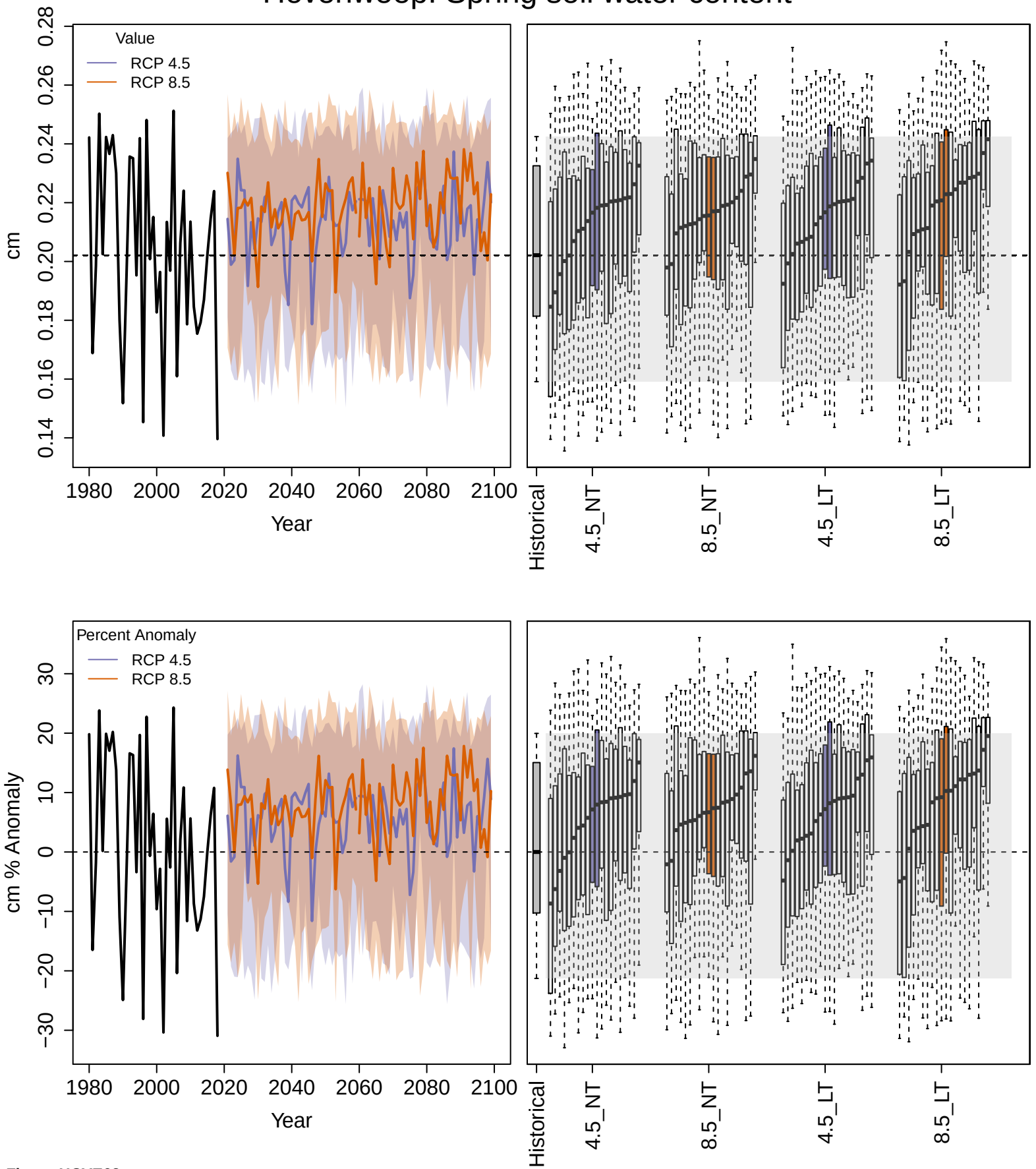


Figure HOVE63:
Past trends and future trajectories of park−wide mean values for Spring soil water content in Hovenweep. Top panels show values, bottom panels show changes from the long−term historical mean. Left: Time series of historical (black) and future projections for RCP 4.5 and 8.5. Shaded areas show spread among climate models. Right: Boxplots of temporal variability over 40−year periods under historical (left box) and individual climate models under two RCPs. Right: Historical time period is 1970−2010; near−term (NT) is 2020−2060; long−term (LT) is 2061−2100.

Hovenweep: Spring soil water content

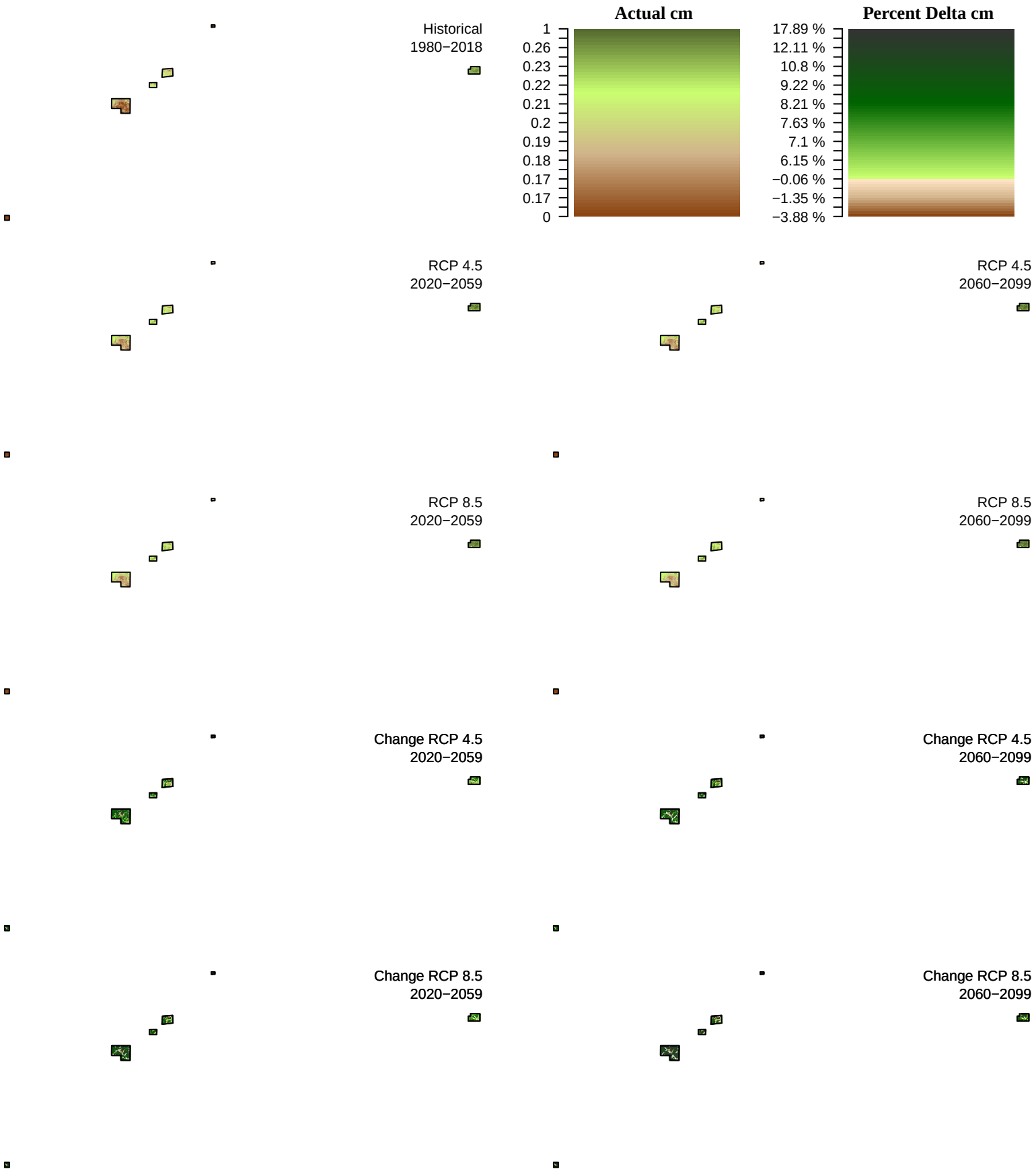


Figure HOVEmap63:
Past trends and future trajectories of park−wide mean values for Spring soil water content in Hovenweep. Topmost panel depicts the historical mean from 1980−2018. Lower four panels show the emission scenarios of RCP 4.5 and RCP 8.5 at near−term and long−term timeframes. Bottom four panels depict the change from the historical mean; cross hatching denotes areas of robust predicitons (90% of models agree in the direction of change).

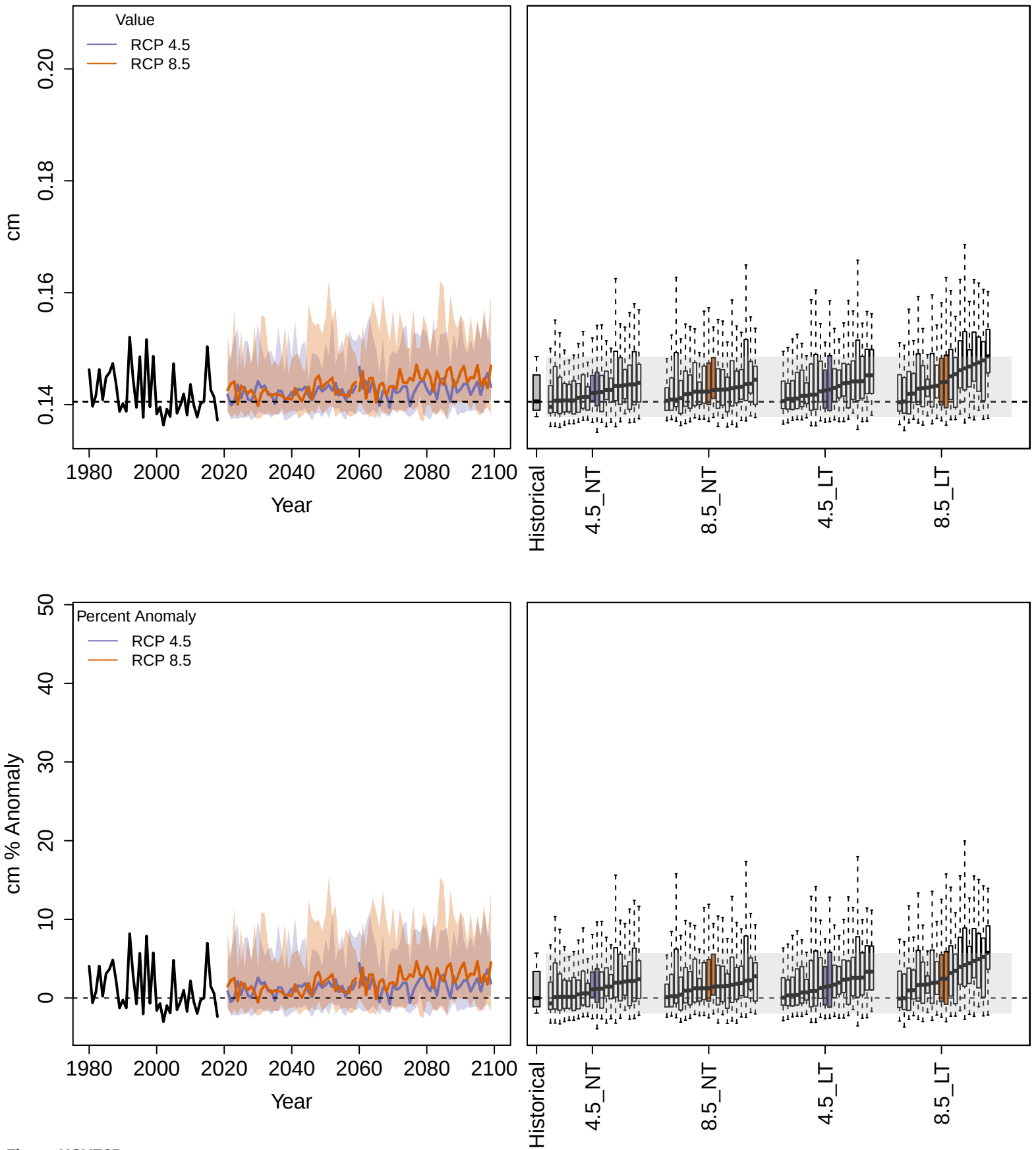


Figure HOVE65:
Past trends and future trajectories of park−wide mean values for Summer soil water content in Hovenweep. Top panels show values, bottom panels show changes from the long−term historical mean. Left: Time series of historical (black) and future projections for RCP 4.5 and 8.5. Shaded areas show spread among climate models. Right: Boxplots of temporal variability over 40−year periods under historical (left box) and individual climate models under two RCPs. Right: Historical time period is 1970−2010; near−term (NT) is 2020−2060; long−term (LT) is 2061−2100.

Hovenweep: Summer soil water content

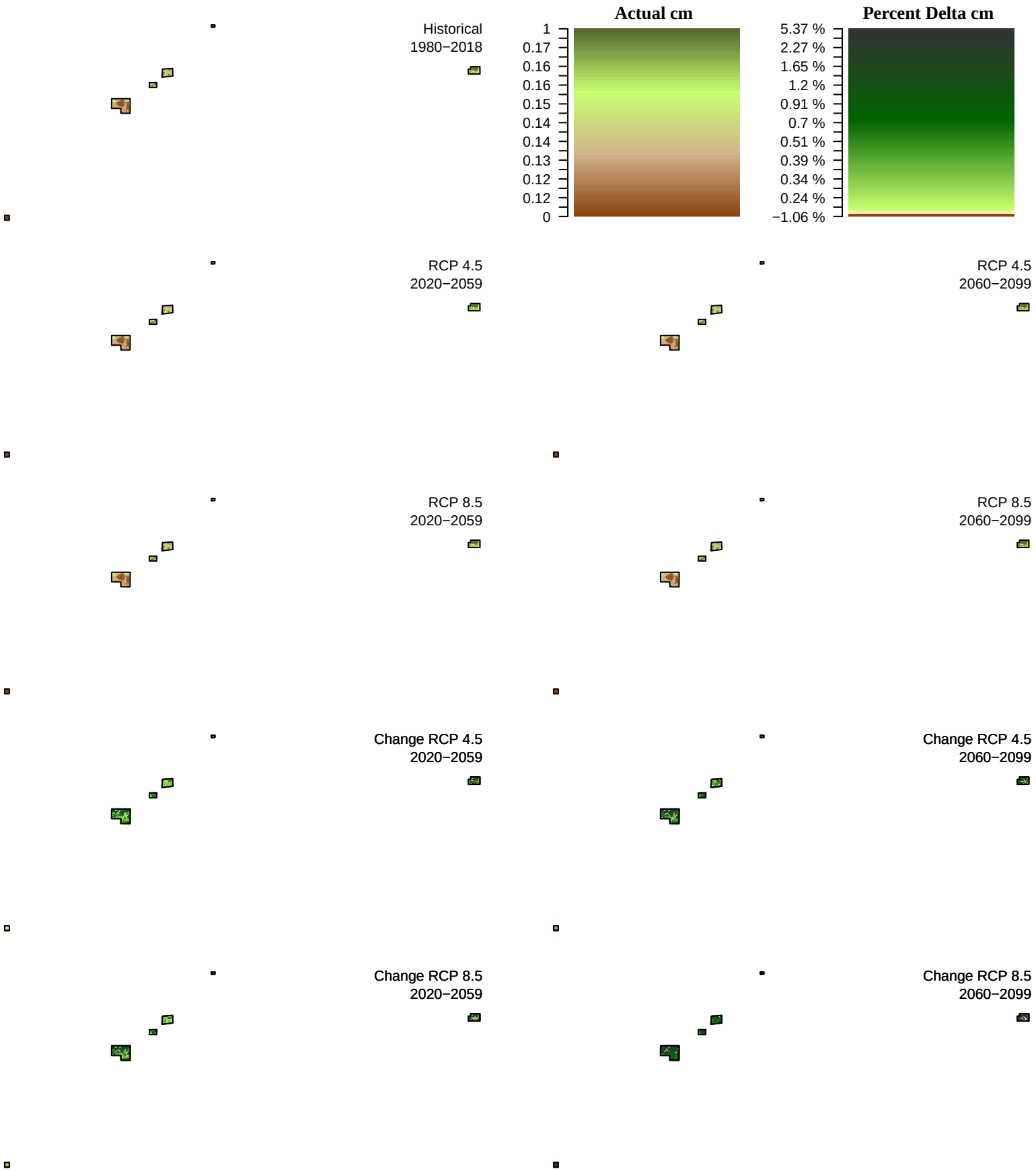


Figure HOVEmap65:
Past trends and future trajectories of park−wide mean values for Summer soil water content in Hovenweep. Topmost panel depicts the historical mean from 1980−2018. Lower four panels show the emission scenarios of RCP 4.5 and RCP 8.5 at near−term and long−term timeframes. Bottom four panels depict the change from the historical mean; cross hatching denotes areas of robust predicitons (90% of models agree in the direction of change).

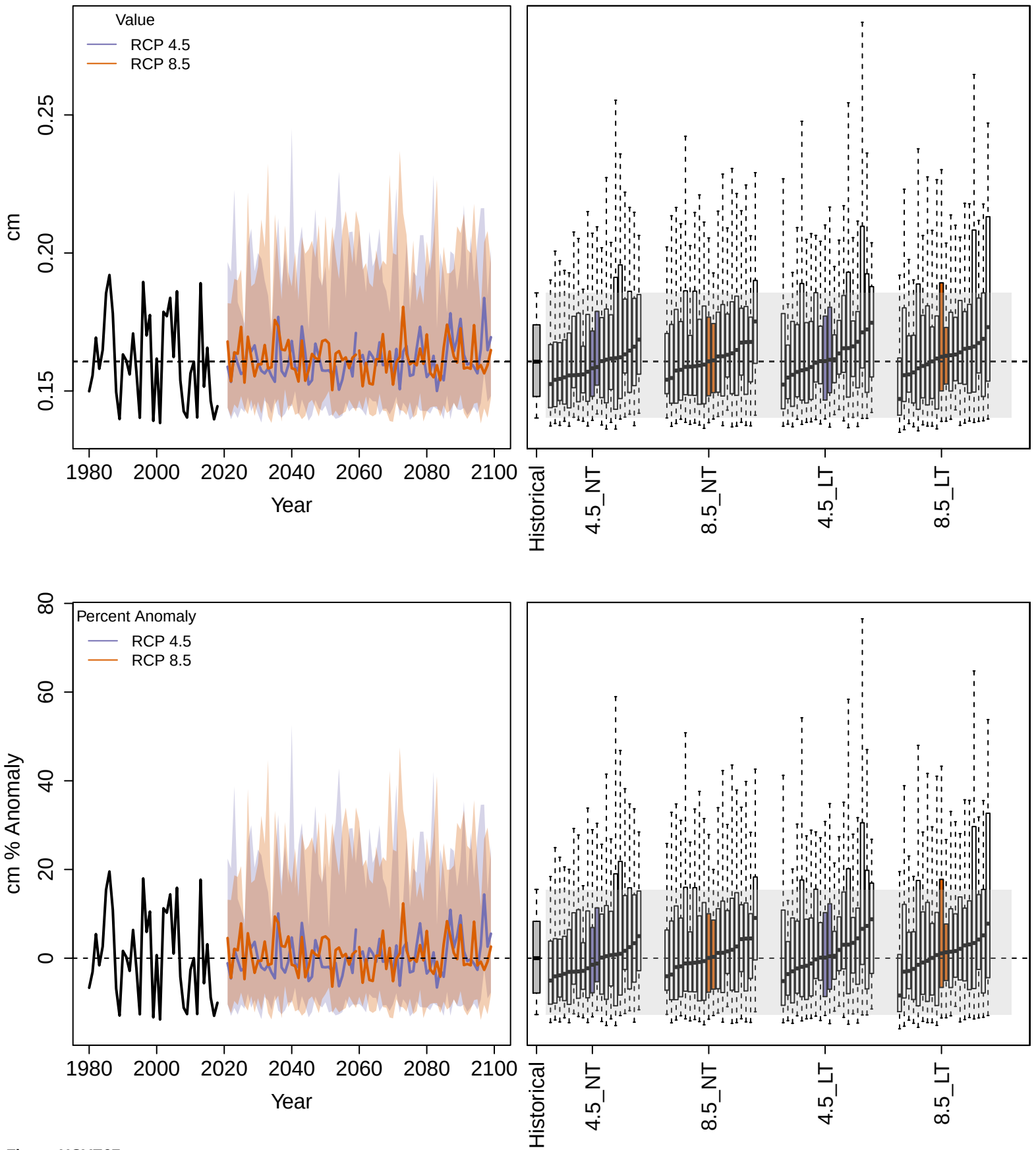


Figure HOVE67:
Past trends and future trajectories of park−wide mean values for Fall soil water content in Hovenweep. Top panels show values, bottom panels show changes from the long−term historical mean. Left: Time series of historical (black) and future projections for RCP 4.5 and 8.5. Shaded areas show spread among climate models. Right: Boxplots of temporal variability over 40−year periods under historical (left box) and individual climate models under two RCPs. Right: Historical time period is 1970−2010; near−term (NT) is 2020−2060; long−term (LT) is 2061−2100.

Hovenweep: Fall soil water content

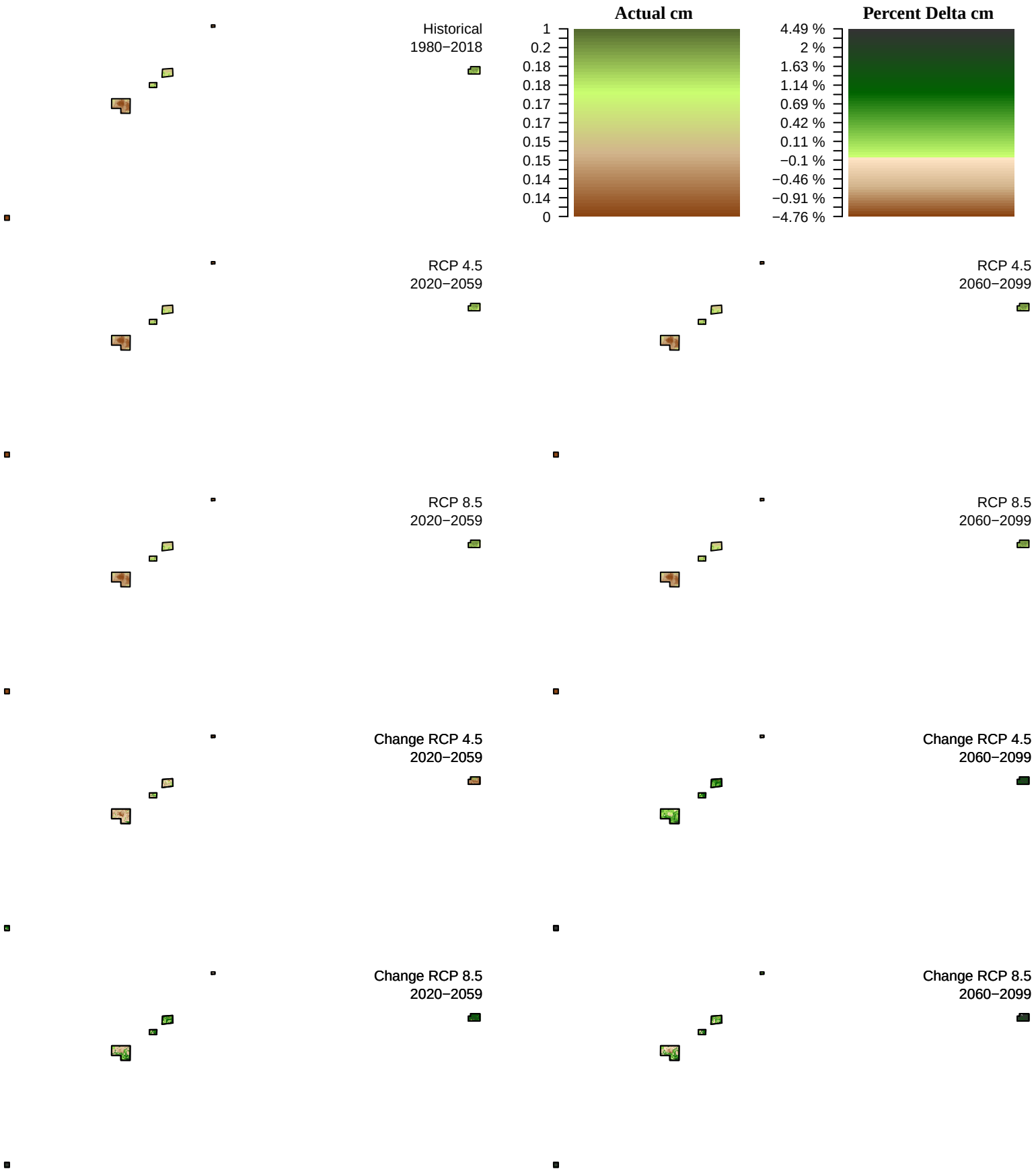


Figure HOVEmap67:
Past trends and future trajectories of park−wide mean values for Fall soil water content in Hovenweep. Topmost panel depicts the historical mean from 1980−2018. Lower four panels show the emission scenarios of RCP 4.5 and RCP 8.5 at near−term and long−term timeframes. Bottom four panels depict the change from the historical mean; cross hatching denotes areas of robust predicitons (90% of models agree in the direction of change).

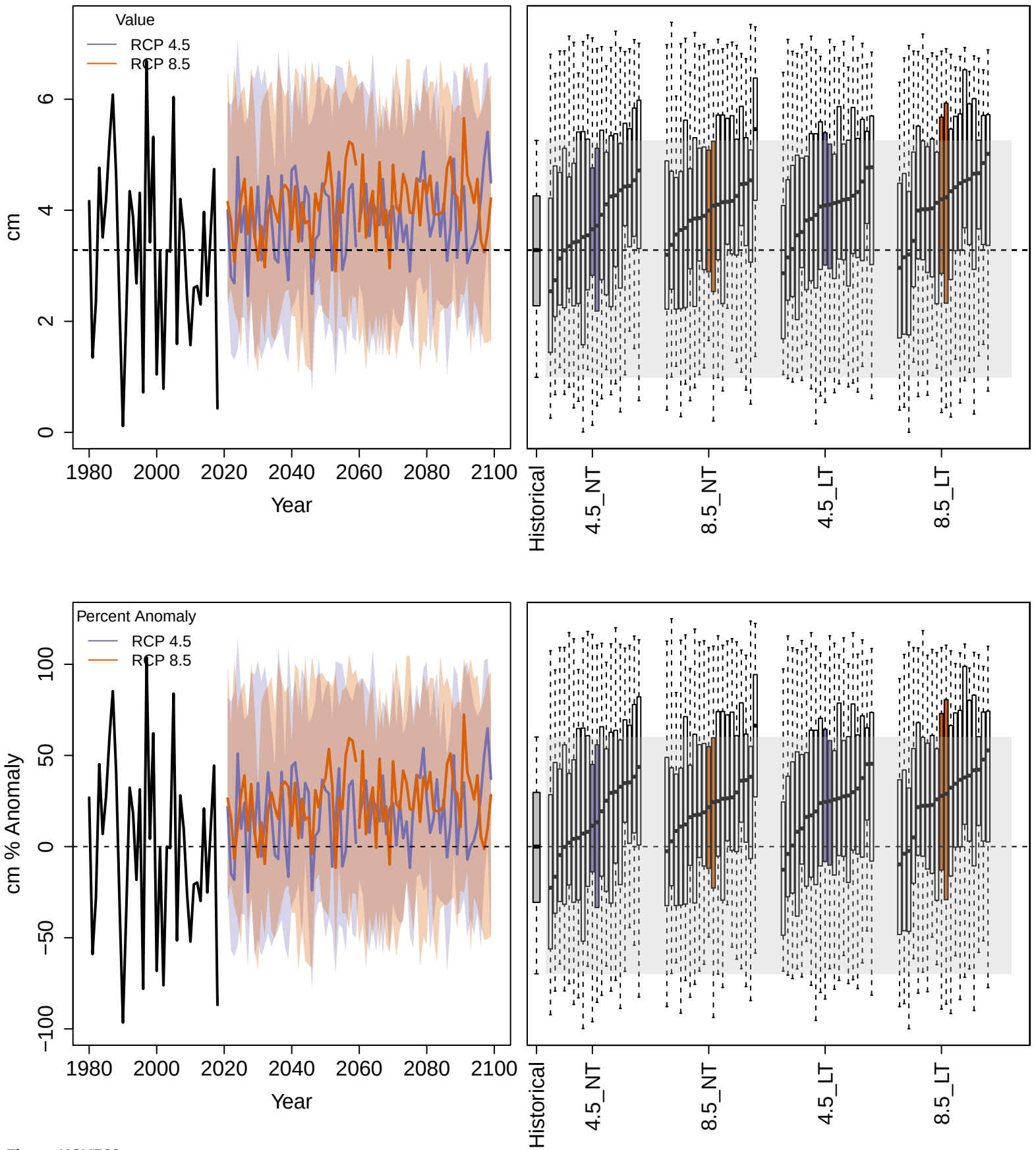


Figure HOVE69:
Past trends and future trajectories of park−wide mean values for Winter available soil moisture: top 50cm in Hovenweep. Top panels show values, bottom panels show changes from the long−term historical mean. Left: Time series of historical (black) and future projections for RCP 4.5 and 8.5. Shaded areas show spread among climate models. Right: Boxplots of temporal variability over 40−year periods under historical (left box) and individual climate models under two RCPs. Right: Historical time period is 1970−2010; near−term (NT) is 2020−2060; long−term (LT) is 2061−2100.

Hovenweep: Winter available soil moisture: top 50cm

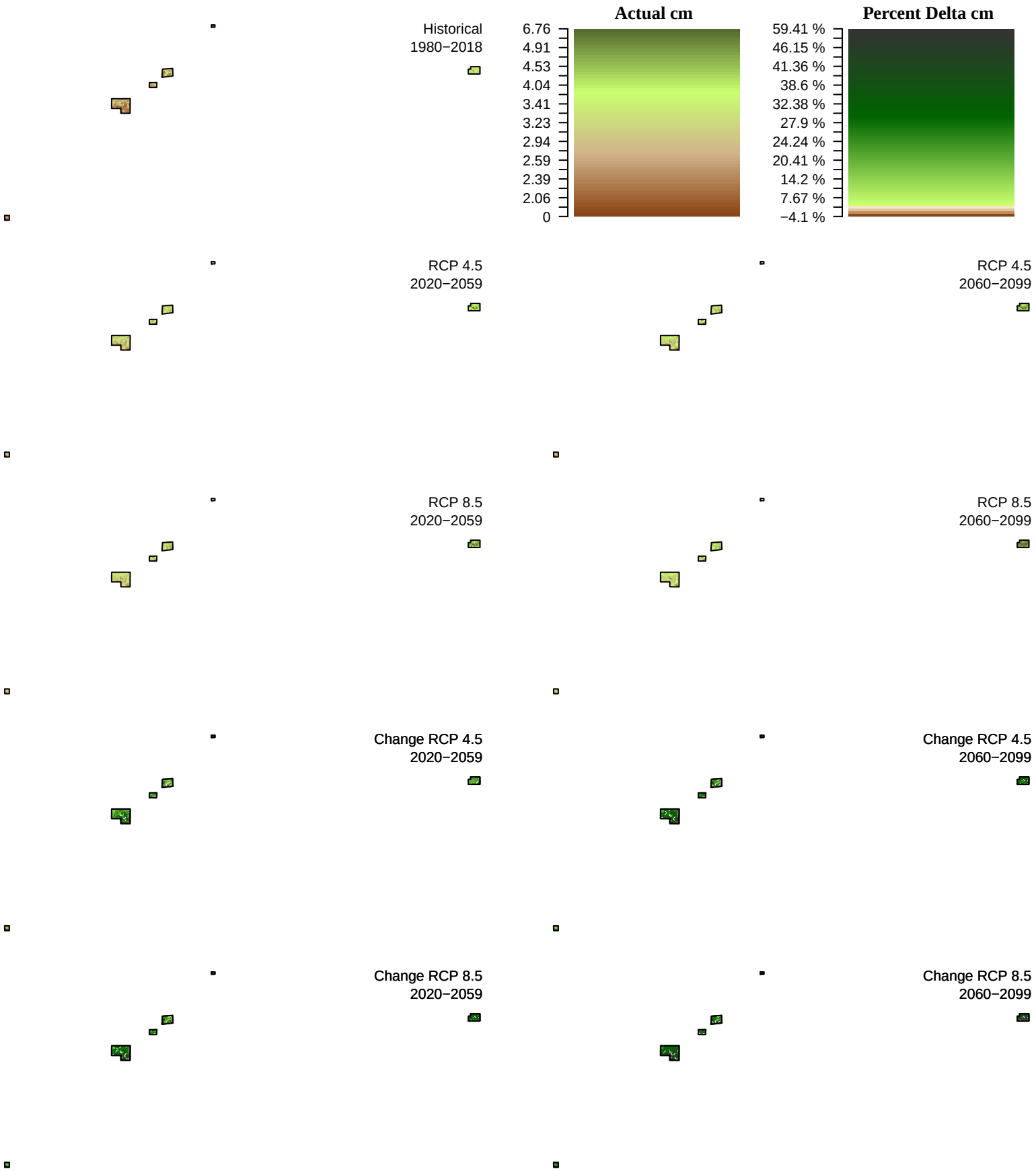


Figure HOVEmap69:
Past trends and future trajectories of park−wide mean values for Winter available soil moisture: top 50cm in Hovenweep. Topmost panel depicts the historical mean from 1980−2018. Lower four panels show the emission scenarios of RCP 4.5 and RCP 8.5 at near−term and long−term timeframes. Bottom four panels depict the change from the historical mean; cross hatching denotes areas of robust predicitons (90% of models agree in the direction of change).

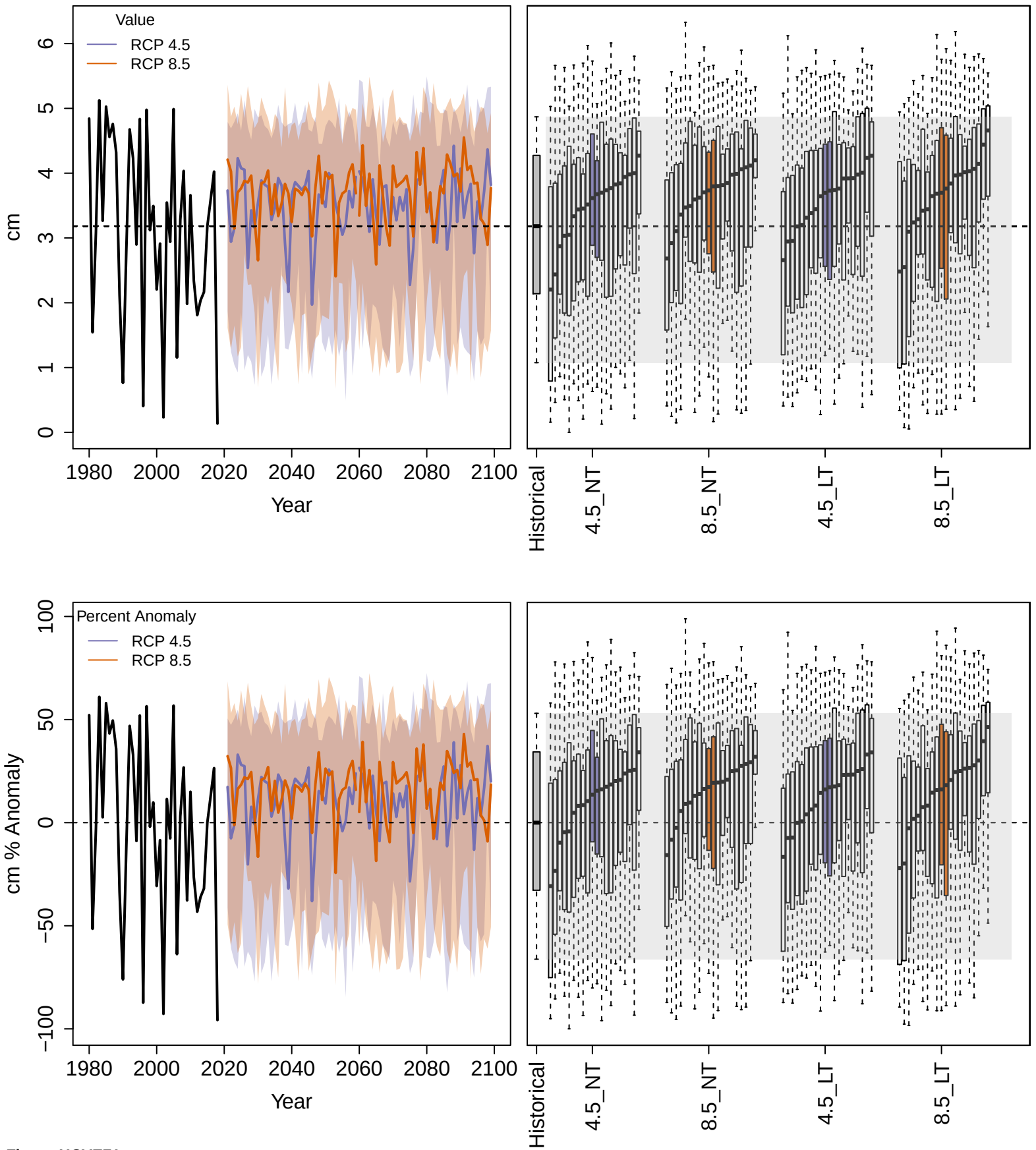


Figure HOVE71:
Past trends and future trajectories of park−wide mean values for Spring available soil moisture: top 50cm in Hovenweep. Top panels show values, bottom panels show changes from the long−term historical mean. Left: Time series of historical (black) and future projections for RCP 4.5 and 8.5. Shaded areas show spread among climate models. Right: Boxplots of temporal variability over 40−year periods under historical (left box) and individual climate models under two RCPs. Right: Historical time period is 1970−2010; near−term (NT) is 2020−2060; long−term (LT) is 2061−2100.

Hovenweep: Spring available soil moisture: top 50cm

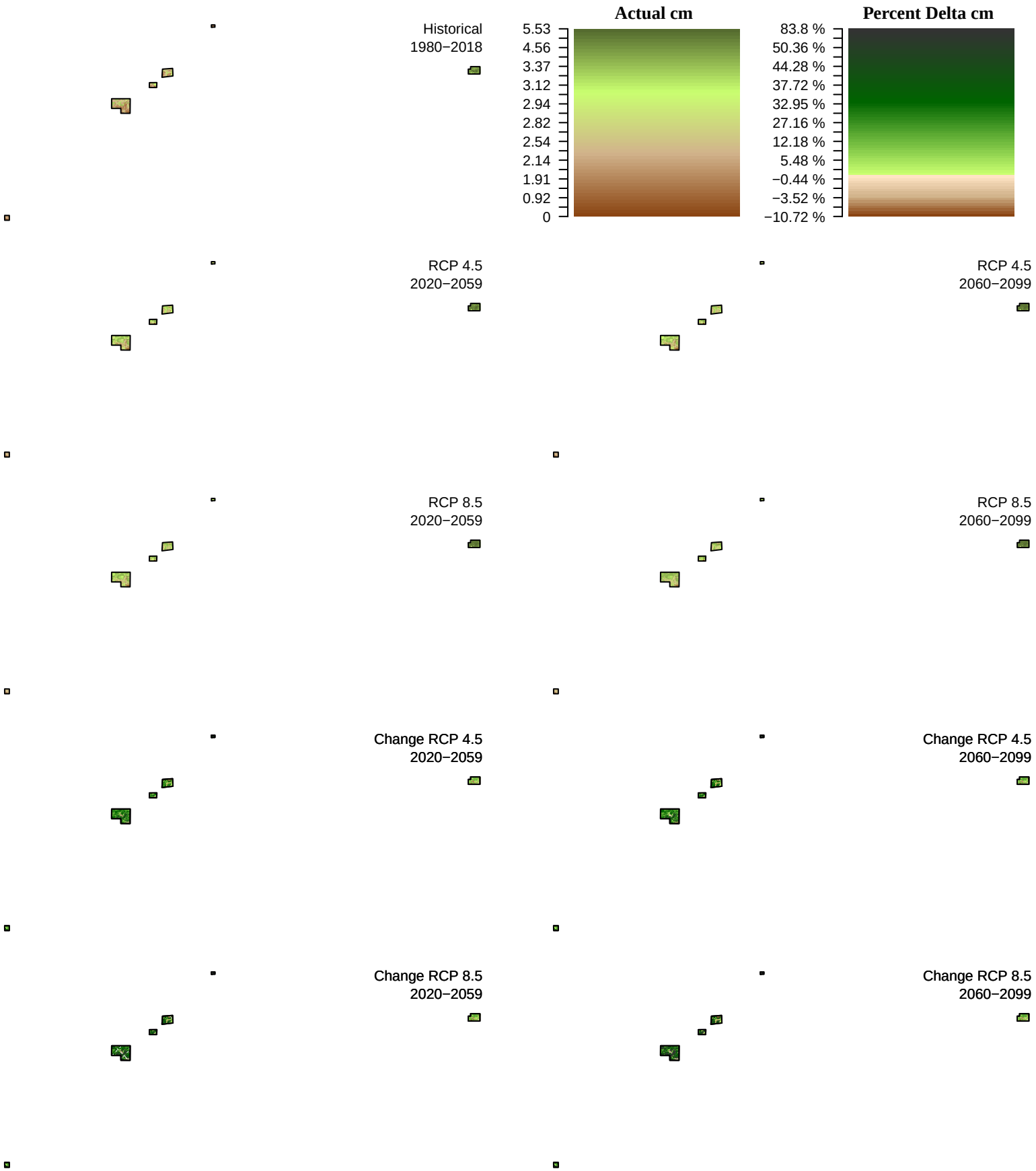


Figure HOVEmap71:
Past trends and future trajectories of park−wide mean values for Spring available soil moisture: top 50cm in Hovenweep. Topmost panel depicts the historical mean from 1980−2018. Lower four panels show the emission scenarios of RCP 4.5 and RCP 8.5 at near−term and long−term timeframes. Bottom four panels depict the change from the historical mean; cross hatching denotes areas of robust predicitons (90% of models agree in the direction of change).

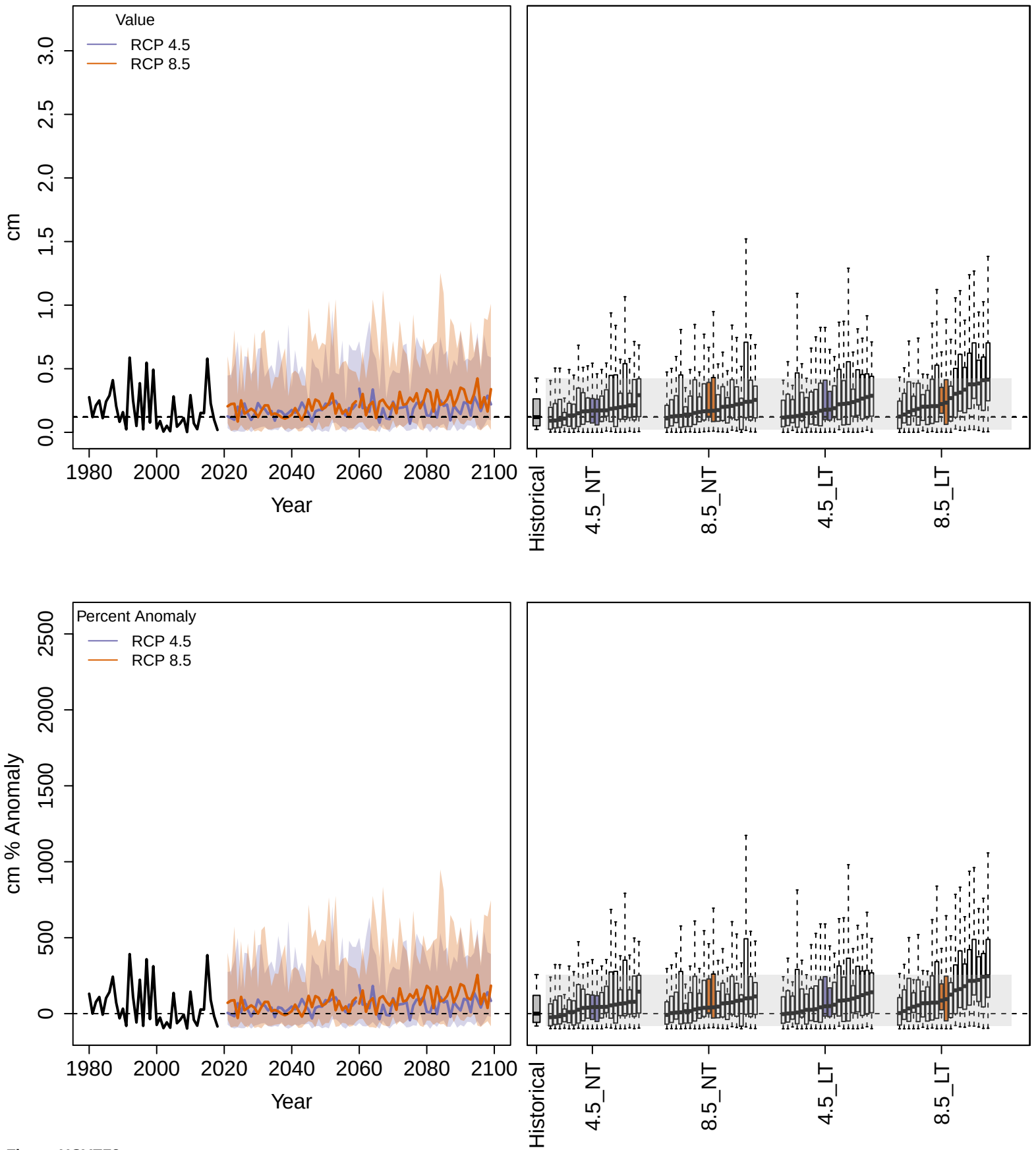


Figure HOVE73:
Past trends and future trajectories of park−wide mean values for Summer available soil moisture: top 50cm in Hovenweep. Top panels show values, bottom panels show changes from the long−term historical mean. Left: Time series of historical (black) and future projections for RCP 4.5 and 8.5. Shaded areas show spread among climate models. Right: Boxplots of temporal variability over 40−year periods under historical (left box) and individual climate models under two RCPs. Right: Historical time period is 1970−2010; near−term (NT) is 2020−2060; long−term (LT) is 2061−2100.

Hovenweep: Summer available soil moisture: top 50cm

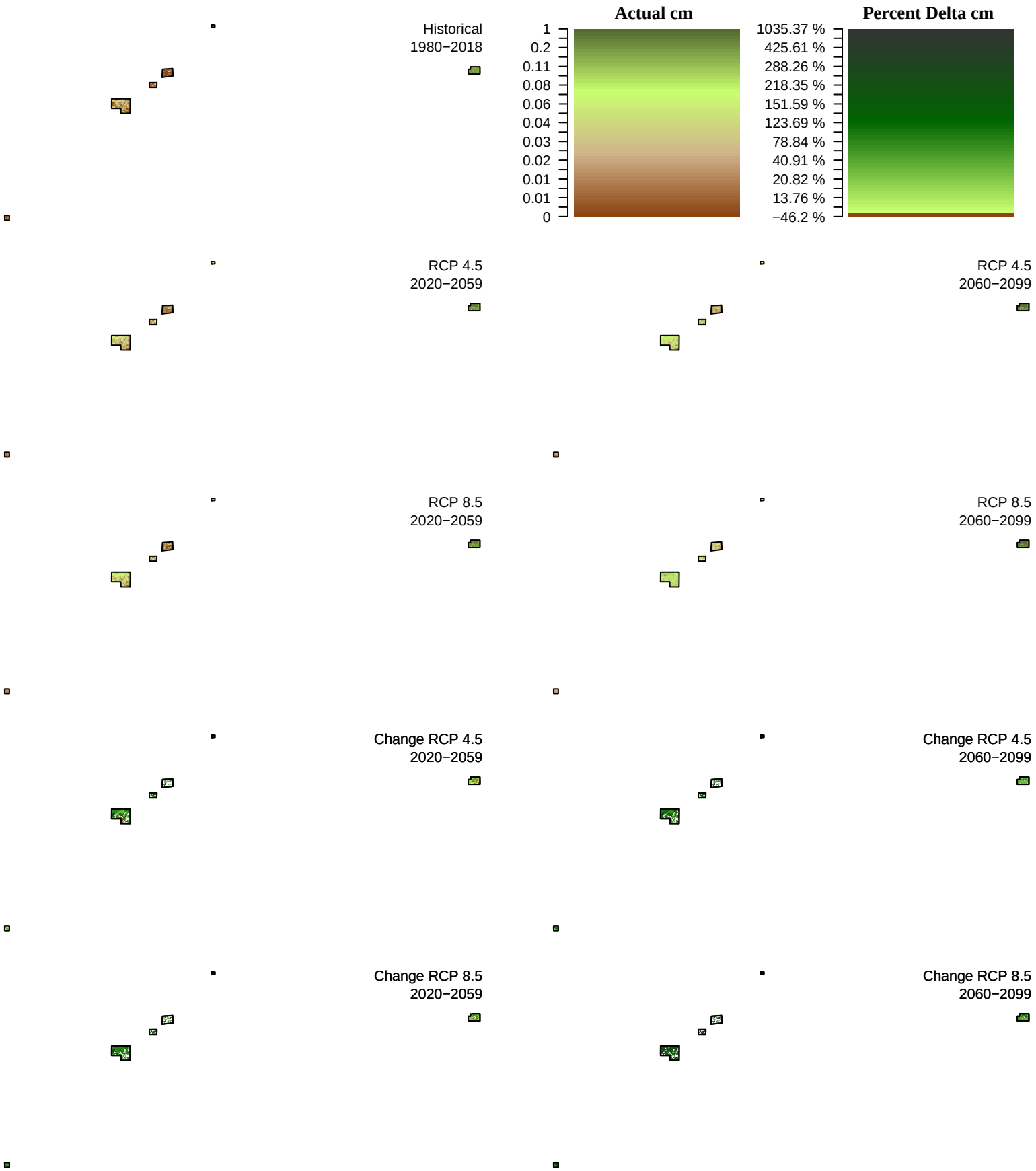


Figure HOVEmap73:
Past trends and future trajectories of park−wide mean values for Summer available soil moisture: top 50cm in Hovenweep. Topmost panel depicts the historical mean from 1980−2018. Lower four panels show the emission scenarios of RCP 4.5 and RCP 8.5 at near−term and long−term timeframes. Bottom four panels depict the change from the historical mean; cross hatching denotes areas of robust predicitons (90% of models agree in the direction of change).

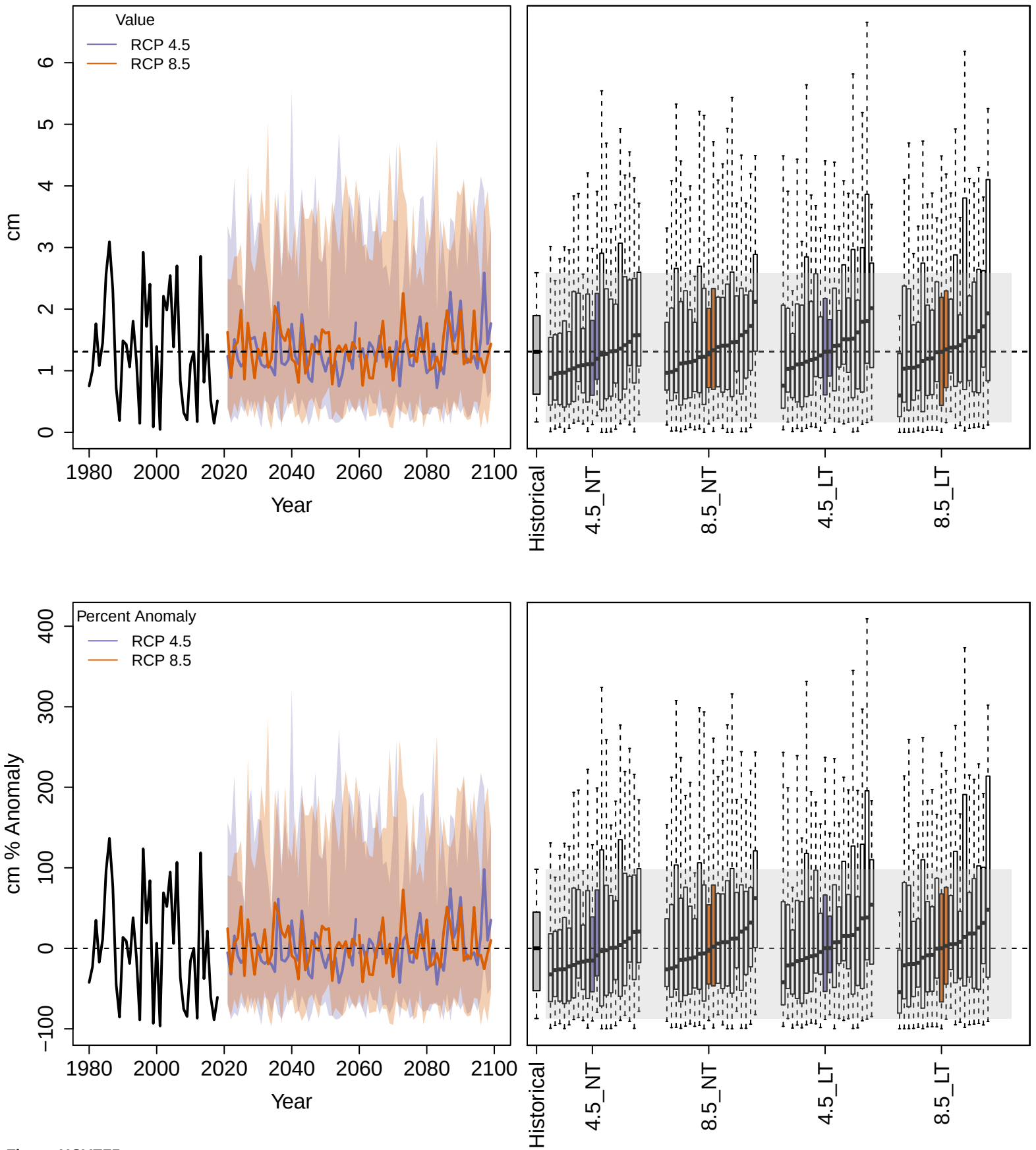


Figure HOVE75:
Past trends and future trajectories of park−wide mean values for Fall available soil moisture: top 50cm in Hovenweep. Top panels show values, bottom panels show changes from the long−term historical mean. Left: Time series of historical (black) and future projections for RCP 4.5 and 8.5. Shaded areas show spread among climate models. Right: Boxplots of temporal variability over 40−year periods under historical (left box) and individual climate models under two RCPs. Right: Historical time period is 1970−2010; near−term (NT) is 2020−2060; long−term (LT) is 2061−2100.

Hovenweep: Fall available soil moisture: top 50cm

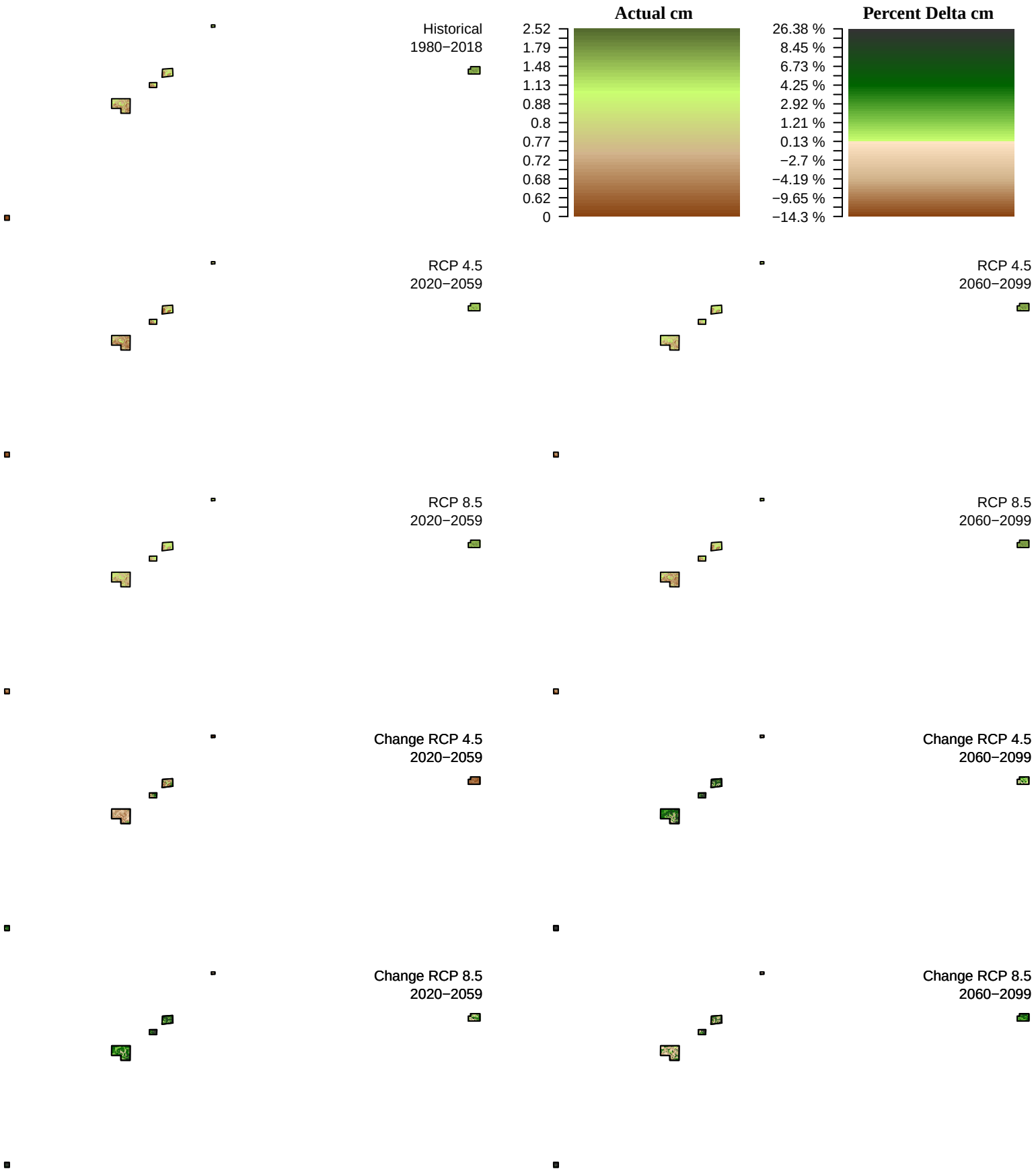


Figure HOVEmap75:
Past trends and future trajectories of park−wide mean values for Fall available soil moisture: top 50cm in Hovenweep. Topmost panel depicts the historical mean from 1980−2018. Lower four panels show the emission scenarios of RCP 4.5 and RCP 8.5 at near−term and long−term timeframes. Bottom four panels depict the change from the historical mean; cross hatching denotes areas of robust predicitons (90% of models agree in the direction of change).

Hovenweep: Winter available soil moisture

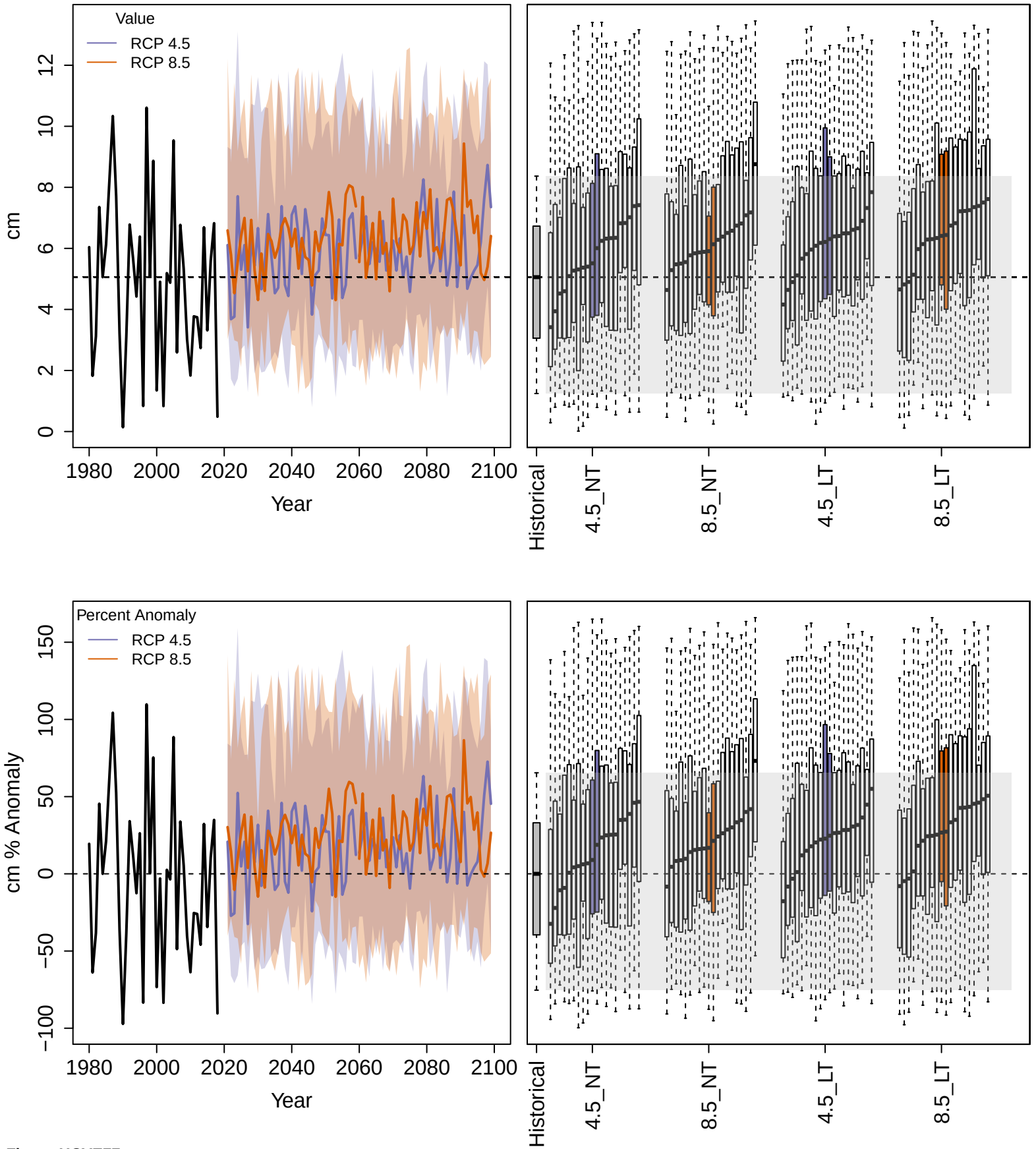


Figure HOVE77:
Past trends and future trajectories of park−wide mean values for Winter available soil moisture in Hovenweep. Top panels show values, bottom panels show changes from the long−term historical mean. Left: Time series of historical (black) and future projections for RCP 4.5 and 8.5. Shaded areas show spread among climate models. Right: Boxplots of temporal variability over 40−year periods under historical (left box) and individual climate models under two RCPs. Right: Historical time period is 1970−2010; near−term (NT) is 2020−2060; long−term (LT) is 2061−2100.

Hovenweep: Winter available soil moisture

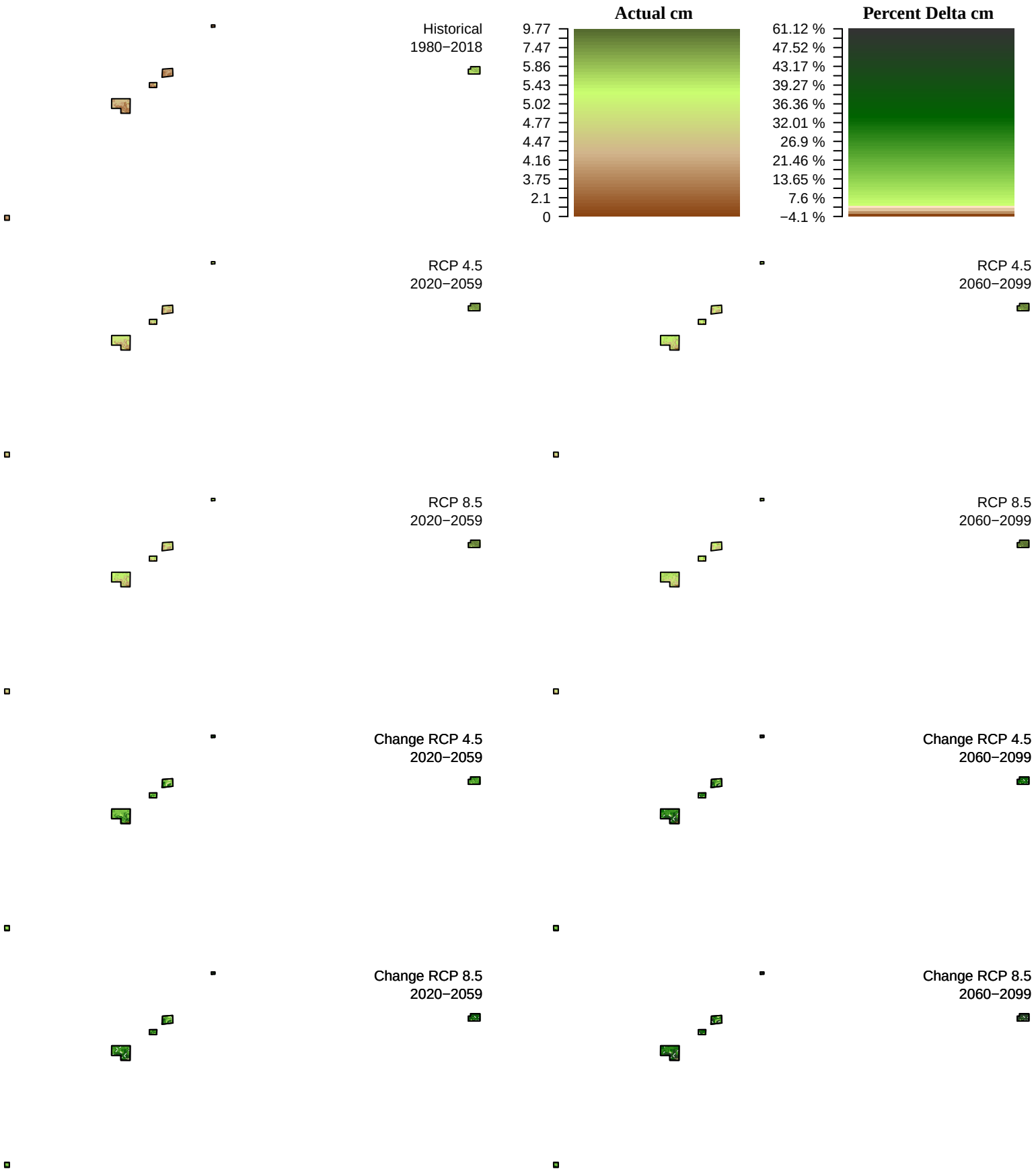


Figure HOVEmap77:
Past trends and future trajectories of park−wide mean values for Winter available soil moisture in Hovenweep. Topmost panel depicts the historical mean from 1980−2018. Lower four panels show the emission scenarios of RCP 4.5 and RCP 8.5 at near−term and long−term timeframes. Bottom four panels depict the change from the historical mean; cross hatching denotes areas of robust predicitons (90% of models agree in the direction of change).

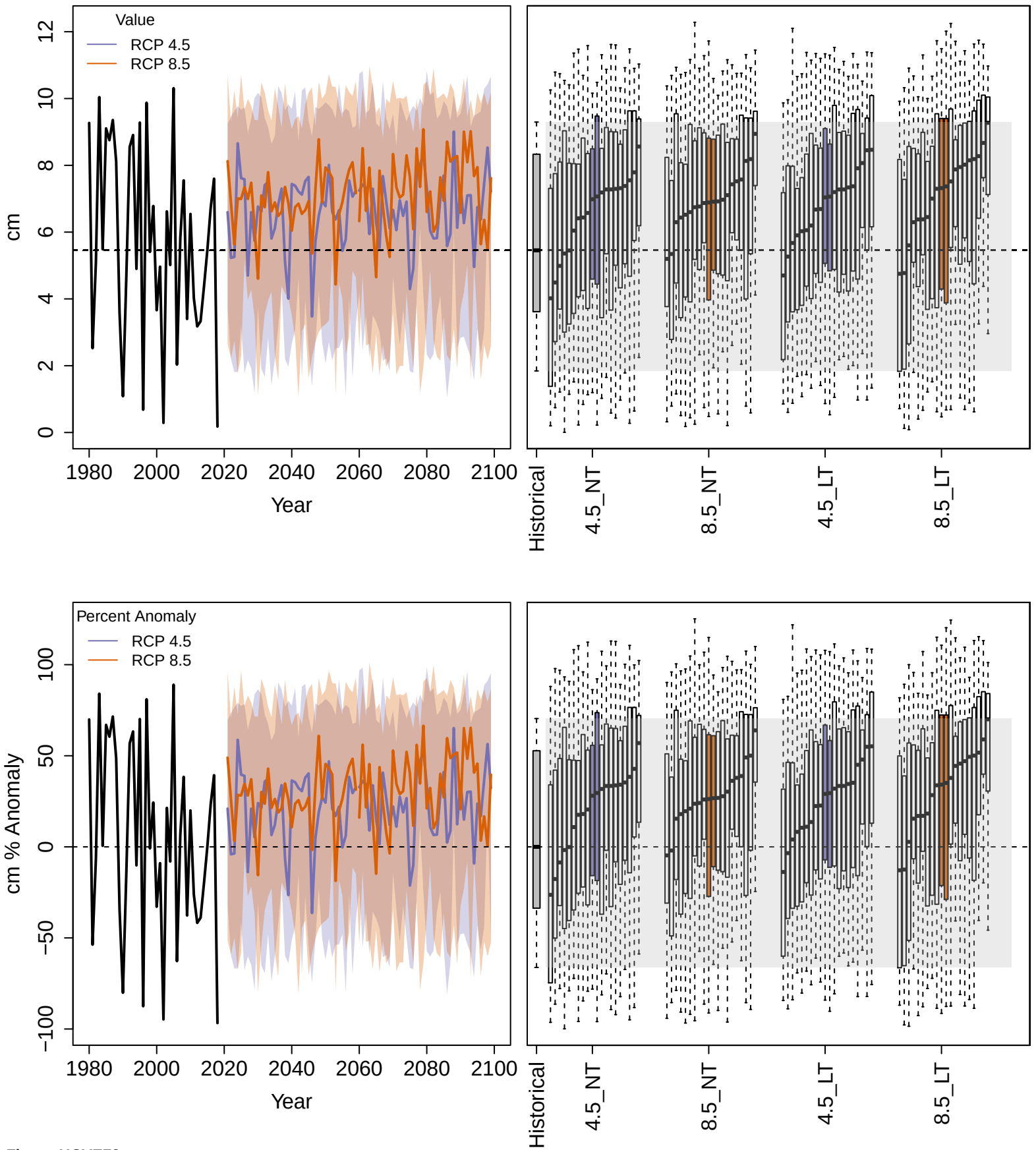


Figure HOVE79:
Past trends and future trajectories of park−wide mean values for Spring available soil moisture in Hovenweep. Top panels show values, bottom panels show changes from the long−term historical mean. Left: Time series of historical (black) and future projections for RCP 4.5 and 8.5. Shaded areas show spread among climate models. Right: Boxplots of temporal variability over 40−year periods under historical (left box) and individual climate models under two RCPs. Right: Historical time period is 1970−2010; near−term (NT) is 2020−2060; long−term (LT) is 2061−2100.

Hovenweep: Spring available soil moisture

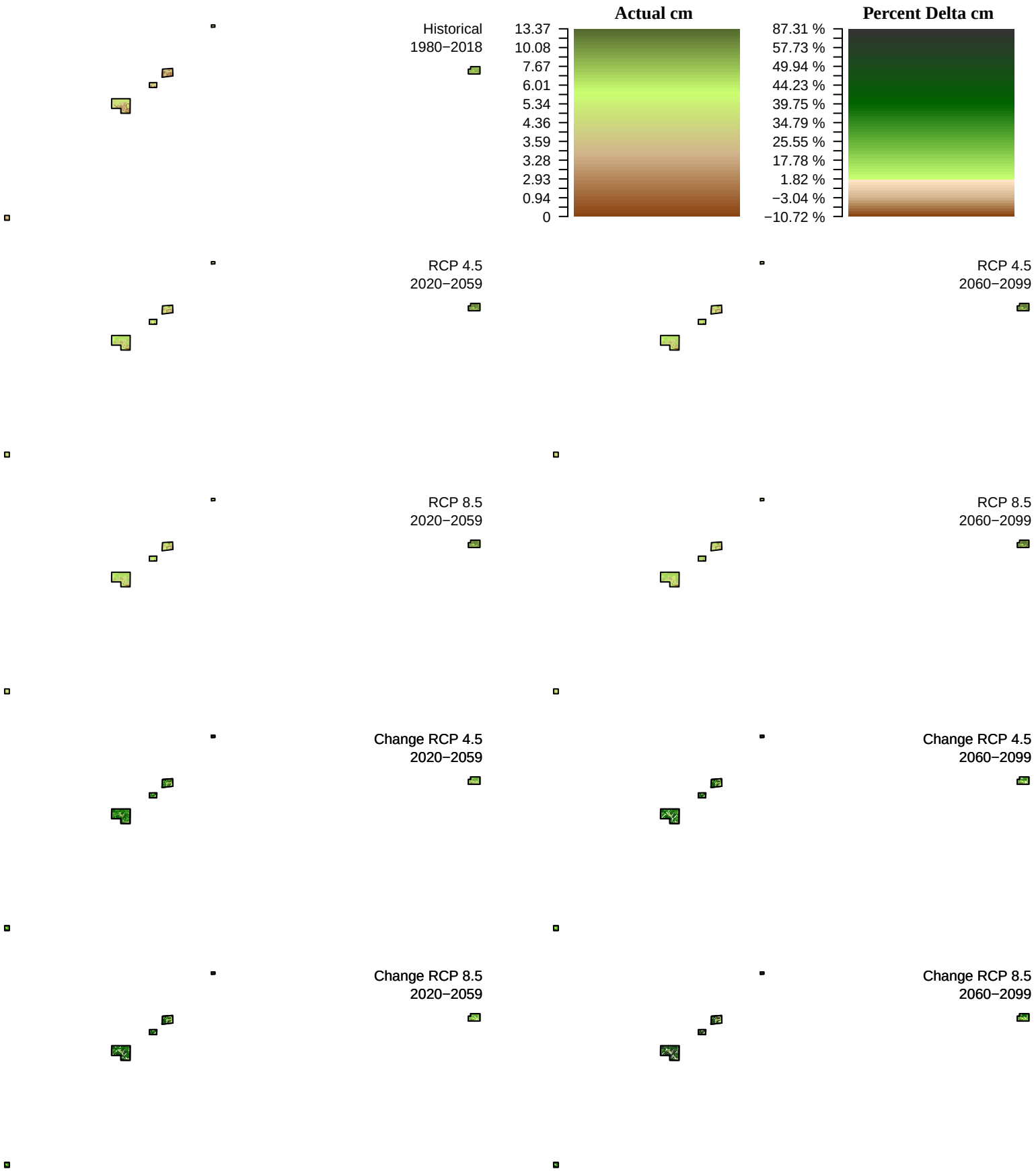


Figure HOVEmap79:
Past trends and future trajectories of park−wide mean values for Spring available soil moisture in Hovenweep. Topmost panel depicts the historical mean from 1980−2018. Lower four panels show the emission scenarios of RCP 4.5 and RCP 8.5 at near−term and long−term timeframes. Bottom four panels depict the change from the historical mean; cross hatching denotes areas of robust predicitons (90% of models agree in the direction of change).

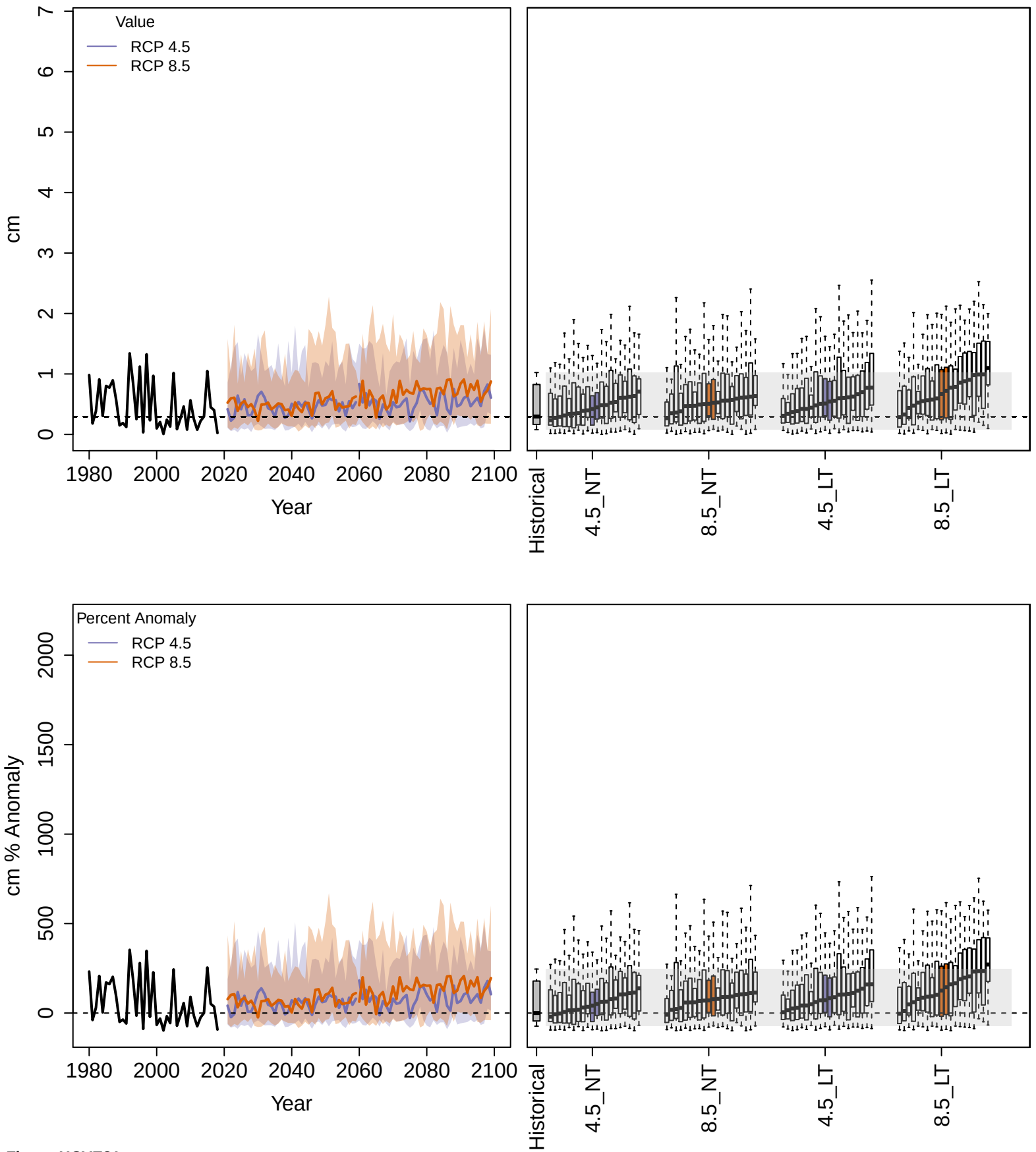


Figure HOVE81:
Past trends and future trajectories of park−wide mean values for Summer available soil moisture in Hovenweep. Top panels show values, bottom panels show changes from the long−term historical mean. Left: Time series of historical (black) and future projections for RCP 4.5 and 8.5. Shaded areas show spread among climate models. Right: Boxplots of temporal variability over 40−year periods under historical (left box) and individual climate models under two RCPs. Right: Historical time period is 1970−2010; near−term (NT) is 2020−2060; long−term (LT) is 2061−2100.

Hovenweep: Summer available soil moisture

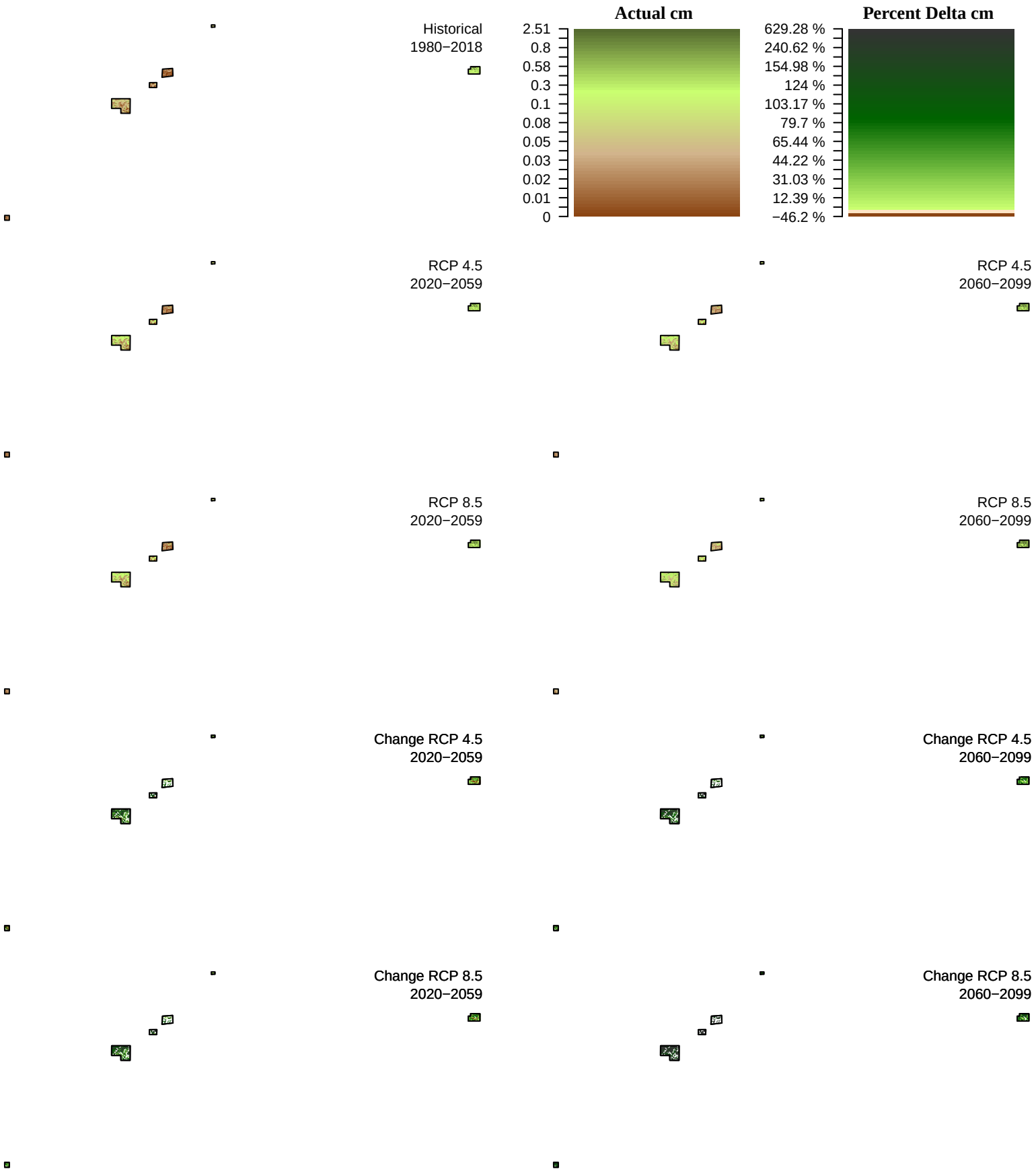


Figure HOVEmap81:
Past trends and future trajectories of park−wide mean values for Summer available soil moisture in Hovenweep. Topmost panel depicts the historical mean from 1980−2018. Lower four panels show the emission scenarios of RCP 4.5 and RCP 8.5 at near−term and long−term timeframes. Bottom four panels depict the change from the historical mean; cross hatching denotes areas of robust predicitons (90% of models agree in the direction of change).

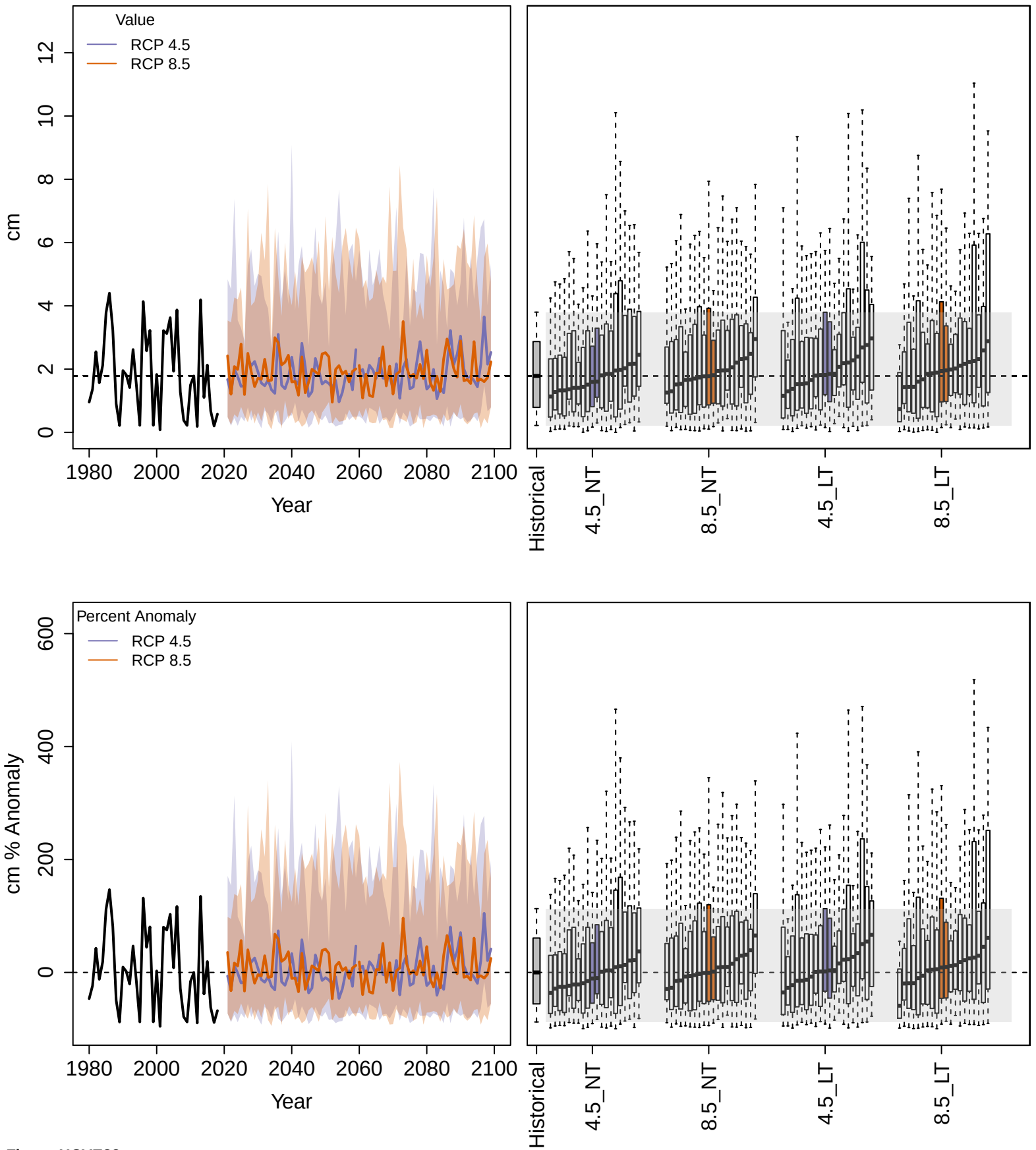


Figure HOVE83:
Past trends and future trajectories of park−wide mean values for Fall available soil moisture in Hovenweep. Top panels show values, bottom panels show changes from the long−term historical mean. Left: Time series of historical (black) and future projections for RCP 4.5 and 8.5. Shaded areas show spread among climate models. Right: Boxplots of temporal variability over 40−year periods under historical (left box) and individual climate models under two RCPs. Right: Historical time period is 1970−2010; near−term (NT) is 2020−2060; long−term (LT) is 2061−2100.

Hovenweep: Fall available soil moisture

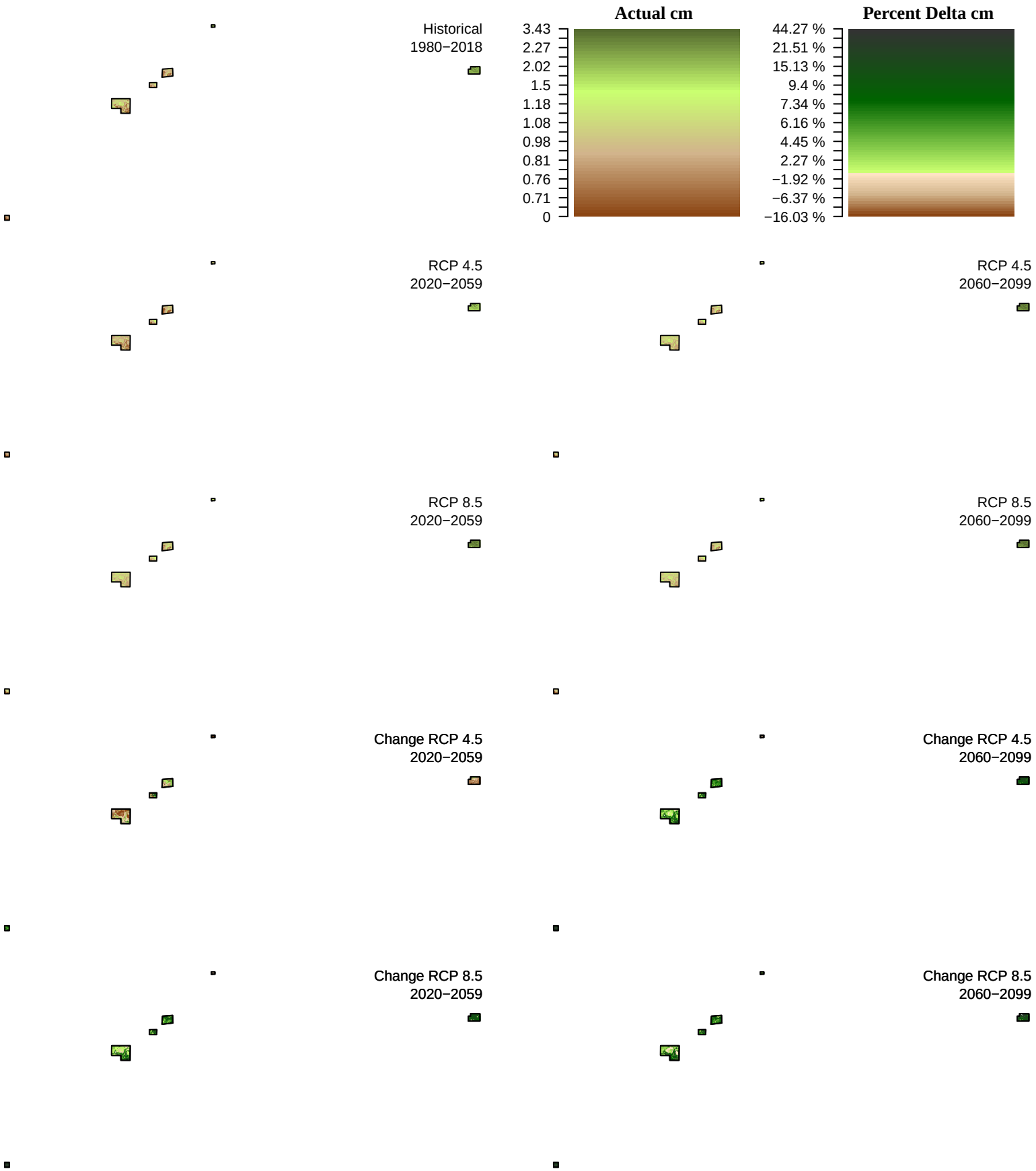


Figure HOVEmap83:
Past trends and future trajectories of park−wide mean values for Fall available soil moisture in Hovenweep. Topmost panel depicts the historical mean from 1980−2018. Lower four panels show the emission scenarios of RCP 4.5 and RCP 8.5 at near−term and long−term timeframes. Bottom four panels depict the change from the historical mean; cross hatching denotes areas of robust predicitons (90% of models agree in the direction of change).

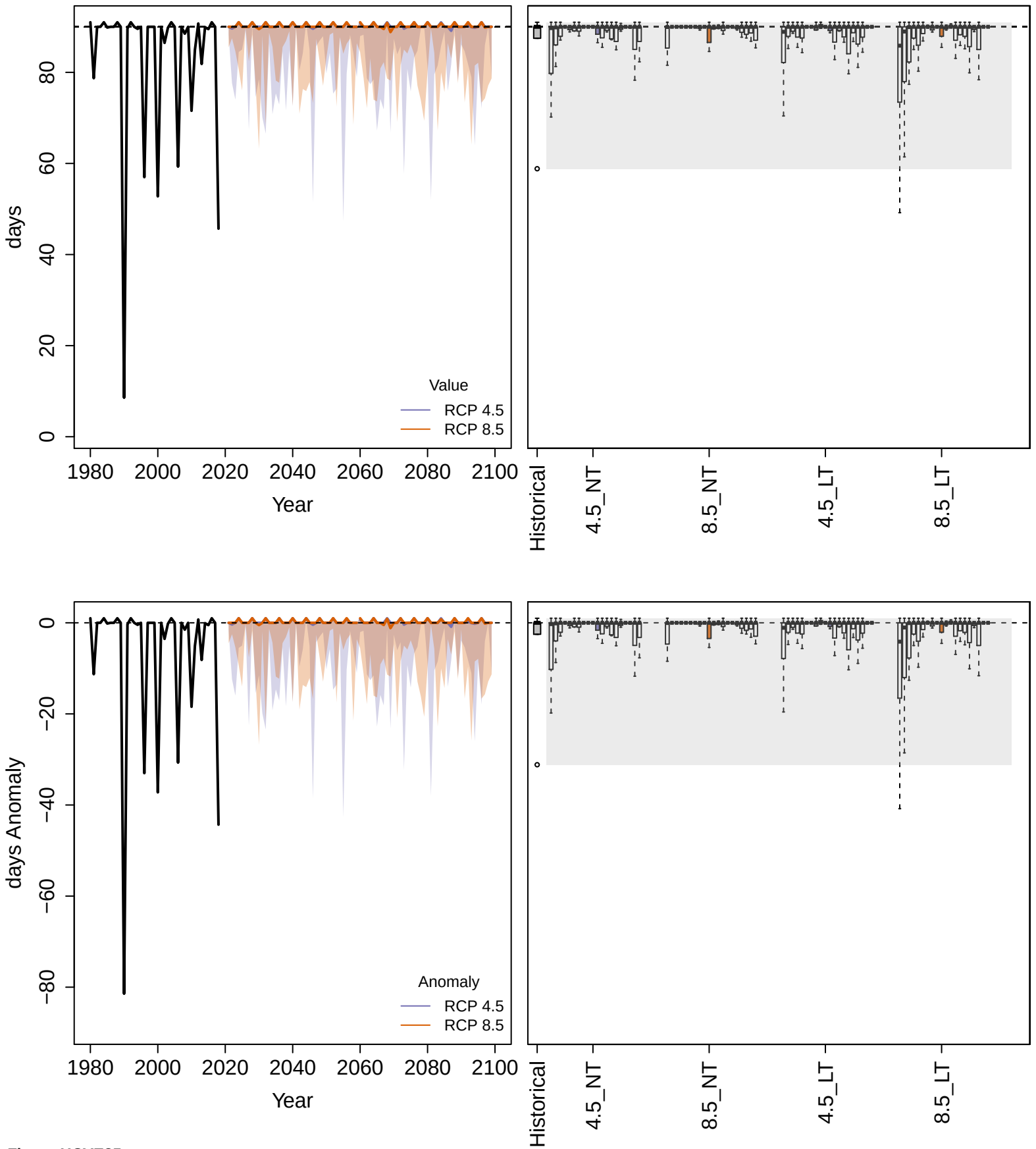


Figure HOVE85:
Past trends and future trajectories of park−wide mean values for Winter wet soil days in Hovenweep. Top panels show values, bottom panels show changes from the long−term historical mean. Left: Time series of historical (black) and future projections for RCP 4.5 and 8.5. Shaded areas show spread among climate models. Right: Boxplots of temporal variability over 40−year periods under historical (left box) and individual climate models under two RCPs. Right: Historical time period is 1970−2010; near−term (NT) is 2020−2060; long−term (LT) is 2061−2100.

Hovenweep: Winter wet soil days

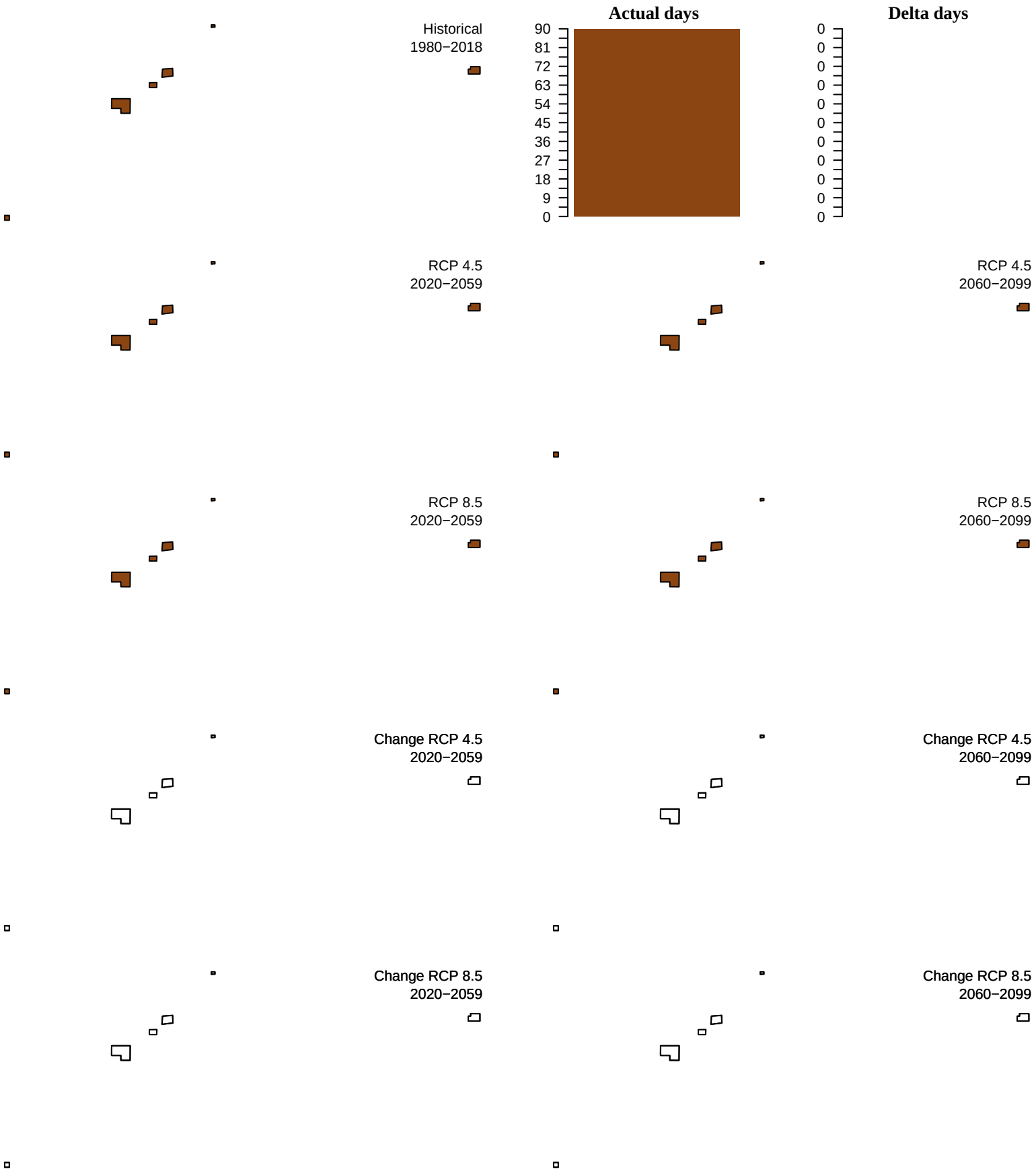


Figure HOVEmap85:
Past trends and future trajectories of park−wide mean values for Winter wet soil days in Hovenweep. Topmost panel depicts the historical mean from 1980−2018. Lower four panels show the emission scenarios of RCP 4.5 and RCP 8.5 at near−term and long−term timeframes. Bottom four panels depict the change from the historical mean; cross hatching denotes areas of robust predicitons (90% of models agree in the direction of change).

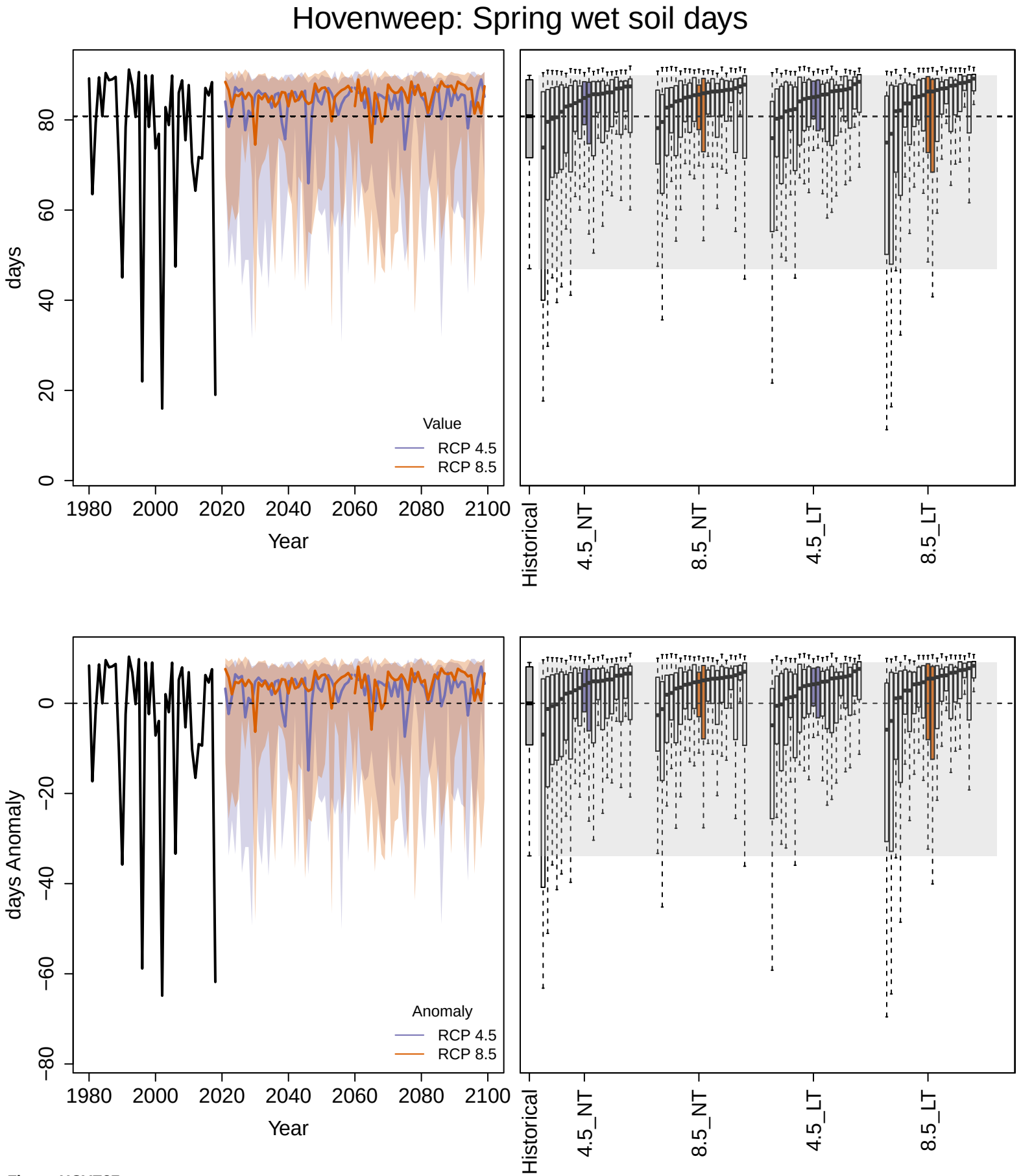


Figure HOVE87:
Past trends and future trajectories of park−wide mean values for Spring wet soil days in Hovenweep. Top panels show values, bottom panels show changes from the long−term historical mean. Left: Time series of historical (black) and future projections for RCP 4.5 and 8.5. Shaded areas show spread among climate models. Right: Boxplots of temporal variability over 40−year periods under historical (left box) and individual climate models under two RCPs. Right: Historical time period is 1970−2010; near−term (NT) is 2020−2060; long−term (LT) is 2061−2100.

Hovenweep: Spring wet soil days

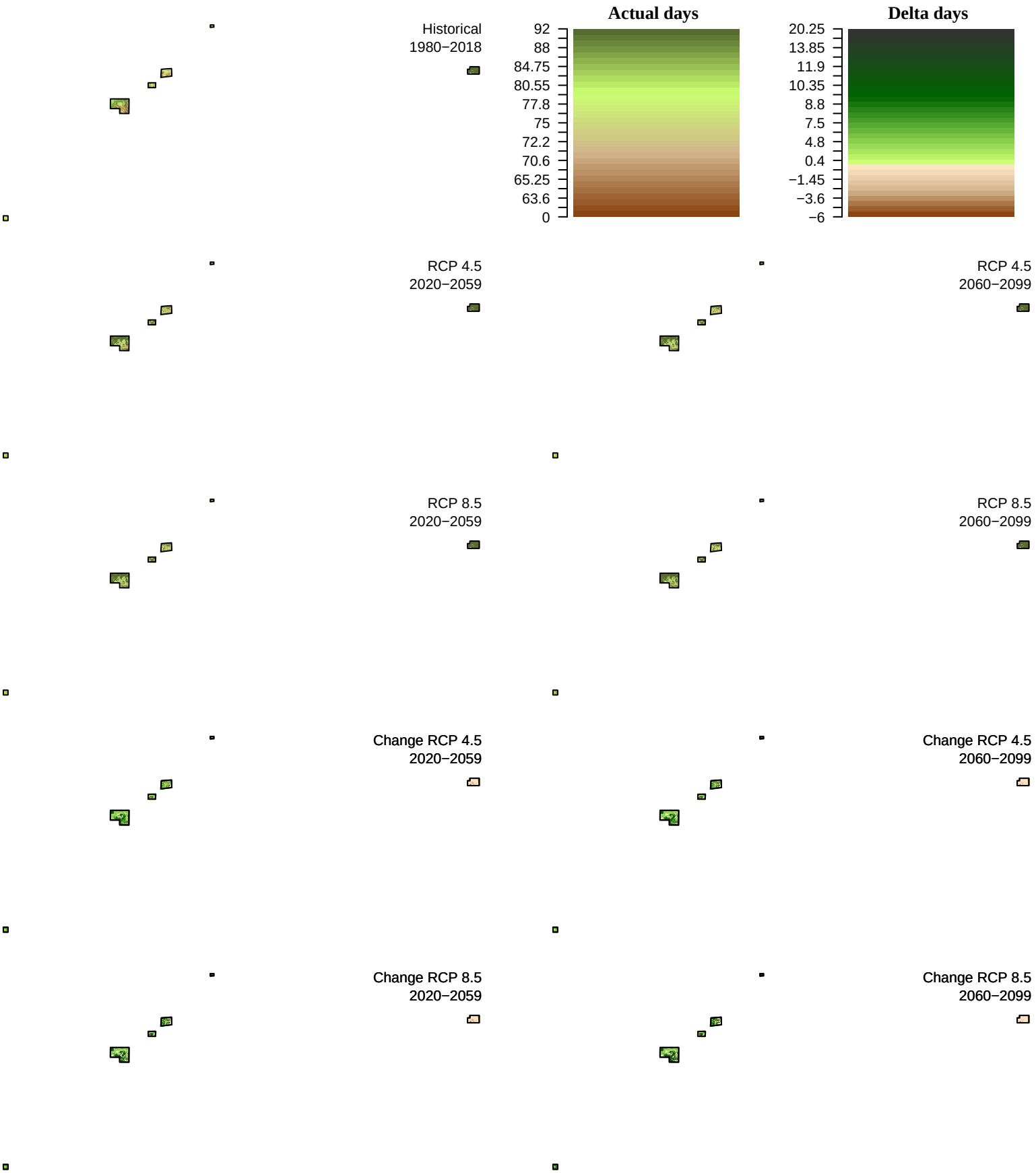


Figure HOVEmap87:
Past trends and future trajectories of park−wide mean values for Spring wet soil days in Hovenweep. Topmost panel depicts the historical mean from 1980−2018. Lower four panels show the emission scenarios of RCP 4.5 and RCP 8.5 at near−term and long−term timeframes. Bottom four panels depict the change from the historical mean; cross hatching denotes areas of robust predicitons (90% of models agree in the direction of change).

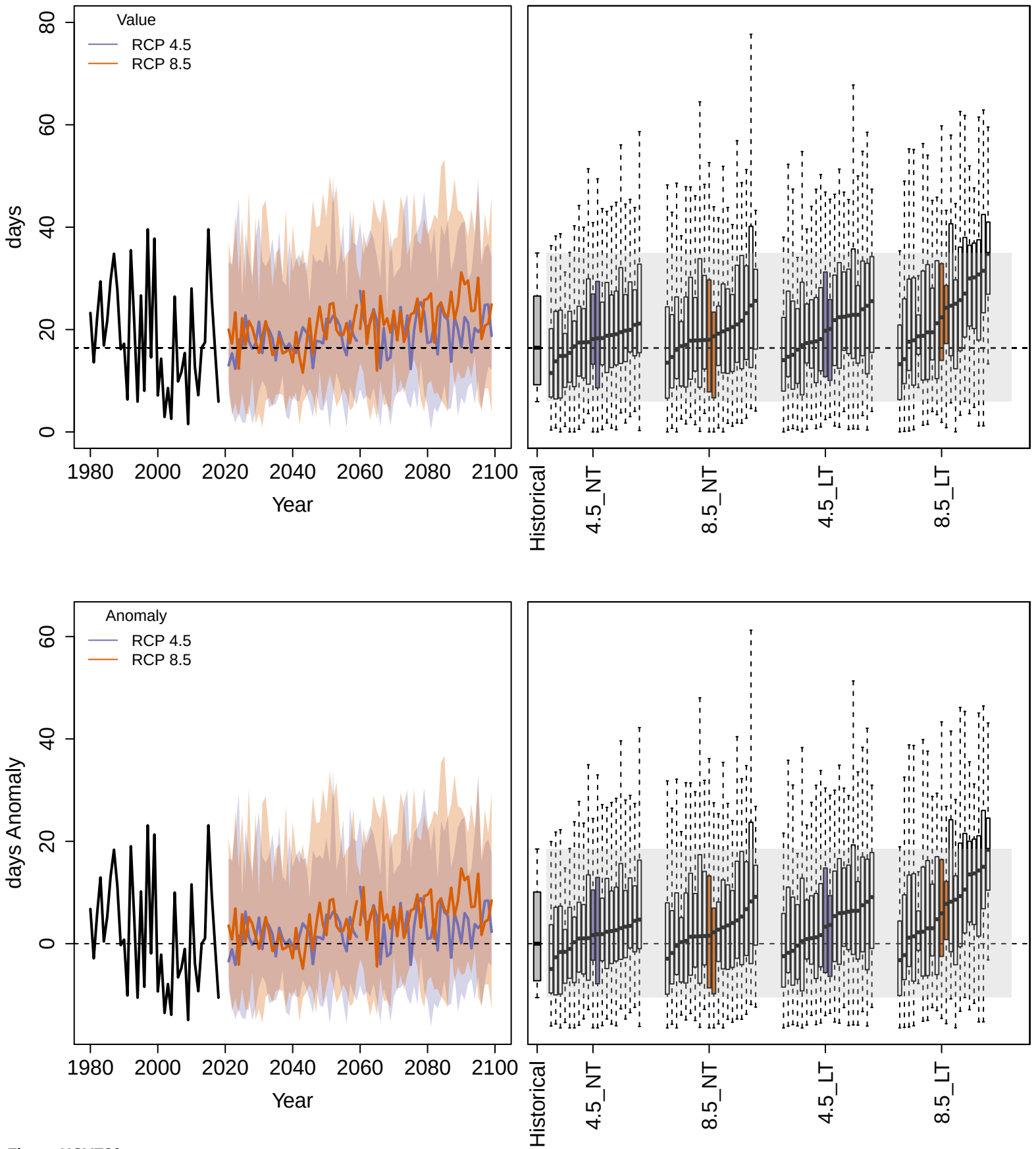


Figure HOVE89:
Past trends and future trajectories of park−wide mean values for Summer wet soil days in Hovenweep. Top panels show values, bottom panels show changes from the long−term historical mean. Left: Time series of historical (black) and future projections for RCP 4.5 and 8.5. Shaded areas show spread among climate models. Right: Boxplots of temporal variability over 40−year periods under historical (left box) and individual climate models under two RCPs. Right: Historical time period is 1970−2010; near−term (NT) is 2020−2060; long−term (LT) is 2061−2100.

Hovenweep: Summer wet soil days

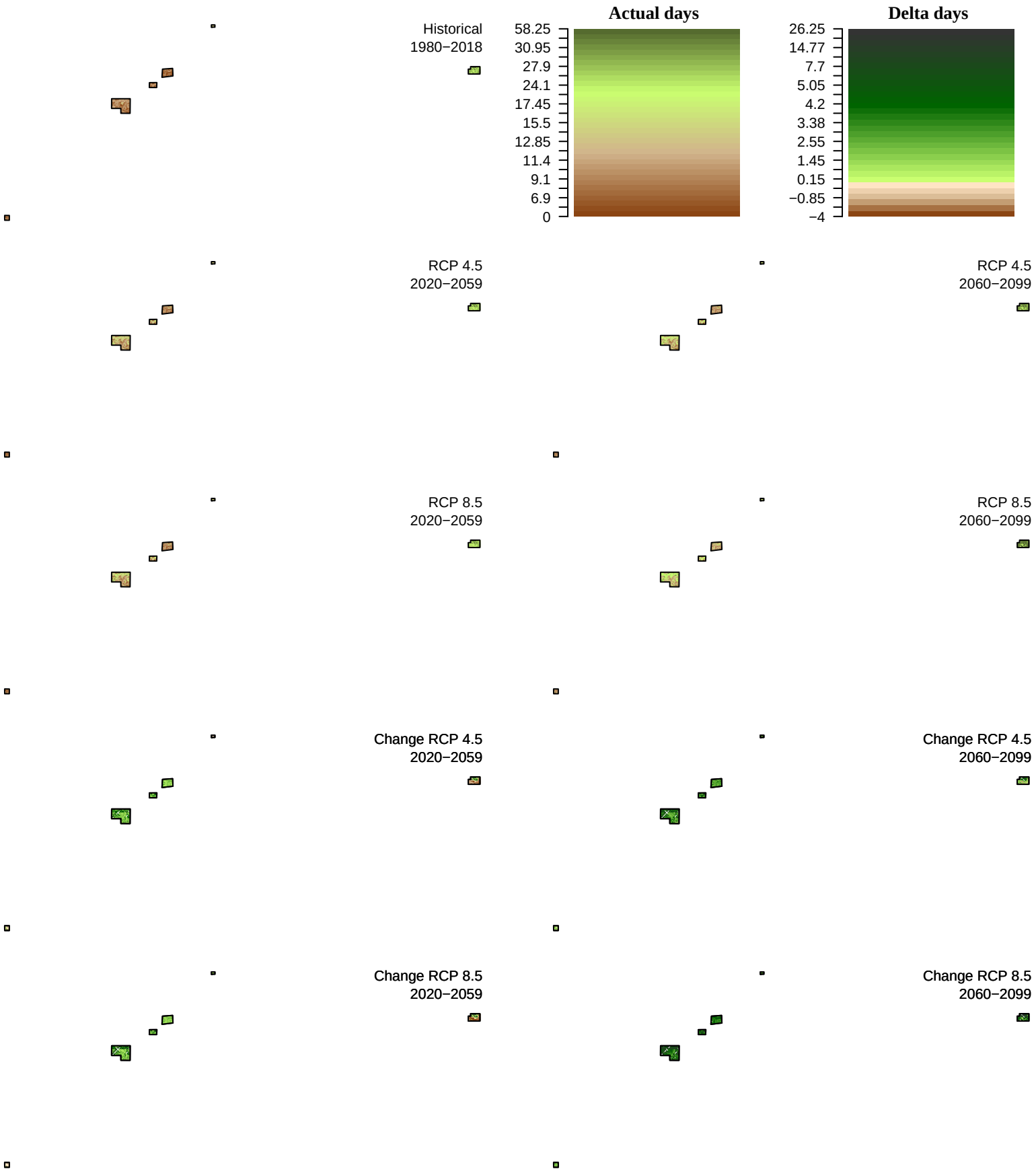


Figure HOVEmap89:
Past trends and future trajectories of park−wide mean values for Summer wet soil days in Hovenweep. Topmost panel depicts the historical mean from 1980−2018. Lower four panels show the emission scenarios of RCP 4.5 and RCP 8.5 at near−term and long−term timeframes. Bottom four panels depict the change from the historical mean; cross hatching denotes areas of robust predicitons (90% of models agree in the direction of change).

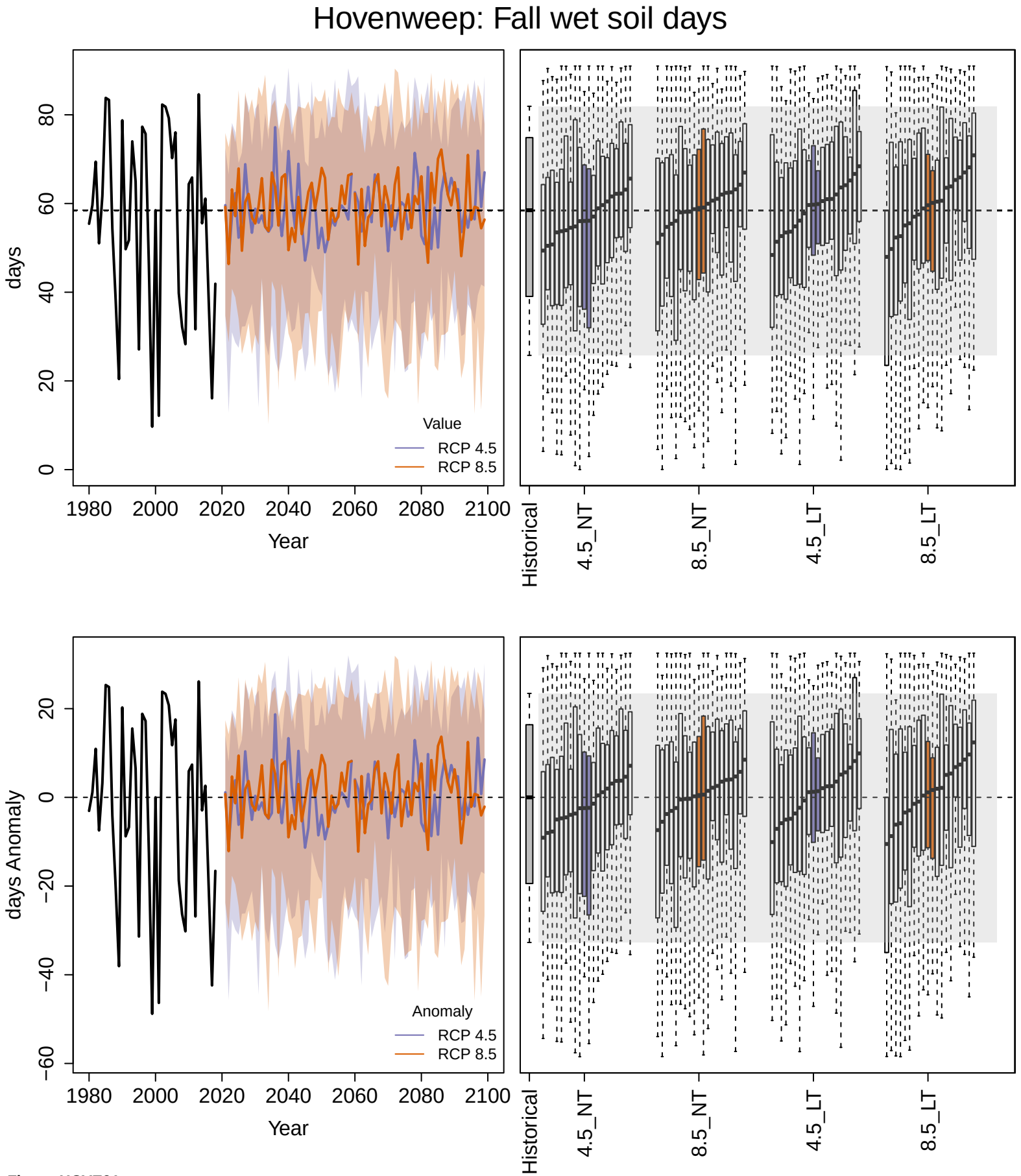


Figure HOVE91:
Past trends and future trajectories of park−wide mean values for Fall wet soil days in Hovenweep. Top panels show values, bottom panels show changes from the long−term historical mean. Left: Time series of historical (black) and future projections for RCP 4.5 and 8.5. Shaded areas show spread among climate models. Right: Boxplots of temporal variability over 40−year periods under historical (left box) and individual climate models under two RCPs. Right: Historical time period is 1970−2010; near−term (NT) is 2020−2060; long−term (LT) is 2061−2100.

Hovenweep: Fall wet soil days

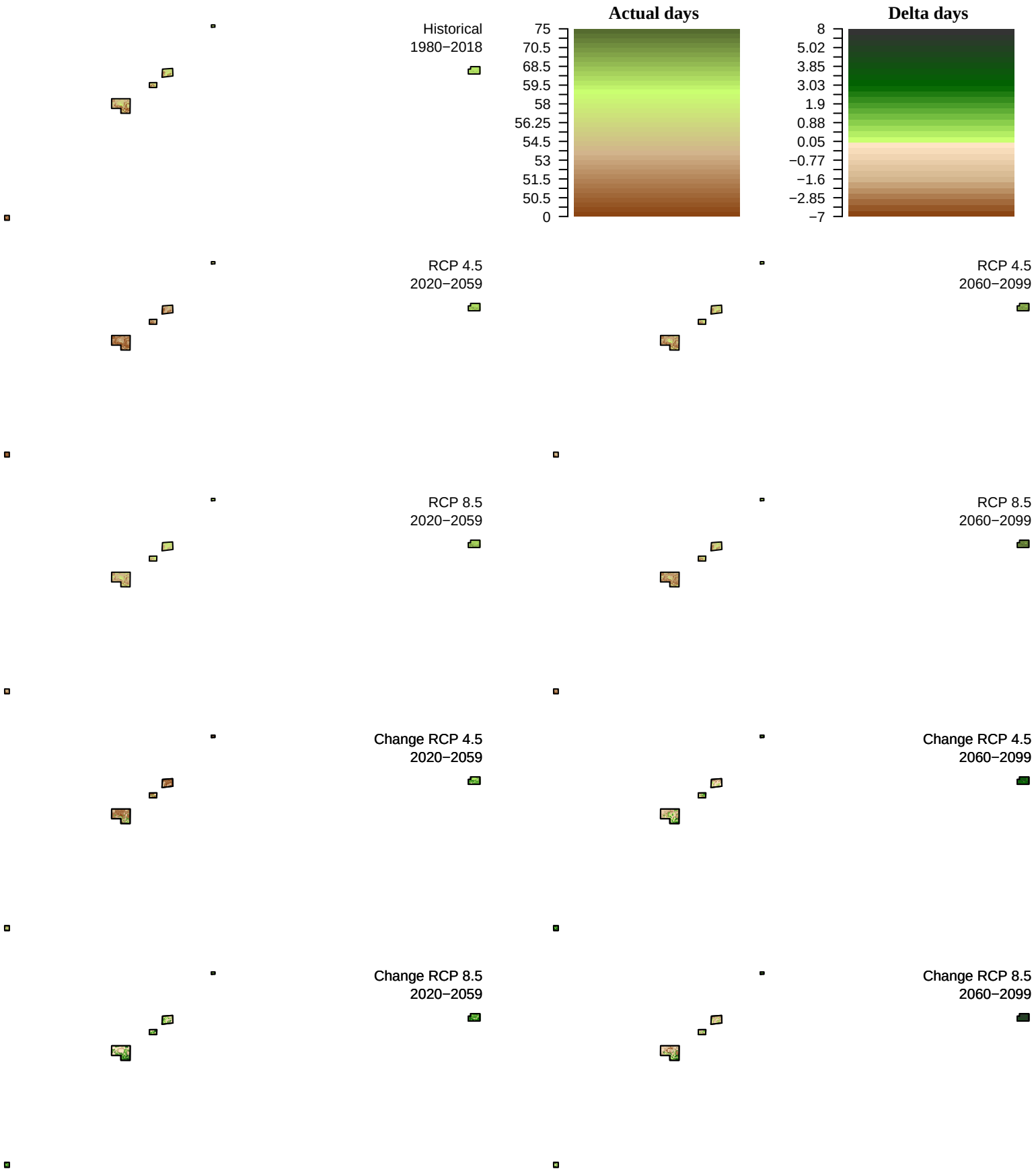


Figure HOVEmap91:
Past trends and future trajectories of park−wide mean values for Fall wet soil days in Hovenweep. Topmost panel depicts the historical mean from 1980−2018. Lower four panels show the emission scenarios of RCP 4.5 and RCP 8.5 at near−term and long−term timeframes. Bottom four panels depict the change from the historical mean; cross hatching denotes areas of robust predicitons (90% of models agree in the direction of change).

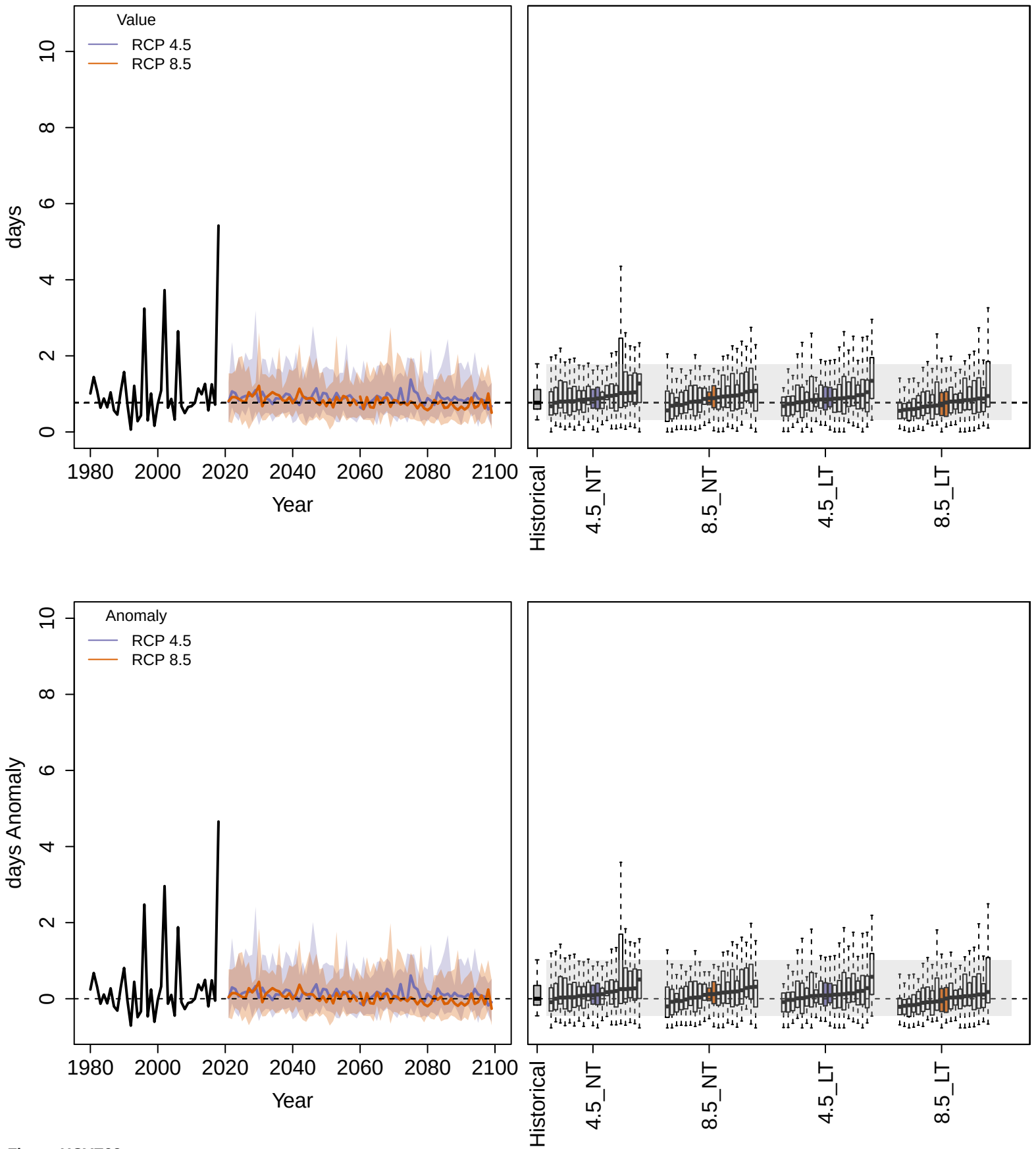


Figure HOVE93:
Past trends and future trajectories of park−wide mean values for Spring dry soil days in Hovenweep. Top panels show values, bottom panels show changes from the long−term historical mean. Left: Time series of historical (black) and future projections for RCP 4.5 and 8.5. Shaded areas show spread among climate models. Right: Boxplots of temporal variability over 40−year periods under historical (left box) and individual climate models under two RCPs. Right: Historical time period is 1970−2010; near−term (NT) is 2020−2060; long−term (LT) is 2061−2100.

Hovenweep: Spring dry soil days

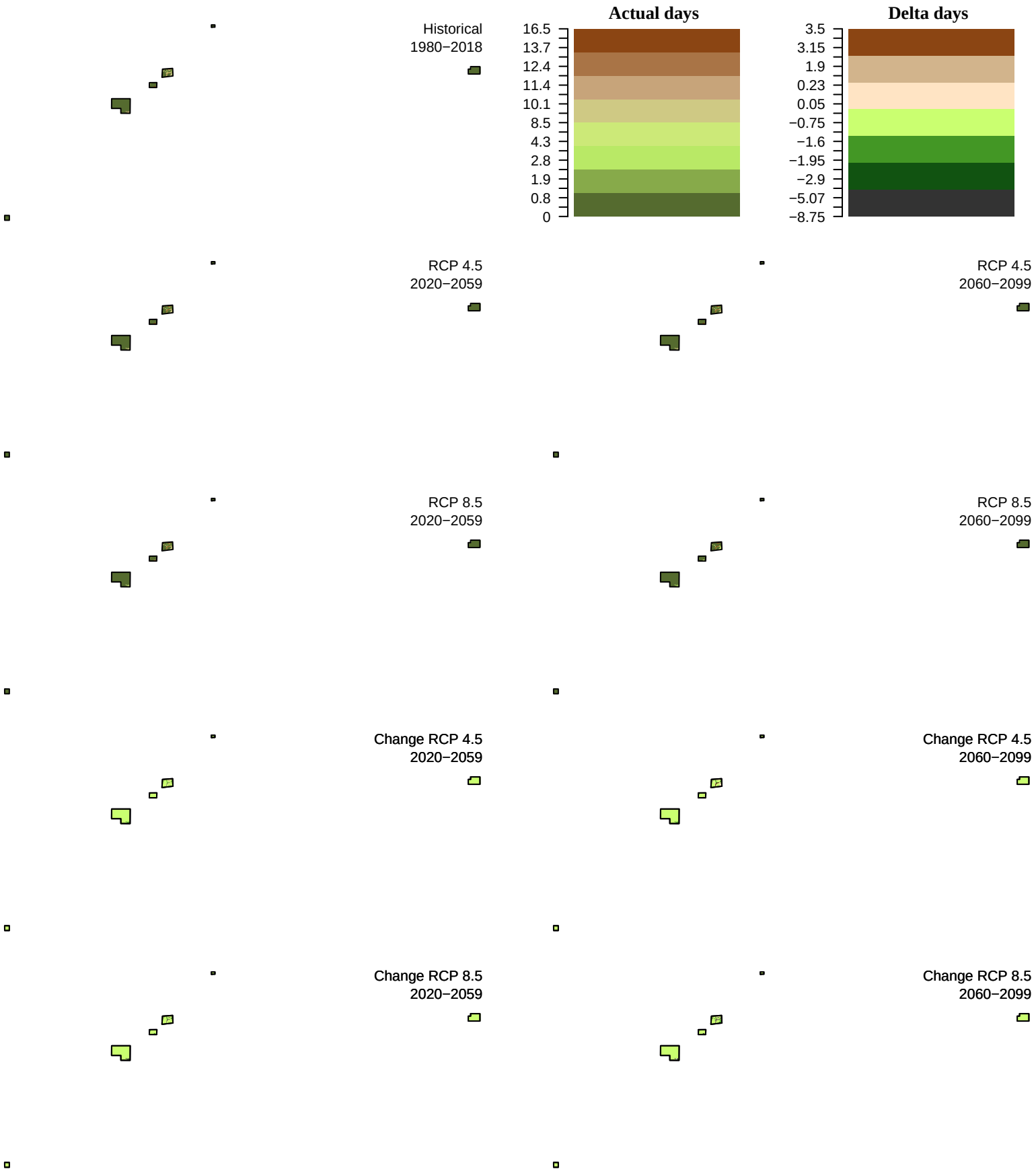


Figure HOVEmap93:
Past trends and future trajectories of park−wide mean values for Spring dry soil days in Hovenweep. Topmost panel depicts the historical mean from 1980−2018. Lower four panels show the emission scenarios of RCP 4.5 and RCP 8.5 at near−term and long−term timeframes. Bottom four panels depict the change from the historical mean; cross hatching denotes areas of robust predicitons (90% of models agree in the direction of change).

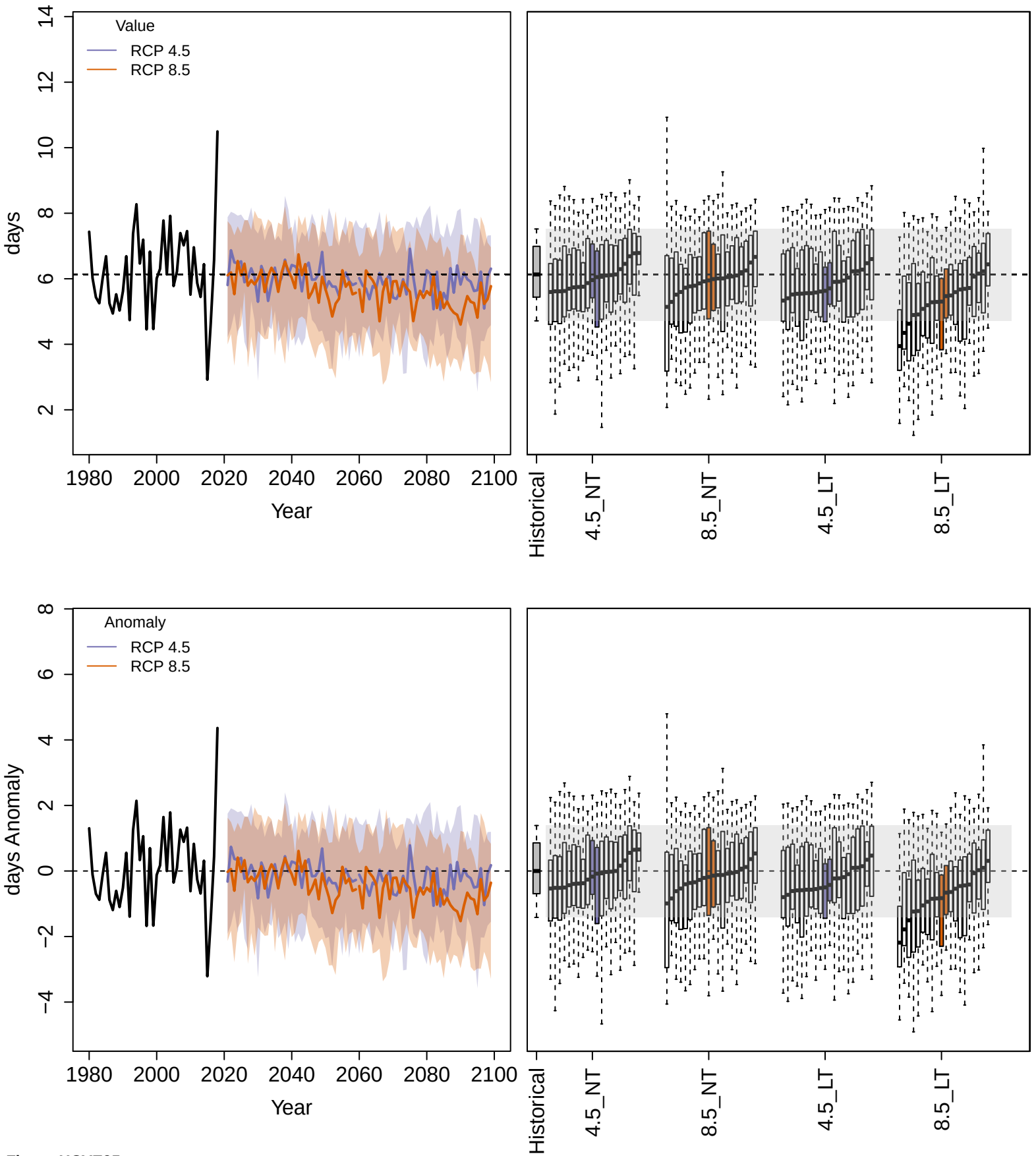


Figure HOVE95:
Past trends and future trajectories of park−wide mean values for Summer dry soil days in Hovenweep. Top panels show values, bottom panels show changes from the long−term historical mean. Left: Time series of historical (black) and future projections for RCP 4.5 and 8.5. Shaded areas show spread among climate models. Right: Boxplots of temporal variability over 40−year periods under historical (left box) and individual climate models under two RCPs. Right: Historical time period is 1970−2010; near−term (NT) is 2020−2060; long−term (LT) is 2061−2100.

Hovenweep: Summer dry soil days

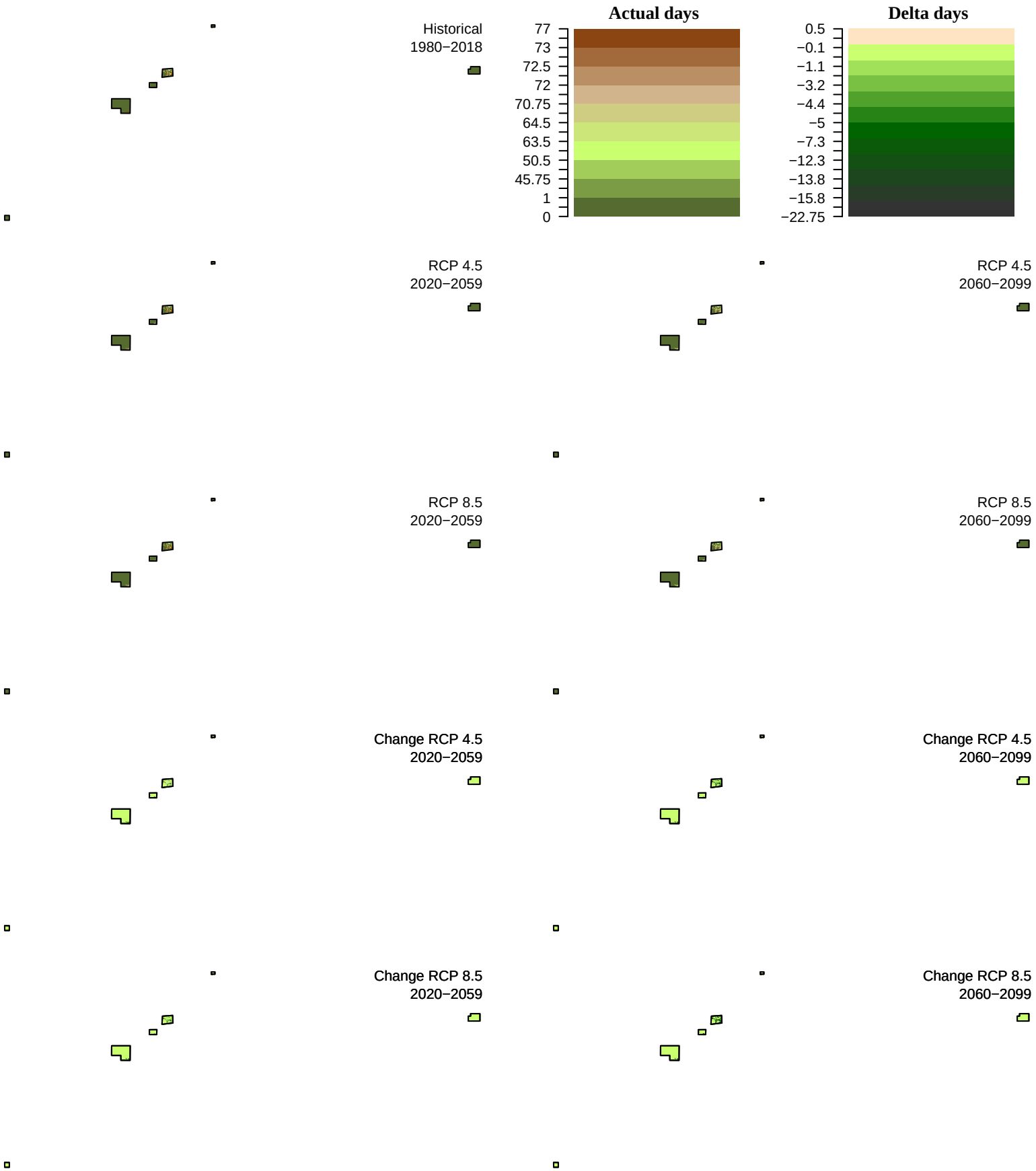


Figure HOVEmap95:
Past trends and future trajectories of park−wide mean values for Summer dry soil days in Hovenweep. Topmost panel depicts the historical mean from 1980−2018. Lower four panels show the emission scenarios of RCP 4.5 and RCP 8.5 at near−term and long−term timeframes. Bottom four panels depict the change from the historical mean; cross hatching denotes areas of robust predicitons (90% of models agree in the direction of change).

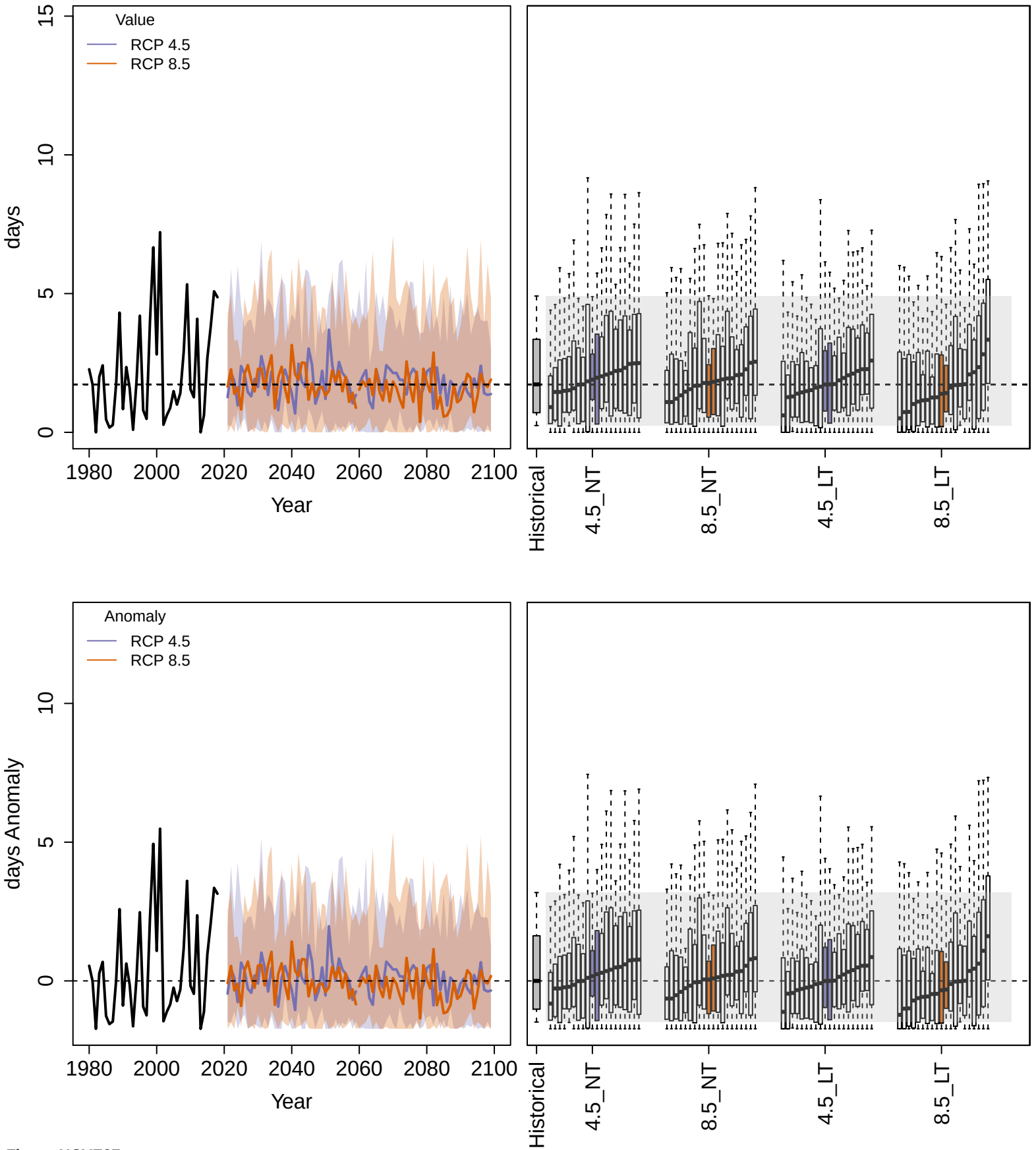


Figure HOVE97:
Past trends and future trajectories of park−wide mean values for Fall dry soil days in Hovenweep. Top panels show values, bottom panels show changes from the long−term historical mean. Left: Time series of historical (black) and future projections for RCP 4.5 and 8.5. Shaded areas show spread among climate models. Right: Boxplots of temporal variability over 40−year periods under historical (left box) and individual climate models under two RCPs. Right: Historical time period is 1970−2010; near−term (NT) is 2020−2060; long−term (LT) is 2061−2100.

Hovenweep: Fall dry soil days

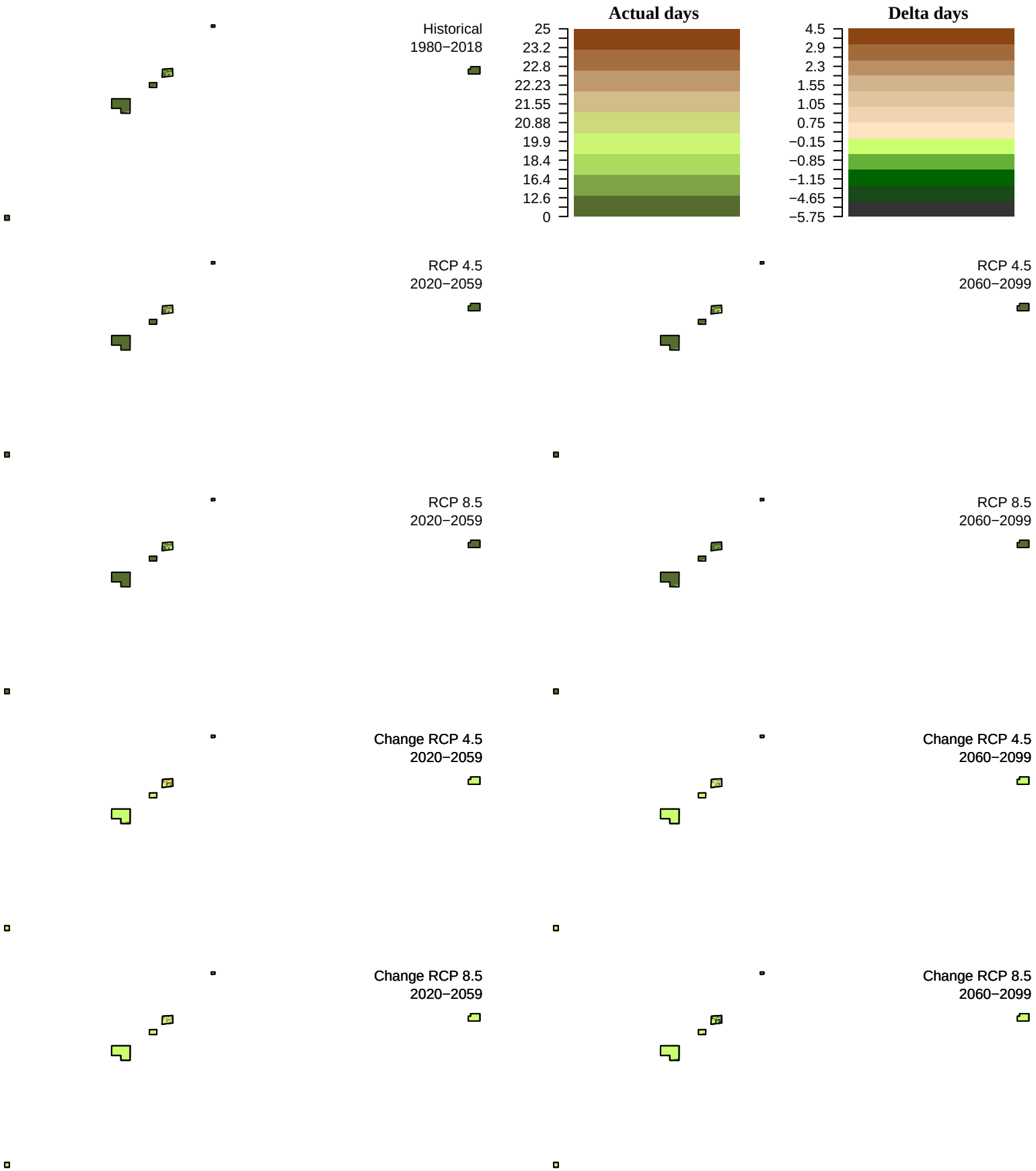


Figure HOVEmap97:
Past trends and future trajectories of park−wide mean values for Fall dry soil days in Hovenweep. Topmost panel depicts the historical mean from 1980−2018. Lower four panels show the emission scenarios of RCP 4.5 and RCP 8.5 at near−term and long−term timeframes. Bottom four panels depict the change from the historical mean; cross hatching denotes areas of robust predicitons (90% of models agree in the direction of change).

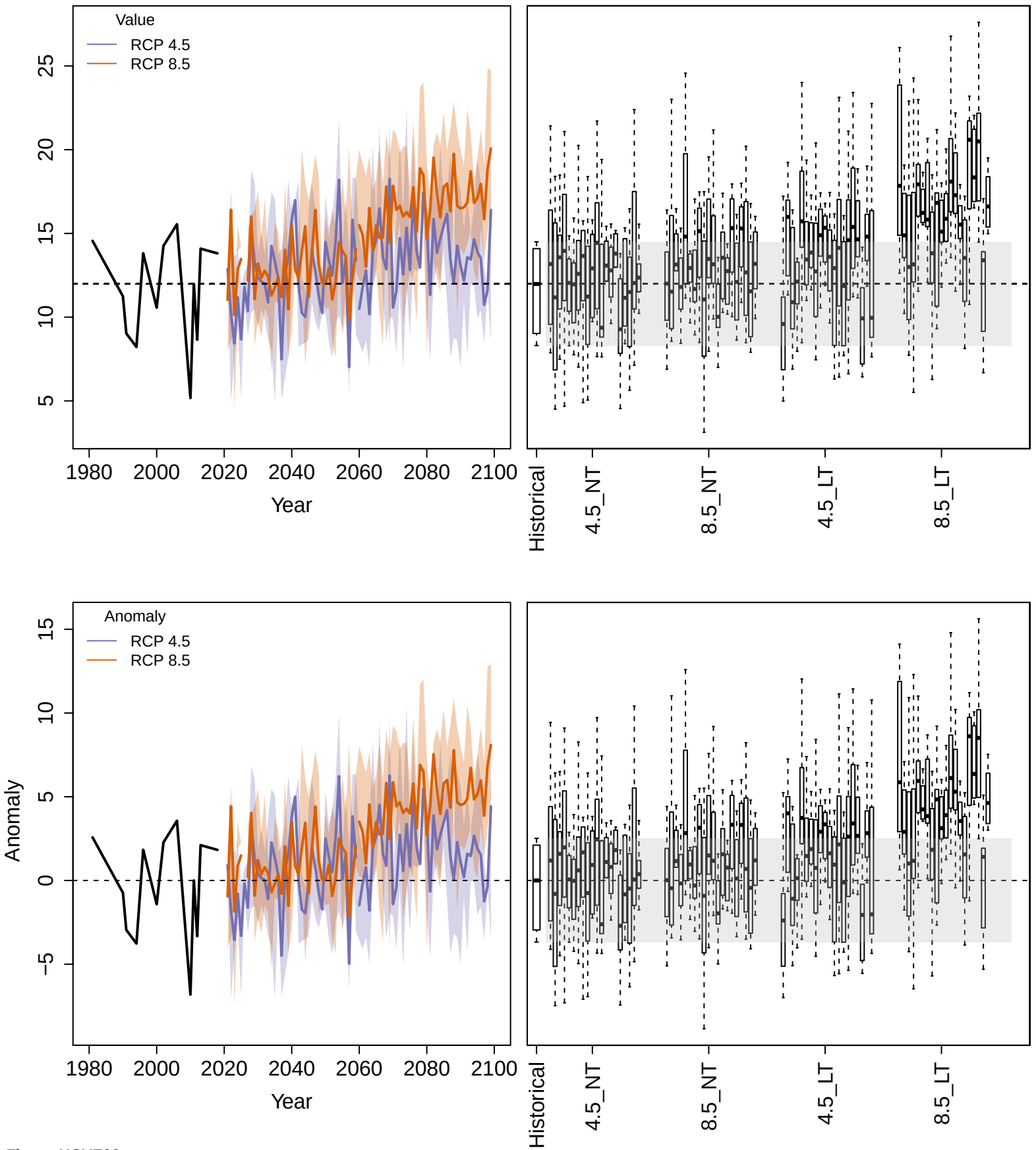


Figure HOVE99:
Past trends and future trajectories of park−wide mean values for Winter extreme short−term dry stress in Hovenweep. Top panels show values, bottom panels show changes from the long−term historical mean. Left: Time series of historical (black) and future projections for RCP 4.5 and 8.5. Shaded areas show spread among climate models. Right: Boxplots of temporal variability over 40−year periods under historical (left box) and individual climate models under two RCPs. Right: Historical time period is 1970−2010; near−term (NT) is 2020−2060; long−term (LT) is 2061−2100.

Hovenweep: Winter extreme short−term dry stress

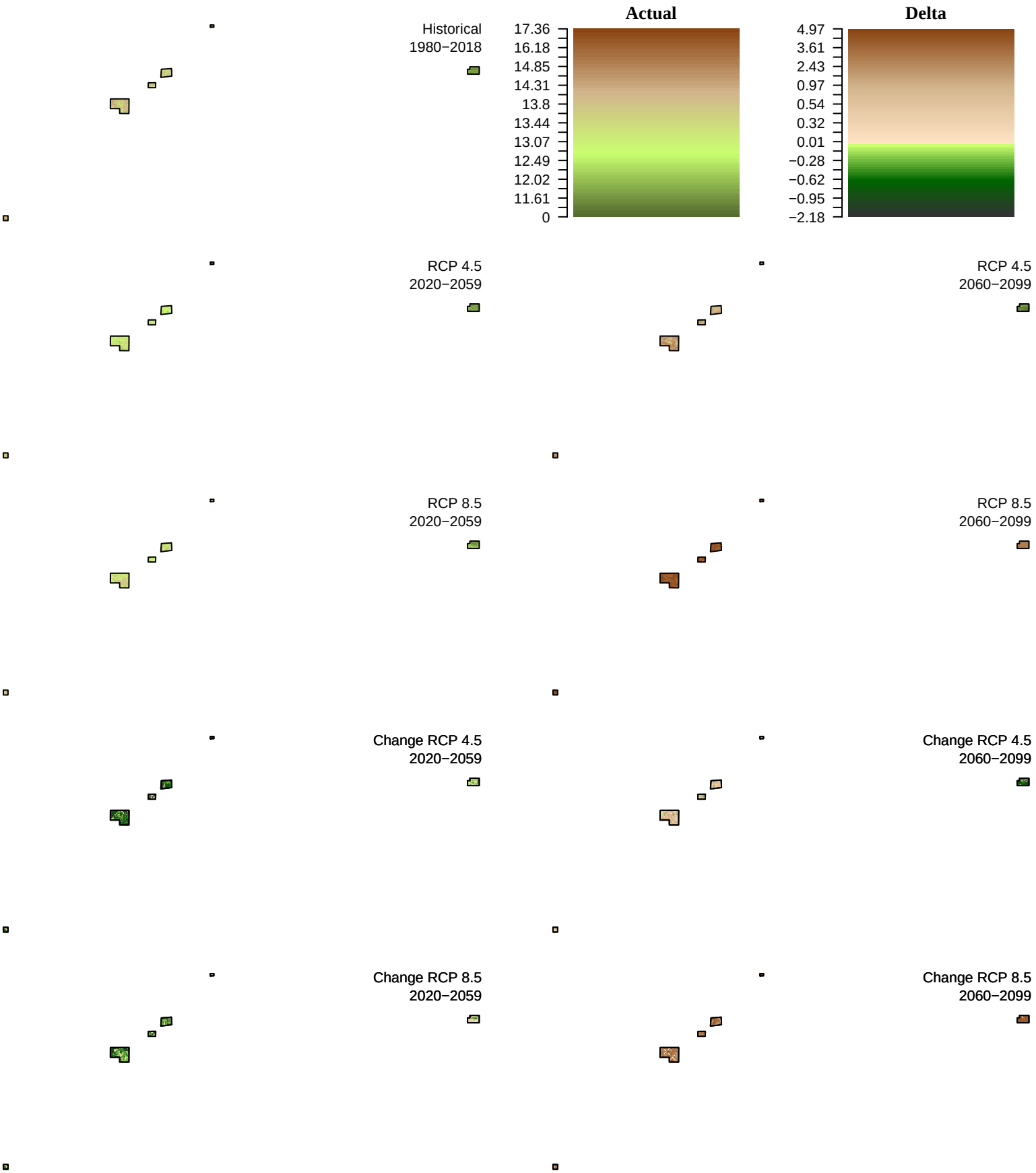


Figure HOVEmap99:
Past trends and future trajectories of park−wide mean values for Winter extreme short−term dry stress in Hovenweep. Topmost panel depicts the historical mean from 1980−2018. Lower four panels show the emission scenarios of RCP 4.5 and RCP 8.5 at near−term and long−term timeframes. Bottom four panels depict the change from the historical mean; cross hatching denotes areas of robust predicitons (90% of models agree in the direction of change).

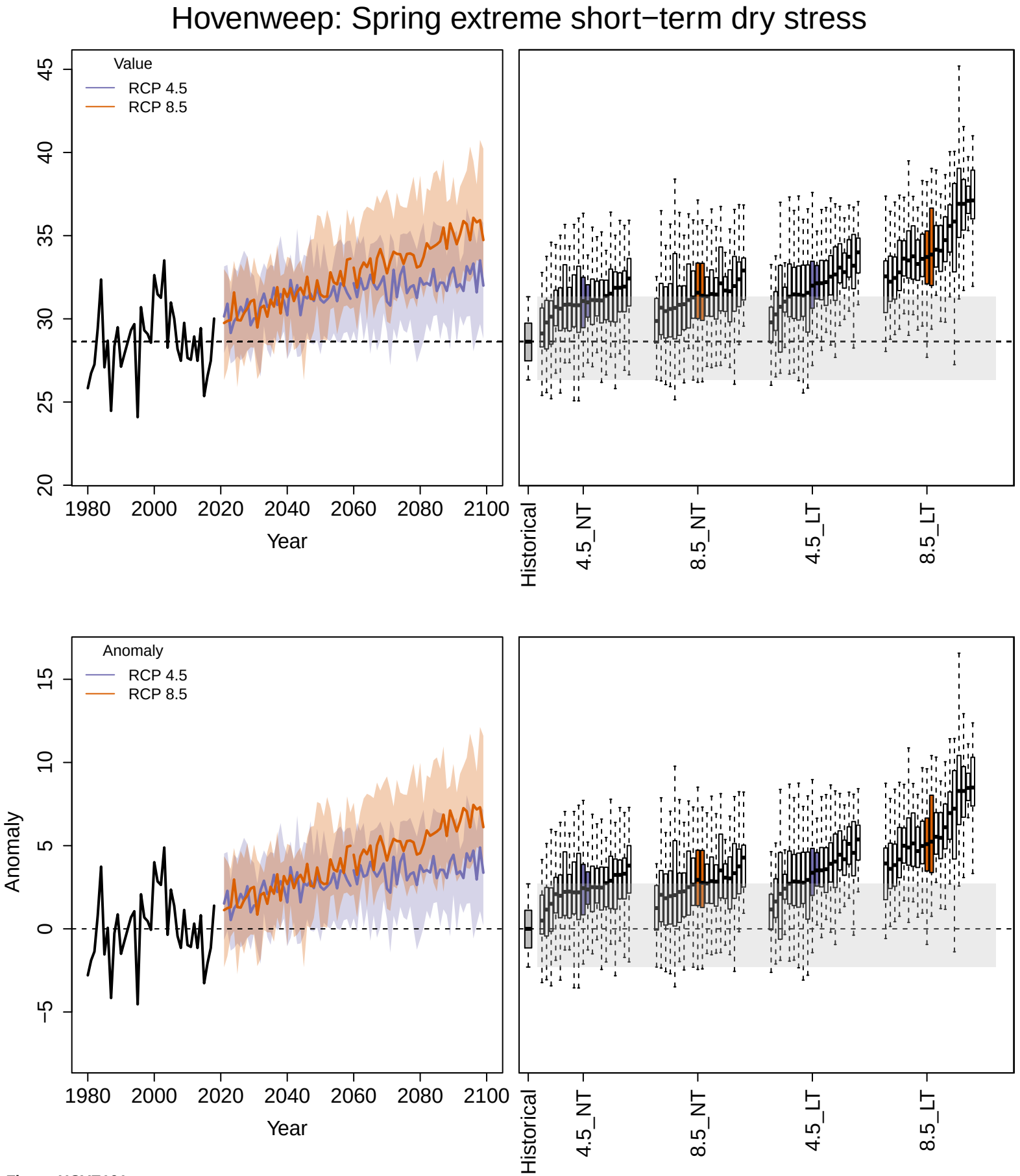


Figure HOVE101:
Past trends and future trajectories of park−wide mean values for Spring extreme short−term dry stress in Hovenweep. Top panels show values, bottom panels show changes from the long−term historical mean. Left: Time series of historical (black) and future projections for RCP 4.5 and 8.5. Shaded areas show spread among climate models. Right: Boxplots of temporal variability over 40−year periods under historical (left box) and individual climate models under two RCPs. Right: Historical time period is 1970−2010; near−term (NT) is 2020−2060; long−term (LT) is 2061−2100.

Hovenweep: Spring extreme short−term dry stress

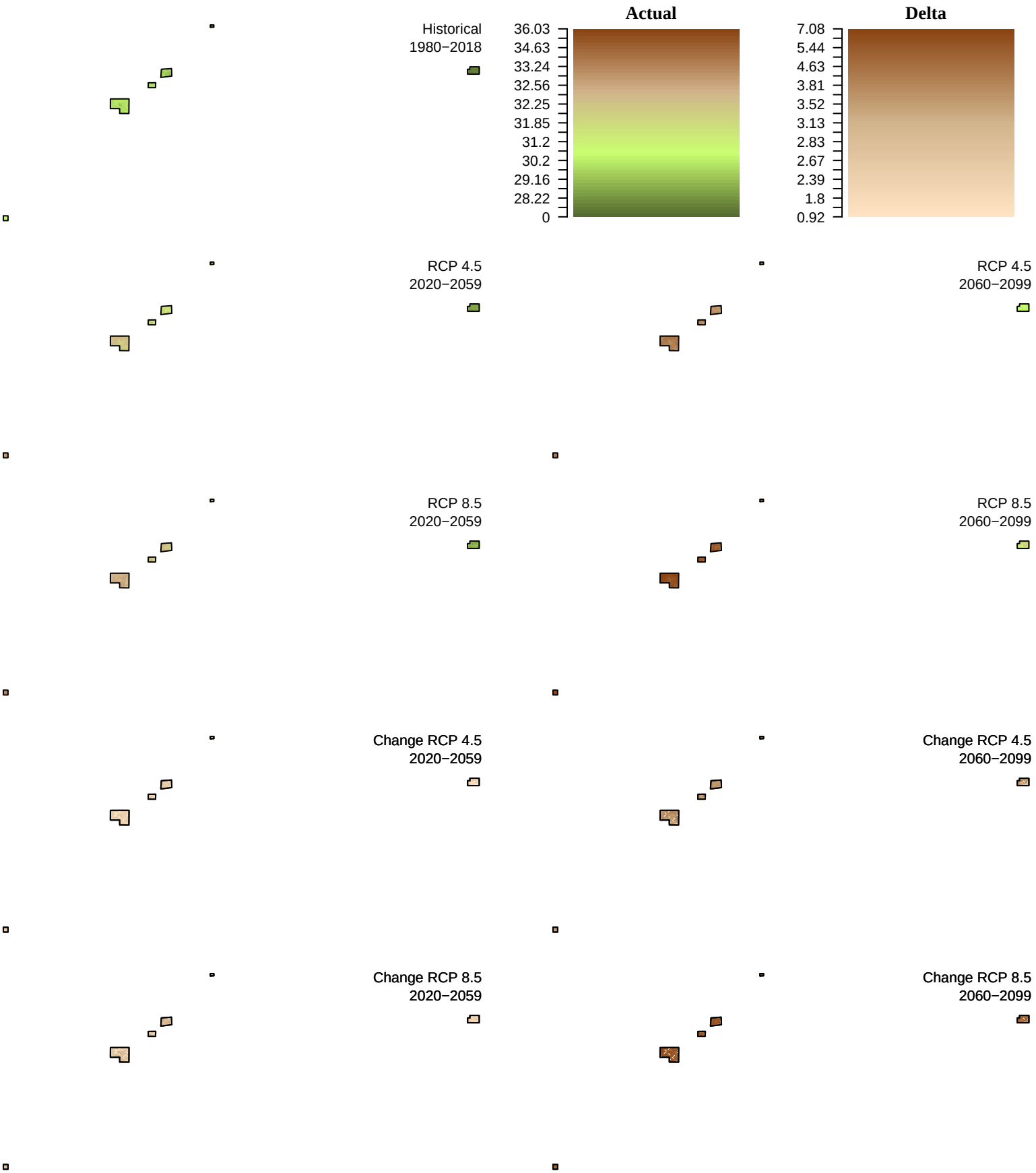


Figure HOVEmap101:
Past trends and future trajectories of park−wide mean values for Spring extreme short−term dry stress in Hovenweep. Topmost panel depicts the historical mean from 1980−2018. Lower four panels show the emission scenarios of RCP 4.5 and RCP 8.5 at near−term and long−term timeframes. Bottom four panels depict the change from the historical mean; cross hatching denotes areas of robust predicitons (90% of models agree in the direction of change).

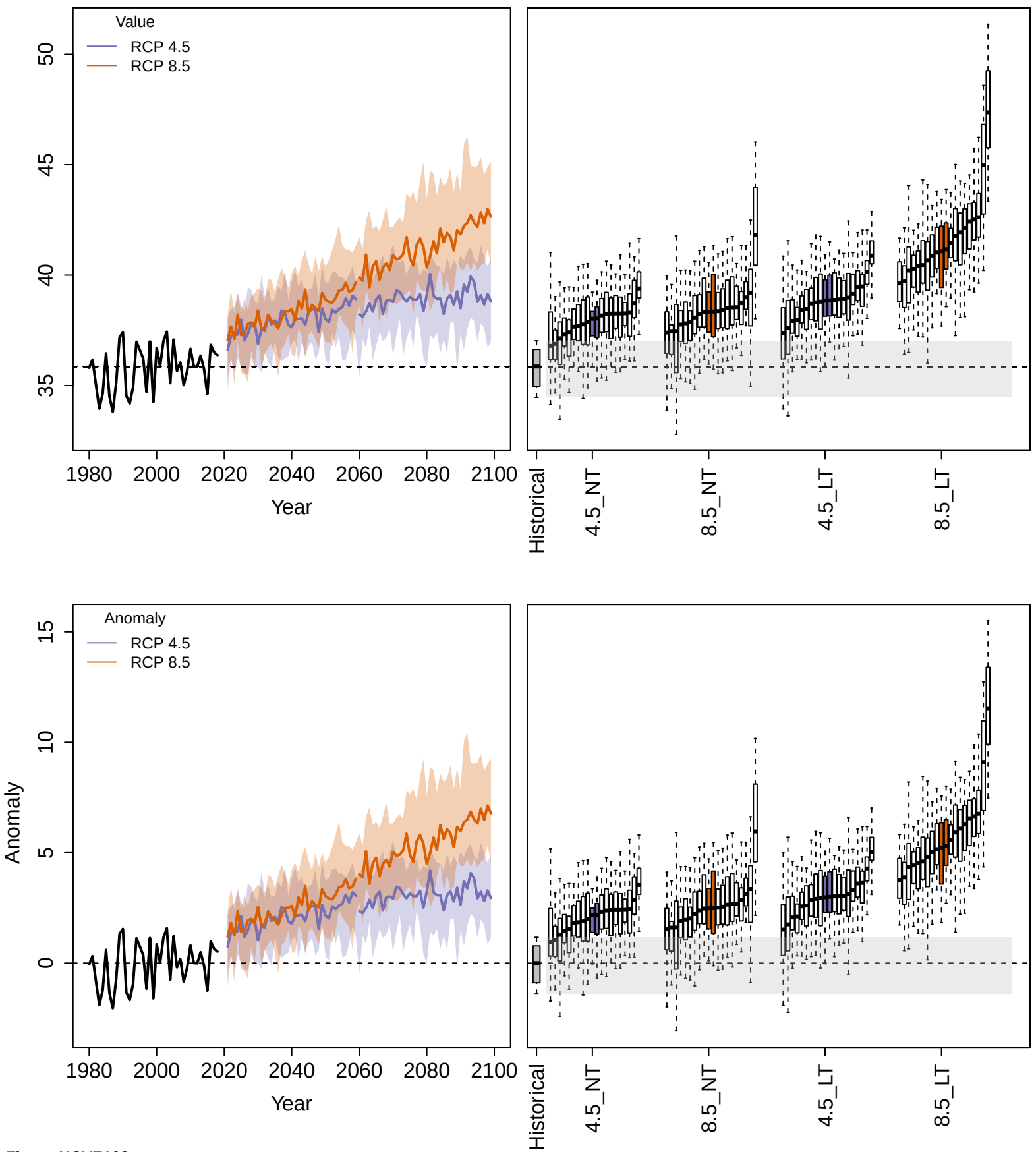


Figure HOVE103:
Past trends and future trajectories of park−wide mean values for Summer extreme short−term dry stress in Hovenweep. Top panels show values, bottom panels show changes from the long−term historical mean. Left: Time series of historical (black) and future projections for RCP 4.5 and 8.5. Shaded areas show spread among climate models. Right: Boxplots of temporal variability over 40−year periods under historical (left box) and individual climate models under two RCPs. Right: Historical time period is 1970−2010; near−term (NT) is 2020−2060; long−term (LT) is 2061−2100.

Hovenweep: Summer extreme short−term dry stress

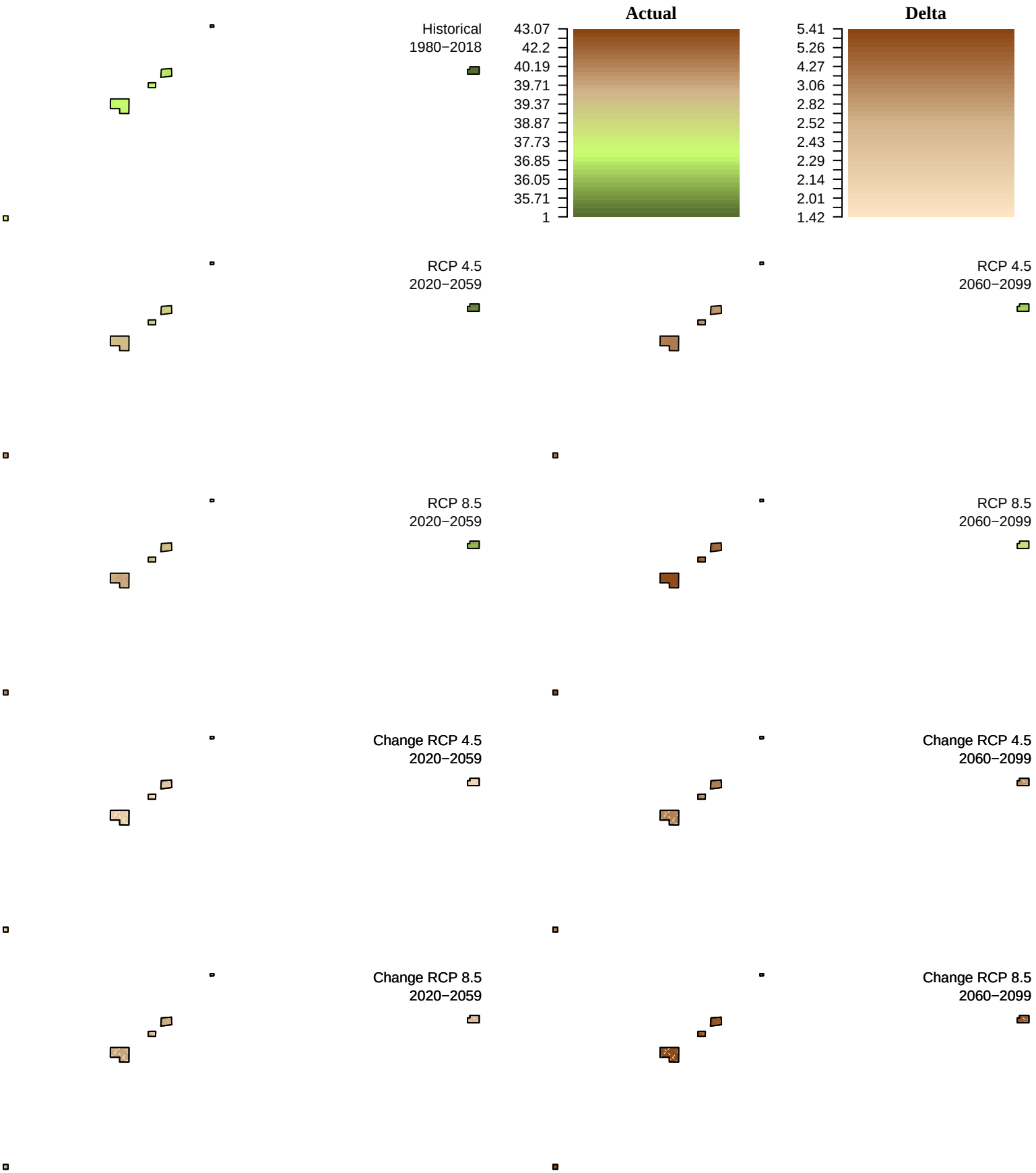


Figure HOVEmap103:
Past trends and future trajectories of park−wide mean values for Summer extreme short−term dry stress in Hovenweep. Topmost panel depicts the historical mean from 1980−2018. Lower four panels show the emission scenarios of RCP 4.5 and RCP 8.5 at near−term and long−term timeframes. Bottom four panels depict the change from the historical mean; cross hatching denotes areas of robust predicitons (90% of models agree in the direction of change).

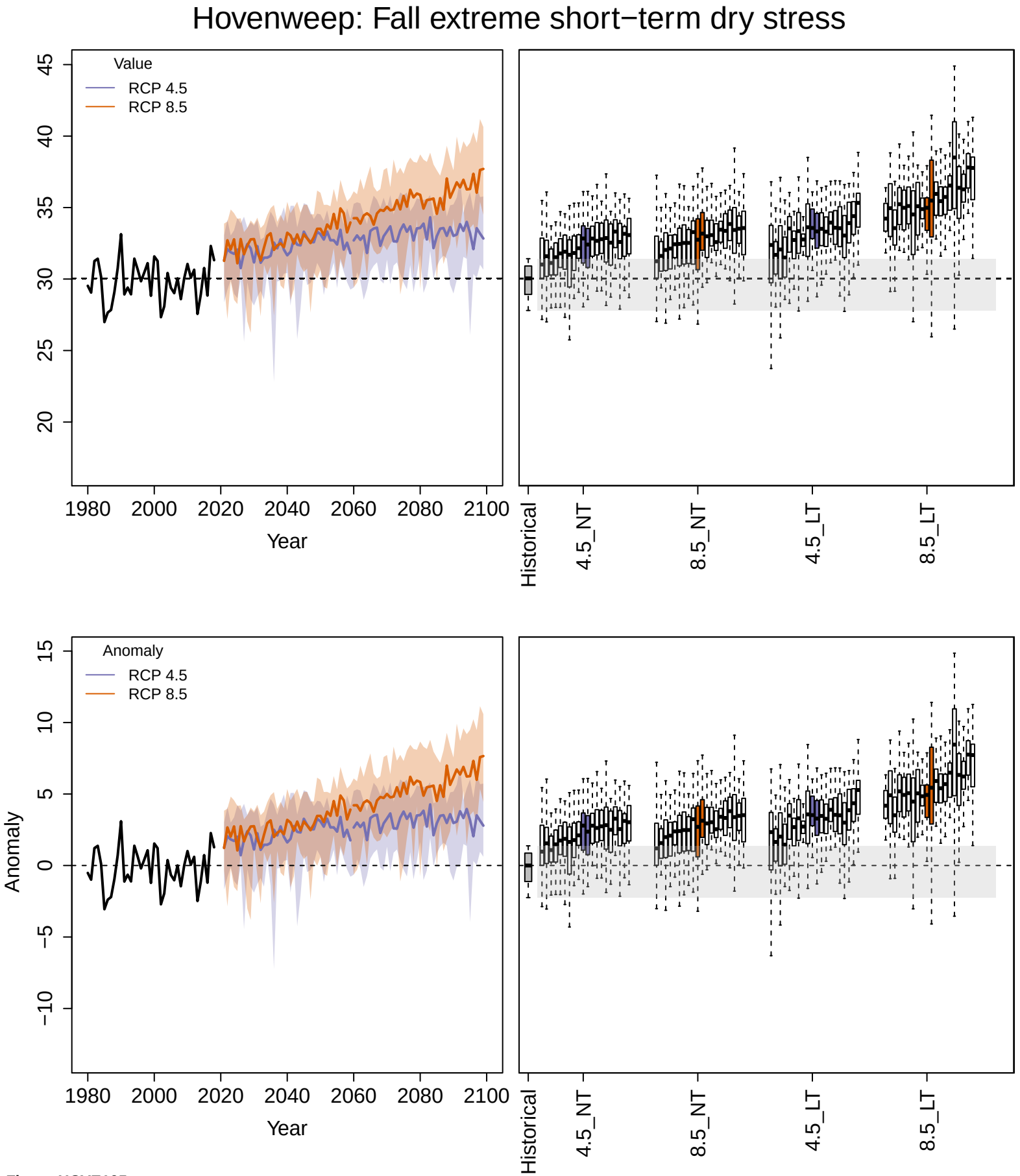


Figure HOVE105:
Past trends and future trajectories of park−wide mean values for Fall extreme short−term dry stress in Hovenweep. Top panels show values, bottom panels show changes from the long−term historical mean. Left: Time series of historical (black) and future projections for RCP 4.5 and 8.5. Shaded areas show spread among climate models. Right: Boxplots of temporal variability over 40−year periods under historical (left box) and individual climate models under two RCPs. Right: Historical time period is 1970−2010; near−term (NT) is 2020−2060; long−term (LT) is 2061−2100.

Hovenweep: Fall extreme short−term dry stress

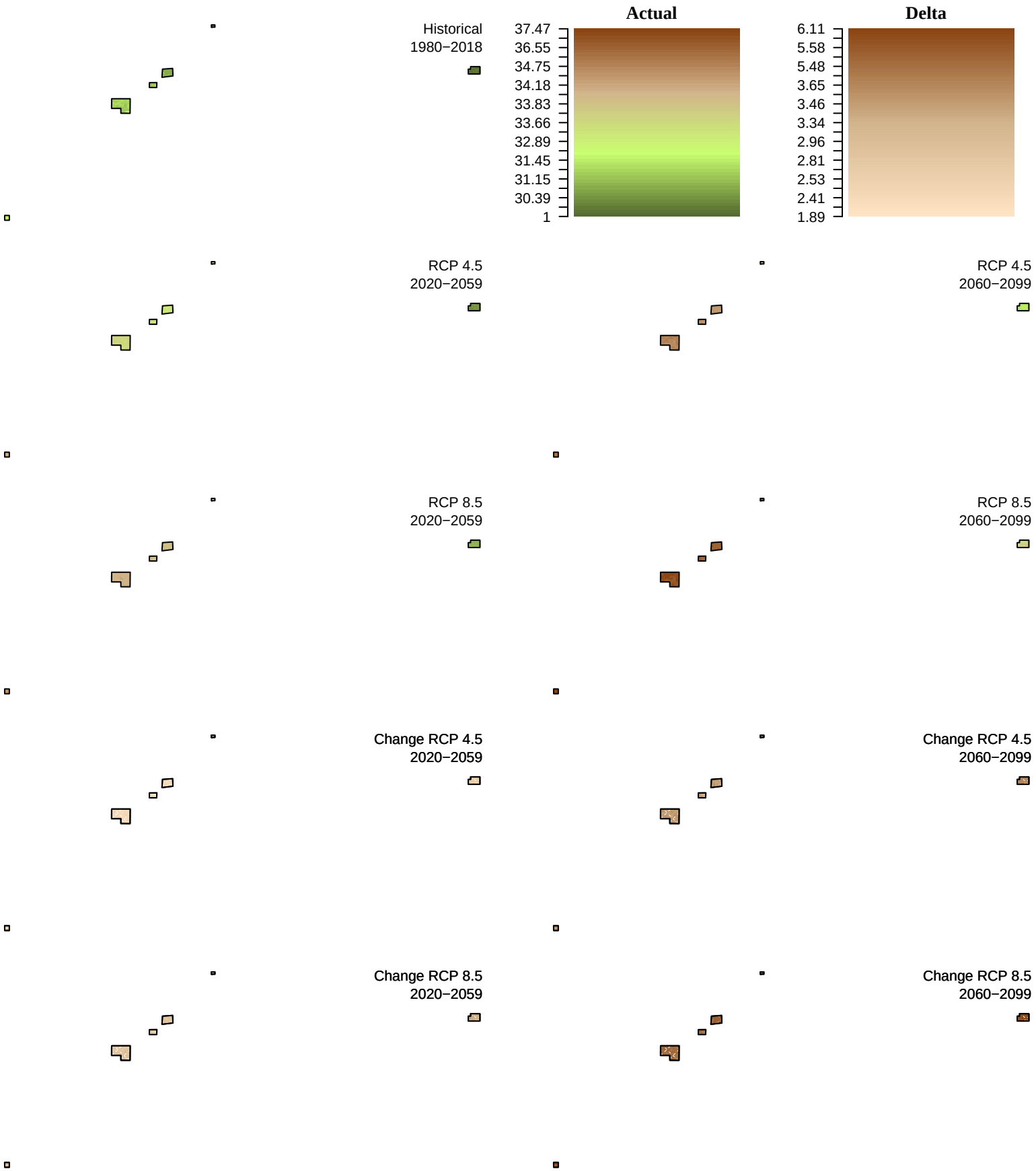


Figure HOVEmap105:
Past trends and future trajectories of park−wide mean values for Fall extreme short−term dry stress in Hovenweep. Topmost panel depicts the historical mean from 1980−2018. Lower four panels show the emission scenarios of RCP 4.5 and RCP 8.5 at near−term and long−term timeframes. Bottom four panels depict the change from the historical mean; cross hatching denotes areas of robust predicitons (90% of models agree in the direction of change).

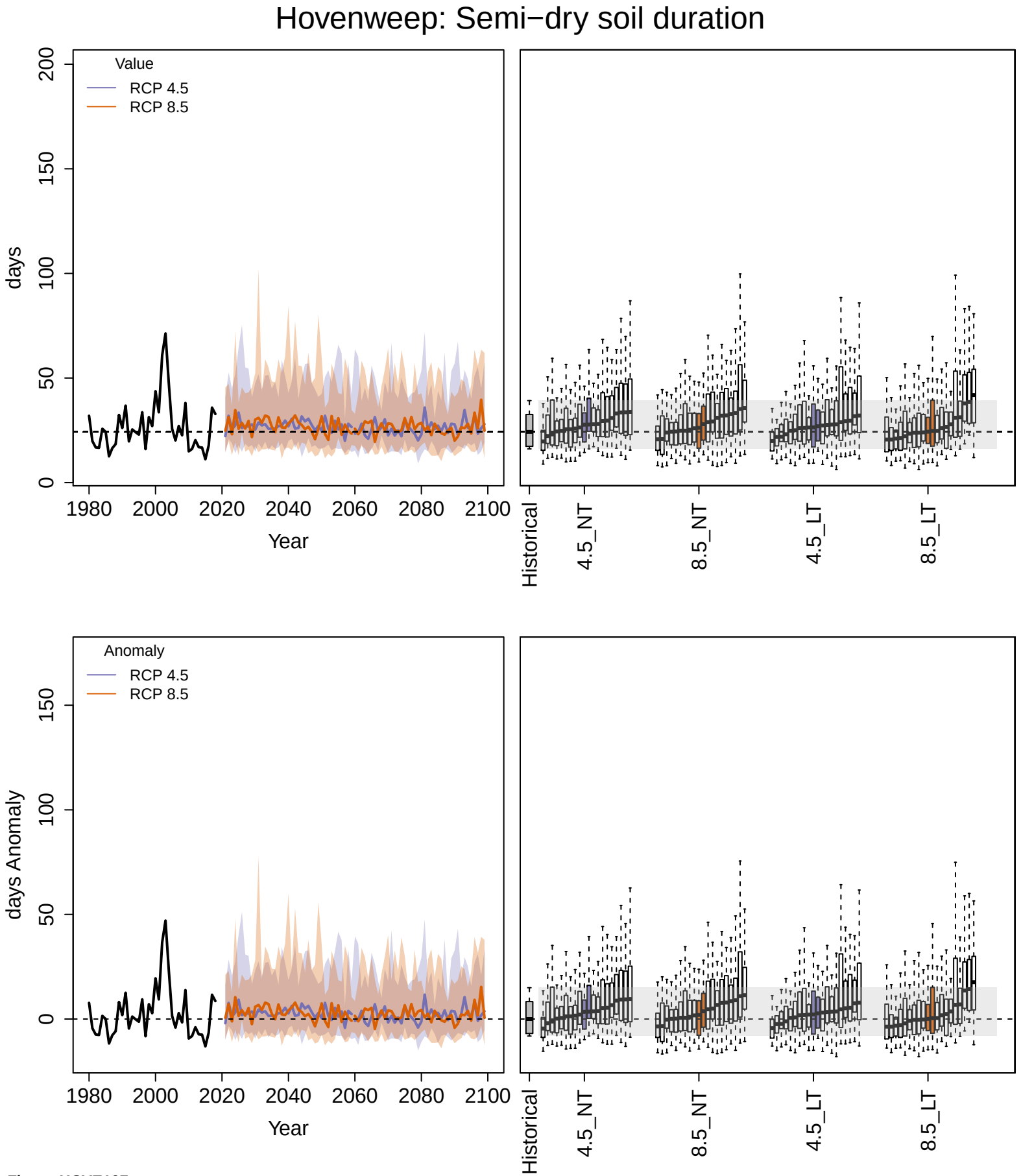


Figure HOVE107:
Past trends and future trajectories of park−wide mean values for Semi−dry soil duration in Hovenweep. Top panels show values, bottom panels show changes from the long−term historical mean. Left: Time series of historical (black) and future projections for RCP 4.5 and 8.5. Shaded areas show spread among climate models. Right: Boxplots of temporal variability over 40−year periods under historical (left box) and individual climate models under two RCPs. Right: Historical time period is 1970−2010; near−term (NT) is 2020−2060; long−term (LT) is 2061−2100.

Hovenweep: Semi−dry soil duration

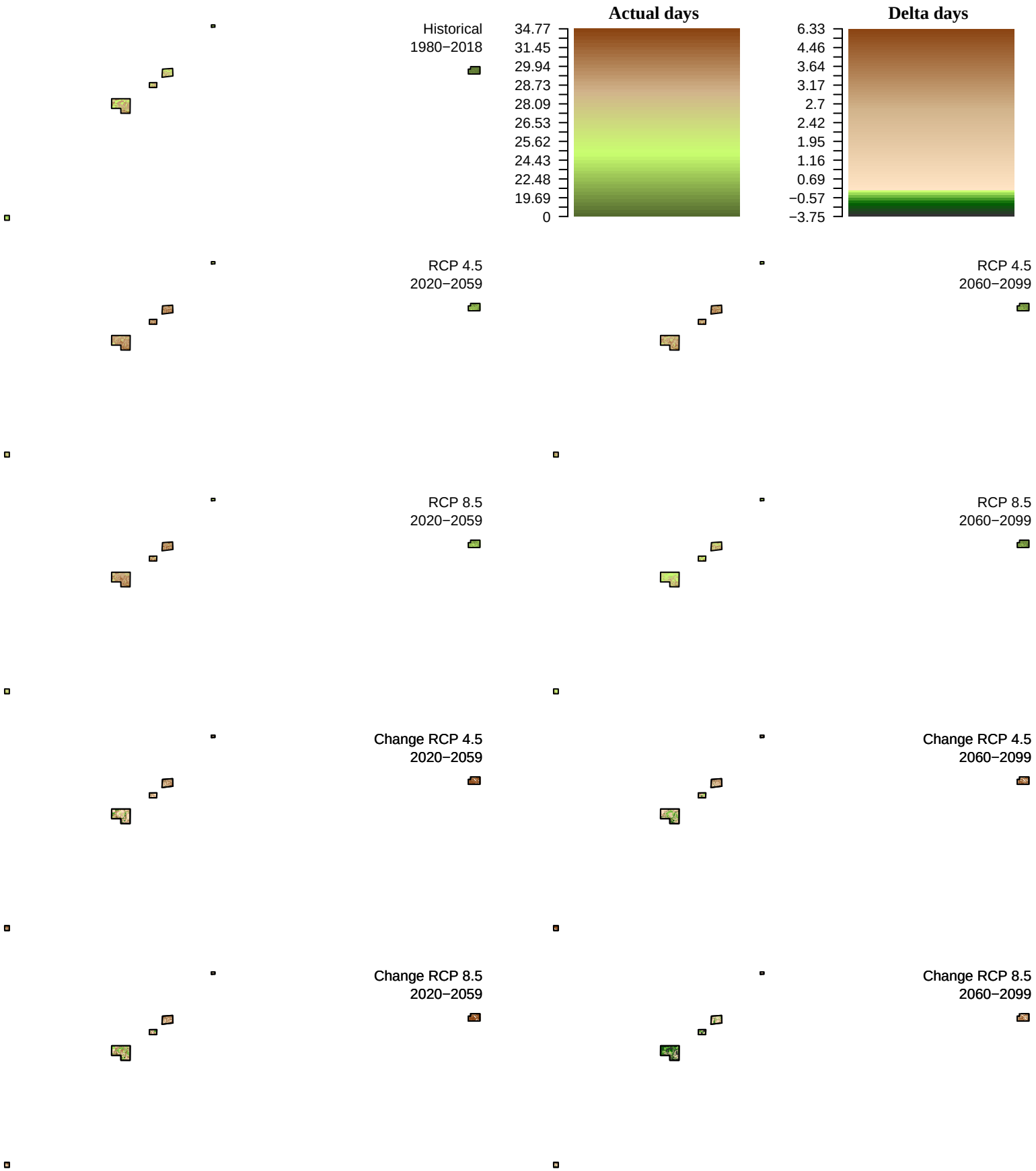


Figure HOVEmap107:
Past trends and future trajectories of park−wide mean values for Semi−dry soil duration in Hovenweep. Topmost panel depicts the historical mean from 1980−2018. Lower four panels show the emission scenarios of RCP 4.5 and RCP 8.5 at near−term and long−term timeframes. Bottom four panels depict the change from the historical mean; cross hatching denotes areas of robust predicitons (90% of models agree in the direction of change).

Hovenweep: Winter evaporation

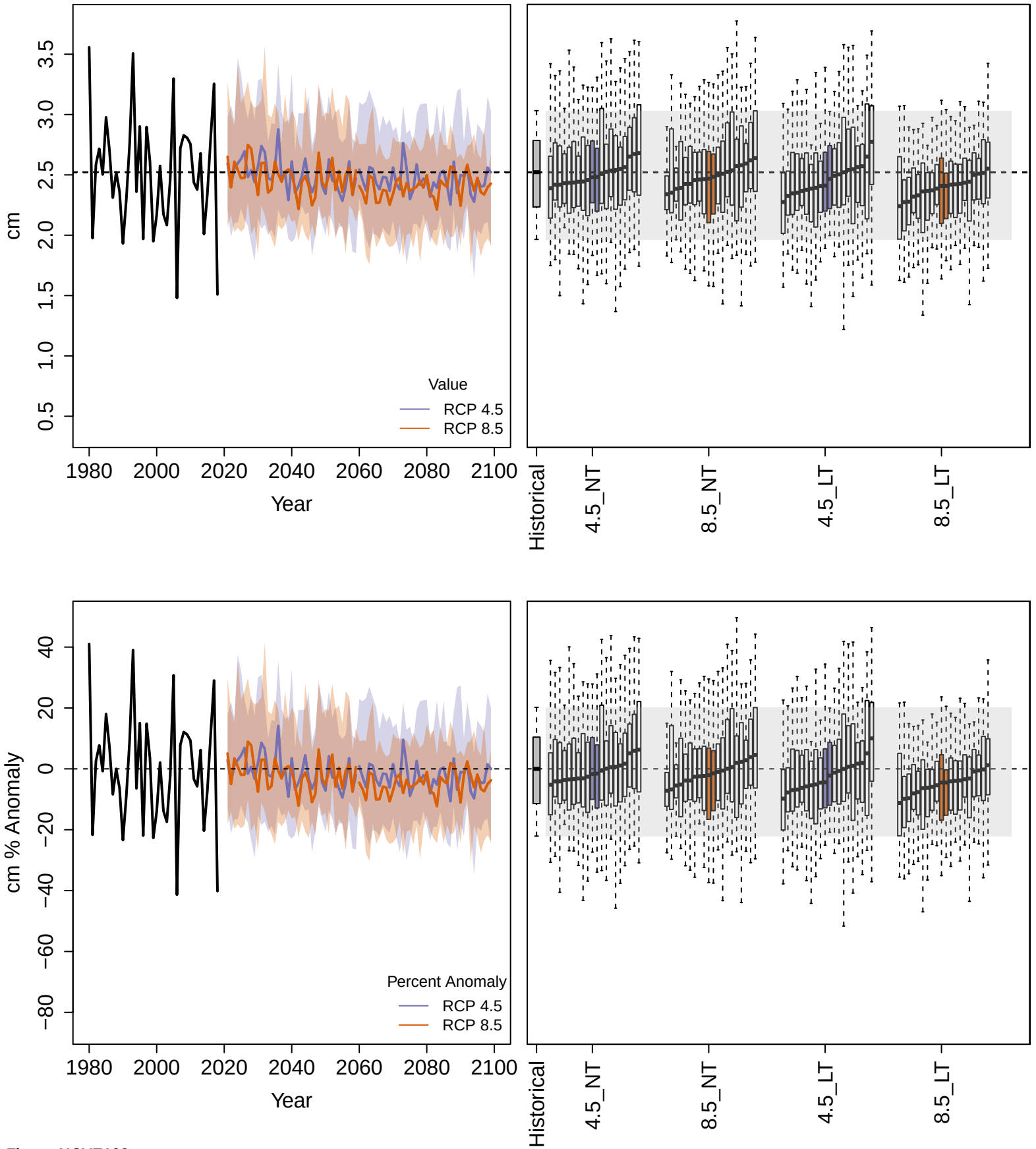


Figure HOVE109:
Past trends and future trajectories of park−wide mean values for Winter evaporation in Hovenweep. Top panels show values, bottom panels show changes from the long−term historical mean. Left: Time series of historical (black) and future projections for RCP 4.5 and 8.5. Shaded areas show spread among climate models. Right: Boxplots of temporal variability over 40−year periods under historical (left box) and individual climate models under two RCPs. Right: Historical time period is 1970−2010; near−term (NT) is 2020−2060; long−term (LT) is 2061−2100.

Hovenweep: Winter evaporation

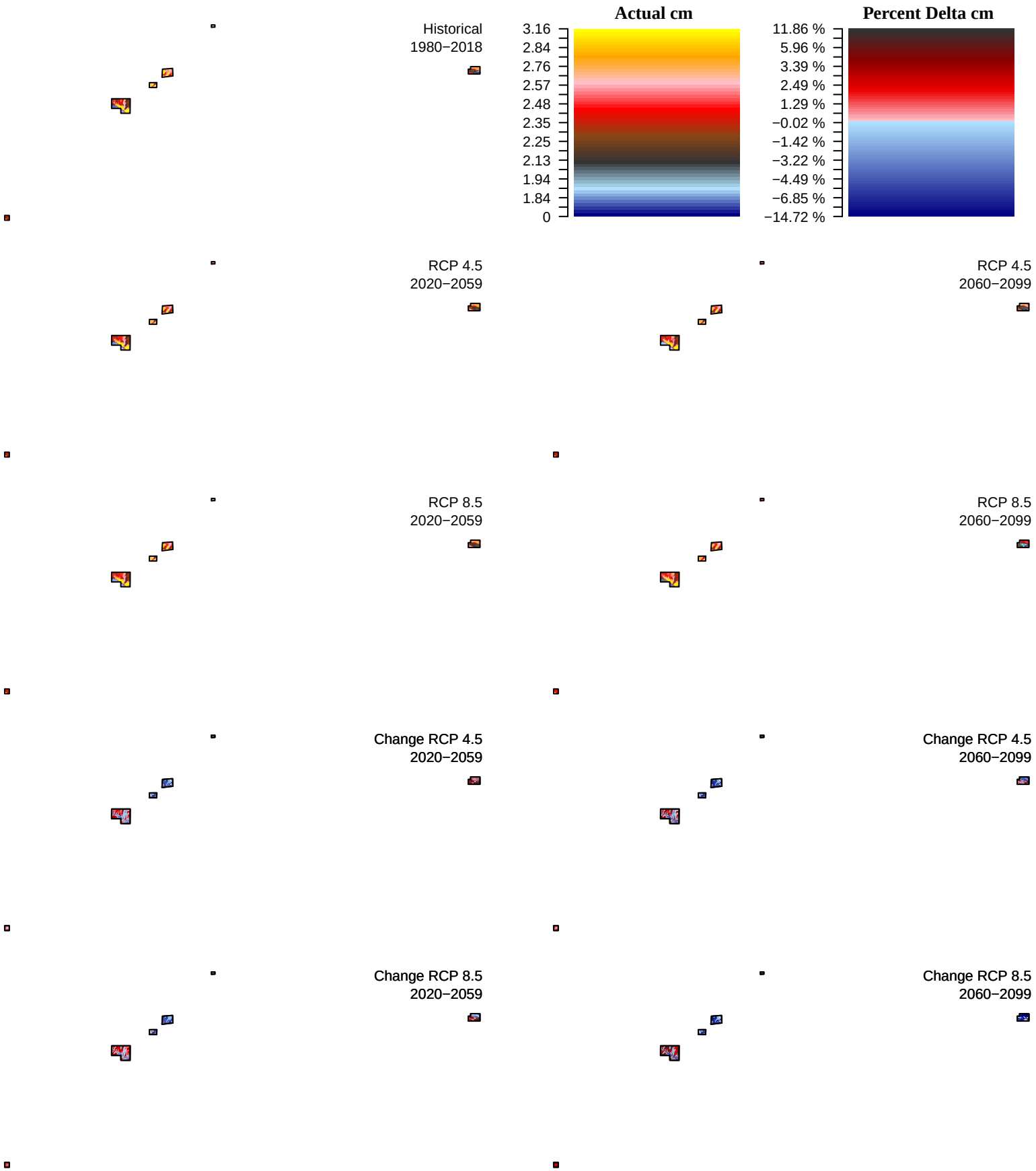


Figure HOVEmap109:
Past trends and future trajectories of park−wide mean values for Winter evaporation in Hovenweep. Topmost panel depicts the historical mean from 1980−2018. Lower four panels show the emission scenarios of RCP 4.5 and RCP 8.5 at near−term and long−term timeframes. Bottom four panels depict the change from the historical mean; cross hatching denotes areas of robust predicitons (90% of models agree in the direction of change).

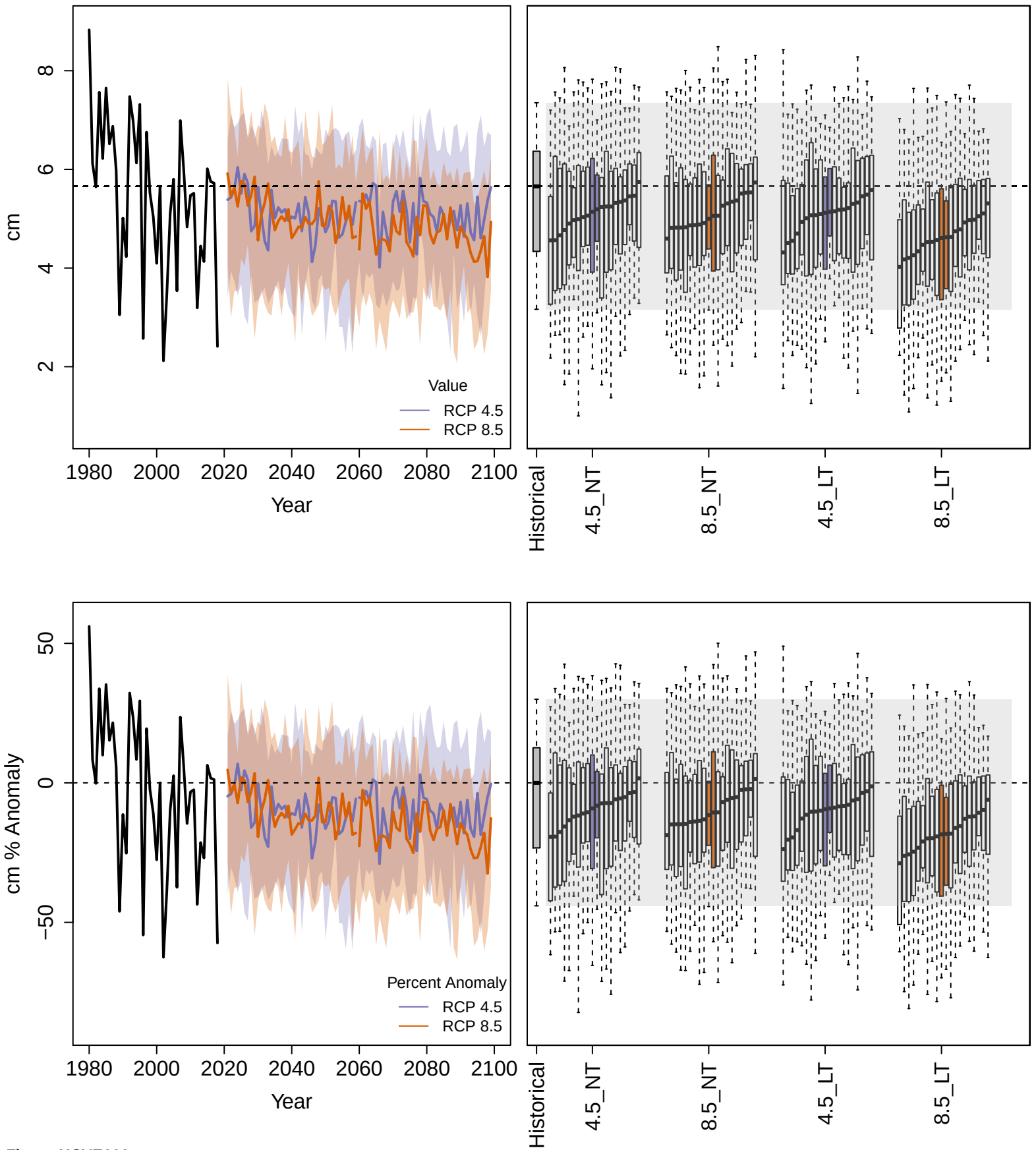


Figure HOVE111:
Past trends and future trajectories of park−wide mean values for Spring evaporation in Hovenweep. Top panels show values, bottom panels show changes from the long−term historical mean. Left: Time series of historical (black) and future projections for RCP 4.5 and 8.5. Shaded areas show spread among climate models. Right: Boxplots of temporal variability over 40−year periods under historical (left box) and individual climate models under two RCPs. Right: Historical time period is 1970−2010; near−term (NT) is 2020−2060; long−term (LT) is 2061−2100.

Hovenweep: Spring evaporation

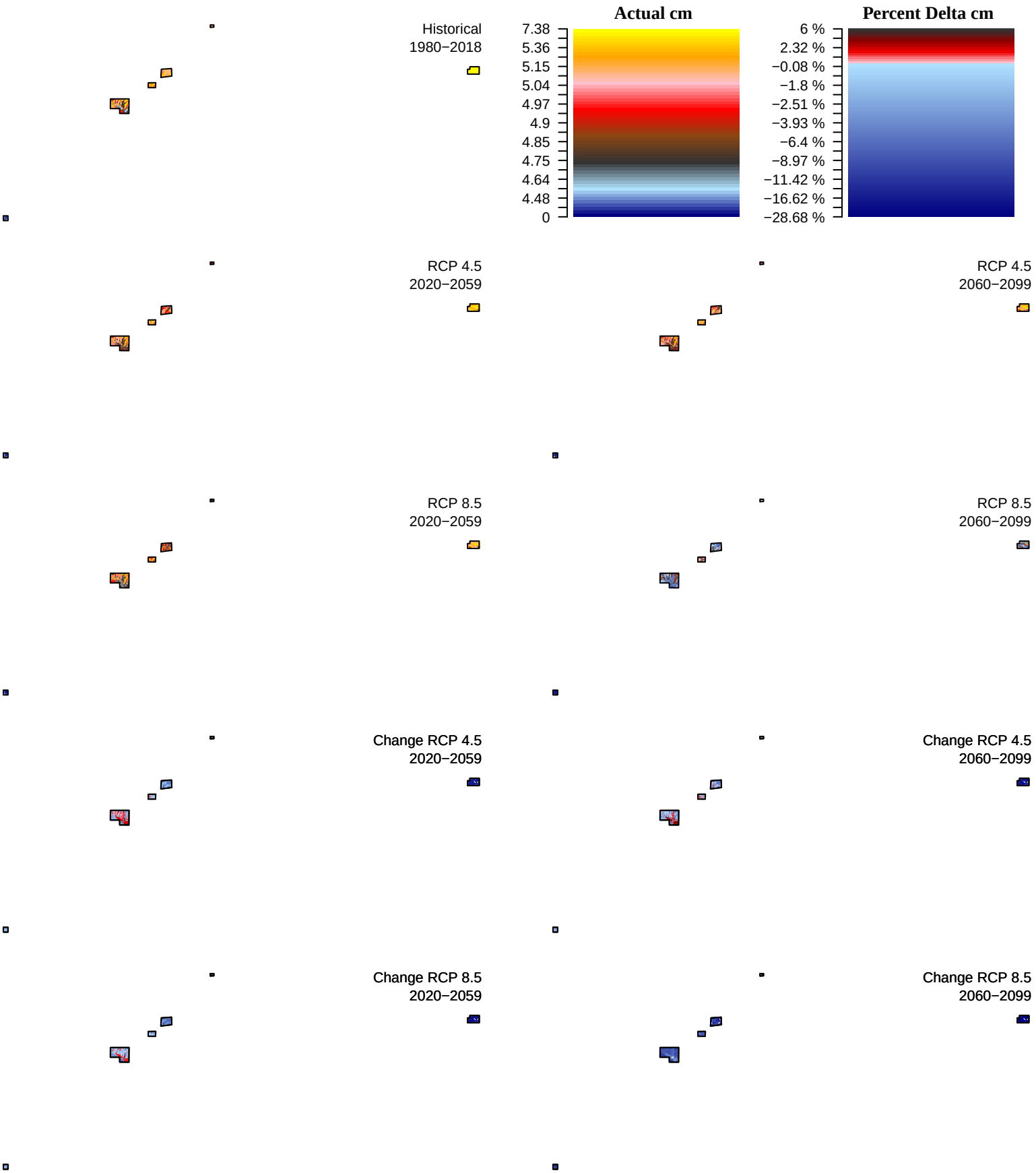


Figure HOVEmap111:
Past trends and future trajectories of park−wide mean values for Spring evaporation in Hovenweep. Topmost panel depicts the historical mean from 1980−2018. Lower four panels show the emission scenarios of RCP 4.5 and RCP 8.5 at near−term and long−term timeframes. Bottom four panels depict the change from the historical mean; cross hatching denotes areas of robust predicitons (90% of models agree in the direction of change).

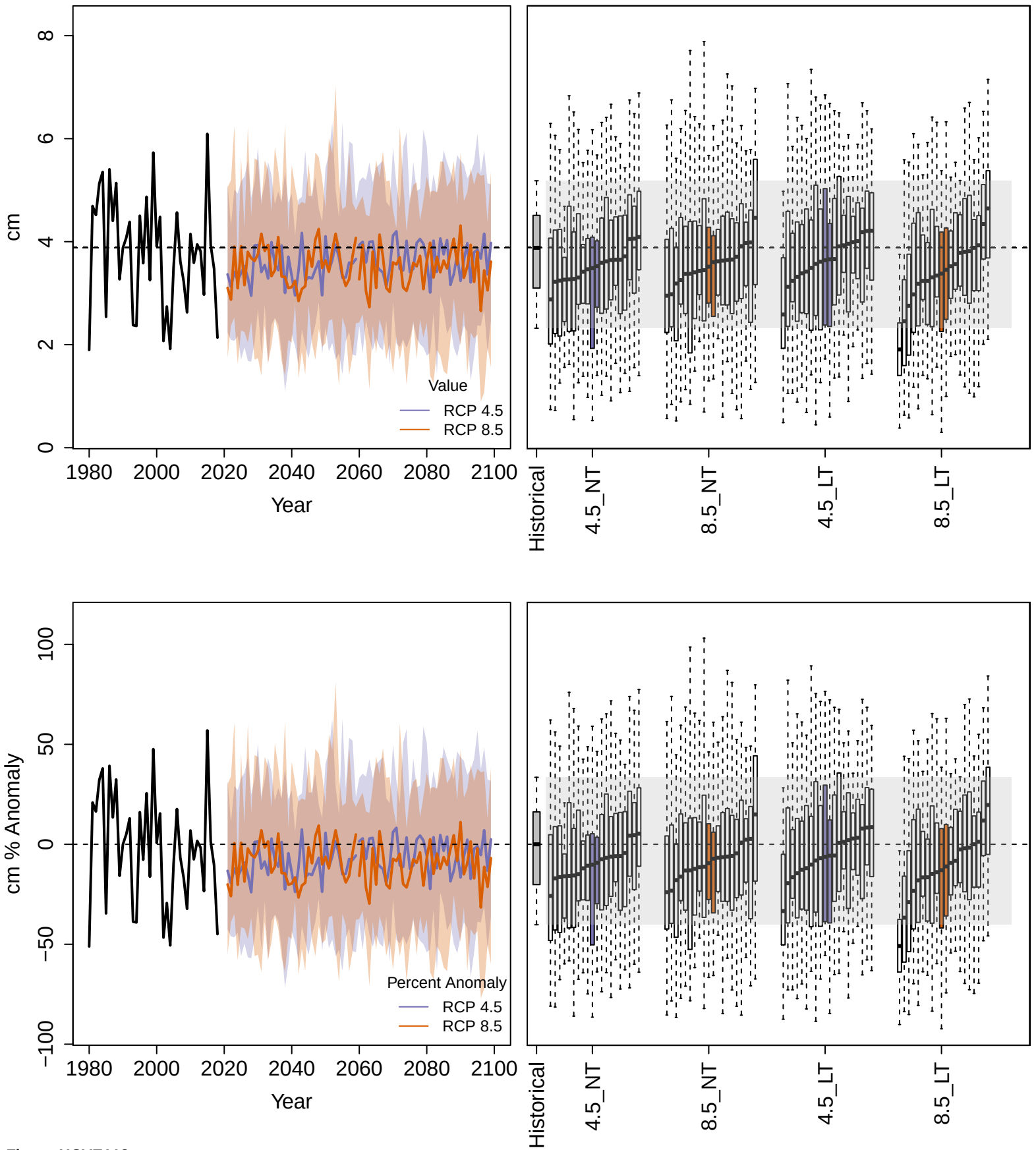


Figure HOVE113:
Past trends and future trajectories of park−wide mean values for Summer evaporation in Hovenweep. Top panels show values, bottom panels show changes from the long−term historical mean. Left: Time series of historical (black) and future projections for RCP 4.5 and 8.5. Shaded areas show spread among climate models. Right: Boxplots of temporal variability over 40−year periods under historical (left box) and individual climate models under two RCPs. Right: Historical time period is 1970−2010; near−term (NT) is 2020−2060; long−term (LT) is 2061−2100.

Hovenweep: Summer evaporation

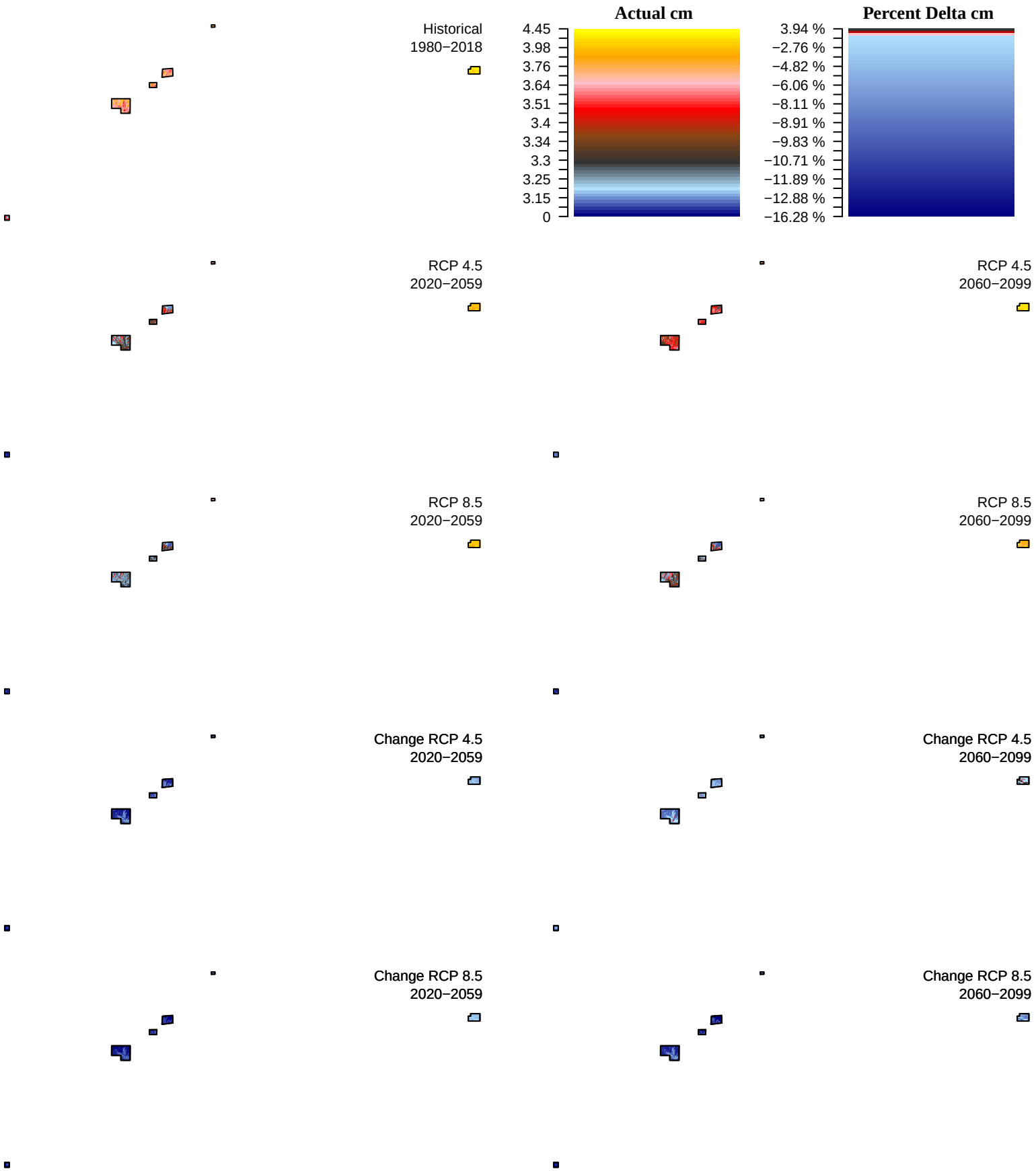


Figure HOVEmap113:
Past trends and future trajectories of park−wide mean values for Summer evaporation in Hovenweep. Topmost panel depicts the historical mean from 1980−2018. Lower four panels show the emission scenarios of RCP 4.5 and RCP 8.5 at near−term and long−term timeframes. Bottom four panels depict the change from the historical mean; cross hatching denotes areas of robust predicitons (90% of models agree in the direction of change).

Hovenweep: Fall evaporation

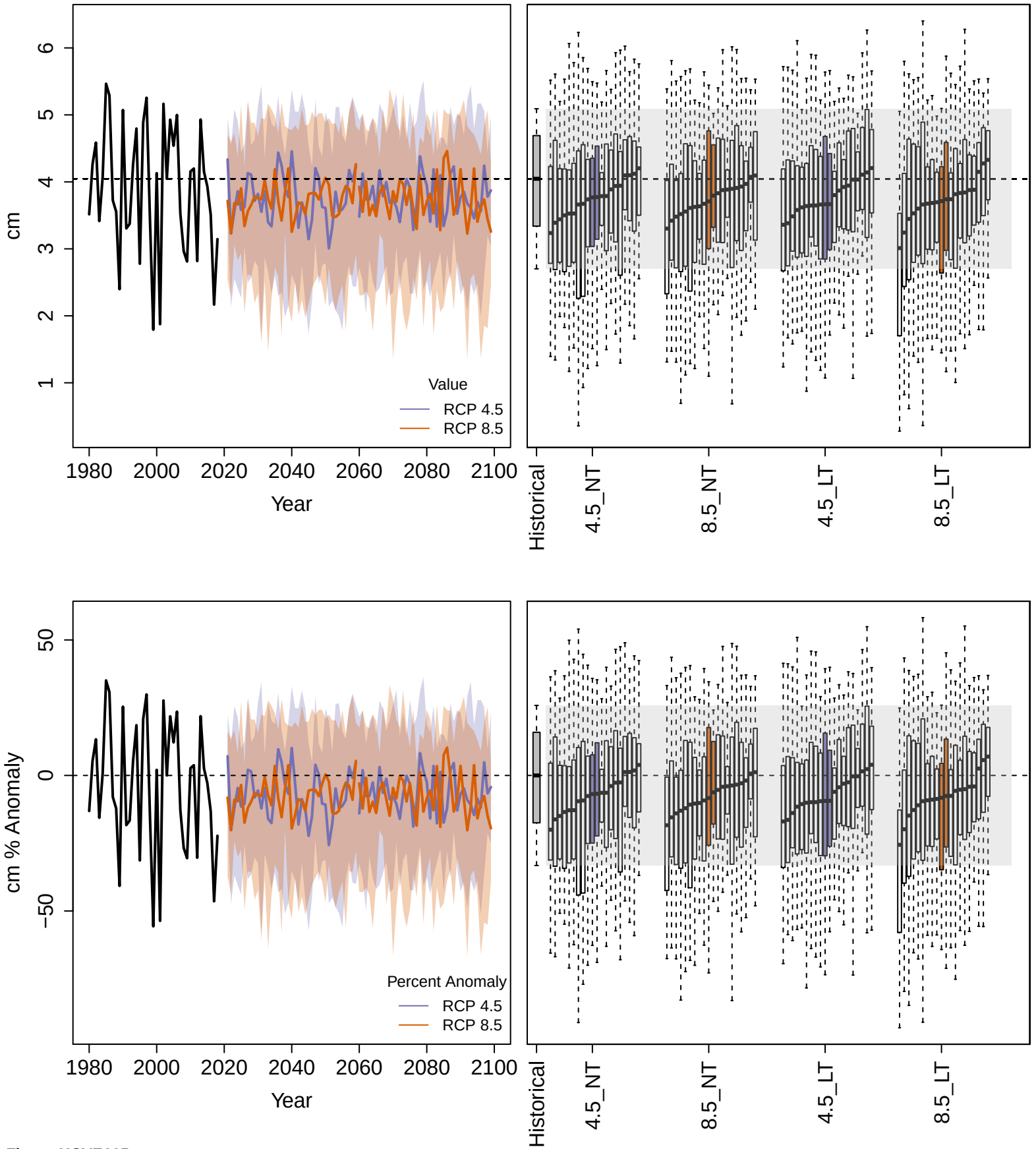


Figure HOVE115:
Past trends and future trajectories of park−wide mean values for Fall evaporation in Hovenweep. Top panels show values, bottom panels show changes from the long−term historical mean. Left: Time series of historical (black) and future projections for RCP 4.5 and 8.5. Shaded areas show spread among climate models. Right: Boxplots of temporal variability over 40−year periods under historical (left box) and individual climate models under two RCPs. Right: Historical time period is 1970−2010; near−term (NT) is 2020−2060; long−term (LT) is 2061−2100.

Hovenweep: Fall evaporation

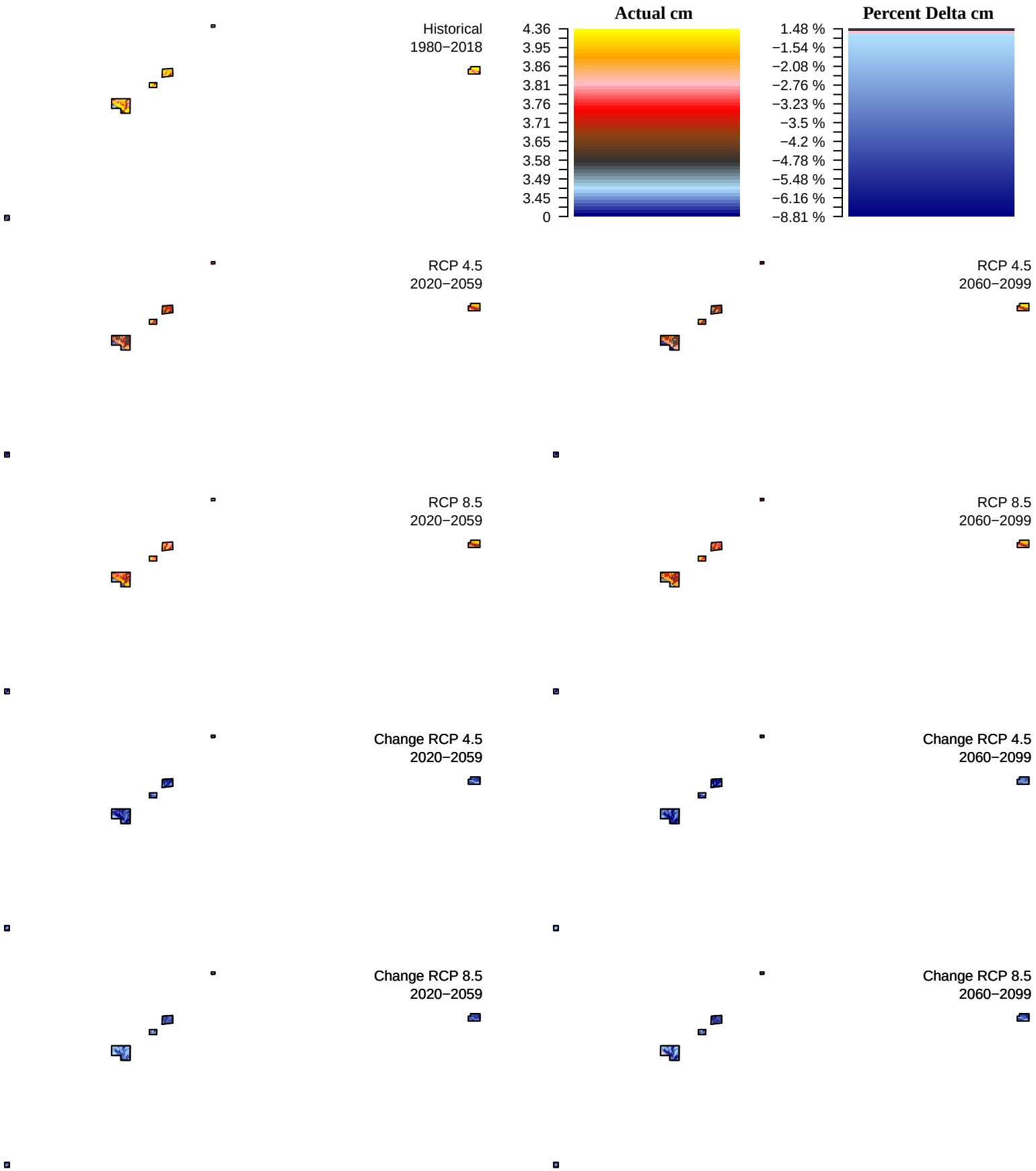


Figure HOVEmap115:
Past trends and future trajectories of park−wide mean values for Fall evaporation in Hovenweep. Topmost panel depicts the historical mean from 1980−2018. Lower four panels show the emission scenarios of RCP 4.5 and RCP 8.5 at near−term and long−term timeframes. Bottom four panels depict the change from the historical mean; cross hatching denotes areas of robust predicitons (90% of models agree in the direction of change).

Hovenweep: Winter transpiration

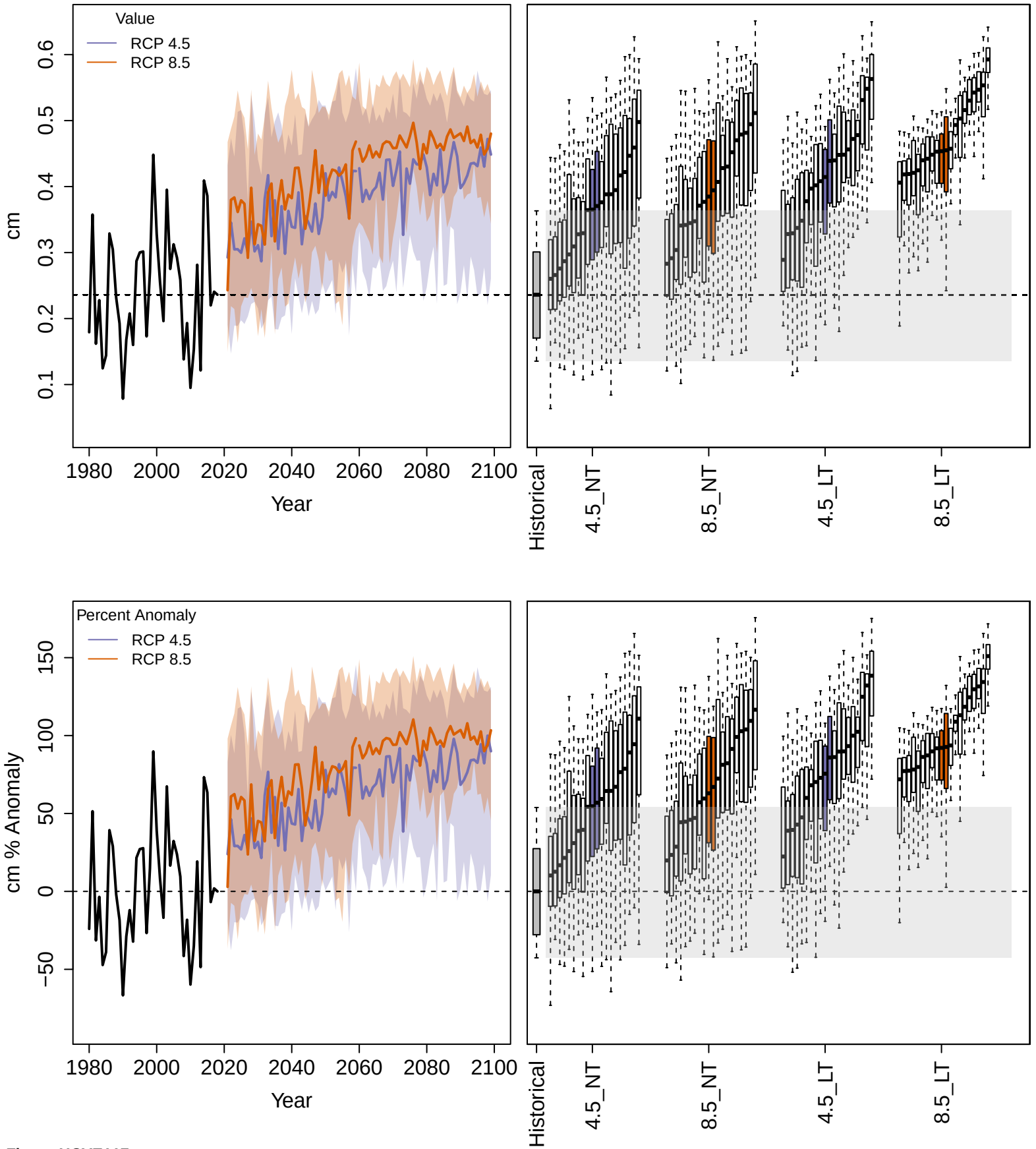


Figure HOVE117:
Past trends and future trajectories of park−wide mean values for Winter transpiration in Hovenweep. Top panels show values, bottom panels show changes from the long−term historical mean. Left: Time series of historical (black) and future projections for RCP 4.5 and 8.5. Shaded areas show spread among climate models. Right: Boxplots of temporal variability over 40−year periods under historical (left box) and individual climate models under two RCPs. Right: Historical time period is 1970−2010; near−term (NT) is 2020−2060; long−term (LT) is 2061−2100.

Hovenweep: Winter transpiration

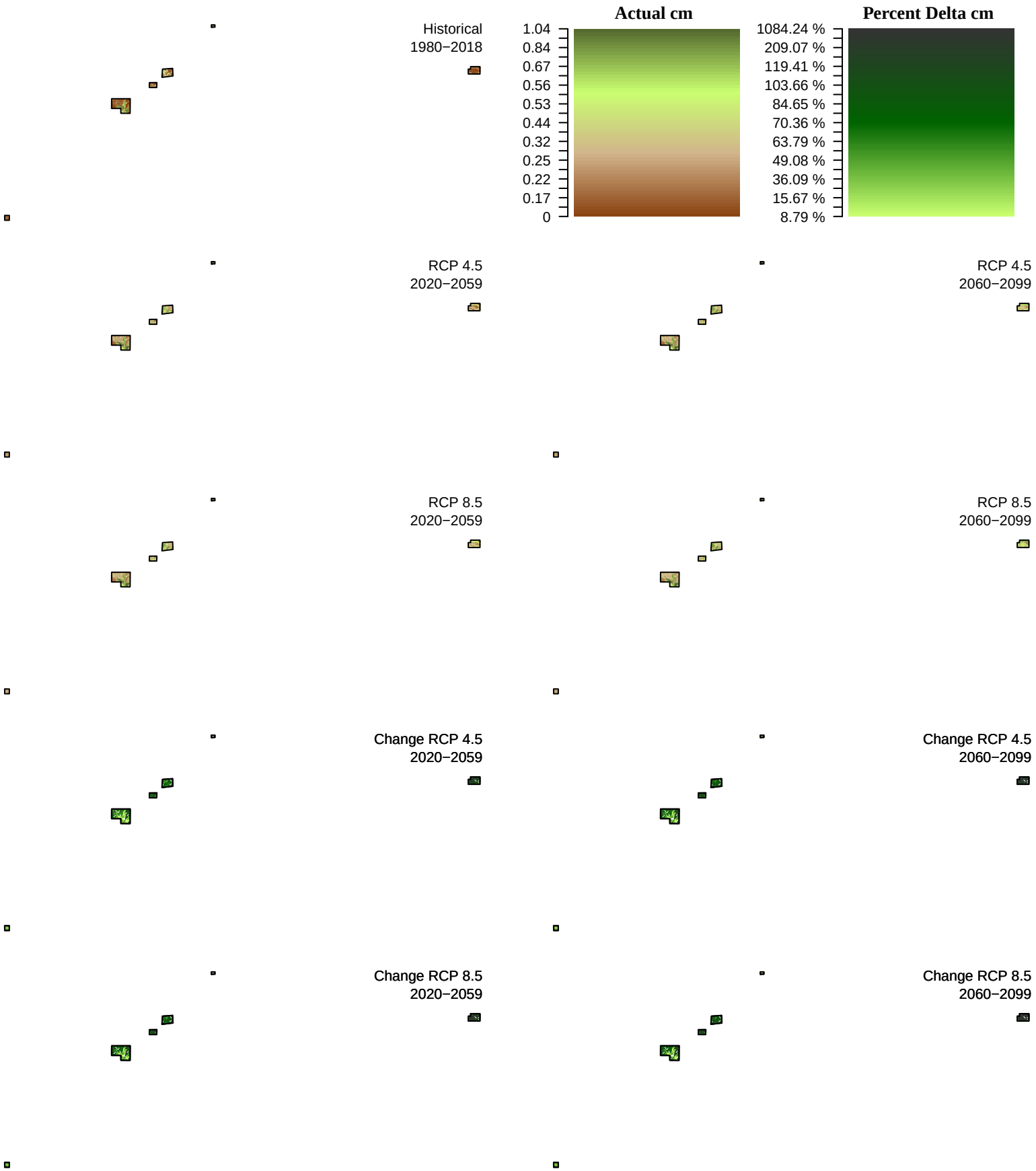


Figure HOVEmap117:
Past trends and future trajectories of park−wide mean values for Winter transpiration in Hovenweep. Topmost panel depicts the historical mean from 1980−2018. Lower four panels show the emission scenarios of RCP 4.5 and RCP 8.5 at near−term and long−term timeframes. Bottom four panels depict the change from the historical mean; cross hatching denotes areas of robust predicitons (90% of models agree in the direction of change).

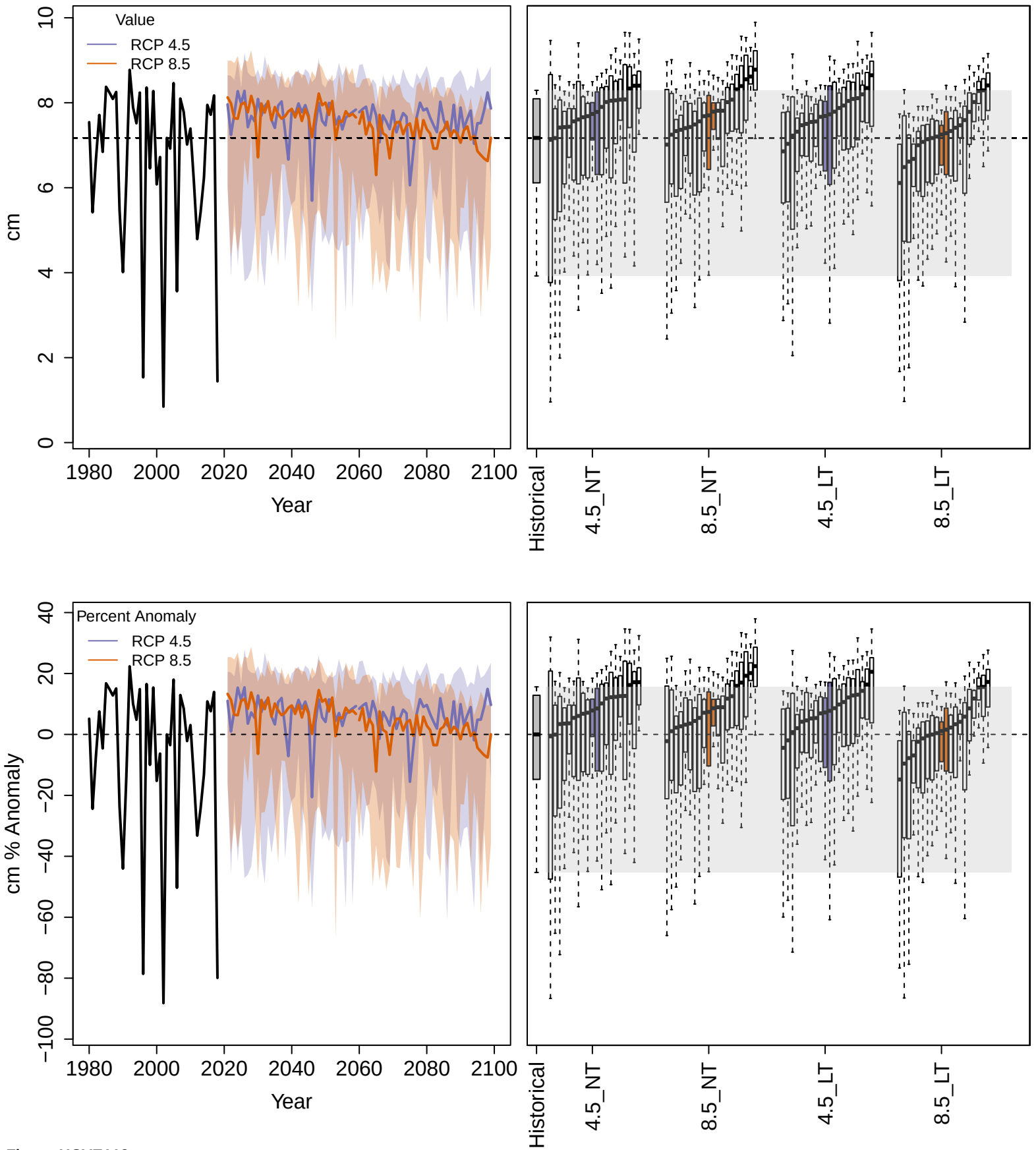


Figure HOVE119:
Past trends and future trajectories of park−wide mean values for Spring transpiration in Hovenweep. Top panels show values, bottom panels show changes from the long−term historical mean. Left: Time series of historical (black) and future projections for RCP 4.5 and 8.5. Shaded areas show spread among climate models. Right: Boxplots of temporal variability over 40−year periods under historical (left box) and individual climate models under two RCPs. Right: Historical time period is 1970−2010; near−term (NT) is 2020−2060; long−term (LT) is 2061−2100.

Hovenweep: Spring transpiration

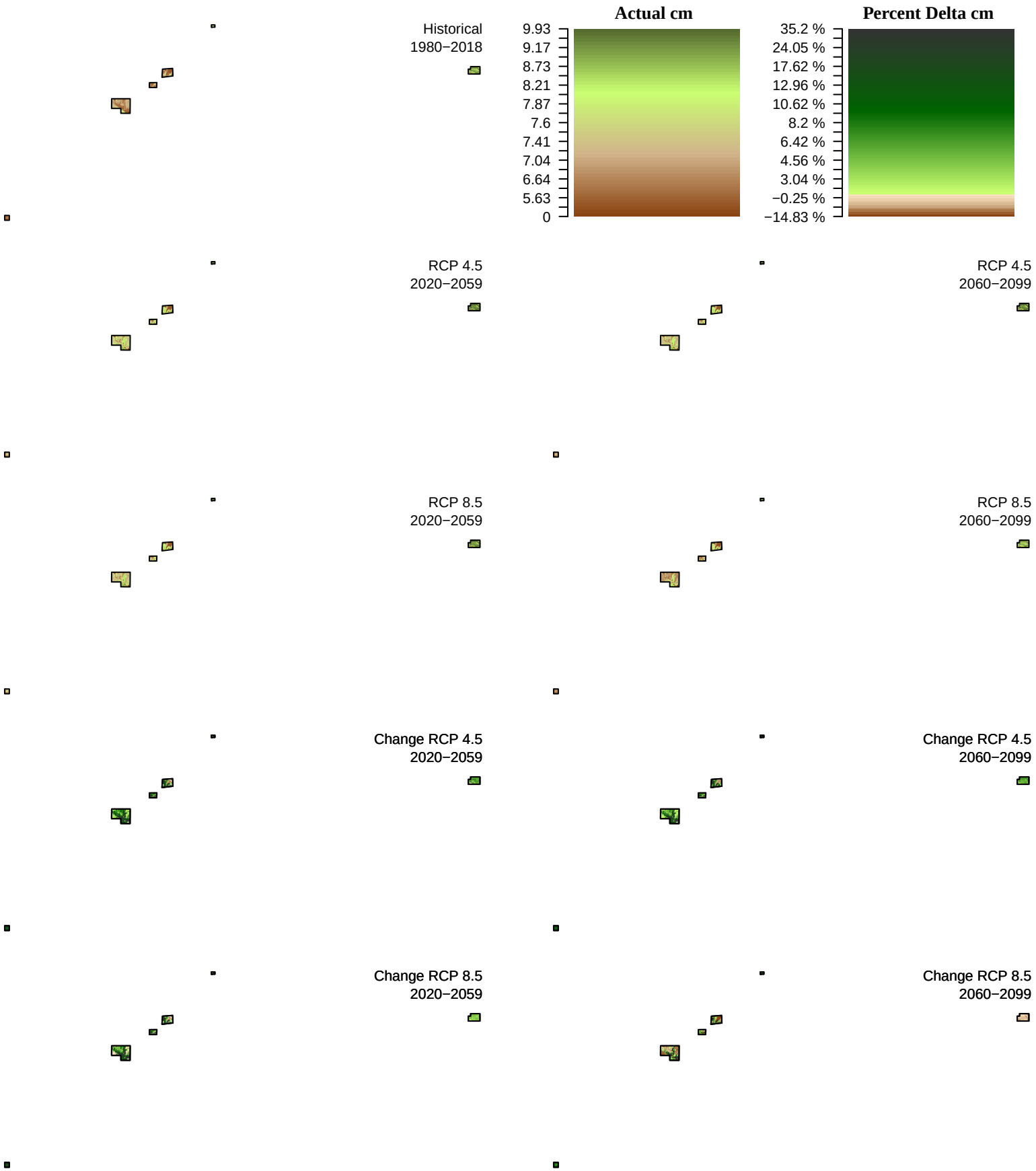


Figure HOVEmap119:
Past trends and future trajectories of park−wide mean values for Spring transpiration in Hovenweep. Topmost panel depicts the historical mean from 1980−2018. Lower four panels show the emission scenarios of RCP 4.5 and RCP 8.5 at near−term and long−term timeframes. Bottom four panels depict the change from the historical mean; cross hatching denotes areas of robust predicitons (90% of models agree in the direction of change).

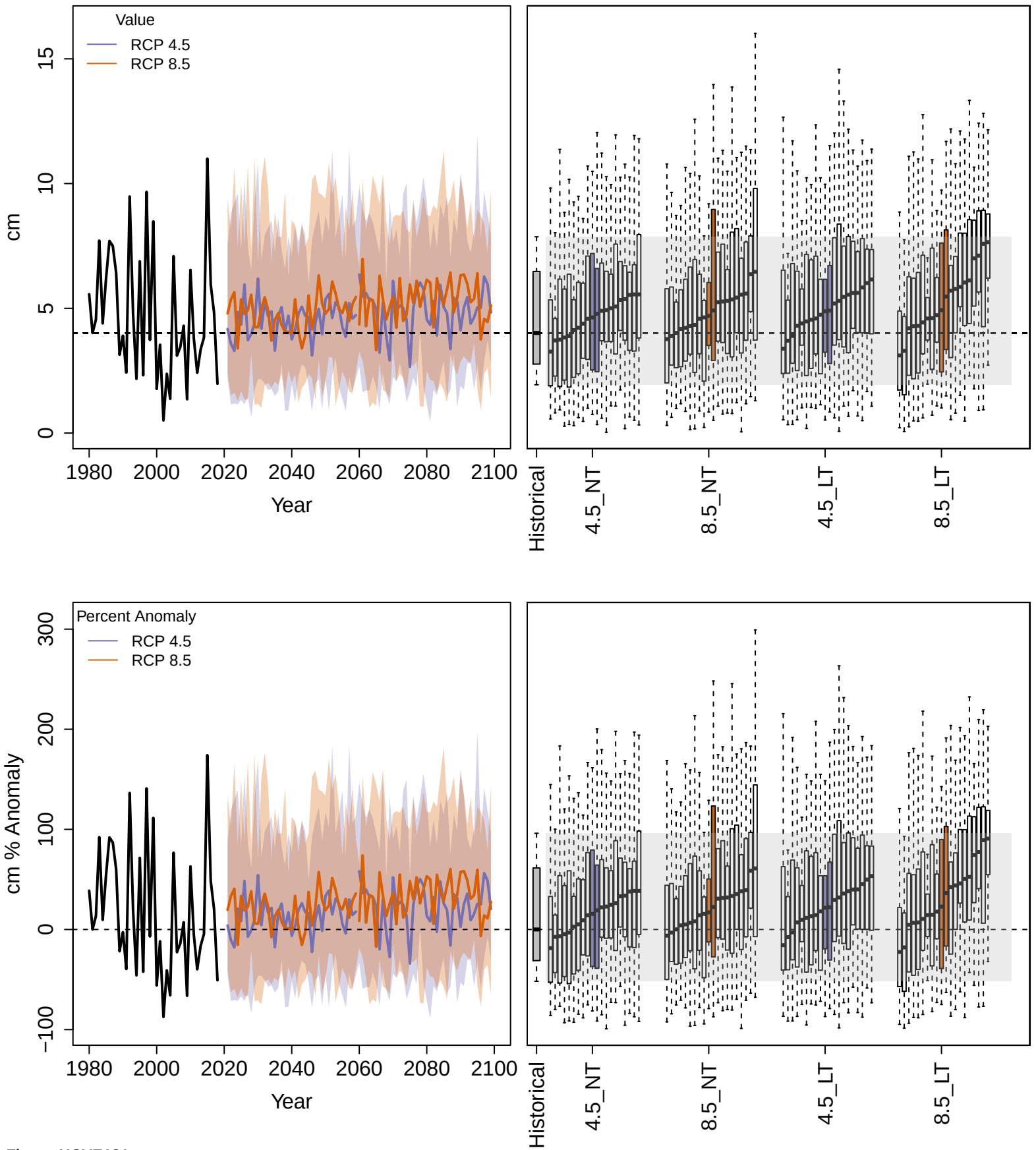


Figure HOVE121:
Past trends and future trajectories of park−wide mean values for Summer transpiration in Hovenweep. Top panels show values, bottom panels show changes from the long−term historical mean. Left: Time series of historical (black) and future projections for RCP 4.5 and 8.5. Shaded areas show spread among climate models. Right: Boxplots of temporal variability over 40−year periods under historical (left box) and individual climate models under two RCPs. Right: Historical time period is 1970−2010; near−term (NT) is 2020−2060; long−term (LT) is 2061−2100.

Hovenweep: Summer transpiration

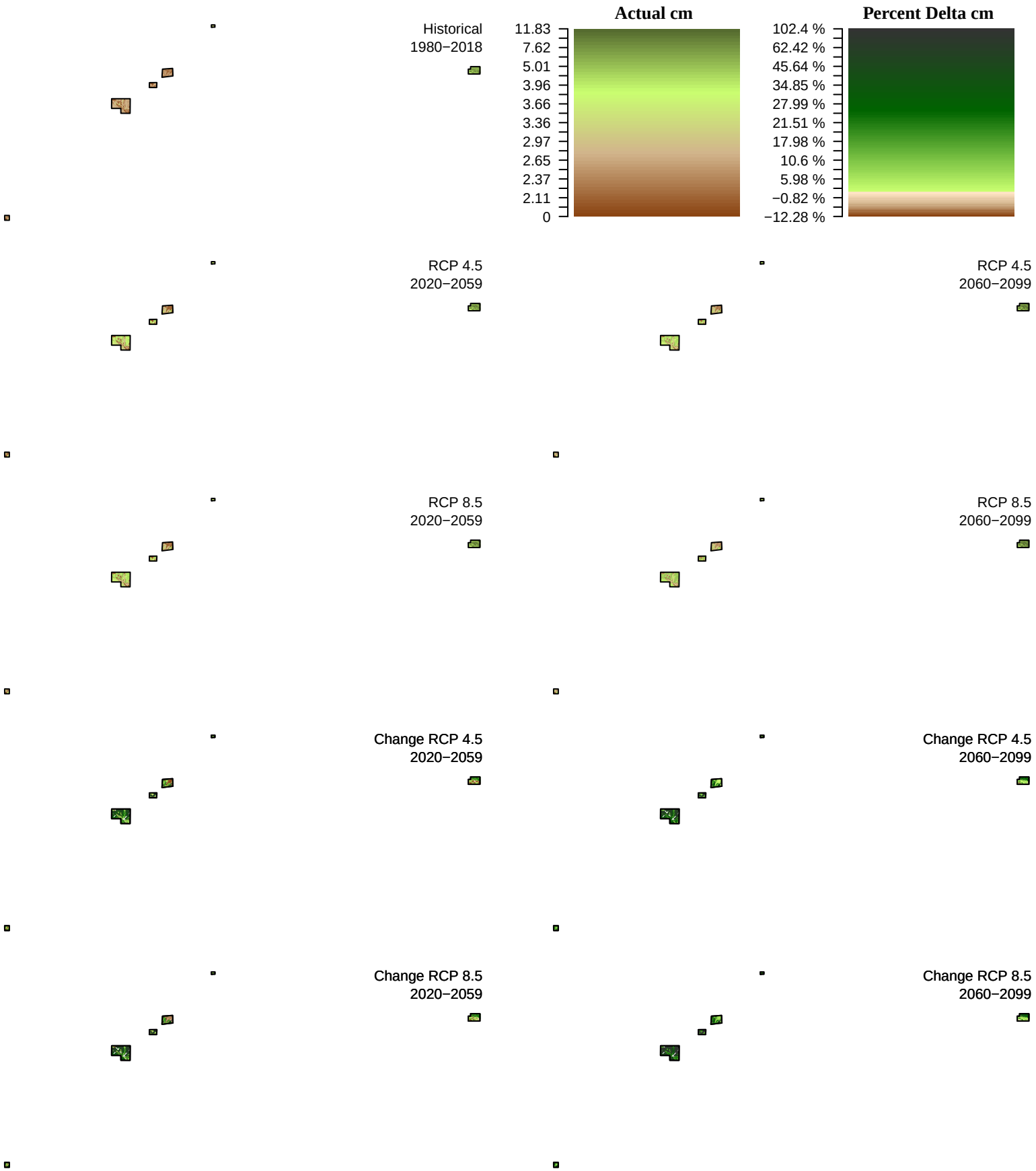


Figure HOVEmap121:
Past trends and future trajectories of park−wide mean values for Summer transpiration in Hovenweep. Topmost panel depicts the historical mean from 1980−2018. Lower four panels show the emission scenarios of RCP 4.5 and RCP 8.5 at near−term and long−term timeframes. Bottom four panels depict the change from the historical mean; cross hatching denotes areas of robust predicitons (90% of models agree in the direction of change).

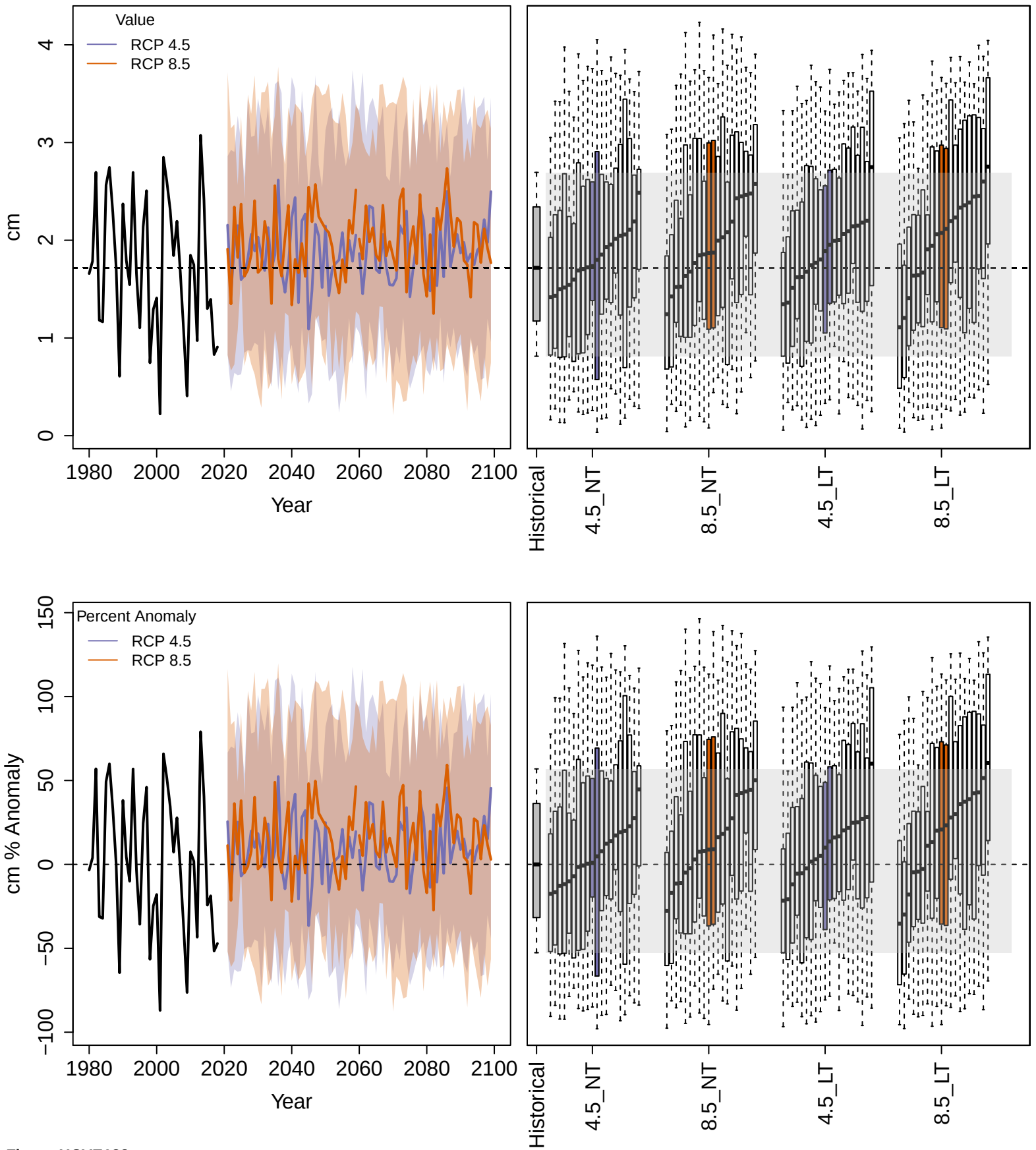


Figure HOVE123:
Past trends and future trajectories of park−wide mean values for Fall transpiration in Hovenweep. Top panels show values, bottom panels show changes from the long−term historical mean. Left: Time series of historical (black) and future projections for RCP 4.5 and 8.5. Shaded areas show spread among climate models. Right: Boxplots of temporal variability over 40−year periods under historical (left box) and individual climate models under two RCPs. Right: Historical time period is 1970−2010; near−term (NT) is 2020−2060; long−term (LT) is 2061−2100.

Hovenweep: Fall transpiration

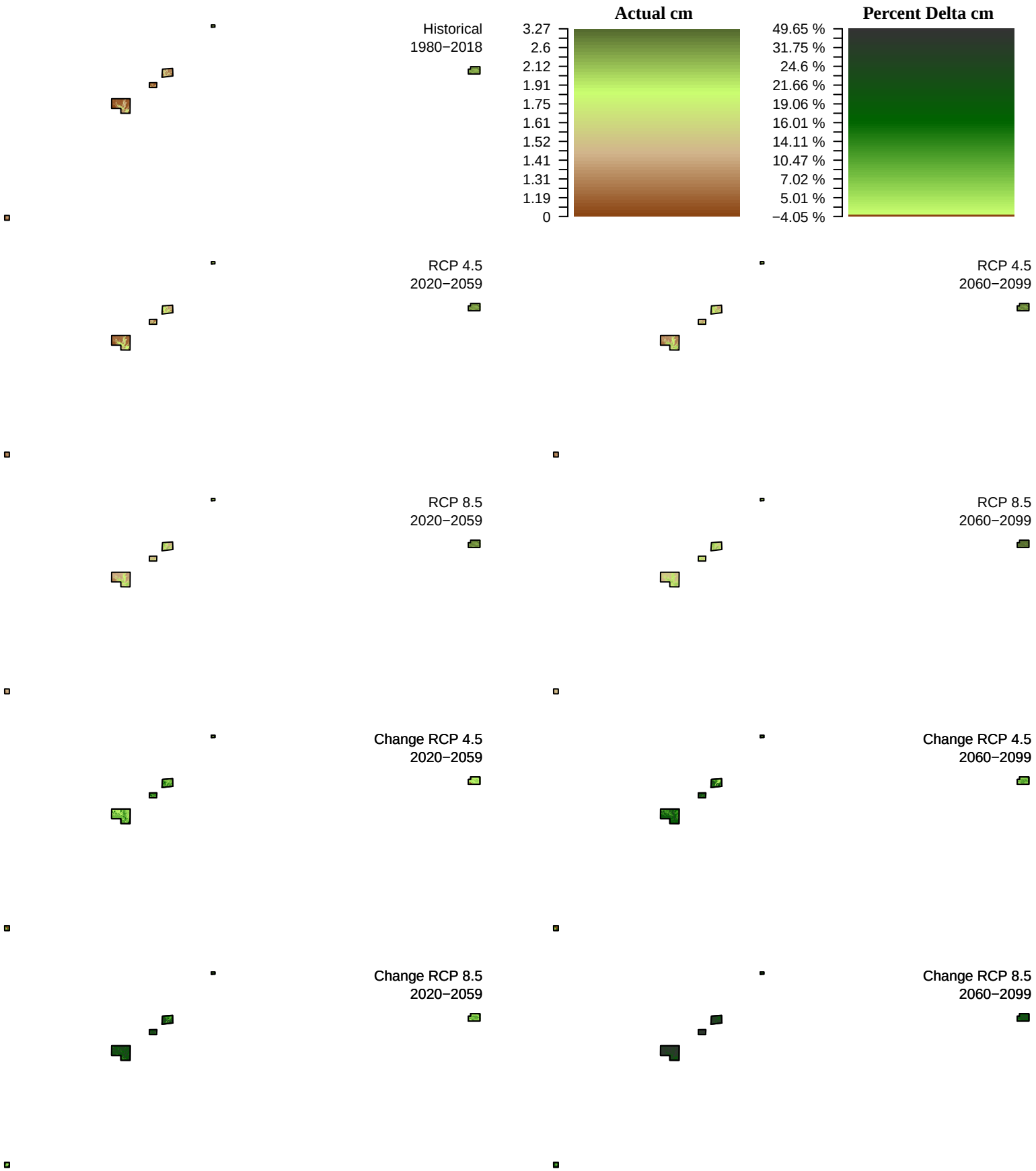


Figure HOVEmap123:
Past trends and future trajectories of park−wide mean values for Fall transpiration in Hovenweep. Topmost panel depicts the historical mean from 1980−2018. Lower four panels show the emission scenarios of RCP 4.5 and RCP 8.5 at near−term and long−term timeframes. Bottom four panels depict the change from the historical mean; cross hatching denotes areas of robust predicitons (90% of models agree in the direction of change).

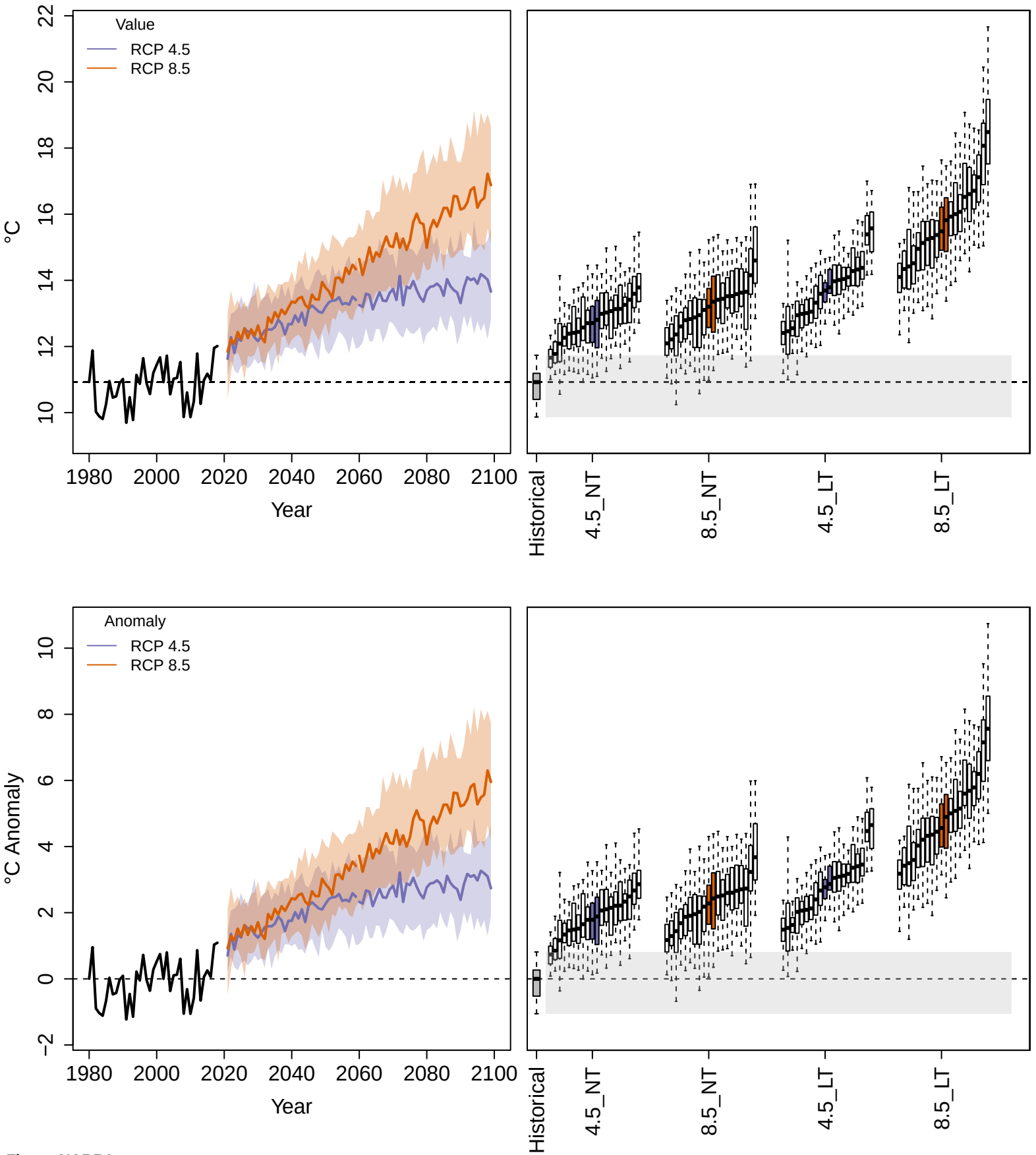


Figure NABR1:
Past trends and future trajectories of park−wide mean values for Mean Annual Temperature in Natural Bridges. Top panels show values, bottom panels show changes from the long−term historical mean. Left: Time series of historical (black) and future projections for RCP 4.5 and 8.5. Shaded areas show spread among climate models. Right: Boxplots of temporal variability over 40−year periods under historical (left box) and individual climate models under two RCPs. Right: Historical time period is 1970−2010; near−term (NT) is 2020−2060; long−term (LT) is 2061−2100.

Natural Bridges: Mean Annual Temperature

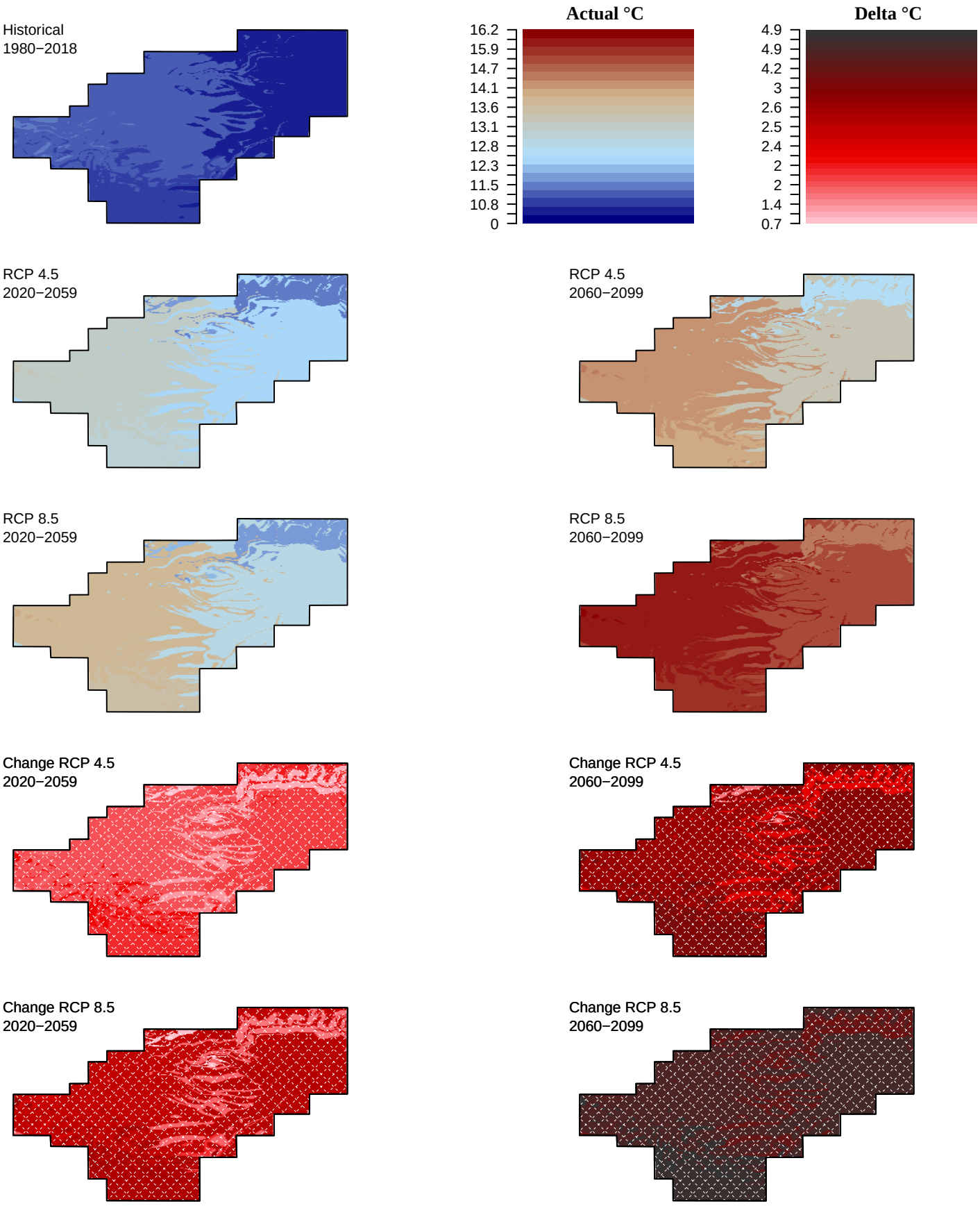


Figure NABRmap1:
Past trends and future trajectories of park−wide mean values for Mean Annual Temperature in Natural Bridges. Topmost panel depicts the historical mean from 1980−2018. Lower four panels show the emission scenarios of RCP 4.5 and RCP 8.5 at near−term and long−term timeframes. Bottom four panels depict the change from the historical mean; cross hatching denotes areas of robust predicitons (90% of models agree in the direction of change).

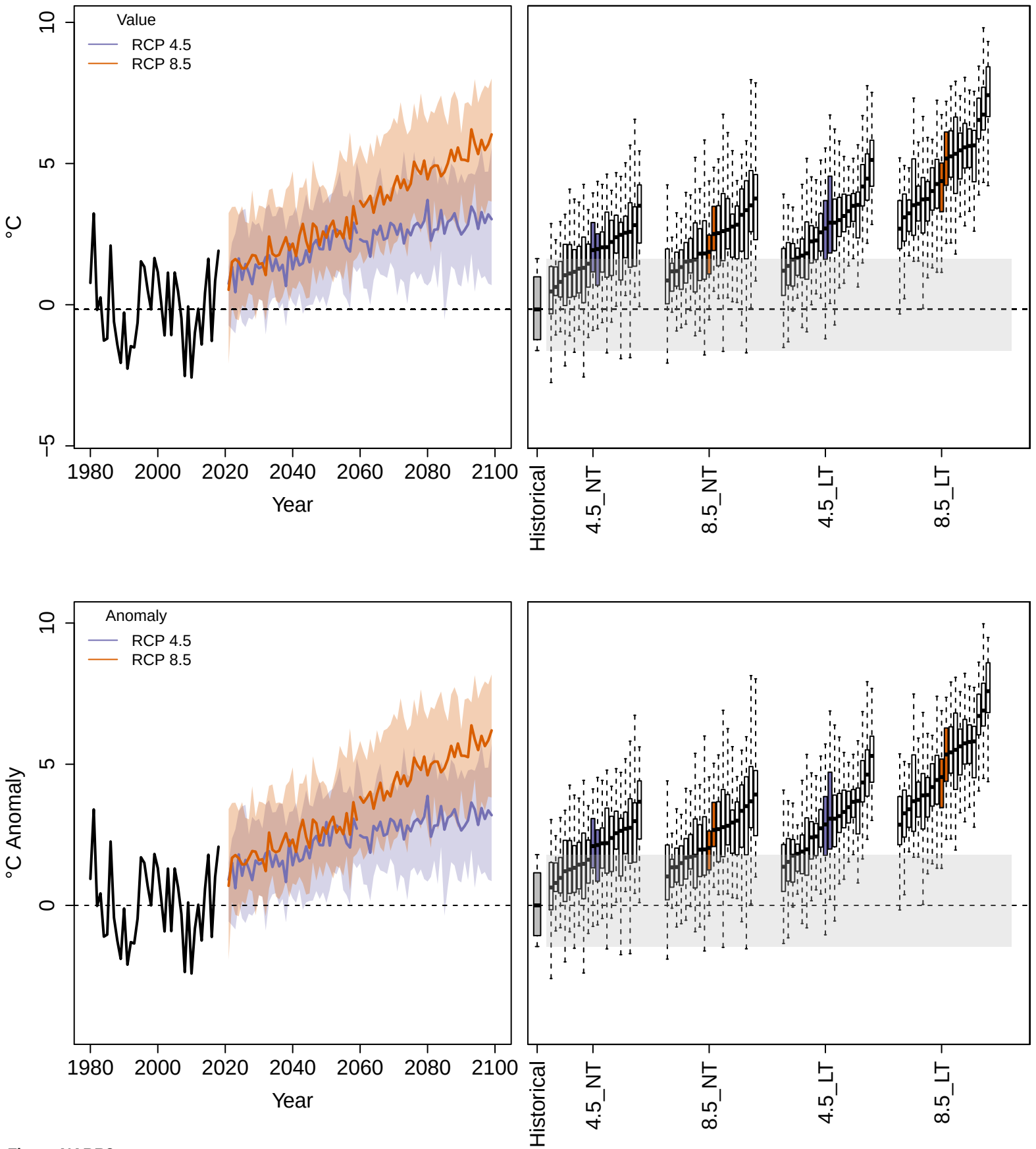


Figure NABR3:
Past trends and future trajectories of park−wide mean values for Winter Temperature in Natural Bridges. Top panels show values, bottom panels show changes from the long−term historical mean. Left: Time series of historical (black) and future projections for RCP 4.5 and 8.5. Shaded areas show spread among climate models. Right: Boxplots of temporal variability over 40−year periods under historical (left box) and individual climate models under two RCPs. Right: Historical time period is 1970−2010; near−term (NT) is 2020−2060; long−term (LT) is 2061−2100.

Natural Bridges: Winter Temperature

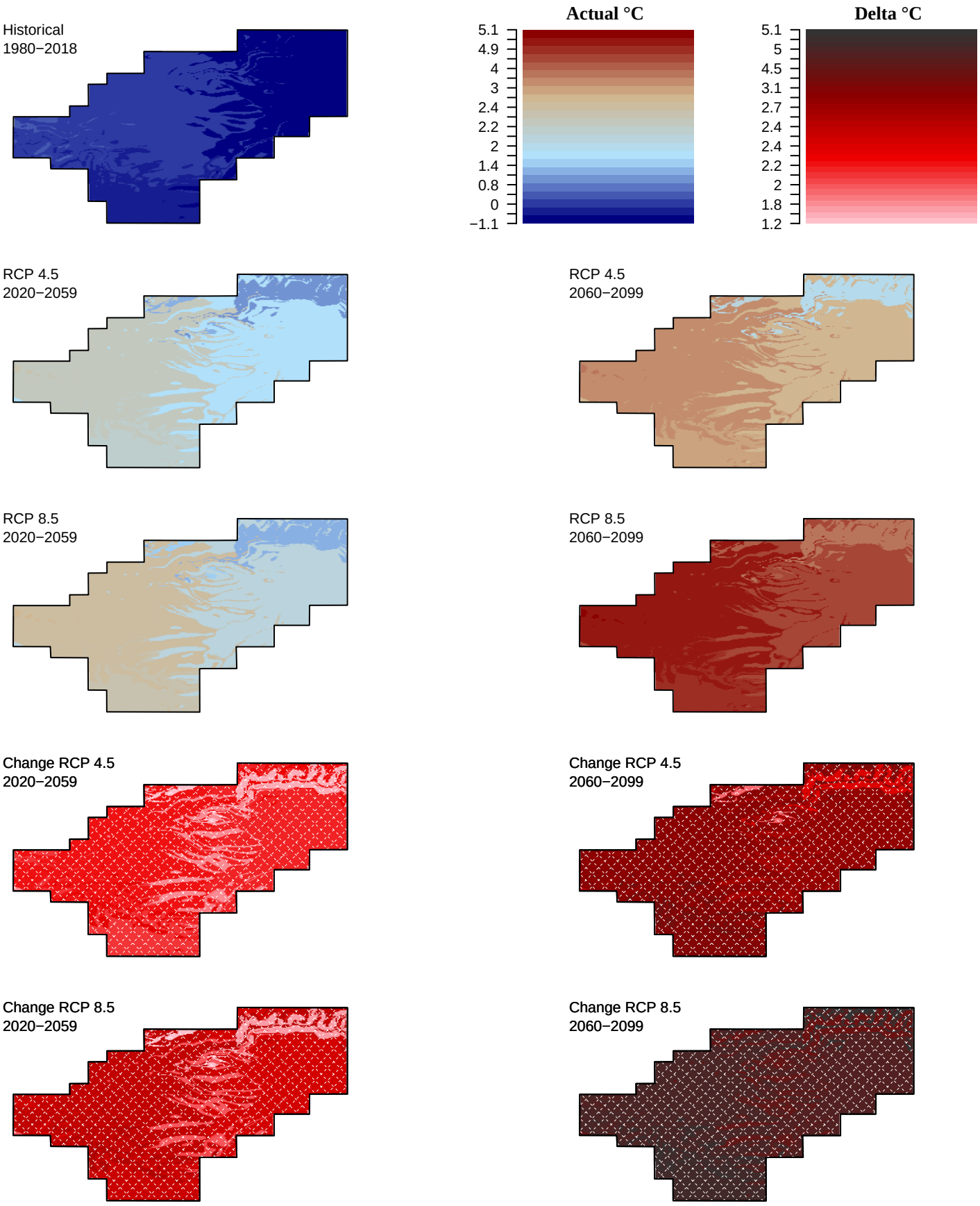


Figure NABRmap3:
Past trends and future trajectories of park−wide mean values for Winter Temperature in Natural Bridges. Topmost panel depicts the historical mean from 1980−2018. Lower four panels show the emission scenarios of RCP 4.5 and RCP 8.5 at near−term and long−term timeframes. Bottom four panels depict the change from the historical mean; cross hatching denotes areas of robust predicitons (90% of models agree in the direction of change).

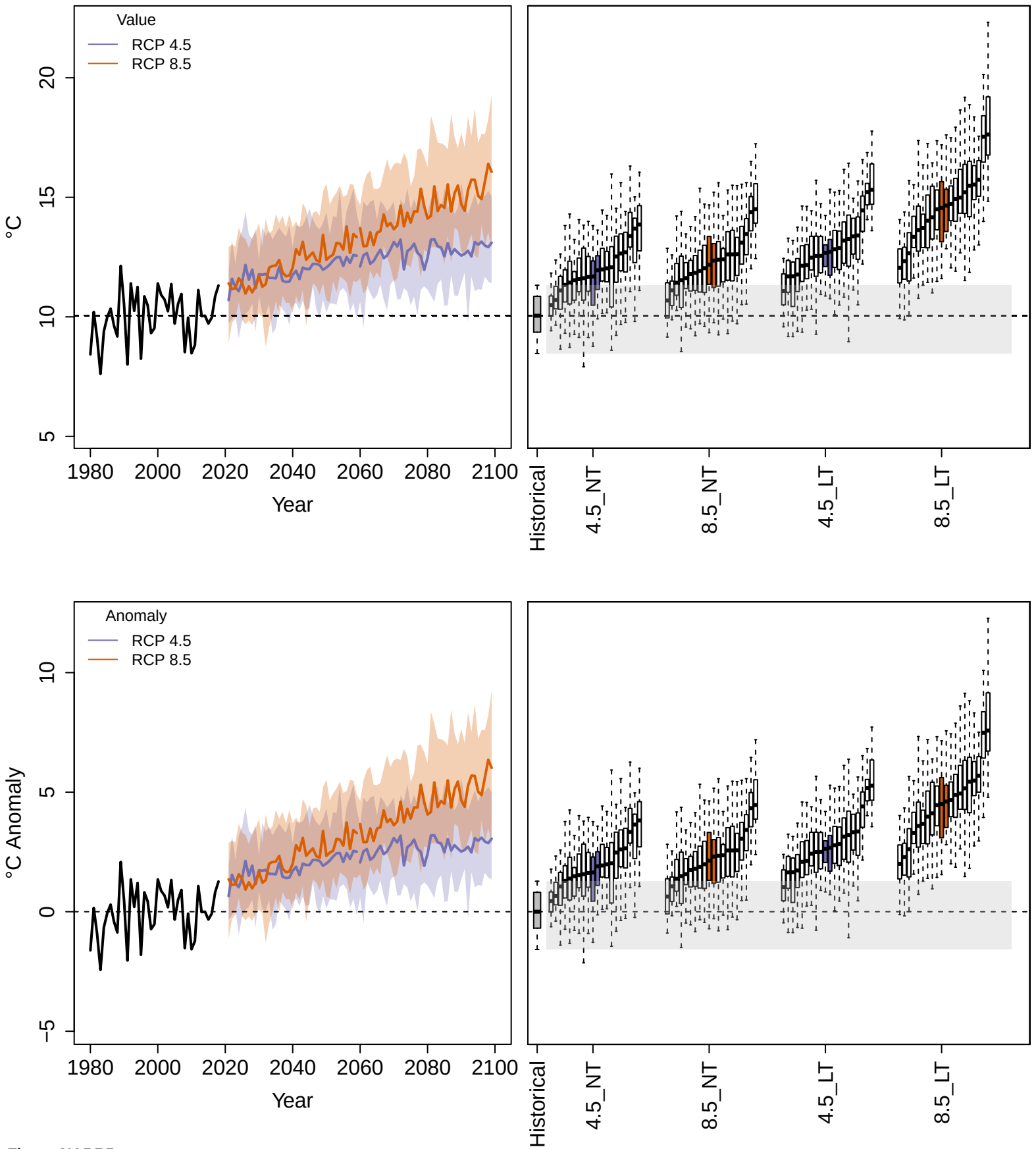


Figure NABR5:
Past trends and future trajectories of park−wide mean values for Spring Temperature in Natural Bridges. Top panels show values, bottom panels show changes from the long−term historical mean. Left: Time series of historical (black) and future projections for RCP 4.5 and 8.5. Shaded areas show spread among climate models. Right: Boxplots of temporal variability over 40−year periods under historical (left box) and individual climate models under two RCPs. Right: Historical time period is 1970−2010; near−term (NT) is 2020−2060; long−term (LT) is 2061−2100.

Natural Bridges: Spring Temperature

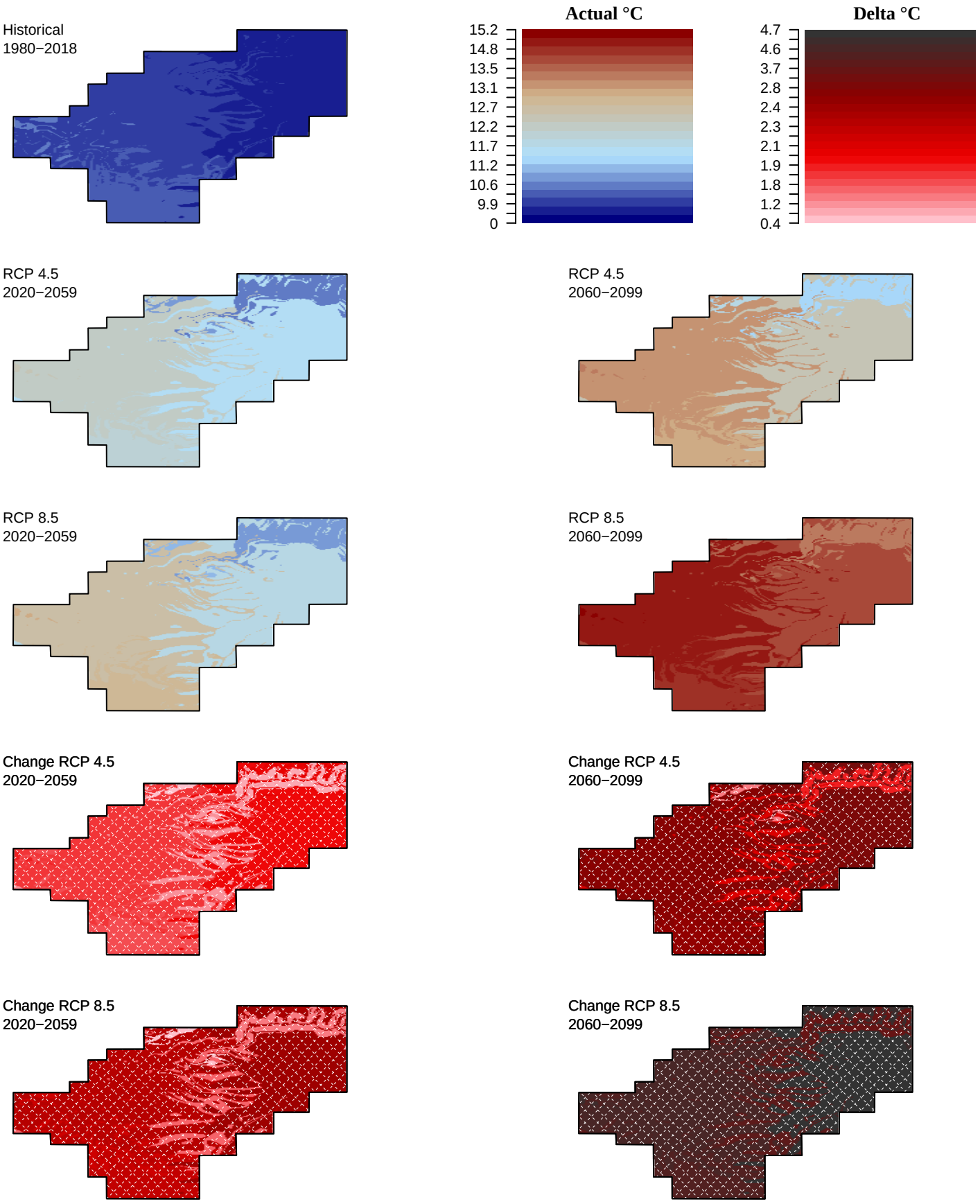


Figure NABRmap5:
Past trends and future trajectories of park−wide mean values for Spring Temperature in Natural Bridges. Topmost panel depicts the historical mean from 1980−2018. Lower four panels show the emission scenarios of RCP 4.5 and RCP 8.5 at near−term and long−term timeframes. Bottom four panels depict the change from the historical mean; cross hatching denotes areas of robust predicitons (90% of models agree in the direction of change).

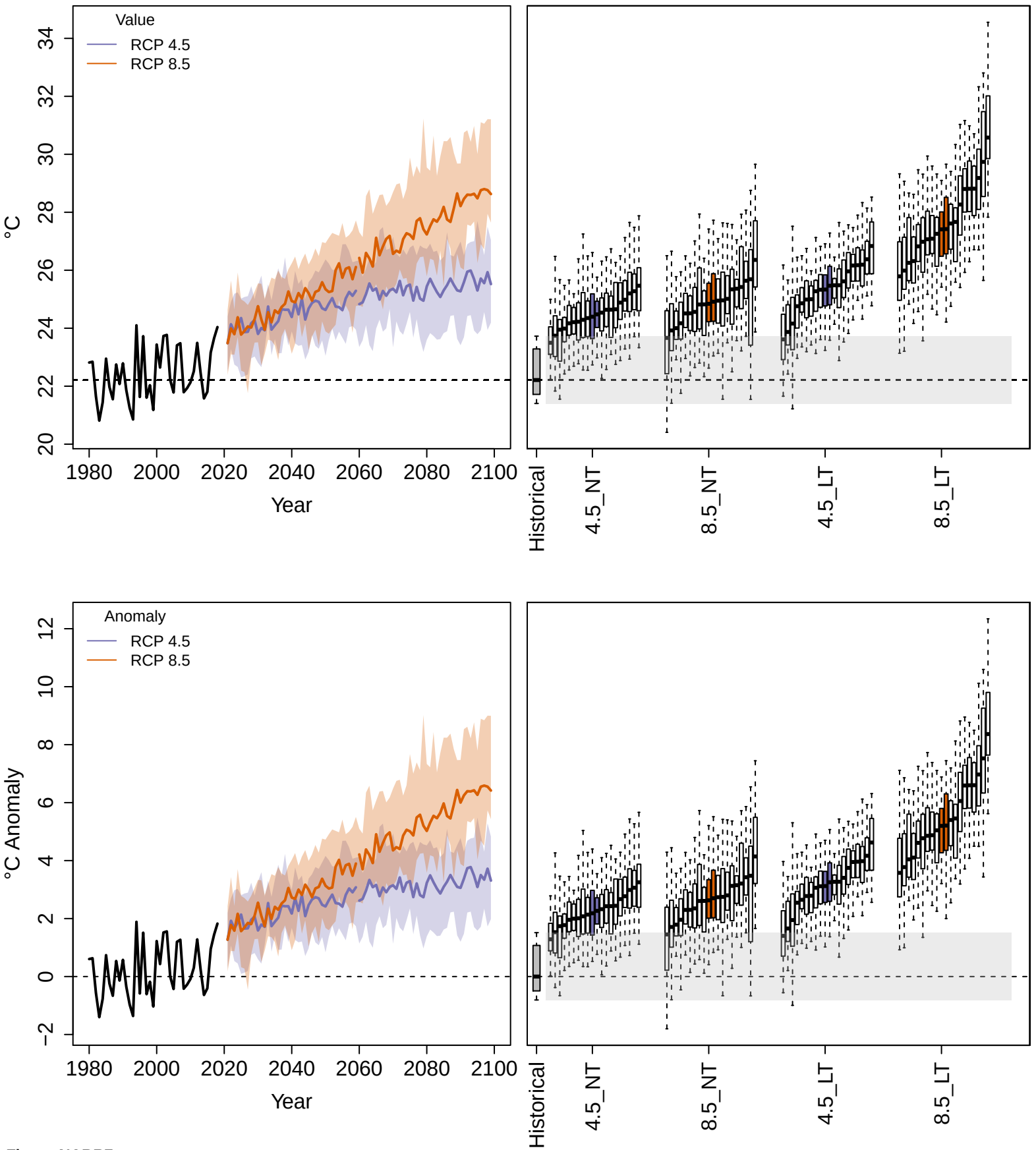


Figure NABR7:
Past trends and future trajectories of park−wide mean values for Summer Temperature in Natural Bridges. Top panels show values, bottom panels show changes from the long−term historical mean. Left: Time series of historical (black) and future projections for RCP 4.5 and 8.5. Shaded areas show spread among climate models. Right: Boxplots of temporal variability over 40−year periods under historical (left box) and individual climate models under two RCPs. Right: Historical time period is 1970−2010; near−term (NT) is 2020−2060; long−term (LT) is 2061−2100.

Natural Bridges: Summer Temperature

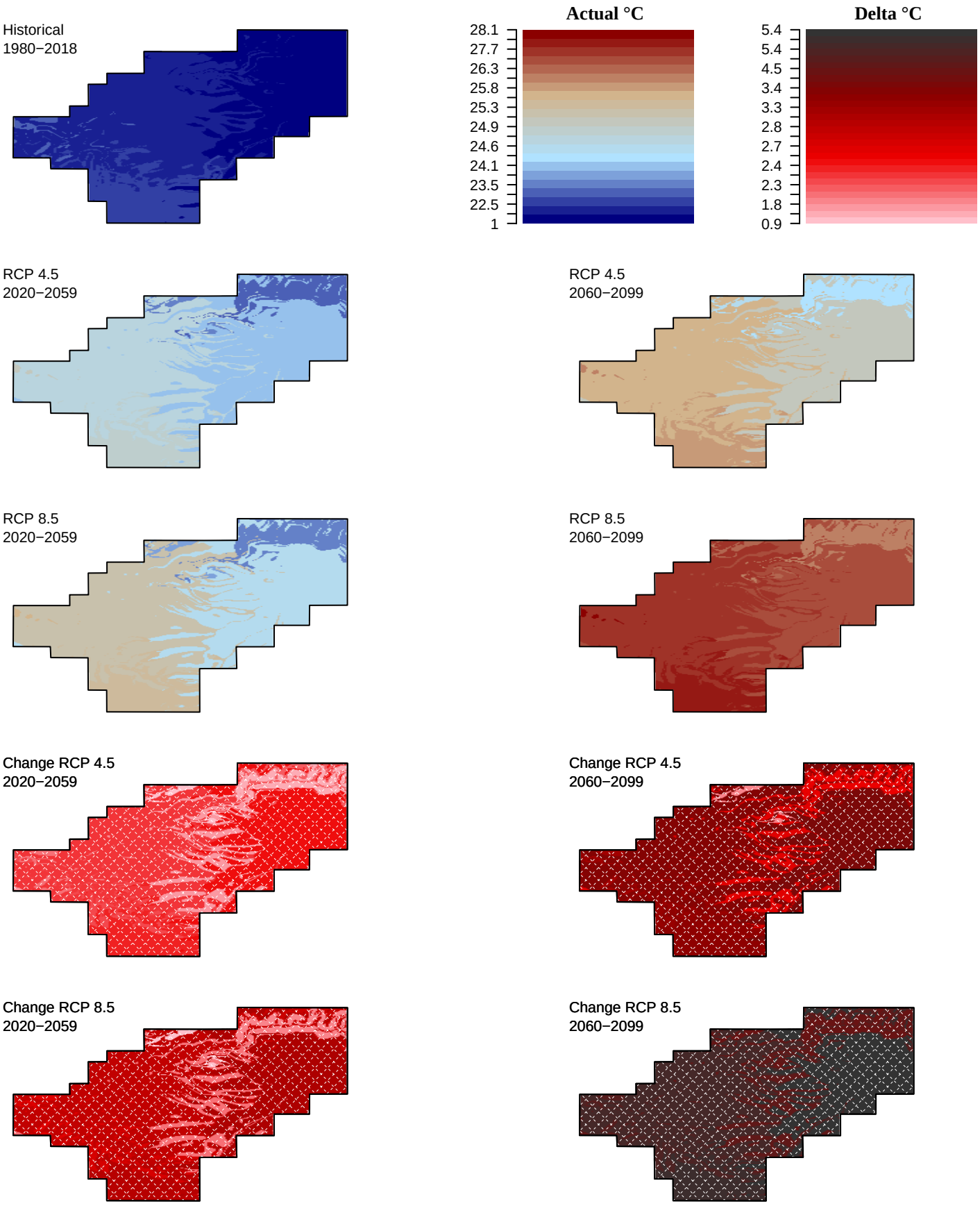


Figure NABRmap7:
Past trends and future trajectories of park−wide mean values for Summer Temperature in Natural Bridges. Topmost panel depicts the historical mean from 1980−2018. Lower four panels show the emission scenarios of RCP 4.5 and RCP 8.5 at near−term and long−term timeframes. Bottom four panels depict the change from the historical mean; cross hatching denotes areas of robust predicitons (90% of models agree in the direction of change).

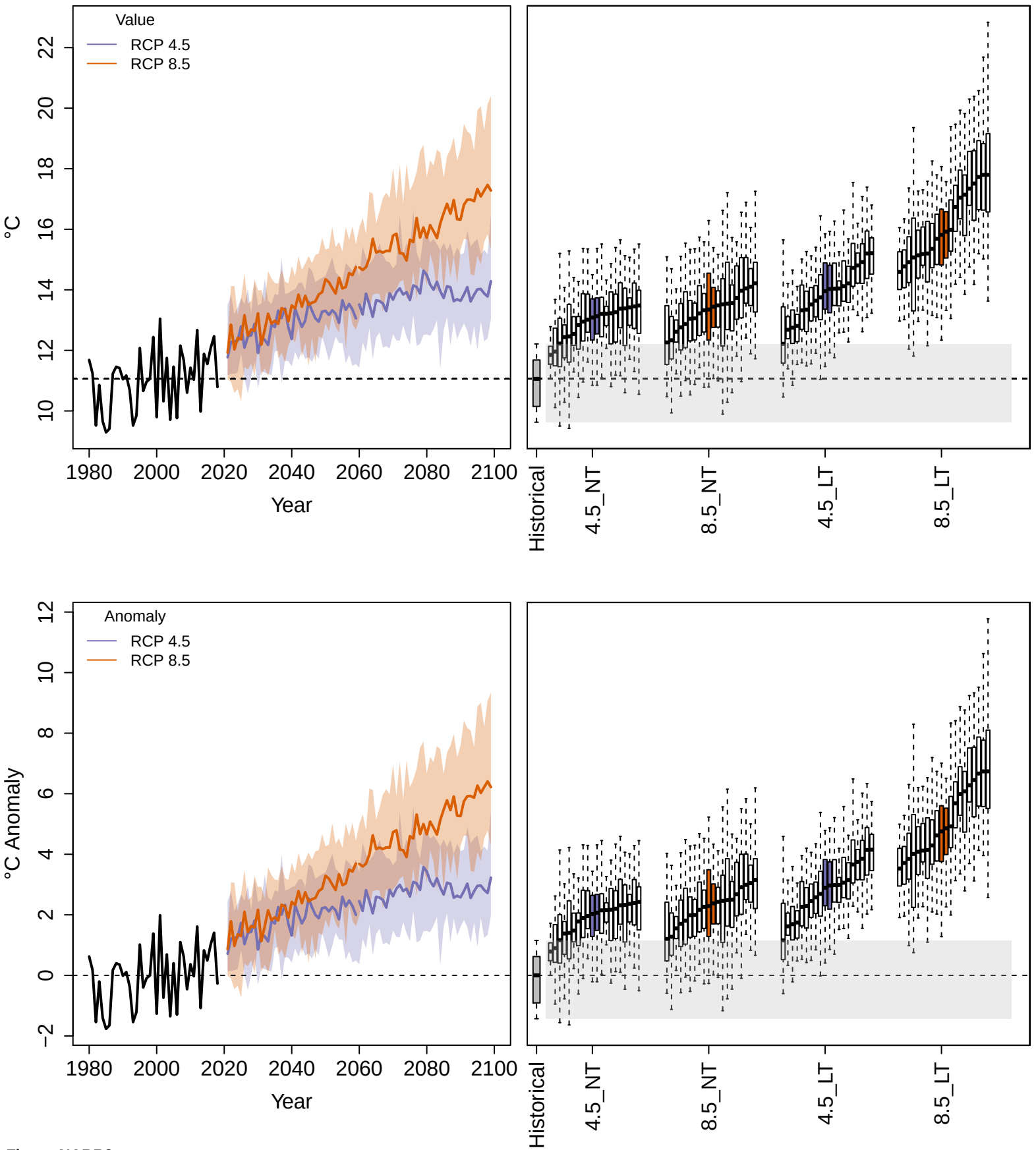


Figure NABR9:
Past trends and future trajectories of park−wide mean values for Fall Temperature in Natural Bridges. Top panels show values, bottom panels show changes from the long−term historical mean. Left: Time series of historical (black) and future projections for RCP 4.5 and 8.5. Shaded areas show spread among climate models. Right: Boxplots of temporal variability over 40−year periods under historical (left box) and individual climate models under two RCPs. Right: Historical time period is 1970−2010; near−term (NT) is 2020−2060; long−term (LT) is 2061−2100.

Natural Bridges: Fall Temperature

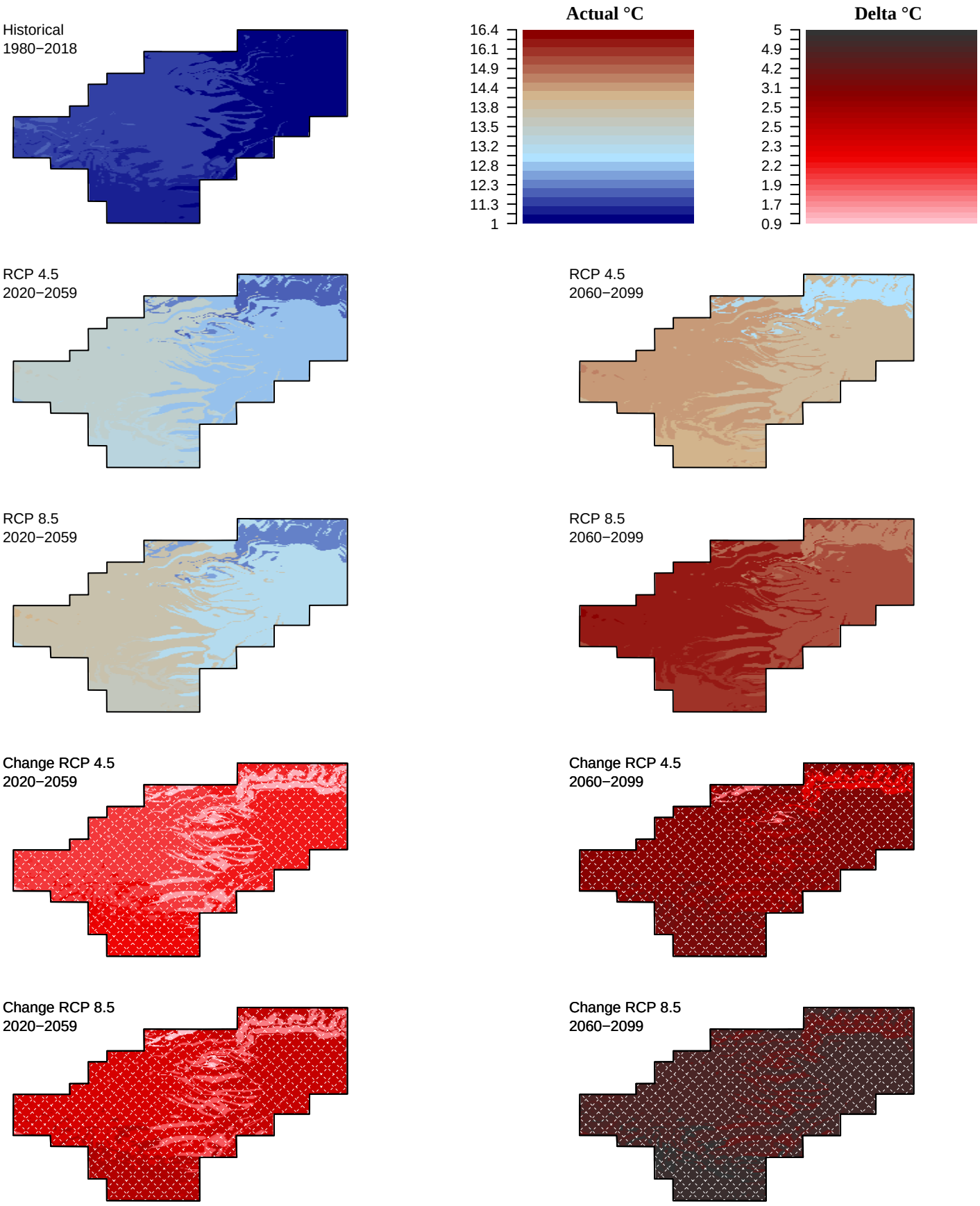


Figure NABRmap9:
Past trends and future trajectories of park−wide mean values for Fall Temperature in Natural Bridges. Topmost panel depicts the historical mean from 1980−2018. Lower four panels show the emission scenarios of RCP 4.5 and RCP 8.5 at near−term and long−term timeframes. Bottom four panels depict the change from the historical mean; cross hatching denotes areas of robust predicitons (90% of models agree in the direction of change).

Natural Bridges: Minimum winter temperature

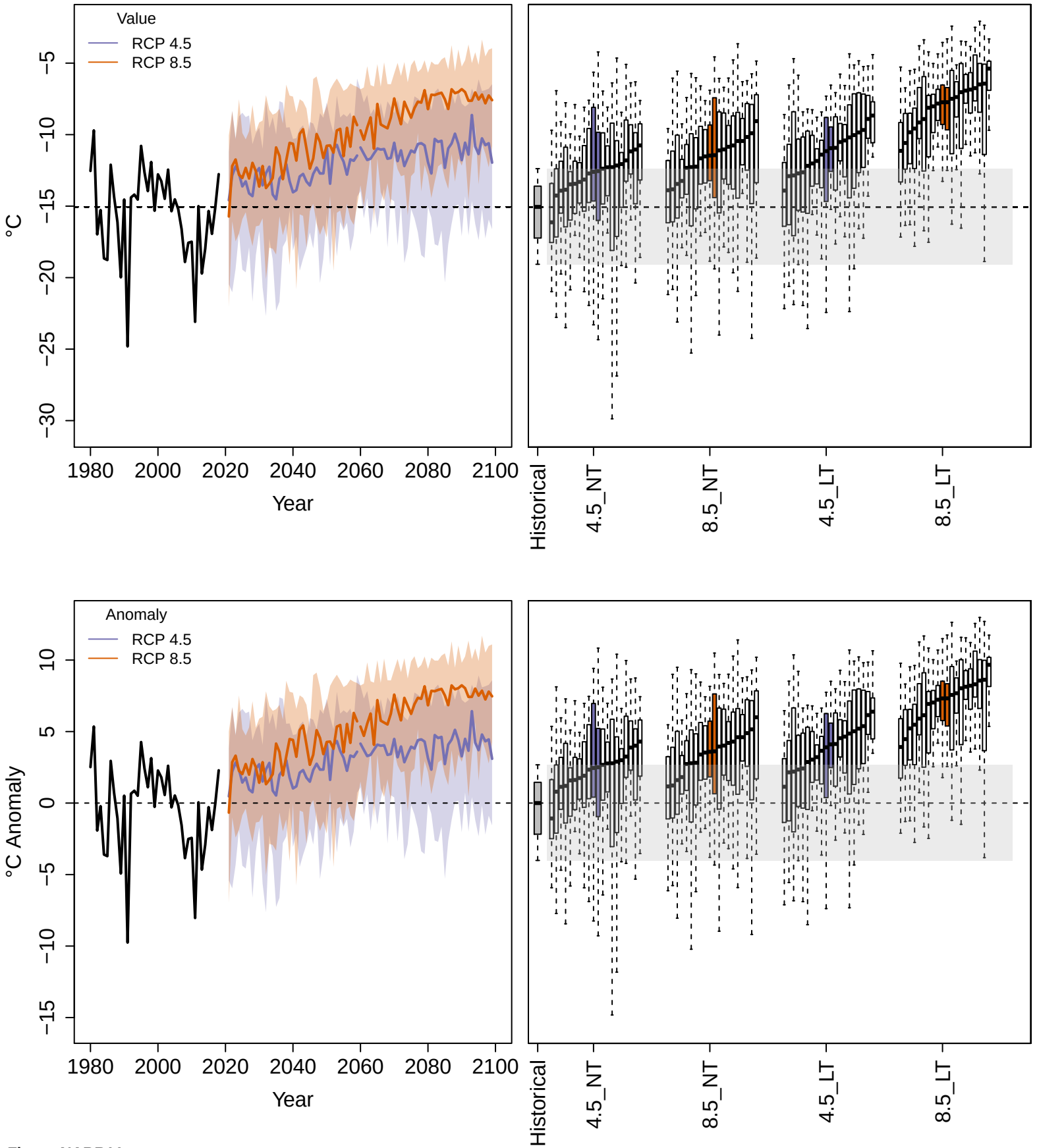


Figure NABR11:
Past trends and future trajectories of park−wide mean values for Minimum winter temperature in Natural Bridges. Top panels show values, bottom panels show changes from the long−term historical mean. Left: Time series of historical (black) and future projections for RCP 4.5 and 8.5. Shaded areas show spread among climate models. Right: Boxplots of temporal variability over 40−year periods under historical (left box) and individual climate models under two RCPs. Right: Historical time period is 1970−2010; near−term (NT) is 2020−2060; long−term (LT) is 2061−2100.

Natural Bridges: Minimum winter temperature

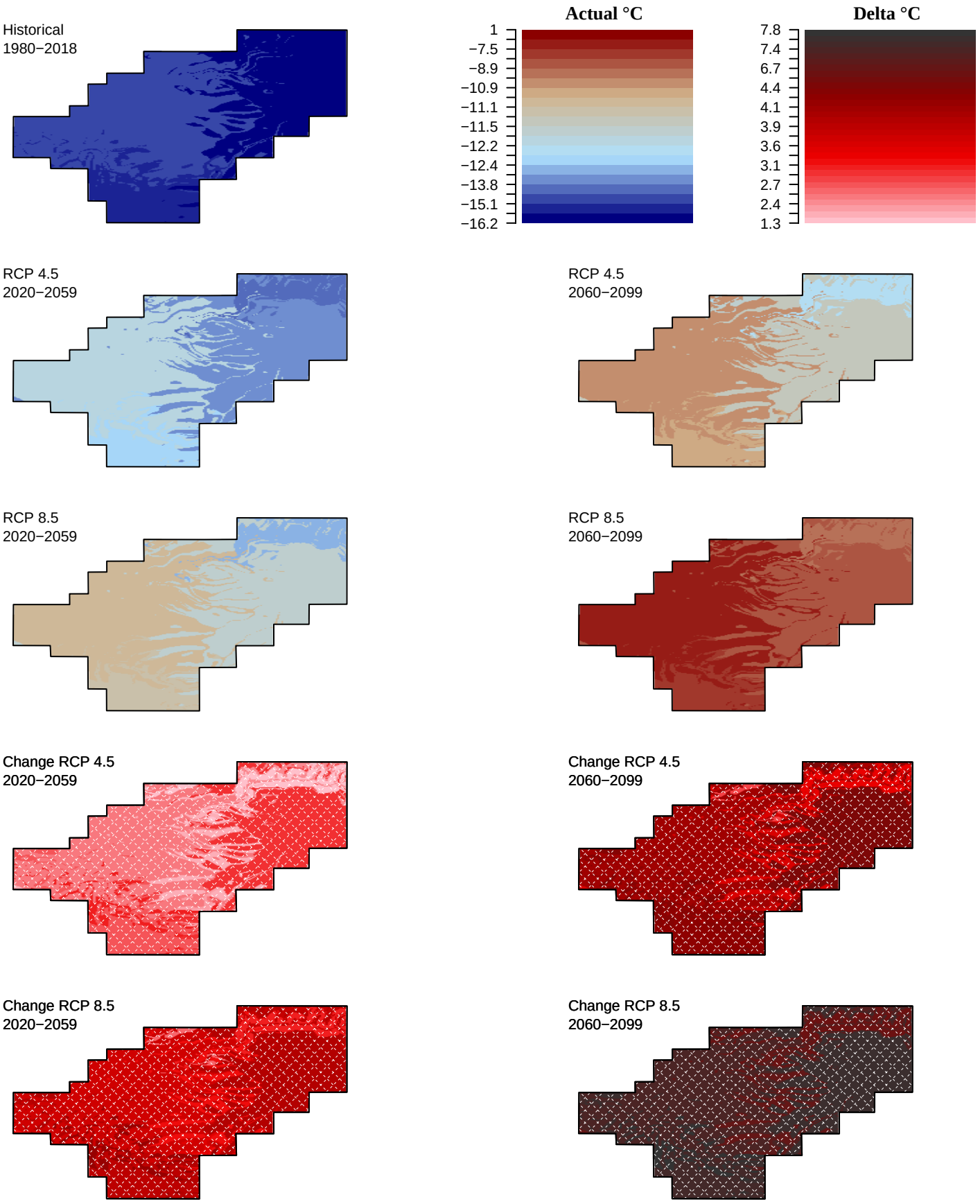


Figure NABRmap11:
Past trends and future trajectories of park−wide mean values for Minimum winter temperature in Natural Bridges. Topmost panel depicts the historical mean from 1980−2018. Lower four panels show the emission scenarios of RCP 4.5 and RCP 8.5 at near−term and long−term timeframes. Bottom four panels depict the change from the historical mean; cross hatching denotes areas of robust predicitons (90% of models agree in the direction of change).

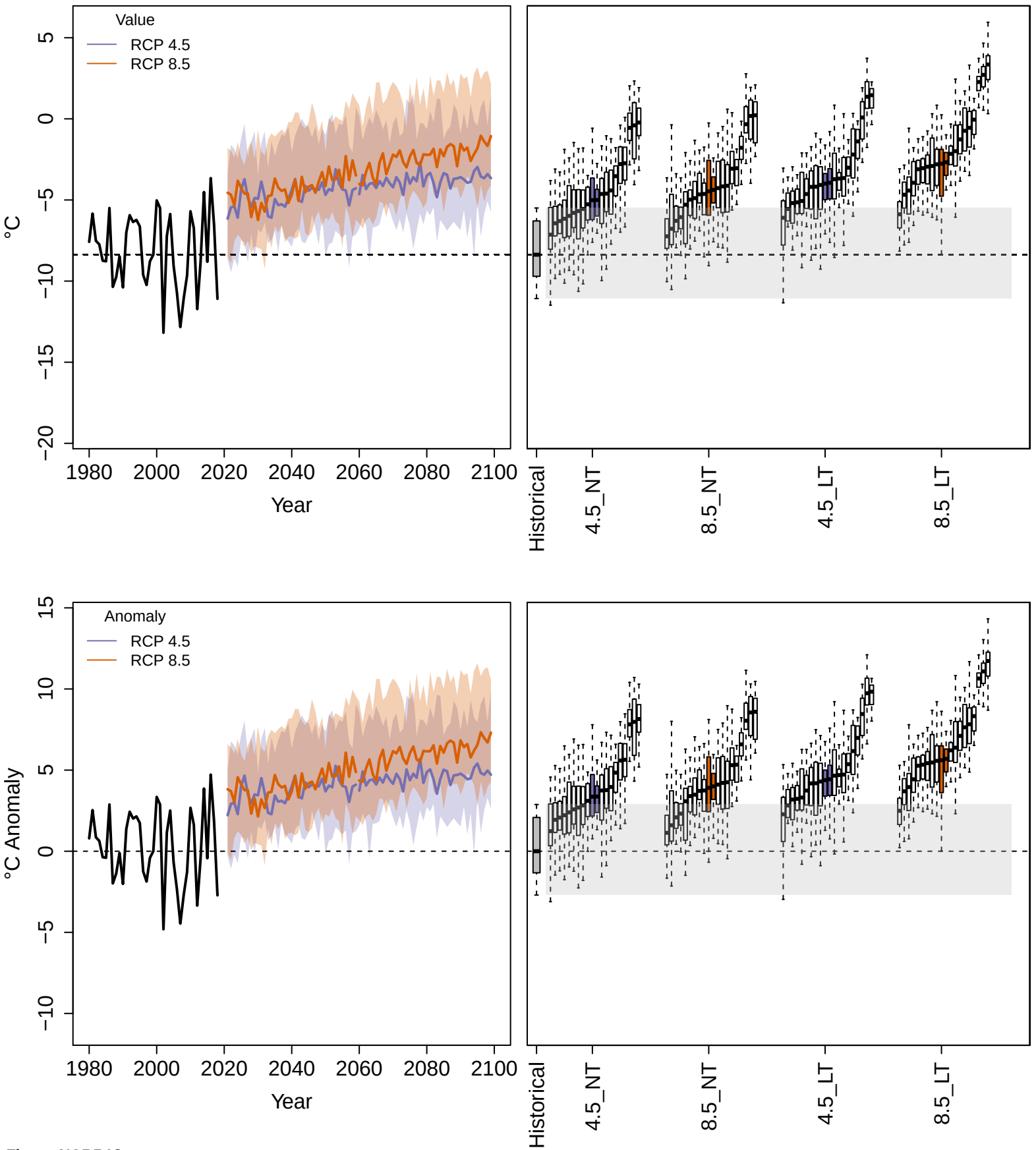


Figure NABR13:
Past trends and future trajectories of park−wide mean values for Minimum spring temperature in Natural Bridges. Top panels show values, bottom panels show changes from the long−term historical mean. Left: Time series of historical (black) and future projections for RCP 4.5 and 8.5. Shaded areas show spread among climate models. Right: Boxplots of temporal variability over 40−year periods under historical (left box) and individual climate models under two RCPs. Right: Historical time period is 1970−2010; near−term (NT) is 2020−2060; long−term (LT) is 2061−2100.

Natural Bridges: Minimum spring temperature

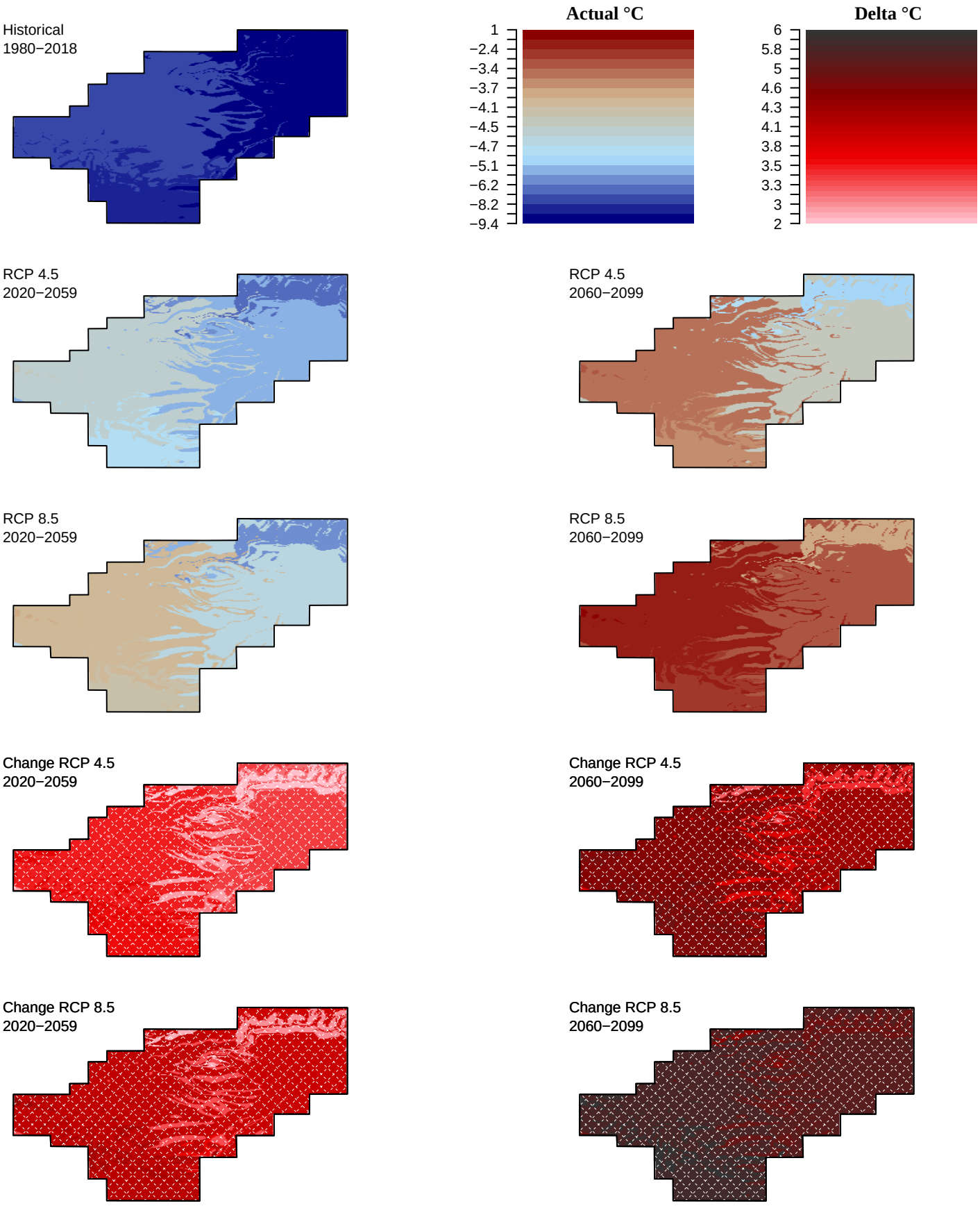


Figure NABRmap13:
Past trends and future trajectories of park−wide mean values for Minimum spring temperature in Natural Bridges. Topmost panel depicts the historical mean from 1980−2018. Lower four panels show the emission scenarios of RCP 4.5 and RCP 8.5 at near−term and long−term timeframes. Bottom four panels depict the change from the historical mean; cross hatching denotes areas of robust predicitons (90% of models agree in the direction of change).

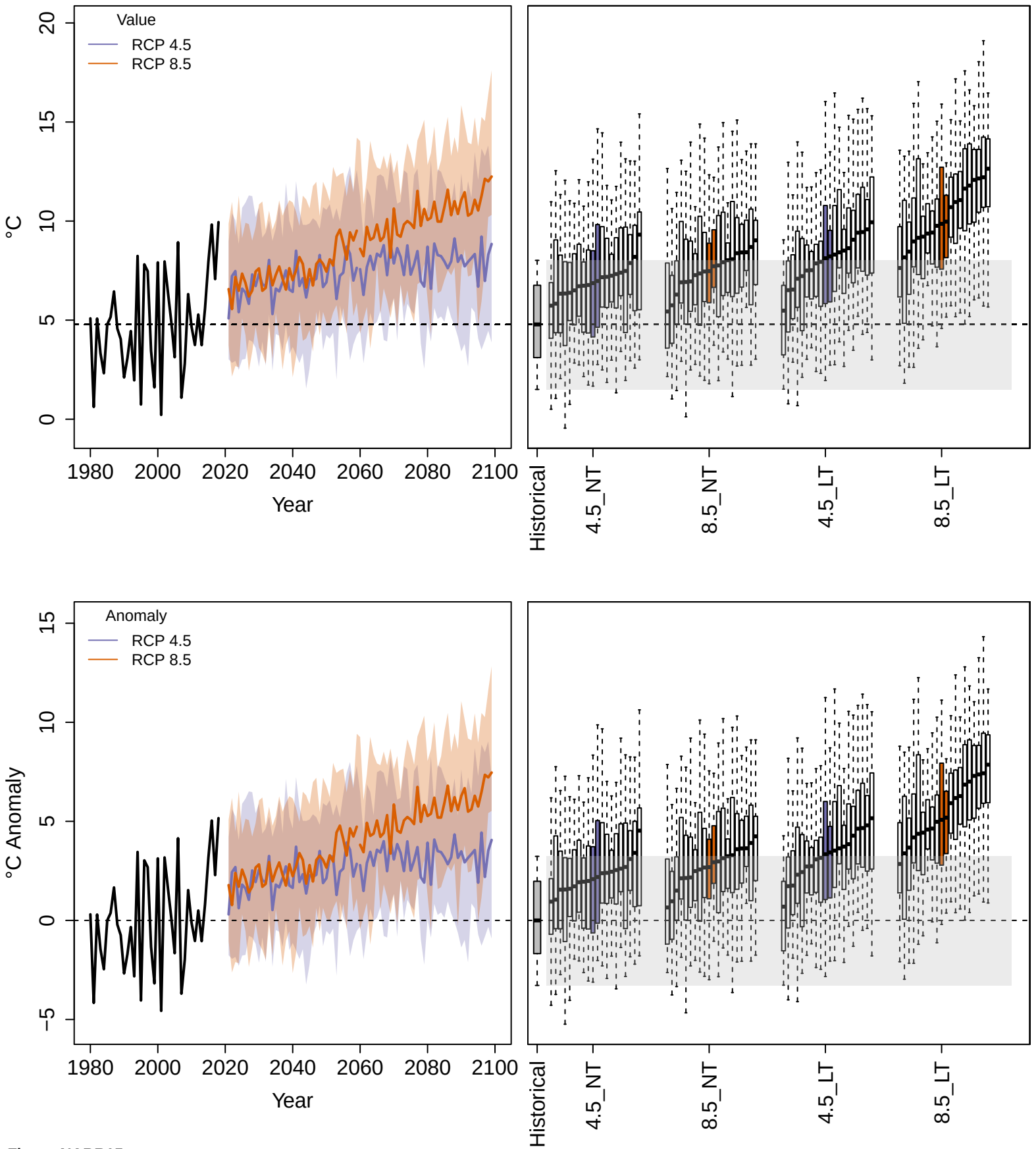


Figure NABR15:
Past trends and future trajectories of park−wide mean values for Minimum summer temperature in Natural Bridges. Top panels show values, bottom panels show changes from the long−term historical mean. Left: Time series of historical (black) and future projections for RCP 4.5 and 8.5. Shaded areas show spread among climate models. Right: Boxplots of temporal variability over 40−year periods under historical (left box) and individual climate models under two RCPs. Right: Historical time period is 1970−2010; near−term (NT) is 2020−2060; long−term (LT) is 2061−2100.

Natural Bridges: Minimum summer temperature

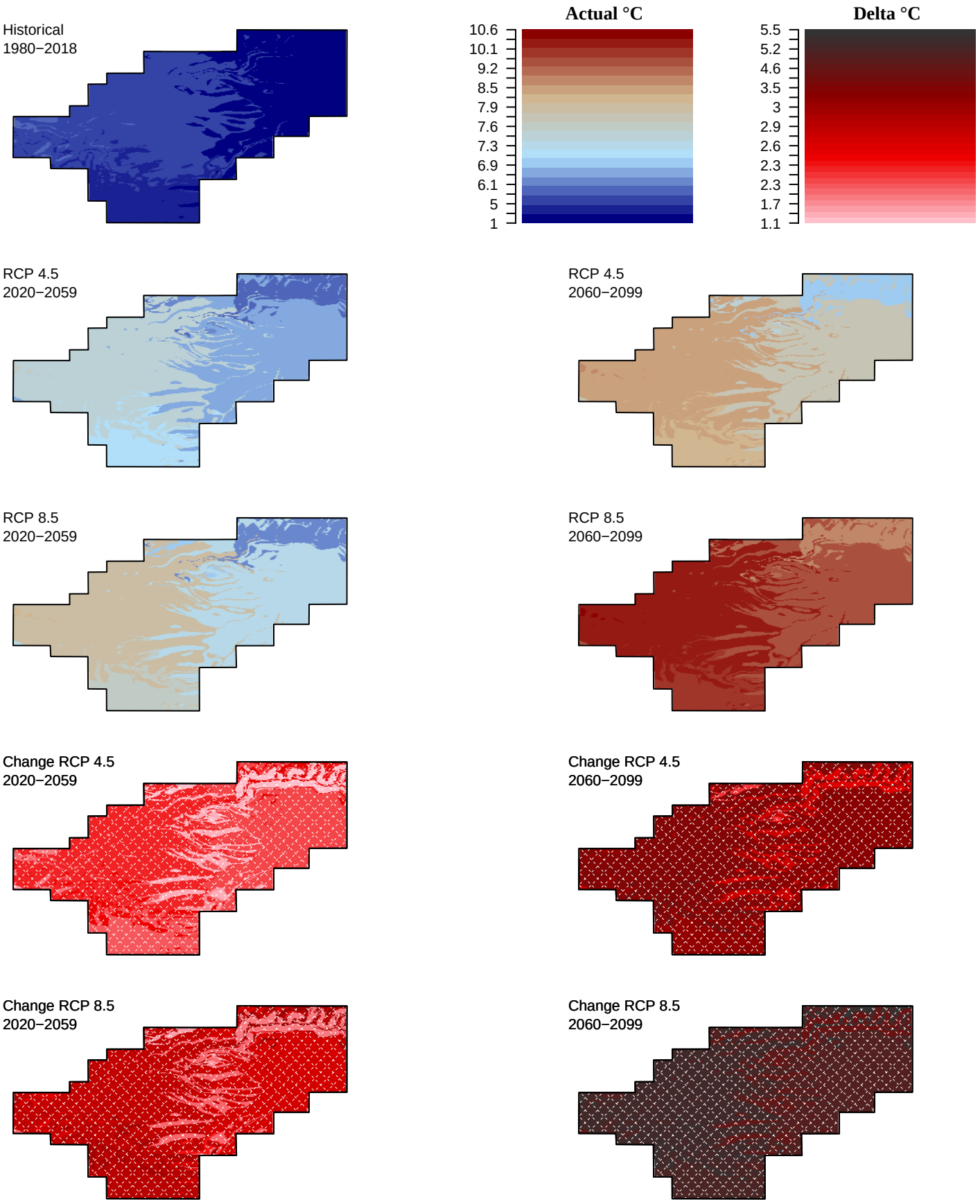


Figure NABRmap15:
Past trends and future trajectories of park−wide mean values for Minimum summer temperature in Natural Bridges. Topmost panel depicts the historical mean from 1980−2018. Lower four panels show the emission scenarios of RCP 4.5 and RCP 8.5 at near−term and long−term timeframes. Bottom four panels depict the change from the historical mean; cross hatching denotes areas of robust predicitons (90% of models agree in the direction of change).

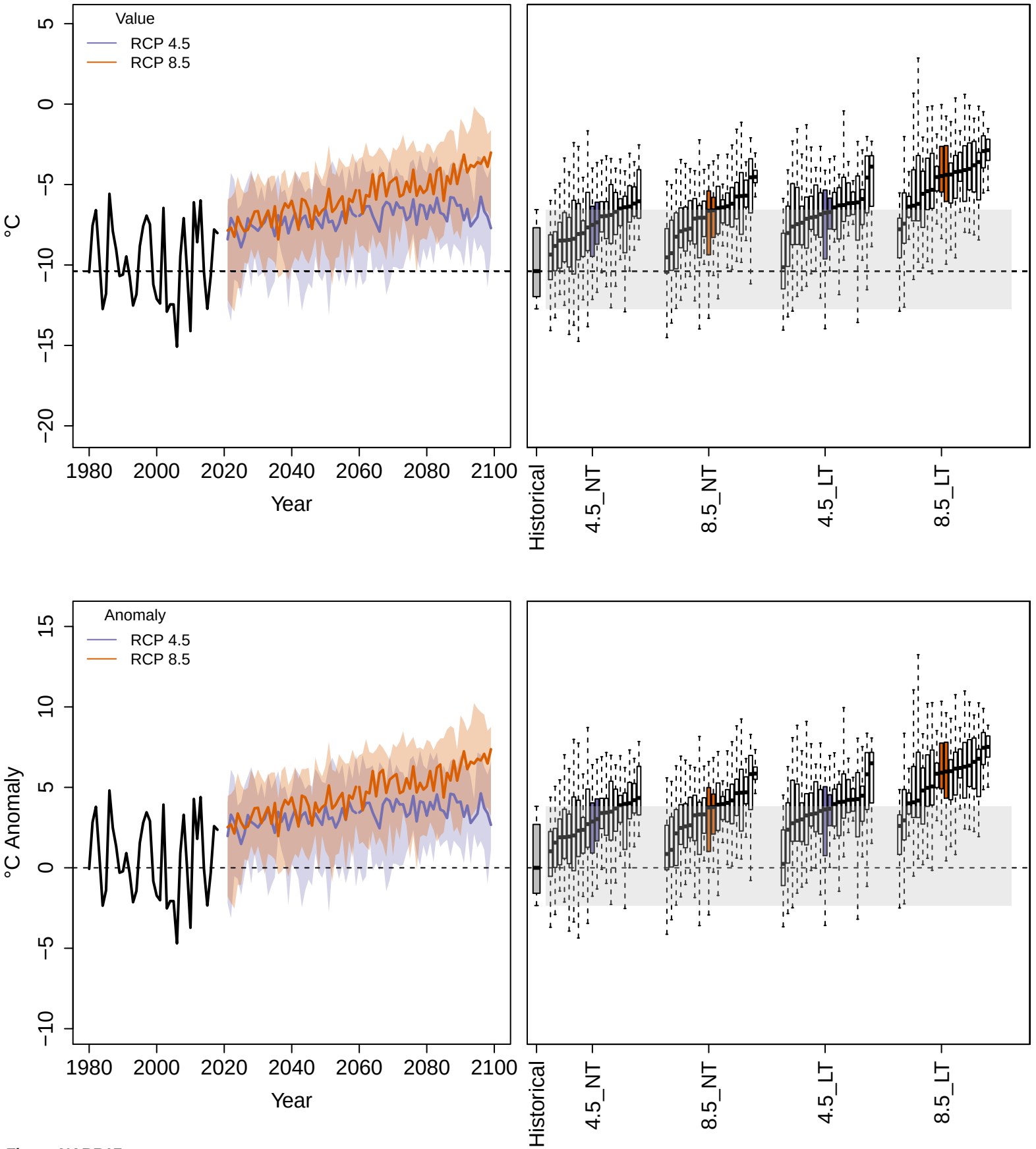


Figure NABR17:
Past trends and future trajectories of park−wide mean values for Minimum fall temperature in Natural Bridges. Top panels show values, bottom panels show changes from the long−term historical mean. Left: Time series of historical (black) and future projections for RCP 4.5 and 8.5. Shaded areas show spread among climate models. Right: Boxplots of temporal variability over 40−year periods under historical (left box) and individual climate models under two RCPs. Right: Historical time period is 1970−2010; near−term (NT) is 2020−2060; long−term (LT) is 2061−2100.

Natural Bridges: Minimum fall temperature

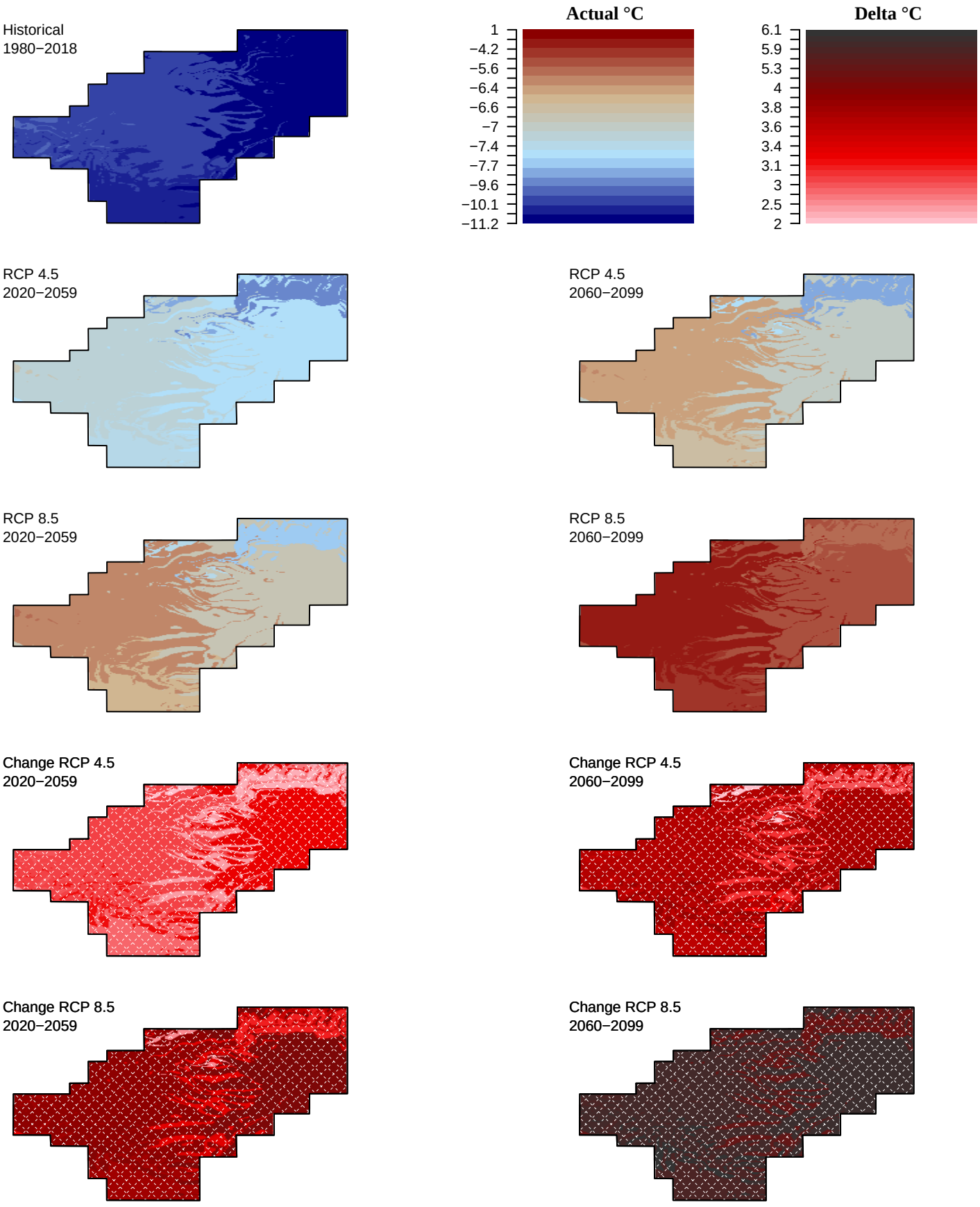


Figure NABRmap17:
Past trends and future trajectories of park−wide mean values for Minimum fall temperature in Natural Bridges. Topmost panel depicts the historical mean from 1980−2018. Lower four panels show the emission scenarios of RCP 4.5 and RCP 8.5 at near−term and long−term timeframes. Bottom four panels depict the change from the historical mean; cross hatching denotes areas of robust predicitons (90% of models agree in the direction of change).

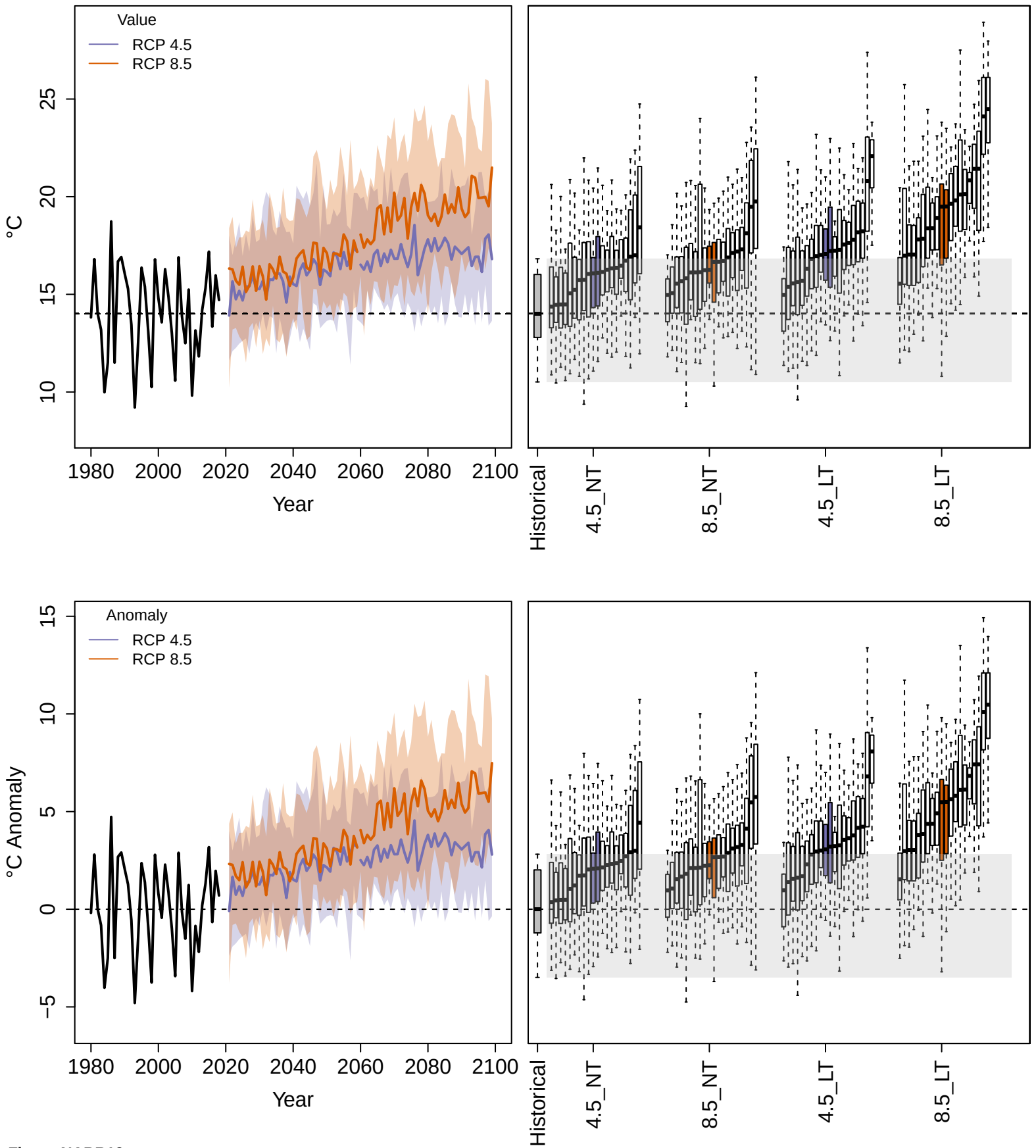


Figure NABR19:
Past trends and future trajectories of park−wide mean values for Maximum winter temperature in Natural Bridges. Top panels show values, bottom panels show changes from the long−term historical mean. Left: Time series of historical (black) and future projections for RCP 4.5 and 8.5. Shaded areas show spread among climate models. Right: Boxplots of temporal variability over 40−year periods under historical (left box) and individual climate models under two RCPs. Right: Historical time period is 1970−2010; near−term (NT) is 2020−2060; long−term (LT) is 2061−2100.

Natural Bridges: Maximum winter temperature

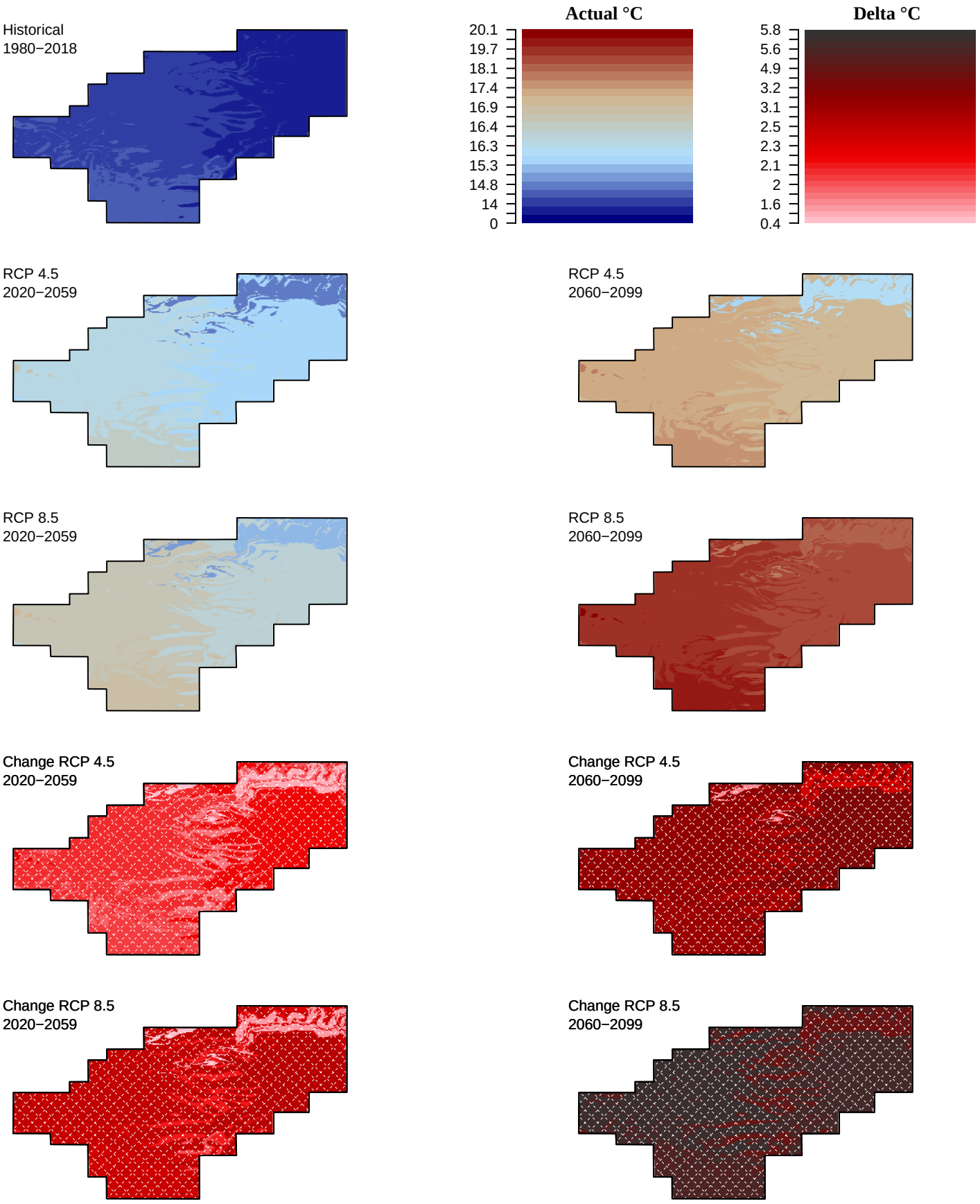


Figure NABRmap19:
Past trends and future trajectories of park−wide mean values for Maximum winter temperature in Natural Bridges. Topmost panel depicts the historical mean from 1980−2018. Lower four panels show the emission scenarios of RCP 4.5 and RCP 8.5 at near−term and long−term timeframes. Bottom four panels depict the change from the historical mean; cross hatching denotes areas of robust predicitons (90% of models agree in the direction of change).

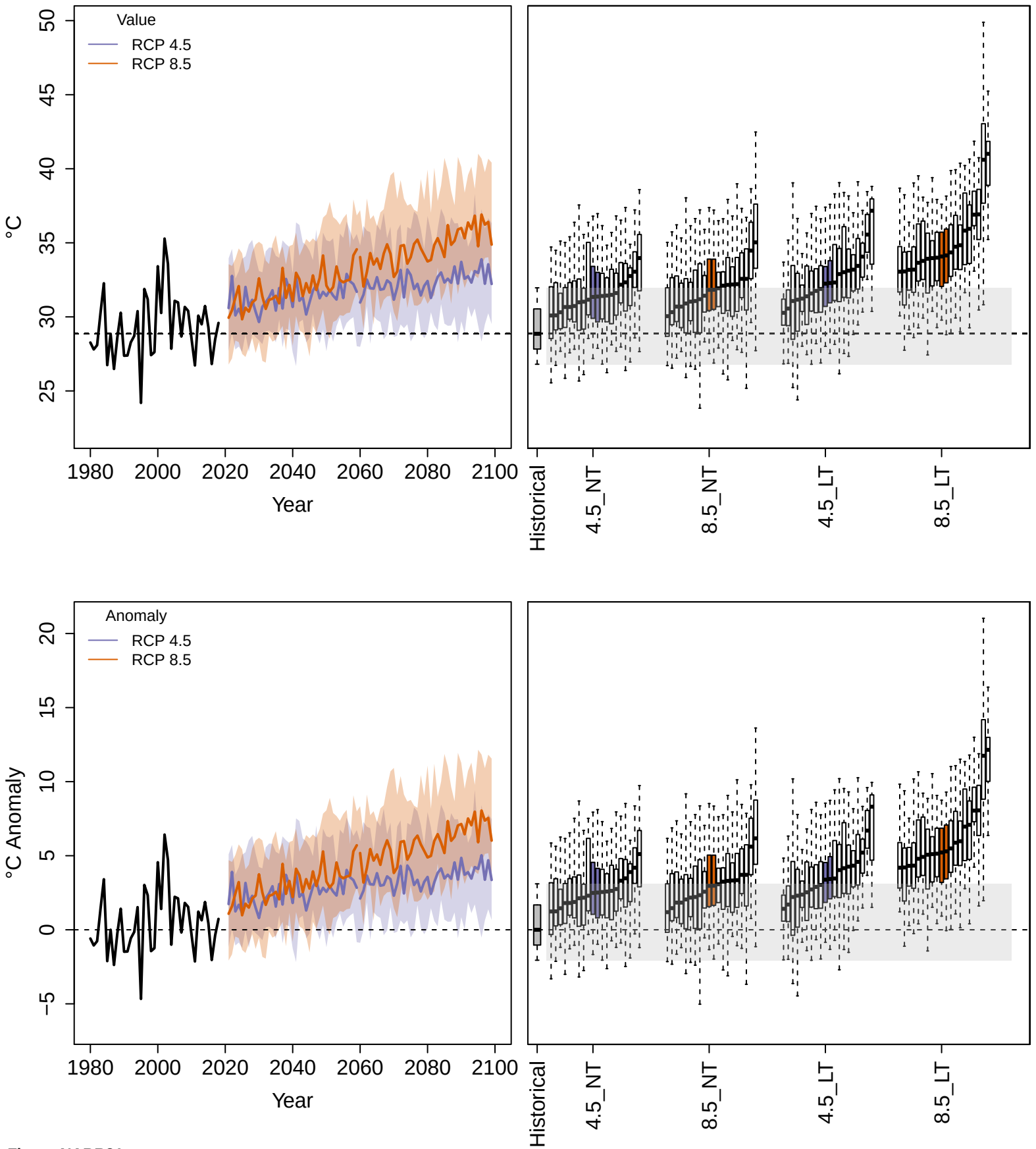


Figure NABR21:
Past trends and future trajectories of park−wide mean values for Maximum spring temperature in Natural Bridges. Top panels show values, bottom panels show changes from the long−term historical mean. Left: Time series of historical (black) and future projections for RCP 4.5 and 8.5. Shaded areas show spread among climate models. Right: Boxplots of temporal variability over 40−year periods under historical (left box) and individual climate models under two RCPs. Right: Historical time period is 1970−2010; near−term (NT) is 2020−2060; long−term (LT) is 2061−2100.

Natural Bridges: Maximum spring temperature

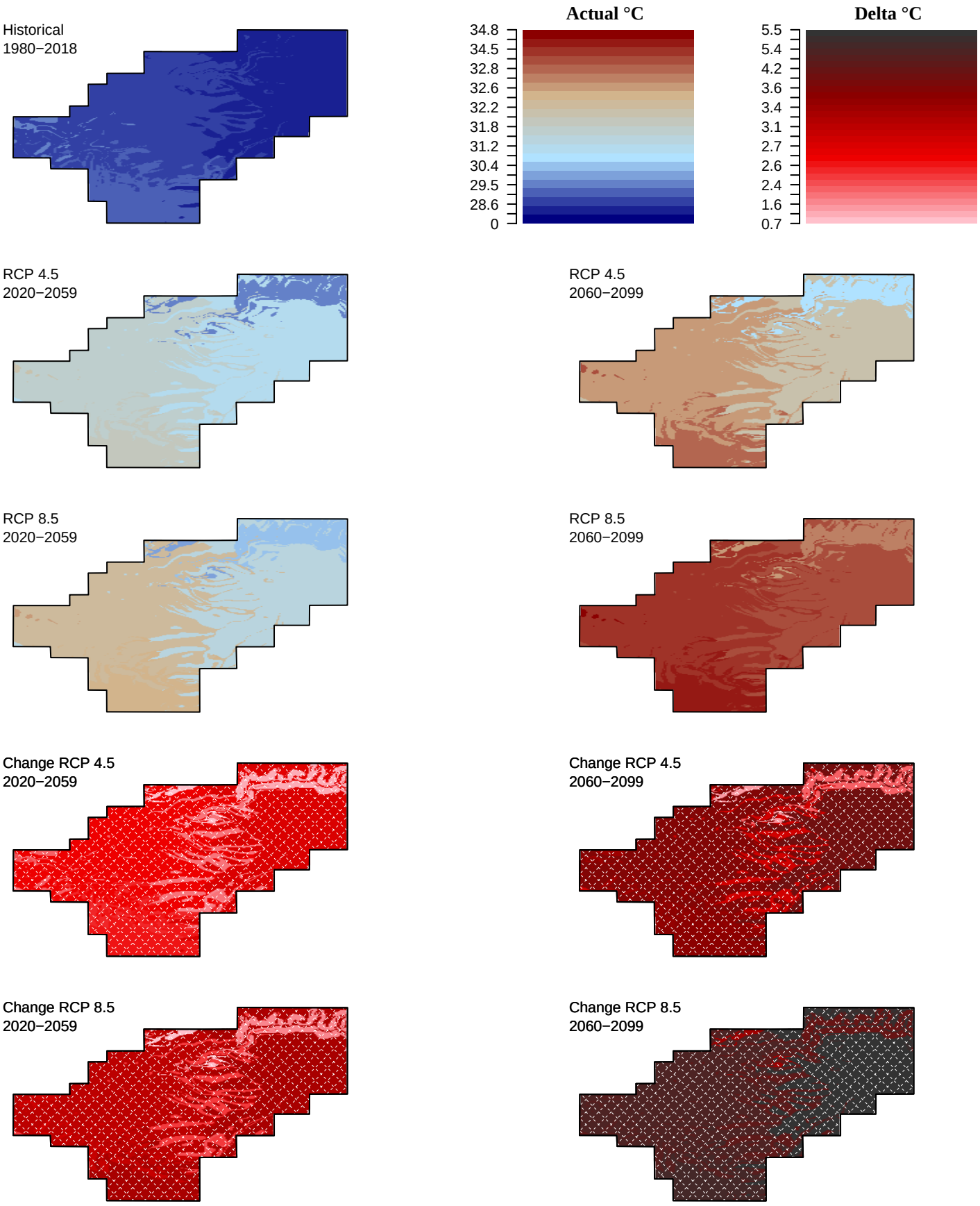


Figure NABRmap21:
Past trends and future trajectories of park−wide mean values for Maximum spring temperature in Natural Bridges. Topmost panel depicts the historical mean from 1980−2018. Lower four panels show the emission scenarios of RCP 4.5 and RCP 8.5 at near−term and long−term timeframes. Bottom four panels depict the change from the historical mean; cross hatching denotes areas of robust predicitons (90% of models agree in the direction of change).

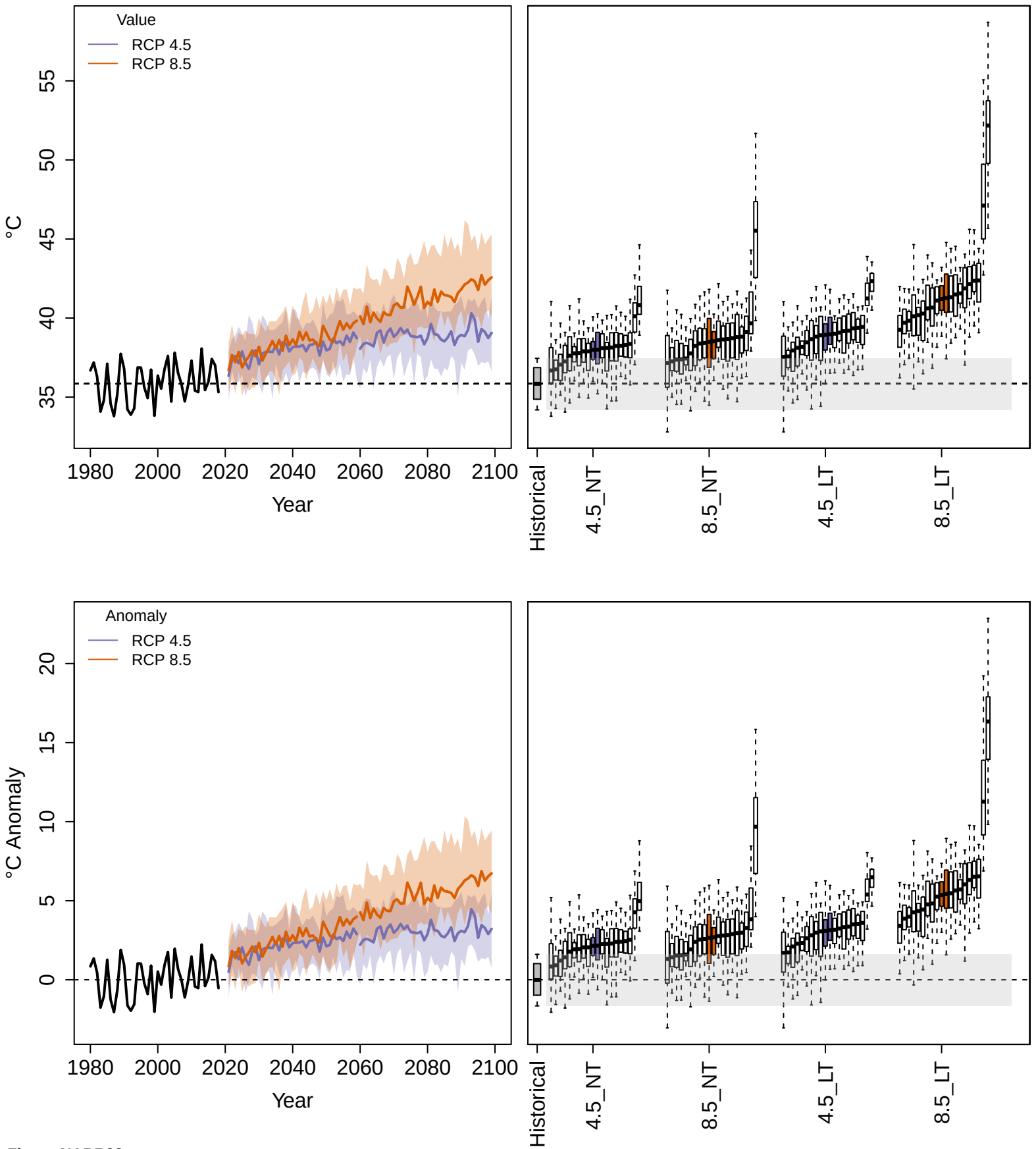


Figure NABR23:
Past trends and future trajectories of park−wide mean values for Maximum summer temperature in Natural Bridges. Top panels show values, bottom panels show changes from the long−term historical mean. Left: Time series of historical (black) and future projections for RCP 4.5 and 8.5. Shaded areas show spread among climate models. Right: Boxplots of temporal variability over 40−year periods under historical (left box) and individual climate models under two RCPs. Right: Historical time period is 1970−2010; near−term (NT) is 2020−2060; long−term (LT) is 2061−2100.

Natural Bridges: Maximum summer temperature

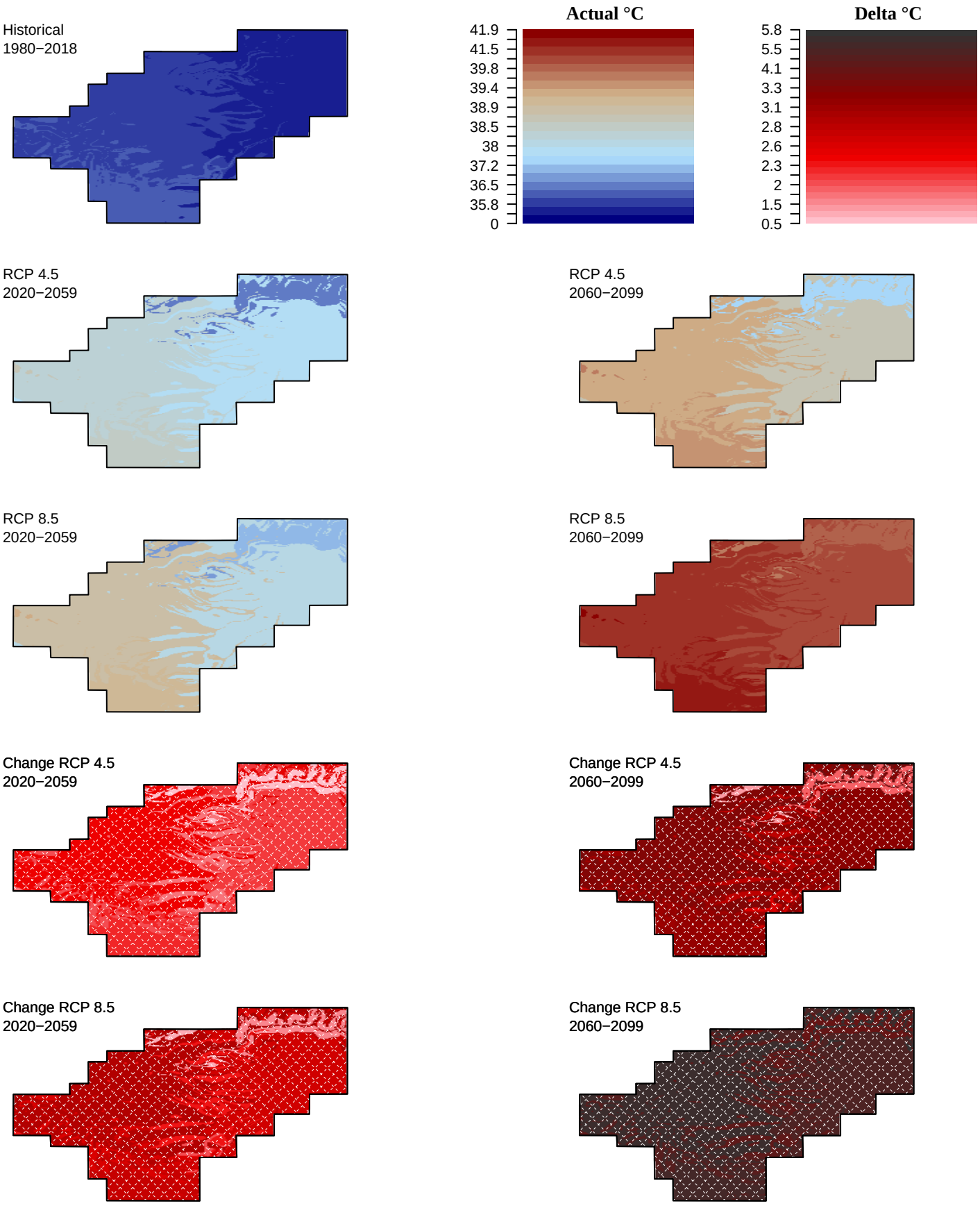


Figure NABRmap23:
Past trends and future trajectories of park−wide mean values for Maximum summer temperature in Natural Bridges. Topmost panel depicts the historical mean from 1980−2018. Lower four panels show the emission scenarios of RCP 4.5 and RCP 8.5 at near−term and long−term timeframes. Bottom four panels depict the change from the historical mean; cross hatching denotes areas of robust predicitons (90% of models agree in the direction of change).

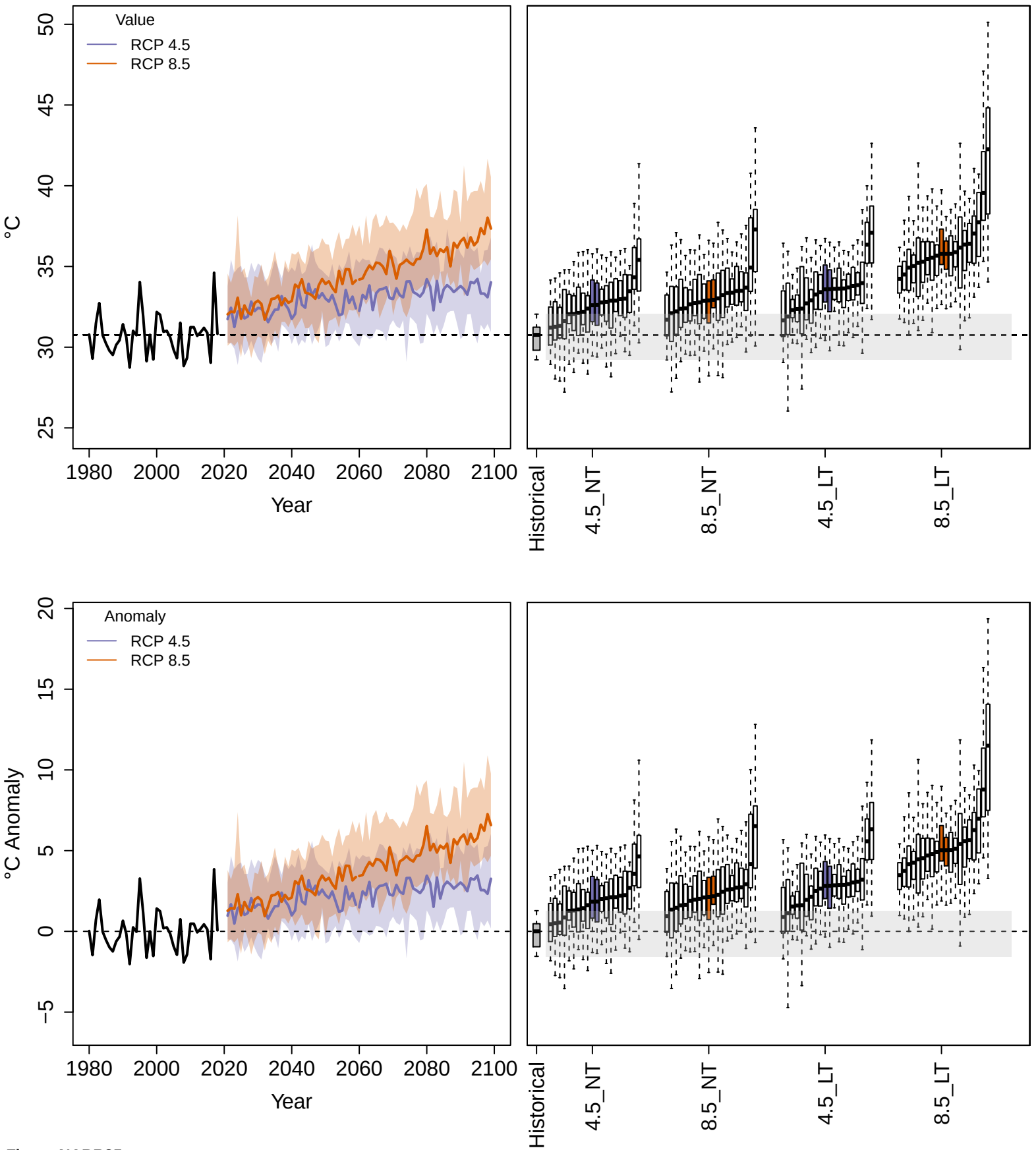


Figure NABR25:
Past trends and future trajectories of park−wide mean values for Maximum fall temperature in Natural Bridges. Top panels show values, bottom panels show changes from the long−term historical mean. Left: Time series of historical (black) and future projections for RCP 4.5 and 8.5. Shaded areas show spread among climate models. Right: Boxplots of temporal variability over 40−year periods under historical (left box) and individual climate models under two RCPs. Right: Historical time period is 1970−2010; near−term (NT) is 2020−2060; long−term (LT) is 2061−2100.

Natural Bridges: Maximum fall temperature

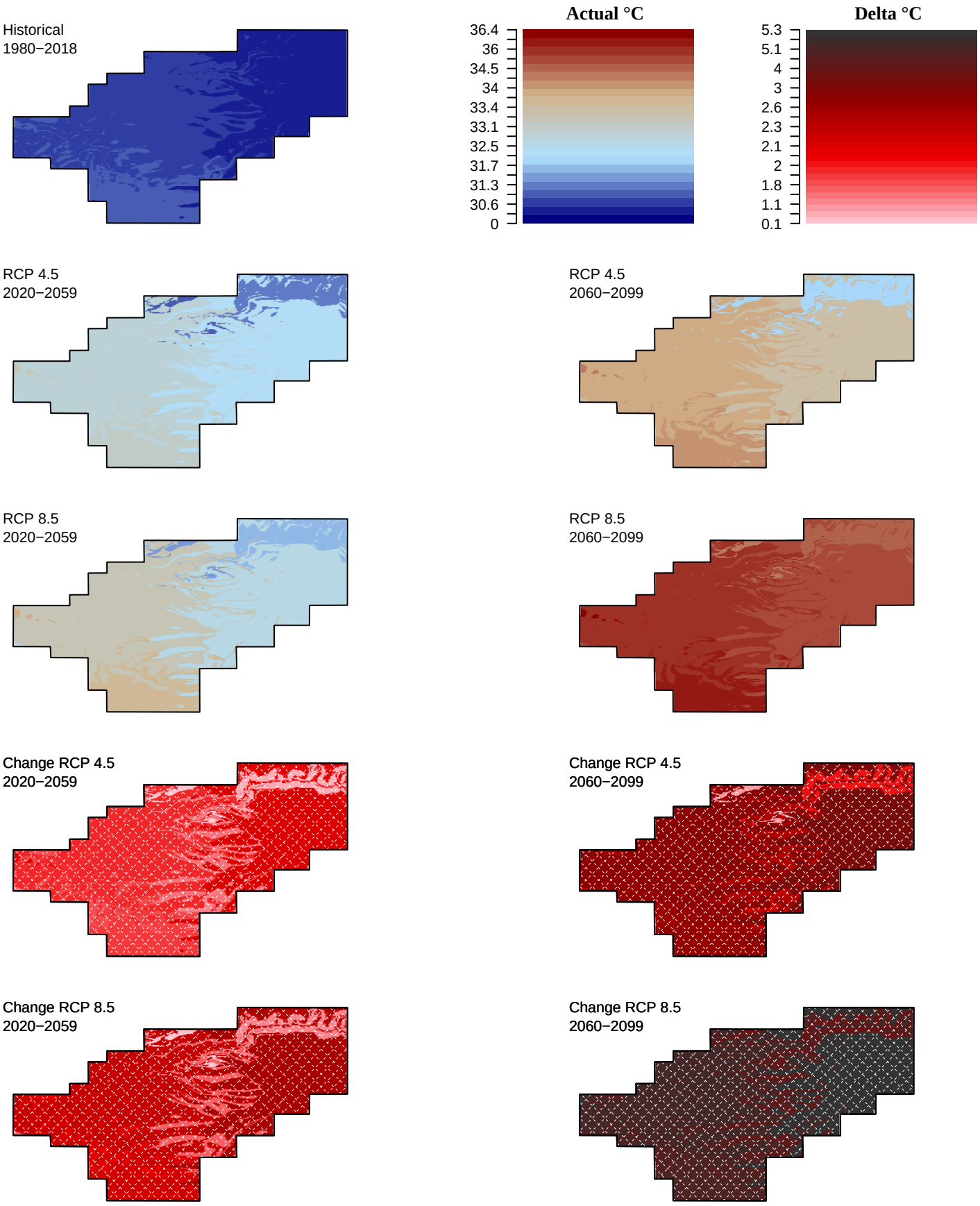


Figure NABRmap25:
Past trends and future trajectories of park−wide mean values for Maximum fall temperature in Natural Bridges. Topmost panel depicts the historical mean from 1980−2018. Lower four panels show the emission scenarios of RCP 4.5 and RCP 8.5 at near−term and long−term timeframes. Bottom four panels depict the change from the historical mean; cross hatching denotes areas of robust predicitons (90% of models agree in the direction of change).

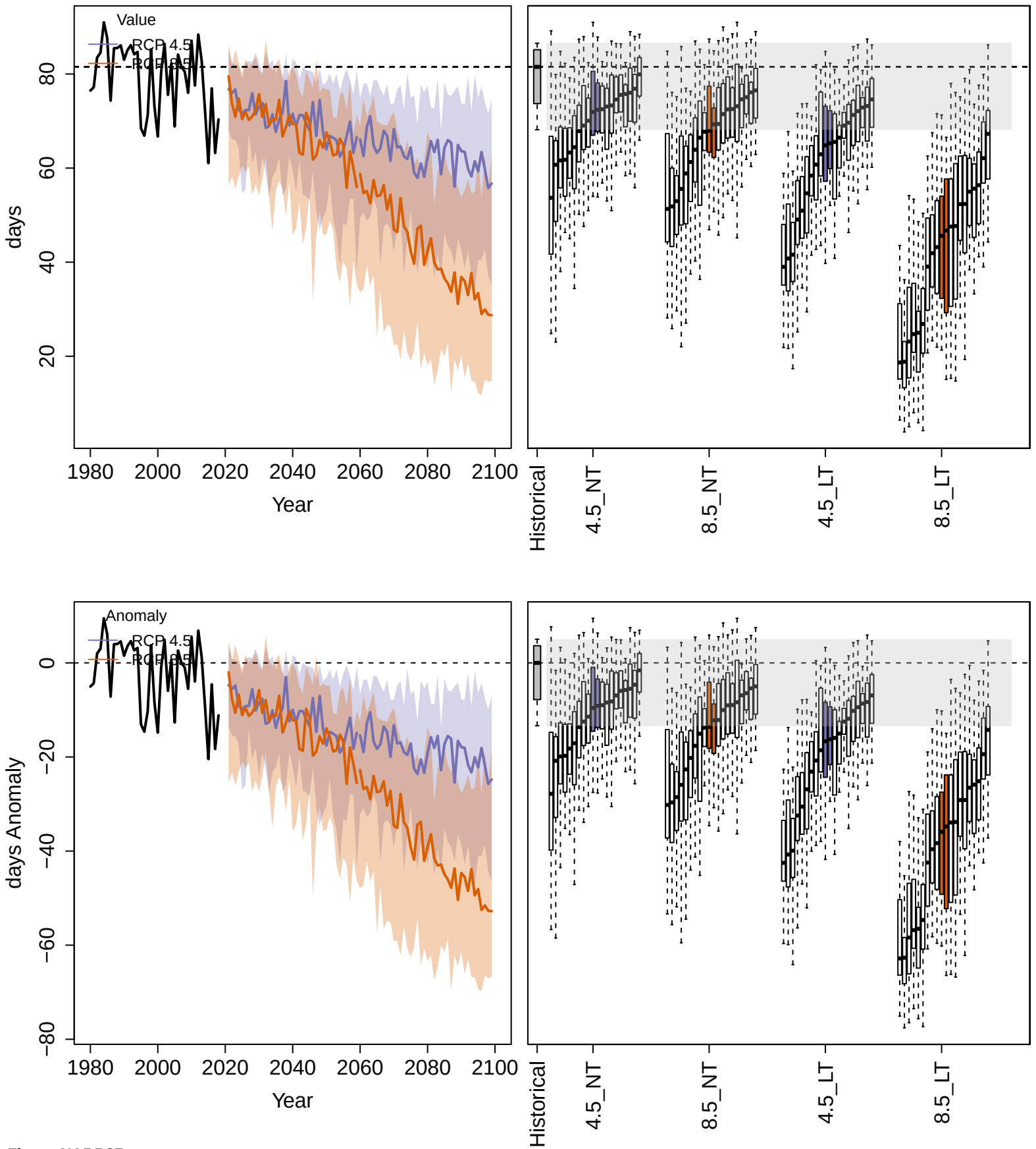


Figure NABR27:
Past trends and future trajectories of park−wide mean values for Winter frost days in Natural Bridges. Top panels show values, bottom panels show changes from the long−term historical mean. Left: Time series of historical (black) and future projections for RCP 4.5 and 8.5. Shaded areas show spread among climate models. Right: Boxplots of temporal variability over 40−year periods under historical (left box) and individual climate models under two RCPs. Right: Historical time period is 1970−2010; near−term (NT) is 2020−2060; long−term (LT) is 2061−2100.

Natural Bridges: Winter frost days

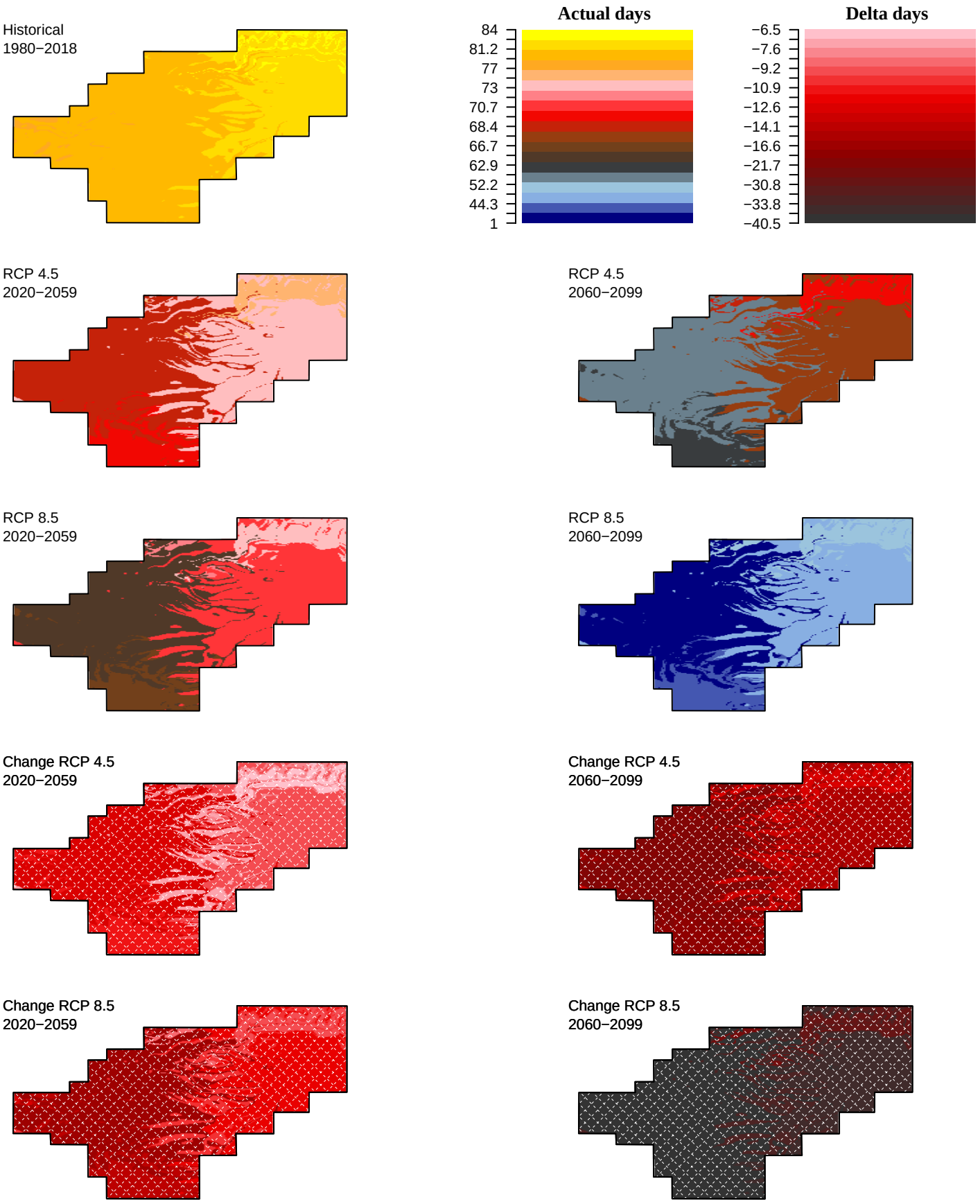


Figure NABRmap27:
Past trends and future trajectories of park−wide mean values for Winter frost days in Natural Bridges. Topmost panel depicts the historical mean from 1980−2018. Lower four panels show the emission scenarios of RCP 4.5 and RCP 8.5 at near−term and long−term timeframes. Bottom four panels depict the change from the historical mean; cross hatching denotes areas of robust predicitons (90% of models agree in the direction of change).

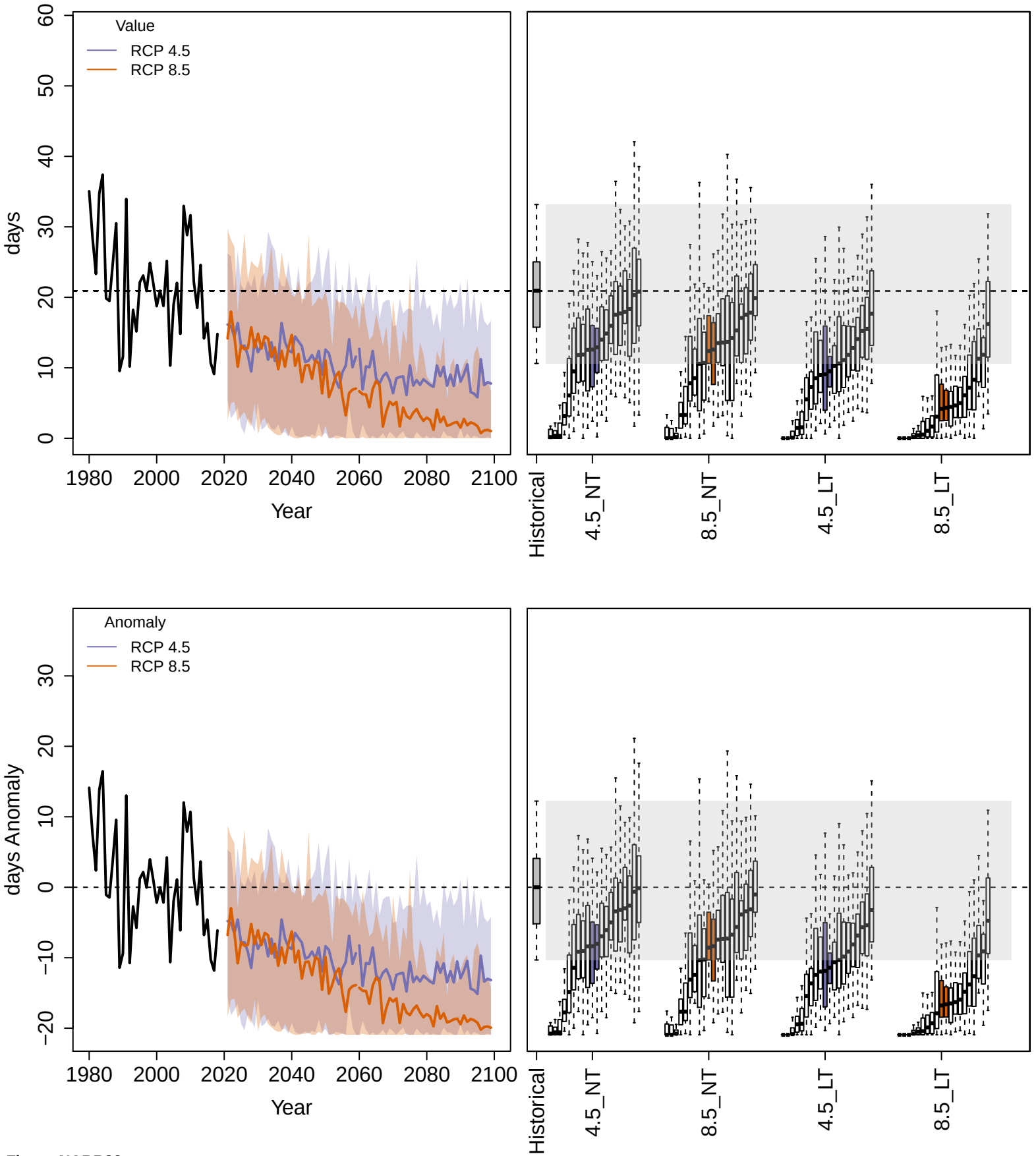


Figure NABR29:
Past trends and future trajectories of park−wide mean values for Spring frost days in Natural Bridges. Top panels show values, bottom panels show changes from the long−term historical mean. Left: Time series of historical (black) and future projections for RCP 4.5 and 8.5. Shaded areas show spread among climate models. Right: Boxplots of temporal variability over 40−year periods under historical (left box) and individual climate models under two RCPs. Right: Historical time period is 1970−2010; near−term (NT) is 2020−2060; long−term (LT) is 2061−2100.

Natural Bridges: Spring frost days

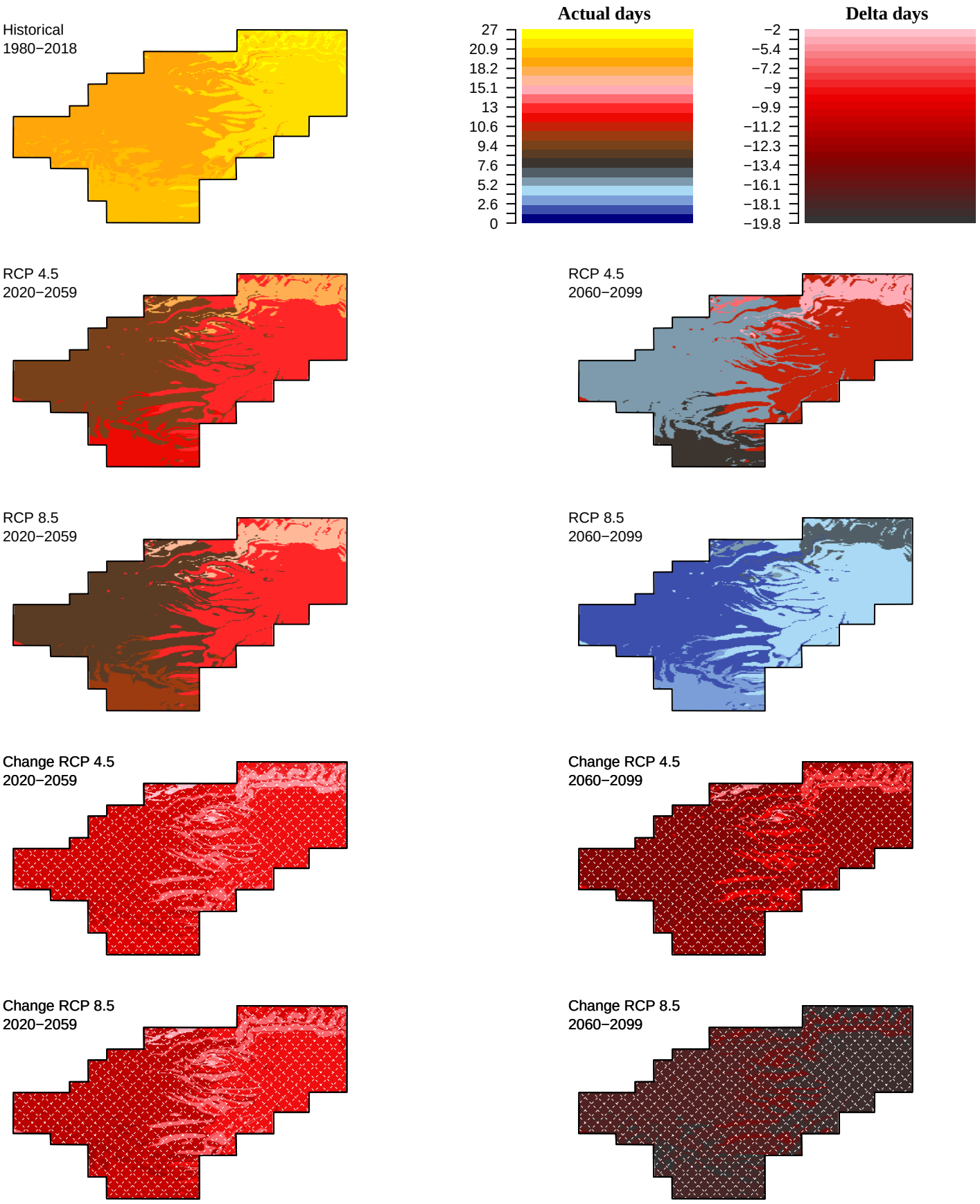


Figure NABRmap29:
Past trends and future trajectories of park−wide mean values for Spring frost days in Natural Bridges. Topmost panel depicts the historical mean from 1980−2018. Lower four panels show the emission scenarios of RCP 4.5 and RCP 8.5 at near−term and long−term timeframes. Bottom four panels depict the change from the historical mean; cross hatching denotes areas of robust predicitons (90% of models agree in the direction of change).

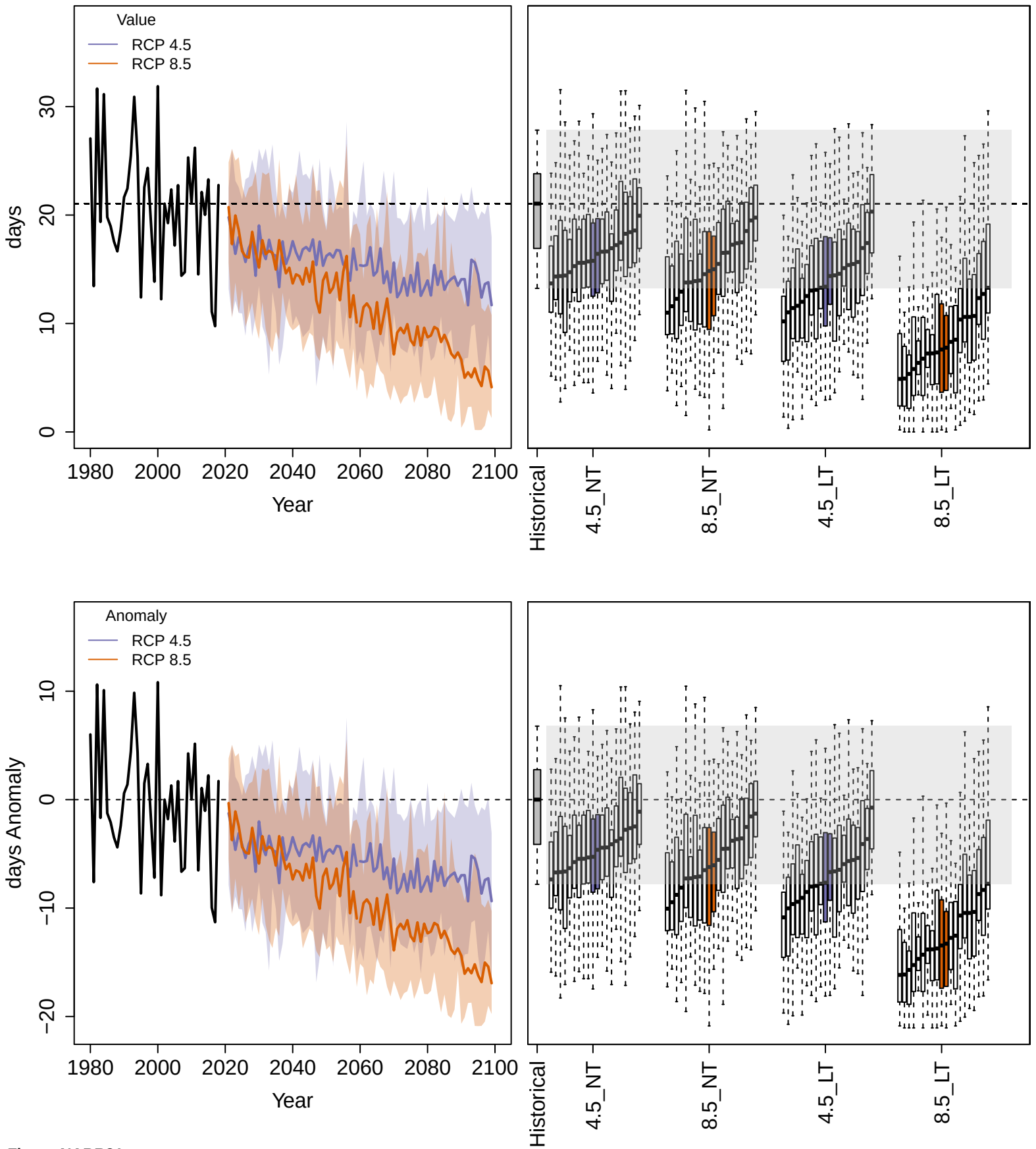


Figure NABR31:
Past trends and future trajectories of park−wide mean values for Fall frost days in Natural Bridges. Top panels show values, bottom panels show changes from the long−term historical mean. Left: Time series of historical (black) and future projections for RCP 4.5 and 8.5. Shaded areas show spread among climate models. Right: Boxplots of temporal variability over 40−year periods under historical (left box) and individual climate models under two RCPs. Right: Historical time period is 1970−2010; near−term (NT) is 2020−2060; long−term (LT) is 2061−2100.

Natural Bridges: Fall frost days

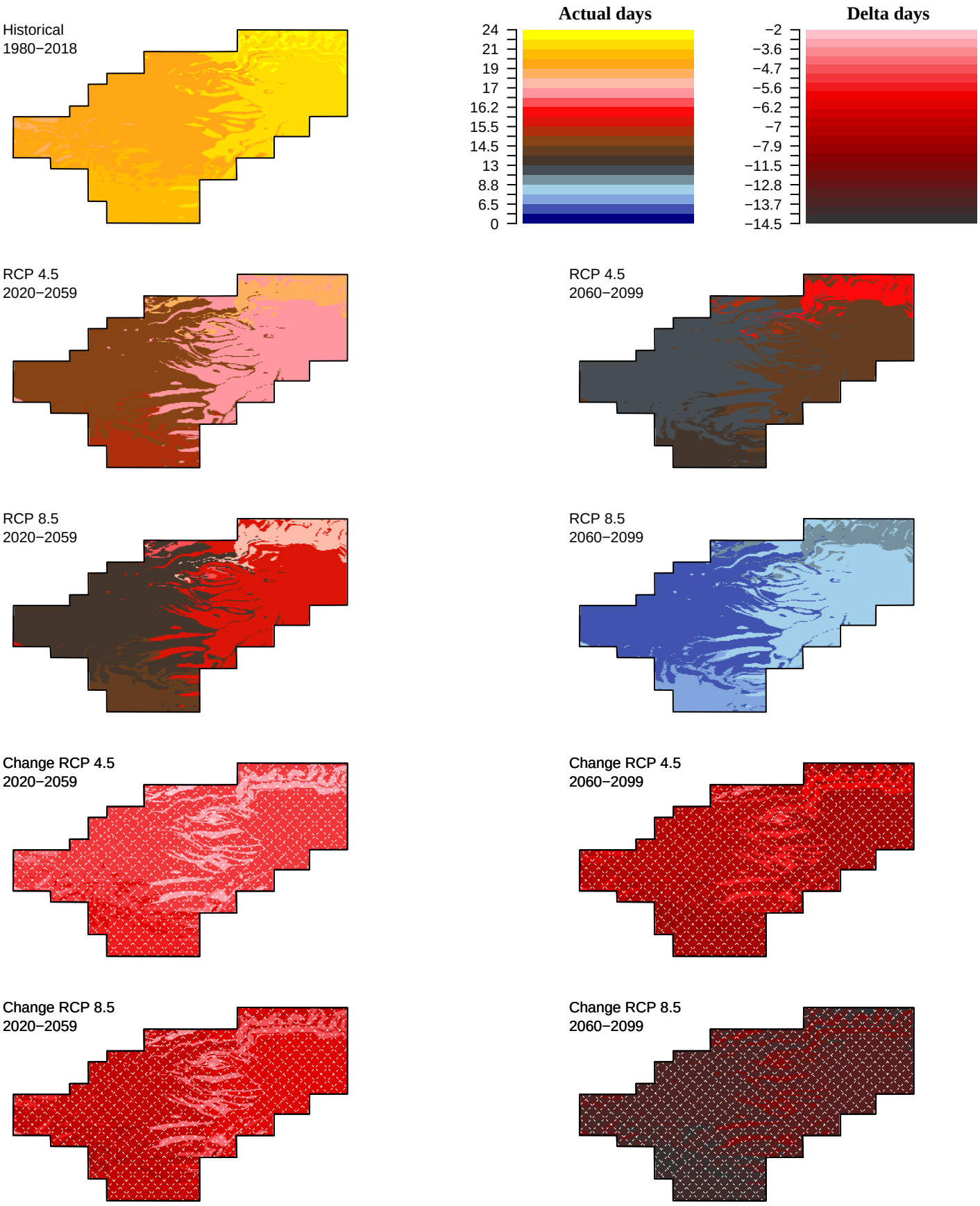


Figure NABRmap31:
Past trends and future trajectories of park−wide mean values for Fall frost days in Natural Bridges. Topmost panel depicts the historical mean from 1980−2018. Lower four panels show the emission scenarios of RCP 4.5 and RCP 8.5 at near−term and long−term timeframes. Bottom four panels depict the change from the historical mean; cross hatching denotes areas of robust predicitons (90% of models agree in the direction of change).

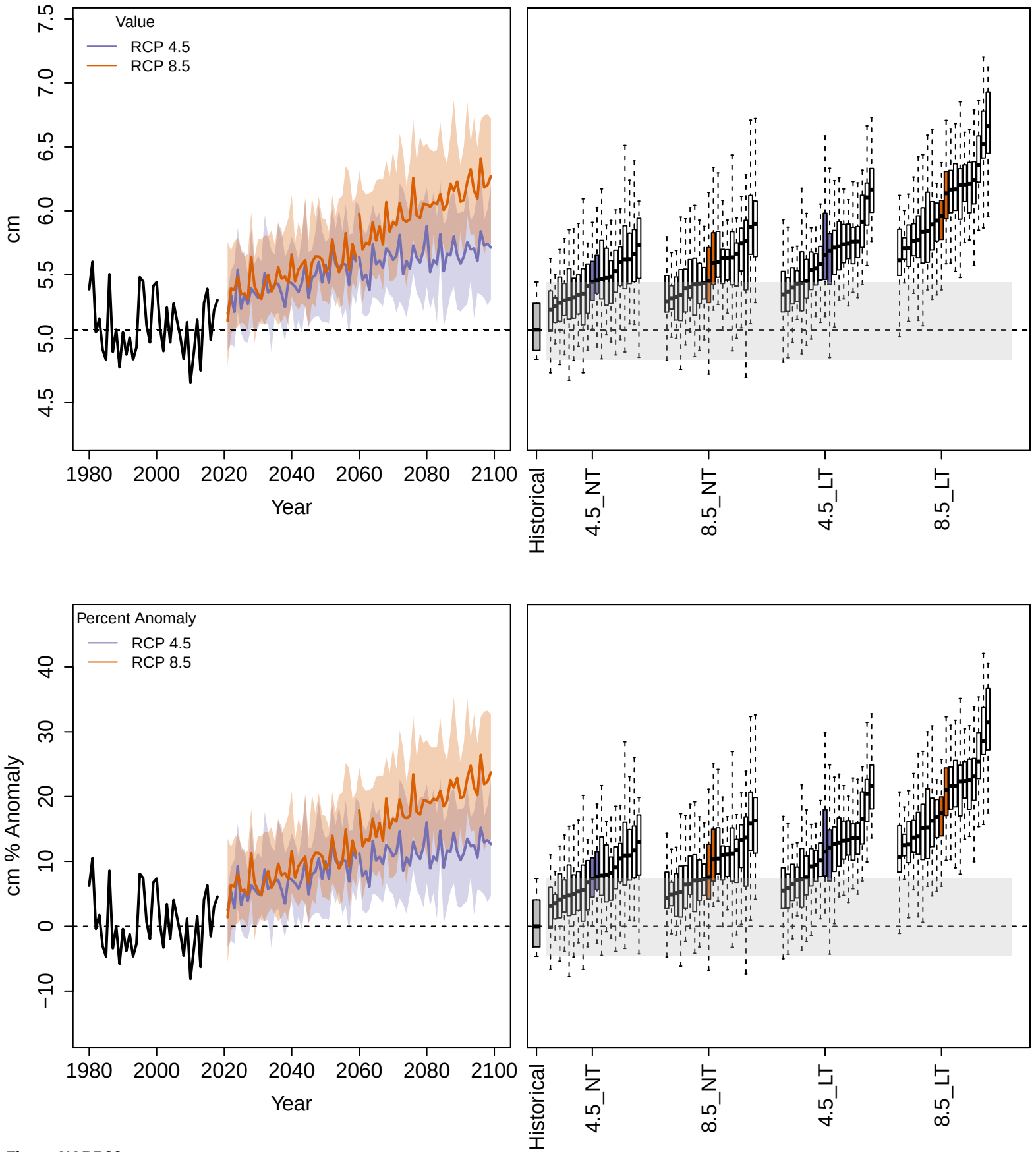


Figure NABR33:
Past trends and future trajectories of park−wide mean values for Winter potential evapotranspiration in Natural Bridges. Top panels show values, bottom panels show changes from the long−term historical mean. Left: Time series of historical (black) and future projections for RCP 4.5 and 8.5. Shaded areas show spread among climate models. Right: Boxplots of temporal variability over 40−year periods under historical (left box) and individual climate models under two RCPs. Right: Historical time period is 1970−2010; near−term (NT) is 2020−2060; long−term (LT) is 2061−2100.

Natural Bridges: Winter potential evapotranspiration

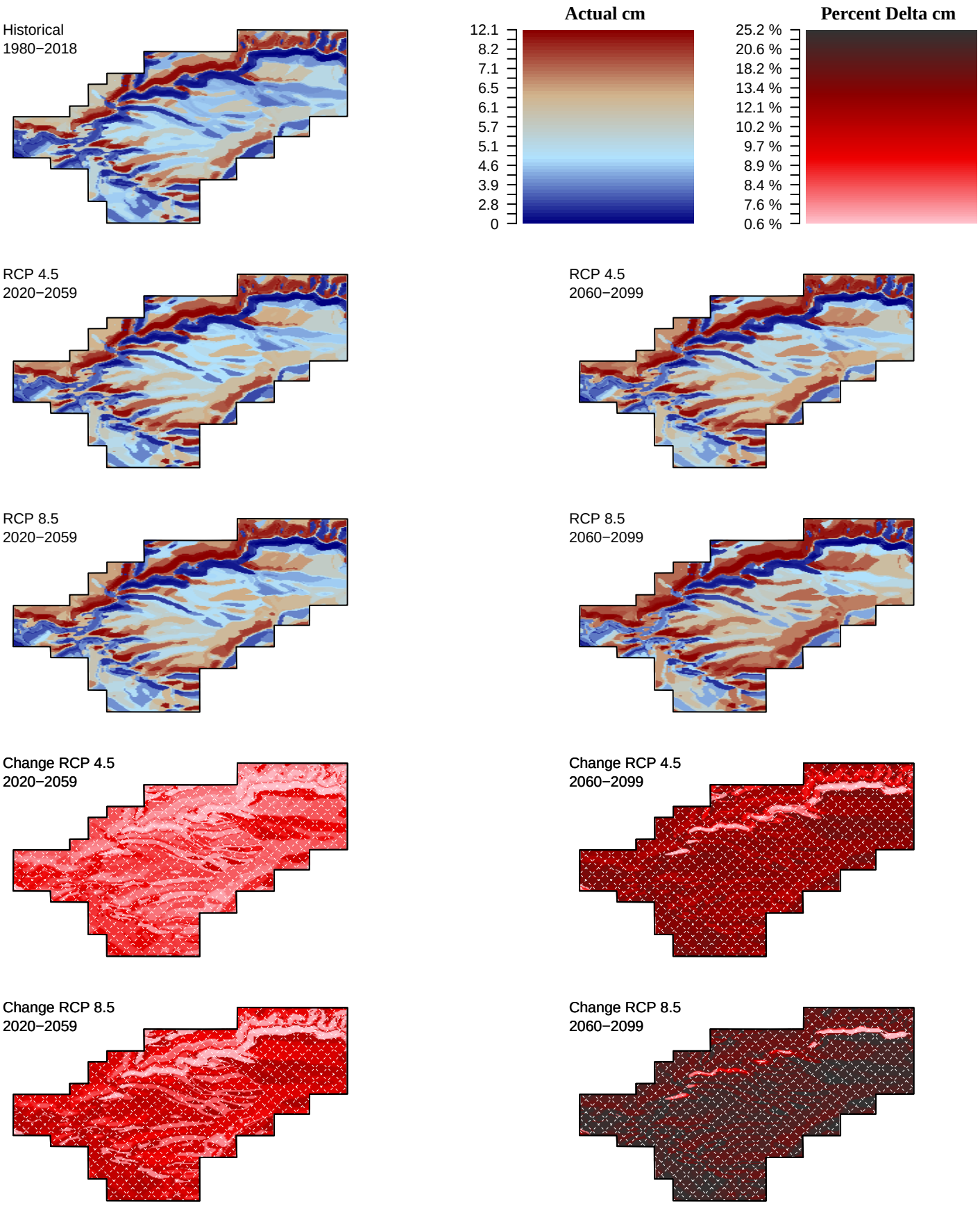


Figure NABRmap33:
Past trends and future trajectories of park−wide mean values for Winter potential evapotranspiration in Natural Bridges. Topmost panel depicts the historical mean from 1980−2018. Lower four panels show the emission scenarios of RCP 4.5 and RCP 8.5 at near−term and long−term timeframes. Bottom four panels depict the change from the historical mean; cross hatching denotes areas of robust predicitons (90% of models agree in the direction of change).

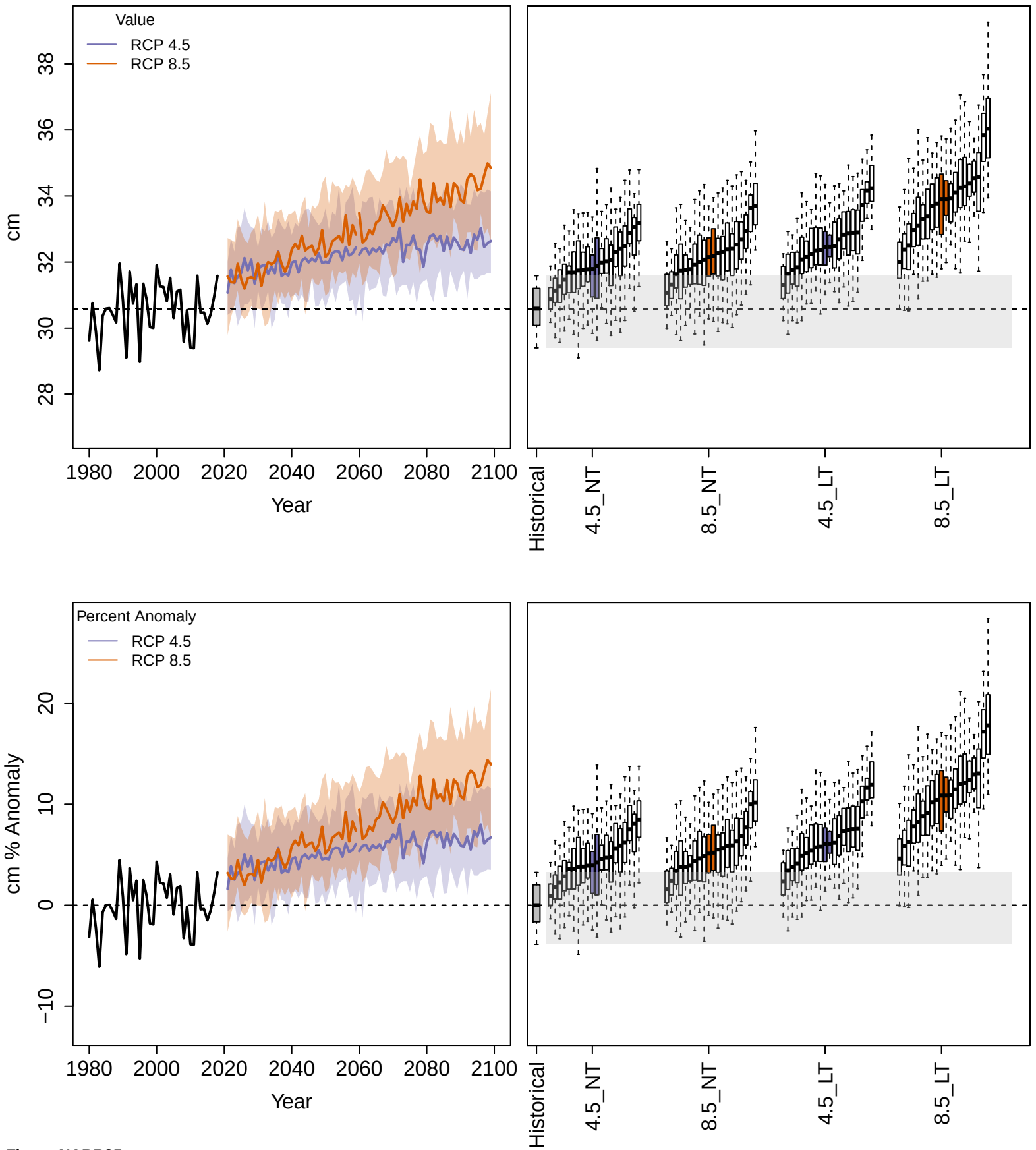


Figure NABR35:
Past trends and future trajectories of park−wide mean values for Spring potential evapotranspiration in Natural Bridges. Top panels show values, bottom panels show changes from the long−term historical mean. Left: Time series of historical (black) and future projections for RCP 4.5 and 8.5. Shaded areas show spread among climate models. Right: Boxplots of temporal variability over 40−year periods under historical (left box) and individual climate models under two RCPs. Right: Historical time period is 1970−2010; near−term (NT) is 2020−2060; long−term (LT) is 2061−2100.

Natural Bridges: Spring potential evapotranspiration

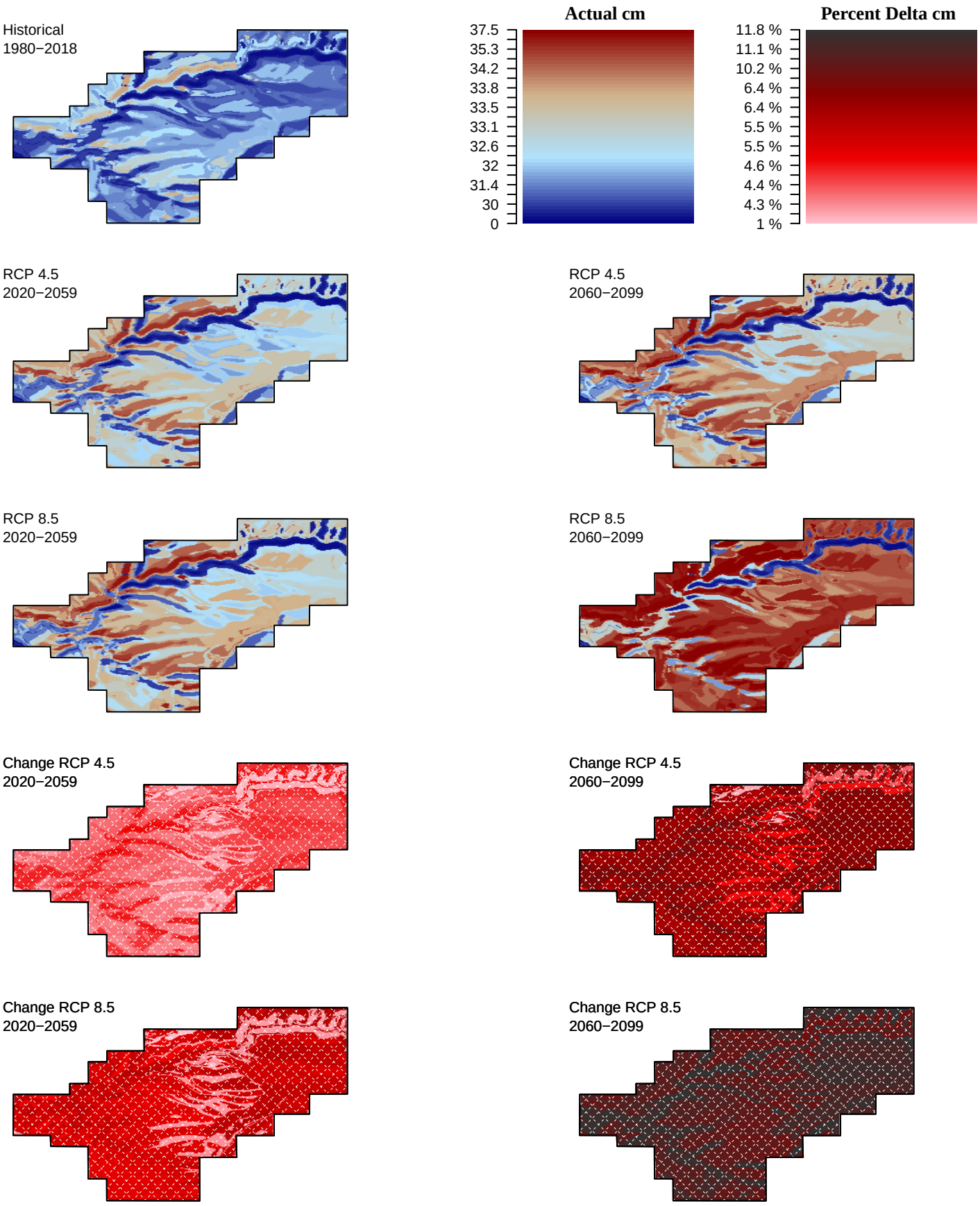


Figure NABRmap35:
Past trends and future trajectories of park−wide mean values for Spring potential evapotranspiration in Natural Bridges. Topmost panel depicts the historical mean from 1980−2018. Lower four panels show the emission scenarios of RCP 4.5 and RCP 8.5 at near−term and long−term timeframes. Bottom four panels depict the change from the historical mean; cross hatching denotes areas of robust predicitons (90% of models agree in the direction of change).

Natural Bridges: Summer potential evapotranspiration

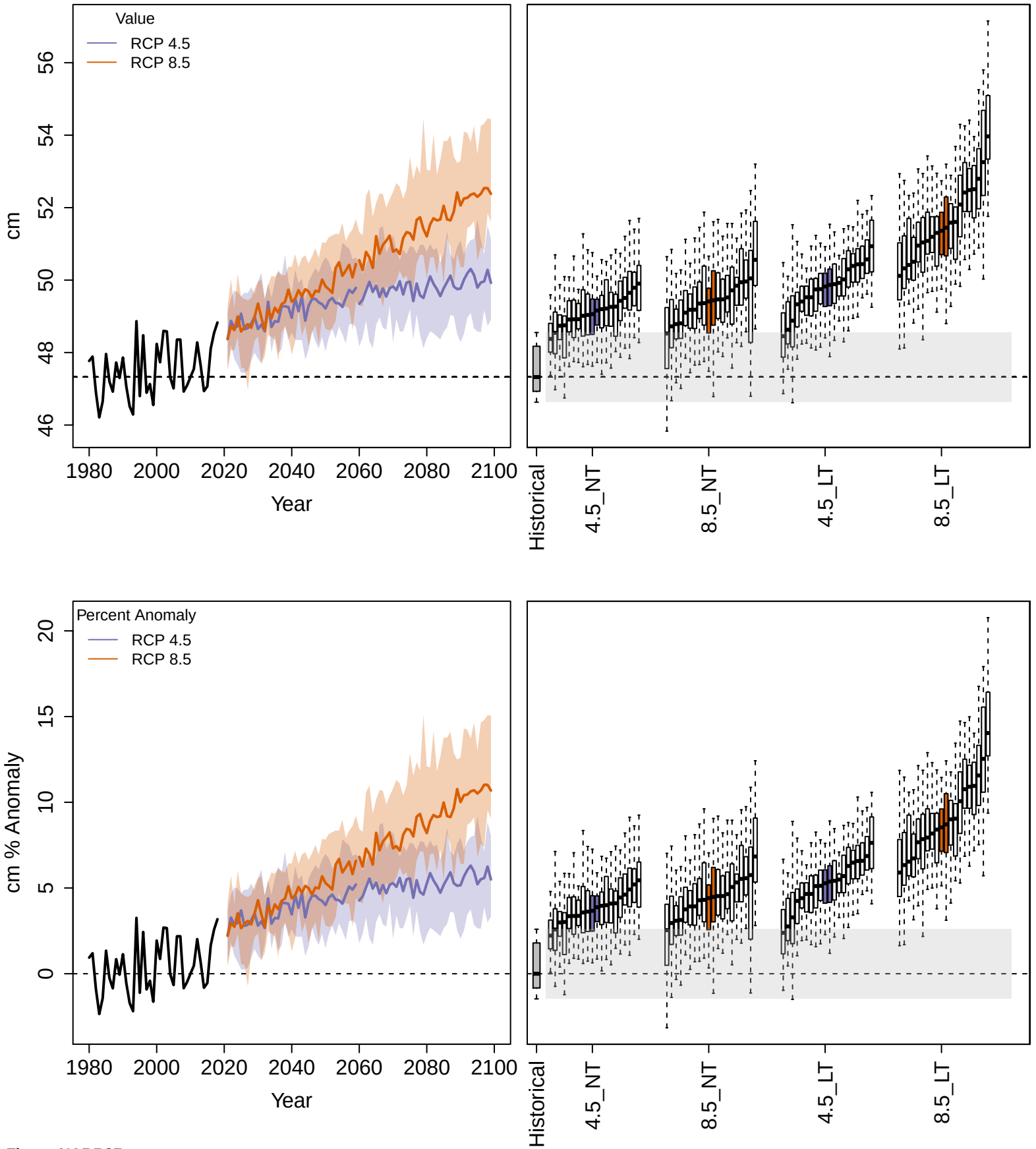


Figure NABR37:
Past trends and future trajectories of park−wide mean values for Summer potential evapotranspiration in Natural Bridges. Top panels show values, bottom panels show changes from the long−term historical mean. Left: Time series of historical (black) and future projections for RCP 4.5 and 8.5. Shaded areas show spread among climate models. Right: Boxplots of temporal variability over 40−year periods under historical (left box) and individual climate models under two RCPs. Right: Historical time period is 1970−2010; near−term (NT) is 2020−2060; long−term (LT) is 2061−2100.

Natural Bridges: Summer potential evapotranspiration

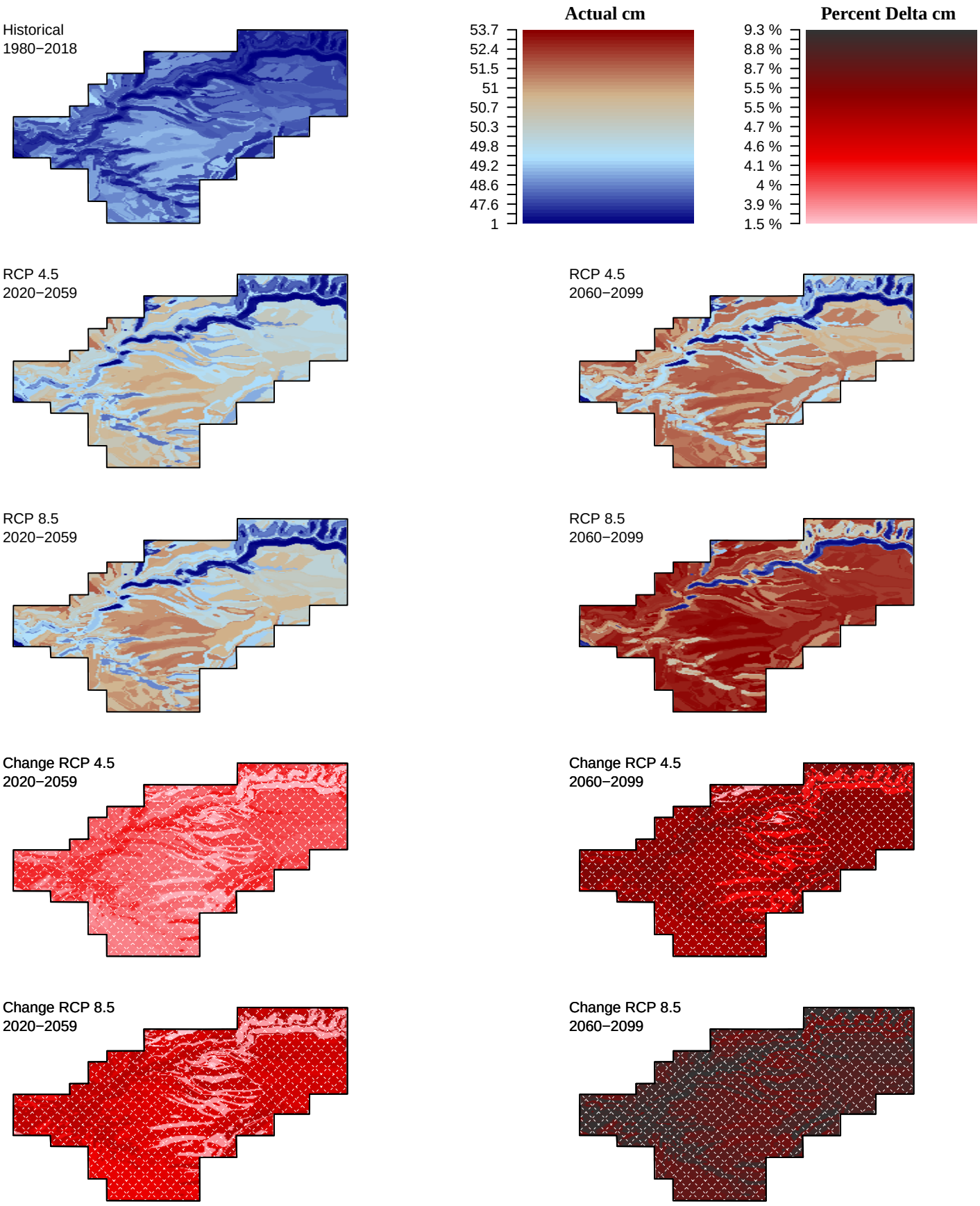


Figure NABRmap37:
Past trends and future trajectories of park−wide mean values for Summer potential evapotranspiration in Natural Bridges. Topmost panel depicts the historical mean from 1980−2018. Lower four panels show the emission scenarios of RCP 4.5 and RCP 8.5 at near−term and long−term timeframes. Bottom four panels depict the change from the historical mean; cross hatching denotes areas of robust predicitons (90% of models agree in the direction of change).

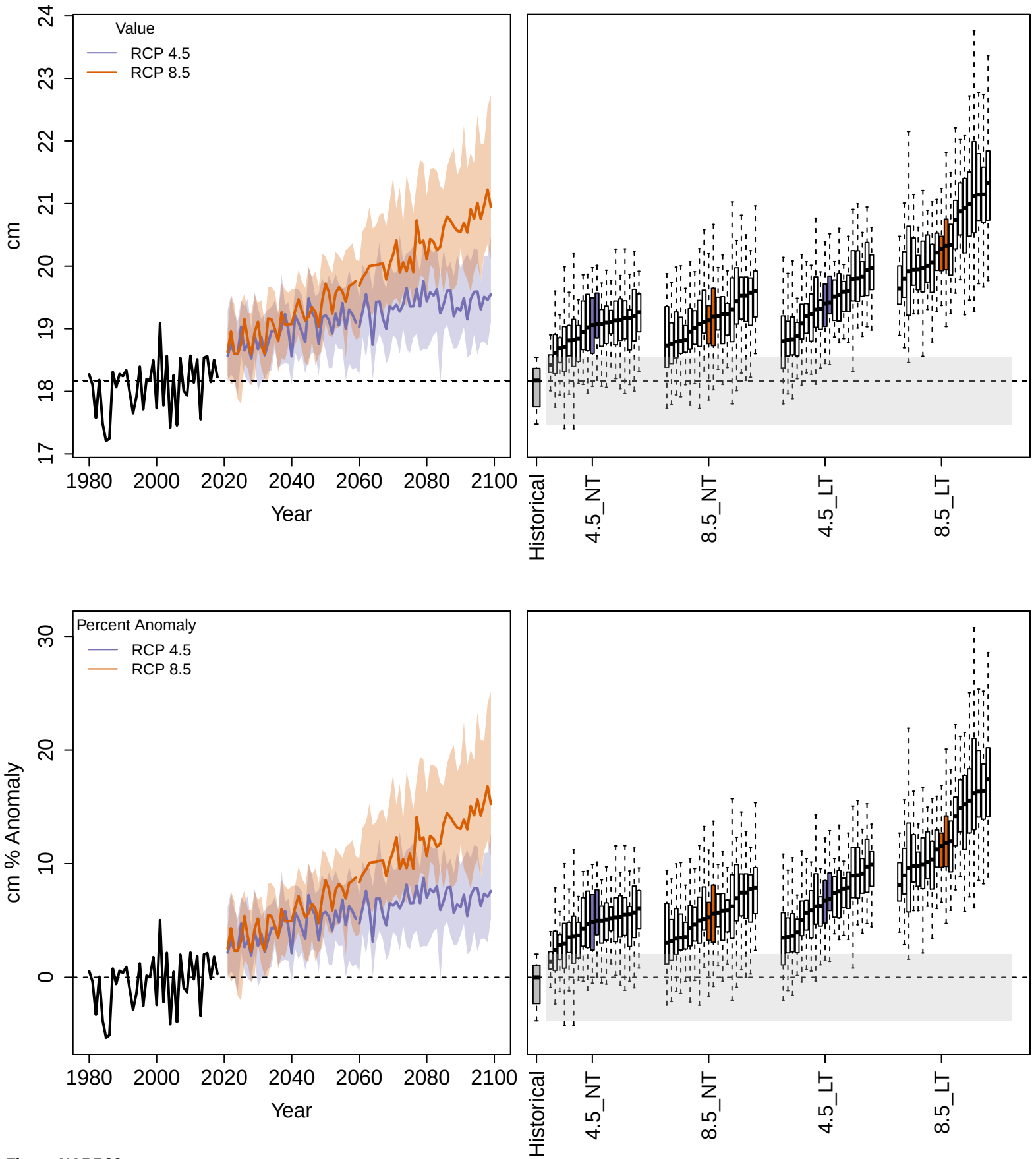


Figure NABR39:
Past trends and future trajectories of park−wide mean values for Fall potential evapotranspiration in Natural Bridges. Top panels show values, bottom panels show changes from the long−term historical mean. Left: Time series of historical (black) and future projections for RCP 4.5 and 8.5. Shaded areas show spread among climate models. Right: Boxplots of temporal variability over 40−year periods under historical (left box) and individual climate models under two RCPs. Right: Historical time period is 1970−2010; near−term (NT) is 2020−2060; long−term (LT) is 2061−2100.

Natural Bridges: Fall potential evapotranspiration

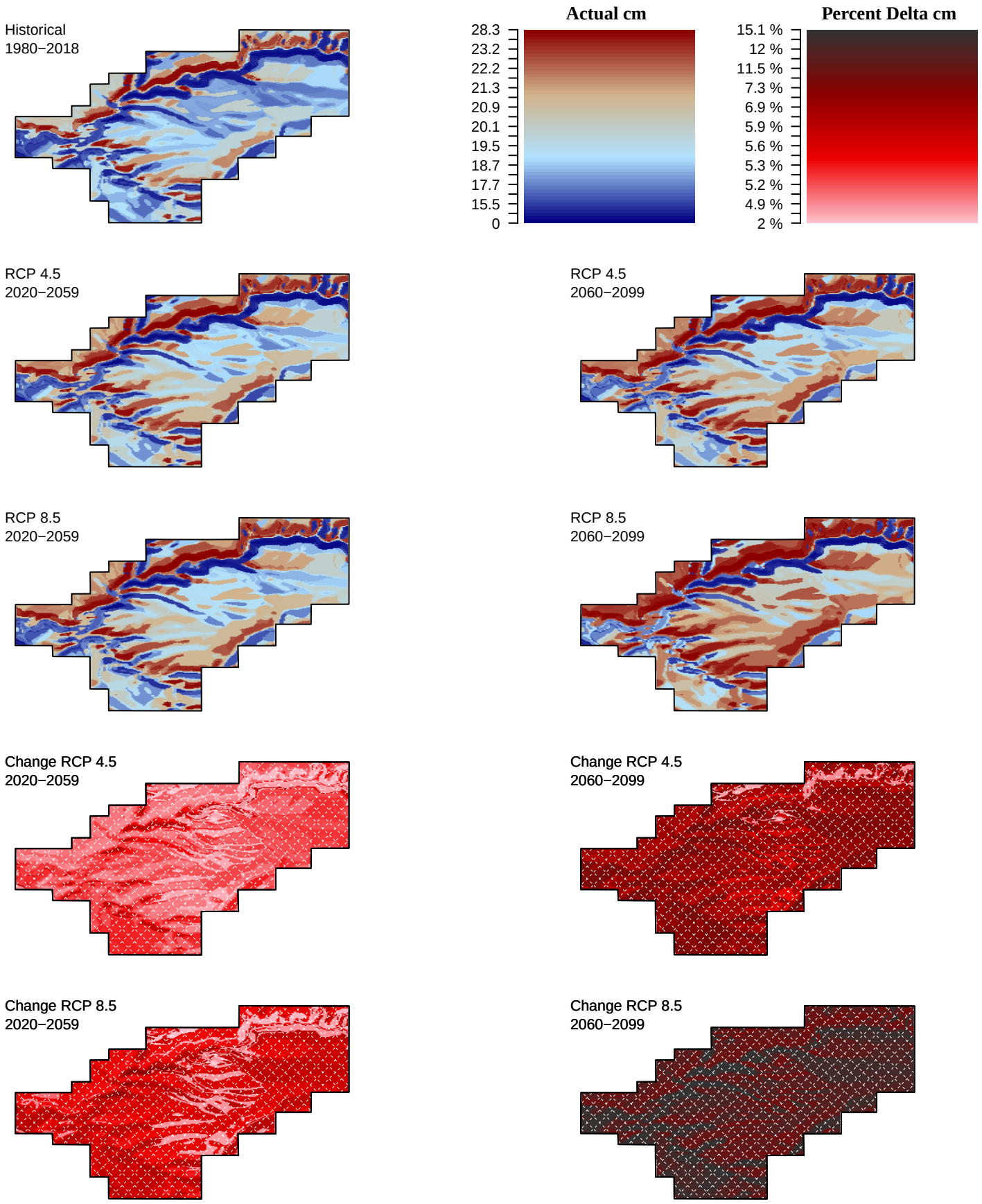


Figure NABRmap39:
Past trends and future trajectories of park−wide mean values for Fall potential evapotranspiration in Natural Bridges. Topmost panel depicts the historical mean from 1980−2018. Lower four panels show the emission scenarios of RCP 4.5 and RCP 8.5 at near−term and long−term timeframes. Bottom four panels depict the change from the historical mean; cross hatching denotes areas of robust predicitons (90% of models agree in the direction of change).

Natural Bridges: Annual Precipitation

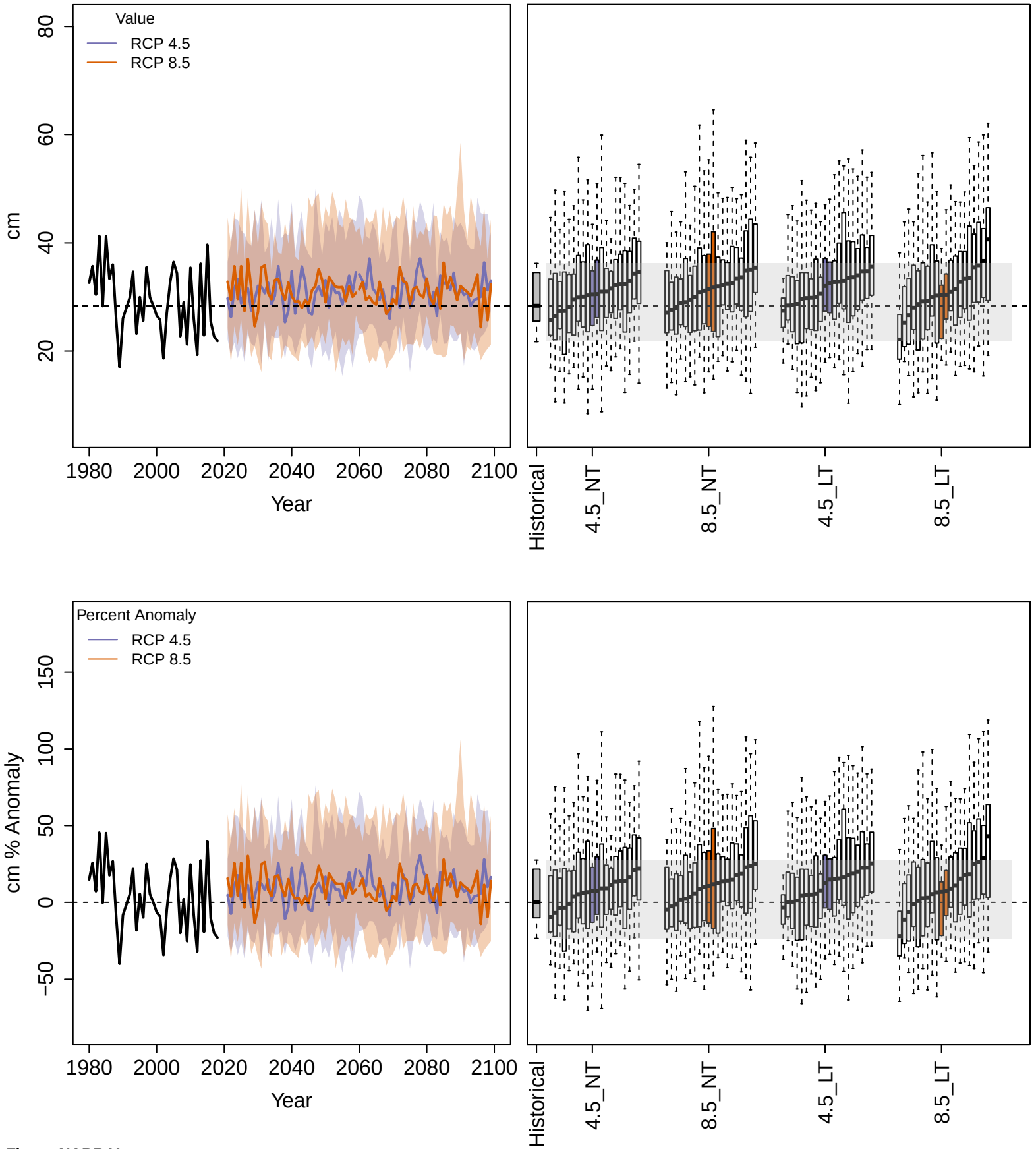


Figure NABR41:
Past trends and future trajectories of park−wide mean values for Annual Precipitation in Natural Bridges. Top panels show values, bottom panels show changes from the long−term historical mean. Left: Time series of historical (black) and future projections for RCP 4.5 and 8.5. Shaded areas show spread among climate models. Right: Boxplots of temporal variability over 40−year periods under historical (left box) and individual climate models under two RCPs. Right: Historical time period is 1970−2010; near−term (NT) is 2020−2060; long−term (LT) is 2061−2100.

Natural Bridges: Annual Precipitation

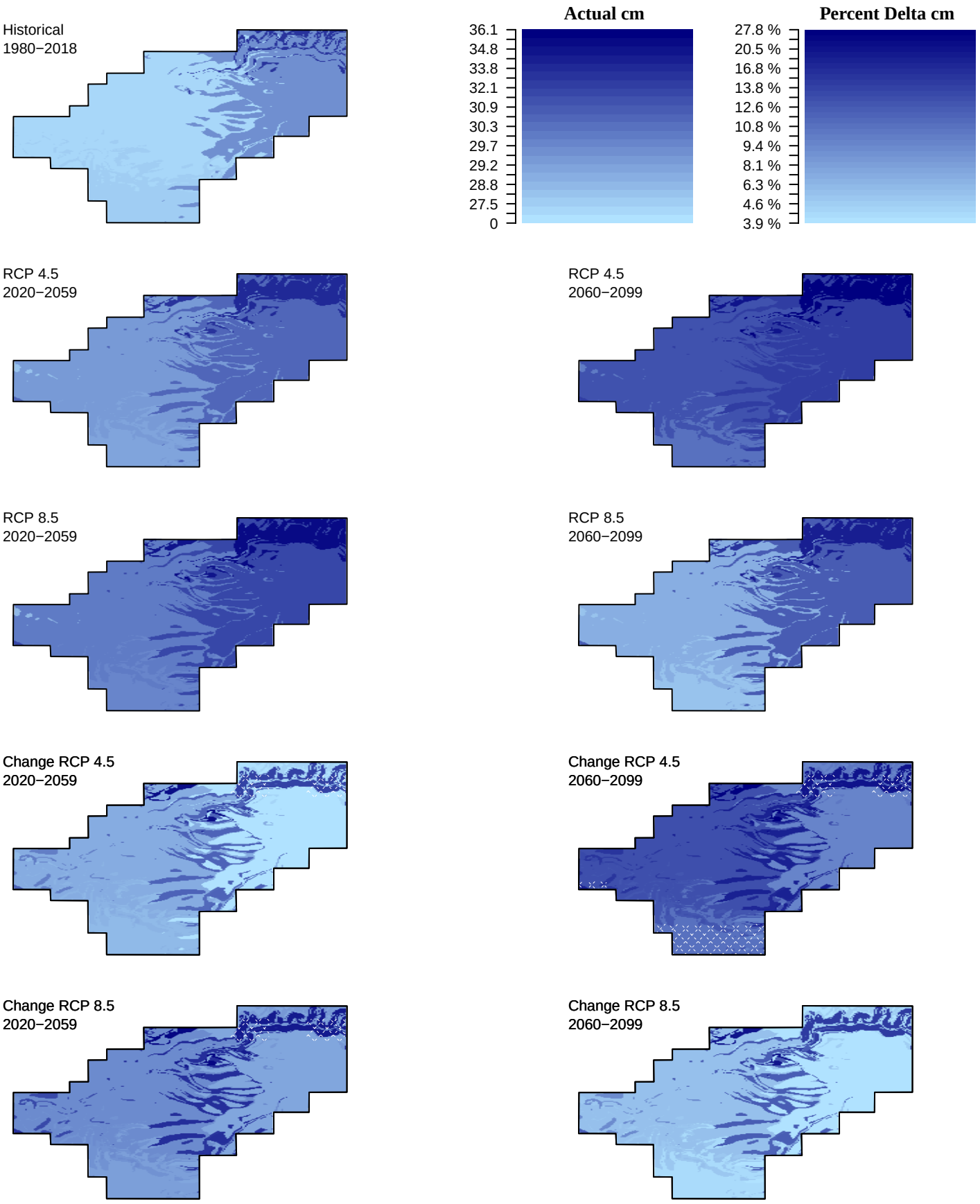


Figure NABRmap41:
Past trends and future trajectories of park−wide mean values for Annual Precipitation in Natural Bridges. Topmost panel depicts the historical mean from 1980−2018. Lower four panels show the emission scenarios of RCP 4.5 and RCP 8.5 at near−term and long−term timeframes. Bottom four panels depict the change from the historical mean; cross hatching denotes areas of robust predicitons (90% of models agree in the direction of change).

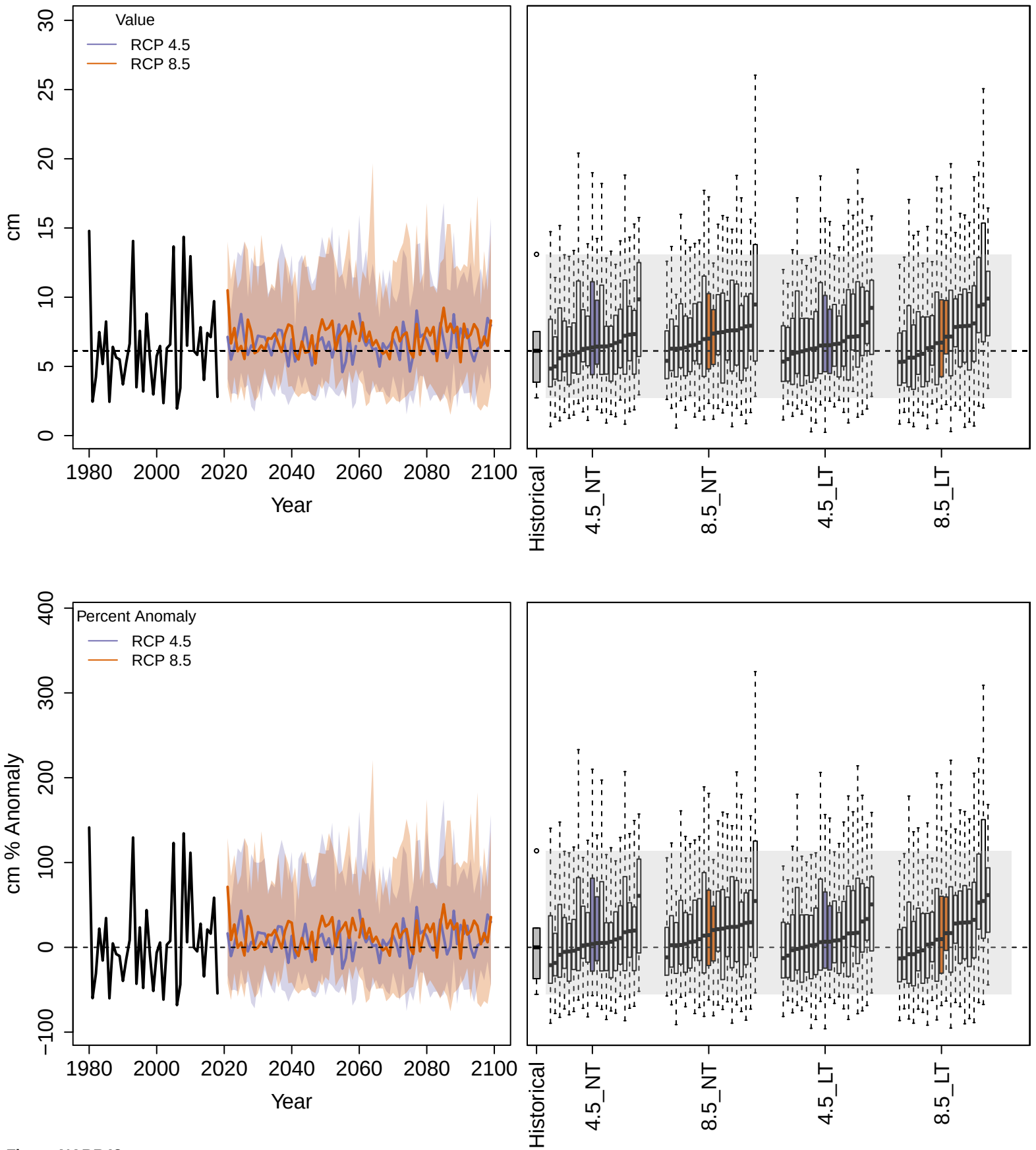


Figure NABR43:
Past trends and future trajectories of park−wide mean values for Winter Precipitation in Natural Bridges. Top panels show values, bottom panels show changes from the long−term historical mean. Left: Time series of historical (black) and future projections for RCP 4.5 and 8.5. Shaded areas show spread among climate models. Right: Boxplots of temporal variability over 40−year periods under historical (left box) and individual climate models under two RCPs. Right: Historical time period is 1970−2010; near−term (NT) is 2020−2060; long−term (LT) is 2061−2100.

Natural Bridges: Winter Precipitation

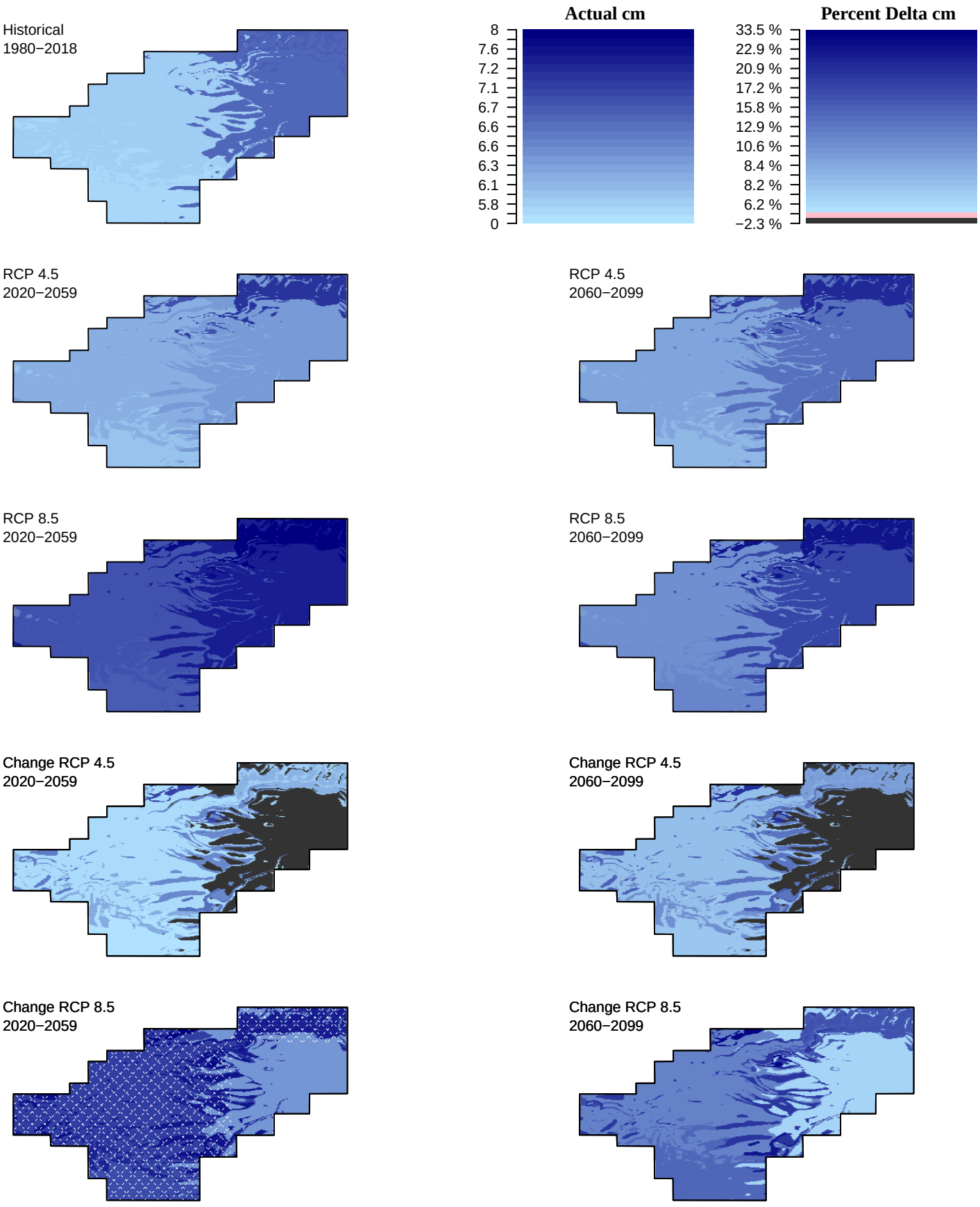


Figure NABRmap43:
Past trends and future trajectories of park−wide mean values for Winter Precipitation in Natural Bridges. Topmost panel depicts the historical mean from 1980−2018. Lower four panels show the emission scenarios of RCP 4.5 and RCP 8.5 at near−term and long−term timeframes. Bottom four panels depict the change from the historical mean; cross hatching denotes areas of robust predicitons (90% of models agree in the direction of change).

Natural Bridges: Spring Precipitation

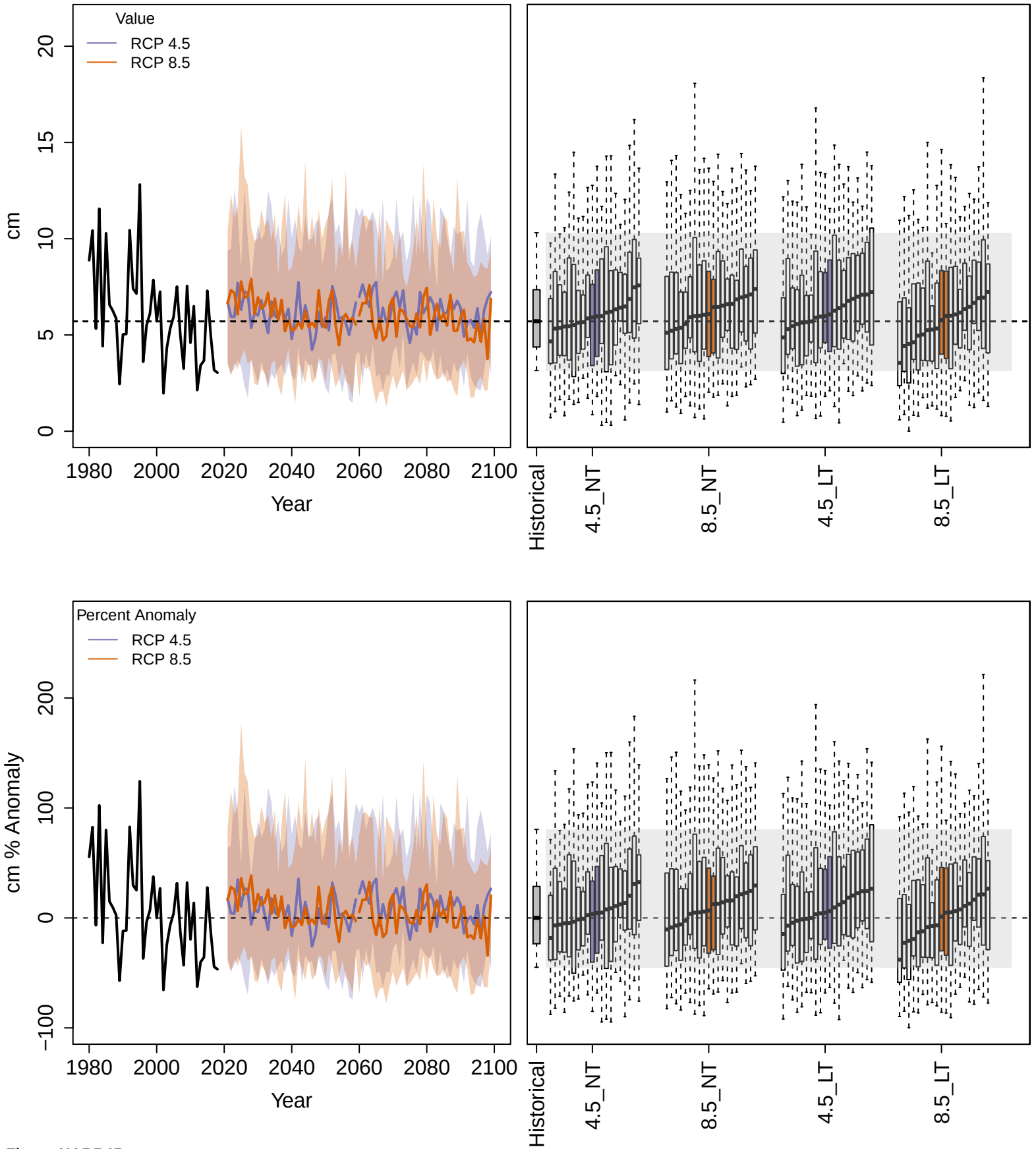


Figure NABR45:
Past trends and future trajectories of park−wide mean values for Spring Precipitation in Natural Bridges. Top panels show values, bottom panels show changes from the long−term historical mean. Left: Time series of historical (black) and future projections for RCP 4.5 and 8.5. Shaded areas show spread among climate models. Right: Boxplots of temporal variability over 40−year periods under historical (left box) and individual climate models under two RCPs. Right: Historical time period is 1970−2010; near−term (NT) is 2020−2060; long−term (LT) is 2061−2100.

Natural Bridges: Spring Precipitation

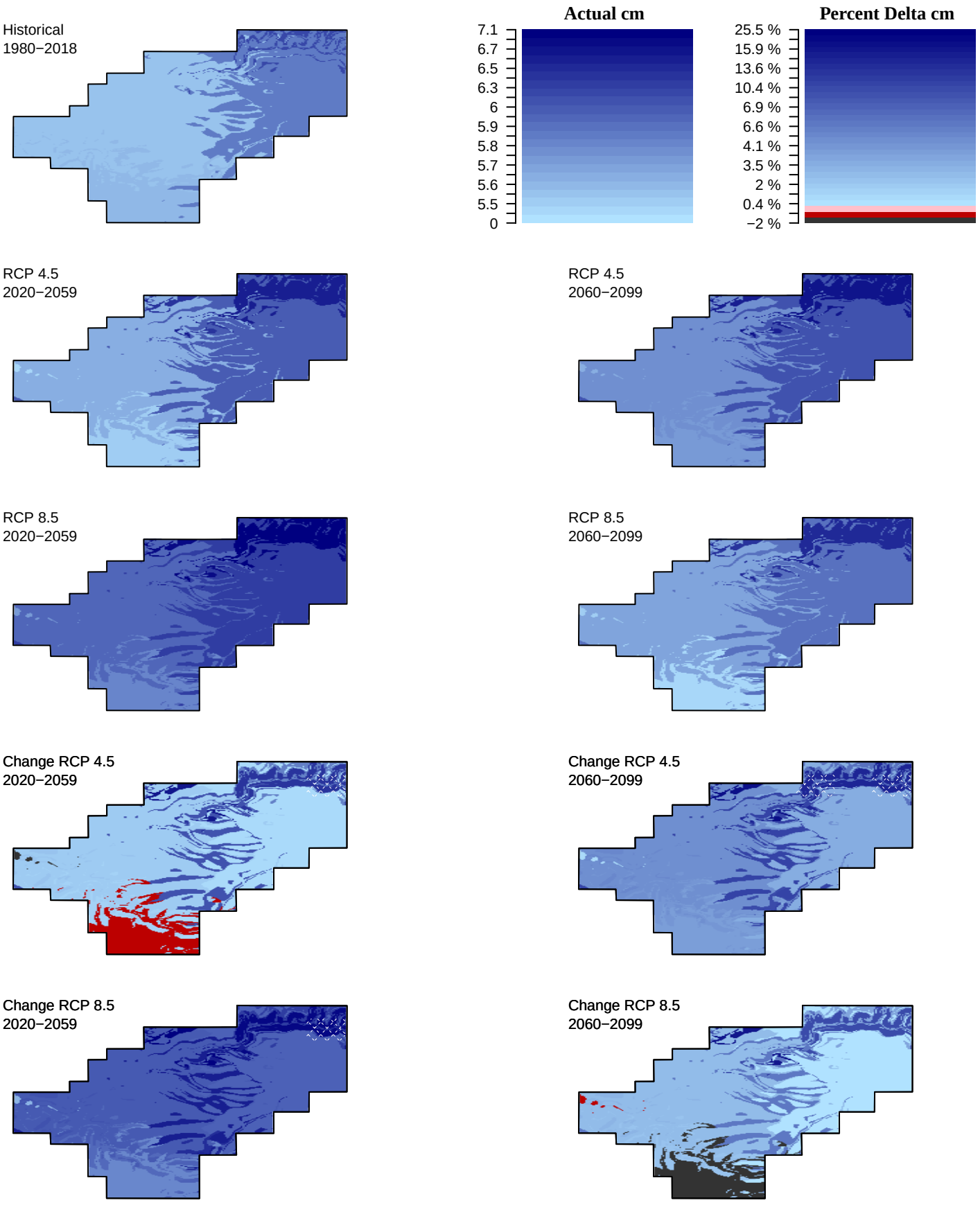


Figure NABRmap45:
Past trends and future trajectories of park−wide mean values for Spring Precipitation in Natural Bridges. Topmost panel depicts the historical mean from 1980−2018. Lower four panels show the emission scenarios of RCP 4.5 and RCP 8.5 at near−term and long−term timeframes. Bottom four panels depict the change from the historical mean; cross hatching denotes areas of robust predicitons (90% of models agree in the direction of change).

Natural Bridges: Summer Precipitation

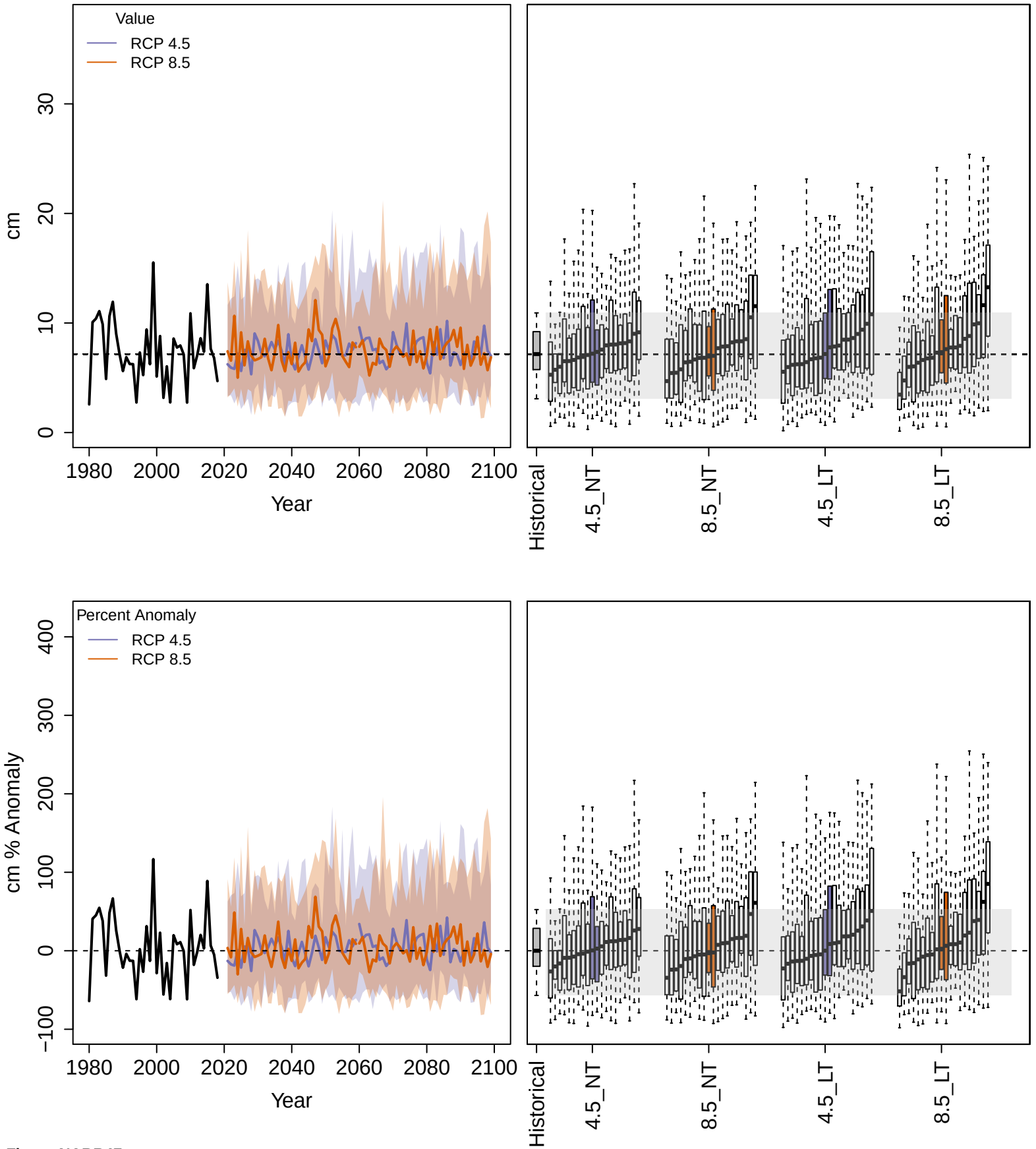


Figure NABR47:
Past trends and future trajectories of park−wide mean values for Summer Precipitation in Natural Bridges. Top panels show values, bottom panels show changes from the long−term historical mean. Left: Time series of historical (black) and future projections for RCP 4.5 and 8.5. Shaded areas show spread among climate models. Right: Boxplots of temporal variability over 40−year periods under historical (left box) and individual climate models under two RCPs. Right: Historical time period is 1970−2010; near−term (NT) is 2020−2060; long−term (LT) is 2061−2100.

Natural Bridges: Summer Precipitation

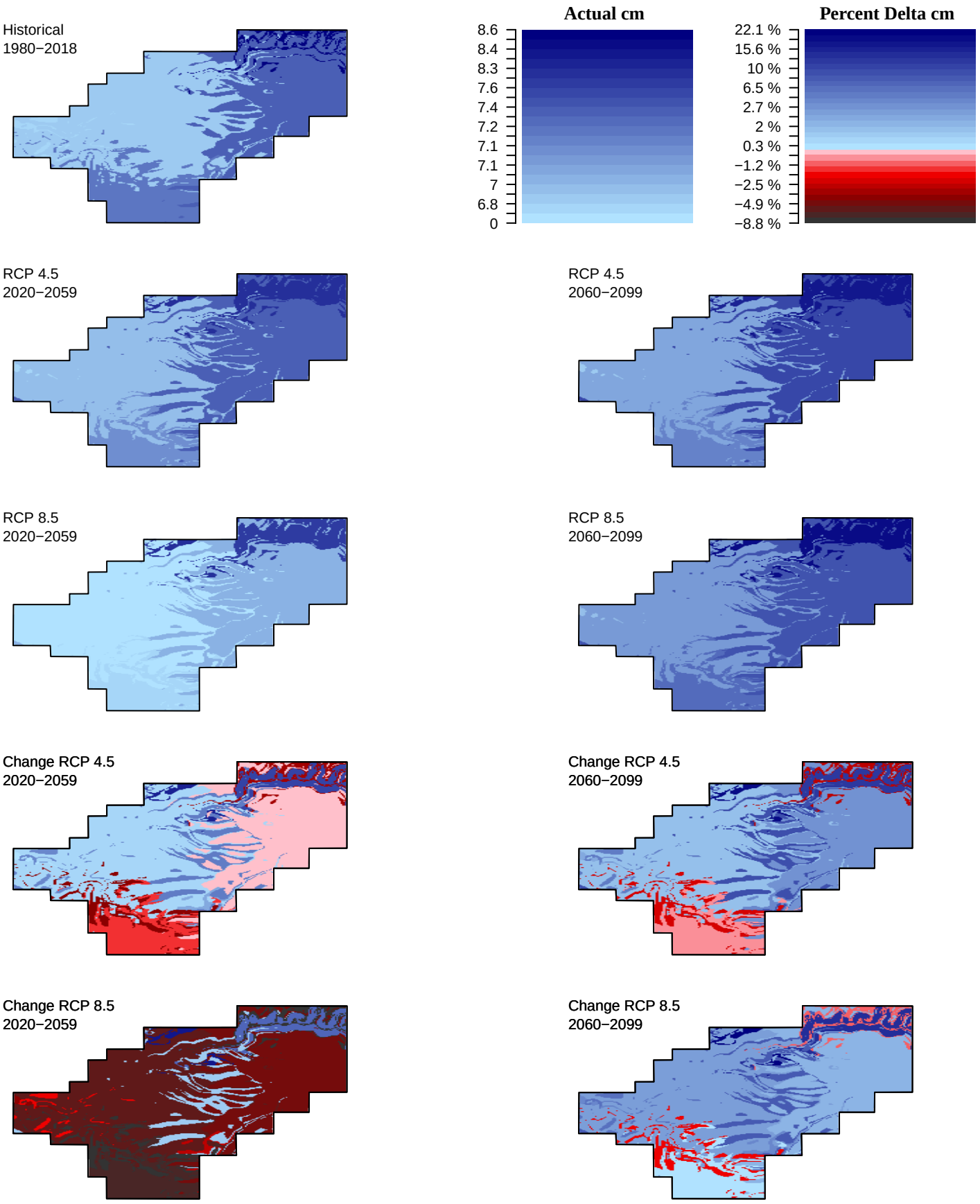


Figure NABRmap47:
Past trends and future trajectories of park−wide mean values for Summer Precipitation in Natural Bridges. Topmost panel depicts the historical mean from 1980−2018. Lower four panels show the emission scenarios of RCP 4.5 and RCP 8.5 at near−term and long−term timeframes. Bottom four panels depict the change from the historical mean; cross hatching denotes areas of robust predicitons (90% of models agree in the direction of change).

Natural Bridges: Fall Precipitation

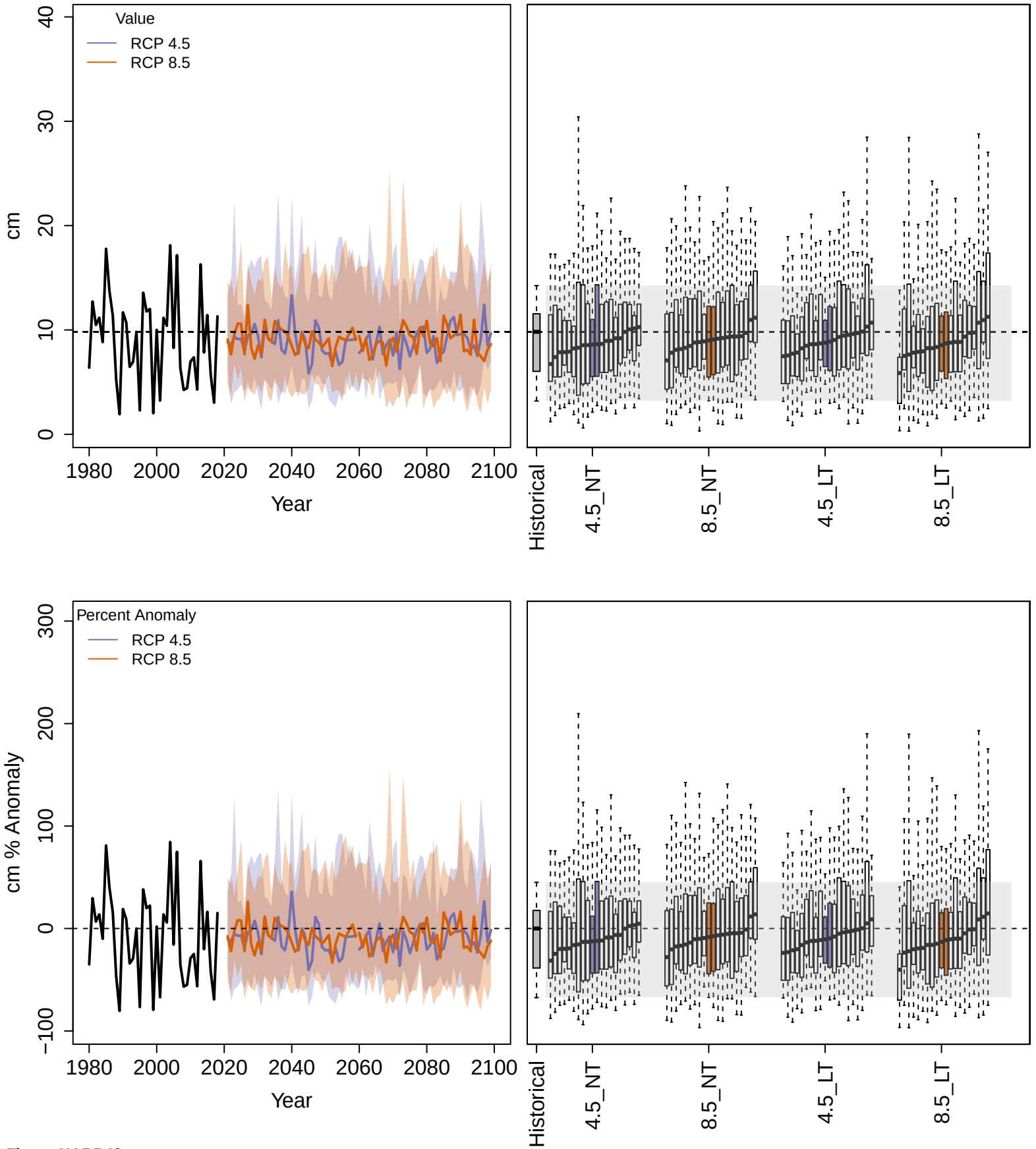


Figure NABR49:
Past trends and future trajectories of park−wide mean values for Fall Precipitation in Natural Bridges. Top panels show values, bottom panels show changes from the long−term historical mean. Left: Time series of historical (black) and future projections for RCP 4.5 and 8.5. Shaded areas show spread among climate models. Right: Boxplots of temporal variability over 40−year periods under historical (left box) and individual climate models under two RCPs. Right: Historical time period is 1970−2010; near−term (NT) is 2020−2060; long−term (LT) is 2061−2100.

Natural Bridges: Fall Precipitation

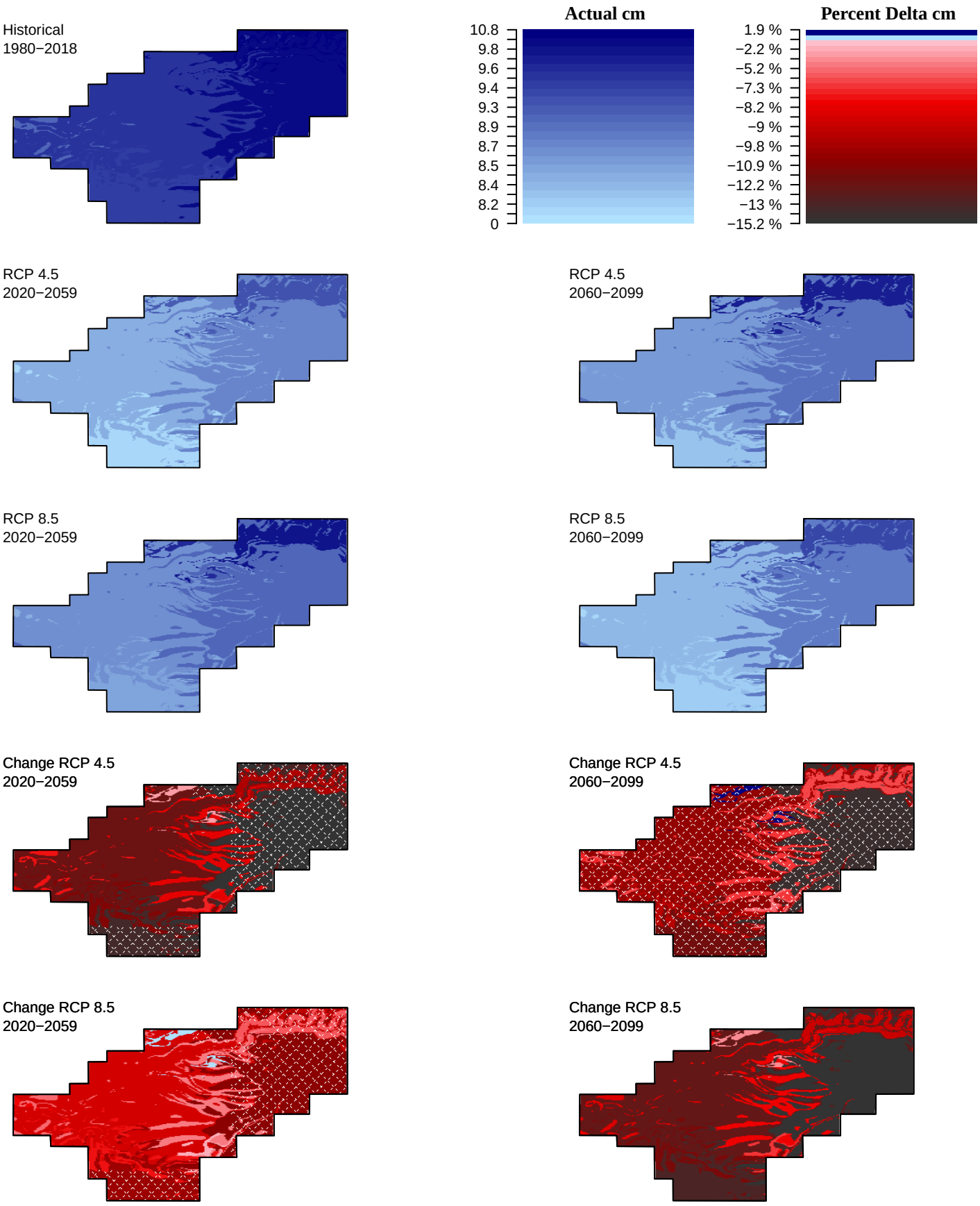


Figure NABRmap49:
Past trends and future trajectories of park−wide mean values for Fall Precipitation in Natural Bridges. Topmost panel depicts the historical mean from 1980−2018. Lower four panels show the emission scenarios of RCP 4.5 and RCP 8.5 at near−term and long−term timeframes. Bottom four panels depict the change from the historical mean; cross hatching denotes areas of robust predicitons (90% of models agree in the direction of change).

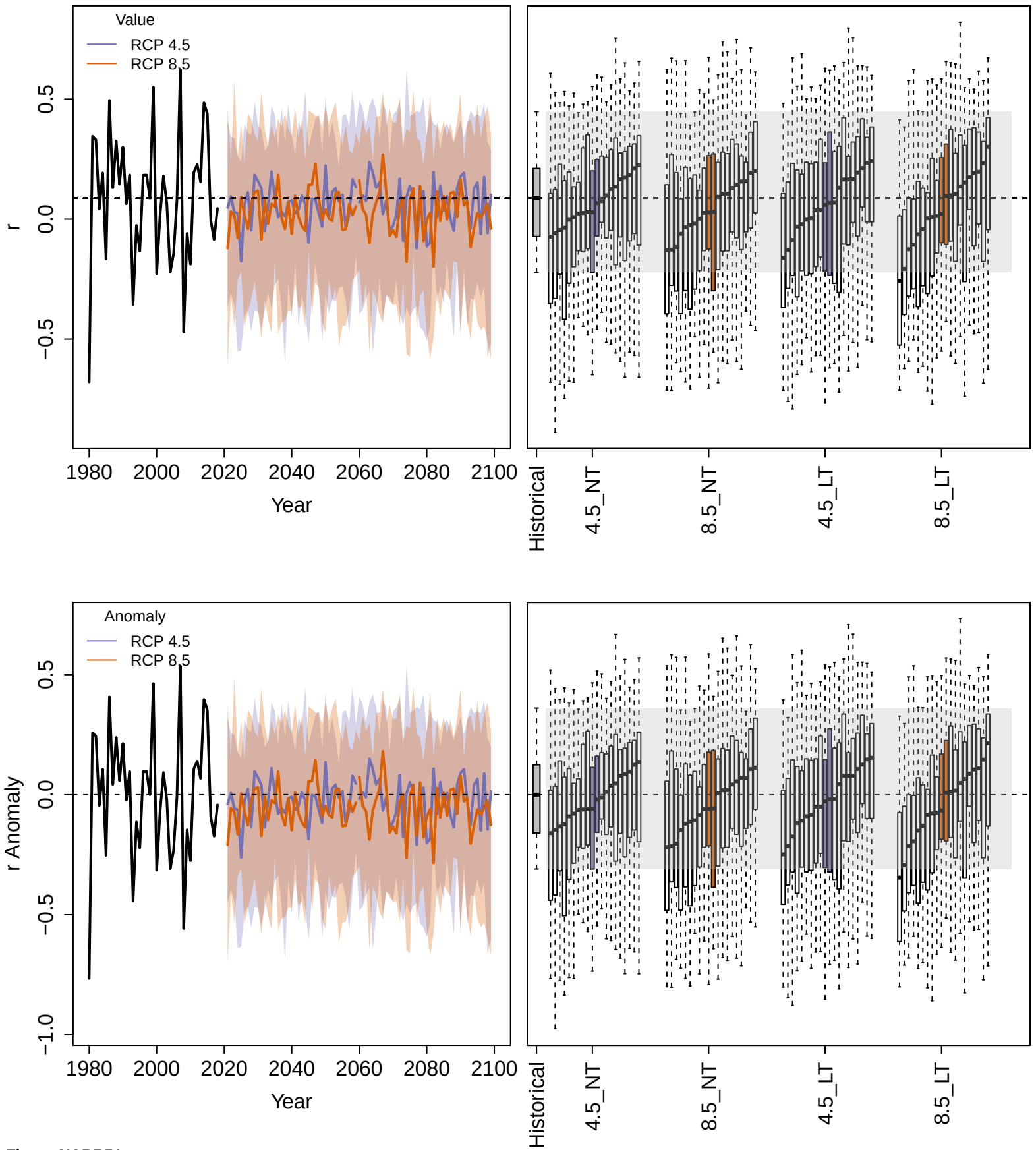


Figure NABR51:
Past trends and future trajectories of park−wide mean values for Monthly temperature−precipitation correlation in Natural Bridges. Top panels show values, bottom panels show changes from the long−term historical mean. Left: Time series of historical (black) and future projections for RCP 4.5 and 8.5. Shaded areas show spread among climate models. Right: Boxplots of temporal variability over 40−year periods under historical (left box) and individual climate models under two RCPs. Right: Historical time period is 1970−2010; near−term (NT) is 2020−2060; long−term (LT) is 2061−2100.

Natural Bridges: Monthly temperature−precipitation correlation

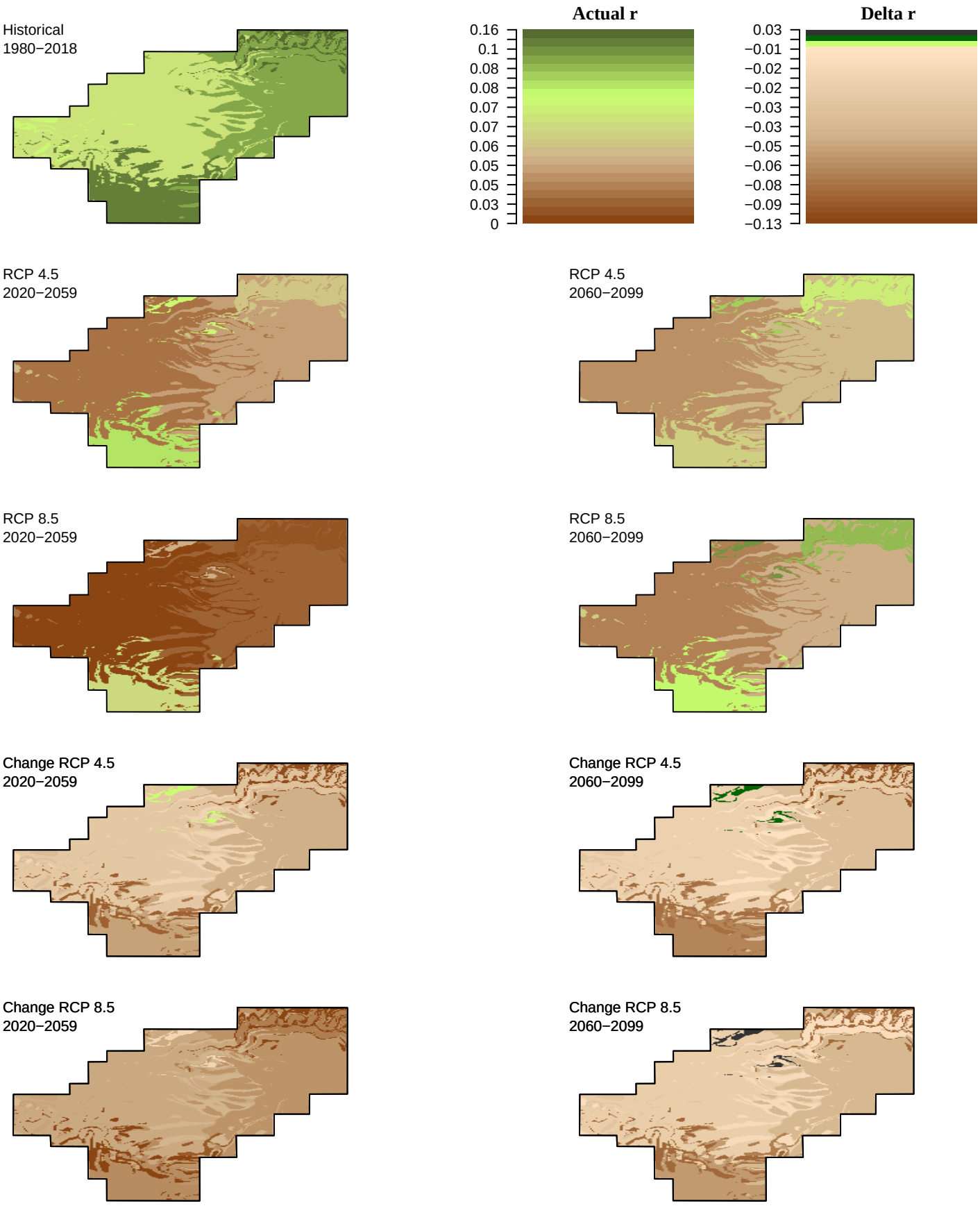


Figure NABRmap51:
Past trends and future trajectories of park−wide mean values for Monthly temperature−precipitation correlation in Natural Bridges. Topmost panel depicts the historical mean from 1980−2018. Lower four panels show the emission scenarios of RCP 4.5 and RCP 8.5 at near−term and long−term timeframes. Bottom four panels depict the change from the historical mean; cross hatching denotes areas of robust predicitons (90% of models agree in the direction of change).

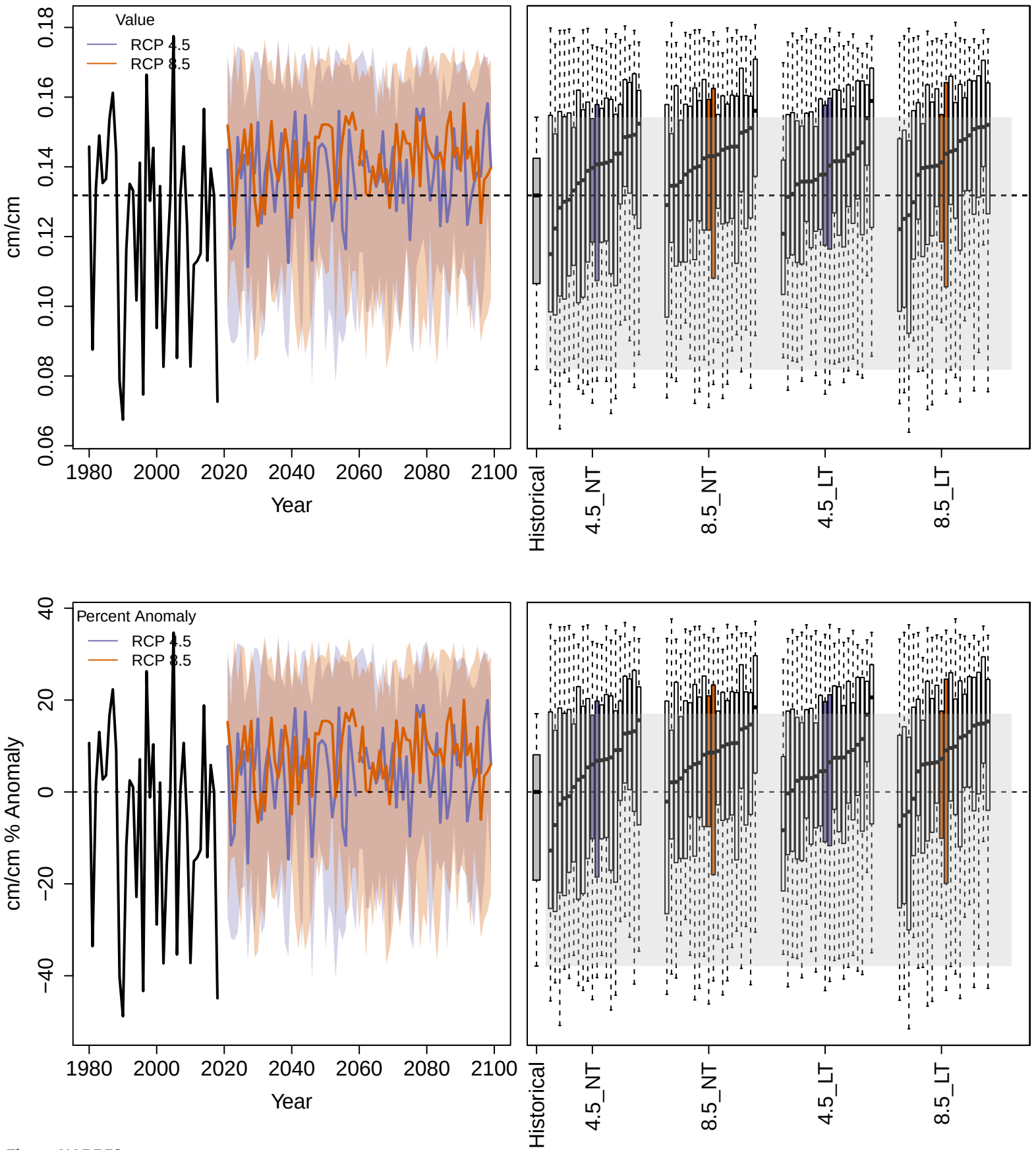


Figure NABR53:
Past trends and future trajectories of park−wide mean values for Winter soil water content: Top 50cm in Natural Bridges. Top panels show values, bottom panels show changes from the long−term historical mean. Left: Time series of historical (black) and future projections for RCP 4.5 and 8.5. Shaded areas show spread among climate models. Right: Boxplots of temporal variability over 40−year periods under historical (left box) and individual climate models under two RCPs. Right: Historical time period is 1970−2010; near−term (NT) is 2020−2060; long−term (LT) is 2061−2100.

Natural Bridges: Winter soil water content: Top 50cm

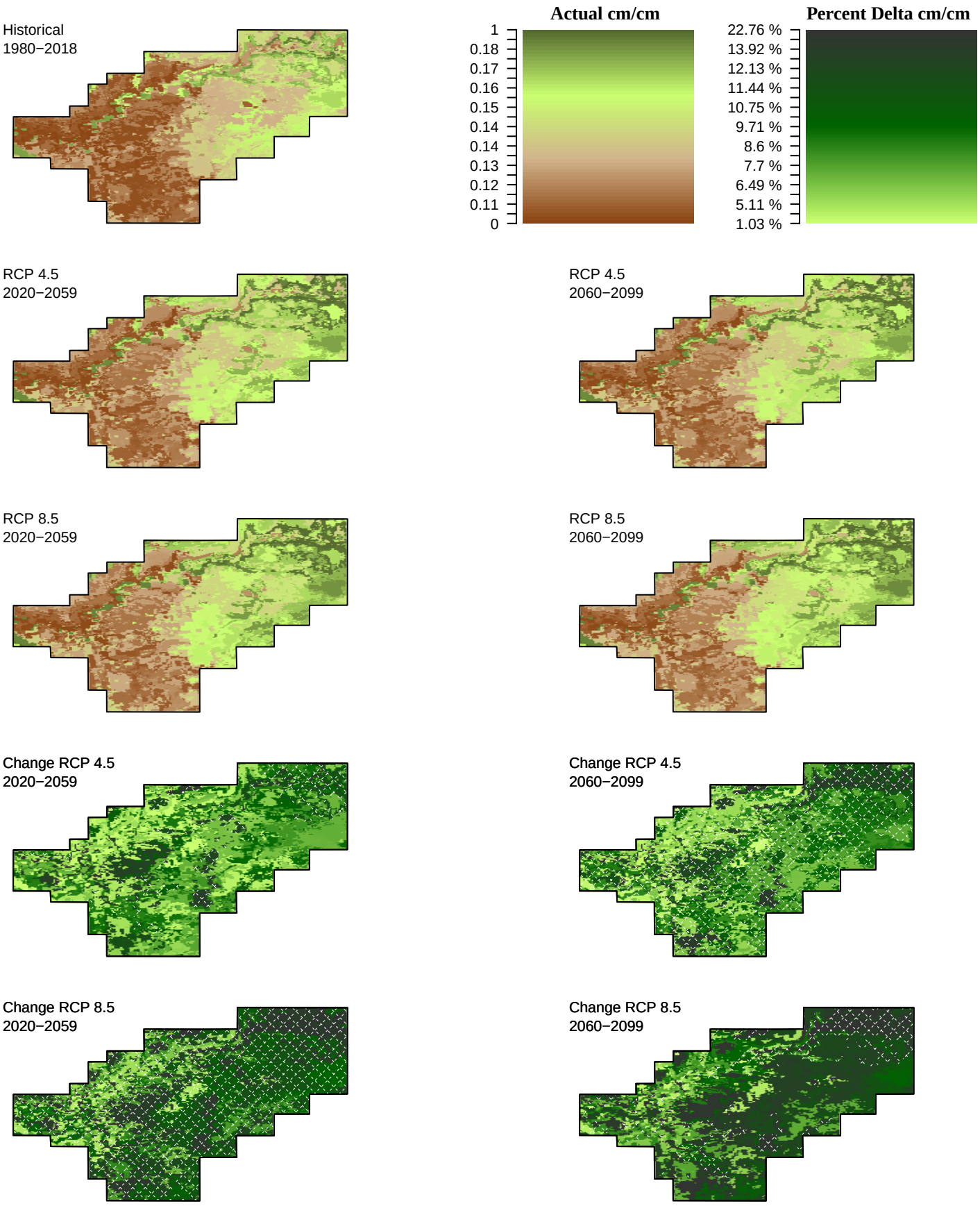


Figure NABRmap53:
Past trends and future trajectories of park−wide mean values for Winter soil water content: Top 50cm in Natural Bridges. Topmost panel depicts the historical mean from 1980−2018. Lower four panels show the emission scenarios of RCP 4.5 and RCP 8.5 at near−term and long−term timeframes. Bottom four panels depict the change from the historical mean; cross hatching denotes areas of robust predicitons (90% of models agree in the direction of change).

Natural Bridges: Spring soil water content:Top 50cm

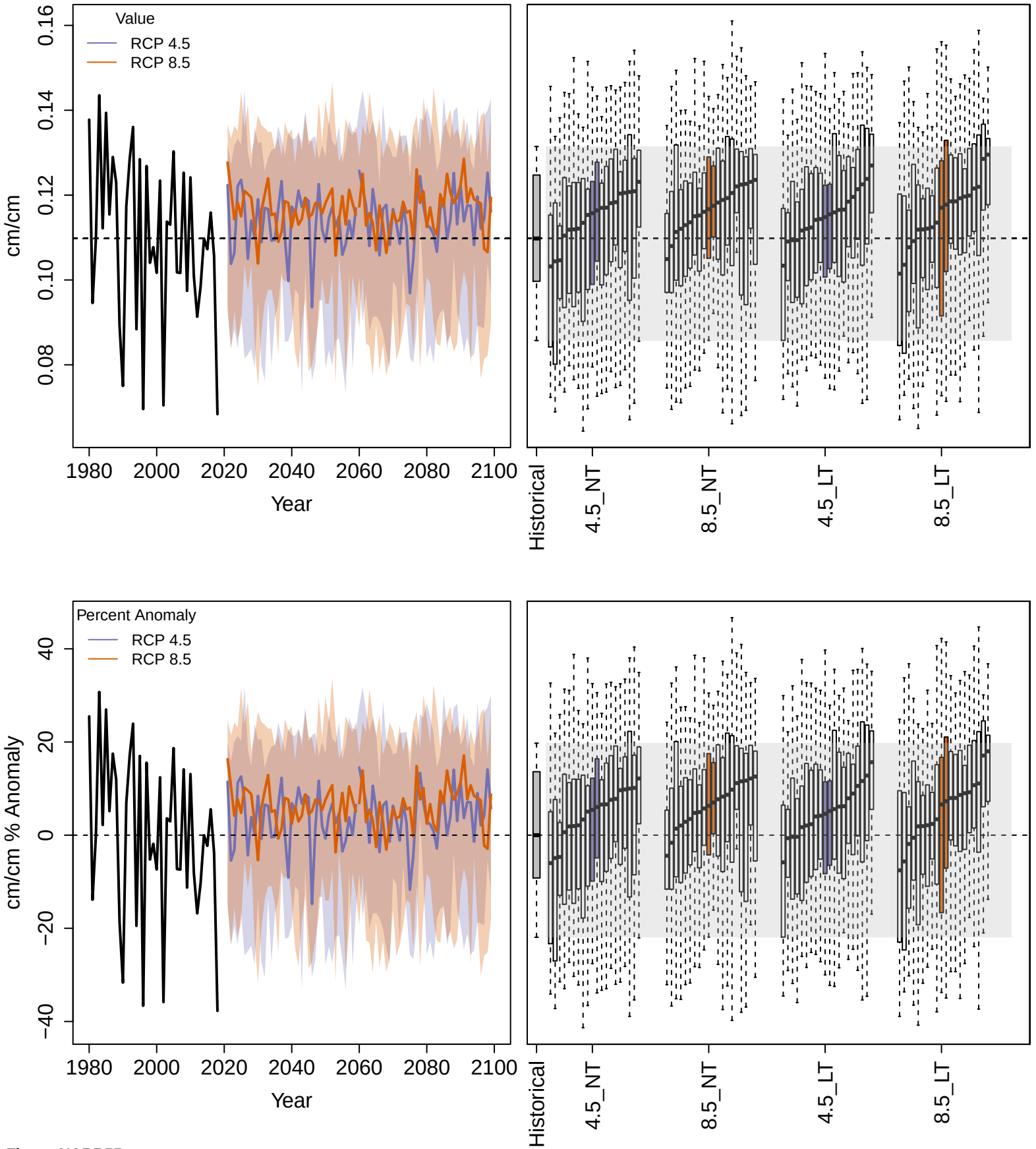


Figure NABR55:
Past trends and future trajectories of park−wide mean values for Spring soil water content:Top 50cm in Natural Bridges. Top panels show values, bottom panels show changes from the long−term historical mean. Left: Time series of historical (black) and future projections for RCP 4.5 and 8.5. Shaded areas show spread among climate models. Right: Boxplots of temporal variability over 40−year periods under historical (left box) and individual climate models under two RCPs. Right: Historical time period is 1970−2010; near−term (NT) is 2020−2060; long−term (LT) is 2061−2100.

Natural Bridges: Spring soil water content:Top 50cm

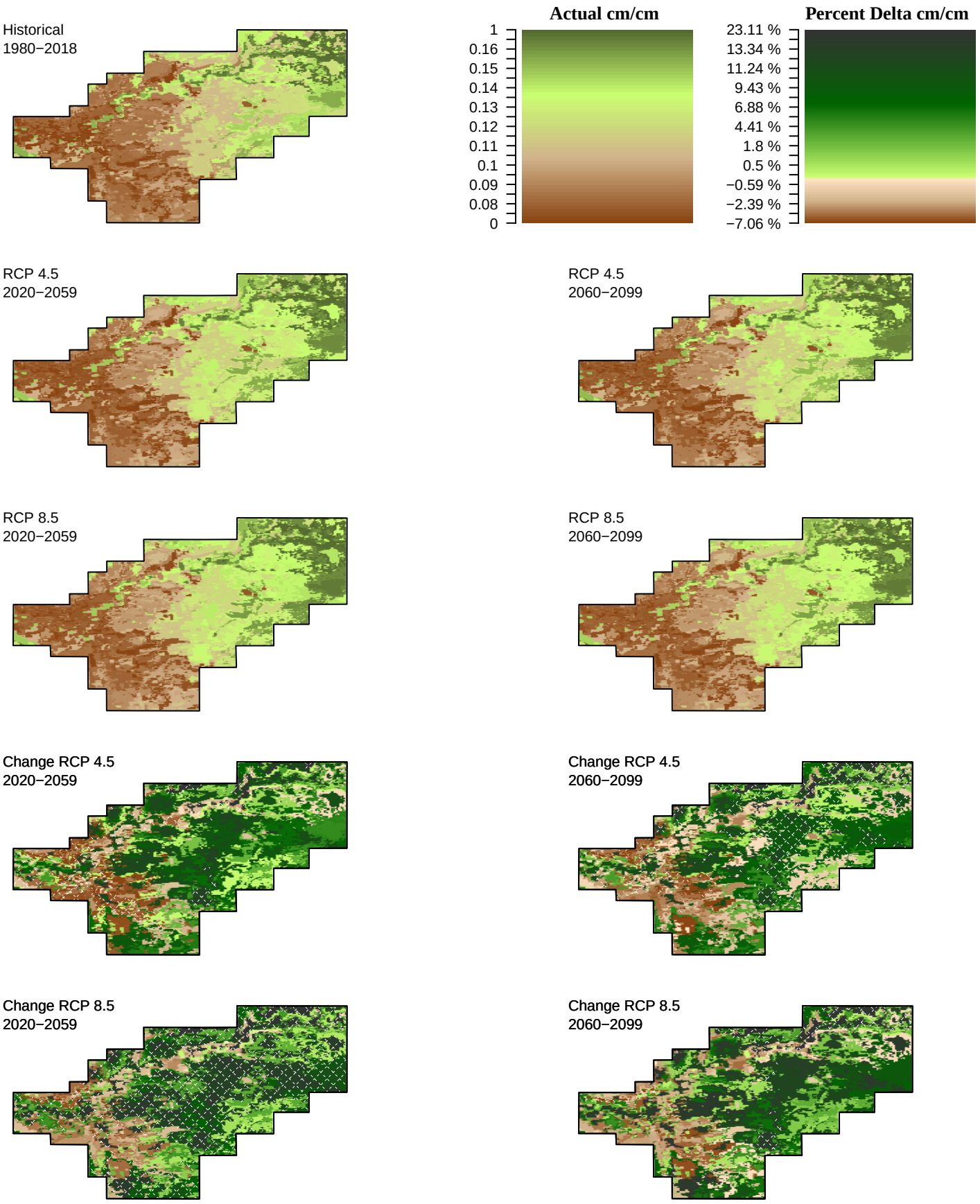


Figure NABRmap55:
Past trends and future trajectories of park−wide mean values for Spring soil water content:Top 50cm in Natural Bridges. Topmost panel depicts the historical mean from 1980−2018. Lower four panels show the emission scenarios of RCP 4.5 and RCP 8.5 at near−term and long−term timeframes. Bottom four panels depict the change from the historical mean; cross hatching denotes areas of robust predicitons (90% of models agree in the direction of change).

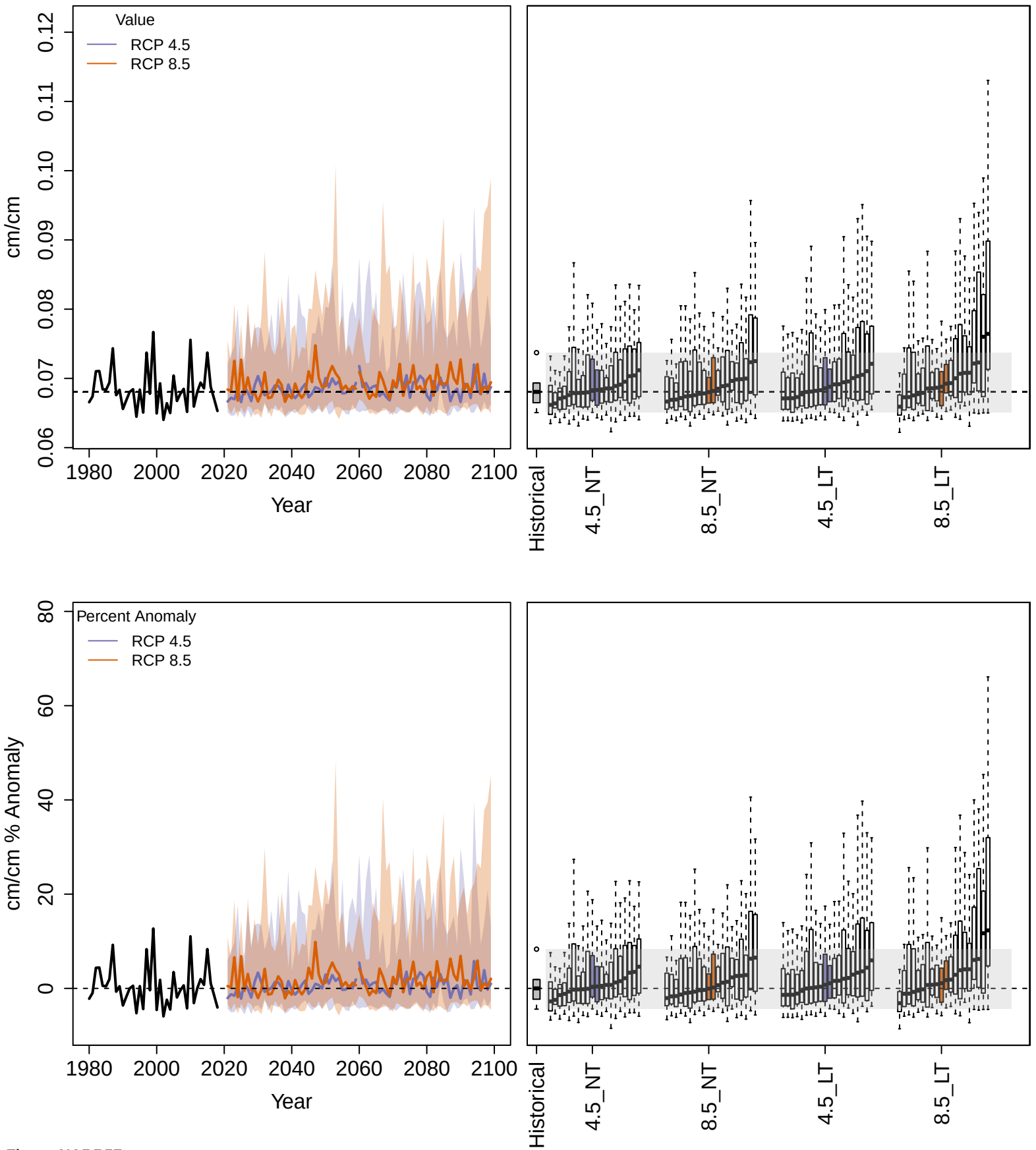


Figure NABR57:
Past trends and future trajectories of park−wide mean values for Summer soil water content:Top 50cm in Natural Bridges. Top panels show values, bottom panels show changes from the long−term historical mean. Left: Time series of historical (black) and future projections for RCP 4.5 and 8.5. Shaded areas show spread among climate models. Right: Boxplots of temporal variability over 40−year periods under historical (left box) and individual climate models under two RCPs. Right: Historical time period is 1970−2010; near−term (NT) is 2020−2060; long−term (LT) is 2061−2100.

Natural Bridges: Summer soil water content:Top 50cm

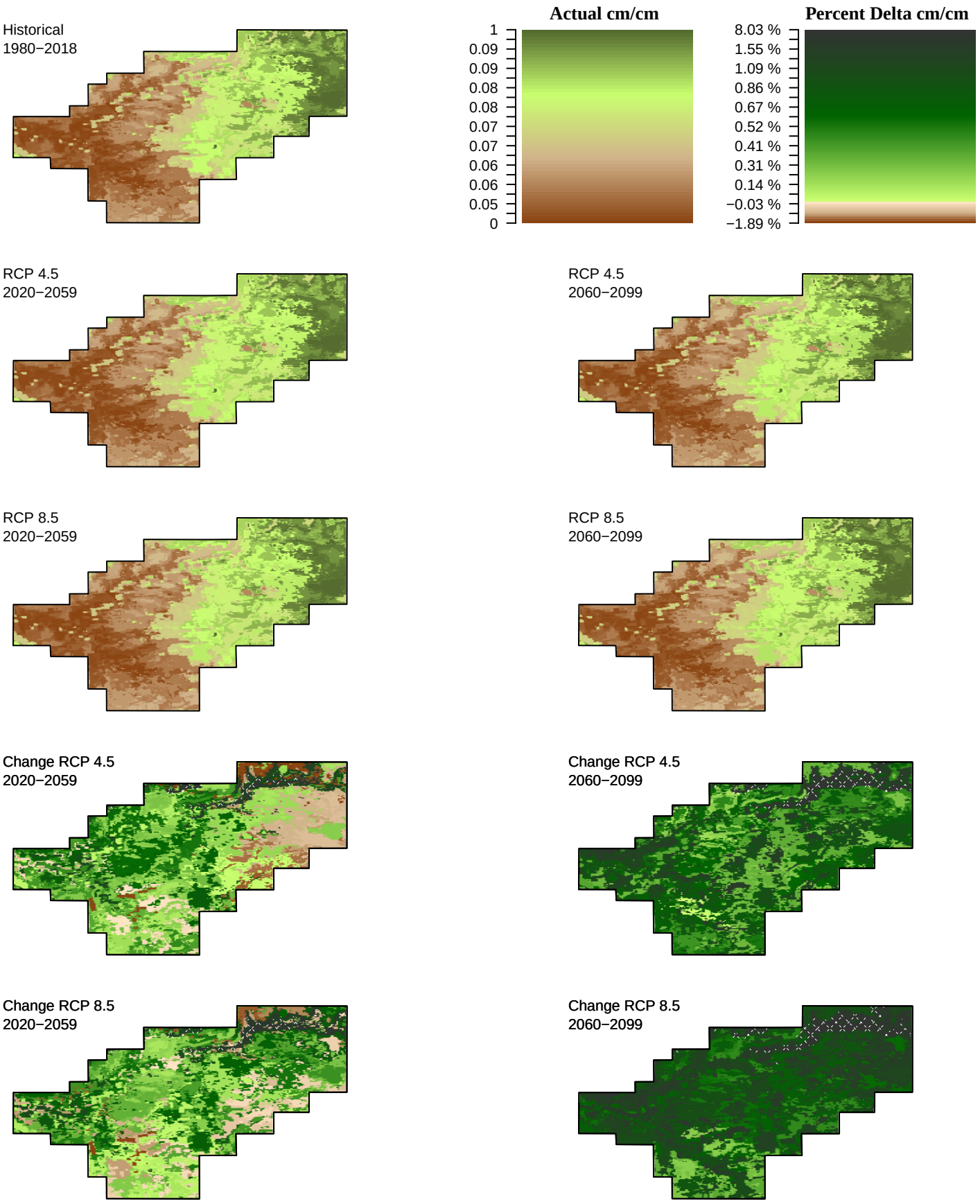


Figure NABRmap57:
Past trends and future trajectories of park−wide mean values for Summer soil water content:Top 50cm in Natural Bridges. Topmost panel depicts the historical mean from 1980−2018. Lower four panels show the emission scenarios of RCP 4.5 and RCP 8.5 at near−term and long−term timeframes. Bottom four panels depict the change from the historical mean; cross hatching denotes areas of robust predicitons (90% of models agree in the direction of change).

Natural Bridges: Fall soil water content:Top 50cm

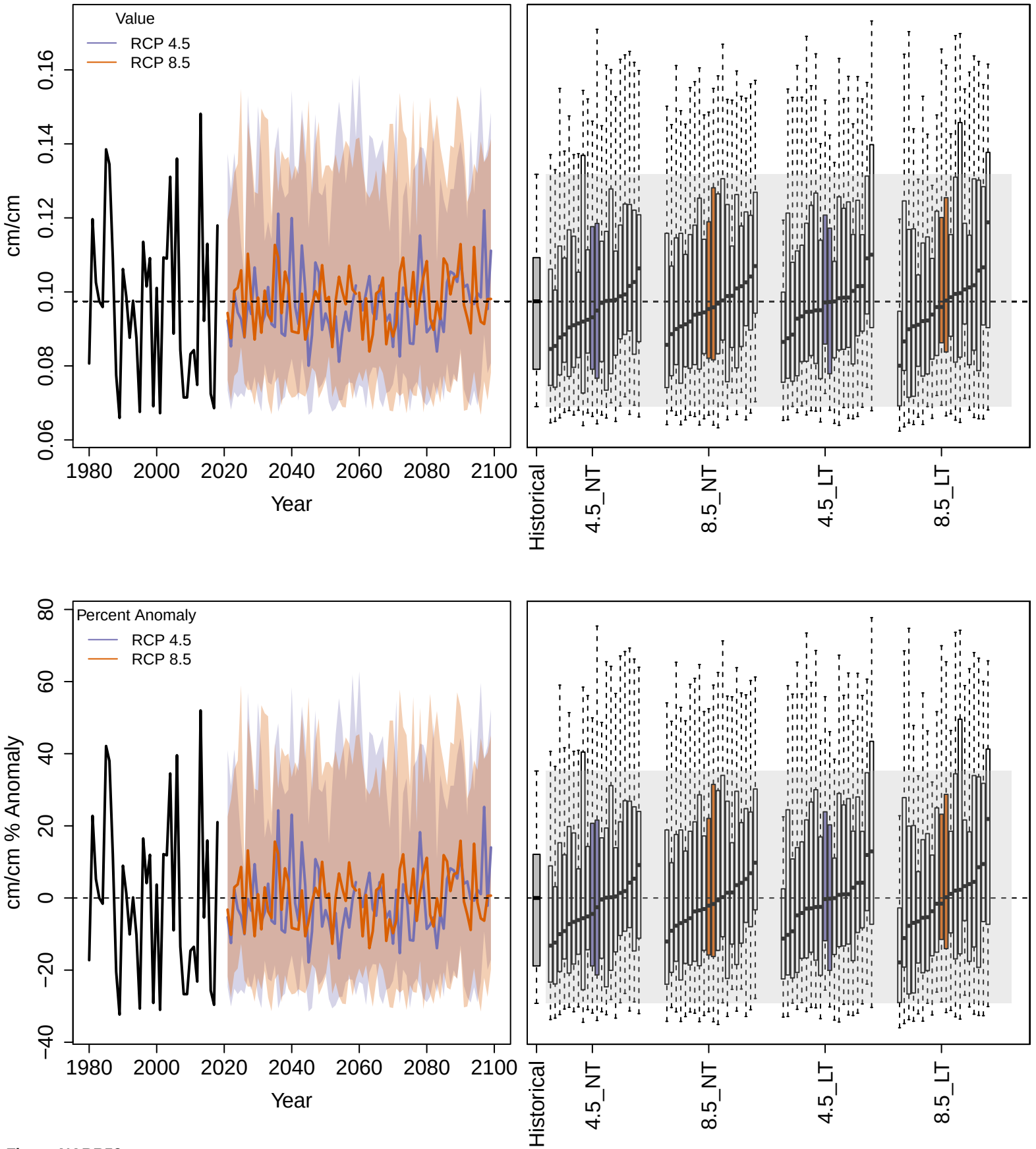


Figure NABR59:
Past trends and future trajectories of park−wide mean values for Fall soil water content:Top 50cm in Natural Bridges. Top panels show values, bottom panels show changes from the long−term historical mean. Left: Time series of historical (black) and future projections for RCP 4.5 and 8.5. Shaded areas show spread among climate models. Right: Boxplots of temporal variability over 40−year periods under historical (left box) and individual climate models under two RCPs. Right: Historical time period is 1970−2010; near−term (NT) is 2020−2060; long−term (LT) is 2061−2100.

Natural Bridges: Fall soil water content:Top 50cm

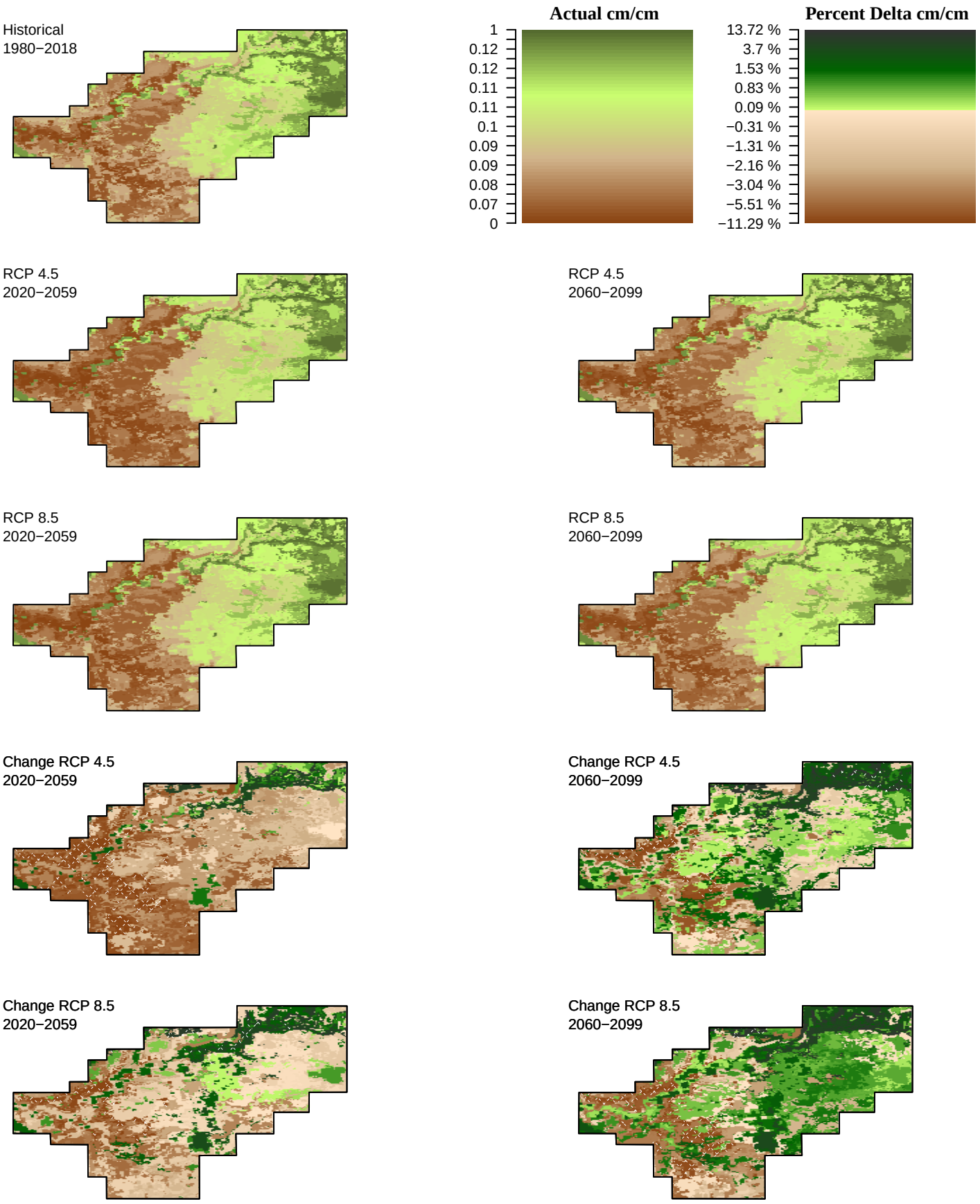


Figure NABRmap59:
Past trends and future trajectories of park−wide mean values for Fall soil water content:Top 50cm in Natural Bridges. Topmost panel depicts the historical mean from 1980−2018. Lower four panels show the emission scenarios of RCP 4.5 and RCP 8.5 at near−term and long−term timeframes. Bottom four panels depict the change from the historical mean; cross hatching denotes areas of robust predicitons (90% of models agree in the direction of change).

Natural Bridges: Winter soil water content

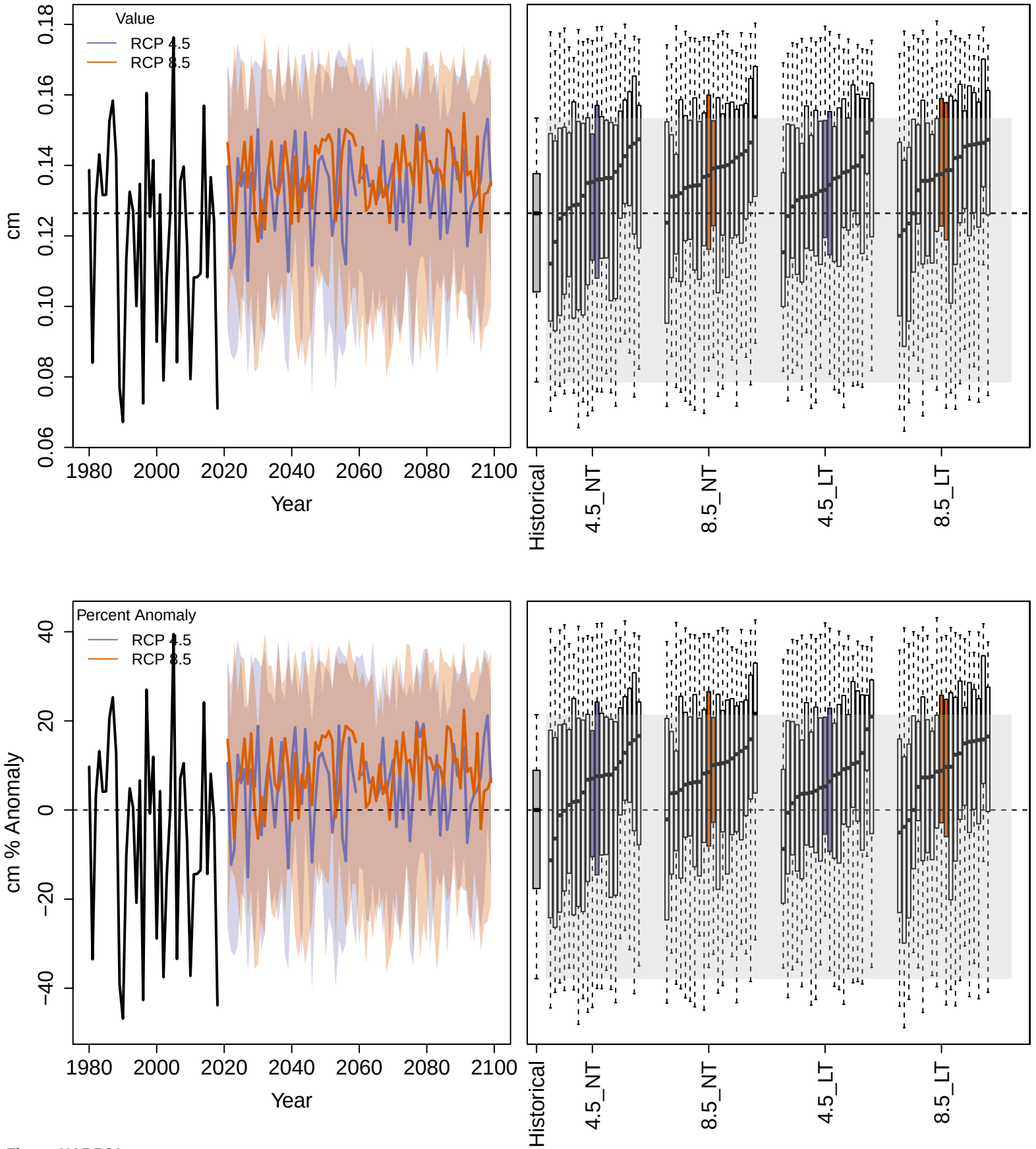


Figure NABR61:
Past trends and future trajectories of park−wide mean values for Winter soil water content in Natural Bridges. Top panels show values, bottom panels show changes from the long−term historical mean. Left: Time series of historical (black) and future projections for RCP 4.5 and 8.5. Shaded areas show spread among climate models. Right: Boxplots of temporal variability over 40−year periods under historical (left box) and individual climate models under two RCPs. Right: Historical time period is 1970−2010; near−term (NT) is 2020−2060; long−term (LT) is 2061−2100.

Natural Bridges: Winter soil water content

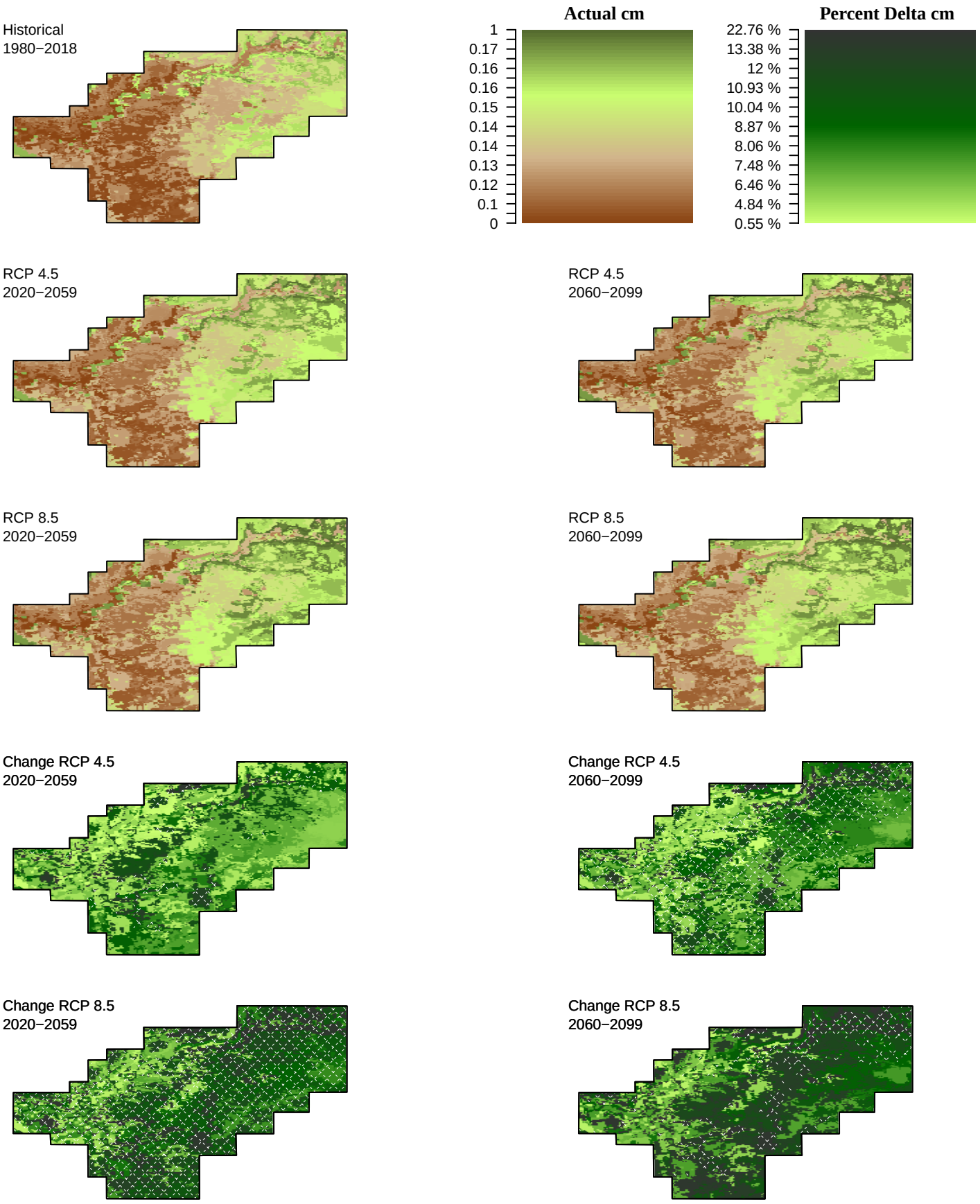


Figure NABRmap61:
Past trends and future trajectories of park−wide mean values for Winter soil water content in Natural Bridges. Topmost panel depicts the historical mean from 1980−2018. Lower four panels show the emission scenarios of RCP 4.5 and RCP 8.5 at near−term and long−term timeframes. Bottom four panels depict the change from the historical mean; cross hatching denotes areas of robust predicitons (90% of models agree in the direction of change).

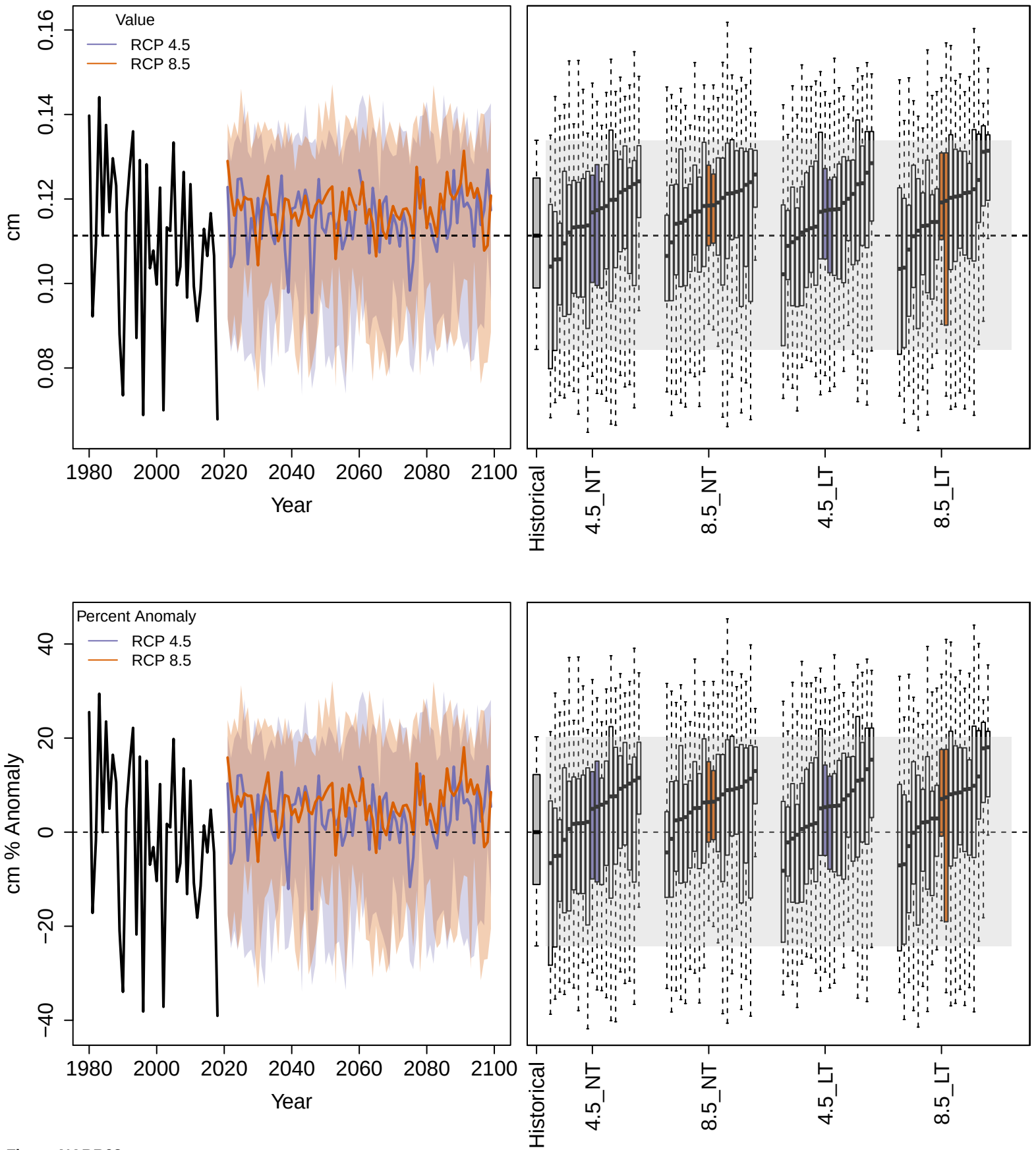


Figure NABR63:
Past trends and future trajectories of park−wide mean values for Spring soil water content in Natural Bridges. Top panels show values, bottom panels show changes from the long−term historical mean. Left: Time series of historical (black) and future projections for RCP 4.5 and 8.5. Shaded areas show spread among climate models. Right: Boxplots of temporal variability over 40−year periods under historical (left box) and individual climate models under two RCPs. Right: Historical time period is 1970−2010; near−term (NT) is 2020−2060; long−term (LT) is 2061−2100.

Natural Bridges: Spring soil water content

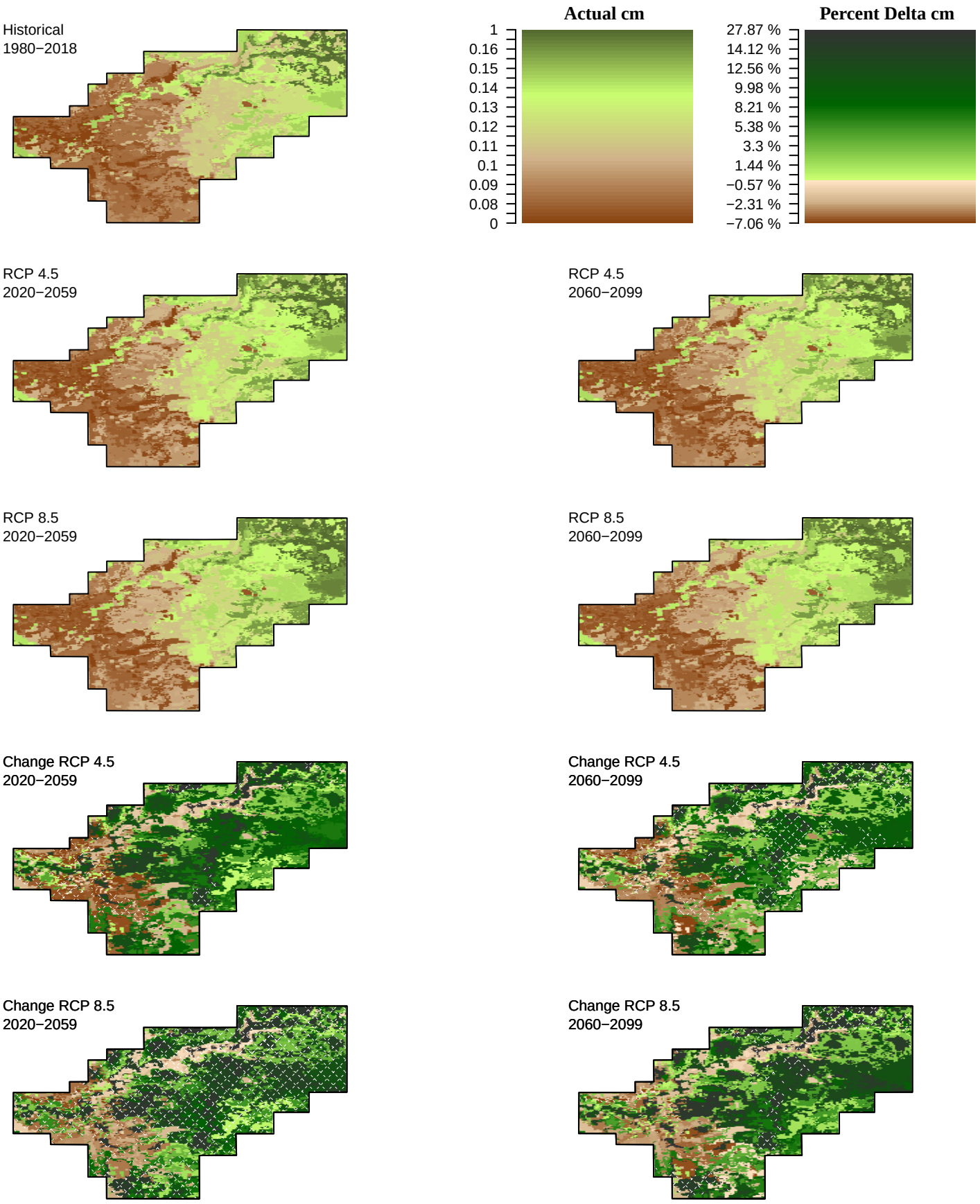


Figure NABRmap63:
Past trends and future trajectories of park−wide mean values for Spring soil water content in Natural Bridges. Topmost panel depicts the historical mean from 1980−2018. Lower four panels show the emission scenarios of RCP 4.5 and RCP 8.5 at near−term and long−term timeframes. Bottom four panels depict the change from the historical mean; cross hatching denotes areas of robust predicitons (90% of models agree in the direction of change).

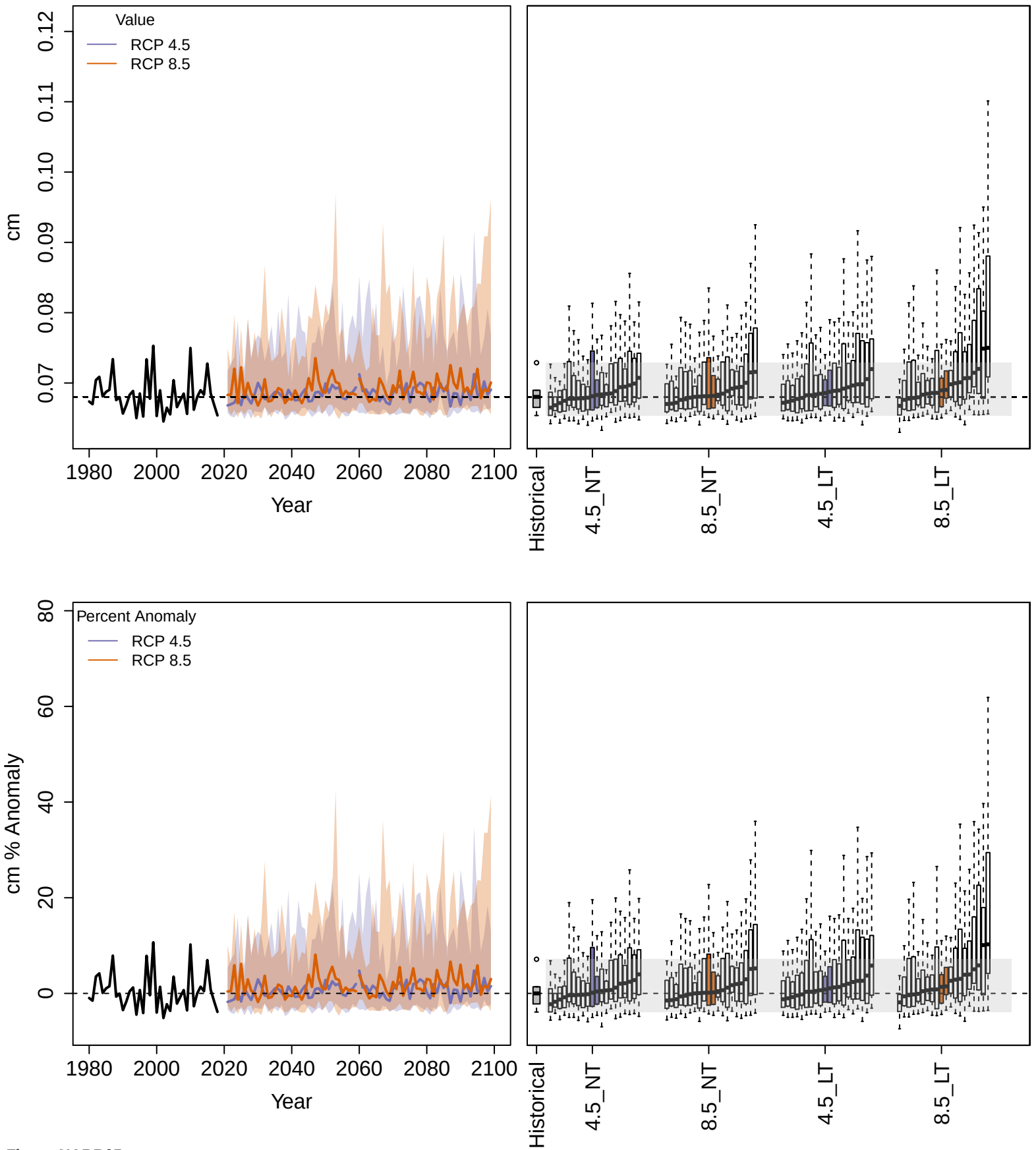


Figure NABR65:
Past trends and future trajectories of park−wide mean values for Summer soil water content in Natural Bridges. Top panels show values, bottom panels show changes from the long−term historical mean. Left: Time series of historical (black) and future projections for RCP 4.5 and 8.5. Shaded areas show spread among climate models. Right: Boxplots of temporal variability over 40−year periods under historical (left box) and individual climate models under two RCPs. Right: Historical time period is 1970−2010; near−term (NT) is 2020−2060; long−term (LT) is 2061−2100.

Natural Bridges: Summer soil water content

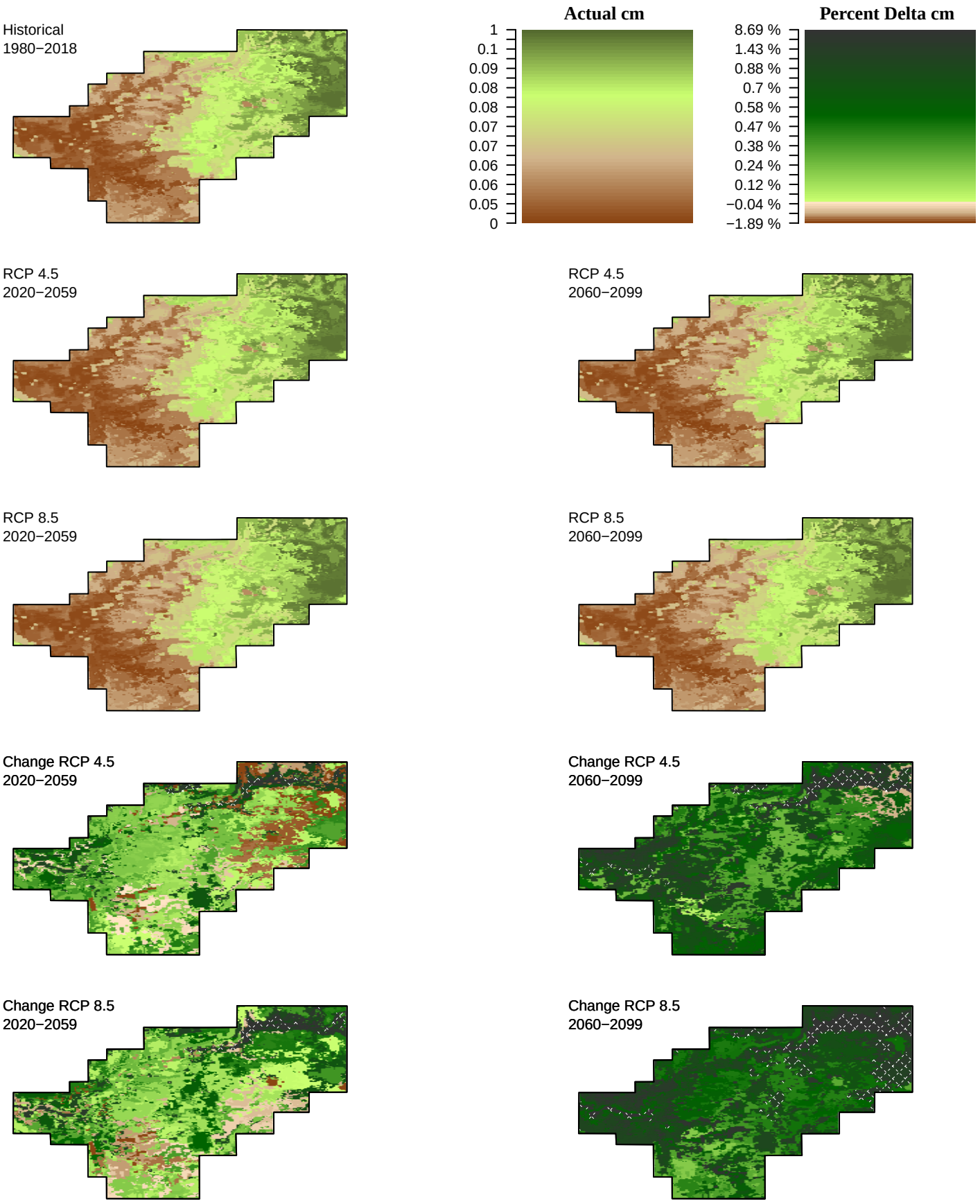


Figure NABRmap65:
Past trends and future trajectories of park−wide mean values for Summer soil water content in Natural Bridges. Topmost panel depicts the historical mean from 1980−2018. Lower four panels show the emission scenarios of RCP 4.5 and RCP 8.5 at near−term and long−term timeframes. Bottom four panels depict the change from the historical mean; cross hatching denotes areas of robust predicitons (90% of models agree in the direction of change).

Natural Bridges: Fall soil water content

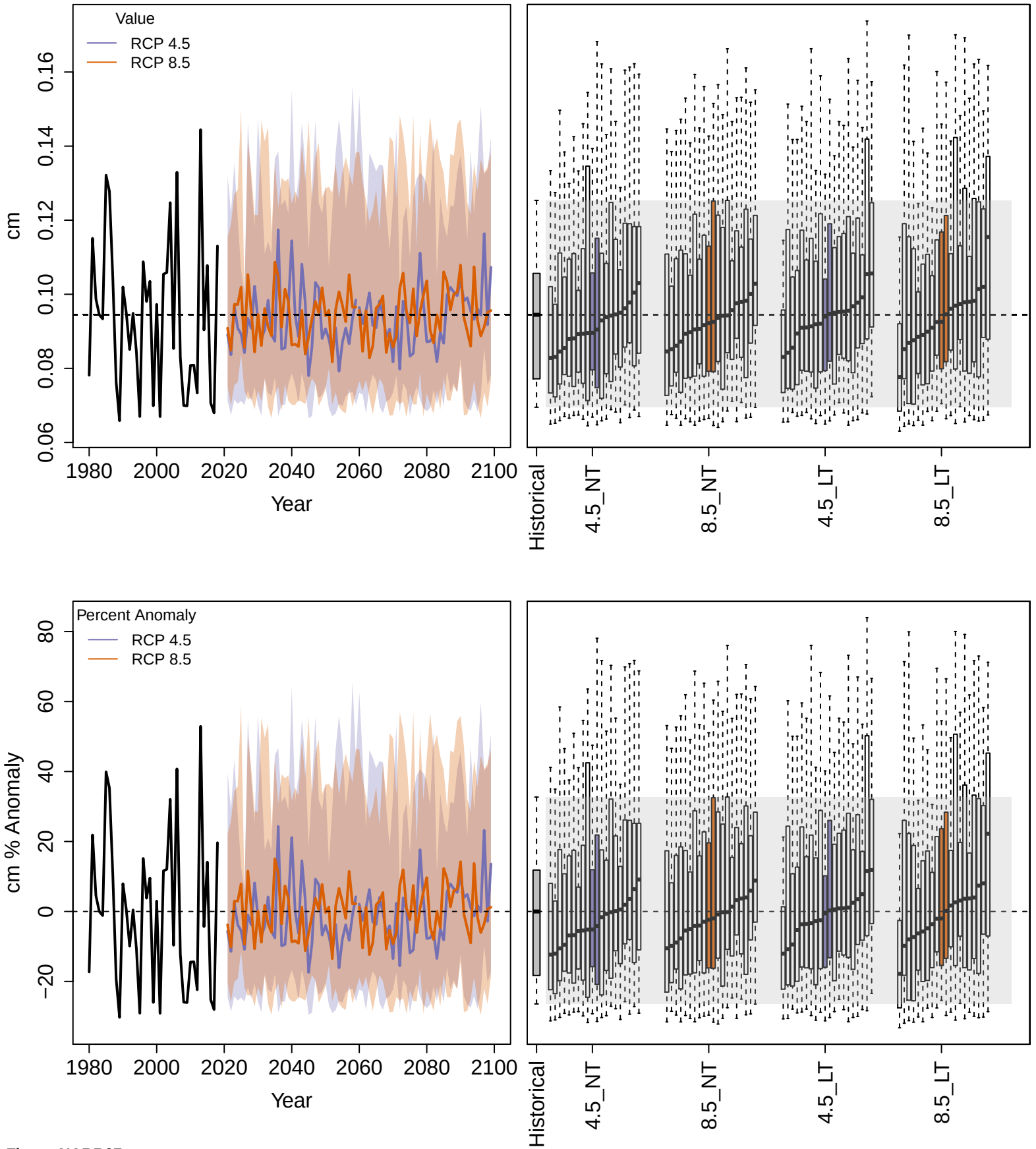


Figure NABR67:
Past trends and future trajectories of park−wide mean values for Fall soil water content in Natural Bridges. Top panels show values, bottom panels show changes from the long−term historical mean. Left: Time series of historical (black) and future projections for RCP 4.5 and 8.5. Shaded areas show spread among climate models. Right: Boxplots of temporal variability over 40−year periods under historical (left box) and individual climate models under two RCPs. Right: Historical time period is 1970−2010; near−term (NT) is 2020−2060; long−term (LT) is 2061−2100.

Natural Bridges: Fall soil water content

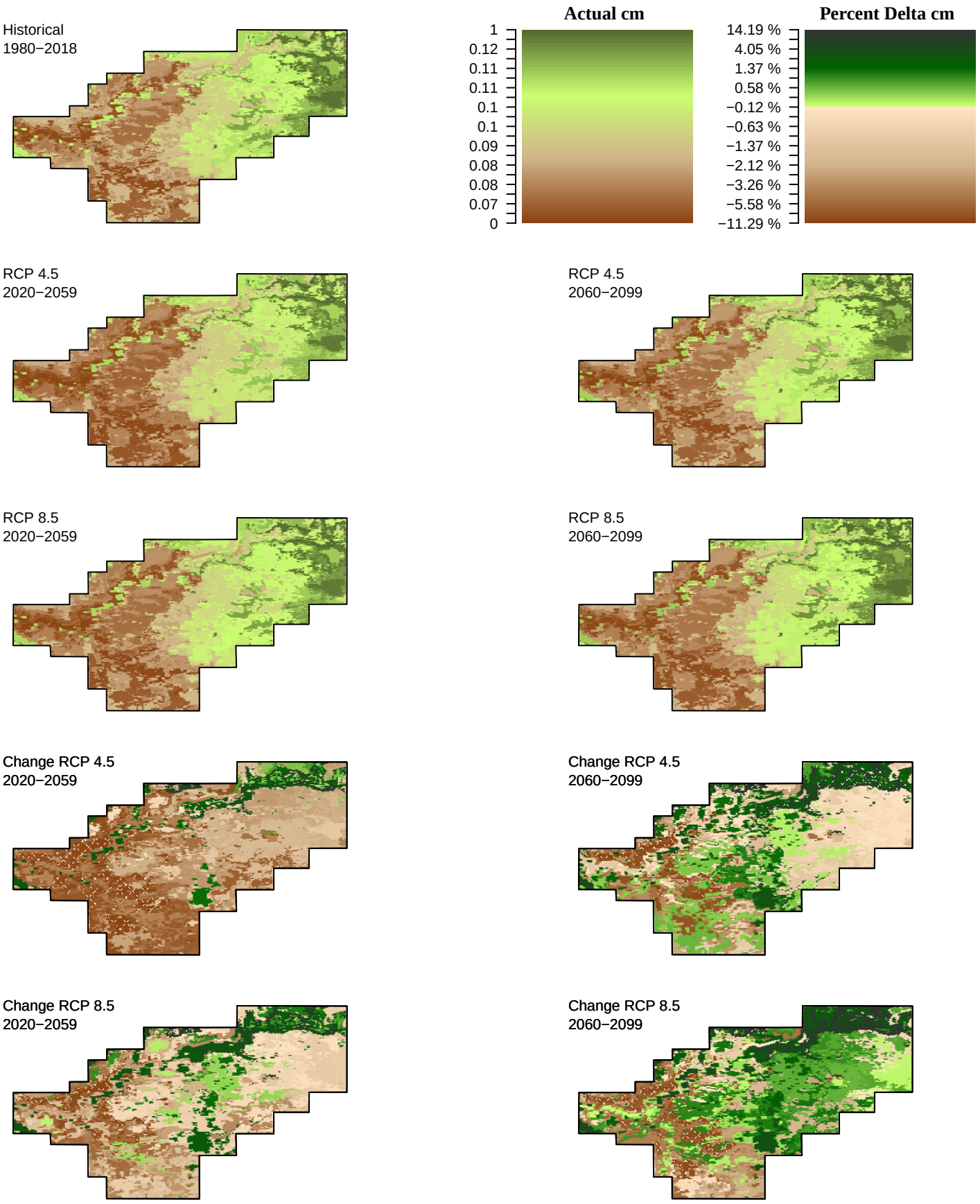


Figure NABRmap67:
Past trends and future trajectories of park−wide mean values for Fall soil water content in Natural Bridges. Topmost panel depicts the historical mean from 1980−2018. Lower four panels show the emission scenarios of RCP 4.5 and RCP 8.5 at near−term and long−term timeframes. Bottom four panels depict the change from the historical mean; cross hatching denotes areas of robust predicitons (90% of models agree in the direction of change).

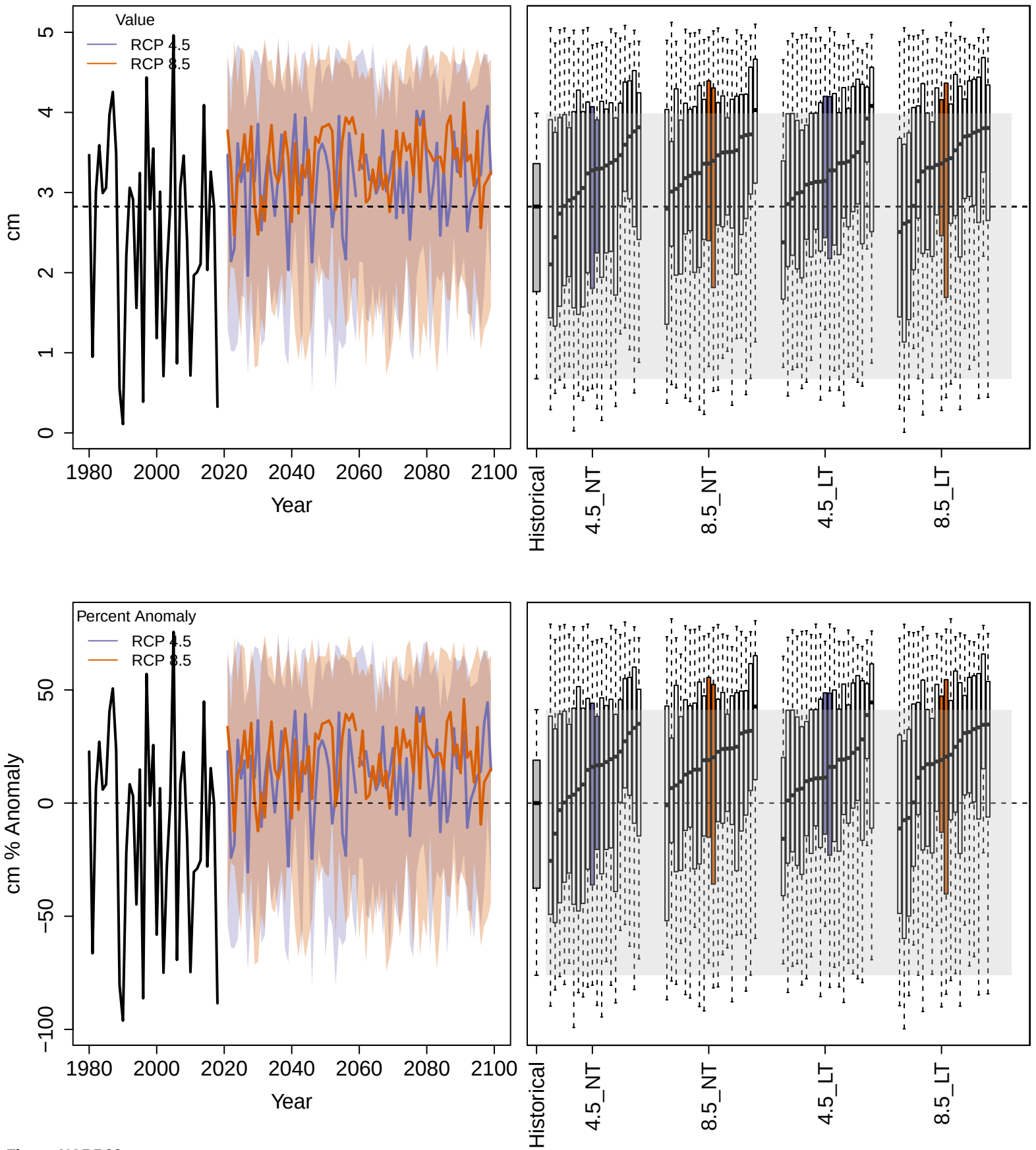


Figure NABR69:
Past trends and future trajectories of park−wide mean values for Winter available soil moisture: top 50cm in Natural Bridges. Top panels show values, bottom panels show changes from the long−term historical mean. Left: Time series of historical (black) and future projections for RCP 4.5 and 8.5. Shaded areas show spread among climate models. Right: Boxplots of temporal variability over 40−year periods under historical (left box) and individual climate models under two RCPs. Right: Historical time period is 1970−2010; near−term (NT) is 2020−2060; long−term (LT) is 2061−2100.

Natural Bridges: Winter available soil moisture: top 50cm

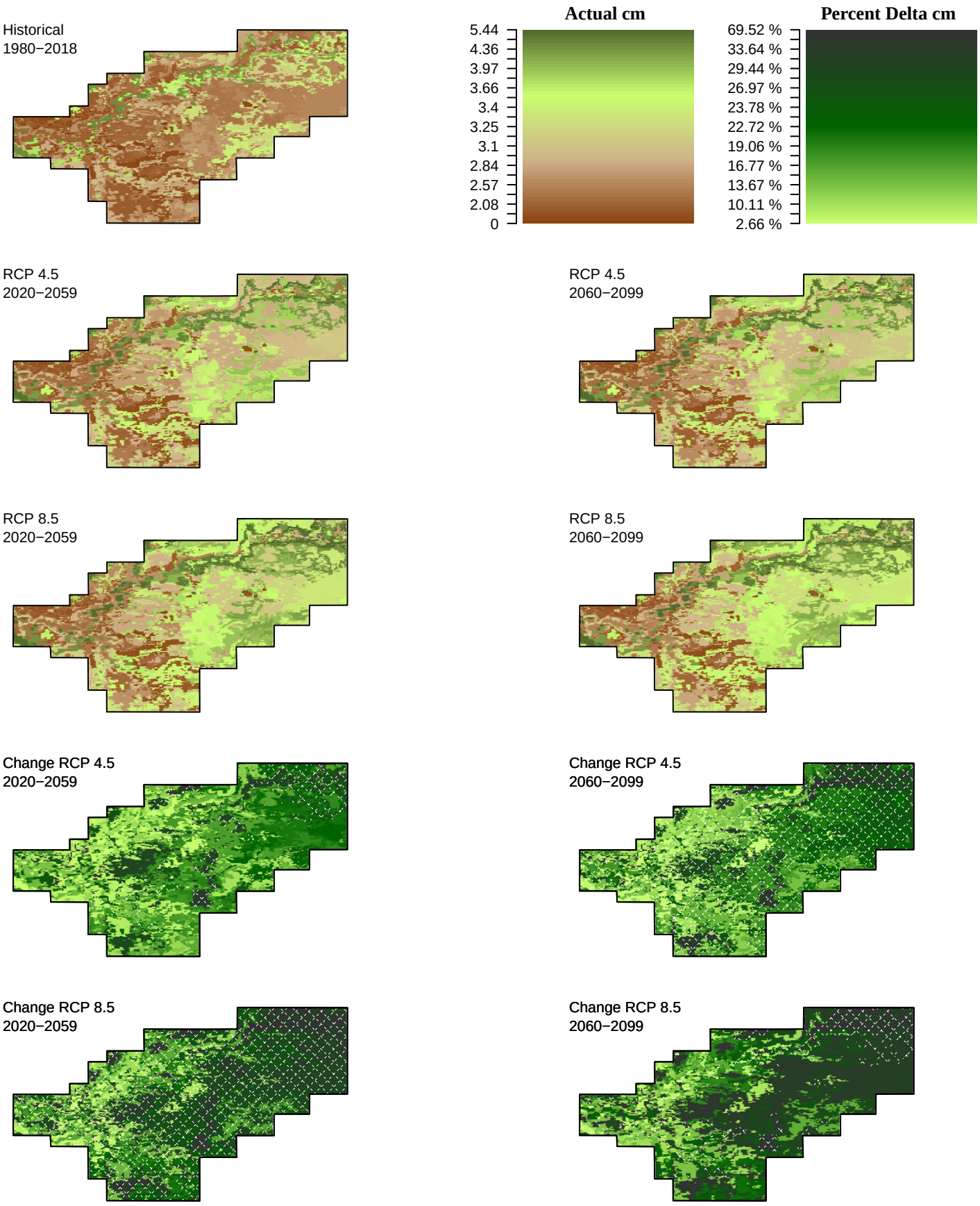


Figure NABRmap69:
Past trends and future trajectories of park−wide mean values for Winter available soil moisture: top 50cm in Natural Bridges. Topmost panel depicts the historical mean from 1980−2018. Lower four panels show the emission scenarios of RCP 4.5 and RCP 8.5 at near−term and long−term timeframes. Bottom four panels depict the change from the historical mean; cross hatching denotes areas of robust predicitons (90% of models agree in the direction of change).

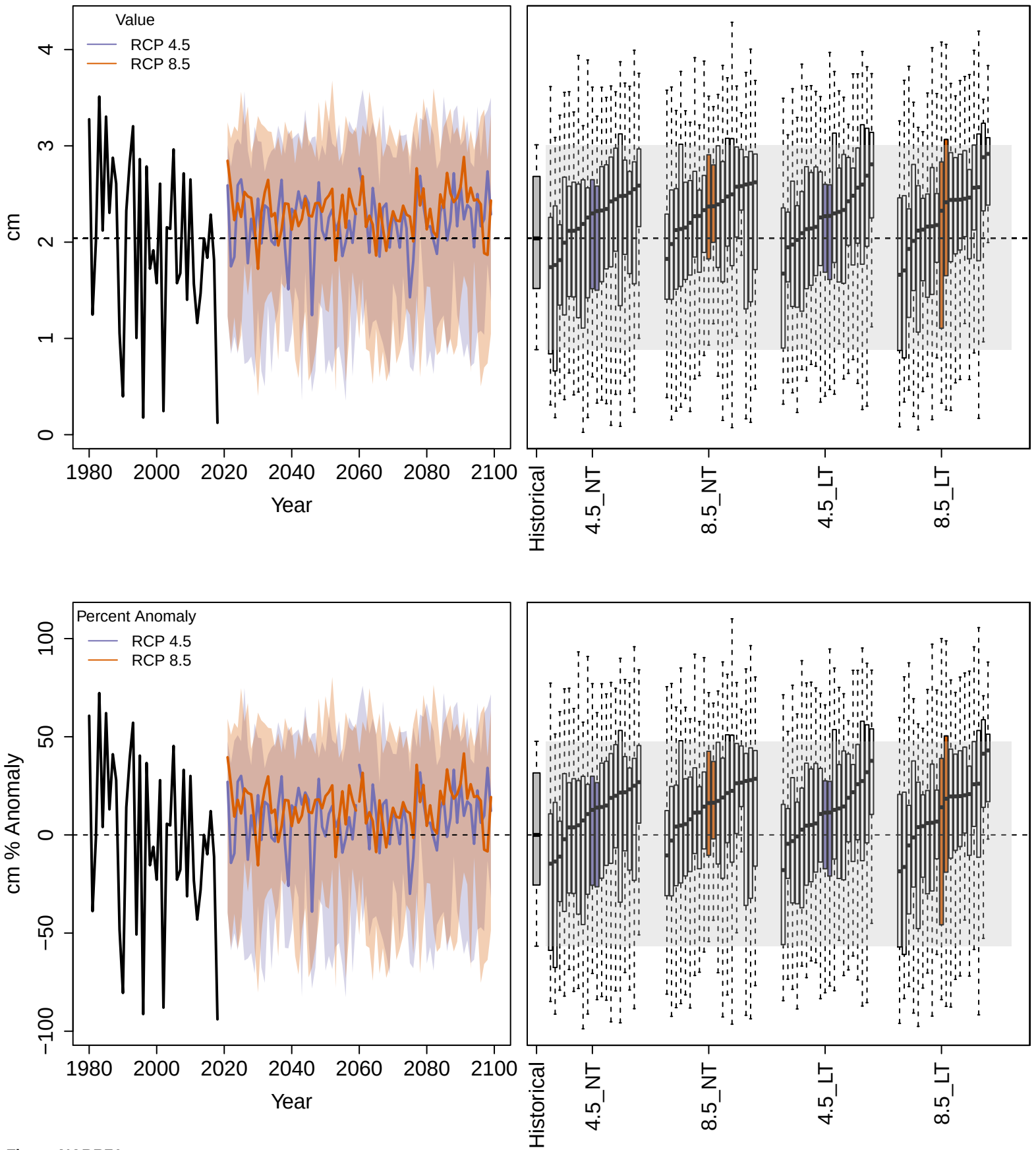


Figure NABR71:
Past trends and future trajectories of park−wide mean values for Spring available soil moisture: top 50cm in Natural Bridges. Top panels show values, bottom panels show changes from the long−term historical mean. Left: Time series of historical (black) and future projections for RCP 4.5 and 8.5. Shaded areas show spread among climate models. Right: Boxplots of temporal variability over 40−year periods under historical (left box) and individual climate models under two RCPs. Right: Historical time period is 1970−2010; near−term (NT) is 2020−2060; long−term (LT) is 2061−2100.

Natural Bridges: Spring available soil moisture: top 50cm

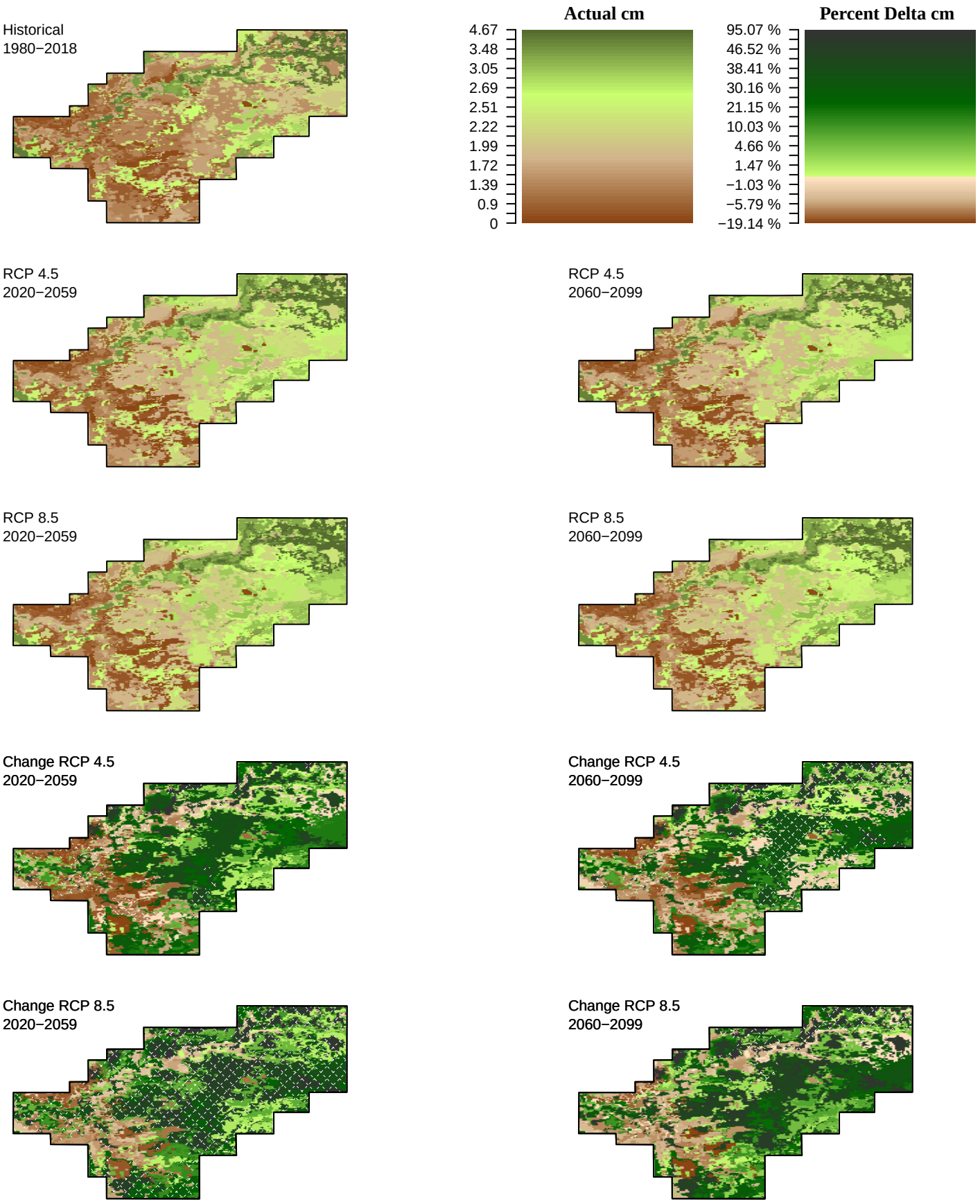


Figure NABRmap71:
Past trends and future trajectories of park−wide mean values for Spring available soil moisture: top 50cm in Natural Bridges. Topmost panel depicts the historical mean from 1980−2018. Lower four panels show the emission scenarios of RCP 4.5 and RCP 8.5 at near−term and long−term timeframes. Bottom four panels depict the change from the historical mean; cross hatching denotes areas of robust predicitons (90% of models agree in the direction of change).

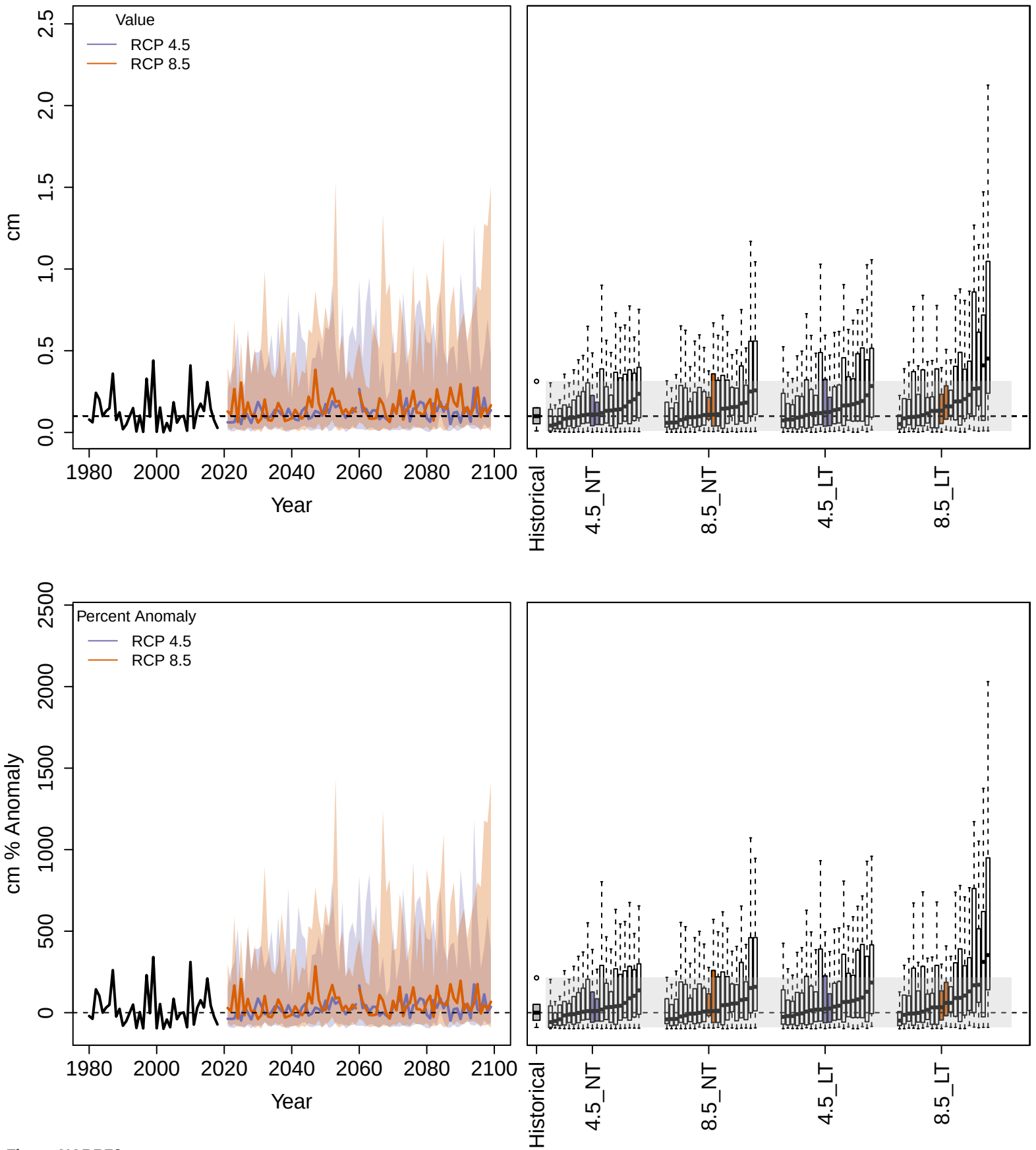


Figure NABR73:
Past trends and future trajectories of park−wide mean values for Summer available soil moisture: top 50cm in Natural Bridges. Top panels show values, bottom panels show changes from the long−term historical mean. Left: Time series of historical (black) and future projections for RCP 4.5 and 8.5. Shaded areas show spread among climate models. Right: Boxplots of temporal variability over 40−year periods under historical (left box) and individual climate models under two RCPs. Right: Historical time period is 1970−2010; near−term (NT) is 2020−2060; long−term (LT) is 2061−2100.

Natural Bridges: Summer available soil moisture: top 50cm

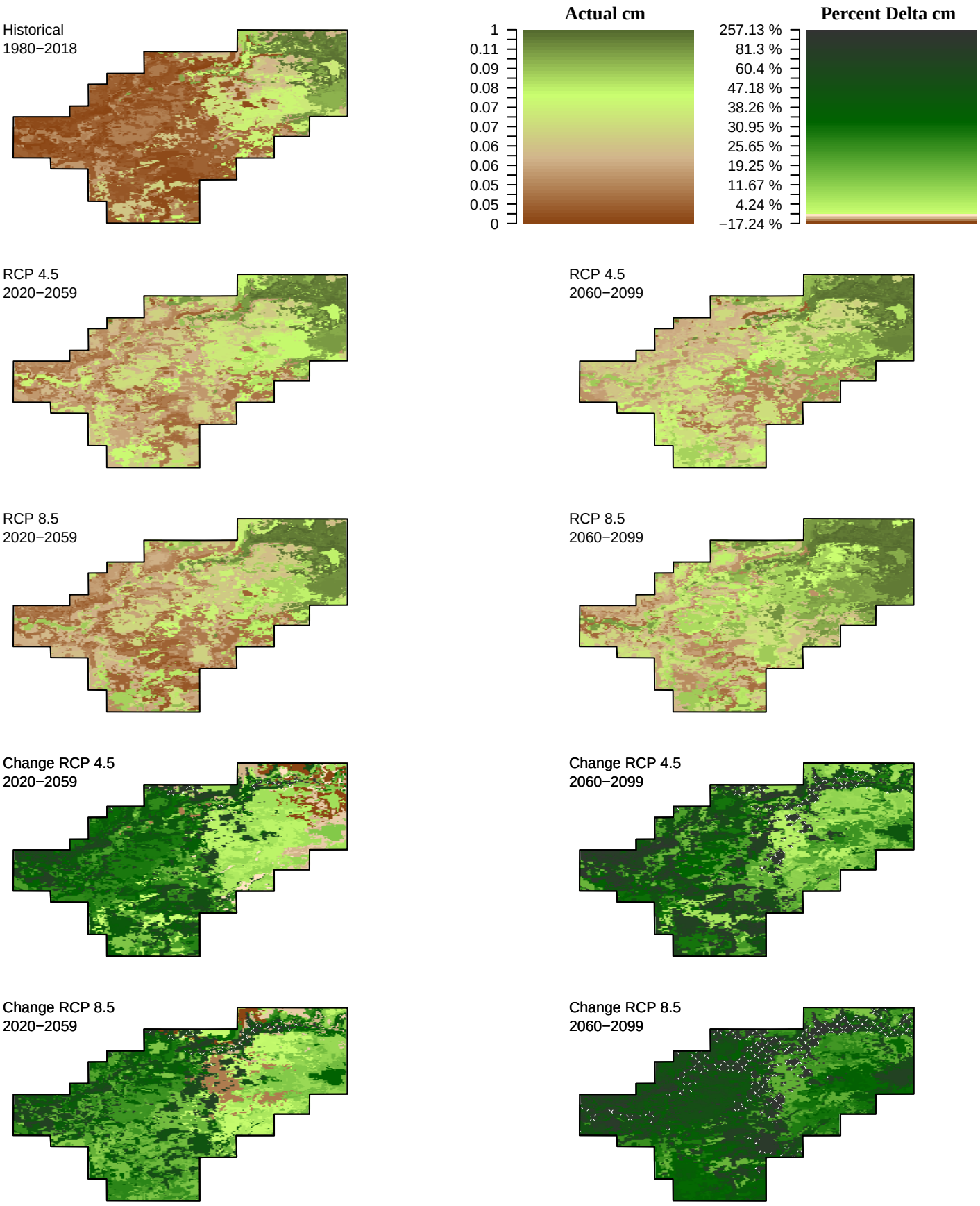


Figure NABRmap73:
Past trends and future trajectories of park−wide mean values for Summer available soil moisture: top 50cm in Natural Bridges. Topmost panel depicts the historical mean from 1980−2018. Lower four panels show the emission scenarios of RCP 4.5 and RCP 8.5 at near−term and long−term timeframes. Bottom four panels depict the change from the historical mean; cross hatching denotes areas of robust predicitons (90% of models agree in the direction of change).

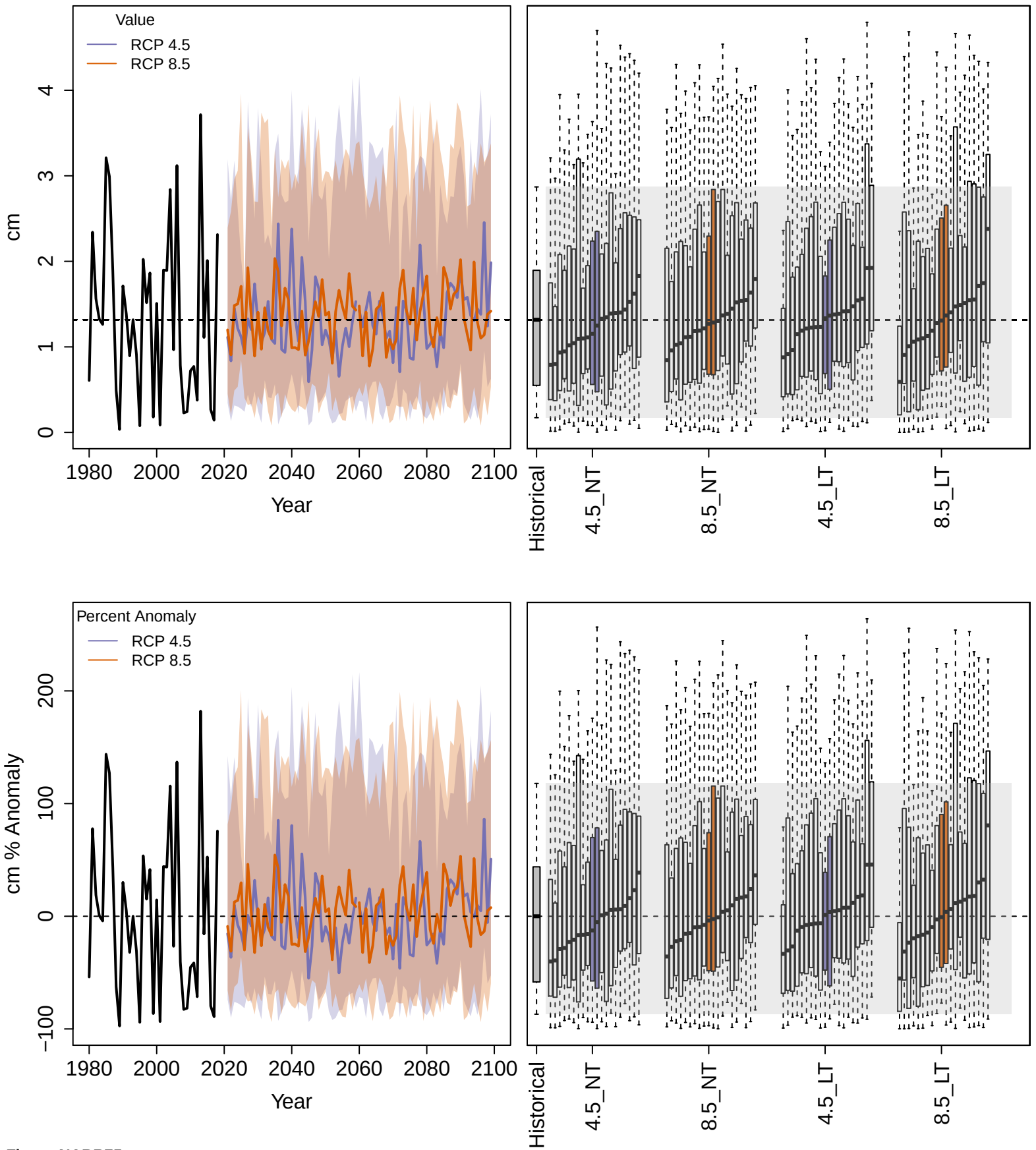


Figure NABR75:
Past trends and future trajectories of park−wide mean values for Fall available soil moisture: top 50cm in Natural Bridges. Top panels show values, bottom panels show changes from the long−term historical mean. Left: Time series of historical (black) and future projections for RCP 4.5 and 8.5. Shaded areas show spread among climate models. Right: Boxplots of temporal variability over 40−year periods under historical (left box) and individual climate models under two RCPs. Right: Historical time period is 1970−2010; near−term (NT) is 2020−2060; long−term (LT) is 2061−2100.

Natural Bridges: Fall available soil moisture: top 50cm

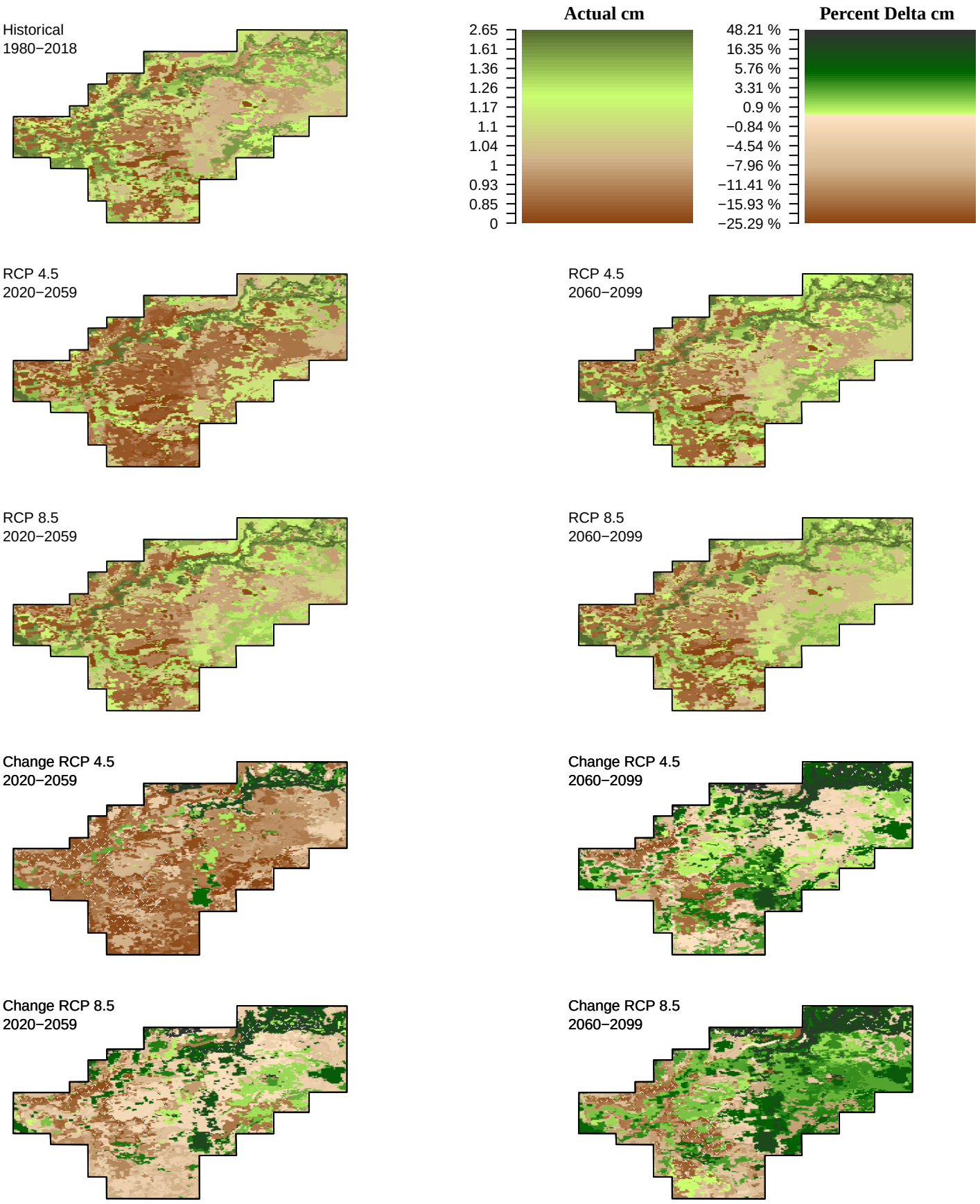


Figure NABRmap75:
Past trends and future trajectories of park−wide mean values for Fall available soil moisture: top 50cm in Natural Bridges. Topmost panel depicts the historical mean from 1980−2018. Lower four panels show the emission scenarios of RCP 4.5 and RCP 8.5 at near−term and long−term timeframes. Bottom four panels depict the change from the historical mean; cross hatching denotes areas of robust predicitons (90% of models agree in the direction of change).

Natural Bridges: Winter available soil moisture

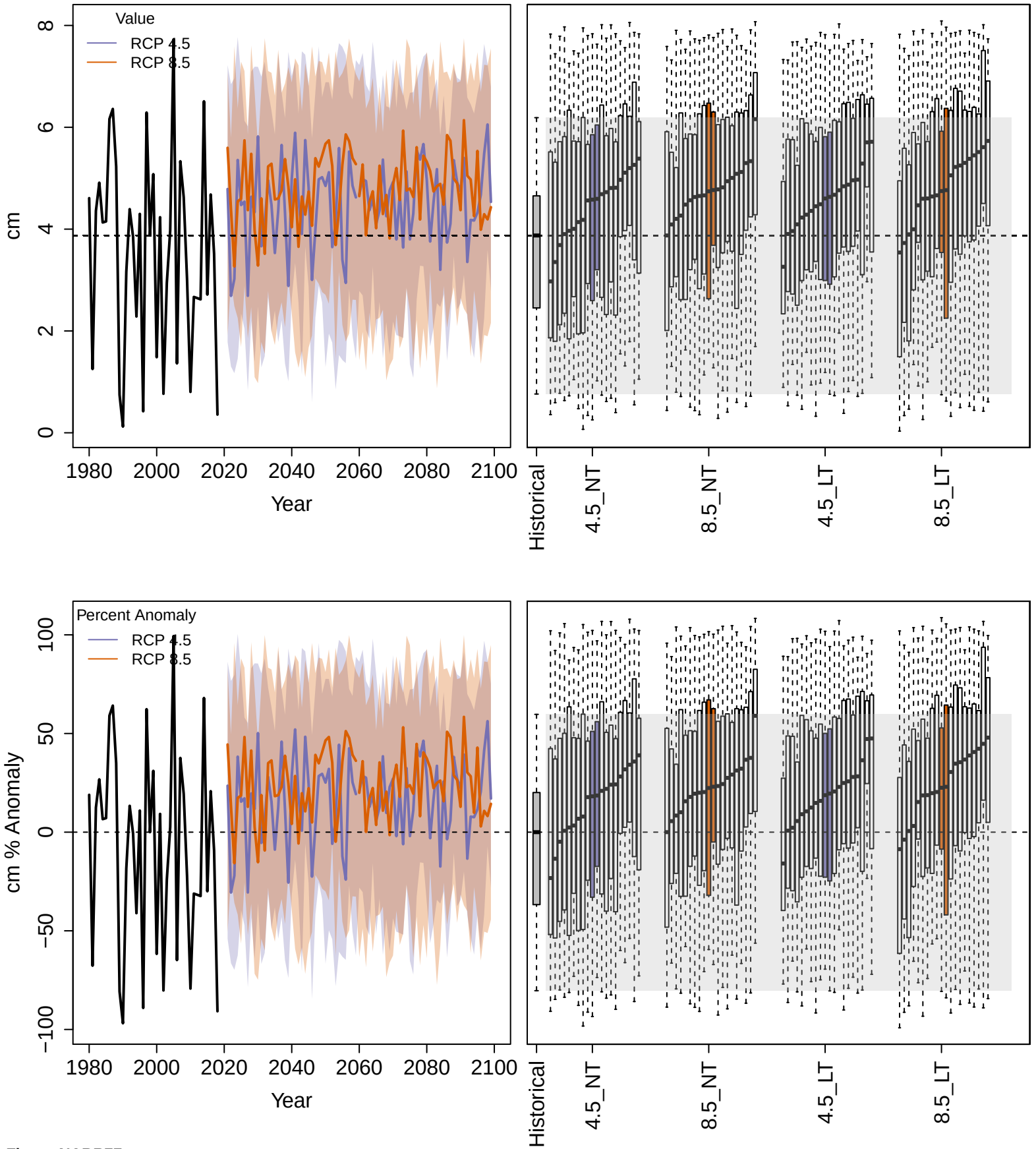


Figure NABR77:
Past trends and future trajectories of park−wide mean values for Winter available soil moisture in Natural Bridges. Top panels show values, bottom panels show changes from the long−term historical mean. Left: Time series of historical (black) and future projections for RCP 4.5 and 8.5. Shaded areas show spread among climate models. Right: Boxplots of temporal variability over 40−year periods under historical (left box) and individual climate models under two RCPs. Right: Historical time period is 1970−2010; near−term (NT) is 2020−2060; long−term (LT) is 2061−2100.

Natural Bridges: Winter available soil moisture

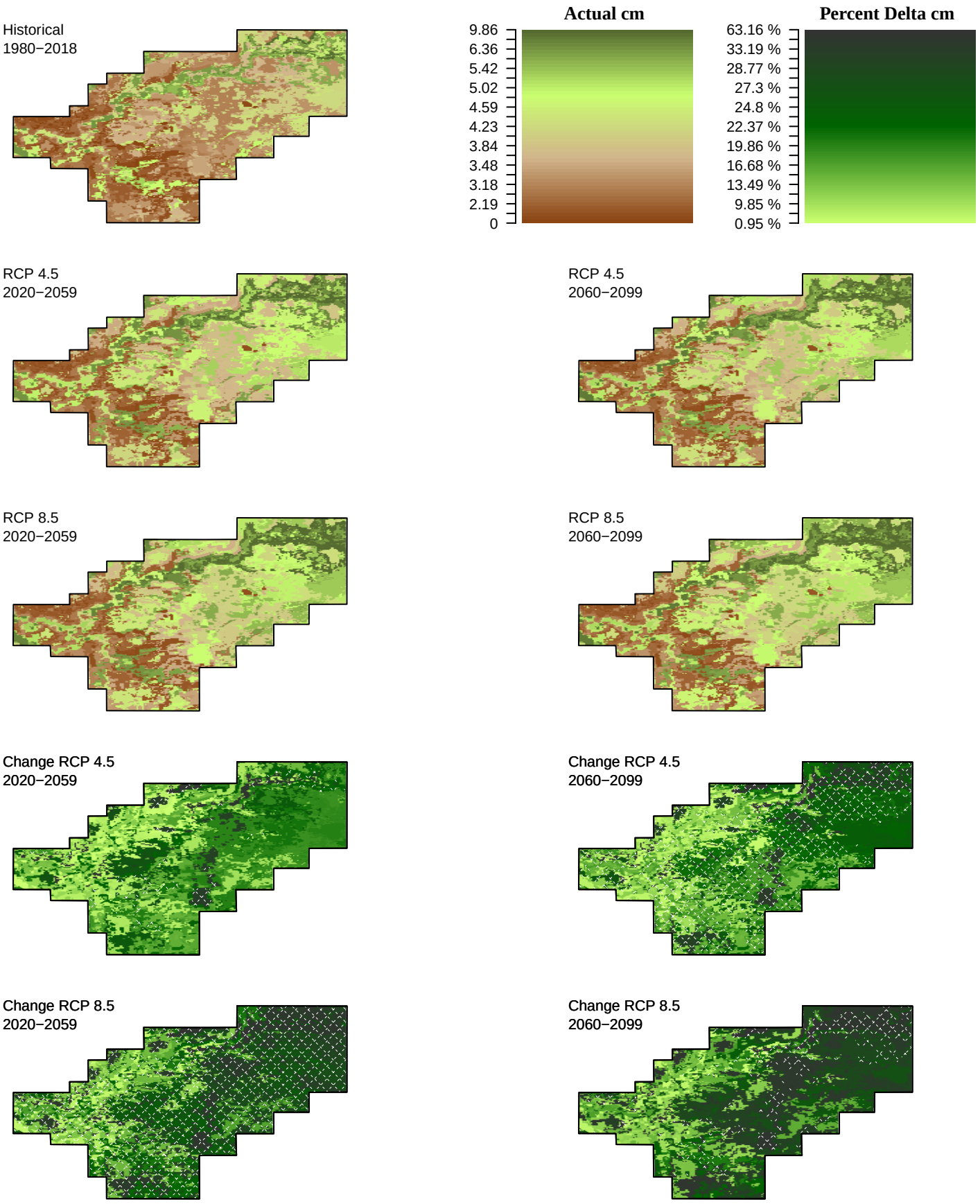


Figure NABRmap77:
Past trends and future trajectories of park−wide mean values for Winter available soil moisture in Natural Bridges. Topmost panel depicts the historical mean from 1980−2018. Lower four panels show the emission scenarios of RCP 4.5 and RCP 8.5 at near−term and long−term timeframes. Bottom four panels depict the change from the historical mean; cross hatching denotes areas of robust predicitons (90% of models agree in the direction of change).

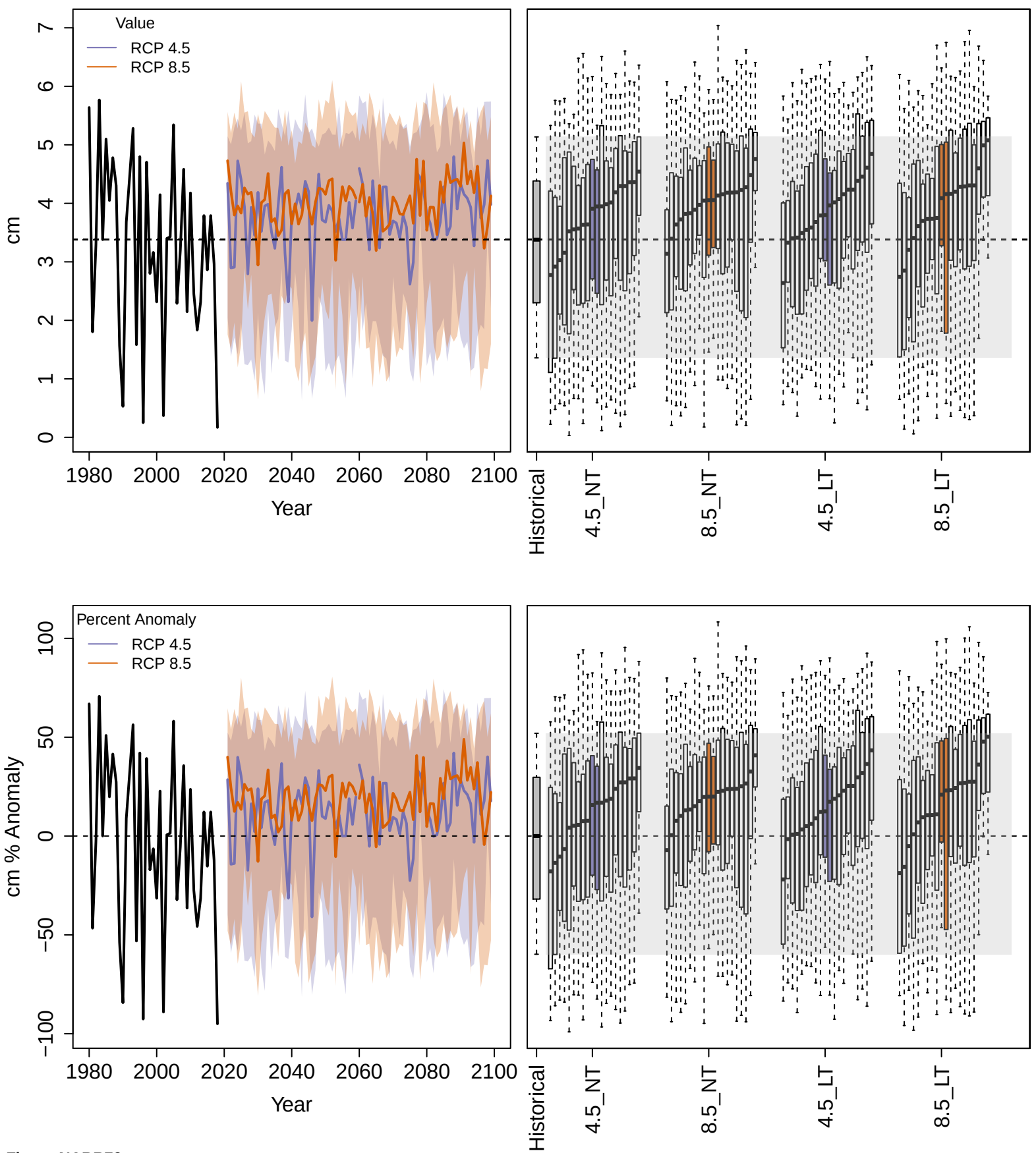


Figure NABR79:
Past trends and future trajectories of park−wide mean values for Spring available soil moisture in Natural Bridges. Top panels show values, bottom panels show changes from the long−term historical mean. Left: Time series of historical (black) and future projections for RCP 4.5 and 8.5. Shaded areas show spread among climate models. Right: Boxplots of temporal variability over 40−year periods under historical (left box) and individual climate models under two RCPs. Right: Historical time period is 1970−2010; near−term (NT) is 2020−2060; long−term (LT) is 2061−2100.

Natural Bridges: Spring available soil moisture

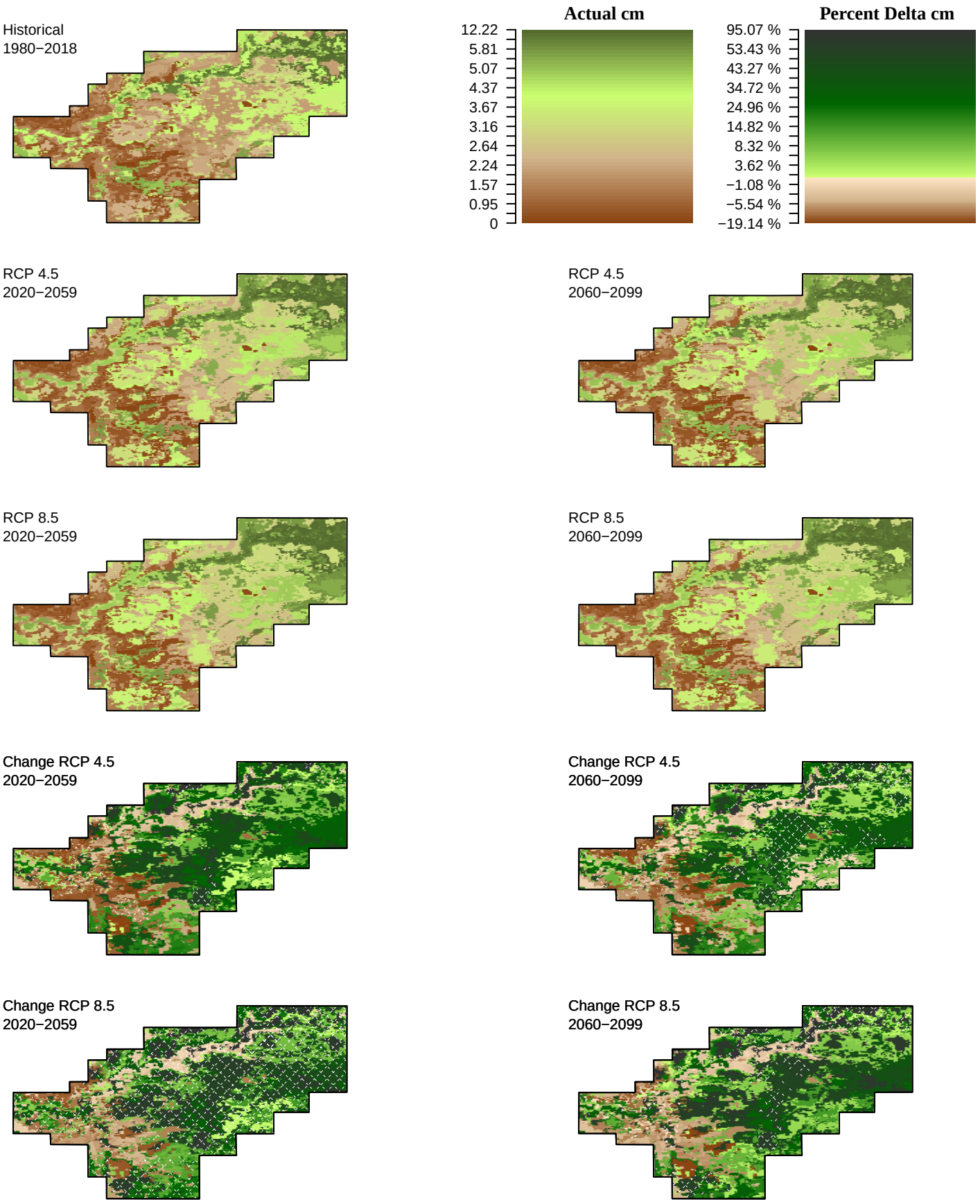


Figure NABRmap79:
Past trends and future trajectories of park−wide mean values for Spring available soil moisture in Natural Bridges. Topmost panel depicts the historical mean from 1980−2018. Lower four panels show the emission scenarios of RCP 4.5 and RCP 8.5 at near−term and long−term timeframes. Bottom four panels depict the change from the historical mean; cross hatching denotes areas of robust predicitons (90% of models agree in the direction of change).

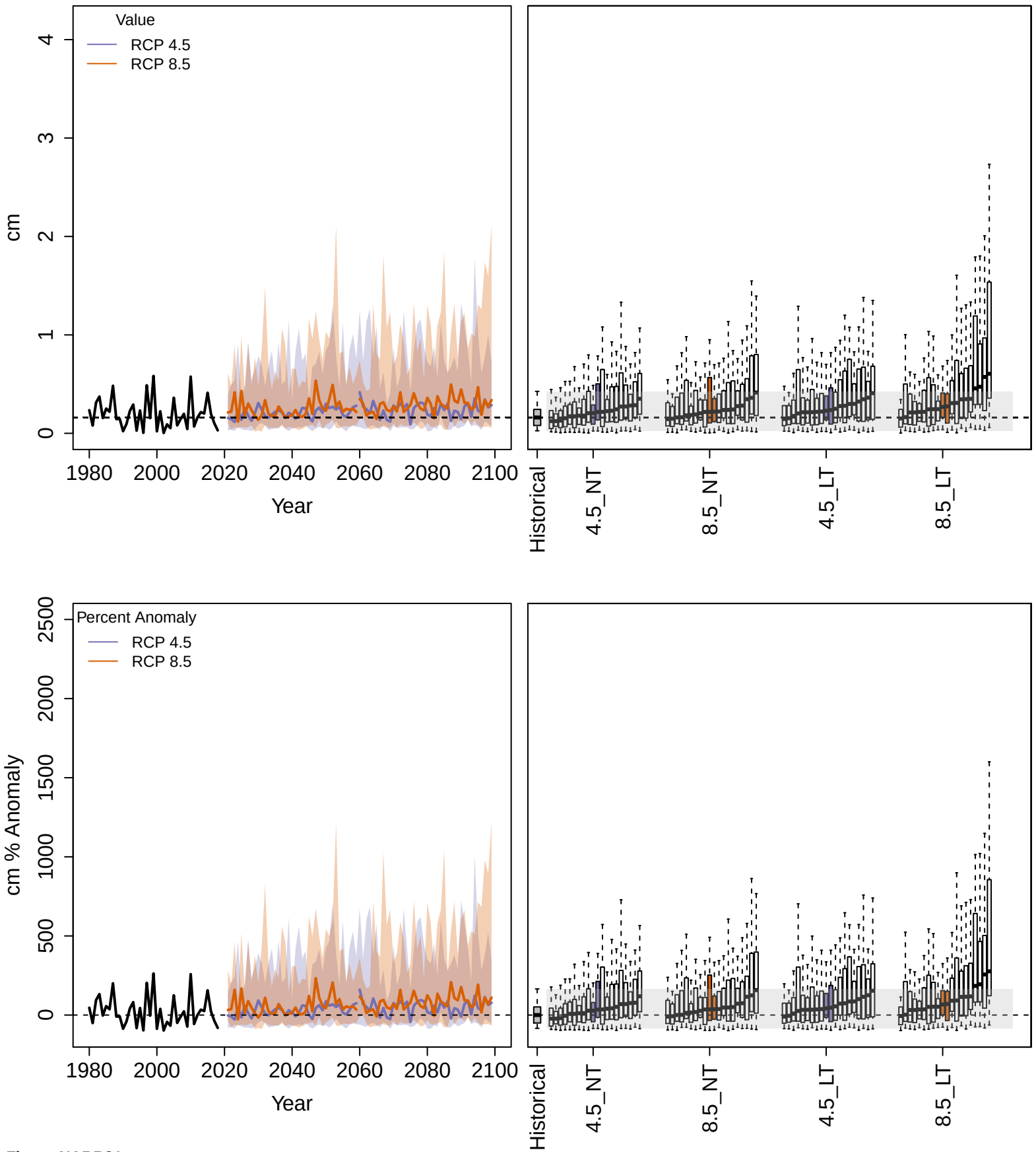


Figure NABR81:
Past trends and future trajectories of park−wide mean values for Summer available soil moisture in Natural Bridges. Top panels show values, bottom panels show changes from the long−term historical mean. Left: Time series of historical (black) and future projections for RCP 4.5 and 8.5. Shaded areas show spread among climate models. Right: Boxplots of temporal variability over 40−year periods under historical (left box) and individual climate models under two RCPs. Right: Historical time period is 1970−2010; near−term (NT) is 2020−2060; long−term (LT) is 2061−2100.

Natural Bridges: Summer available soil moisture

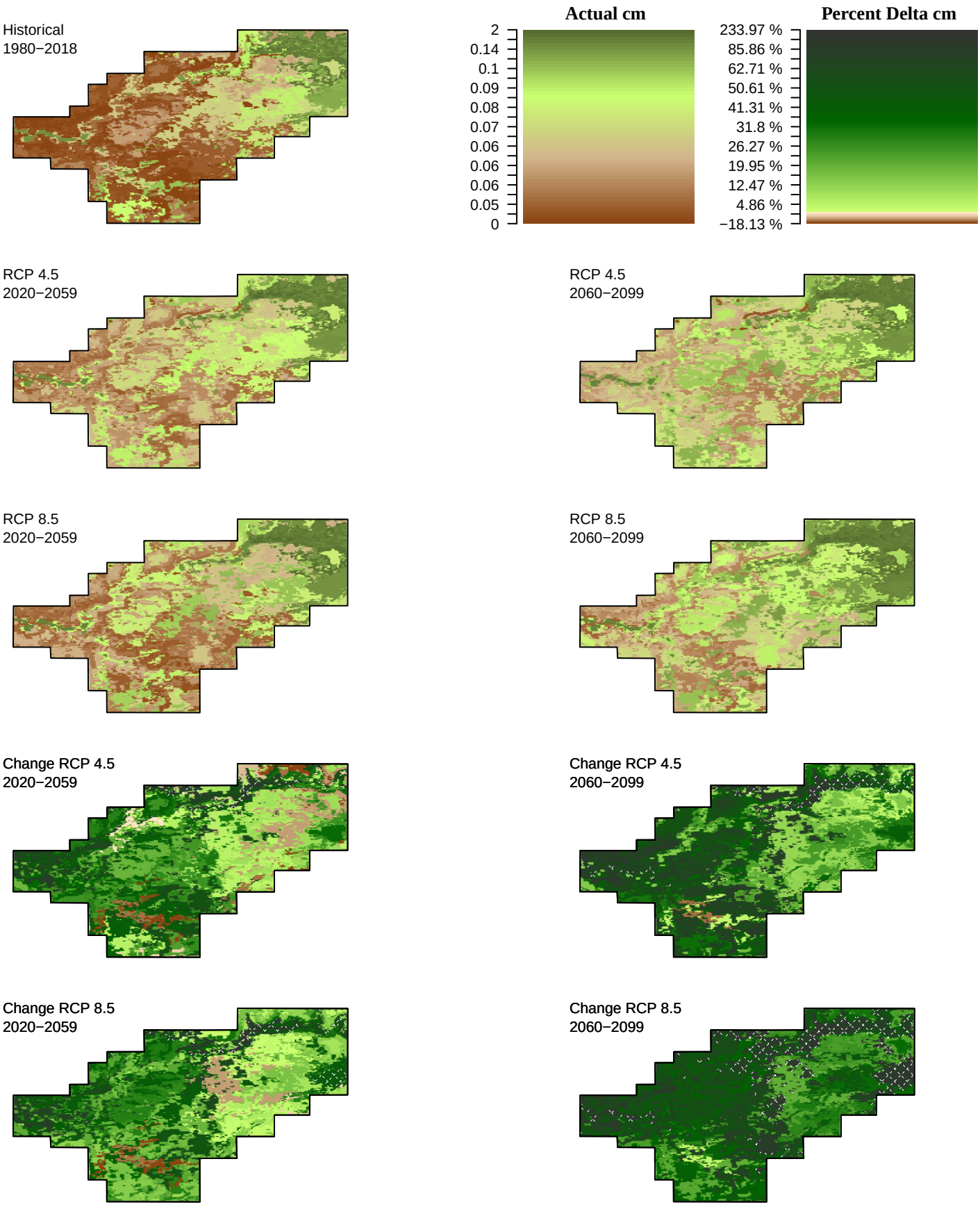


Figure NABRmap81:
Past trends and future trajectories of park−wide mean values for Summer available soil moisture in Natural Bridges. Topmost panel depicts the historical mean from 1980−2018. Lower four panels show the emission scenarios of RCP 4.5 and RCP 8.5 at near−term and long−term timeframes. Bottom four panels depict the change from the historical mean; cross hatching denotes areas of robust predicitons (90% of models agree in the direction of change).

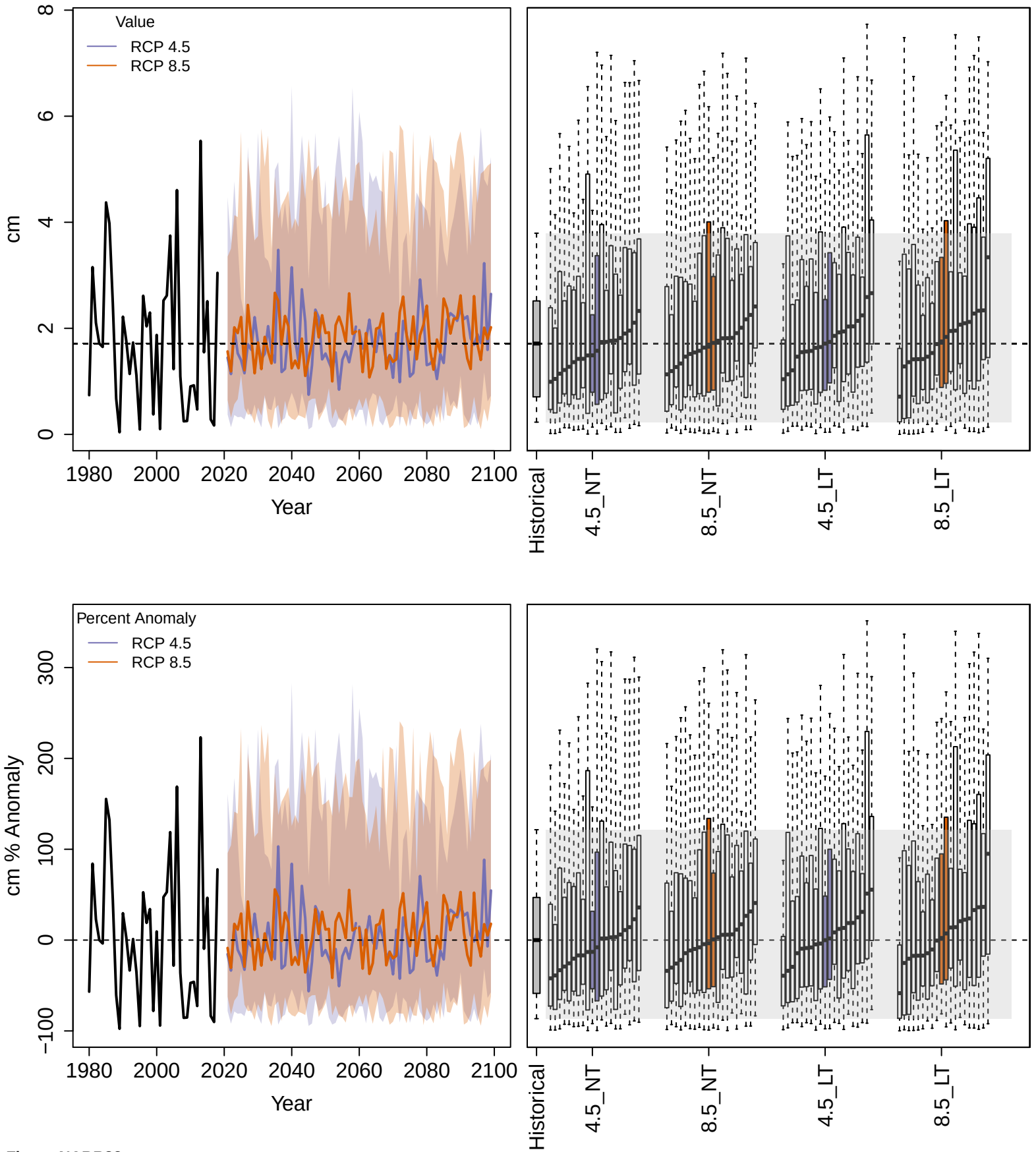


Figure NABR83:
Past trends and future trajectories of park−wide mean values for Fall available soil moisture in Natural Bridges. Top panels show values, bottom panels show changes from the long−term historical mean. Left: Time series of historical (black) and future projections for RCP 4.5 and 8.5. Shaded areas show spread among climate models. Right: Boxplots of temporal variability over 40−year periods under historical (left box) and individual climate models under two RCPs. Right: Historical time period is 1970−2010; near−term (NT) is 2020−2060; long−term (LT) is 2061−2100.

Natural Bridges: Fall available soil moisture

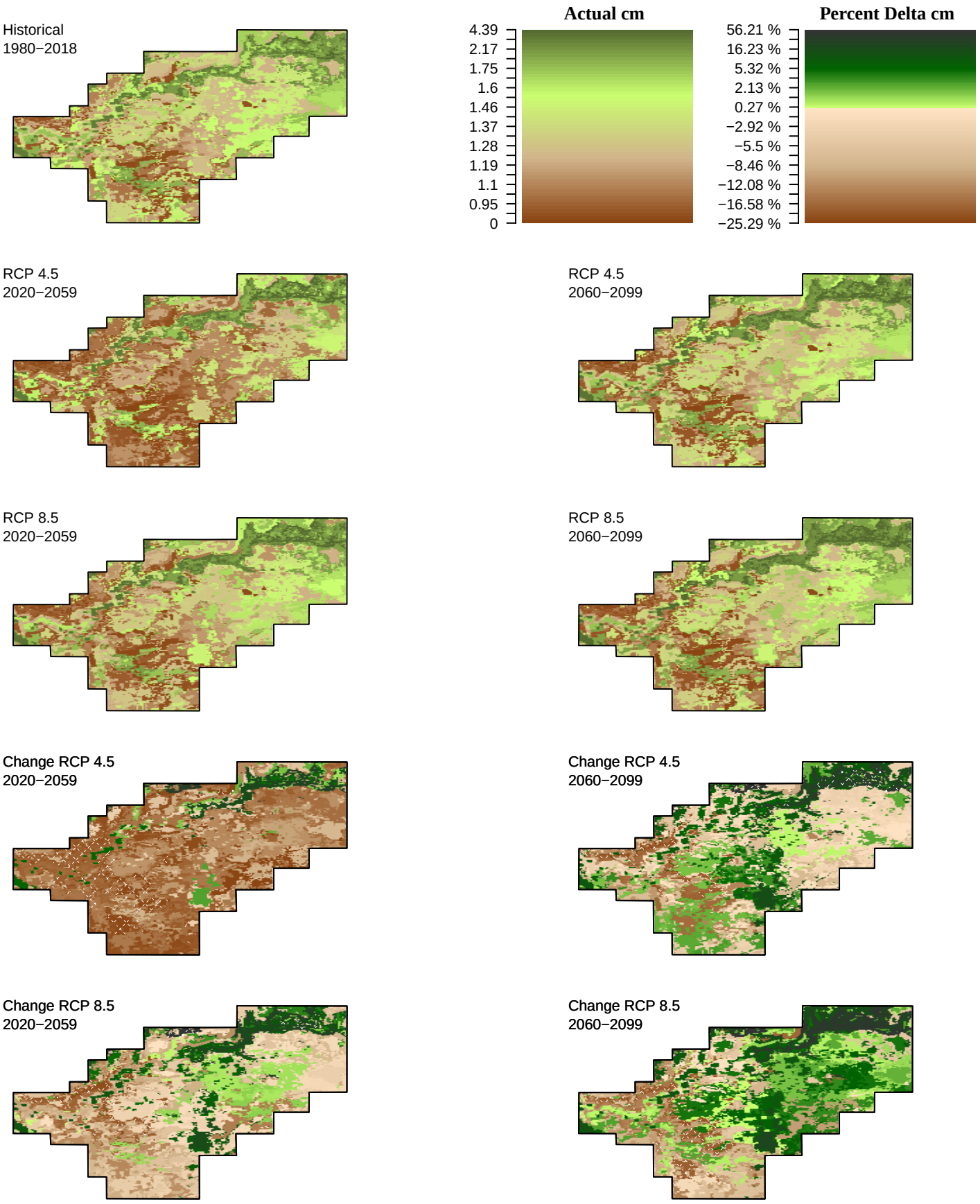


Figure NABRmap83:
Past trends and future trajectories of park−wide mean values for Fall available soil moisture in Natural Bridges. Topmost panel depicts the historical mean from 1980−2018. Lower four panels show the emission scenarios of RCP 4.5 and RCP 8.5 at near−term and long−term timeframes. Bottom four panels depict the change from the historical mean; cross hatching denotes areas of robust predicitons (90% of models agree in the direction of change).

Natural Bridges: Winter wet soil days

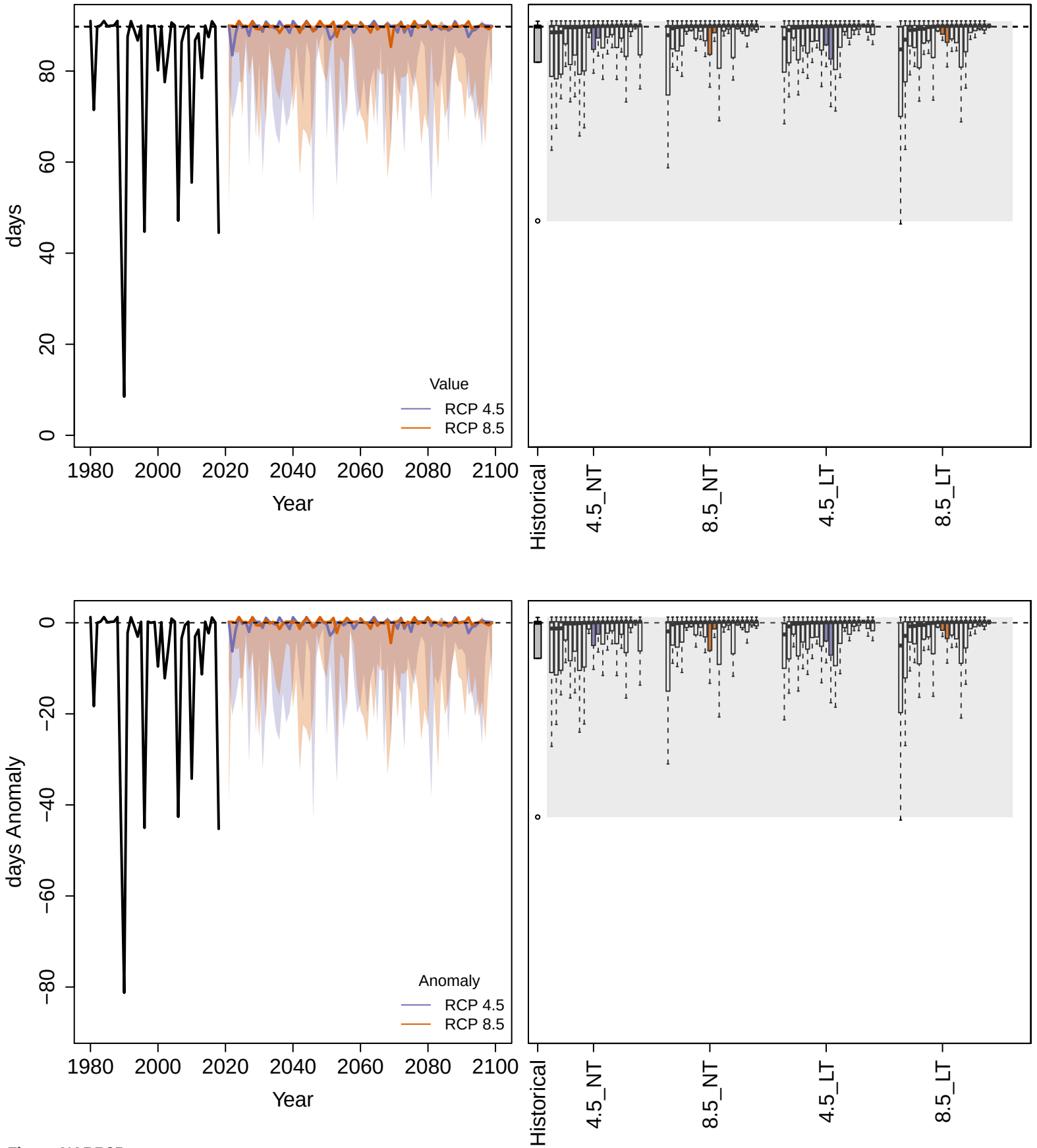


Figure NABR85:
Past trends and future trajectories of park−wide mean values for Winter wet soil days in Natural Bridges. Top panels show values, bottom panels show changes from the long−term historical mean. Left: Time series of historical (black) and future projections for RCP 4.5 and 8.5. Shaded areas show spread among climate models. Right: Boxplots of temporal variability over 40−year periods under historical (left box) and individual climate models under two RCPs. Right: Historical time period is 1970−2010; near−term (NT) is 2020−2060; long−term (LT) is 2061−2100.

Natural Bridges: Winter wet soil days

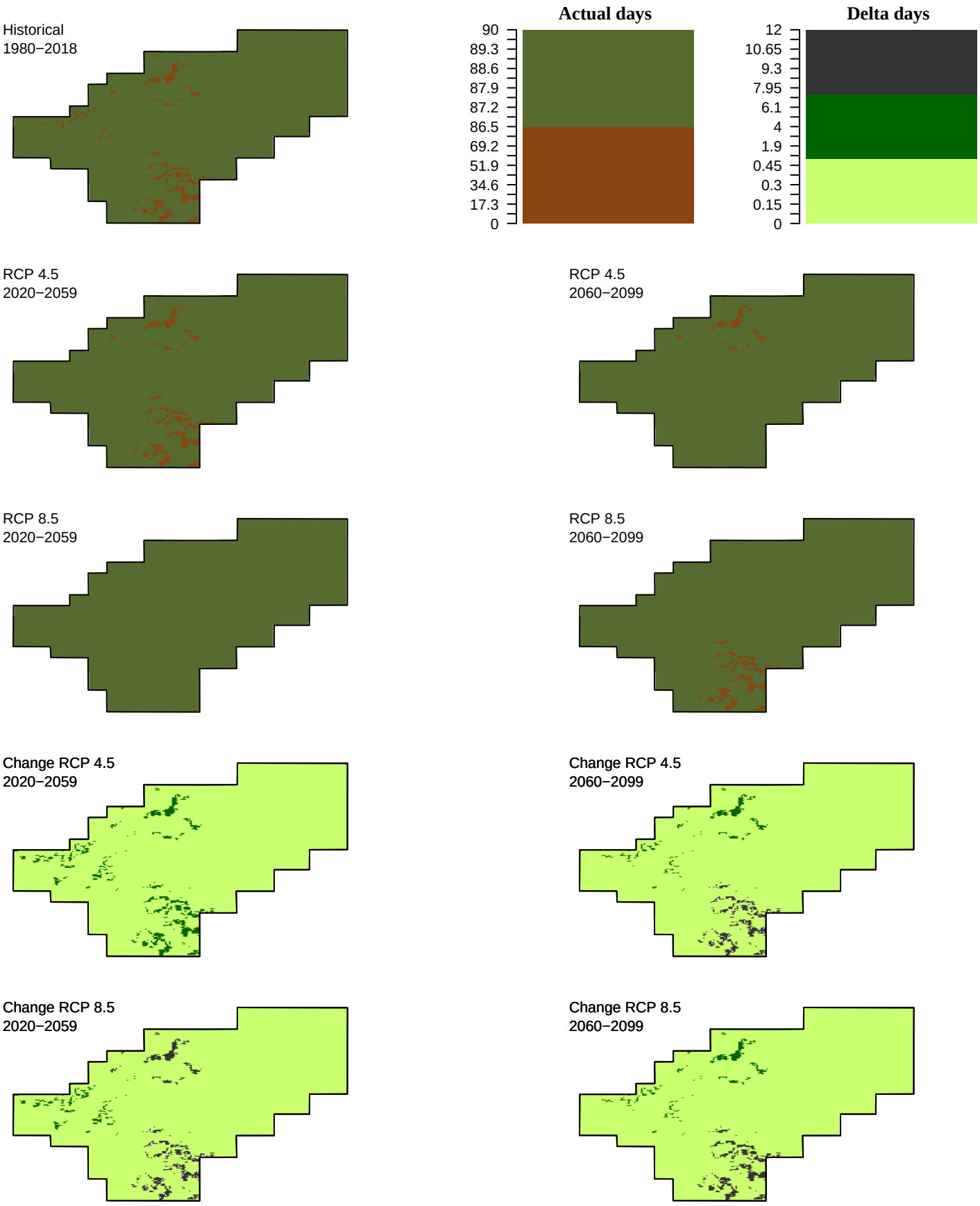


Figure NABRmap85:
Past trends and future trajectories of park−wide mean values for Winter wet soil days in Natural Bridges. Topmost panel depicts the historical mean from 1980−2018. Lower four panels show the emission scenarios of RCP 4.5 and RCP 8.5 at near−term and long−term timeframes. Bottom four panels depict the change from the historical mean; cross hatching denotes areas of robust predicitons (90% of models agree in the direction of change).

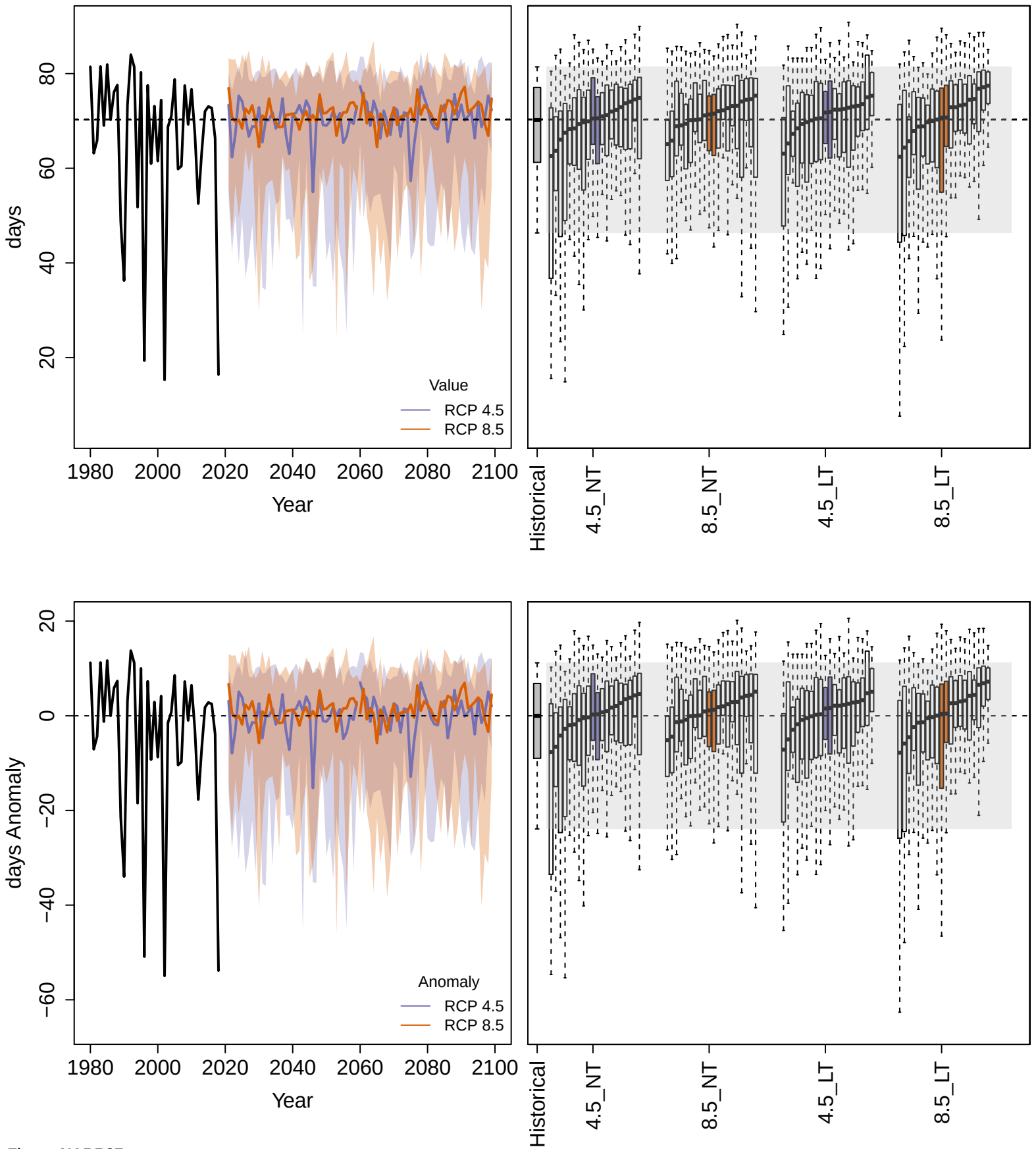


Figure NABR87:
Past trends and future trajectories of park−wide mean values for Spring wet soil days in Natural Bridges. Top panels show values, bottom panels show changes from the long−term historical mean. Left: Time series of historical (black) and future projections for RCP 4.5 and 8.5. Shaded areas show spread among climate models. Right: Boxplots of temporal variability over 40−year periods under historical (left box) and individual climate models under two RCPs. Right: Historical time period is 1970−2010; near−term (NT) is 2020−2060; long−term (LT) is 2061−2100.

Natural Bridges: Spring wet soil days

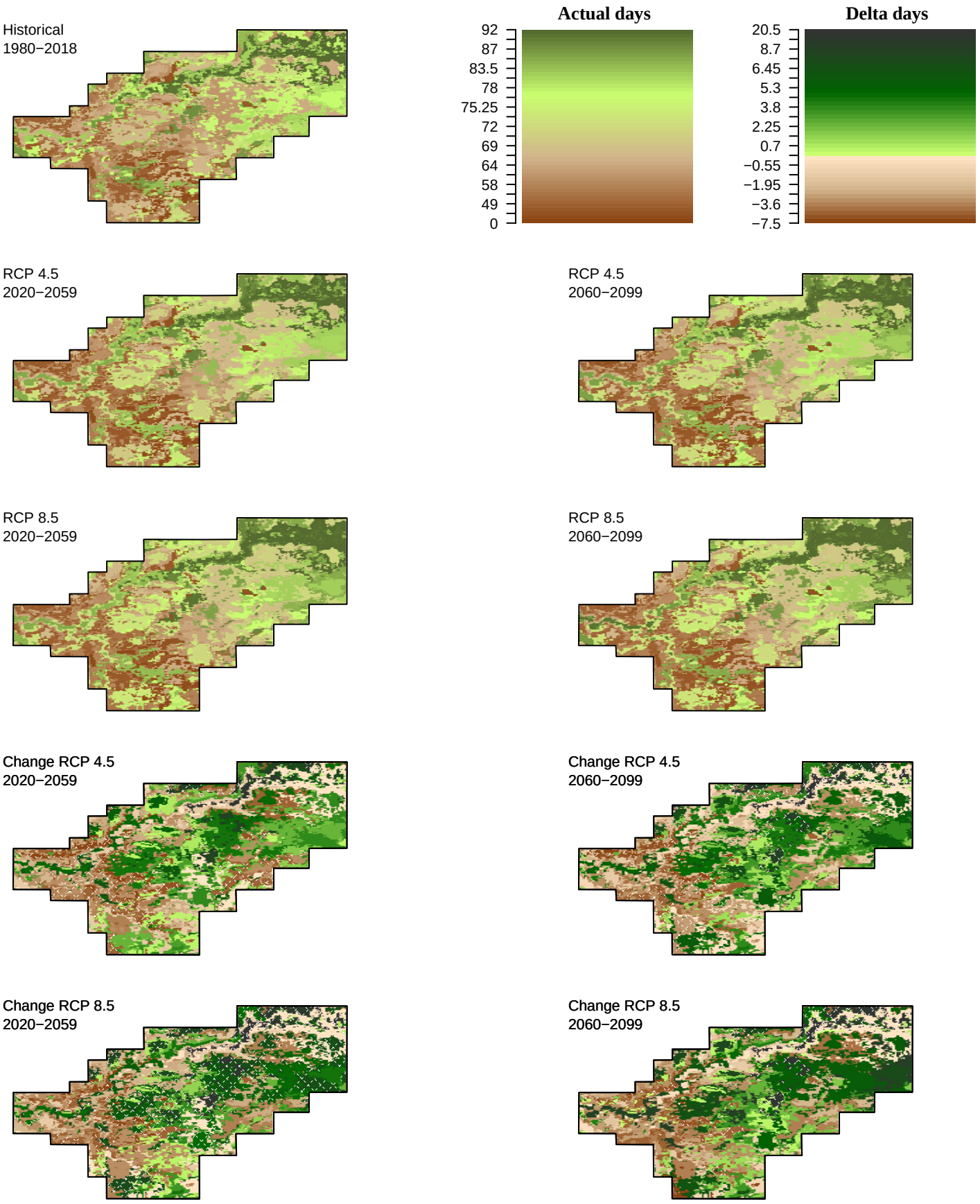


Figure NABRmap87:
Past trends and future trajectories of park−wide mean values for Spring wet soil days in Natural Bridges. Topmost panel depicts the historical mean from 1980−2018. Lower four panels show the emission scenarios of RCP 4.5 and RCP 8.5 at near−term and long−term timeframes. Bottom four panels depict the change from the historical mean; cross hatching denotes areas of robust predicitons (90% of models agree in the direction of change).

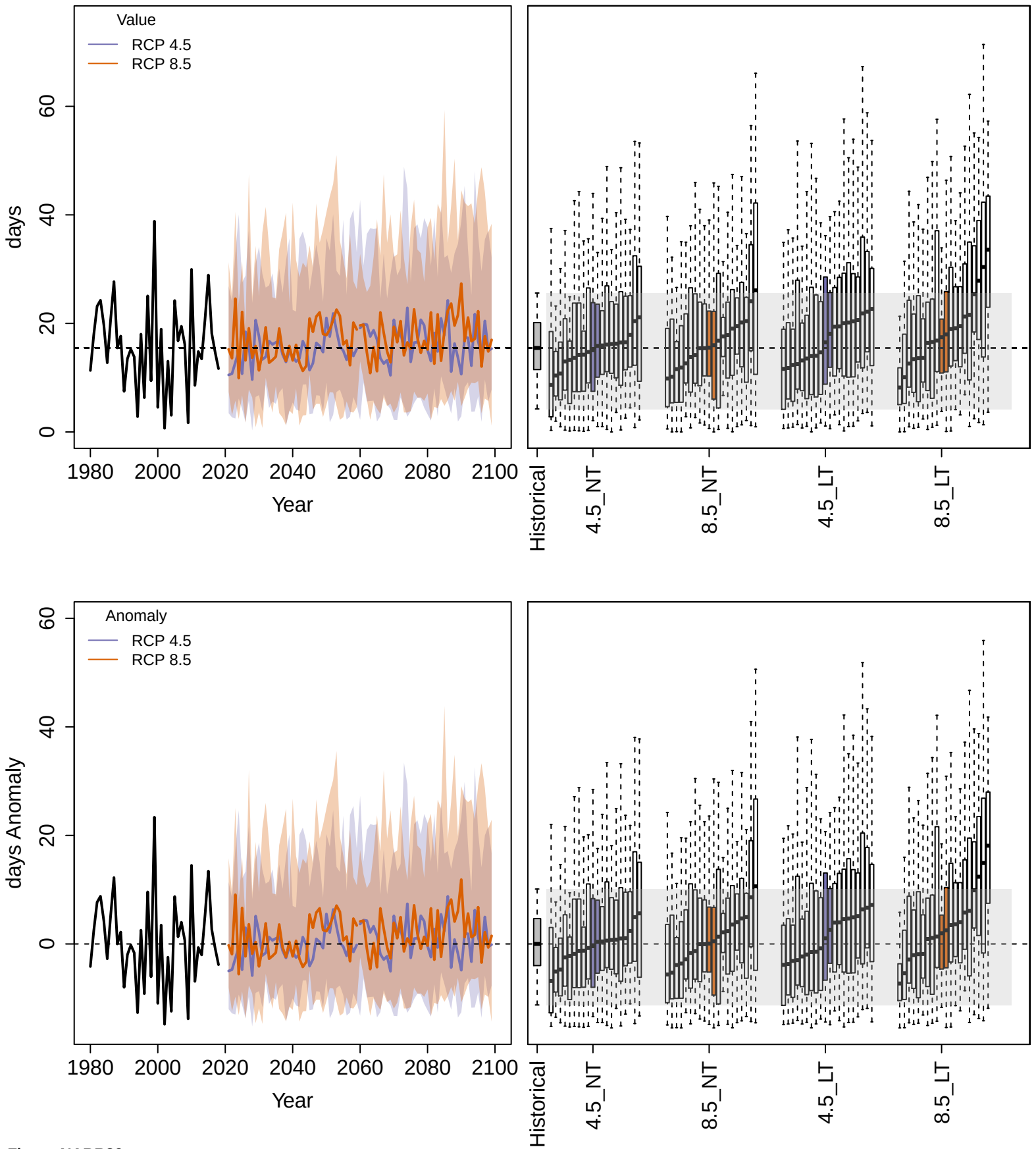


Figure NABR89:
Past trends and future trajectories of park−wide mean values for Summer wet soil days in Natural Bridges. Top panels show values, bottom panels show changes from the long−term historical mean. Left: Time series of historical (black) and future projections for RCP 4.5 and 8.5. Shaded areas show spread among climate models. Right: Boxplots of temporal variability over 40−year periods under historical (left box) and individual climate models under two RCPs. Right: Historical time period is 1970−2010; near−term (NT) is 2020−2060; long−term (LT) is 2061−2100.

Natural Bridges: Summer wet soil days

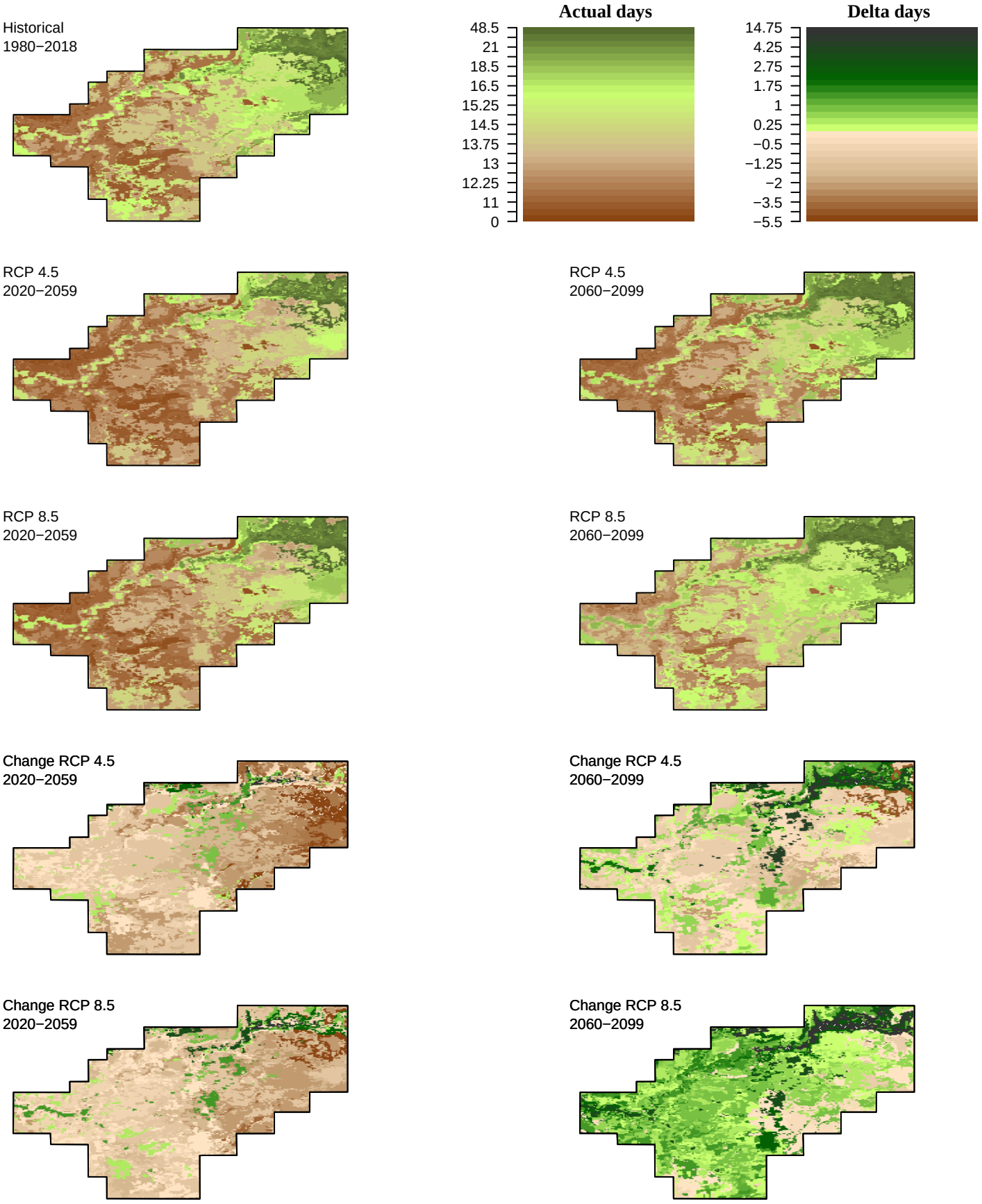


Figure NABRmap89:
Past trends and future trajectories of park−wide mean values for Summer wet soil days in Natural Bridges. Topmost panel depicts the historical mean from 1980−2018. Lower four panels show the emission scenarios of RCP 4.5 and RCP 8.5 at near−term and long−term timeframes. Bottom four panels depict the change from the historical mean; cross hatching denotes areas of robust predicitons (90% of models agree in the direction of change).

Natural Bridges: Fall wet soil days

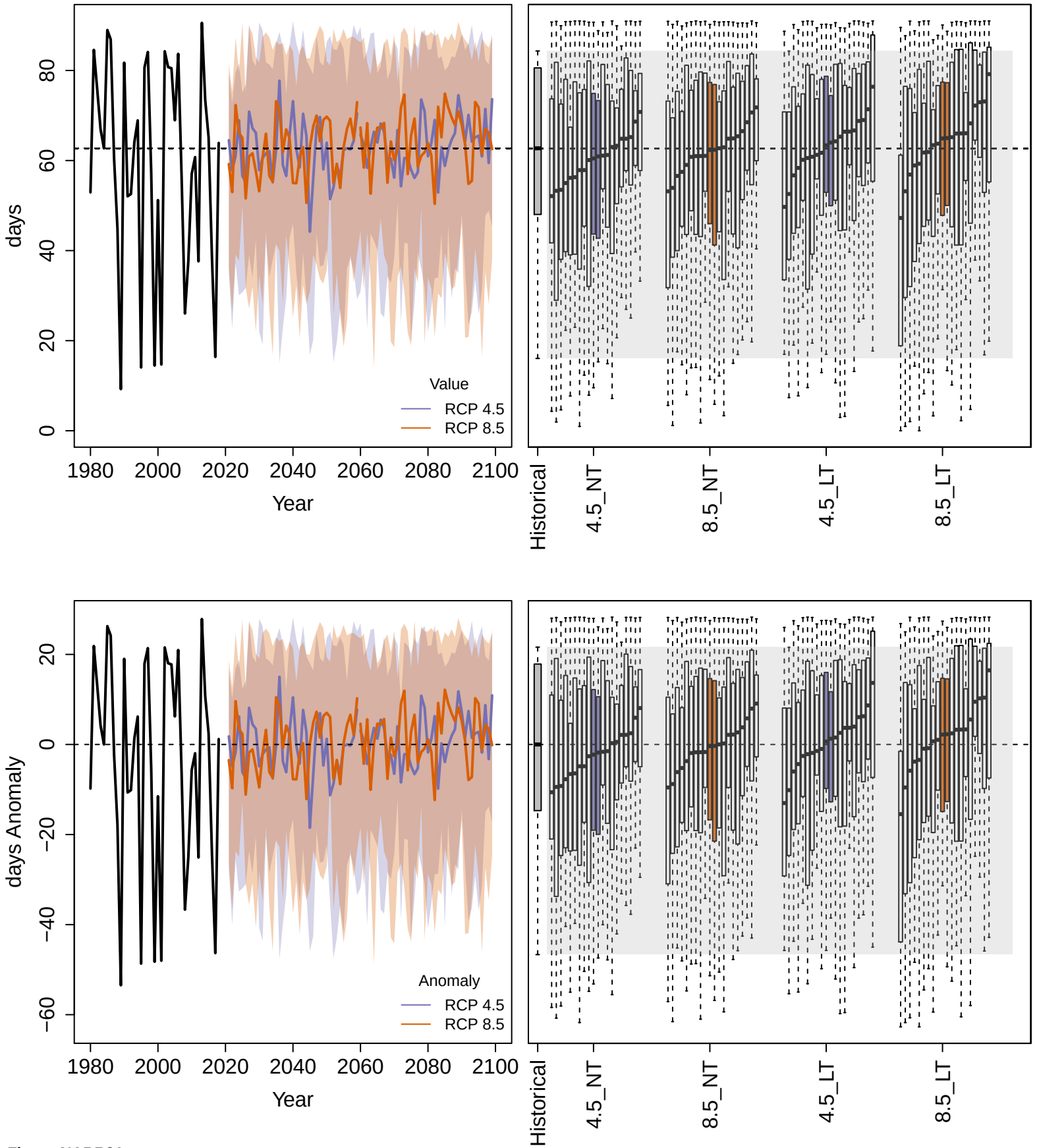


Figure NABR91:
Past trends and future trajectories of park−wide mean values for Fall wet soil days in Natural Bridges. Top panels show values, bottom panels show changes from the long−term historical mean. Left: Time series of historical (black) and future projections for RCP 4.5 and 8.5. Shaded areas show spread among climate models. Right: Boxplots of temporal variability over 40−year periods under historical (left box) and individual climate models under two RCPs. Right: Historical time period is 1970−2010; near−term (NT) is 2020−2060; long−term (LT) is 2061−2100.

Natural Bridges: Fall wet soil days

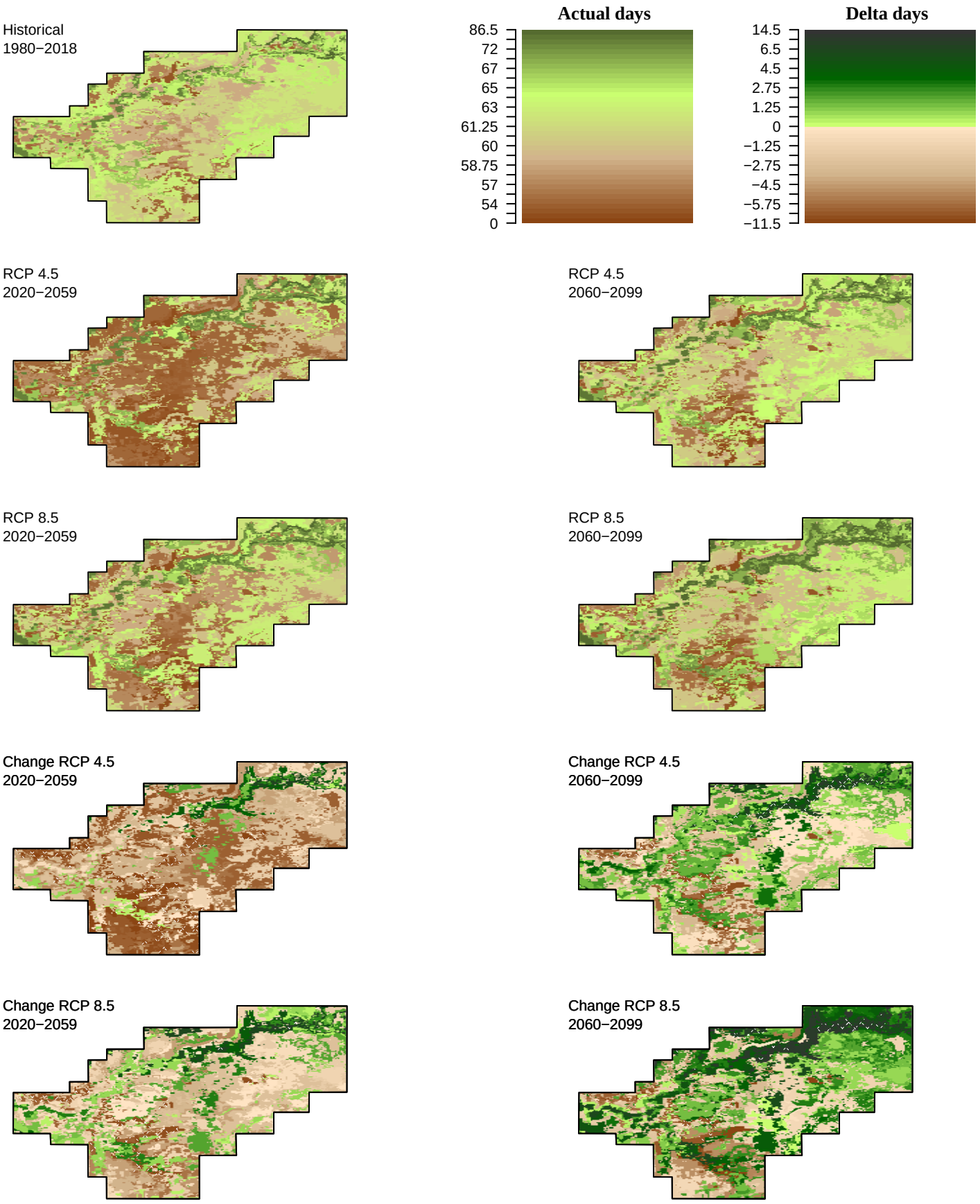


Figure NABRmap91:
Past trends and future trajectories of park−wide mean values for Fall wet soil days in Natural Bridges. Topmost panel depicts the historical mean from 1980−2018. Lower four panels show the emission scenarios of RCP 4.5 and RCP 8.5 at near−term and long−term timeframes. Bottom four panels depict the change from the historical mean; cross hatching denotes areas of robust predicitons (90% of models agree in the direction of change).

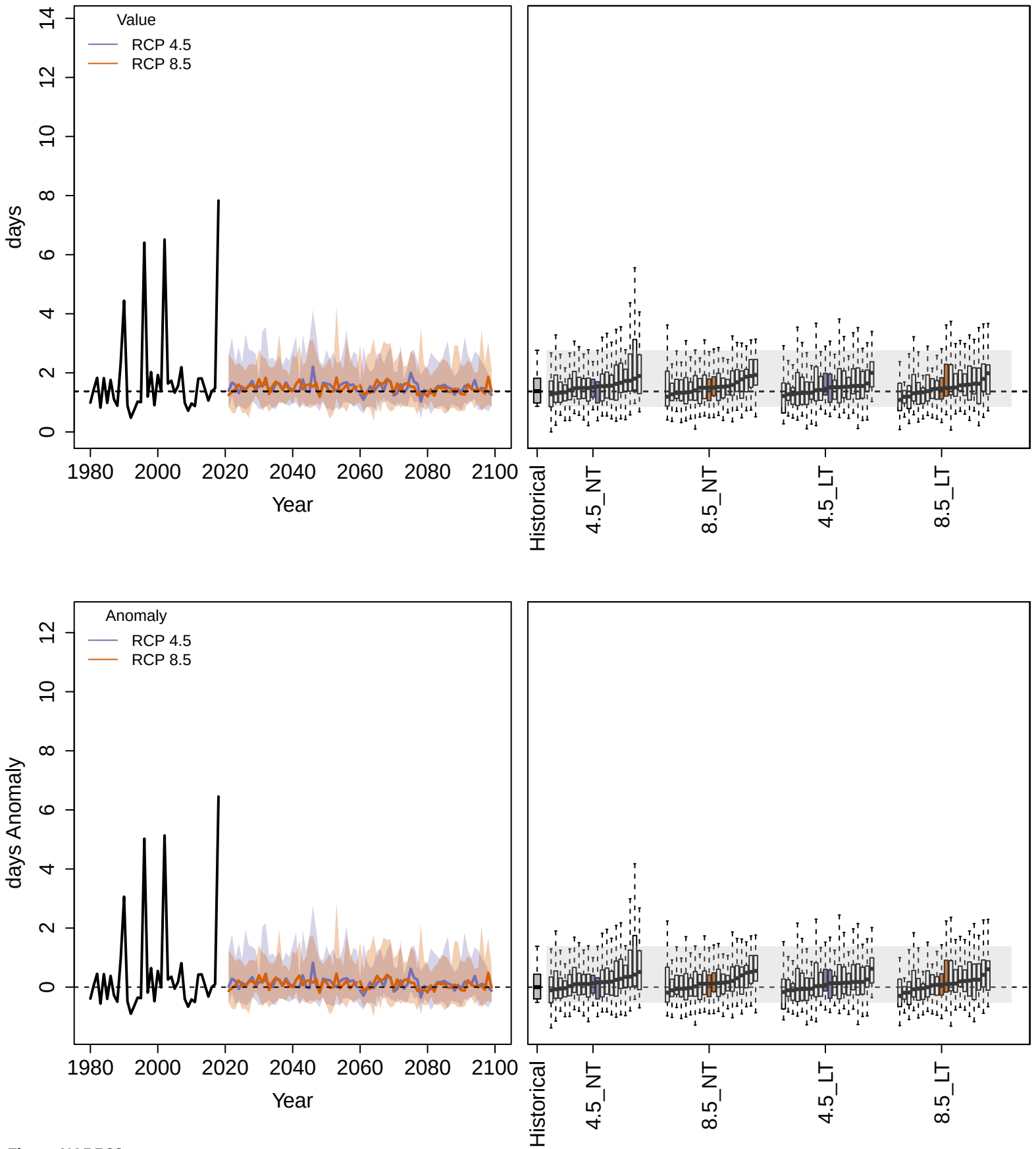


Figure NABR93:
Past trends and future trajectories of park−wide mean values for Spring dry soil days in Natural Bridges. Top panels show values, bottom panels show changes from the long−term historical mean. Left: Time series of historical (black) and future projections for RCP 4.5 and 8.5. Shaded areas show spread among climate models. Right: Boxplots of temporal variability over 40−year periods under historical (left box) and individual climate models under two RCPs. Right: Historical time period is 1970−2010; near−term (NT) is 2020−2060; long−term (LT) is 2061−2100.

Natural Bridges: Spring dry soil days

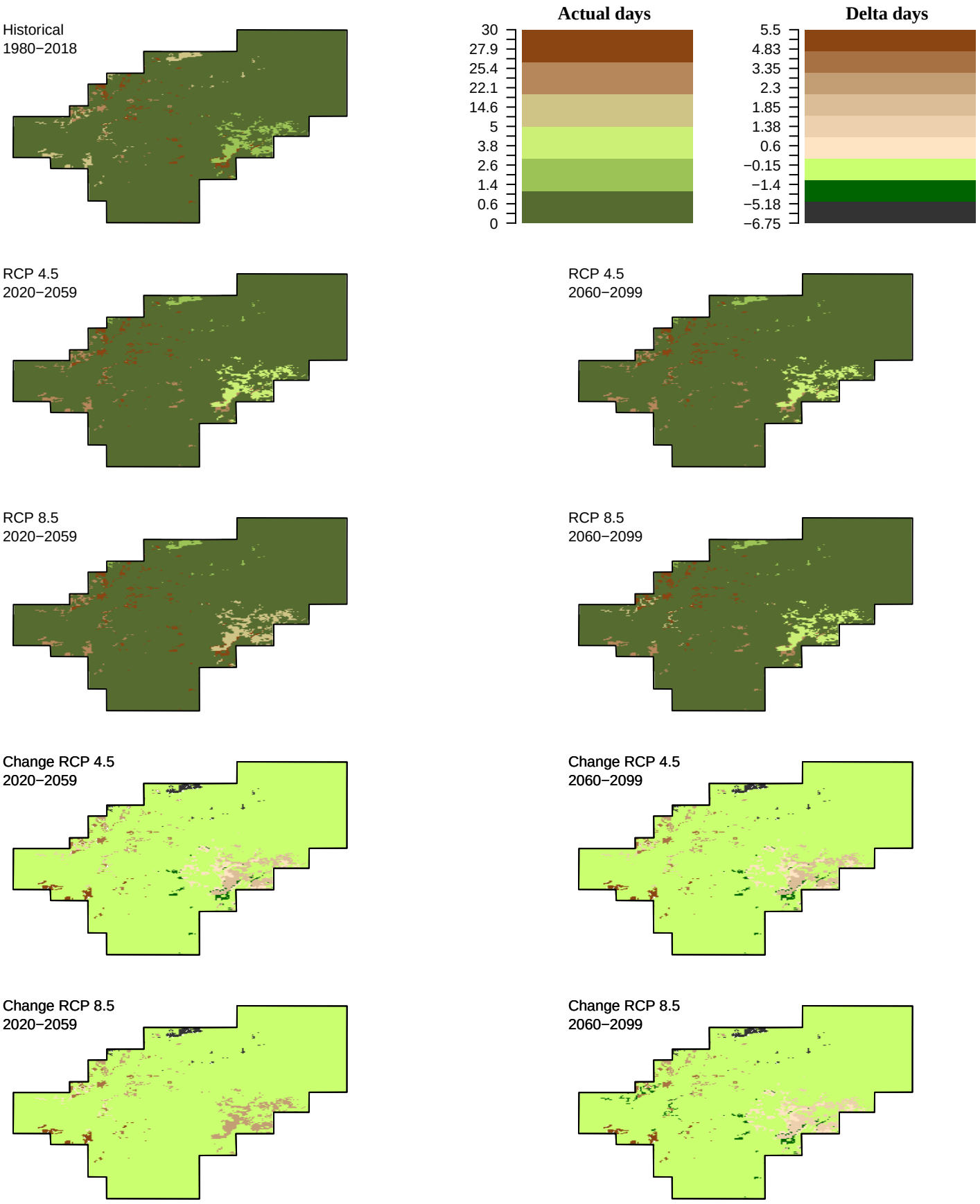


Figure NABRmap93:
Past trends and future trajectories of park−wide mean values for Spring dry soil days in Natural Bridges. Topmost panel depicts the historical mean from 1980−2018. Lower four panels show the emission scenarios of RCP 4.5 and RCP 8.5 at near−term and long−term timeframes. Bottom four panels depict the change from the historical mean; cross hatching denotes areas of robust predicitons (90% of models agree in the direction of change).

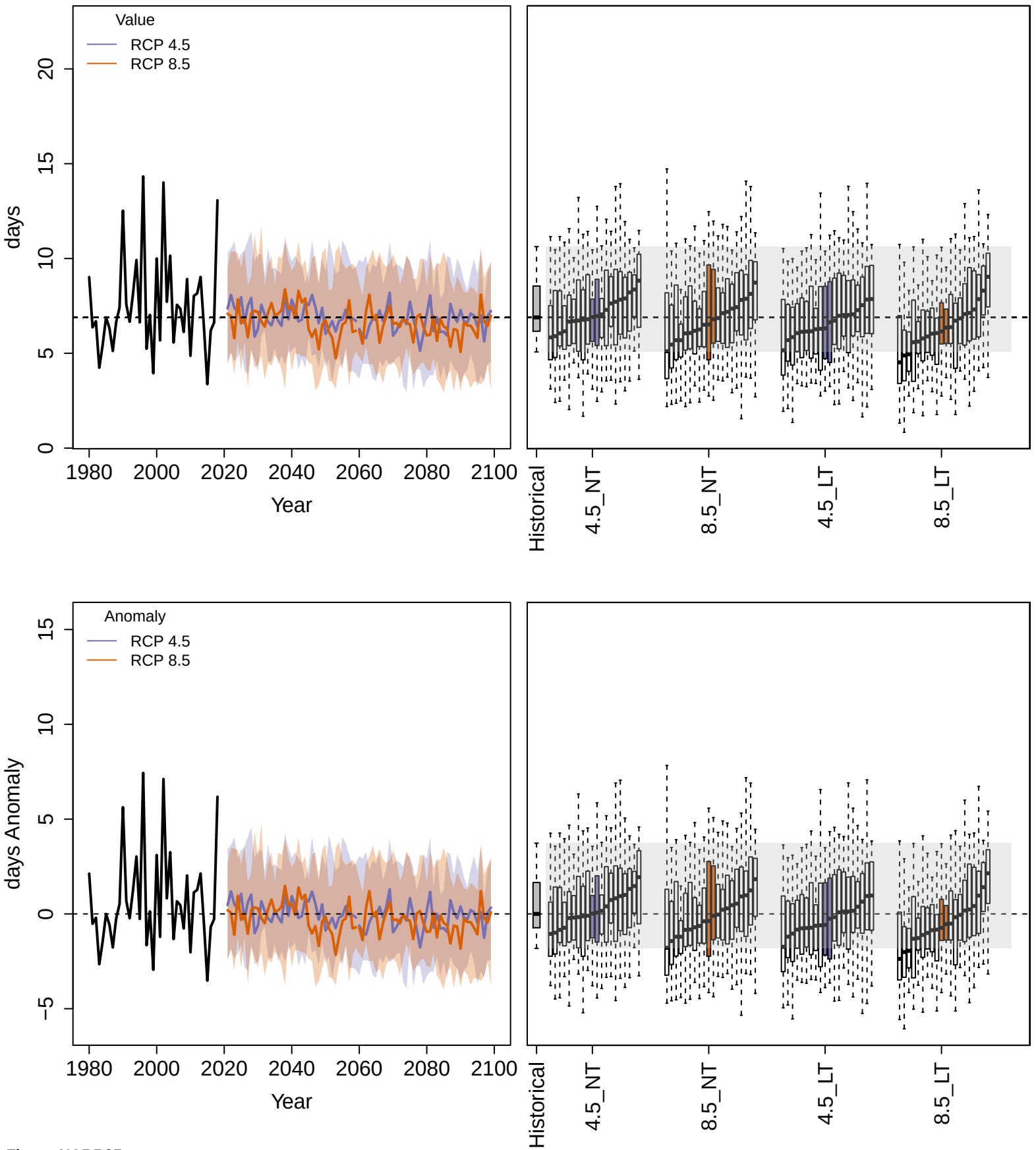


Figure NABR95:
Past trends and future trajectories of park−wide mean values for Summer dry soil days in Natural Bridges. Top panels show values, bottom panels show changes from the long−term historical mean. Left: Time series of historical (black) and future projections for RCP 4.5 and 8.5. Shaded areas show spread among climate models. Right: Boxplots of temporal variability over 40−year periods under historical (left box) and individual climate models under two RCPs. Right: Historical time period is 1970−2010; near−term (NT) is 2020−2060; long−term (LT) is 2061−2100.

Natural Bridges: Summer dry soil days

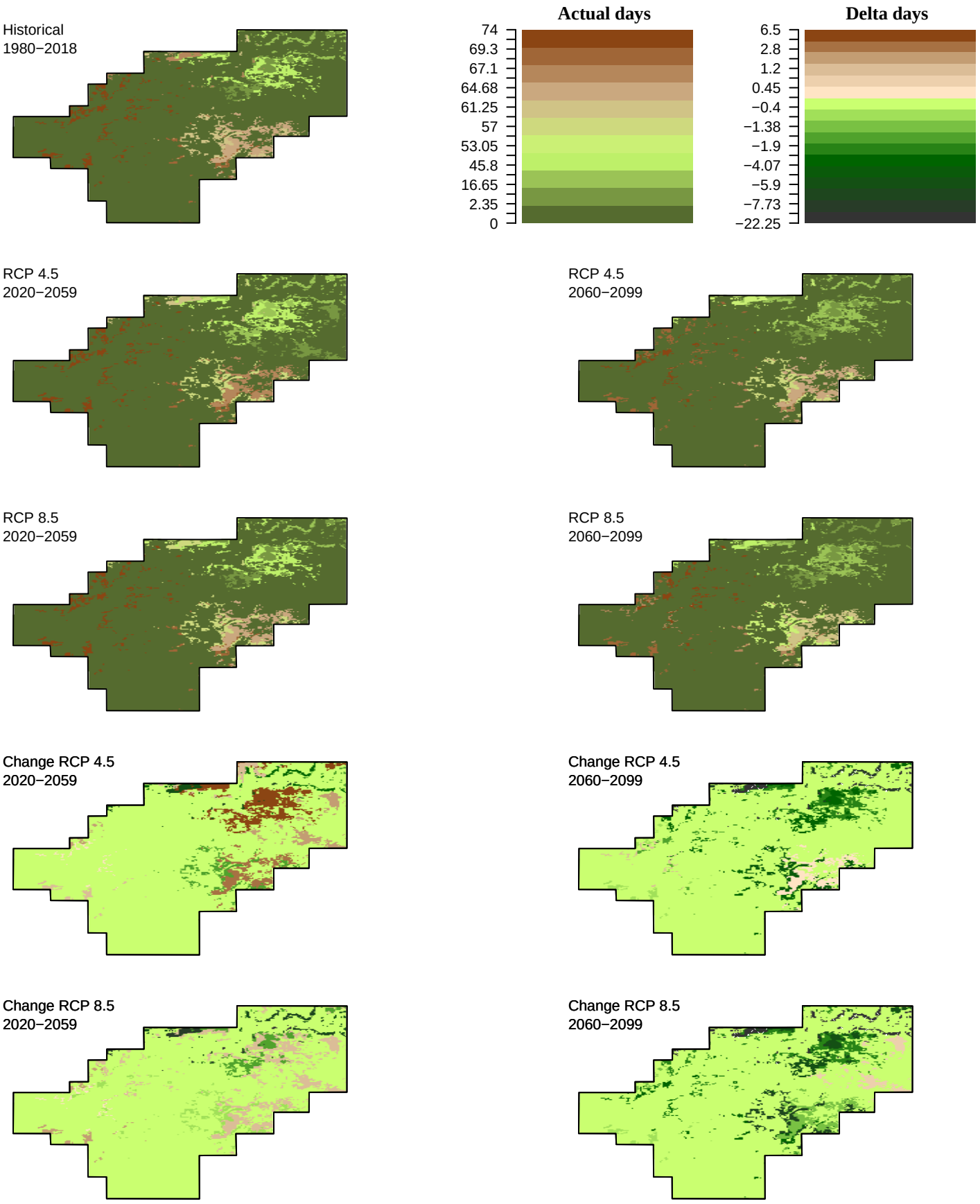


Figure NABRmap95:
Past trends and future trajectories of park−wide mean values for Summer dry soil days in Natural Bridges. Topmost panel depicts the historical mean from 1980−2018. Lower four panels show the emission scenarios of RCP 4.5 and RCP 8.5 at near−term and long−term timeframes. Bottom four panels depict the change from the historical mean; cross hatching denotes areas of robust predicitons (90% of models agree in the direction of change).

Natural Bridges: Fall dry soil days

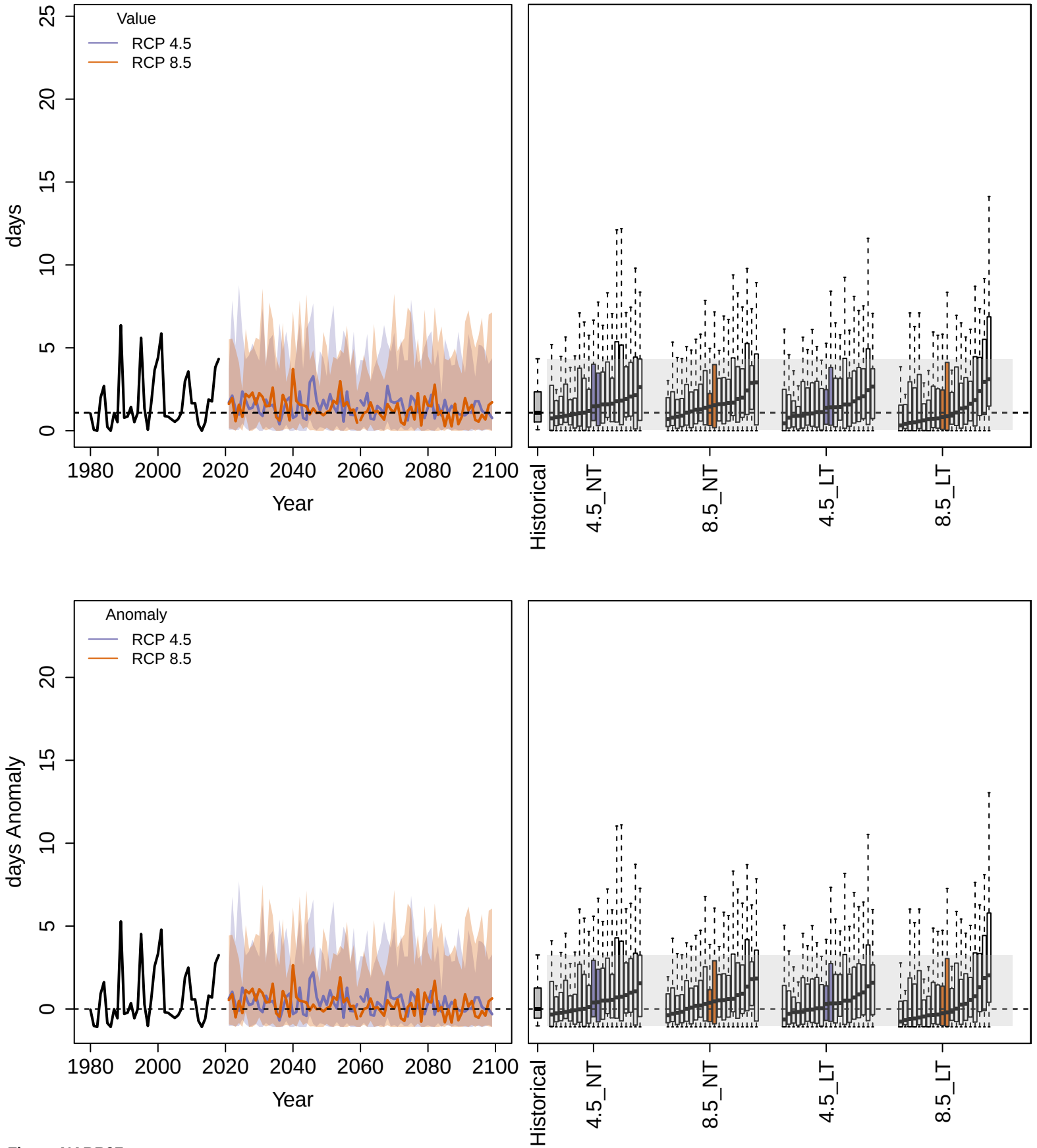


Figure NABR97:
Past trends and future trajectories of park−wide mean values for Fall dry soil days in Natural Bridges. Top panels show values, bottom panels show changes from the long−term historical mean. Left: Time series of historical (black) and future projections for RCP 4.5 and 8.5. Shaded areas show spread among climate models. Right: Boxplots of temporal variability over 40−year periods under historical (left box) and individual climate models under two RCPs. Right: Historical time period is 1970−2010; near−term (NT) is 2020−2060; long−term (LT) is 2061−2100.

Natural Bridges: Fall dry soil days

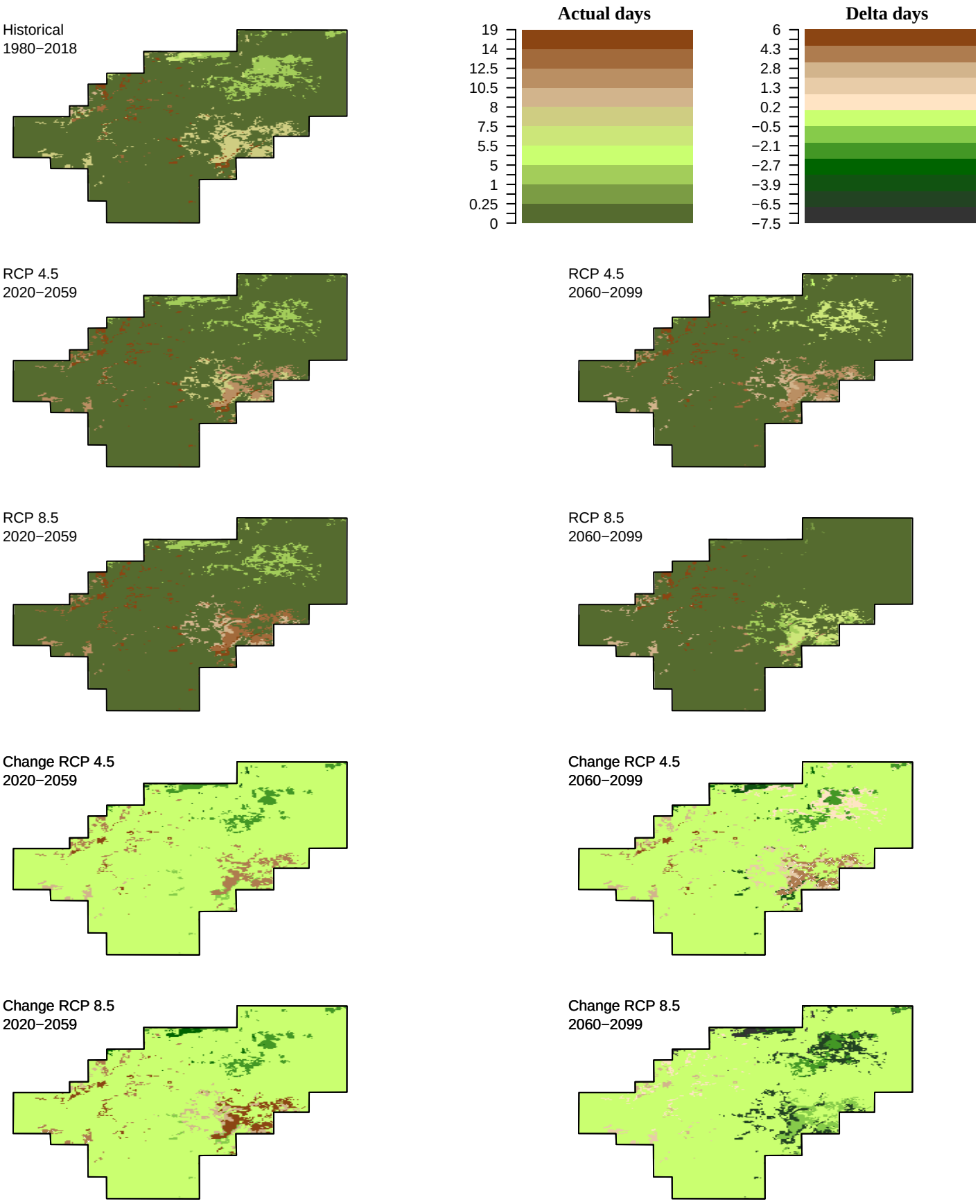


Figure NABRmap97:
Past trends and future trajectories of park−wide mean values for Fall dry soil days in Natural Bridges. Topmost panel depicts the historical mean from 1980−2018. Lower four panels show the emission scenarios of RCP 4.5 and RCP 8.5 at near−term and long−term timeframes. Bottom four panels depict the change from the historical mean; cross hatching denotes areas of robust predicitons (90% of models agree in the direction of change).

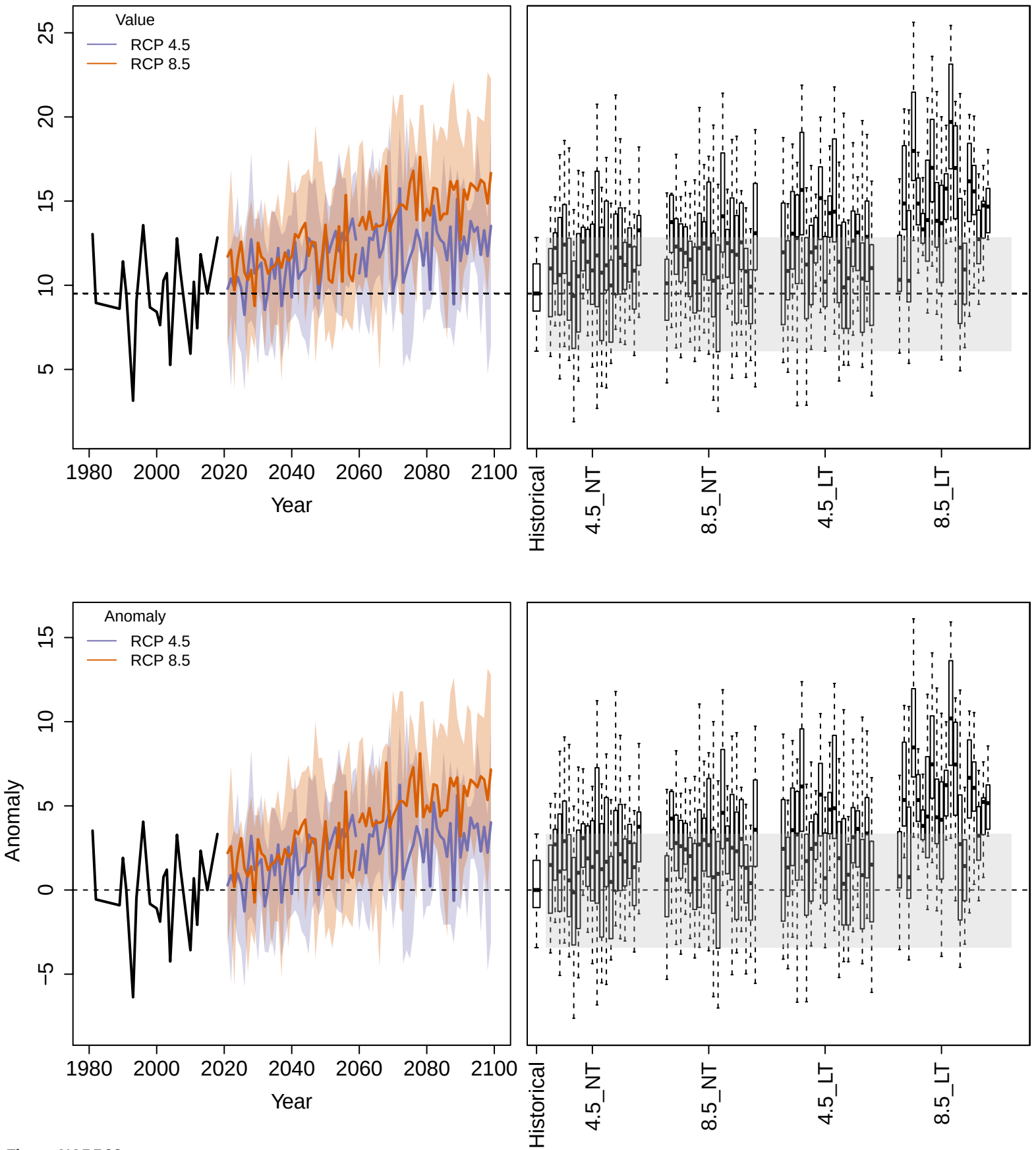


Figure NABR99:
Past trends and future trajectories of park−wide mean values for Winter extreme short−term dry stress in Natural Bridges. Top panels show values, bottom panels show changes from the long−term historical mean. Left: Time series of historical (black) and future projections for RCP 4.5 and 8.5. Shaded areas show spread among climate models. Right: Boxplots of temporal variability over 40−year periods under historical (left box) and individual climate models under two RCPs. Right: Historical time period is 1970−2010; near−term (NT) is 2020−2060; long−term (LT) is 2061−2100.

Natural Bridges: Winter extreme short−term dry stress

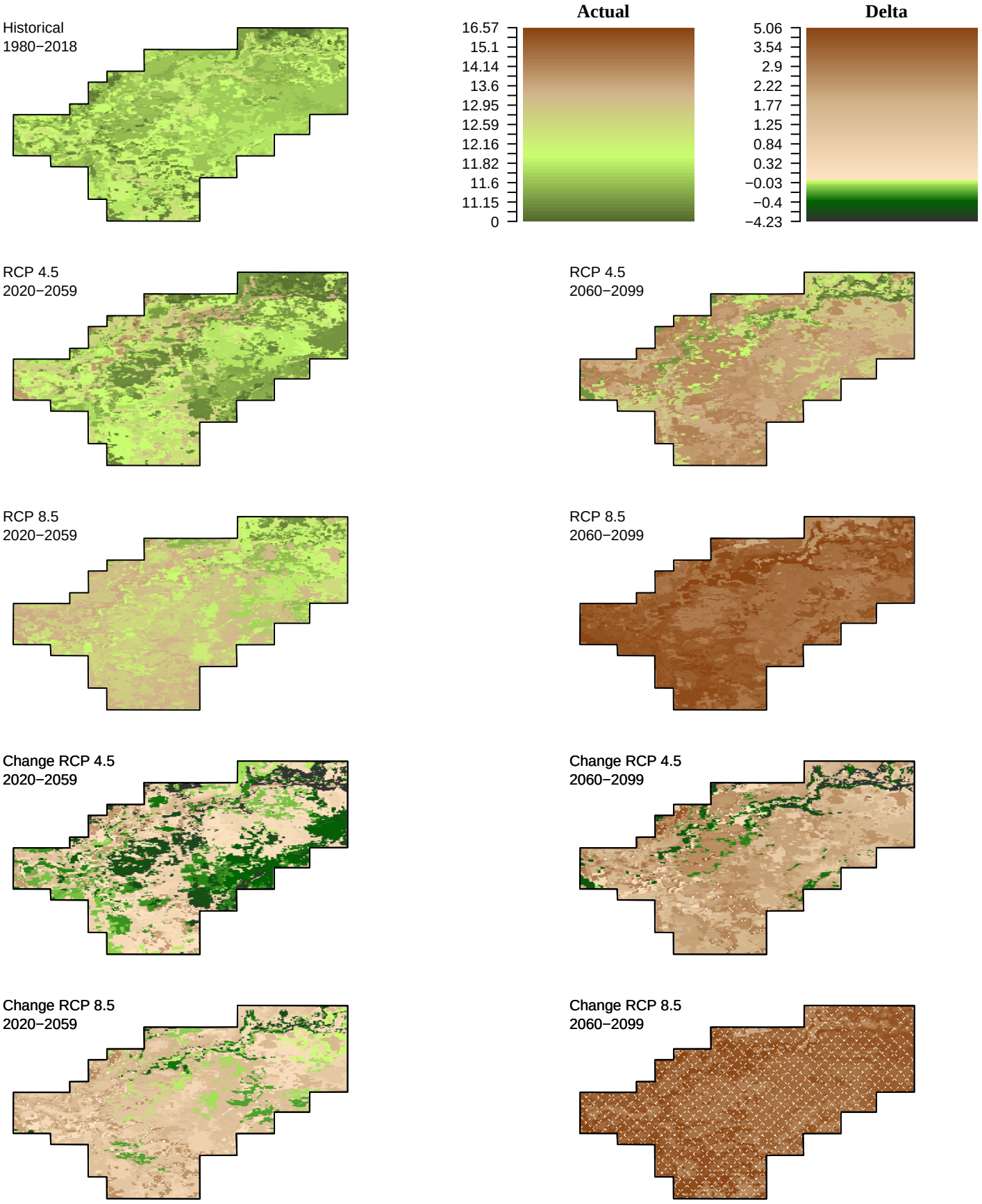


Figure NABRmap99:
Past trends and future trajectories of park−wide mean values for Winter extreme short−term dry stress in Natural Bridges. Topmost panel depicts the historical mean from 1980−2018. Lower four panels show the emission scenarios of RCP 4.5 and RCP 8.5 at near−term and long−term timeframes. Bottom four panels depict the change from the historical mean; cross hatching denotes areas of robust predicitons (90% of models agree in the direction of change).

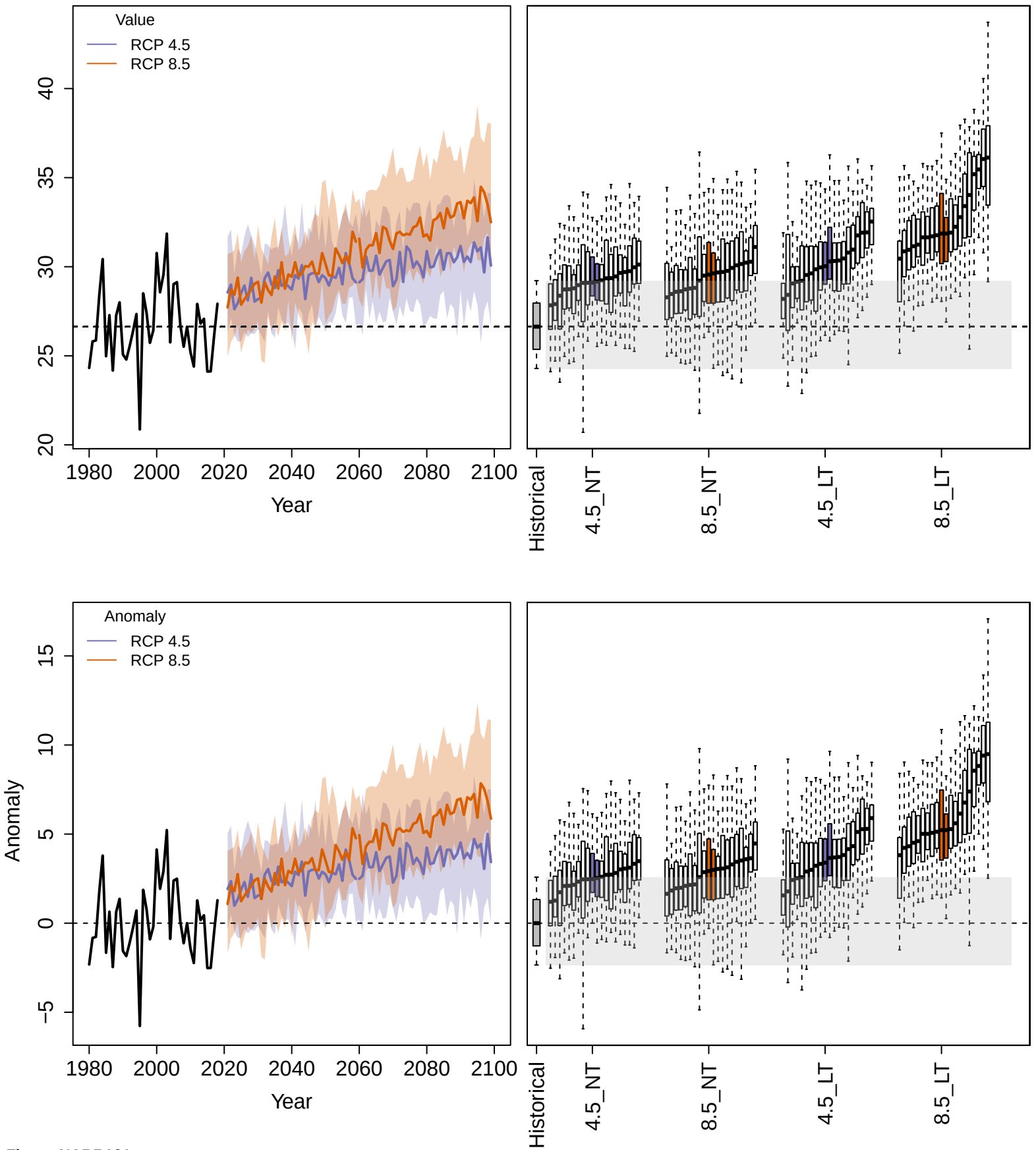


Figure NABR101:
Past trends and future trajectories of park−wide mean values for Spring extreme short−term dry stress in Natural Bridges. Top panels show values, bottom panels show changes from the long−term historical mean. Left: Time series of historical (black) and future projections for RCP 4.5 and 8.5. Shaded areas show spread among climate models. Right: Boxplots of temporal variability over 40−year periods under historical (left box) and individual climate models under two RCPs. Right: Historical time period is 1970−2010; near−term (NT) is 2020−2060; long−term (LT) is 2061−2100.

Natural Bridges: Spring extreme short−term dry stress

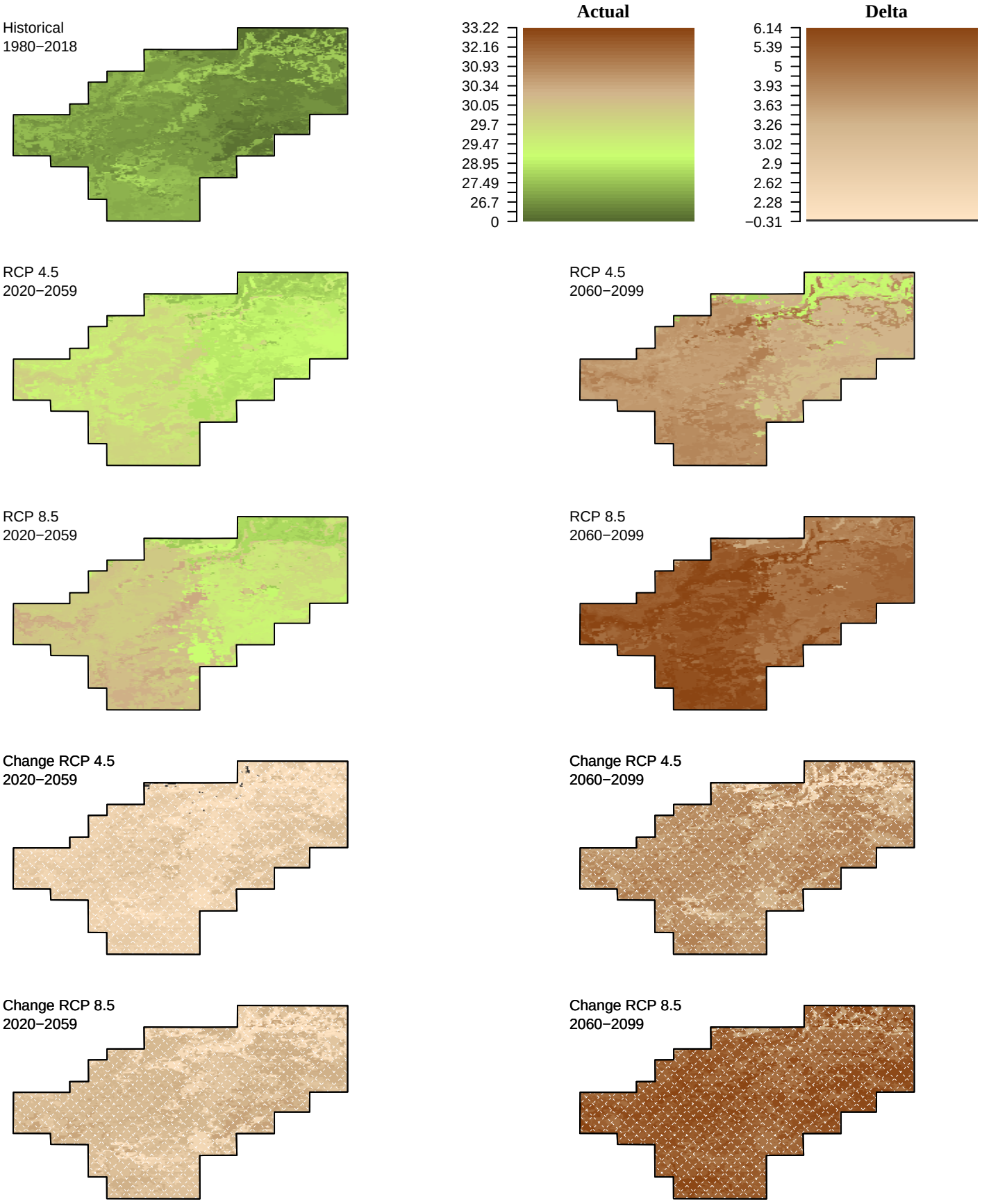


Figure NABRmap101:
Past trends and future trajectories of park−wide mean values for Spring extreme short−term dry stress in Natural Bridges. Topmost panel depicts the historical mean from 1980−2018. Lower four panels show the emission scenarios of RCP 4.5 and RCP 8.5 at near−term and long−term timeframes. Bottom four panels depict the change from the historical mean; cross hatching denotes areas of robust predicitons (90% of models agree in the direction of change).

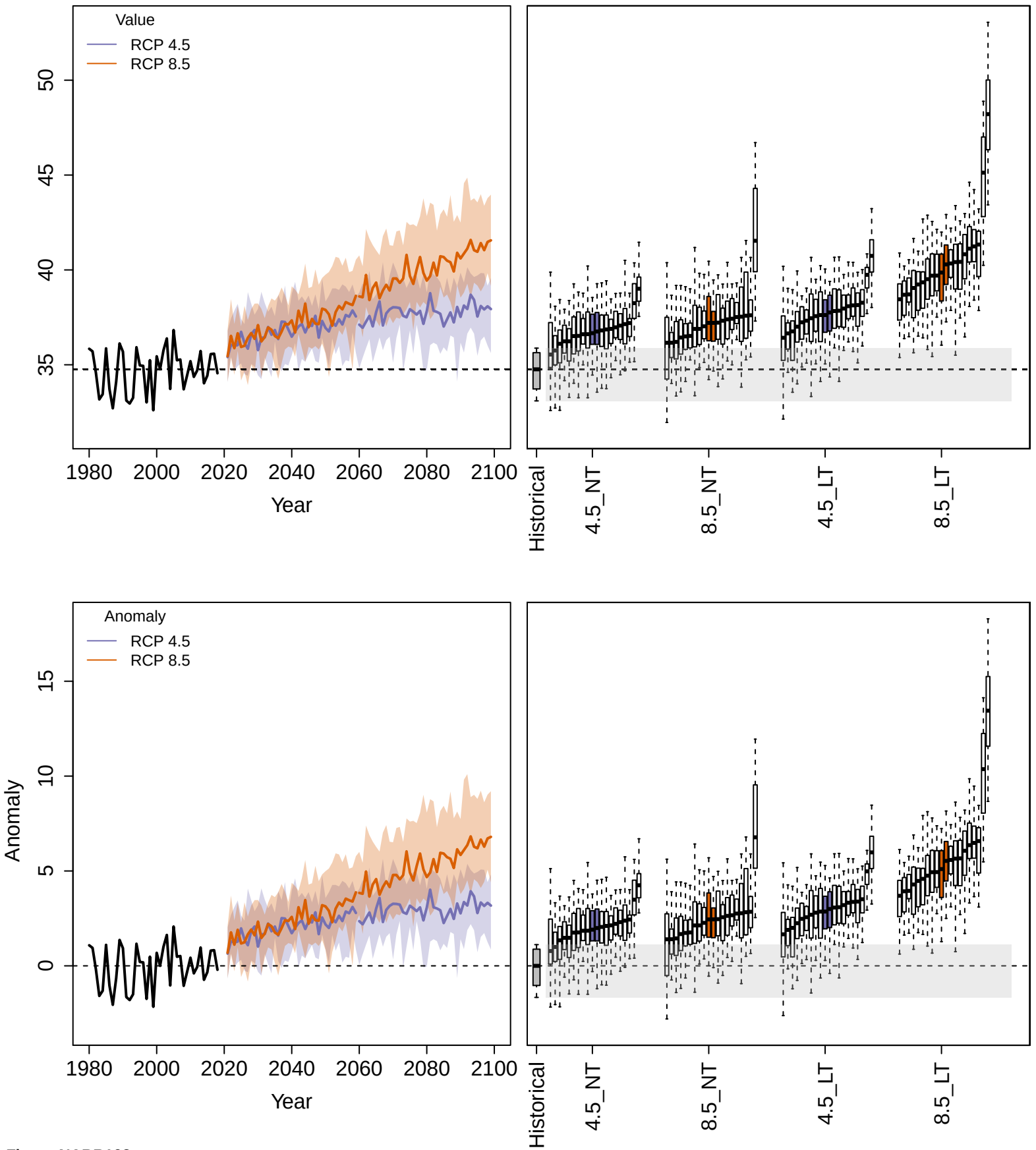


Figure NABR103:
Past trends and future trajectories of park−wide mean values for Summer extreme short−term dry stress in Natural Bridges. Top panels show values, bottom panels show changes from the long−term historical mean. Left: Time series of historical (black) and future projections for RCP 4.5 and 8.5. Shaded areas show spread among climate models. Right: Boxplots of temporal variability over 40−year periods under historical (left box) and individual climate models under two RCPs. Right: Historical time period is 1970−2010; near−term (NT) is 2020−2060; long−term (LT) is 2061−2100.

Natural Bridges: Summer extreme short−term dry stress

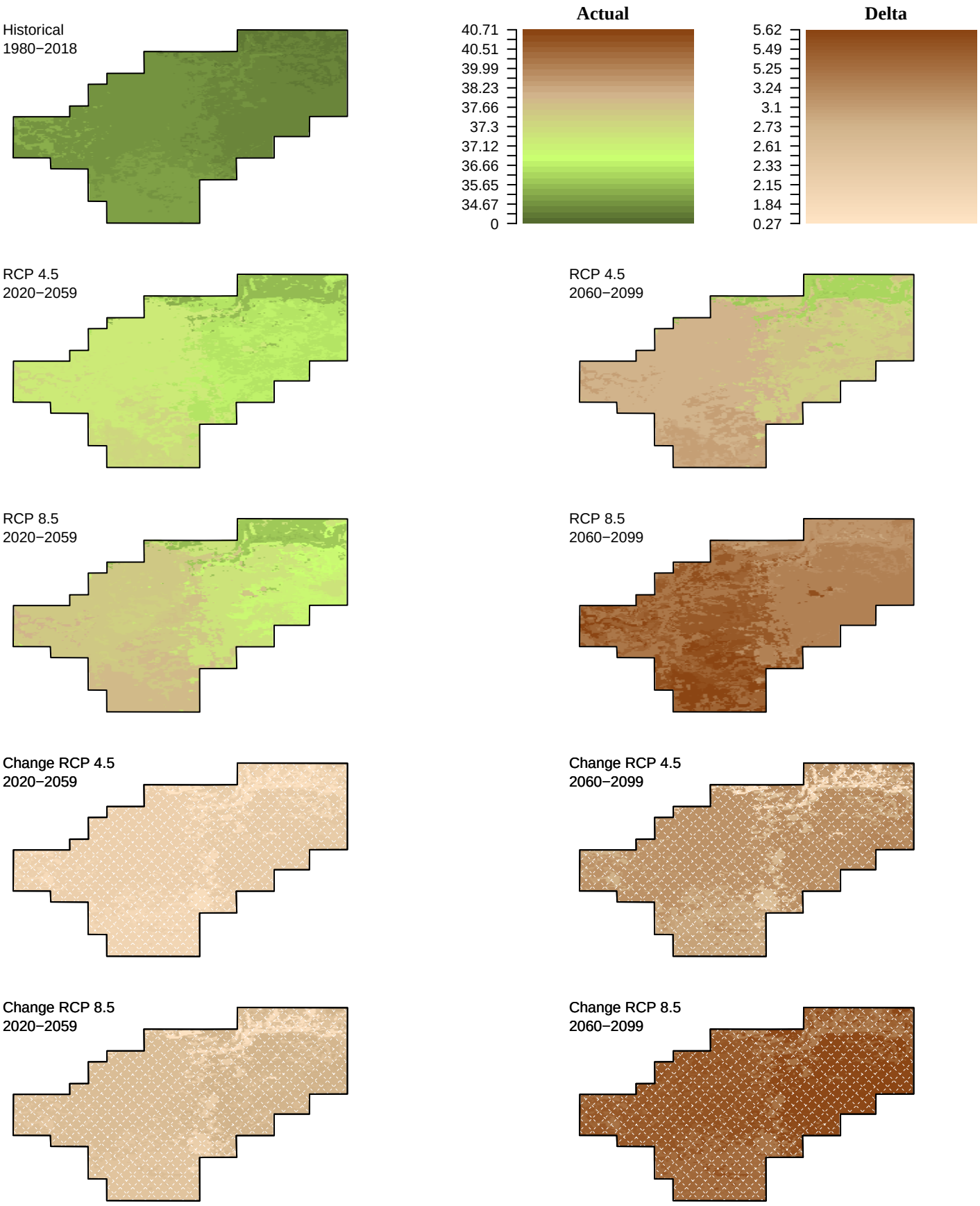


Figure NABRmap103:
Past trends and future trajectories of park−wide mean values for Summer extreme short−term dry stress in Natural Bridges. Topmost panel depicts the historical mean from 1980−2018. Lower four panels show the emission scenarios of RCP 4.5 and RCP 8.5 at near−term and long−term timeframes. Bottom four panels depict the change from the historical mean; cross hatching denotes areas of robust predicitons (90% of models agree in the direction of change).

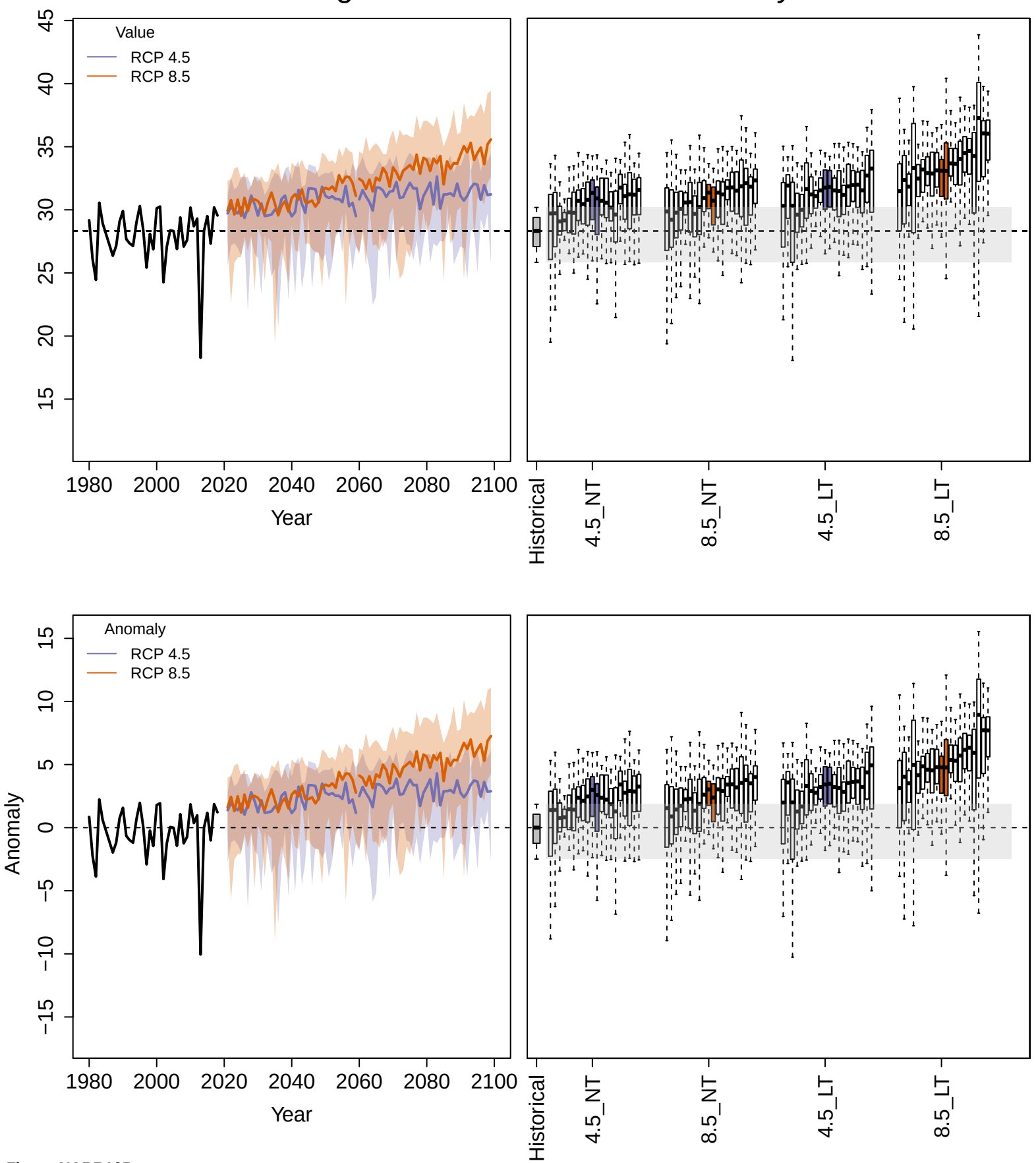


Figure NABR105:
Past trends and future trajectories of park−wide mean values for Fall extreme short−term dry stress in Natural Bridges. Top panels show values, bottom panels show changes from the long−term historical mean. Left: Time series of historical (black) and future projections for RCP 4.5 and 8.5. Shaded areas show spread among climate models. Right: Boxplots of temporal variability over 40−year periods under historical (left box) and individual climate models under two RCPs. Right: Historical time period is 1970−2010; near−term (NT) is 2020−2060; long−term (LT) is 2061−2100.

Natural Bridges: Fall extreme short−term dry stress

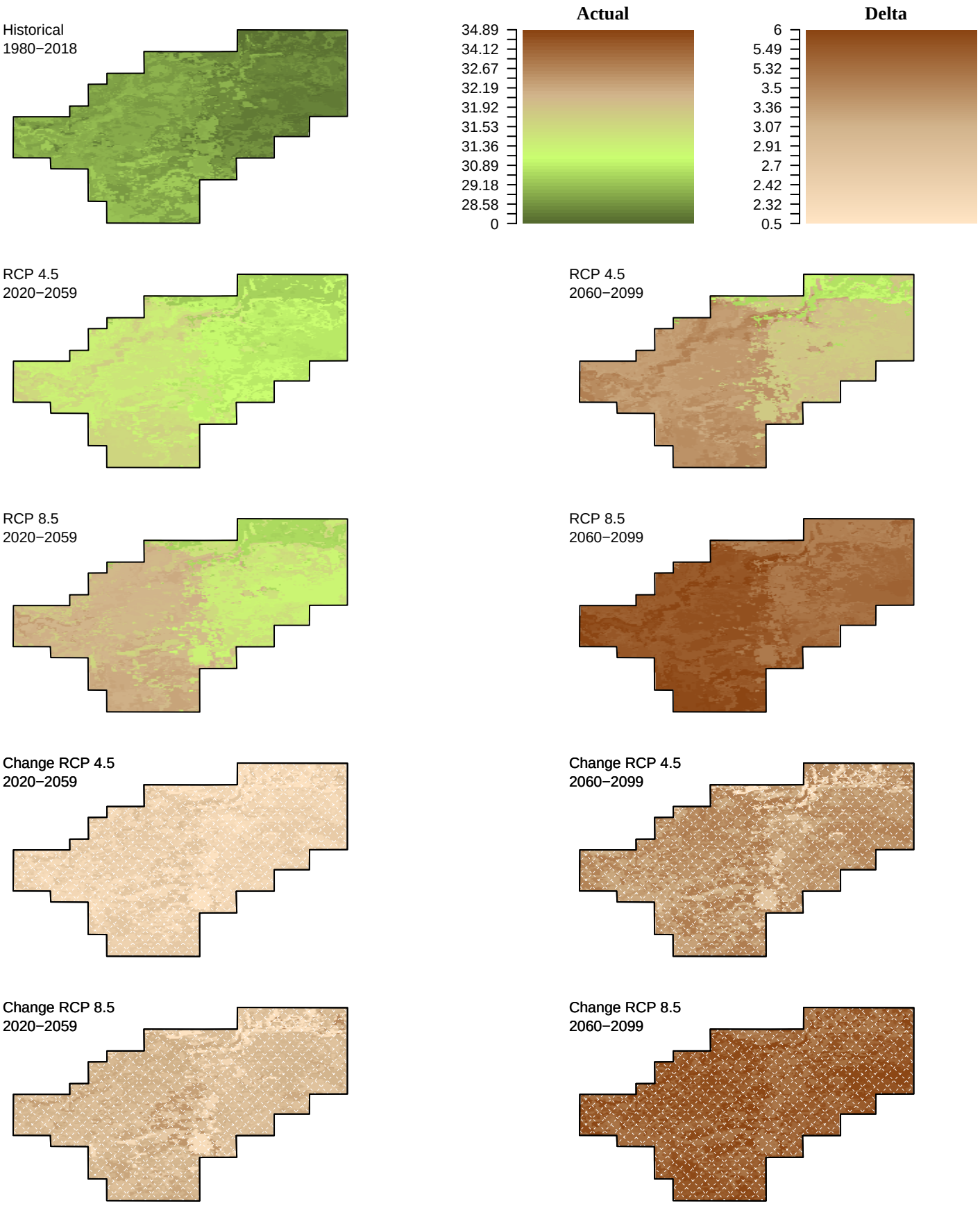


Figure NABRmap105:
Past trends and future trajectories of park−wide mean values for Fall extreme short−term dry stress in Natural Bridges. Topmost panel depicts the historical mean from 1980−2018. Lower four panels show the emission scenarios of RCP 4.5 and RCP 8.5 at near−term and long−term timeframes. Bottom four panels depict the change from the historical mean; cross hatching denotes areas of robust predicitons (90% of models agree in the direction of change).

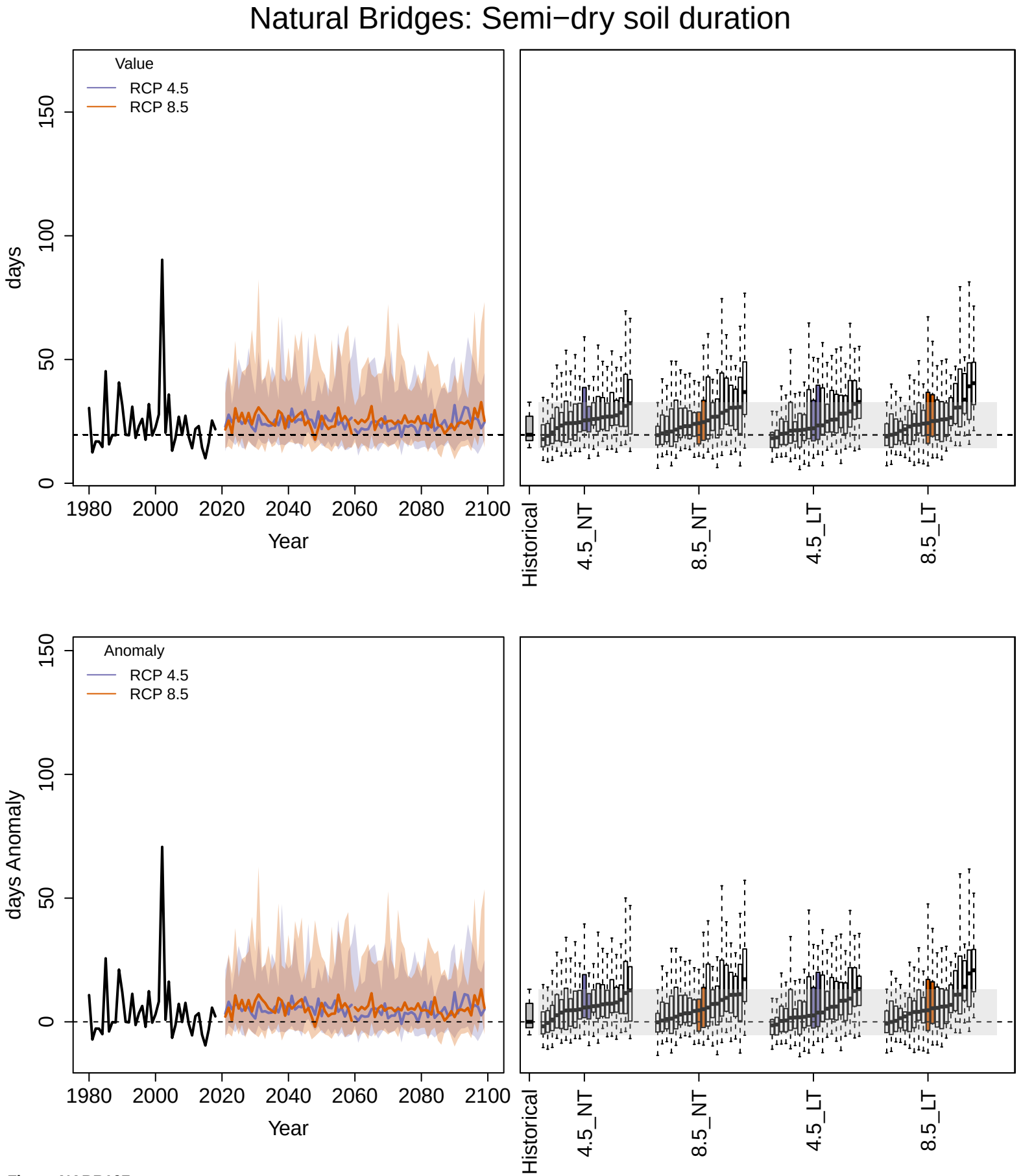


Figure NABR107:
Past trends and future trajectories of park−wide mean values for Semi−dry soil duration in Natural Bridges. Top panels show values, bottom panels show changes from the long−term historical mean. Left: Time series of historical (black) and future projections for RCP 4.5 and 8.5. Shaded areas show spread among climate models. Right: Boxplots of temporal variability over 40−year periods under historical (left box) and individual climate models under two RCPs. Right: Historical time period is 1970−2010; near−term (NT) is 2020−2060; long−term (LT) is 2061−2100.

Natural Bridges: Semi−dry soil duration

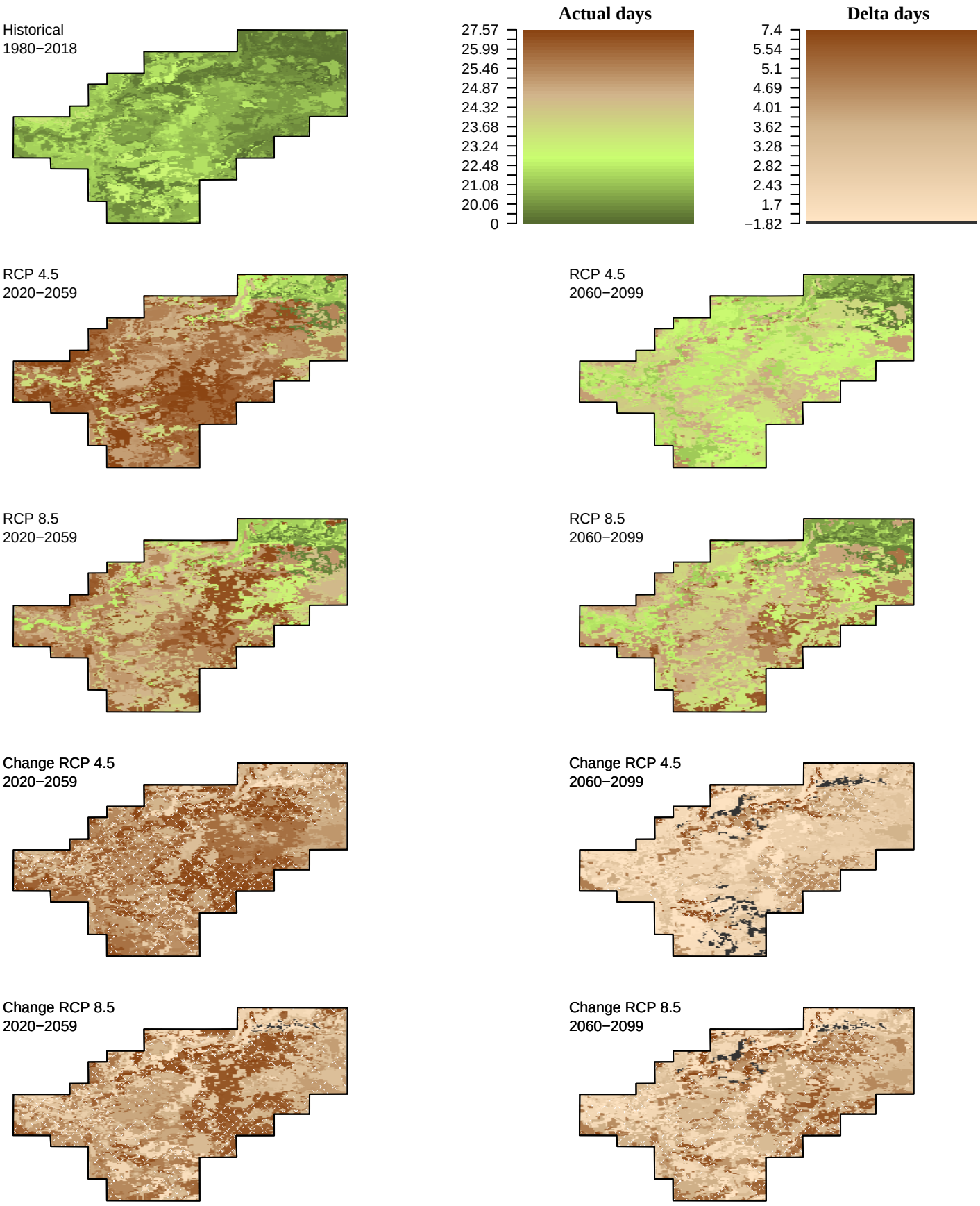


Figure NABRmap107:
Past trends and future trajectories of park−wide mean values for Semi−dry soil duration in Natural Bridges. Topmost panel depicts the historical mean from 1980−2018. Lower four panels show the emission scenarios of RCP 4.5 and RCP 8.5 at near−term and long−term timeframes. Bottom four panels depict the change from the historical mean; cross hatching denotes areas of robust predicitons (90% of models agree in the direction of change).

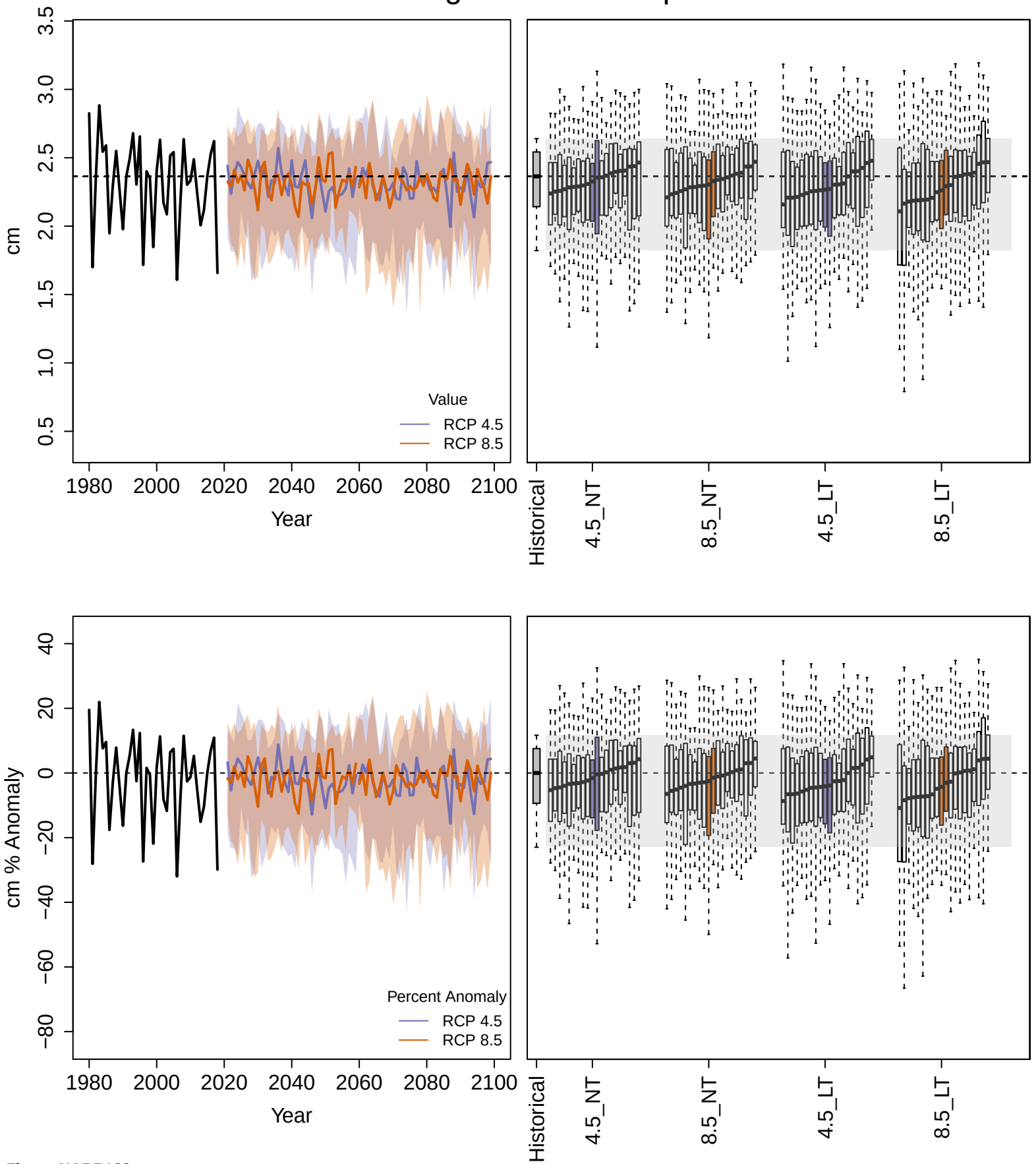


Figure NABR109:
Past trends and future trajectories of park−wide mean values for Winter evaporation in Natural Bridges. Top panels show values, bottom panels show changes from the long−term historical mean. Left: Time series of historical (black) and future projections for RCP 4.5 and 8.5. Shaded areas show spread among climate models. Right: Boxplots of temporal variability over 40−year periods under historical (left box) and individual climate models under two RCPs. Right: Historical time period is 1970−2010; near−term (NT) is 2020−2060; long−term (LT) is 2061−2100.

Natural Bridges: Winter evaporation

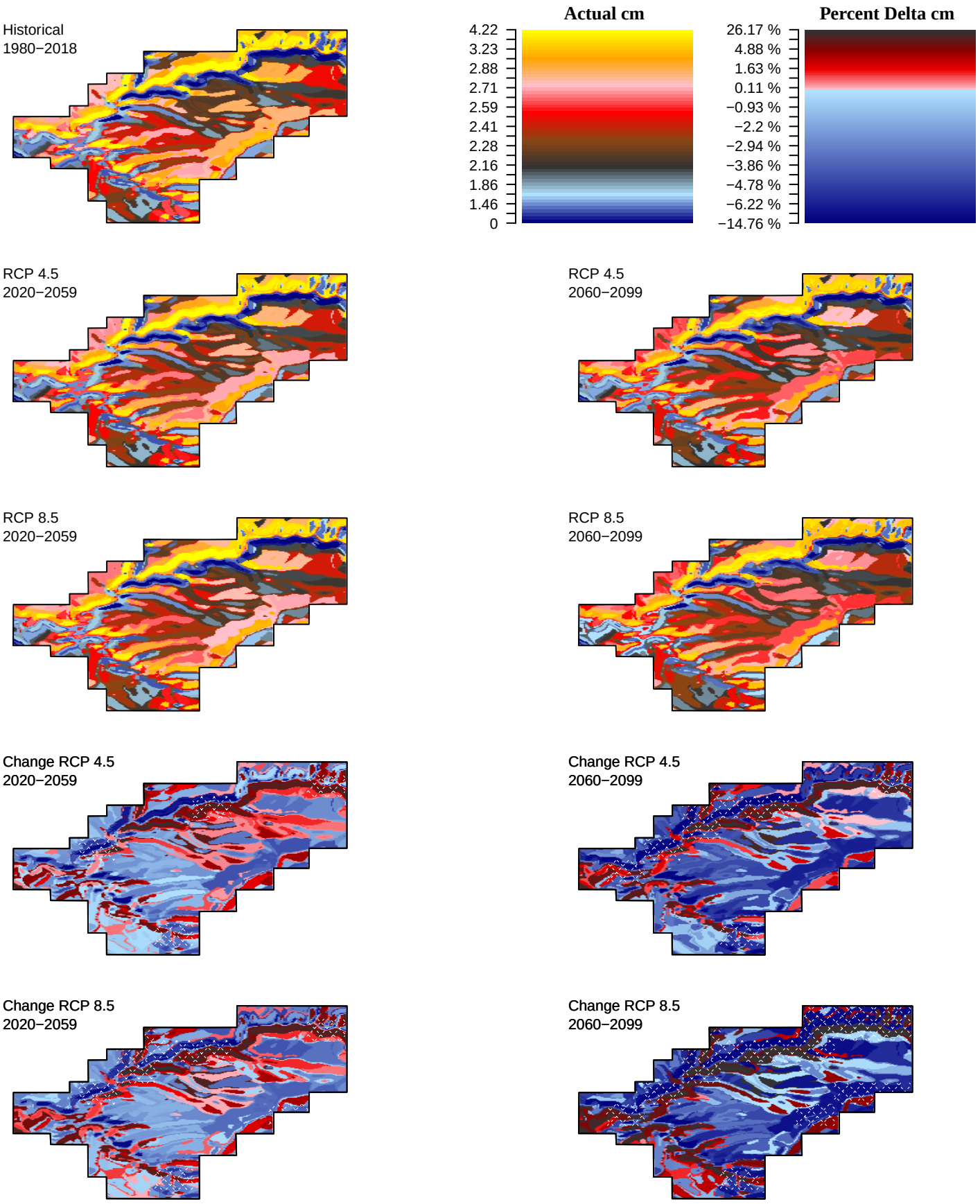


Figure NABRmap109:
Past trends and future trajectories of park−wide mean values for Winter evaporation in Natural Bridges. Topmost panel depicts the historical mean from 1980−2018. Lower four panels show the emission scenarios of RCP 4.5 and RCP 8.5 at near−term and long−term timeframes. Bottom four panels depict the change from the historical mean; cross hatching denotes areas of robust predicitons (90% of models agree in the direction of change).

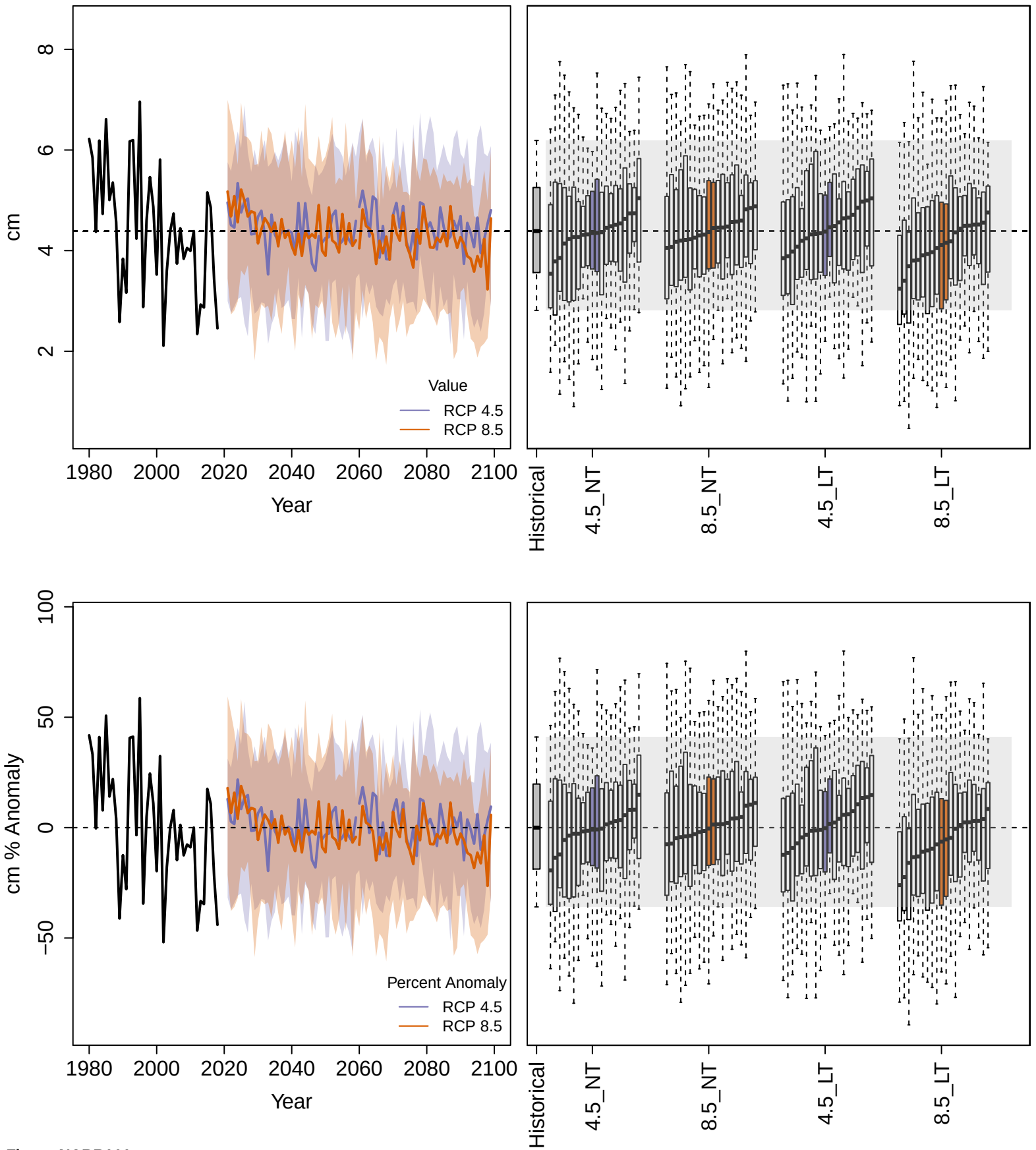


Figure NABR111:
Past trends and future trajectories of park−wide mean values for Spring evaporation in Natural Bridges. Top panels show values, bottom panels show changes from the long−term historical mean. Left: Time series of historical (black) and future projections for RCP 4.5 and 8.5. Shaded areas show spread among climate models. Right: Boxplots of temporal variability over 40−year periods under historical (left box) and individual climate models under two RCPs. Right: Historical time period is 1970−2010; near−term (NT) is 2020−2060; long−term (LT) is 2061−2100.

Natural Bridges: Spring evaporation

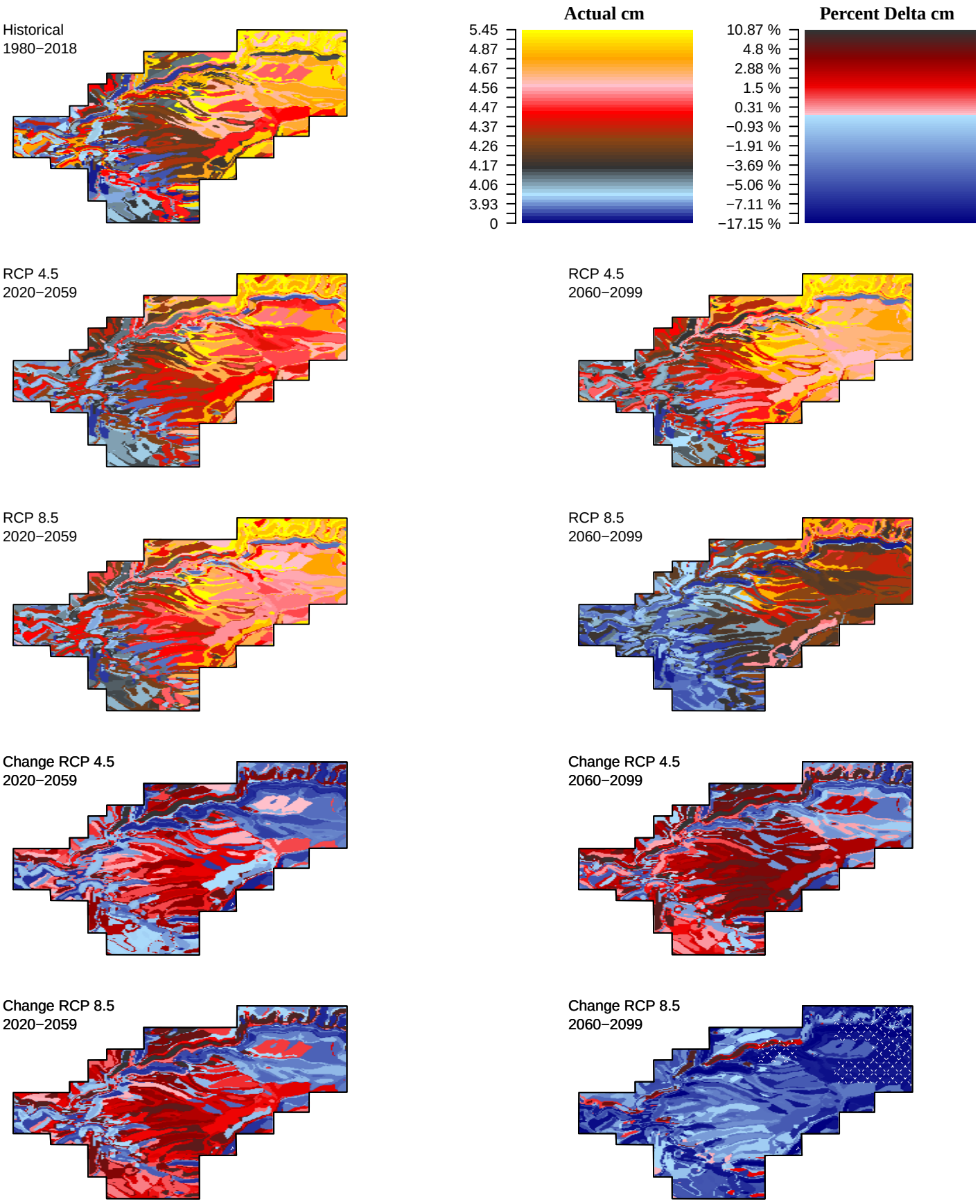


Figure NABRmap111:
Past trends and future trajectories of park−wide mean values for Spring evaporation in Natural Bridges. Topmost panel depicts the historical mean from 1980−2018. Lower four panels show the emission scenarios of RCP 4.5 and RCP 8.5 at near−term and long−term timeframes. Bottom four panels depict the change from the historical mean; cross hatching denotes areas of robust predicitons (90% of models agree in the direction of change).

Natural Bridges: Summer evaporation

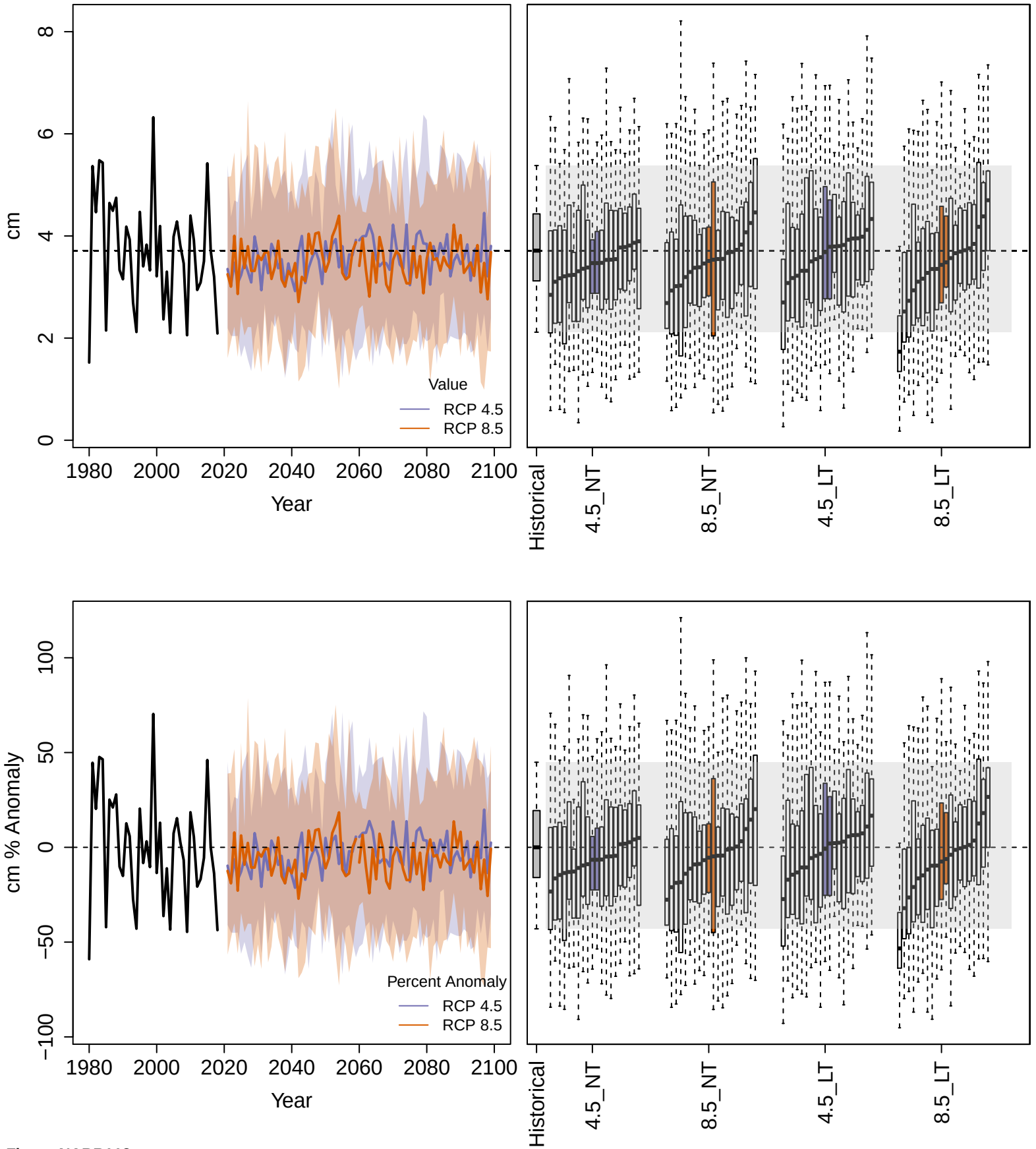


Figure NABR113:
Past trends and future trajectories of park−wide mean values for Summer evaporation in Natural Bridges. Top panels show values, bottom panels show changes from the long−term historical mean. Left: Time series of historical (black) and future projections for RCP 4.5 and 8.5. Shaded areas show spread among climate models. Right: Boxplots of temporal variability over 40−year periods under historical (left box) and individual climate models under two RCPs. Right: Historical time period is 1970−2010; near−term (NT) is 2020−2060; long−term (LT) is 2061−2100.

Natural Bridges: Summer evaporation

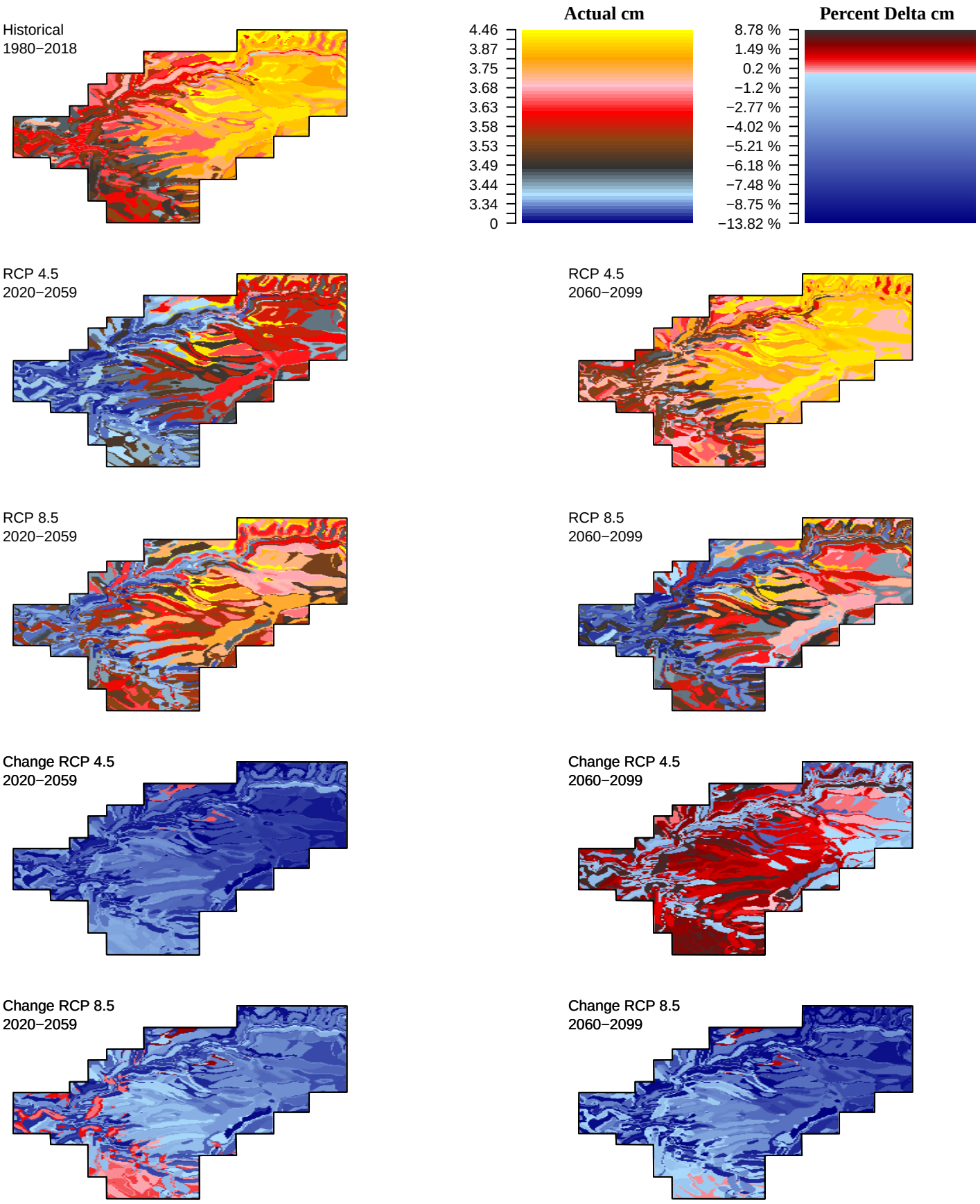


Figure NABRmap113:
Past trends and future trajectories of park−wide mean values for Summer evaporation in Natural Bridges. Topmost panel depicts the historical mean from 1980−2018. Lower four panels show the emission scenarios of RCP 4.5 and RCP 8.5 at near−term and long−term timeframes. Bottom four panels depict the change from the historical mean; cross hatching denotes areas of robust predicitons (90% of models agree in the direction of change).

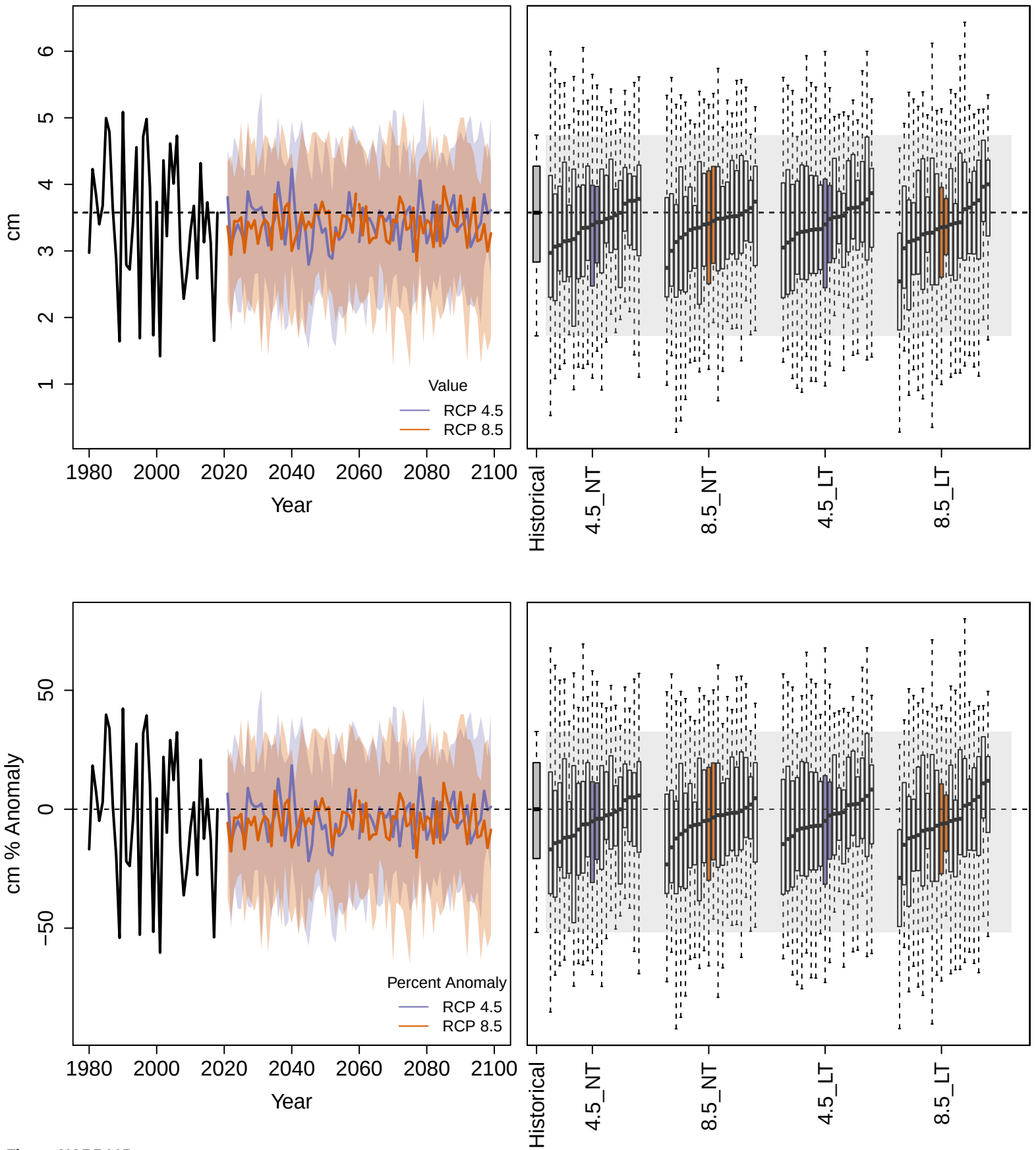


Figure NABR115:
Past trends and future trajectories of park−wide mean values for Fall evaporation in Natural Bridges. Top panels show values, bottom panels show changes from the long−term historical mean. Left: Time series of historical (black) and future projections for RCP 4.5 and 8.5. Shaded areas show spread among climate models. Right: Boxplots of temporal variability over 40−year periods under historical (left box) and individual climate models under two RCPs. Right: Historical time period is 1970−2010; near−term (NT) is 2020−2060; long−term (LT) is 2061−2100.

Natural Bridges: Fall evaporation

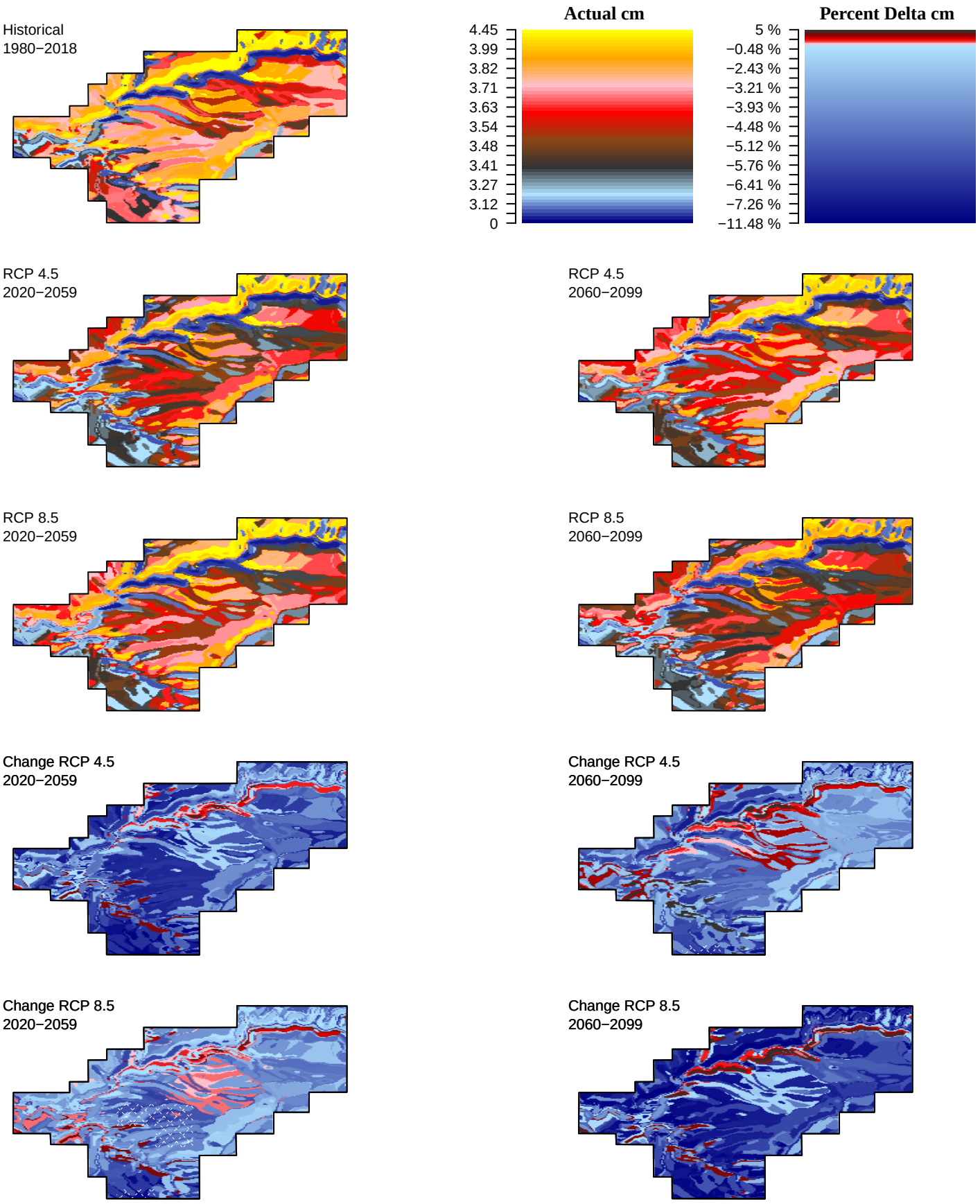


Figure NABRmap115:
Past trends and future trajectories of park−wide mean values for Fall evaporation in Natural Bridges. Topmost panel depicts the historical mean from 1980−2018. Lower four panels show the emission scenarios of RCP 4.5 and RCP 8.5 at near−term and long−term timeframes. Bottom four panels depict the change from the historical mean; cross hatching denotes areas of robust predicitons (90% of models agree in the direction of change).

Natural Bridges: Winter transpiration

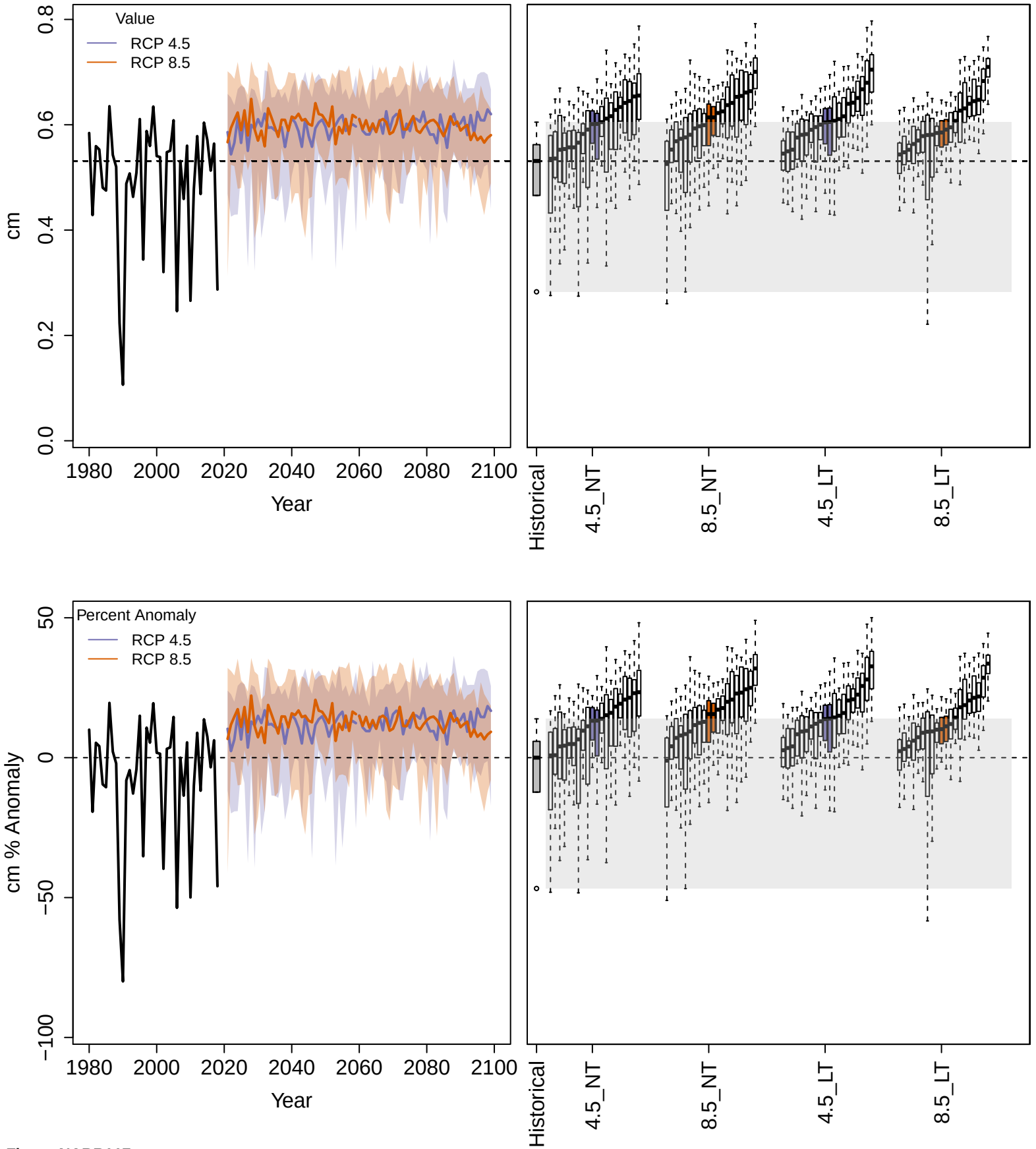


Figure NABR117:
Past trends and future trajectories of park−wide mean values for Winter transpiration in Natural Bridges. Top panels show values, bottom panels show changes from the long−term historical mean. Left: Time series of historical (black) and future projections for RCP 4.5 and 8.5. Shaded areas show spread among climate models. Right: Boxplots of temporal variability over 40−year periods under historical (left box) and individual climate models under two RCPs. Right: Historical time period is 1970−2010; near−term (NT) is 2020−2060; long−term (LT) is 2061−2100.

Natural Bridges: Winter transpiration

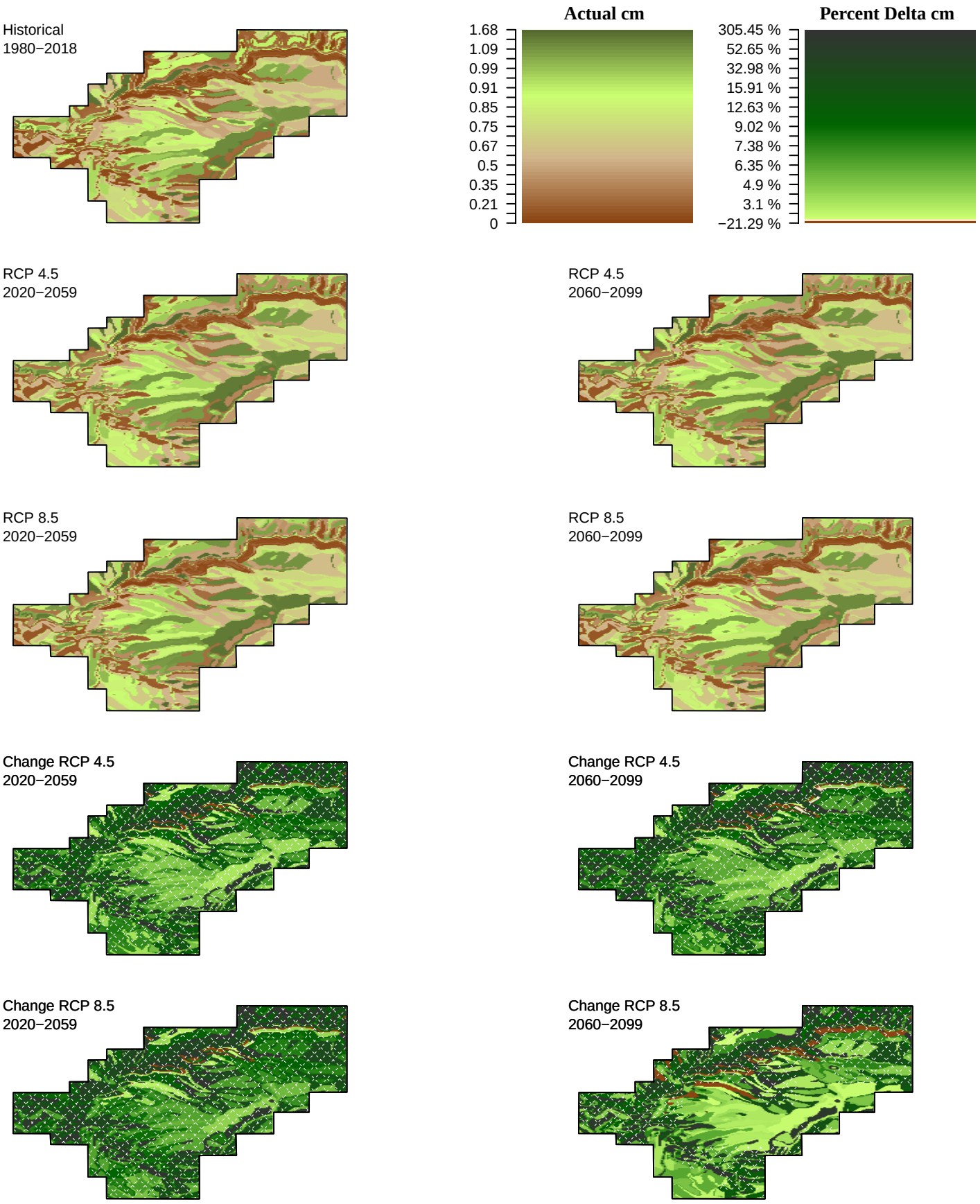


Figure NABRmap117:
Past trends and future trajectories of park−wide mean values for Winter transpiration in Natural Bridges. Topmost panel depicts the historical mean from 1980−2018. Lower four panels show the emission scenarios of RCP 4.5 and RCP 8.5 at near−term and long−term timeframes. Bottom four panels depict the change from the historical mean; cross hatching denotes areas of robust predicitons (90% of models agree in the direction of change).

Natural Bridges: Spring transpiration

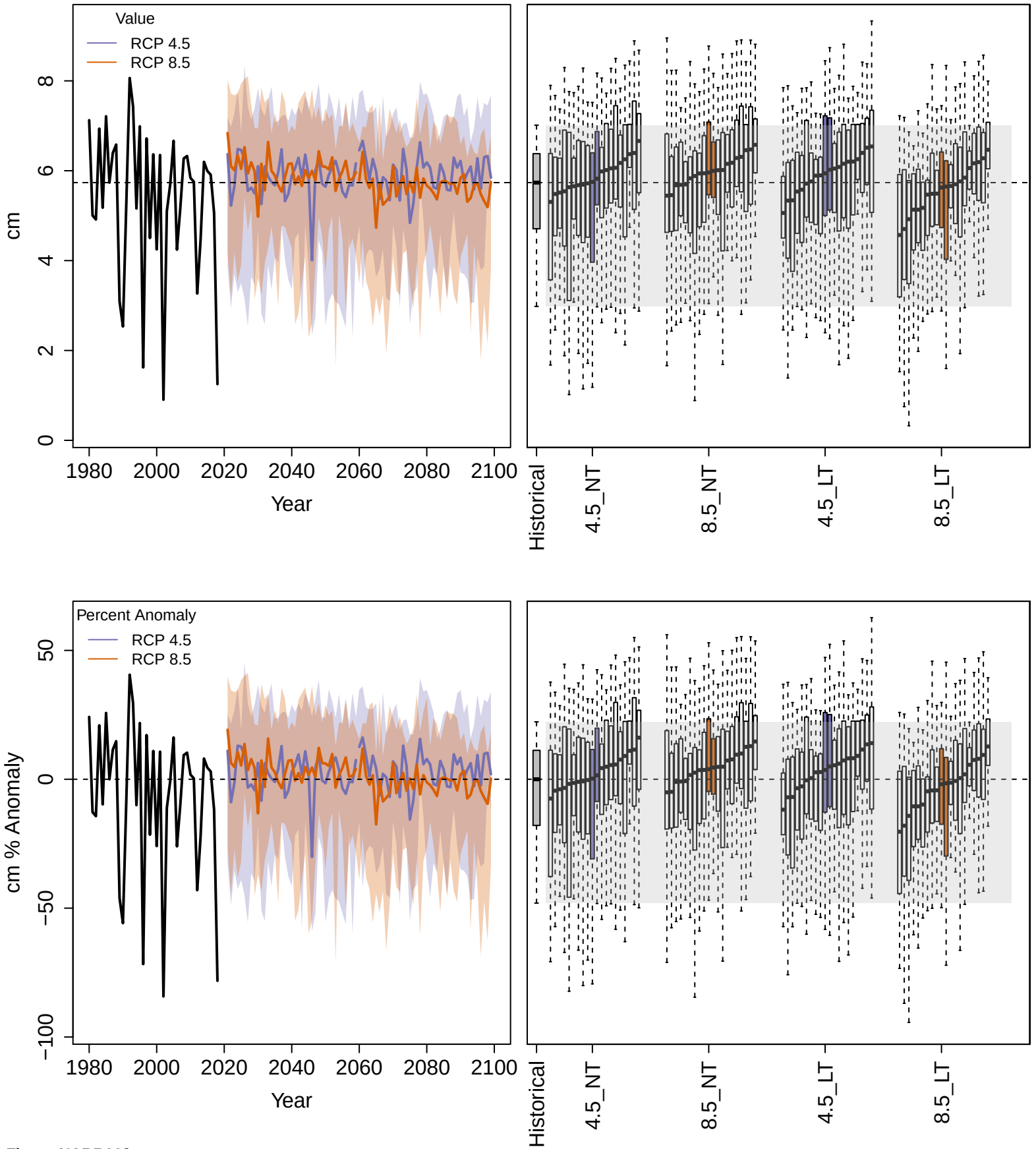


Figure NABR119:
Past trends and future trajectories of park−wide mean values for Spring transpiration in Natural Bridges. Top panels show values, bottom panels show changes from the long−term historical mean. Left: Time series of historical (black) and future projections for RCP 4.5 and 8.5. Shaded areas show spread among climate models. Right: Boxplots of temporal variability over 40−year periods under historical (left box) and individual climate models under two RCPs. Right: Historical time period is 1970−2010; near−term (NT) is 2020−2060; long−term (LT) is 2061−2100.

Natural Bridges: Spring transpiration

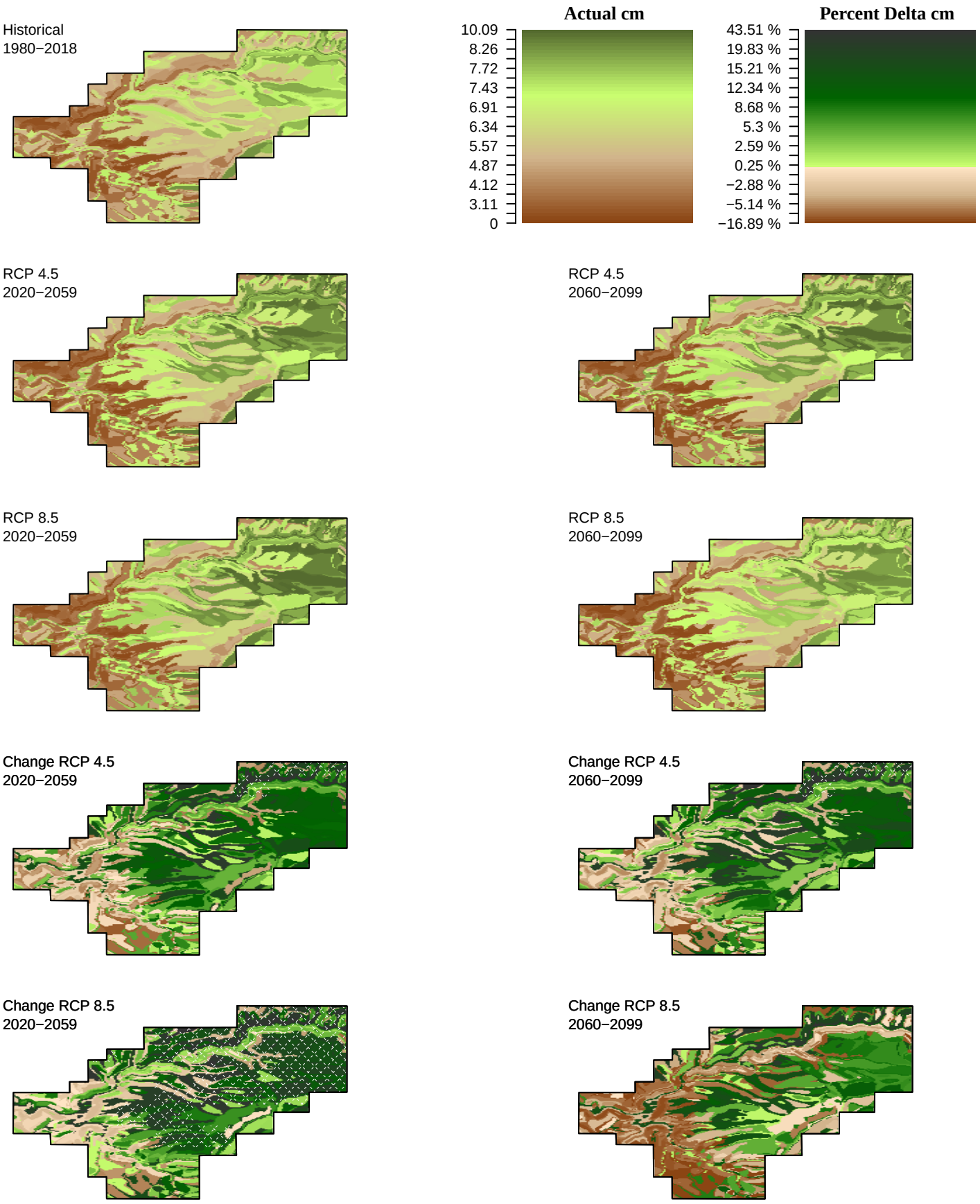


Figure NABRmap119:
Past trends and future trajectories of park−wide mean values for Spring transpiration in Natural Bridges. Topmost panel depicts the historical mean from 1980−2018. Lower four panels show the emission scenarios of RCP 4.5 and RCP 8.5 at near−term and long−term timeframes. Bottom four panels depict the change from the historical mean; cross hatching denotes areas of robust predicitons (90% of models agree in the direction of change).

Natural Bridges: Summer transpiration

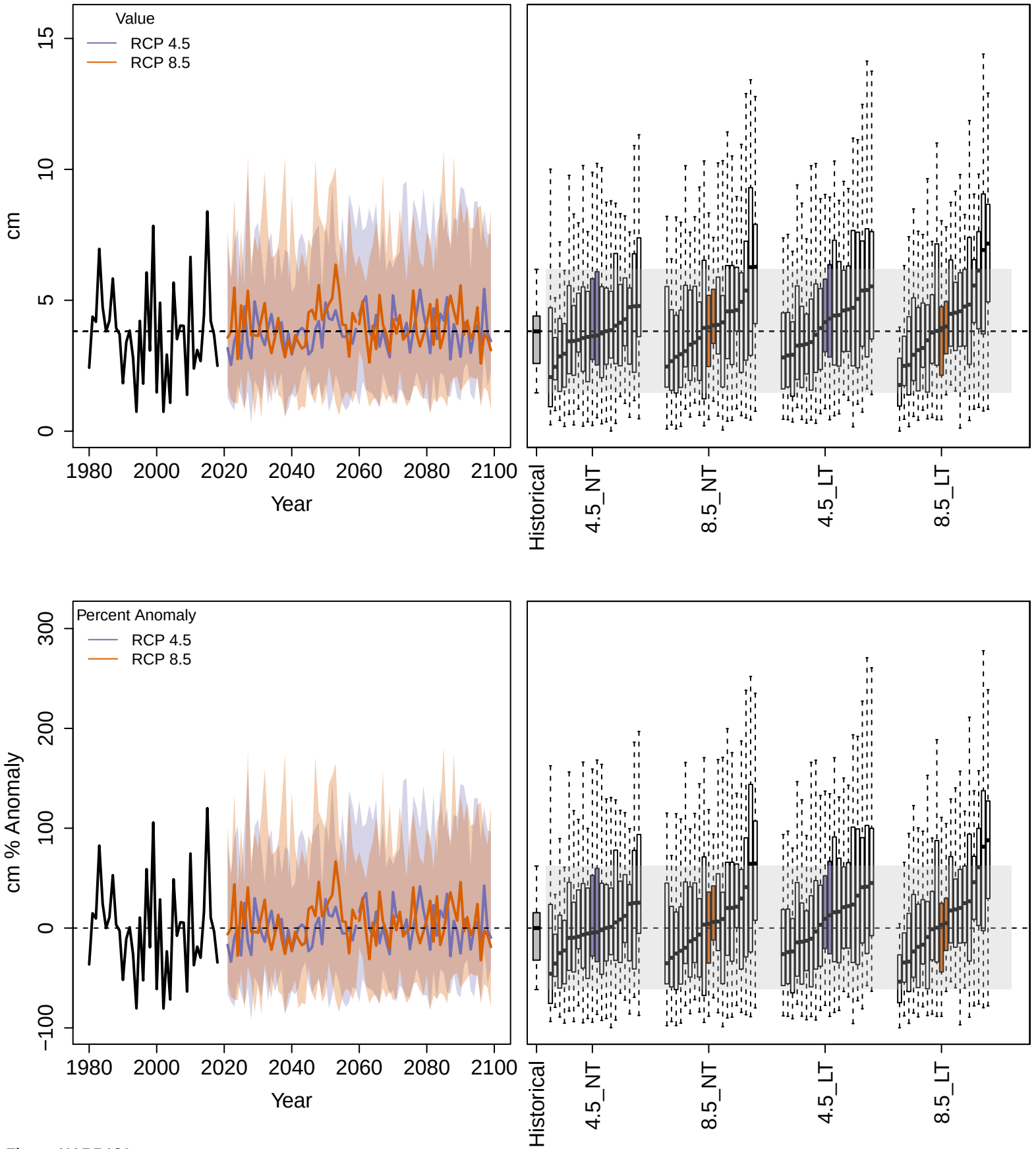


Figure NABR121:
Past trends and future trajectories of park−wide mean values for Summer transpiration in Natural Bridges. Top panels show values, bottom panels show changes from the long−term historical mean. Left: Time series of historical (black) and future projections for RCP 4.5 and 8.5. Shaded areas show spread among climate models. Right: Boxplots of temporal variability over 40−year periods under historical (left box) and individual climate models under two RCPs. Right: Historical time period is 1970−2010; near−term (NT) is 2020−2060; long−term (LT) is 2061−2100.

Natural Bridges: Summer transpiration

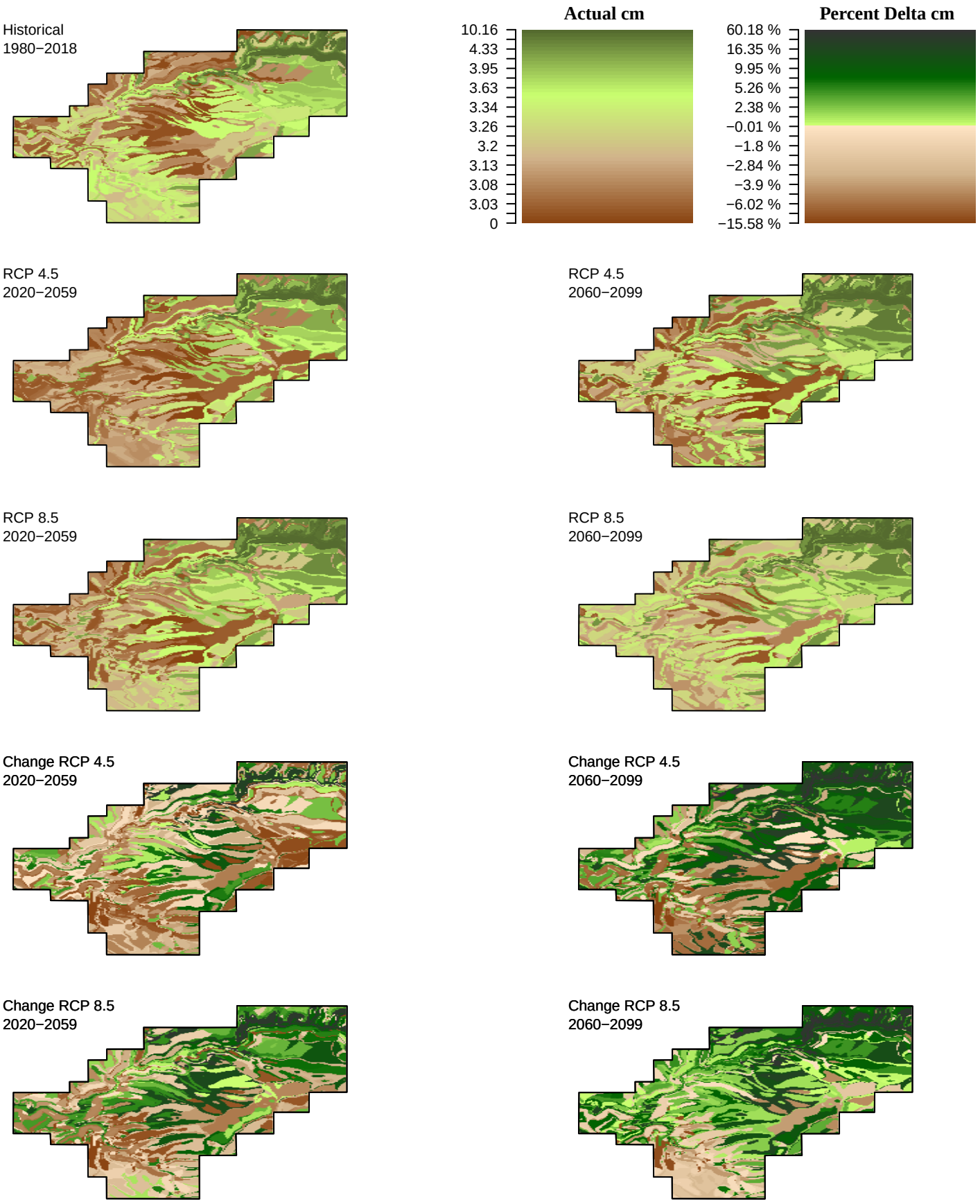


Figure NABRmap121:
Past trends and future trajectories of park−wide mean values for Summer transpiration in Natural Bridges. Topmost panel depicts the historical mean from 1980−2018. Lower four panels show the emission scenarios of RCP 4.5 and RCP 8.5 at near−term and long−term timeframes. Bottom four panels depict the change from the historical mean; cross hatching denotes areas of robust predicitons (90% of models agree in the direction of change).

Natural Bridges: Fall transpiration

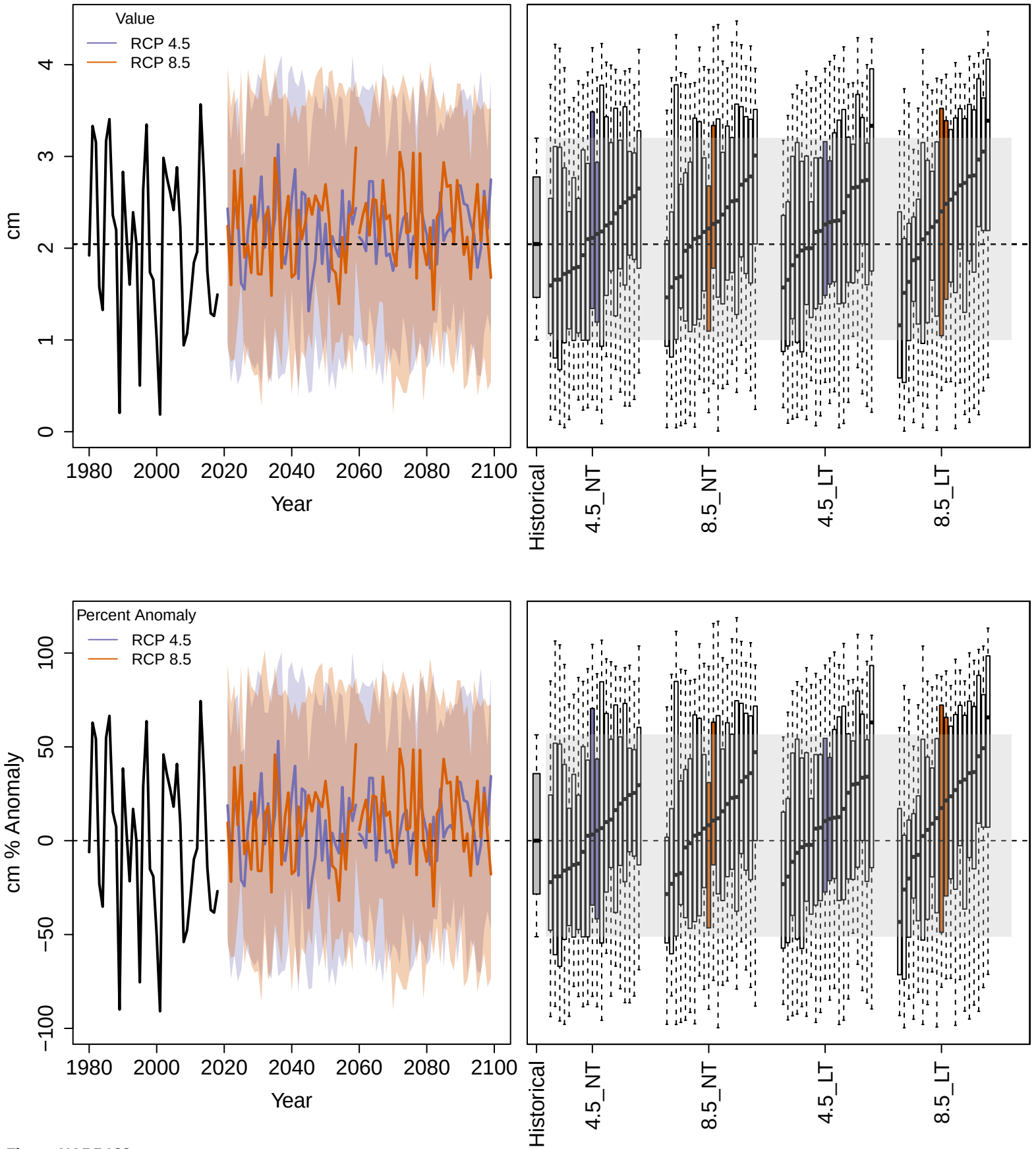


Figure NABR123:
Past trends and future trajectories of park−wide mean values for Fall transpiration in Natural Bridges. Top panels show values, bottom panels show changes from the long−term historical mean. Left: Time series of historical (black) and future projections for RCP 4.5 and 8.5. Shaded areas show spread among climate models. Right: Boxplots of temporal variability over 40−year periods under historical (left box) and individual climate models under two RCPs. Right: Historical time period is 1970−2010; near−term (NT) is 2020−2060; long−term (LT) is 2061−2100.

Natural Bridges: Fall transpiration

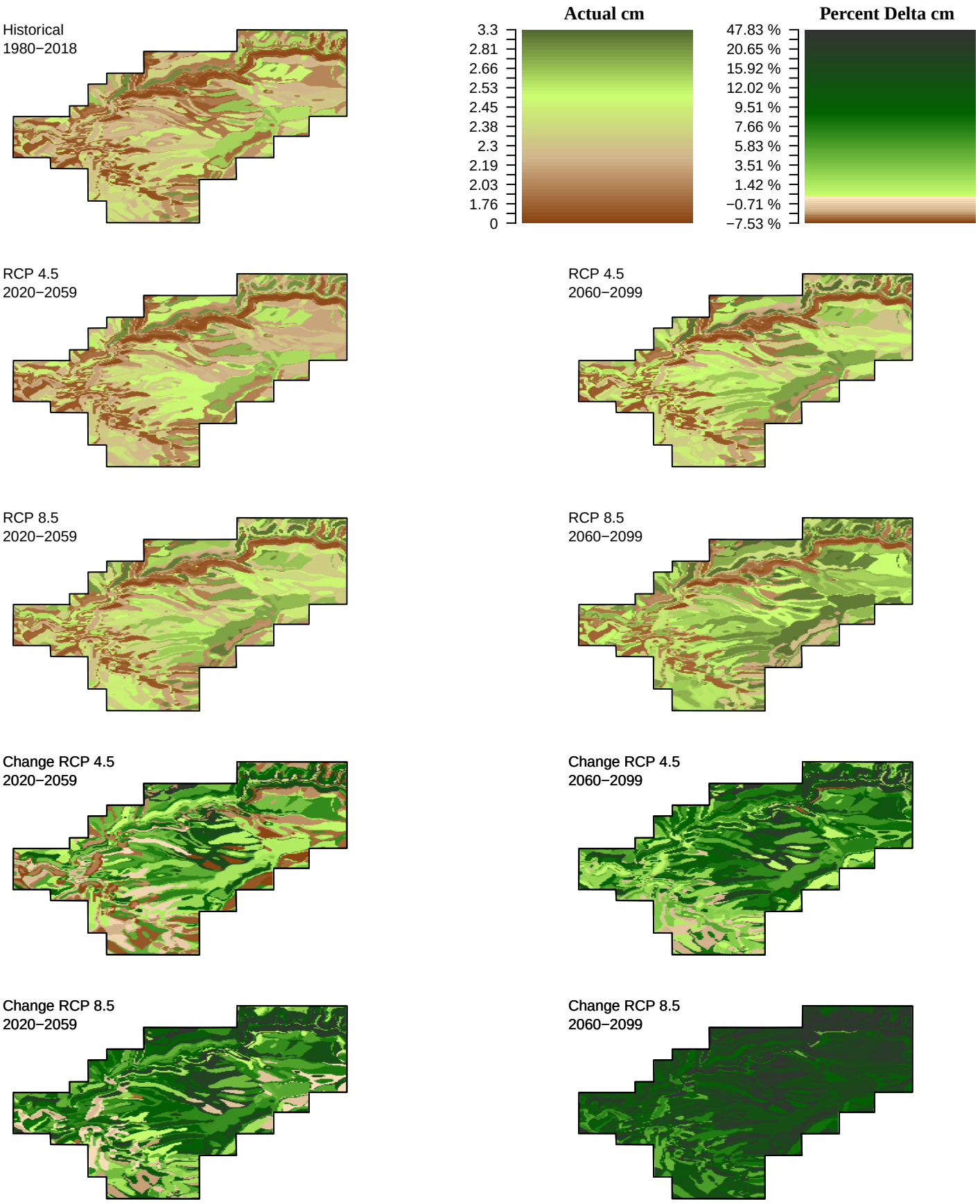


Figure NABRmap123:
Past trends and future trajectories of park−wide mean values for Fall transpiration in Natural Bridges. Topmost panel depicts the historical mean from 1980−2018. Lower four panels show the emission scenarios of RCP 4.5 and RCP 8.5 at near−term and long−term timeframes. Bottom four panels depict the change from the historical mean; cross hatching denotes areas of robust predicitons (90% of models agree in the direction of change).